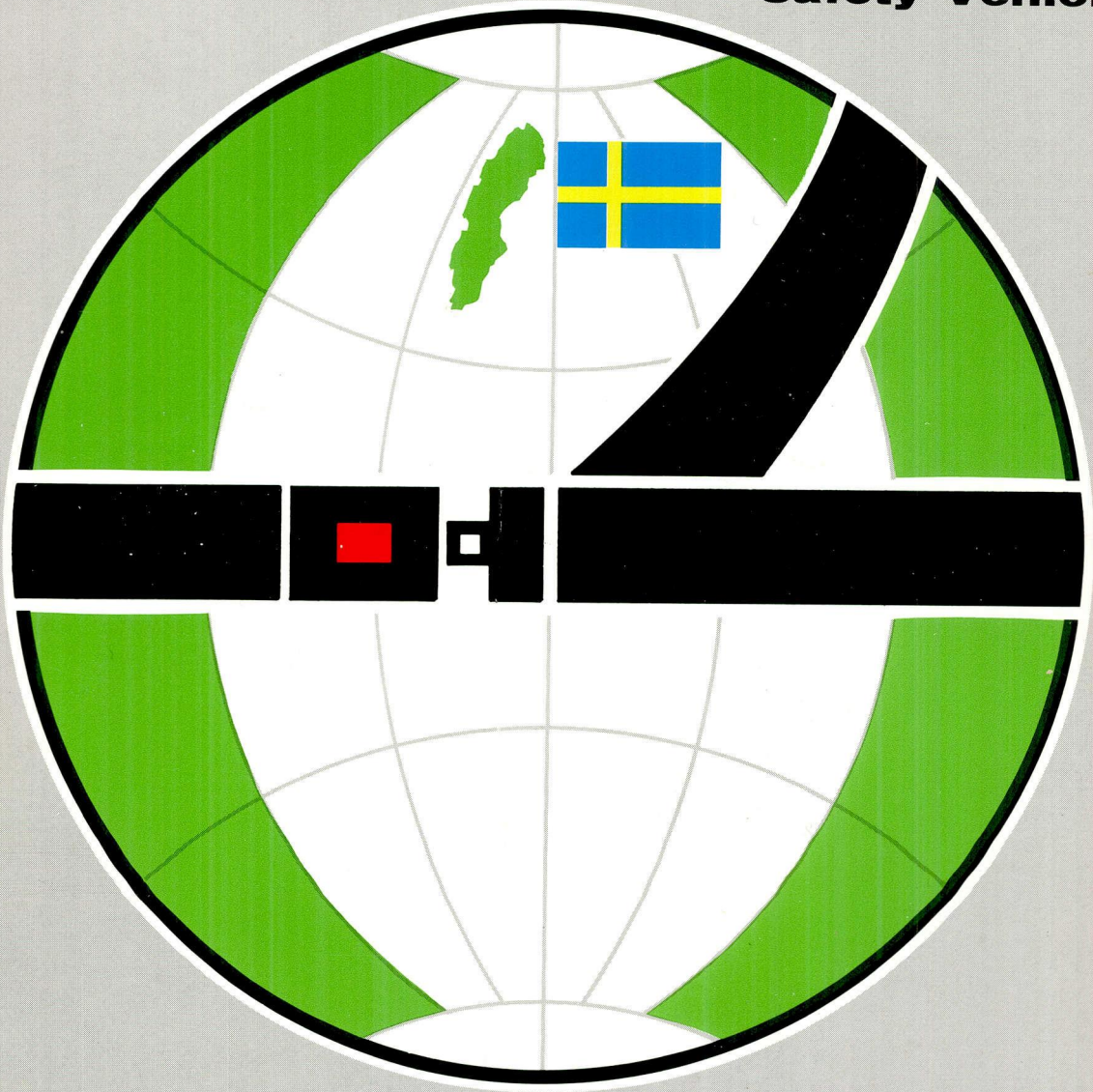




U.S. Department  
of Transportation

**National Highway  
Traffic Safety  
Administration**

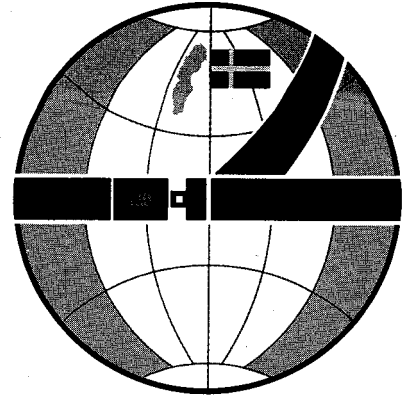
**Twelfth  
International  
Technical  
Conference on  
Experimental  
Safety Vehicles**



Proceedings Vol. 2  
May 29—June 1  
Göteborg, Sweden  
1989



U.S. Department  
of Transportation  
**National Highway  
Traffic Safety  
Administration**



# **The Twelfth International Technical Conference on Experimental Safety Vehicles**

**Sponsored by:**  
U.S. Department of  
Transportation  
National Highway Traffic  
Safety Administration

**Hosted by:**  
Swedish Government

**Held at:**  
Göteborg, Sweden  
May 29—June 1, 1989

# Foreword

This report of the proceedings of the Twelfth International Technical Conference on Experimental Safety Vehicles was prepared by the National Highway Traffic Safety Administration, U.S. Department of Transportation.

We wish to thank the authors and all those responsible for the excellence of the material submitted, which aided materially in the preparation of this report.

For clarity and because of some translation difficulties, a certain amount of editing was necessary. Apologies are, therefore, offered where the transcription is not exact.

# Introduction

The International Experimental Safety Vehicles (ESV) Program originated under NATO's Committee on the Challenges of Modern Society (CCMS) and was implemented through bilateral agreements between the United States Government and the governments of France, the Federal Republic of Germany, Italy, the United Kingdom, Japan, and Sweden. The participating nations agreed to develop experimental safety vehicles to advance the state-of-the-art in safety engineering and to meet periodically to exchange technical information on their progress.

To date, eleven international conferences have been held, each hosted by one of the participating Governments. These conferences have drawn participants from government, the worldwide automotive industry, and the motor vehicle safety research community. International cooperation in motor vehicle safety research continues at the highest level. As work on experimental safety vehicles was completed, the research program was expanded to cover the entire range of motor vehicle safety. The ESV Conferences now serve as the international forum through which progress in motor vehicle safety technology is reported.

The proceedings of each Conference have been published by the United States Government and distributed worldwide. These reports, which detail the safety research efforts underway worldwide, have been recognized as the definitive work on motor vehicle safety research. We are sure that this outstanding example of international cooperation seeking reductions in motor vehicle deaths and injuries will continue its past success.

## **Attendees**

---

### **BELGIUM**

---

Noritoshi Arai  
Toyota Motor Corporation

Johan De Vidts  
Honda Motor Co., Ltd.

Tetsuo Hasegawa  
Nissan Motor Co. LTD

Herbert Henssler  
Commission of the European

Pieter W. Hoekstra  
Commission of the European

Kizu  
Toyota Motor Corporation

Kondo  
Toyota Motor Corporation

Willy Maes  
Drive Office

Henk Mannekens  
Nissan Motor Co. LTD

Horst-Georg Marks  
CCMC

Yutaka Matsumoto  
Toyota Motor Corporation

André Meganck  
Honda Motor Co., Ltd.

Kengo Nishikata  
Mazda Motor Repres. Office

Keichi Okabayashi  
Toyota Motor Corporation

R.J. Peeters  
Commission of the European

Hans Van Driessche  
Honda Motor Co., Ltd.

---

### **CANADA**

---

Ray Boulding  
Hastings & Boulding

Dainius Dalmotas  
Transport Canada

John C. Hastings  
Hastings & Boulding, Consl. Eng.

Michael Macnabb  
U.B.C. Accident Investigation Team

James A. Newman  
Biokinetics and Assoc.

Edwin S. Nowak  
The University of Western Ontario

Jocelyn Pedder  
Biokinetics and Assoc.

Andre St-Laurent  
Biokinetics and Associates Ltd.

A. Lloyd Thompson  
McGill University

André Viel  
Régie de l'assurance automobile

Christopher S. Wilson  
Transport Canada

---

### **DENMARK**

---

Ib Rasmussen  
Ministry of Justice

---

### **FINLAND**

---

Jukka Sundberg  
Electrolux Klippan

---

### **FRANCE**

---

Claude Aubry  
Autoliv Klippan

Jean-Jacques Azuar  
Peugeot S.A.

Marc Behaghel  
Chambre Syndicale

Farid Bendjellal  
Lab. Physiologi Biomecanique

Jean Bloch  
INRETS—LCB

Serge Bohers  
Peugeot SA/Etudes

Miss Bohers  
Peugeot SA/Etudes & Recherches

Patrick Botto  
Laborat. Physiologie Biomecanique

Francoise Brun Cassan  
Laboratoire de Physiologie ET

Gilles Brutel  
PSA Etudes-Et-Recherches

Dominique Cesari  
INRETS—LCB

Georges Dobias  
Inst. National de Recherche

Leonce Evin  
Autoliv Klippan

Hélène Fontaine  
INRETS

Bruno Foret  
Laborat. Physiologie Biomecanique

Jean Fructus  
UTAC

Bernard Gauvin  
Direction de la Securite

Claude Henry  
Laborat. Physiologie Biomecanique

Mrs. Herve  
Peugeot SA/Etudes & Recherches

Serge Koltchakian  
Laborat. Physiologie Biomecanique

Michel Kozyreff  
Autoliv Klippan

Philippe Mack  
Lab. Physiologie Biomec.

Gerard Mauron  
PSA Études et Recherches

John Phelps  
O.I.C.A.

Nicholas Rogers  
IMMA, Int. Motorcycle Manuf. Assoc.

Shigeru Sasaki  
JAMU; Japan Automobile

Jean Pierre Spagnol  
Autoliv Klippan

Georges Stcherbatcheff  
Renault

Christian Steyer  
Regie Renault

Claude Tarriere  
Laborat. Physiologie Biomecanique

Kyriakos Vavalidis  
Autoliv Klippan

---

### **GREAT BRITAIN**

---

Raymond Attwood  
B.S.R.D. Ltd.

Gordon Bacon  
Motor Industry Research Association

Bill Baker  
Ford Motor Company, Ltd.

John Bidgood  
RAC Motoring Service, Ltd.

Philip Bly  
Transport and Road Research Laboratory

Mo Bradford  
Institute for Consumer Ergonomics

David Burleigh  
Britax Child Care

John Cart  
Lucas Car Braking Systems

Bryan Chinn  
Transport and Road Research Laboratory

Keith Clemo  
Motor Industry Research Association

David Coates  
Motor Industry Research Association

Tony Denniss  
Norton Motors Limited

Bill Dixon  
SMMT Ltd.

Gerald Doe  
Lotus Cars Ltd.

Eric Dunn  
Department of Transport

Malcolm Eden  
Ford Motor Company Limited

Stanley J. Edge  
Sheller Clifford Ltd.

Douglas Foot  
Department of Transport

James Stephen Frampton  
Jaguar Cars Ltd.

Robert W. Fraser  
Ford Motor Co., Ltd

Nicholas Grew  
Austin Rover

John Harris  
Transport and Road Research Laboratory

Kenneth Hill  
Middlesex Polytechnic

C. Adrian Hobbs  
Transport and Road Research Laboratory

Fred Hope  
Hope Technical Developments Ltd.

David Jeffery  
Transport and Road Research Laboratory

Rachel Jelly  
Lotus Cars Ltd.

Paul Jennison  
SMMT, Society of Motor

Christopher Paul Kavanagh  
Marling Industries PLC

John Lee  
Ford Motor Company Ltd.

Richard Lewis  
Ford Motor Co., Ltd.

Richard Lowne  
Transport & Road Research Laboratory

Murray Mackay  
Accident Research Unit

Annabel Macleod  
Oxford Metrics Ltd.

Terry McGowan  
Land Rover Ltd.

Pat Murphy  
Department of Transport

Ian D. Neilson

Fred Nicod  
Electrolux Klippan Ltd.

Andrew Parkes  
Husat Research Centre

Chris J. Patience  
Automobile Association

Geoffrey Platten  
Ogle Design Ltd.

Tracy Ramsey  
Husat Research Centre

Mostafa Rashidy  
Cranfield Impact Centre

Stephen Richins  
Land Rover Ltd.

Brian Robinson  
Transport and Road Research Laboratory

Peter Roy  
Middlesex Polytechnic

Majid M. Sadeghi  
Cranfield Impact Centre

Ram Singh  
K.L. Jeenay P.L.C.

Bruce Smallbone  
Leylands Bus Ltd.

Derek Spragg  
Department of Transport

John A. Stubbs  
Automobile Association

Gary D. Suthurst  
Ford Motor Company, Ltd.

Brian Teece  
Jaguar Cars Ltd.

John Temple

Alan Vaughan Thomas  
Jaguar Cars Limited

Pete Thomas  
Institute for Consumer Ergonomics

Sadayuki Ujihashi  
University of Strathclyde

Simon Valkenburg  
Marling Industries PLC

---

## IRELAND

---

Kotaro Kitai  
European Components Corp.

Patrick Mc Donagh  
European Components Corporation

Denis P. Wood  
Wood & Associates

---

## ISRAEL

---

Zvi Eshel  
Ministry of Defence Tel Aviv

---

## ITALY

---

Domenico Chirico  
Alfa Lancia Industriale

Andrea Costanzo  
Universita di Roma "La Sapienza"

Gaetano Danese

Giancarlo Ferrero  
Fiat Auto

Ardoino Pierluigi  
Fiat Auto SpA-DT-SP-Centro  
Sicurezza

Ubaldo Quaranta  
Ministero dei Trasporti  
Ubaldo Quaranti

---

## JAPAN

---

Kiyoshi Fujii  
Suzuki Motor Co., Ltd.

Yoshiichi Fujimura  
Takata Corporation

Tatsuya Futamata  
Nissan Motor Co., Ltd.

Junji Hasegawa  
Toyota Motor Corporation

Masayuki Higuchi  
Toyota Motor Corporation

Yosiiti Huzimura

Yoshikazu Ide  
Mazda Motor Corporation

Toshihiro Ishikawa  
Mazda Motor Corporation

Masahiro Itoh  
Japan Automobile Research Inst., Inc.

Hiroshi Kizawa  
JAMA

Yutaka Kondoh  
Toyota Motor Corporation

Ono Koshiro  
JARI, Inc.

Masakazu Kume  
Jap. Automob. Standards Intern.

Keiji Kusaka  
Kawasaki Heavy Ind., Ltd.

Fumio Matsuoka  
Toyota Motor Corporation

Akihiro Miyajima  
Subaru Research Center

Taizo Miyake  
Suzuki Motor Co., Ltd.

Masanobu Mizuguchi  
Ashimori Industry Co., Ltd.

Yoshiyuki Mizuno  
Nissan Motor Co Ltd

Shinji Mori  
Tokai Rika Co., Ltd.

Masanori Motoki  
Japan Automobile Research Inst., Inc.

Masonori Murata  
Fuji Autoliv Co., Ltd.

Kosuke Nagao  
Ashimori Industri Co., Ltd.

Hiroshi Nagao  
Mazda Motor Corporation

Masakazu Nakada  
Traffic Safety Policy Office

Masakazu Nakada  
Traffic Safety Policy Office

Yukinori Nakamura  
Nissan Motor Co., Ltd.

Akihisa Nakamura  
IATSS

Yousuke Nishida  
Honda R&D Co., Ltd.

Hideo Obata  
Century Research Center Corporation

Kenji Ogata  
Toyota Motor Corporation

Kizu Ryohei  
Toyota Motor Corporation

Kiminori Saito  
Toyota Motor Corporation

Kazutoshi Sakamoto  
Daihatsu Motor Co., Ltd.

Shinichi Sakamoto  
Suzuki Motor Co., Ltd.

Hikota Sakamoto  
Nissan Motor Co., Ltd.

Minoru Sakurai  
Japan Automobile Research Ins., Inc.

Toshiaki Sakurai  
Mitsubishi Motors Corporation

Hiroshi Sato  
Fuji Autoliv Co., Ltd.

Tsutomu Sawada  
Nissan Motor Co., Ltd.

Munemasa Shimamura  
Nissan Motor Co., Ltd.

Nobuyoshi Shimoda  
Honda R&D Co., Ltd.

Shuji Shiraishi  
Honda R&D Co., Ltd.

Yoichi Sugimoto  
Honda R&D Co., Ltd.

Koji Taga  
Mazda Motor Corporation

Moriyuki Taguchi  
Yamaha Motor Co., Ltd.

Taka  
Director, Land Transport Engineering  
Dep

Kazuhiko Takada  
Takata Corporation

Noboru Takahashi  
Fuji Heavy Industries, Ltd.

Matsui Takashi  
Yamaha Motor Co., Ltd.

Naofumi Takashige  
Ministry of Transport

Tetsuo Teramoto  
Toyota Motor Corporation

Masanobu Wada  
Nissan Motor Co., Ltd.

Kuniyuki Watanabe  
Nissan Motor Co., Ltd.

Kazuo Watanabe  
Takata Corporation

Eiichi Yaguchi  
Nissan Motor Co., Ltd.

Tsuyoshi Yamaguchi  
Nissan Motor Co., Ltd.

Yoshikazu Yamaguchi  
Ministry of Intern. Trade & Ind.

Yoshido Yamakawa  
Takata Corporation

Takenari Yamamoto  
Honda R&D Co., Ltd.

Shuichi Yamazaki  
Honda Promotion Center

Hiroaki Yoshida  
Mitsubishi Motors Corporation

Keigo Yoshida  
Honda R&D Co. Ltd.

Ryoichi Yoshida  
Takata Corporation

---

## NETHERLANDS

---

Arjaan Buijk  
Pisces International B.V.

Frans Campman  
Volvo Car B.V.

Frans Christophe  
Volvo Car B.V.

Jos De Ceuster  
Volvo Car B.V.

Hans Huybers  
Rykwaterstaat

Paul Jacobs  
Volvo Car B.V.

Edgar Janssen  
TNO Road-Vehicles Research Institute

Jaap Maartense  
Volvo Car B.V.

Gerard J.M. Meekel  
Rijksdienst voor het Wegverkeer

John Nieboer  
TNO Road-Vehicles Research Institute

Henk Oskam  
Volvo Car B.V.

Bernard Reys  
TNO Road-Vehicles Research Institute

Leo Shloser  
Rykswaterstaat

Constantijn Sneathlage  
Pisces International B.V.

Gerard Steegers  
Van Oerle Alberton B.V.

Jan Stoop  
Volvo Car B.V.

Gerrit Tanis  
TNO Road-Vehicles Research Institute

Maarten Van Der Velden MM

Boudewyn Van Kampen  
Institute for road safety research swov

Carla van Moorsel  
Rijksdienst voor het Wegverkeer

Eric van Oorschot  
TNO Road-Vehicles Research Institute

A.G.M. van Vliet  
Yamaha Motor Europe N.V.

Fred Wegman  
Institute for Road Safety Research

Theo Verbruggen  
TNO Road-Vehicles Research Institute

Jac Wismans  
TNO Road-Vehicles Research Institute

---

## NORWAY

---

Per Georg Karlsen  
Teknologisk Institut

---

## SPAIN

---

Javier Alvarez-Montalvo  
Ministerio de Industria y Energia

Ricardo Chicharro  
I.N.T.A.

Julian Soria  
Nissan Motor Iberica SA

---

## SWEDEN

---

Rickard Adlercreutz  
Volvo Car Corporation

Bertil Aldman  
Chalmers University

Åke Almgren  
Elektrolux Autoliv AB

Rune Almqvist  
Volvo Car Corporation

Per Andersson  
Autoliv Development AB

Sture Andersson  
Electrolux Autoliv AB

Tommy Andersson  
Autoliv Stil AB

Georg Andersson  
Kommunikationsdepartementet

Göran Andersson  
Trafiksäkerhetsverket

Bo Appelqvist  
Chalmers Tekniska Högskola

Hans-Olof Arvidsson  
Volvo Car Corporation

Kjell Astergård  
Volvo Car Corporation

Peter Augustsson  
Volvo Car Corporation

Claes Avedal  
Volvo Car Corporation

Robert Bell  
AB Akta

Marisa Benedek  
Swedish Trade Council

Sven Bengtson  
Volvo Car Corporation

Stefan Berge  
Volvo Car Corporation

Eddy Bergenheim  
Volvo Car Corporation

Laura Bidussi-Mancini  
Swedish Trade Council

Jarl Bill  
Bil AB Atlas

Jan Billig  
Volvo Car Corporation

Jan-Olof Blomfeldt  
Bilindustriföreningen

Nils Bohlin  
OBE Engineering Co.

Kent Bovellan  
Saab Personbilsdivision

Gunnar Bringfeldt  
Volvo Car Corporation

Olle Bunketorp  
Östra Hospital

Staffan Calsson  
AB Bofors

Nicole Candelier  
Swedish Trade Council

Gerd Carlsson  
Volvo Car Corporation

Gunnar Carlsson  
VTI

Serge Cavanna  
Swedish Trade Council

Gustaf Celsing  
Autoliv Stil AB

Magnus Dahl  
Volvo Car Corporation

Sverker Dahl  
Förenade Landsortstidningar

Olivier Daillant  
Swedish Trade Council

Heidlore Drathen  
Swedish Trade Council

Izumi Duggal-Takagi  
Swedish Trade Council

Gertrud Dürkop  
Swedish Trade Council

Lars Eggertz  
Swedish Road Safety Office

Mats Ekholm  
Volvo Car Corporation

Björn Eklind  
Volvo Personvagnar AB

Jan-Inge Eliasson  
Volvo Car Corporation

Olof Englund  
Volvo Car Corporation

Anders Englund  
FSAB / TRK

Bengt Engström  
Volvo Car Corporation

Sture Ericson Saab-Scania AB	Erik Hang Autoliv Stil AB	Peter Jakobsson Autoliv Development AB
Anders Eriksson Volvo Car Corporation	Thomas Hansson Volvo Car Corporation	Mille Jeltin Saab-Scania AB
Anders Eugensson Volvo Car Corporation	Lars-Åke Haraldsson Saab-Scania AB	Lennart Johansson Volvo Car Corporation
Sven-Erik Flyborg SLG Produkter AB	Thomas Harne Saab-Scania AB	Rune Johansson Volvo Car Corporation
Hans Folkesson Saab-Scania AB	Sören Hedberg Swedish Road Safety Office	Eva Johansson Saab-Scania AB
Peter Follin Volvo Car Corporation	Lars-Olof Hellgren Saab Personbilsdivision	Tommy Johansson Trelleborg AB
Eva Forsberg Volvo Car Corporation	Tore Helmersson Saab-Scania	Göran Johansson Volvo Car Corporation
Tord Forsgren Volvo Car Corporation	Håkan Helsner Volvo Car Corporation	Magnus Jonsson Saab-Scania AB
Stig Franzén Saab-Scania Consult AB	Susan Hilton Swedish Trade Council	Tony Jonsson Autoliv Development AB
Lennart Fremling Trafiksäkerhetsverket	Ulla Hjelmblad Swedish Trade Council	Janusz Kajzer Chalmers University of Technology
Rune Fritsby Volvo Car Corporation	Maria Hjohlman Autoliv Development AB	Leif Karlbrink Electrolux Klippan
Lars Gardell Saab-Scania AB	Jutta Hoffman-Zobel Swedish Trade Council	Rune Karlsson Volvo Truck Co
Jonas Gawell Bilindustriföreningen	Alf Holgers Saab-Scania AB	Walter Keiser Swedish Trade Council
Ulf Granström Volvo Car Corporation	Björn Holthe Volvo Car Corporation	Reinhard Klose Swedish Trade Council
Peder Grell Göteborgs Posten	Lotta Hultberg Volvo Personvagnar AB	Magnus Koch Volvo Car Corporation
Tore R Gullstrand Saab-Scania AB	Christer Hydén Lunds Universitet	Johnny Korner Volvo Car Corporation
Leif Gunnarsson Autoliv Development AB	Alf Håkansson Volvo Truck Corporation	Jörgen Krabbe Volvo Car Corporation
Monica Gustafson Volvo Car Corporation	Yngve Håland Autoliv Development AB	Anders Kullgren Folksam
Rune Gustafsson Volvo Car Corporation	Bosse Händel Volvo Svenska Bil	Ulrika Landelius Volvo Car Corporation
Hans Gustavsson Volvo Car Corporation	Kristina Höije Saab-Scania AB	Bengt Landin Saab-Scania
Henrik Gustavsson Saab-Scania AB	Carl-Axel Höjer Volvo Car Corporation	Lars Larson Volvo Car Corporation
Jan Eric Gyllenram Kommunikationsdepartementet	Bertil Ilhage Saab Scania Car Division	Johnny Larsson Volvo Car Corporation
Sören Haglund Autoliv Development AB	Chieko Imasato Swedish Trade Council	Thomas Lekander Swedish Road Safety Office
Anders Hallén Volvo Car Corporation	Jan Ivarsson Volvo Car Corporation	Anders Lie Metimur AB

Lars G-R Lind Volvo Car Corporation	Petter Nilsson Volvo Car Corporation	Klaus Rieger Trelleborg AB
Bo Lind Volvo Truck Corporation	Richard Nilsson Volvo Car Corporation	Per-Olof Rosén Autoliv Development AB
Jörgen Lindberg Saab-Scania AB	Anders Nilsson Volvo Truck Corporation	Agneta Roth Kvällsposten Malmö
Stig Linde Volvo Personvagnar AB	Gert Nilsson Chalmers University of Technology	Kåre Rumar VTI, Swedish Road Traffic Research
Thomas Lindskog Volvo Personvagnar AB	Stig-Håkan Nilsson Autoliv Cipro	Svante Runberger Volvo Bussar AB
Inger-Lise Lundberg Bilindustriföreningen	Larsgunnar Nilsson Saab-Scania AB	Camilla Rygaard Volvo Car Corporation
Björn Lundell Volvo Car Corporation	Stefan Nilsson Volvo Car Corporation	Stephan Ryrberg Volvo Car Corporation
Ulf Lundqvist Volvo Car Corporation	Curt Nordgren Bilindustriföreningen	Lasse Sandvik Autoliv Development AB
Lars-Göran Löwenadler Volvo Truck Corporation	Ingalill Nordlander Volvo Car Corporation	Venti Saslecov Volvo Car Corporation
Per Lövsund Chalmers University of Technology	Olle Nordström Statens Väg- och Trafikinstitut (VTI)	Bengt Schultz Volvo Car Corporation
Olle Magnusson Volvo Car Corporation	Hans Norin Volvo Car Corporation	Ebbe Skarin Volvo Car Corporation
Thomas Magnusson Autoliv Stil AB	Harry Nygren Volvo Car Corporation	Torbjörn Skånberg Autoliv Development AB
Martin Marklund Volvo Lastvagnar AB	Lars Näsman Bilindustriföreningen	Lars-Gunnar Skötte Autoliv Stil AB
Holger Mattsson Volvo Car Corporation	Jörgen Olsson Autoliv Stil AB	Peter Spitz Swedish Trade Council
Hans Åke Mattsson Volvo Car Corporation	Jan Olsson Autoliv Stil AB	Lars-Gunnar Stadler Statens Väg- och Trafikinstitut (VTI)
Hugo Mellander Volvo Car Corporation	Leif Ottosson Klippan Team AB	Ingemar Stig Autoliv Development AB
Lennart Moberg Volvo Car Corporation	Elsie Parker Swedish Trade Council	Eilert Storm Saab-Scania AB
Mats Moberg Volvo Car Corporation	Elfi Perkhofer Swedish Trade Council	Lennart Strandberg Swedish Road & Traffic Research
Svante Mogefors Autoliv Development AB	Jan Crister Persson Volvo Car Corporation	Lars Strandäng Volvo Car Corporation
Hans Mohlin Swedish Road Safety Office	Michael Persson Volvo Car Corporation	Åke Sundberg Trafiksäkerhetsverket
Viktor Nesterov c/o Matreco HAB	Torsten Persson A.B. Bofors	Lennart Svenson Volvo Truck Corporation
Hans-Ove Nilson Volvo Car Corporation	Ingrid Planath Volvo Car Corporation	Sven-Erik Svensson Volvo Car Corporation
Ulf Nilsson Volvo Car Corporation	Jacqueline Recker Swedish Trade Council	Mats Svensson Chalmers University of Technology
	Göran Reinstam Trafiksäkerhetsverket	Erik Söderbaum Volvo Car Corporation

Bo Söderberg  
Caran Alpha AB

Yoko Teichler-Urata  
Swedish Trade Council

Carl-Olof Ternryd  
Bilindustriföreningen

Börje Thor  
Volvo Car Corporation

Lennart Thorngren  
Chalmers University of Technology

Kjell Thunberg  
Saab-Scania AB

Hans Thörnqvist  
Saab-Scania AB

Lars Runo Tillback  
Volvo Car Corporation

Claes Tingvall  
Folksam

Igor Titkov  
c/o Matreco HAB

Claes Tjäder  
Kommunikationsdepartementet

Thomas Turbell  
VTI

Per Törneld  
Volvo Car Corporation

Ingmar Wallin  
Centaur AB

Stephen Wallman  
Volvo Car Corporation

Roger Warolin  
Trafiksäkerhetsverket

Johan Wedlin  
Volvo Car Corporation

Jan Wenäll  
VTI, Statens väg/trafik inst.

Christer Wilén  
Volvo Car Corporation

T D Yamamoto  
Swedish Trade Council

Kazuko Yoshida-Ingham  
Swedish Trade Council

Kensuke Yoshimura  
Swedish Trade Council

Ann-Lil Åhsberg  
Trafiksäkerhetsverket

Sven Åsander  
AB Svensk Bilprovning

Anders Öhlund  
Volvo Car Corporation

Ingemar Örtendahl  
Volvo Car Corporation

Åke Östgren  
Volvo Car Corporation

---

## SWITZERLAND

---

Masakazu Kume  
Director, Japan Automobile Standards

---

## WEST GERMANY

---

Peter Alber  
Daimler-Benz AG

Horst Albrecht  
Volkswagen AG

Christian Bader  
Daimler-Benz AG

Ernst Bauer  
ACE LENKRAD Auto Club Europa  
ACE

Christian Boder  
Daimler-Benz A.G.

Hermann Brandsch  
Dr.ing.h.c.F.Porsche AG

Bert Breuer  
Technische Hochschule

Helmut Carli  
Volkswagen AG

Bo Cavell  
Autoliv GmbH

Volkmar Cott  
Adam Opel AG

Horst Dalibor  
Volkswagen AG

Hans-Harald Eggelmann  
Daimler-Benz AG ENZ

Bernd Friedel  
Bundesanstalt fuer Strassenwesen

Artur Föhl  
TRw Repa GmbH

Hans Albert Graefe  
Akzo/Enka AG

Jürgen Grandel  
DEKRA

Lothar Groesch  
Daimler Benz AG

Dieter Grunow  
TÜV Rheinland e.V.

Johann Guggenberger  
Siemens AG

Oswald Haase  
ASSEV

Josef Haberl  
BMW AG

Toshifumi Haraguchi  
Mazda Motor Corporation

Hansjoachim Hartwig  
Bundesverkehrsministerium

Wolfgang Helbach  
TRW Repa GmbH

Appel Hermann  
Berlin University of Technology

Roland Herrmann  
Daimler-Benz AG

Richard Heydenreich  
BMW AG

Rainer Hoffmann  
Engineering System Intern. GmbH

Masahiro Homma  
Mitsubishi Motors Corp.

Peter Hora  
MBB GmbH

Thomas Hummel  
HUK-Verband

Wolfgang Kleemann  
BMW AG

Walter Knabel  
Autoliv-Kolb GmbH & Co.

Hubert Koch  
Institut für Zweirad

Hans Kocherscheidt  
BMW AG

Bernhard Koonen  
Tüv Rhenland E. V.

Axel Kootz  
Ford-Werke AG

Martin Kreuzer  
KS-Lenkradwerk

Wolf Krummheuer  
Akzo/Enka AG

Hans-Joachim Krüger  
TÜV Rheinland E. V.

Heinz Kunert  
Sekurit-Glas Union GmbH

Klaus Langwieder  
HUK-Verband

Josef Mayer  
Autoliv-Kolb GmbH & Co.

Günther Menzel  
Volkswagen AG

Charles Merlino  
Merco, Inc.

Jürgen Mitzkus  
TRW Repa GmbH

Karl Erik Nilsson  
Bayern Chemie GmbH

Klaus Oehm  
Volkswagen AG

Olaf H. Peters  
Bergische Universität

Anton Poth  
BMW A.G.

Heinrich Praxenthaler  
Bundesanstalt fuer Strassenwesen

Horst Roesler  
BMW AG

Dietrich Rück  
TRW Repa GmbH

Minoru Saeki  
c/o Subaru Deutschland GmbH

Takuya Saigo  
Nippon Oil & Fats Co., Ltd.

Dieter Schaper  
Autoliv GmbH

Hans-Joachim Schmidt-Clausen

Walter Schneider  
A.S.S.e.V.

Günter Schröder  
Bundesministerium für Forschung

Karl Heinz Schwedes  
BMW AG

Ruprecht Sinnhuber  
Volkswagen AG

Alexander Spörner  
HUK-Verband

Armin Starck  
DEKRA, Deutscher Kraftfahrzeug

Carl-Christian Steger

Ichirou Tateno  
c/o Subaru Deutschland GmbH

Michael Thiem  
Honda R&D Europe GmbH

Hans-Eggert Tonnesen  
Anton Ellinghaus GmbH & Co. KG

Karl Unterforsthuber  
Bayern-Chemie

Uwe Wagner  
Ford-Werke Aktiengesellschaft

Alois Weidele  
Technische Hochschule

Bernd Werner  
Bayern Chemie

Harald Wester  
Volkswagen AG

Ulrich Wezel  
Dr.-Ing.h.c.F.Porsche AG

Tomasz Wierzbicki  
BMW AG

Walter Wohnig  
BMW AG

Frank Wolf  
Daimler-Benz AG

Elmar Vollmer  
AUDI AG

Egon-Christian Von Glasner  
Daimler-Benz AG

Akimasa Yasuoka  
Honda R&D Europe GmbH

---

## USA

---

Eiji Amito  
Honda North America, Inc.

Eiji Amito  
American Honda Motor Co., Inc.

Thomas Baloga  
Mercedes-Benz of North America

James Bennett  
General Motors Research Labs

Frances Bents  
Dynamics Science, Inc.

Thage Berggren  
Volvo GM Heavy Truck Corporation

David Biss  
David James, Ltd.

James Blaker  
Transportation Research Center

David Breed  
Automotive Technologies Intern.

Ria Breed  
Automotive Technologies Intern.

Howell Brewer  
NHTSA

August Burgett  
NHTSA

Alex Butt  
American Suzuki Motor Corporation

Rino Castelli  
Automotive Technologies Intern.

Raymond Champagne

Benjamin Cohen  
Committee on Energy and Commerce

Neil K. Cooperrider  
Failure Analysis Associates

Sheryl Cooperrider  
Failure Analysis Associates

Jerry Curry  
NHTSA

Gregory Dana  
Automobile Importers of America

Robert Davis  
General Motors Corporation

Adele Derby  
NHTSA

Kennerly Digges  
NHTSA

James P. Donovan  
Wilson, Elser, Moskowitz

William R. Edwards  
Chrysler Motors Corporation

Leonard Evans  
General Motors Research Laboratories

Karl-Heinz Faber  
Mercedes-Benz of North America Inc.

Eugene Farber  
Ford Motor Co.

Michael Finkelstein  
NHTSA

Michael Fitzpatrick  
Fitzpatrick Engineering

John Fleck  
J & J Technologies Inc.

Donald Friedman  
Liability Research, Inc.

Peter Fuller  
University of Louisville

Stephen Godwin  
Transportation Research Board

Peter Griskivich  
Motor Vehicle Macs Ass., Inc.

Charles Griswold C J Griswold Engineering	John Leinonen Ford Motor Co.	Elaine Petrucelli Association for Advancement of ?
James Hackney NHTSA	JR Leisure NHTSA	George G. Pitarra Humanetics, Inc.
Chet Hale American Honda Motor Co., Ltd.	Diane Lestina Insurance Inst for Highway Safety	Gordon Plank DOT/Transportation Systems Center
Peter Hancock University of Southern California	Paul A. Lisovicz Morgan, Melhuish & Lisowski	Priyaranjan Prasad Ford Motor Co.
Toni Harrington Honda North America	John I. Lisowski Morgan, Melhuish & Lisowski	Nagarajan Rangarajan Gesac, Inc.
James E Hofferberth NHTSA-VRTS	Alan Maness U.S. Senate Committee on Commerce and Transportation	Gaylene Reed Automotive Occupant Restraints
Robert Hoffman General Motors Technical Center	Artie Martin General Motors, CPC	Donald Reed SAE "Automotive Engineering"
Teiji Iida Toyota Motor Corporate Services	John Melvin General Motors Research Labs.	Ron Robbins Ron Robins
Kazuo Iwasaki Nissan Research and Development, Inc.	Patrick M. Miller MGA Research Corporation	Robert Rogers General Motors Technical Center
H. George Johannessen Automotive Occupant	Ralph Millet Saab Scania of America	David Romeo Autoliv N. America, Inc.
Jan Karlsson Volvo Monitoring & Concept Center	David Mislan CSPI	Gary W. Rossow Freightliner Corporation
Hiroshi Kato Mitsubishi Motors America Inc.	Craig Morgan Robert A. Denton, Inc.	Anthony Sances, Jr. Medical College of Wisconsin
Joseph Kennebeck Volkswagen of America, Inc.	Rudolf Mortimer University of Illinois	John Secrest Kohl, Secrest, Wardle, Lynch
William K. King Ford Motor Co.	Robert Munson Ford Motor Company	William Shapiro Volvo Cars of North America
Rolland King Battelle	John Musgrave Coburn, Croft & Putzell	Philip Sheets Kawasaki Motors Corp., USA
Sean Kinsey Fitzpatrick Engineering	Andrzej Nalecz University of Missouri	Andy Sklover NHTSA
Jim Koike Yamaha Motor Corp., USA	Alberto Negro FIAT AUTO	Albert J. Slechter Chrysler Corporation
Hikomichi Kosato Kawasaki Motors Corporation	George Nield Automobile Importers of USA, Inc.	John Smreker MVMA/Chrysler Motors
Stephen F. Krystoff Chrysler Motors Corporation	Satoshi Nishibori Nissan Research and Development, Inc.	Jerry Sonosky Hogan and Hartson (Mercedes-Benz)
Leo Lake Yamaha Motor Corp., USA	Linda O'Connor NHTSA	Melvin Stahl Motorcycle Industry Council
Linda Lance U.S. Senate Committee on Commerce, Science	Stephen O'Toole General Motors Corporation	Dean P. Stanley Navistar International
Gunnar Larsson Volvo Monitoring & Concept Center	Lonney Pauls Fitzpatrick Engineering	James Stone Morton-Thiokol, Inc.
William Leasure National Highway Traffic	Helen Petrauskas Ford Motor Company	Jean Tennant Automotive Systems Laboratory, Inc.
		Terry M. Thomas Failure Analysis Associates

Douglas Toms  
American Honda Motor Co., Inc.

Pin Tong  
DOT Transp. Systems Center

Francis J Turpin  
NHTSA

Paul Utans  
Subaru of America

Barry Wade  
Humanetics, Inc.

Michael J Walsh  
Hartley Associates Inc.

Ronald Wasko  
Motor Vehicle Manufacturers Assoc.

Emroy Watson  
Yamaha Motor Corp., USA

Kathleen Weber  
Child Passenger Protection

David Weir  
Dynamic Research, Inc

Mukul Verma  
General Motors—CPC Engineering

Gaetano J. Verrastro  
Somers, Hall, Verrastro & Kern

Richard P. White, Jr.  
Systems Research Laboratories, Inc.

David Viano  
General Motors Research Laboratories

William Willen  
American Honda Motor Co., Inc.

Richard Wilson  
Packer Engineering

T. Albert Yamada  
Mike Masaoka Associates, Inc.

Sharon Yukevich  
Volvo Cars of N. America

James Yukevich  
Lester-Schwab-Katz & Dwyer

John Zellner  
Dynamic Research, Inc.

Karl-Heinz Ziwica  
BMW of North America, Inc.

---

# Volume 1 Opening Ceremony Thru Sessions 4A

## Contents

---

Foreword .....	iii
Introduction .....	v
Attendees .....	vii

### **SECTION 1: OPENING CEREMONY**

#### **Welcoming Address**

The Honorable Jerry R. Curry, Head of United States Delegation and Administrator Designate, National Highway Traffic Safety Administration .....	1
---	---

#### **Keynote Address**

The Honorable Georg Andersson, Minister of Transport and Communications, Sweden .....	2
---	---

#### **Awards for Engineering Excellence**

Conference Chairman: Michael M. Finkelstein .....	5
---	---

### **SECTION 2: GOVERNMENT STATUS REPORTS**

Chairman: Professor Dr. Bertil Aldman, Sweden .....	11
---	----

#### **JAPAN**

Naofumi Takashige, Ministry of Transport .....	11
---	----

#### **THE EUROPEAN EXPERIMENTAL VEHICLES COMMITTEE**

Professor Dr. Bernd Friedel, Director, Bundesanstalt für Strassenwesen .....	14
--	----

#### **UNITED KINGDOM**

Eric Dunn, Chief Mechanical Engineer, Department of Transport .....	16
---	----

#### **ITALY**

Dr. Gaetano Danese, Direttore Generale della Motorizzazione, Civile e dei Trasporti in Concessione, Ministero dei Trasporti .....	19
--	----

**FRANCE**

George Dobias,  
Director General,  
Institut National de Recherche sur les Transports et leur Securite . . . . . 19

**FEDERAL REPUBLIC OF GERMANY**

Heinrich Praxenthaler,  
Der President,  
Bundesanstalt fur Strassenwesen . . . . . 22

**CANADA**

S. Christopher Wilson,  
Director General,  
Road Safety and Motor Vehicle Regulation Directorate,  
Transport Canada . . . . . 27

**UNITED STATES**

Michael M. Finkelstein,  
Conference Chairperson and Associate Administrator for Research and  
Development,  
National Highway Traffic Safety Administration . . . . . 29

**SWEDEN**

Lennart Fremling,  
Conference Chairperson and Head, Vehicle Department,  
Swedish Road Safety Office . . . . . 36

**SECTION 3: TECHNICAL SESSIONS**

Chairman: Lennart Fremling, Sweden

**Technical Session 1A:**

**Motor Vehicle Safety of Children and the Elderly**

**Children in Cars—Their Injury Risks and the Influence  
of Child Protection Systems**

K. Langwieder, Th. Hummel,  
HUK-Verband,  
Federal Republic of Germany . . . . . 39

**Lives Saved by Child Safety Seats From 1982 Through 1987**

S. Partyka,  
National Highway Traffic Safety Administration,  
United States . . . . . 50

**The Performance of Child Restraint Systems in Side Impacts**

A. Roy, (Middlesex Polytechnic); R. W. Lowne, (TRRL); K. Hill,  
United Kingdom . . . . . 55

<b>Comparison of Carbed and Rear-Facing Infant Restraint Systems</b> K. Weber, University of Michigan, United States .....	61
<b>Protection of Children in Cars</b> H. J. Krueger, N. Hackenberg, TUEV Rheinland, Federal Republic of Germany .....	67
<b>Integrated Child Restraints in Cars for Children 0–10 Years Old</b> L. Karlbrink, (Electrolux Autoliv); M. Krafft, (Folksam Ins. Co.); C. Tingvall (Chalmers University, Sweden) .....	73
<b>Protection of Children More Than Three Years Old: Presentation of a Concealable Device Integrated in a Seat</b> B. Weber, G. Stcherbatcheff, F. Brun-Cassan, Renault, France .....	76
<b>Improving Traffic Safety for Older Driver in the United States</b> A. Derby, National Highway Traffic Safety Administration, United States .....	79
<b>Traffic Accidents of Elderly People in The Netherlands; They Really Are More Vulnerable Than Other Road Users</b> L. vanKampen, Institute of Road Safety Research, The Netherlands .....	85
<b>Improving Traffic Safety for an Aging Society</b> S. Godwin, Transportation Research Board, United States .....	91
<b>Age and Risk of Injury</b> B. Brorsson, MFR, Sweden .....	101
<b>Designing Controls for Older Drivers</b> A. Yanik, General Motors Corp, United States .....	104

## Written Only Papers

### **An Econometric Estimate of the Lifesaving Effect of Child Restraint Legislation**

J. Graham, W. Evans,  
Harvard School of Public Health,  
United States ..... 108

### **Transportation Requirements of Medically Fragile Infants**

M. Walsh, B. Kelleher,  
Hartley Associates, Inc.  
United States ..... 115

### **Restraint Systems for Transporting Medically Fragile Children**

M. Bull, K. Bruner Stroup, J. Stout,  
Indiana University, K. Weber, University of Michigan,  
United States ..... 123

### **The Quantitative Effect of Age on Injury Outcome**

J. Pike,  
Ford Motor Company,  
United States ..... 128

### **Motor Vehicle Headlighting: Considerations of Older Drivers**

R. Mortimer,  
University of Illinois,  
United States ..... 132

### **Elderly Drivers and Accident Involvement**

B. Brorsson,  
MFR,  
Sweden ..... 135

### **Technical Session 1B:**

#### **Heavy Truck Safety**

Chairman: William Leasure, United States

### **Braking Characteristics of 400 Heavy Trailer Combinations from Denmark, Finland, Norway and Sweden**

L. Strandberg, L. Stadler, K. Karlsson,  
Road and Traffic Research Institute,  
Sweden ..... 139

### **Heavy Vehicle Braking Philosophies: U.S. vs. Europe**

R. Radlinski, M. Flick,  
National Highway Traffic Safety Administration,  
United States ..... 159

<b>Behaviour of Different Coaches During Steering and Braking Maneuvers</b> D. Grunow, TUEV Rheinland, Federal Republic of Germany .....	167
<b>Truck Front-end Protection Systems</b> S. Gruettert, V. Middelhauve, H. Appel, Technische Universitaet Berlin, Federal Republic of Germany .....	173
<b>Passive Safety Measures for Trucks—Effectiveness and Priorities</b> M. Danner, K. Langwieder, HUK Verband, Federal Republic of Germany .....	179
<b>Accident Tests With a View to the Analysis of and Further Development in the Safety of Road Transport Tankers</b> J. Grandel, F. A. Berg, DEKRA, Federal Republic of Germany .....	192
<b>A Concept of Heavy Truck Safety—Its Realization and Markets</b> H. Eggelmann, P. Alber, F. Wolf, Daimler-Benz AG, Federal Republic of Germany .....	201
<b>Road Safety in Heavy Goods Haulage</b> L. Gardell, SAAB-Scania AB, Sweden .....	214

**Panel**

<b>Safety Implications of the Application of High Technology Electronics in Heavy-Duty Trucks</b>	
<b>Peter Griskivich (Moderator)</b> Vice President, Motor Truck Manufacturers Division Motoral Vehical Manufacturers Association United States Oral Presentation Only .....	220
<b>Dean P. Stanley</b> Vice President, Corporate Technology Navistar International Transportation Corporation United States Oral Presentation Only .....	220

**Christian Bader,**  
General Manager, Commercial Vehicle Concept Development,  
Daimler-Benz A.G.,  
Federal Republic of Germany ..... 220

**Thage Berggren,**  
President and Chief Executive Officer,  
Volvo GM Heavy Truck Corporation,  
United States ..... 222

### Written Only Papers

**Safety Situation of Heavy Truck Occupants in Traffic Accidents**  
D. Otte, H. Appel,  
Medifiuische Hochschule Hannover University,  
Federal Republic of Germany ..... 223

**Improvements in the Front-Frontal Collision between Personal Vehicle  
(PV) and Heavy Duty Vehicle (HDV)**  
P. Soret,  
Renault,  
France ..... 229

**Technical Session 2A:  
Frontal Crash Protection**  
Chairman: Kennerly Digges, United States

#### **Panel A: General Frontal Crash Protection**

**Analysis of Frontal Crash Safety Performance of Passenger Cars, Light Trucks and Vans  
and an Outline of Future Research Requirements**  
J. Hackney, D. Cohen, W. Hollowell,  
National Highway Traffic Safety Administration,  
United States ..... 233

**Inadequacy of 0° Degree Barrier Test with Real World Frontal Accidents**  
S. Koltchakian, C. Thomas, C. Tarriere,  
Laboratory of Physiology and Biomechanics, APR,  
France ..... 241

**Reference Frontal Impact**  
G. Stcherbatcheff, D. Pouget, C. Thomas;  
Renault,  
France ..... 252

**Experimental Investigation of Rear Seat Submarining**  
T. MacLaughlin, L. Sullivan,  
National Highway Traffic Safety Administration,  
United States ..... 261

**An Experimental Study of Crashworthiness of Vehicle Front Structure**

N. Takahashi, A. Miyajima,  
FUJI Heavy Industries, Ltd.,  
Japan ..... 271

**Safer Steering Wheels to Reduce Face Bone Fractures,**

M. White, K. Clemo,  
Motor Industry Research Association,  
S. Penoyre, TRRL,  
United Kingdom ..... 275

**Panel B: Restraint System Technology**

**The Inertial Flow Crash Sensor and its Application to Air Bag Deployment**

D. Breed, R. Castelli,  
Automotive Technologies,  
United States ..... 287

**Vehicle Tests Required For Air Bag System Design**

D. Romeo,  
Autoliv North America,  
John Morris, NHTSA,  
United States ..... 293

**The Development of an Advanced Air Bag Concept**

L. Johansson, J. Billig, H. Mellander  
Volvo Car Corporation,  
B. Werner, P. Nora,  
Bayern Chemic GmbH  
Sweden ..... 299

**The Passive Restraint Approach**

R. Munson,  
Ford Motor Company,  
United States ..... 303

**Panel C: Simulation Applications**

**Crash Simulation Methods for Vehicle Development at Nissan**

T. Futamata, N. Takahashi, H. Okuyama,  
Nissan Motor Co. Ltd.,  
Japan ..... 309

**Simulation of Vehicle Crashworthiness and Its Application**

K. Kurimoto, K. Taga, H. Mutsumoto, Y. Tsukiji,  
Mazda Motor Corp.,  
Japan ..... 315

<b>Occupant Simulator Preprocessors: Parameter Studies Made Easy</b> E. Sieveka, W. Pilkey, University of Virginia, W. Hollowell, NHTSA, United States .....	320
--	-----

<b>On the Safety Body Structure of Finite Element Method Analysis</b> T. Sakurai, T. Aoki, Mitsubishi Motors Corporation, Japan .....	327
--	-----

<b>Identification of Safety Problems for Restrained Passengers in Frontal Impacts</b> D. Cohen, NHTSA, L. Simeone, Transportation Systems Center, United States .....	333
---	-----

<b>Computational Crash Analysis at the SAAB Car Division</b> L. Nilsson, SAAB-SCANIA AB, Sweden .....	349
--	-----

**Written Only Papers**

<b>Intrusion Effects on Steering Assembly Performance in Frontal Crash Testing</b> C. Ragland, NHTSA, G. Klemer, TSC, United States .....	358
--	-----

<b>Influence of Corrosion on the Passive Safety of Private Cars</b> W. Sievert, E. Pullwitt, D. Wobben, Bundesanstalt fuer Strassenwesen, Federal Republic of Germany .....	388
--	-----

<b>The Breed All-Mechanical Driver Air Bag Evaluation</b> J. Kossar, National Highway Traffic Safety Administration, United States .....	397
---	-----

<b>Design of a Crash Attenuation System for a Lightweight Commuter Car</b> D. L. Beaudry, L. Watson, P. Hertz, University of Saskatchewan, Canada .....	408
--	-----

<b>Passenger Car Crashworthiness in Moose-Car Collisions</b> P. Lovsund, G. Nilson, M. Svensson, J. Terins, Chalmers University, Sweden .....	410
--	-----

**Investigation, Development and Evaluation of Advanced Concepts in Three Point Belt Comfort Enhancement Devices**

D. Biss,  
David James, Ltd,  
United States ..... 416

**Investigation of Fire in Cars**

E. Johansson,  
Saab Car Division,  
Sweden ..... 442

**The Effect of Restraint Design and Seat Position on the Crash Trajectory of the Hybrid III Dummy**

C. Freeman, D. Bacon,  
Motor Industry Research Association,  
United Kingdom ..... 451

**Technical Session 2B:  
Accident Investigation and Data Analysis**  
Chairman: S. Christopher Wilson, Canada

**In-Depth Study of Motor Vehicle Accidents in Japan**

M. Itoh, K. Ono, JARI,  
Y. Irie, TSNRI,  
Japan ..... 459

**The Crash Avoidance Rollover Study: A Database for the Investigation of Single Vehicle Rollover Crashes**

E.A. Harwin, L. Emery,  
National Highway Traffic Safety Administration,  
United States ..... 470

**Rollover Crashworthiness Classification and Severity Indices**

K. Digges and D. Cohen, NHTSA,  
R. Nichols, COMIS,  
United States ..... 477

**Photogrammetric Measurement of Damaged Vehicles in Road Traffic Accidents**

S. Johansson, S.O. Johansson, A. Lie, C. Tingvall,  
Metimur Ab, Chalmers University of Technology, and Folksam Ins. Co.,  
Sweden ..... 488

**The Gothenburg Traffic Injury Register**

O. Bunketorp, B. Romanus,  
The Traffic Injury Register,  
Sweden ..... 493

**Police Reports: First Step Towards Investigation**

A. Viel,  
Regie de l'assurance automobile du Quebec,  
Canada ..... 500

**Passenger Car Weight and Injury Severity in Single Vehicle Non-Rollover Crashes**

S. Partyka, W. Boehly,  
National Highway Traffic Safety Administration,  
United States ..... 507

**Panel**

**Consequences of Accident Research for Vehicle Safety Measures**

R. Herrmann, R. Stadelmann,  
Daimler-Benz, AG,  
Federal Republic of Germany ..... 519

**Situation of Road Traffic Accidents and the Prevention Measures in Japan**

M. Suzuki,  
N. Koba Traffic Safety Policy Office,  
Japan ..... 523

**Characteristics of Fatal Frontal Impacts and Future Countermeasures in Great Britain**

P.F. Gloyns, S. J. Rattenbury,  
Vehicle Safety Consultants,  
I. Jones,  
Forensic Technologies International,  
United States ..... 529

**Written Only Papers**

**A Relational Database for Use on a Personal Computer in Processing Motorway Accident Data**

D. Vulin, S. Olivier,  
I.N.R.E.T.S.,  
France ..... 536

**Rollover of Passenger Cars in France**

R. Biard, D. Cesari, J. Bloch,  
I.N.R.E.T.S.,  
France ..... 541

<b>A System for Automated Coding of Injuries</b> R. Tong, L. Applebaum, L. Balcom, Advanced Decision Systems, J. Marcus, NHTSA, United States .....	553
<b>Interior Safety of Truck Cabs—Results of an In-Depth Study</b> J. Grandel, DEKRA, Federal Republic of Germany .....	558
<b>Head Risks in Frontal Impacts: Similarities and Differences Between Tests and Real-Life Situations</b> G. Walfisch, D. Pouget, Renault, C. Thomas, C. Tarriere, Laboratory of Physiology and Biomechanics, APR, France .....	563
<b>Technical Session 3A: International Harmonization—The Current Approach and The Future</b> Chairman: Bernard Gauvin, France	
<b>Statements by Panelists</b>	
<b>Kåre Rumar,</b> Professor, Road and Traffic Research Institute, Sweden .....	571
<b>Francis J. Turpin,</b> Director, International Harmonization, National Highway Traffic Safety Administration, United States .....	571
<b>Roger J. Peeters,</b> Transportation Equipment Industries, Commission of European Communities, Belgium .....	571
<b>Masakazu Kume,</b> Director, Japanese Automobile Standards International Center, Geneva Office, Japan .....	571

**Horst Albrecht,**  
Manager, Research and Development,  
Vehicle Regulations Department,  
Volkswagen, AG,  
Federal Republic of Germany ..... 571

**Technical Session 3B:**  
**Future Motor Vehicle Safety Research Needs**  
Chairman: R. Dir. Hansjoachim Hartwig, Federal Republic of Germany

**Statement by Panelists**

**Panel A: Crash Avoidance**

**Robert Rogers,**  
Director, Automotive Safety Engineering,  
Environmental Activities Staff,  
General Motors Corporation,  
United States ..... 573

**Michael M. Finkelstein,**  
Associate Administrator for Research and Development,  
National Highway Traffic Safety Administration,  
United States ..... 575

**Eiichi Yaguchi,**  
Manager,  
Technical Strategic Planning Office,  
Nissan Motor Company,  
Japan ..... 577

**W. Maes,**  
Directorate General XIII Drive Office,  
Commission of the European Communities,  
Belgium ..... 578

**Tore Gullstrand,**  
SAAB-SCANIA AB,  
Sweden ..... 578

**Christer Hyden,**  
Lund Institute of Technology,  
Sweden ..... 580

**Panel B: Crashworthiness in the Nineties**

**John N. Leinonen,**  
Representative of the Motor Vehicle Manufacturers Association,  
United States ..... 585

**Research Priorities in Crashworthiness**

**Adele Derby,**

Associate Administrator for Plans and Policy,  
National Highway Traffic Safety Administration,  
United States .....

586

**Yataka Kondo,**

General and Project Manager,  
Corporate Technical/Planning Office,  
Toyota Motor Company,  
Japan .....

588

**Bertil Aldman,**

Professor,  
Chalmers University of Technology,  
Sweden .....

590

**George Dobias,**

Director,  
I.N.R.E.T.S.,  
France .....

591

**Herbert Henssler,**

Director General,  
Internal Market and Industrial Affairs,  
Commission of the European Communities,  
Belgium .....

593

**Technical Session 4A:**

**Biomechanics and Dummy Development**

Chairman: Richard Lowne, United Kingdom

**Panel A: Facial Injury**

**Restrained Drivers' Facial Skeleton Injuries Resulting From Steering**

**Assembly Contact: A Conspectus**

D. Zuby,  
Transportation Research Center,  
R. Saul,  
NHTSA,  
United States .....

597

**A Comparison of Human Facial Fracture Tolerance With the Performance of a  
Surrogate Test Device**

E. Welbourne,  
Transport Canada,  
M. Ramet,  
INRETS,  
M. Zarebski,  
University of De Lyon .....

603

**Facial Injury Assessment Techniques**

J. Melvin, T. Shee,  
General Motors Corporation,  
United States ..... 608

**Panel B: Head/Neck Injury**

**Finite Element Modeling of Head Injury Caused by Inertial Loading**

P. Tong,  
Transportation Systems Center,  
R. Eppinger, J. Marcus, C. Galabraith,  
NHTSA,  
United States ..... 617

**Toward a Biomechanical Criterion for Functional Brain Injury**

T. Anderson, J. Lighthall, J. Melvin, K. Ueno,  
General Motors Corporation,  
United States ..... 627

**Injury Biomechanics of the Head-Neck Complex**

A. Sances, N. Yoganandan, F. Pintar, J. Reinartz, D. Maiman, S. Larson,  
Medical College of Wisconsin,  
United States,  
W. Rauschnig,  
University Hospital,  
Sweden ..... 634

**Multi-Directional Dummy Neck Prototype**

H. Pritz,  
NHTSA,  
R. Stalnaker, K. Mendis,  
Ohio State University,  
United States ..... 645

**Panel C: Thorax Performance Panel**

**Thoracic Deflection of Hybrid III: Dummy Reponse for Simulations of Real Accidents**

J. Foret-Bruno, F. Brun-Cassan, C. Brigout, C. Tarriere,  
Laboratory of Physiology and Biomechanics, APR,  
France ..... 650

**Problem and Improvement of Hybrid III Dummy Rib Cage Features**

F. Matsuoka, H. Takahashi, K. Kumagai,  
Toyota Motor Corporation,  
Japan ..... 660

**Computed Dynamic Response of the Human Thorax From a Finite Element Model**  
 G. Plank,  
 Transportation Systems Center,  
 R. Eppinger, NHTSA,  
 United States ..... 665

**Measurement of Seat Belt Loads Sustained by the Dummy in Frontal Impact with Critical Pelvic Motion: Development of a 2-D Transducer**  
 F. Bendjellal, D. Gillet, J. Foret-Bruno, C. Tarriere,  
 Laboratory of Physiology and Biomechanics, APR,  
 France ..... 673

**Human Cadaver Patella-Femur-Pelvis Injury Due to Dynamic Frontal Impact to the Patella**  
 R. Morgan, R. Eppinger, J. Marcus,  
 National Highway Traffic Safety Administration,  
 United States ..... 683

**Panel D: Side Impact Dummy**

**Involvement of Older Drivers in Multi-Vehicle Side Impact Crashes**  
 D. Viano, C. Culver, L. Evans, M. Frick, R. Scott,  
 General Motors Corporation,  
 United States ..... 699

**Development of a Modelization of Human Beings in Lateral Impact, to Mitigate the Insufficiencies of Actual Side Impact Dummies**  
 F. Chamouard, C. Tarriere, P. Mack, F. Bendjellal,  
 Laboratory of Physiology and Biomechanics, APR,  
 France ..... 705

**Comparison of EUROSID and Cadaver Response in Side Impacts**  
 E. Janssen, P.J.A. deCoo, J. Wismans,  
 TNO Road-Vehicles Research Institute,  
 The Netherlands ..... 726

**Report on EUROSID 1989**  
 A. Roberts,  
 Transport and Road Research Laboratory,  
 France ..... 743

**Written Only Papers**

**Three-Dimensional Computerized Tomography Analysis of Steering Wheel Induced Facial Trauma**  
 A. Sances, N. Yoganandan, F. Pintar, G. Harris, S. Larson, M. Mahadevappa,  
 Medical College of Wisconsin,  
 United States ..... 752

---

# Volume 2 Sessions 4B Thru 6B

## Contents

---

### Technical Session 4B:

#### Crash Avoidance

Chairman: Ubaldo Quaranta, Italy

#### Panel A: Visibility Problems

#### Relationship Between Visibility Needs and Vehicle-Based Roadway Illumination

R. VanInderstine, M. Ulman, A. Burgett,

National Highway Traffic Safety Administration,

United States ..... 765

#### Using PCDETECT to Compare United States and European Beam Patterns

E. Farber, C. Matle,

Ford Motor Company,

United States ..... 774

#### Vehicle Conspicuity

K. Rumar,

Road and Traffic Research Institute,

Sweden ..... 781

#### Why the Windshield Should Be Included in Motor Vehicle Inspection (§ 29 St.

#### VZO = Motor Vehicle Approval and Traffic Registration

W. Schneider,

Forschungsgemeinschaft Auto-Sicht-Sicherheit,

Federal Republic of Germany ..... 785

#### Large Scale Experiment About Improving The Night-time Conspicuity of Trucks

H. J. Schmidt-Clausen, H. Finsterer,

Technische Hochschule Darmstadt,

Federal Republic of Germany ..... 791

**Panel B: Stability of Vehicles**

**Assessment of Experimental Methods of Determining Braking Efficiency**

R. Radlinski,  
National Highway Traffic Safety Administration,  
United States ..... 794

**Dynamic Analysis of Vehicle Rollover**

A. Nalecz and A. Bindemann  
University of Missouri-Columbia,  
H. Brewer,  
NHTSA,  
United States ..... 803

**Real World Rollovers—A Crash Test Procedure and Vehicle Kinematics  
Evaluation**

T. Thomas, N. Cooperrider, S. Hammoud, P. Woley,  
Failure Analysis Association,  
United States ..... 819

**Skidding Accidents and Their Avoidance with Different Cars**

L. Strandberg,  
Road and Traffic Research Institute,  
Sweden ..... 825

**Volvo Concept for Active Safety**

L. Tillback, J. Wedlin,  
Volvo Car Corporation,  
Sweden ..... 829

**Braking and Stability Performance of Cars Fitted with Various Types of  
Anti-Lock Braking Systems**

J. Robinson, B. Riley,  
Transport and Road Research Laboratory,  
France ..... 836

**Control Concept for Traction Control System (TCS) and its Performance**

S. Shiraisi, O. Yamamoto, H. Kiryu, T. Nishihara, M. Satoh,  
Honda R&D Co., Ltd.,  
Japan ..... 846

**Active Safety Through Traction Control of 4WD Vehicles**

E. Yaguchi, K. Ozaki, G. Naito, S. Torii,  
Nissan Motor Co., Ltd.,  
Japan ..... 853

## **Panel C: Driver Support Systems**

### **Active Safety Research on Intelligent Driver Support Systems**

S. Franzen, B. Ilhaye,  
SAAB-SCANIA, AB,  
Sweden ..... 859

### **The Driver Vigilance State Control: A Key Aspect of the Driver-Vehicle Environment Interface**

D. Chaput, C. Poilvert, D. Tamalet, C. Tarriere,  
Renault,  
France ..... 865

### **Human Factor Capabilities for Avoiding Traffic Accidents**

A. Costanzo,  
University La Sapienza,  
Italy ..... 876

### **Accident Reduction with New Driving Aids—Efficiency Assessment**

H. Fontaine, G. Malaterre, P. Van Elslande,  
INRETS,  
France ..... 880

### **Study of Laser Radar**

T. Teramoto, K. Fujimura, Y. Fujita,  
Toyota Motor Corporation,  
Japan ..... 888

## **Written Only Papers**

### **An Investigation on a Torque Bias-Limited Slip Differential and Assessment of its Influence on Vehicle Handling**

A. Robertson, D. Rahani,  
Cranfield Institute of Technology,  
United Kingdom ..... 896

### **Analysis of Optimum Low-Beam Illumination Pattern Based on Human Visual Perception Characteristics**

Y. Seko, H. Iizuka, T. Saito,  
Nissan Motor Co., Ltd.,  
Japan ..... 902

### **Steering and Traction Control for Accident Avoidance Maneuverability**

M. Tani, T. Tanaka, H. Yuasa, H. Yoshida,  
Mitsubishi Motors Corporation,  
Japan ..... 909

**Technical Session 5A:**

**Side Impact Occupant Protection**

Chairman: Professor Dr. Bernd Friedel, Federal Republic of Germany

**Panel A: Accident Analysis and Biomechanics in Side Impacts**

**Side Impacts: Expected Benefits of Planned Standards**

C. Henry, C. Thomas, C. Tarriere,

Laboratory of Physiology and Biomechanics, APR,

France ..... 913

**Side Impact Regulations—How Do They Relate to Real World Accidents?**

P. Thomas, M. Bradford,

Institute for Consumer Ergonomics

United Kingdom ..... 919

**Side Impacts: Test Crashes and Real-World Collisions**

A. German, Z. Gorski, R. Green, E. Nowak,

University of Western Ontario,

Canada ..... 929

**Upper Interior Head Protection: A Fleetwide Characterization**

H. Gabler, D. Willke,

National Highway Traffic Safety Administration,

United States ..... 934

**Biomechanics of the Human Chest, Abdomen and Pelvis in Lateral Impact**

D. Viano, I. Lau, C. Asbury,

General Motors Corp.,

A. King, P. Begeman,

Wayne State University,

United States ..... 943

**Panel B: Crash Tests, Test Procedures and Dummies**

**EEVC Working Group a Report on the EEVC Side Impact Test Procedure**

R. Lowne,

Transport and Road Research Laboratory,

United Kingdom ..... 950

**The Influence of Car Structures and Padding on Side Impact Injuries**

C. Hobbs,

Transport and Road Research Laboratory,

United Kingdom ..... 954

<b>Effect of Belt Restraint Systems on Occupant Protection Performance in Side Impact Crashes</b> N. Shimoda, A. Akiyama, Y. Nishida, Honda R&D Co., Ltd., Japan .....	963
<b>Side Impact Protection System—A Description of the Technical Solutions and the Statistical and Experimental Tools</b> H. Mellander, J. Ivarsson, J. Korner, S. Nilsson, Volvo Car Corporation, Sweden .....	969
<b>Airbag System for Side Impact Protection</b> J. Olsson, L. Skotte, Electrolux Autoliv AB, S. Svensson, Volvo Car Corp., Sweden .....	976
<b>Study on Side Impact Test Methods</b> M. Sakurai, H. Ohmae, Y. Nakamura, K. Watanabe, T. Harigae, Japan Automobile Research Institute Inc., Japan .....	983
<b>DEPTH: A Relationship Between Side Impact Thoracic Injury and Vehicle Design</b> H. Gabler, J. Hackney, T. Hollowell, National Highway Traffic Safety Administration, United States .....	994
<b>Variability of Results of the Same Test Conducted in Three Different Laboratories</b> J. Bloch, D. Cesari, E. Pullwitt, R. Lowne, INRETS, France .....	1007
<b>Influence of Driving Speed of Side Impacted Vehicle on Dummy Loading</b> E. Faerber, Bundesanstalt fuer Strassenwesen, Federal Republic of Germany .....	1012
<b>Panel C: Simulation of Side Impacts</b>	
<b>Developments in the Simulation of Side Impact</b> M. G. Langdon, Transport and Road Research Laboratory, United Kingdom .....	1018

<b>Mathematical Modeling of Side Collisions</b> C. Steyer, P. Mack, P. DuBois, R. Renault, Renault, France .....	1032
<b>Side Impact SubSystem Thoracic Impactor Evaluation</b> D. Willke, M. Monk, J. Kianianthra, National Highway Traffic Safety Administration, United States .....	1043
<b>Safety Performance Evaluation of Production Vehicles in Side Impacts Using the Modeling Approach</b> J. Kianianthra, T. Trella, S. Edwards, National Highway Traffic Safety Administration, United States .....	1055
<b>Side Impact Simulation Analysis Using an Improved Occupant Model</b> J. Hasewaga, T. Fukatsu, T. Katsumata, Toyota Motor Corporation, Japan .....	1071
<b>The Composite Test Procedure (CTP)—State of the Art</b> B. Richter, CCMC, Belgium .....	1077
<b>An Assessment of a Composite Test Procedure for Side Impact</b> J. Bennett, Y-C. Deng, K. Lin, J. Stocke, General Motors Corporation, United States .....	1087
<b>Application of Finite Element Method to the Design of a Light Weight Composite Passenger Car Door</b> M. Rashidy, M. Sadeghi, Cranfield Impact Centre Ltd, United Kingdom .....	1097
<b>Analysis of Factors Effecting Dummy Readings in Side Impact Tests</b> T. Yamaguchi, K. Watanabe, Nissan Motor Company, Japan .....	1104
<b>Reconstitution With Partial Testing of a Full-Scale Side Impact Test Severity</b> J. Bloch, D. Cesari, R. Biard, INRETS, France .....	1114

## Written Only Papers

### **A Methodology for Enhancing Side Impact Crashworthiness**

R. Hardy,  
Cranfield Impact Centre,  
H. Mellander,  
Volvo Car Corp.,  
Sweden ..... 1119

### **Technical Session 5B:**

#### **Evaluation and Assessment**

Chairman: Gunnar Carlsson, Sweden

### **A Mechanical Buckle Pretensioner to Improve a Three Point Seat Belt**

Y. Håland, T. Skånberg,  
Electrolux Autoliv AB,  
Sweden ..... 1125

### **Estimating Effectiveness of Increased Seat Belt Usage on the Number of Fatalities**

F. Wegman, J. Bos, F. Bijleveld,  
Institute for Road Safety Research SWOV,  
Sweden ..... 1132

### **The Effect of Fully Seat-Integrated Front Seat Belt Systems on Vehicle Occupants in Frontal Crashes**

J. Havberl, F. Ritzl, S. Eichinger,  
BMW AG,  
Federal Republic of Germany ..... 1138

### **Rear Seat Occupant Protection. A Study of Children and Adults in the Rear Seat of Cars in Relation to Restraint Use and Car Characteristics**

C. Tingvall, M. Krafft, A. Nygren,  
Folksam,  
Sweden ..... 1145

### **Passive Compared to Active Approaches to Reducing Occupant Fatalities**

Leonard Evans,  
General Motors Corporation,  
United States ..... 1149

### **Impairment Resulting From Motor Vehicle Crashes**

S. Luchter,  
National Highway Traffic Safety Administration,  
United States ..... 1157

### **Status of Costs of Injury Research in the United States**

S. Luchter, B. Faigin, D. Cohen, L. Lombardo,  
National Highway Traffic Safety Administration,  
United States ..... 1184

**Proposal of a Motor Vehicle Safety Assessment**

H. Appel, W. Glatz, F. Kramer,  
Technische Universitaet Berlin,  
Federal Republic of Germany ..... 1196

**Low Speed Rear Impacts and the Elastic Properties of Automobiles**

F. Navin, D. Romilly, M. Macnabb, R. Thomson,  
Accident Research Team, Univ. of British Columbia,  
Canada ..... 1199

**Written Only Papers**

**Effects of Internal Fittings on Injury Value of Unrestrained Occupants**

K. Oho, I. Sugamori, K. Yamasaki,  
ISUZU,  
Japan ..... 1205

**Consideration of Potential Safety Effects for a New Vehicle-Based Roadway  
Illumination Specification**

G. Stewart, A. Burgett,  
National Highway Traffic Safety Administration,  
United States ..... 1209

**The Effect of Occupant Restraints on Children and the Elderly in Motor Vehicle Crashes**

E. Orsay, T. Turnbull, M. Dunne, J. Barrett, P. Langenberg, C. Orsay,  
University of Illinois,  
United States ..... 1213

**Technical Session 6A:**

**Pedestrian Impact Protection**

Chairman: Dominique Cesari, France

**A Study of Test Methods to Evaluate Pedestrian Protection for Cars**

J. Harris,  
EEVC Working Group 10,  
EEVC Representative from The United Kingdom ..... 1217

**National Highway Traffic Safety Administration Pedestrian Head Injury Mitigation  
Research Program—Status Report**

J. Kessler,  
Transportation Research Center of Ohio,  
M. Monk,  
NHTSA,  
United States ..... 1226

<b>National Highway Traffic Safety Administration Pedestrian Thoracic Injury Mitigation Program—Status Report</b> J. Elias, Transportation Research Center of Ohio, M. Monk, NHTSA, United States .....	1237
<b>Evaluation of the Round Symmetrical Pedestrian Dummy Leg Behaviour</b> D. Cesari, C. Cavallero, H. Roche, INRETS, France .....	1244
<b>Bumper System Evaluation Using an Experimental Pedestrian Dummy</b> J. Kajzer, B. Aldman, H. Mellander, K. Jonasson, Chalmers University, Sweden .....	1246
<b>The Influence of Car Shape on Pedestrian Impact Energies and its Application to Sub-System Tests</b> G. Lawrence, Transport and Road Research Laboratory, United Kingdom .....	1253
<b>Bumper Configurations for Conflicting Requirements: Existing Performance vs. Pedestrian Protection</b> L. Groesch, W. Heiss, Daimler-Benz, AG, Federal Republic of Germany .....	1266

**Written Only Papers**

<b>Pedestrian Casualties: The Decreasing Statistical Trend</b> H. Vallee, C. Thomas, C. Tarriere, Laboratory of Physiology and Biomechanics, APR, France .....	1273
<b>Technical Session 6B: Motorcycle Safety</b> Chairman: Hiroshi Kizawa, Japan <b>Risk of Leg Injuries of Motorcyclists—Present Situation and Countermeasures</b> A. Sporner, K. Langwieder, J. Polauke, HUK-Verband, Federal Republic of Germany .....	1279

<b>Leg Protection and its Effect on Motorcycle Rider Trajectory</b> B. Chinn, P. Hopes, M. Finnis, Transport and Road Research Laboratory, United Kingdom .....	1287
<b>Motorcycle Accident Impact Conditions as a Basis for Motorcycle Crash Tests</b> J. Pedder, H. Hurt, D. Otte, Biokinetics & Associates, Canada .....	1297
<b>Design of a Motorcyclist Anthropometric Test Device</b> A. St. Laurent, J. Newman, T. Szabo, Biokinetics & Associates, Canada .....	1308
<b>A Combined Anti-Lock Brake System for Motorcycles</b> G. Donne, Transport and Road Research Laboratory, United Kingdom .....	1316
<b>Car Driver Behavior During Differing Driving Maneuvers</b> P. Hancock, G. Wulf, D. Thom, University Southern California, P. Fassnacht, Motorcycle Safety Foundation, United States .....	1320
<b>Difficulties in Leg Protection Research</b> S. Sakamoto, Japan Automobile Manufacturers Association, Japan .....	1328
<b>A Study on Required Field of View for Motorcycle Rear-View Mirror</b> M. Motoki, T. Tsukisaka, Japan Automobile Manufacturer Association, Japan .....	1335
<b>ESM 4—A Lightweight Safety Motorcycle</b> P. Watson, G. Donne, Transport and Road Research Laboratory, United Kingdom .....	1352
<b>Assessment of Motorcycle Braking Performance and Technical Perspectives for Enhanced Braking Safety</b> A. Weidele, Technische Hochschule Darmstadt, Federal Republic of Germany .....	1357

## Written Only Papers

<b>Load Measuring Method of Motorcyclists Leg During Motorcycle Collision</b> S. Sakamoto, K. Miyazaki, M. Kubota, Japan Automobile Manufacturers Association, Japan .....	1368
<b>The Application of a New Data Recovery System for Automotive/Motorcycle Dynamic Testing</b> R. White, T. Gustin, Arvin/Calspan, United States .....	1372
<b>Study on Antilock Brake Systems for Motorcycles</b> T. Okayama, T. Nishimi, T. Katayama, A. Aoki, Japan Automobile Research Inst., Inc., Japan .....	1383
<b>Riders' Control Behavior of Lane Change</b> T. Nishimi, T. Katayama, T. Okayama, A. Aoki, Japan Automobile Research Institute, Inc., Japan .....	1393
<b>Leg Injuries and Mechanisms in Motorcycling Accidents</b> P. Harms, Transport and Road Research Laboratory, United Kingdom .....	1408

# Technical Session 4B

## Crash Avoidance

Chairman: Ubaldo Quaranta, Italy

### Relationship Between Visibility Needs and Vehicle-Based Roadway Illumination

---

**August Burgett, Linda Matteson, Marian Ulman, and Richard Van Iderstine,**  
National Highway Traffic Safety Administration

#### Abstract

Nighttime accident data was studied to determine priorities for accident reduction through the use of improved vehicle roadway illumination. The relationship between the driver, vehicle, environment and target was then modeled, resulting in thousands of conflicting, yet high priority target points. Prioritized accident data and target similarity was then used to reduce the number of targets to a more manageable number for specification purposes. The resulting specification, based on safe driving needs during nighttime driving conditions, will be the basis for developing future lighting throughout the world.

#### Introduction

In a Request for Comments that was published on August 14, 1987, the National Highway Traffic Safety Administration (NHTSA) announced a plan for a long-term effort to develop a vehicle-based roadway illumination performance requirement. A Notice of Proposed Rule-making (NPRM) was published on May 9, 1989 (54 FR 20084) which proposed such a vehicle-based roadway illumination specification for inclusion as an option to the current headlamp photometrics required by Federal Motor Vehicle Safety Standard (FMVSS) No. 108, *Lamps, Reflective Devices, and Associated Equipment*.

Several factors and events have coalesced to form the basis for this action. These include the analysis of accident data which shows the potential for reduction in accidents and injuries from improved headlighting and the volume of petitions from vehicle and headlighting manufacturers to have new headlighting systems that are different from those that already exist. Attendant with new systems are new photometric specifications because the headlighting systems are either intended to provide better light for customers or have optical systems that can not meet the current requirements. There is also an entirely different beam pattern required for the lower beam in Europe. Additionally, a research paper by John Arens (1)\* showed that there may be a problem with visibility of roadway guide signs due to insufficient upward light from new headlighting designs. This potential sign visibility problem

exists because there are no specifications for minimum light intensities above the horizontal. A similar concern in Europe about the lack of overhead sign visibility adds hope that this need for some minimum, but non-glaring illumination might be the common basis for this performance-based specification to help achieve harmonization of worldwide specifications.

The approach, as proposed in the NPRM, is based on the visibility needs of night driving. The basic needs are to stay on the roadway, to avoid pedestrians and other objects on or near the roadway, and to see signs to the side and above the roadway. A review of these needs, including a detailed analysis of accident files, led the NHTSA to evaluate the lighting requirements for a variety of conditions and situations. These conditions include the presence of either an approaching or a following glare-producing vehicle and driving on curved and hilly roads as well as roads that are straight and level. This paper presents an overview of this effort. The results are two new vehicle-based specifications for roadway illumination which have the potential of improving the level of safety of night driving, one which is compatible with today's headlamps, the other based solely on visibility needs. This paper discusses only the latter.

The effort consisted of developing and using a computer model of visibility to determine the necessary amount of light that the vehicle must produce to enable the driver to see important features, such as pedestrians and lane markers. The necessary amount of light for each of a large number of driving situations was determined.

This approach has the advantage of providing a basis for developing any of several vehicle-based options, including specifications that are compatible with the performance of existing lamps or specifications that provide an improvement in safety. This approach also provides a basis of comparison with performance of existing lighting systems, addresses the concern about illumination of signs, and provides a basis for continuing international discussions on harmonization of headlighting specifications.

In order to develop the model and to then condense the myriad of resulting targets into a manageable specification, nighttime accidents needed to be more fully understood. A key question associated with the analysis of accident data is how motor vehicle headlighting is related to the various types of accidents that occur. These relationships are most easily understood if accidents are divided into single-vehicle and multiple-vehicle categories. For multiple-vehicle accidents, headlighting may be involved in several ways. Headlamps help prevent accidents by enhancing the

\*Numbers in parentheses designate references at end of paper.

conspicuity of vehicles and by marking their edges. On the other hand, it is possible that headlamps that produce excessive glare, whether from misaim or poor design, may cause accidents. While such excessive glare is undesirable, some light is needed to provide for sign illumination and for silhouetting targets otherwise not visible. There appears to be no clear and concise way to determine the involvement of these effects in multiple-vehicle collisions.

For single-vehicle accidents, headlighting is more directly involved in the ability of the driver to see the road and roadway features and obstacles. Thus, lack of proper roadway illumination can contribute to a driver failing to stay on the road or to a vehicle hitting a person or other object on or near the road. Although existing accident data bases rarely contain accident-avoidance information such as the illumination that is provided by headlights, or the relationship of headlighting to the accident, it is believed that improved illumination will reduce the number of most types of single-vehicle nighttime accidents. For these reasons, the analysis of accident data for this project was limited to single-vehicle accidents. This analysis is reported in a companion paper, "Estimation of Reductions in Accident and Severity Rates for a New Vehicle-Based Roadway Illumination Specification" (Paper No. 89-5B-W-011).

From the analysis of accident data, it is apparent that any evaluation of roadway illumination needs for night driving, must address the visibility of pedestrians. It is also apparent that the visibility of roadway features, such as lane markings, that can assist the driver in maintaining the vehicle within the driving lane must be considered. The visibility of lane markings will also help reduce the number of rollover accidents and other accidents where the vehicle hits a tree or some other offroad object. It was assumed that when sufficient illumination is provided to see pedestrians, then that same level of illumination will also provide visibility of larger or more reflective inanimate roadway objects, therefore no additional targets were modeled.

After using the accident-data analysis for developing the model, the accident data was used to eliminate many close or overlapping test points with conflicting illumination needs, i.e. a pedestrian and an oncoming driver's eyes. It also helped by reducing the total number of test points that resulted from exercising the model. The resultant condensation became the vehicle-based roadway illumination specification. A complete technical report detailing the development of the models, instructions for use, the computer program coding, and the accident data analysis is available in Docket 85-15; Notice 7, at the Docket Section, Room 5109, Nassif Building, 400 Seventh Street, SW, Washington, DC 20950, USA.

## The Modeling

The approach of this project was to determine the vehicle forward lighting necessary to view critical roadway targets at night by modeling night driving scenarios. This reflects a reversal of the method used in the Comprehensive Headlamp Environment Systems Simulation Model

(CHESS), a popular headlighting model written by the Ford Motor Company (2). CHESS examines various visibility situations and various glare situations and determines whether a specified headlighting system provides sufficient illumination to see a pedestrian or a stretch of lane marking or whether the glare produced by the vehicle lighting system causes discomfort of another driver. The performance of the lighting system in each situation is noted, and from a compilation of the results of all the roadway situations, a Figure of Merit (FOM) score is calculated for the headlighting system. This number represents the percentage of the simulated distance traveled in the model over which the headlights performed adequately. The FOM is most useful for comparing the performances of two different headlighting systems. Whereas CHESS begins with a headlighting system and a set of roadway situations and generates a number representing the adequacy of the headlighting system, this project requires a program which starts with a set of roadway situations and calculates a set of roadway illumination specifications; thereby defining an adequate headlighting system.

CHESS incorporates the work of many other researchers. The key components of CHESS are the DeBoer discomfort criterion (3), the Fry equation for veiling brightness (4), the Blackwell equation for threshold contrast (2, 5), and an equation for actual contrast. Though CHESS could not be used in its current form for this project, the same building blocks are used in the program described here and are used for determining road illumination requirements.

## Glare and visibility algorithm

The approach combines the glare effects with the determination of necessary illumination for target visibility. Considering glare limitations and visibility requirements at the same time requires that the program must simultaneously solve the equations for determining the necessary illumination and acceptable glare intensity. For instance, the discomfort an observer experiences as a result of light from the glare vehicle is dependent, in part, on the luminance to which the observer is adapted. This "adaptation brightness" is the brightness of the observer's surroundings which is influenced by the intensity of the headlights of the observer vehicle. On the other hand, the headlighting system of the observer vehicle must generate sufficient illumination so that the contrast between a target and its background are greater than a threshold value. The contrast is decreased by the presence of veiling brightness produced by the headlights of other vehicles.

The intensities for the two vehicles are calculated using an iterative approach. The approach consists of eight steps, as follows:

1. The placement of the observer vehicle, a target, and a glare vehicle are determined. Positions are based on target type, road geometry, velocity of the observer vehicle, and the type of glare situation, either oncoming or following.

2. An initial intensity is assumed for the headlighting system of the observer vehicle. This intensity may not be close to the final intensity for that specific target, but it provides a number to use in calculations in the first iteration of the algorithm.

3. The background brightness and target brightness for the specified observer vehicle intensity are calculated.

4. Using a specified DeBoer value and an adaptation brightness (equal to background brightness), the maximum allowable intensity for the glare vehicle is determined.

5. The veiling brightness from the glare vehicle is calculated.

6. The actual contrast and threshold contrast are calculated from target brightness, background brightness and veiling brightness.

7. The actual contrast and threshold contrast are compared to determine if the target is visible.

8. If not visible, (i.e., the estimated actual contrast is less than the threshold contrast) the observer vehicle light intensity value is adjusted by the model and steps 3 through 7 are repeated until the target is visible and the necessary observer vehicle light intensity has been determined, to the nearest 10 candela.

The program results include a minimum forward-lighting intensity for the observer vehicle, a maximum forward-lighting intensity for the glare vehicle, and angular coordinates relating the vectors for the lighting intensities to the vehicle coordinate system.

## The target types

Three types of targets were examined in this project. These are: pedestrians, signs, and lane markings. Eight programs were written to implement the basic visibility algorithm described previously as well as the variations on the algorithm necessary for evaluating visibility of the different targets.

### A. Pedestrian targets

A pedestrian is considered to be a stationary target, standing on the right shoulder of the road. The visibility criterion is that a driver should see a pedestrian target at a sufficient distance that the vehicle may be stopped before it reaches the target. Therefore the pedestrian is separated from the observer vehicle by a distance equal to the stopping distance, the combination of the reaction time and the deceleration time, of the observer vehicle at a specified velocity.

For each of the programs, the representation of a pedestrian is 2.5 feet tall and 1.0 feet wide, with a reflectance of 12%. The small target size was selected as representing that part of a pedestrian which is most likely to fall into the lower, brighter portion of a headlight beam. In the model, the driver's eyes focus on a point on the simulated pedestrian which is 1.0 foot above the ground. Use of this height reduces the occurrence of high intensities at or above driver

eye-height, which would conflict with glare restrictions. The use of a focus point which was lower than one foot would have decreased the distance between target and background, thus reducing the contrast and increasing illumination requirements.

For the simulation of the oncoming glare situation, the glare vehicle is separated from the observer vehicle by twice the distance between the observer vehicle and the pedestrian. Two glare situations with the glare vehicle following the observer vehicle are also considered. Vehicle locations for each of the glare situations will be discussed in a subsequent section ("Fixed Program Parameters").

### B. Lane markings

Lane markings are also handled with the eight-step algorithm, but a lane marking is modeled differently than a pedestrian target. A fifty-foot segment of lane marking is considered as the target. This agrees with the method used in CHESSE. The fifty-foot segment is centered at a point two seconds traveling distance ahead of the observer vehicle. The two-second rule agrees with the criterion used in CHESSE. The fifty-foot segment of lane marking is centered at the two-second distance on the assumption that a driver's eyes will tend to be focused on the center of a target. Third, the angular size (area) of the target is calculated.

For lane marking visibility, oncoming-glare vehicles are located at twice the distance from the observer vehicle as the central point on the target. Glare vehicles following, are located at the same positions as in pedestrian-viewing situations. This will be discussed more completely in a later paragraph (Fixed Program Parameters).

### C. Signs

The eight-step algorithm was not used to evaluate sign visibility. It was decided to treat signs differently from the other visibility targets. The method chosen is based on a 1987 SAE Paper written by John Arens (5). The retroreflectance values used in that paper are also used in the simulations of this project. Against a background of limited complexity, a sign should be legible if the luminance from it is greater than 1 fL. (1). The intensity from the observer vehicle necessary to cause a minimum luminance of 1 fL. on the sign may be calculated from the distance to the sign and the specific intensity per unit area (SIA) of the signing material.

Most guide and warning signs need to be legible for five to ten seconds before reaching them in order for drivers to evaluate a sign before reaching it and then react. Stop signs must be visible at the stopping distance.

## Fixed program parameters

Many constants and variables are needed for the various roadway situations. Values for characteristics such as ambient brightness of the sky, reflectance of a target, target dimensions, and driver eye-height had to be selected. When possible, these values were selected based on design guidelines of associations such as the American Association of State Highway and Transportation Officials (AASHTO).

Driver eye height is among these parameters. Driver eye-height was chosen to be 3.5 feet because this agrees with the eye-height used as a basis for highway design (6). Mirror locations were determined based on measurements of locations of mirrors in 12 cars representing about 35% of the 1986 U.S. automobile sales. Values for the reflectance of mirrors were based on Federal Motor Vehicle Safety Standard No. 111, *Rearview Mirrors*. The reflectance of the interior mirror was set at 80%, slightly more than twice the minimum in Standard No. 111 and the reflectance of the exterior mirrors was set at 60%, slightly less than twice that minimum. For overhead signs, the specific intensity per unit area (SIA) values used are characteristic of High-Intensity Grade sheeting recommended for permanent highway signs. This sheeting has an SIA of 200–250 cd/ft<sup>2</sup>.

Locations of the glare vehicle in the various roadway situations were selected so that the glare vehicle would be present most of the time as the observer vehicle approached the target. In mirror situations, two following distances were used. A distance relating to two seconds traveling time at the specified velocity was used because this is recognized in driver training courses and state driver's handbooks as the minimum safe following distance. A second following distance of 25 feet was considered because this situation is likely to occur in rush-hour traffic.

Roadway reflectances were selected based on research findings of the Ford Motor Company. Information on reflectances was sought from other sources, but the only information found appropriate for this project was in *Modeling Vision with Headlights in a Systems Context* by Bhise, et al. (2)

Values used for the other parameters were based on the best information available. All these values are incorporated directly into the programs, and may be changed only by editing the source code.

## Program outputs

The output data from each program include the distance from the observer vehicle to the target, the distance from the glare vehicle to the observer, angles from the vehicles to the targets, the minimum illuminance required to be produced by the observer vehicle, and the maximum illuminance allowed to be produced by the glare vehicle. The output angles may be expressed in either a vehicle-coordinate system or a lamp-coordinate system. In the vehicle-coordinate system, angles are referenced to the center, front of the vehicle at ground level. In the lamp-coordinate system, angles are referenced to the center of each headlamp.

## Using The Models

The programs discussed above were written with ease-of-use in mind. User inputs were minimized without limiting flexibility. The user is required to select the target type and the coordinate system—vehicle or headlamp—in which the program results will be described. Then, the user must enter several other parameters required by the program. The

necessary parameters differ with target type and road situation.

For this project, a variety of speeds was used for each target type. Velocities were generally selected after it was determined what range of speeds produced program results (illumination levels) which seemed practicable for current headlighting technology. For pedestrian situations, the greatest speed which produced an illumination level which seems achievable is 40 miles per hour. Because of the higher retroreflectance of signs, lower light is required to achieve visible luminance. The criterion for necessary visibility was also different. It was discovered that, for speeds up to 65 miles per hour, lighting requirements for sign visibility would likely be practicable.

In situations involving glare—all but sign situations—the user must enter a DeBoer glare value. A criterion value of 4, representing deBoer's perception of 'just unacceptable' glare, was selected so that any glare achieved would be deemed to be 'just acceptable' (2, 3).

Deceleration and driver-reaction time must be entered in situations in which visibility distances must be equal to vehicle stopping distance. This includes pedestrian situations and situations involving stop signs. To avoid accidents, a driver must stop before or upon reaching these targets. The vehicle stopping distance is a function of vehicle speed, driver reaction time, and vehicle deceleration. Driver reaction time was chosen to be 1.42 seconds. This corresponds to the mean value used in CHES. The source for this value is a table published by L.M. Forbes (7). This reaction time represents a combination of data from Mortimer (8) and Normann (9). The original work by Normann includes only the time required for a driver's foot to travel from the accelerator to the brake pedal. Mortimer's work centered on perception time. The combination of the two includes both perception time and physical reaction time. Deceleration (0.5 g's) also corresponds to the value used in CHES. Moreover, 0.5 g's is less than that required by Federal Motor Vehicle Safety Standards for new automobiles (FMVSS No. 105, *Hydraulic Brake Systems*, Paragraph S5.1).

Pedestrian locations and lane marking locations are prescribed within the programs as functions of road geometry. Lane markings are always located on either edge of the lane in which the observer is traveling. Pedestrians are always located on the right shoulder, two feet to the right of the lane in which the observer is traveling. Sign locations, however, are to be entered by the user. For this project, sign locations were selected from Section 2A–16 of the Manual on Uniform Traffic Control Devices (MUTCD) (10). A range of locations meeting the MUTCD guidelines was selected to represent a variety of sign types. The seven signs examined are:

1. Stop sign mounted on the right side of the road, 12 feet from the right edge of the observer vehicle's lane of travel.
2. Guide sign mounted on the right, 12 feet from the right edge of the observer vehicle's lane of travel.

3. Guide sign mounted on the right, 30 feet from the right edge of the observer vehicle's lane of travel.
4. Warning sign mounted on the left, 2 feet from the left edge of the observer vehicle's lane of travel.
5. Warning sign mounted on the left, 12 feet from the left edge of the observer vehicle's lane of travel.
6. Overhead guide sign, directly over observer vehicle's lane of travel.
7. Overhead guide sign, mounted over lane adjacent on the right to the observer vehicle's lane of travel.

The program permits a series of curved road segments, but for this project, a single curve with a constant radius of curvature of 1000 feet was used. According to the American Association of State Highway and Transportation Officials (AASHTO), this is a minimum curvature for a roadway with a design speed of 60 miles per hour (6). For hills, the grade of the slope is user-entered, and the user is required to select a 'hill type'. Maximum hill slope for this project was selected to be 10 percent. According to AASHTO, this is the maximum slope for a 40 mile per hour design speed (6). There are four possible selections for hill types, and these differ somewhat for oncoming vehicle and following vehicle glare situations. In each glare situation, either the glare vehicle or the observer vehicle is located at the extreme, crest or sag, of the hill. This causes requirement of illumination from the headlights at the greatest vertical angles. For sign visibility situations, either the sign or the observer vehicle is located at the crest or sag of a hill.

Table 1 defines the abbreviations used for describing the roadway and target scenarios in the tabulated outputs of the models. This table should be used with subsequent tables for identifying the scenarios chosen.

**Table 1. Terminology.**

For use in understanding the terminology use in some of the tables the following key is provided.

The items in the DRIVING SITUATION column are velocity, driver age, DeBoer level, road geometry, road grade, target type, and glare situation. Abbreviations are defined as follows:

First 2-digit # - Vehicle speed  
 STRT - Straight roadway  
 RCUR - Right curve  
 LCUR - Left curve  
 LL - Level roadway  
 C1 - Hill situation Crest 1 as described in Figure 1A-1.  
 C2 - Hill situation Crest 2 as described in Figure 1A-1.  
 S1 - Hill situation Sag 1 as described in Figure 1A-1.  
 S2 - Hill situation Sag 2 as described in Figure 1A-1.  
 PED - Pedestrian target.  
 CT LM - Center lane marking target.  
 RT LM - Right lane marking target.  
 SIGN--OTHER - A sign target than a stop sign.  
 GLR CAR APPR - Glare is caused by an oncoming vehicle.  
 GLR CA - Glare is caused by an oncoming vehicle.  
 LT 2 S FOLLO - Glare is caused by reflection in the left mirror of the lights of a vehicle following at 2 seconds.  
 CT 2 S FOLLO - Glare is caused by reflection in the center mirror of the lights of a vehicle following at 2 seconds.  
 RT 2 S FOLLO - Glare is caused by reflection in the right mirror of the lights of a vehicle following at 2 seconds.

## Development of the Roadway-Illumination Specification

Given the large number of scenarios, each with a distinct

target, that result from exercising of the model, a basis for determining how to prioritize and then combine many of them was necessary. The basis for deleting a target was initially the analysis of accident data. The target specifications for a driving situation with a higher priority would pre-empt target specifications for lower priorities. Based on these results and a preliminary review of the modeling results, it was determined that only scenarios representing three priority driving situations would be used for establishing the final specifications. The driving situations modeled are visibility of lane edge marking on straight/level roads, visibility of pedestrians on straight/level roads, and visibility of lane edge marking on curved/level roads. Speeds of 20, 30, 35, 40, and 55 miles per hour are considered. Glare-producing vehicles, either approaching or following, are present for each of these situations. Signs were also included as necessary targets. By limiting the driving conditions to the highest priorities, the number of points with lighting specifications is substantially reduced.

The minimum amount of light needed to see targets and the maximum amount of glare light that should be present was calculated for each driving situation. The large number of specifications was then reduced to a smaller number for regulatory purposes through a multistage condensation process. The processes for reducing the number of maximum intensity specifications, the number of minimum intensity specifications for pedestrian and lane marker targets, and the number of minimum intensity specifications for sign target were slightly different, however the basis for each reduction was similar.

Though the visibility needs-based requirements are not specifically limited by the design of current headlighting systems, some roadway-illumination requirements were eliminated because they appear impractical to achieve. For example, unrealistically large illumination requirements generally occur when the source of glare is aligned with the roadway feature that is to be seen. One situation in which this occurs is for visibility of the right edge marker on a right curve when traveling at 55 miles per hour. The model indicates that the vehicle must provide the equivalent of 71,910 cd. Because of the impracticability of this specification for low beam headlighting, this group of points has been dropped from the overall specification. The other group of points which is dropped corresponds to avoiding a pedestrian when traveling at 55 miles per hour. With an approaching vehicle, this would require an equivalent intensity of 214,020 cd. for the observer vehicle.

The selection of *minimum* intensity specifications for pedestrian and lane marker targets started with the compilation of all of the specifications. From this list it was seen that for each combination of road geometry, vehicle speed and target location, the angular location of the specification for the observer vehicle remained the same while the angular location of the light for the glare vehicle changed for each of the seven glare situations. This led to seven (usually different) minimum specifications for the

same point for the observer vehicle. Requirements for the glare vehicle varied both in location and in intensity. The largest of the seven minimum intensity requirements for the observer vehicle was retained, and the other six points were dropped. The selected point consistently corresponded to

the minimum intensity needed to see when a glare vehicle was approaching, rather than following. This step in the process led to a total of 33 minimum intensity specifications. The driving situations for these points are shown in table 2. The total number of specifications was reduced further by

Table 2. Minimum intensity situations.

DRIVING SITUATION	TARGET ILLUM (f-c)	MAX/MIN	TARGET DISTANCE (ft)	HORIZONTAL ANGLE (degree)	VERTICAL ANGLE (degree)
20, AGE=35. W=4. STRT LL PED, GLR CAR APPR	0.435	MIN	68.84	6.67	0.83
30, AGE=35. W=4. STRT LL PED, GLR CAR APPR	0.633	MIN	122.86	3.73	0.47
35, AGE=35. W=4. STRT LL PED, GLR CAR APPR	0.791	MIN	154.94	2.96	0.37
40, AGE=35. W=4. STRT LL PED, GLR CAR APPR	1.002	MIN	190.36	2.41	0.30 *
20, AGE=35. W=4. STRT LL RT LM, GLR CAR APPR	0.322	MIN	58.97	5.84	0.00
20, AGE=35. W=4. STRT LL CT LM, GLR CAR APPR	0.546	MIN	58.97	-5.84	0.00
30, AGE=35. W=4. STRT LL RT LM, GLR CAR APPR	0.425	MIN	88.20	3.90	0.00
30, AGE=35. W=4. STRT LL CT LM, GLR CAR APPR	0.814	MIN	88.20	-3.90	0.00
35, AGE=35. W=4. STRT LL RT LM, GLR CAR APPR	0.502	MIN	102.84	3.35	0.00
35, AGE=35. W=4. STRT LL CT LM, GLR CAR APPR	0.998	MIN	102.84	-3.35	0.00
40, AGE=35. W=4. STRT LL RT LM, GLR CAR APPR	0.595	MIN	117.49	2.93	0.00 *
40, AGE=35. W=4. STRT LL CT LM, GLR CAR APPR	1.221	MIN	117.49	-2.93	0.00
55, AGE=35. W=4. STRT LL RT LM, GLR CAR APPR	0.984	MIN	161.45	2.13	0.00
55, AGE=35. W=4. STRT LL CT LM, GLR CAR APPR	2.158	MIN	161.45	-2.13	0.00 *
20, AGE=35. W=4. RCUR LL RT LM, GLR CAR APPR	0.386	MIN	63.75	7.23	0.00 *
20, AGE=35. W=4. RCUR LL CT LM, GLR CAR APPR	0.61	MIN	64.13	-3.53	0.00 *
20, AGE=35. W=4. LCUR LL RT LM, GLR CAR APPR	0.345	MIN	64.13	3.55	0.00 *
20, AGE=35. W=4. LCUR LL CT LM, GLR CAR APPR	0.578	MIN	63.75	-7.21	0.00 *
30, AGE=35. W=4. RCUR LL RT LM, GLR CAR APPR	0.675	MIN	92.88	6.38	0.00
30, AGE=35. W=4. RCUR LL CT LM, GLR CAR APPR	0.812	MIN	93.44	-1.00	0.00
30, AGE=35. W=4. LCUR LL RT LM, GLR CAR APPR	0.427	MIN	93.44	1.03	0.00
30, AGE=35. W=4. LCUR LL CT LM, GLR CAR APPR	0.877	MIN	92.88	-6.35	0.00
35, AGE=35. W=4. RCUR LL RT LM, GLR CAR APPR	0.967	MIN	107.46	6.30	0.00
35, AGE=35. W=4. RCUR LL CT LM, GLR CAR APPR	0.885	MIN	108.11	-0.07	0.00
35, AGE=35. W=4. LCUR LL RT LM, GLR CAR APPR	0.48	MIN	108.10	0.11	0.00
35, AGE=35. W=4. LCUR LL CT LM, GLR CAR APPR	1.022	MIN	107.46	-6.26	0.00
40, AGE=35. W=4. RCUR LL RT LM, GLR CAR APPR	1.391	MIN	122.03	6.34	0.00 *
40, AGE=35. W=4. RCUR LL CT LM, GLR CAR APPR	0.927	MIN	122.77	0.73	0.00 *
40, AGE=35. W=4. LCUR LL RT LM, GLR CAR APPR	0.526	MIN	122.77	-0.69	0.00
40, AGE=35. W=4. LCUR LL CT LM, GLR CAR APPR	1.111	MIN	122.04	-6.30	0.00
55, AGE=35. W=4. RCUR LL RT LM, GLR CAR APPR	1.003	MIN	166.75	2.74	0.00
55, AGE=35. W=4. RCUR LL CT LM, GLR CAR APPR	0.68	MIN	166.75	-2.68	0.00
55, AGE=35. W=4. LCUR LL RT LM, GLR CAR APPR	1.184	MIN	165.76	-6.80	0.00 *

\* POINTS THAT WERE RETAINED IN THE FINAL VEHICLE SPECIFICATION.

geometrically grouping these points and judiciously selecting the maximum value of the specifications within each of the groups, leaving 10 minimum value specifications for the final requirement.

The process for reducing the number of *maximum* specifications that correspond to pedestrian and lane marker targets was similar. In this case however, the points were grouped geometrically using approximately common vertical angular locations.

The minimum of the maximum values of intensity within each group was selected to represent that group. This produced 17 maximum value specifications. The driving situations for these points are shown in table 3. The total number of specifications which were maximums, was reduced further by judiciously selecting points that generally covered the angular area in front of the vehicle, leaving 6 maximum-value specifications for the final requirement.

For visibility of signs, a total of 13 minimum value

specifications spanned the entire region in front of the vehicle where signs occur, and these were used for the final requirement. These may be seen in table 4.

A foreground *maximum* illumination point at 32 feet was chosen because it represents the foreground at about half the distance to the quartet of nearest points located at 64 feet. The specification for illuminance directed at this foreground point must not exceed the average of the illuminance directed at those four points located at about 64 feet.

The compiled set of specifications for the vehicle requirement is shown in table 5, and a graphic representation is in figure 1.

## Implementation of the Specifications

There was almost universal agreement among commenters to the Notice of Request for Comments (50 FR 42735) that any new performance requirement should not test the vehicle as a whole, but should test the headlighting

Table 3. Driving conditions for maximum grouping values.

DRIVING SITUATION	TARGET ILLUM (f-c)	TARGET DISTANCE (ft)	HORIZONTAL ANGLE (degree)	VERTICAL ANGLE (degree)	MAX/MIN	
20, AGE=35. W=4. STRT LL	PED, CT, SEP=25 FT	0.146	26.44	0.00	8.69	MAX
20, AGE=35. W=4. STRT LL	PED, RT, SEP=25 FT	0.228	26.82	5.83	6.74	MAX
20, AGE=35. W=4. STRT LL	CT LM, LT SEP=25 FT	0.187	26.82	-5.83	6.74	MAX
20, AGE=35. W=4. RCUR LL	RT LM, CT 2 5 FOLLO	0.158	72.09	2.08	3.21	MAX
20, AGE=35. W=4. STRT LL	PED, CT 2 5 FOLLO	0.146	72.11	0.00	3.21	MAX *
20, AGE=35. W=4. LCUR LL	RT LM, CT 2 5 FOLLO	0.162	72.09	-2.05	3.21	MAX *
20, AGE=35. W=4. RCUR LL	RT LM, RT 2 5 FOLLO	0.246	72.28	4.24	2.51	MAX
20, AGE=35. W=4. STRT LL	PED, RT 2 5 FOLLO	0.228	72.39	2.16	2.51	MAX *
20, AGE=35. W=4. RCUR LL	CT LM, LT 2 5 FOLLO	0.195	72.48	-0.07	2.50	MAX
20, AGE=35. W=4. STRT LL	PED, LT 2 5 FOLLO	0.198	72.39	-2.16	2.51	MAX
20, AGE=35. W=4. LCUR LL	CT LM, GLR CAR APPR	0.067	121.40	-1.49	1.65	MAX
20, AGE=35. W=4. STRT LL	CT LM, GLR CAR APPR	0.059	122.29	-4.93	1.64	MAX *
20, AGE=35. W=4. RCUR LL	CT LM, GLR CAR APPR	0.064	123.02	-8.39	1.63	MAX *
30, AGE=35. W=4. LCUR LL	CT LM, GLR CAR APPR	0.074	179.36	1.79	1.12	MAX
30, AGE=35. W=4. STRT LL	CT LM, GLR CAR APPR	0.058	180.80	-3.33	1.11	MAX *
40, AGE=35. W=4. LCUR LL	RT LM, LT 2 5 FOLLO	0.236	130.77	-4.92	1.39	MAX
30, AGE=35. W=4. RCUR LL	CT LM, GLR CAR APPR	0.066	181.77	-8.50	1.10	MAX

\* POINTS THAT WERE RETAINED IN THE FINAL VEHICLE SPECIFICATION

Table 4. Sign visibility driving situations.

DRIVING SITUATION	TARGET ILLUM (f-c)	TARGET DISTANCE (ft)	HORIZONTAL ANGLE (degree)	VERTICAL ANGLE (degree)	MAX/MIN	
VEL= 65, AGE= 35. LCUR C1	SIGN--OTHER	0.002	468.58	-14.50	0.50	MIN *
VEL= 65, AGE= 35. LCUR S2	SIGN--OTHER	0.002	481.22	-9.00	2.00	MIN
VEL= 65, AGE= 35. STRT S2	SIGN--OTHER	0.002	477.05	-2.50	2.00	MIN
VEL= 65, AGE= 35. STRT C2	SIGN--OTHER	0.002	477.05	-2.50	0.50	MIN
VEL= 65, AGE= 35. STRT S1	SIGN--OTHER	0.002	476.67	0.00	3.50	MIN *
VEL= 65, AGE= 35. STRT C1	SIGN--OTHER	0.002	478.26	4.50	0.50	MIN
VEL= 65, AGE= 35. STRT S2	SIGN--OTHER	0.002	478.26	4.50	2.00	MIN
VEL= 65, AGE= 35. RCUR C2	SIGN--OTHER	0.002	472.70	12.50	0.50	MIN *
VEL= 65, AGE= 35. RCUR LL	SIGN--OTHER	0.002	472.11	13.50	2.50	MIN *
VEL= 55, AGE= 35. RCUR S1	SIGN--OTHER	0.002	397.31	11.50	4.00	MIN
VEL= 65, AGE= 35. LCUR S1	SIGN--OTHER	0.002	466.52	-16.00	2.00	MIN *
VEL= 65, AGE= 35. LCUR S1	SIGN--OTHER	0.002	470.60	-13.50	3.50	MIN *
VEL= 40, AGE= 35. LCUR S2	SIGN--OTHER	0.002	289.00	-8.50	5.00	MIN *
VEL= 30, AGE= 35. LCUR S2	SIGN--OTHER	0.002	216.20	-3.00	6.50	MIN *
VEL= 20, AGE= 35. STRT S2	SIGN--OTHER	0.002	146.67	0.00	9.50	MIN *
VEL= 20, AGE= 35. STRT S2	SIGN--OTHER	0.002	147.16	4.50	9.50	MIN *
VEL= 30, AGE= 35. RCUR S2	SIGN--OTHER	0.002	213.62	9.50	6.50	MIN *
VEL= 65, AGE= 35. RCUR S1	SIGN--OTHER	0.002	467.80	15.00	3.50	MIN *
VEL= 65, AGE= 35. RCUR S2	SIGN--OTHER	0.002	462.82	18.50	2.00	MIN *

\* POINTS THAT WERE RETAINED IN THE FINAL VEHICLE SPECIFICATION

devices individually. To respond to these comments, a procedure which tests components was developed for verifying the performance of the vehicle in meeting its roadway-illumination-performance requirements. This is accomplished by trigonometrically converting the location of test points from a vehicle coordinate to a roadway-illumination device (headlamp) coordinate system. The actual illumination performance from each device would be determined by the vehicle designer in such a way that the roadway-illumination-performance requirement for the vehicle is met. For each headlighting system, the designer's task includes the apportionment of the illumination task between contributing roadway-illumination devices

(RID's); i.e. each RID must provide the necessary illumination for the vehicle requirements. Locational aspects such as height above the ground and distance from the vehicle centerline also affect the individual RID performance. These would be established by the vehicle and lamp designers. Depending on the actual locations, the required performance of the RIDs could be very different from present headlamps, but it does not have to be if lamp locations and numbers are similar to those used today.

A visual representation of the trigonometric conversion of a target specification from the vehicle reference to a headlamp reference may be seen in figure 2 and figure 3, where side and top views, respectively, are shown. The

**Table 5. Roadway illumination test points (vehicle coordinate system).**

TARGET ILLUMINANCE (fc)	TARGET DISTANCE (ft)	HORIZONTAL ANGLE (deg)	VERTICAL ANGLE (deg)
>=2.158	161.45	-2.13	0.00
>=1.002	190.36	2.41	0.30
>=1.184	165.76	-6.80	0.00
>=1.391	122.03	6.34	0.00
>=0.927	122.77	0.73	0.00
>=0.595	117.49	2.93	0.00
>=0.610	64.13	-3.53	0.00
>=0.578	63.75	-7.21	0.00
>=0.386	63.75	7.23	0.00
>=0.345	64.13	3.55	0.00
>=0.002	472.70	12.50	0.50
>=0.002	468.58	-14.50	0.50
>=0.002	476.67	0.00	3.50
>=0.002	472.11	13.50	2.50
>=0.002	467.80	15.00	3.50
>=0.002	470.60	-13.50	3.50
>=0.002	466.52	-16.00	2.00
>=0.002	462.82	18.50	2.00
>=0.002	289.00	-8.50	5.00
>=0.002	213.62	9.50	6.50
>=0.002	216.20	-3.00	6.50
>=0.002	146.67	0.00	9.50
>=0.002	147.16	4.50	9.50
<=0.058	180.80	-3.33	1.11
<=0.228	72.39	2.16	2.51
<=0.064	123.02	-8.39	1.63
<=0.059	122.29	-4.93	1.64
<=0.162	72.09	-2.05	3.21
<=0.146	72.11	0.00	3.21
*	32.00	0.00	0.00

\* Target Illuminance is less than or equal to the average of the target illuminance values actually measured at the 64.13, 63.75, 63.75, and 64.13 foot targets.

**NOTE:** when designing the system, the Roadway Illumination Device (RID) intensity values are to be apportioned by the lighting designer among the RID(s) within the system so that the total system illuminance at each test point above falls within the required limits.

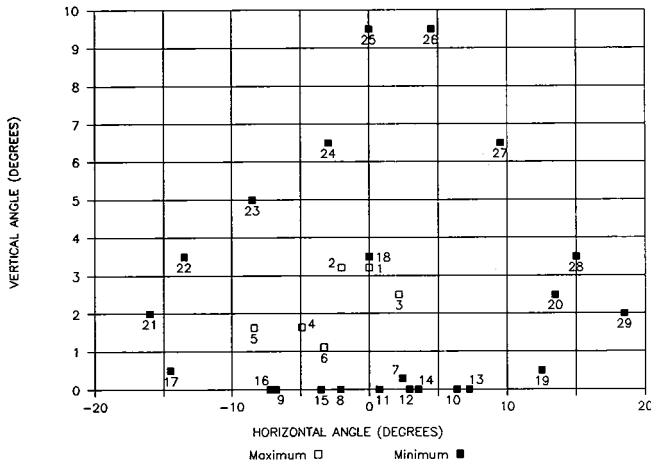


**Figure 1. Vehicle-based test points.**

reference for measurement is now the axis through the center of the RID instead of the vehicle centerline at the road surface. In the side view the vertical angles (RIDVA) are identical for each test point, but in the overhead view, the test points, either illumination or glare, do not have the same horizontal angle (RIDHA), since the reference axis now is the axis of each light producing device. Even though the two RID's illuminate the same target in space, the angles from each to that target are different. When testing on a screen at 60 feet as is presently done, the beams of light projected to that object in space pass through two different locations on that screen giving different photometric performance requirements for left and right RID's. For the example point,

using two RID's 22 inches from the ground spaced 48 inches apart, the values for left and right respectively, are: RIDVA = 0.75 deg. down, RIDHA = 3.50 deg. right, and RIDVA = 0.75 deg. down, RIDHA = 2.00 de. right, with a combined intensity value of  $\geq 27,890$  cd. to be apportioned by the lamp designer between the two lamps.

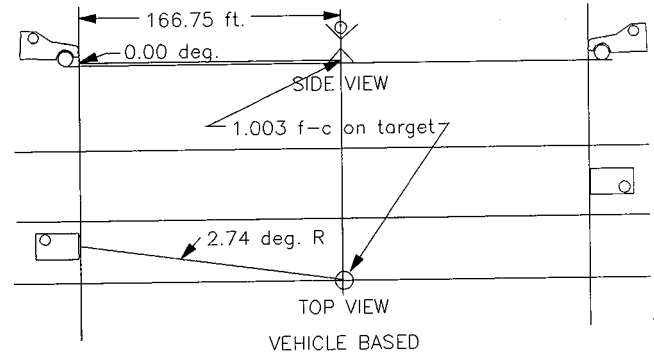


**Figure 2. Conversion from vehicle to RID performance.**

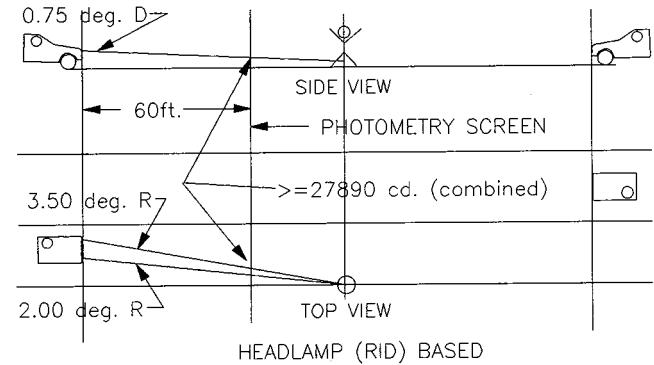


**Figure 3. Conversion from vehicle to RID performance 22" RID HT., 48" separation.**

Taking the final vehicle specifications of table 5, and using headlamps that are 24 inches from the ground spaced 48 inches apart, the conversion to a lamp-based reference is shown in table 6, and the test points for left and right are graphically shown in figures 4 and 5 respectively.

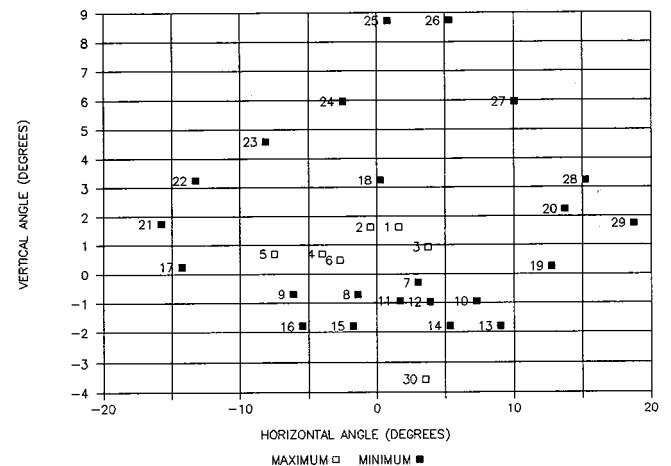


**Figure 4. Left RID test points.**

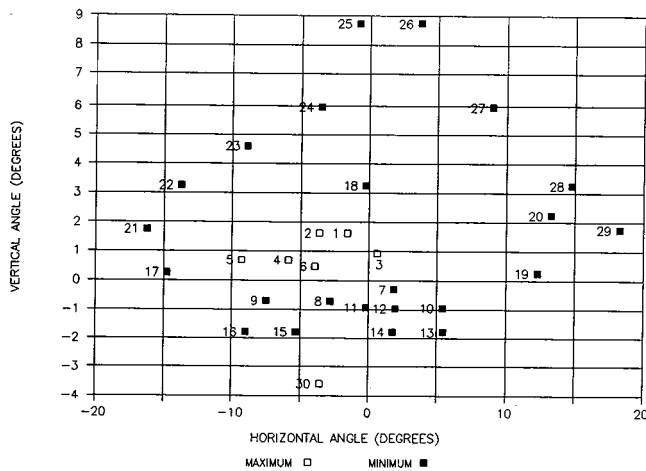


Figure 5. Right RID test points.

## Summary and Conclusions

A relationship between the nighttime visibility needs of drivers and vehicle-based roadway illumination has been established through the study of nighttime accident data in the United States, and by modeling the parameters and events of seeing and driving at night. The resultant set of important targets was reduced in number through the use of prioritized accident data and the judicious elimination of targets with similar illumination requirements. The resulting 30 targets and associated locational and illumination specifications for vehicles offer significant freedom of headlighting system design while assuring all vehicle drivers consistent roadway illumination for safer nighttime driving. This work should provide a sound basis for developing future vehicle-roadway lighting throughout the world.

Table 6. Vehicle specifications with RID specifications 2-lamp system, 28" HT., 24" from centerline.

TEST POINT NUMBER	TARGET ILLUM <f-c>	TARGET MAX/MIN	TARGET DISTANCE <ft>	HORIZONTAL ANGLE <degree>	VERTICAL ANGLE <degree>	TOTAL CANDELA <cd>***	LEFT RIDHA 24"SEP	RIGHT RIDHA 24"SEP	RIDVA 28"HT
1	0.146	MAX	72.11	0.00	3.21	761	1.58	-1.58	1.63
2	0.162	MAX	72.09	-2.05	3.21	845	-0.46	-3.63	1.63
3	0.228	MAX	72.39	2.16	2.51	1196	3.74	0.58	0.93
4	0.059	MAX	122.29	-4.93	1.64	887	-4.00	-5.86	0.71
5	0.064	MAX	123.02	-8.39	1.63	962	-7.47	-9.31	0.70
6	0.058	MAX	180.80	-3.33	1.11	1905	-2.70	-3.96	0.48
7	1.002	MIN	190.36	2.41	0.30	36310	3.01	1.81	-0.30
8	2.158	MIN	161.45	-2.13	0.00	56260	-1.42	-2.84	-0.71
9	1.184	MIN	165.76	-6.80	0.00	32520	-6.11	-7.48	-0.69
10	1.391	MIN	122.03	6.34	0.00	20710	7.27	5.41	-0.94
11	0.927	MIN	122.77	0.73	0.00	13970	1.66	-0.20	-0.93
12	0.595	MIN	117.49	2.93	0.00	8210	3.90	1.96	-0.97
13	0.386	MIN	63.75	7.23	0.00	1570	9.00	5.45	-1.79
14	0.345	MIN	64.13	3.55	0.00	1420	5.32	1.77	-1.78
15	0.61	MIN	64.13	-3.53	0.00	2510	-1.75	-5.30	-1.78
16	0.578	MIN	63.75	-7.21	0.00	2350	-5.43	-8.98	-1.79
17	0.002	MIN	468.58	-14.50	0.50	460	-14.26	-14.74	0.26
18	0.002	MIN	476.67	0.00	3.50	460	0.24	-0.24	3.26
19	0.002	MIN	472.70	12.50	0.50	460	12.74	12.26	0.26
20	0.002	MIN	472.11	13.50	2.50	460	13.74	13.26	2.26
21	0.002	MIN	466.52	-16.00	2.00	440	-15.76	-16.24	1.76
22	0.002	MIN	470.60	-13.50	3.50	440	-13.26	-13.74	3.26
23	0.002	MIN	289.00	-8.50	5.00	170	-8.11	-8.89	4.61
24	0.002	MIN	216.20	-3.00	6.50	95	-2.47	-3.53	5.98
25	0.002	MIN	146.67	0.00	9.50	45	0.78	-0.78	8.74
26	0.002	MIN	147.16	4.50	9.50	45	5.27	3.73	8.74
27	0.002	MIN	213.62	9.50	6.50	95	10.03	8.97	5.97
28	0.002	MIN	467.80	15.00	3.50	440	15.24	14.76	3.26
29	0.002	MIN	462.82	18.50	2.00	440	18.73	18.27	1.75
30	×	MAX	32.00	0.00	0.00		3.57	-3.57	-3.57

× ILLUMINANCE AT THIS POINT CANNOT EXCEED THE AVERAGE OF THE ILLUMINANCE ACTUALLY PRODUCED AT POINTS 13, 14, 15, AND 16.

\*\*\* TOTAL CANDELA MUST BE APPORTIONED BY RID SYSTEM DESIGNER AMONG THE RID'S WITHIN THE SYSTEM. FOR EXAMPLE, IN THIS TWO LAMP SYSTEM, THE CANDELA VALUE FOR EACH RID COULD BE 50% OF THE TOTAL. OR, FOR THOSE TEST POINTS TO THE LEFT OF THE VEHICLE CENTERLINE, THE LEFT RID COULD BE DESIGNED TO CONTRIBUTE 75% OF THE CANDELA AND THE RIGHT RID ONLY 25%. CONVERSLY, THE RIGHT RID WOULD THEN HAVE TO PROVIDE 75% OF THE LIGHT TO THE RIGHT OF THE CENTERLINE, AND ONLY 25% TO THE LEFT. ANY APPORTIONMENT COULD BE USED THAT WOULD FULFILL THE VEHICLE REQUIREMENTS.

## References

(1) Arens, J.B., *The Potential Impact of Automotive Headlight Changes on the Visibility of Reflectorized Highway Signs*, Society of Automotive Engineers Report No. 870238.

(2) Bhise, V.D., et al., *Modeling Vision with Headlights in a Systems Context*, Society of Automotive Engineers Report No. 770238, 1977.

(3) Schmidt-Clausen, H.J. and Bindels, J.T.H., "Assessment of Discomfort Glare in Motor Vehicle Lighting," *Lighting Research and Technology*, Vol. 6, No. 2, 1974.

(4) Fry, G.A., "Evaluating Disabling Effects of Approaching Automobile Headlights," *Highway Research Board Bulletin No. 89*, 1954.

(5) Blackwell, H.R., "Use of Performance Data to Specify Quantity and Quality of Interior Illumination," *Illuminating Engineering*, Vol. 50, No. 6, June, 1955.

(6) American Association of State Highway and Transportation Officials, *A Policy on Geometric Design of Highways and Streets*, Washington, D.C., 1984.

(7) Forbes, L.M., *Field of View from Automotive Vehicles*, Society of Automotive Engineers Report No. SP-381, May, 1973.

(8) Mortimer, R.G., *Dynamic Evaluation of Automobile Rear Lighting Configurations*, Highway Safety Research Institute, University of Michigan, 1969.

(9) Normann, O.K., "Newest Stopping Ability Tables," *Traffic Safety*, January, 1968.

(10) *Manual on Uniform Traffic Control Devices*, United States Federal Highway Administration, 1978.

## Using PCDETECT to Compare United States and European Beam Patterns

Eugene Farber and Calvin Matle,  
Ford Motor Company

### Abstract

This paper describes the results of comparison of the performance of U.S. and European low beams with the PCDETECT seeing distance model developed by the Ford Motor Company. PCDETECT is a revised version of the DETECT seeing distance model, developed by Ford in 1975, and is programmed to run on IBM PCs and compatibles. The beam patterns studied were the U.S. H4656 low beam and the European Granada H4 low beam. These lamps have very similar performance as measured by the Ford CHES headlamp evaluation program. PCDETECT was used to compare the seeing distance performance of the lamps, under conditions likely to reflect the differences in the beam patterns.

On level roads and in mild horizontal curves, a correctly aimed European low beam performed as well as or better than U.S. beams for objects on or near the road surface. The European beam provided substantially less illumination of overhead traffic signs than the U.S. beam, resulting in shorter legibility distances. Also, the European beam was generally much more sensitive to misaim than the U.S. beam and gave significantly lower seeing distances to pedestrians and pavement lines. Finally, seeing distance to pedestrians and pavement delineation on sag vertical curves (valleys) was substantially less with the European beam.

### Introduction

The beam patterns of U.S. and European low beams are distinctly different. This dissimilarity reflects a difference

in emphasis: the European low beam is shaped to provide bright, uniform foreground illumination with minimum glare; the U.S. low beam produces more of a spotlight effect to illuminate obstacles and delineation along the right edge of the roadway. These differences notwithstanding, U.S. and European lamps can produce very similar overall results when evaluated by CHES (1).\* CHES (Comprehensive Headlamp Evaluation Simulation System) is a computer program developed by Ford that evaluates headlight beam patterns by conducting thousands of simulated seeing distance and glare "tests" on a simulated test route. Given that a particular European low beam produces CHES scores typical of U.S. low beam, should it be regarded as acceptable for U.S. driving conditions?

CHES results by themselves may not provide a completely valid basis for determining the acceptability of European lamps on North American roads. There are two reasons for this. First, because the figure-of-merit is an overall score, situations in which a particular beam pattern may be very poor or even unacceptable may be offset by other situations in which the beam performs especially well. Second, CHES does not take into account the visibility of traffic signs and certain other traffic control devices. The visibility of unilluminated overhead signs is an especially pertinent issue in comparing U.S. and European low beams. This is because these signs are common in the U.S., and European low beams characteristically direct little candlepower above the horizon.

The purpose of the research described here was to use the Ford PCDETECT Seeing Distance Model (1) to compare the performance of U.S. and European lamps in encounters that might be expected to produce a significant advantage or disadvantage for either beam.

\*Numbers in parentheses designate references at end of paper.

## The PCDETECT Seeing Distance Model

The PCDETECT Seeing Distance Model was used to calculate seeing distances for European and U.S. low beams under a range of conditions for several different types of visibility 'targets'.

PCDETECT was developed by the Ford Motor Company and is written in QuickBASIC for IBM-compatible personal computers. It is a revised version of the DETECT seeing distance model developed by Ford as a FORTRAN program for mainframe application (2). PCDETECT calculates the distances at which a driver can see various objects on the road at night, as illuminated by the headlamp system specified by the user. It incorporates revised visibility algorithms and geometric routines. The revised visibility algorithms are based on more recent and comprehensive formulations for calculating contrast thresholds, including new formulations relating age and individual differences to contrast sensitivity and disability glare effects (3). The revised model also incorporates more elaborate geometry routines to insure accurate projection of sight lines and candlepower on hills and curves. PCDETECT also calculates the discomfort glare experienced by the observer-driver in opposed situations, as expressed by the DeBoer glare index.

PCDETECT provides a series of interactive menus that allow the user to define the conditions of observation in detail. The menus address such factors as observer and glare vehicle headlamp type, misaim and configuration, roadway geometry and characteristics, visibility target type, characteristics and location, glare parameters, and driver characteristics.

### Headlamp Beam Patterns

The beam patterns used in the study were as follows:

*United States Beam*—The U.S. beam pattern is an average H4656 halogen low beam. The candlepower at each point on the grid is the average of the corresponding points from 25 samples of H4656 lamps. The candlepower distribution of this beam is shown in figure 1. The "hotspot", i.e., the point of peak intensity, is located at  $H = 2.0^\circ$  right,  $V = 1.5^\circ$  down and has a value of 20,121 candlepower. The average intensity of this lamp, calculated by adding up all of the candlepower values in the grid and dividing by the number of points is 2310 candlepower.

*European Beam*—The European beam pattern is the average of two Ford Granada H4 low beams. This particular system was selected to represent European low beams in this study because its overall performance, as measured by CHESSE, is almost identical to the U.S. average H4656 lamp. The hotspot of this beam is located at  $H = 2.0^\circ$  right,  $V = 0.5^\circ$  down and has a value of 14533 candlepower. The average intensity, as defined above, is 2154 candlepower. The

candlepower distribution of this lamp is shown in figure 2.

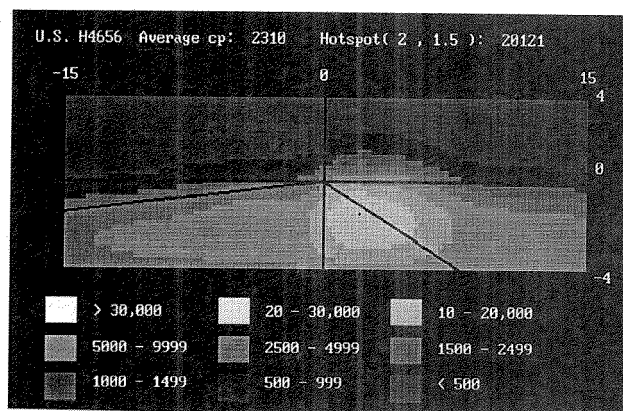


Figure 1. H4656 low beam.

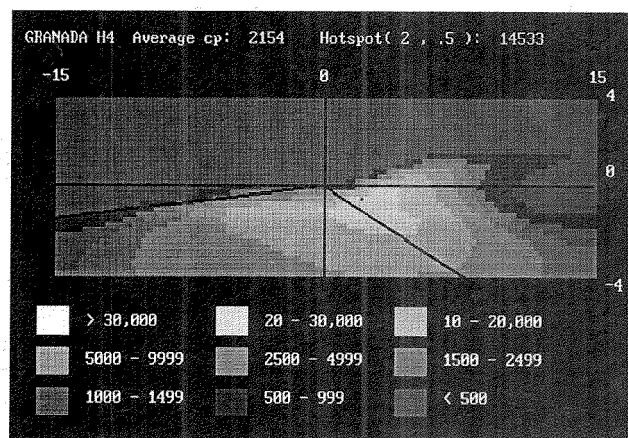


Figure 2. Granada H4 low beam.

The characteristic differences between U.S. and European low beams are evident in the figures. The European beam has a much sharper vertical candlepower gradient than the U.S. lamp, providing less candlepower above the horizon and more candlepower just below the horizon than the U.S. beam. Also, the European beam has a more uniform horizontal candlepower distribution than the U.S. beam and provides more illumination to the left of centerline. The U.S. beam, by contrast, concentrates more illumination in an intense spot that is aimed at the right edge line.

### Visibility Targets and Road Conditions

PCDETECT was exercised with the U.S. and European beam patterns for various visibility targets, locations and road conditions. The visibility targets studies were as follows:

#### Adult pedestrian

Pedestrian reflectance: 0.025 cd/lux/m<sup>2</sup>

Road surface (background) reflectance: 0.019 cd/lux/m<sup>2</sup>

Height: 1.77m  
 Road type: two-lane highway, 3.7m lanes  
 Location: six lateral locations from 3.7m left to 5.5m right of the road centerline (see figure 3)

Road surface reflectance: 0.019 cd/lux/m<sup>2</sup>  
 Length: 30m  
 Width: 10cm

**Traffic signs (element legibility)**

Element reflectance: 9.5 cd/lux/m<sup>2</sup>  
 Sign panel (background) reflectance: 1.9 cd/lux/m<sup>2</sup>  
 Element size (stroke width): 7.6cm  
 Road type: four-lane divided highway, 3.7m lanes, 2.4m median  
 Overhead sign location (center of sign): 5.9m high, centered over left edge of right lane (see figure 9).  
 Roadside sign location (center of sign): 2.7m high, 9.1m right of right edge of rightmost lane (see figure 9).

**Other baseline conditions**

Baseline conditions common to most of the runs were as follows:  
 Ambient luminance: .0003 cd/m<sup>2</sup>  
 Driver age: 35  
 Driver contrast sensitivity: 50th percentile  
 Glare car distance (when present): 91m  
 Road alignment: level and tangent, except as noted  
 Headlamp height: 0.61m  
 Headlamp separation: 1.22m

**Post-mounted delineator (PMD)**

Reflectance: 3.2 cd/lux/m<sup>2</sup>  
 Area: 100 cm<sup>2</sup>  
 Road type: two-lane highway, 3.7m lanes  
 Location 1.8m to the right of edge of rightmost lane  
 Height: 0.9m

**CHES Results**

Both beams were evaluated by CHES to develop an overall figure of merit for each. Results of the CHES runs are summarized in table 1. These runs were made with random misaim based on U.S. data (5). The CHES Figure of Merit scores are essentially identical for the two lamps. The U.S. lamp produced discomforting levels of glare slightly less often than the European lamp and were slightly better for detecting pavement delineation. The European lamp was slightly better for detecting pedestrians. On the basis of these overall scores, the performance of the two lamps is very similar.

**Pavement delineation (right edge line)**

Delineation reflectance: 0.025 cd/lux/m<sup>2</sup>

Table 1. Results of CHES exercises with United States and European low beams.

Beam Pattern	Overall Figure of Merit	Percentage of Encounters Meeting Visibility Criteria				Opposing Drivers Discomforted
		Unopposed (Without Glare)		Opposed (With Glare <sup>a/</sup> )		
		Delineation	Pedestrians	Delineation	Pedestrians	
U.S.	65.2	88.3	37.7	87.2	28.1	4.0
European	65.1	87.6	39.2	86.7	29.5	5.0

<sup>a/</sup>(glare is from identical beam pattern)

**PCDETECT Results**

**Pedestrians**

*Effect of Pedestrian Location*—PCDETECT results for the pedestrian are summarized in figures 3 to 6. Figure 3 shows seeing distance to the pedestrian as a function their lateral location on the roadway for the U.S. and European low beams with and without glare from corresponding lamps (i.e., from lamps that are the same as the observer's lamps). The pedestrian locations range from the leftmost edge of the left (opposing lane) to a point 1.8m off the roadway to the right.

Going from right to left, the seeing distances ranged from about 125m to 75m for both lamps in the absence of glare. The seeing distances were slightly greater for the U.S. beam for pedestrians located to the right of the centerline and slightly longer with the European beam for pedestrians to the left of centerline.

In the presence of glare from a corresponding lamp, the European lamp produced somewhat longer seeing distances than the U.S. lamp at all lateral locations. The differences ranged from 5m to 15m. Note the ""dip"" in the seeing distances for pedestrians located on the centerline. This occurs because at this location, the pedestrian is close to the driver's line-of-sight to the opposing lamps and glare is at a maximum.

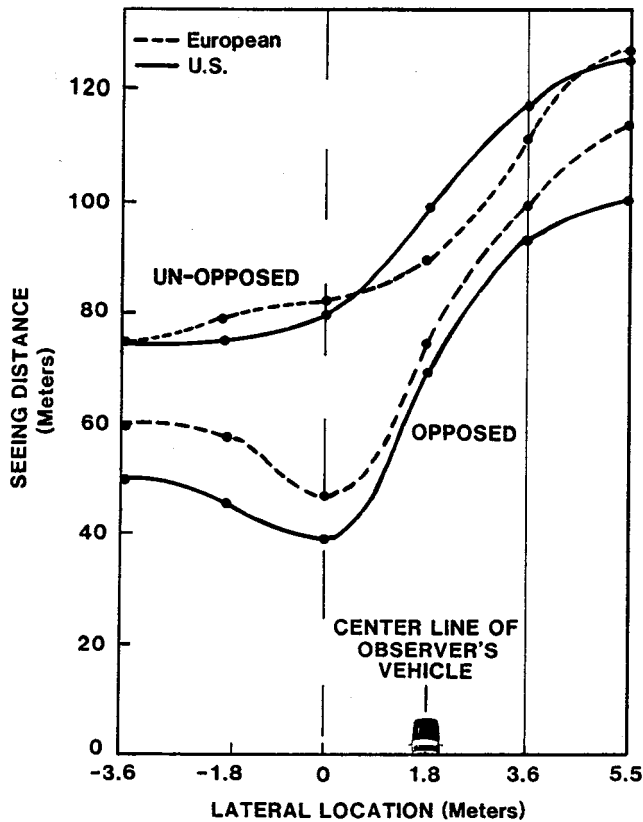


Figure 3. Seeing distance to pedestrian with U.S. and European low beams with and without glare from same beam.

These results are consistent with the differences between the beams described above.

*Mixing United States and European beams*—One of the concerns expressed regarding the mixing of U.S. and European beams under U.S. conditions is that the driver of the vehicle with the European beams would be at a relative disadvantage in meeting situations with U.S. beams because of the higher glare levels of the U.S. beams and the lower peak candlepower of the European beam. Figure 4 shows seeing distances for the U.S. and European beams, each against glare from the other lamp. Under these conditions, the two lamps gave very similar results: the U.S. beam gives slightly longer seeing distances (5 to 10m) than the European lamp for pedestrians to the right of centerline, while for pedestrians further to the left the results were almost identical.

*Headlamp misaim*—Figure 5 compares seeing distances for U.S. and European lamps with and without glare from corresponding lamps under 'worst case' misaim conditions. Under this condition, the observer car lamps were misaimed 1-degree down and the glare lamps were aimed 1-degree up. Based on headlamp misaim distributions in the U.S., this or a worse misaim condition would occur in about 2.5% of encounters. In the no-glare case, seeing distances were much less than with properly aimed lamps for both beams. However, the European beam provided seeing distances that were substantially (25% to 50%) lower than the U.S. beam. Under glare, the seeing distances were further diminished, with the European lamp

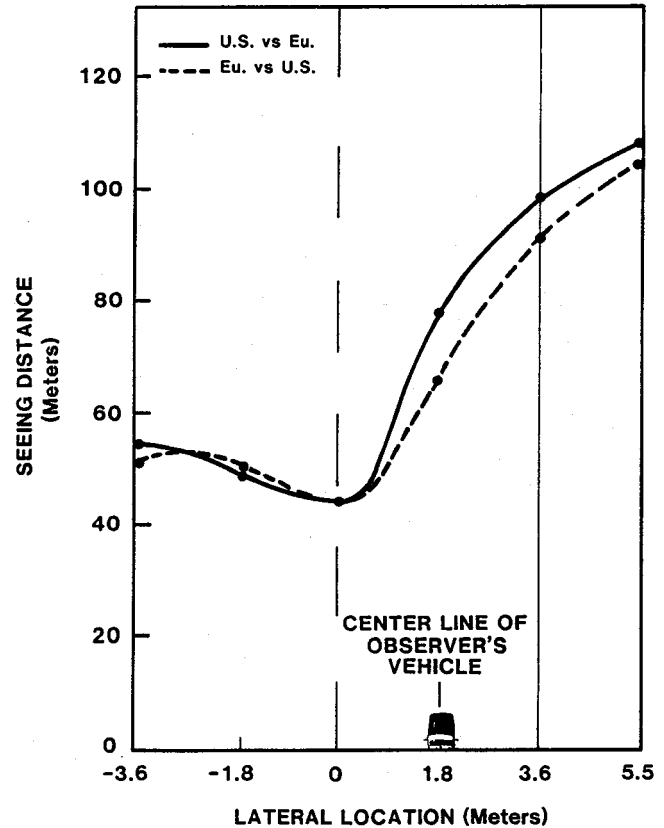


Figure 4. Seeing distance to pedestrian for U.S. and European low beams with glare from opposite beam.

yielding seeing distances as much as 40% less than the U.S. beam.

*Horizontal curves*—Figure 6 shows seeing distances to pedestrians on mild right- and left-hand curves (radius = 1745m). On both curves, the European beam produced consistently longer seeing distances than the U.S. lamp. It is clear that the European lamp, with its horizontally spread-out pattern, is less sensitive to mild curvature than the U.S. beam.

### Delineators on vertical curves

Because of the steep candlepower gradient of European beams close to the horizontal, they can be expected to perform somewhat differently than U.S. beams on both crest and sag vertical curves (i.e., hill tops and valleys). Figure 7 depicts a 400 meter crest vertical curve connecting opposite 3% slopes. The included table gives seeing distances and DeBoer discomfort glare values for the U.S. and European beams for both the vertical curve and a straight road. The design speed for this vertical curve and the sag curve discussed is 90 kph. The target was a 100 cm<sup>2</sup>, 1m-high post-mounted delineator having a reflectance of 3.2 cd/lux/m<sup>2</sup>, and located 2m off the roadway to the right.

On a level road there was no difference in seeing distance between the two beams, but the U.S. lamp produced somewhat more discomfort glare. On the vertical curve, the European lamp gave 8% longer seeing distances and almost as much discomfort glare as the U.S. beam. The European

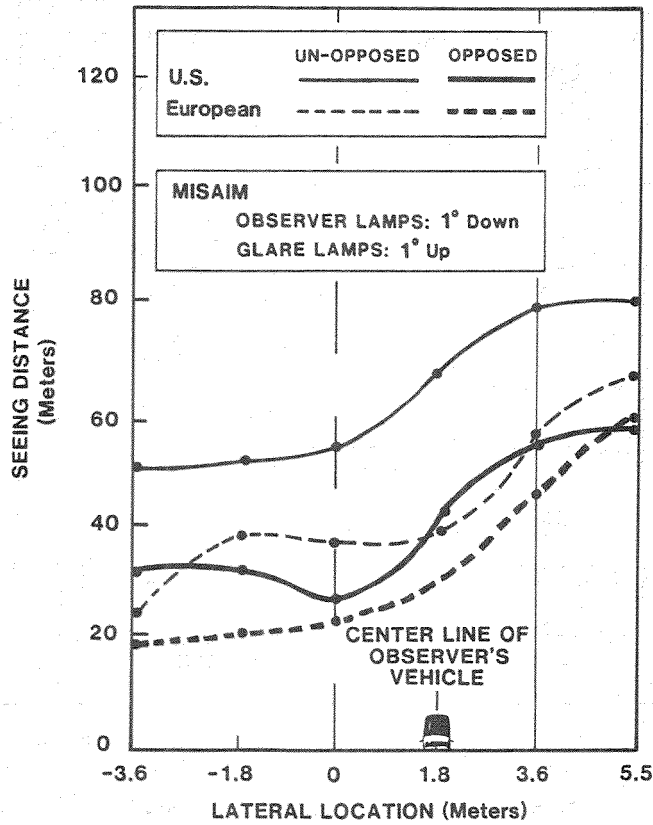


Figure 5. Seeing distance to a pedestrian with misaimed U.S. and European low beams with and without glare from corresponding beam.

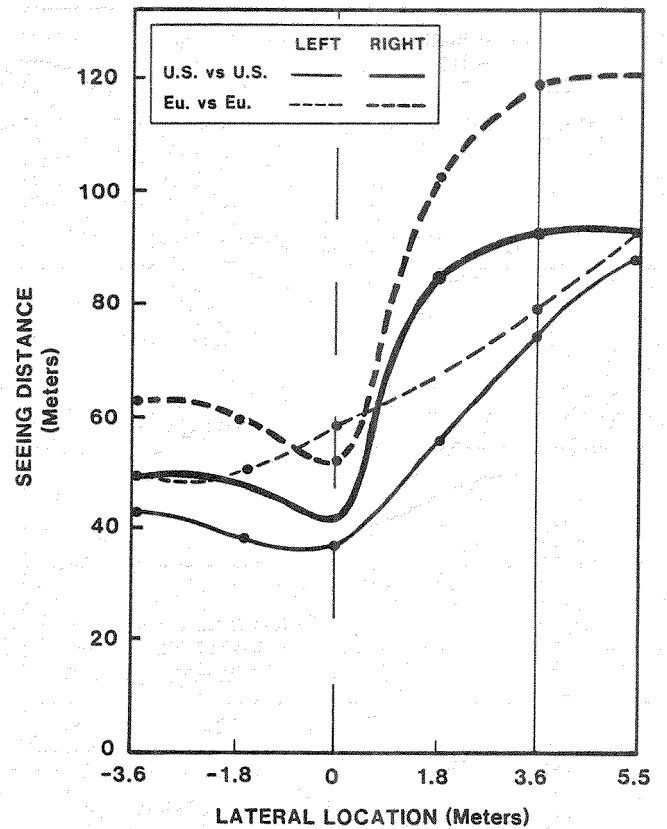


Figure 6. Seeing distance to a pedestrian with U.S. and European low beams on 1745m radius left and right curves with glare from corresponding beam.

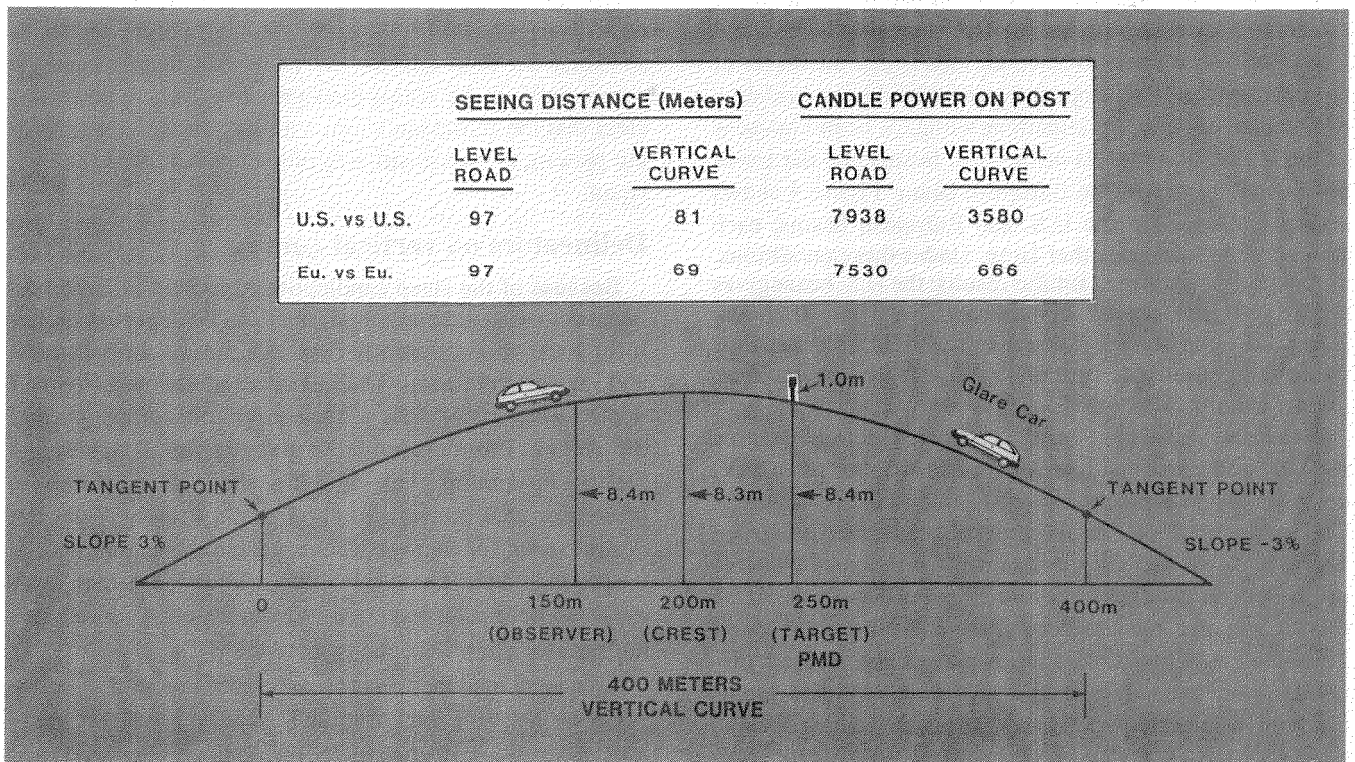


Figure 7. Seeing distance to a post mounted delineator and discomfort glare level on a 400 meter crest vertical glare with U.S. and European low beams.

beam was certainly not at any disadvantage under these conditions.

Figure 8 depicts a 244m sag vertical curve, also connecting 3% slopes. Seeing distances to the post-delineator target are given for the vertical curve and straight road for the U.S. and European beam. No glare was introduced because with this geometry, glare effects are nil for properly aimed lamps. Both lamps gave shorter seeing distances on the sag

curve. However, the decrease was greater for the European lamp (29%) than for the U.S. lamp (16%). Also shown on the figure are the incident on-target candlepower totals produced by the two lamps. On a level road, there was little difference between the two lamps; however, on the sag curve, the European beam produced only a fraction (less than 20%) of the candlepower produced by the U.S. lamp. This is because under these conditions, the target was above the cutoff line of the European beam.

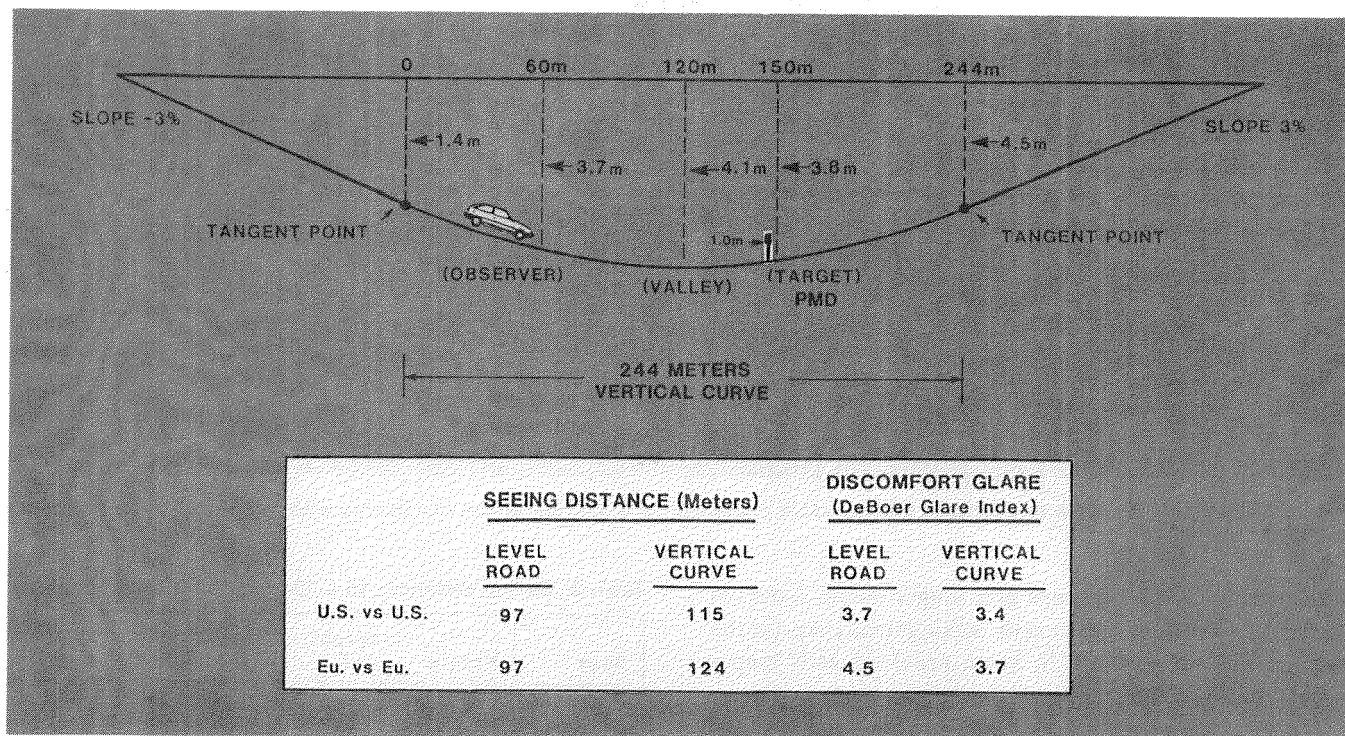


Figure 8. Seeing distance to a post-mounted delineator on a 244m sag vertical curve with U.S. and European low beams.

### Traffic signs

Because of the sharp cutoff of the European beam, it would not be expected to perform as well as the U.S. beam in illuminating unlighted overhead guide signs, which are common on U.S. Interstate Highways and freeways. Figure 9 shows a ground-level view of a four-lane divided roadway with an overhead sign and a roadside sign. Glare is from a platoon of three opposing vehicles in the inside lane, a reasonable worst case condition. Visibility and illumination data are given in the incorporated tables. The legibility distances given in the figure represent the distance at which the sign lettering first becomes readable.

The results are consistent with the differences in the beam pattern. The U.S. low beam put more than twice the candlepower on the overhead sign than the European beam and provided 23% longer legibility distance against glare from corresponding lamps. In the case where the European lamp is opposed by glare from U.S. lamps the difference was 29%. The U.S. lamp also provided better illumination and visibility distances to the road side sign.

### Pavement delineation

A series of PCDETECT exercises were carried out to calculate seeing distances to a pavement delineation target—a painted right edge line. The runs were made with the U.S. and European lamps under four geometric conditions: straight road, left and right curves of 872m radius and the 244m sag vertical curve described earlier. All of these conditions were run with and without glare from the corresponding lamp, and with and without misaim. The misaim condition was the same as used in earlier exercises: observer lamps aimed one degree down, glare lamps aimed one degree up.

The results are summarized in table 2.

*No misaim*—On a straight road and with correctly aimed lamps, the U.S. and European beams yielded identical seeing distances. On the left and right hand curves, the European beam gave longer seeing distances than the U.S. beam by 15% and 12%, respectively. The difference is of more significance for the left curve than for the right curve because in the latter case, both beams give ample seeing

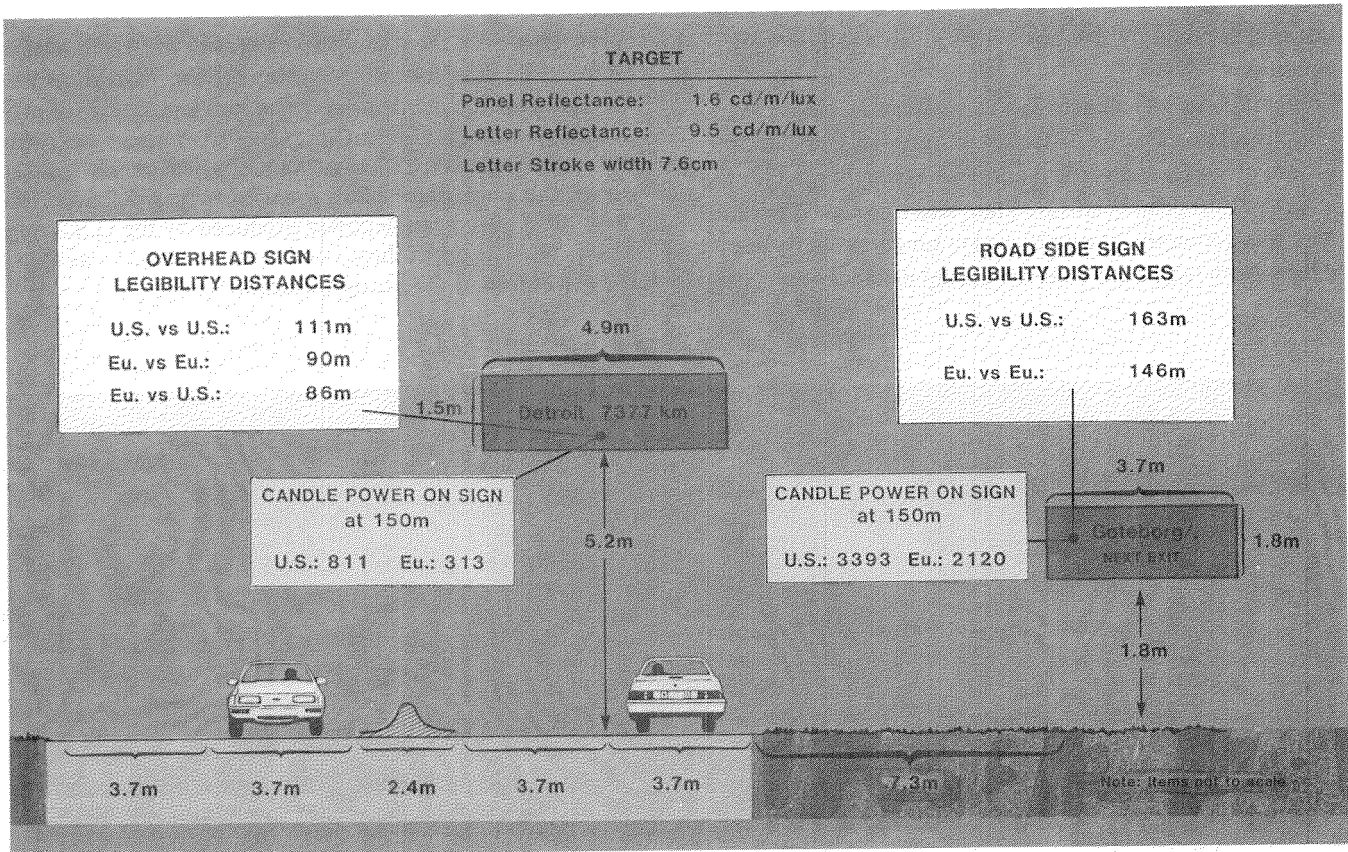


Figure 9. Legibility distance to overhead and roadside signs with U.S. and European low beams with glare from three opposing vehicles.

distances. In fact, both lamps give longer seeing distances on the right hand curve than in the straight road case. On the sag vertical curve, the U.S. beam provided 26% longer seeing distances than the European beam.

*With misaim*—Both beams produced considerably shorter seeing distances to the edge line under the worst case glare conditions studied. However, the European low beam was much more sensitive to misaim than the U.S. low beam. On the straight road, the seeing distance was 37% longer with the U.S. beam. On the left curve and the sag vertical curve the U.S. lamp resulted in seeing distances that were, respectively, 17% and 38% longer than the European beam. On the right curve, the European beam gave 16% longer seeing distance. Again it needs to be pointed out that this difference is of less significance than the differences observed under other conditions because the seeing distances on the right curve are, in any case, relatively long.

### Summary and Conclusions

On level roads and in mild horizontal curves, a correctly aimed European low beam performed as well or better than U.S. beams for targets on or near the road surface. In particular, because of the horizontal spread of candlepower, the European lamp produced longer seeing distances to pedestrians to the left of the (two-lane) roadway centerline. Mixing correctly aimed U.S. and European low beams in traffic does not appear to cause a problem. In situations

Table 2. Seeing distances to a 30-meter long right edge line.

Beam	Misaim	Straight Road	Curve Left	Curve Right	Vertical Sag
U.S.	No	125m	94m	152m	101m
European	No	125	108	171	80
U.S.	Yes	78	74	111	72
European	Yes	57	63	129	52

where vehicles with correctly aimed U.S. and European low beams were each exposed to glare from each other, the performance of the two systems was nearly identical.

However, there are conditions under which the European low beam, because of its steep vertical candlepower gradient, is at a disadvantage compared to the U.S. beam. First, the European lamp, with its sharp cutoff of candlepower above the horizon, provides substantially less illumination of overhead traffic signs, than the U.S. beam, resulting in shorter legibility distances.

Second, the European lamp is generally much more sensitive to misaim than U.S. lamps. Under the reasonable worst case misaim conditions used in this research, the European lamp provided significantly lower seeing distances to pedestrians and pavement lines than the U.S. beam.

Finally, on sag vertical curves (valleys), targets that lie beyond the point where the cutoff line is intercepted by the

roadway are not as well illuminated by the European lamp. The result in this study was that seeing distances to delineation elements was substantially less with the European beam.

Based on these findings it would appear that in order for the European type low beam to be suitable for the U.S. conditions it would be necessary to (1) control misaim more closely than is necessary with U.S. low beams and (2) provide more intensity above the horizon line to better illuminate overhead signs.

## References

(1) V. Bhise, et. al., Modeling Vision with Headlights in a Systems Context, Society of Automotive Engineers, SAE 770238, 1977.

(2) E. Farber and C. Matle, PCDETECT: A Revised Version of the DETECT Seeing Distance Model. Transportation Research Board—68th Annual Meeting, 1989—Paper No. 880547.

(3) V. Bhise, E. Farber and P. MacMahan, Predicting Target Detection Distance with Headlights, Transportation Research Record 611, Transportation Research Board, National Academy of Sciences, 1976.

(4) Commission Internationale De L'Eclairage, An analytical model for describing the influence of lighting parameters upon visual performance, Publication CIE No 19/2.1, 1981.

(5) P. Olson, A survey on the Condition of Lighting Equipment on Vehicles in the United States, Society of Automotive Engineers, Inc., SAE 850229, March 1985.

## Vehicle Conspicuity

**Kåre Rumar**

Swedish Road and Traffic Research Institute

### Abstract

Collisions between road users are the most serious and frequent road traffic accidents. When trying to look deeper into the question why a collision really happened a frequent and true answer is that the other road user was not detected until too late. Certainly accidents may happen in spite of detection, e.g. due to misjudgement of speed and/or distance. But early detection is a necessary condition for safe road traffic.

For most road users the most dangerous vehicle in road traffic is the automobile (the truck, the bus, the passenger car). Therefore, the most important conspicuity is that of the automobile. It is true that the highest risk is that for the motorcycle. But even if the risk is high the accident frequency and the risk for others are low.

Vehicle conspicuity can be obtained at least four ways:

- Contrast (brightness, colour)
- Motion (against background or internal)
- Size (angular)
- Information technology (radar, microwaves, infrared, ultrasound, etc)

For several reasons internal motion and angular size are not workable variables. Information technology is probably the solution of the future—but not today. Contrast can be obtained by choice of colour. But the effects in some situations are not too good. Another way is the use of lights on the vehicle. Specially in levels of lower ambient illumination lights on vehicles (DRL: Daytime Running Lights) call attention in the periphery of the visual field—detection!

In Sweden, Finland, and Norway DRL has been successfully tried as a conspicuity enhancing and accident

reducing measure. In Canada, the Netherlands, and Austria the question of compulsory DRL is close to a solution. An account will be made of the advantages and problems with DRL.

### Introduction

According to official statistics (UN 1986) collisions between road users constitute about two-thirds of all road accidents in many countries. These accidents cause heavy economic losses and human suffering. A very common explanation for most accidents is of the type "I did not see . . . , I detected too late . . . , Suddenly he was there . . . ". Increased vehicle conspicuity is really one of the primary problems in road safety work.

Another support for treating vehicle conspicuity as one of the main road safety problems is found in the results from the accident-in-depth studies carried out in road traffic. The two largest and best controlled studies known (Sabey & Staughton 1975; Treat 1980) are unanimous in pointing out the human error as the main contributing factor (60–90%). Recognition errors dominate and typical errors mentioned are (ranked):

1. Improper lookout
2. Excessive speed
3. Inattention
4. False assumption
5. Improper manoeuvre
6. Internal distraction

At least (1), (3), (6) could be classified as being closely related to vehicle conspicuity, to detection of other road users.

In road safety work many efforts have been carried out and are still carried out to try to reduce these human errors by information, education, and training. But even if it is

possible to increase driver attention by such means it will never solve the problem because it is of a more basic perceptual nature.

## Conspicuity

Road traffic due to its speed has a built in inertia that requires driver action based on predictions. Otherwise the traffic would become very jerky. Predictions in turn require early detection. Otherwise there is no time for mental simulations of various possible outcomes.

By visibility in this context is meant the possibilities of road user to detect and identify the relevant objects and events in front of him. By conspicuity is meant the ability of a road user to make himself visible and conspicuous to other road users. Consequently visibility and conspicuity is the same problem from two sides.

Conspicuity and to some extent visibility contain a cognitive aspect. But in this paper only the main visual function is treated. The reasons are that the visual problems are more basic and have to be solved first, and that it is probably possible to compensate for deficiencies in the cognitive function (mainly expectancy based on experience and knowledge) by enhanced perceptual conspicuity.

The detection process may be split up into two categories: peripheral detection and central detection.

During the history of man we have been both hunted and hunters. In those two roles the detection of moving creatures (attacking or escaping) in the peripheral visual field was a matter of life and death. And according to Darwin what was important to survival soon became a characteristic feature of the species. Consequently motion is a key stimulus for human detection. We even have special receptors for various types of motion.

## Vehicle detection

However, in present road traffic the "attacking" vehicles are sneaking up on us at a very high speed, silently and without any inherent motion. Therefore this inherited talent of ours does not function for survival in traffic. We have to replace the historic motion by something that gives a corresponding peripheral conspicuity to motor vehicles.

Daylight detection of other vehicles in central vision where the resolution capacity and the contrast sensitivity is high is normally no problem. But in strong shadows and with dark backgrounds detection may be a problem even when we look straight at the vehicle—in central vision.

However, when another approaching vehicle appears where we do not expect it, we are not looking for it, and if we do not detect it in peripheral vision the situation might develop into a critical one. Consequently peripheral detection is considered the crucial visual function concerning detection of other unexpected approaching vehicles.

From a psychophysical point of view the detection of a visual target is determined by its

- contrast against background,
- angular size,
- motion.

Modern information technology applied in road traffic (RTI) may offer still other possibilities; radar, microwaves, infrared, ultrasound, etc.

We cannot change the size of vehicles (even if we from the conspicuity point of view would like e.g. the frontal area of motorcycles to be larger). Some efforts have been made to introduce motion on the front of vehicles, but designers do not like the idea. Information technology is probably a good solution in the future—but not today! Consequently what remains to manipulate is contrast.

## Contrast

Experiments to study the effect on conspicuity of the colour of the car against various backgrounds have been carried out (Dahlstedt & Rumar, 1973). The results show a marked effect of contrast. A colour which is good in one situation (e.g. black in winter) may be bad in another situation (e.g. forest road in summer). This is of course quite in line with all the laboratory studies that have been carried out (e.g. Blackwell, 1946). But the most interesting result was that with low beams all cars (irrespective of colour) reached the same conspicuity as the best colour for each background. Consequently some kind of daytime running lights (DRL) seem to be a possible way to improve vehicle detection.

The effect on detection of lights on motor vehicles is dependent on several variables such as ambient daylight illumination level, landscape and background reflectance factors, colours, etc. Ambient illumination primarily depends on the sun's altitude and the weather. The sun's altitude is a function of time of day and of latitude and season, while weather has a more complex background. The closer to the poles, the longer are the periods of low ambient illumination. In December the ambient illumination at noon is five times higher in Rome (40°N) than in Stockholm (60°N). Also the twilight periods are longer. But in the Swedish analyses of accident reduction after introduction of DRL no difference was found between good ambient illumination conditions and bad ambient illumination conditions. Landscape reflectance factor and colour is varying with snow, frost, rain, fog, vegetation, etc and angle of sun, shadows, etc. But also weather (overcast, rain, haze, etc) has influence. There are also daytime glare situations such as low opposing sun when DRL may have an important effect on vehicle conspicuity.

## Lights

Most studies of vehicle detection as a function of light intensity have been carried out in central (foveal) vision (e.g. Allen & Clark, 1964, King & Finch, 1969, Hörberg & Rumar, 1975, Attwood, 1981, SAE, 1984). The results from these studies indicate that in central vision on the one hand, even very low DRL intensities ( $\leq 100$  cd each) might increase vehicle conspicuity, but on the other hand quite high intensities ( $\leq 5000$  cd each) are even more effective and

create no problem. Now on this later point there is some disagreement. Hörberg & Rumar (1975) and Attwood (1981) argue that if DRL are to be accepted in dawn and dusk glare problems might occur and they suggest a maximum value of 1000–1500 cd for DRL in dawn and dusk.

Rumar, Hörberg and their co-workers have in several studies systematically investigated the peripheral conspicuity of oncoming vehicles as a function of vehicle lighting intensity and as a function of level of ambient illumination. The results from these studies indicate that in broad daylight ( $\geq 3000$  lx sky illumination) the intensity correspondent to an ordinary low beam (about 400 cd) is needed to improve vehicle conspicuity in  $30^\circ$  peripheral vision. In  $60^\circ$  peripheral vision more than 1000 cd is needed to increase vehicle conspicuity.

In another study using  $20^\circ$  peripheral vision it was shown that when the ambient illumination level decreases (dawn and dusk  $\leq 1000$  lx sky illumination) considerably lower intensities are needed to substantially increase peripheral vehicle conspicuity at 600 lx about 300 cd, at 400 lx about 200 cd.

Since 1984 the SAE Lighting Committee is carrying out special DRL-studies in connection with their meetings. In one study (April 1985) peripheral conditions were also investigated. Their results seem to favour higher values than those recommended by Hörberg & Rumar and by Attwood. Maximum intensities in the H–V point of about 5000 cd are discussed. It should be noted that their studies are normally carried out at higher levels of daylight illumination.

In general it is agreed that the maximum intensity of DRL should be in the horizontal plane and concentrated in the HV point (rural situations) or slightly to the left (in right hand traffic).

The light can also change over time either by flashes (as in emergency and maintenance vehicle warning lights) or by modulated light (changes between high and low levels of intensity).

Such means to improve vehicle conspicuity have been extensively and successfully used for emergency and maintenance vehicles. Here colour has been used to separate different categories of vehicles from each other. We know that especially peripheral vision is sensitive to this type of change of stimulation. There are several studies of emergency beacons but since flashing lights are reserved for special vehicle signals they are not suitable as DRL.

For normal road vehicles the idea of modulated light is applied on motorcycles. Proposals have been presented in several countries, e.g. USA, Australia (e.g. Tratner 1980, Jenkins & Wigan 1985).

### **Lights: colour and size**

As far as is known the only studies of the effect of colour and luminous area of DRL have been carried out by Hörberg & Rumar (1975) and SAE (1986).

On colour, their results indicate that in subjective evaluations observers say they find the yellow or amber DRL more

conspicuous than the white one. But in objective detection studies, colour (white and yellow) seems unimportant. What influences the results is light intensity, not colour of light. From the legislative point of view both colours could be accepted.

Concerning area, their results again indicate no difference between  $70$  cm<sup>2</sup> (special daytime running lights) and  $200$  cm<sup>2</sup> (headlights). Swedish and Norwegian standards and most studies with special daytime running lights use  $40$  cm<sup>2</sup> as the minimum area. But in Finland the minimum required area is  $70$  cm<sup>2</sup>.

### **Some positive effects except conspicuity**

DRL have many positive effects besides the main one, improved peripheral and central detection.

One is that an oncoming DRL-car is estimated to be closer than an unlighted car (Attwood, 1976).

Another is that it is easier to estimate the lateral position on the road of a DRL-car compared to an unlighted car (Attwood, 1976).

It is easy to identify an opposing DRL car as moving and not stationary. An unlighted car might be stationary or moving, it is hard to tell at long distances.

Those road users that probably benefit most from DRL are pedestrians and cyclists. Andersson & Nilsson (1981) have shown that the accident reduction for those groups as an effect of the compulsory DRL in Sweden 1977 is larger than that for motor vehicles (see table 1). These groups probably use their peripheral vision more than drivers. Furthermore these road user categories often have visual degradation which give a visual status that is lower than that of drivers.

### **Accident analysis**

Early studies in US and Sweden give positive results of DRL but are not well controlled. Later studies in Finland, Sweden, US, and Norway are however carried out as well as is possible considering that a fully experimental rotated design is not possible. They all support each other and present corresponding effects. A review of the evaluation studies is given in Helmers (1988).

Here we only present a Swedish representative study (Andersson & Nilsson 1981). They used single vehicle accidents and night-time accidents as controls, thereby balancing for irrelevant factors that may have varied during the before and after periods (DRL was made compulsory in Sweden 1977). Table 1 gives the results.

### **Some negative effects**

Some possible negative effects are often discussed. The most common ones are:

- No effect if everyone has them (the novelty effects disappear)
- Worse for those not having them (effect of expectation and masking)

**Table 1. The accident reduction of daytime collisions as an effect of introduction of DRL in Sweden 1977.**

	DAY	NIGHT
Single Acc Collisions	Control - 13 %	Control
Subgroups		
{ Head on		- 10 %
{ Angular		- 9 %
{ Rear end		- 2 %
{ Car-bicycle		- 17 %
{ Car-pedestrian		- 21 %

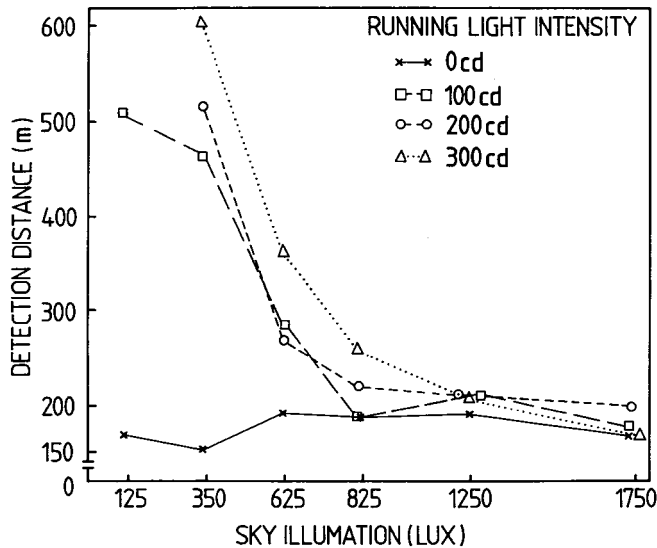


**Figure 1. Peripheral (20°) detection distance (m) of oncoming vehicles as a function of sky illumination (lux) and DRL intensity (cd).**

- Glare in dawn and dusk periods (masking effects)
- Masking of signal lights such as direction indicators and brake lights (if rear position lights go on at the same time)
- Increased petrol and bulb consumption (economy)
- Auxiliary DRL quickly lose their efficiency due to dirt, corrosion, bad aiming, etc (durability)

The following comments can be made on these arguments:

- The daytime running lights as a whole are no doubt more effective for the larger proportion that have them. Results vary from 10–30% reduction of daylight collisions but they are all clearly positive.
- Those few that are not using DRL when most vehicles have them will in certain cases be in a worse position than previously. But this is rather an argument for and not against compulsory DRL and must be considered against the total reduction of accidents obtained.
- Glare in dark dawn and dusk periods might occur with DRL over about 100 cd (Attwood, 1979). But

either we accept an upper limit for DRL at or above 1000 cd or we prohibit the use of DRL in dawn and dusk and prescribe ordinary low beam during these periods.

- Masking or rear signal lights such as brake lights does not seem to constitute any problem (Färber et al, 1976). Masking of front direction indicators might be a problem with very high (>5000 cd) DRL intensities (SAE 1986). At longer distances these problems may appear already at a DRL-intensity of 1000 cd if they are mounted too close to the direction indicators. Again if we prohibit the use of DRL during dawn and dusk there is little need for having position lights on.
- Petrol consumption is naturally increased by DRL. Estimates and empirical studies concerning the size of this effect vary. USDOT (1981) calculated the cost increase of DRL to be 2–3 per cent. But there seems to be a fair agreement that the increase is of the order of less than one per cent (Rumar 1981, Transport Canada 1985). Also bulb replacement needs will be increased by DRL.
- The bad experiences in Sweden with separate auxiliary DRL (dirt, corrosion, etc) indicate the advantage of integrating the DRL in the car construction, as a part of the standard light equipment.

## DRL: legislation and trends

Present legislation concerning DRL mainly concerns motorcycles (Australia, France, Canada, several states in USA, Denmark and some others) and only specifies conventional low beam (300–625 cd in HV in Europe) except for USA where modulated low beam is accepted.

Finland and Sweden have laws on compulsory DRL for motor vehicles with special lights although low beam is permitted in both countries. (In Sweden even reduced low beam.) Sweden specifies 300–800 cd at HV while the Finnish standard specifies 600–1200 cd at HV. Norway and Canada have introduced DRL-laws for new vehicles. (In Norway valid from January 1, 1985 in Canada valid from December 1, 1989.)

Sweden and Finland are trying to reach an international (ECE) agreement on the illumination requirement for DRL.

Presently discussions and studies are carried out in the Netherlands and in Austria with the intention to investigate the feasibility of a DRL legislation.

## Conclusion

The basic assumptions behind DRL are:

1. That they increase vehicle conspicuity/detectability.
2. That increased vehicle conspicuity decreases the risk user collisions.

The studies carried out support both hypothesis. Furthermore, the introduction of DRL seems to be very efficient also from cost benefit point of view.

## References

Allen, M J and Clark J R. Automobile running lights—a research report. *Am J Optometry and Archives Am Acad Optometry* 41(5), May 1964.

Andersson, K and Nilsson, G. The effects on accidents of compulsory use of running light driving daylight in Sweden. VTI, Report 208A, 1981.

Attwood, D A. Daytime Running-Lights Project IV: Two-lane passing performance as a function of headlight intensity and ambient illumination. Canadian Ministry of Transport, Road Safety Unit Rep RSU 76/1, Toronto, Canada, 1976.

Attwood, D A. The effects of headlight glare on vehicle detection at dusk and dawn. *Human Factors* 21(1), 35–45, 1979.

Attwood, D A. The potential of daytime running lights as a vehicle collision countermeasure. SAE Technical Paper No 810190, 1981.

Blackwell, H R. Contrast thresholds of the human eye. *J Opt Soc Am* 36, 624, 1946.

Dahlstedt, S and Rumar, K. Vehicle colour and front conspicuity in some simulated rural traffic situations. Department of Psychology, University of Uppsala, Sweden, 1973.

Färber, B et al. Brake Lights—Daylight Detectability with and without Lighted Tail-Lights. Unpublished report from Dept of Psychol, Univ of Uppsala, Sweden, 1976.

Helmers, G. Daytime Running Lights—A potent traffic safety measure? VTI Report 3331 VTI, Linköping, Sweden, 1988.

Hörberg, U and Rumar K. Running lights—conspicuity and glare. Rep 178. Department of Psychology, University of Uppsala, Sweden, 1975.

Jenkins, S E & Wigan, M R. The applicability of a motorcycle headlamp modulator as a device for enhancing daytime conspicuity. *Transportation Research Record* 1985 (in press).

King, L E and Finch, D M. Daytime running lights. *Highway Res Rec* No 275, 1969.

Rumar, K. Daylight running lights in Sweden—pre-studies and experiences. SAE Technical Paper No 810191, 1981.

Sabey, B E and Staughton, G C. Interacting roles of road environment, vehicle, and road user in accidents. 5th International Conference of the International Association for Accident and Traffic Medicine, London, 1975.

SAE (Society of Automotive Engineers, USA) Lighting Committee. DRL tests 1984.

SAE Committee. DRL tests 1986.

Transport Canada. A Study of Daytime Running Lights. Transport Canada, Road Safety and Motor Vehicle Directorate, Ottawa, Canada. TP 67 16 E, 1985.

Tratner, A A. Review of options currently available and suggestions for future research directions for increasing motorcycle conspicuity. Proceedings, International Motorcycle Conference 1980, 1085–1105, Motorcycle Safety Foundation, Linthicum, Maryland, USA.

Treat, J R. A study of precrash factors involved in traffic accidents. Highway Safety Research Institute (HSRI). HSRI 10/11, 6/1. Ann Arbor, Michigan, 1980.

U N. Road Accident Statistics 1986.

U S Department of Transportation. A Cost/Benefit Study of a Potential Automotive Safety Program on Daylight Running Lights. DOT-HS-805 888. 1981.

## Why the Windshield Should Be Included in Motor Vehicle Inspection (§ 29 St. VZO = Motor Vehicle Approval and Traffic Registration)

Walter Schneider,  
Auto-Sicht-Sicherheit, Cologne,  
Federal Republic of Germany

### Abstract

Windshields are subject to wear and tear which leads to stray light values which, according to legal court demands, engender unusually slow speed limits. They disregard reality.

Windshields must be considered as a wear and tear part insofar as their condition as regards traffic safety is variable and unreliably predictable so that a periodical inspection within the meaning of § 29 of the Motor Vehicle Approval and Traffic Registration Code (=StVZO) is necessary for the preservation of traffic safety.

### Establishment of Standards for Authorized Windshields

The legislative body has provided protection against the consequences of production-caused faults in optical media used in vehicles by the establishment of § 40 StVZO (=Motor Vehicle Approval and Traffic Registration Code), para. 1, clause 3: "Windshields made of safety glass which are significant for the vision of the vehicle driver must be clear, transparent and free of distortions." The necessary transmission degree is to be measured by vertical radiation course, in accordance with the technical guidelines for inspection under this regulation of § 40 StVZO (=Motor Vehicle Approval and Traffic Registration Code).

Since, however, the transmission degree decreases with the inclination of the windshield, it is then high time that, in

view of windshields inclined at 60°, the regulation as regards inspection of the necessary degree of transmission be reviewed; then the retardation of recognition of obstacles on the street under the influence of inclined windshields is a long known fact which I would like to recall here by reference to figure 1.

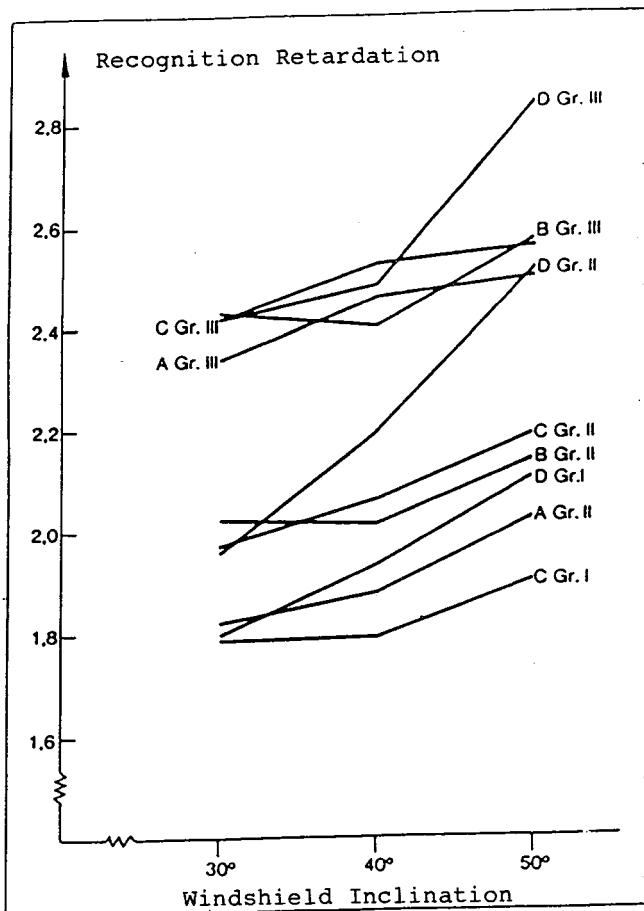


Figure 1. Recognition retardation by various windshields and various groups of test persons in relation to inclination of the windshield (excerpted from Schneider 1976, 350).

At that time, experiments were made with inclinations only up to 50°. On the other hand, the time—by darkness—up to recognition of an obstacle in one's own low beam light before the observer on the street by oncoming light was also differentiated between young and older test persons and people who wear glasses. Then, times up to recognition of obstacles with an average up to 2,8 seconds were measured.

## The Significance of Recognition Retardation by Stray Light

The experimental measuring procedure for the establishment of time up to the recognition of obstacles was continuously used and may, in view of this, be considered as the standard. By field tests, as used many times particularly by the Swedish Traffic Research Institute "VTI" for research into vision by night, the shortening of the available brake distance can then be realistically ascertained. "Recognition distances of obstacles on the street as seen

through windshields in various degrees of wear" was also the theme of a test in Sweden executed by Helmers and Lundquist whose results were published at the end of 1988 (VTI-Rapport 339a).

Experiments were made in Sweden among other things with a windshield whose share of stray light lay by 3,04 cd/lux×m<sup>2</sup>. The reduction of the recognition visual range by this stray light value amounts to approximately 15% as compared with free vision.

## Distribution of Stray Light Values in the Vehicle Inventory

Are stray light values of this sort to be found in practice? A glance at the stray light data of 896 vehicles which were tested in a very differentiated manner in the area of Cologne may help to answer this question. The results of this study will be presented in detail by H. Derkum at the conference "VISION IN VEHICLES" in Aachen. His measurements, made with the stray light analyzer of A. Timmermann, included 6 measurements each of stray light (at first in a soiled condition) in the main area of vision. The distribution of the mean values of this measurement is reflected in figure 2. 12% of the measured vehicles have a stray light value of over 3 cd/lux×m<sup>2</sup>.

This value of 3 cd/lux×m<sup>2</sup> by a safety helmet visor was, following an accident, object of legal assessment in view of the existing authorized speed. The Regional Court of Appeal in Hamm (Federal Republic of Germany) established that the driver was allowed to drive not faster than 30 km/h due to the limited visibility caused by stray light (written decision attached).

Since one may hardly expect, however, that such a legal judgement can attain a decisive behavioral strength, the possibility of solving the problem of limited visibility lies rather in the replacement of this kind of obstructive optical media.

Returning to the data from H. Derkum: Further, he tested the cleaned windshields. By half of the windshields only the inside resp. the outside was cleaned at the outset. As may be seen in figure 2 there is a stray light index of over 3 cd/lux × m<sup>2</sup> by approximately 7% of the vehicles when only the outside of the windshield is cleaned.

By completely cleaned windshields there remains finally 0,4% of the vehicles with a stray light index of over 3 cd/lux × m<sup>2</sup> (figure 3).

## Distribution of stray light values by cleaned windshields

One may well say, as regards the results of this test: It appears that the limited visibility caused by stray light is for the most part a problem that can be easily solved through education. How does one motivate and convince drivers that for their own safety it is necessary to clean the windshields regularly, particularly on the inside? An answer to this question will not be attempted here, instead it is to be passed on to the people of the media.

Comparison  
soiled, exterior resp. interior cleaned

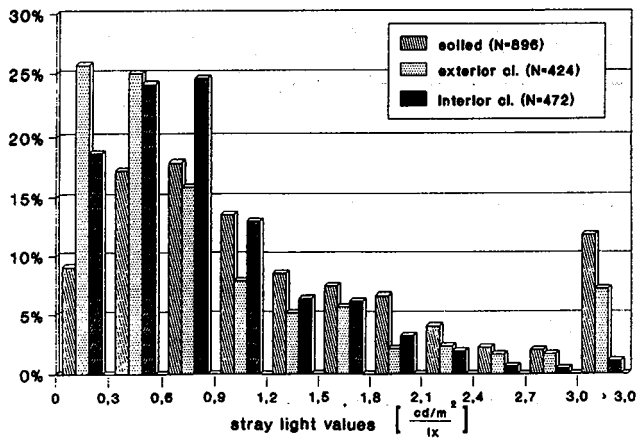


Figure 2. Stray light values (Average of 6 measurements each, random sample of passenger vehicles from the Cologne area—N 896), H. Derkum (1989).

Distribution of Stray Light Values  
by cleaned windshields

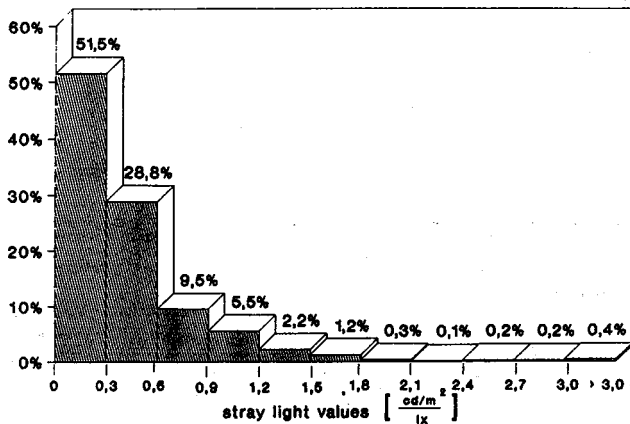


Figure 3. Stray light values (Average from 6 measurements each vehicle) from 896 passenger vehicles in the Cologne area (Derkum 1989).

## Is the Demand for the Replacement of Worn Windshields Reasonable?

Should the demand of the Regional Court of Appeal in Hamm (which was made on the motorcycle driver), that in view of the worn safety helmet visor he should drive not faster than 30 km/h in darkness, be transferred to drivers of passenger vehicles who have similarly bad windshields on their vehicles, one would surely share my decided expectation that this demand will not be met. For the owner of a vehicle with such a worn windshield there remains then only the alternative of replacing it. Who then is to bring the driver to do this? In view of the regularly recurring "Inspection of Motor Vehicles and Trailers" in accordance with § 29 of StVZO (=Motor Vehicle Approval and Traffic Registration Code) this question may take on concrete form. The so-called worn parts receive particular attention in § 30 StVZO (=Motor Vehicle Approval and Traffic Registration Code). Until now it has not been the norm to treat the

windshields as a part of the vehicle which wears. The facts, particularly the measurements of Derkum, teach us better. In this respect, it remains open as to whether a far lower stray light index as the one mentioned in the decision of the Regional Court of Appeal in Hamm should lead to replacement of the windshield. It is still a great difference between the demanded highest speed of 30 km/h and the usually driven speed by low beam light. The question as regards which threshold value should lead to the refusal of a test sticker by the inspection in accordance with § 29 StVZO (=Motor Vehicle Approval and Traffic Registration Code) should remain open here. Only the question as to whether the possibility now exists for the motor vehicle specialist to refuse a test sticker is to be more closely examined here.

## Legal Basis for Inspection of Windshields and Judging According to Administrative Law

The legal situation appears to me—in particular after being informed by experienced administrative lawyers—to be as follows:

In order to consider motor vehicle windshields as a part which wears in legal assessment, § 30, para. 3 of StVZO (=Motor Vehicle Approval and Traffic Registration Code) is to be observed. This stipulation reads:

"For traffic and operational safety, important motor vehicle parts, which in particular can wear easily or be easily damaged, must be so constructed that they may be easily (simply) inspected and replaced."

This version exists since 1973. The explanation for its introduction states:

"The new version of para. 3 emphasizes the currently recognized principle that, in particular by technical inspection in accordance with § 29 (StVZO = Motor Vehicle Approval and Traffic Registration Code), it is necessary that the named vehicle parts may be inspected without fundamental loss of time."

As regards the windshields, this possibility exists only since measuring facilities resp. evaluation methods exist which are also capable of evaluating installed windshields. This possibility now exists, on the one hand, with the measuring instrument of A. Timmermann and, on the other, with a photographic procedure for which an atlas with comparative examples of exact measured windshields is at the present time in preparation.

What then is the stand of legal clarity as regards the wording of the regulation in § 30 StVZO (=Motor Vehicle Approval and Traffic Registration Code) as well as its substantiation.

The person who applies this regulation is, according to a questioned administrative lawyer, well advised when he, due to failing explicit directions, attempts to ascertain from the tenor of the wording those cases in which § 30, para. 3 StVZO (=Motor Vehicle Approval and Traffic Registration Code) was applied in administrative practice and in which manner. It could, however, only be established that below

the ordinance level no binding definition for “easily worn” (“wear easily”), “easily inspected” and “easily replaced” in connection with § 30, StVZO (=Motor Vehicle Approval and Traffic Registration Code), and insofar generally valid, may be found.

When, nevertheless, the criteria of § 30, para. 3, StVZO (=Motor Vehicle Approval and Traffic Registration Code) are brought into connection with the subject of windshields as parts which easily wear, an interesting legal comparison of required and existing criteria will then be possible by way of the concept technical stand. Due to failing absolute standards for “simply” and “easily” one must limit oneself to approximate comparisons.

For the legal examination which is to be made it is practical to classify the regulated criteria, i.e. criteria for windshields which are defined by the regulations, into two groups. The first group includes those criteria which are described by the paragraphs 22a (approved construction details for vehicle parts) and 40 (windshields and windshield wipers) of the StVZO (=Motor Vehicle Approval and Traffic Regulation Code) as well as the TA Nr. 29 or the equally valid requirement of the ECE-Regulation Nr. 43. § 22a, para. 1 reads:

“The installments listed hereafter, irrespective of whether they are used on vehicles which require registration or those which require no registration, must be produced in an officially approved design: . . . 3. glass plates made of safety glass (§ 40).”

§ 40, para. 1 of StVZO (=Motor Vehicle Approval and Traffic Registration Code) reads:

“All glass plates—excepting mirrors as well as covering plates for lighting equipment and instruments—must be made of safety glass. Glass or material similar to glass whose broken pieces cause no serious injury is considered to be safety glass. Plates made of safety glass which is of significance for the vehicle driver must be clear, transparent, and free of obstructions.”

The criteria of group 1 need no particular interpretation as regards wear and tear. Some of these criteria are those with which changes during the operational time of the plate, the wear and tear relevant to traffic safety are to be shown on which the final decision is based to replace the glass plate with a safer one.

The criteria classified in the second group are those from § 30, para. 3 StVZO (=Motor Vehicle Approval and Traffic Registration Code) which are to be developed. These criteria are to be described so that they correspond with the technical stand, which is determined particularly by the criteria of the first group and at the same time are comparable to the indefinite legal terms of § 30, para. 3 StVZO (=Motor Vehicle Approval and Traffic Registration Code) and suitable for making these concrete.

§ 30, para. 3 StVZO (=Motor Vehicle Approval and Traffic Registration Code) deals with important vehicle parts for traffic or operational safety. Presumably it is indisputable

that windshields belong to these parts, as may be described through the connection of 6 of the Traffic Law (=StVG), paragraphs 22a, 40 StVZO (=Motor Vehicle Approval and Traffic Registration Code).

From the comparison of new windshields with those in use in traffic one recognizes which criteria are subject to change. Here in particular is the stability against outside influences of interest. One of the criterion from the first group belonging to stability against outside influences is defined, based on regulations for abrasion testing (ECE-R 43, para. 8.1.3, Appendix 3, para. 4, Appendix 6, para. 5.1.3, appendix 9, para 2.3), as a measurable factor, namely light scattering. Exactly this, however, has now become assessable with currently available measuring and evaluation instruments. Interesting in this connection is the opinion of an administrative lawyer which may be summarized as follows:

As increasing portions of stray light influence traffic safety, an approved upper limit was added to light scattering in windshields through the stipulation of the ECE-Regulation 43, in particular Appendix 6, para. 5.1.3. The accompanying abrasion test is, in accordance with its nature, a simulation test which, under reproducible laboratory conditions, imitate traffic influences in a time-lapse procedure, which substitutes for the actual encumbrance later. The standard threshold value of 2% for light scattering which was set by the distribution of design approval for windshields is therefore an official measurement for stray light portions which are not yet considered as dangerous to traffic.

By such simulation tests only a standardized wear and tear can be considered and the results (i.e. the model approval) loses significance when the actual conditions for usage deviate. Should such deviations become significant, the examination of the approved item should then be recommended for the maintenance of traffic safety.

The light scattering of 2% which is mentioned in this regulation also corresponds approximately with a magnitude order of two stray light units with the A. Timmermann measuring instrument, as comparative measurements have shown.

According to § 30, para 3 of the Motor Registration Code (StVZO) the inspection should be easily reached. Due to the relationship with § 29 of the Motor Vehicle Approval and Traffic Registration Code the standard “easily tested” (“simple to test”) is to be fixed within the framework of the periodical § 29 inspection. The inspection of the bright-dark-limit condition of low beam headlights, in practice now for decades, is suggested for use as a comparison. As long as expenditures for personnel and apparatus for the measuring of stray light in windshields lies in this magnitude, it may be qualified as simple.

As regards the requirement for easy replacement, a comparison with other parts which wear is also given, namely brake linings and brake shoes. The expenditures correspondent with the individual technical stand cannot—and in the past were not—be questioned according to § 30, para. 3 of

the Motor Vehicle Approval and Traffic Registration Code (=StVZO). The currently available techniques for installation and removal of windshields also may not be questioned (according to wording and administrative practice) in light of § 30, para 3 of the Motor Vehicle Approval and Traffic Registration Code (=StVZO).

## References

Derkum, H. (1989)—“Stray Light in Windshields—Measurement and Effect.” Lecture announced for the conference Vision in Vehicles 3, Aachen, September 1989.

Helmers, G. & S.-O. Lundkvist (1988)—Direction Distances to Obstacles on the Road Seen through Windscreens in Different States of Wear—VTI rapport 339A, Linköping (S).

Regional Court of Appeal, Hamm (1989)—Grund- und Teil-Urteil (=Judgement on the Substance of the Claim and Part Judgement) from June 30, 1988 27 U 232/85 in: ZVS 35, 1989, p. 37–38.

Schneider, W. (1976)—Sportliches Styling verschlechtert die Sicht im Auto. (=Sporty Styling Impairs Visibility in Auto) in: UMSCHAU 76, Heft 16, p. 529–530.

Timmermann, A. (1986)—Direct Measurement of Windscreen Surface Wear and the Consequences for Road Safety—Vision in Vehicles I, Elsevier Science Publishers B.V. (North-Holland), 1986, p. 331–342.

## Appendix: Law and Justice in Service to Traffic Safety

### Regional Court of Appeal, Hamm

Helmet visors reduce visual range, particularly in rain.

Judgement on the substance of the claim and Part Judgement pronounced on June 30, 1988, (27 U 232/85 Regional Court of Appeal, Hamm)

Statement of facts (edited)

On November 16, 1988 at approximately 16.45 hours the appellee drove with his light motorcycle on a 6.45 m wide street. He wore glasses as well as a crash-helmet with lowered visor. On the vehicle of the appellee dimmed headlights were switched on. Extremely bad weather prevailed, the sky was heavily overcast. It rained heavily. Due to advanced twilight resp. darkness, street lights were switched on—on the edge of the right lane (for the appellee the direction of traffic) whip lights were switched on.

At the same time the, at that time, almost six-year-old complainant wanted to cross the Gütersloher Straße from left to right—for the appellee the direction of traffic—(southwest to northeast). The children wore light green resp. light yellow-brown jackets and brown resp. red pants. The complainant held the hands of her siblings. She had observed the traffic before beginning to cross the street. She saw vehicles approaching from the left at a greater distance. With her siblings she attempted to cross the street quickly. Before the children reached the other side of the street, however, the complainant and her brother were caught by

the light motorcycle of the appellee and thrown to the ground. The highest speed in the area of the accident is . . . limited to 60 km/h. By reason of the collision the complainant was seriously injured.

The complainant is of the opinion that the appellee is at fault for the accident thereby that he did not adjust his speed to the particularly adverse conditions of the street and weather. He is also at fault because he did not apply the brakes and did not attempt to make way for the children.

Grounds of the decision (edited)

“The appellee is at fault through negligence for the serious bodily injury to the complainant. He, having caused the accident, is in violation against § 3, para. 1, part 2 of the Traffic Regulations (StVO). According to these regulations, he was duty bound to adjust his driving speed to the extremely difficult conditions of the street, traffic, visibility and weather as laid out in the case. He did not meet these stipulations sufficiently.

According to the convincing statement of the expert witness, the speed of the light motorcycle driven by the appellee was at least 55 km/h before the collision. This result was determined convincingly by the expert based on the skid marks of the motorcycle and using as a basis 3,5 to 4 m/sec<sup>2</sup>. According to this, the accident took place at least 26 m before the final position of the motorcycle as shown in the traffic accident sketch. The speed area determined by the expert is essentially in accord with the expert opinion which was the basis of the preliminary proceedings. This expert has also determined the driving speed of the appellee to be approximately 50 km/h. Finally, the appellee himself has conceded his held speed to be 50 to 60 km/h. According to this, the speed of at least 55 km/h for the light motorcycle was, however, in view of the generally adverse weather conditions which prevailed at the time, but also in view of the clearly impaired visibility of the appellee caused by these conditions, decisively too fast. This the appellee must have been aware of and it should have caused him to make a clear reduction of his speed to not essentially faster than 30 km/h. The circumstances necessary for such a speed reduction were also clear to the appellee. The heavy rain, the tar asphalt wet from rain, the impaired visibility caused by mist and twilight, the light reflections on the street caused by the street lights on the edge of one side of the street and finally the fact that he was driving wearing glasses and with a lowered helmet visor must have given the appellee the impression of strongly reduced visibility and the necessity for a clear reduction of his driving speed. Moreover, the clearly impaired visibility caused by rain on the visor of the safety helmet stood unmistakably in the forefront.

The expert, established specialist in the field of “Vision and Traffic”, has, by request of the Senate (i.e. the court), given an opinion on the visibility conditions at the time of the accident and, at the same time, has examined the visor of the safety helmet. Summarizing, the expert has concluded that stray light is considerably heightened through water drops on the viewing shield which are unavoidable during rain. Dependent upon the head wind and posture of the head,

stray light coefficients would result which could go beyond the critical threshold of 3,0 and at times also reach 6,0. Thereby, an obvious obstruction of view is at hand which, of course, still allows one to recognize head lights and tail lights of other road users as well as strong contrasts quite well in the dark, but by oncoming light, i.e. glare, could make the recognition of weak contrasts by dark background impossible. In the case at litigation, possible sources of glare would be (1) the head lights of the oncoming passenger car of the witness Hanschmidt and, to an even stronger degree, (2) the street lights fitted with high pressure lamps. The latter guarantee flawless lighting during dry weather conditions, however, by wet pavement they pose a traffic safety disadvantage. The individual drops on the visor scattered the light from the street lamps and the oncoming passenger car so that a glare condition appeared. The field of vision is then broken into particles (visually considered) which lead to a situation in which weak contrasts could no longer be recognized. The appellee should have, under these conditions, raised his visor, at least in part, so that he, on the one hand, would have been protected from the rain and, on the other, would not have to look through the visor, whereby admittedly the water drops on the glasses worn by the appellee could have eventually caused an obstruction of his view. During oral commentary and supplementation of his written opinion the expert stated that under the given circumstances—closed visor, rain, pedestrians who were essentially clothed in dark garments—the appellee should not have driven faster than 30 km/h.

The Senate (i.e. the court) agrees with this opinion without reservation. The basic principle of the regulation of § 3, para. 1 of the StVO (=Traffic Regulations) is the law of driving by sight, the “golden rule” of traffic. Driving by sight means being able to stop within the area visible at a glance. The primary law, driving by sight, is valid by day and by night, by all weather conditions and for vehicles of every kind (cf. BGH = Federal Supreme Court, NJW 1961, 1588). A motorist who drives at dusk on a city street wet from rain must expect that pedestrians will cross the street. Should, by the given visibility conditions, observation of the street and recognition of obstacles be complicated by interference from lighted oncoming vehicles, the driver must then make allowance for this situation by lowering the speed and a heightening of attention. He must be able to stop on visual range and is not allowed to drive blindly into uncertainty (cf. BGH = Federal Supreme Court, VersR 1969, 373; 1976, 189).

In the case at litigation, the existing considerable obstruction of vision due to rain, dusk and stray light through a closed visor wet from rain must obtrude upon the mind of the appellee. The fact is that it also has not remained concealed from him. On the contrary, as his statement in the written charges of the traffic accident shows, he referred expressly to such an obstruction of vision to the police officer who made the on-the-spot investigation of the accident. In that case nothing was more obvious than the law

of driving by sight and driving adjustments to the street, traffic, visibility and weather conditions (§ 3, para. 1, StVO = Traffic Regulations), the improvement of visibility possibility by raising—in part—the visor and, above all, to allow for the difficult visibility conditions by clearly reducing the driving speed. This should have been clear to every responsible driver and also to the appellee. Also, no reasonable doubt exists as to the degree of the required reduction of speed. It was obvious, indeed most urgent, that in any case a speed was to be chosen not much higher than 30 km/h, therefore corresponding with that speed limit which is increasingly being stipulated for purely residential streets and zones with traffic abatement, but also corresponds in general with that speed which is demanded by difficult visibility and traffic conditions for the protection of other participants in traffic, in particular the pedestrians. Accordingly, the appellee has, through negligence, violated against his incumbent obligation to exercise due care in accordance with § 3, para. 1 of the Traffic Regulations.

This violation of obligation by the appellee also was the cause of the accident. The appellee could and should have recognized the complainant and her siblings in time and—by a clearly reduced speed—reacted in a manner that would have prevented resp. diminished the results.

In accordance with the results of the evidence the Senate (i.e. the court) assumes the speed of the oncoming vehicle toward the appellee to be approximately 40 km/h. The speed of the complainant and her siblings, based on the evidence, is set at ca. 1,5 m/sec—quick walking. Proceeding from the given values, the expert has come intelligibly and convincingly to the conclusion that the complainant was recognizable practically by the appellee exactly one second before the collision thus—by a calculated speed of the appellee of at least 55 km/h—ca. 15 m before the place of impact—as she discovered the outer right head light thus attempting a reaction demand.

The expert did, however, raise some doubts as regards discernibility and explained, among other things, the following: The covering of a head light of an oncoming vehicle by a pedestrian crossing the street from the left is of course visible when one stands at the place of the accident, watching and waiting for the event. This in no way means that a driver in the actual traffic situation also must see the covering. One is dealing with a peripheral event whose conspicuousness is not designed to necessarily demand the attention of a driver. The expert confirmed this fundamental opinion also during his oral explanations and additions to his written opinion before the Senate (i.e. the court), however qualifying his observations: Whether or not the occurrence may be distinguished in an individual case resp. must be distinguished depends, among other things, above all on the distance; it is, for example, noticeable when it occurs nearby in an area of ca. 20 m and the head lights as well as the approaches would be concealed by the person on short notice.

It is exactly this nearby area which is the object of the

conflict in this case. The expert convincingly explained—as mentioned—that the complainant became visible to the appellee ca. 15 m before the collision. In this nearby area the visibility was given by the concealing of the right head light of the passenger vehicle of the witness also following the comments of the expert. It is a case of a noticeable concealing of a head light from the oncoming passenger vehicle in the nearby area of 15 m before the motorcycle driver.

In addition, the appellee—at 15 m—could and should have seen the complainant and her siblings even in the direct light beam of his headlights. The expert has stated as regards the capability of motorcycle head lights (low beam light) that, according to his experience, these (head lights) offer, under the given conditions by poor contrast objects, a visibility of approximately 15 m, admittedly only then when the object is found to be directly in front of the vehicle. So was the arrangement of this case.

According to this, the appellee, with the required attention, should have and could have recognized the complainant approximately 15 m before the collision—the opinions of both experts agree in this matter. The attention of the appellee was, however, missing. He did not see the children at all before the collision, as he himself admits. Instead he recognized only a shadow of his motorcycle directly before the collision. The accident could have been

avoided by an adjusted speed. The expert has made a statement as regards the avoidability.

The expert has come to the conclusion intelligibly and convincingly that even at a speed of 40 km/h for the motorcycle the accident would not have happened.

Assuming a speed of 35 km/h, according to the Senate (i.e. the court), the highest speed at which the appellee should have been permitted to drive, an area for bringing the vehicle to a standstill of 9,73 m (1 sec. reaction time) + 7,9 m (purely area for braking by a brake retardation of 6 m/sec<sup>2</sup> which the expert described as realistic for this motorcycle even when the street is wet), results, a total then of 17,62 m. In this case, the time avoidability resulted from the following consideration: The motorcycle needed at 35 km/h a time to bring the vehicle to a standstill totalling 2,6 sec. (1 sec. reaction time + 1,6 sec. time for braking). In this time (2,6 sec.) the complainant and her siblings, at a walking speed of 1,5 m/sec. would have already gone 3,9 m and would have crossed the street long before. According to this, the accident would have been clearly avoided. Using a speed of only 30 km/h as the basis, the avoidability appears even clearer.

Finally, the appellee could have swerved to the left within his own lane. This was easily possible and reasonable. Here also the accident would certainly have been avoided.

## **Large Scale Experiment About Improving the Night-Time Conspicuity of Trucks**

**Schmidt-Clausen, H.J., Finsterer, H.,**  
Technical University, Darmstadt

### **Abstract**

Based on the experiments in the laboratory about marking of trucks with passive retroreflective materials for better conspicuity during night-time driving, a large scale experiment is started in the Federal Republic of Germany.

About 1,000 trucks are equipped with special markings of different shapes. The accident rate of these trucks and the rate of unequipped trucks will be compared. In addition the aging and the pollution of these materials shall be investigated.

The planned time of duration of the tests is about two years with the aim to improve the relevant International Regulations on behalf of light signalling devices.

### **Introduction**

Starting from the accident-rates of trucks, an investigation about additional marking of trucks was performed. This investigation led to so-called contour-markings, which enables the driver to recognize the car in front as a truck over a large distance.

This kind of contour-marking shall be tested in a large scale experiment, marking roughly 1,000 trucks and

compare their accident-rates with unequipped trucks. This experiment shall be finished in 1991.

### **Accident-rates of trucks**

Starting the first experiment about additional markings of trucks for better conspicuity during night-time driving, it was found that especially trucks with a low silhouette (for example platformbody trucks) were involved in much more night-time accidents than other trucks. For an investigation in Germany in the early 80th (when these experiments were started) the results are plotted in figure 1 (1).\*

For both, side- and rear-impact, the accident-rates are the highest for the platformbody type. This drew the attention to the fact that there is a need for an additional marking of trucks either with passive materials or lamps based for example on LED.

### **Optimum Luminances of Rear Position Lamps**

In figure 2 the main results about an assessment/experiment "optimum luminances of rear position lamps" are plotted (2).

The results show that there are still possibilities for improvement of the "light values" of rear position lamps.

\*Numbers in parentheses designate references at end of paper.

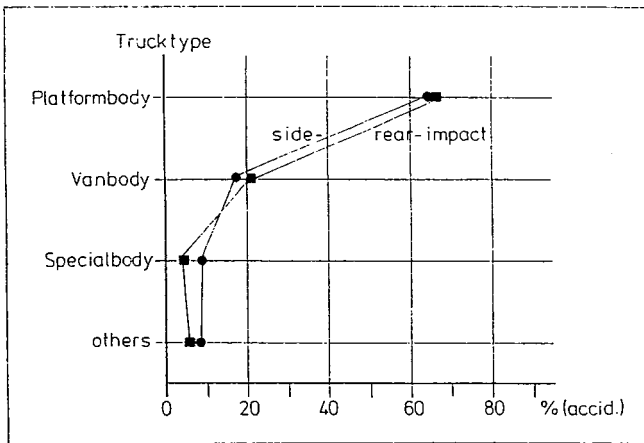


Figure 1. Accident-rates in percent for different types of trucks.

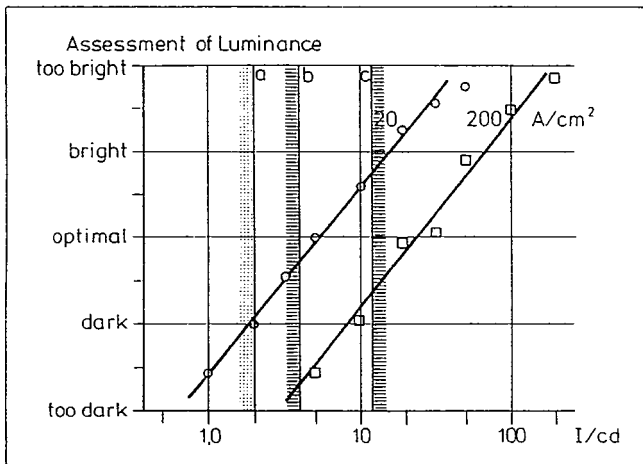


Figure 2. Assessment of luminances of rear position lamps with different light intensities during night-time driving. A: size of the rear position lamp. a, b, c: minimum/maximum light intensities required in the ECE-Regulation.

The boundaries "a" and "b" in figure 2 mark the minimum light intensities ( $I = 2cd$ ,  $I = 4cd$ ), "c" the maximum of  $I = 12cd$ .

In the traffic situation the light intensities as plotted in figure 3 are found (3). "a" and "b" describe the minimum value of the light intensity of rear position lamps, "c" the maximum value. As shown in this figure there is an aging effect of lamps due to different reasons. It seems that there is a need for improvement and checking of lamps of trucks.

### Additional marking of trucks

In a down-scale experiment the improvement of conspicuity of trucks by additional markings was investigated. Out of a series of different markings in figure 4, 4 different side markings are plotted (5, 6, 7). The results for the necessary luminances are shown in figure 5 where the luminance  $L$  in dependence of the recognition distance of a truck is plotted.

The results show that the contour-marking "c" needs the lowest luminance values, that means it is the best additional marking.

The barr-marking seems to be second. The results are roughly the same for rear- and side-marking of trucks.

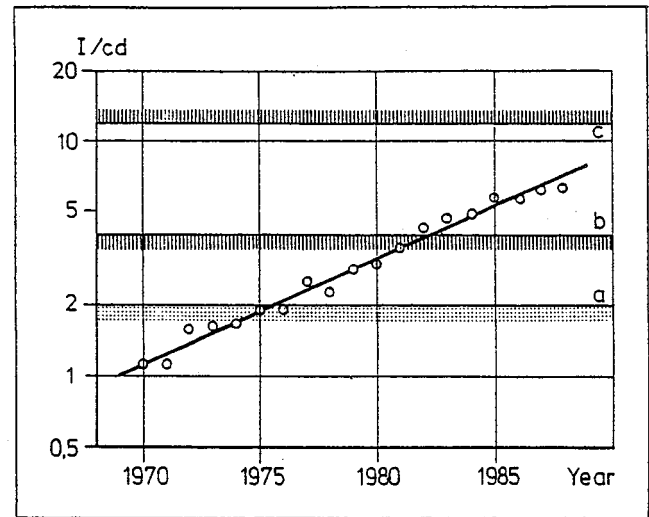


Figure 3. Axial light intensities of rear position lamps of different production years. a, b, c: minimum/maximum light intensities required in the ECE-Regulation.

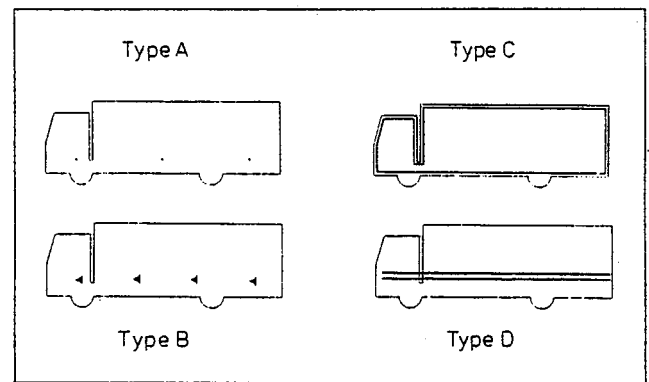


Figure 4. Samples of marking of trucks.

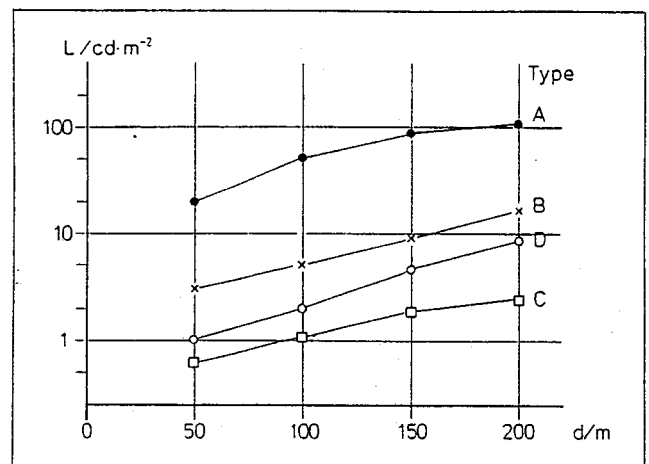


Figure 5. Necessary luminance  $L$  for marking of trucks for different viewing distances. A, B, C, D: Different types of marking (figure 4).

### Large scale experiment

To prove the improvements of conspicuity of trucks dur-

ing night-time traffic, a large scale experiment was initiated in Germany by the Ministry of Transport. The aim is to equip 1,000 trucks of different types with barr- or contour-markings on the basis of retroreflective materials of different types. Parallel a control group of 500 trucks of similar types is chosen for comparison of accident-rates. Due to legal (national and international) problems at this moment, only 200 trucks are equipped, but up till autumn 1989 all 1,000 trucks will be equipped.

Beside the comparison of accident-rates of the different types of truck accidents, other effects like aging of the used materials and of headlamps of cars are investigated. From other experiments about aging on behalf of "light values" of traffic signs, the reduction of the retroreflective factor  $R'$  is known. The results for a white material of a special type is shown in figure 6. The reduction is nearly  $20\text{cd} \cdot \text{lx}^{-1} \cdot \text{m}^{-2}$  per 5 years.

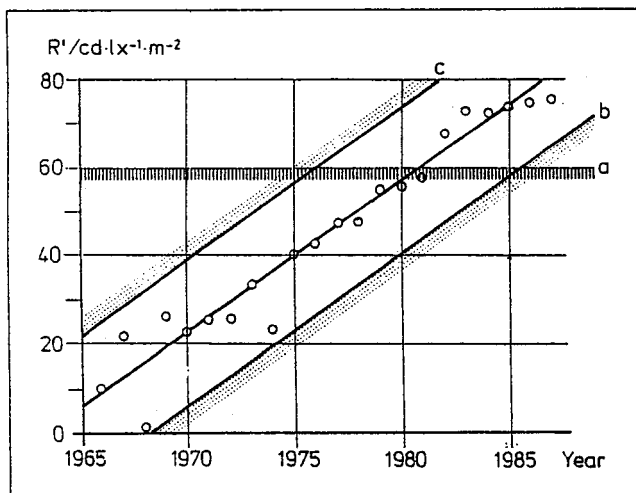


Figure 6. Aging of retroreflective materials during use in traffic. a: minimum required value for retroreflection factor  $R'$ . b, c: confidence levels for 95%.

The aging of materials fixed on trucks may differ from these results. So in addition the aging of retroreflective materials will be investigated.

To get the optimum luminances of markings, the low beam headlamps must emit a minimum amount of light above the cut-off (glare zone). Up till now there are no requirements for these values in the relevant regulations. From early experiments (3) it is known that the glare value of a low beam headlamp is nearly independent of the age of the headlamp (figure 7).

The hatched boundary (a) in figure 7 marks the maximum value of glare in the point B50L. In addition in this large

scale experiment in other points of the "glare zone" of low beam headlamps the change of "light value" will be measured.

## Conclusion

The accident-rates of trucks during night-time traffic indicate that there is a need for an additional marking of

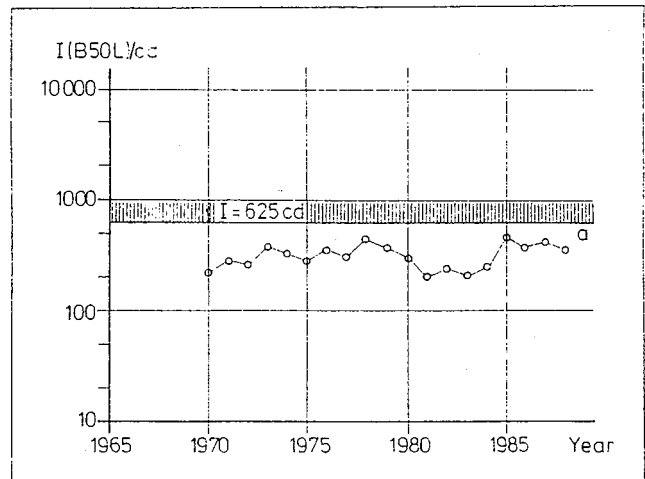


Figure 7. Changes in glare values of low beam headlamps. a: maximum permissible glare-intensity.

trucks. In a large scale experiment the accident-rates of equipped and unequipped trucks will be compared. In addition the change of "light values" of retroreflective materials and low beam headlamps will be checked in normal traffic situations.

## References

- (1) Gauss, F. a.o.: Äußere Sicherheit von LKW und Anhängern, FAT-Report Nr. 27, 1982.
- (2) Schmidt-Clausen, H.J.: Optimum Luminances and Areas of Rear Position Lamps and Stop Lamps, ESV-Conference Oxford, 1986.
- (3) Schmidt-Clausen, H.J. a.o.: Leuchten- und Scheinwerferüberprüfung im Verkehr, Deutsche Kraftfahrtforschung Heft 297, 1987.
- (4) Erke, H.: Ein Konzept zur zusätzlichen Sicherung von LKW-Hecks, International Report, 1977.
- (5) Schmidt-Clausen, H.J. a.o.: Seitenbeleuchtung von LKW, Deutsche Kraftfahrtforschung Heft 302, 1987.
- (6) Schmidt-Clausen, H.J. a.o.: Rückwärtiges Signalbild von LKW, Deutsche Kraftfahrtforschung Heft 303, 1987.
- (7) Hartge, J.E. a.o.: Rückwärtige und seitliche Kenntlichtmachung von LKW durch retroreflektierende Materialien, CIE-Report 415, Venice, 1987.

# Assessment of Experimental Methods for Determining Braking Efficiency

Richard W. Radlinski,  
Vehicle Research and Test Center,  
National Highway Traffic Safety Administration

## Abstract

Six different experimental methods for measuring braking efficiency have been utilized and evaluated by the National Highway Traffic Safety Administration at its Vehicle Research and Test Center. This work has been performed in support of international efforts to harmonize passenger car braking regulations. Four of the methods are similar in that they measure brake force distribution at one or more braking rates on high coefficient of friction surfaces and calculate braking efficiency as a function of a hypothetical peak tire/road coefficient of friction ( $\mu$ ). The other two methods measure maximum non-locked wheel deceleration of the vehicle on a particular surface and then rely on measurement of  $\mu$  to calculate efficiency for that particular surface. Generally, the four methods utilizing the brake force measurement approach produce similar results, although one of these four is a very low-speed test that does not necessarily predict efficiency at higher speeds. The other two maximum deceleration-based methods do not necessarily produce similar results due to the fact that they measure a somewhat "different" braking efficiency.

## Introduction

Recent international efforts to harmonize passenger car braking regulations have stimulated considerable interest in methods for determining braking efficiency or the ability of a vehicle to utilize available tire/road friction without wheel lockup. At the present time the European braking regulations, Economic Commission for Europe (ECE) Regulation No. 13 and European Economic Community (EEC) Directive 71/320, contain requirements for wheel lockup sequence and acceptable ranges of braking efficiency, but these requirements do not specify a method for determining brake performance data needed to verify that the requirements are being met. Because of this lack of a specific or objective test method for measuring the necessary braking parameters, the United States has been unwilling to accept the European proposal to adopt the ECE/EEC requirements "as is" in a harmonized regulation.

Throughout the world there appear to be many different methods being used to obtain the necessary brake performance or "brake factors," but there appears to be little agreement on any particular approach. Methods being employed range from calculation of brake factors starting from some measured or assumed lining coefficient of friction to inertia dynamometer tests of complete brake assemblies to full-scale vehicle tests. The United States has favored the full-scale vehicle test approach because it evaluates all of the braking-related components together as a complete system and is the method most likely to provide

an accurate representation of how the vehicle will perform in the hands of the consumer.

Although the National Highway Traffic Safety Administration (NHTSA) has issued two notices of proposed rulemaking for a harmonized braking regulation (FMVSS No. 135), and both of these notices have proposed methods for determining brake balance via full-scale vehicle tests, final agreement among the various parties in the harmonization process has yet to be achieved. In the course of the harmonization process NHTSA has evaluated a number of different vehicle test methods to measure braking efficiency. This work was performed at NHTSA's Vehicle Research and Test Center (VRTC) in East Liberty, Ohio. The purpose of this paper is to describe the methods evaluated and to summarize the results of the evaluation in each case.

## Brake Balance, Adhesion Utilization and Braking Efficiency

"Brake balance," "adhesion utilization" and "braking efficiency" are all terms which have been used somewhat interchangeably during the harmonization process to refer essentially to the same aspect of braking system performance. Although they are closely related they are not equivalent. It is important to understand the relationship between these three terms as well as several other basic terms as they will be used throughout this paper.

Brakes generate *brake torque* at the wheels in response to brake system inputs. Brake torque is transmitted via the tire and wheel assembly to the ground or tire/road interface, where the retarding force for that particular wheel is developed. This longitudinal force, commonly referred to as the *brake force*, divided by the normal force at the wheel cannot be larger than the peak tire/road coefficient of friction ( $\mu$ ). Attempting to increase this ratio (i.e., increase brake force or reduce normal force) so that it exceeds  $\mu$  results in wheel lockup.

*Brake force distribution* or *brake balance* simply refers to the distribution of brake forces front to rear (or axle to axle in vehicles with more than two axles). Brake forces by design are equal left to right so that it is not necessary to work in terms of distribution on a wheel-by-wheel basis. By knowing the brake force at each axle it is possible to calculate the vehicle deceleration by simply summing these forces to obtain the total retarding force acting on the vehicle. At this point it is possible to account for other forces such as aerodynamic drag and rolling resistance in the total retarding force, although usually these "parasitic" forces are assumed to be insignificant and are neglected.

Once the vehicle deceleration is determined, it is then possible using simple rigid body dynamics and static weight distribution to calculate the dynamic normal force at each axle. The ratio of the brake force to the calculated normal force at the axle is referred to by the ECE/EEC regulations

as the *adhesion utilization (AU)*. The European regulations contain requirements for adhesion utilization as a function of deceleration for all vehicles that do not have antilock braking systems. The adhesion utilization "curves" for each axle must fall within specified ranges.

Once the deceleration of the vehicle is known and the corresponding adhesion utilization for each axle has been calculated, it is possible to calculate the *braking efficiency* for that particular operating condition. Braking efficiency or the percentage of available surface friction that can be utilized without wheel lockup is 100 times the ratio of the maximum vehicle deceleration without wheel lockup divided by  $\mu$ . To calculate efficiency from deceleration and adhesion utilization (AU), it is simply a matter of finding which wheel has the highest AU (this is the wheel that will lock first and it will do so when  $\mu = AU$ ) and then dividing this value into the deceleration and multiplying the ratio by 100. It should be pointed out that in this particular case efficiency is being calculated based on rigid body assumptions.

It is also possible to determine efficiency more directly by measuring the deceleration that a vehicle can achieve without wheel lockup on a particular surface and measuring the peak coefficient of friction of the vehicle's tires on the same surface. ECE/EEC regulations utilize this approach to determine the braking efficiency of vehicles with antilock braking systems (ABS). They then specify a minimum *measured* efficiency that must be achieved.

Since for vehicles without ABS, ECE/EEC regulations specify that AU for each axle must fall within certain limits over a broad range of decelerations, this in effect places requirements on *calculated* braking efficiency. It is important to make a distinction between calculated and measured efficiency because if the rigid body assumption does not hold, the two values of braking efficiency may not be the same.

## The Methods

With the above background as a basis for better understanding the fundamental differences in various approaches to measuring braking efficiency, the methods studied by VRTC will now be discussed. The following different methods have been evaluated:

- Torque Transducers
- Single-Axle Snubs
- In-Road Force Transducers
- Low-Speed Roller Dynamometer
- Skid Checks and Stopping Distance Tests
- ECE Regulation No. 13, Annex 13 Efficiency

The first four methods are similar in that they involve the determination of brake force at each wheel or axle (either by direct or indirect measurement); it is then possible to calculate adhesion utilization and braking efficiency using simple rigid body dynamic equations. The equations typically used in the analyses are essentially the same as

those that appear in Annex 10 of ECE Regulation No. 13, the "brake distribution annex" for vehicles without ABS. In all of the first four methods, brake applications are made on relatively high- $\mu$  surfaces at braking levels below the lockup point of any of the wheels. By utilizing a high- $\mu$  surface, brake force distribution and braking efficiency can be determined over the broadest possible range of braking levels. It is not necessary to know the exact value of  $\mu$  for these tests, only that it is high. The calculations then make it possible to predict efficiency on lower- $\mu$  surfaces.

The last two methods are fundamentally different in that they involve tests at braking rates right up to the point of wheel lockup (or beyond in the case of skid checks) on a particular surface. In these methods it is important to know the exact value of  $\mu$  for the test surface; without this information it is not possible to calculate efficiency. Different surfaces must be employed if efficiency is to be determined at different braking rates as it is not possible to extrapolate results on one surface to another. Another fundamental difference is the fact that measurements for these last two methods take into account road surface friction and roughness and the performance of the vehicle's tires and suspension, as well as the brakes, in the test results. This is not the case for the first four methods, which essentially just measure the brakes and calculate efficiency for a hypothetical situation (rigid body vehicle, smooth road, given tire/road  $\mu$ ).

Each of the six methods will now be discussed in more detail:

### Torque transducers

Torque transducers are typically strain gage transducers that bolt onto the brake drum or rotor via the wheel studs. The wheel-and-tire assembly is then bolted to the transducer with a separate set of studs on the transducer. In some cases the transducer is not a separate component but is built into a special wheel. This type of transducer is usually referred to as a *torque wheel*. A device of this type is shown in figure 1. Since either type rotates with the wheel, slip rings or rotary transformers must be employed to provide a path for excitation and output signals. In addition, because different vehicles have different wheel bolt patterns, various adaptors (or different sets of transducers) are needed to enable a broad range of vehicles to be tested. Some installations also require spacers to prevent the transducer from interfering with brake calipers. Unless special wheels with a "deep dish" offset are used with the universal type transducer (as opposed to a torque wheel customized for a particular application), installing the transducer results in a wider axle tread width. This is not a particular problem, however, unless the tires interfere with the body; tread width has no effect on brake force distribution.

Commercially available transducer-slip ring assemblies for passenger cars and light trucks cost in the neighborhood of \$10,000 per wheel, not including signal conditioning or data recording equipment. Torque transducers are available for heavy trucks but are not widely used because of high cost

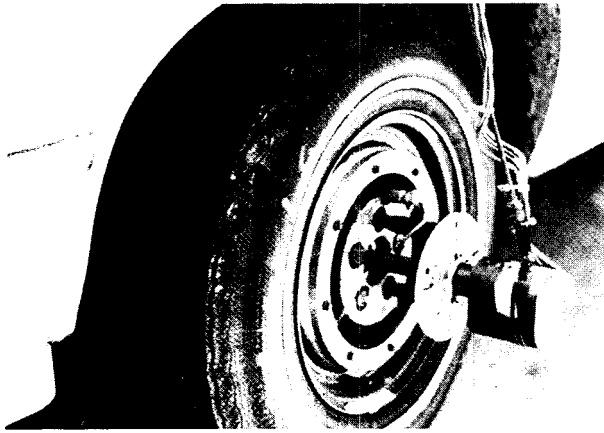


Figure 1. Torque wheel and slip rings installed on vehicle.

(\$15,000 or more per wheel) and the difficulty of adapting them to the many wheel-end configurations that exist on this class of vehicles.

Torque transducers can be used either with or without transducers for measuring hydraulic brake-line pressures. If they are used with pressure transducers it is possible to determine the torque-versus-pressure relationship of effectiveness for each brake. Typically a linear relationship is assumed and regression techniques are employed to "fit" the data. The slope of the best-fit line is the parameter used to describe brake effectiveness. Although this linear assumption can introduce some degree of error, the magnitude of the error is generally considered to be small. The slope is divided by the tire's rolling radius to give effectiveness in terms of brake force instead of brake torque. Since tires are flexible elements that change their rolling radius as forces acting on them change, assuming a constant rolling radius at this point (this is how most torque data analyses are done) also introduces some error in the process. As is the case with the linear assumption on the torque-pressure relationship, it is generally assumed that this error is small.

If pressure information is available, it is also possible to determine the front-versus-rear brake pressure relationship and then to use that information with the brake effectiveness factors to relate the front and rear brake forces. Although this appears to be a redundant process since the brake forces can be related directly from the transducer measurements at any point in time without any pressure data, measuring pressures and using this approach has the advantage that it provides an indication of brake system input-output characteristics and separates the performance of the foundation brakes from the brake pressure proportioning valve(s). In effect, it provides a building-block or component performance superposition approach as opposed to an overall system efficiency measurement approach.

Vehicle road testing with torque transducers can be done in basically two different ways: (1) ramp brake apply or (2) steady-state (constant-input) brake apply. Either approach can be used with or without pressure transducers utilizing the analyses described above. With the ramp apply approach, one stop that progresses up to the point of wheel

lockup on a high-coefficient surface provides continuous brake force distribution data over the entire range of braking levels that a vehicle will experience in normal use. The constant-input approach measures forces at one braking level per stop, but if the linear torque-versus-pressure assumption is made, and if pressure data is available, it is possible to extrapolate torque-versus-pressure data from one constant-input stop to all possible braking rates. A line is simply fit from the point where braking starts (i.e., brake force threshold) up to the data point generated by the single stop. A better approach is to make several constant-input stops at various braking rates and to fit all the data with the line; this minimizes the risks inherent with large extrapolations.

If pressure information is not available, a single constant-input stop only provides brake force distribution, adhesion utilization and braking efficiency data at one braking level and, since none of these parameters are necessarily linear with respect to braking rate, extrapolation to other braking rates is not possible. By making stops at various braking rates, however, it is possible to assume a linear relationship between "points" and to approximate the nonlinear relationship with straight line segments. The more braking rates that are utilized, the better the approximation of the nonlinear relationship will be.

When the constant-input test approach is utilized, torque data is usually collected for the entire period of time that the brakes are applied and then time-averaged for each brake over the period after the initial transient dies out. If pressure is being recorded, it is also usually averaged over the same time period. The average torques (and pressures if available) are then used in the calculations of brake effectiveness.

With a ramp application, continuous brake force distribution-versus-deceleration data is developed in a single stop, and thus, by making calculations at small deceleration steps, nearly continuous relationships can be established for adhesion utilization and braking efficiency. This approach does not require brake pressure information but does lend itself to digital data acquisition methodology and digital computing techniques due to the high number of computations required.

Although VRTC has not performed an extensive experimental comparison of the constant-input and ramp apply approaches, we have examined a great deal of data generated by General Motors where both methods were performed consecutively on the same vehicles. This analysis indicates that both apply methods give essentially the same brake force distribution-deceleration relationship.

The bulk of the torque transducer testing that has been performed by VRTC has employed the constant-input approach with pressure transducers. In the most recent testing that has been performed, which will be discussed later, three repeat stops were run at each of four different braking rates. Effectiveness was then determined by the slope of the line best fitting the resulting torque-pressure data points and the threshold point (determined from a static test).

## Single-axle test

The single-axle approach involves making brake applications with brakes operational on only one axle at a time. The same input levels are used on each axle in order to be able to relate the braking forces. Vehicle deceleration is measured and then brake force for that axle is calculated knowing vehicle mass. In order to account for parasitic drag, a coast-down or no-brake test is run and the deceleration measured in this test is subtracted from the braking tests before the force calculation is made. Deceleration can be measured with a decelerometer or it can be calculated from vehicle speed data by differentiation. The latter approach is most frequently used because it produces a high level of accuracy; decelerometers lack accuracy due to vehicle pitch effects, mechanical noise and road gradient effects.

This approach has been used for a number of years for heavy trucks. SAE Recommended Practice, "Brake System Torque Balance Code-Commercial Vehicles-SAE J225," first published in 1971, specifies this method. A more detailed and comprehensive version of the test for commercial vehicles was developed by an SAE committee in the early 1980's and was published as Recommended Practice, "Brake Force Distribution Test Code-Commercial Vehicles-SAE J1505," in 1985. VRTC was deeply involved with SAE in the development of SAE J1505 at the same time that the first Notice of Proposed Rulemaking (NPRM) for a harmonized braking regulation for passenger cars (FMVSS No. 135) was being developed and decided to apply the truck approach to passenger cars. Reference 1 describes the result of this VRTC effort. The first NPRM (Notice 1) for FMVSS No. 135 included the VRTC procedure, and it became known as the "single-axle" procedure. Comments received by NHTSA relative to Notice 1 indicated that many commenters did not particularly like the single-axle procedure because they felt it was time consuming, required disruption of the hydraulic system (to install pressure transducers and shut-off valves for each axle) and was prone to experimental error.

The instrumentation required to run the single-axle procedure consists of an accurate speed measuring system, a timer or time-base recorder in order to determine the time between two preselected speeds and pressure transducers to measure brake pressures. In addition valves are required in the hydraulic system to permit the brakes on each axle to be shut off. As is the case with torque transducers, pressure instrumentation is not required if extrapolation of results to other significantly different braking rates is not necessary. If pressure is not measured, a pedal force transducer must be used to measure input level so that the same input level can be used on each axle and the various forces can be related. It is desirable, but not absolutely necessary, to use a brake applier to ensure that a constant input is achieved.

## In-road force transducers

In the early 1980's General Motors (GM) developed a highly sophisticated system for measuring brake force dis-

tribution at normal driving speeds that utilizes instrumented plates installed in the test track and requires essentially no instrumentation onboard the test vehicle. This system, called the road transducer plate (RTP) facility, can be utilized to test vehicles up to 10,000 lbs GVWR. GM has constructed four of these facilities, although two of these were earlier designs that are no longer in use. The basic concept is not new; instrumented plates have been used in inspection stations for a number of years to measure brake force at each wheel. With these inspection station testers, the vehicle is driven on at walking speed and then stopped while still on the plates. GM has taken this basic concept, developed very accurate, low-friction transducers and integrated them with a microcomputer-based data acquisition system to permit highway-speed drive-over testing and highly automated data analyses. The GM transducers measure brake force as well as vertical (normal) force and lateral (side) force at each wheel, although side force data is not being utilized for any particular purpose at the present time. The RTP computer sums braking forces to determine vehicle deceleration and calculates vehicle speed by timing the start of normal force for each axle, having been given the axle spacing (wheelbase) of the vehicle as input information.

GM agreed to share its RTP technology with NHTSA in the form of drawings, schematics, material lists, software, etc., and in 1987 VRTC completed construction of a facility similar to those at GM. The NHTSA/VRTC facility is located at the Transportation Research Center (TRC) of Ohio, where it is available for use by others through TRC. Round robin testing has shown that the GM and NHTSA RTPs produce equivalent results. Figure 2 shows the NHTSA facility; the GM facility is described in detail in Reference 2.



Figure 2. NHTSA light-vehicle RTP.

Although the GM and NHTSA systems incorporate four individual transducer plates that measure all four wheels simultaneously, tests conducted by both GM and VRTC indicate that essentially the same results can be achieved with only two plates (a left and a right) operational. Apparently brake force distribution does not change by a significant amount during the short time period between front and rear axle crossings. Conceivably, it might even be possible to achieve satisfactory results with a single wide plate since the brake forces are usually summed on each axle prior to calculating brake efficiency.

When testing on the RTP, the driver starts his brake application at a fixed point approximately 70 feet ahead of the plates. He must select a vehicle speed at the point of brake application such that the crossing speed is as close as possible to the target speed. Both GM and VRTC have been using 40 mph as the target speed. The first snub is usually made at 0.2g at an initial speed of 45 mph and in each successive application the deceleration is increased by 0.1g and the initial speed is increased by 2.5 mph until wheel lockup occurs (at which point the test run is aborted and the data from the snub discarded). The driver uses the vehicle's speedometer for judging speed and a U-tube decelerometer for deceleration. Exact decelerations are not really necessary as long as a reasonably well-spaced broad range of braking rates are achieved during the test, and because of this experienced drivers can run satisfactory tests without the decelerometer.

It is possible to test at crossing speeds as low as 25 mph, but below that speed the driver has a difficult time judging the application of the brakes without stopping on or before the plates. The upper limit on crossing speed is a function of how fast an approach speed is practical (at 0.8g the initial speed must be approximately 20 mph above the desired crossing speed). VRTC has successfully run tests at 50 mph crossing speed.

Only minimal driver training is required with the RTP. Although it does take some level of skill, drivers who are given brief instruction and allowed an hour of practice can usually perform quite satisfactorily. One key instruction that should be given to drivers is that they must maintain a constant or slightly increasing input force on the brake pedal when crossing the RTP. If a driver reduces pedal force, hysteresis in the brake system results in erroneous results.

At the present time the vertical (normal) force measurement capability of the RTPs is primarily being employed for vehicle static weighing. Although vertical forces are monitored during braking runs, the data is not being utilized in calculations of adhesion utilization or braking efficiency (rigid body dynamics are used to calculate vertical forces). This is due to the fact that vertical forces fluctuate considerably due to road irregularities and suspension dynamics and the frequency of this variation is so low that the RTP does not capture a complete cycle. RTP dynamic vertical force data is therefore not necessarily representative of the average dynamic normal forces existing on the vehicle during braking. To a certain extent, dynamic vertical forces measured by the RTP are influenced by the profile of the approach road immediately ahead of the plates.

Figure 3 provides an example of the difference that exists between calculated vertical force distribution and that actually measured by the RTP vertical force transducers. This data is typical, and higher and lower levels of fidelity between calculated and measured results have been experienced. Figure 3 indicates that the weight transfer off of the rear axle as measured by the RTP is greater than the calculated transfer. A review of over 900 RTP tests conducted by VRTC indicates that this greater transfer of weight off of the

rear occurs on the RTP in the majority (but not all) of the tests. One hypothesis is that braking is initiated too close to the RTP plates and that vehicle pitch is not at its steady-state level before the vehicle "hits" the RTP; however, this hypothesis has been checked with four significantly different vehicles instrumented to measure pitch and found not to be the case.

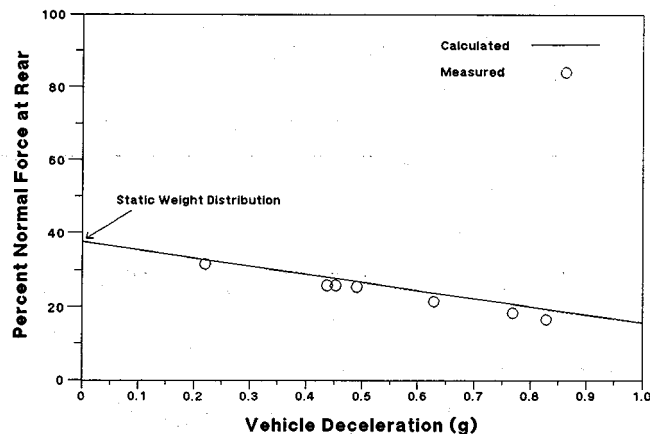


Figure 3. Comparison of calculated and measured normal force distribution.

The cost of reproducing the GM-designed four-plate RTP at TRC was approximately \$300,000 including a building for the data acquisition/computer system, pit excavation and minor paving work around the pit. Although it would appear that the cost of employing RTP technology is high, this is not necessarily the case. Since testing has shown that only two plates are necessary, and since vertical force during braking can be (and usually is) calculated from rigid body equations knowing vehicle static wheel weights, an RTP facility could be constructed at a much lower cost. The current RTPs employ a total of 32 transducers for four plates; it is conceivable that a two-plate facility could be constructed with only two transducers. This would greatly simplify the data acquisition hardware requirements and reduce system cost significantly. It is estimated that a light-vehicle facility could be constructed for less than \$50,000.

VRTC is currently developing a road transducer plate facility for heavy vehicles adjacent to the light-vehicle facility. This system shares the data acquisition system and computer with the light-vehicle RTP. Rather than design transducer plates from scratch, commercially available transducer plates manufactured in Europe that are sold for use in inspection stations are being evaluated. These plates are respectively low cost (approximately \$12,000 per pair). They measure longitudinal (braking) forces only and employ electronic load cell technology. The transducers are much more accurate and have a faster response than the hydraulic plates that have been in use for a number of years in inspection stations. VRTC performed a comprehensive static calibration of these plates in the laboratory and as a result of obtaining positive results, installed them outside in a pit on the test track for dynamic evaluation. Since the

plates are 2.5 inches thick, only a very shallow pit is required.

Figure 4 shows the heavy-vehicle transducer plates installed in the pit on the track. Each transducer is actually two separate plates each supported on strips of roller bearings and placed end to end to provide a total length of approximately thirteen feet. Only one of the two plates is instrumented with a single load cell; the other is spring loaded against the instrumental plate. In running over the plates, the vehicle encounters the plate without the load cell first so that it can transmit the braking force to the instrumented plate. The total length of the transducer allows approximately one full wheel revolution to be recorded so that the brake torque variation that typically occurs in a single wheel revolution can be averaged out.



Figure 4. NHTSA heavy vehicle RTP.

Although the dynamic evaluation is still not complete, the initial results look very promising. Figure 5 shows brake force recorded on one of the plates during a test of a five-axle tractor semitrailer loaded to 80,000 lbs. The signal has been filtered with a 50 Hz low-pass filter identical to that used with the light-vehicle RTP and the quality of signal is comparable to that recorded with the light-vehicle transducers. Assuming that the dynamic calibration phase produces positive findings, two more transducers will be obtained and installed approximately 35 feet away on the track in another pit. This will enable the facility to measure the brakes on a tractor and its trailer (or trailers) at approximately the same time. With the existing single pair of transducers there can be as much as a ten mph speed drop before the trailer wheels cross the plates.

### Low-speed roller dynamometers

Roller Dynamometers are very common in Europe in garages and inspection stations, but they are rarely found in the U.S. They consist of roller sets that cradle one axle of a vehicle at a time and drive the wheels independently left and right with electric motors (usually at speeds below 5 mph). The motors drive against the brakes and are mounted so that their reactive torque is transmitted through transducers that are calibrated to read out directly in terms of brake force. These devices are not expensive and can be purchased for

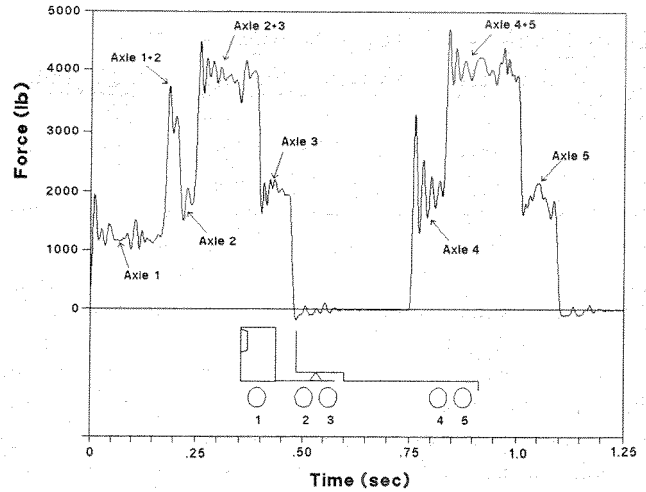


Figure 5. Brake forces recorded on one heavy-vehicle transducer plate during crossing by five-axle tractor semitrailer rig.

less than \$10,000 for light vehicles and less than \$20,000 for heavy vehicles.

A roller dynamometer (light-vehicle model) currently in use at VRTC is shown in figure 6. This tester is quite old (about 20 years) and is shown installed above the floor. Most of the installations overseas are in pits, so that ramps are not required. The original VRTC tester employed hydraulic load cells that were connected to pressure gauges calibrated to read in force units, but these have been replaced with electronic cells such as those used in testers produced today.



Figure 6. Low-speed roller dynamometer.

In order to measure brake force distribution with such a single-axle tester, it is necessary to add a transducer to measure input to the brake system so that the front- and rear-axle brake forces can be related. The most convenient way to do this is with a pedal force transducer. This device must have relatively high resolution since brake pedal forces to be measured are relatively low. Either a ramp brake apply or a constant-input apply at various levels can be adopted. In most testing conducted by VRTC the constant-input approach has been utilized.

## Skid checks and stopping distance tests

Skid checks are simply vehicle braking tests to determine which axle locks first on a particular surface. When coupled with a non-locked wheel, minimum-stopping distance tests on the same surface, a relative measure of overall vehicle braking efficiency can be obtained. However, unless the coefficient of friction of the test vehicle's tires is known, tire properties cannot be separated from brake system properties. For example, a vehicle that has poor brake balance but good performing tires may exhibit the same stopping distance on a particular surface as a vehicle that has good brake balance and poor tires. Although it can be argued that minimum stopping distance on a particular surface is the most meaningful braking performance metric because it provides an evaluation of the stopping performance of the entire vehicle system, the fact remains that it is not necessarily an indicator of the braking efficiency metric calculated from brake force distribution. Suspension properties also exert an effect on stopping distance but do not enter into the braking efficiency calculation, which assumes the vehicle to be a rigid body on a flat road.

The skid check-stopping distance test approach determines braking performance at only one braking level per surface. In order to cover a range of braking levels it is necessary to test on several different surfaces.

The second major proposal by the U.S. for a harmonized braking regulation (FMVSS 135 Notice 4) incorporated the skid check-stopping distance approach as a method for regulating braking efficiency. This proposed rulemaking specified skid checks on two low-coefficient surfaces and stopping distance tests on one (the lower  $\mu$ ) of these surfaces. This is in addition to the stopping distance tests on a high-coefficient surface which have appeared in all proposals. NHTSA is presently considering comments (most of which express concern about definition of test surfaces and repeatability of this approach) before proceeding with additional rulemaking action for a harmonized braking regulation.

### ECE Regulation 13/Annex 13 efficiency

This approach is defined in the portion of the regulation that specifies the requirements for vehicles equipped with antilock braking systems (ABS). An identical procedure is specified in EEC Directive 71/320, Annex X. In this approach, tests are first run with brakes on only one axle at a time operational to determine the coefficient of friction of the test surface. (By determining the maximum deceleration with brakes on one axle and calculating axle normal force using rigid body equations, it is possible to calculate coefficient of friction,  $\mu$ ). Once  $\mu$  is determined, stops are made with all brakes operational and the ABS cycling on the surface to determine the resulting deceleration. The ratio of the deceleration with cycling ABS to the theoretical maximum based on  $\mu$  (i.e.,  $\mu \times g$ ) determines the braking efficiency.

This basic procedure can be applied to vehicles without ABS by simply replacing the second step with a test to

determine the maximum deceleration possible (with all brakes operational) without wheel lockup. Several stops can then be added in order to determine which axle locks first. Such an approach has been recently evaluated by VRTC and the results are presented in Reference 3. This report indicates that the procedure for determining surface coefficient (i.e., the first step in the process) does not produce results that are consistent with those measured with a traction trailer on the same surface with the same tires. Generally, the results obtained from the vehicle test are significantly lower than those obtained with a traction trailer, a device which is considered to be more accurate because it directly measures horizontal and vertical forces. The report hypothesizes that a major cause of this difference is the rigid body assumption in the calculation procedure for  $\mu$ . Since the vehicle is not a rigid body and does not operate on a perfectly smooth road during testing, axle normal forces can drop below the calculated values, and thus wheel lockup will occur at lower than expected decelerations.

Another possible way of implementing this procedure would be to replace the first step with a test to determine  $\mu$  by means of a traction trailer or other reliable friction measuring device. This would then remove the need to make the rigid body assumption.

## Comparison of Results from the Various Methods

The first four methods discussed should in theory provide comparable results because they are all designed to measure brake force distribution either directly or indirectly, and to then utilize this information with the same basic equations to calculate adhesion utilization and braking efficiency. The skid check-stopping distance method does not really produce a braking efficiency metric although it should be possible to calculate efficiency if tire/road peak  $\mu$  and brake system apply time is known for the stop. Even so, this efficiency might be different than efficiency from the first four methods because suspension performance enters into stopping performance. The final method discussed (Annex 13) appears flawed because of its inability to measure  $\mu$  accurately. If this problem could be corrected (by using a traction trailer, for example) then the efficiency should be comparable to that determined by the stopping distance method.

Although VRTC has performed tests using all six methods over the last several years, no single vehicle or group of vehicles has been subjected to all six methods in a systematic fashion. This is primarily due to the fact that the various methods have evolved and have been evaluated at different times during the harmonization process. There have been many cases, however, where two or three of the methods have been used on the same vehicle or group of vehicles and from the results of these tests it is possible to infer something about how the methods compare.

Five different vehicles, each with ten sets of burnished original equipment (OE) linings and proportioning valves,

have each been tested using three of the methods: torque transducers, RTP and low-speed roller dynamometer. Figure 7 shows the results for one of the vehicles and indicates that agreement between the three methods is quite good. Similar agreement was found on the other four vehicles.

One disadvantage with the low-speed roller tester is that because it is a static test device, it cannot be utilized for testing vehicles with load- or deceleration-sensing rear brake pressure proportioning valves; vehicle deceleration and weight transfer during braking is not simulated in a static test. This lack of weight transfer also means that vehicles with front brake bias (most passenger cars) lock their front wheels at a relatively low braking level; braking levels equivalent to those on dry pavement cannot be simulated. This is why the roller tester results in figure 7 represent lower decelerations than the RTP or torque transducers.

One concern that has been expressed about the roller tester is the fact that it measures brake performance at low speed (3 mph). In the tests of the five cars with burnished OE brakes it did not appear that brake balance at 3 mph was significantly different than at higher speeds. The RTP tests were run at 40 mph and the torque transducer tests were run at 45 mph, and they are very similar to the roller tester results at 3 mph. However, in another series of tests where the RTP and roller tester were both used on a group of 68 vehicles, many of which were different models, the RTP and roller tester results were significantly different for a number of the vehicles. Figure 8 shows an example of the level of difference that was found. Apparently some vehicles do experience a change in brake balance with speed and in such cases the results from the roller tester will not predict higher-speed performance.

The single-axle test and the RTP have both been run on a group of eleven vehicles (Reference 3) and for nine of these vehicles the two different methods produced similar results. For the remaining two vehicles, however, there were significant differences that could not easily be explained. Speed difference was not a factor as test speed was the same for both tests. Since the single-axle method is a much less direct method of measuring brake balance and it involves more steps than the RTP approach it is possible that some form of measurement errors were introduced into the single-axle test measurement process.

VRTC has not conducted any tests that would allow a direct comparison between the skid check-stopping distance approach and the other methods, but tests have been performed comparing the Annex 13 efficiency test to the RTP. Since the skid check-stopping distance approach is fundamentally the same as the Annex 13 approach (both approaches involve making stops to determine maximum deceleration on a particular surface) this comparison provides some insight as to how both of these methods would compare to the RTP.

The Annex 13 versus RTP comparison is described in Reference 3, which indicates that the two methods do not produce the same results. However, as was mentioned

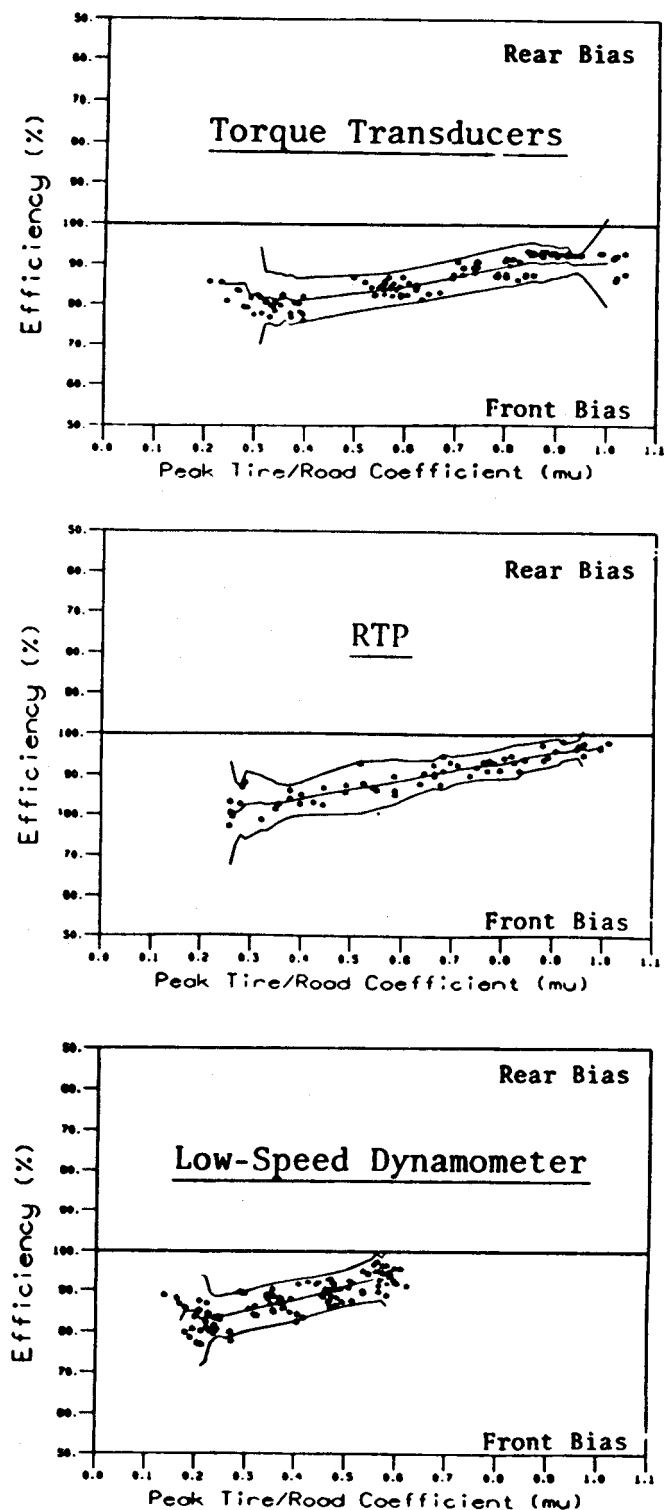


Figure 7. Comparison of torque transducer, RTP and low-speed roller dynamometer test results—one vehicle with 10 sets OE brakes.

above, the Annex 13 procedure is flawed in its method for measuring  $\mu$ . To evaluate the effect of correcting the  $\mu$  measurement problem in Annex 13, ASTM traction trailer data collected during the test program has been utilized to recalculate efficiency. Figure 9 shows the comparison between the RTP and this modified Annex 13 result for one of the three surfaces used in the test program. It can be seen

that there are still significant differences between the two methods. Similar difference exist on the other surfaces as well. Figure 9 illustrates the result of the fundamental differences between methods which measure brake force distribution and calculate efficiency from rigid body dynamics and methods which measure maximum vehicle deceleration on a particular surface and use this information along with  $\mu$  to determine efficiency.

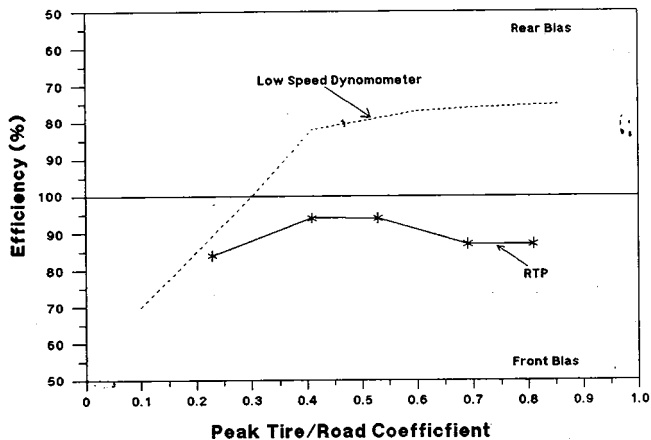


Figure 8. Example of difference between RTP and low speed roller dynamometer results as found on some vehicles.

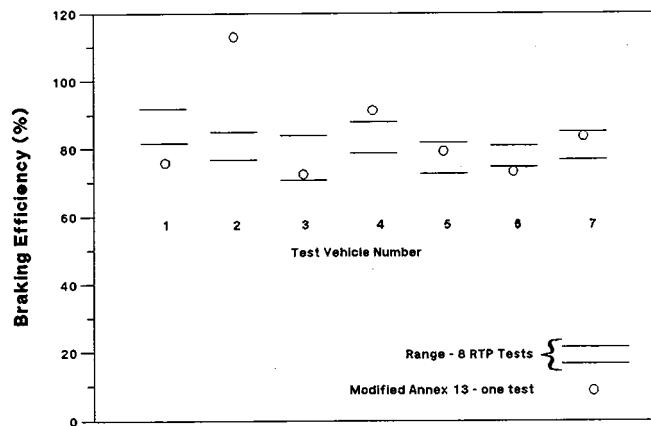


Figure 9. Comparison between RTP and Annex 13 methods (Annex 13 modified to utilize traction trailer data for  $\mu$ ).

## Summary and Conclusions

Six different approaches to measuring braking efficiency have been extensively evaluated by NHTSA/VRTC. These six methods fall into two basic categories: (1) methods which determine brake force distribution and then calculate efficiency from rigid body dynamics equations as a function of  $\mu$  (tire/road coefficient of friction) and (2) methods which determine maximum deceleration capability of the vehicle on a particular surface. In the latter category, braking efficiency can be calculated only if  $\mu$  is known.

Methods that employ torque transducers, RTP, single-axle snubs and low-speed roller dynamometers fall into the first category. Torque transducers make it possible to accurately record torque output at each brake for an entire stop. Although an assumption must be made about tire

rolling radius to convert torque to force, this does not appear to introduce any significant error. Torque transducers are relatively expensive (\$40,000 or more per vehicle), however, and adapting them to different vehicles can be difficult.

The single-axle test method measures brake forces at each axle indirectly. Measurements of the deceleration of the vehicle during a small speed change (about 5 mph) with brakes on only one axle at a time operational are used to calculate brake forces on each axle. Instrumentation required to run the test is minimal (speed vs. time and brake pressures or pedal force must be determined), and its cost is relatively low compared to the other methods. This approach requires that the vehicle's hydraulic system be "disturbed" to install shut-off valves (and pressure transducers if utilized) to enable the brakes on each axle to be disabled. Tests that have been run to compare this method to other methods indicate reasonable agreement in most but not all cases. Because it is an indirect method for measuring brake forces, it may be more susceptible to the introduction of experimental error.

Road transducer plates (RTP) measure brake forces at each wheel directly without the need for onboard instrumentation. RTP technology has been perfected to the point that measurement and data reduction process is highly automated, and a single RTP is able to test many different types of vehicles. Although the RTPs currently in operation are quite expensive (\$300,000 or more), it appears that adequate facilities could be constructed at a much lower cost (\$50,000 or less). Because the instrumented plates are seven feet long, the RTP only measures brake forces for about one full wheel revolution. It also has a somewhat restricted useful speed range (25 to 50 mph for NHTSA's RTP) but tests that have been performed indicate that the RTP measurements compare well with those from torque transducers.

Low-speed roller dynamometers are relatively low-cost (\$10,000 or less) static test devices that directly measure braking on one axle at a time at speeds less than five mph. As is the case with the single-axle procedure, a transducer must be employed to measure brake system inputs to ensure that front and rear axle results can be related and superimposed. The low-speed roller tester produces brake balance measurements that agree well with those from higher-speed tests with torque transducers and the RTP, but only when the vehicle does not have a load- or deceleration-sensing proportioning valve and only when the vehicle's brake balance does not change with speed. This limits the utility of the device, as many vehicles appear to fall into the category where the low-speed static tester will not accurately predict dynamic performance at highway speeds.

Skid checks provide a measure of brake bias, and stopping distance tests give a metric that is an indicator of a vehicle's overall stopping performance. Nevertheless, this information only applies to the particular surface that is used for the tests. Various surfaces must be utilized if the

results are to be generalized over a broad range of operating conditions (this is not the case for the first four methods, where all testing can be done on one high- $\mu$  surface). Constructing and maintaining several surfaces for testing can be a very costly proposition, but it offers a very realistic condition in terms of how the consumer will operate the vehicle. Tire/road peak  $\mu$  and brake application time must be known in order to calculate braking efficiency from stopping distance, but this value may differ from braking efficiency derived from the first four methods because of vehicle suspension effects and road roughness.

The Annex 13 approach to measuring efficiency is flawed in its technique for measuring tire/road coefficient or friction. If this problem is corrected the approach may be viable, but as is the case with stopping distance approach, a number of surfaces will be required to cover a range of braking rates. Also, for the reasons given above, the

approach will not necessarily produce the same braking efficiency as the brake force measurement-based methods.

## References

(1) Radlinski, Richard W. and Flick, Mark A., "A Vehicle Test Procedure for Determining Adhesion Utilization Properties," SAE Paper No. 840334, 1984.

(2) Wolanin, Michael J. and Baptist, Thomas A. "Road Transducer—Objective Brake Balance Measurement Without Vehicle Instrumentation," SAE Paper No. 870266, February 1987.

(3) Flick, Mark A. and Radlinski, Richard W., "Harmonization of Braking Regulations—Report Number 6: Testing to Address Surface Friction and Vehicle Braking Efficiency Comments to the SNPRM," Vehicle Research and Test Center, Final Report No. DOT HS 807 393, March 1989.

## Dynamic Analysis of Vehicle Rollover

Andrzej G. Nalecz and Alan C. Bindemann,  
University of Missouri-Columbia

Howell K. Brewer,  
National Highway Traffic Safety Administration

### Abstract

Statistical analyses of collected accident data have shown that incidents involving rollover represent a major safety concern based on both the frequency of occurrence and the severity level of occupant injury. Computer based models can be used to provide valuable insight into the dynamic behavior of vehicle rollover and determine the influence of basic vehicle design parameters on vehicle rollover propensity. This paper describes two computer based models which can be used to investigate vehicle rollover. The first of these models represents the Intermediate Tripped Rollover Simulation (ITRS). This computer simulation is capable of determining the response of a vehicle which slides laterally into a rigid curb, initiating vehicle rollover. The second model is the Intermediate Maneuver Induced Rollover Simulation (IMIRS) and is used to investigate untripped vehicle rollover accidents caused by sudden or excessive steering and braking inputs. Results obtained from each model are shown and general purpose sensitivity methods are applied to each model in order to investigate the relative influence of various vehicle design parameters on vehicle rollover propensity. The use of Rollover Prevention Energy Reserve (RPER) as a measure of vehicle stability is explained and demonstrated using each model.

### Introduction

Accidents involving vehicle rollover have been and continue to be one of the most hazardous types of vehicle accidents. The serious nature of the rollover problem is

documented in the various collections of rollover accident data compiled by the National Highway Traffic Safety Administration (NHTSA) (1-4)\*. According to data collected from the Fatal Accident Reporting System (FARS) rollover was identified as being a factor in over 20 percent of all non-collision fatalities in single vehicle accidents which occurred in 1986. Data collected using the National Accident Sampling System (NASS) in 1985 shows that 20 percent of the 18,400 fatalities which occurred that year were in accidents involving rollover, while at the same time, rollover occurred in less than 7 percent of all accidents. Several studies of accident data show a strong correlation between vehicle size and/or type and the likelihood of its involvement in a rollover accident (5-12). A report by Snyder et al. (6) shows that utility vehicles have the highest likelihood of rolling over in an accident. Other reports indicate that small utility vehicles, those having a wheelbase which is less than 100 inches, have the highest number of occupant deaths per 10,000 vehicles registered. The Insurance Institute for Highway Safety (IIHS) has concluded that the major reason behind this high death rate is associated with the propensity of small utility vehicles to rollover and eject occupants in an accident. The Institute study attributes 46 percent of all occupant deaths associated with utility vehicles to single vehicle accidents which involve rollover with ejection (7). The Institute also found that the fatality rate due to rollover in single vehicle accidents of light pickup trucks, those weighing less than 3200 pounds, and intermediate utility vehicles, those with a wheel base between 100 and 120 inches, is substantially higher than the rates associated with the different classes of passenger cars. The fatality rate associated with passenger cars in rollover accidents was found to decrease as vehicle size increased.

\*Numbers in parentheses designate references at end of paper.

Because accidents which involve rollover occur frequently and typically impart serious injuries to vehicle occupants it is both beneficial and necessary to investigate and identify the factors which contribute to rollover. In general, these issues might be related to human factors such as age, alcohol involvement, or driver reaction in an accident situation; they might also be related to environmental factors such as pavement conditions, curb profile, and embankment conditions. Finally they may be related to factors associated with vehicle design such as track width, suspension geometry, and minimum acceptable ground clearance. Research into each of these safety issues is imperative since utility vehicles and light pickup trucks make up a growing share of the American new car market and the domestic passenger car fleet continues to undergo a rapid reduction in size and weight. The results of such investigations can be used to lower the number of rollover accidents and to find ways to mitigate occupant injuries when rollovers do occur.

A considerable amount of research into the factors which influence rollover propensity attempts to find correlations between vehicle parameters such as weight, wheelbase, and track width with rollover statistics from accident data bases compiled by organizations such as NHTSA and IIHS. The Texas Transportation Research Institute (8, 9) examined rollover risk of passenger cars as a function of road type and vehicle weight and found that vehicle rollover did increase with decreasing vehicle weight. However, this study could not make any conclusions relating vehicle weight to the dynamic behavior associated with rollover since weight could simply correlate with one or more vehicle parameters such as track width, wheelbase or moments of inertia.

There have also been numerous experimental studies of rollover behavior. Habberstad, Wagner and Thomas (13) investigated the influence of occupant ejection and roof crush on occupant injury in a tripped rollover test. Calspan Corporation (14) examined the rollover behavior of a Volkswagen Rabbit on a sloping soil embankment in order to determine the effect of roadside features on rollover propensity. Prompted by litigation, American Motors Corporation performed both tripped and untripped rollover tests on a variety of vehicles in an effort to demonstrate that a wide range of vehicles could be made to rollover. More recently, several experimental tests have been performed to demonstrate the rollover stability of several popular utility vehicles. While tests of this nature can sometimes provide useful information, they frequently provide inadequate information regarding test conditions and are not always sponsored or performed by totally impartial organizations; therefore these tests must be examined critically.

Experimental tests can provide useful knowledge on the dynamic behavior of rollover accidents, but like statistical tests, they are poorly suited for determining the influence of vehicle design parameters on rollover behavior since it is often difficult to vary vehicle parameters one at a time. Experimental repeatability is also an extremely important when trying to access the influence of different design

parameters. Finally, the high costs associated with full scale rollover testing can preclude extensive parametric investigation.

Analytical investigation into the dynamic behavior of vehicles is the most effective method of determining the influence of design parameters on vehicle response. While analytical methods have found only limited use in the investigation of human factors, these methods are quite useful in the study of environmental and design factors. Computer based simulation models can be used to predict vehicle response in a variety of conditions, gain insight into the fundamental reasons behind dynamic phenomenon such as rollover, and provide information on the influence of design parameters on dynamic response.

There have been numerous analytical studies into the causes of vehicle rollover. Jones of Calspan Corporation (15) analyzed the mechanics of rollover as the result of curb impact. Calspan (16) also used its Highway Vehicle Object Simulation Model (HVOSM) to investigate the influence of roadway features on rollover. Systems Technology Incorporated (STI) (17) developed a tripped rollover model which simulated response of a vehicle which slides laterally into a curb. Later the University of Missouri-Columbia (18) used this model to analyze the influence of design parameter variations on rollover response using sensitivity models.

This paper presents an overview of current rollover research sponsored by NHTSA and being performed at the University of Missouri-Columbia. The Intermediate Tripped Rollover Simulation (ITRS) is described and demonstrated for the cases of simultaneous and oblique curb impacts. An energy based rollover stability measure known as Rollover Prevention Energy Reserve (RPER) is introduced and the influence of basic vehicle design parameters on this measure is determined using sensitivity methods. The paper also illustrates the Intermediate Maneuver Induced Rollover Simulation (IMIRS). This model can be used to investigate the rollover propensity of vehicles which are subjected to severe cornering and braking accelerations. Results obtained from the IMIRS simulation in J and S turn maneuvers are presented. Sensitivity methods are used to determine the influence of several basic vehicle design parameters on a dynamic measure of rollover stability. Finally, the paper describes the development of the Advanced Vehicle Rollover Model (AVRM).

## **Intermediate Tripped Rollover Simulation**

An extensive review of accident statistics has shown that a majority of vehicle rollovers are initiated by an excursion into a roadside feature such as a curb, ditch, or embankment. Most frequently, a driver loses control of the vehicle and it skids at a large sideslip angle when it strikes or crosses the tripping roadside feature. Vehicle contact with these roadside discontinuities can result in high levels of deceleration that generate large inertia forces which act on

the vehicle. These inertia forces generate rolling moments about the roadside discontinuity and if these moments exceed inertia couples and gravitational forces which resist vehicle roll then the vehicle will leave a four wheel stance and can rollover. The purpose of the Intermediate Tripped Rollover Simulation (ITRS) is to investigate the tripped rollover motion of a vehicle which slides into a curb. The simulation permits investigation of impacts at different sideslip angles as well as different angles of incidence with the curb. The ITRS has been used extensively to investigate rollover behavior by examining the energy exchange which occurs in tripped rollover situations.

A moderate level of detail was used during the formulation of the ITRS. This represented a compromise between an overly simplistic model which would be incapable of examining the influence of vehicle subsystem design on rollover propensity, and a highly detailed model, which would require that extensive vehicle measurements be performed in order to obtain the data required to drive the simulation. Also, because there is very little experimental investigation into the impact forces which occur when the tire and wheel contact a roadside feature it is unrealistic to develop highly detailed vehicle models until more is known about these impact forces.

Work on the ITRS was initiated after performing a sensitivity analysis (18) of an existing tripped rollover simulation (17). This rollover simulation program was intended to investigate the rollover behavior of a vehicle which was skidding, at a sideslip angle of 90 degrees, into a curb. The simulation permitted small variations in the heading angle of the vehicle as measured relative to the curb at the instant of impact. After performing the sensitivity analysis of this model it was decided that an improved tripped rollover model should be developed based on the previous one. Improvements in this new model include the addition of forward dynamics, the inclusion of all dynamic couplings in the equations of motion and the addition of a more sophisticated curb impact model. These additions permit investigation of tripped rollover accidents over a full range of vehicle sideslip angles and incidence angles with the curb.

### ITRS model description

The ITRS simulation utilizes an 8 degree of freedom model to represent the vehicle. The model (figure 1) consists of two masses, one representing the vehicle's sprung mass and a second mass which represents the combined unsprung masses of front and rear suspension systems. The masses are connected using two pins attached to the front and rear of the sprung mass which can slide in vertical slots located in the unsprung mass. The pins permit the sprung mass to move vertically relative to the unsprung mass and also allow relative rotation between the two masses. The pins represent the vehicle roll axis, whose position is determined from the kinematics of the front and rear suspension systems. The suspension model assumes that the vehicle's

roll axis is parallel to the ground and lies in the vehicle's plane of symmetry at all times. The sprung mass is attached to the unsprung mass using four springs and four viscous dampers. There are also four upper bump stops and four lower bump stops attached to the unsprung mass to prevent excessive relative motion between both masses. Each bump stop consists of an elastic element placed in parallel with a viscous damping element. The suspension model is illustrated in figure 1.

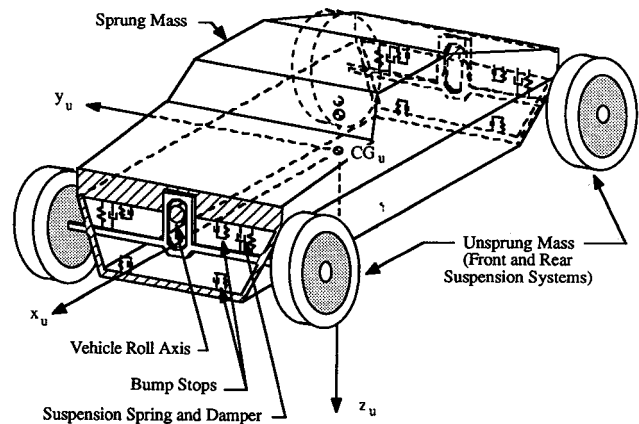


Figure 1. The ITRS vehicle model and non-inertial reference system assumed.

No planes of symmetry were assumed in the analysis, therefore all elements of the inertia matrices describing the sprung and unsprung masses were included in the equations of motion. The degrees of freedom include three angles of rotation and three linear translations of the unsprung mass, the vertical position of the sprung mass, and the roll angle of the sprung mass. The model assumes that the pitch and yaw angles of the two masses are identical. The following eight generalized coordinates are used in the model.

- q1 = x longitudinal position of unsprung mass c.g. in the absolute reference system
- q2 = y lateral position of unsprung mass c.g. in the absolute reference system
- q3 = z<sub>u</sub> vertical position of unsprung mass c.g. in the absolute reference system
- q4 = z<sub>s</sub> vertical position of sprung mass roll axis in the absolute reference system
- q5 = φ<sub>u</sub> unsprung mass roll angle
- q6 = φ<sub>s</sub> sprung mass roll angle
- q7 = θ vehicle pitch angle
- q8 = Ψ vehicle yaw angle

### Equations of motion

The equations of motion for the ITRS model were formulated using the Newton-Euler approach. Provided the origin of the non-inertial reference system attached to the rigid body (point P) is located at the body's center of mass (i.e.  $\bar{P}_c = 0$ ) or is not accelerating, the rigid body equations of motion can be written in the following form:

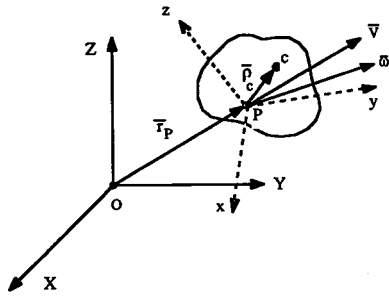


Figure 2. General rigid body motion.

$$\begin{aligned}
 F_x &= m(\dot{v}_x + v_z \omega_y - v_y \omega_z) \\
 F_y &= m(\dot{v}_y + v_x \omega_z - v_z \omega_x) \\
 F_z &= m(\dot{v}_z + v_y \omega_x - v_x \omega_y) \\
 M_x &= I_{xx} \dot{\omega}_x + I_{xy}(\dot{\omega}_y - \omega_x \omega_z) + I_{xz}(\dot{\omega}_z + \omega_x \omega_y) + (I_{zz} - I_{yy}) \omega_y \omega_z + I_{yz}(\omega_y^2 - \omega_z^2) \\
 M_y &= I_{yy} \dot{\omega}_y + I_{xy}(\dot{\omega}_x + \omega_y \omega_z) + I_{yz}(\dot{\omega}_z + \omega_x \omega_y) + (I_{xx} - I_{zz}) \omega_x \omega_z + I_{xz}(\omega_z^2 - \omega_x^2) \\
 M_z &= I_{zz} \dot{\omega}_z + I_{yz}(\dot{\omega}_y + \omega_x \omega_z) + I_{xz}(\dot{\omega}_x - \omega_y \omega_z) + (I_{yy} - I_{xx}) \omega_x \omega_y + I_{xy}(\omega_x^2 - \omega_y^2)
 \end{aligned} \quad (1)$$

If the origin of the non-inertial reference system does not satisfy either one of the two conditions listed above then the Newton-Euler equations of motion must be extended to the following form:

$$\begin{aligned}
 F_x &= m[\dot{V}_{P_x} + V_{P_z} \omega_y - V_{P_y} \omega_z + \rho_z \dot{\omega}_y - \rho_y \dot{\omega}_z + \omega_y(\omega_x \rho_y - \omega_y \rho_x) - \omega_z(\omega_z \rho_x - \omega_x \rho_z)] \\
 F_y &= m[\dot{V}_{P_y} + V_{P_x} \omega_z - V_{P_z} \omega_x + \rho_x \dot{\omega}_z - \rho_z \dot{\omega}_x + \omega_z(\omega_y \rho_z - \omega_z \rho_y) - \omega_x(\omega_x \rho_y - \omega_z \rho_x)] \\
 F_z &= m[\dot{V}_{P_z} + V_{P_y} \omega_x - V_{P_x} \omega_y + \rho_y \dot{\omega}_x - \rho_x \dot{\omega}_y + \omega_x(\omega_z \rho_x - \omega_x \rho_z) - \omega_y(\omega_y \rho_z - \omega_z \rho_y)] \\
 M_x &= I_{xx} \dot{\omega}_x + I_{xy}(\dot{\omega}_y - \omega_x \omega_z) + I_{xz}(\dot{\omega}_z + \omega_x \omega_y) + (I_{zz} - I_{yy}) \omega_y \omega_z + I_{yz}(\omega_y^2 - \omega_z^2) + m(\rho_y a_z - \rho_z a_y) \\
 M_y &= I_{yy} \dot{\omega}_y + I_{xy}(\dot{\omega}_x + \omega_y \omega_z) + I_{yz}(\dot{\omega}_z + \omega_x \omega_y) + (I_{xx} - I_{zz}) \omega_x \omega_z + I_{xz}(\omega_z^2 - \omega_x^2) + m(\rho_z a_x - \rho_x a_z) \\
 M_z &= I_{zz} \dot{\omega}_z + I_{yz}(\dot{\omega}_y + \omega_x \omega_z) + I_{xz}(\dot{\omega}_x - \omega_y \omega_z) + (I_{yy} - I_{xx}) \omega_x \omega_y + I_{xy}(\omega_x^2 - \omega_y^2) + m(\rho_x a_y - \rho_y a_x)
 \end{aligned} \quad (2)$$

where,  $\rho_x$ ,  $\rho_y$  and  $\rho_z$  represent the x, y, z components of the vector  $\vec{P}_c$  and  $a_x$ ,  $a_y$  and  $a_z$  are the x, y, z acceleration components of the non-inertial reference system origin (point P).

It should be noted that all velocity components in both sets of equations are measured in the non-inertial reference system. Also, in both sets of equations  $F_x$ ,  $F_y$ ,  $F_z$ ,  $M_x$ ,  $M_y$ , and  $M_z$  represent the x, y, z components of the external forces and moments which act on the rigid body as seen in the non-inertial reference system. In the case of interconnected multi-body systems, the bodies can be split apart and

the Newton-Euler equations can be applied separately to each of the bodies. If this approach is used then the reactions which occur at the connections between the rigid bodies must be determined. Additional equations of motion obtained from separating the system into subsystems can be used to solve for the reactions which occur at the system connections.

The ITRS model is a multi-body dynamic system in which the first body represents the unsprung mass, and the second represents the sprung mass. These bodies are interconnected through the vehicle roll axis, and by numerous spring and damping elements which comprise the suspension system. The origin of the non-inertial reference system attached to the unsprung mass is located at the unsprung mass c.g. Therefore the first form of the Newton-Euler equations (1) of motion were used to formulate the equations of motion of the unsprung mass. The origin of the non-inertial reference system attached to the sprung mass is located in the same longitudinal plane as the sprung mass c.g., however, the longitudinal axis (the x axis) of the non-inertial reference system coincides with the vehicle roll axis, and does not pass through the c.g. of the sprung mass. Since the origin of this non-inertial reference system does not coincide with the sprung mass c.g., and the origin of the system is expected to accelerate, the second form of the Newton-Euler equations of motion (2) had to be used to formulate the sprung mass equations of motion. The resulting equations include all moments and products of inertia and also include all dynamic couplings.

## External forces

The external forces which act on the vehicle include gravitational forces, the normal reactions at the wheels, the frictional forces of tires, and the impact forces which occur when the vehicle strikes the curb. The tire normal reactions are calculated using a linear spring and damping element. The normal reaction is dependent on the radial deformation of the tire, as well as the rate of radial tire deformation (index  $i = 1, \dots, 4$  is used to denote each of the four wheels):

$$\begin{aligned}
 F_{z_i} &= K_z \Delta T_{r_i} - B_z \dot{\Delta T}_{r_i} & \Delta T_{r_i} > 0 \\
 F_{z_i} &= 0 & \Delta T_{r_i} \leq 0
 \end{aligned} \quad (3)$$

The radial deformation of each tire is dependent on the vertical position, roll angle and pitch angle of the unsprung mass.

The x and y components of the tire frictional forces are computed using the following relations:

$$\begin{aligned}
 F_{x f_i} &= \mu_x F_{z_i} f_x(v_{x_i}) \\
 F_{y f_i} &= \mu_y F_{z_i} f_y(v_{y_i})
 \end{aligned} \quad (4)$$

where,  $\mu_x$  and  $\mu_y$  are the sliding coefficients of friction of the

tire in the x and y directions and  $f_x(v_{x_i})$ ,  $f_y(v_{y_i})$  represent nonlinear functions of the tire sliding velocity. These functions are introduced to insure that the frictional forces act to oppose vehicle motion and prevent the sudden reversal of tire frictional forces if velocities  $v_{x_i}$  or  $v_{y_i}$  change signs. The form of functions  $f_x(v_{x_i})$  and  $f_y(v_{y_i})$  is shown in figure 3.

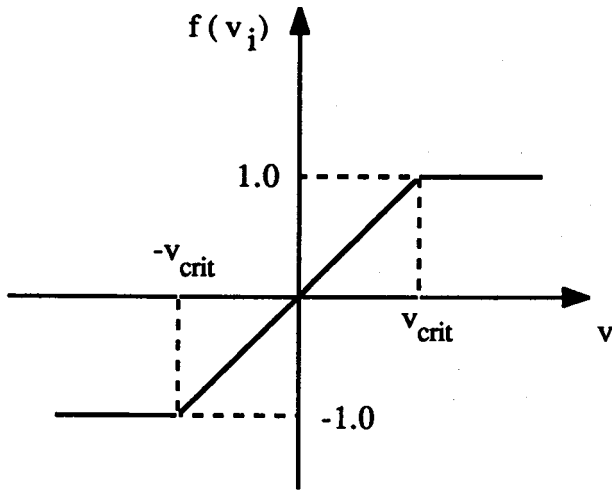


Figure 3. Velocity dependent tire frictional function.

The force which occurs when the tire comes into contact with the curb consists of two components, an impact force which is perpendicular to the curb, and a scrub force which acts parallel to the curb. The impact force is dependent on the amount of deformation as well as the time rate of change in the deformation. The deformation is determined based on the location and orientation of the vehicle relative to the curb. A force displacement curve having three linear slopes in three regions is used to determine the elastic portion of the impact force and is shown in figure 4. The first region of the force displacement curve is totally elastic and is used to represent wheel compliance. The second region represents a zone where plastic deformation occurs as the wheel and suspension elements undergo permanent crush. As the amount of deformation increases, more solid members of the vehicle such as the frame and powertrain are deformed and the third region of the curve is utilized. If the vehicle rebounds after impact the force displacement curve will unload using one of two slopes. If the deformation is totally elastic, i.e. in region I, then the force displacement curve will unload at slope  $K_1$ . If the deformation is plastic, i.e. in regions II or III, then the curve will unload at slope  $K_4$ . If plastic deformation does occur then the amount of permanent deformation is noted and the force deformation curve will reload using slope  $K_4$  on subsequent impacts. Thus in subsequent impacts the impact force is computed as a function of previous plastic deformation.

The portion of the impact force which is dependent on the time rate of change in the deformation is modelled using a viscous damping characteristic. The force component which is dependent on deformation and the force component dependent on the rate of deformation are added together to obtain the total impact force.

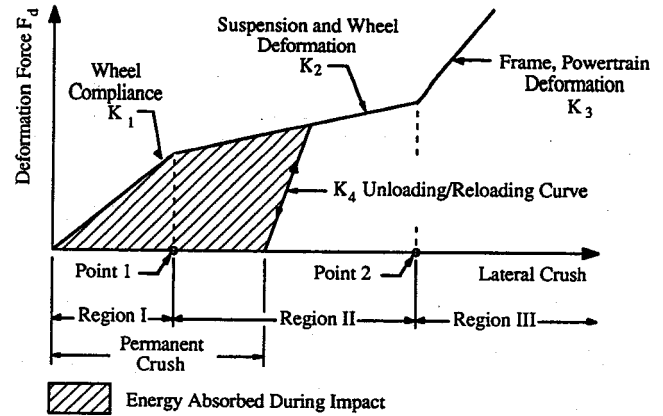


Figure 4. Force deflection characteristic used in the ITRS for curb impact.

The scrub force which is generated during a curb impact is determined using the following relationship:

$$F_{\text{scrub}_i} = \mu_s F_{\text{impact}_i} f(v_{X_i}) \quad (5)$$

where,  $\mu_s$  represents the tire friction coefficient along the curb,  $F_{\text{impact}_i}$  is the impact force normal to the curb, and  $f(v_{X_i})$  represents a non-linear function of the tire's scrub velocity shown in figure 5.

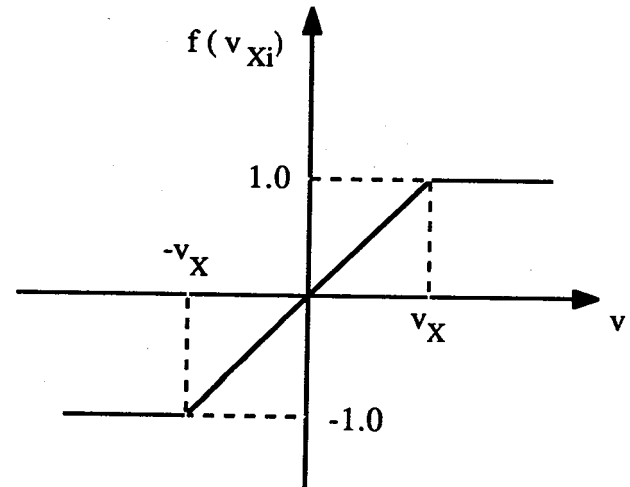


Figure 5. Velocity dependent tire scrub force function.

### Energy based rollover stability criteria

In order to analytically investigate the influence of design parameters on a vehicle's rollover stability, decisions must be made regarding the criteria which will be used to quantitatively measure vehicle rollover stability. One widely used rollover stability criteria known as the Static Rollover Stability Factor (SRSF) is defined:

$$\text{SRSF} = \frac{\text{Track Width}}{2 \text{ Height}_{\text{cg}}} \quad (6)$$

As shown above, the SRSF is a function of two easily measured vehicle parameters and, as the name implies, is a purely static measure of rollover stability. Because of its simplicity, the SRSF cannot be used to determine the influ-

ence of vehicle design parameters on the dynamic rollover behavior and has mainly been used in statistical studies which attempt to find correlations between SRSF and rollover propensity.

Vehicle rollover is essentially a problem associated with stability. In a rollover situation, a vehicle which generates small roll angles will return to a four wheel stance and is considered stable, however at larger roll angles the vehicle can tip over and is considered unstable. Classical stability theory states that the stability of a system's equilibrium position can be investigated based on the change of the system's potential energy caused by small perturbations of its stated variables. If this change is positive then the system is stable, if negative then the system is unstable. For example, when a vehicle has a roll angle of zero an increase in the roll angle raises its center of gravity position, thus increasing the potential energy of the system, which indicates that the initial position is stable. However, when a vehicle's roll angle equals the static tip over angle then increasing the roll angle will lower the center of gravity position and decreases the system's gravitational potential energy, making the system unstable. The example illustrated above refers to stability of an equilibrium position and could be extended to the more general case of stability of motion. However, this would necessitate investigation into complex and difficult issues related to dynamic analysis (Nalecz (19), (20)). While it is not always practical to perform a classical stability analysis on a complex, non-linear dynamic model it is possible to gain useful information on vehicle response and stability by examining the time history of the vehicle's kinetic and potential energies.

In a majority of tripped rollover accidents, a vehicle's kinetic energy before impact with the tripping obstacle is largely translational. As a result of impact a portion of this translational energy is converted into rotational kinetic energy. If the vehicle gains enough rotational kinetic energy it will roll past its static tip over angle, which represents an unstable equilibrium position. At this point gravitational force acting on the vehicle begins to exert a destabilizing influence, rather than stabilizing, and will pull the vehicle over.

The concept of Rollover Prevention Energy Reserve (RPER) was first introduced by Nalecz et al. (18) and was used as a measure of vehicle rollover stability in the sensitivity analysis of a tripped rollover model. This energy based stability measure examines the difference between the potential energy required to bring the vehicle to the static tip over position and the rotational kinetic energy of the vehicle created as a result of vehicle impact with the curb. If the vehicle has a sufficient amount of rotational kinetic energy to raise the vehicle to its static tip over position and overcome any energy dissipation which might reduce rotational kinetic energy then RPER will become negative, and rollover will occur. RPER is dependent on both static factors such as track width and center of gravity height, and is also dependent on the dynamic response of the vehicle. This makes the time history of RPER dependent on

vehicle and environmental parameters as well as the initial conditions of the tripped rollover test. The utilization of RPER in analysis enables determination of the influence of all vehicle design and environmental characteristics on vehicle rollover propensity using a time varying measure of dynamic stability.

During the development of the ITRS the first RPER function (described in (18)) was refined to account for the change in the elastic potential energy of the suspension system and tires as well as to include the effect of suspension crush on the center of gravity position at the static tip over angle. This new measure of RPER was designated RPER3 and is described in (27).

### Sensitivity analysis

A vehicle's dynamic system and subsystems (suspensions, brakes, and steering for example) are comprised of many elements whose characteristics directly or indirectly affect its dynamic response. Understanding how design characteristics affect a vehicle's dynamic response is a fundamental step in the design process. Unfortunately, the influence of system parameters on a vehicle's response in a particular maneuver is not always obvious. Sensitivity methods can be used to determine the influence of any vehicle design parameter on its dynamic response, making them very useful in the analysis and synthesis of a complex mechanical system (23-26).

There are various types of sensitivity measures which can be used to investigate the influence of design parameters on vehicle response. These include first order standard, first order percentage, first order logarithmic, and second order standard sensitivity functions (26).

The first order standard sensitivity function is equal to the partial derivative of a system variable taken with respect to a particular system parameter and is useful for determining the influence of a single design parameter on a particular system variable. The first order percentage sensitivity function is calculated by finding the variable change associated with a parameter change of some user specified percentage. Percentage sensitivity functions are useful for comparing the influence of several parameters on a particular system variable. For example, if a designer wished to investigate whether a 2% increase in track width would influence the vehicle's roll angle more than a 2% reduction in center of gravity height then percentage sensitivity could be used. The first order logarithmic sensitivity function is determined by multiplying the first order standard sensitivity function by the parameter value and dividing this product by the variable value. Logarithmic sensitivity functions are dimensionless, making them useful when comparing and ranking the influence of various parameters on system variables. Second order sensitivity functions are determined by calculating the second partial derivative of a system variable with respect to a system parameter. Second order sensitivity functions can be used to gain additional insight into sensitivity results when two or more parameters exhibit

similar first order sensitivity. Table 1 summarizes each sensitivity function.

**Table 1. Summary of different sensitivity functions.**

Sensitivity Type	Analytical Expression	Numerical Expression	Units
1st Order Standard	$\frac{\partial V}{\partial P}$	$\frac{\Delta V}{\Delta P}$	$\frac{V}{P}$
1st Order Percentage	$\frac{\delta V}{\delta P} \delta P$	$\Delta V$	V
1st Order Logarithmic	$\frac{\partial V}{\partial P} \frac{P}{V}$	$\frac{\Delta V}{\Delta P} \frac{P}{V}$	None
2nd Order Standard	$\frac{\partial^2 V}{\partial P^2}$	$\frac{\Delta (\frac{\Delta V}{\Delta P})}{\Delta P}$	$\frac{V}{P^2}$

### ITRS results

The initial conditions which must be supplied to the ITRS simulation include the vehicle heading angle measured relative to the curb, the initial distance of the vehicle from the curb (measured from the front right tire), and initial velocity of the vehicle center of mass (figure 6).

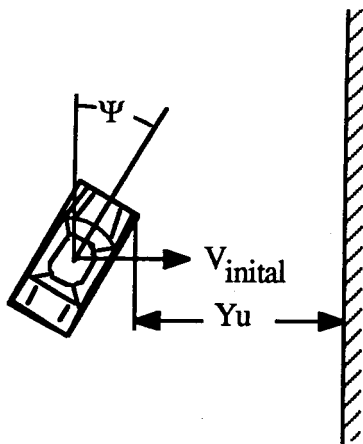


**Figure 6. Initial conditions used in intermediate tripped rollover simulation.**

The time histories of RPER obtained from the ITRS simulation using data typical of a full size passenger vehicle are illustrated in figures 7 and 8. Figure 7 shows the RPER of a vehicle initially located 7.5 feet from the curb ( $Y_u = 7.5$  feet) and parallel to the curb ( $\psi = 0$ ). These initial conditions produced simultaneous front and rear wheel contact with the curb. RPER was computed using initial velocity values of 17, 20, 22.13, 25 and 27 ft/s. In the 17 ft/s case the vehicle came to a stop before reaching the curb and vehicle impact occurred in all cases with initial speeds higher than 47 ft/s. The instant of vehicle impact with the curb can be identified on each curve at the point where RPER begins to decrease. The initial velocity of 23.13 ft/s was found to be the threshold speed for tripped rollover in simultaneous impact cases. For initial speeds smaller than 23.13 ft/s vehicle rollover did not occur and the RPER curves for these speeds always remained positive. However, the results obtained using initial velocities greater than or equal to 23.13 ft/s resulted in

rollover and the RPER reached negative values. At 23.13 ft/s the minimum value of RPER is only slightly negative, but as the speed increases the minimum values of RPER become strongly negative. These results indicate that RPER is a very useful dynamic function for assessing the rollover potential of a vehicle in a simultaneous tripped rollover situation.

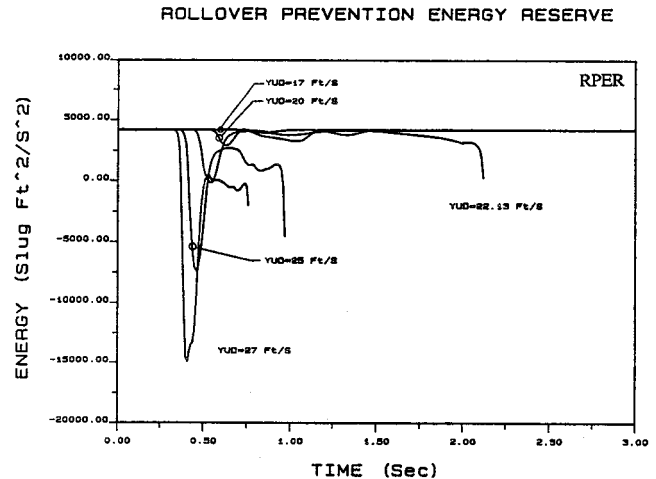


**Figure 7. RPER of ITRS in simultaneous impact case ( $\psi = 0$  degrees).**

The curves shown in figure 8 illustrate the RPER of a vehicle which is initially located 7.5 feet away from the curb ( $Y_u = 7.5$  ft) and has an initial yaw angle  $\psi = 25$  degrees. The values of RPER were computed using initial velocities of 17, 20, 23.73, 25 and 27 ft/s. As before, the vehicle came to a stop prior to impact with the curb in the 17 ft/s case. Rollover occurred in the 23.73, 25 and 27 ft/s cases, however, the 20 ft/s case did not result in rollover. The initial velocity of 23.73 ft/s was found to be the rollover threshold speed for the initial conditions of this oblique impact. In the oblique impact the minimum value of RPER at the rollover threshold speed falls below the minimum value of RPER which occurs in the simultaneous impact case. This is because when the vehicle strikes the curb at a positive oblique angle the front wheels of the vehicle strike the curb first, the vehicle then yaws until the rear wheels strike the curb, and then the vehicle rolls over. A palpable amount of energy is dissipated during the time period between the front and rear wheel impacts and the vehicle must possess enough excess kinetic energy to overcome this dissipation if a rollover is to occur.

The sensitivity methods developed by the University of Missouri-Columbia (Nalecz and Bindemann (21, 22)) have been utilized to determine the influence of various vehicle design parameters on the time history of a vehicle's RPER in tripped rollover maneuvers. The sample sensitivity results presented in figures 9-12 have been obtained in simultaneous impact at the rollover threshold speed of 22.13 ft/s. The percentage sensitivity functions which have been chosen for analysis represent the variable change caused by a 1 percent parameter change and can be interpreted in the following manner. If the percentage sensitivity function is positive then this indicates that an increase the parameter

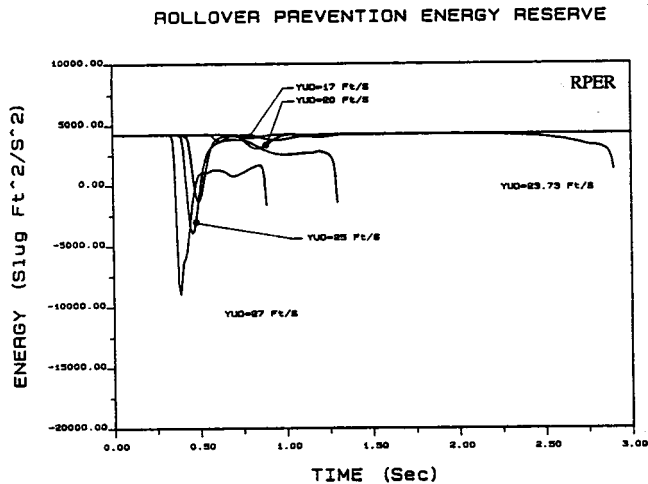


Figure 8. RPER of ITRS in oblique impact case ( $\psi=25$  degrees).

value results in an increase in the variable, which in this case, is RPER. If the sensitivity function is negative this indicates that an increase of the parameter value will decrease the variable value.

The time period on these sensitivity graphs which provides the greatest amount of information on how parameter changes can influence the rollover propensity of a vehicle begins at the start of the curve ( $t=0$ ) and ends at the point of rollover initiation. This paper designates the point of rollover initiation as the instant when RPER becomes negative.

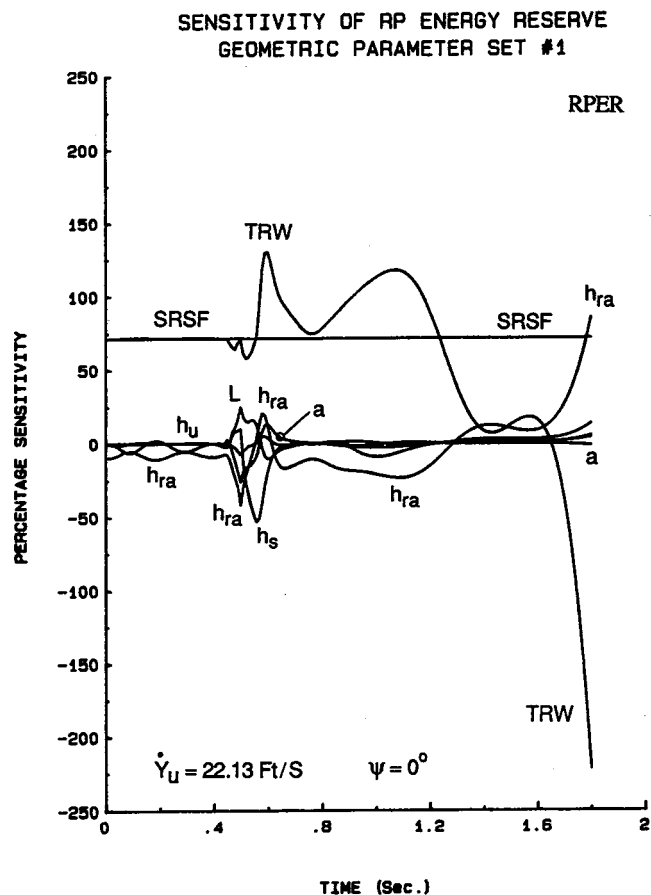


Figure 9. Sensitivity of ITRS RPER for geometrical parameters set No. 1.

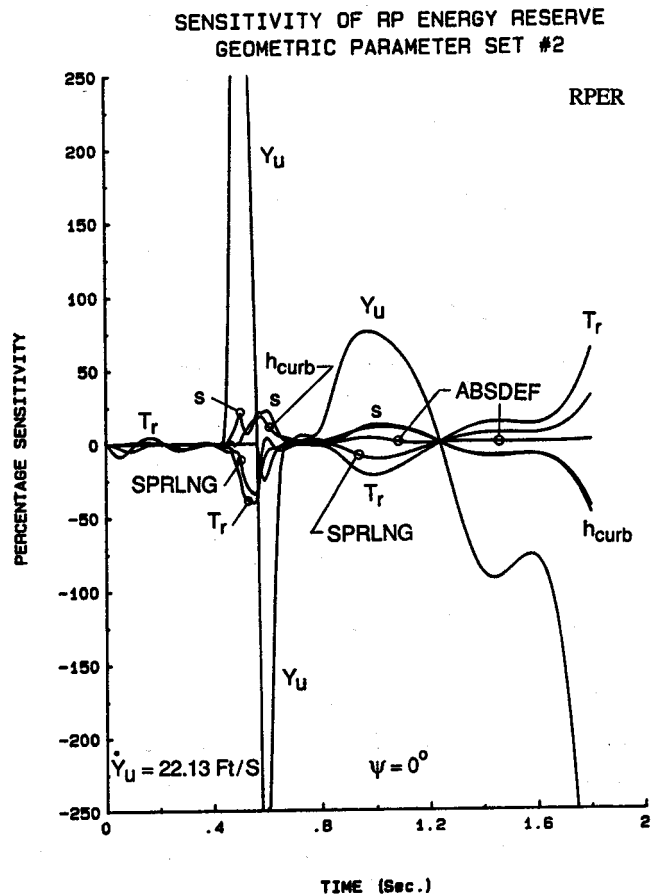


Figure 10. Sensitivity of ITRS RPER for geometrical parameter set No. 2.

For the initial conditions used to generate the sensitivity functions shown in figures 9–12 the point of rollover initiation occurs at approximately 0.58 seconds. The primary reason for limiting the analysis to this time period is this; what happens to the vehicle in this time period determines whether or not rollover will occur.

Figures 9 and 10 show the influence of geometric parameters on RPER. The most important parameters in figure 9 are the track width TRW and the static stability rollover factor SRSF. Because the SRSF is a purely static measure of rollover stability its sensitivity function remains constant and does not change with time. Track width TRW, however, does exert a dynamic influence on the system and its sensitivity function changes with time. The results show that vehicle rollover stability can be increased by increasing the vehicle track width (and therefore its static stability rollover factor). The influence of other parameters in figure 9 are much smaller than those of TRW and SRSF.

Figure 10 shows that the initial distance from the curb  $Y_u$  has a very large influence on RPER and that increasing  $Y_u$  results in a very large transient increase of RPER. The reason for positive values of sensitivity functions of  $Y_u$  is that a vehicle which is farther away from the curb must slide a longer distance before impact, and therefore it will dissipate a greater amount of its translational kinetic energy before impact and will strike the curb at a lower speed than a vehicle which begins its motion closer to the curb. However,

SENSITIVITY OF RP ENERGY RESERVE  
MASS PARAMETER SET

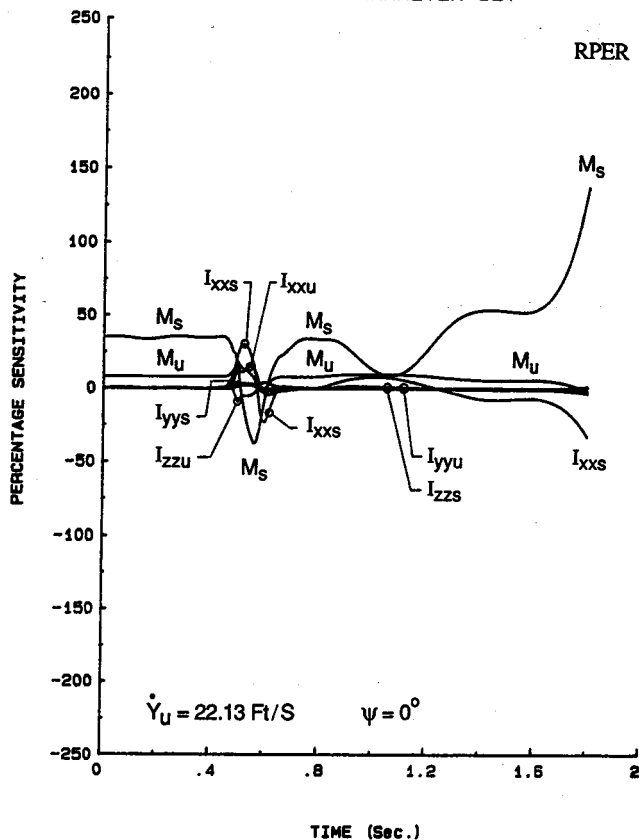


Figure 11. Sensitivity of ITRS RPER for mass/inertia parameter set.

the transient behavior (and relatively large values) of the sensitivity function increase is caused by the nature of the sensitivity methods used in this analysis (see Nalecz and Bindemann (21, 22)). Other influential parameters on figure 10 are the undeformed suspension spring length SPRLGN and tire radius  $T_r$ . The figure indicates that increasing either of these parameters will decrease RPER, which is very reasonable since increasing  $T_r$  or SPRLGN parameters has a secondary effect of raising the vehicle center of gravity.

Figure 11 illustrates the influence of vehicle mass and inertia parameters on RPER. The figure shows that increasing the sprung mass initially increases the vehicle's RPER, however, after impact the sprung mass exerts a negative influence on RPER. This is because after impact the inertia force of the vehicle tends to rotate the vehicle about the curb, and therefore a larger sprung mass will produce a larger inertia force as a result of impact. The increases of the roll moments of inertia of sprung and unsprung masses  $I_{xxs}$  and  $I_{xxu}$  produced increases of vehicle RPER during impact, which was expected, since the roll moments of inertia oppose the roll acceleration of the vehicle.

The influence of impact and force parameters on vehicle RPER is illustrated in figure 12. As seen in this figure the pavement friction coefficient  $\mu_y$  exerts a strong positive influence on RPER. This is logical since the majority of kinetic energy which is lost prior to impact with the curb is

SENSITIVITY OF RP ENERGY RESERVE  
FORCE PARAMETER SET

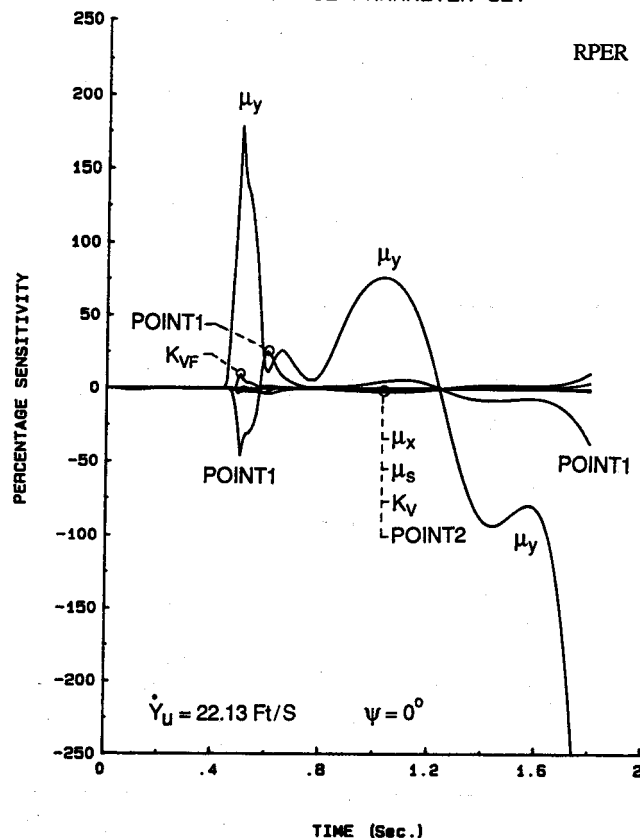


Figure 12. Sensitivity of ITRS RPER for force parameter set.

dissipated by the frictional forces generated by the tires. A higher friction coefficient will produce higher friction forces and the loss of additional kinetic energy prior to impact, resulting in lower impact speeds. Figure 12 also shows that increasing the elastic region of the impact force deformation curve (Point 1, figure 4) will decrease vehicle RPER. Because plastic deformation during impact will dissipate a portion of the vehicle's kinetic energy plastic deformation helps to reduce the risk of rollover and the onset of plastic deformation can be hastened by reducing the size of the elastic deformation region.

### Intermediate Maneuver Induced Rollover Simulation

In the past, there has been a considerable amount of debate and controversy surrounding the phenomenon of maneuvered induced rollover. These are rollover accidents which typically occur on smooth pavement and are initiated by driver steering and braking inputs, rather than an excursion into a roadside feature. While maneuver induced rollover accidents occur infrequently in comparison to tripped rollover accidents, it is justifiably argued that a vehicle should not rollover as a result of steering and braking inputs which might occur in a collision avoidance situation. Much of this controversy centers around off-road utility vehicles and light pick-up trucks. Critics of these vehicles claim that the high ground clearances associated with these vehicles

result in a high center of gravity, and increase their rollover propensity.

The Intermediate Maneuver Induced Rollover Simulation (IMIRS) developed by Nalecz (28) can be used to investigate vehicle maneuver induced rollover as well as limit handling maneuvers. The IMIRS represents an extension of the Lateral Weight Transfer Simulation (LWTS) described in (29). Like the ITRS the IMIRS utilizes a vehicle model of intermediate detail, which requires a modest amount of vehicle data and computation time.

### IMIRS model description

The IMIRS simulation utilizes two coupled vehicle dynamic models to simulate handling and rollover behavior; an illustration of each model is given in figures 13 and 14. The vehicle handling model has 3 degrees of freedom, while the rollover model is a 5 degree of freedom model.

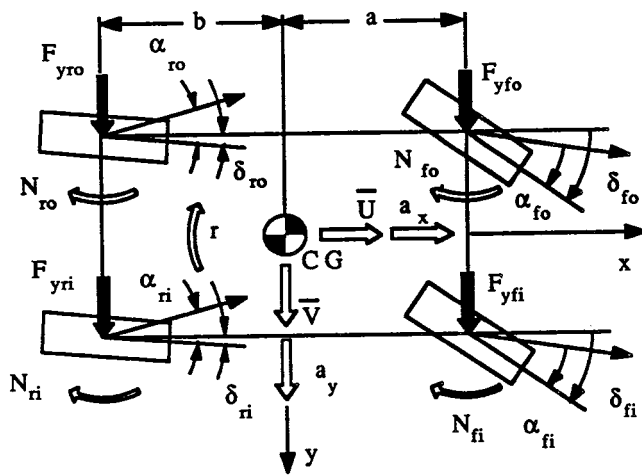


Figure 13. IMIRS handling model.

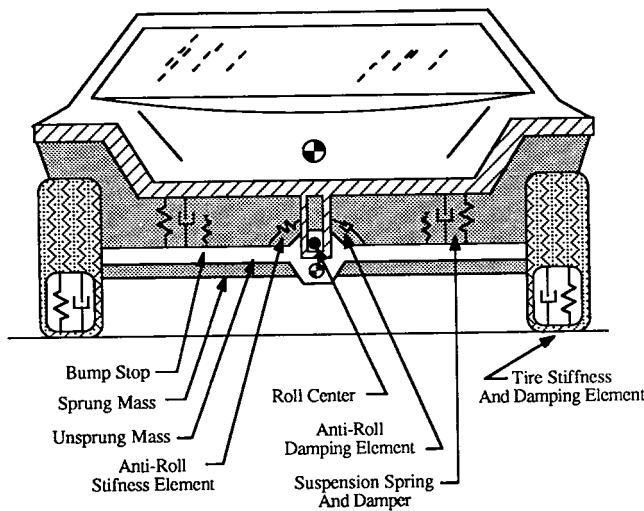


Figure 14. IMIRS rollover model.

The generalized velocities used in the handling model are forward velocity  $U$ , lateral velocity  $V$  and yaw rate  $r$ . The equations of motion employed in the vehicle handling model have been obtained from the Newton-Euler formulation: The external forces and moments which act on the IMIRS

$$\Sigma F_x = m (\dot{U} - r V)$$

$$\Sigma F_y = m (\dot{V} + r U) \quad (7)$$

$$\Sigma M_z = I_z \dot{r}$$

handling model are those generated by pneumatic tires, gravitational and aerodynamic effects. A non-linear tire model based on the non-dimensional slip angle approach was employed in the simulation. The tire model determines the side force, braking force, and aligning moment generated by a tire in combined cornering and braking maneuvers based on the conditions of normal load, longitudinal slip, slip angle, and camber angle which are imposed on the tire. Example plots of side force versus slip angle and braking force versus slip ratio are shown in figures 15 and 16.

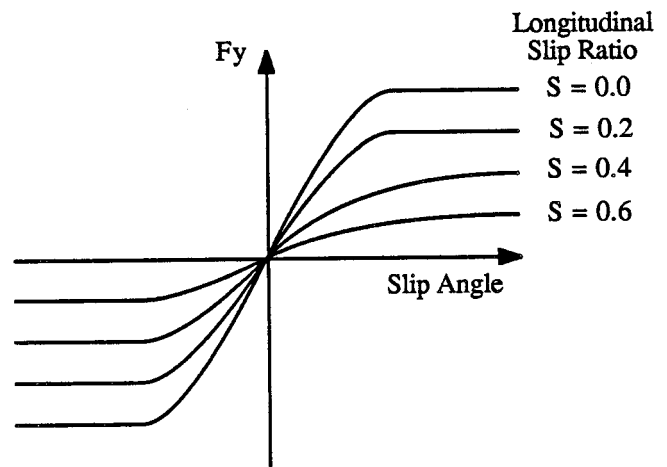


Figure 15. Tire side force versus slip angle in IMIRS simulation.

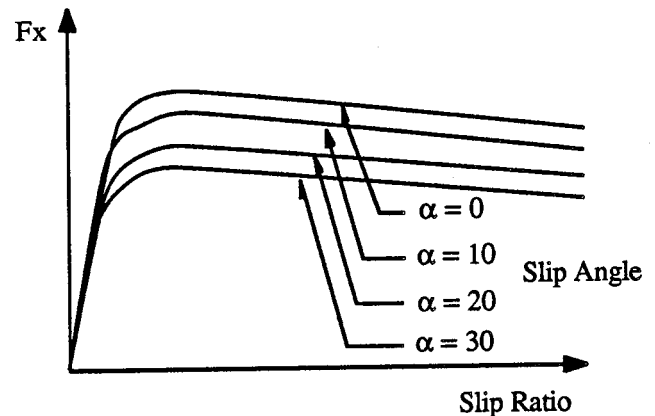
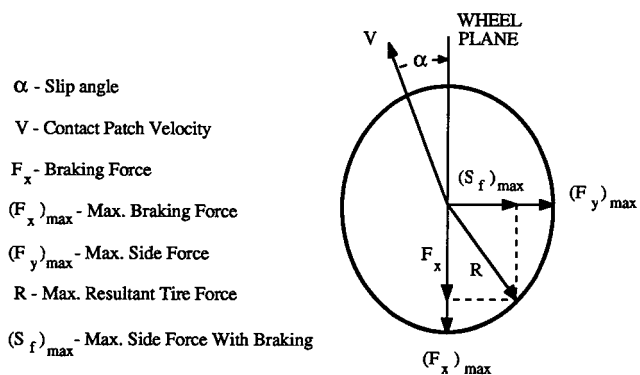


Figure 16. Tire braking force versus slip ratio in IMIRS simulation.

If the applied brake torque exceeds the frictional torque produced by the force generated at the tire/pavement interface then the tire is assumed to become locked and the sliding frictional force is assumed to act in a direction opposite the tire's direction of motion. If the applied thrust torque exceeds the tires traction ability then the tire is assumed to begin spinning and the tire thrust force acts in the direction

of the wheel plane. The friction ellipse is used to determine the tire limits of adhesion in all directions and is shown in figure 17.



- $\alpha$  - Slip angle
- V - Contact Patch Velocity
- $F_x$  - Braking Force
- $(F_x)_{max}$  - Max. Braking Force
- $(F_y)_{max}$  - Max. Side Force
- R - Max. Resultant Tire Force
- $(S_f)_{max}$  - Max. Side Force With Braking

**Figure 17. Friction ellipse in combined cornering and braking conditions.**

The size and aspect ratio of the ellipse is dependent on the peak braking and cornering friction coefficients, pavement conditions, and tire normal load. The IMIRS tire model uses Calspan tire data to determine the following tire characteristics:

- Cornering Stiffness
- Camber Stiffness
- Peak Cornering Friction Coefficient
- Peak Braking Friction Coefficient
- Sliding Friction Coefficient
- Slip Ratio at Peak Braking
- Aligning Moment

These characteristics are computed as functions of tire normal and side loads. The aerodynamic side force together with aerodynamic yaw damping are also included in the model.

In order to investigate untripped vehicle rollover behavior, a vehicle rollover model has been added to the IMIRS to work in conjunction with the handling model. It is a planar model and consists of two masses, sprung and unsprung, which are connected through the various elements of the suspension system. The rollover model is coupled to the vehicle handling model through the external forces which are applied to the planar model. These forces include the side forces generated by the tires, the inertial forces acting on the sprung and unsprung masses, and gravity. The degrees of freedom used in the IMIRS rollover model include:

- $\phi_u$ —Roll angle of the unsprung mass
- $y_u$ —Lateral displacement of the unsprung mass center of gravity
- $z_u$ —Vertical location of the unsprung mass center of gravity
- $\phi_s$ —Roll angle of the sprung mass relative to the unsprung mass
- $z_s$ —Heave of sprung mass relative to the unsprung mass

The equations of motion of the rollover were derived using the Lagrangian formulation (28).

The suspension system used in the rollover model is similar to that used in the ITRS and is illustrated in figure 14. The sprung mass motion is constrained using a pin which slides in a vertical slot in the unsprung mass. Two linearly elastic springs and viscous dampers support the sprung mass. Bump stops limit the relative motion of the sprung mass in roll and heave. These bump stops are modelled using non-linear, hardening springs which become infinitely stiff if compressed to zero length. The front and rear tires are combined at the left and right sides of the vehicle and are modelled using a linearly elastic spring placed in parallel with a viscous damping element.

**IMIRS rollover prevention energy reserve**

Rollover prevention energy reserve was used in the ITRS simulation as a dynamic measure of vehicle stability in tripped rollovers. The concept of RPER has also been applied to the IMIRS to assess vehicle stability in maneuver induced rollover situations. The formulation of RPER used in the IMIRS differs slightly from that used in the ITRS because of the differences between the two maneuvers. The IMIRS determines RPER by subtracting the kinetic energy of vehicle rolling motion, obtained from the Lagrangian formulation of the rollover model, from the amount of potential energy required to raise the vehicle center of gravity from its instantaneous position to the static tip over position. This measure of RPER is designated RPER<sub>a</sub>.

**Results obtained from IMIRS**

The IMIRS was used to simulate a J-turn maneuver using vehicle data typical of a small off-road utility vehicle. This maneuver simulates a vehicle being driven in a straight line at 58.67 ft/s (40 miles per hour) and given a ramp steering wheel input of 240 degrees in 0.5 seconds. The steering wheel was then held stationary. The pavement conditions used in the simulation had a moderately high coefficient of friction (SN = 110). A high coefficient of friction was chosen so that the vehicle could generate a value of lateral acceleration sufficient to cause rollover. If the road surface had a low coefficient of friction, such as that of wet pavement, then the vehicle would tend to skid or spin out rather than rollover. The roll angle of the unsprung mass as well as the roll angle of the sprung mass measured relative to the unsprung mass are shown in figure 18.

The time history of RPER<sub>a</sub> obtained in the J-turn maneuver is presented in figure 19. The shape of this RPER curve is qualitatively different from the characteristic shape produced in the tripped rollover cases. These dissimilarities are caused by fundamental differences between tripped and maneuver induced rollover behavior. RPER in its most basic form represents the change in potential energy required to raise the vehicle center of gravity to the static tip over position minus the rotational kinetic energy of the vehicle. In the case of tripped rollover the rotational kinetic energy of the vehicle reaches a maximum value shortly after impact with the curb and then decreases as the vehicles rotate to the static tip over angle. In maneuver induced rollover acci-

dents the rotational kinetic energy of the vehicle tends to increase continuously.

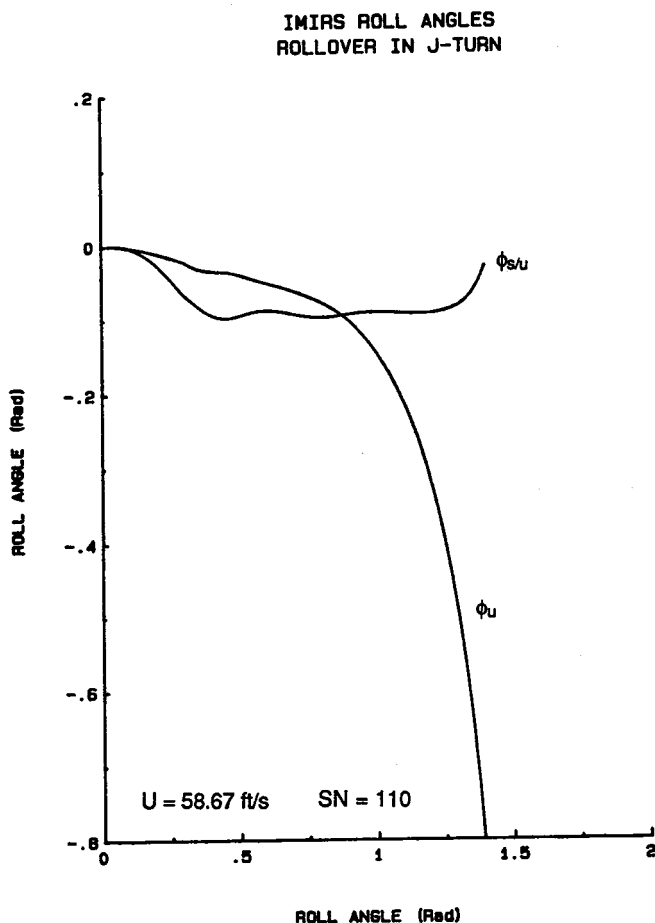


Figure 18. IMIRS vehicle roll angle in J-turn rollover.

The sensitivity of vehicle  $RPER_a$  to selected parameter groups in the 40 mile per hour J-turn maneuver has been performed utilizing percentage sensitivity functions. The influence of two groups of vehicle geometrical parameters on  $RPER_a$  is shown in figures 20 and 21. Figure 20 indicates that an increase of the sprung mass center of gravity height decreases vehicle  $RPER_a$ , while an increase in the front and rear track widths increases  $RPER_a$ . The influence of geometrical parameter set #2 is shown in figure 21 from which it is seen that  $RPER_a$  can be raised by increasing spring track widths. Changes in front and rear roll center heights  $RC_f$  and  $RC_r$ , static suspension spring length  $SPRLNG$ , and undeformed bump stop length  $BSLNG$  appear to have very little effect on  $RPER_a$  in the J-turn maneuver induced rollover. The most influential geometrical parameters appear to be, in order of importance, sprung mass center of gravity height, front and rear track width, suspension spring track width, the distance from the front axle to the vehicle c.g. a, and the unsprung mass center of gravity heights  $H_{UF}$  and  $H_{UR}$ .

The influence of vehicle mass/inertia parameters on  $RPER_a$  is presented in figure 22. The results show that the sprung mass initially has a beneficial effect, however, when the vehicle begins to roll an increase in the sprung mass

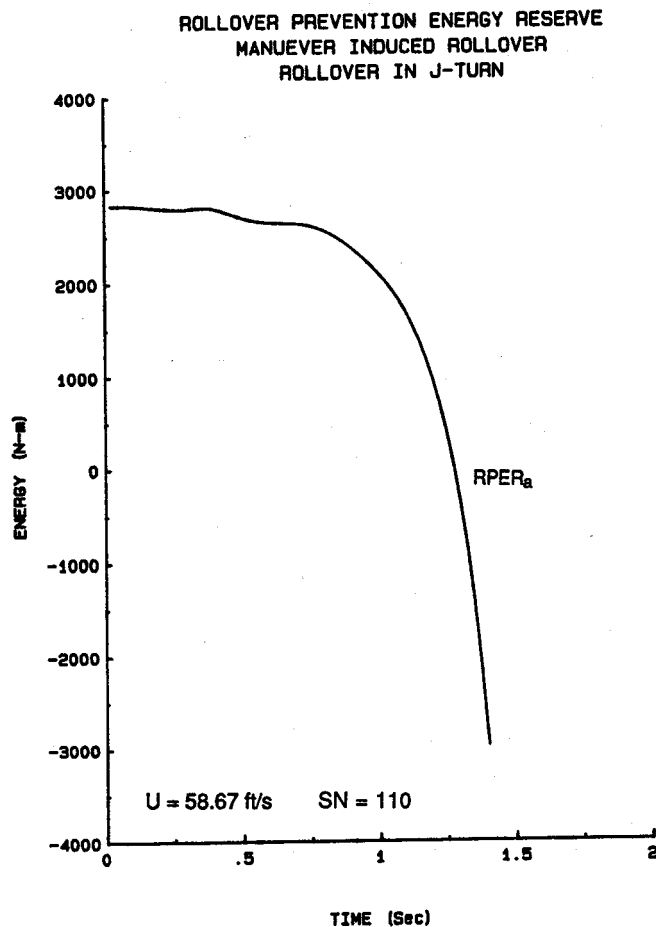


Figure 19. IMIRS vehicle  $RPER_a$  in J-turn rollover.

reduces  $RPER_a$ . Increases in the unsprung masses ( $M_{uf}$  and  $M_{ur}$ ) and yaw moment of inertia  $I_{zz}$  seem to have a positive influence on  $RPER_a$ , however, an increase of the sprung mass roll moment of inertia  $I_{xxs}$  tends to reduce  $RPER_a$ . This seems to contradict the results obtained from the sensitivity analysis of the ITRS where an increase in the vehicle roll moment of inertia raised vehicle  $RPER$ . One reason for this difference is that in the maneuver induced rollover the sprung mass roll acceleration changes signs as the sprung mass rolls to the outside and is then stopped by the suspension elements which oppose this motion. Since inertia tends to oppose acceleration it may exert a negative influence in a maneuver induced rollover. The figure also shows that shifting the vehicle weight distribution toward the rear of the vehicle increases  $RPER_a$ , in agreement with the sensitivity of parameter as shown on figure 20.

The sensitivity of  $RPER_a$  to changes in the stiffness parameters is illustrated in figure 23. The figure shows that  $RPER_a$  can be increased by increasing the stiffness of the suspension springs and tires  $K_1$  and  $K_2$  and by shifting the vehicle roll stiffness distribution  $KR_{dist}$  toward the front of the vehicle. The stiffness of the bump stops  $K_2$  as well as the auxiliary roll stiffness contribution from anti-roll bars  $K_{rf}$  and  $K_{rr}$  had little influence on vehicle  $RPER_a$  in the rollover induced by the J-turn.

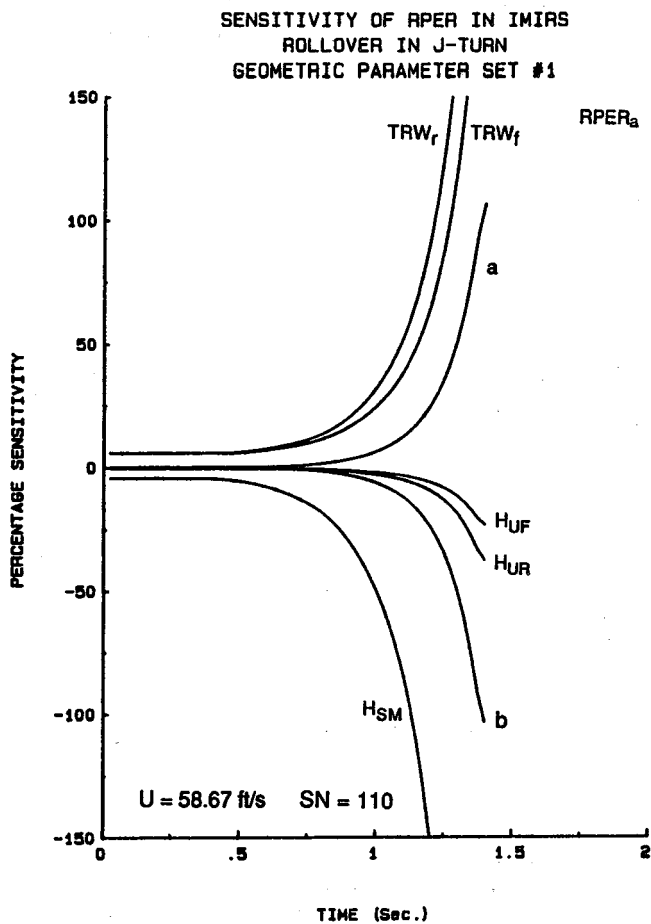


Figure 20. Sensitivity of IMIRS  $RPER_a$  for geometrical parameter set No. 1.

## An Overview of the Advanced Vehicle Rollover Model (AVRM)

The University of Missouri-Columbia is currently in the process of developing a complex simulating program (30) which will be capable of providing detailed analysis into all of the most common types of rollover accidents. The Advanced Vehicle Rollover Simulation (AVRM) will be able to simulate maneuver induced rollovers, as well as rollovers caused by vehicle excursions into roadside features such as curbs, soft soil, and embankments. The vehicle model assumed in the AVRM simulation has 14 degrees of freedom. The sprung mass has 6 degrees of freedom, three translational and three rotational. Each suspension system has 2 degrees of freedom and each wheel has a rotational degree of freedom. All phases of various rollover events will be simulated including pre-rollover motion, rollover initiation, rollover and post impact motion. The simulation will be able to provide an estimate of rollover impacts severity using a sprung mass/ground impact model.

The AVRM will be capable of simulating virtually any type of independent suspension system through an equivalent swing arm suspension model (figure 24). The pivot point of each swing arm is placed at the wheel's instant

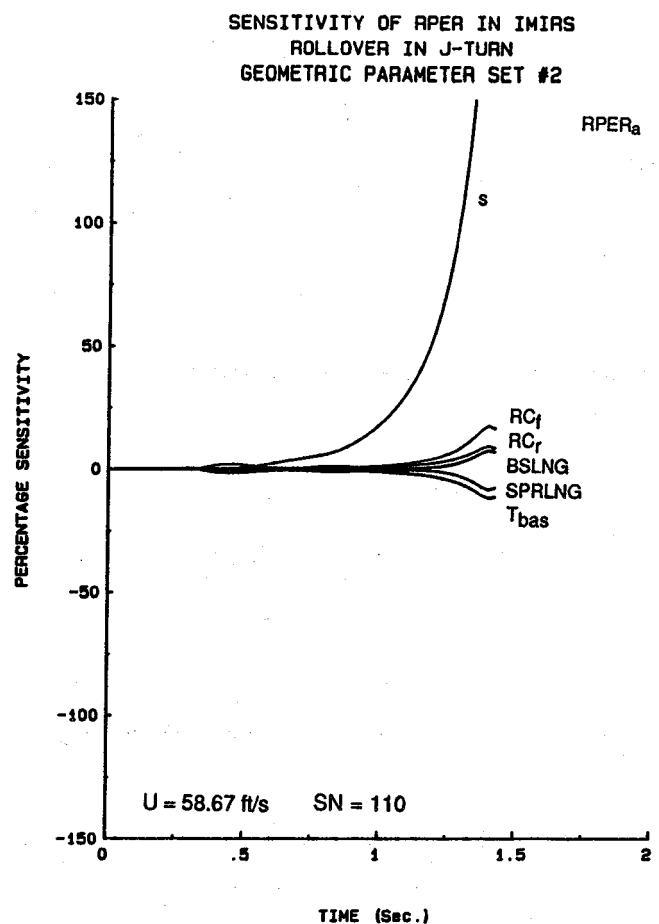


Figure 21. Sensitivity of IMIRS  $RPER_a$  for geometrical parameter set No. 2.

center in static conditions and this location is determined based on a kinematic analysis of the suspension system. Dependent suspension systems are modeled using a beam axle representation (figure 25). The beam axle is assumed to pivot about the static roll center of the suspension and can translate in a vertical direction relative to the sprung mass. The suspension springs have non-linear stiffness characteristics which are computed using polynomial functions of displacement with coefficients which are determined experimentally. The damping rate of each shock absorber is a quadratic function of the damper's rate of displacement. Both independent and dependent suspension systems have elastic and viscous damping anti-roll elements. Both types of suspensions, independent and dependent, can be employed in any combination at the front and rear of the vehicle.

The frictional tire model used in the AVRM is based on the non-dimensional slip angle approach and utilizes a dual friction ellipse concept to determine the limits of adhesion in different directions under combined conditions of cornering and braking or thrust. This model includes modifications to account for the large values of camber angles, as well as overload conditions which can occur during tire impacts with roadside features such as a curb. Several discontinuities which existed in the previous

SENSITIVITY OF RPER IN IMIRS  
 ROLLOVER IN J-TURN  
 MASS-INERTIA PARAMETER SET

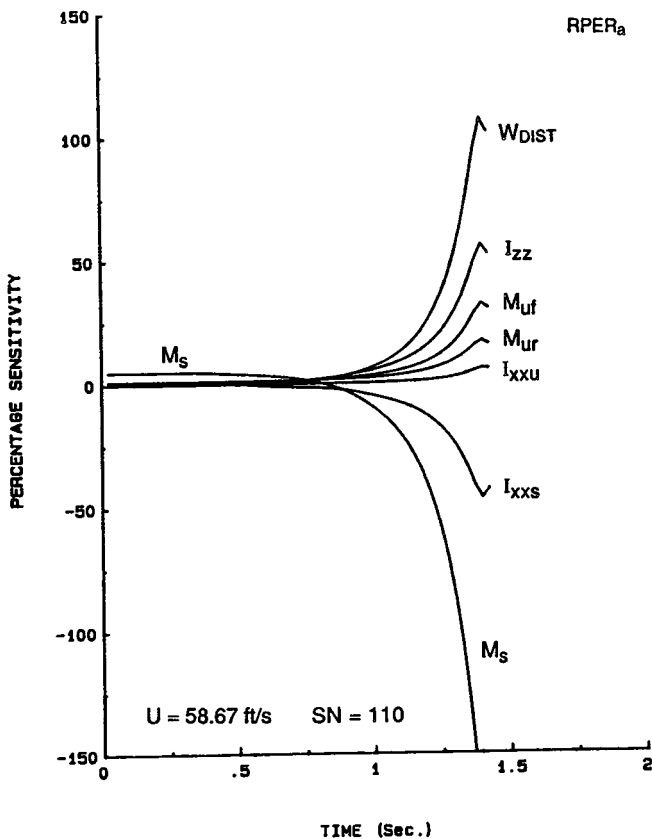


Figure 22. Sensitivity of IMIRS RPER<sub>a</sub> for mass/inertia parameter set.

version of the tire frictional model under conditions of combined cornering and braking have been eliminated through the development of a dual friction ellipse representation. Figure 26 and 27 show examples of side force vs. slip angle at various camber angles in both free rolling and heavy braking conditions.

The forces and moments generated during vehicle impact with roadside features are computed based on the three dimensional state of the tire caused by interference with the terrain profile. The tire impact model is illustrated in figures 28 and 29. Figure 28 shows the three dimensional representation of the tire impacting with a curb at an oblique angle. The impact model consists of numerous springs which have been specially arranged to ensure that the generated impact reactions are adequate in various vehicle maneuvers including those which produce excessive camber angles and overloads. A radial cross section detailing the spring locations and orientations used in the tire model can be seen in figure 29. The deformation of each spring is determined based on the wheel's orientation relative to the terrain surface. The forces and moments produced by each elastic element are then totalled to obtain the net reaction of each wheel.

A vehicle/ground impact model employs 21 node points

SENSITIVITY OF RPER IN IMIRS  
 ROLLOVER IN J-TURN  
 STIFFNESS PARAMETER SET

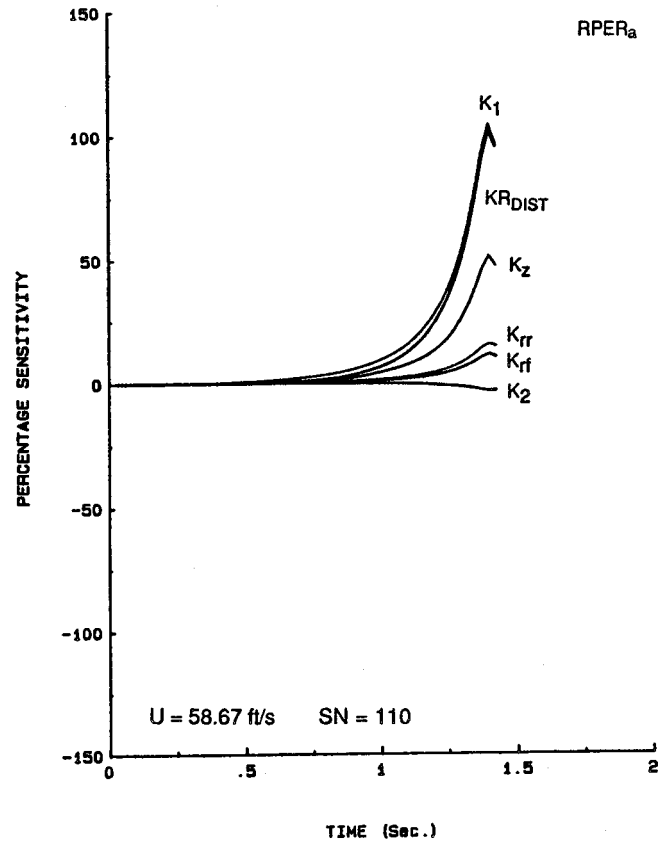


Figure 23. Sensitivity of IMIRS RPER<sub>a</sub> for stiffness parameter set.

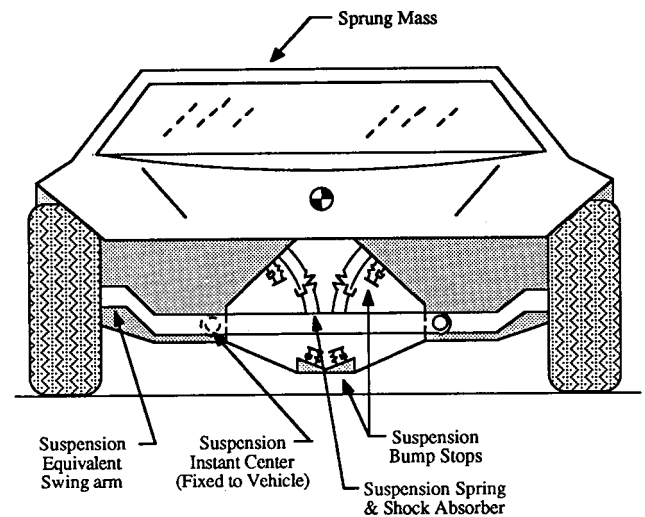


Figure 24. AVR equivalent swing arm representation of independent suspension.

to generate reactions during sprung mass contact with the ground. The forces produced by each node are based on both the amount and rate of change of deformation. The force/deflection characteristics of each node are similar to those used in the wheel/curb impact model of the ITRS (figure 4).

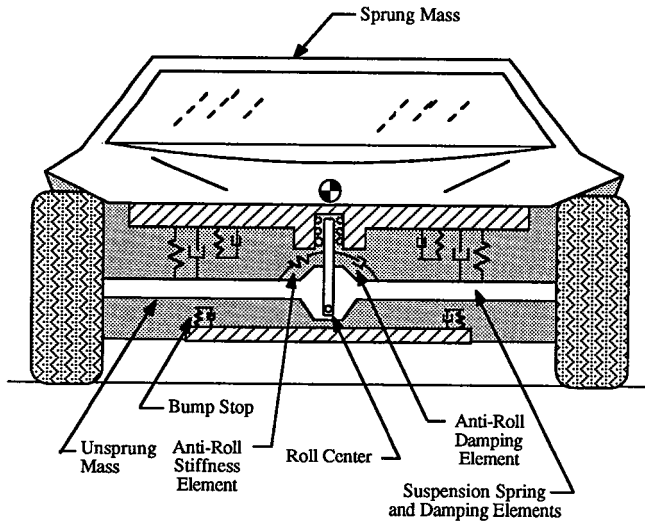


Figure 25. AVRM representation of dependent suspension system.

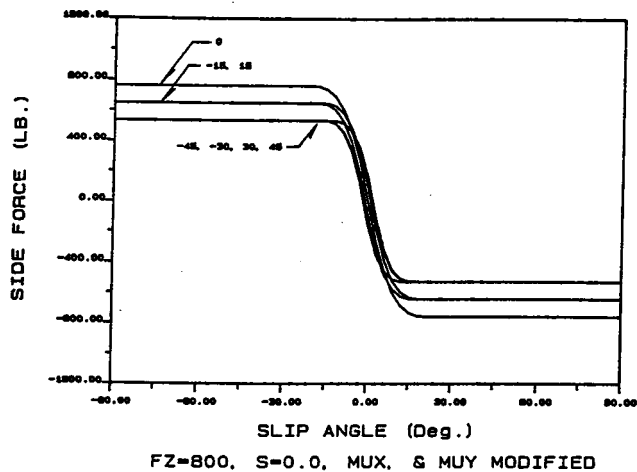


Figure 26. Side force versus slip angle in free rolling conditions at various camber angles.

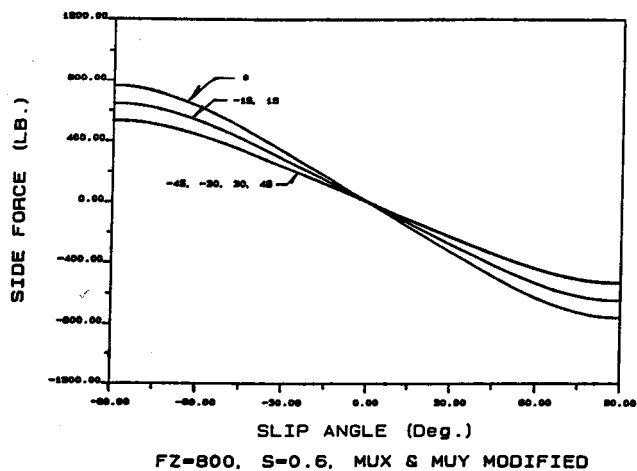


Figure 27. Side force versus slip angle in heavy braking conditions at various chamber angles.

These deformation characteristics account for both elastic and plastic deformation at each node and can be used to

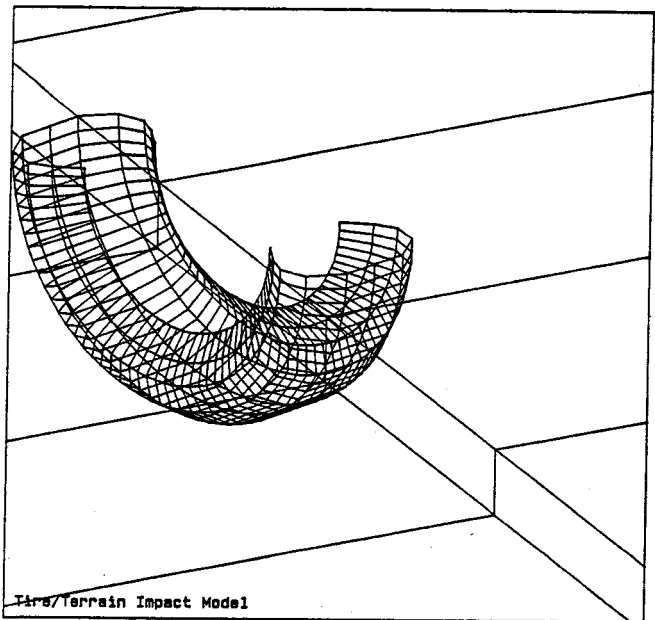


Figure 28. AVRM tire terrain impact model.

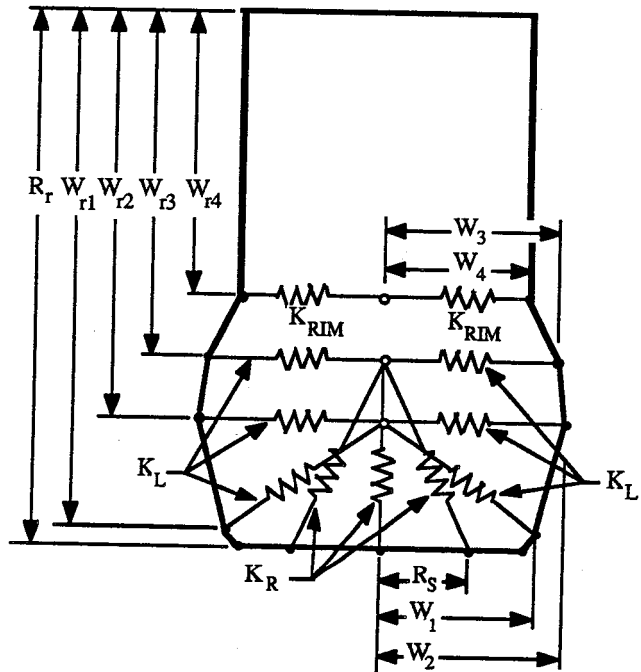


Figure 29. Cross section of tire impact model.

estimate the severity of the rollover event. The frictional scrub force generated by each node are calculated as a function of the normal reaction and sliding velocity of each node. Examples obtained during testing of the sprung mass ground impact model are shown in figures 30 and 31.

The equations of motion for the AVRM are derived using the Lagrangian formulation in quasi-coordinates. In addition to sprung and unsprung masses the AVRM model permits inclusion of 6 additional masses which can be used to investigate the effects of various passenger/payload configurations.

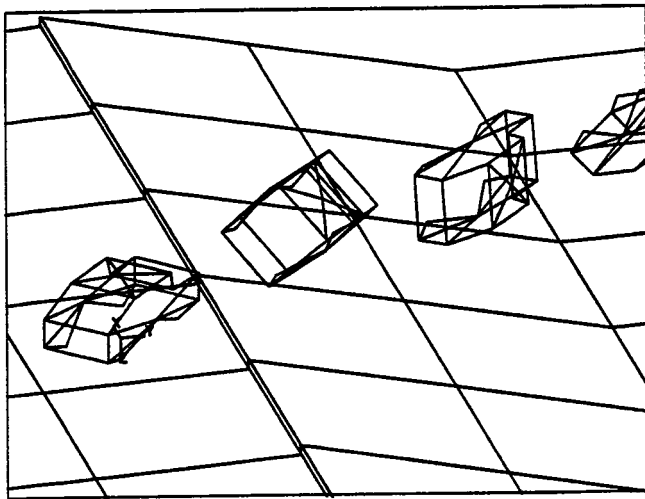


Figure 30. AVRMM tripped rollover simulation.

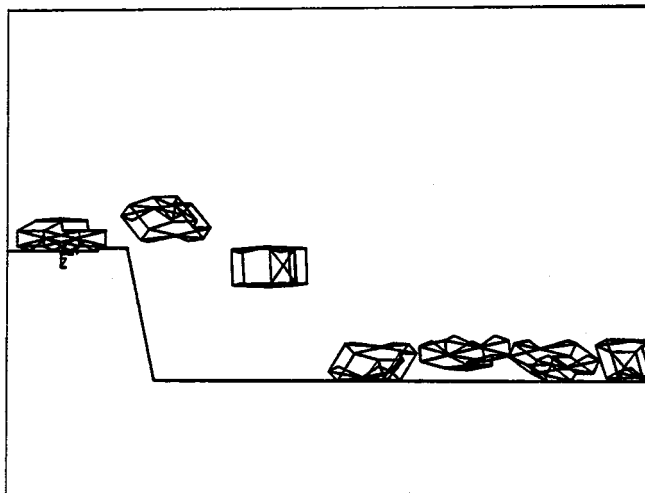


Figure 31. AVRMM sprung mass ground impact model test.

## Conclusions

The results presented in this paper show that ITRS and IMIRS simulations are very useful for predicting the occurrence of rollover and, when used in conjunction with sensitivity methods, represent powerful tools which can determine the influence of vehicle design parameters on dynamic rollover behavior.

The concept of Rollover Prevention Energy Reserve is a reliable indicator of dynamic rollover stability. The results reveal that the minimum value of RPER approaches zero at the threshold of rollover and if this minimum falls below zero then vehicle rollover will occur. Finding the effects of parameter variations on RPER using sensitivity methods represents a practical, productive approach when investigating the influence of vehicle and environmental parameters on rollover propensity. The vast majority of results obtained using this approach have agreed with statistical observations and prevailing opinion.

A great deal of useful experience was gained during the development of the ITRS and IMIRS simulations and has proved most useful while developing the AVRMM model.

Preliminary results obtained while testing AVRMM subsystem models are quite promising and indicate that it will be a very useful tool for investigating of all types of rollover accidents.

## References

- (1) Maryland State Police, "Maryland Rollover Data File," Accident Data Collected for NHTSA R&D, U.S. DOT, Washington D.C., 1988.
- (2) National Accident Sampling System (NASS) 1985 Data Base, National Center for Statistics and Analysis, NHTSA, U.S. DOT, Washington D.C., 1985.
- (3) Edwards, M.L., "A Database for Crash Avoidance Research," SAE Special Publication NO. 699, 1987.
- (4) NHTSA—U.S. DOT, "Fatal Accident Reporting System 1986," A Review of Information on Fatal Traffic Accidents in the United States in 1986, Washington D.C., 1986.
- (5) Jones, I.S., "Vehicle Stability Related to Frequency of Overturning for Different Models of Cars," Proc. Australian Road Research Board, Vol. 7, Part 5, 1974.
- (6) Snyder, R.C., et al., "On-Road Crash Experience of Utility Vehicles," HSRI, University of Michigan, Report No. UM-HRSI-80-14, February 1980.
- (7) Insurance Institute for Highway Safety, "Small Passenger Vehicles a Problem," IIHS Status Report, Vol. 22, No. 2, February 1987.
- (8) Griffin, L.I., III, "Probability of Overturn in Single Vehicle Accidents as a Function of Road Type and Passenger Car Curb Weight," Traffic Accident Research and Evaluation Program, Texas Transportation Institute, Texas A&M University System, November 1981.
- (9) Griffin, L.I., III, "Probability of Driver Injury in Single Vehicle Collisions with Roadway Appurtenances as a Function of Passenger Car Curb Weight," Texas Transportation Institute, Texas A&M University System, October 1981.
- (10) Reinfurt, D.W., et al., "A Comparison of the Crash Experience of Utility Vehicles, Pickup Trucks and Passenger Cars," Highway Safety Research Center, University of North Carolina, September 1981.
- (11) Reinfurt, D.W., et al., "A Further Look at Utility Vehicle Rollover," Highway Safety Research Center, University of North Carolina, August 1984.
- (12) Malliaris, A.C., et al., "Problems in Crash Avoidance Research," SAE International Congress & Exposition, Detroit, Michigan, SAE Paper No. 830560, 1983.
- (13) Habberstad, J.L., Wagner, R.C., Thomas, T.M., "Rollover and Interior Kinematics Test Procedures Revisited," SAE Paper No. 861875, 1986.
- (14) Segal, D.J., "Highway Vehicle Object Simulation Model," FHWA—U.S. DOT Final Report No. FHWA-RD-76-162, 1976.
- (15) Jones, I.S., "The Mechanics of Rollover as the Result of Curb Impact," SAE Paper 7650461, 1975.
- (16) DeLeys, N.J., Parada, L.O. "Rollover Potential of

Vehicles on Embankments, Sideslopes, and Other Roadside Features," FHWA—U.S. DOT Final Report No. FHWA—RD-86-164, 1986.

(17) Rosenthal, T.J., et al., "User's Guide and Program Description for a Tripped Roll Over Vehicle Simulation," NHTS—U.S. DOT Report No. DOT HS 807140, 1987.

(18) Nalecz, A.G., et al., "Sensitivity Analysis of Vehicle Tripped Rollover Model," NHTSA—U.S. DOT Report No. DOT HS 807 300, July 1988.

(19) Nalecz, A.G., "The Nonholonomic Constraints of a Vehicle on Pneumatic Tires," *Vehicle System Dynamics*, v. 12, n. 1-3, July 1983, 8th IAVSD Symp on the Dyn of Veh on Roads and Tracks, MIT, Aug. 14-19, 1983.

(20) Nalecz, A.G., "Dynamic Equilibrium of a Motor Car Vehicle Under Action of Oblique Airflow," *Nonlinear Vibration Problems*, Vol. 18, No. 9, pp. 107-145, 1977.

(21) Nalecz, A.G., Bindemann, A.C., "Sensitivity Analysis of Vehicle Design Attributes that Affect Vehicle Response in Critical Accident Situations—Part I: User's Manual," Final Report NHTSA—U.S. DOT No. DOT HS 807229, October 1987.

(22) Nalecz, A.G., Bindemann, A.C., "Sensitivity Analysis of Vehicle Design Attributes that Affect Vehicle Response in Critical Accident Situations—Part II: Technical Report," Final Report NHTSA—U.S. DOT No. DOT HS 807 230, November 1987.

(23) Nalecz, A.G., Wicher, J., "Design Sensitivity Analysis of Mechanical Systems in Frequency Domain,"

*Journal of Sound and Vibration*, Vol. 120, No. 3, pp. 517-526, 1988.

(24) Wicher, J., Nalecz, A.G., "Second Order Sensitivity Analysis of Lumped Mechanical Systems in the Frequency Domain," *International Journal for Numerical Methods in Engineering*, Vol. 24, No. 12, pp. 2357-2366, 1987.

(25) Nalecz, A.G., "Sensitivity Analysis of Vehicle Design Attributes in Frequency Domain," *International Journal of Vehicle System Dynamics*, Vol. 17, No. 3, pp. 141-163, 1988.

(26) Nalecz, A.G., "Application of Sensitivity Methods to Analysis and Synthesis of Vehicle Dynamic Systems," State of the Art Paper at 11th IAVSD Symp on the Dyn of Veh on Roads and Tracks, Kingston, Canada, August 1989.

(27) Nalecz, A.G., Bare, C., "Development and Application of ITRS," NHTSA—U.S. Department of Transportation, Contract No. DTNH22-87-D27174, Final Report 1989.

(28) Nalecz, A.G., "Intermediate Maneuver Induced Vehicle Rollover Simulation," TSC—U.S. Department of Transportation, Contract No. DTRS57-88-P-82668, Final Report, 1989.

(29) Nalecz, A.G., "Investigation into the Effects of Suspension Design on Stability of Light Vehicles," *SAE Transactions*, Vol. 96, No. 1, Paper No. 870497, 1987.

(30) Nalecz, A.G., et al., "Advanced Dynamic Rollover Model," NHTSA—U.S. Department of Transportation, Contract No. DTNH22-87-D-27174, Final Report 1989.

## Real World Rollovers—A Crash Test Procedure and Vehicle Kinematics Evaluation

T. M. Thomas,  
N. K. Cooperrider,  
S. A. Hammoud,  
P. F. Woley,

Failure Analysis Associates, Inc.

### Abstract

Until recently, crash tests to study real world rollover accidents have used either snubbed dollies or guided ramps. Neither method accurately represents what occurs during a curb trip rollover accident. This paper discusses a series of rollover tests conducted by Failure Analysis Associates, Inc. (FaAA), in which the test vehicles are slid sideways, released from tow, and tripped by a curb, as could occur in a real accident. Another vehicle was launched from a FMVSS 208 dolly for comparison. The test vehicles contained unrestrained front seat anthropomorphic dummies.

The tests were documented with real time and high speed photography. Vehicle kinematics was found by analysis of

the high speed film. The vehicles tested represent a range of vehicle geometries from passenger cars to utility vehicles. The vehicle kinematics results include presentation of position, velocity, and energy profiles. The results are compared with those from the dolly rollover test at similar speeds with a similar vehicle.

### Introduction

Automobile rollover accidents have been a subject of research for more than 50 years (1)\*. Despite years of study, the mechanics of vehicle rollover remains poorly understood, a situation that can be attributed to the complexity of the rollover process. Many factors influence the likelihood of vehicle rollover, including vehicle characteristics, pre-rollover vehicle dynamic motion, and the nature of the mechanism initiating rollover. It is well known that a vehicle's propensity to rollover depends on vehicle characteristics that include geometric dimensions, inertial properties, and suspension characteristics. Pre-

\*Numbers in parentheses designate references at end of paper.

rollover dynamic conditions including orientation, sideslip angle, and both translational and rotational velocities affect rollover occurrence. To further complicate matters, vehicle rollover may be initiated by a number of different mechanisms including tripping on the roadway surface under forces generated by tire-pavement interaction, tripping due to impact with a curb or other object, and tripping due to forces generated off road by tire-soil interaction.

A research project focusing on the mechanics of automobile rollover is underway at FaAA. This paper reports a portion of that effort concerned with understanding how rollovers are initiated and how different initiation mechanisms affect the subsequent vehicle rollover mechanics. In particular, this paper reports results of tests conducted to investigate rollovers tripped by a curb and to compare the vehicle behavior in this situation with vehicles launched from a FMVSS 208 dolly.

Analysis of accident statistics provides insight into the rollover initiation mechanisms involved in real world accidents. Most researchers agree that the majority of rollover accidents occur off the roadway (2,3,4). The most frequent off-road trip mechanism involves the vehicle tires plowing through soil, often on a sideslope (2,3,4). A less frequent, but not uncommon situation is tire and wheel impact with a curb or other object (2,3,4,5). The research reported here concerns the mechanism of rollover initiation by curb contact. A study of rollovers tripped by tires in soil is planned for the future.

## Background

The mechanics of vehicle rollover has been approached from both an analytical and experimental viewpoint. Several proposed analytical models treat the rollover initiation process as an abrupt trip where the wheels of the impacting vehicle are suddenly stopped by an object such as a curb (5,6). These analyses produce an expression for the minimum velocity needed to trip the vehicle, although the values computed with these methods are much lower than the minimum velocities found from testing and accident experience. More complex models that treat the vehicle suspension and tire properties in detail have also been developed (6,7,8). These models provide more realistic evaluations of rollover mechanics, although the authors are not aware of studies that report close agreement between analytical and experimental results. The lack of agreement can be attributed to the poor state of understanding of real world rollover initiation mechanics.

Most automobile rollover testing has been directed toward evaluation of occupant protection in rollover accidents. Far less effort has been spent on tests to provide an understanding of real world rollover mechanics. The objective of test procedures such as the SAE J857 Jun 80 ramp rollover test (9), the FMVSS 208 dolly rollover test (10), and other dolly test procedures (11,12) is to evaluate the occupant protection capability of a vehicle and its

restraint systems in a rollover situation. These procedures are not designed to replicate real world rollover initiation mechanisms, and in fact research indicates that substantial differences in rollover mechanics may exist (13). A better understanding of real world rollover behavior will be useful in designing for occupant protection and developing analysis and test procedures to evaluate occupant protection.

## Test Description

In order to examine curb tripped rollover mechanics, five curb impact tests and one dolly rollover test were conducted. The tests and test vehicles are identified in table 1. The test vehicles were chosen to cover a wide range of vehicle sizes from a sub-compact automobile to a full size van. A second compact size vehicle of the same make and model as used in the curb test series was rolled in the dolly rollover test. The center of gravity heights were measured for each vehicle in their test condition and are reported in table 1. Test vehicle weights, wheelbase, and track width are also given in this table.

**Table 1. Test vehicle description.**

Test Number	1	2	3	4	5	6
Test Type	Curb	Curb	Curb	Curb	Curb	Dolly
Test Speed (mph)	29.9	29.6	29.3	29.6	30.2	30.2
Vehicle Model	1981 Challenger (2 dr)	Same as #1 with steel wheels	1979 B210 (2 dr)	1972 C20 (van)	1981 Impala (4 dr)	Same as #1
Vehicle Weight (lbs)	2630	Same as #1	1930	4360	3490	2787
Wheelbase (in)	99.8	Same as #1	91.4	125.	115.	Same as #1
Track Width (in)	55.8	Same as #1	52.3	67.9	61.5	Same as #1
CG Height (in)	20.9	Same as #1	20.3	30.3	21.7	Same as #1
Anthropomorphic Dummies	2	2	2	2	2	0

The tests were conducted in the crash test facility at the FaAA Test and Engineering Center. The nominal speed for all tests was 30 mph. In the curb trip tests, the test vehicles were towed sideways and released just before curb impact. A soap solution on the concrete track reduced the coefficient of friction, making it possible to stably tow the test vehicles laterally. The dolly rollover followed the FMVSS 208 procedure.

The tests were documented with high speed movie cameras. Vehicle and ground based targets were placed in camera view to permit film analysis to determine vehicle positions, orientations, and velocities. Pre-test and post-test photographs documented the vehicle and test conditions. Rest position measurements were made in all tests.

## Test Methodology

The test vehicles described in table 1 were free of previous major damage and modified only to allow installation of onboard cameras and, in the case of the curb trip test vehicles, underbody tow and guidance hardware. The two types of tests, the curb trip and the dolly rollover test, require substantially different test set-ups and procedure.

The test vehicles and the rollover dolly are guided by attachment to a tow-shoe through a bridal assembly. The tow-shoe, captured on a monorail, is propelled along the monorail by a continuous wire rope cable driven by internal combustion engines. Tow-shoe speed is controlled by following a predetermined acceleration schedule. The towed vehicle or dolly is released from the tow system and tow-shoe only a few feet from impact with the curb or the rollover dolly snubber system.

The curb used to trip the test vehicles was a 6-inch square section of steel tubing rigidly affixed to the monorail and surrounding concrete roadway. The test speeds for the curb impacts were nominally 30 mph. The vehicles were oriented to impact the curb while sliding sideways with the right side leading as shown in figure 1.



Figure 1. Curb test vehicle.

Typically, to accelerate vehicles laterally for laboratory impact testing a set of dolly wheels replaces the test vehicle's original tires and wheels to permit the vehicle to be rolled sideways. However, this method clearly cannot be used for curb trip tests because the wheels and tires are not in place to contact the curb and trip the vehicle. For this series of tests, the vehicles were slid sideways on a film of soap applied to the concrete roadway just prior to conducting the test, a test method first identified in (13).

In order to more closely represent the attitude of a side-sliding vehicle in a real world accident, a slight roll angle, as would result from the tire-ground interaction, was built into the test vehicles by extending the off side suspension with wood blocks. A 2.5 degree pre-impact roll angle was built into each vehicle.

In the curb trips, onboard high speed cameras recorded the motion of the two 50th percentile male hybrid II

dummies occupying the left and right front seat positions. In addition to the onboard cameras, five ground-based, high speed cameras and a shuttered video camera were positioned as shown in figure 2 to document the vehicle motion for later film analysis. To facilitate the film analysis, inch tape and targets were applied to the vehicle at selected locations, and stationary targets were placed in the foreground of the overlapping camera views.

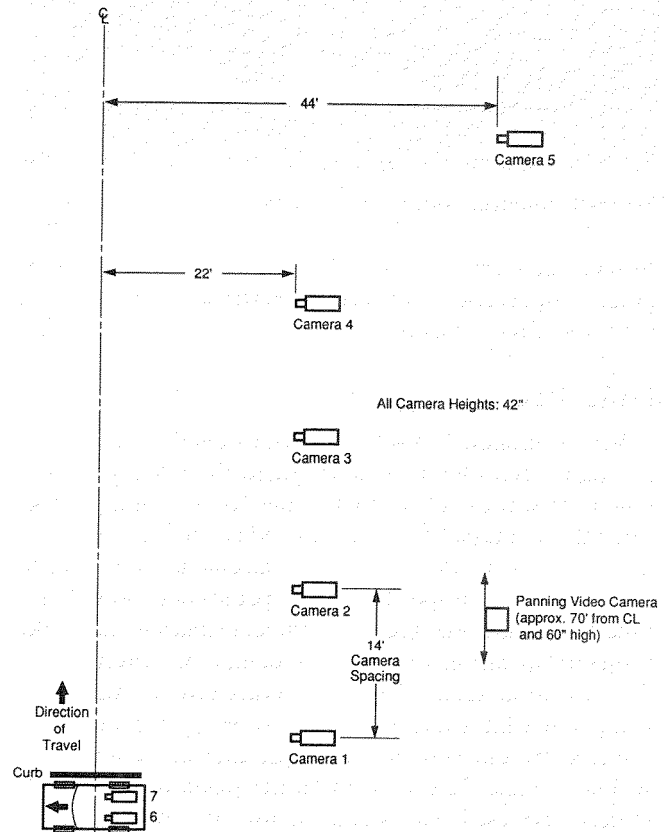


Figure 2. Camera locations.

The dolly rollover test was set up and conducted in accordance with the guidelines contained in FMVSS 208. The vehicle was launched from the dolly and rolled laterally with the right side leading. The dolly inclined the vehicle at an angle of 23 degrees and elevated the bottom of the leading tire 9 inches above ground. The dolly fixture is shown with the test vehicle in figure 3.

Rotation of the vehicle was induced by the 4-inch trip lip on the dolly, which applied loads to the tire when the dolly was rapidly decelerated. The dolly fixture was accelerated to the selected test speed of 30 mph by the same vehicle tow system used in the curb trip tests. When the dolly was stopped suddenly by a snubber system of energy absorbing material, the test vehicle was launched onto a dry concrete surface.

The motion of the dolly rollover test vehicle was recorded by five high speed ground cameras and a video camera. Inch tape and targets also were placed on the car to enhance film analysis. The high speed cameras were parallel to the vehicle roll axis and spaced with overlapping fields of view.

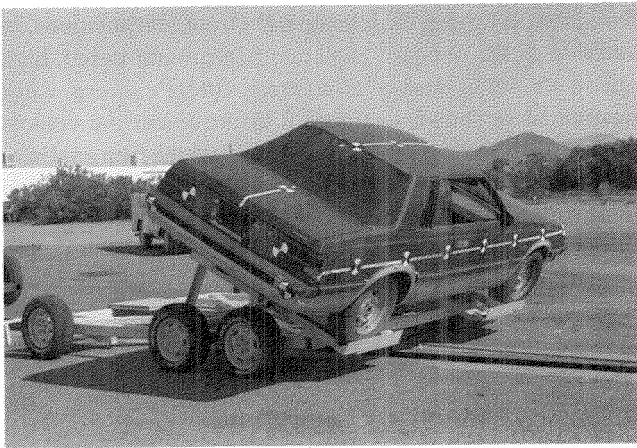


Figure 3. Rollover dolly with test vehicle.

In both the curb trip and dolly rollover tests, a series of ground targets and event correlation flashes were placed in the view of the cameras.

## Data Processing

Vehicle motion data was obtained by detailed analysis of the high speed film using a Vanguard Film Analyzer. The time base was established using the 100 Hz timing marks generated in the cameras and exposed on the film edge. The timing marks and the Vanguard frame counter were used to determine the film speed in frames per second, providing a time base. The horizontal and vertical displacements of the projected position of vehicle's center of gravity were determined at selected time intervals through the event using the film analyzer. In determining the distances traveled by the vehicles, multiple-measurement scales within a single field of view in the plane of the vehicle targets were used. This was done for each camera view, a procedure that helped compensate for out-of-plane views and lens distortion. The overlapping cameras were synchronized by a series of ground based flashes that occurred simultaneously and appeared in the view of each camera.

A table containing time, horizontal travel, vertical travel, and roll angle was generated through film analysis for each test. Time intervals ranged from a few milliseconds to 80 milliseconds, depending on the vehicle's position and motion. Vehicle to ground contacts, along with airborne events, were noted. Test data was converted to computer data files and a computer program was used to calculate various vehicle motion parameters. The following time histories were generated for each test from the computer analysis:

- Vehicle center of gravity displacement in the horizontal and vertical planes;
- Roll angle;
- Horizontal, vertical, and rotational velocities; and
- Kinetic, potential, and total energy.

This data was used to produce the plots presented in this paper.

## Test Results

The five curb trip tests, conducted on four vehicles, resulted in two rollovers. The vehicles that did not rollover did not sustain the minimum force impulse necessary to cause a rollover due to failures of their wheels or axles under the curb impact loads. When these events occurred, the vehicles would roll slightly, clear the curb, and slide to rest.

The vehicles that did rollover in Tests 2 and 3, rolled 1 and 1½ revolutions, respectively, over an average distance of 47 feet. The vehicle launched from the rollover dolly, Test 6, rolled three times, coming to rest on its tires 70 feet from roll initiation. Figure 4 shows the cumulative vehicle roll angle versus distance for the Test 2, 3, and 6 vehicles. The curb tripped vehicles tended to roll in a more purely lateral manner, resulting in damage primarily to the off-side roof and A-pillar area. The dolly rollover vehicle developed some yaw and end-to-end contact during the rollover sequence, resulting in damage to the off-side front fender and the leading side roof and door frame area.

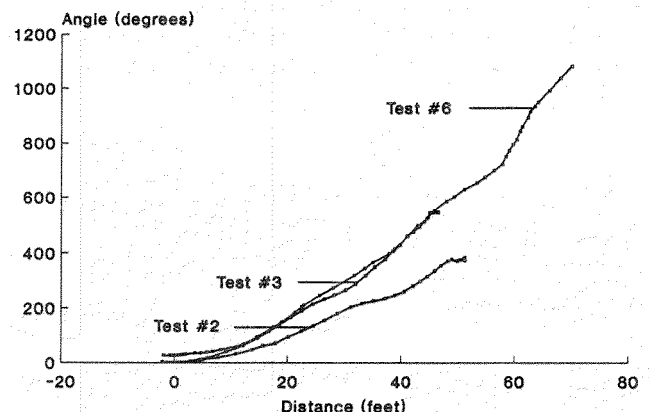


Figure 4. Roll angle distance.

## Vehicle Kinematics

Horizontal velocity versus time plots are presented in figures 5, 6, and 7 for the tests that resulted in rollover. The horizontal velocity plots for Tests 2, 3, and 6, are annotated to reflect the occurrence of significant vehicle-to-ground impacts. Differences between curb trips and dolly rollover tests become apparent when viewing the respective horizontal velocity versus time plots. When the vehicles impacted the curb, a velocity change of approximately 20 feet per second (fps) over .060 seconds resulted in Test 2, and a change of 18 fps over a period of .040 seconds in Test 3. The average decelerations for these events were 12.4 g's and 13.2 g's, respectively.

These decelerations are in sharp contrast to the dolly rollover test, where the initial velocity loss caused by the vehicle contacting the ground of 18 fps occurred over a much longer period of time, .43 seconds, a 1.3 g average deceleration rate for the event.

The deceleration rates experienced during curb impact by the vehicles that did not roll were approximately half the values of the Test 2 and Test 3 vehicles. In Test 1 the curb

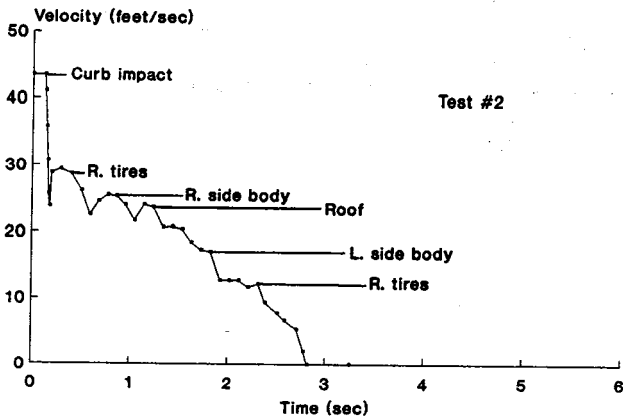


Figure 5. Horizontal velocity v time, curb trip.

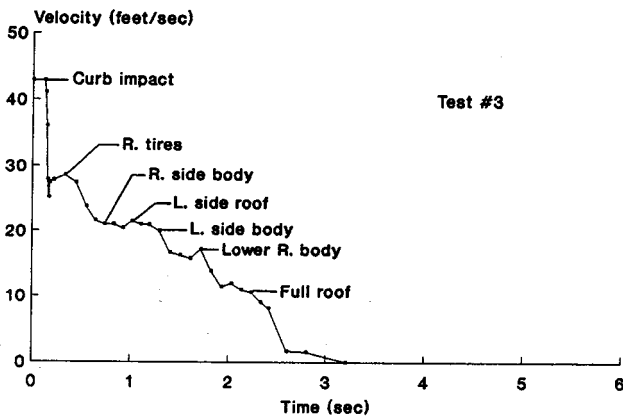


Figure 6. Horizontal velocity v time, curb trip.

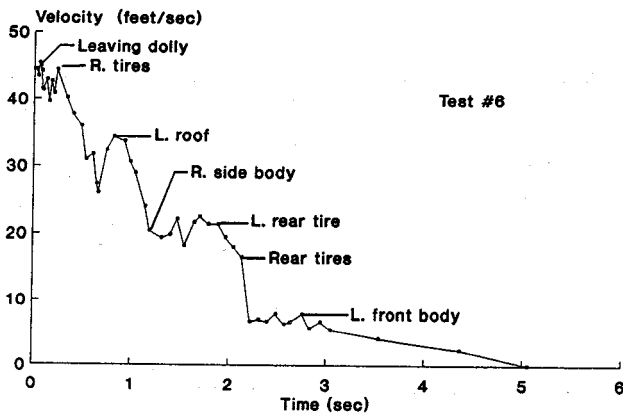


Figure 7. Horizontal velocity v time, dolly rollover.

impact deceleration was 6.0 g's; in Test 4, 5.5 g's; and in Test 5, 5.4 g's.

Average decelerations for the rolling vehicles can be determined for portions of the rollover event from linear regression analysis of the horizontal velocity versus time data. Generally, the deceleration values have been reported over the entire rollover event rather than over selected ranges. Orłowski (14) reported an average deceleration for the rolling vehicles in a series of FMVSS 208 dolly rollover tests as .43 g between dolly launch and point of rest. Hight (4) reported deceleration rates ranging from 0.40 to 0.65 for vehicles in actual rollover accidents on level ground. Linear

regression of the data in figures 5 and 6 for the curb trip tests resulted in an average deceleration over the entire event of 0.32 g. However, the vehicle decelerations and the resulting relative velocities between the occupant and vehicle as a result of discrete occurrences during the rollover sequence often are more significant in addressing the occupant protection issue. The rapid deceleration during a curb impact may result in occupant motions or impacts with the vehicle interior that result in injuries.

The dolly rollover event produced an average deceleration of 0.31 g from launch to rest. In figure 7, two distinct deceleration regions are seen. From initial launch to approximately 2.1 seconds, the vehicle decelerated more rapidly, 0.39 g, than in the subsequent travel to rest where the average deceleration was 0.08 g. During this final period in which the vehicle rotated 360 degrees, but only traveled 7 feet before landing on its tires, the rotational kinetic energy was greater than the translational kinetic energy. The most significant deceleration of the dolly rollover vehicle occurred during initial tire-to-ground contact, an average deceleration of 1.3 g over about 0.43 seconds. The dolly rollover tests conducted by Orłowski (14) utilizing vehicles of similar size to that used in Test 6 produced similar trends in horizontal velocity loss.

Figures 8, 9, and 10 depict the rotational velocities versus time for Tests 2, 3, and 6. While the two curb trip vehicles responded similarly, with peak roll velocities of 260 and 300 deg/sec, the dolly rollover vehicle achieved a peak roll rate of 460 deg/sec. Because the velocity lost during the impact with the curb is of similar magnitude to that lost by the dolly rollover vehicle impacting the ground, the horizontal force impulses must also be similar. However, the difference in roll rates can be attributed to the 48 degree roll angle of the dolly rollover vehicle when it strikes the ground that results in a larger moment arm from the point of impact to the center of gravity of the vehicle.

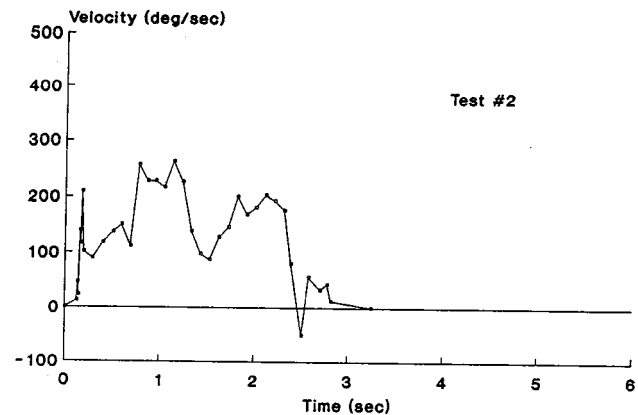


Figure 8. Rotational velocity v time, curb trip.

The initial total energy of the dolly rollover vehicle was greater than that of the curb trip vehicles, as can be seen in figure 11. The total energy shown here is the sum of the kinetic energy from the vertical, horizontal, and rotational velocities; and the potential energy. Most of the energy is

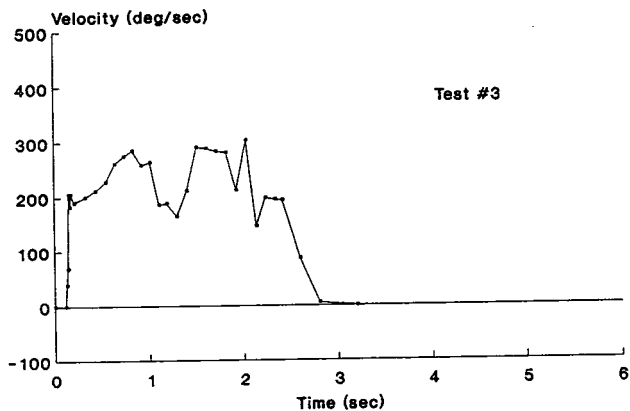


Figure 9. Rotational velocity v time, curb trip.

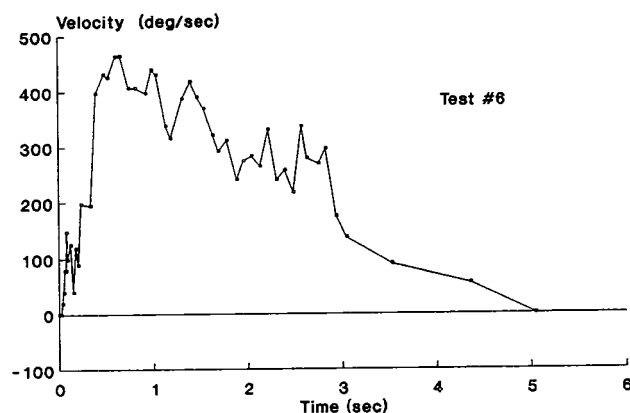


Figure 10. Rotational velocity v time, dolly rollover.

associated with the horizontal velocity, therefore, these plots are similar in form to the horizontal velocity plots. The primary reason for the added energy in the dolly rollover vehicle is the potential energy resulting from its position on the dolly fixture at a 23 degree initial roll angle.

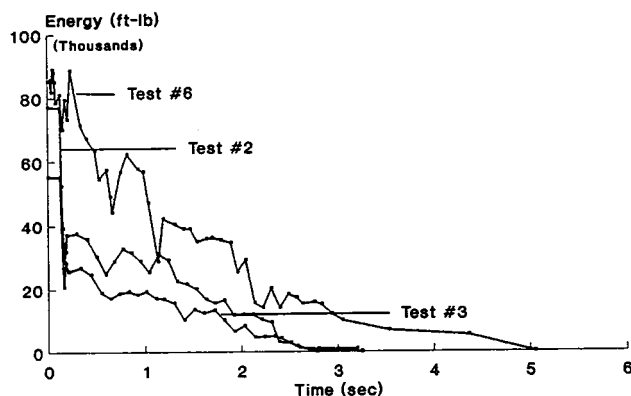


Figure 11. Total energy v time.

## Discussion

Insight into several aspects of real world rollover behavior can be obtained from the results presented in this paper. Some vehicles do not rollover after curb impact as seen in Tests 1, 4, and 5. Very large forces are generated during the curb impact, and vehicle components may fail under these forces. When such failures occur, the forces

tending to roll the vehicle are relieved allowing the vehicle to slide over the curb. An average deceleration of about 13 g's and corresponding force of approximately 35,000 lbs. occurred in the curb impact of Test 2. In Test 1, the same vehicle that rolled in Test 2, but equipped with cast aluminum wheels, did not roll because the wheels fractured under a deceleration of about 6 g's and a corresponding force of 16,000 lbs. Deceleration levels of about 5.5 g's occurred in Tests 4 and 5, where component failures also prevented rollover.

Several differences were seen between the vehicle behavior in the curb trip rollovers and the FMVSS 208 dolly rollover including:

- Much higher deceleration rates during curb impact than in the corresponding first ground contact of the dolly launched vehicle.
- Higher angular velocities experienced by the dolly launched vehicle.
- Higher initial energy in the dolly launched vehicle due to its initial c.g. elevation approximately 1.5 feet above the ground.

These differences should be considered when using dolly rollover test results to analyze real world rollover events.

Although occupant kinematics is not the focus of this paper, the differences in occupant behavior in dolly rollovers and curb tripped rollovers should be noted. The higher initial deceleration and lower angular velocities experienced by the curb tripped vehicles will result in very different occupant behavior than seen in a dolly launched vehicle. This difference was apparent in the rollover test reported in (13).

Although differences exist between dolly launched and real world rollovers, the work reported here and the test project discussed in (13) illustrate that such tests are not difficult to perform.

## Future Work

Many areas for future investigation into rollover behavior remain. FaAA intends to continue research into the effect of other sideslip angles on curb trip behavior, occupant kinematics in curb tripped rollovers, the behavior of additional vehicles in such tests, and also plans to conduct a similar investigation into the rollover behavior of vehicles tripped by tire-soil interaction.

## References

- (1) Wilson, R.A. and Gannon, R.R., "Rollover Testing," SAE Paper 720495, May 1972.
- (2) DeLays, N.J. and Brinkman, C.P., "Rollover Potential of Vehicles on Embankments, Sideslopes, and Other Roadside Features," SAE Paper 870234, February 1987.
- (3) Terhune, K., "Rollover and Ejection Study," Presentation to Rollover Subcommittee, Motor Vehicle Safety Research Advisory Committee, NHTSA, March 16, 1989.

(4) Hight, P.V., Siegel, A.W., and Nahum, A.M., "Injury Mechanisms in Rollover Collisions," SAE Paper 720966, Proceedings of Sixteenth Stapp Car Crash Conference, November 1972, p. 204-227.

(5) Jones, I.S., "The Mechanics of Rollover as the Result of Curb Impact," SAE Paper 750461, February 1975.

(6) McHenry, R.R., "Speed Estimates in Vehicle Rollovers," Calspan Report No. ZQ-5639-V-1, January 1976.

(7) Nalcezk, A., "Status Report on NHTSA Sponsored Research on Computer Modeling of Rollover Vehicle Dynamics," Presentation to Rollover Subcommittee, Motor Vehicle Safety Research Advisory Committee, NHTSA, March 16, 1989.

(8) Allen, R.W., "Vehicle Characteristics and Maneuver Conditions Affecting Rollover," Presentation to Rollover Subcommittee, Motor Vehicle Safety Research Advisory Committee, NHTSA, August 31, 1988.

(9) "Roll-Over Tests Without Collision," SAE J857 Jun

80, Society of Automotive Engineers Recommended Practice, June 1980.

(10) Federal Motor Vehicle Safety Standard No. 208, "Occupant Crash Protection," Part 571, S208.

(11) Griffin, R. and Enserink, E., "Evaluation of Rollover Procedures," National Highway Traffic Safety Administration Report No. DOT HS 803 262, October 1977.

(12) Segal, D.J. and Kamholz, L.R., "Development of a General Purpose Rollover Test Device," National Highway Traffic Safety Administration Report No. DOT HS-806 550, September 1983.

(13) Habberstad, J.L., Wagner, R.C., and Thomas, T.M., "Rollover and Interior Kinematics Test Procedures Revisited," SAE Paper 861875, 1986.

(14) Orlowski, K.F., Bundorf, R.T., and Moffatt, E.A., "Rollover Crash Tests—The Influence of Roof Strength on Injury Mechanics," SAE Paper 851734.

## Skidding Accidents and Their Avoidance with Different Cars

**Lennart Strandberg,**  
Swedish Road and Traffic Research Institute,  
VTI

### Abstract

In Swedish statistics from 1985 and 1986, the percentage of "oncoming vehicle" accidents is four times greater on snowy/icy roads (16%) than on dry clear roads (4%). The percentage "rear end" accidents is the same (6%) for both road conditions. Also the fatality numbers (364 people in "oncoming vehicle" versus 26 in 'rear end' accidents) indicate that more emphasis should be put on instability and skidding problems (typical for oncoming vehicle accidents) than on braking distances and steering-while-braking problems (rear end accidents).

Vehicle dynamics show that the cornering performance of the rear wheels must be superior to that of the front wheels, if a car is to be stable at all speeds. This is illustrated by some hydroplaning fatality cases, where the tyre pattern was much deeper at the front than at the rear. Since traction or braking forces reduce the side force, skid recovery will be more difficult in a front wheel driven car, if the driver depresses the clutch pedal before countersteering. Experiments with experienced drivers offered an explanation to why such a behaviour still is recommended in many driver training courses.

Influence on stability from vehicle design and equipment is being even more pronounced with antilock (ABS-) brakes, 4 wheel steering, cruise control, etc. This must be considered in research on vehicle black spots in accidents,

in vehicle inspection and testing, and in driver training programs.

### Focus on Safety Relevant Properties in Vehicle Technology Development

An increasing number of investigators claim that improvements of crash avoidance properties in cars do not increase the net driver-vehicle safety. For instance, the distinct improvements with antilock (ABS-) brakes in experimental driving tests found by Rompe et al (1987) were contradicted by accident records from real traffic according to Aschenbrenner et al (1988).

It has also been concluded that training of drivers on skid pads and in advanced evasive manoeuvres may increase the accident risk in real traffic. Glad (1988) found that drivers with skidpad training were involved in more accidents per mileage unit than comparable drivers without such training.

However, controllability (steering and braking) performance had been emphasized with a disregard for the directional stability properties both in the tests by Rompe et al (1987) and in the skidpad training evaluated by Glad (1988). This may explain the paradoxical findings by Glad (1988) and by Aschenbrenner et al (1988), since there are evidence from Swedish accidents and driving experiments that poor stability may contribute to a much greater number of serious accidents than what poor controllability does.

Therefore, the question on stability versus controllability may be decisive both of safety and of public demands on vehicle technology developments in the future.

Influence on stability from vehicle design and equipment

is being even more pronounced with ABS brakes, with front/rear or four wheel drive, with cruise control, with four wheel steering, with (prohibitions on) studded tyres, with increased differences in tyre adhesion between wet and dry conditions, etc. This must be considered in research on vehicle black spots in accidents, in vehicle inspection and testing, and in driver training programs.

## Directional Stability Versus Controllability in Accident Statistics

In official statistics of Sweden from 1985 and 1986, the percentage of "oncoming" vehicle accidents with personal injury is four times greater on snowy/icy roads (16%) than on dry clear roads (4%), SCB (1986) and SCB (1987). The percentage "rear end" accidents is the same (6%) for both road conditions. When considering the Swedish accident numbers from 1985 and 1986 to be representative samples of these accident types, Strandberg (1988) found that their difference in road slipperiness sensitivity was significant on the 0.001 level (chi-square 173 and 253 respectively).

Perhaps it is contrary to common belief, but slippery road conditions are much more overrepresented in "oncoming" than in "rear end" accidents. See figure 1. This indicates that more emphasis should be put on instability and skidding problems (typical for oncoming vehicle accidents) than on braking distances and steering-while-braking problems (rear end accidents).

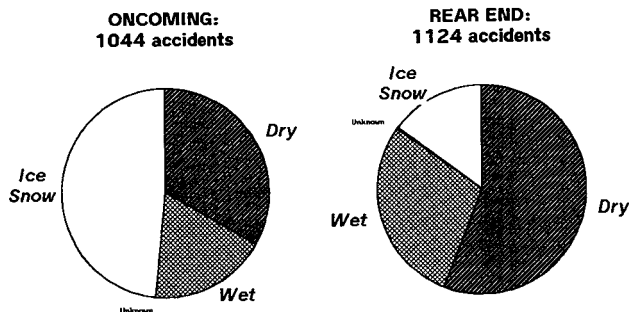


Figure 1. Distribution of road surface conditions in two types of police reported accidents with personal injury, Sweden 1986. Data from SCB (1987).

Also the fatality numbers in multiple vehicle crashes are dominated by "oncoming" accidents. According to Swedish statistics from 1985 and 1986, "oncoming" vehicle accidents killed 364 people, while 26 persons died upon "rear end" accidents. Figure 2 gives the division of fatalities during 1986 between different types of accidents between motor vehicles.

## Superior Front Wheel Cornering Performance Threatens Stability

A vehicle is stable if the resultant of external forces applies to the rear of the centre of gravity (figure 3). When aerodynamic forces are negligible, this condition is fulfilled in a car at any speed (and without demands on compensating

steering), if the cornering performance (or cornering stiffness coefficient as defined by SAE, 1975) of the front wheels is inferior to that of the rear wheels. See Strandberg (1983) and Strandberg et al (1983) for mathematical details.

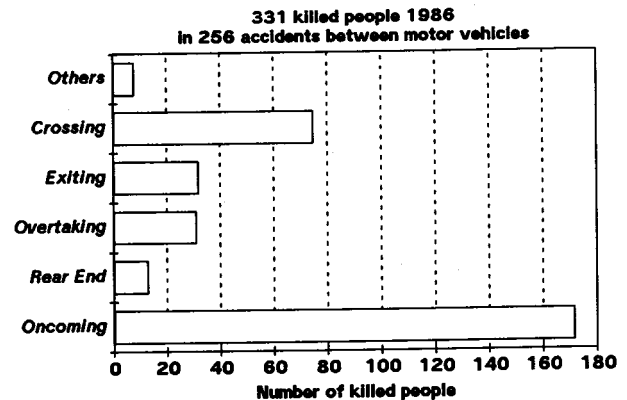


Figure 2. Number of killed persons in different types of accidents between motor vehicles, Sweden 1986. Data from SCB (1987).

Since lateral tyre forces are reduced by longitudinal ones, stability may be reinforced also if the front wheels are overpowered or overbraked compared to the rear wheels.

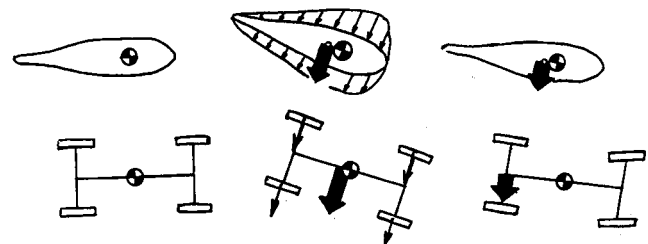


Figure 3. External forces and their resultant acting on a vehicle (air- or waterborne ship above, and car below). Stability and spontaneous return to original direction, since the resultant force applies to the rear of centre of gravity. Sequence of events and direction of motion from left to right.

Superior front wheel cornering performance, on the other hand, may initialize spontaneous skidding and spin-outs. That has been confirmed in a considerable number of accident case descriptions. A pilot investigation of some hydroplaning fatality cases, revealed that the tyre tread pattern of the skidding and outspinning cars was much deeper at the front than at the rear (table 1).

In the year of 1986, 327 car drivers and 155 passengers were killed in Swedish traffic accidents, that is 9 car occupant fatalities per week. According to table 1, rear wheel skids and poor rear tyres may contribute about a quarter of this average during certain time periods. However, a more scientific and systematic approach is needed before any general conclusions can be drawn on the relative influence from the front tyres compared to the rear ones. Therefore, a case-control investigation is being planned to study if poor rear tyres are overrepresented in accidents on slippery road surfaces. See the last paragraph of this paper.

**Table 1. A sample of car occupant fatalities reported as hydroplaning accidents, where it has been attempted to assess the tyre tread pattern depth. Cases (2-8) discovered in Swedish newspapers from four summer weeks in 1988, and an additional accident (Acc. ref. no. 1) from 1987, the documents of which were investigated on request from a local Court.**

Acc. Ref. No.	Date	No. of Killed People	DEVIATING CAR		TYRE PATTERN (mm)				Comments
			Skid at	Wheels Driven	Rear Left	Rear Right	Front Left	Front Right	
1	July 25, 1987	3	Rear	Front	2?	< 1.6	New	New	BHN 794. Rear tyre photos only.
2	July 25, 1988	1	Rear	Rear	0-1	Burned	> 6	> 6	KYM 965. Car on fire.
3	July 29, 1988	1	Rear	Front	0-1	2	4	4	MUP 991.
4	July 29, 1988 (1)	1	Front	Rear	2.5	2.5	3	3	GZJ 434. Plow out (front skid).
5	July 30, 1988	1	Rear	Rear	Tyres burned & destroyed				KHD 343. Minibus skidding.
6	Aug. 4, 1988	3	Rear	Rear	0.5-1	1	4-5	4-5	EBK 322.
7	Aug. 15, 1988	1	Rear	Rear	2	2	7	7	MZD 964. Single vehicle acc.
8	Aug. 20, 1988	2	Rear	Rear	1	1	3-4	3-4	TSU8854.
No.2-8:		10	Hydroplaning fatalities in 4 weeks discovered in this survey.						
No.2-8 but no.4:		9	Rear wheel skid fatalities in 4 weeks discovered in survey.						
No.1-8 but no.4:		12	Rear wheel skid fatalities. Total number discovered in survey.						

## Stability and Controllability in Different Situations and Cars

Directional (yaw) stability is often reduced when controllability is improved. Therefore, some measures on the car may deteriorate safety, though they are based on many individuals' experience from normal driving and though they aim at increasing the driver's control over the vehicle.

Also contributing to the contradiction is that skilled drivers are able to better control the motion of the car by forcing it into an unstable state. For instance, in competition driving or the like it may be advantageous to turn the car quickly and precisely. Then the throttle may be used to spin the wheels and the hand controlled (parking) brake to lock them up.

This was demonstrated in a television program (Billing, 1988), where the VTI test driver kept the car spinning in about nine revolutions while its speed decreased from 70 km/h to standstill. The car was front wheel driven and the hand brake acted on the rear wheels.

In the same broadcast it was made clear that severe yaw motions, being extremely dangerous in real traffic, may occur unintentionally and suddenly if the rear wheels are overpowered or overbraked. Such cases may well be initialized on icy roads by the automatic cruise control devices, though they are considered contributing to safety by helping the driver to keep the speed limits.

It has also been observed (Strandberg, 1988) that rear skid recovering may be simplified by braking in certain ABS-equipped cars. Since overbraking of the front wheels reduces their side forces, the need of precise countersteering becomes less pronounced.

## Front Wheel Drive and Studded Tyres

Common driving experience indicates that severe yaw and rear wheel skids are unlikely to occur in front wheel driven cars. However, irrespective of front or rear drive, Strandberg (1988) found spin outs more frequent than plow outs in double lane change tests on ice with ordinary studded tyres. Since then it has been observed that the stud protrusion tends to increase at the driven wheels and to decrease at the other ones, particularly in front wheel driven cars. Therefore, front wheel driven cars with studded tyres may be more susceptible to unexpected loss of stability on winter roads.

Stud protrusion was measured by the VTI during the winter 1988/89 on a sample of 200 cars in Sweden. To achieve results representative for the Swedish tyre population, police officers selected the cars randomly from the normal traffic flow on suitable roads. The average stud protrusion was greater at the driven wheels. The difference was most pronounced and statistically significant for front wheel driven cars. See table 2, confirming that front wheel driven cars with studded tyres tend to be less stable on ice, when longitudinal tyre forces are negligible.

The corresponding hazard of front wheel drive is reinforced by the fact that common education recommends drivers (even of front driven cars) to depress the clutch pedal before countersteering in a rear wheel skid. The recommendation may stem from successful tests with experienced drivers, who are unlikely to resist countersteering until the skid is fully developed and to avoid any recovering action before depressing the clutch pedal. See Strandberg (1988) for further details.

Nevertheless, studded tyres on today's average car seem to improve safety on ice and snow according to the preliminary results from a case-control (pilot) study carried out in two Swedish police jurisdictions from November 1988 to

Table 2. Stud-protrusion-statistics. Data from Random selection of 200 cars in traffic on Swedish roads during winter 1988-89. (Report by Samuelsson in preparation.)

Driven wheels	Average Tyre Stud Protrusion (Variable Definition)	No. of Cars	Variable Mean (mm)	Std. Dev. (mm)	Std. Error (mm)	Min. value (mm)	Max. value (mm)	Comments
Rear	Rear Right	90	0.89	0.46		0.00	2.00	
Rear	Rear Left	90	0.90	0.47		0.00	1.90	
Rear	Front Right	86	0.84	0.44		0.00	1.70	
Rear	Front Left	86	0.83	0.46		0.00	1.90	
Front	Rear Right	72	0.75	0.50		0.00	2.30	
Front	Rear Left	71	0.80	0.50		0.00	2.30	
Front	Front Right	75	1.01	0.51		0.10	2.60	
Front	Front Left	75	0.96	0.50		0.00	2.60	
Rear	Rear minus Front	86	+0.06	0.34	0.04	-0.95	+1.05	
Front	Rear minus Front	71	-0.21	0.27	0.03	-1.15	+0.45	Mean signif. < 0

April 1989 (Strandberg & Junghard, in preparation). Based on the share of studded tyres in 30 accident involved cars and in 126 cars bypassing the accident site, the accident risk was assessed 90% greater for cars without studs. However, the safety superiority on ice with studded tyres was not significant ( $0.1 < p < 0.2$ ), and the relative risk is expected to be different (from 1.9) when more data are available for analysis.

## References

- Aschenbrenner M, Biehl B, Wurm G (1988): Mehr Verkehrssicherheit durch bessere Technik? Felduntersuchungen zur Risikokompensation am Beispiel des Antiblockiersystems (ABS). Unpublished, Mannheim, 1988.
- Billing P (1988): Slipperiness. Feature of the Channel 1 program "Science". (In Swedish: Halka. Inslag i Kanal 1-programmet "Vetenskap".) Swedish Television Broadcasting Company, Stockholm, January 30, 1988.
- Glad A (1988): Phase 2 in Driver Education. Effects on Accident Risk. (In Norwegian: Fase 2 i Føreropplæringen. Effekt på ulykkesrisikoen.) Report no. 0015/1988, Transportøkonomisk Institutt, Oslo.
- Rompe K, Schindler A, Wallrich M (1987): Advantages

of an Anti-Wheel Lock System (ABS) for the Average Driver in Difficult Driving Situations. Proceedings (pp. 442-448) on the 11th ESV Conference, Washington DC, May 12-15, 1987.

SAE—Society of Automotive Engineers (1975): Vehicle Dynamics Terminology. SAE J670D, Warrendale, PA 15096.

SCB—Statistiska Centralbyrån (1986): Traffic Injuries 1985. Official Statistics of Sweden S-115 81 Stockholm.

SCB—Statistiska Centralbyrån (1987): Traffic Injuries 1986. Official Statistics of Sweden, S-115 81 Stockholm.

Strandberg L (1983): Danger, Rear Wheel Steering. Journal of Occupational Accidents, vol. 5, pp. 39-58. Elsevier Scientific Publishing Company, Amsterdam.

Strandberg L (1988): On Skidding Accidents and Skidpad Training. Theoretical Analysis and Tests with Experienced Drivers. (In Swedish: Om sladdolyckor och halkutbildning. Teoretisk analys och körförsök med vana forare.) Note TF 60-04, Swedish Road and Traffic Research Institute, Linköping, October 24, 1988.

Strandberg, L, Tengstrand G, Lanshammar H (1983): Accident Hazards of Rear Wheel Steered Vehicles. In Johanssen G & Rijnsdorp JE (eds.): IFAC Analysis, Design and Evaluation of Man-Machine Systems, pp. 399-405, Pergamon Press, Oxford and New York.

# Volvo Concept for Active Safety

Lars-Runo Tillback, Johan Wedlin,  
Volvo Car Corporation, Göteborg, Sweden

## Abstract

As a background for the following discussion some of the most significant limitations which affect driving safety are pointed out. Conventional chassis design compromises are analysed and the resulting property levels are described.

As a result of this a number of areas, in which improvements are specifically desirable, are identified.

Active suspension and four wheel steering are two relatively new techniques. Active suspension has been studied at Volvo during several years in the CCS (Computer Control Suspension) version. Four wheel steering has been added to this study at a later stage. Specific emphasis has been put on the potential to achieve new and better compromises in the interest of driving safety.

Simulation and test results are presented which show some of the potentials of each system.

After that a synthesis of the desired property improvements and the possible improvements from active systems is done.

This results in a special project—Volvo Concept for Active Safety (VCAS). This project also includes a study of tyre development as an important part in improving driving safety.

The ideas which went into this project are described more in detail and the principal design is presented. Test results which support the ideas are shown.

Finally it is concluded that a combination of active suspension, four wheel steering and purpose developed tyres can give a significant improvement of driving safety.

## Introduction

Accidents with cars depend on several factors, separately or in combination:

- Surroundings (road, sight, other vehicles)
- The vehicle
- The driver

As a car manufacturer our task is to influence the vehicle and its adaptation to the surroundings and the driver.

This paper deals partly with the problem of adapting the vehicle to changing road conditions and partly with the adaption of the vehicle properties to the driver.

A lot is still to be learned about the driver's behaviour in different situations. Volvo has however established the following basic rules regarding the handling properties:

- The control properties should be as *consistent* as possible.
- The *feed back* signals through the normal controls (steering wheel, brake pedal, accelerator) should be *distinct* and together with feed back from

lateral/longitudinal accelerations and yaw velocity give good indication when limits of adhesion are approached.

- The vehicle and its control system should be *unsensitive to disturbances*.

It is well known and accepted that the lateral and longitudinal accelerations of a vehicle are limited by the available tyre/road friction. On a smooth and dry asphalt road the maximum acceleration at braking and curve driving is around 0.8–1.0 g for most cars.

Since the required accelerations during normal driving are 0.2–0.4 g this gives a good safety margin (figure 1). Other road conditions may however change this. Ice, snow and water on the road decreases the friction to, in some cases, very low values. The safety margin is then drastically decreased or even negative if the driver does not change his driving strategy, i.e. lowers the speed and brakes and accelerates more gently. Since the common trend has been towards wider tyres, the difference in safety margins on dry roads respectively icy or wet roads has increased.

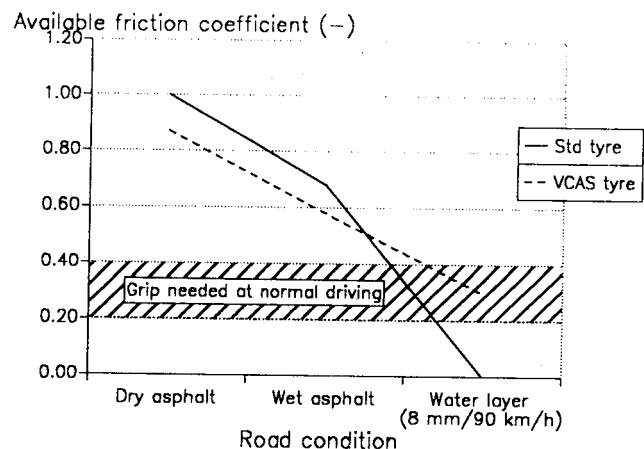


Figure 1. Available friction on different road conditions.

The above facts are the main reason for the creation of the Volvo Concept for Active Safety—VCAS. Other limitations of the conventional vehicle are pointed out in the following.

## Limitations of the Conventional Vehicle

One of the significant factors regarding the adaption of a vehicle to the surroundings is the variation of friction between tyre and road. Snow and ice are of course well known reasons for decreased friction. The use of winter tyres, with or without studs, is an accepted solution to get higher friction. This type of tyres, however, gives a number of drawbacks. Apart from increased road surface wet and higher tyre/road noise, the steering and stability on non-covered roads deteriorate.

There is no similar solution regarding lower friction

caused by water layer on the road. Wide tyres, which are required for the high speed stability (and fashion), combined with very smooth road surfaces and longitudinal tracks on the road, can result in very low friction values already at moderate speeds when the road is covered by water.

Another factor which reduces the effective friction on a conventional vehicle is the fact that the car is rolling during curve driving and pitching during braking and acceleration, which gives two effects:

One is caused by restricted wheel travels. Wheel travel is "consumed" by the roll motion in curve driving. The inner wheel comes closer to the rebound stop and a relatively small unevenness can cause the spring action of the body to lift the inner wheel. Since this risk increases with higher lateral acceleration it can result in sudden change of characteristics.

The other one is caused by the induced tyre camber. Practically all wheel suspensions, except live axles, give a camber angle change of the tyre against the road when the body is rolling or pitching. This results in a decreased friction level as compared to the maximum capability of the tyre.

Uneven or bumpy roads cause variations in the tyre to road force. Because of the tyres degressive vertical force/friction characteristic, the result is a net loss of friction, figure 2.

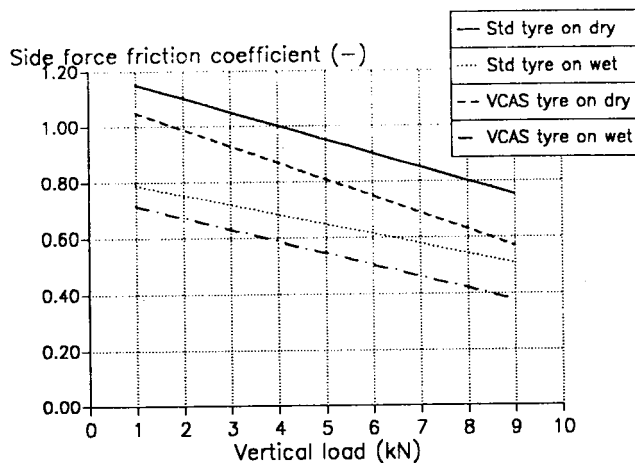


Figure 2. Friction coefficients on dry and wet asphalt roads.

This can be quite severe when the car is excited with the sprung mass frequency. The amplitude of body movements can be so high that the wheels are lifted from the ground. This is especially significant on cars with shock absorbers set primarily for good ride comfort.

These problems are true limitations of the conventional car in the sense that they can only be minimized at the sacrifice of other properties. The Volvo Concept for Active Safety aims at solving them without this sacrifice.

## Purpose-Developed Tyres

The tyres are involved in many sub-properties of the vehicle, like ride comfort, noise isolation etc, apart from

handling requirements. They also have to fulfill demands on wear resistance, rolling resistance etc.

The undoubtedly most important task of the tyres is to interact with the road surface to give a friction level which is high enough to assure safe use in traffic.

It is therefore the intention of this work to create an overall concept which allows the best possible use of the existing tyre grip and to lower the demands on the other tyre properties in favour of raised friction on bad road conditions. In other words, to change the tyre property profile towards a more friction oriented one.

Tyres of this type exist already. In many countries winter tyres, with or without studs, are used during winter periods. These tyres are of course optimized to get higher friction on snow and ice. They have more open and deeper tread patterns and are also often more narrow than the corresponding standard tyres. As a result of this they have lower cornering stiffness (figure 5) and lower maximum friction on dry asphalt road (figures 2 and 3), which cause degradation of steering and stability properties. This type of tyres, however, gives also a significant improvement regarding hydroplaning (figure 4).

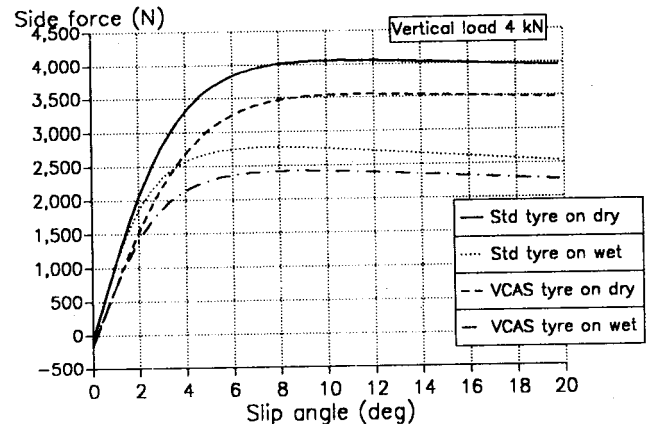


Figure 3. Side forces as function of slip angle.

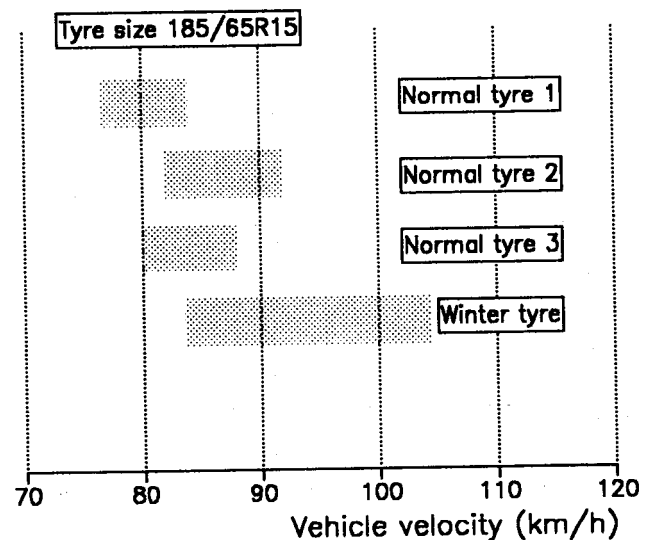


Figure 4. Velocities for initial resp final loss of adherence on water layer.

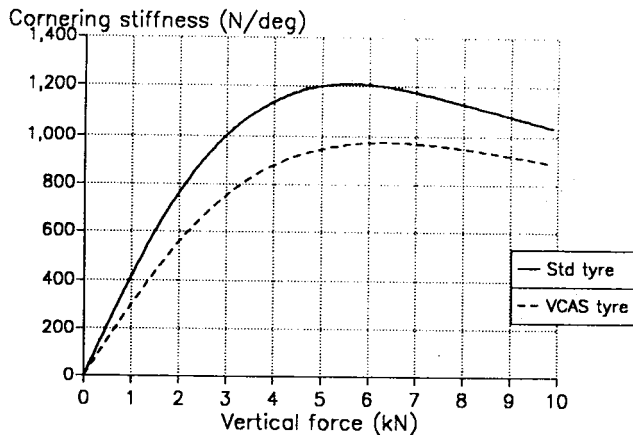


Figure 5. Cornering stiffnesses as function of load.

These facts have led to the idea to develop a tyre which is similar to a winter tyre regarding hydroplaning properties, cornering stiffness and friction on dry asphalt road but which fulfill normal demands (or better) regarding other properties. The demands on steering and stability properties, maximum lateral acceleration etc. will be supported by the action of the active suspension and the four wheel steering system, according to the following chapters, in order to fulfill high demands on these properties.

The result of this philosophy is a prototype of the VCAS-tyre. A development program is set up with the tyre manufacturer Michelin with the intention to fully explore a new optimization of tyre properties, towards more grip orientation.

The tests presented in this paper are run on tyres with data according to figure 2, 3, 4, 5.

Tyre data are measured and implemented in the tyre model described in reference (4)\*. This tyre model and data are used for the simulations presented in this paper.

## The Effect of Active Suspension

The Volvo active suspension, CCS (Computer Controlled Suspension), is described by Tillback and Brodd (5). It allows control of body motions in the vertical, roll and pitch modes. It also allows control of semi-static vertical force distribution between the wheel and the dynamic force variation between tyre and road.

The improvements regarding tyre-road grip are derived from the following facts:

### Body roll

The body roll is kept at zero roll during curve driving. The wheel travel in a conventional car is partly consumed by the roll movement so that the outer wheel comes closer to full bump and the inner wheel closer to full rebound. By eliminating the roll the free movement before the suspension goes to full wheel travel is increased and the tyre to road force variations are minimized.

Another important effect of the zero roll is that the tyre is kept at zero camber angle. This reduces the slip angles and

increases the maximum lateral force which can be produced by the tyre, figure 6. A tyre with lower cornering stiffness and friction can hence give the same cornering behaviour on an active suspension car as a "tougher" tyre on a conventional car.

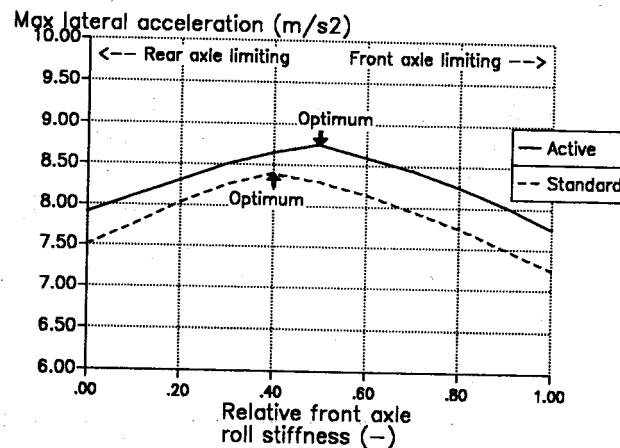


Figure 6. Maximum lateral force as function of relative roll distribution.

## Roll moment distribution

The roll moment, caused by lateral acceleration, can be controlled by an algorithm which uses the yaw velocity overshoot as an error signal:

$$\psi_e = \psi_m - \frac{U \cdot \beta_r}{L}$$

where:

$\psi_e$	Yaw velocity error
$\psi_m$	Measured yaw velocity
$U$	Vehicle velocity
$\beta_r$	Front wheel steer angle
$L$	Wheelbase

The vehicle is then effectively steered at high lateral accelerations by the change in roll moment distribution. The result of this method is that both the steering response and the stability are improved. The nominal roll moment distribution can be closer to the optimum according to figure 6, which further increases the available lateral grip compared to a conventional vehicle.

## Controlling the sprung mass

The sprung mass is controlled in all modes by a "sky-hook"-algorithm, as shown in the first part of the expression below.

This makes it possible to use very high relative damping compared with a conventional car without deterioration in ride comfort while, more important in this case, reducing the body to wheel motion so that the tyre to road force is not

\*Numbers in parentheses designate references at end of paper.

$$I_{dem} = k_a \cdot V_{dem} = k_a \cdot \left( \frac{F - C_s \cdot X}{D_s} \right) + (k_u \cdot V_{vu} + k_{mu} \cdot a_{vu})$$

where:

$I_{dem}$	Required valve current	$D_s$	Simulated damping
$k_a$	Actuator/valve coefficient	$k_u$	Unsprung mass vertical velocity coefficient
$V_{dem}$	Computed actuator velocity demand	$V_{vu}$	Vertical velocity of unsprung mass (integrated from $a_{vu}$ )
$F$	Measured force between actuator and sprung mass	$k_{mu}$	Unsprung mass vertical acceleration coefficient
$X$	Measured actuator position	$a_{vu}$	Vertical acceleration of unsprung mass
$C_s$	Simulated stiffness		

affected by the suspension going to full rebound or full compression.

The effect of body motion is illustrated in figure 7, which shows the superior body control at lower frequencies for the CCS system.

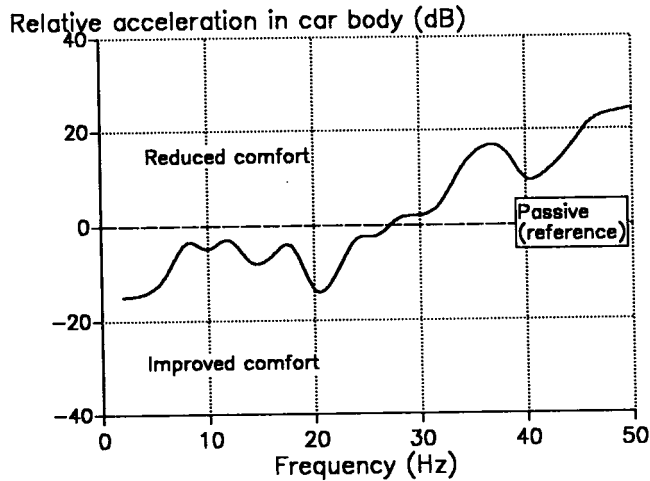


Figure 7. Comparison between CCS car and passive car from road measurements.

## Controlling the unsprung mass

Tyre to road force variations which are normally caused by unsprung mass to road resonances are minimized by the ability of the active suspension to control the vertical movement of the wheels separately. The second part of the expression above controls the unsprung mass.

## The Effect of Four-Wheel Steering

### Existing systems

Four wheel steering systems (4WS) have been the subject of intense studies in later years, both theoretically and in the presentation of a number of experiment and production vehicles. Most of the earlier work emphasized using 4WS for improving the high speed handling, often used the concept of minimizing the vehicle slip angle, as well as the low speed manoeuvrability (parking manoeuvres).

The high speed handling has been improved, but not to a significant degree since most modern cars already have good stability and steering properties. Also, the concept of minimizing the vehicle slip even further makes one of the inputs used by the driver to monitor the vehicle behaviour, weaker.

The turning radius can of course be significantly reduced.

This is presently not regarded as very important for Volvo cars since they have a turning diameter of less than 10 m (between kerbs).

It is however clearly shown that it is possible to influence the car behaviour significantly by using 4WS.

## Volvo dynamic control steer (DCS)

The Volvo concept of using 4WS, hereby introduced in the VCAS, is aimed at compensating for the improvements in properties *other* than the pure handling on dry surfaces, primarily the aquaplaning resistance and wet grip properties of the tyres, described in the tyre section above. The aim is also to keep the feeling of the car familiar, rather like a standard Volvo.

Later studies have pointed out the potential of giving the car an initial yawing motion when entering a curve, then stabilizing it when in the curve. Landreau (3) suggests a proportional steering with a delay, while Nalecz and Bindemann (1, 2) show the potentials of using a so called rear advance steering system. Both of these systems are open-loop but have the advantage of using simple input signals. Closed-loop 4WS systems would of course have a greater potential, but these demand more expensive transducers and a more error-sensitive control loop.

For the VCAS we have adopted a rear advance steering system, which we have called Dynamic Control Steer (DCS). This system can be described by the equation

$$\beta_r = k_1(U) \cdot \beta_f + k_2 \cdot \dot{\beta}_f$$

where  $\beta_r$  is the rear wheel steer angle,  $\beta_f$  is the front wheel steer angle and  $\dot{\beta}_f$  is the front wheel steer velocity.  $U$  is the vehicle velocity while  $k_1$  and  $k_2$  are parameters controlling the system. Positive rear wheel steer angle is defined as in-phase steering (understeer effect).

$$k_1(U) = k_3 \cdot U - k_4$$

Parameter  $k_1(U)$  is the so called *steady-state factor*. It gives a rear wheel steer angle proportional to the front wheel angle and is velocity-dependent in the way that it increases with vehicle velocity, as shown in figure 8. This dependence is designed to give a more *consistent* steering feel and increased stability with increasing speed.

Parameter  $k_2$  is the *transient factor*. It controls the *addition* of yaw motion when entering a curve which gives faster vehicle response, and the *counteraction* of the yaw motion when leaving the curve which gives improved stability. It has no effect in steady-state conditions.

The principle of the Volvo DCS is shown in figure 9.

Since  $k_1$  increases with speed while  $k_2$  does not, the vehicle is increasingly stabilized with speed, as compared with a conventional 2WS vehicle. Figure 10 shows the gain between steering wheel angle and lateral acceleration for a 2WS Volvo with standard high performance tyres and with the special tyres, and the VCAS with special tyres.

As seen in the figure, the gain is decreased for the VCAS compared with the standard car. This can be compensated

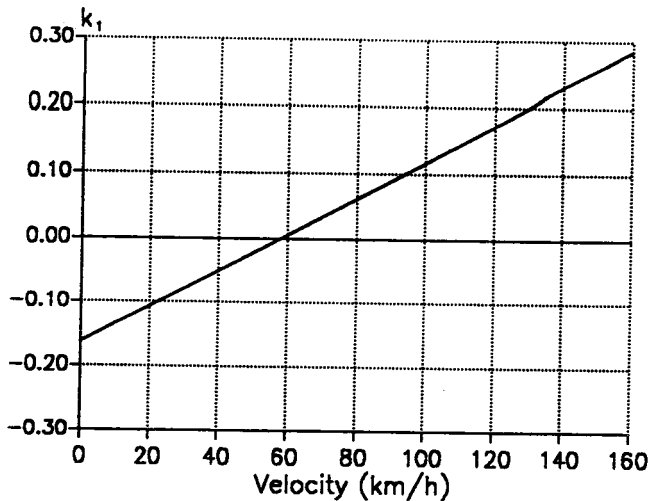


Figure 8. Variation of steady-state factor  $k_1$  with vehicle velocity.

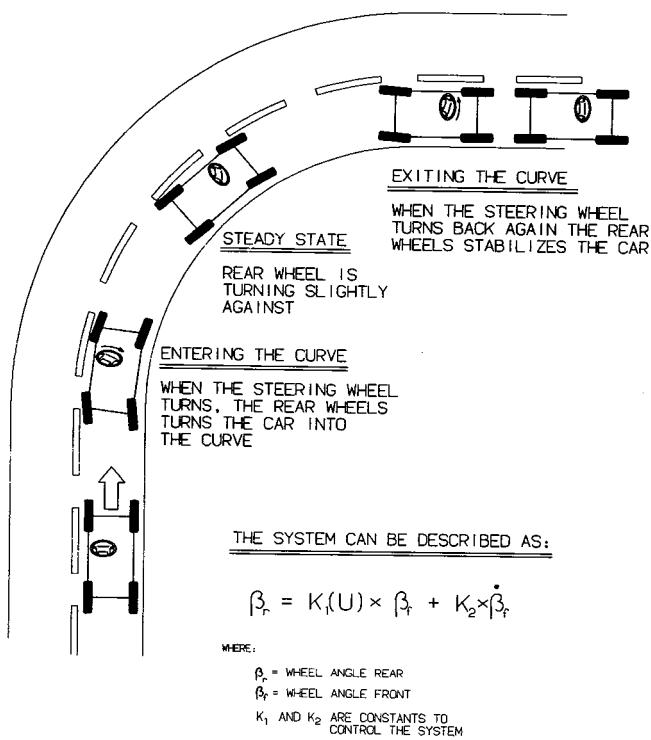


Figure 9. Principle of Volvo DCS.

by changing the front steering ratio. An example of this is also shown in the figure above.

The two factors  $k_1(U)$  and  $k_2$  have to be carefully tuned to get the desired properties for driving safety (stability) and course stability for different driving situations. The 4WS vehicle has been computer simulated and tested, with the special tyres. The simulations have been made with the vehicle and tyre model described in (4). The tests have been made, subjectively together with Michelin at the Michelin test tracks in France, and objectively at the Volvo test tracks in Sweden.

The two factors  $k_1(U)$  and  $k_2$  have been chosen to give the desired properties, while avoiding giving the vehicle the typical "4WS behaviour" for the reasons mentioned earlier.

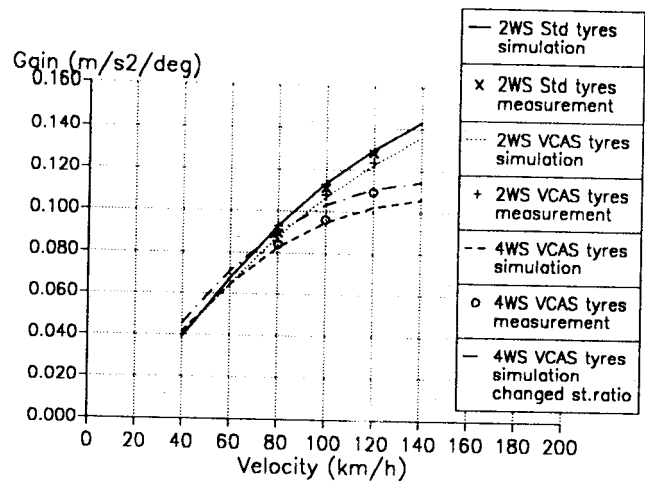


Figure 10. Lateral acceleration gain.

The rear wheel steer angle is limited to 2 degrees, which is quite sufficient to create good stability. We have chosen not to go further to achieve a smaller turning radius, also for the reasons described above. The possible 2 degrees rear steer angle thus gives a turning radius decrease by about 0.16 m.

### System layout

The Volvo DCS system, as described above, is entirely controlled by electronic input signals, derived from (a) the front wheel steer angle, (b) the front wheel steer angle velocity and (c) the vehicle velocity. The signals are processed within the onboard main CCS computer (5). The resulting output signals is then fed into the rear wheel steering actuator, which acts on the track rods of the Volvo Multilink rear suspension (described by Andersson, Bane and Larsson (6)) figure 11.

The control system of the actuator is doubled in order to check for system errors. In case of any error detection, the actuator is pushed to initial (mid) position by stiff springs and then locked in that position, resetting the car to 2WS. This system is necessary since a malfunctioning rear wheel steering system would make the car potentially unstable. More research in the field of reliability is necessary before putting any electronically controlled rear wheel steering into production.

### Test and Simulation Results

In the following section, we will show with simulation and test results how handling is affected for 3 cases:

- (1) 2WS with standard high performance tyres
- (2) 2WS with special aquaplaning resistant and high wet grip tyres
- (3) 4WS with special aquaplaning resistant and high wet grip tyres (VCAS)

The simulation model used is described by Bakker, Pacejka and Lidner (4) and includes the tyre model developed by Volvo and the University of Technology in Delft, the Netherlands. The 4WS system is modelled as an

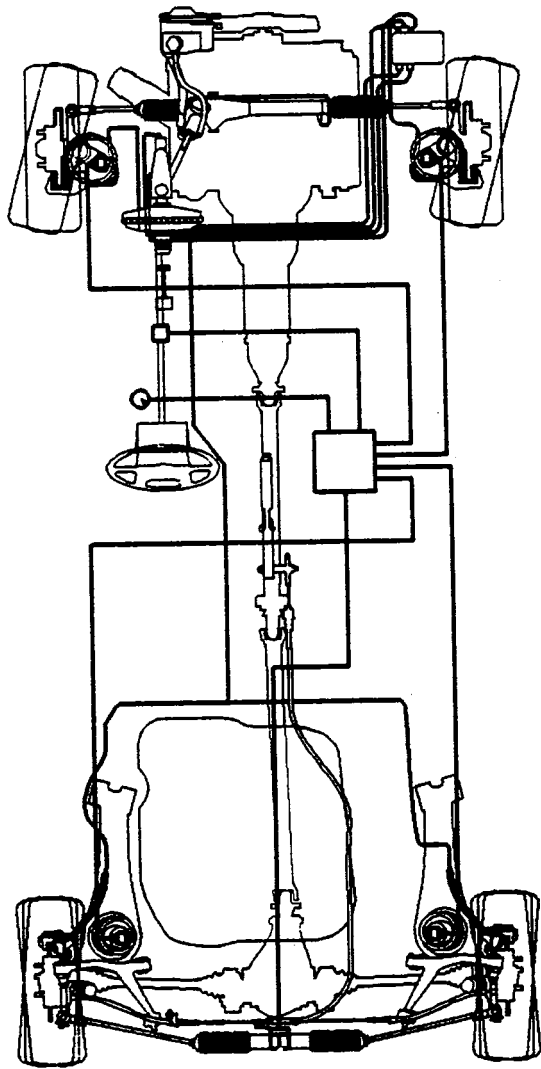


Figure 11. DCS system layout.

analog system, while the CCS system is not modelled at this stage.

Measurements are run on a CCS car equipped with DCS, which can be disengaged when applicable. The test equipment consists of a steering machine and a gyro platform measuring yaw velocity, lateral acceleration, roll angles etc.

### Sine time lags according to ISO/TR 8725 (lane change test)

The car is driven at 80 km/h on wet asphalt road. A sinusoidal steering input is given at a frequency of 0.5 Hz. The test is repeated with different steering wheel angle amplitudes. This test includes the dynamic behaviour of the car, and it is our opinion that it correlates well with the subjective assessments of the vehicle handling. The test mainly evaluates the steering properties at normal curve driving, but also the avoidance manoeuvre stability at higher lateral accelerations. Many properties can be extracted from the test results; we have chosen to show the sine time lags (second peak time lags) to yaw velocity and lateral

acceleration as functions of the peak lateral acceleration, figure 12 and figure 13.

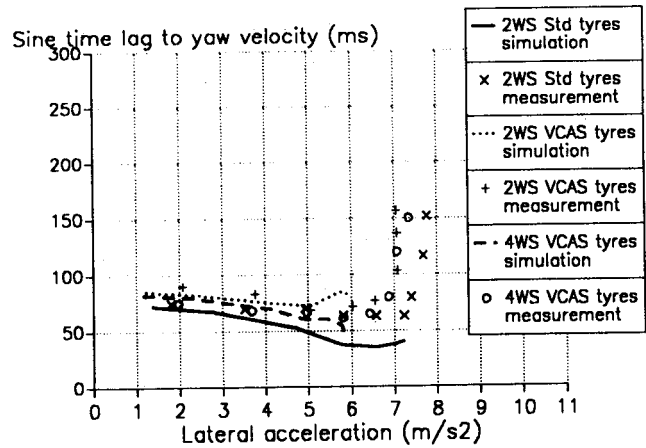


Figure 12. Lane change test. Sine time lags to yaw velocity.

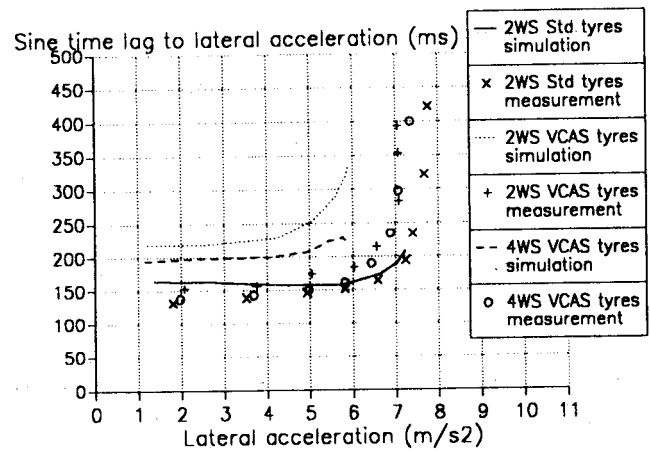


Figure 13. Lane change test. Sine time lags to lateral acceleration.

The correlation between simulations and measurements is quite good regarding time lags to yaw velocity; for these the DCS system has a strong influence. The correlation regarding time lags to lateral acceleration is not so good; this is probably due to that the CCS system is not included in the simulation model. The advantages of the CCS system makes it possible to make better use of the tyres, here showing as decreased time lags to lateral acceleration.

The diagrams show that the time lags of the 2WS car with standard tyres are more or less retained by the 4WS vehicle with special tyres. The 2WS car with special tyres has higher time lags, especially to lateral acceleration. The 4WS vehicle, however, is not quite so good as the standard 2WS at higher lateral accelerations, which indicates that the maximum available grip of the special tyres is, as expected, not quite so high as the standard tyres on dry asphalt road, but still good enough.

### Step response

This test is mainly for evaluating the vehicle stability, which in our case is mainly controlled by the CCS system but also by the transient parameter of the 4WS system. The

car is driven straight ahead at 80 km/h when a steering step input is given. The yaw velocity overshoot, defined as the difference between the yaw velocity and the lateral acceleration divided by the vehicle velocity, and the vehicle slip angle are calculated for different steering wheel amplitudes, figure 14 and figure 15.

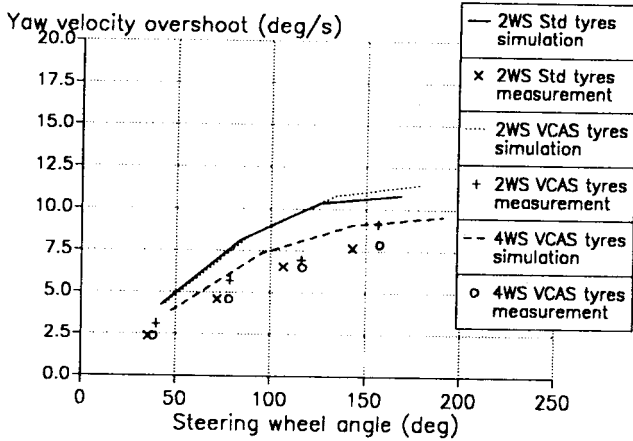


Figure 14. Step response. Yaw velocity overshoot.

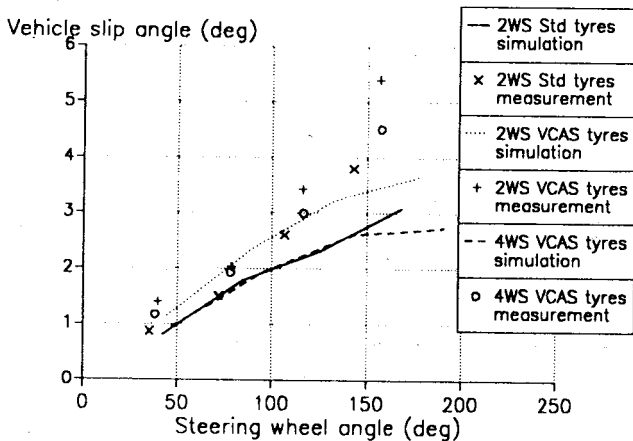


Figure 15. Step response. Vehicle slip angle.

The diagrams show that the stability of the VCAS is as good as that of the car equipped with 2WS and standard tyres. The correlation between simulations and measurements are not so good in this case, due to the fact that the CCS system is not modelled. Since the yaw stability is mainly controlled by the CCS system, the measurements show better results than the simulations. The trends are however still the same. A more detailed model including the CCS system will be set up in order to create better prediction possibilities also for avoidance manoeuvres.

### Side wind stability

The car is driven in natural side wind stochastic disturbances. RMS-values of the yaw velocity and wind velocity are calculated and the yaw coefficients  $RMS_{yaw}/RMS_{wind}$  are calculated. The coefficients are compared with, and referenced to, the 2WS car with standard tyres, figure 16. No simulations of this test have been made.

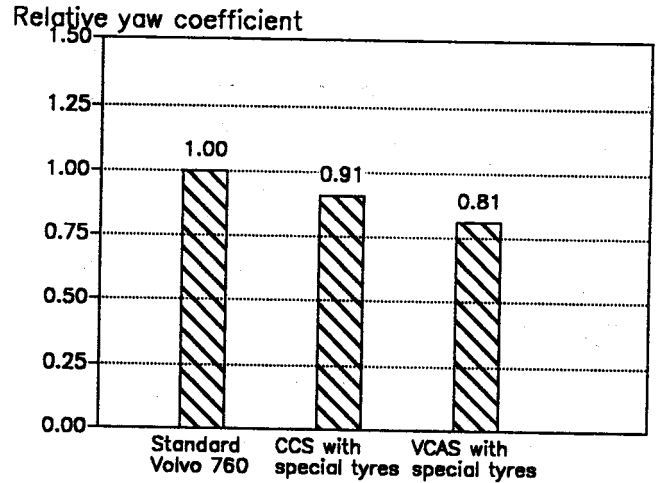


Figure 16. Side wind stability. Yaw coefficients.

The diagrams show that already the CCS with the softer special tyres stabilizes the car with a yaw coefficient that is 91% of that of the standard Volvo 760. The VCAS is even better with a yaw coefficient of only 81% of the reference car. This test has been used for the first set-up of the parameters  $k_1$  and  $k_2$  since it involves many normal driving situations.

### Conclusions

The work presented in this paper shows that a *symbiosis* of the CCS, DCS and the tyre systems gives a significant improvement of important properties.

The DCS system described in this paper would have given a slight improvement of steering characteristics in combination with normal tyres. By combining tyres with special characteristics with DCS and CCD, much more significant improvements in several properties are achieved.

Figure 17 is a synthesis of the results and illustrates clearly the gains which are achieved. Driving safety, driving pleasure and comfort properties are improved. These gains are made without deterioration in other properties. It is therefore to be considered as a *true step forward* in the application of new technology in passenger cars.

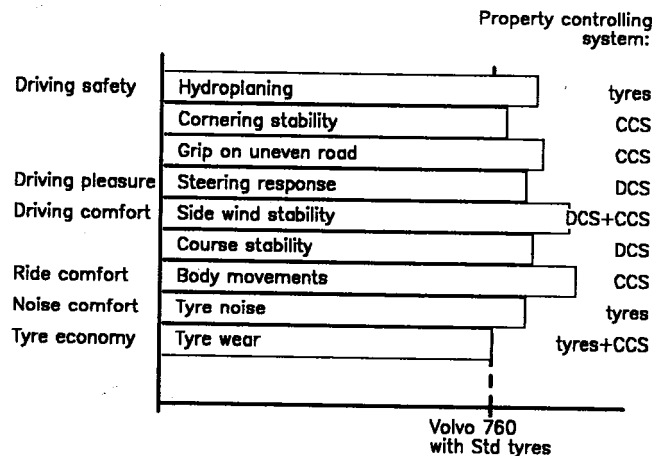


Figure 17. Property profile compared with standard.

## References

- (1) Nalecz A.G., Bindemann A.C.: Investigation into the Stability of Four Wheel Steering Vehicles. *Int.J. of Vehicle Design*, Vol. 9, No. 2, pp. 159–178, 1988.
- (2) Nalecz A.G., Bindemann A.C.: Handling Properties of Four Wheel Steering Vehicles. SAE Paper No. 890080.
- (3) Landreau T: Simulation of Dynamic Behaviour of a Four Wheel Steering Vehicle by Means of a Vehicle and Driver Model. SAE Paper No. 890078.
- (4) Bakker E., Pacejka H.B., Lidner L.: A New Tire Model with an Application in Vehicle Dynamics Studies. SAE Paper No. 890087.
- (5) Tillback L.-R., Brodd S.: Active Suspension—The Volvo Experience. SAE Paper No. 890083.

- (6) Andersson J.-E., Bane O. Larsson A.: Volvo 760 GLE Multi-link Rear Axle Suspension. SAE Paper No. 890082.
- (7) Takahashi T., Pacejka H.B.: Cornering on Uneven Roads. 10th IAVSD Symposium, 1987.
- (8) Jaksch F.O.: The Influence of Different Vehicle Parameters on Steering Controllability and Stability. IMechE Road Vehicle Handling Conference, 1983.

## Acknowledgements

The authors wish to thank all people involved in the Volvo-Michelin co-operation group, Mr. Lars Lidner for doing all simulations, Mr. Alf Söderström for performing the objective handling tests, Mr. Jan van Oosten for work on the tyre model and to all other people who have given their help in producing this paper.

## Braking and Stability Performance of Cars Fitted with Various Types of Anti-Lock Braking Systems

**B.J. Robinson, B.S. Riley,**  
Transport and Road Research Laboratory,  
Department of Transport,  
United Kingdom

### Abstract

The effectiveness of four modern anti-lock braking systems has been assessed in an extensive programme of track tests. The performance of the systems in three different manoeuvres, on a range of road surfaces, has been compared to that attainable by the vehicles with the systems wholly or partially disabled. It is shown that while the deceleration performance of an anti-lock system is closely related to its degree of complexity, the improvement in controllability that is provided by any system ensures that the accident avoidance potential of all of the vehicles tested is greater than that of the non anti-lock vehicles. This potential is shown to be higher for the complex, and expensive, electronic systems but still significant for a cheap and simple mechanical system.

### Introduction

Over a period of many years car anti-lock braking systems have been developed to improve vehicle stopping distances and to provide controllability under all braking conditions. By not allowing some or all of the wheels on a vehicle to lock, sufficient side forces can always be maintained to enable the vehicle to be steered. Releasing wheel lock can, in principle, be achieved very easily (by disconnecting the brakes) but unless this is done in a tightly controlled way there is likely to be a penalty, which can be serious in terms of increased stopping distances. Much of the development work has therefore been devoted to

providing improved stopping distances as well as controllability.

Stopping distances can only be reduced if the anti-lock system comes into play when the locked wheel tyre-road friction coefficient is not the maximum achievable. On the vast majority of road surfaces, which exhibit characteristics similar to the Brake Force curve of figure 1, the braking force coefficient is less when the wheels are locked than when they are rolling, new snow and loose gravel being two exceptions. An anti-lock braking system will minimise stopping distances if it can maintain the braking force on each wheel at that force necessary to provide the maximum tyre-road friction coefficient. A system will achieve this by transferring the wheel from conditions of high braking slip to those of high brake force.

Controllability is at a maximum when the available side-forces are at a maximum. This is when the wheels are freely rotating (zero slip in figure 1). When a brake force is applied the available side-forces are reduced (1)\*. Consequently, if an anti-lock system is set up to minimise stopping distances by always applying the brake force required for peak friction coefficient, then the available side-forces may be insufficient to retain stability (see figure 1). It may be necessary therefore to operate at levels of braking slip lower than those which achieve maximum braking force coefficient, so that a compromise must be reached between stopping distance reduction and controllability under panic braking. The balance between the two in a commercial anti-lock system will depend on the relative importance that the system designer attaches to each.

This paper sets out to describe work carried out at the Transport and Road Research Laboratory to investigate the

\*Numbers in parentheses designate references at end of paper.

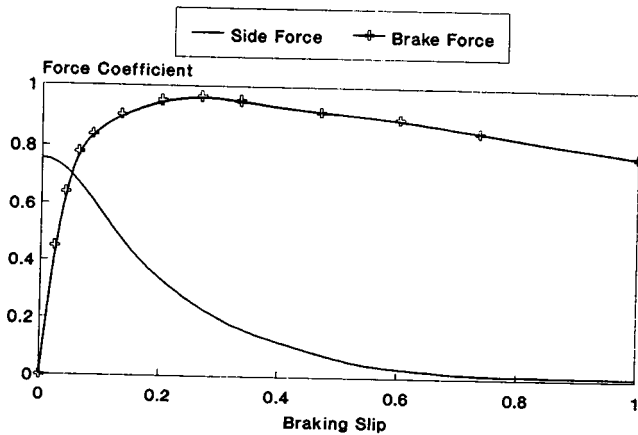


Figure 1. A typical relationship between brake force coefficient and available side force coefficient as braking slip increases from 0 (free rolling) to 1 (locked wheel).

stopping distances and controllability that some existing anti-lock systems can achieve.

## The Test Vehicles

Four vehicles have been tested. Table 1 describes each model, including details of its anti-lock system, its tyres, and its weights as tested. All the vehicles were loaded in such a way that for the laden tests the rear axle weight and gross vehicle weight were both as near to the manufacturer's recommended maximums as possible. This was done with two front seat occupants, a full petrol tank and the remaining load made up of metal weights or gravel filled containers.

Table 1. The test vehicles.

Vehicle (anti-lock system)	Tyre Type	Weights (kg)			
		Unladen		Laden	
		Front (Total)	Rear (Total)	Front (Total)	Rear (Total)
Ford Escort 1.4L (Lucas-Girling)	155 SR 13	615	460 (1075)	665	660 (1325)
Mazda 626 GT (Girling-Sumitomo)	195/60 R 15	814	560 (1374)	982	870 (1852)
Honda Prelude EX-M (Honda)	185/70 HR 13	705	475 (1180)	765	725 (1490)
BMW 320i (Bosch)	195/60 HR 14	675	550 (1225)	680	820 (1500)

The BMW and the Mazda both have three channel electronic systems, two of which independently control wheel lock on each front wheel with the third channel controlling the rear axle using the "select low" principle. "Select low" on an axle ensures that the brake pressure to that axle is regulated by whichever wheel is in the greatest danger of locking. The result is that neither of the wheels are allowed to lock.

The Honda also has an electronic system, but it is only two channel. The rear wheels are again controlled using the "select low" principle but the front wheels are jointly controlled on the "select high" principle. This regulates the brake pressure to the front axle such that one wheel may lock (usually the one on the lowest friction coefficient

surface or the one with the lowest down-force acting on it) but never both.

The Ford Escort has the mechanical two channel system which is described fully by Newton and Riddy (2). Summarising, the two front wheels are independently controlled, but the rear axle does not have its own separate wheel lock detection capability. Instead, each rear wheel is linked, via an apportioning valve, to the diagonally opposite front wheel. This arrangement is designed to ensure that under conditions of panic braking it may be possible to lock one of the rear wheels, but never both.

## The Test Procedures

Tests were carried out on a variety of surfaces (described in table 2), with the cars both unladen (driver and front seat passenger only) and laden (defined earlier). For the purposes of the wet tests, the track was watered by means of a hose and sprinkler system. This ensured that the track was covered by a uniform layer of water rather than being merely damp in some places. The test programme is shown in table 3. The full test programme could not be carried out on some vehicles due to inclement weather or unavailability of the vehicle or the relevant test surface. Nevertheless, useful comparisons have been achieved in all the important areas.

Table 2. The test surfaces.

Name	Texture	Tested Wet/Dry
Bridport Rounded Gravel Macadam Carpet	Rough, polished	Wet
Smooth Mastic Asphalt	Smooth, polished	Wet
Fine Textured Asphalt (FTA)	Smooth, harsh	Wet and Dry
Motorway Surface	Rough, fairly harsh	Wet and Dry

Table 3. The test programme.

Surface	Test	Unladen			Laden		
		No A/L	A/L	Half A/L	No A/L	A/L	Half A/L
Wet Bridport	Straight	EMHB	EMHB	E	EMHB	EMHB	E
	Curve	-	EMHB	E	-	EMHB	E
Wet Mastic	Straight	EMHB	EMHB	E	EMHB	EMHB	E
	Curve	-	EMHB	E	-	EMHB	E
Wet FTA	Straight	EMHB	EMHB	E	EMHB	EMHB	E
	Curve	-	EMHB	E	-	EMHB	E
Dry FTA	Straight	EMHB	EMHB	E	EM B	EM B	E
	Curve	-	EMHB	E	-	EMHB	E
Wet Motorway	Straight	EM	EM	E	EM	EM	E
	Curve	EM	EM	E	EM	EM	E
Dry Motorway	Straight	EM	EM	E	EM	EM	E
	Curve	EM	EM	E	EM	EM	E
Bridport/FTA	Split	EMH	EMHB	E	EM	EMHB	E
	Split	EM	EMHB	E	EM	EMHB	E

E - Escort, M - Mazda, H - Honda, B - BMW

Three separate braking tests were performed on each vehicle. These involved "straight line braking", "braking on curve", and "split surface braking". They are described in detail later in this section.

In all the tests the results, in the form of speed and stopping distance, were taken from a fifth wheel device connected to the rear of the vehicle. An electronic processing unit inside the vehicle was connected to both the fifth wheel and the foot brake pedal. The unit gave a digital read-out of the velocity at which the brakes were applied

and of the distance travelled between application of the brakes and the vehicle coming to a halt. The initial velocity and the stopping distance could then be used to calculate the average deceleration.

Most of the testing was done to compare the performance of a vehicle with its anti-lock system functioning to that with it disabled. The nature of the mechanical system fitted to the Escort is such that a complete failure of both anti-lock circuits is highly unlikely. The two halves of the diagonally split system are completely independent, and hence a failure in one half, such as a broken drive belt, or stuck valve, can only affect that half. As a result, extra tests were done with the Escort to investigate its performance with one of the wheel-lock detectors disabled as well as with both disabled. These extra tests are referred to as "half" anti-lock in table 3.

The electronic systems fitted to the other three vehicles could all be completely disabled by simply disconnecting part of their electrical systems. There are obviously many more partial or complete failure modes possible but the test programme did not investigate them.

On all the vehicles tested the failed anti-lock condition is equivalent to having a conventional, non anti-lock, system. It is not, however, necessarily equivalent to the standard, non anti-lock, version of the vehicle as some or all of the individual components of the braking systems may vary from one model type to the other.

### Straight line braking

This test involved driving the vehicle at constant speeds increasing from 20 km/h to 100 km/h in roughly 10 km/h increments and applying the foot brake as hard and as fast as possible while all four wheels of the vehicle were on the same test surface. The initial velocity and stopping distance were found in the manner described above. This test was performed on the surfaces detailed in table 3 with the anti-lock system functioning and with it disabled and with the vehicles unladen and laden.

The purpose of this test was to compare the average decelerations achievable with the anti-lock system functioning with those achievable should the system fail.

As explained in the Introduction, an anti-lock system with good stopping distance characteristics should show an improved average deceleration when braking from any initial speed when compared to the deceleration obtained with the wheels locked, provided that the locked wheel friction coefficient is not the maximum possible. On all the surfaces tested friction coefficients in excess of the locked wheel value should indeed be possible, and hence in principle an anti-lock system should be able to provide improved decelerations. For reasons explained in the Introduction, however, even if an anti-lock system is unable to achieve such an improvement, it may still provide better controllability, and this should be evident from the other tests in the programme.

The detailed results, showing decelerations obtained from three particular speeds, are given separately for each vehicle in tables 4 to 7.

Table 4. The test results—Escort—straight line braking.

Test Surface	Loading	Anti-lock	Average Deceleration (g)		
			30 km/h	60 km/h	90 km/h
Wet Bridport	Unladen	None	0.41	0.35	0.30
		Half	0.37	0.32	0.31
		Full	0.32	0.31	0.30
	Laden	None	0.40	0.35	0.30
		Half	0.38	0.34	0.30
		Full	0.29	0.30	0.29
Wet Mastic	Unladen	None	0.40	0.26	0.22
		Half	0.38	0.30	0.24
		Full	0.41	0.33	0.23
	Laden	None	0.43	0.24	---
		Half	0.38	0.28	0.23
		Full	0.36	0.28	0.23
Wet FTA	Unladen	None	0.88	0.81	0.67
		Half	0.82	0.78	0.63
		Full	0.78	0.71	0.58
	Laden	None	0.85	0.81	0.63
		Half	0.79	0.76	0.58
		Full	0.66	0.67	0.53
Wet Motorway	Unladen	None	0.80	0.62	0.55
		Half	0.70	0.63	0.57
		Full	0.55	0.61	0.57
	Laden	None	0.76	0.60	0.56
		Half	0.70	0.59	0.53
		Full	0.50	0.56	0.51
Dry FTA	Unladen	None	0.82	0.83	0.84
		Half	0.79	0.83	0.82
		Full	0.68	0.81	0.79
	Laden	None	0.79	0.78	0.80
		Half	0.75	0.77	0.72
		Full	0.64	0.75	0.72
Dry Motorway	Unladen	None	0.81	0.77	0.70
		Half	0.78	0.82	0.81
		Full	0.71	0.84	0.84
	Laden	None	0.78	0.75	0.68
		Half	0.78	0.78	0.67
		Full	0.72	0.79	0.75

Table 5. The test results—Mazda—straight line braking.

Test Surface	Loading	Anti-lock	Average Deceleration (g)		
			30 km/h	60 km/h	90 km/h
Wet Bridport	Unladen	None	0.42	0.38	0.32
		Full	0.44	0.46	0.47
		None	0.36	0.34	0.31
	Laden	Full	0.38	0.43	0.47
		None	0.49	0.38	0.30
		Full	0.53	0.57	0.48
Wet Mastic	Unladen	None	0.42	0.30	0.23
		Full	0.43	0.42	0.40
		None	0.72	0.74	0.56
	Laden	Full	0.69	0.83	0.69
		None	0.63	0.61	0.46
		Full	0.63	0.72	0.56
Wet Motorway	Unladen	None	0.61	0.58	0.54
		Full	0.57	0.66	0.70
		None	0.52	0.49	0.51
	Laden	Full	0.52	0.59	0.68
		None	0.76	0.77	0.79
		Full	0.74	0.86	0.90
Dry FTA	Unladen	None	0.62	0.64	0.68
		Full	0.64	0.70	0.75
		None	0.69	0.72	0.72
	Laden	Full	0.70	0.82	0.83
		None	0.63	0.64	0.65
		Full	0.62	0.75	0.81

Table 6. The test results—Honda—straight line braking.

Test Surface	Loading	Anti-lock	Average Deceleration (g)		
			30 km/h	60 km/h	90 km/h
Wet Bridport	Unladen	None	0.46	0.39	0.34
		Full	0.47	0.44	0.39
		None	0.44	0.40	0.33
	Laden	Full	0.44	0.44	0.39
		None	0.44	0.32	0.26
		Full	0.53	0.51	0.43
Wet Mastic	Unladen	None	0.41	0.32	0.26
		Full	0.51	0.50	0.38
		None	0.67	0.64	0.56
	Laden	Full	0.65	0.67	0.62
		None	0.61	0.58	0.52
		Full	0.63	0.63	0.60
Wet FTA	Unladen	None	0.68	0.70	0.71
		Full	0.71	0.75	0.80

**Table 7. The test results—BMW—straight line braking.**

Test Surface	Loading	Anti-lock	Average Deceleration (g)		
			30 km/h	60 km/h	90 km/h
Wet Bridport	Unladen	None	0.34	0.31	0.33
		Full	0.43	0.49	0.45
	Laden	None	0.41	0.36	0.33
		Full	0.46	0.51	0.46
Wet Mastic	Unladen	None	0.33	0.26	----
		Full	0.42	0.54	0.54
	Laden	None	0.40	0.27	----
		Full	0.46	0.47	0.48
Wet FTA	Unladen	None	0.65	0.54	0.56
		Full	0.56	0.72	0.69
	Laden	None	0.64	0.64	0.63
		Full	0.65	0.74	0.75
Dry FTA	Unladen	None	0.70	0.71	0.72
		Full	0.75	0.86	0.88
	Laden	None	0.65	0.71	0.72
		Full	0.74	0.82	0.86

**Braking on a curve**

This test involved driving the vehicle at constant speeds increasing in 5 or 10 km/h increments through a curved path marked out by cones. The radius of this curved path was 60m to the inside of the lane and 63m to the outside. Whilst the vehicle was within the lane, the foot brake was applied as hard and as fast as possible. Readings of initial velocity were taken in the usual way.

The purpose of this test was to investigate the controllability of the anti-lock equipped vehicles under conditions of combined cornering and heavy braking. To give some idea of how well the systems were performing the maximum speed at which the test could be completed under braking was compared to the maximum speed at which the vehicle could be driven through the course without application of the brakes (referred to as the Unbraked Breakaway Speed, UBS). A vehicle was deemed to have failed the test if any of the marker cones were disturbed, that is if the vehicle could not be steered to stay within the lane. The UBS was found before the braking tests were carried out as it gave an idea of the upper limit of speeds that would be achievable.

It would be impossible for a non anti-lock vehicle to complete this manoeuvre successfully as with both the front or rear wheels locked the vehicle would inevitably disturb cones. Because of this, tests were only conducted with the anti-lock systems functioning. The Escort was also tested in both its "half" anti-lock modes, that is with the front inside wheel only sensing (referred to as "inner") and then with the front outside wheel only ("outer").

Table 8 gives the results of each test on each surface in the form of maximum successful braked speed as a percentage of the Unbraked Breakaway Speed. A result equal to 100 percent would indicate that even when the vehicle is braked while at its controllability limit the anti-lock system can provide sufficient side-forces to allow control of the vehicle to be maintained.

**Split surface braking**

This test is similar to the straight line braking test but rather than being carried out on a single surface, it is conducted with the near-side wheels on a different surface to the off-side wheels. The layout of the TRRL track allows for

**Table 8. The test results—braking on a curve.**

Vehicle	Loading	Anti-lock	Maximum possible speed (%UBS)			
			Wet Bridport	Wet Mastic	Wet FTA	Dry FTA
Escort	Unladen	inner	75	84	85	89
		outer	76	87	87	84
	Laden	inner	96	100	100	98
		outer	78	86	85	88
		full	75	75	85	90
		full	93	99	99	99
Mazda	Unladen	full	94	100	100	98
	Laden	full	93	100	100	100
Honda	Unladen	full	89	80	93	96
	Laden	full	98	80	93	99
BMW	Unladen	full	89	97	95	96
	Laden	full	90	98	100	94

two combinations of surfaces to be tested, and these are shown in table 3.

Once again the procedure involved driving the vehicle at various constant speeds gradually increasing from 20 km/h in 5 or 10 km/h increments, onto the split surface area and then applying the foot brake as hard and as fast as possible. Initial velocity and stopping distance were found in the usual way.

A car not fitted with anti-lock is likely to spin violently during this manoeuvre if all four wheels lock. This is because the two wheels on the more slippery of the two surfaces will not be slowed down as quickly as the wheels on the higher grip surface, and hence one side of the vehicle will try to move faster than the other. For this reason not all the cars were tested with their anti-lock systems wholly disabled.

Again the Escort was tested in its two "half" anti-lock modes. By disabling one or other of the anti-lock sensors, the system could be made to provide anti-lock to the front wheel on the low grip surface only (referred to as low  $\mu$  anti-lock in table 9), or to that on the high grip surface only (high  $\mu$  anti-lock in table 9).

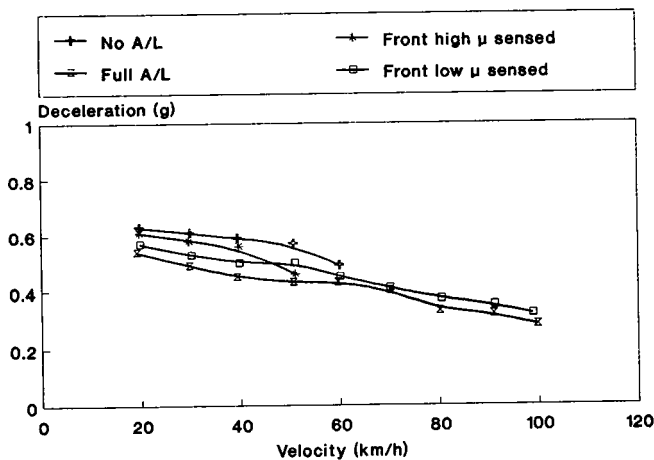
The primary purpose of this test was to examine the controllability of an anti-lock equipped vehicle when it is braked heavily on a split high-low grip surface. This type of braking condition can easily be encountered for example when snow, ice or water lies to one side of an otherwise dry road.

Table 9 shows the maximum speed at which the manoeuvre could be performed for the various anti-lock conditions. For the manoeuvre to be performed successfully the driver had to be able (with some steering correction if necessary) to bring the vehicle to halt in a straight line, that is with either side of the vehicle remaining on the surface it was on when braking commenced. Speeds over 100 km/h were not investigated, so for an anti-lock system with good controllability characteristics we would expect to see speeds up to 100 km/h shown in table 9. If a system has been designed to minimise stopping distance at the expense of controllability we would expect to see a lower speed when the lack of

**Table 9. The test results—split surface braking.**

Vehicle	Loading	Anti-lock	Maximum speed (km/h)	
			Bridport/FTA	Mastic/FTA
Escort	Unladen	None	50	60
		Low $\mu$	100	100
		High $\mu$	70	70
		Full	100	100
Laden	None	60	70	
	Low $\mu$	100	100	
	High $\mu$	50	70	
	Full	100	100	
Mazda	Unladen	None	70	50
		Full	100	100
	Laden	None	70	50
		Full	100	100
Honda	Unladen	None	50	--
		Full	100	100
	Laden	Full	100	100
		Full	100	100
BMW	Unladen	Full	100	100
	Laden	Full	100	100

controllability makes the successful completion of the manoeuvre impossible. At the lower speeds, however, we would expect the better stopping distances to be evident. Some of the speeds and stopping distances are shown in graphical form in figures 2, 3 and 4.



**Figure 2. Escort—split surface tests—Bridport/FTA—Laden.**

## Discussion of the Test Results

The purpose of the programme of tests described above was to investigate the effectiveness of anti-lock braking systems as fitted to a number of modern passenger cars. The nature of the investigation was to compare the performance of a vehicle with its anti-lock system fully operational to that with it partly or wholly disabled. Different makes of vehicles are bound to produce different results, even under the same external conditions. Because of this, it is only possible to make a general comparison of the performance of the four anti-lock systems. Such a general comparison is made at the end of this section, but first the performance of each individual vehicle is discussed in turn.

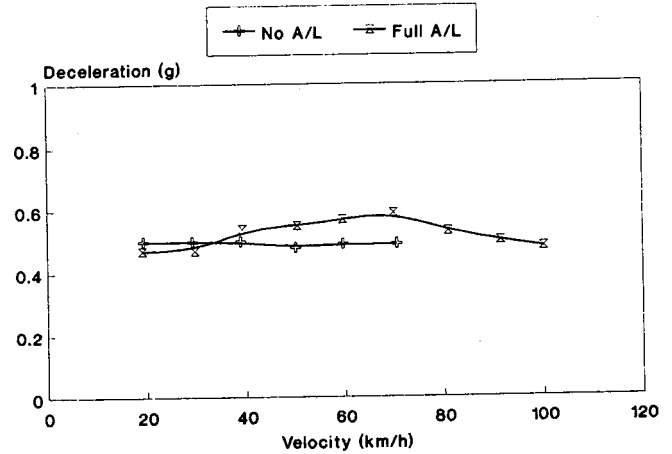


**Figure 3. Mazda—split surface tests—Bridport/FTA—Laden.**

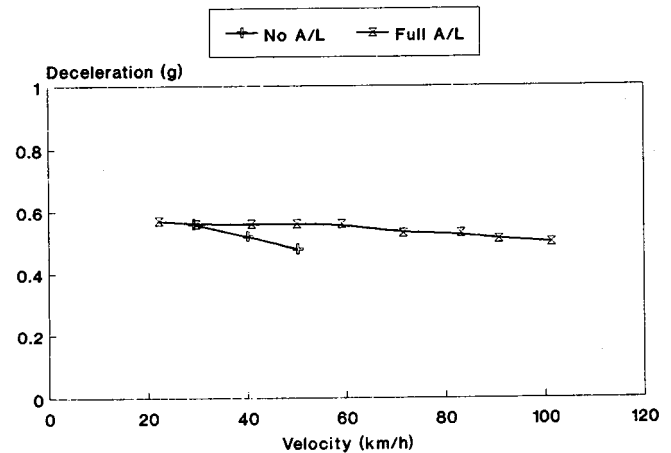


**Figure 4. Honda—split surface tests—Bridport/FTA—Unladen.**

## Escort

### Escort—straight line braking

The results of these tests are given in table 4. From the table two general trends emerge. First, the results obtained with the vehicle laden are very similar to those with it unladen. Second, the average decelerations are higher with locked wheels (no anti-lock) than with the anti-lock partly or wholly operational.

The fact that the unladen and laden results are similar is not entirely surprising. It indicates that the load-sensing valves on the rear axle are able to maintain the braking force coefficients on that axle at the same level regardless of loading.

The second of the observed trends, that is that on many surfaces decelerations are not improved by the anti-lock system, is not so expected. This result implies that the anti-lock braking system does not generally maintain the brake effort at each wheel at a sufficiently high level to ensure better adhesion than can be obtained by allowing the wheels to lock. On all but two of the surfaces at 30 km/h decelerations without anti-lock (referred to in table 4 as "none" anti-lock) are higher than the half anti-lock values and these are higher still than the full anti-lock values. The

only exceptions are the Wet Mastic, unladen, and the Dry Motorway, laden, results.

At 60 km/h the deceleration without anti-lock is still appreciably better than the two anti-lock cases on the Wet FTA surface, and slightly better on the Wet Bridport. There are negligible differences between the three cases on the Wet Motorway and Dry FTA. A slight improvement is obtained with the two anti-lock operational cases when the vehicle is braked from 60 km/h on the Dry Motorway or Wet Mastic.

At 90 km/h the Wet FTA surface still produces better decelerations when the anti-lock system is disabled. This is also the case, though to a lesser extent, on the Dry FTA. No significant performance differences were found at this speed on the Wet Bridport, Wet Mastic (unladen), or Wet Motorway surfaces. The Dry Motorway surface once again showed better decelerations achievable with the anti-lock operational.

The vehicle was prone to rotate as it slid with all wheels locked on the Wet Mastic and Wet Bridport surfaces. This made the taking of results at higher speeds on these surfaces very difficult when the anti-lock system was disconnected. Indeed in the laden case speeds in excess of 70 km/h could not be attempted on the Wet Mastic, hence the deceleration value at 90 km/h could not be established and so no entry is shown here in table 4.

When operating, the two channel mechanical anti-lock system fitted to the Ford Escort car provides better deceleration characteristics on only two of the surfaces tested and then only at certain speeds. These were at speeds between 30 and 90 km/h on the Wet Mastic surface and at 40 km/h and over on the Dry Motorway surface. At all other speeds and on all other surfaces tested the anti-lock system did not attain the objective of increasing the decelerations. Indeed, at low speeds (less than 50 km/h) the decelerations obtained with locked wheels were often significantly better than those with the anti-lock system functioning.

The reason for the enhanced performance on the Mastic may be that the ratio of peak to locked wheel tyre/road friction coefficient is quite high, allowing the anti-lock system to operate within a larger range of brake pressures that produce brake force levels in excess of the locked wheel value. This locked wheel value can be further diminished by the fact that the surface is smooth and so it is easier for a layer of water to get between the tyre and the road. If the wheel is rotating the tyre tread will be able to disperse most of this water, but this process will not be as effective if the wheel is locked.

As is explained in the Introduction any anti-lock system has to achieve a compromise between good deceleration and good controllability. This test shows that the Escort system does not, generally, manage to reduce stopping distances. It should be stressed, however, that the stopping distances achieved with the anti-lock system are still perfectly acceptable for a modern passenger car. The further testing outlined below shows what effect this anti-lock

system has on the controllability characteristics of the vehicle.

The decelerations were generally better with only half the anti-lock system functioning than with the whole system. The controllability of the vehicle was better with half anti-lock than with no anti-lock at all, though not as good as with full anti-lock. These results suggest that the performance of the car does not deteriorate noticeably when only half the anti-lock system functions, and indeed may perform better in conditions where reduced stopping distances (high decelerations) are considered to be more important than increased controllability.

### **Escort—braking on a curve**

The results of these tests are given in table 8. Once again, as was the case in the straight line braking, there is negligible difference between the results achieved with the vehicle laden and unladen. There is also negligible difference between the results obtained with the two half anti-lock conditions, implying that either condition gives substantially the same degree of controllability.

The main conclusion that can be drawn from table 8 is that the results for the full anti-lock case are significantly better than those from the two half anti-lock cases. Speeds of between 93 and 100 percent of the UBS were achieved with the anti-lock system fully operational.

The two half anti-lock cases produced speeds of between 75 and 90 percent of the UBS. This implies that, at relatively low speeds, a vehicle with part of its anti-lock system disabled will still be controllable under conditions of panic braking, but at higher speeds (or higher lateral accelerations) the vehicle will be no more controllable than it would be if the whole system were disabled. Stopping distances were also measured but, unlike in the straight braking tests, only small differences were found between any of the three anti-lock conditions.

In summary, therefore, we can say that the mechanical anti-lock system fitted to this Escort car, when fully operational, provides significantly more controllability under conditions of panic braking on a curve than is possible with half of the system disabled. Even this half anti-lock condition, however, provides an appreciable degree of controllability which would be impossible in a car that allowed both wheels on any one axle to be locked at the same time. In the previous (straight braking) tests, the half anti-lock condition performed better than the full system. The braking on a curve test, however, shows that the full system is preferable under conditions where the amount of available side-force (and hence controllability) is important.

### **Escort—split surface braking**

The results of these tests are given in table 9 and figure 2. As can be seen from the table maximum speeds of between 50 and 70 km/h were achievable, with both loading conditions and on both surface pairs, when the anti-lock system was completely disabled. Very similar results were achieved when only the front wheel on the high grip (FTA)

surface was able to detect wheel-lock (high  $\mu$  in table 9). At speeds above the figures shown (that is the maximum), the vehicle would have rotated violently through angles exceeding 90 degrees.

The results obtained from the other half anti-lock mode, that is with the front low grip wheel sensed, were considerably different. Speeds of 100 km/h were achieved with no violent instabilities apparent. This means that the vehicle could be braked hard from 100 km/h and could, with minimal steering corrections, be brought to a halt in a straight line. This was the case on both surface pairs and both unladen and laden. Identical results were obtained when the full anti-lock system was operational.

It is evident, therefore, that the half anti-lock mode can provide significantly more controllability under conditions of panic braking on split coefficient surfaces than can be derived from the no anti-lock mode, but only provided the sensed wheel is on the low grip surface. If the sensed wheel is on the high grip surface, the controllability is no more than can be obtained from the vehicle with no anti-lock.

Figure 2 shows the Deceleration versus Velocity curve for one of the test conditions. Similar results were obtained for the remaining three conditions. It can be seen that the decelerations achieved by the two low controllability modes (no anti-lock and front high  $\mu$  sensed) were generally slightly higher than those achieved by the other two modes over the speed ranges in common. The deceleration capabilities of the two high controllability modes are seen to be similar.

The conclusion that has to be drawn from the series of split surface tests is that the full anti-lock mode is significantly better than either of the two half anti-lock modes or the no anti-lock mode. It allows the vehicle to be braked safely from high speeds on hazardous combinations of high and low grip surfaces regardless of which side of the vehicle is on the low grip area.

### **Escort—summary**

The straight line braking tests indicated that the Escort gave, generally, slightly lower decelerations when the two channel mechanical anti-lock system was operational, than those achieved with the system disabled. The Wet Mastic and Dry Motorway were the only surfaces on which the reverse was true. The results also show that the half anti-lock mode performed better than the full system in this respect.

Results from the tests involving braking on a curve and on split surfaces suggest that the increased controllability that can be obtained from the full anti-lock system, when compared to half anti-lock mode and particularly the no anti-lock mode, offers significant benefits.

The system offers the further advantage that a failure is only likely to affect one-half of the braking system. The performance of such a failed vehicle has been shown to be significantly better than without anti-lock (both halves of system failed).

## **Mazda**

### **Mazda—straight line braking**

The results of these tests are given in table 5. Two important trends emerge from the table. First, the decelerations achieved with the laden vehicle are appreciably lower than those achieved with it unladen. This is the case on all surfaces and at all speeds except the Wet Bridport at 90 km/h.

It was found that, even with the anti-lock system disconnected, the rear wheels could not be made to lock. This indicates a degree of under braking to the rear axle that is probably sufficient to produce the deterioration in braking experienced when the vehicle was loaded to the very high maximum levels specified by the manufacturer, as listed in table 1.

The second, and more interesting trend from table 5 is that on all surfaces, under both loading conditions, and at speeds of 60 and 90 km/h, the anti-lock system considerably increases the decelerations achievable when compared with the non anti-lock case. At 30 km/h there is little difference between the anti-lock and non anti-lock cases on any of the surfaces tested.

The results indicate that at speeds of below about 40 km/h the stopping distances achievable are about the same with and without anti-lock. As the speed increases from this value, the advantages of the anti-lock system become more apparent. In general, the higher the speed, the more significant is the increase in deceleration that may be obtained from the system.

It can be concluded, therefore, that the three channel electronic anti-lock system fitted to the Mazda has very good deceleration capabilities. This shows that the system is able to operate at average tyre/road friction values in excess of those achievable with wheels locked.

### **Mazda—braking on a curve**

The results of these tests are given in table 8. Unlike the straight braking tests there is no significant difference between the unladen and laden results. The maximum speeds achieved range from 93 to 100 percent of the UBS, indicating that the anti-lock system provides a very high degree of controllability at all speeds up to very near the limit of control of the unbraked vehicle.

### **Mazda—split surface braking**

The results of these tests are given in table 9 and figure 3. The results in table 9 are seen to be identical for the unladen and laden cases.

With the anti-lock system disabled the vehicle could not be brought to a halt in a straight line at speeds over 70 km/h on the Bridport/FTA and 50 km/h on the Mastic/FTA.

As for the straight braking tests the rear wheels could not be made to lock. This affected the stability of the vehicle such that at these higher speeds it merely pulled over onto the high grip (FTA) surface, rather than spin violently as it would have done had both rear wheels locked. This demon-

strates that the non anti-lock vehicle has good stability characteristics but with the front wheels locked there is very little controllability for the driver.

In contrast, with the anti-lock system operational, the vehicle could be braked hard from 100 km/h and brought to a rapid, fully controllable, halt. Figure 3 shows the decelerations achieved with and without anti-lock under one particular test condition. Similar results were obtained from the other three conditions, though once again deceleration levels were slightly lower in the laden case. The figure shows that the results of this test are very similar to those of the straight braking tests. The decelerations obtained with and without anti-lock are similar at speeds below about 40 km/h. At higher speeds the results with the anti-lock operating are significantly better than without it.

### **Mazda—summary**

There can be no doubt that the three channel anti-lock system fitted to the Mazda car greatly increases both the stopping power and the controllability of the vehicle under panic braking conditions on all of the surfaces, through all of the manoeuvres tested, and at all but quite low speeds (less than 40 km/h). At these lower speeds there are no significant differences in the stopping power of the anti-lock and non anti-lock vehicle, though controllability is still enhanced by the operation of the anti-lock system.

## **Honda**

### **Honda—straight line braking**

The results of these tests are given in table 6. Three surfaces were tested both unladen and laden. The Dry FTA surface could only be tested unladen. The limited availability of the vehicle and bad weather prevented the dry surface laden tests from being carried out.

The Wet Bridport and Mastic surfaces both show only small differences in the two loading conditions. There is a slight loss in deceleration capability when laden on the Wet FTA. The deceleration performance on this higher coefficient surface may be adversely affected by the tendency of the non anti-lock vehicle to lock rear wheels when unladen but not when laden.

The decelerations achieved at 30 km/h are roughly the same with and without the anti-lock operating on all surfaces except the Wet Mastic. On this surface there is a significant improvement in the decelerations achievable when the anti-lock system is operational. The same improvement is evident on all the surfaces at speeds of 60 and 90 km/h, though the differences on the Bridport, Wet FTA and Dry FTA are less marked than those on the Mastic.

The results therefore indicate that at speeds over about 40 km/h anti-lock achieves a definite increase in deceleration on all surfaces. On the Wet Mastic, in particular, there is a considerable increase at all speeds.

In the unladen, non anti-lock condition, the rear wheels were able to lock, causing instability problems on the low grip (Bridport and Mastic) surfaces. This instability was not

present when the vehicle was laden or when the anti-lock was operational. The "select high" system operating on the front axle did allow one of the front wheels to lock, but never both. When the anti-lock was functioning, the vehicle therefore remained controllable and stable on all the surfaces tested and at all speeds.

It is apparent that the two channel electronic anti-lock system fitted to the Honda has good deceleration capabilities, particularly on the Wet Mastic, and provides a degree of stability and controllability that is not possible with the system disabled.

### **Honda—braking on a curve**

The results of these tests are given in table 8. On all the surfaces and with both loading conditions, the maximum achievable speeds were at least 80 percent of the UBS. This 80 percent level was achieved on the Wet Mastic, the other surfaces produced results ranging from 89 to 99 percent.

These results may slightly underestimate the true performance of the vehicle as shortage of time allowed only one attempt to be made at each speed. The speed was increased in 5 km/h increments, hence if the course was successfully completed at, for example, 60 km/h the driver would then have one attempt at 65 km/h. If this run was unsuccessful then 60 km/h was taken to be the maximum, whereas 64 km/h may have been possible. The UBS, on the other hand, was found by gradually increasing the speed in 1 or 2 km/h steps.

The "select high" system operating on the front, steered, axle allows one wheel to lock up. The inside wheel (the one with the lowest down-forces acting on it) did occasionally lock during this manoeuvre, particularly on the Mastic. Having one wheel locked on the steered axle is bound to reduce the available side-forces that allow the vehicle to be steered. This helps to explain the slightly lower maximum speeds that were found to be achievable on the Mastic surface.

Overall it has been found that, despite the inherent possibility of one front wheel locking, the controllability of the Honda car, fitted with this two channel electronic anti-lock system, remains very high under conditions of panic braking on a curve.

### **Honda—split surface braking**

The results of these tests are given in table 9 and figure 4. It is clear from the table that on both surface combinations and under both loading conditions the anti-lock equipped vehicle remained fully controllable when braked hard from a speed of 100 km/h.

With the anti-lock system disabled the vehicle was prone to spin violently. Only one test of this condition was carried out and the maximum speed was found to be 50 km/h. At this speed the car spun through almost 90 degrees.

Figure 4 shows that the decelerations achieved by the anti-lock vehicle were slightly better over the speed range at which the non anti-lock vehicle could successfully complete the manoeuvre.

The fact that the front wheel on the low coefficient sur-

face could lock would suggest that the controllability may be adversely affected, in that the side-forces available are reduced. It was found that a fairly large degree of steering correction was needed by the driver, but control of the vehicle could nevertheless be maintained. The degree of correction needed was found to be greater in the unladen case. This is probably due to the increased level of brake force necessary to cause rear wheel lock-up in this condition, causing a reduction in the available rear axle side-forces, and a resulting reduction in the vehicle's stability.

### **Honda—summary**

The two channel electronic anti-lock system fitted to the Honda car was designed to perform in a similar way to the more complicated three channel systems but cost about half the price. The results indicate that the system's performance is indeed likely to be comparable with that of its more complex rivals.

The straight line stopping distances were found to be significantly improved, particularly at speeds in excess of 40 km/h.

The controllability during the braking on a curve test was found to be slightly restricted by the "select high" control of the steered axle. Nevertheless the vehicle was still found to have a significant degree of controllability at lateral acceleration levels that would have rendered control of the non anti-lock vehicle quite impossible.

Control of the vehicle could only be maintained on the split surface tests with a degree of driver steering input, particularly when unladen. With this steering input, however, control of the vehicle was maintained when braked hard from 100 km/h. Without anti-lock the vehicle was uncontrollable when braked on the split coefficient surfaces.

## **BMW**

### **BMW—straight line braking**

The results of these tests are given in table 7. There is quite a wide scatter when comparing the unladen to laden results, but there is no consistent variation between the two.

At 30 km/h there is generally a slight improvement in decelerations when the anti-lock system is operational. The Wet FTA (unladen) was the only condition that showed a reduction in the decelerations attainable. At speeds of 60 and 90 km/h there was a substantial improvement on all the surfaces and under both loading conditions.

The rear wheels were prone to lock on the Wet Mastic surface when the anti-lock system was disabled. This caused the vehicle to rotate through an angle of almost 90 degrees at speeds of about 80 km/h. The test was therefore not performed at higher speeds on this surface with the system disabled. No such stability problems were found with the anti-lock system operational.

The three channel electronic anti-lock system fitted to the BMW seems to have excellent deceleration capabilities,

and this test suggests that it also has good stability characteristics.

### **BMW—braking on a curve**

The results of these tests are given in table 8. On all surfaces and with both loading conditions the maximum speeds at which the course could be completed were between 89 and 100 percent of the UBS. This demonstrates clearly that the anti-lock system provides a high degree of controllability when the vehicle is braked heavily from speeds that are very near the limit of control for the unbraked vehicle.

### **BMW—split surface braking**

The results of these tests are given in table 9. The violent instabilities that this test caused with the anti-lock system disabled meant that the manoeuvre was only performed with the system operational. As can be seen from the table the vehicle, with anti-lock, could be braked heavily from speeds of 100 km/h without any significant loss of stability or controllability. Some steering correction was necessary at higher speeds, but this could not be considered excessive.

### **BMW—summary**

The three channel electronic anti-lock system fitted to the BMW is complicated and expensive. We would therefore expect it to perform well, and indeed the results are excellent.

The improvements in stopping distances were very impressive, with only one condition (Wet FTA, unladen, 30 km/h) showing a slight reduction in performance.

The controllability that the system provides when the vehicle is braked heavily on a curve or split coefficient surface is also excellent.

## **Overall Summary of Results**

It has been shown that the three channel electronic anti-lock systems fitted to the Mazda and BMW cars have excellent performance characteristics. Both systems reduced stopping distances and increased the stability and controllability of the vehicles to a significant extent under the great majority of braking conditions to which they were subjected.

The two channel electronic system fitted to the Honda car has also performed very well. The stopping distances were reduced, particularly at higher speeds (over 40 km/h). The controllability was found to be slightly hindered by the "select high" principle acting on the front axle, but in extreme conditions it was still very much greater than that of the non anti-lock vehicle.

The two channel mechanical system fitted to the Escort was found to provide very good controllability. At speeds below about 50 km/h the stopping distances were found to increase on the majority of surfaces when the full anti-lock system was operational. Even so, the stopping distances achieved with anti-lock were always acceptable and were

generally comparable with the locked wheel distances achieved by the other vehicles. Moreover, the most likely failure mode of this system is still capable of providing anti-lock for one half of the diagonally split braking circuit. This mode was also thoroughly tested and found to provide good controllability. It was also found to exhibit stopping distance capabilities that were often better than those of the full anti-lock system.

If we consider the degree of complexity and resulting cost of each system we would expect the more expensive and complicated systems to perform better than the cheaper, simpler, systems. The theoretical performance analyses by Oppenheimer (3) provide further evidence, and the results of the tests conducted at the Transport and Road Research Laboratory confirm, that this is indeed the case. However, even the simplest and cheapest system, as fitted to the Escort, showed a level of performance that should greatly increase the accident avoidance potential for a driver in many common emergency braking situations.

It was clear from the testing that all systems provided much improved steering ability and stability while braking. Producing an anti-lock braking system that will decrease stopping distances as well as improve controllability under a range of loading and road surface conditions is not a simple matter. The test programme of work described in this paper indicates that these objectives are met in full by the three electronic systems. The mechanical system meets both objectives on some surfaces only, but has considerable cost advantages over the other systems. It may also have reliability advantages because of its greater simplicity.

The relative importance of shorter stopping distances as against better controllability in reducing the number and severity of road accidents is not clear. Controllability in this context means the ability to steer out of trouble and/or the retention of vehicle stability. Road accidents which may be prevented or reduced in severity by anti-lock brakes are basically of two types. Firstly, accidents in which the driver of a car fitted with anti-lock brakes might have been able to steer around an obstacle or continue on a bend in the road while still braking. Also in this category are accidents where vehicle instability (spinning out of control) makes the consequences of the accident worse. Secondly, accidents in which there is no space available to steer out of trouble but where a shorter stopping distance would have reduced the severity of the accident or might have prevented it altogether.

The relative numbers of these two types of accident determines whether improved controllability or reduced stopping distance is the more important. If accidents are nearly all of the second type then it may be counter-productive in terms of accident costs to introduce anti-lock braking systems which result in longer stopping distances, since the severity of accidents would be made worse. On the other hand, there must be many accidents caused because a driver tries to steer around an object but the front wheels lock under braking and the car continues in a straight line. The steering under braking offered by antilock is of course

only of use if drivers do try and steer in emergency conditions and do not simply "freeze."

In the absence of detailed accident data it is not possible to say for certain which is the more important. Obviously it is preferable to have both shorter stopping distances and better controllability, but it is the authors' opinion that the advantages of the ability to steer and the improved stability while braking are probably sufficient to outweigh the small loss in braking deceleration found under some circumstances with the Escort in these tests.

## Conclusions

1. Four modern anti-lock braking systems have been tested on a variety of road surfaces, with the vehicle both unladen and fully laden, and at speeds ranging from 20 to 100 km/h.

2. The performance of each system has been compared to that of the same vehicle with the system partially or wholly inoperative.

3. The deceleration characteristics have been assessed by heavily braking the vehicles from a known speed to rest whilst driving in a straight line on several surfaces having single (that is uniform) coefficients of friction.

4. The controllability of the systems has been assessed by heavily braking whilst driving on a curved path on single coefficient surfaces and whilst driving in a straight line over split coefficient surfaces.

5. The vehicle controllability provided by all the anti-lock braking systems was found to be excellent.

6. The deceleration characteristics were found to be closely related to the degree of complexity and cost of the systems.

7. Both the expensive three channel electronic systems significantly increased the deceleration levels attainable on all the surfaces and at all but quite low speeds. An appreciable increase at all but low speeds was also provided by the cheaper two channel electronic system. There was a slight increase provided by the two channel mechanical system on some of the test surfaces but on most, particularly at lower speeds, the anti-lock actually reduced the braking deceleration slightly, although never to an unacceptable level.

8. Detailed analysis of accident data is required before any definite conclusions can be drawn regarding the relative importance of greater controllability compared with reduced stopping distances.

9. The enhanced controllability that anti-lock provides, and the wide variation in car deceleration capabilities that exists, means that even the cheap and simple mechanical system is considered to provide a substantial improvement in accident avoidance potential. This potential is greater for the more expensive and complex systems.

## References

- (1) Holmes, K.E. and R.D. Stone, *Tyre Forces as*

*Functions of Cornering and Braking Slip on Wet Road Surfaces.* TRRL Report No. LR 254. Transport and Road Research Laboratory, Crowthorne, 1969.

(2) Newton, W.R. and F.T. Riddy, *Evaluation Criteria for Low Cost and Anti-Lock Brake Systems for FWD Passenger Cars.* SAE Paper No. 840464. Detroit, 1984.

(3) Oppenheimer, P., *Comparing Stopping Distances of Cars With and Without Anti-Lock Braking Systems.* SAE Paper No. 880324. Detroit, 1988.

## Control Concept for Traction Control System (TCS) and Its Performance

S. Shiraishi, O. Yamamoto, H. Kiryu,  
T. Nishihara, and M. Satoh  
Honda R&D Co., Ltd.

### Abstract

Typical traction control systems (TCSs) are mainly designed to maintain the longitudinal acceleration performance of motor vehicles on slippery roads, particularly snow-covered ones. If emphasis is placed on traction, this may result in inadequate vehicle handling performance or, if undue priority is given to vehicle handling, it may lead to insufficient traction performance. Also, the TCS, essentially a spin velocity control system for the driven wheels, may not work stably on a gravel or bumpy road if the wheel rotation receives an external disturbance from vibrations of the suspension.

An improved TCS should provide both satisfactory traction and handling performance whatever the road condition.

This paper gives an example of a control concept which realizes the required system capability, followed by discussions of an experimental vehicle based on this concept. Then it studies the control performance of the example TCS using this experimental vehicle.

### Introduction

We have been conducting diversified research, primarily focusing on accident-avoidance capabilities of motor vehicles, with the goal of adapting vehicles to satisfy driver demands and increasing the ease of operation. One of the major results from this research is a prototype traction control system (TCS) incorporating a new control concept.

The TCS discussed here is an automatic control system which helps prevent loss of traction to the driven wheels and enables the car to accelerate with good efficiency. Moreover, for rear wheel drive automobiles, the system may help to avoid a reduction in directional stability during longitudinal acceleration, and for front wheel drive vehicles, it helps maintain steerability during acceleration. Of course, there are some conditions so adverse that TCS is

### Acknowledgements

The work described in this paper forms part of the programme of the Transport and Road Research Laboratory and the paper is published by permission of the Director.

### Crown Copyright

Any views expressed in this paper are not necessarily those of the Department of Transport. Extracts from the text may be reproduced, except for commercial purposes, provided the source is acknowledged.

unlikely to be an effective countermeasure, and it is always up to the driver to recognize such situations and drive accordingly. In any case, all of the TCSs so far put on the market offer some compromise between satisfactory traction and handling performance, and all of them generally rely on the wheel-slip-control concept.

To achieve an improved system, we tried to work out an integrated control concept with adequate consideration given to the vehicle dynamics and then develop possible alternative technical features to put the concept to practical use.

Some existing TCSs have a tendency to overcontrol on bumpy and slippery roads, such as graveled ones, and vehicles, when negotiating these rough roads, often have more traction without TCS. The development of an advanced TCS that can more adequately maintain satisfactory performance both on smooth and rough roads might benefit from techniques which clearly distinguish these road surface conditions and which make suitable control responses to varying states of road surface.

This report discusses an integrated control technique aimed at meeting these requirements, and compares it with the conventional methods used for the existing TCSs. This is followed by a brief description of an experimental vehicle incorporating our control technique, and then by a study using this vehicle of the actual response and performance with the new integrated control technique.

### Control Concept for TCS

As noted earlier, past TCSs have been primarily intended to maintain longitudinal acceleration performance on slippery roads, and therefore, they are sometimes unable to provide satisfactory vehicle handling performance, specifically good stability and steerability during acceleration. If undue priority is given to vehicle handling, on the other hand, a system may fail to offer sufficient longitudinal acceleration performance.

Since the longitudinal acceleration performance of motor vehicles depends on driving forces working on the tires,

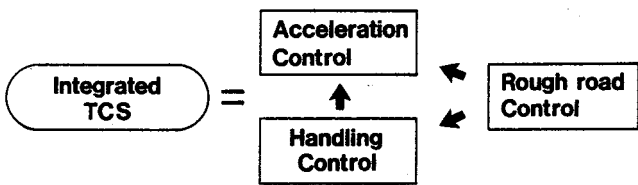
such performance could be improved by controlling tire longitudinal slippage as will be discussed later. At the same time, the handling performance and the steering response characteristics need to be considered. Therefore, using steering response as one of the control parameters, we need to seek a better compromise between longitudinal acceleration and handling performances during traction.

On the other hand, some TCS configurations may neither work stably nor provide sufficient acceleration performance on gravel or other irregular roads because vibrations of the suspension give external disturbances to the control action of the system, which may result in excess control of the driven wheels.

To get over these difficulties and develop an improved TCS that can maintain satisfactory acceleration and handling performance on a variety of road surfaces, we divided the TCS control concept into three elements comprising "acceleration," "handling" and "rough road" controls. Then we decided on a system configuration with a longitudinal acceleration control element at the center as a wheel-slip-control unit, which is supplemented by handling and rough-road controls (see figure 1).



• TCS Allows Ease of Acceleration on Slippery Roads.



• TCS Provides Ease of Acceleration and Cornering on a Variety of Road Conditions.

Figure 1. Control concept for TCS.

More specifically, the handling control subsystem monitors the steering response characteristics of the vehicle, to judge whether desirable steering response is being maintained, and transmits the results to the acceleration control element. Based on these data, the acceleration control element adjusts its control target. Meanwhile the rough-road control subsystem monitors the response to the road surface condition and sends the results to the acceleration control element and also to the handling control subsystem. Control parameters are then corrected according to the transmitted information.

This is our INTEGRATED CONTROL CONCEPT, which is discussed in more detail in the following sections, with respect to its working mechanism and control technique.

## Working Mechanism of the System

### Tire frictional force

While a motor vehicle is moving, the tires generate driving forces for longitudinal acceleration and lateral forces for cornering. The resultant of these two forces, a frictional force working between the tire treads and the road surface, is limited and declines as the road surface becomes more slippery (see figure 2).

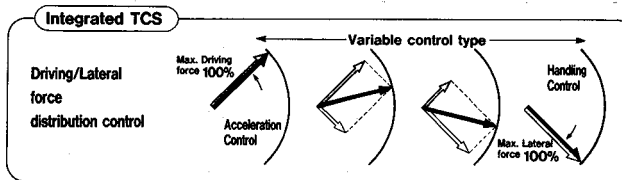
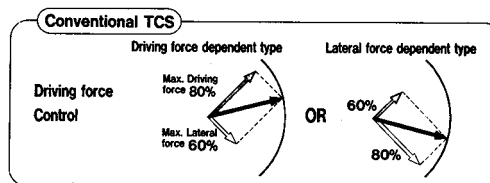
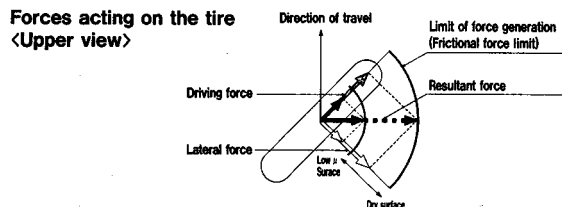


Figure 2. Example TCS function for the distribution of the tire frictional force.

Any attempt to give the tires a greater force than this limit might not only make the tires skid and fail to transmit the expected traction force, but might also adversely affect the vehicle handling performance. The essential function of the TCS is to try to automatically keep the frictional force within the limit noted above by curbing excess engine power during longitudinal acceleration so as to preclude the skidding of the driven wheels.

In some existing TCSs, however, a substantial portion of the lateral force for cornering remains even when only straight-ahead acceleration is desired because driving and lateral forces, the two components of the resultant frictional force, are always distributed at a fixed ratio. For instance, the driving-force-dependent TCS example in Figure 2 assigns 80 percent of the resultant frictional force to the maximum driving force and 60 percent of the resultant to the maximum lateral force. In the other TCS example which gives priority to directional stability and steerability of the vehicle, an 80-percent equivalent of the resultant is distributed to the lateral force and a 60-percent equivalent to the driving force.

Understandably, however, the lateral force limits needed for straight line acceleration may be low, and use of the residual lateral force as an additional driving force would enable the vehicle to accelerate more efficiently. If a

sufficient lateral force is not generated in cornering, on the other hand, the diversion of driving force into additional lateral force might help improve cornering performance.

Taking note of this relationship between driving and lateral forces, we decided to study an integrated TCS concept which combines the control of acceleration and handling into a whole system to try to make nearly 100-percent driving and lateral forces available for acceleration and cornering, respectively. In other words, it is a concept of variable force distribution TCS which controls the distribution of the resultant frictional force between driving and lateral forces. To realize this integrated TCS concept, we first had to develop a specific technique to set the distribution ratios for driving and lateral forces, and secondly we had to work out a method for actually assigning the resultant frictional force to driving and lateral forces according to these ratios. Of these techniques, the former is discussed in more detail in the next section from the viewpoint of vehicle dynamics, and the latter is dealt with in the next subsection in terms of tire skidding or slip ratio.

### Wheel slip control

Figure 3 describes the example TCS working mechanisms in terms of wheel slip ratio.

During longitudinal acceleration, the tires may slip on the road surface, resulting in a velocity differential (slip velocity) between the tire spin velocity and the vehicle velocity at the contact point. The ratio of this slip velocity to the tire spin velocity is generally known as the wheel "slip ratio."

The diagrams in figure 3 show the possible relationship between the slip ratio and the force generated at the tires, with the former given on the abscissa and the latter on the ordinate. The upper diagram is for the working mechanism of a conventional TCS and the lower diagram is for that of an integrated TCS. The solid curves indicate the driving force and the dashed lines represent the maximum lateral force.

The relationship between the tire slip ratio and driving force shows that, in the lower range of slip ratio, the driving force increases in proportion to a rise in slip ratio, but as this ratio increases further, the driving force levels off and then begins decreasing gradually. A look at the relationship between the slip ratio and the maximum lateral force indicates that the closer the slip ratio is to zero, the greater the lateral force, or the higher the slip ratio the smaller the lateral force.

For the existing TCS example dealt with here, the driving force oriented system in the upper diagram performs its control function using only the shaded range where the driving force reaches its peak. This can result in a lower maximum lateral force, putting narrower limits on the cornering performance.

Meanwhile the integrated TCS example in the lower diagram tries to extend the available range of slip ratios as much as possible so that full range of driving and lateral forces from zero to 100 percent might be used for acceleration and cornering. With such variable desired slip ratio, the

### Forces acting on the tire

<Side-view>

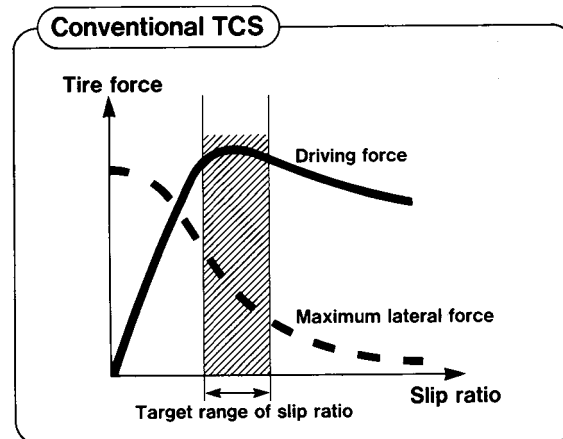
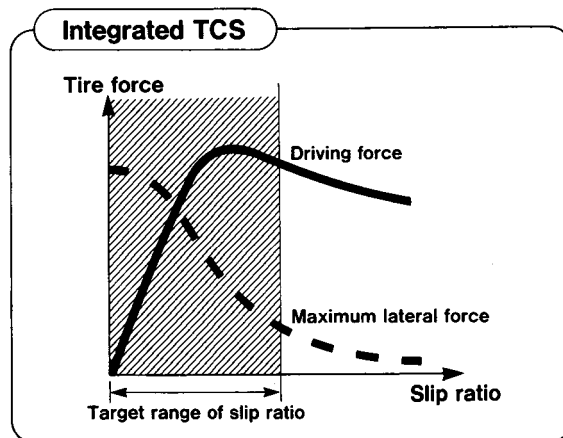
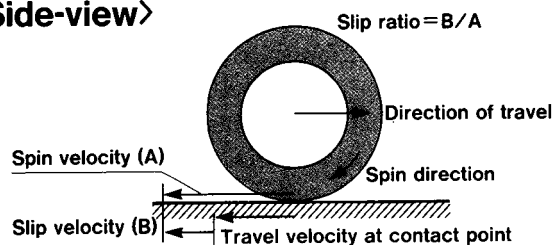


Figure 3. Example TCS function as the wheel-slip control.

integrated TCS tries to make an efficient distribution of driving and lateral forces, and the desired slip ratio is set by the handling control technique within the extended available range.

The handling control technique using the control algorithm for the example integrated TCS is discussed below.

### Control Algorithm for the Integrated TCS

The control algorithm for the integrated TCS is shown in figure 4. It consists of three blocks—the acceleration, handling and rough road control units. Of these components, the acceleration control unit plays a leading role in system operation, and based on information from the handling and rough road control units, its purpose is to

provide integrated control of traction, taking into consideration the "driver-vehicle-road system."

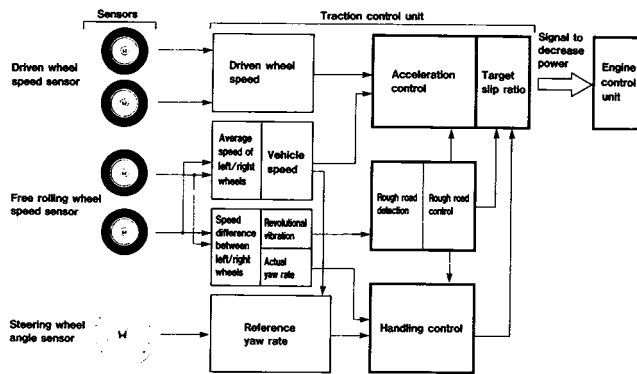


Figure 4. Control algorithm of integrated TCS.

### Acceleration control

This unit first measures the spin velocity of the free rolling wheels—the vehicle velocity—and that of the driven wheels using four wheel speed sensors. Then the slip ratio of the driven wheels is estimated from the vehicle and driven wheel velocities. This is followed by the calculation of feed back control to bring the slip ratio to the desired level, and the calculated results are transformed into an engine power reduction signal to the engine control unit. At the same time, the desired slip ratio is first set from the vehicle speed and then adjusted as necessary based on information from the handling and rough road control units. Feedback gains are also corrected according to the results of rough road control.

### Handling control

The vehicle handling control technique is schematically described in the lower part of figure 4. This unit is designed to minimize the difference between the reference yaw response when the steering wheel is turned and the estimated yaw response that actually results from the vehicle.

The handling unit calculates a reference yaw rate every moment using precomputed values and based upon the steering wheel angle and vehicle velocity. This process is reflected in the "reference yaw rate" block in the diagram of figure 4. The reference yaw rate, an essential element of the handling control concept, represents a precomputed estimate of the nominal yaw rate that should result when the driver turns the steering wheel. These precomputed steering response characteristics of the vehicle, which are used to calculate the reference yaw rate, are stored in the TCS computer memory. These response characteristics can be estimated, for instance, by steering response tests on an example vehicle chosen for TCS installation under dry and other road surface conditions. They might also be hypothetically determined from ideal response characteristics or derived from the basic vehicle specifications and tire characteristics.

The actual yaw rate of the vehicle is estimated from velocity differences between the right and left free rolling wheels. Comparison of the reference and actual yaw rates

shows if the vehicle response is suitable. From the magnitude and sign of their difference, changes in the transient steering characteristics can be estimated and serve as a parameter for assessing the moment-to-moment changes in vehicle handling performance. Using this parameter, the final evaluation of the handling performance is determined from a weighting function that takes into account the information provided by the rough road control unit. The results of the evaluation are sent to the acceleration unit.

In this process, the velocity difference between the two free rolling wheels is used to estimate the yaw rate. However we do not think the correlation between the actual yaw rate and the velocity difference between the right and left wheels is an important consideration in terms of traction control, because the velocity difference itself is among those vehicle response parameters which represent the lateral motion of the vehicle, and the reference steering response of which can be set through road or proving-ground tests. Since its measurement does not require an additional sensor, this velocity difference is practically very useful, compared with such alternatives as yaw rate, lateral acceleration or side slip angle.

### Rough road control

When accelerating the vehicle on a bumpy road, such as a gravelled one, a greater driving force can be generated usually if the driven wheels are allowed to slip and skid more than on a smooth hard road. Accordingly, a TCS capable of detecting road irregularities and reducing its control authority, when on a rough road, might not only enable the vehicle to accelerate more, but it could also make it less affected by external disturbances from vibrations of the wheels. Noting that unsprung components of the motor vehicle tend to vibrate at their resonance frequency during rough road driving, we decided to use a technique which, with a band pass filter, would monitor vibrations of these components through oscillations from wheel revolution, and based on the monitored results, adjust the control gain and change the control reference as necessary. This is the basic concept of our rough road control which sends the results of the calculation to the acceleration and handling control units.

No additional sensors are needed to find oscillations from wheel revolution as they can be monitored by wheel speed sensors.

## Experimental Vehicle Equipped with TCS

The experimental vehicle we have built on the basis of the integrated TCS concept is a front-wheel-drive car powered by a 2.7-liter normal aspirated engine. It has a wheel base of 2.7 meters and a weight of 1,400 kgw.

### TCS configuration

In a broad sense, the TCS possibilities include all types of systems designed to control excess power generated by the engine. As shown in figure 5, TCS configurations in general

may be divided into three main control areas, namely engine, transmission and brake controls. These can be subdivided further. The TCS used for the experimental vehicle is a simple system based on our engine control technique combined with fuel and ignition timing controls.

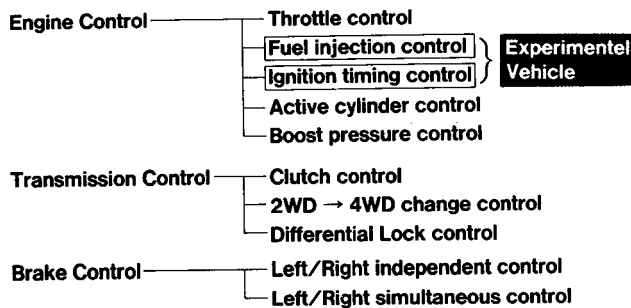


Figure 5. TCS configuration for experimental vehicle.

### System construction

The construction of our TCS is shown in figure 6. It uses wheel speed sensors installed at each of the four wheels, and a steering wheel angle sensor based on our unique idea. The steering angle sensor measures only the incremental angle. The steering wheel angle is estimated by the TCS computer which monitors the steady state yaw rate response to steer inputs, and adjusts the null value of the steering angle gradually based on the memorized steady-state gain and the yaw rate value every time the steady state is detected. Therefore this element comprises both hardware and software. The estimation program serves to automatically increase the accuracy, and the settling time of the estimations is quick enough for practical use. A major advantage of this method is that adjustment of the steer angle sensor is not needed when it is installed on the production line. These features are important elements of the technology needed to make the handling control concept suitable for practical purposes.

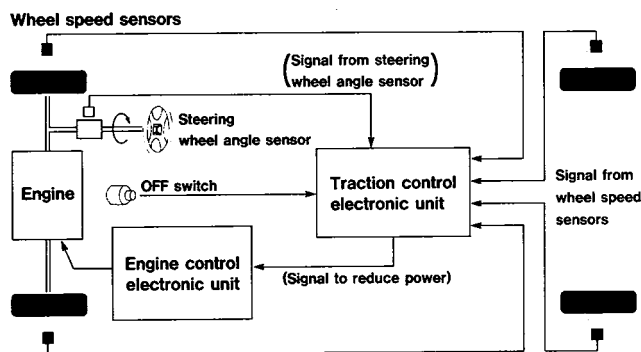


Figure 6. TCS structure for experimental vehicle.

The TCS computer unit receives signals from these sensors, makes the control calculations noted above, and sends power reduction signals to the engine control unit whenever necessary. In response to these signals, the engine control computer unit determines suitable values of fuel injection and ignition timing, taking into account the ever-changing operating condition of the engine.

The TCS has a manual shutoff switch to keep it unactuated when unnecessary or undesired, but the system can not be shutoff by the driver if it is actually operating (in a TCS mode). Ordinarily, when the ignition key is turned on, the TCS is automatically switched on, ready to work at any moment.

### Effects of Integrated TCS

The integrated TCS has three control functions; acceleration control, handling control and rough road control. This section discusses the effects of these control units, compared with more conventional TCS designs.

#### Effect of acceleration control

When negotiating a low  $\mu$  road, specifically a snow-covered one, the driver usually has to operate the accelerator carefully to avoid tire skidding. Among major features of the TCS is its capability to modulate the engine power on a low  $\mu$  road. If the driven wheels tend to skid during start-up or longitudinal acceleration on such a slippery road, the TCS automatically reduces the engine power and regulates tire skidding to ensure that the driving force will be efficiently transmitted to the road surface even if the driver does not make careful accelerator inputs. Figure 7 compares the traction performances of TCS and conventional vehicles during start-up and acceleration on a low  $\mu$  road with the steering wheel angle at zero or in the neutral position. The driven wheels of the vehicle equipped with TCS skid very little even though the throttle of the engine is wide open. The diagram also indicates that the TCS vehicle reaches higher speed and in a shorter time after the standing start. The system enables anyone to achieve such efficient traction performance.

When receiving information from the handling control unit that the vehicle is on a straight road, the acceleration control unit of the integrated TCS sets the target slip ratio so that the maximum driving force will be generated. The system may therefore achieve better acceleration efficiency than more conventional TCS configurations under some adverse conditions, and may provide at least as good traction performance as when operated by a skilled driver. These test findings are schematically described in figure 8. In this test, 4 example drivers were given a task to start and accelerate the vehicle as quickly as they could over a given length of a narrow, straight course, and they were told to keep on the course from end to end. The time required by each test car to go through the specified test course was recorded. The test was conducted with 4 drivers each of whom made five tries on the course. In the diagram, the average time of the five tries is marked with a circle, and the best and worst performances are shown at either end. The effects of the acceleration control unit are clearly reflected in the diagram.

#### Effect of handling control

To examine the effects of the handling control unit, another

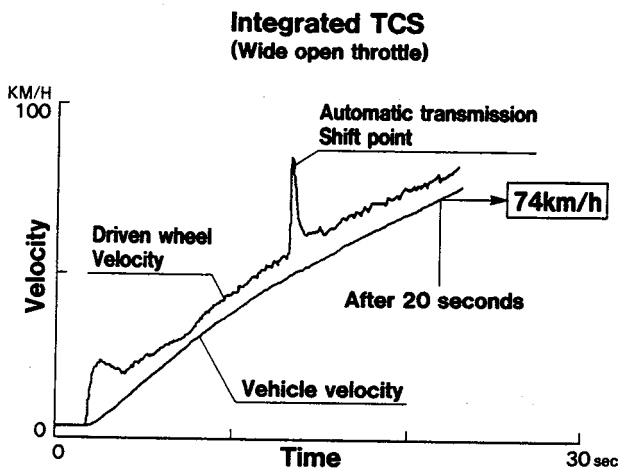
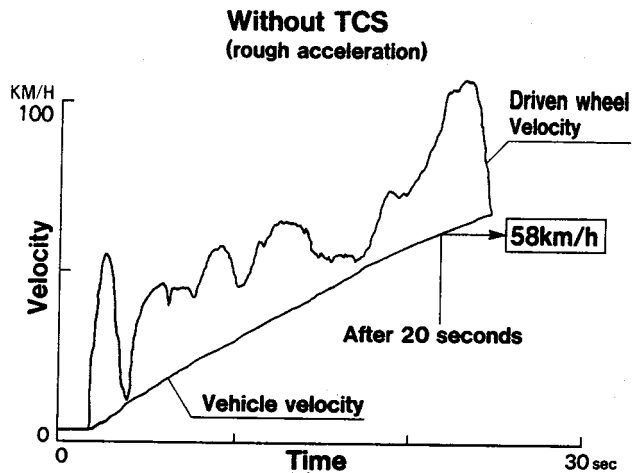


Figure 7. Straight line acceleration performance.

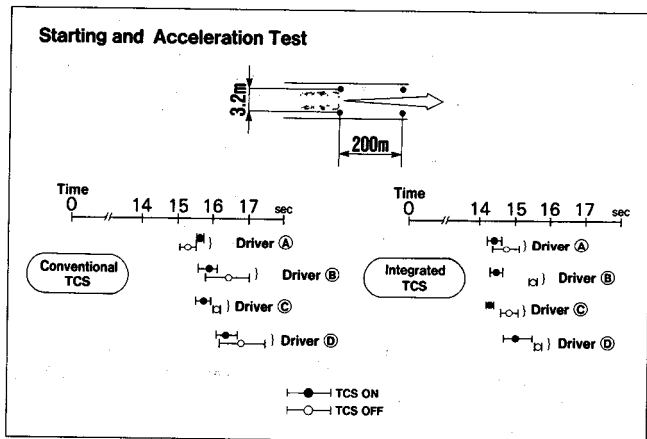


Figure 8. Task performance on low  $\mu$  surface.

er test was conducted on the experimental vehicle with the TCS set in two different ways, one with the handling control unit actuated and the other with this unit deactivated. An open-loop test was conducted. The driver started and accelerated the vehicle straight ahead at wide open throttle on a low  $\mu$  course, and when the vehicle velocity reached 20 km/h, he turned the steering wheel 180 degrees to perform cornering during acceleration. Measures of steering wheel

angle, yaw rate, and driving and lateral forces at the driven wheels, were recorded.

In the case of the TCS with its handling control unit deactivated, as indicated by dashed lines in figure 9, the tire driving force did not decline significantly even after the steering wheel was turned and the vehicle began cornering, but the tire lateral force decreased gradually until the vehicle was unable to maintain the expected yaw rate. In this example, this means that if no handling control is provided, the steering response is less than expected.

In the case of the TCS with the handling control unit actuated, the example shows that the tire driving force decreases while the tire lateral force capability, given priority, is maintained when the vehicle starts cornering, as indicated by solid lines in the diagram. As a result, the yaw rate and steering response of the vehicle are about the same as the case with no longitudinal acceleration.

If the integrated TCS was actuated, therefore, the vehicle was able to turn without getting off the course appreciably in this example. This is the effect of the handling control unit.

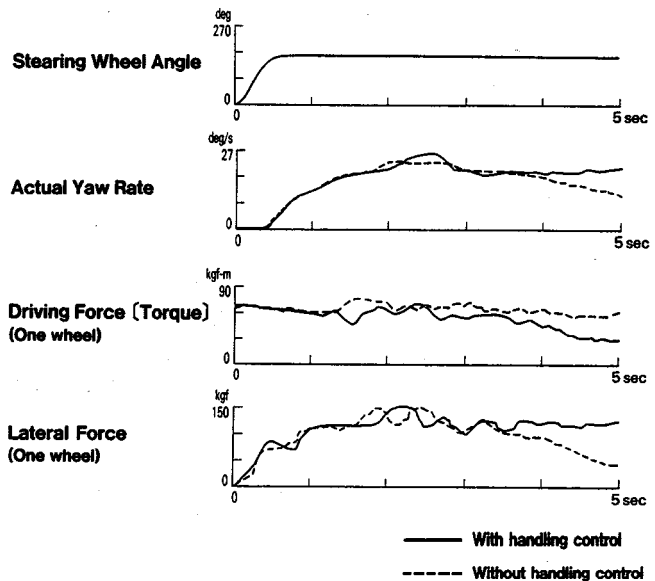


Figure 9. Effect of handling control.

### Effect of rough road control

A test was conducted on the experimental vehicle alternately equipped with two different configurations of TCS, one with rough road control capability and the other without this control function. An open-loop test was conducted (see figure 10). The driver started and accelerated the vehicle at wide open throttle on an example gravel road to provide test data for comparing the longitudinal acceleration performance of the experimental vehicle alternately set in two different TCS configurations. The TCS with the rough road control unit offered a little greater slip ratio than the other TCS which did not have this control function. Accordingly the vehicle with the integrated TCS showed better acceleration performance and reached a higher speed in the same

time on the example course. This demonstrates that the rough road control unit can give the vehicle greater capability to negotiate typical rough roads.

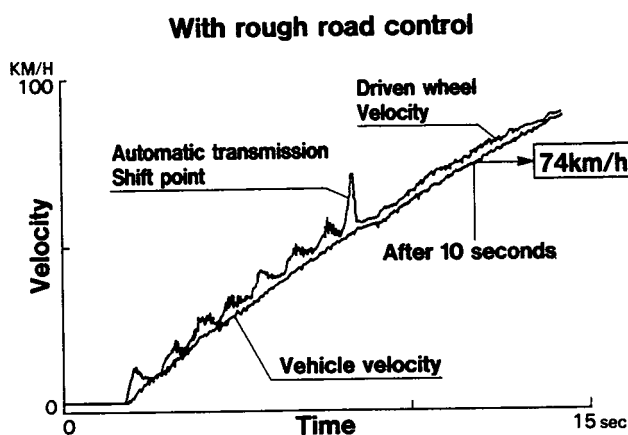
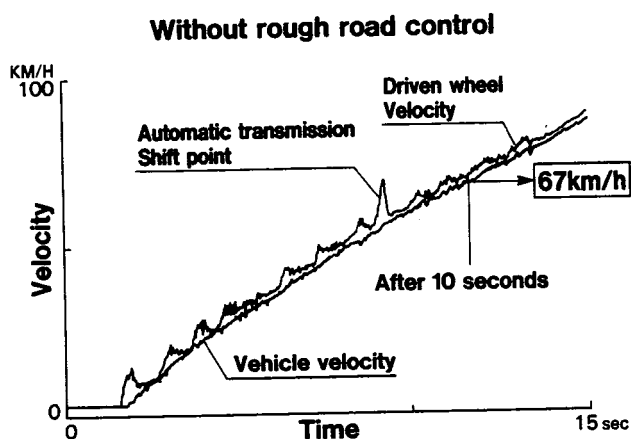


Figure 10. Effect of rough road control.

The rough road control unit of the integrated TCS senses if the vehicle is on a bumpy road, and sends corresponding information to the acceleration and handling control units. In response to such information, these units adjust their control parameters to try to ensure that the TCS will not overcontrol. Compared with more conventional TCSs, therefore, the integrated TCS can help improve vehicle performance during its operation. This favorable effect of the rough road control unit is shown in figure 11. In an example test on this control function, the drivers were given the same task as in figure 8, but the road surface and course length differed from those used in the previous test.

As is apparent from figure 11, the rough road control unit was effective in precluding overcontrol for this example roadway.

## Summary and Conclusion

We have presented a control concept for an integrated TCS, a method for realizing the concept, and an actual system based on that concept; that can provide a combination of satisfactory traction and vehicle handling performances for a variety of road surface conditions. A series of tests have also been conducted on the integrated

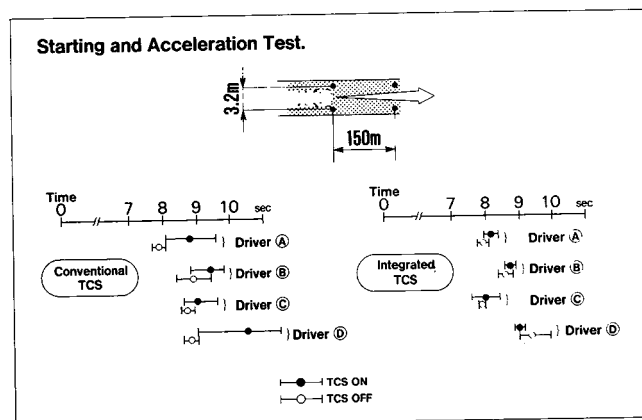


Figure 11. Task performance on rough road.

TCS. The findings of the tests and studies discussed in the foregoing sections may be summarized as follows:

1. The control concept and the appropriate control techniques for the integrated TCS have been established through a study of the vehicle dynamics and vibration.
2. The acceleration control unit of the integrated TCS can provide longitudinal acceleration performance that is about as good as an expert driver under a variety of adverse conditions, because, based on information from the handling control unit, it can adjust the slip ratio in a suitable way.
3. The handling control unit can observe moment-to-moment changes in the steering response characteristics of the vehicle, determine the values for handling evaluation using these changes, and send information to the acceleration control unit on the values thus determined. The acceleration control unit regulates the engine power based on this information. Therefore, it can provide better steerability for front-wheel-drive vehicles during acceleration under most conditions, compared with more conventional TCS configurations.
4. The rough road control unit senses if the vehicle encounters a bumpy road, such as a gravelled one, and this information enables the acceleration and handling control units to change their control parameters as appropriate. Therefore the integrated TCS can accelerate the vehicle to greater degree than more conventional TCSs, and it can also avoid overcontrolling.
5. The research efforts discussed here have led to the establishment of important technological elements for making an integrated TCS available for practical purposes. These elements include:

- Steering wheel angle sensor and position estimation which does not require adjustment of the sensor neutral point.
- Digital filter technique for estimation of vehicle yaw rate using velocity differences between the right and left wheels: and

- Band pass filter technique to improve rough road operation.

It is hoped that the integrated TCS can give full play to its control and performance capabilities under various conditions which make the driven wheels liable to skid, and thereby help contribute to future progress in the area of accident-avoidance capability of motor vehicles.

## References

- (1) M. Sato, S. Shiraishi, "Performance of A Simplified Control Technique for Antilock Brakes", 9th International Technical Conference on ESV, 1982, Kyoto.
- (2) S. Sano, Y. Furukawa, S. Shiraishi, "Modification of Vehicle Handling Performance by Four-Wheel Steering System" 10th International Technical Conference on ESV, 1985, Oxford.
- (3) J.H. Moran, R.A. Grimm, "Max Trac—Wheel Spin Control by Computer", SAE 710612.
- (4) L. Lind, "The Volvo Electronic Traction Control—Concept for Safe Driving", 9th International Technical Conference on ESV, 1982, Kyoto.
- (5) B. Thomson, "The Increase of Cornering Force and Traction by a Wheel-Slip-Control-system", 9th IAVSD-Symposium, June 1985, Sweden.
- (6) H.-J. Schoepf, J. Paul, "ASR Acceleration Skid Control—A Further Contribution Towards Increasing The Active Safety of Daimler-Benz Vehicle", SAE 885050.
- (7) Y. Inoue, H. Minegishi, K. Ise, H. Miyazaki, "A Traction Control System for Use in Rear-Wheel-Drive Vehicles with Automatic Transmission", C366/88 IMechE, 1988.
- (8) H. Wallentowitz, G. Egger, H. Herb, H. Krusche, "Stability and Traction Control for Four-Wheel-Drive Passenger Vehicles", C365/88 IMechE, 1988.
- (9) D.H. Weir, R.J. DiMarco, "Correlation and Evaluation of Driver/Vehicle Directional Handling Data", SAE 780010.
- (10) Fifth Draft Proposal for an International Standard. Road Vehicles—Braking in a Turn—Open Loop-Test Procedure, ISO/TC/22/SC9, N213, March 1981.
- (11) R.A. Hamming, "Digital Filters" Prentice-Hall, 1977.
- (12) Y. Takahashi, "Digital Control" (in Japanese) Iwanami Shoten, 1985.

## Active Safety Through Traction Control of 4WD Vehicles

Eiichi Yaguchi, Shuji Torii,  
Kiyotaka Ozaki, Genpei Naito,  
Nissan Motor Co., Ltd.

### Abstract

Three performance areas can be singled out in the human-machine system, consisting of the driver and the vehicle, as key factors for improving active safety. (1) The vehicle should provide good response and controllability in relation to the driver's operational inputs. (2) Vehicle behavior should be highly stable and free of any sudden changes. (3) There should be a sufficient flow of information from the vehicle to the driver to assure accurate recognition of present vehicle conditions and good predictability of subsequent vehicle behavior. Based on this framework, an analysis was made of the torque split between the front and rear wheels of a 4WD vehicle, and an optimum traction control method was devised for improving the performance areas noted above. That method was incorporated into an electronically controlled torque split 4WD system which employs a wet multiplate clutch in the 4WD transfer assembly to achieve optimum traction control. Vehicle tests conducted with the system confirmed that it significantly improves cornering properties and ABS performance under all road surface conditions, and thereby contributes to improved active safety.

### Introduction

There are many reports in the literature dealing with the vehicle dynamics of 4WD vehicles (1, 2, 3).<sup>\*</sup> However, most of them concern analyses of the stability of mechanical 4WD systems or analyses of vehicle behavior during braking. This paper presents the Nissan concept for active safety from the standpoint of vehicle dynamics. It also describes the construction and performance of a new-generation electronically controlled torque split 4WD system which contributes to a significant improvement in active safety. This system was developed on the basis of results obtained in a fundamental analysis of the relationship between traction control of a 4WD vehicle and the resulting vehicle dynamics.

### Nissan Concept for Active Safety

The Nissan concept for active safety from the standpoint of vehicle dynamics is outlined in figure 1.

This concept strikes a good balance among the following three performance requirements in terms of the human-machine system comprising the driver and the vehicle, and thus contributes to higher levels of active safety.

(1) The vehicle should move as the driver expects. This means providing good response and controllability in

<sup>\*</sup>Numbers in parentheses designate references at end of paper.

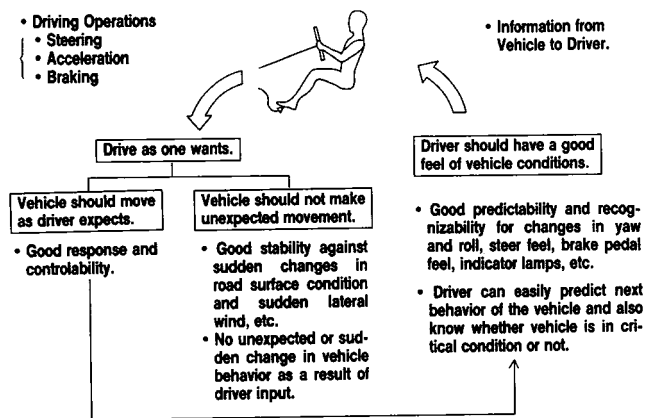


Figure 1. Nissan concept for active safety from the standpoint of vehicle dynamics.

relation to driving operations executed by the driver.

(2) The vehicle should not make any unexpected movement. This involves providing good stability against sudden changes in the road surface condition, sudden lateral wind or other external disturbances. There should not be any unexpected or sudden change in vehicle behavior as a result of operational inputs by the driver.

(3) There should be a sufficient flow of information from the vehicle to the driver so as to give the driver a good feel of the vehicle conditions. This means allowing the driver good recognizability and predictability based on changes in yaw and roll, steer feel, brake feel and indicator lamps. Such information enables the driver to easily predict subsequent vehicle behavior and to feel the critical performance limits of the vehicle.

In achieving enhanced active safety, it is essential to improve performance levels simultaneously in all three areas noted above, not simply attain higher absolute values for individual performance indices. A more detailed explanation will be given later of the significant improvements that can be obtained in all performance areas in figure 1 through the application of optimum traction control to a 4WD vehicle.

## Effect of Traction Control (Torque Split) on Vehicle Dynamics: Results of Basic Analysis

### Tractive performance

The tractive performance of a vehicle when traveling straight ahead can be analyzed in terms of the skid limit and the maximum powertrain torque limit. The former limit is determined by the level of friction between the tires and the road surface. The tractive force at the front and rear wheels can be calculated using a model like the one shown in figure 2. The latter limit is determined by the maximum engine torque, gear ratio and tire diameter. The relationship between tractive performance on high and low friction road surfaces and the torque split ratio is shown in figure 3 for a typical passenger car.

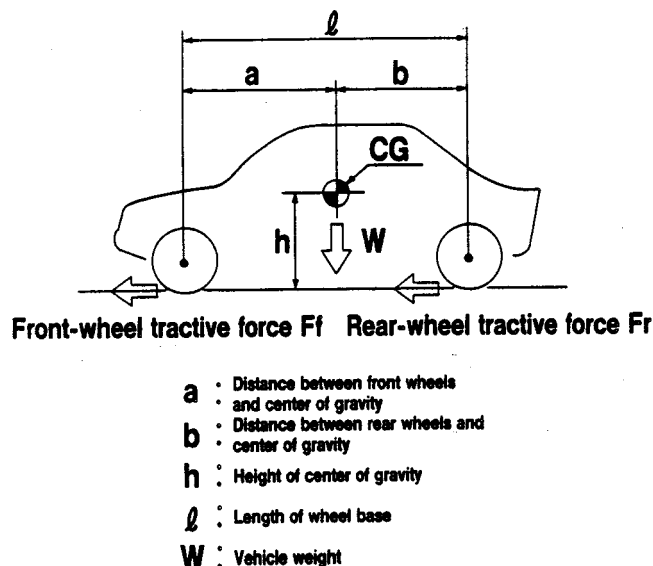


Figure 2. Calculation model.

From this figure the following observations can be made.

(1) The highest skid limit is obtained with the rigid 4WD mode when the front and rear wheels are directly coupled. The front-rear torque split when traveling straight ahead in the rigid 4WD mode is virtually equal to the weight distribution ratio between the front and rear axles (4, 5).

(2) The torque split ratio has little effect on vehicle dynamics on a high friction road surface because the maximum powertrain torque limit is lower than the skid limit.

(3) By contrast, the torque split ratio has a large influence on vehicle dynamics on a low friction road surface because the skid limit is lower than the maximum powertrain torque limit. As a result, a 4WD system with a torque split ratio of (f)50 : (r)50 is capable of providing approximately twice the tractive performance of a 2WD system.

(4) From (2) and (3) above, it can be concluded that optimum tractive performance can be obtained from a vehicle by controlling the torque split ratio to match the road surface and driving conditions, rather than trying to maintain a constant 4WD state with a (f)50 : (r)50 torque distribution.

### Cornering performance

An analysis of cornering performance and anti-lock brake system performance was carried out using a computer simulation model having 16 degrees of freedom. Six degrees of freedom were applied for body motion, four for wheel revolution, four for wheel toe change and two for the steering system.

It was found that the torque split ratio had very little effect on cornering behavior under a constant speed or on cornering behavior under gradual acceleration where the tractive force does not exert much influence. However, under a condition of rapid acceleration where the tractive force does exert a large influence, the torque split ratio was found to have a significant effect on cornering behavior.

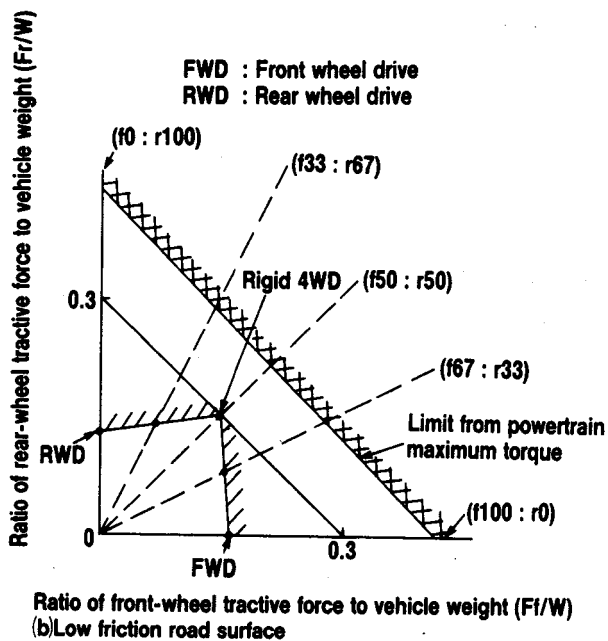
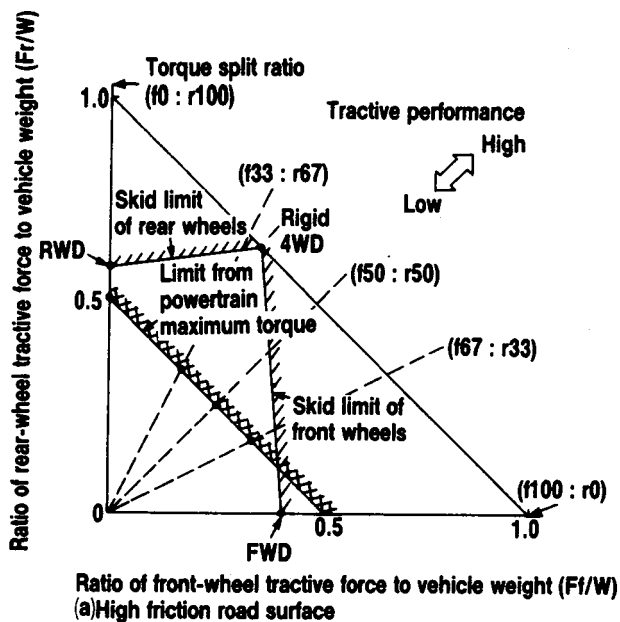


Figure 3. Maximum tractive performance.

Figure 4 illustrates the relationship between lateral gravity ( $G$ ) and vehicle cornering behavior,  $R/R_0$ , under a condition of rapid acceleration during cornering. Here,  $R_0$  is the turning radius of the vehicle at low speed with a certain steering angle and  $R$  is the turning radius of the vehicle while accelerating with the same steering angle. From this figure, the following points are made clear.

(1) The torque split ratio has a large effect on cornering behavior in the high lateral  $G$  region. The range of influence of the torque split ratio is indicated by the shaded area in the figure.

(2) Increasing the torque split ratio to the front wheels results in a larger  $R/R_0$  value and produces a drift out tendency. On the other hand, increasing the torque ratio distributed to the rear wheels produces a spin tendency.

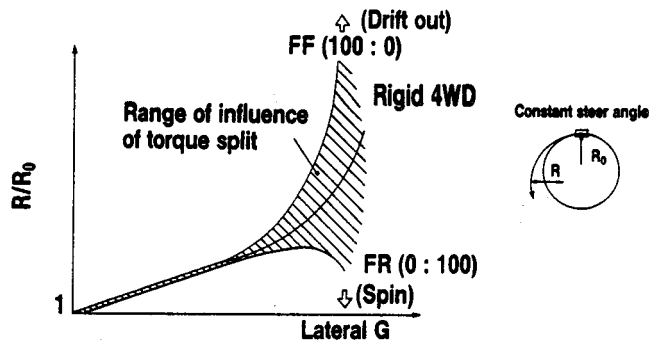


Figure 4. Cornering behavior under rapid acceleration.

The differences in cornering behavior observed in figure 4 result from the interrelationship between the longitudinal and lateral forces of the tires. Under this interrelationship, the lateral force of the tires decreases, as the longitudinal force increases.

The foregoing discussion has considered cornering behavior from the viewpoint of absolute performance values. When considered from the standpoint of active safety, it is important to examine cornering behavior on the basis of the physical values actually felt by the driver. The physical quantity selected here as the evaluation standard was the change in yaw velocity,  $\Delta \Psi$ , that occurred when a step tractive force was applied while cornering under a constant speed. Using the evaluation method shown in figure 5, an analysis was made of the relationship between the torque split ratio and cornering performance. Typical analytical results obtained under various road surface conditions are presented in figure 6. The reference line in figures 5 and 6 indicates the optimum  $\Delta \Psi$  change, for which there is no change in the turning radius within one second following acceleration.

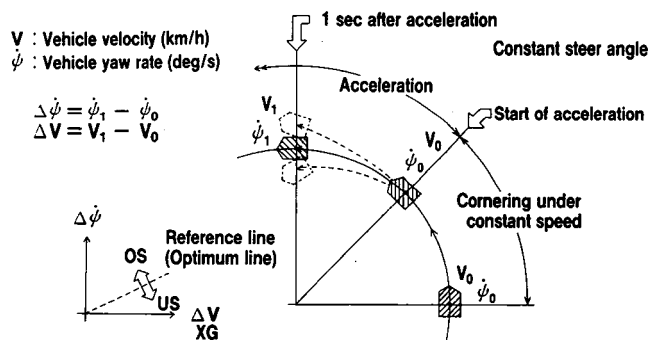


Figure 5. Evaluation method.

The following observations can be made from figure 6.

(1) Depending on the magnitude of the tractive force (longitudinal acceleration), the torque split ratio should be varied continuously in order to obtain cornering behavior that is acceptable to the driver. The desired cornering behavior suppresses the spin and drift out tendencies when the vehicle is accelerated during cornering. A sample torque split control pattern is indicated by points A, B and C in figure 6.

(2) The optimum torque split ratio depends on the coefficient of friction of the road surface. On a high friction road

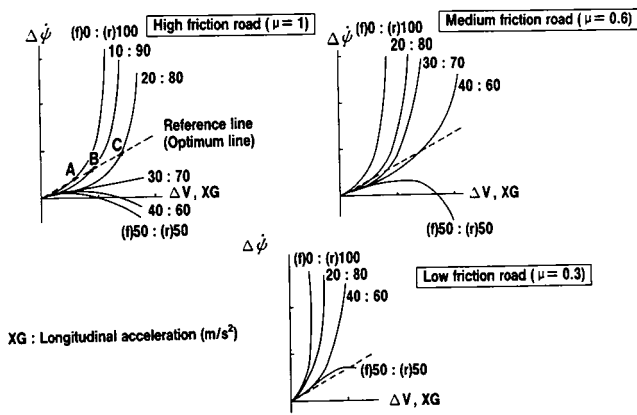


Figure 6. Influence of torque split ratio on cornering behavior under various road surface conditions.

surface, the torque split ratio should be controlled within a range from (f)0 : (r)100 to (f)20 : (r)80; on a low friction road surface, it should be controlled within a range from (f)0 : (r)100 to (f)50 : (r)50.

These observations can be explained in terms of the concept of the tire friction circle illustrated in figure 7. It is seen from the figure that the optimum torque split ratio roughly corresponds to the size of the friction circles for the front and rear inner wheels. The reason for this is related to the fact that greater lateral and longitudinal acceleration can be generated as the coefficient of friction of the road surface increases; thus, with the resulting increase in load movement, the tire capacity of the rear wheels rises, allowing a larger portion of the tractive force to be distributed to the rear wheels.

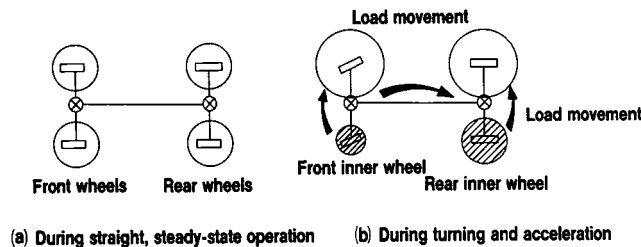


Figure 7. Size of friction circle of four wheels during turning and acceleration.

### Performance of anti-lock braking system (ABS)

A 4WD vehicle requires greater braking performance to match its higher tractive force capability, and thus there is an especially strong requirement to incorporate ABS in 4WD vehicles. An anti-lock braking system calculates the velocity of the vehicle body and controls the velocity of each wheel accordingly, based on the concept that each wheel rotates independently.

Attempts to apply ABS to 4WD vehicles have run into the problem of unacceptable performance degradation caused by the occurrence of a coupling force between the front and rear wheels that restricts wheel rotation. Figure 8 shows the changes in wheel velocity calculated for a rigid 4WD vehi-

cle equipped with an anti-lock braking system having three channels and four wheel speed sensors. (7)

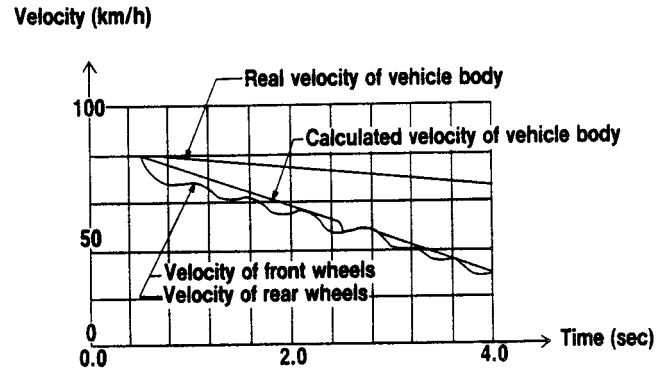


Figure 8. ABS performance (rigid 4WD) on icy road surface.

In this example, since the inertia of the engine and transmission is applied to all four wheels, it takes longer for the wheels to recover their rotational velocity after slipping occurs. As a result, this degrades the accuracy of the vehicle velocity calculations, particularly on a road surface with a low coefficient of friction. Since the slip ratio of all four wheels becomes excessively large, ABS performance deteriorates drastically. One approach to avoiding this problem when ABS is actuated is to switch to a rear-wheel-drive condition by controlling the transfer unit so as to release the coupling force between the front and rear wheels. (6)

This approach makes it possible to achieve good control over the front wheels because the vehicle velocity can be calculated accurately. However, it has the disadvantage that vehicle stability deteriorates (figure 9), particularly on a road surface with a low coefficient of friction. This problem is caused by the excessively large slip ratio that occurs at the rear wheels owing to the fact that they receive all of the engine brake torque. While a similar problem is also observed with a conventional rear-wheel-drive vehicle, it is more serious in the case of a 4WD vehicle. This is because the actuation of ABS would cause a sudden loss of the high level of vehicle stability felt by the driver until just prior to braking. In order to resolve this problem, it is necessary to transfer a certain portion of the braking torque generated by the engine brake to the front wheels.

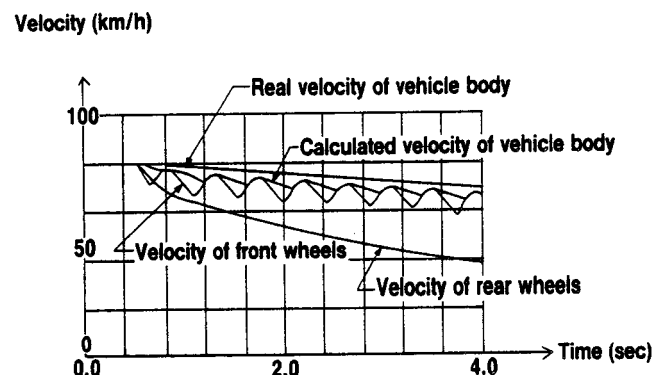


Figure 9. ABS performance (rear wheel drive condition) on icy road surface.

Figure 10 shows the relationship between the maximum transfer torque to the front wheels,  $T_c$ , and the average slip ratio of all four wheels two seconds after the onset of braking on an icy road surface. It is seen that the slip ratio of the front wheels,  $S_f$ , increases with increasing  $T_c$ , while the slip ratio of the rear wheels,  $S_r$ , decreases. However, beyond the point where  $T_c = T_o$ , the rear wheel slip ratio switches to an increasing curve. The combined slip ratio of the front and rear wheels,  $S_f + S_r$ , shows a minimum, i.e. optimum, value at the point where  $T_c = T_o$ .

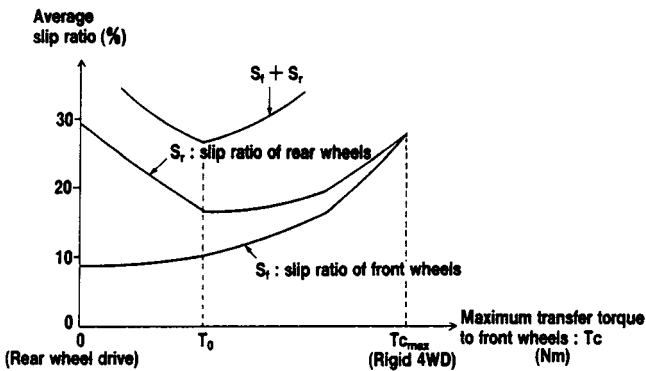


Figure 10. Relationship between maximum transfer torque to front wheels and average slip ratio of each wheel on icy road surface.

## New electronically controlled torque split 4WD system

The foregoing analytical results provided the basis for the development of a new electronically controlled torque split 4WD system. Not only does this system improve tractive performance, it also provides excellent controllability, stability and predictability of vehicle behavior during cornering and braking.

### System outline

An outline of the system configuration is given in figure 11. The output of the transmission is transmitted directly to the rear differential gear to drive the rear wheels. Meanwhile, the transmission output is transmitted to the differential gear of the front axle via a multiplate clutch built into the transfer assembly. The engagement pressure of the multiplate clutch is controlled by a hydraulic piston in the transfer assembly.

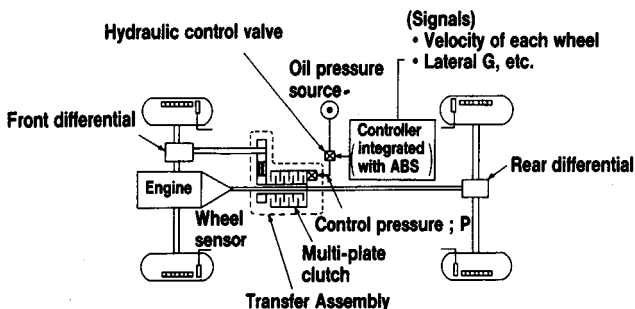


Figure 11. Outline of electronically controlled torque split 4WD system.

Letting  $T$  represent the torque input to the transfer assembly, the torque transmitted to the front and rear wheels,  $T_f$  and  $T_r$ , can be given the following expressions:

$$T_f = T_c \quad (1)$$

$$T_r = T - T_c \quad (2)$$

where,  $T_c$  is the transfer torque of the multiplate clutch. Since  $T_c$  is proportional to the clutch pressure,  $P$ , controlling  $P$  enables the torque split ratio to be varied over a range from a rear wheel drive condition ( $T_f : T_r = 0 : 100$ ) to a 4WD condition close to the weight distribution ratio between the front and rear axles ( $T_f : T_r = 50 : 50$ ).

The multiplate clutch is oil-cooled and electronically controlled. This clutch management system design is fully capable of withstanding the level of heat generated during operation. Heat generation is equivalent to the product of the transfer torque ( $T_c$ ) and the difference in rotational speed between the front and rear wheels that occurs during driving.

A motor-driven oil pressure source is provided to generate hydraulic pressure which is controlled by a compact electromagnetic hydraulic control valve to produce the control pressure ( $P$ ) for the multiple clutch. Based on signal inputs from wheel speed sensors, a lateral G sensor and the ABS unit, the controller sends a signal to the control valve to regulate the clutch pressure. Integrated control with ABS is provided for the wheel speed sensors, controller and most of the control logic.

### Control strategy

An outline of the control strategy used in this system is given in figure 12. In the figure  $N_r$  indicates the average velocity of the rear wheels (km/hr),  $N_f$  the average velocity of the front wheels and  $K$  the gain of  $N_r - N_f$  and the clutch pressure,  $P$ , or the clutch transfer torque,  $T_c$ .

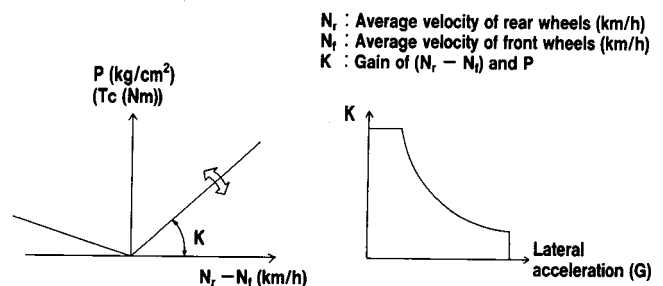


Figure 12. Control strategy.

As indicated in the figure, in the region where  $N_r - N_f$  is positive, gain  $K$  is controlled such that it is high when lateral  $G$  is low and low when lateral  $G$  is high. Consequently, with this control strategy, large driver torque is transmitted to the front wheels under operating conditions where gain  $K$  is large because lateral  $G$  is small. This occurs, for example, under conditions where the drive torque must be split between the front and rear wheels, such as when accelerating while driving straight ahead or when traveling on a snowy road surface. On the other hand, when accelerating during cornering on a dry road surface, where large lateral  $G$  oc-

curs, the amount of torque transferred to the front wheels is relatively small because the value of gain  $K$  is small. As a result, this makes it possible to obtain excellent cornering performance.

Since control is carried out continuously, it does not cause any sudden changes in vehicle behavior. When ABS is actuated, the clutch transfer torque is controlled to a certain fixed level.  $T_o$ , based on the analytical results presented in the previous section. This measure works to enhance ABS performance. The control strategy has also been designed to avoid sudden changes in vehicle behavior when the driver lets up on the accelerator pedal during high-speed cornering. In this case,  $N_r - N_f$  in figure 12 is in the negative region and gain  $K$  is low. The control system increases the clutch pressure,  $P$ , rapidly so as to distribute a suitable torque ratio to the front wheels.

The wind up phenomenon that can occur in the rigid 4WD mode during low speed operation is effectively suppressed because gain  $K$  is small when  $N_r - N_f$  is negative.

### Experimental results

Figure 13 shows the experimental results for cornering performance on dry and icy road surfaces. It is seen that excellent cornering performance was obtained under various road surface conditions as a result of providing optimum traction control over the 4WD vehicle equipped with the electronically controlled torque split 4WD system.

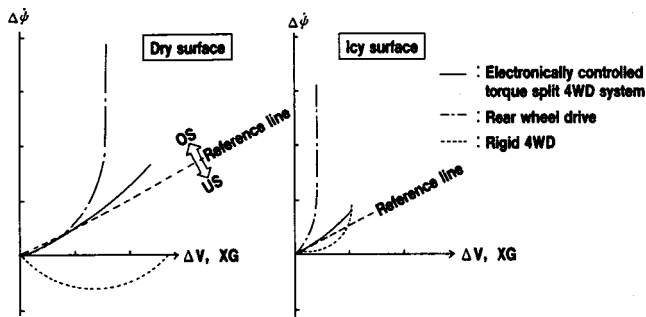


Figure 13. Cornering performance (experimental) yaw rate change in acceleration from steady-state cornering.

Specifically, the gradual change provided from neutral steer to moderate oversteer assures high predictability, which means the driver can easily feel the cornering limits of the vehicle. Second, good controllability is achieved because linear yaw rate changes are achieved relative to accelerator pedal inputs.

The tractive force distribution between the front and rear axles of the 4WD vehicle is shown in figure 14 in relation to the road surface conditions of figure 13. It is seen in the figure that the change in the tractive force distribution was controlled in a smooth, continuous manner and that the torque split ratio was varied to match the road surface conditions.

Figure 15 shows the relationship between the cornering characteristic,  $R/R_0$ , and lateral  $G$  when a step steering input was applied during steady-state cornering. The vehicle equipped with the electronically controlled torque split

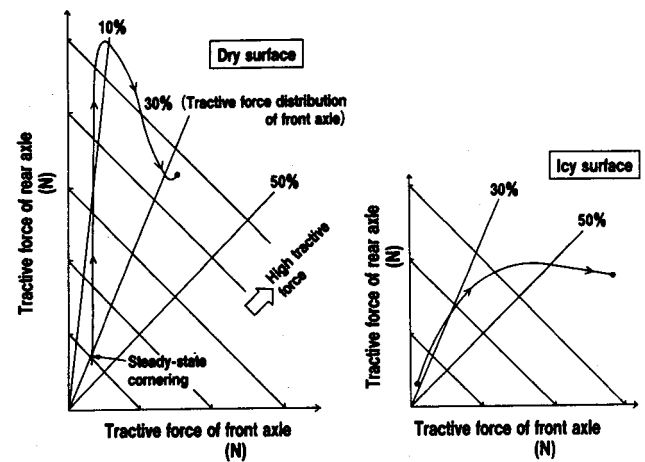


Figure 14. Tractive force distribution between front and rear axles (experimental) acceleration from steady-state cornering.

4WD system shows a smaller  $R/R_0$  value than the vehicle equipped with a conventional 4WD system. This result confirms that the electronically controlled torque split 4WD system provides better steerability than a conventional 4WD system even under a condition of high lateral  $G$ .

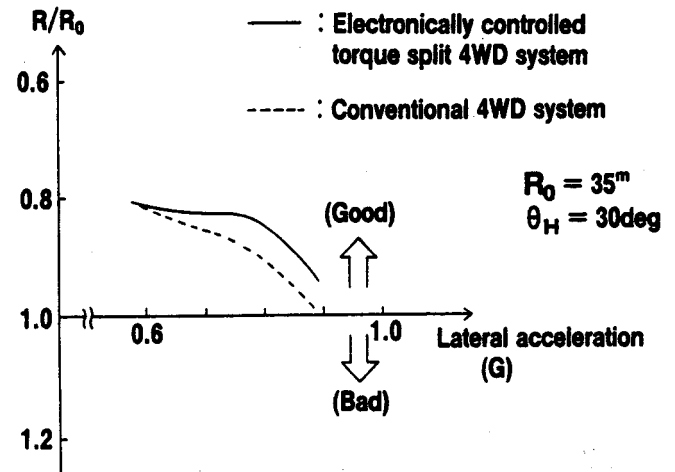


Figure 15. Steerability.

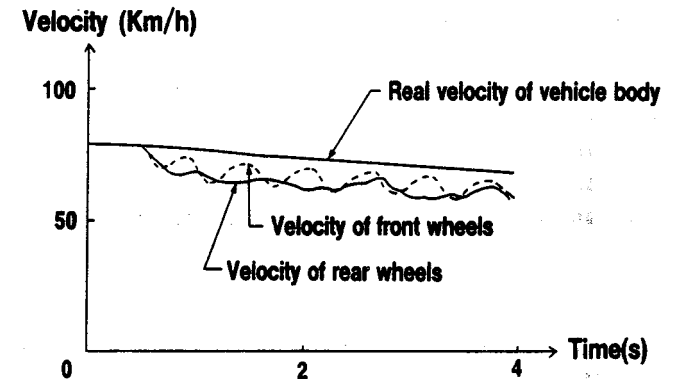


Figure 16. ABS performance ( $T_c = T_o$ ) on icy road surface.

Figure 16 shows the ABS performance obtained on an icy surface. The slip ratio of the front and rear wheels was controlled to a suitable value through the control strategy of

$T_c = T_0$ , as outlined in the previous section for ABS operation. It is clear from the figure that this strategy achieves good ABS performance.

## Conclusion

The conclusions of the present work are summarized below.

(1.) In the human-machine system made up of the driver and the vehicle, it is essential to fulfill the following performance requirements in order to obtain higher improved levels of active safety.

- The vehicle should provide good response and controllability in relation to operational inputs by the driver.
- Vehicle behavior should be highly stable and free of any sudden changes.
- There should be a sufficient flow of information from the vehicle to the driver to assure accurate recognition of present vehicle conditions and good predictability of critical performance limits.

(2.) The results of an analysis carried out with a simulation model showed that suitable traction control between the front and rear wheels would contribute greatly to performance improvements in all three areas noted above.

(3.) Based on the foregoing analytical results, a new electronically controlled torque split 4WD system was developed. This system provides continuous control over the torque split ratio to the front and rear wheels using a multiplate clutch incorporated in the transfer assembly. Control is carried out according to information provided by

wheel speed sensors, a lateral G sensor and a signal from the ABS unit.

(4.) Vehicle tests on this new system have confirmed that it provides high tractive performance, good steerability in response to steering wheel and accelerator pedal inputs (i.e. good response and controllability), excellent ABS performance, superb high-speed vehicle stability and excellent cornering performance on all types of road surfaces, allowing good predictability of the performance limits of the vehicle.

## References

- (1) R. Matsumoto, et al., "Increase of Driving Safety through New Concept 4WD Vehicle," 9th ESV Conference, Kyoto, November 1982.
- (2) M. Otake, et al., "Maneuverability and New suspension for Four-Wheel Drive Vehicles," 10th ESV Conference, Oxford, July 1985.
- (3) K. Kodama, et al., "4WD Vehicle Behavior during Braking in a Turn," 11th ESV Conference, Washington, May 1987.
- (4) K. Isoda, et al., "Handling Characteristics of 4WD Passenger Cars," (in Japanese), JSAE, Vol. 40, No. 3, (1986).
- (5) H. Minabe, et al., "Dynamic Performance of 4WD Vehicles", (in Japanese), JSAE, Vol. 40, No. 3 (1986).
- (6) A. Zomotor, et al., "Mercedes-Benz 4-Matic, an Electronically Controlled Four-Wheel Drive System for Improved Active Safety," SAE Paper 86131.
- (7) T. Suzuki, et al., "A Study for Applying an Anti-Lock Braking System for Four-Wheel Drive Cars," SAE Paper 89032.

## Active Safety Research on Intelligent Driver Support Systems

Stig Franzén, Bertil Ilhage,  
SAAB-SCANIA AB

### Abstract

The rapid development of new information technology makes it realistic to look for more advanced driver support systems to increase the active safety of modern vehicles. Application oriented R&D work must be stimulated in the areas of advanced micro-electronics, new communication techniques, AI-type software, and automotive human engineering.

The design of a driver-vehicle interface where the information flow to the driver and the control actions taken by the driver could be supported in an intelligent and selective way is the long-term goal. Research on optimal design of the driver-vehicle interface, where also the adaptive dimension of the driver-vehicle dialogue (or interaction) can be addressed, will therefore be of specific interest.

Some examples of active safety research and development work within the SAAB-SCANIA Group in the past, at present, and in the future are discussed.

### Introduction

Safe driving has been one of the main goals of Saab Car Division since the beginning of the Saab car history in the mid 40s. The original concept with front wheel drive, precise rack steering gear and aerodynamic styling are early characteristics of the Saab car design related to active safety. Other visible signs of Saab Car Division concern for active safety solutions are the introduction of the world's first headlamp wiper/washer in 1970 and the running light in 1974.

The passive safety issues have also been dealt with at an early stage. Protection of the driver and the car passengers in traffic accidents by the early introduction of safety belts

and by the basic design of the mechanical structure of the car body are examples of such steps.

Today the development of new advanced solutions based on information technology may be a tool for further improvements of the active safety of road traffic. These new "IT-tools" may be used for methodological improvements of the R&D process for the design of better vehicle dynamics and man-machine interface.

A more frequent use of dynamic modelling and simulations of the driver-vehicle-environment system can be foreseen. The development of forceful methods and criterias for the evaluation of the principles of new systems as early as possible in the car design process may also be accomplished.

Advanced micro-electronics, new sensors and communication techniques, new light sources, powerful signal and data processing, AI-type software, smart power supplies, etc. may be used in future vehicles to improve the "active safety competence" of the vehicle and of the total road environment.

### The total road traffic system

The total road traffic system is a dynamic system composed of several subsystems or elements. You can identify the driver, the vehicle, the road, the weather condition, the traffic situation, other road users, etc. The driving tasks will be dynamically influenced by the interaction driver-vehicle-environment. The driver is and will also in the future be responsible for how the vehicle is controlled.

The driving tasks must be analyzed in detail and the driver's behaviour in different tasks must be studied. The driver has a goal for the trip and makes a plan for the route to be followed. The driver then manoeuvres the vehicle in intersections and in lanes, overtakes and tries to follow traffic regulations etc. These tasks can be defined as tertiary and secondary tasks, while the actual handling and stabilizing of the car on the road is the primary task. Rasmussen (1983) has presented a three echelon model of an operator (or driver) related to knowledge-based, rule-based and skill-based human actions (or planning, manoeuvring and handling) in man-machine systems (figure 1).

The drivers and other road users of future road traffic systems will probably not find the traffic situation simpler than today. Subsequently the driving task will not become easier. The driver therefore needs active support in the driving tasks. More information about the driving environment and assistance in the actual driving task can if realized make driving easier and hence actively influence the driver behaviour in such a way that road traffic safety is enhanced (figure 2).

There is also need for coordinated actions of the different types of road users. If the road traffic system is better understood, smoother traffic flow and effective route guidance can be accomplished by intelligent traffic control input and by intelligent driver support systems introduced in the vehicle.

The vehicle should also be equipped with systems which

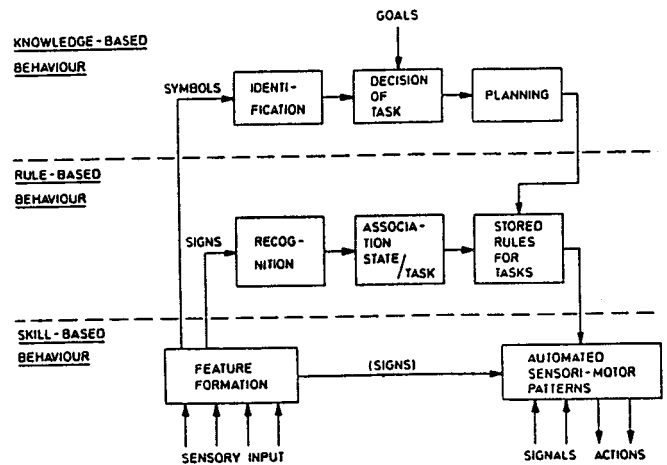


Figure 1. Illustration of the three levels of performance of skilled human operators (Rasmussen, 1983).

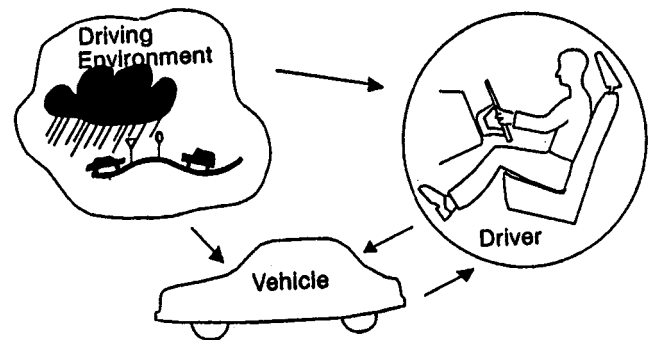


Figure 2. The total road traffic system.

support the driver in the primary driving tasks, i.e. handling and stabilizing the vehicle on the road. High-frequency control of longitudinal and lateral motion of the vehicle could help the driver control the vehicle in a better way.

### Active Safety Research

Active safety is concerned about the reduction of the number of accidents and casualties/injuries in road traffic by supporting the driver in the driving tasks. The reduction of the negative effects of an accident if it should occur (i.e. passive safety) is also important, but is not treated in this paper.

The task to improve the active safety in road traffic is obviously a multi-science problem with the involvement of many actors with different competences. The central focus must be on the needs of the different road users, and consequently human-oriented sciences and the area of man-machine interaction are important and central. One new research area where these aspects are concentrated is *cognitive science engineering* or *cognitive engineering* (figure 3).

### Cooperation basic research—car industry

The Saab Car Division started collaboration with universities and research institutes with active safety topics about 20 years ago. One example is the work together with the Psychology Department of Uppsala University in the areas

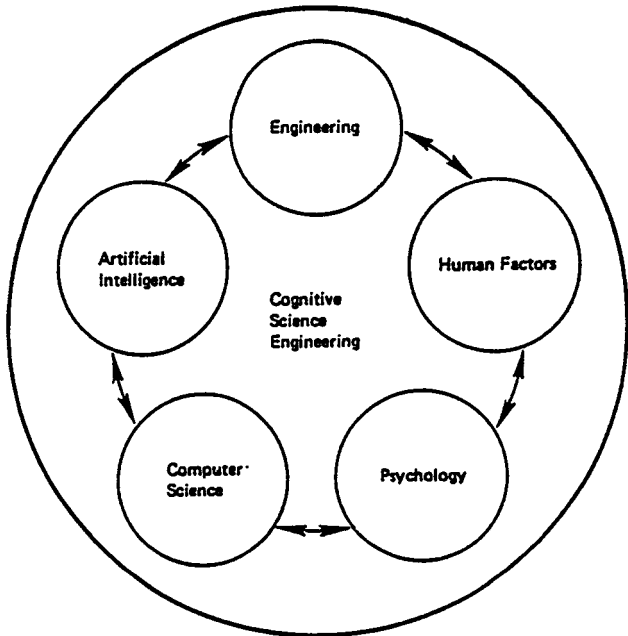


Figure 3. Cognitive science engineering or cognitive engineering (1987).

of lighting and man-machine interface design. The practical results were an improved light distribution on low beam, the running lights, and an improved organization of instruments and controls. However, due to the slow and complicated legislation process, many interesting research results were not possible to implement in real road traffic at that time.

One example today is the cooperation with VTI (Swedish Road and Traffic Research Institute) in the area of driver modelling, especially the cognitive process of the driver. The complex structure of human (or driver) behaviour can for example be indicated in a block diagram (figure 4).

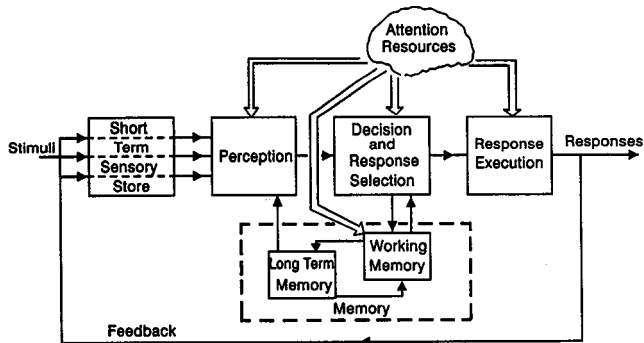


Figure 4. A human operator model (Wickens 1984).

Another example is the contact we have with Delft University, The Netherlands in the area of vehicle dynamics.

The SAAB-SCANIA participation in European research programmes on road traffic systems of the future (Prometheus and DRIVE), will certainly increase our close cooperation with many other universities and research institutes in Europe over the years to come. The research programmes have the objectives to increase the safety of road traffic, to make the total traffic system more effective, and to decrease

environmental negative effects caused by road traffic by means of advanced information technology systems.

### Automotive human engineering

By tradition the automotive human engineering activities are mainly directed toward the ergonomical and perceptual areas. The driver's seat, the steering wheel, the instrumentation, the controls, and the driver's visual view through the windscreen are all elements and subsystems related to active safety.

But today and even more in the future the psychological and cognitive aspects of different driving tasks will become more important in order to obtain a good man-machine interface design.

A better understanding of different driver's behaviour in all possible road traffic situations must be developed. There is no such thing as an "average driver" and consequently no average way to design the interface between the driver and the vehicle. The variation of experience, age, skill, education, etc. of drivers is very large. The conclusion is that the driver-vehicle interface must be adaptive to this variation in order to really make a solution for enhanced active safety possible.

Especially the driver's own understanding of different driving tasks must be better known. To develop a model or a description of the driver's tasks from a cognitive point of view is therefore necessary. A structured and comprehensive understanding of these tasks is essential to identify all safety relevant variables and to arrive to appropriate solutions for task allocation between intelligent driver support systems and the driver.

In order to structure the work in the area of automotive human engineering, concept studies related to the new functions developed for future road traffic systems must be performed. But these studies must be supported by relevant related basic research on driver behaviour as well as R&D work on potential technical solutions to implement the functions (figure 5).

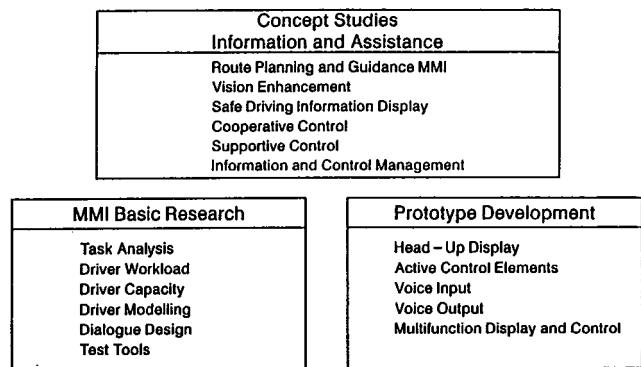


Figure 5. Structure of future R&D work in the area of automotive human engineering (Prometheus-WG4).

### Methodological research

New information technology has made it possible to make considerable improvements in methods and tools for

active safety R&D. Modelling, simulations (both on computers and in simulators), computer aided engineering and testing in general have been substantially improved.

However, there is still much to gain in these areas, i.e. in driver-vehicle modelling, driver task analysis, simulation and test tools. An introduction of new intelligent driver support systems will add new requirements for methods and tools. One example is the recently started modification of the VTI driving simulator to better fit research work with new systems for driver support. Saab-Scania is partly financing this modification.

Procedures and techniques for performing task analysis by both modelling and practical analysis of real driving situations must be developed. Simulation in both simple and advanced driving simulators as well as analysis of film or video recordings of real driving situations are two such methods.

New software packages can be used as an early input in the design process for "rapid prototyping" of displays, controls, and for dialogue studies. Different ideas and principles can be tested in a simple manner and speed up the design process of the driver-vehicle interface noticeably.

### Intelligent Driver Support Systems

The driver as a part of the road traffic system needs support to improve active safety and other important aspects of road traffic. The support systems must however be introduced step by step. We have tried to identify some of these steps in terms of vehicle competences or vehicle copilot functions.

The first step is "informative competences" where new sensing systems and communication links will make it possible to improve the quality and increase the quantity of information for the operation of different vehicle systems. An "informative copilot" should be used to select and present information to the driver relevant mainly to safety and/or the driving task.

One example in this area can be to present local weather information and information about road conditions in winter time. Also real-time road friction could be measured and then presented to the driver. The selection of information and the way the information is presented must be optimally related to the driver's needs, the driving environment and the vehicle status.

The development of new sensing systems is essential. New physical principles, advanced signal and data processing, and the use of AI-techniques must be introduced and be better understood. These ideas are presented in figure 6.

The next step can be the introduction of "communicative competences" where the copilot system can communicate with other road users and the infrastructure in a standardized way (preferably world wide standard). The system should also have the competence to perform a dialogue with the driver according to the driver's needs and actual workload.

Introduction of assisting systems or "cooperative

- New sensors needed
- 4 main groups of sensors:
  - Environment
  - Road Surface
  - Vehicle Status
  - Driver Status

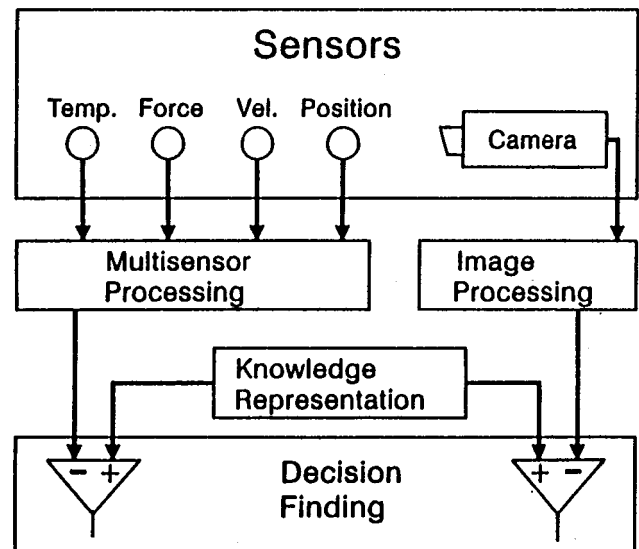


Figure 6. Research on new sensing systems (Prometheus-WG1).

competences" could be the next step. Such systems have already been introduced partly as autonomous subsystems like ABS and Traction Control. But in our context the "cooperative copilot" should be able to interact with the driver, other road users, and the infrastructure systems in a cooperative and adaptive way. Examples in this area are emergency warnings after an accident and adaptive speed keeping according to actual traffic flow and/or speed limits.

A long term goal would be the introduction of "predictive competences" in vehicles and the road traffic systems. Significant for a good and experienced driver is the ability to make correct predictions and judgements regarding what will happen on the road traffic scene. A "predictive copilot" as a support system may help the driver to expand the prediction capabilities in critical situations. One example could be driving in bad weather conditions and in darkness where "artificial enhanced vision" may improve prediction and reduce the reaction time for the driver.

The vehicle competences or copilot functions described can be realized as an *information and assistance system* (figure 7). Such a system will act as a linkage between all subsystems and elements in the total road traffic system. In all cases the responsibility will remain with the driver and the system will make use of the capabilities of the human

being in an adaptive way. At the same time the system will support the driver in situations where the human senses and the human motor system have limitations.

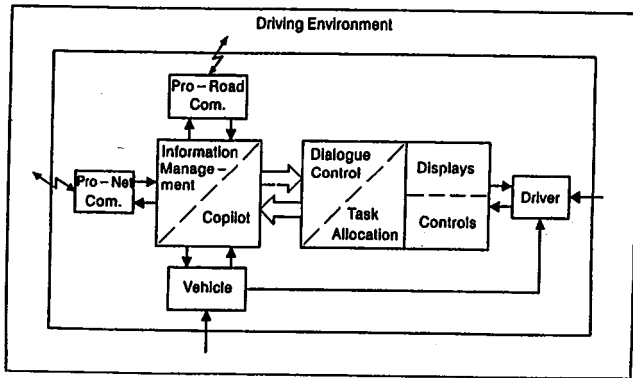


Figure 7. The principle structure of an information and assistance system (Prometheus-WG4).

### Some Research Examples

The SAAB-SCANIA Group of today consists of the Car, Truck, and Aircraft Divisions as well as the Combitech Group with small high-tech companies for the design of space, advanced military, and automotive electronics subsystems and equipment. Historically the Saab Car Division emanated from the Saab Aircraft Division. The first Saab car therefore includes many for the automotive industry at that time unconventional and high technology solutions (figure 8).

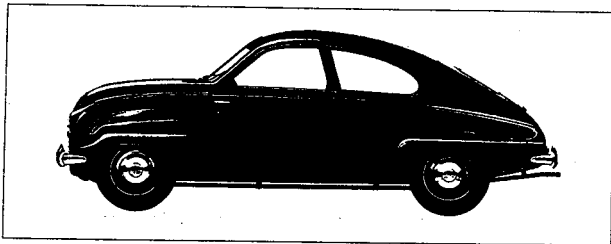


Figure 8. The first Saab car, Saab 92, introduced 1949.

The dashboard and the instrumentation of the Saab car have from the very beginning been designed with the driver's needs in mind. By tradition the pilot of a military aircraft has been supported by a well designed instrumentation. The ultimate goal has been to make the combination of pilot and aircraft as effective as possible in fulfilling the military mission set out. The instrumentation of the new Saab jet fighter JAS 39 Gripen is a good example of such work (figure 9).

The aerospace industry has been leading in the introduction and application of information technology. As the SAAB-SCANIA Group includes both aircraft and space industries the Saab Car Division has been able to profit from their activities in this area.

We have tried to accomplish synergy effects, more or less successful over time. Some examples are mentioned in the following sections. Two on-going research projects in the

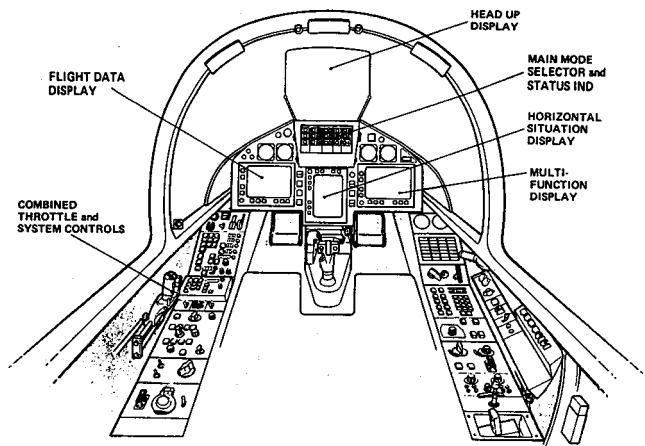


Figure 9. Instrumentation of Saab JAS 39 Gripen.

area of active safety which now show intermediate results are also presented.

### Synergy from aerospace activities

The core of the first engineering team of the Saab Car Division in the late 40s was coming from the Saab Aircraft Division. Unconventional and for that time highly sophisticated technical solutions were applied from the start. That tradition is still alive. Some examples of activities close to the technology front in the active safety area can be mentioned.

The Saab Space Company and the Saab Car Division developed our own ABS system already in the beginning of the 70s, and the Saab Car Division did in that time also research on a "Speedometer for peripheral vision", invented by Mr. L Nordstöm, Saab Aircraft Division. In both cases the ideas were perhaps developed too early to be implemented in serial production at an acceptable cost level in the 70s.

Another example is our "Friction Tester Car" developed together with the Saab Aircraft Division about 15 years ago. This equipment is mainly used at airfields worldwide, but some "cars" have been sold to road administrations in Europe and USA (figure 10).

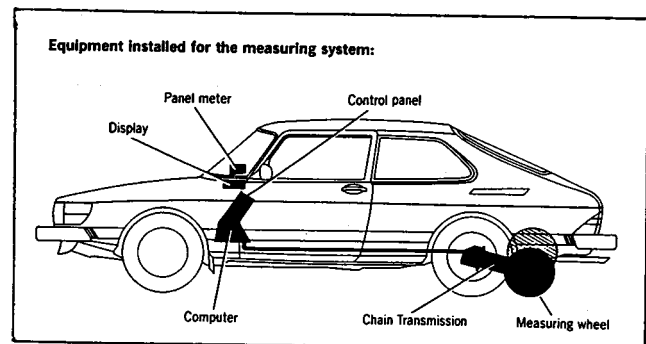


Figure 10. Saab friction tester car.

A new generation of the "Friction Tester Car" with mobile telecommunication systems has a potential to be used as a tool for improving road safety. The equipment can

provide real-time road friction information to other road users through traffic information centres and local radio transmissions.

### Saab EV-1

The EV-1 was presented in 1985. It was a "test bed for new technology" within an experimental Saab sports coupé car. Improvements of the passive safety were made by introducing energy-absorbing front and rear sections and collision protection in the doors based on the experience of new materials that had been gained in the Aircraft Division. A solar cell roof supported an advanced climate control system of the car.

With the assistance of VDO, the principle of "black panel" instrumentation was further developed for the EV-1. The speedometer, which no longer included a trip meter and odometer, was fitted right in front of the driver. So the driver's attention should not be distracted from the readings he wants—the speed of the car. Due to a segmented light conductor illumination, only the speed range at which the car was travelling was visible on the instrument.

### Saab traction control system, TCS

The goals with the project TCS have been and is to improve driving performance and vehicle stability on split friction and low friction road surfaces in low and medium speeds. These goals are achieved by combining the ABS braking system with a smart throttle and wheel slip control system.

The system has been developed together with Alfred Teves ATE (brakes) and Hella (electronic throttle control). There are a number of unique features which also are relevant for the improvement of road safety (figure 11).

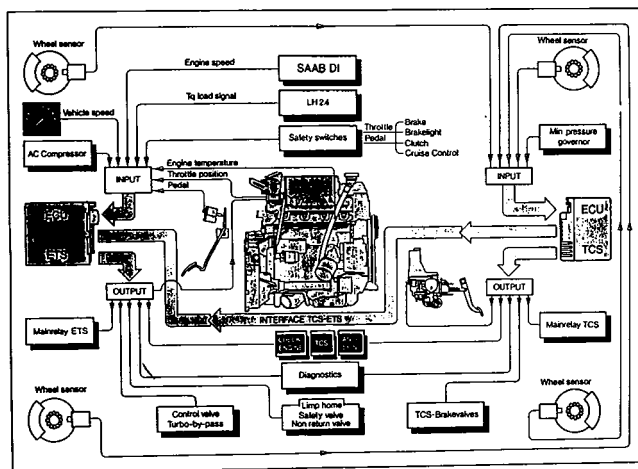


Figure 11. Saab traction control system, TCS.

It will be possible to pass a crossing or intersection more quickly or to make a fast and safe merging manoeuvre into high density road traffic from a side road also on snow and ice with split friction conditions.

The system will also give more stable and safe manoeuvres while overtaking or when passing through curves on snow, ice and split friction road surfaces. Finally, there will be

integrated speed control with adjustments of the speed to the actual traffic flow or speed limit.

### Ultraviolet headlamps

Traffic accident rates on roads are much higher during nights compared to daytime. It is also a fact that road traffic during dark hours is rather large in Scandinavia.

The Saab Car Division started a study on UV-headlamps in 1984 based on a proposed idea from Mr. L. Bergqvist, Labino Patent AB. The first results were not so promising due to the lack of light sources with the UV-content needed. There were also problems with matching UV-filters and with the high voltage supply.

Later on Philips (NL) presented a new small discharge lamp with part of the light in an interesting UV-region. After some tests we found that the UV-content did not have the right power and the spectral distribution. However, last year Philips presented a number of new prototype lamps with higher near-UV content. In combination with optimized filters they show considerable improvements in visibility range and optical guidance.

A lot of research is still needed and an expanded research group has now been formed. VTI, TFB (Swedish Transport Research Board), Swedish National Road Administration, and VOLVO among others are now joining the original Labino and SAAB-SCANIA team. The Swedish UV-light project is a part of the Swedish research programme in the framework of Prometheus/DRIVE. One of the present test vehicles is a bus in the Malmö City urban traffic system.

Further UV-light research is now performed to optimize the characteristics of bulbs, filters, headlamps, and electronic drive units in the vehicles. Also research on fluorescent pigments on clothes, road signs, markings and other items in the road traffic environment is carried out. In parallel the degree of visibility improvement by UV-light will be investigated under various conditions (figure 12).

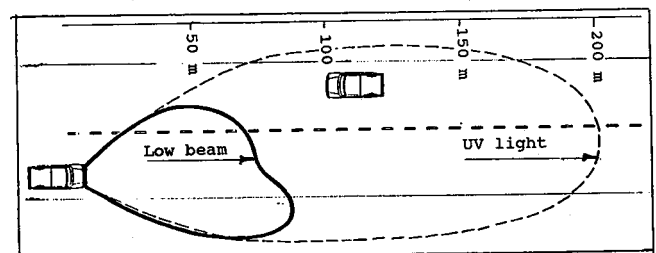


Figure 12. Improvements of visibility range by the introduction of UV-lights.

### Future Outlook

The development of intelligent driver and traffic support systems is now starting all over the world. For example, the actual status in Europe, USA and Japan was indicated recently both in Europe and in the USA at three conferences. Ideas about active safety systems based on future information technology elements and subsystems were presented. The conferences were "Elektronik im Kraftfahrzeug", Baden-Baden, FRG, September 1988,

"Convergence 88", Dearborn, Mi., USA, October 1988, and the Human Factors Society 32nd Annual Meeting, Anaheim, Ca., USA, October 1988.

The automotive industries have joined forces with electronic industries, universities, research institutes, and governmental authorities to develop the information technology in traffic systems applications. In parallel to the long-term research work (Prometheus, DRIVE, etc.) many engineers all over the world are now engaged in the development of new active safety systems for medium-term serial production.

## References

Bulliger, H.-J., Schackel, B. (Eds.) (1987) Proceedings of the 2nd IFIP Conference on Human-Computer Interaction, Stuttgart, FRG, 1-4 September, 1987.

Human Factors Society (1988). Proceedings of the Human Factors Society 32nd Annual Meeting, Anaheim, Ca., USA, October 24-28, 1988.

IEEE, SAE (1988). Proceedings of the International Congress on Transportation Electronics "Convergence 88," Dearborn, Mi., USA, October 17-18, 1988.

Rasmussen, J. (1983). Skills, Rules, and Knowledge; Signals, Signs, and Symbols, and Other Distinctions in Human Performance Models, IEEE Transactions on Systems, Man, and Cybernetics, Vol. SMC-13, No. 3, May/June 1983.

VDI-Gesellschaft Fahrzeugtechnik (1988). VDI Berichte 687, Elektronik im Kraftfahrzeug, Baden-Baden, FRG, 8-9 September, 1988.

Wickens, C.D. (1984). Engineering psychology and human performance, Charles Merrill, Columbus, Oh., USA.

## Driver Vigilance State Control: A Key Aspect of the Driver-Vehicle-Environment Interface

---

**C. Tarrière, D. Chaput, C. Poilvert,  
D. Tamalet,**  
Renault, France

### Abstract

At a time when interest in extending the use of computer technology and "smart" electronics in road transport systems is growing, it should not be forgotten that, on the road, man still remains at the wheel.

Even the most sophisticated and efficient systems still require input from the driver and the driver's efficiency obviously depends upon the state of alertness of the central nervous system. The driver's ability to use information will be the key point of all future safety systems.

How will drinking and dozing off, which are two very worrying facts, and which have a tremendous effect on road safety, be integrated into the workings of the system as a whole? Such a question explains why, at the same time as proposing a system such as CARMINAT to generate information useful to the driver. Renault is also endeavouring to develop a system which will monitor the driver's level of alertness, and allow continuous measurement of the constant fluctuations of vigilance which occur during the time spent at the wheel.

The Driver Vigilance State Control System is described in its latest form, incorporating the most recent improvements. All the available results obtained for validation of the system are given and discussed in terms of the likelihood of meeting the safety requirements for such a system.

### Introduction

Statistical analysis of accidents shows the frequency and the

special severity of accidents affecting automotive vehicles, utilities and lorries, for which "fatigue" or loss of alertness can be assumed. This is the main cause of 18% of accidents on motorways and 26% of fatalities. For example, the significant frequency of accidents involving a single vehicle is observed (65% of fatalities) due to leaving the road (35% of fatalities) and impacting against side barriers. These accidents are twice as frequent at night, especially in the second part of the night, often after a long trip and long hours at the wheel, in relatively monotonous driving conditions. "Fatigue" is a factor in 21% of severe or fatal accidents studied in the REAGIR surveys, and it is a factor in 40% of weekend and holiday accidents, and in 66% of night accidents!

### Brief Background to Research

Fluctuations in vigilance levels in real or simulated vehicle driving conditions have been the subject of almost constant research in France since the end of the 1950s.

At Régie Renault, F. Picard, then R&D Manager, initiated experimental work to try and understand the nature of nervous fatigue of the driver, and if possible to develop means of limiting its adverse effects. This was the subject of our initial automotive work in 1957, with the principle aim of showing the drop in alertness during driving in monotonous conditions, and studying the influential factors involved.

Moreover, as early as 1960, when the ONSER was founded, with G. Michaut, we endeavoured to verify in real driving conditions the observations made in laboratory-simulated conditions.

Laboratory work (1 to 25)\* and field work (26 to 36) provide very useful contributions to our understanding of lapses of attention in car and lorry drivers.

In particular, such studies have pinpointed the effects of driving time, halts (31), the nycterohemeral cycle and habituation (3), headlight dazzle in night driving conditions (33), radio noise (music and speech) (3), (4), (8), (9), (23 to 25), and tobacco (11 to 17). Studies being carried out jointly by Renault and the INRETS under EEC contracts aim at analyzing the effect of cumulative nuisances, where the effects of noise, vibration and heat are combined (figure 1).

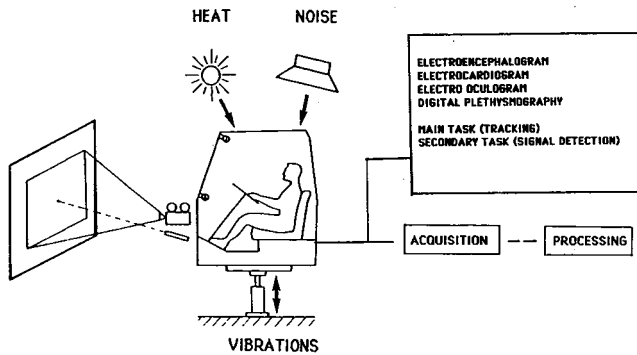


Figure 1. Synergic effect of noise, vibration and heat on the driver's vigilance.

An essential characteristic of this work by Renault (14 to 17) and ONSER (26 to 36) (known as INRETS since 1985) is the association of behavioural indicators (analysis of driver performance) and physiological indicators describing the driver's condition (analysis of the electroencephalogram, the heart rate, the electromyogram and eye movements) (figures 2 to 5). This dual approach provided at least a partial explanation of the phenomenon observed, and supplied the data which justify the present research paper. This accumulated knowledge gave rise to the Prevent Driver Dozing Project, through the selection of one or more functions in normal driving practice which may vary depending on the driver's level of alertness. The present paper describes the implementation of that project.

## The Renault System for Detection of Hypoalertness and Prevention of Dozing

### Objective of the study

The objective of the study is to develop a Driving Aid system to detect lapses in driver vigilance and to prevent him from dozing.

Driving a vehicle involves complex activities of detection of any change in the environment to allow constant anticipation relative to the instantaneous situation perceived by the driver. Now the quality of this brain activity which involves continuously integrating all available data and using them to predict possible changes in

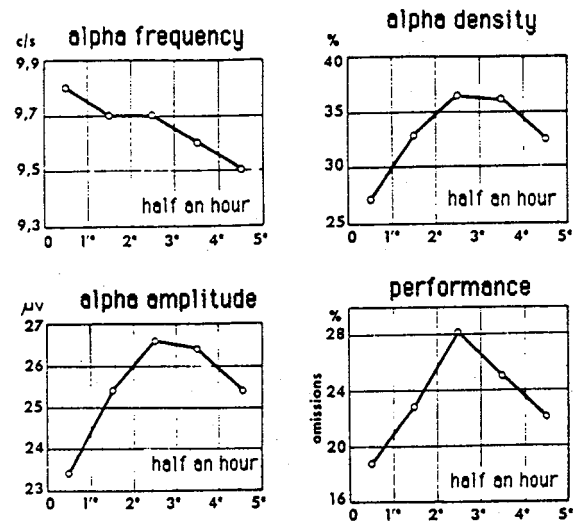


Figure 2. Compared evolutions of the performance and the alpha waves evolution during a monitoring task (12 subjects) (reference 15).

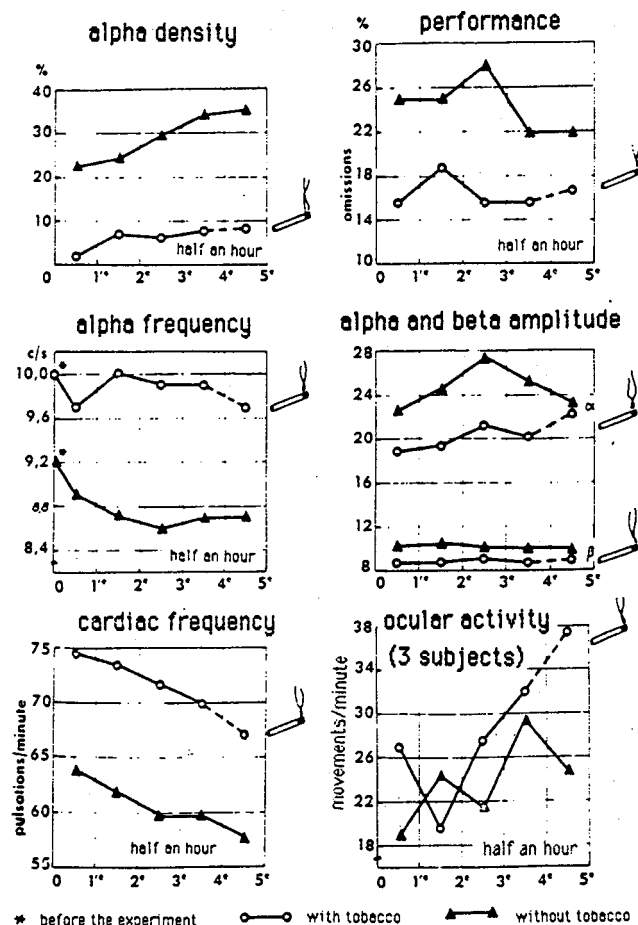


Figure 3. Attendant variations of the performance and of several physiological criteria during a monitoring task (reference 15).

situation depends very much on the driver's level of physiological alertness. Any deterioration in alertness detracts from driving safety. In an extreme case, for driving in monotonous conditions and/or when fatigued, during certain periods of the nycthemeron, dozing occurs.

\*Figures in parentheses designate references at the end of paper.

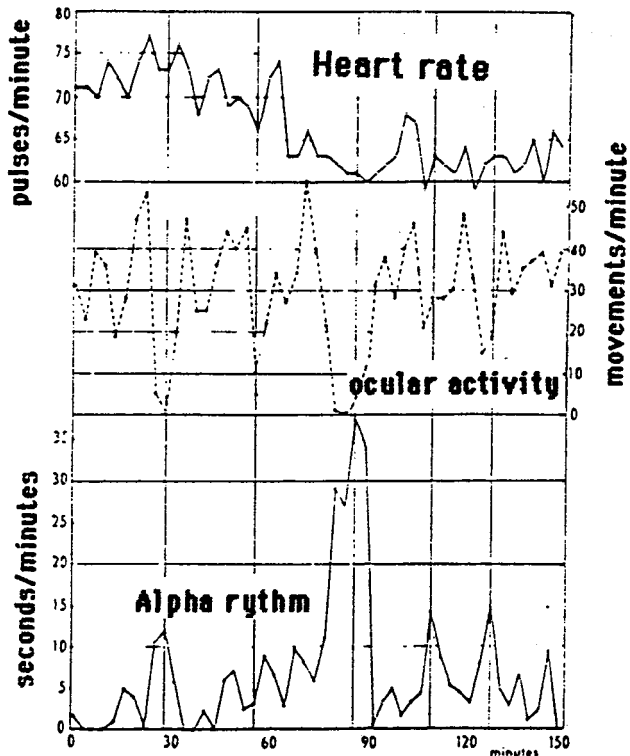


Figure 4. Example of concomitant fluctuations in cortical, cardiac and ocular activities manifested by a subject during a supervisory task (reference 15).

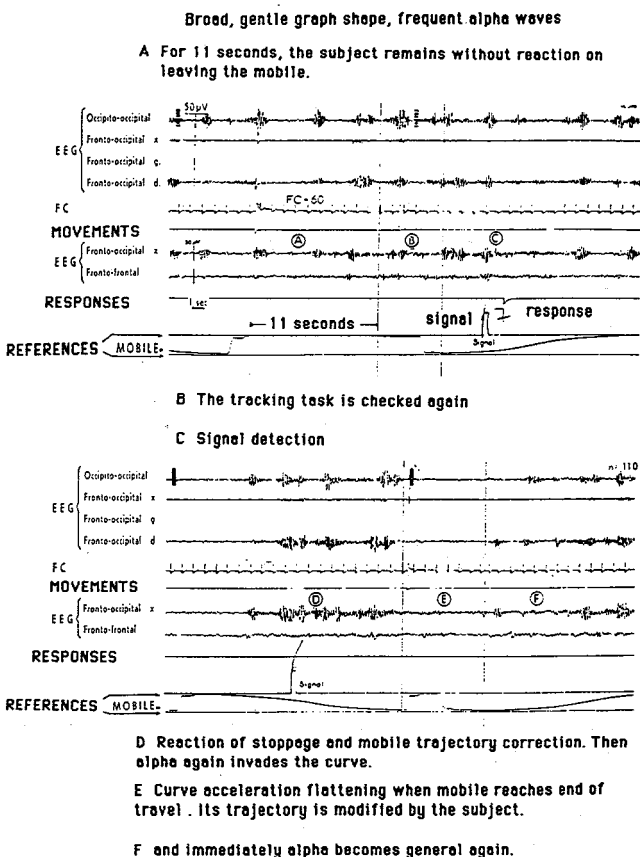


Figure 5. Examples of fluctuations of attention during a supervisory and tracking task (reference 15).

## Principle of the study system

The driving aid system Renault would like to propose on its vehicles is based on the observation of a correlation between the way in which the driver performs minor corrections of direction (made necessary, even on a straight road, by irregular road surfacing and the effect of wind) and his state of alertness.

It is as though steering wheel micro-movements of small amplitude, only a few degrees, but very frequent under "high alertness" conditions, became fewer in "low alertness" conditions and were compensated for by corrections of large amplitude. This is what we can all sometimes see on the road. A car ahead drifts slowly and even dangerously towards a side railing or another vehicle and then suddenly and brusquely swerves back into its lane.

The following system is therefore proposed. An on-board microprocessor prepares for each driver and, if necessary, for each trip, a so-called "high alertness" reference for the function of steering wheel movement analysis during the first 20 or 30 minutes of travel on the highway or motorway.

The system then indicates any change in driving patterns in the following hours, relative to the reference.

The system, which consists of a steering wheel angle transducer, a speed transducer and a microprocessor calculating the steering wheel function best adapted to the psycho-physiological indices describing the state of alertness, continuously compares the instantaneous "steering wheel" values and the "high alertness" reference.

Any change in driving pattern triggers alarms for present thresholds of the "steering wheel" function.

## Justification for study orientations

*Desired properties.*—The aim is to obtain a system having the following properties:

- The index detected must be inherent to the driving task.—The indicator must not influence the driving task.
- Relevance of the detected index.—The indicator must be significant of the driving task and the driver's psycho-physiological condition.
- Preventive.—The system must be able to detect any deterioration in driver alertness sufficiently early.
- Personalizable.—A reliable system must be able to allow for driving differences from one individual to another.
- Informative.—The system must be able to inform the driver (visual indicator, audible alarm, etc.) of any deterioration in his driving ability.

Note: This type of system is also designed for intervention. One could, for example, envisage automatic speed limiting if a series of alarms were to occur without the driver stopping (such interventions should of course be tested with respect to their utility and possible detrimental side-effects).

*Constraints accepted by the driver for system selection.—*

- Convenience: The system must be easy to use, and usable only at the driver's request.
- Constraint: The system must not cause a nuisance and especially no extra fatigue.

Hence the choice of a system based on an index inherent in the driving task (steering wheel movement and speed), not requiring the installation of any electrode or any other constraint such as holding the hand on the steering wheel, or, again, any mental or percepto-cognitive overload which could be represented, for example, by a task added on to evaluate availability for driving.

*Credibility of the basic systems.—*The suitability of steering wheel movement analysis to account for variations in alertness levels is based on numerous experimental observations described in the scientific literature (21), (22), (26), (35) and (37).

However, there remained the task of defining and selecting functions deduced from analysis of the steering wheel movements most suitable for predicting dozing and therefore, in practice, suitable for triggering an alarm before it could be too late.

This was the subject of an initial stage of study entrusted by Renault to the ONSER, which was performed in real driving conditions on the motorway, here called "Experimental phase 1."

## Description of the Study

### Experimental phase 1 in real driving conditions

This experimental phase involved motorway travel by night for long periods (5 to 6 hours) performed on a Renault 18 station wagon equipped with a steering wheel angle transducer, a speed transducer and physiological recording equipment allowing simultaneous recording on magnetic media of not only the two parameters mentioned above but also the EEG, heart rate, nape electromyogram and eye movements (figure 6).

An experimental researcher sitting in the rear could also collect observations concerning driving quality or the apparent condition of the driver, and even intervene in the event of dangerous behaviour.

We may note, for example, that for 5 subjects in a preliminary study by the ONSER in 1978, and for 12 subjects in this preliminary phase, 3 out of 17 underwent states of drowsiness close to complete inattention leading to loss of control of the vehicle:

- One subject had to be replaced by the experimental researcher.
- Another subject went into the ditch.
- A third subject had to be wakened (comment of the experimental researcher: "I was very afraid at

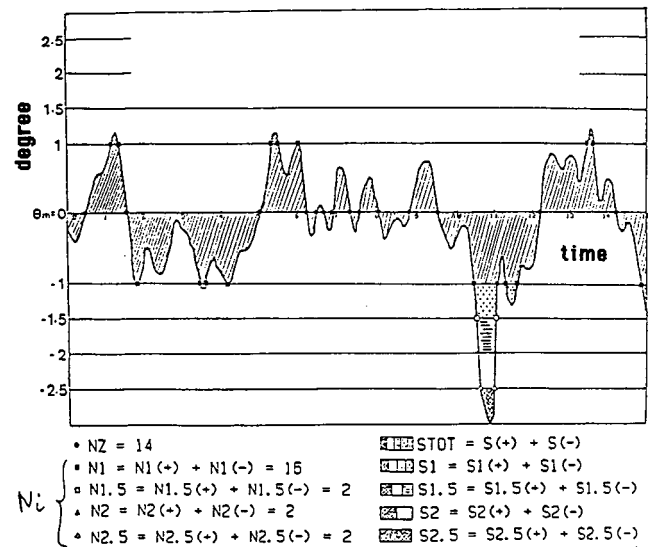


Figure 6. Definition of "steering wheel" parameters for axes offset by 1, 1.5, 2 and 2.5 degrees relative to  $O_m$ .

No. 64—the straight line number—I had to tap the subject on the shoulder; it was frightening").

At certain times, most of the subjects also took risks or had sluggish reflexes associated with fatigue, resulting in "oscillations" or "sudden swerves" sometimes causing "close shaves."

It is important to emphasize the nature of the concomitant neurophysiological data for these driver "failings." The EEG showed peaks of greater density at alpha or theta rhythms known as hypoalertness indicators.

### Definition of functions describing steering wheel movements in relation to speed

On the basis of ONSER experimental study 1, functions were created which combine the frequencies and amplitudes of steering wheel movements and the speed of the vehicle (figure 6).

Statistical studies have shown significant correlations between the most pertinent steering wheel functions and psycho-physiological variables. Hence, for all subjects, provided only the cumulative High and Low Alertness areas are adopted, a population of 228 "steering wheel function/EEG variable" pairs was tested. For the best three functions, the correlation factors vary between .64 and .68 significant at a threshold of  $P = .01$ . These are the factors which were adopted for the validation tests of Experimental Phase 1.

Finally, alarm thresholds were set relative to the high alertness reference period for each of the steering wheel functions.

## Experimental Validation of Research Products

The new phase at present being carried out involves validating, in real driving conditions, the steering wheel

functions shown to be the best by statistical correlation tests.

This research phase is performed under contract between Renault and SERT, on behalf of the Ministries responsible for Transportation and Research.

### Validation tools

*Objective* validation with direct reference to the neuro-physiological condition of the driver analyzed simultaneously.

The objective, indisputable way of proving the quality of the Doze Prevention System might well be to show that the alarm generated by it occurs at the same time as signs of brain hypoalertness.

This is precisely what we do, in various ways.

By having the system perform post-reading in laboratory of magnetic tapes containing records, during night driving hours on the motorway, of:

- micro-movements of the steering wheel for analysis;
- vehicle speed;
- electroencephalogram changes with high and low alertness phases. It should be mentioned that experimental researcher observations are also available, marked on the same time base (data collected prior to 1983 under the initial contract between Renault and ONSER).
- Direct implementation of this comparison in real time during driving (simultaneous recording of steering wheel functions and EEG).

An example of the results obtained will be described in the following section.

*Subjective* validation in real driving conditions by asking the driver to permanently define the relevance of alarms relating to his own evaluation of his alertness level.

An example will also be described in the next section. However, the procedure should first be explained.

For this subjective validation test, a car was specially instrumented and equipped with a data acquisition and processing computer. This system was called "VIVRE" (Vigilance-Véhicule Renault Expérimental). The functional description of the "VIVRE" system is given in figure 7.

The main component is an on-board computer which is sufficiently plastic to present several steering wheel functions and allow them to be modified if any optimization is required. In this way, 9 different alarm tripping thresholds can be tested.

During the trip which must last several hours, the driver must select and retain one of the 3 "steering wheel" functions which can be selected,  $Y_1$ ,  $Y_3$  or  $Y_{3M}$ . The experiment instructions require that he test the alarm thresholds from 0 to 9, knowing that it is possible to move on to the higher threshold only after 5 alarms have occurred for any given threshold.

Each alarm is validated by the driver, who must actuate one of the 3 pushbuttons available to him:

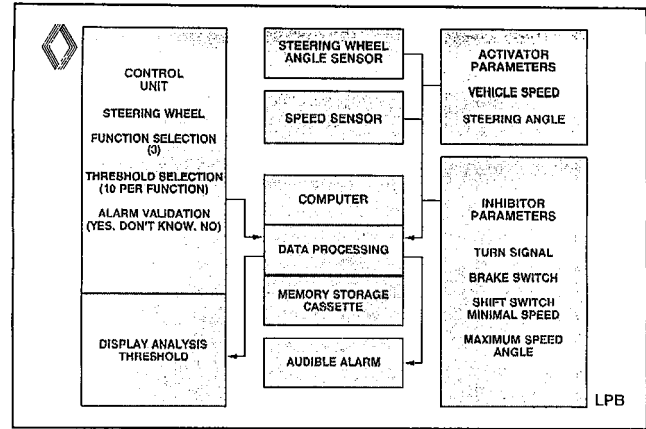


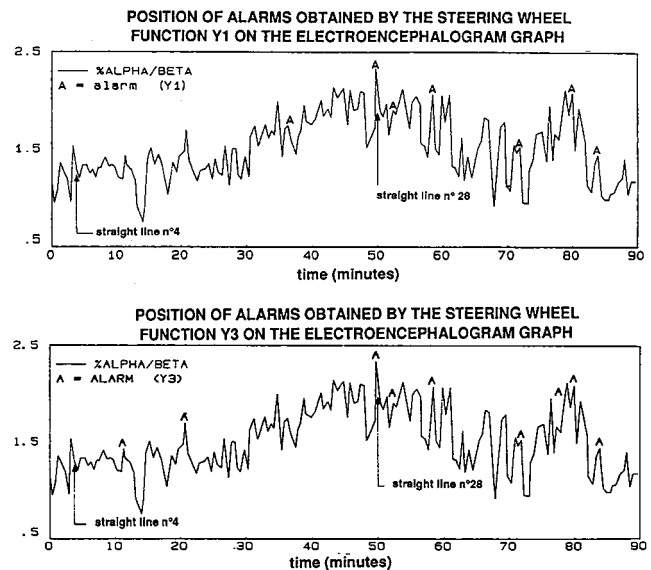
Figure 7. Experimental flowchart of driving aid system.

- "Yes" button, meaning "I am tired," which is a relevant alarm;
- "No" button which is not a relevant alarm;
- "Don't know" button, when the answer is not obvious.

By means of this procedure, the frequency of false alarms can be analyzed as a function of the alarm threshold "height" and the necessary data can be acquired to select the most suitable threshold for the end system to be defined.

### Initial results of objective validation

The example described shows the relevance of alarms with respect to the concomitant state of the driver's electroencephalogram (graph A).



Graph A

The EEG is an excellent indicator of the driver's state of alertness. A high density of alpha waves (1) in the electroencephalogram is characteristic of hypoalertness, while beta waves predominate during a period of good alertness (2).

*A good correlation therefore exists between the physiological condition of the driver and the occurrence of the alarms.*

(1) Alpha waves (frequency in the range between 8 and 12 Hz) appear in gusts of sinewaves of high amplitude.

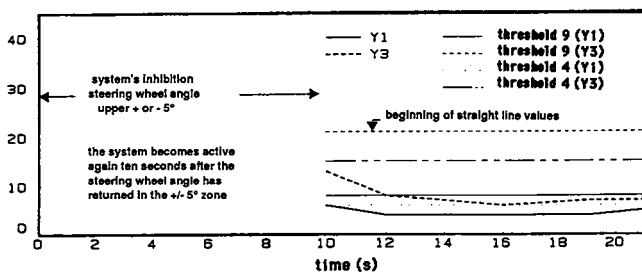
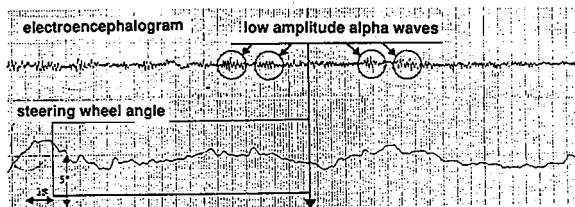
(2) Beta waves are more irregular, of smaller amplitude, and their frequency is in the range between 13 and 25 Hz.

The alpha/beta ratio thus fluctuates in inverse proportion to the driver's alertness; it can be seen here that this ratio increases with driving time.

The alarms, which correspond to what the system perceives as a state of hypoalertness, appear at the same time as the alpha/beta peaks.

*Period of high alertness (graph B).*—The electroencephalogram is characteristic of a normal state of alertness; the gusts of alpha waves are rare and of small amplitude.

ELECTROENCEPHALOGRAPH AND STEERING WHEEL ANGLE'S EVOLUTION ON THE STRAIGHT LINE N°4



EVOLUTION OF THE STEERING WHEEL FUNCTIONS ON THE STRAIGHT LINE N°4

### HIGH VIGILANCE PERIOD

Nowadays, the system is working only in straight lines. It calculates constantly the steering wheel functions during the ten seconds before and inhibits all angle values upper or equal to  $\pm 5$  degrees. The straight lines specific values take place after the arrow indicating "beginning of straight lines values".

### Graph B

Steering wheel movements are not sharp.

The steering wheel functions (1), developed from the steering wheel movements to predict the appearance of a drop in alertness, do not exceed the alarm thresholds.

As a guide, threshold No. 4 is an intermediate threshold and threshold No. 9 is the maximum threshold. The higher the threshold, the more it is typical of hypoalertness.

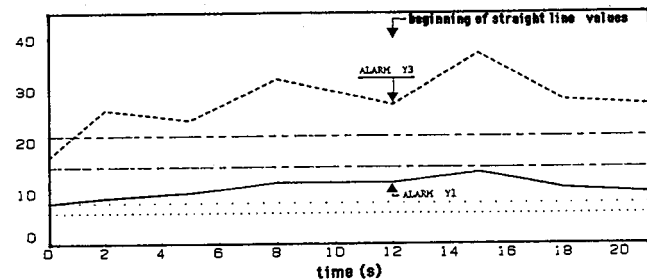
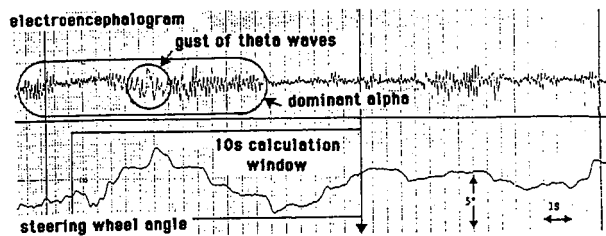
(1) The steering wheel functions were established on the basis of:

- The amplitude of steering wheel movements;
- The frequency of intersection of steering wheel angles from  $0^\circ$  to  $2.5^\circ$ ;
- The vehicle's speed.

*Period of low alertness (graph C).*—The electroencephalogram is rich in alpha waves, which characterize a lowered state of alertness. One also observes the appearance

of a gust of theta waves, which are slower and characterize the first stage of sleep, that is, falling asleep.

ELECTROENCEPHALOGRAPH AND STEERING WHEEL ANGLE'S EVOLUTION ON THE STRAIGHT LINE N°2B



EVOLUTION OF THE STEERING WHEEL FUNCTIONS ON THE STRAIGHT LINE N°2B

### LOW VIGILANCE PERIOD

The window located on the steering wheel angle graph delimites the values used for the steering wheel function calculation when the alarm appears. The steering wheel function crosses the alarm's threshold n°9 a long time before the indication: "alarm Y3", but, at this time, the Y3 values are not specific of straight lines. However, when the indication "beginning of straight line values" appears, steering wheel functions are still above the alarm's threshold n°9. So, they generate a straight line specific alarm.

### Graph C

Steering wheel movements recorded at the same moment are of large amplitude.

The steering wheel functions both exceed the maximum alarm threshold.

*Conclusions concerning objective validation.*—These positive results lead us to believe that validation of the Renault system is well underway.

The alarms occur at the moment at which the high density of alpha waves indicates a state of hypoalertness.

The steering wheel functions, calculated on the basis of steering wheel movements, are clearly closely correlated to the state of alertness.

The alarm threshold values appear to be suitably chosen, since the alarms occur at the expected times.

The basic assumption (correlation between steering wheel movements and alertness levels) appears to be justified. The steering wheel functions and the thresholds of the Renault system are hence at least partially validated.

These initial results require confirmation:

- For other subjects, and
- By extension of the system to bends.

## Initial results of subjective validation

These results, already published (38) will be summarized here. The study concerned a trip between Limoges and Paris, driver D.C., function selected  $Y_3$ .

For the sake of example, we give the "yes," "no" and "don't know" answers.

*Validated alarm: "don't know" at time 7:04.40 p.m.*—The alarm was due to passage over a road surface irregularity. Since the driver has a plausible explanation, he classified it as "don't know" and not as "no."

The plotted graph corresponding to this  $Y_3$  alarm just exceeds the threshold (figures 8a and 8b); 15 seconds earlier, it had already reached the threshold, without, however, exceeding it and without triggering the alarm.

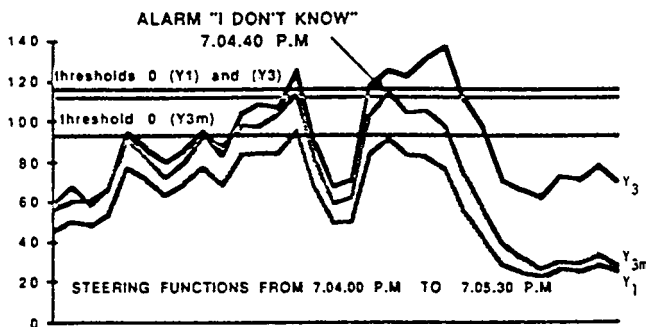


Figure 8a. Steering functions from 7:04.00 p.m. to 7:05.30 p.m.

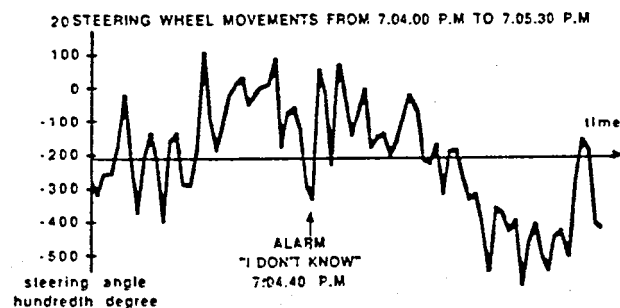


Figure 8b. Steering wheel movements from 7:04.00 p.m. to 7:05.30 p.m.

The other two functions,  $Y_1$  and  $Y_{3M}$ , are also recorded simultaneously, even if these do not produce alarms in this experiment. It is of interest to note that  $Y_1$  would also have produced the alarm and not  $Y_{3M}$ .

Since the threshold then selected by the driver was 0, the lowest, and therefore the least selective, it can be observed that, according to the functions (in this case  $Y_1$  and  $Y_3$ ), some alarms can occur, but only just, and that these would have been avoided by a slightly higher threshold, e.g., 1 for  $Y_3$ , and 2 or 3 for  $Y_1$ .

*"No" validated alarm at time 7:20.11 p.m.*—The driver, who has been driving for approximately 3 hours, did his driving at speeds of between 100 and 140 km/h, depending on traffic conditions.

An alarm sounded, for which there was no apparent justification. The function barely exceeded the alarm threshold which was set to level 2 for this period.

At level 3, this alarm would have been avoided (figure 9a).

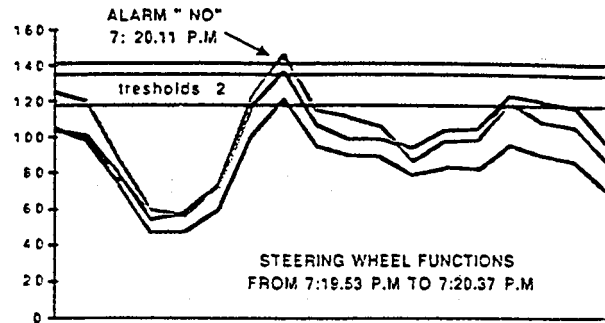


Figure 9a. Steering functions from 7:19.53 p.m. to 7:20.37 p.m.

An analysis of steering wheel movements (figure 9b) revealed a major angular variation preceding the alarm. Just after the alarm, another major angular variation was recorded, but it was insufficient to pass the thresholds (figure 9a).

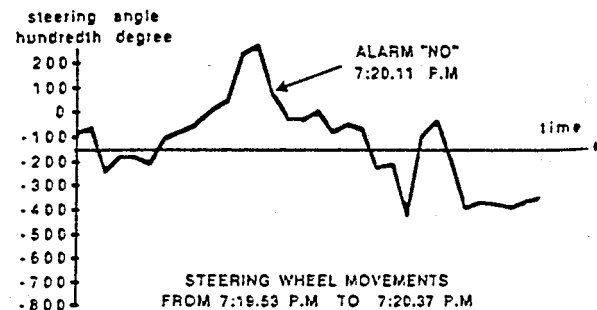


Figure 9b. Steering wheel movements from 7:19.53 p.m. to 7:20.37 p.m.

*"Yes" validated alarm at time 7:47.12 p.m.*—The driver, still on the highway, is driving at a very moderate speed as required by traffic conditions.

An alarm sounded, which he confirmed as "yes" since he was surprised in a state of inattention.

The alarm threshold is then set to 1.

The response on  $Y_3$  is of large amplitude (figure 10a). This also applied to  $Y_{3M}$ , while  $Y_1$  just barely exceeds the threshold. It can be observed, in spite of the increase in the threshold from 0 to 1 with respect to the previous example, how the "yes" alarm corresponds to a very clear and significant response to  $Y_3$ .

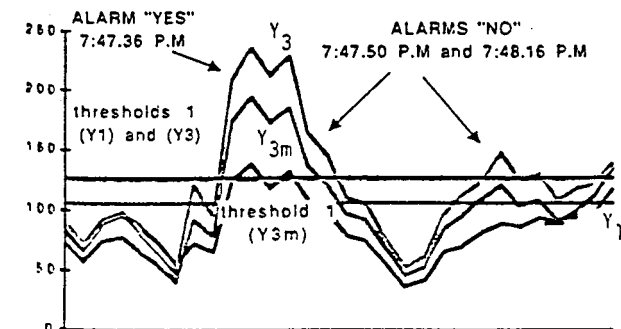


Figure 10a. Steering functions from 7:46.39 p.m. to 7:48.30 p.m.

Two “no” alarms occurred during the same period of time. The first, in fact, corresponds to the same cause as the “yes” alarm, since the function had not returned to zero. The second “no” alarm is of low amplitude; this alarm would be eliminated by a higher threshold.

## Validation on Simulator

The validation experiments in real driving conditions described above represent an essential but difficult method, since they depend on the experimental researcher’s luck (!). For an experiment to be conclusive, a deterioration in vigilance must occur during the programmed trip. This is far from being always the case.

One can therefore understand the advantage of performing the same work of objective and subjective validation on a driving simulator.

In such conditions, it is possible to programme a very monotonous trip, and it will be very hard for the subject to retain a high level of vigilance during 2 or 3 hours of driving.

In any case, it is then possible to speed up the deterioration of vigilance by depriving the subject of sleep or even administering a tranquilizer or a hypnotic drug.

Of course, the simulator must be sufficiently realistic for the driving behaviour to be representative of real road driving conditions.

A trial has been programmed on the Swedish simulator of VTI at Linköping as part of the DRIVE programme.

## Evaluation of the Renault System for Monitoring the Driver’s Internal Condition to Detect Alcohol Intake

An initial test was performed on the Valéo simulator. Simulation is performed by coupling the vehicle directly to the system. The vehicle’s powerplant is used. Two side cylinders monitor transverse movements in relation to the vehicle’s centre of gravity.

The experiment involved two test-bench driving phases, in the morning without alcohol, and after lunch with a monitored alcohol rate of 1 g/litre, slightly above the fixed legal rate in France of 0.8 g/litre.

Figure 11 is very eloquent in this respect.

Function  $Y_1$  obtained during two 10-minute phases representative of behaviour with and without alcohol shows two strongly contrasted driving patterns.

Further experiments are planned on the same simulator to refine this initial result with other test subjects.

## Experimental Development

In addition to experiments planned for the VTI and Valéo simulators, experiments are continuing on the highway and motorway.

Four vehicles are now equipped, allowing:

- Extension of the system’s operation from straight lines to curves;

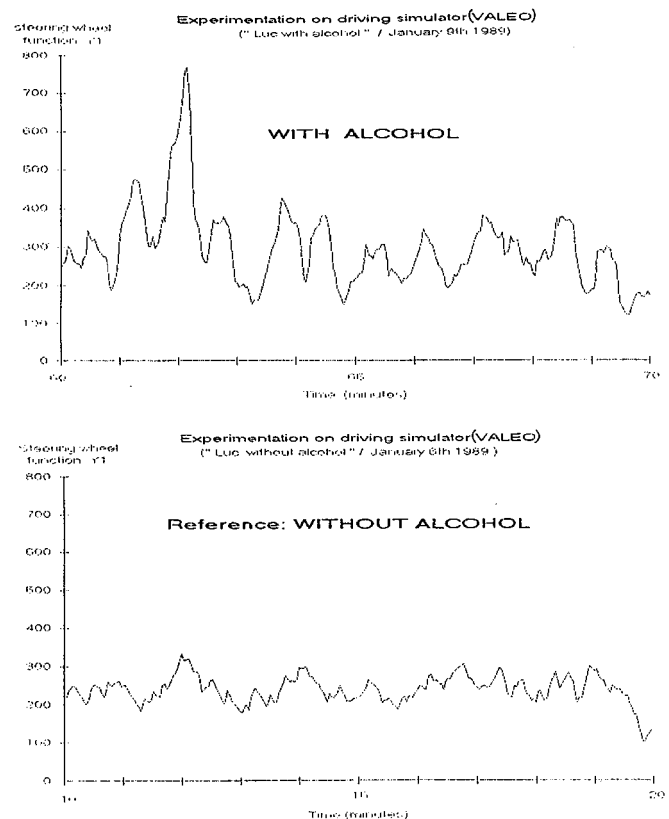


Figure 11.

- Comparison of the results obtained with and without power-assisted steering;
- And, in particular, rapid multiplication of available results for validation either on the road or on simulator.

## Critical Analysis of an Alternative to Ensure Detection of Lowered Alertness

In a previous publication, the authors briefly mentioned some existing experiments. A more exhaustive description is given below.

### Previous attempts based on an analysis of steering wheel movements

“Safety drive adviser”, Nissan (Japan), 1985 (39).— Principle: Diminished vigilance is accompanied by steering wheel movements different from those performed in states of high vigilance. It was demonstrated that, after a period of absence of steering corrections, the shape of the correction and counter-correction movement curves would be different, depending on whether the vigilance level is high or low. These special characteristics, which correspond to steering wheel movement speeds, were entered in the new steering wheel “pattern” built into the “safety drive adviser” available in 1985–1986 on the Bluebird, as sold in Japan. A reference period is determined during which the amplitude and speed of steering wheel movements are recorded. If, during a low vigilance phase, the driver exceeds both a threshold value and a movement amplitude value, an alarm

is triggered. The process operates in the same manner along straight sections and bends, but the threshold crossing value on bends is higher.

Comments: This is the only system already marketed. However, it seems astonishing that, in spite of the sale of several thousand vehicles equipped with the device, no publications have yet appeared to confirm the efficiency of the system.

*"Driver Alertness Aid"*—USA—1974.—An attempt was made to market this device in the U.S.A. in cooperation with Ford.

Principle: the frequency of steering wheel movements is counted from two contactors set at  $+2^\circ$  and  $-2^\circ$  with respect to the steering wheel position at which the front and rear wheels are aligned. A reference frequency is established over the first 3 minutes of use, then:

- If the frequency drops below a certain percentage of the reference, an audible alarm indicates that the driver is tired;
- If the frequency exceeds a certain percentage of the reference, an orange light indicates that the driver is "overexcited."

Comments: Excessive operation of the audible and visual signals during the tests conducted by us would have tended to invalidate the system. This can be explained as follows: the reference frequency corresponds to the sum of the various actions (trajectory control movements, changes of lane, bends, etc.). Now this reference frequency is established over 3 minutes, a period which is not sufficient to take all the different driving situations into account. Therefore, it suffices that during these 3 minutes, the driver perform numerous lane changes, or that the number of bends be high, so that, as soon as conditions change (clear highway, for example), the steering wheel movements decrease and the "fatigue" alert operates. The results of these tests further confirm what Nissan seems to be demonstrated: the frequency of steering wheel movements cannot alone provide an indication of momentary attention level (39).

### Recent proposals based on direct recording of a physiological parameter

*"Dormalert"*—U.K. (1985).—Principle: The basic hypothesis is that cutaneous resistance is clearly correlated to the level of vigilance. The system analyzed changes in skin resistance during driving time. The calibration duration is 10 to 15 minutes, during which a detection threshold is set at a level such as to eliminate false alarms. Any drop in vigilance causes an increase in cutaneous resistance, and therefore triggers an audible alarm.

Apparatus: Two electrodes, fitted to form a ring around one finger (or big toe, in the shoe), are connected by wires to a unit the size of a large matchbox, that might be carried in a pocket of the driver's clothing.

Comments: Tests conducted by our Laboratory were not conclusive, since the alarm did not operate in the drowsiness phase just before sleeping. Moreover, the cutaneous

resistance is directly affected by environmental thermal variations, and the manner in which the spurious factor is taken into account is not clearly explained. Finally, the problem of the hindrance that a system of this type might cause to drivers should be considered.

*"Magneto Encephalo Grammetry"*—Sweden—1987.—Principle: With electrodes worn not on, but simply close to the head, it is possible to record a magneto encephalogram (MED) whose signals, very similar to those obtained in electroencephalograms, are characteristic of the state of vigilance of an individual. This system can be miniaturized and associated with an alarm so as to prevent diminished vigilance while driving.

Comments: The recording of a magnetic field corresponding to the cerebral dipole requires sensitivities of  $10^{-12}$  or  $10^{-13}$  Tesla, which constitutes a laboratory or highly protected site performance. To extrapolate to the electromagnetic environment of our roads seems rather audacious.

Some French specialists in cerebral activity and analysis do not consider that it is possible to master the problem involved in application of MEG to car driving in the near future.

*Other recent proposals.*—More than 200 devices have been patented in the USA, which claim to detect diminished vigilance. A rather amusing version involved the idea of transmitting forward bending of the head to a bell. This would seem to be the same idea used with the "Slarner" in France (1980) attached to the ear, or by the Majima-CO system in Japan (1984): a sensor attached to the head and a buzzer. If the bending movement exceeds a certain angle, the alarm sounds.

*Vigilynx*—France (1987).—Principle: This is an electronic device, the special feature of which is that it actuates a visual and/or audible alarm for any unintentional drift of the vehicle. The use of a flashing light, a sign of an intentional change in trajectory, neutralizes the device.

The system operates by analyzing contrast according to the colour and distance (height) from the ground. It uses electronic filters, so that the system reacts to spurious contrasts such as differences in light and shade, partial reworking of the roadway, puddles of water, etc.

Conversely, the sensors detect change from tarmac to grass on the side of the road, or crossing of a continuous or broken white line.

Comments: The fact that the alarm triggers when the vehicle crosses a white line or the edge of the road gives rise to questions concerning its efficiency. In fact, when driving at 130 km/h, is it not too late to be alerted only when a white line is crossed? In this situation, does one have the time to take corrective action before reaching the shoulder or safety preventive system? Moreover, it is liable to be intrusive, for the slightest omission in using the direction indicator to change lanes (which is a frequent occurrence) causes the alarm to operate.

*Use of "Artificial Skin"*—recent French proposal (1987).—Principle: This would consist of tactile instrumentation on the pedals, driver's seat and steering wheel by

means of a pressure sensor known as an "artificial skin". No experimental results have been published, but the authors claim that a multisensorial approach (pressure on pedals, steering wheel and seat) is more likely to give responses to a change in the state of vigilance, in opposition to the single-sensory approaches proposed previously.

Comments: We can reply that any accumulation of parameters unrelated to the level of cerebral activity is certainly less interesting than the study of a single but pertinent parameter. There is nothing in our experience, and in the literature, to allow us to think that pressure on the steering wheel, pedals or seat can be an indication of diminished vigilance. Moreover, the major drawback is to impose a constraint on the driver, obliging him to exert a minimum constant and permanent pressure to the steering wheel, so as not to trigger the alarm.

Nissan has demonstrated that the pressure applied to the steering wheel is not correlated to changes in vigilance.

## Conclusions

The evaluation tools developed by Renault should now allow acquisition of data required for validation of the research hypotheses and products.

The initial available results are already very encouraging. They must still be verified with a sufficiently high number of subjects.

The initial objective of this research is to detect hypoalertness to prevent dozing at the wheel. The high frequency of accidents linked to fatigue and falling asleep, especially on the motorway and at night, fully justifies this research effort.

It would not be surprising if the same system could also very effectively detect alcohol intake during driving. The first observation performed seems to confirm this.

However, beyond prevention of dozing, it is easy to imagine what could be the usefulness of a system for continuous monitoring of the driver's internal condition, at a time when ambitious projects such as CARMINAT and Prometheus are under development.

In a motor car, the utility of multiple continuously updated information systems will depend directly on the driver's ability to receive and process the data and react appropriately and quickly.

This means that the neurophysiological and psychological characteristics of the drivers must also be taken into account in all their diversity and in the frequently non-optimum conditions in which the effects of nervous fatigue due to prolonged driving appear.

The most sophisticated and most efficient systems still require intervention by the driver, and his effectiveness obviously depends on the alertness of his central nervous system. Hence the interest of continuously recording fluctuations in driver vigilance, to warn him of any negative change, of which he is frequently unaware or which he underestimates (40 to 42), and to prevent dozing, which

represents the extreme but not exceptional condition of deterioration in driver efficiency.

Technological advances will lead to significant traffic safety progress only if one remembers that man is the essential link in the chain, since he is the responsible element in the overall traffic system.

## References

- (1) Tarrière C. and Wisner A., "L'épreuve de vigilance", in *Psychologie Française*, 1959, Vol. 4, 261-283.
- (2) Tarrière C., "Un moyen d'étude des accidents inexplicables: l'épreuve de vigilance", thèse médicale, Paris, 1960, édit. R.N.U.R.
- (3) Tarrière C. and Wisner A., "Effets des bruits significatifs et non significatifs au cours d'une épreuve de vigilance", in *Travail Humain*, 1962, XXV, 1-2, 2-28.
- (4) Tarrière C., "Les effets non auditifs du bruit sur le comportement", in *Bulletin du C.E.R.P.*, 1962, XI, 4, 335-378.
- (5) Tarrière C., "Conditionnement du véhicule et vigilance du conducteur dans la prévention des accidents d'automobile", S.B.I.A., FISITA, Brussels, 1963.
- (6) Tarrière C., "Confrontation de données objectives et subjectives relatives à des épreuves de vigilance", in *Travail Humain*, 1964, XXVII, 1-2, 1-36.
- (7) Tarrière C., "Les recherches effectuées dans le domaine de l'attention et de l'inattention", in "La Santé chez l'Homme," 1964, 134, 21-25.
- (8) Tarrière C. and Moreau E., "Influence d'Ambiances Sonores Variées sur le Système Nerveux Central de Rats en Préparation Chronique" Renault-DRME Contract, 1964, 107 pages.
- (9) Wisner A and Tarrière C., "Les effets des bruits sur la vigilance en fonction de leurs caractéristiques physiques et psycho-physiologiques," *Acustia*, 1964, XIV, 4, 216-226.
- (10) Tarrière C., "La simulation de la conduite automobile. Présentation d'un ensemble expérimental original", *Revue des Corps de Santé*, 1965, 6, 1, 115-127.
- (11) Hartemann F, Niarfeix M. and Tarrière C., "Influence de la fumée de tabac dans une épreuve de vigilance," in *Travail Humain*, 1965, XXVIII, 1-2, 147-148.
- (12) Hartemann F and Tarrière C., "Etude des effets de l'oxyde de carbone et de la nicotine contenus dans la fumée de tabac sur l'exécution d'une tâche simulant la conduite automobile", *Cahiers d'Etudes de l'O.N.S.E.R.*, 1965, 14, 1-27.
- (13) Tarrière C. and Hartemann F, "Investigations into the Effects of Tobacco Smoke on a Visual Vigilance Task", in *Proceedings of the 2nd International Congress on Ergonomics*, Dortmund, 1964, Supplement to "Ergonomics", 1965, 525-530, Ed. Taylor & Francis Ltd., London.
- (14) Tarrière C., Hartemann F and Niarfeix M., "Influence de la fumée de tabac sur l'évolution de la performance au cours d'une tâche de surveillance. Intérêt de la fréquence cardiaque comme élément complémentaire d'interprétation", *Travail Humain*, 1966, XXIX, 1-2, 1-21.

(15) Tarrière C. Hartemann F and Niarfeix M., "Recherche de corrélations entre données de vigilance opérationnelle et physiologique. L'électroencéphalographie comme source d'information sur l'évolution de l'efficacité du conducteur", Cahiers d'Etudes de l'O.N.S.E.R., 1966, 1-38.

(16) Hartemann F and Tarrière C., "Essai de détermination par analyse de l'E.E.G. du degré de liaison entre niveau d'activation et performance à une tâche de vigilance", paper presented at S.E.L.F., Marseilles, Oct. 1966, in Travail Humain, 1967, 1-2, 141-142.

(17) Tarrière C. and Hartemann F. "Importance du niveau de vigilance physiologique dans l'exécution d'une tâche de surveillance" in Le Travail Humain, 1968, XXXI, 1-2, 125-156.

(18) Tarrière C., Manigault B. and Valentin M., "Contribution à l'étude de la fatigue nerveuse par l'enregistrement de l'électroencéphalogramme et de la fréquence cardiaque sur des postes en chaîne", paper presented at S.E.L.F., Paris 1968, in Le Travail Humain, 1968, 31, 3-4.

(19) Hartemann F. Manigault B. and Tarrière C., "An Endeavour to Evaluate the Nervous Load at Work Stations in Line Production", in the International Journal of Production Research, 1969, 8, 1, 3-10.

(20) Hartemann F and Tarrière C., "Presentation d'un modèle expérimental pour l'étude de la prise de décision en conduite automobile", Ergonomics in Machine Design, printed by International Labour Office, Geneva, 1969, 163-169.

(21) Michel B, 1980, "Aides à la conduite—Mouvements du volant indices de vigilance". Unpublished study. Edition RNUR, September 1980.

(22) Sfez E., "Fatigue et Baisse de Vigilance en Conduite Automobile de Longue Durée". Mémoire de DEA en Ergonomie de l'Ingénierie, Université Paris Nord, 196 pages, 1983.

(23) André A., Contet C., Tarrière C., "Effets du Bruit sur le Système Cardio-Vasculaire, les Performances Visuelles et la Vigilance"—Publication Interne RNUR, Renault-Reginov Contract, Ministère de l'Environnement, 1985.

(24) André A., Tamalet D., Tarrière C., "Etude des variations Interindividuelles dans les Effets ExtraAuditifs du Bruit sur les Fonctions Cardio-Vasculaires, Cérébrales, Neuromusculaires, Oculaires et Comportementales dans une Situations de Vigilance Prolongée", EDF-IRBA Contract No. 1C7504, 1986.

(25) Petit C., Tamalet D., Tarrière C., "Intérêt de la Réponse Vasomotrice dans l'Evaluation de la Susceptibilité au Bruit—Mesure des Variations Inter et Intra-Individuelles", EDF-IRBA Contract No. 1C7504, March 1987.

(26) Michaut G. and Pottier M., "Etude du comportement des conducteurs d'automobiles: Conduite en situation monotone", ONSER-Bulletin No. 8, 1964.

(27) Michaut G. and Pottier M., "La notion de fatigue au

cours de la conduite", Annales de Médecine des Accidents et du Trafic, 4ème trimestre, 1966.

(28) Pin M.C., "Application de techniques électro-physiologiques à l'étude de la conduite automobile", Cahiers d'Etudes de l'ONSER, 15, 1966.

(29) Michaut G., "Conduite automobile et charge mentale", Cahier d'Etude de l'ONSER No. 18, 1968.

(30) Lecret F., Pin M.C., Cura J.B., and Pottier M., "Les variations de la vigilance au cours de la conduite sur autoroute". Paper presented at the 6th S.E.L.F. Congress, October 1968.

(31) Lecret F. and Pottier M., "Conduite de longue durée et pauses", Paper presented at the 7th S.E.L.F. Congress, October 1969.

(32) Lecret F. and Pottier M., "La vigilance, facteur de sécurité dans la conduite automobile", le Travail Humain 34, 1, 58-68, 1971.

(33) Lecret F., "La conduite sur autoroute: effet des signaux lumineux sur le niveau de vigilance", 5th Congress of the International Ergonomics Association, Amsterdam, June 1973.

(34) Neboit M., 1973, "Role de l'anticipation perceptive dans la conduite automobile", Etude bibliographique de l'ONSER No. 5.

(35) Lecret F., "La fatigue du conducteur", Cahier d'Etude de l'ONSER No. 38, 1976.

(36) Grillon F., "La Vigilance et ses Variations lors d'une Tâche de Longue Durée : le cas de la Conduite Automobile", Thèse de Doctorat de 3ème Cycle Académie de Paris, Université René Descartes, December 1985, 190 pages.

(37) Wildervanck C., Mulder G. and Michon J.A., 1977, "Une tentative en vue de dresser la" carte de la charge mentale "de la conduite automobile", le Travail Humain, 40, 2, 273-278.

(38) Tarrière C., Hartemann F., Sfez E., Chaput D., Petit-Poilert C., "Some Ergonomic Features of the Driver-Vehicle-Environment Interface", FISITA'88, Paper No. 885051, September 25-30, Dearborn, Michigan.

(39) Yabuta F. and coll., "The Development of Drowsiness Warning Devices", in Proceedings of the International Technical Conference on Experimental Safety Vehicles, July 1-4.

(40) Steiner J., Jarvis M. and Parrish J., 1970, "Risk Taking and Arousal Regulation", British Journal of Medical Psychology, Dec. 1970, 43/4, 333-348.

(41) L'Hoste, Moget, Monsoeur, 1976, "L'alcool et la sécurité routière, préparation d'une campagne d'information", Cahier d'Etude de l'ONSER, Dec. 1976, Bulletin No. 40.

(42) O'Hanlon J.F. and Kelley G.R., 1977, "Comparison of performance and physiological changes between drivers who perform well and poorly during prolonged vehicular operation" in R.R. Mackie, "Vigilance, Theory, Operational performance, and physiological correlates", 87-109.

# Human Factor Capabilities for Avoiding Traffic Accidents

---

**Andrea Costanzo, M.D.,**  
Rome University, Italian Department of  
Transportation

## Abstract

This paper is essentially aimed to analyse the influence of human factor in the contest of preventing the accidents.

In addition to that in this paper has also taken into consideration the possibility to give appropriate instruction in order to improve the road safety.

After a short analysis of the general problem concerning the safety both active and passive ones, we have concentrated our attention on the specific area of the physical capabilities of the driver for the control of the vehicle over all the time.

Therefore the biomechanics of the human body has been discussed and analysed in the most important functions of the body which are particularly involved in the vehicle's management.

The reduced capabilities of the driver is a consequence of the stress which is related not only to the time involved but essentially to the environment including also the interface between the driver and the structure of the vehicle, such as the seat and the angle of visibility.

Incorrect physiological posture of the driver or inadequacy of the structure, will stress or pain during the driving time with a consequence of reducing the capabilities for the vehicle's control. Obviously this situation will increase the probabilities of crashes and accidents.

The areas of the human body particularly involved for stressing the driver, are the two parts of the spine which have more possibilities of movements: these are the cervical and lumbar ones.

In order to give the possibilities of analysing as deeply as possible the problem, an appropriate appendix has been prepared for discussing mathematical and analytical methods for calculating forces, stresses and displacement of the most significant vertebrae.

As a conclusion of this paper the real possibilities of the driver to keep the control of the vehicle at a sufficient level can be envisaged.

## Introduction

Road safety can be discussed and analyzed taking into account two specific aspects that concern the human capacity to manage and control the car as well as the conditions of the vehicle and the structures that are involved in the problem of road traffic.

These aspects specifically concern active safety in the sense that an adequate training of the driver in the best possible conditions contribute positively to the reduction of accidents. In the same terms, even though with different assumptions, reference should be made to the characteristics of vehicle and infrastructure which if correctly studied

and analysed can also contribute to limiting the number of accidents.

The range of factors that we have examined, and that is, those connected to the possibility that man has in the control of the vehicle and technical characteristics of both vehicle and infrastructure, represent the fundamental elements that define active safety, that is to say, safety intrinsically connected to the environment in which the vehicle operates and to the various possibilities of managing the vehicle itself.

This work is essentially dedicated to the analysis of those problems which come within this sphere of influence and therefore, at a later stage, we shall return to this topic to examine it in greater detail. It is worth it however, to complete the picture and present a balanced argument, to mention that another type of safety comes into play in the management of motorway traffic. This type of safety is defined as passive safety. Passive safety concerns the means available to reduce the consequences of an accident once it has taken place. The elements that are taken into account in this type of safety are again the characteristics of the vehicle and of the infrastructure in the sense that suitable structural design of the vehicle can appreciably reduce the consequences of an accident.

Besides these elements, it is necessary to mention the possibilities that exist for an intervention in favour of the accident victim from the medical and traumatological point of view. From the moment in which an accident occurs, it is thought that there should be set into motion a whole organization which is capable of intervening at the site of the accident, wait for first-aid to be given and later, work with available hospital resources depending on the case.

The general problem that we have dealt with has served to give an idea in terms that define the problem of road safety, but to remain within the scope of this work, it is necessary to approach more specifically the aspect of the physical and psychological characteristics of the driver in controlling the vehicle for the whole time that it is being driven. In conceptual terms, this topic falls within the framework of active safety, but it represents an aspect that undoubtedly aims at an analysis of a sector that has not been approached but which, in our opinion, deserves careful analysis. We believe it our duty to point out, before entering into a detailed discussion on the topic, that it is extremely difficult to quantify the level of the entity of responsibility that should be attributed to the human factor in the general context of an accident. Perhaps this is the reason why up to now no mention has been made of this specific aspect, but this does not mean that the matter is of no importance.

## The Physical Stress of the Driver of a Motor Vehicle: Biomechanical Analysis

The term stress is used to define that complex of

pressures, suffering and tiredness derived from the activity of driving a motor vehicle.

Two fundamental aspects exist in the general context of stress, one connected to the period of time for which the automobile is used and the other to the condition in which the driver finds himself when seated in the driver's seat. Naturally it is the second problem that constitutes the heart of the problem in that the possibility of shortening the period of time spent driving is a simple solution to the first aspect of the problem. On the other hand, the second aspect, which concerns the condition in which the driver finds himself in the driver's seat, deserves careful analysis.

Problems arising from the driver's position at the steering wheel are linked both to the geometry of his posture and the mechanical characteristics of the structure that interfaces with him.

The topic should be dealt with in all its details but for reasons of simplicity and for its relative importance in the general context of the argument, we have concentrated on the fundamental element represented by tiredness deriving from an incorrect posture of the vertebral column and in particular of its two mobile sections: cervical and lumbar regions.

With the aim of setting out the problem in the simplest terms we have correlated the two postures to two particular conditions.

With regard to the cervical column, we will examine the position of the optical axis in relation to the level of the road as an element of evaluation of the configuration that the cervical column adopts in order to adjust itself to the existing driving conditions. For the lumbar region of the spinal column, we believe that the configuration assumed (both in relation to the articulation of the hip joint as well as to the point of contact with the seat), is the fundamental cause of disturbance of the natural physiological equilibrium to which the spinal column is accustomed.

Physiologically, the cervical tract of the spinal column is curved in lordosis as regards as the equilibrium of the forces exerted on it and on the stability that it has to maintain, (figure 1). The position therefore, which this tract of the spinal column assumes, is compromising in itself, in the sense that the slight curving that it assumes places extra stress on the seven vertebrae that form the curve and in particular on the central ones. These, therefore, are under additional stress as a result of the offsetting of the pressures exerted on them. Though initially, this situation causes differentiated tiredness in the vertebrae, in the end, the difference is neutralized and there is a condition of equilibrium brought about by the involvement of ligaments and muscles.

Each time that these conditions are modified so that the motorist has to adjust his gaze in such a way as to shift the optic axis from its initial position, there is a negative feedback.

An extreme case of this situation is that of the driver who find himself in a position that is rather elevated from the level of the road (e.g. bus drivers and lorry drivers) and

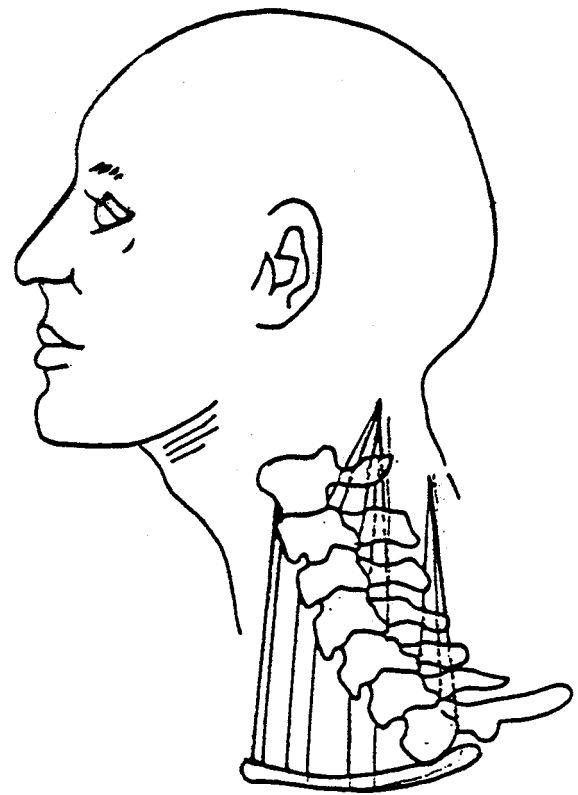


**Figure 1. Outline of the cervical column with its muscular and ligament support system.**

consequently he is forced to fix his gaze at a point that is relatively close to the vehicle. This means a straightening of the spinal column to such an extent the cervical curve disappears or is inverted. In this position, the system of pressure of the vertebrae is completely upset to the point of creating additional stress on top of the basic ones. This is due to the fact that the weight of the head is not in equilibrium with the base of the column and therefore the muscles have to undergo greater tension in order to maintain a balance.

Figure 2 shows the different positions of the cervical column in respect of the angle of focusing and in figure 3 is shown the progression of the gamma's angle on the optical axis with the level of the road with regard to the distance of the object to be observed from the perpendicular of the driver's seat. From an examination of this diagram it can be observed that as the height of the seat is gradually increased, the angle of inclination of the cervical tract of the spinal column also increases.

The lumbar region of the spinal column presents a more complex condition of load-bearing compared to the cervical region for two fundamental reasons. Firstly, because it has to bear a greater weight that is above it and secondly, because the reactions which are passed on to the column must be taken into consideration.

However, conceptually, the problem is the same as that of the cervical column, and that is to say, an artificial configuration of the column as a result of the posture that the driver is forced to maintain in the driver's seat which causes

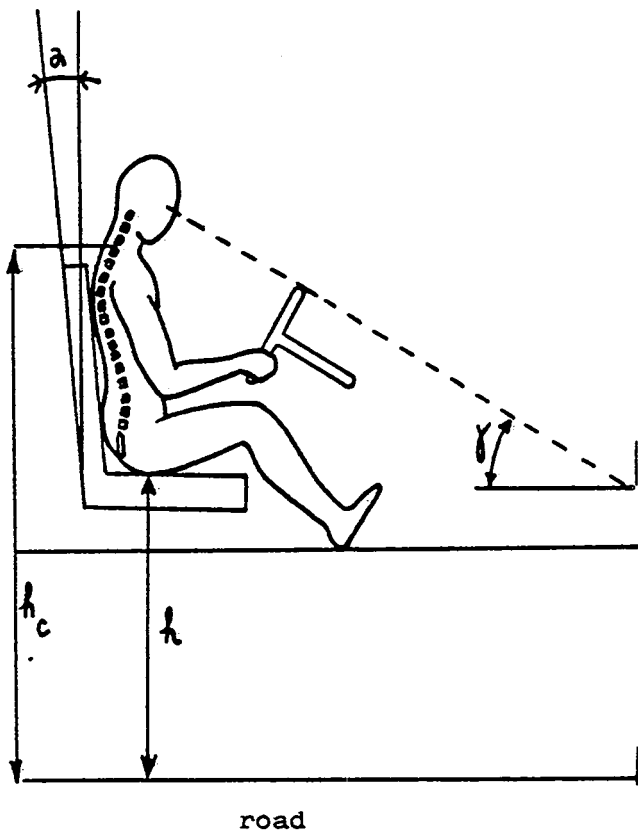


Figure 2. Posture of the driver with the optic axis inclined at an angle  $\theta$  with respect to the level of the road, this posture shows the corresponding complete disappearance of the cervical curve.

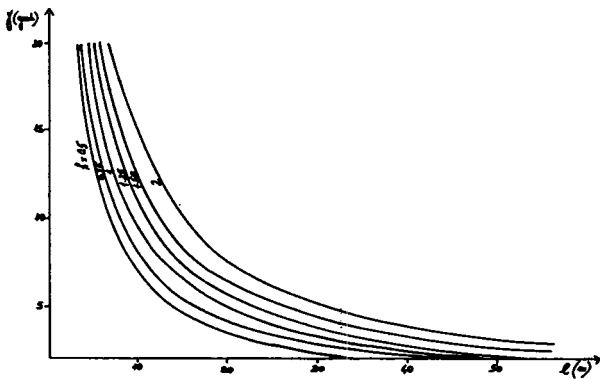


Figure 3. Progression of  $\theta$  as a function of  $\gamma$  for various heights of the cushion within the limits between half a metre and two metres.

disturbance of the normal physiological configuration in the sense that a variation in the angle between the vertebrae creates a condition of tiredness.

A study of the configuration of the column is more complex, because, besides taking into consideration the different orientation of the vertebrae that make up the spinal column, shifts from the support base must also be taken into account. This condition is particularly important in cases where the driver must vary the lumbo-sacral angle in relation to the different positions he must assume when seated in the driver's seat.

To be able to study the biomechanical behaviour of the lumbo-sacral system, it is necessary to refer movements to a fixed point (point H) which for our purposes corresponds to the point of articulation of the hip joint. In this framework, it is possible to define the various angulation that the delimiting points of support of the vertebrae assume and on which the pressures that induce vertebral stress depend.

In figure 4, three extreme configuration are set out, also on an experimental basis, from which the angulation and deformation which the column undergoes can be seen. With regard to the lumbar region, there can be a reduction or inversion of the lordosis also involving notable shifting from point H; this gives rise to bending stress of inflexion the vertebrae and therefore to fatigue.

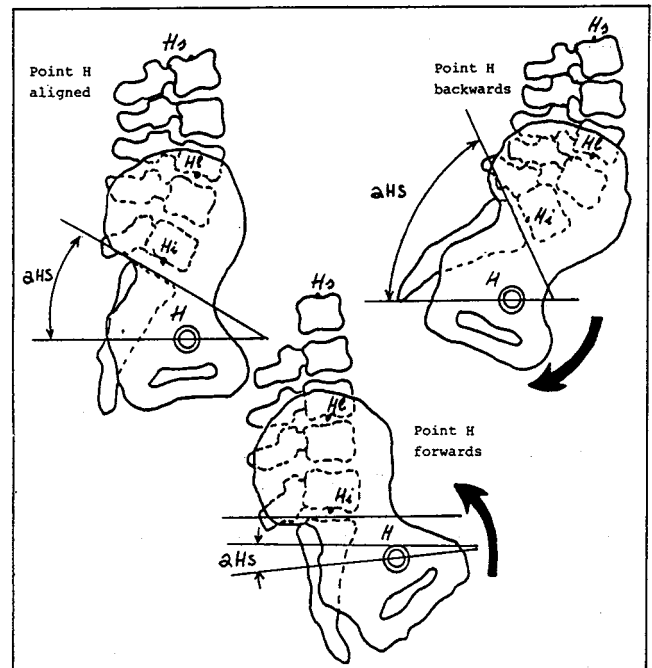


Figure 4. Influence of the position relative to the point H in respect of the extreme upper part of the column in relation to mechanical pressures. HS: angle of reference of the superior arrow of  $S_1$  with the horizontal plane.

## Physiopathological Analysis

No matter how much effort the driver makes to maintain the best driving position, his wrapping line will not always correspond to the structure of the vertebrae, a condition necessary for the physiologically even distribution of load on all the vertebral discs. In order to maintain static equilibrium, an opposite or contrary action is required on the part of the extensor muscles of the column, together with the elastic resistance of the legaments (intertrasversal, interapophyseal and interspinal processes, the yellow legament, the posterior longitudinal legament) and of the posterior articulations.

After a period of driving, during which the driver has maintained the same position, muscular fatigue takes place and therefore further resistance will be entrusted to the legaments only, these, depending on the biological make-up

of each particular subject, will be deformed in a manner that is more or less irreversible.

An abnormal, static position of the driver, therefore, inevitably gives rise to painful suffering. This depends, in fact, on the irritation of one or more of the pain-sensitive tissues of the neighbouring structures. A similar irritation will, to a greater or lesser degree, compromise the function of the spinal column and consequently, the safety of driving. From a general point of view, the origins of the fatigue and the behaviour of the spinal column are essentially similar both for the cervical and lumbar regions of the vertebral column.

This notwithstanding, in the following part of this work, we will refer mainly to the pathology of the lumbar region for the more important cases.

The painful conditions of the lumbar region originating from posture are generally caused by an increase in the lumbo-sacral angle and therefore to an increase in the lordosis of the lumbar region. This increase in the angulation of the sacrum also causes an intensification of sharing stress at the lumbo-sacral level.

The anterior longitudinal ligament limits the extensor mobility of the lumbar region. Its insertions are such that the anterior intervertebral spaces are relatively restricted. It is evident that if the extension is stretched, the anterior opening of the spaces will correspond to their posterior closing. This closure will cause not only the narrowing of the posterior angles but also that of the posterior articular surfaces.

The pain in the vertebral column which accompanies over-lordosis of the lumbar region is the result of posterior mechanical constriction of the functional unit and therefore, at least in part, of the irritation and the distortive use of the posterior articulations.

The narrowing of the intervertebral space and the shortening of the distance between facets can also cause pain because of the irritation provoked in the nerve roots near the intervertebral foramen.

Hyperextension of the lumbar region can also be responsible for irritation and pain in the nerve endings independently of the posterior articulations, and that is through direct compression of the roots or of the meningeal nerve in the passage where they unite. Such a situation may occur in the case of a totally normal disc but it occurs more early where an increase of angulation is associated with a restriction of the intervertebral space.

The foregoing physio-pathological interpretation of the pain provoking posture of the lumbar, may be common to all the alterations, static and dynamic, of the vertebral column in various working activities.

In the case of the driver of a motor vehicle, there also occurs a situation which is the contrary of that described above, as for all other activities, and that is to say, similar unfavourable effects can be provoked by a relaxed stance, a fact commonly observed in habitual drivers of motor vehicles where the trunk is brought forward to the point of causing tension in the forked ligament, with the pelvis

excessively inclined and therefore out of balance in respect of the perpendicular line. In such a situation, the angle of the sacrum is increased and the lumbar region is constricted, in compensation, to force in lordosis. So, almost paradoxically, from a posture of repose is derived an insidious stressful action on the lumbar region of the spine.

It is precisely in this phase that the peripheral section of the spinal body will experience a greater pressure than at the beginning in that the interface between the two adjoining cartilage discs is contracted. In the long run, this brings about atrophy of the cartilage itself and the beginning of phenomena of degeneration which give rise to certain forms of marginal osteofitosis sclerotic, thickening of tissues with deformations of the whole spinal body.

Abnormal postures and movements in persons who are driving are factors that contribute unfavourably on the trophic state and on the structure of the vertebrae. Its degeneration begins with separation of the connection between the concentric fibre of the anulus and dehydration of the nucleus material.

The compression on the posterior surface on the disc and on the posterior ligament causes lumbo-sacral pain. Direct pressure on the nerve roots causes pain in the corresponding cutaneous area.

Apart from the involvement of the intervertebral disc, pain can also originate from suffering in the posterior intervertebral articulation; this in fact will assume the form of lumbago with irradiation of the pain to the thigh and sometimes even to the leg. Suffering in the interspinal ligament causes pain which spreads along the lumbar region and resulting in a form of renal colic and painful contraction of the inferior wall of the abdomen.

## Conclusions

The biomechanical analysis carried out and the physiopathological interpretation given of the phenomena examined, demonstrate a clear situation of intolerance of the driver when he is forced to take up positions that are significantly different from the physiological one.

This state of perturbation creates notable intolerance which is reflected in a lack of concentration on his driving activity and therefore on his capacity of control.

The geometry and the structure of the cabin must therefore be correctly studied to be able to evaluate all the possible consequences that they are likely to produce in the human factor. On the other hand, it is also necessary bear in mind that a position of extreme repose in the driver can reduce certain pressures but it may also provoke a state of lack of concentration.

These considerations supplemented by the technical, biomechanical and physiopathological observations allow for a construction of the complete picture of the situation with possible indicators for a theoretical and experimental study.

It may be recalled that in the introduction to this work we pointed out the lack of quantitative evaluation of road accidents caused by tiredness or stress.

We believe that the statistical analyses obtained up to now to identify the possible causes of an accident should be properly amplified by including this factor.

## References

Bonaccorsi, S., Costanzo A.: La patologia vertebrale nel conducente abituale di autoveicoli (analisi biomeccanica e fisiopatologica) Pag. 379–410. Atti I Congresso Naz. Medicina del Traffico. Fiuggi Terme 6–7–8 Giugno 1974.

Costanzo A.: La colonna cervicale nel conducente di autoveicoli (postura, funzione e sollecitazioni). ATA Ingegneria Automotoristica n.11–12 Vol.36, 1983.

Costanzo A.: Posto di guida (postura e patologia del rachide). Bollettino del Collegio Medici Italiani dei Trasporti, n.4, 1983.

Costanzo A.: La patologia cervicale del conducente di automezzi pesanti (importanza dell'altezza del posto di guida). Bollettino del Collegio Medici Italiani dei Trasporti, n.2, 1984.

Costanzo A.: La colonna lombare: funzioni, carichi, sollecitazioni. Bollettino del Collegio Medici Italiani dei Trasporti, n.3, 1984.

Costanzo A.: La colonna lombare del conducente al posto di guida (criteri di ottimizzazione del sedile). Bollettino del Collegio Medici Italia ni dei Trasporti, n.1, 1985.

Costanzo A.: Analisi diomeccanica della patologia vertebrale per sovraccarichi funzionali derivanti da sollevamento e spostamento pesi. Ed. Roma Medica 1988.

Fielding J.W.: Cinerontgenography of the normal cervical spine. *J.Bone Joint Surg.* 39 A: 1280, 1957.

Johnson, R.M.: Crelin F.S., White A.A. and Paniabi M.M.: Some new observation on the functional anatomy of the lower cervical spine. *Clin. Ortop.* 111:192; 1975

(Review of some important aspects of the surgical and biomechanical anatomy).

Leonardi A.: Le protrusioni posteriori del disco intervertebrale. Atti 51° Congresso S.I.O.T. Catania 22–25 ottobre 1966.

Munro D.: The factors that govern stability of the spine. *Paraplegia* 3:219, 1965.

Paniabi M.M., White A.A. AND Johnson R.M.: Cervical spine mechanics as a function of transection of components. *J. Biomech.* 8: 327, 1975.

Paniabi M.M., White A.A., Keller D., Southwick W.O. and Friedlaender G.: *Clinical Biomechanics of the cervical spine 75–WA BIO–7 Am Soch Mech. Eng.*; New York, 1975 (Experimental basis for presumptions about the usefulness of the strecht test).

Wells E. Luttgens: *Kinesiologia*, Verduci Editore 1978.

White A.A. and Hirsch C.: The significance of the vertebral posterior elements in the mechanics of the thoracic spine. *Clin. Ortop.* 81: 2, 1971.

White A.A., Johnson R.M., Paniabi M.M. and Southwick W.O.: Biomechanical analysis of clinical stability in the cervical spine. *Clin. Ortop.* 109: 85, 1975.

White A.A., Paniabi M.M., Hausfeld J. and Southwick W.D.: Clinical instability in the thoracic and thoracolumbar spine. Review of past and current concepts. Presented at the American Orthopaedic Association Meeting Boca Ratan, Florida 1977.

White A.A., Southwick W.O., Paniabi M.M. and Johnson R.M.: Practical biomechanics of the spine for orthopaedic surgeons (Chapter Instructional Course Lecture. American Academy of Orthopaedic Surgeons). St. Louis C.V. Mosby 1974.

White A.A. and Paniabi M.M.: *Clinical Biomechanics of the spine* ed. J.B. Lippincott Company Philadelphia—Toronto 1978.

## Accident Reduction With New Driving Aids: Efficiency Assessment

**Hélène Fontaine, Gilles Malaterre,  
Pierre Van Elslande,**  
Institut National de Recherche sur les Transports  
et leur Sécurité

### Abstract

The aim of the research presented here is to assess what benefits may be derived from new devices in terms of accidents avoidance. We focused on the driving aids specially designed to improve safety.

A first research project, based on in-depth accident analyses, showed that in most accidents a driver "weakness" could be identified in the behavioural chain. We determined which were the needs corresponding to every class of situa-

tions, and hence what driving aids would be likely to reduce or eradicate the accidents concerned. This qualitative approach allowed us to point out the major categories of driving situations, accidents, needs and potential aids, but had to be corroborated by statistical analyses based on national accident records.

Thus, we extended this type of approach to a representative sample of police reports, tried to make a quick reconstruction of the accident, and attempted to determine in which way various driving aids could have been efficient. We worked on 350 accidents, and then we added the results of the analyses to a computer file which already contained the description of these accidents. By appropriate means (correspondence analysis), we specified the efficiency of each driving aid, in each situation and condition, etc . . . in

order to determine what is globally at stake, but also to get an idea of more precise targets: that is driving aids particularly fitted to specific problems. A typology of accidents, drivers' needs and efficient aids is analysed. Conclusions are drawn about devices that appear the most promising.

## Introduction

Research into transport is tending to become more European, and several programmes are being developed at the present time which are putting emphasis on the problems of safety. These are, firstly, PROMETHEUS (Program for European Traffic with Highest Efficiency and Unprecedented Safety), set up on the initiative of 14 car manufacturers, and secondly, DRIVE (Dedicated Road Infrastructure for Vehicle Safety in Europe), launched by the European Commission.

One of the difficulties in evaluating the potential value of these projects comes from the fact that most of the systems suggested don't exist, and are often not yet even clearly defined as a principle. The stated aims of the promoters are based on assumptions about driver behaviour in the relevant situations, and demand a high level of reliability for the different equipment as well as an optimal level of equipping for the vehicles. Some reservations have to be made about the change in behaviour which will automatically follow the introduction of this equipment. However, failing anything better, it should be possible, initially to evaluate the advantages expected of this equipment using studies which have been carried out from analyses of accidents. The reasoning used is the following: would the accident have taken place, or have been as serious if any of the parties involved had had one of the aids which we are describing at his disposal? Of course, this type of reasoning applies in other respects, everything being equal, in other words, that the potential advantages are evaluated, hypothesizing that the results will not be canceled out by side-effects. Taking possible side-effects into account is a totally different problem which must be treated separately.

We can see straight away that such an approach raises two questions:

Are the analyses of the accidents accurate enough to be able to make predictions about what would have happened if a driving aid had been used?

Can equipment as yet non-existent for which technical documents are not yet available be accurately described?

There is no easy answer to these questions, in so far as accident analyses can be detailed to varying degrees according to the source material used, i.e. detailed accident files from in-depth study, police reports, national or local statistical file data, etc, and the driving aids envisaged don't have the same degree of complexity nor the same innovative character. The level of analysis can be even anticipatory in character by spot-lighting more the needs of the driver in an accident, rather than the assumed efficiency of a particular piece of equipment.

The aim of this study has been, therefore, to attempt an evaluation using accident police reports, but also referring to results obtained already from files of the in-depth accident studies. The conclusions focus on the identified needs for driver aids and the efficiency of 14 driver aids whose functions we have defined. Here, we are presenting the first available findings.

## Methodology

Few studies are available on this subject. In 1987, Hitchcock provided some evaluation. This author used two files:

The "at the scene" file containing the accidents in a radius of 25 kilometres around the Transport and Road Research Laboratory, and for which detailed information is gathered on site with 2468 statements recorded in a period of about two years.

The "stats 19" file, the national file on injuries from accidents in Great Britain. It contains about 250,000 accidents for each year. Only 1987 was used for this study.

He selected four aid functions:

In the vehicle:

"Electrical vision" which detects and signals any object or vehicle present on the roadway.

"Override", the anti-collision device which activates the brakes automatically or takes lateral avoiding action in the case of an obstacle.

Between vehicles:

Communication of the position of the speed of the vehicles nearby on the same road or on an adjacent road.

Between the vehicle and the road:

Local information about the weather, ice, etc.,

He then researched into how many of these accidents could have been affected by these aids by examining the 1429 "at the scene" drivers' interviews (1042 accidents) one by one and only taking into account rear-end collisions for the second file.

A study was also carried out at INRETS by Van Elslande and Malaterre in 1987 on about thirty in-depth accident studies from the data bank at Salon-de-Provence. It aimed to identify the mechanisms such as "didn't see", "didn't understand", "didn't judge properly", and the corresponding factors such as restricted visibility conditions, negligence in signaling, . . . , and to deduce the main classes of elementary needs. Nevertheless, since the accident file of Salon-de-Provence is not representative nationally, no qualitative conclusions could be drawn.

In the research presented here, our objective was to go from a qualitative to a quantitative phase, using not only the in-depth accident studies from Salon-de-Provence, but also the police reports available to INRETS. The problem was to use the relatively well defined categories of needs in the in-depth accident studies and then to try to evaluate them using

a much briefer type of document, but which is representative of accidents nationally. Furthermore, we have defined 14 driving aids, as well as their intended ways of use in such a way as to estimate, according to the accident, which ones could have been used and which could have stopped the accident happening. The defining phase of the needs categories is inspired from the preliminary study of in-depth analyses and the definition of the aids comes from the various texts in DRIVE and PROMETHEUS. A statistical analysis was then undertaken so as to evaluate the potential gain from the aids studied, on the one hand, and to underline the links between certain types of accidents, needs and driver aids, on the other hand, by using a multi-criteria approach.

### The Data Base Used for the Evaluation

Whenever a personal injury takes place, the Police make out two types of documents:

a statistical sheet: "Bulletin d'Analyse d'Accident Corporel de la Circulation Routière" (BAAC). These sheets are then entered into a computer. This national computer file makes a great deal of information available about all personal accidents. This information concerns the general features of the accident, the infrastructure, the vehicles and the road-users involved.

a police report, which forms the basis of later legal action. It's about 18 pages long on average, and describes the facts very precisely. Moreover, the document contains the declarations of the parties in question, plans and also, sometimes photos; it gives an overall view of the accident, without being as complete as the in-depth accident studies.

A police report file, representative of accidents in France, was set up at INRETS (Fontaine, Gourlet, Jurvillier, 1989) with the aim of making an intermediate data base available between the exhaustive documents and information supplied by specific enquiries. Since the beginning of 1987, the Association TRANS-PV which has the task of receiving, photocopying and sending all the police reports to the insurance companies concerned, has also assumed the task of picking out one in every 50 police reports at random and to send them to INRETS. The corresponding BAAC sheet was also retrieved from the computer file. The sub-file obtained is then improved by more relevant additional statistics for the analysis of accidents and they are structured on a relational data base.

For our study, we decided to draw a sample at random of a tenth of this file which represents 350 accidents. We don't claim, at this stage that it is perfectly representative nationally. Our aim was first to set up a method on a small sample, before extending the study to all the file. However, the representativity was examined for the principle variables of the study, and the statistics from the exhaustive national accident file were referred to. Our sample does not

contain any bias. The procedure followed is shown in figure 1.

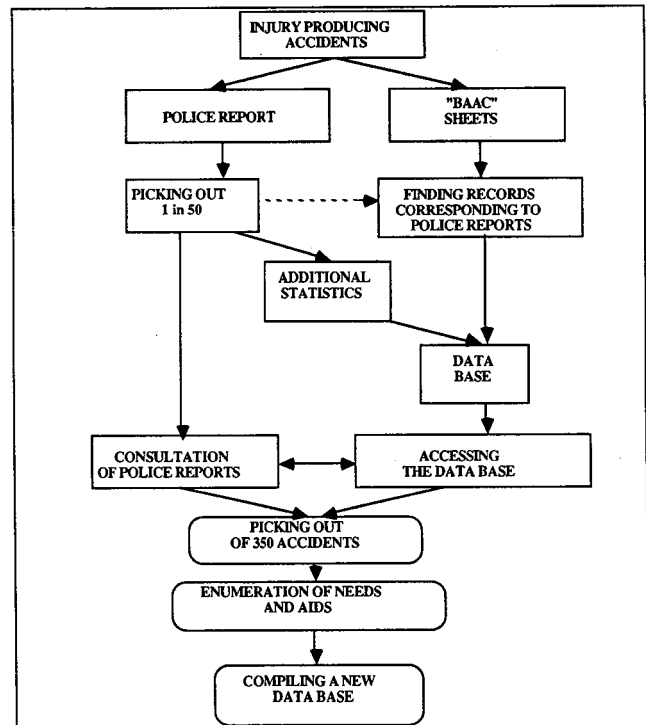


Figure 1. The data base used.

### The Driver Assistance Needs

We got our inspiration from the study of driver assistance needs quoted above as well as a report which had followed it up (Marion, 1987). We delineated 13 significant needs, in this way, which seemed to cover all the cases examined up to now. These needs are the following:

1. To maintain a sufficient level of arousal.
2. To detect a dangerous point (to increase warning).
3. To detect an obstacle on the roadway (debris, animals, pedestrians, stationary vehicles).
4. To detect an oncoming vehicle.
5. To detect a vehicle on a side road.
6. To detect an obstacle, behind or to the side.
7. To detect the catching up of a slower moving vehicle.
8. To indicate that the vehicle is on a collision course with another one at an intersection.
9. To detect the slowing down or an incident at the head of a platoon.
10. To evaluate the right speed for a punctual difficulty.
11. To indicate the intention of a visible road-user not to stop or to move away at an intersection where he doesn't have the priority.
12. To indicate a visible road-user's intention of moving to the right, the left, or straight ahead.
13. To indicate a visible road-user's intention to pass.

Categories 2 to 6 correspond to the detection of the simple presence of an object or objects, categories 7 to 10 correspond to an evaluation of a relative movement, and categories 11 to 15 to a diagnosis of the likely intentions of

another road user. When several needs could be chosen, we have chosen the more simple.

To encode needs, we added 3 categories to the list above which are not, strictly speaking, needs but allow us to cover all of the cases envisaged:

- non-equitable road-user (two wheels or pedestrians).
- indeterminable need (road-user not interviewed for example).
- no need identified or belonging to the list above.

## The Devices Considered in the Evaluation

In the same way, we have compiled a list of 14 aids which we have tried to define in terms of their functions and uses, using the rare and imprecise documents already existing on the subject. Whenever the documentation didn't allow a fair enough idea about how these devices work, we were compelled to try to define their possibilities for ourselves. These driver aids can be divided into two categories:

Information equipments (aids No. 1 to No. 7): improve the driver's information which he cannot get alone, or by simply making the system more reliable thanks to a certain redundancy or, on the other hand, a selective presentation of the right information when and where it is necessary.

Assistance equipments (aids No. 8 to No. 14): can take over a part of the driving themselves, either permanently, or voluntarily, or switching in when the automatic co-pilot detects an emergency situation.

### Information equipment

*Electric vision No. 1.*—Equipment intended to amplify senses, and more particularly vision. It enables the driver to see in unstable weather conditions (at night and in fog) using infra-red or ultrasonic devices. In principle, it enables any object to be seen that could be seen by an eye in optimal conditions, in other words, anything which is not masked. This is an active system not requiring any installation in the road or of other road-users.

The main information used by the driver, in normal conditions, is gathered through the windscreen. However, this information can be difficult to gather under certain conditions: i.e. darkness when driving at night, dazzling from other car headlights, rain, fog, etc. With this equipment the degree of information available through the windscreen doesn't depend on the environmental conditions and the information gathering activities are maintained.

*Active rear-view mirrors No. 2.*—Work on the same lines as above. They eliminate blind spots to the side or behind.

*Cooperative detection No. 3.*—Different from the above devices in that hidden road-users can be detected (limited visibility), as long as they are equipped with a co-pilot and a transmitter.

This device should enable road-users hidden by another vehicle, trees or buildings to be detected, particularly at an

intersection, on a bend or on the brow of a hill. It, therefore, allows obstacles to be located.

*Intersection control No. 4.*—Considers the respective speeds and trajectories and warns of the risk of collision. It can also prevent moving off if the way is not clear. This device is based on intervehicle communication, from co-pilot to co-pilot, but also takes into account priority factors, such as red lights and stop signs.

This type of device switches in when two vehicles approach an intersection and both intend to continue without stopping. This is a cooperative device which necessitates inter-vehicle communication up to 100 metres.

*Detection of incidents No. 5.*—Enables vehicles involved in accidents or bottlenecks to be detected. This feature is sometime included in more general centralized information devices, such as Road Service Information, which includes traffic flow, diversions and weather information, etc.,

This device combines visual warnings with a radio transmission of information at various distances from critical areas, such as accidents, bottlenecks, road-works PRO-ROAD and ROAD-NET have both offered devices fulfilling these functions. The techniques aren't the same, but the results are very similar.

*Detection of situations No. 6.*—Messages sent by the road or by a transmission system and displayed inside the vehicle: e.g. a dangerous point, speed restrictions, ice, snow, stops or priority. It's no longer a question of inter-vehicle but of road-vehicle communication. Such equipment involves the setting up of public data transmission systems.

*Automatic detection No. 7.*—Diagnosis of the state of the vehicle, warning of tyre pressure loss, bad state of the brakes, of the engine, etc. These are intra-vehicle communication devices.

A vehicle monitoring device would supply information about critical components in safety and engine performance. The sensors would be installed for the vehicles in general.

### Assistance equipments

*Monitoring of driver condition No. 8.*—Detects a fall in attention, fatigue, the effects of alcohol, etc. The equipment sounds an alarm in the case of deviation from the road.

This device should prevent a driver under the influence of alcohol or unable to drive from taking the wheel. The methods contemplated which would measure fitness for driving are of two types:

direct: measuring the alcohol breathed into the air.

indirect: checking of driver performance by identifying abnormal behaviour (swerving, abnormal movements of the steering wheel, etc). We choose to assess the second type of device.

*Anti-collision radar No. 9.*—Sounds an alarm when relationship of distance and speed become critical in regard to a potential obstacle.

An anti-collision and anti-obstacle radar was contemplated as part of PROMETHEUS. The sensor is defined as a long-range sensor (50 to 200 metres) which would work

through the Doppler effect using a high frequency band (which is less sensitive to atmospheric conditions) or with a laser (which gives better spatial localization of obstacles).

*Overtaking No. 10.*—Warns of the presence of obstacles in an adjacent file of traffic, either going in the same or the opposite direction, so as to aid passing.

Passing aid equipment was put forward by PRO-CAR with the same principle as the obstacle detection device described above.

PRO-NET anticipates a cooperative system which would assist in communication between vehicles. This system would make up a communication network of up to 10 vehicles in a 500 m zone in front and behind.

*Speed keeping No. 11.*—Enable the vehicle's speed to be stabilized at the desired level or in relation to the guidance signals described in No. 6.

The legal or recommended speed limit is received by the vehicle and displayed. When this speed limit is reached, an effective limit is applied with the hardening of the action of the accelerator pedal or by the absence of response when it is depressed to the floor. (cf Malaterre and Saad, 1984)

*Car following No. 12.*—In driving in a line, it automatically adapts the vehicle speed to that of the vehicle in front of the line so as always to keep a safe distance. It only applies to motorways. The device for checking distances, such as that described for the detection of obstacles and for aid in passing should also compare the vehicle speed in front with that behind in order to maintain the correct distance in the case of motorway driving.

A vehicle following device should be capable of combining information about the distance and speed of the vehicle in front with data concerning the atmospheric conditions, the road surface and the condition of the vehicle.

*Lane keeping No. 13.*—Allows driving in a given lane without having to move the steering wheel. Only applies to motorway driving.

Ove Sviden described such a device in Automatic Fast Lane Chaffering (cf. PRO-GEN 1987). A vehicle equipped with a multi-sensor system and an anti-collision device could go into a fast lane in which the automatic co-pilot would take over the steering and control of the speed and distances. The co-pilot would also warn the road-user when he should change to a manual system.

*Navigation aids No. 14.*—Helps to prepare the journey, also indicates the direction to follow once the itinerary has been chosen.

The aim of this device is to supply the following information. Information about the trip and the time taken during its planning. The device considers the places of the departure and destination, and during the driving, the directions to follow as well as the different alternatives possible at each intersection.

Real time information on the traffic. It considers the traffic speed and delays due to road-works or accidents. It also calculates the estimated time of arrival according to the chosen route.

Precise and timely information about the direction to be taken at any moment. It recommends the route to be taken at each intersection according to the user's choice.

These navigation aid devices can be autonomous or assisted from outside.

To encode the police reports, we adopted the following scale. A figure was attributed to each aid ranging between 0 and 4 depending on the following criteria.

0. No, the aid cannot be used for this type of situation.

1. The aid would have had an effect in advance of the accident (such that the accident situation may not have arisen).

2. Unlikely to be effective for technical reasons: the aid would work but wouldn't be enough to prevent the accident, since the information or assistance was little suited, or too limited technically, or too late.

3. Unlikely to be effective for human reasons: the aid would work but might not be sufficient for the driver, considering his work-load, his state or intentions. Or even, the aid supplied is useless or redundant.

4. Probable effectiveness: the aid would have worked and probably prevented the accident.

## Statistical Treatment of the Data

First of all, we evaluated the effectiveness of each of the aids. Then, in the second stage, we followed a multi-dimensional approach, in order to bring out the homogeneous groups of vehicle drivers involved in accidents as well as relevant needs and aids.

### The evaluation of the devices

We first assessed the potential efficiency of the aids in avoiding the accidents (the evaluation was made at the accident level), and then we evaluated the drivers' needs satisfaction (the evaluation was made for each driver).

*The accidents avoided.* Below (figure 2) are the percentages of the accidents which could probably have been prevented for each of the aids. Some driving aids have a previous influence coming from their delineation. This means that they wouldn't have had an influence on the accident itself, but would have prevented the accident situation from coming about. The results below concern both direct and indirect influence. It has to be emphasized immediately that these are maximum estimates, which suppose the optimal working of the driving aids. The lack of information in some police reports has, in giving them the benefit of the doubt, led to an overestimation of the level of effectiveness. There would be a case in applying a coefficient to reduce the level, especially for the less well defined aids.

Five aids show a high percentage of effectiveness. These are:

- Intersection control (16%). This is an aid for which the performance limits are not well-known. It was, therefore, assumed that this aid would regulate practically all misunderstandings at intersections or when the priority or traffic signals aren't respected except when done deliberately.

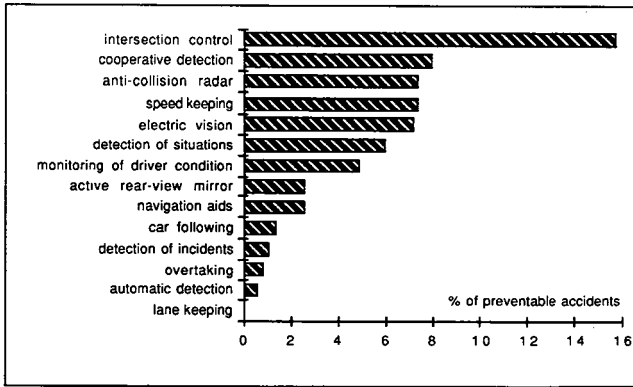


Figure 2. The percentage of accidents which could have been avoided by driving aids.

Figure 2. The percentage of accidents which could have been avoided by driving aids.

- This explains the high level of effectiveness.
- Cooperative detection (8%), which detects hidden oncoming road-users or those in side-roads. However, there again, we don't know if such a device might not overload the driver with information, especially in a built-up area not all of which is relevant. This could reduce its effectiveness.
- The anti-collision device (7%) which would have worked in a much larger number of cases (in almost all the car crashes), but which would not have prevented the accident, in particular when the obstacle cuts too close across the electronic beam of the vehicle. This is true of most of the accidents involving pedestrians.
- Speed keeping (7%) which have in most cases a previous influence.
- The electric vision aid 7%, is probably exaggerated in as much as frequent statements such as "I saw the pedestrian crossing too late" can sometimes be categorized as a vision or detection problem, but we know from experience of in-depth accident studies that it is not always detection which is at fault, rather the realization too late that the other road-user constitutes a potential hazard. As long as he is immobile or on the pavement, he isn't "seen" in the sense that he's included in the relevant elements in the driving process.

Some aids are very specific to types of accidents which are little represented here (motorways accident for example). These driving aids specific to particular situations, such as motorway and bad weather conditions would need studies using a suitable sample which we could not do using our 350 police reports.

Globally the effect of the 14 devices together is equal to 44%, but it should be noticed that the results obtained present two types of errors: a statistical error coming from the small sample, and an error coming from the lack of information in the police report and in the definition of the aids. The latter is difficult to assess. We tried for "electric vision" (Fontaine, Malaterre, Van Elslande 1988). The statistical error gives the following result: 7% [ $\pm 3\%$ ] of accident prob-

ably preventable. And, in this case, what we mean by "probably preventable" is 3/4 of the accident avoided.

*The assistance of the drivers.* This was a matter of evaluating the effectiveness of the driving aids in meeting the needs of assistance for the individual road users. It is clear that driving aids can sometimes be redundant in connection with an accident, for example where they respond effectively to the needs of the two road users involved. The results of this evaluation are given in table 1:

Table 1. Assessment of the assistance to the drivers.

need	size	direct efficiency or indirect (beforehand) (number of users)	% of drivers assisted by at least one aid
1 - level of arousal	30	13	43%
<b>detection</b>			
2 - dangerous point	13	11	85%
3 - obstacle on the road	75	26	35%
4 - oncoming vehicle	32	23	72%
5 - vehicle on side road	73	35	48%
6 - obstacle behind, to the side	17	11	65%
<b>relative movement</b>			
7 - catching up moving vehicle	10	10	100%
8 - collision course (inter)	33	18	55%
9 - incident	7	7	100%
10 - right speed	16	13	81%
<b>evaluation of intention</b>			
11 - non stop or move away	27	8	30%
12 - moving right or left	30	7	23%
13 - passing intention	3	2	67%
<b>TOTAL</b>	<b>366</b>	<b>184</b>	<b>50%</b>

The sample is composed of 621 vehicles (two or four wheels). A need of assistance has been identified for 366 road users and between them, 45% [ $\pm 5\%$ ] could have been directly assisted by at least one of the 14 studied aids. If we consider now the direct and indirect (beforehand) possible effect of the aids, this proportion reach to 50% [ $\pm 5\%$ ]. The more complex needs are the less correctly satisfied. We must not forget, here again, that the results present two types of errors, a statistical one and one coming from the lack of information.

### Multi-dimensional analysis

We analysed all the drivers and vehicles involved in accidents. We tried to bring out homogeneous classes and to situate needs and aids in relation to these categories. The process consists, in its initial stage, in making a correspondence analysis, then, in its second stage, we made a hierarchical classification using the factors determined previously in the analysis of correspondences. Thus, categories are obtained which are markedly different from the contributory factors of each of them. The programmes used belong to SPAD software (Portable System for the Analysis of Data—Lebart and Morineau—CESIA 1985)

*The correspondence analysis.* The analysed sample comprises 621 vehicles involved in accidents. An analysis of the 350 accidents has also been undertaken (Fontaine, Malaterre, Van Elslande, 1988), but it is not presented here. We chose as "active variables" those which describe the accident objectively, and the "illustrative variables" were the evaluations of needs and the effectiveness of the driver aids, with the aim of placing them in the different groups of vehicles involved in accidents."

Active variables are, therefore, those describing the vehicle and driver involved (category and age of the vehicle, age, sex, profession and condition of the driver). We added the relative variables of the accident in which the vehicle is involved (day, lighting, atmospheric conditions, whether in a built-up area or not, at an intersection or not, type of road, cross-section, ground plan, result of the accident).

The other criteria were put down as illustrative variables. They could be variables which we are trying to explain, for example the needs or the effectiveness of the aids, or highly correlated with active variables. In this last case, active and additional items were determined after several previous analyses which enabled the most relevant criteria to be selected for the axes. The illustrative variables play no part in the fixing of the analysis axes, but they do appear on the plan of factors and in the categories of the typology. The plan of the factors formed by the first two axes is represented by figure 3.

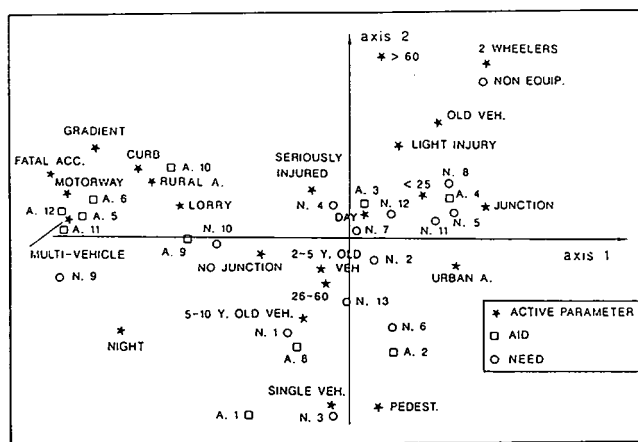


Figure 3. Correspondence analysis on vehicles involved in accidents—axis 1 and 2.

The first axis is that of the location of the accident. It distinguishes the vehicles involved outside a built-up area, not at an intersection, and vehicles involved in a built-up area, at an intersection.

On one side we see accidents happening in open country, on the motorway, which are fatal, involving more than 3 vehicles, at night, on a bend and on a slope. The needs identified are the detection of slowing down in the traffic and the evaluation of a suitable speed for the conditions. The driving aids appearing at this side of the axis are car following (No. 12), the detection of incidents (No. 5), speed keeping (No. 11) and detection of the situation (No. 6).

On the other side, in built-up areas, we can identify the two wheeled vehicle. The need to detect a vehicle in a side-road, as well as driving aid No. 4 (intersection control) are on this side of the axis.

The second axis indicates the road-users. On the one hand, there are the vehicles involved in accidents with pedestrians, on the other hand, accidents with two wheelers. The need for detection of an obstacle on the roadway, driving aid No. 1 (electric vision) concern accidents involving pedestrians.

*Typology of vehicles and drivers involved in accidents.* The examination of results of the classification drawn up from the factors obtained in the analysis above, shows the number of groups selected to be 6.

*Class 1 (240 vehicles).* This deals with vehicles involved in accidents between several vehicles at intersections in built-up areas. The needs most often identified are the following:

- Detection of a vehicle on a side-road.
- Detection of the intention of a visible road-user at an intersection not to stop.
- Detection of a collision course at an intersection.

The individual manoeuvres most often found in this category are the change in direction and parking. Driving aid No. 4 (intersection control) is identified twice as often here as for the accidents as a whole.

*Class 2 (103 vehicles).* This category includes a large number of 2 wheelers, which are most often involved in accidents at intersections and in built-up areas. The riders and drivers are often under 25 and are only slightly hurt. The most common manoeuvre is parking and moving away from a parked position. No aid was possible because we didn't consider the two-wheeled road-user to be equitable.

*Class 3 (80 vehicles).* This category deals mainly with collisions between several vehicles, outside built-up areas and intersections on major roads during the day. The accidents often happened on a bend or on a slope. The needs represented in this category are:

- Evaluation of the suitable speed on a difficult route.
- Detection of an oncoming vehicle.

Driving aid No. 3 (cooperative detection) would probably have prevented the accident in 14% of these cases;

*Class 4 (64 vehicles).* This class is that of the vehicle involved in an accident against a pedestrian in a built-up area. The identified need is that of the detection of obstacles on the roadway. Driving aid No. 1 (electric vision) would have probably prevented the accident in 11% of cases. However, we repeat that our method of evaluating using the police reports probably exaggerated this aid to the detriment of an aid detecting the intentions of another road-user. However, we do not see, how such an aid could work.

*Class 5 (56 vehicles).* This category consists mainly of vehicles involved in accidents caused through loss of control, away from intersections, out of built-up areas, at night.

The driver, who is under 25 in almost half the cases, is killed or seriously injured. In this category, there are most often accidents in the cold season or at weekends. The needs which are most linked to this category are the maintenance of a high level of arousal and the evaluation of the suitable speed at a road difficulty. Aid No. 6 (detection of situation) would probably concern 7% of the cases, or almost three times as much as for the vehicles as a whole. Driving Aid No. 8 (monitoring of driver condition) and No. 11 (speed keeping) would work indirectly.

Class 6 (78 vehicles). This group is represented by vehicles in accidents on the motorway in multiple pile-ups. The cause is either a slowing down (in half the cases) or a lane change (in a third of cases). These accidents are often serious and happen in the warm season. There doesn't appear to be any need specific to this group. Aid No. 9 (anti-collision radar) would prevent the accident in 19% of cases and driving aid No. 6 (detection of situation) in 10% of cases.

The categories of vehicles, the identified needs and the aids which could be used are shown in table 2.

**Table 2. Categories of vehicles involved, needs of drivers, and aids.**

categories of vehicles involved (the most contributing forms)	identified needs	usable aids
collisions involving several vehicles in a built up area at an intersection	detection of veh. on a side road detection of an intention not to stop detection of a collision course	intersection control (n°4)
two wheelers in built up area at intersections		non equipable road-user
collisions between several vehicles, outside built up areas, away from intersection, on major roads during the day	suitable speed to negotiate a road difficulty detection of an oncoming vehicle	cooperative detection (n°3)
vehicles involved with pedestrians in built up area	detection of obstacles on the road	electric vision (n°1)
single vehicle, loss of control away from intersections outside built up areas, at night	suitable speed to negotiate a road difficulty	detect. of situation (n°6) speed keeping (n°11) monitoring cond (n°8)
multiple accidents on motorway		anti-collision radar (n°9) detection of situation (n°6)

In each category, we have indicated the most contributing forms, however, this presentation is of course very much reduced: the forms indicated apply generally to the majority of the vehicles of the category and not to all of them. In the same way, some vehicles belonging to other categories can use the same forms. It will be noticed that there is no single need for accidents on motorways. This is due to the heterogeneity of needs.

## Synthesis of the Results

The typology emphasized by a multi-criteria approach makes the most discriminating variables appear from the vehicles involved in accidents, as a whole. However, the groups obtained are not completely satisfactory, in so far as regrouping the vehicles and drivers involved in accidents from a national statistical file is not possible. We, therefore, had to find a simpler typology based on only two or three criteria. The choice of these new criteria was made, on the one hand, by considering the results of the classification and, on the other hand, by relating to the possible application of certain driving aids: for example, the type of road-users concerned or the type of place. This new, simpler typology comprise 4 groups:

The vehicles involved in accidents with 2 wheelers or pedestrians (252 vehicles of which 106 two wheelers).

These accidents take place mainly in built-up areas, in warm weather, on working days. The participation of young drivers is greater than for the other accidents as a whole. The most commonly found needs are the detection of an obstacle on the road-way or a vehicle on a side-road. The aids which are likely to be useful are electronically improved vision (No. 1) and active rearview mirrors (No. 2).

Four wheeled vehicles involved in single vehicle accidents (49 vehicles). These are serious accidents. The driver is under-25 in almost half the cases. Accidents at weekends, at night, in bad weather, outside built-up areas, away from intersections and on bends are all very common in this category. Two needs are apparent: the maintenance of driver arousal and the evaluation of speed to negotiate a road difficulty. The aids in this class are electric vision (No. 1), monitoring of driver condition (No. 8), the detection of the situation (No. 6), and speed keeping (No. 11).

Four wheeled vehicles in multiple accidents in towns (199 vehicles). They are mainly non-serious accidents at intersections. The driver needs are the detection of a vehicle on a side-road and the indication of a collision course. Three types of aids could be effective here: intersection control (No. 4), cooperative detection (No. 3) and anti-collision radar (No. 9).

Four-wheeled vehicles involved in multiple accidents outside built-up areas (121 vehicles). We find here a great number of accidents away from intersections, on bends, in bad weather, an also on the motorway. The main need of the drivers is the detection of an oncoming vehicle. A large number of aids would function efficiently: anti-collision radar (No. 9), car following (No. 12), cooperative detection (No. 3), the detection of incidents (No. 5), intersection control (No. 4), the detection of situation (No. 6) and speed keeping (No. 11).

These 4 categories are represented by figure 4.

## Conclusion

This typology should make it possible to evaluate needs from files of national statistics. It should not be forgotten, all the same, that this evaluation of the needs *strongly depends on the precision with which the driving aids are defined*. The vaguer a definition of an aid is, the more difficult is the estimation of its effectiveness. We think that we overestimated the performance of several aids.

We worked on a relatively small sample. We were able to take into account a limited number of categories in proportion to the small number studied. Certain aids are very specific to types of accidents which are little represented here (motorway accidents for example). This is not problematic when making a general evaluation of the aids but can be for a specific analysis of the individual needs of these categories. This is why this study should only be seen as a preliminary step in the analysis of a 1/50th sample in a whole year's police reports which should be undertaken soon. A more precise analysis of the unsatisfied needs will be carried out in order to specify new potential aids.

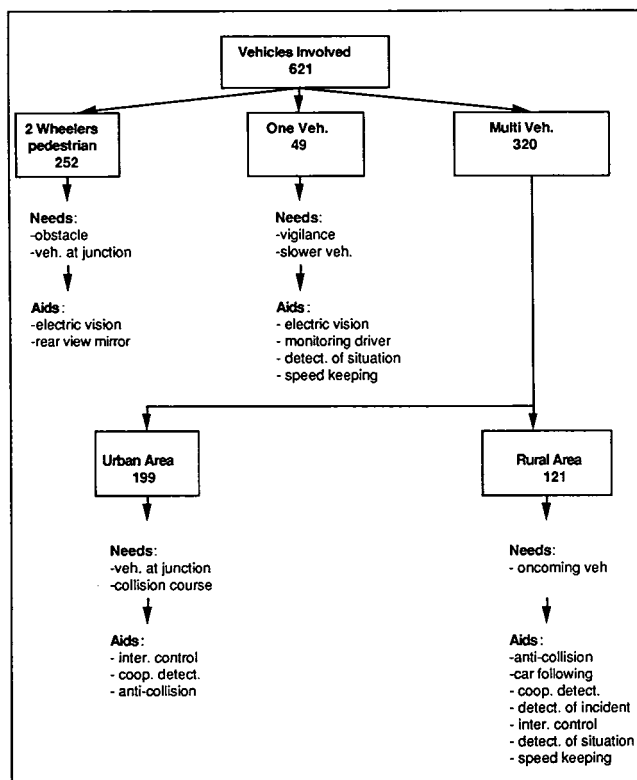


Figure 4. Typology of the vehicles and drivers involved in accidents.

## References

- Drive, 1988, Workplan, Draft of 26 April, edited by the Commission of the European Communities.
- Fontaine, H., Gourlet, Y., Jurvillier, J.C., (1989). Le fichier des procès-verbaux d'accidents corporels de l'année 1987, Rapport Inrets.
- Fontaine, H, Malaterre, G, Van Elslande, P, (1988). Evaluation de l'efficacité potentielle des aides à la conduite—Rapport Inrets No. 85.
- Hitchcock, A. (1987). Potential safety implications of the Prometheus project.
- Lebart, L. et Morineau, A. (1985). Spad, Cesia
- Malaterre, G., Saad, F. (1984). Contribution à l'analyse du contrôle de la vitesse. Evaluation de deux limiteurs de vitesse. Cahier d'études Onser No. 62.
- Marion, E. (1987). Contribution de l'étude détaillée d'accidents de la route, et de l'approche psychologique utilisée, à la conception d'un système d'aides à la conduite. Rapport de stage Inrets.
- Pro-gen LP 71250, Final Draft, 1987.
- Prometheus (1987) Actes du 2<sup>ème</sup> symposium (9 documents).
- Van Elslande, P., Malaterre, G. (1987). Les aides à la conduite, analyse des besoins en assistance des conducteurs, Rapport Inrets.

## Study of Laser Radar

Tetsuo Teramoto,  
Toyota Motor Corporation  
Keiji Fujimura, Yasuhiro Fujita,  
Fujitsu Ten Limited

### Abstract

We have made a prototype of a headway control radar using a pulsed semiconductor laser and have confirmed its feasibility.

The transmitter of this radar transmits two beams having radiation angles of  $\pm 0.5$  and  $\pm 1.4$  degrees. The transmitter uses an aspherical plastic lens, and the receiver uses a wide aperture Fresnel lens for improved detection performance. The receiver has automatic gain control (AGC) and sensitive time control (STC) circuits. AGC decreases measurement errors caused by fluctuations in target reflectivity. STC decreases misdetection errors caused by rain or snowfall. An 8-bit microprocessor simplifies the range measurement block. Vehicle tests have shown that the maximum detection range is 350 m from the rear of a static vehicle and the measurement error was 2 m or less in the range of 100 m and above. Since lost targets occurred in the field tests, it will be necessary to examine the beam scanning methods.

## Introduction

Recent car electronics developments have made vehicles faster, safer, and more comfortable. One car electronics field is crash avoidance or headway control, a safety-oriented dream technology. Since 1960 various headway control devices have been studied. We announced a "headway control millimeter-wave radar system" at the Tokyo Motor Show in 1981. This was an FM-CW radar using radio waves in the 50 GHz millimeter-wave band; its V-type transmitting/receiving antenna was installed on the front grille of a car.

In this paper we report a radar headway control system, this time using a laser. Although laser and radio-wave sensing technique may seem different, light rays and radio waves are both electromagnetic waves, differing only in wavelength. The wavelengths of millimeter wave are 1 to 10 mm; the wavelengths of ultraviolet and near-infrared rays are 0.1 to several microns. The wavelengths of the rays generated by the semiconductor laser described in this paper are about 1  $\mu\text{m}$ . The wavelengths of visible rays, 0.4 to 0.7  $\mu\text{m}$ , are close to those of the rays generated by the laser. Since the wavelengths of these rays are shorter than those of millimeter wave, these rays are more effective when used to detect smaller objects.

The history of the laser is comparatively short. Discovered in 1960, the laser is considered one of the greatest discoveries of this century. Since 1960, various laser oscillators and applications have been studied and developed. Range measuring techniques using lasers have been used in the military and in meteorology. The advent of the digital audio disk (DAD) in 1982 triggered remarkable progress in laser device development. Today, light receiving/emitting devices such as semiconductor lasers, PIN photodiodes, and small, high precision optical components are inexpensive and readily available. Lasers for radar applications have the following advantages:

- They are not subject to the regulations of the Wireless Telegraphy Act.
- They are comparatively easy to obtain.
- The transmitted beam is easily controlled.
- They will continue to be made smaller and lighter.

How our prototype laser radar for vehicle installation was designed and evaluated is outlined below.

## Outline System

Figure 1 shows a Toyota concept car called the FXV-II. The headway control system installed in the car is described first.

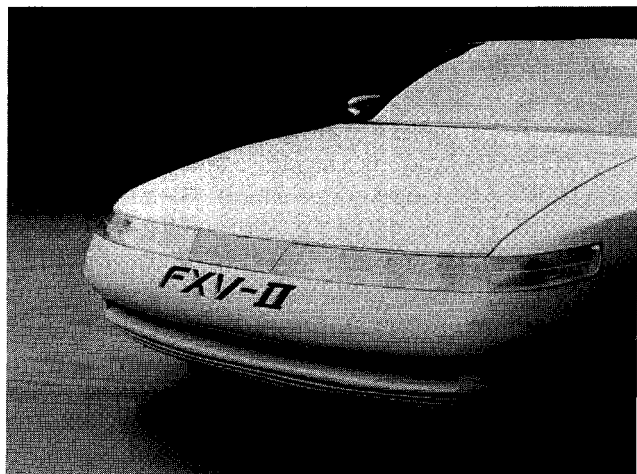


Figure 1. Experimental Toyota FXV-II with laser radar installed. (The radar is installed inside the Toyota insignia on the front grill.)

The total vehicle movement control system concept of the FXV-II car is summarized in figure 2. Various sensors, ECUs and actuators are arranged around a man-machine interface that enables the system to be tailored to the individual driver's needs. This concept car provides more drive control and uses state-of-the-art control technology. The laser radar in this system assists the driver's brain and eyes. The radar cruise control system shown in figure 3 has actuators that control the throttle and brakes. In addition to this radar cruise control system, the FXV-II has the following functions:

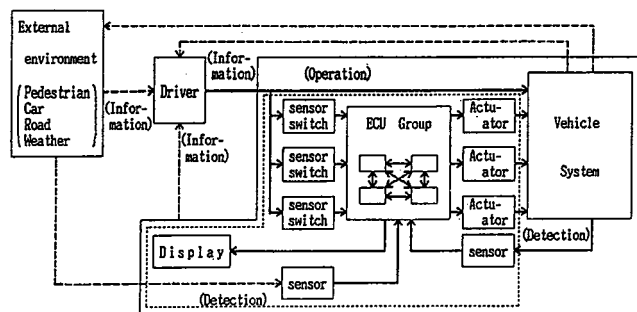


Figure 2. Concept of total control system for vehicle movement.

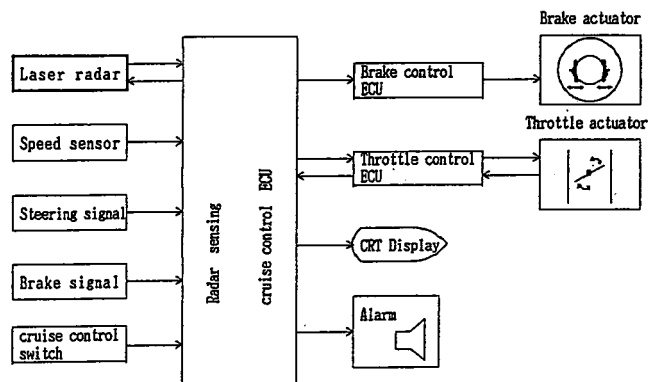


Figure 3. Radar sensing cruise control system configuration.

- A headway control function that maintains the optimum range from the motorist or obstacle ahead.
- An alarm function that warns the driver of the presence of a motorist or obstacle ahead.
- A laser radar system self-diagnosis function.

Range information from the laser radar, information on the driver's activity, e.g., steering and brake signals, and information on the activity of other system ECUs are input to the control computer (ECU). The radar ECU processes the information to selectively control the throttle and brakes to provide smooth control without confusing the driver. Headway information and information about how the system is being controlled are sent to the CRT display located at the center of the instrument panel.

## Basic Characteristics

### Principle of measurement

Radar devices focus an electromagnetic wave on a target, receive the reflected wave, and measure the target's range and direction.

Range is determined from the time it takes for the wave to reach the target and return to the radar receiver. Typical measuring methods are:

*Pulsed method.*—A pulsed electromagnetic wave is transmitted and the time difference between the transmitted pulse and the received pulse is measured.

*CW method.*—A continuous high-frequency sine wave is transmitted and the phase difference between the transmitted wave and the received wave is measured.

Our laser radar prototype uses the pulsed method because:

- Investigations of typical optical radars for detection of numerous and non-specific targets show that the pulsed method is most often used (the CW method is used in some applications, but in most a special reflecting mirror is attached to the target to ensure adequate received power).
- Since cars, guardrails, and people are to be detected, the laser must have a wide power margin.
- Many types of high-power semiconductor lasers for pulsed operation are available.
- Pulsed radar signals are processed in a comparatively simple manner and the system is easily constructed.

Figure 4 shows the principle of pulsed radar measurement. The range (R) to the target, is given by:

$$R = \frac{t \times C}{2} \quad (1)$$

where t is the time difference between the transmitted wave and the received wave and C is the velocity of light ( $3 \times 10^8$  m/s).

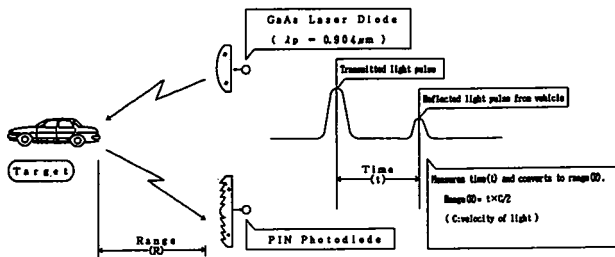


Figure 4. Principle of measurement by pulsed laser radar.

## Laser radar equations

Radar equations describe the relationship between the transmitted and received signal. Sensors are designed according to these equations. For a laser radar, either of the following equations is used depending on the relationship between the cross section ( $A_o$ ) of the target on which the laser beam falls and the cross section (A) of the beam:

(1) When  $A_o < A$  (target < beam)

$$Pr = \frac{Ar \sigma Gt T^2 Pt}{(4\pi)^2 R^4} \quad (2)$$

Where

Pr: Received Power

R: Range to the target

Gt: Gain of the transmitting lens

Ar: Aperture area of the receiving lens

T: Transmission constant of air

$\sigma$ : Scattering cross section of the target

Pt: Transmitted power

(2) When  $A_o > A$  (target > beam)

$$Pr = \frac{Ar N \sigma K T^2 L Y Pt}{R^2} \quad (3)$$

Where

N: Number of particles

$\sigma$ : Particle scattering cross section

K: Transmitter/receiver efficiency

(including the gain of the transmitting lens)

L:  $c \times \tau/2$  ( $\tau$ : laser pulse width, C: velocity of light)

Y: Geometrical efficiency of the transmitting/receiving optical block Y = 1 when the field of view of the transmitting block completely matches that of the receiving block

That is, if a fixed power is transmitted when the laser beam is larger than the target, the received power is inversely proportional to the fourth power of the range. If the laser beam is smaller than the target, the received power is inversely proportional to the square of the range. Equation (3) is often used when the target is a gas or aerosol. For detection of a car, equation (2) should be used. When the range to the target is short, however, equation (3) gives the relationship between the transmitted power and received power.

## Target reflection characteristic

Reflection characteristics obtained by radiating laser beams at a vehicle are shown below.

Figure 5 shows the relationship between the range and the received power. If a beam of  $\pm 0.5$  degrees is transmitted, the diameter of the transmitted beam is about 1 m at a range of 60 m and the beam covers a significant portion of the target vehicle. When the range is 60 m or more, the received power is inversely proportional to the fourth power of the range. When the range is less than 60 m, the received power is inversely proportional to the second or third power of the range, that is, the reflection characteristic is given by equations (2) and (3).

Figure 6 shows the reflection characteristic of the rear of a target vehicle. The characteristic represents the reflection cross-section ( $\sigma$ ). The reflection intensity from the rear of the target vehicle is very high at the reflectors<sup>1</sup> and chrome or decorative trim. Reflections from these areas can be 100 times greater than that from other areas.

Radar equations tell how much power is received when the transmitted beam is sharp and the area of reflection is inversely proportional to the second or third power of the range. If the beam is excessively sharp, however, the received power fluctuates considerably because it is affected by the reflection cross section, and a stable power cannot be received. Beams which are excessively sharp do not conform to the Safety Standard for Laser Beams (described later).

<sup>1</sup> The Japanese Vehicle Safety Standard rules that reflectors be installed on all vehicles.

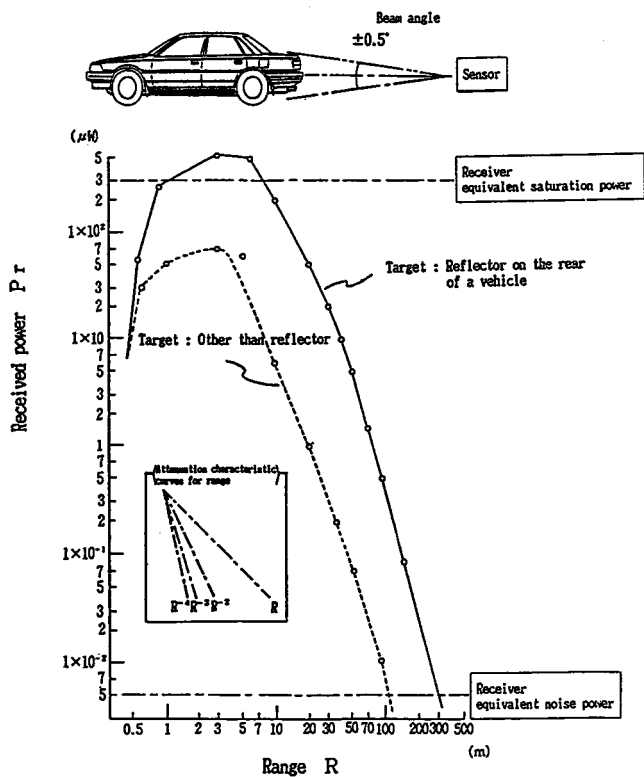
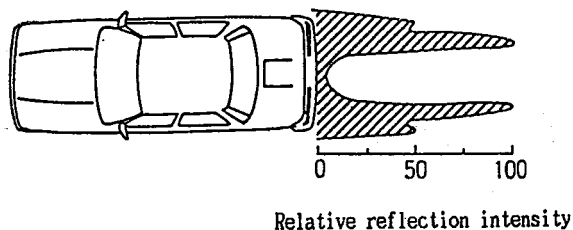


Figure 5. Relationship between range and received power.



The characteristic was measured by scanning the  $\pm 0.5$ -degree laser beam at a distance of 25m.

Figure 6. Reflection characteristic for rear of vehicle.

## Sensor Configuration

### Basic configuration

Figure 7 is a block diagram of the laser radar sensor. The sensor consists of four sections: a laser beam transmitter, a receiver that collects and amplified the reflected light pulses, a range pulse generating section that generates the transmission-reception time difference pulse, and a range calculating section that converts the time difference pulse into range data. Table 1 shows the major sensor specifications. Figure 8 shows the prototype sensor and its internal structure.

Each section is outlined below.

### Transmitter

*Transmitting optical block.*—To extend the detection range and to ensure stable target detection while the vehicle is moving, the block uses two beams of 0.5 and 1.4 degrees.

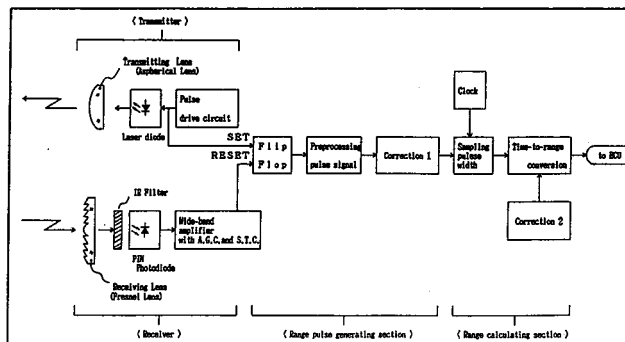


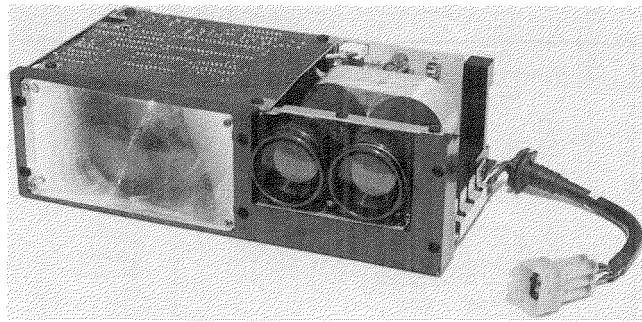
Figure 7. Laser radar sensor block diagram. Table 1. Major laser sensor specifications.

Table 1. Major laser sensor specifications.

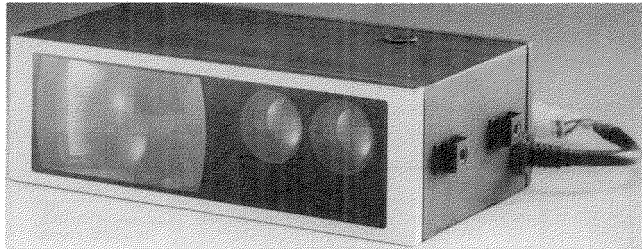
	Item	Specification	Remarks
Transmitter	Lens aperture	Diameter : 34mm	Aspherical plastic lens
	Radiation power (peak value)	10 W or less each	Conforms to class 1 in IEC825 standard
	Beam angle (full angle)	$\pm 0.5^\circ$ , $\pm 1.4^\circ$	Two-beam system
	Pulse width	70 nsec	
	Repetition rate	2 msec	
	Oscillation wavelength	0.904 $\mu$ m	GaAs laser diode
Receiver	Lens aperture	100 $\times$ 55 mm	Plastic Fresnel lens
	Preamplifier band (-3dB)	10 MHz	Light receiving element PIN photodiode
	AGC range	70 dB	
Performance	Detection range	80m or more	Target : Rear of vehicle.
	Range resolving power	0.5 m	
	Range error	$\pm 2$ m or less	
	Data transmission rate	7812 bps	Data such as range data is sent serially to the ECU.
General	Operating voltage range	+10 ~ +16 V	
	Operating temperature range	-20 ~ +70 $^\circ$ C	
	Current consumption	0.7 A or less	
	Dimensions	60 (D) (D) 240 $\times$ 75 $\times$ 130 mm	
	Weight	2.5 kg	
	Installation location	Inside of front grille	

The lens used in the block is an aspherical plastic lens designed by Fujitsu Ten. Each beam angle is obtained by changing the gap (called the lens block) between the laser diode and the lens.

The aspherical lens minimizes spherical aberration and enables efficient transmission of the beam from the laser diode. A conventional single lens causes much spherical aberration and uneven intensity distribution of the radiated beam. An optical block consisting of two or three lenses can suppress spherical aberration but is expensive and heavy and is not suitable for installation in a vehicle. Figure 9 shows the shape of transmitted beam measured by an infrared television camera. The shape of the beam in Figure 9(a) looks like an ellipse because the laser diode chip has an oblong cleaved surface (called the laser oscillation edge). Figure 9(b) shows the cross section pattern at the center of each beam (0.5-degree beam and 1.4-degree beam). These patterns resemble a Gaussian beam.



8(b). Interior view.



8(a). Exterior view.

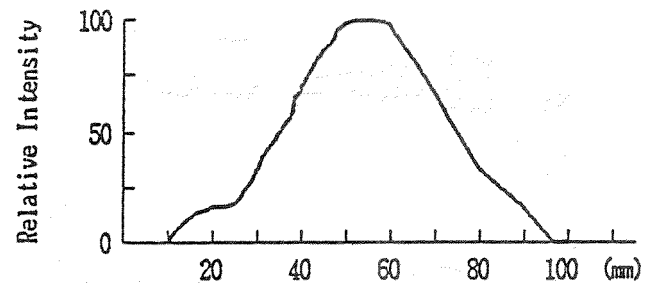
Figure 8. Prototype of laser radar sensor.

**Laser diode.**—The laser diode in prototype is a GaAs (gallium-arsenide) semiconductor laser diode and has a single hetero-junction structure. The laser generates near infrared rays (invisible rays) with a peak wavelength of 0.904  $\mu\text{m}$ . A stacked chip is obtained by stacking three diode chips in series tripling the laser output power for the same drive. This technique produces a high-power laser.

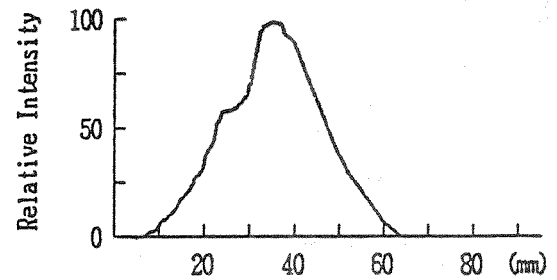
**Pulsed drive circuit.**—Unlike a light emitting diode (LED), the laser diode generates laser beams only when the drive current exceeds a threshold value. A pulsed-type laser diode requires drive currents in the tens of amperes.

The drive pulse width is about 70 nanoseconds wide. This high-current, high-speed pulse drive circuit uses a high-speed silicon controlled rectifier (SCR). Figure 10 shows the basic drive circuit, which is the same as the flash circuit for a camera. The charge on the capacitor is applied to the laser diode when the SCR is triggered. Since the drive circuit is a high-current, high-speed circuit, not only the components shown in figure 10 but the other components must be carefully designed. For example, the patterns on the PC board for the circuit should be as wide and as short as much as possible. A pattern that is 1 mm and 5 mm wide long has an inductive component of about 25 nH. When the drive pulse width is 70 ns and the drive current is 20 A, a voltage drop of about 7 V occurs. This lowers the laser power and generates noise. It is important to select low-inductance components.

**Safety standard for laser beam.**—The laser sensor was designed on the basis of the IEC825 standard which dictates that sensors installed in vehicle must be "totally safe" and have a Class 1 rating. Devices (e.g., this device) that generate rays of short pulse-duration must satisfy the limit for laser radiation flux level based on the maximum permissible exposure (MPE). Increasing the diameter of the transmitted

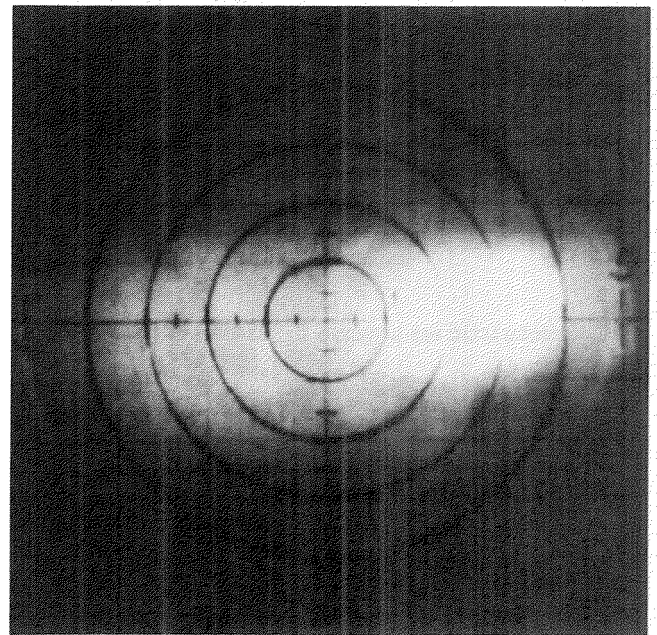


$\pm 1.4^\circ$  Beam



$\pm 0.5^\circ$  Beam

9(b). Beam cross-section pattern.



9(a). Beam shape.

Figure 9. Shape of beam transmitted from laser—set distance: 1m.

beam or the width of the transmit pulse raises the radiation flux level. When the aperture of the lens used is 34 mm and the pulse width is 70 ns, the permissible laser radiation flux level based on the MPE is 10 W. This means that at this level and below, the radiation is not harmful to the eye even if it should be pressed against the transmitting lens. The further the distance from the device, the higher the safety. For example, in the prototype the effect of the laser beam is

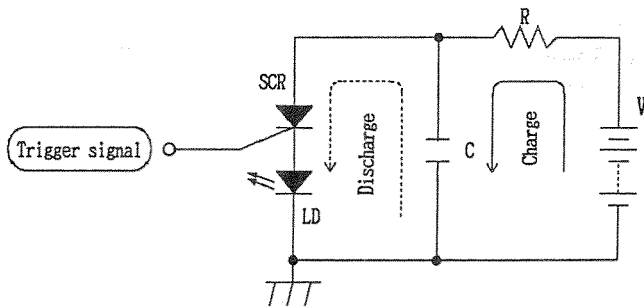


Figure 10. Laser diode pulse drive circuit.

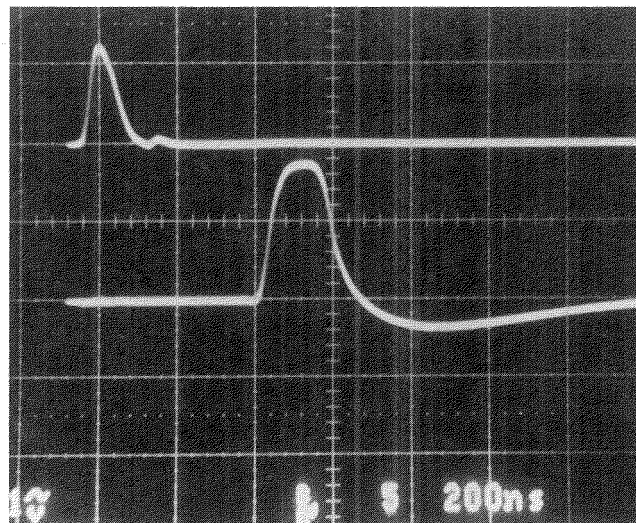
halved 1 m from the lens. Therefore, the prototype is a safe device conforming to the IEC regulations for a Class 1 device.

## Receiver

**Receiving optical block.**—Like the transmitting optical block, the receiving optical block uses a plastic Fresnel lens designed by Fujitsu Ten. The reflected light from the target passes through the aperture ( $100 \times 55$  mm) of the lens and is focused on the light receiving surface ( $1.1 \times 1.1$  mm) of a PIN photodiode. When the range to the target is 10 m or more, the incident light is nearly parallel. An ideal lens collects parallel rays at its focal point. However, the diameter of the spot where the rays are collected is increased by the spherical aberration and the diffraction due to the Fresnel pitch. The spherical aberration of the lens designed for this optical block is one-tenth that of the conventional Fresnel lens. This lens can focus almost the entire incident light beam on the light receiving surface. The lens between the Fresnel lens and the light receiving element can be designed so that the back error is about  $\pm 0.5$  mm and requires little adjustment when assembled. The infrared filter in front of the light receiving element suppresses external light such as the sun's rays. This suppresses the optical noise currents (shot noise), improving the performance of the receiving optical block.

**Receiving amplifier.**—Transmitted light can be regarded as a single pulse (pulse repetition rate: 2 ms, pulse width: 70 ns). Regenerating the pulse without loss requires an amplifier having a bandwidth larger than the half of the reciprocal of the pulse width. The receiver uses a wideband (10 MHz) amplifier.

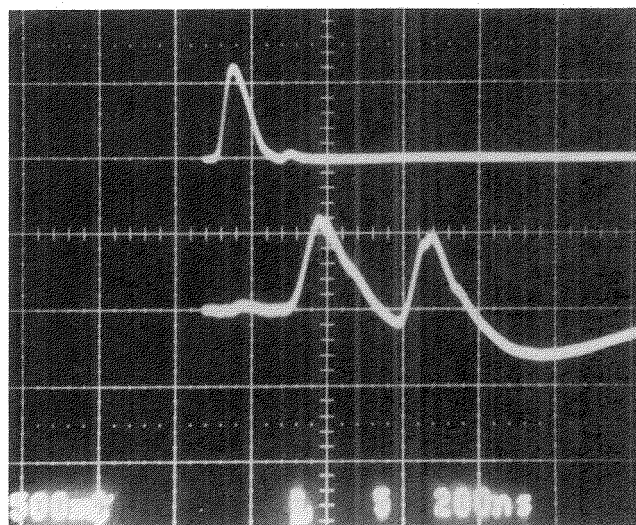
The received optical power can vary as much as 100 dB (figure 5). The dynamic range of the amplifier is about 30 dB. To absorb the level difference, the receiving amplifier has about 70 dB of automatic gain control (AGC). To prevent misdetection caused by dirt on the grille of the vehicle or by light reflected by rain or snow, the receiver amplifier also has a sensitivity time control (STC) circuit. This circuit is similar to that used in conventional radar receivers to increase the sensitivity of the receiver as the range to the target increases. Figure 11 shows examples of transmitted/received waveforms. The waveforms shown in (a) obtained when the reflector on the rear of the target vehicle was completely detected.



The reflector on the rear of a vehicle at a range of about 60 m was detected.

Figure 11(a). Example of transmitted/received waveforms.

The waveforms shown in (b) were obtained when one side of the rear of the vehicle and a wall further from the vehicle we detected, i.e., when the reflected light from multiple targets was received.



A vehicle at a range of about 20 m and a wall at a range of 60 m were detected at the same time.

Figure 11(b). Example of transmitted/received waveforms.

## Range pulse generating section

As shown by equation (1), a range of 1 m corresponds to 6.7 ns, the time difference ( $t$ ) between the transmitted wave and the received wave. To measure the time difference, an ECL counter and a 1-GHz clock are required. This block uses a special analog processing technique. In this technique, the time difference pulse width obtained with an RS flip-flop can be multiplied precisely. This enables the pulse width to be measured using clocks from a microcomputer.

Since the received signal is delayed by each signal processing block, there is an error in the time difference pulse. Since the error varies with the radar set due to the variation

in component tolerances, each set is self-correcting (correction 1, figure 7).

### Range calculating section

This section uses an 8-bit microcomputer to convert the transmission-reception time difference signal into range data. The range is measured at intervals of 2 ms, and the results are smoothed by taking the average of several intervals. If successive abnormal data is detected, the data to be sent to the radar ECU is invalidated, and an instruction is issued to prevent incorrect control.

Final range correction is performed. That is, a standard target is installed at a range of several meters, and the bias error included in the range data is corrected. Error caused by the difference in reception level is also corrected so that an abrupt change in the reflection cross section of the target does not lower the accuracy of detection.

Moreover, whether the sensor is normal is diagnosed by monitoring the transmitted and received signals.

Calculation information, including range data, is sent as serial data to the radar sensing cruise control ECU. The transmission rate is 7812 bps and data is updated at intervals of about 20 ms.

### Evaluation of Performance

Figure 12 shows the areas in which a target (20 × 20 cm reflector) can be detected. The width of the horizontal area is ±0.5 to 1 m; that of the vertical area is ±0.5 m or less. This difference is caused by the oblong beam pattern (figure 9) transmitted. The pattern is favorable because it is little affected by the light reflected from the road surface.

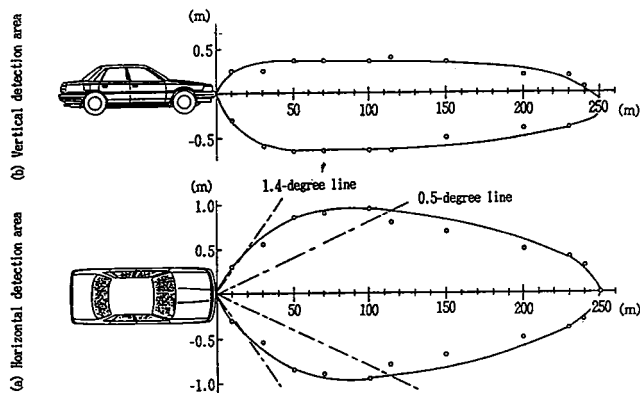


Figure 12. Detection area—target: 20 × 20 cm reflector.

When the range is 100 m or more, the width of the horizontal area gradually decreases within the area enclosed by the 0.5-degree line. That is, the power of the 1.4-degree beam is attenuated and the target is detected chiefly with the 0.5-degree beam. Figure 13 shows the detection limit characteristics for static targets. The rear of a vehicle can be detected at a range of about 350 m. Other targets can be detected at a range of 50 to 130 m. The data shows that the sensor ensures a sufficient detection area.

Figure 14 shows the accuracy of target (vehicle) detection. The detection error is 2 m or less when the

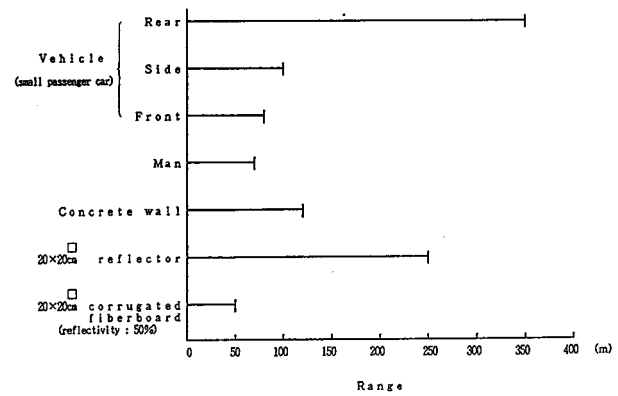


Figure 13. Detection limit ranges for static targets.

distance to the target is 100 m or less. Figure 15 shows an example of how the field test data. The data shown in (a) was obtained when the vehicle approached a concrete wall and receded from it at a fixed speed (5km/h). Lost targets (missing targets) occurred in the area where the range to the target was 60 m or more. The data shown in (b) was obtained with the vehicle pursuing a small truck. In this test, lost targets occurred when the range to the truck was 40 m or more. The vibration (pitch and roll) of the vehicle is thought to be the cause of the lost targets. A sufficient detection area cannot be ensured if vibration cannot be controlled. A countermeasure is to increase the angle of the transmit beam or to scan the beam. Increasing the angle causes a great loss in received power. If the angle is doubled, three-fourths of the received power will be lost. For targets other than the reflector on the rear of a vehicle, the detection limit range that depends on the equivalent noise power of the receiver should be taken into consideration.

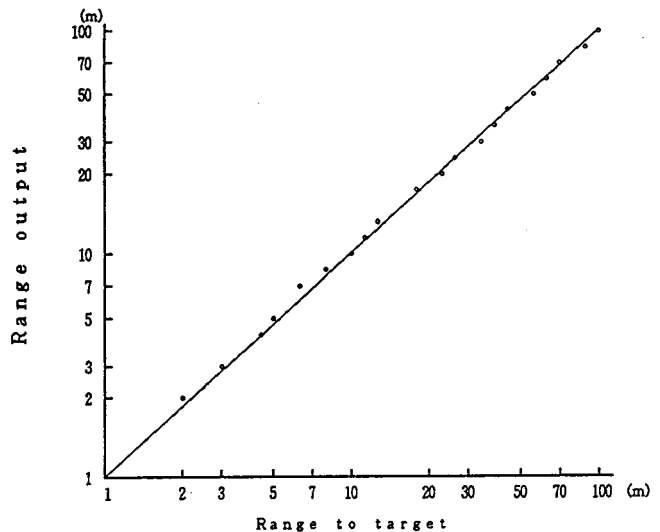


Figure 14. Range measuring accuracy—Target: reflector on the rear of a vehicle.

Scanning the beam enables the detection area to be expanded without sacrifice of the detection limit range. The beam may be scanned using a mirror or an ultrasonic wave. It is necessary to establish a high-stability scanning method.

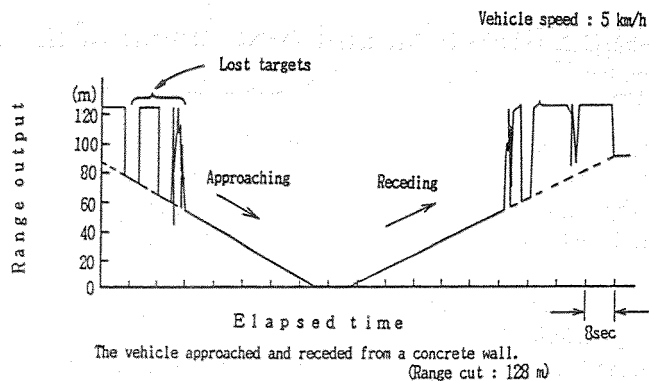


Figure 15(a). Example of obtained in field test.

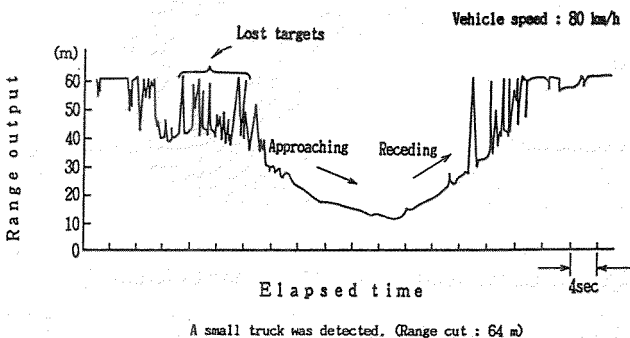


Figure 15(b). Example of obtained in field test.

Which of the two methods (increasing the beam angle or scanning the beam) is most effective should be checked by experiment. The data shown in figure 15(c) was obtained when the laser radar was detecting guardrails of a median strip while the vehicle was driven along a curve. It was difficult to distinguish such fixed objects from the vehicle by range output only. Therefore, the steering signal input to the radar ECU was used to recognize the curve, and the vehicle was run at a fixed speed to ensure stable control.

## Conclusion

Although there is room for performance improvement,

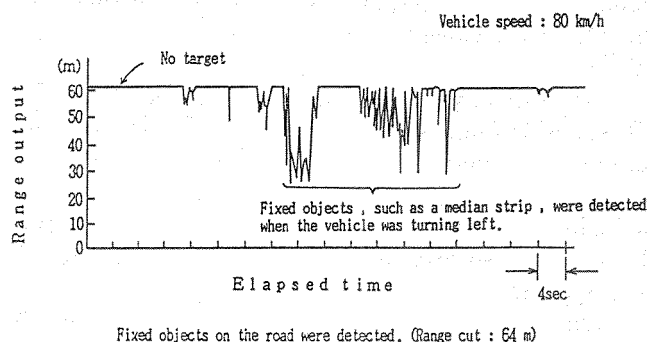


Figure 15(c). Example of obtained in field test.

the feasibility of the headway control using a laser was confirmed. Subjects to be tackled in the future are:

- The stability of the headway control should be improved by taking measures to prevent lost targets.
- The detection characteristic in rain or snow should be examined.
- Setting of the system control specifications for the features which reflect the laser should be examined.

We do not know how the public will receive our headway control system, but we think that it will effectively prevent accidents.

## References

- Nogami, et al., "Application of mm Wave Radar for Automotive," Fujitsu Ten Technical Report Vol. 2, No. 2, 1984.
- The Laser Society of Japan, "Laser Handbook," Ohm-Sha, 1982.
- D. Smith, "Electronic Distance Measurement for Industrial and Scientific Applications," HP Journal, Vol. 31, No. 6, 1980.
- S. Uda, "Exercise on Radar Engineering," Gakken-Sha, 1976.

# An Investigation on a Torque-Bias-Limited-Slip Differential and Assessment of its Influence on Vehicle Handling

Written Only Paper

**D. Rahani,**  
**A.J. Robertson,**  
Cranfield Institute of Technology, England

## Abstract

In recent years there has been a growing interest in the control of wheel spin under adverse road conditions. Some manufacturers are investigating complex control systems to limit or prevent wheel spin by integrating with the anti-lock brake systems. Other manufacturers are fitting limited slip differential mechanisms of various designs.

This paper contains an analysis of a particular type of Torque-Bias-Limited-Slip Differential, showing that for differential action to occur across the unit there must always be a difference of torque at the two output shafts. Parameters affecting this torque difference or Torque Bias Ratio (TBR) between the two shafts are evaluated and the most significant specified.

Verification of the analysis is obtained from measurements recorded on a 2.8 Ton Van fitted with the differential. The existence of the Torque Bias Ratio was established for a number of driving conditions.

Finally the magnitude of the yawing moment applied to the vehicle due to the Torque Bias Ratio is evaluated.

## Introduction

In recent years safari rallies and off-road racing have increased in popularity and the experience of these has highlighted the value of Anti-Spin Regulation (ASR). The benefits of maintaining drive traction and control of the vehicle under low coefficient of friction and differing coefficient of friction conditions become obvious. Lessons learned have been incorporated in road going two-wheel drive and four-wheel drive cars by fitting limited slip differentials. These differentials fall into three basic categories, (1) Mechanical Lock, where the two halves of the system are mechanically locked to form a solid axle (2) Viscous Coupling, where plates attached to each half-shaft rotate relative to each other in a viscous fluid (3) Friction Control where the geometry of the system generates high frictional forces.

The subject of this paper is one of type (3) relying on high friction forces to prevent wheel spin on one side of the system.

A vehicle travelling along a curved path requires the wheels on the side furthest from the centre of turn to rotate faster than those on the side closest to the centre. The magnitude of the difference between the rotations is relatively small in normal driving but can be quite large for parking manoeuvres or when negotiating obstacles. For an "open" differential such as one consisting of two sets of bevel gears the torques transmitted by each side of the

system are equal. The disadvantage of this equality is that if the torque to one wheel is reduced by low friction at the wheel/ground interface the torque on the other side is also reduced leaving little tractive force. But the advantage of equal torque means no yawing moment is applied about the vehicle centre of gravity.

A friction control limited slip differential on the other hand has the advantage that if the torque on one side of the system is reduced by low friction a higher torque can still be transmitted by the other wheel maintaining a reasonable total tractive force. The disadvantage however is the difference in torque and hence tractive effort between each side resulting in a yawing moment on the vehicle which is always present while differential action takes place. Therefore whenever the vehicle turns a corner a yawing moment is applied to the vehicle.

The particular type of differential used in this investigation was the Gleason Torsen (figure 1).

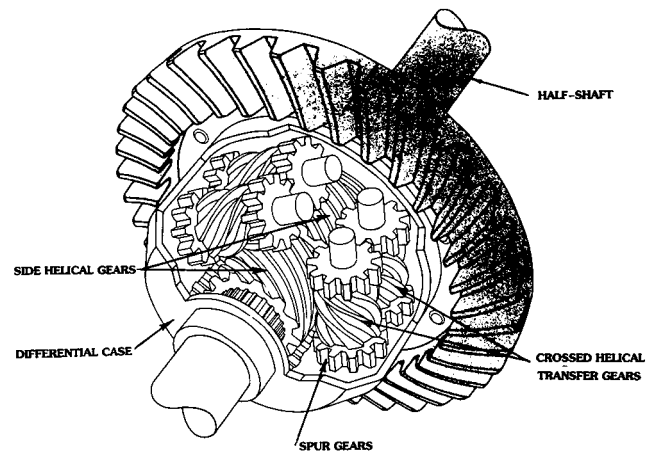


Figure 1. Construction details of a Torsen Differential.

## Torque-Bias Ratio

The ratio of the torque on one side of the differential relative to that on the other is known as the Torque-Bias Ratio (TBR). By definition we choose this value to be the higher torque divided by the lower and therefore TBR is always greater than unity.

We can explain how the TBR occurs by considering the differential used as a gearbox as shown in figure 2. After fixing the casing of the gears, rotate the right-hand shaft anti-clockwise with torque  $T_{WR}$  the left-hand shaft will rotate clockwise with a torque output  $T_{WL}$ . The diagram (figure 2) is shown with the left-hand shaft torque as the reaction torque i.e. the torque necessary to prevent or resist rotation. The reaction torque on the casing  $T_{RG}$  will be the sum of  $T_{WR} + T_{WL}$ . Because of the friction forces developed by the geometry of the differential the value of  $T_{WL}$  will be less than  $T_{WR}$ .

When the differential is used in an axle  $T_{RG}$  is the input

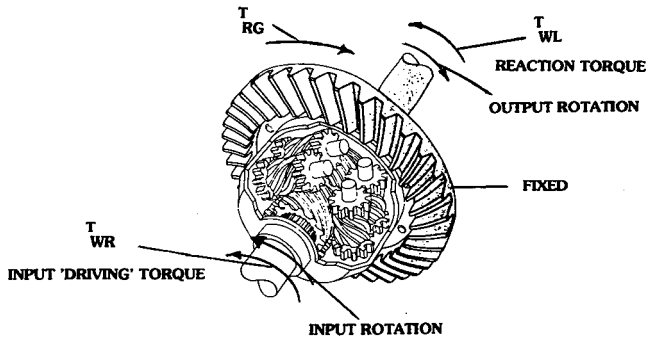


Figure 2. Differential used as a reversing gearbox.

torque from the ring gear while  $T_{WR}$  and  $T_{WL}$  are the right and left-hand wheel torques respectively, as occur when the vehicle is making a right-hand turn. Note that the wheel closest to the centre of the turn carries the largest torque. For a left-hand turn the left-hand wheel becomes the 'driving' side because the relative rotation is reversed, and has the higher torque.

To determine the value of the TBR we need to examine the forces generated at the gear contact points and determine the equations of statics for each of the gear wheels.

### Forces at right-hand helical gear

Consider the right-hand side helical gear attached to the right-hand half-shaft which in the situation shown in figure 2 is the input gear. Figure 3 illustrates the forces generated at the tooth contact point and the reaction thrust force at the left-hand face.

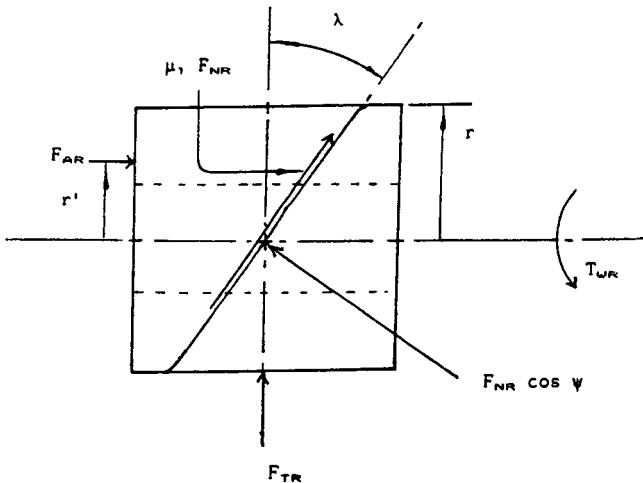


Figure 3. Free body diagram of right-hand helical gear.

The tangential (circumferential) reaction force

$$F_{TR} = 3 F_{NR} A \quad (1)$$

There are 3 transfer gears in contact with the side helical gears. As these are equally spaced around the side helical gear no resultant radial load occurs on the side gear.

The Axial force

$$F_{AR} = 3 F_{NR} B \quad (2)$$

The torsion equation is

$$F_{TR} r + \mu_2 F_{AR} r' = T_{WR} \quad (3)$$

Combining these equations we can express the normal force at the gear contact points

$$F_{NR} = \frac{T_{WR}}{3(Ar + \mu_2 B r')} \quad (4)$$

### Forces at right-hand crossed helical transfer/spur gears

The normal forces and friction forces generated at the tooth contact points by the right-hand side helical gear are applied to the three right-hand crossed helical transfer gears. Figure 4 shows these forces and the reaction forces on the spur gears and end thrust face.

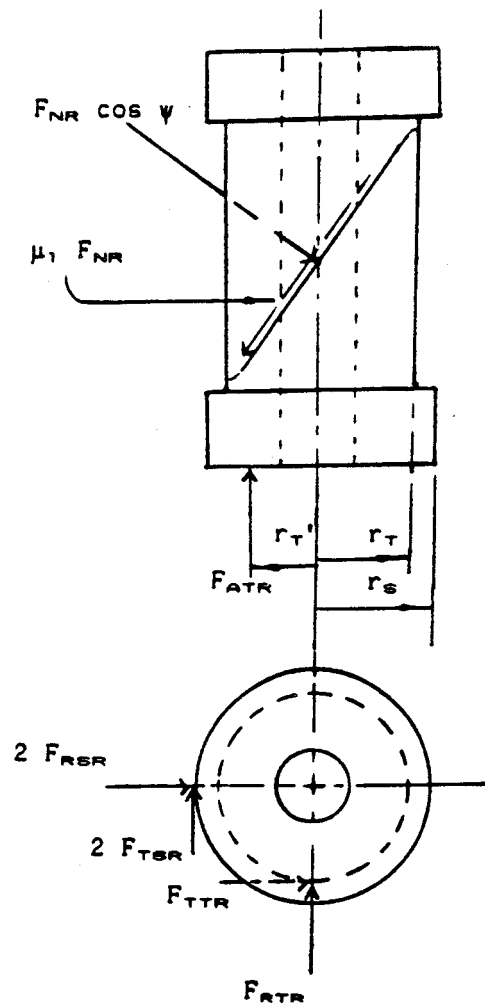


Figure 4. Free body diagram of right-hand transfer gear.

Tangential force on the right-hand crossed helical transfer gears

$$F_{TTR} = F_{NR} B \quad (5)$$

Axial force on end thrust face

$$F_{ATR} = F_{NR} A \quad (6)$$

Separating force on crossed helical gears

$$F_{RTR} = F_{NR} \sin \Psi \quad (7)$$

The tangential force on each of the two spur gears attached to the crossed helical transfer gear is obtained from

$$F_{TSR} = \frac{F_{TTR} r_T}{2 r_s} \quad (8)$$

hence the normal force on the spur gear

$$F_{NSR} = \frac{F_{TSR}}{\cos \Psi_s} \quad (9)$$

and the separating force on the spur gear

$$F_{RSR} = F_{NSR} \sin \Psi_s \quad (10)$$

From the tangential and normal forces on the crossed helical gear and spur gears we can determine the radial load on the shaft and supporting journals

$$F_{RR} = [(F_{TTR} + 2 F_{RSR})^2 + (F_{RTR} + 2 F_{TSR})^2]^{1/2} \quad (11)$$

Hence the friction torque on each crossed helical/spur gear assembly can be found

$$T_{FTR} = \mu_3 F_{ATR} r'_r + \mu_4 F_{RR} \frac{d_p}{2} \quad (12)$$

The torque output from the right-hand spur gears must be the input torque to the crossed helical gear less the friction torque

$$T_{OS} = F_{TTR} r_T - T_{FTR} \quad (13)$$

We ignore any losses in the meshing of the spur gears as these will be small so the input to the left-hand crossed helical/spur gear assembly will be equal to  $T_{OSE}$ .

The Left-Hand Crossed Helical Transfer/Spur Gears can be examined in a similar way while the main forces acting on the assembly are shown in figure 5. For brevity we will not list all the equations here.

The forces generated at the crossed helical gears transmit the driving torque to the left-hand helical gear attached to the left-hand half-shaft.

The Forces at the Left-Hand Helical Gear are shown in figure 6. Again as there are three gears equally spaced around the side gear no resultant radial load exists. However it is most interesting to note that the left-hand side helical gear is forced to the left by the thrust  $F_{AR}$  from the right-hand side wheel and by the axial component of the gear tooth force resulting in  $F_{AL}$  the left-hand axial force being high. Hence the frictional torque is very high. There is a friction torque generated at the right side  $\mu_2 F_{AL} r'$  and also at the left  $\mu_2 F_{AL} r'$ .

$$\text{The axial force } F_{AL} = 3 F_{NL} C + F_{AR} \quad (14)$$

$$\text{The friction torque } T_{FL} = \mu_2 F_{AR} r' + \mu_2 F_{AL} r' \quad (15)$$

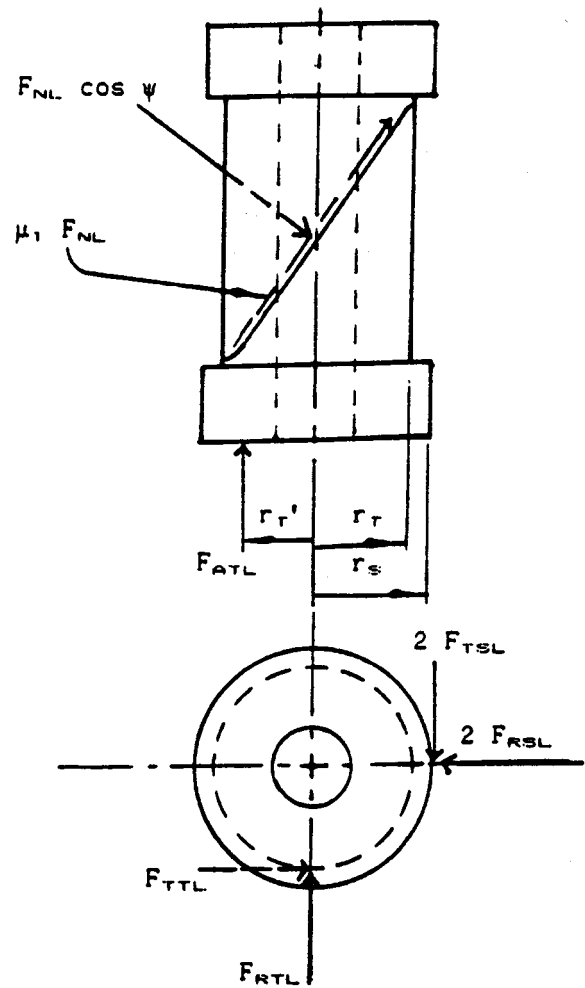


Figure 5. Free body diagram of left-hand transfer gear.

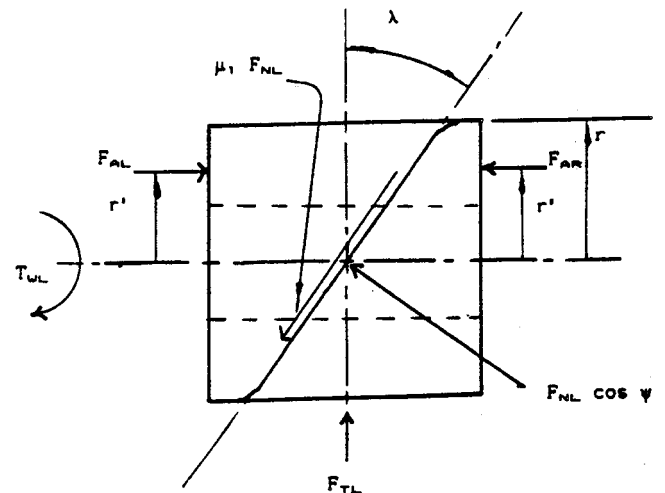


Figure 6. Free body diagram of left-hand helical gear.

$$\text{The input torque } F_{TL} r = 3 F_{NL} D r \quad (16)$$

The output torque to the left-hand half-shaft must equal the input torque less the friction torque.

$$T_{WL} = 3 F_{NL} D r - \mu_2 F_{AR} r' - \mu_2 F_{AL} r' \quad (17)$$

$$\text{Now the Torque Bias Ratio (TBR)} = \frac{T_{WR}}{T_{WL}}$$

and can be expressed in terms of the many parameters as follows:

$$\begin{aligned} \text{TBR} = & \{ \{ D r - \mu_2 C r' \} \times \{ B r_T - \mu_3 A r_T' \} \\ & - \mu_4 \frac{d_p}{2} \left[ B^2 \left( 1 + \frac{r_T \tan \psi_s}{r_s} \right)^2 + \left( \sin \psi + B \frac{r_T}{r_s} \right)^2 \right] \} + \\ & \{ A r + \mu_2 B r' \} \times \{ C r_T + \mu_3 D r_T' \} \\ & + \mu_4 \frac{d_p}{2} \left[ C^2 \left( 1 - \frac{r_T \tan \psi_s}{r_s} \right)^2 + \left( \sin \psi - C \frac{r_T}{r_s} \right)^2 \right] \} \\ & - \frac{2 \mu_2 B r'}{(A r + \mu_2 B r)} \}^{-1} \dots (18) \end{aligned}$$

## Parametric Study

As seen in the previous section there are many parameters in the TBR so the equations were assembled into a computer program so that a parametric study could be made to determine the most important parameters. The differential functions primarily by the lead angle of the helical gears generating axial forces which cause high thrust reactions and high friction torques.

The geometry of the Torsen Differential was taken from the actual unit that was tested except that gear tooth pressure angles were estimated.

Coefficient of Friction at Crossed Helical Gear Teeth was varied from 0 to 0.30 and the variation in TBR is shown in figure 7. The nominal coefficient of friction for steel on steel gear teeth can be of the order of 0.18 which would give a TBR of 10. This value would occur if the relative sliding velocity is very low which is the condition occurring in the differential.

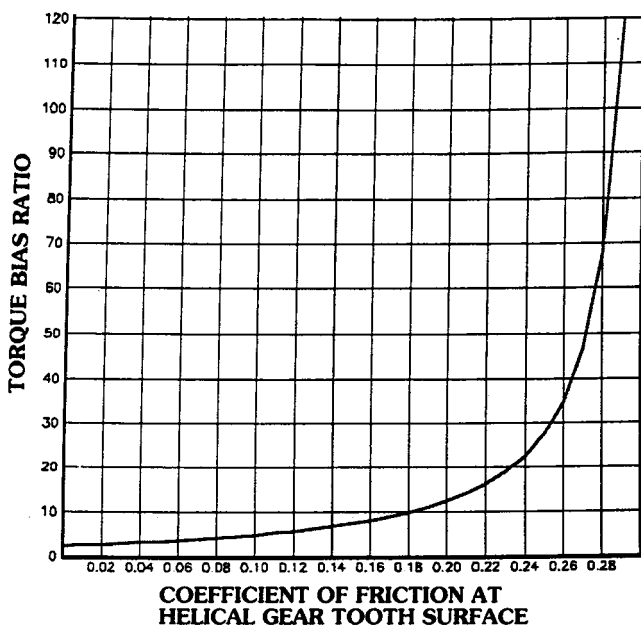


Figure 7. Variation of torque bias ratio with coefficient of friction at crossed helical gear teeth.

Examination of figure 7 shows that with a variation of coefficient of friction at the teeth from 0.1 to 0.2 which

could occur in practice gives TBR from 5.0 to 12.0. If the friction coefficient were to rise to 0.3 the TBR rises to over 100 and the system would effectively lock-up. All the drive is taken by one wheel only—the inner wheel closer to the centre of turn.

Coefficient of Friction at the Side Helical Gear Thrust Face shows an even more dramatic rise in TBR, figure 8. When the friction coefficient is as low as 0.18 the TBR is over 100 and hence the differential has effectively locked-up and will drive on one wheel only.

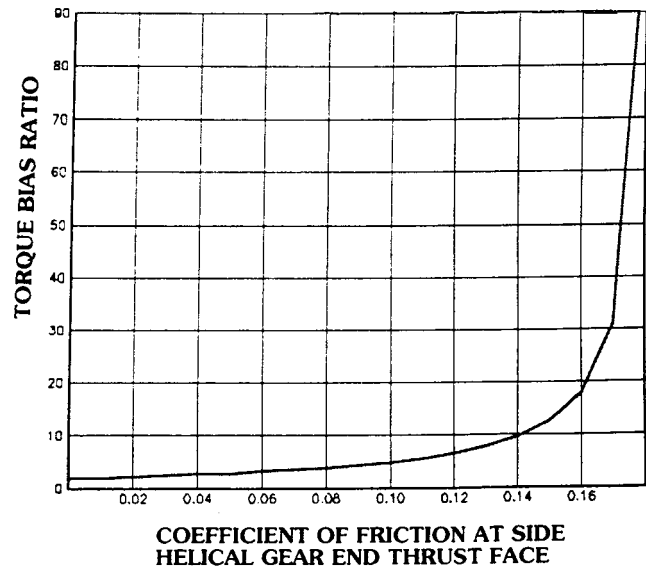


Figure 8. Variation of torque bias ratio with coefficient of friction at side helical gear end thrust face.

The Lead Angle of the Helical Gears is very much in the control of the designer. Figure 9 shows the effect of varying the lead angle between 25° and 75°. When the angle is 25° i.e. the gear is approaching a worm gear, high TBR occurs, while the minimum TBR is given by a lead angle of about 52°. Large lead angles of 75° will result in the helical gears approaching straight spur gears and high end thrust will occur on the transfer gears which approximate to worm gears, reducing the overall efficiency. It is interesting to note that the range of lead angles from 40° to 60° have little influence on the TBR.

## Experimental Tests

A Torsen Differential unit was adapted to fit the Bedford CF2 van shown in figure 10. The adaptations consisted of a ring for mounting the final drive ring gear and sleeves for the support bearings—the Torsen unit was designed for a smaller axle unit.

These modifications were necessary for installation purposes in the available vehicle but of course did not affect the function of the unit. The primary aim of the experimental tests was to verify that the predicted Torque Bias Ratio (TBR) occurred during various turning conditions of the vehicle. Three types of test were conducted, simple steady state turns at various speeds and

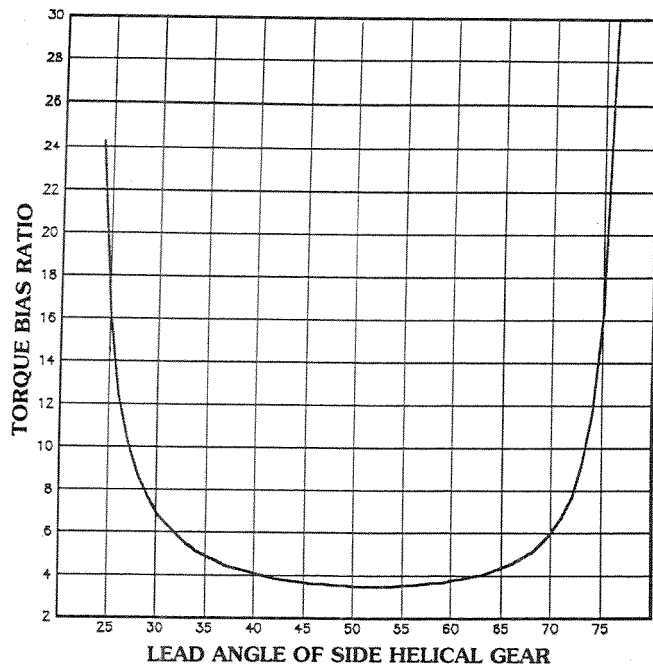


Figure 9. Variation of torque bias ratio with lead angle of side helical gear.



Figure 10. Bedford CF2 Van with Torsen Differential and instrumentation.

radius of turn, lane manoeuvres and turns on a Hill Climb when the torque throughput is relatively higher.

### Steady state turns

The greatest speed ratio between the outer and inner wheels on the axle will occur when the vehicle is turned on full lock. Figure 11 shows the measured wheel torques and speed when the vehicle was travelling at a nominal speed of 3 m/s (10.8 km/h) at full right-hand lock.

The lower graph shows the right-hand (inner) wheel torque at 450 N-m with the left-hand (outer) wheel transmitting about 45 N-m, hence the TBR is approximately 10. The upper graph shows the speed ratio of outer to inner wheel of 1.43.

An interesting observation from this result is the oscillations on both the speed and torque signals from the right-hand or inner wheel indicating vibrations probably caused by a stick-slip action in the differential mechanism. Alter-

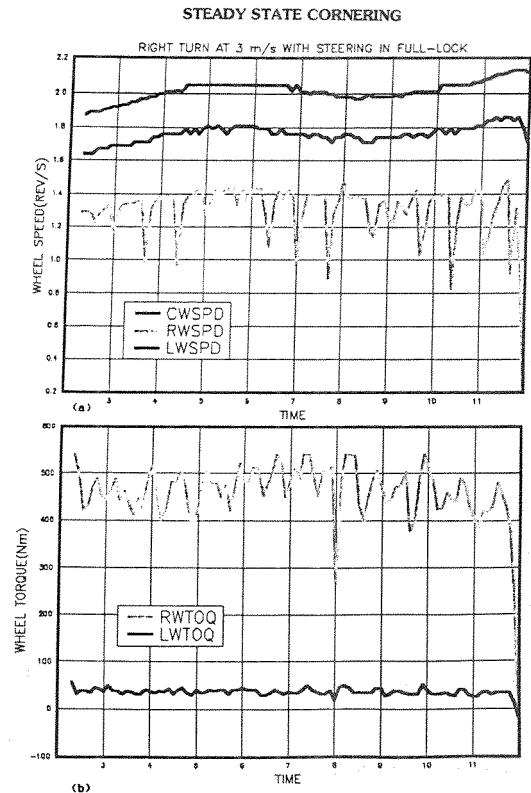


Figure 11. Right turn at 3 m/s with steering in full lock.

natively the inner tyre may have been stick/slipping on the road surface.

Results taken at a higher speed of 6 m/s (21.6 km/h) on a 20m radius of turn are shown in figure 12. The left-turn results show a Torque Bias Ratio (TBR) of approximately 4.5 while the right-turn results show virtually zero torque being transmitted by the outer left-hand wheel i.e. all the tractive effort is transmitted by the inner wheel. Oscillations in both the speed and torque of the inner wheel were again observed for both directions of turn.

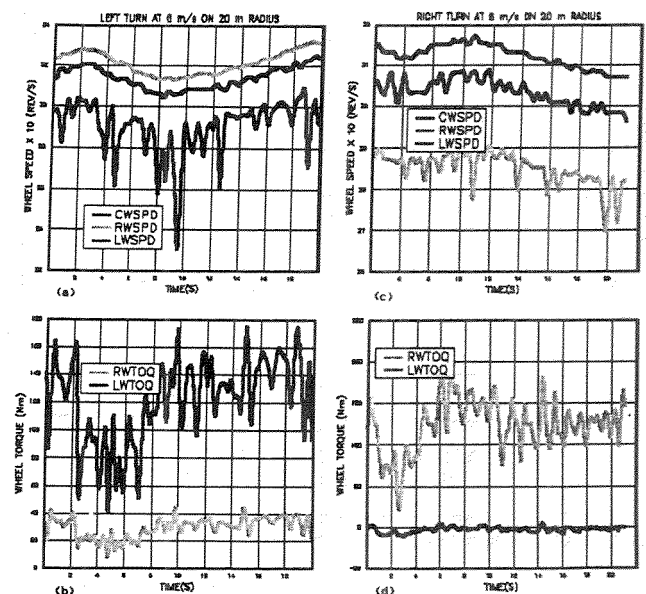


Figure 12. Left and right turns at 6 m/s on a circle of radius 20m.

## Lane change manoeuvres

This test was carried out on a gradient of 7.2% with a turn to the right, a short straight, a second turn to the right followed by a turn to the left. The turns were typical of turns on hilly roads and so the relative speeds of the two wheels differed by only small amounts (figure 14 top graph).

The torques in each drive shaft varied considerably with the Torque Bias Ratio at 11 for right-hand turns and 4.5 for left-hand turns.

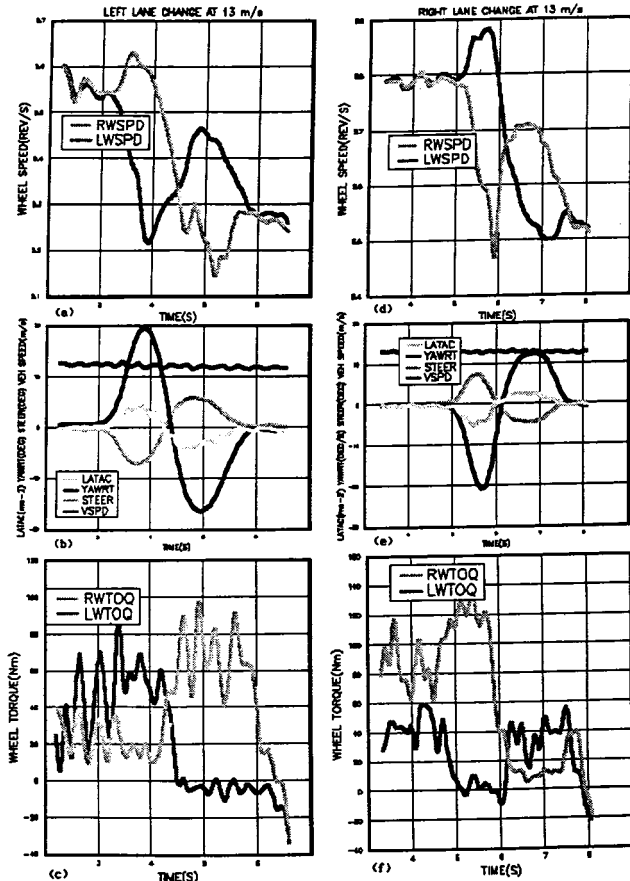


FIGURE 13. Left and Right Lane Change Manoeuvre at 13 m/s.

Figure 13. Left and right lane change manoeuvre at 13 m/s.

## Yawing moment of vehicle

The sections on the theoretical analysis and the practical test results have both shown that when differential motion occurs the torque transmitted by the two wheels differs by the TBR. Both theoretical and practical results show the higher torque is transmitted by the wheel closer to the centre of turn. This will result in a yawing moment applied to the vehicle tending to turn the vehicle out of turn i.e. make the vehicle tend to understeer.

The highest torque difference measured during the tests occurred on the hill climb when the inner and outer wheel torques were 540 N-m and 40 N-m respectively. This vehicle has a track of 1.646 m which results in a Yawing Moment = 410 N-m. With a wheelbase of 3.2 m the change in side force generated at the front and rear axles will be 128 N. Tyre Cornering Stiffness for the tyres fitted to this vehicle

will be of the order of 1000 N/degree of slip angle. Therefore changes in tyre slip angle due to the Yaw Moment caused by the TBR of the differential will be only about 0.128 degrees which will cause only small changes in vehicle handling characteristics.

## HILL CLIMBING TEST RESULTS

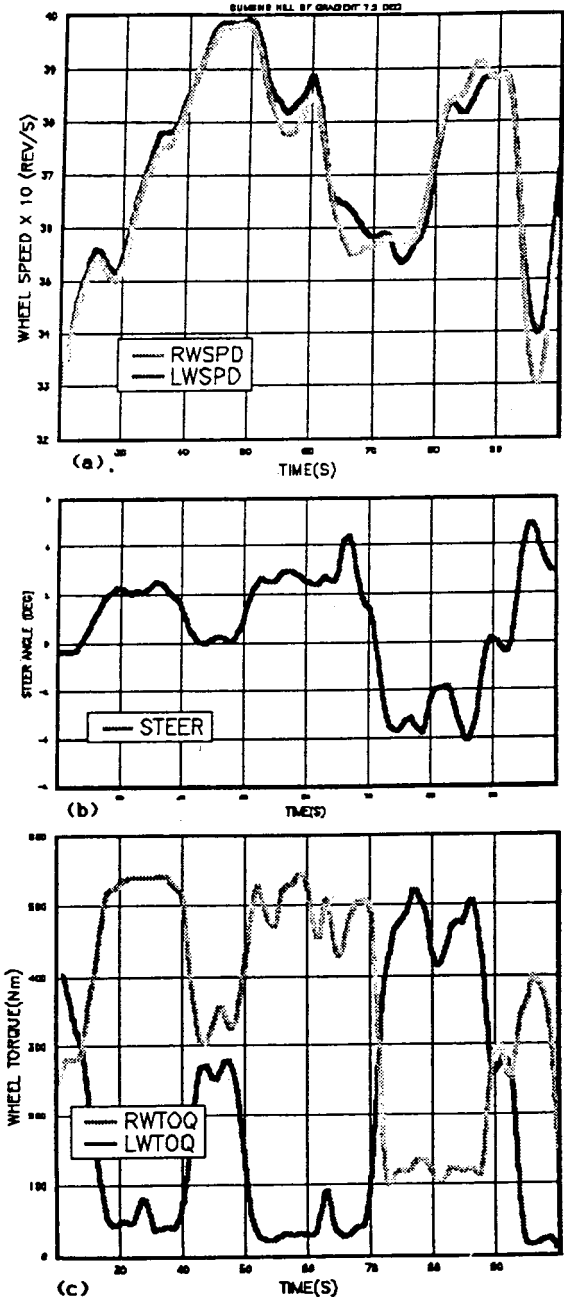


Figure 14. Hill Climbing test on a gradient of 7.2%.

Tests at high lateral accelerations were not conducted. Further investigations are required to determine the conditions that will cause the torque to transfer from the inner wheel to the centre of turn to the outer wheel due to weight transfer from the inner wheel caused by increasing lateral acceleration. There may be a condition when the understeer-

ing Yaw Moment reverses to become an oversteering Yaw Moment.

## Conclusions

The investigations have proved both theoretically and practically that for all conditions of turning when relative rotation occurs across the differential there is a higher torque on the wheel closer to the centre of turn. The TBR is dependent upon many parameters but is influenced mainly by the Lead Angle on the helical side gears, and the coefficients of friction at the end faces of the side helical gears and at the gear teeth. Under normal driving conditions the TBR causes an understeering Yawing Moment on the vehicle which has little influence on the vehicle handling characteristics. Further investigations are required for extremes of cornering condition.

## Reference

D. Rahani, Analysis and Measurement of Torque-Bias and Speed Difference of a Limited Slip Differential. Cranfield Institute of Technology, M.Sc. Thesis, 1988.

## Notation

$d_p$	Diameter of transfer gear shaft
$F_{AL}$	Axial force on left hand helical gear
$F_{AR}$	Axial force on right hand helical gear
$F_{ATL}$	Axial force on left hand crossed helical gear
$F_{ATR}$	Axial force on right hand crossed helical gear
$F_{NL}$	Normal force on left hand helical gear
$F_{NR}$	Normal force on right hand helical gear
$F_{NSR}$	Normal force on right hand spur gear
$F_{RR}$	Resultant force on right hand transfer gear shaft
$F_{RSL}$	Radial separating force on left hand spur gear
$F_{RSR}$	Radial separating force on right hand spur gear
$F_{RTL}$	Radial separating force on left hand transfer crossed helical gear
$F_{RTR}$	Radial separating force on right hand transfer crossed helical gear

$F_{TL}$	Tangential force on left hand helical gear
$F_{TR}$	Tangential force on right hand helical gear
$F_{TSL}$	Tangential force on left hand spur gear
$F_{TSR}$	Tangential force on right hand spur gear
$F_{TTL}$	Tangential force on left hand transfer crossed helical gear
$F_{TTR}$	Tangential force on right hand transfer crossed helical gear
$r$	Pitch circle radius of helical gear
$r'$	Effective friction radius on helical gear end thrust face
$r_s$	Pitch circle radius of spur gear
$r_T$	Pitch circle radius of transfer worm wheel
$r_T'$	Effective friction radius of crossed helical transfer/spur gear end thrust face
$T_{FL}$	Friction torque on left hand helical gear
$T_{FTR}$	Friction torque on right hand crossed helical transfer/spur gear
$T_{OSR}$	Output torque on right hand spur gear
$T_{WL}$	Left hand wheel torque
$T_{WR}$	Right hand wheel torque
TBR	Torque bias ratio
$\lambda$	Lead angle of helical gear
$\mu_1$	Coefficient of friction at helical gear tooth surface
$\mu_2$	Coefficient of friction at helical gear end thrust faces
$\mu_3$	Coefficient of friction at crossed helical transfer/spur gear end thrust face
$\mu_4$	Coefficient of friction at crossed helical transfer/spur gear journal bearing
$\Psi$	Pressure angle of crossed helical gears
$\Psi_s$	Pressure angle of spur gear

For brevity the following symbols used are:

$$A = \cos \Psi \sin \lambda + \mu_1 \cos \lambda$$

$$B = \cos \Psi \cos \lambda - \mu_1 \sin \lambda$$

$$C = \cos \Psi \cos \lambda + \mu_1 \sin \lambda$$

$$D = \cos \Psi \sin \lambda - \mu_1 \cos \lambda$$

## Analysis of Optimum Low-Beam Illumination Pattern Based on Human Visual Perception Characteristics

Written Only Paper

Yasutoshi Seko, Tomoko Saito,  
Haruhiko Iizuka

Vehicle Research Laboratory, Central  
Engineering Laboratories, Nissan Motor Co.,  
Ltd.

### Abstract

An analysis was made of the factors influencing the driver's subjective judgment of illumination pattern quality for

the purpose of determining the optimum illumination pattern of low-beam headlamps. The results indicated that obstacle visibility distance is not the only factor influencing the driver's judgment of the quality an illumination pattern. The perceived brightness of the road surface, especially in zones near the vehicle and at an intermediate distance, was also found to have a large effect on the driver's judgment.

This paper first describes a new methodology for simulating low-beam illumination patterns which employs an image processing system. It then presents an analysis of

perceived brightness and describes an attempt to devise a brightness quantification method.

## Introduction

In order to determine the optimum low-beam illumination pattern for nighttime driving, it is necessary to clarify what illumination conditions are needed by the driver for good visibility. A considerable amount of research has already been carried out concerning this subject. Typical examples of the work done to date include analyses of visibility distance for recognizing obstacles or pedestrians in the road ahead. These analyses have been based on human visual perception characteristics, such as the ability to distinguish differing degrees of luminance.

The aim of this work was to clarify the optimum illumination pattern for low-beam headlamps by analyzing the illumination conditions perceived to be necessary by the driver as seen from the driver's seat. As the first step in this research, a methodology for simulating illumination patterns was developed for use in evaluating the illumination patterns of low-beam headlamps. With this methodology, various road surface luminance patterns are first calculated by computer simulation. These patterns are then synthesized with a background photograph of a real-world landscape using an image processing system. As the second step, the new methodology was used to analyze different road surface luminance patterns.

## Illumination Pattern Simulation Using Image Processing System

Evaluations of low-beam illumination patterns are usually carried out in nighttime driving tests using actual vehicles. This approach by itself, however, is rather inefficient and it is not easy to construct various illumination patterns for confirming how well the driver can see the road.

To overcome these problems, we have developed a methodology for simulating illumination patterns using an image processing system. This methodology makes it possible to create and display different types of forward visibility conditions on a CRT screen.

## Outline of Illumination Pattern Simulation

### Incorporation of background photograph

A daytime photograph of a forward scene as viewed from the driver's eye point (1) in (figure 1) was first input into the image processing system (Nexus 6510). Daytime luminance distribution data,  $L_D(XS, YS)$ , were then found from a shading pattern image of the photograph. Here,  $(XS, YS)$  indicates the coordinate system on the CRT screen (figure 2).

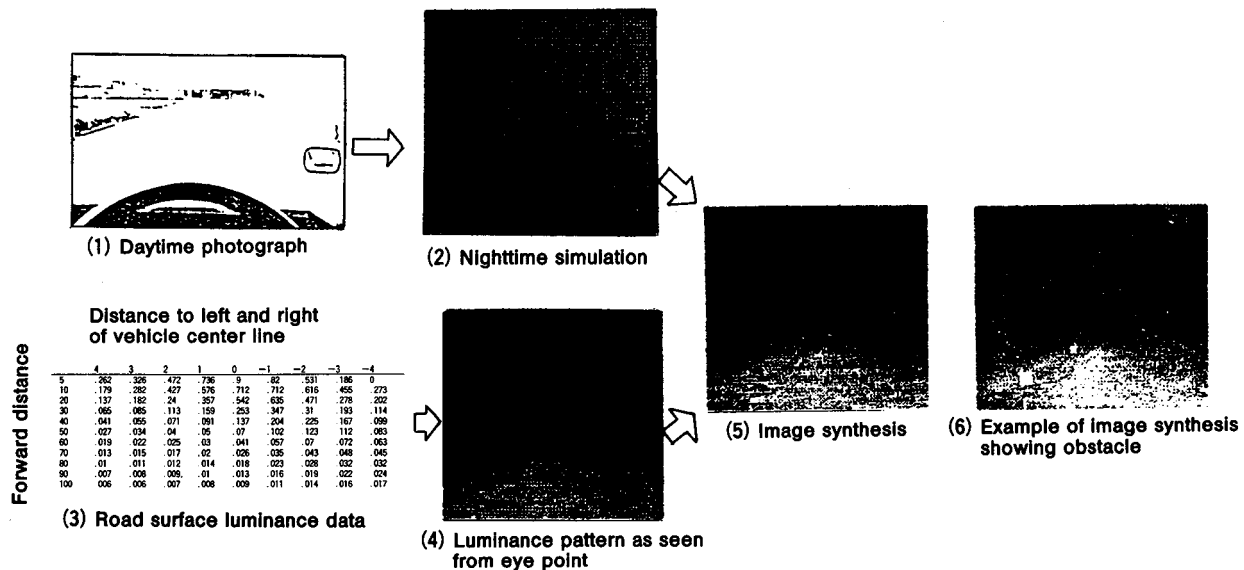


Figure 1. Simulation of illumination patterns using image processing system.

### Simulation of daytime background image

The daytime luminance distribution data,  $L_D(XS, YS)$ , found in paragraph above were multiplied by a coefficient to reduce the overall luminance level. This resulted in luminance distribution data,  $L_{NS}(XS, YS)$ , for a background image that simulated a nighttime driving condition (2) in (figure 1).

$$L_{NS}(XS, YS) = k \times L_D(XS, YS) \quad (1)$$

where,  $k$  is a coefficient.

### Calculation of road surface luminance values

Simulations were performed to calculate illuminance distribution data,  $E(x, y)$  and road surface luminance distribution data,  $L(x, y)$ , from headlamp luminous intensity distri-

bution data,  $I(\theta, \phi)$  and the installation position of the headlamps and the angle of the optical axis ((3) in figure 1).

$$E(x, y) = f(I(\theta, \phi))$$

where,  $\theta$  is the horizontal angle of the luminous intensity output of the headlamps and  $\phi$  is the vertical angle of the luminous intensity.  $(x, y)$  are the coordinates of a distance coordinate system, which has as its starting point the center line of the vehicle. This point is at the front-end of the vehicle when the vehicle and the road surface are viewed from above.  $x$  is the distance to the left and right from the center of the vehicle front-end (left = minus; right = plus), and  $y$  is the distance in the forward direction from the vehicle front-end (figure 2).

$$L(x, y) = \alpha \times \beta \times E(x, y) \quad (2)$$

where,  $\alpha$  is the coefficient of luminance reflected back from the road surface and  $\beta$  is the transmissivity of the windshield.

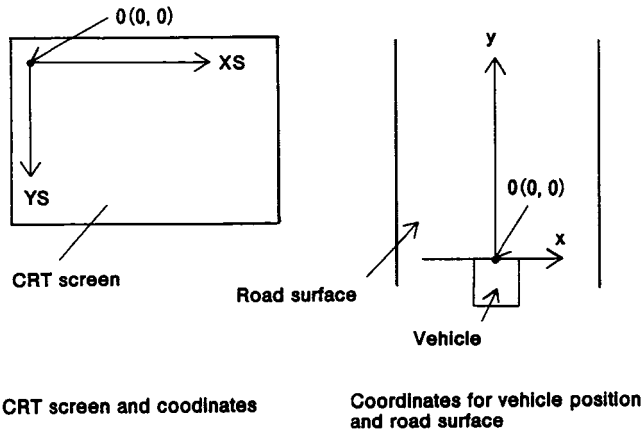


Figure 2. Coordinate system on CRT screen and coordinate system for actual distance.

A coordinate conversion operation was then performed on the coordinates of the road surface luminance distribution data,  $L(x, y)$ , to translate them to the luminance distribution data of the coordinate system on the CRT screen,  $L(XS, YS)$ . The purpose of this operation was to generate image data corresponding to the road visibility as seen from the driver's eye point (4) in (figure 1).

$$L(XS, YS) = F(L(x, y))$$

### Calculation of road surface coefficient

Road surface brightness in the real world undergoes subtle and irregular changes caused by road surface irregularities. A synthesized image, generated by simply adding the background luminance distribution data,  $L_{NS}(XS, YS)$ , found with equation (1) and road surface luminance distribution data,  $L(XS, YS)$ , found with equation (2), is not capable of indicating such delicate changes. Thus it would not provide a realistic depiction of a road surface illuminated by headlamps at night. In order to create such irregular changes in road surface brightness, a road surface coefficient,  $r(XS, YS)$ , was devised. This was done by finding the distribution of the relative luminance ratio for each CRT screen pixel from road surface luminance distribution data of the background image.

Based on the road surface luminance distribution data,  $L(XS, YS)$  found with equation (2) and the road surface coefficient,  $r(XS, YS)$ , road surface luminance distribution data,  $L_{Nr}(XS, YS)$ , were found for the synthesized image. That result was then added to the background luminance distribution data,  $L_{NS}(XS, YS)$ , to synthesize an image of the road surface ahead when illuminated by the headlamps at night ((5) in figure 1).

### Image synthesis

The luminance distribution data,  $L_N(XS, YS)$ , of the synthesized image of the road surface ahead can be given as

$$L_{Nr}(XS, YS) = L(XS, YS) \times r(XS, YS)$$

The luminance distribution data,  $L_N(XS, YS)$ , of the synthesized image of the road surface ahead can be given as

$$L_N(XS, YS) = L_{Nr}(XS, YS) + L_{NS}(XS, YS)$$

### Obstacle image synthesis

The size and reflectivity of an obstacle and the coordinates of its position  $(x, y)$  were also input into the image processing system. Luminous intensity values for the obstacle were determined from the luminous intensity distribution data for the headlamps. An image containing the obstacle was then synthesized using the same procedure as outlined above. As a result, this made it possible to display an obstacle in front of the vehicle, in addition to the road surface.

An example of a synthesized image showing an obstacle is illustrated in (6) in figure 1. The obstacle used was the target recommended by the International Illumination Committee (CIE), having dimensions of 20 cm  $\times$  20 cm and a reflectivity of 5%.

### Comparison of road surface luminance distribution of synthesized image and that found from luminous intensity distribution data

Figure 3 compares the road surface luminance data, calculated by simulation from the luminous intensity distribution data, and the luminance data of the synthesized image shown on the CRT screen. It is seen that the two sets of luminance data show good agreement. This result indicates that the image obtained in the illumination pattern simulation using the image processing system is capable of simulating the nighttime road surface luminance distribution.

### Analysis of low-beam illumination patterns

Four types of illumination patterns were found by simulation for low-beam headlamps currently in use. These patterns were for different road surface illumination zones ranging from a zone immediately in front of the vehicle to a distant zone. In each case, it was assumed that the luminous flux was the same and that the headlamps illuminated a lane

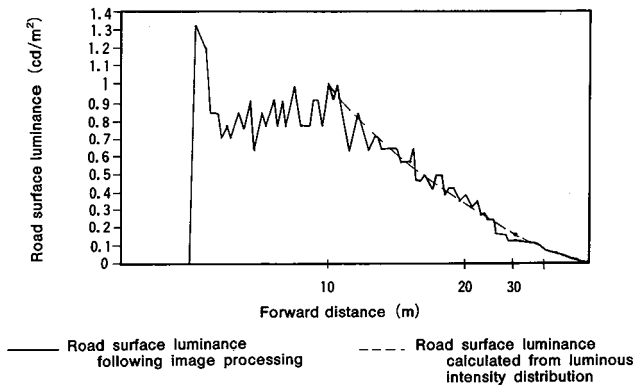


**Figure 3. Comparison of road surface luminance calculated from luminous intensity distribution and road surface luminance found with image processing system.**

width of two meters to the left and right of the vehicle's center line. Images were then synthesized and shown on the CRT screen for evaluation of the low-beam illumination patterns. An analysis was made of the factors thought to influence the evaluation of the optimum low-beam illumination pattern.

The characteristics of the four types of illumination patterns are outlined in table 1. Road surface luminance data are shown in figure 4 for a zone immediately in front of the vehicle (one meter to the left and right) and examples of the road surface illumination patterns displayed on the CRT screen are shown in figure 5.

**Table 1. Characteristics of various illumination patterns.**

Pattern	Characteristics
A	Luminance gradient is twice as great as that of pattern B
B	Has a luminance gradient equal to that of current low-beam headlamp
C	Ease of obstacle recognition is virtually the same for different forward distance
D	Luminance gradient is twice as great as that of pattern C

### Subjective evaluation of illumination patterns

The different illumination patterns of low-beam headlamps result in different feelings of brightness in the road surface ahead that are generally perceptible to drivers. In this work, it was assumed that this perceived feeling of brightness also affected the driver's subjective judgment of the quality of the illumination pattern, in addition to obstacle visibility difference. The following experiment and analysis were carried out to examine this assumption.

In the experiment, the four types of illumination patterns were shown on the CRT screen to six subjects. The subjects were asked to evaluate the quality of the illumination pattern, obstacle visibility distance and brightness of the road surface. The evaluation of road surface brightness included the perceived brightness of the entire road surface as well as that for three different zones: a near zone (8 ~ 20 m) an intermediate zone (20 ~ 40 m) and a far zone (40 ~ 100 m).

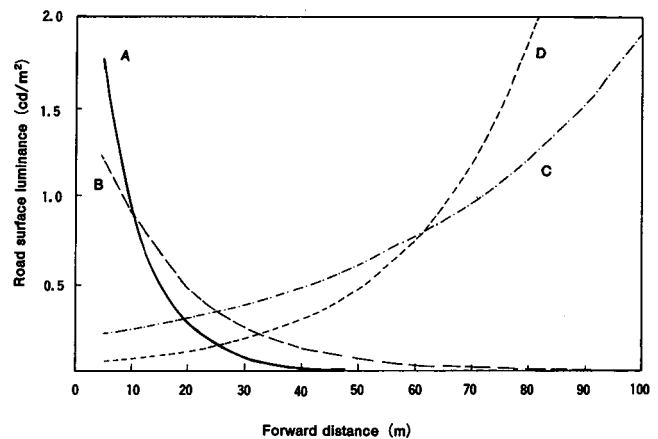


**Figure 4. Road surface luminance level for various illumination patterns.**

### Obstacle Visibility

The subjects were shown an image containing an obstacle on the road in front of the vehicle and were asked to indicate the visibility distance. As mentioned earlier, the obstacle was a target 20 cm X 20 cm in size and with 5% reflectivity. The visibility distance with pattern A was approximately 30 m, with pattern B approximately 50 m and with patterns C and D more than 70 m. The subjects indicated that patterns C and D provided a greater visibility distance than pattern A or pattern B. On the other hand, in their evaluations of illumination pattern quality, pattern B received the highest rating followed by pattern C. Patterns A and D received the lowest ratings.

The relationship between obstacle visibility distance and illumination pattern quality is shown in figure 6. It is seen that the rating of illumination pattern quality has a low correlation with obstacle visibility distance. This result suggests that the optimum low-beam illumination pattern cannot be determined solely on the basis of an evaluation of obstacle visibility distance.

### Perceived road surface brightness

The relationship between the perceived brightness of the entire road surface and illumination pattern quality is shown in figure 7. It is seen that there is a strong relationship between the rating the subjects gave to the brightness of the entire road surface and their evaluation of the illumination pattern quality. This suggests that the perceived brightness of the entire road surface has a major influence on the evaluation of low-beam illumination quality. Thus it indicates that the perceived road surface brightness is an important factor which should be evaluated in making a determination of the optimum illumination pattern for low-beam headlamps.

An analysis was then made of factors influencing the subjects' evaluation of the brightness of the entire road surface. This was done by examining the correlation between their evaluation of the brightness of each zone, i.e., near, intermediate and distant, and their evaluation of the brightness of the entire road surface. The results are shown

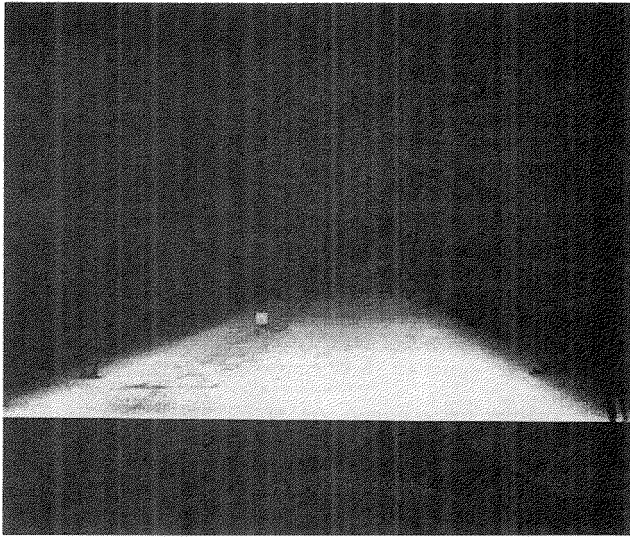


Figure 5. Pattern B—luminance pattern created by image processing.

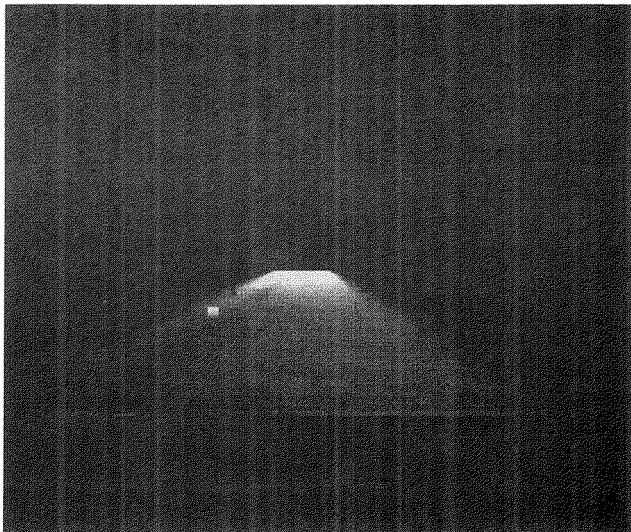


Figure 5. Pattern C—luminance pattern created by image processing.

in figure 8. The coefficients of correlation between their evaluations of the brightness of the entire road surface and evaluations of the brightness of each zone are given in table 2.

The evaluation of the brightness of the near zone and of the intermediate zone show a stronger correlation with the entire road surface brightness evaluation than that of the far zone. These results thus indicate that the perceived brightness of the near and intermediate zones has a large effect on the perceived brightness of the entire road surface.

In summary, the obstacle visibility distance is not the only important factor to consider when determining the

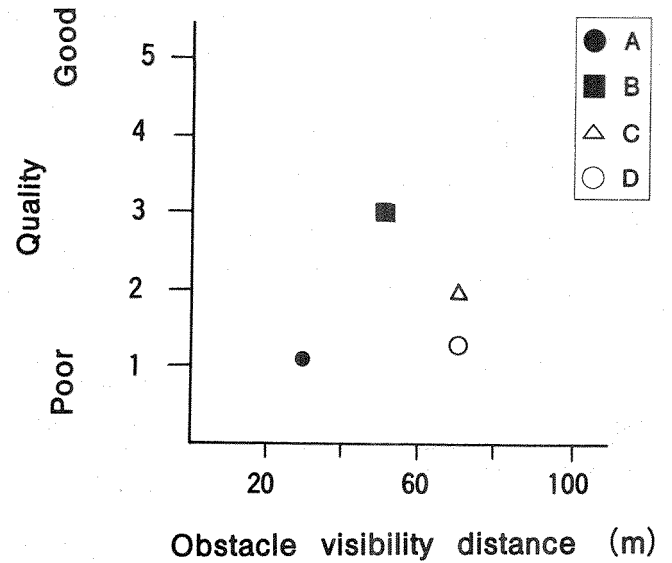


Figure 6. Illumination pattern quality versus obstacle visibility distance.

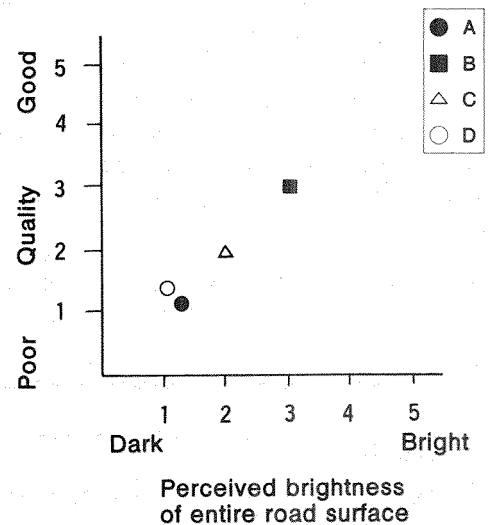


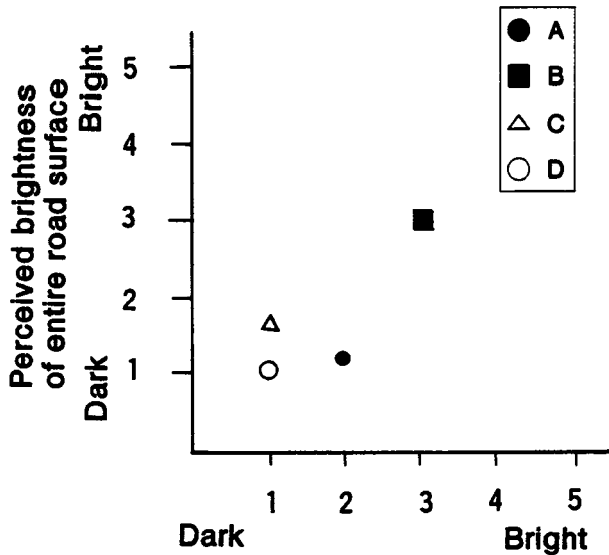
Figure 7. Illumination pattern quality versus perceived brightness of entire road surface.

optimum low-beam illumination pattern. Evaluations of perceived brightness in near and intermediate zones, which appear to have little relationship with the obstacle visibility distance, are also important factors that must be considered.

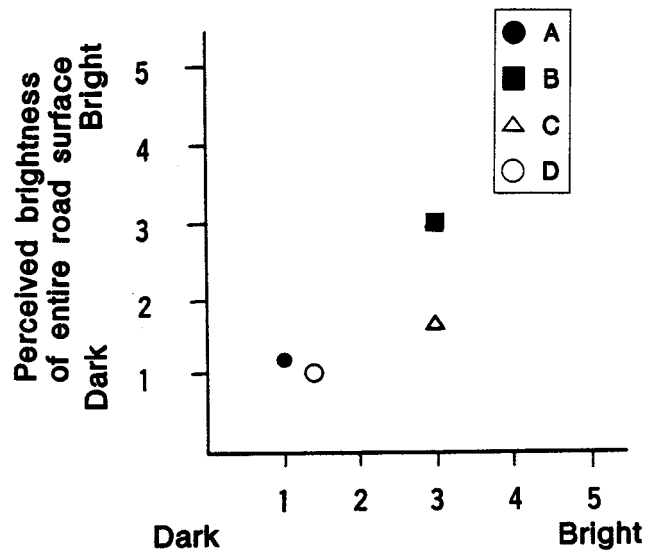
The foregoing results indicated that there was a need to quantify the feeling of road surface brightness in order to determine the optimum illumination pattern for low-beam headlamps. The following section describes an attempt to devise such a quantification technique.

### Trial calculations of perceived brightness for each illumination pattern

Calculations were made of the total road surface luminance using the following three methods in order to determine the amount of light entering the driver's eyes from the road surface. It was thought that this value could be used as a yardstick for quantifying perceived brightness:

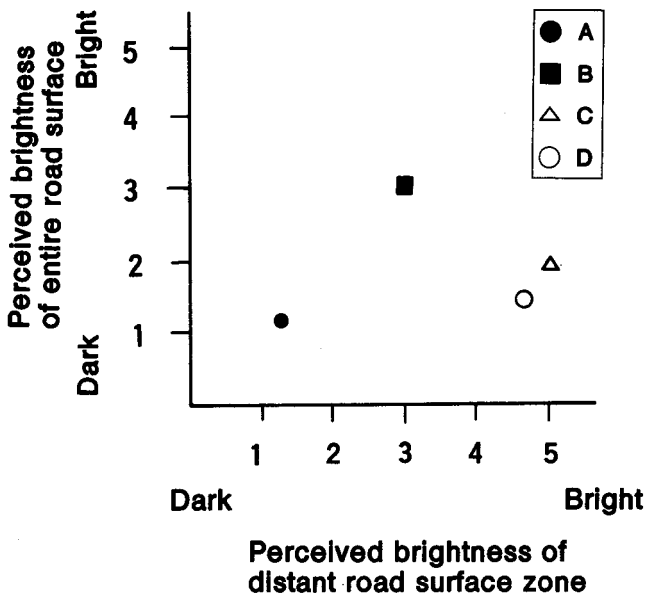


Perceived brightness of near road surface zone



Perceived brightness of intermediate road surface zone

Figure 8. Correlation between perceived brightness of various road surface zones and perceived brightness of entire road surface (1/2).



Perceived brightness of distant road surface zone

Figure 8. Correlation between perceived brightness of various road surface zones and perceived brightness of entire road surface (2/2).

Table 2. Coefficients of correlation for perceived brightness of various road surface zones relative to perceived brightness of entire road surface.

Road surface zone	Correlation coefficient
Perceived brightness of near road surface zone	0.68
Perceived brightness of intermediate road surface zone	0.57
Perceived brightness of distant road surface zone	0.06

(1) The total road surface luminance was found for the entire stretch of road (i.e., two meters on either side of the vehicle and from 8 to 100 m in front of it) when seen from directly over the road.

(2) The total road surface luminance was found for the entire road as seen from the driver's eye point (downward angle of vision of  $0^\circ \sim 8^\circ$  and horizontal angle of  $20^\circ$  left and  $13^\circ$  right as seen from driver's eye point).

(3) The total road surface luminance was found for the road surface in front of the vehicle (one meter to the left and right of the vehicle) as seen from the driver's eye point looking at the road ahead.

Figure 9 shows the relationship between the luminance values calculated for the four illumination patterns with the first method and the subjects' evaluations of the perceived brightness of the entire road surface. With this method, the calculated luminance values for patterns C and D, which have a high road surface luminance level for the distant zone, are larger than the calculated luminance values for patterns A and B. The magnitude relationship of the calculated values does not agree with that of the subjects' evaluations of road surface brightness.

The reason for this discrepancy can be explained as follows. When the road ahead is viewed from the driver's eye point, the apparent area of the distant zone is smaller than that of the near or intermediate zone. However, in calculating the total road surface luminance, each zone was treated as having the same area.

Figure 10 shows the relationship between the luminance values calculated for the four illumination patterns with the second method and the subjects' evaluations of the bright-

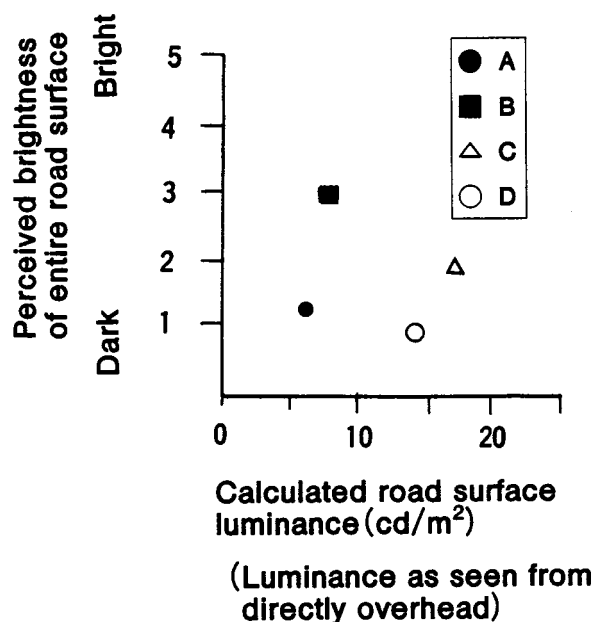


Figure 9. Correlation between perceived brightness of entire road surface and calculated road surface luminance.

ness of the entire road surface. With the second method, the total road surface luminance value is calculated according to the apparent area of the road surface as seen from the driver's eye point. It is seen in the figure that the magnitude relationship of the calculated luminance values for patterns B, C and D corresponds to that of the subjects' evaluations of the brightness of the entire road surface. However, this correlation is not seen for pattern A.

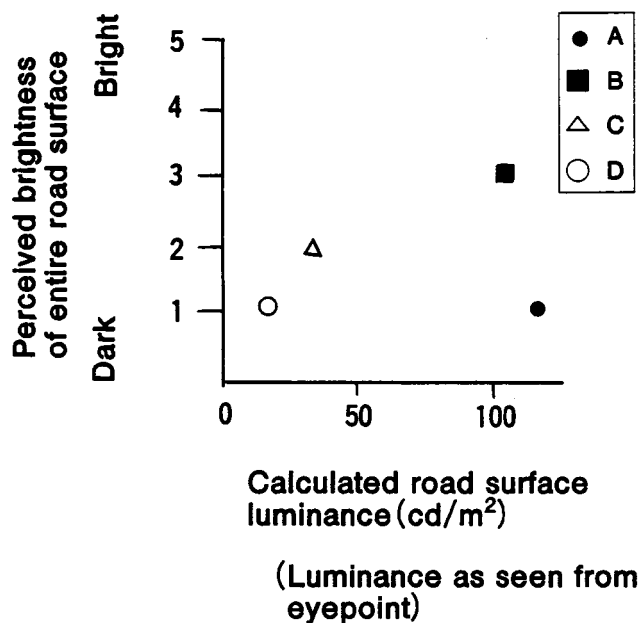


Figure 10. Correlation between perceived brightness of entire road surface and calculated road surface luminance.

With the second method, the total road surface luminance was calculated for a distance of up to 8 m ahead of the vehicle and for a lane width of 4 m (20° left ~ 13° right).

When the subjects evaluated road surface brightness, such as in the first zone to a distance of approximately 8 m ahead of the vehicle, it is thought that they did not necessarily make an evaluation for the full lane width from one side to the other. In their actual evaluations, they may have looked at changes in road surface brightness that occurred in a smaller field of vision and based their ratings on that visual information.

In these experiments, it was not clear what the subjects' field of vision was when they evaluated the road surface brightness. However, with the third method, an attempt was made to calculate the total road surface luminance only for the area in front of the vehicle.

Figure 11 shows the relationship between the luminance values calculated for the four illumination patterns with the third method and the subjects' evaluations of the brightness of the entire road. The magnitude relationship of the calculated values for patterns A and C still runs counter to that of the subjects' evaluations of entire road surface brightness. However, in comparison with the results in figure 10, a stronger correlation is seen between the subjects' evaluation of the brightness of the entire road surface and the calculated values.

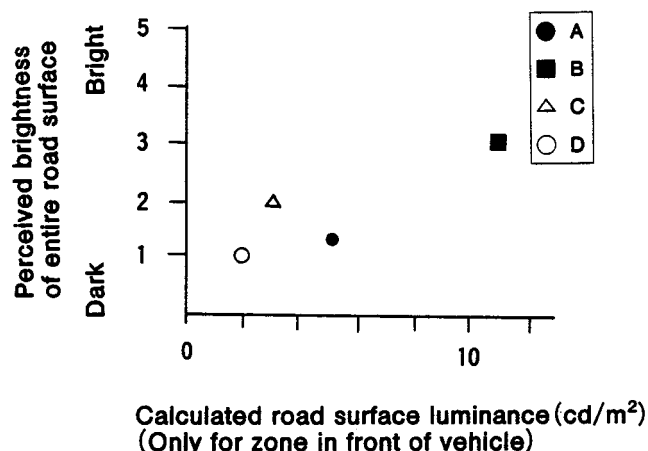


Figure 11. Correlation between perceived brightness of entire road surface and calculated road surface luminance.

Further investigation will have to be made of a method for quantifying perceived brightness, but it is thought that the third method described above for calculating brightness can serve as a general approach to brightness quantification.

## Conclusion

This paper has presented a new methodology for making immediate evaluations of road surface luminance distribution patterns using the results of illumination pattern simulations obtained with an image processing system.

It is shown that the obstacle visibility distance is not the only important factor to be considered when determining the optimum low-beam illumination pattern. The perceived brightness of the road surface, particularly for near and intermediate zones, has a large effect on evaluations of illumination pattern quality. Therefore, an evaluation of

perceived road surface brightness in these two zones is also a significant factor that should be taken into account when determining the best low-beam illumination pattern.

An attempt was made to devise a methodology for quantifying perceived brightness by calculating the total road surface luminance according to the apparent area of different distance zones as seen from the driver's eye point.

## Steering and Traction Control for Accident Avoidance Maneuverability

Written Only Paper

**Masanori Tani, Tadao Tanaka,  
Hiroo Yuasa, Hiroaki Yoshida,**  
Mitsubishi Motors Corporation

### Abstract

In order to evaluate an obstacle avoidance performance of a vehicle, behavior was studied in steering maneuver, such as lane change.

A vehicle with four wheel steering (4WS) was found to contribute to improvement of the vehicle transient response in steering maneuver on a dry road surface. On a slippery road surface, 4WS was also effective to improve vehicle maneuverability.

Effect of traction force control to front and rear wheels on vehicle dynamics was also discussed.

### Introduction

Vehicle behavior is determined by the forces acting between tires and a road surface. In steering maneuvers, active control of cornering force distribution in front and rear wheels improves the transient response of a vehicle. Among many functions of four wheel steering system (4WS), improvement of the vehicle transient response should be emphasized from the accident avoidance point of view, such as quick lane change maneuverability (1, 2, 3).\*

In-phase four wheel steering system generates cornering forces almost simultaneously in front and rear wheels by steering the rear wheels actively in the same direction as the front. The vehicle with 4WS showed higher lane change maneuverability than 2WS on a dry road surface.

The vehicle behavior in steering maneuver on a slippery road surface is studied in this paper. Lane change maneuverability is discussed from the experimental results together with analytical consideration.

As to the vehicle dynamics on a slippery road surface, compatibility of traction force with cornering force acting on each tire is important for accident avoidance maneuverability. This paper also discusses about effect of traction force distribution to front and rear wheels on the maneuverability of a vehicle with 4WS.

A method for calculating the total road surface luminance of the area immediately in front of the vehicle was one of the techniques examined. It is concluded that this method provides a general approach to quantifying brightness, although further investigation of quantification methods will have to be made in future work.

### Lane change maneuverability

Vehicle behavior in lane change maneuver on a dry road surface was reported by the authors to evaluate the performance of 4WS (4) (5). A vehicle with 4WS showed smaller phase delay on the lateral acceleration to the steering angle as compared with a conventional (2WS) vehicle as shown in figure 1 and 2.

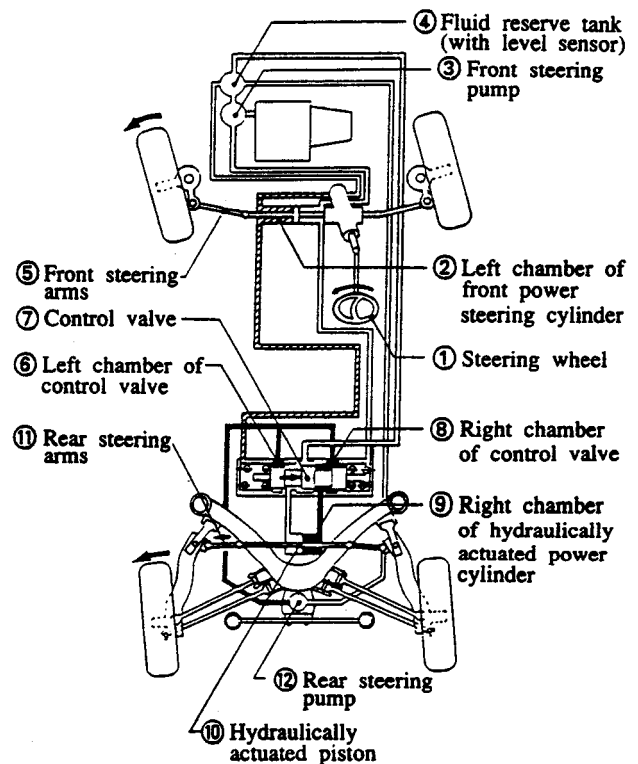


Figure 1. Structure and operating method of Mitsubishi Galant 4WS.

This can be interpreted as improvement of safety that a driver allows a margin of an instant for avoiding an obstacle on a road as shown in figure 3.

### Maneuverability on a slippery road surface

Effect of in-phase 4WS on lane change maneuverability was examined on a slippery road surface. Figure 4 shows typical results of vehicle running tests on an icy road.

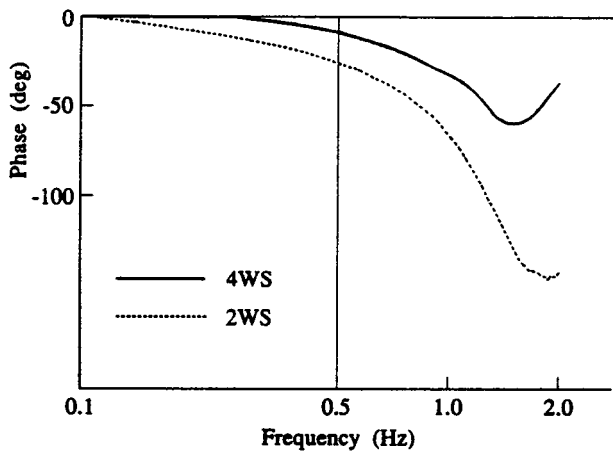


Figure 2. Phase of lateral acceleration to steering input.

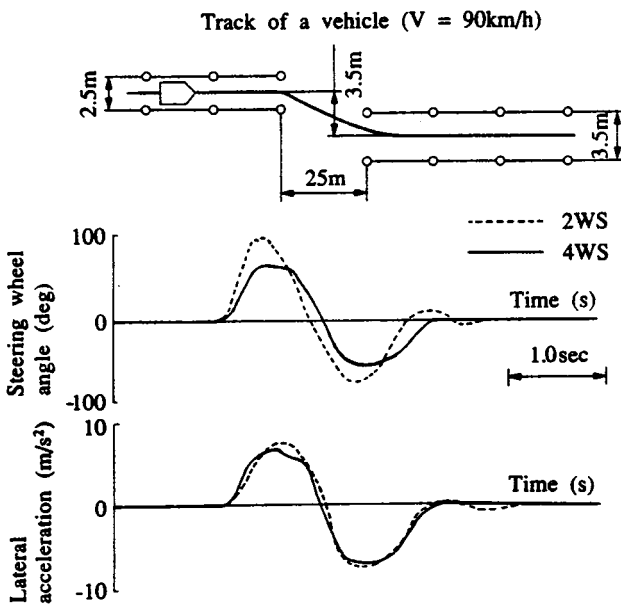


Figure 3. Lane change behavior on a dry road surface.

As can be seen from figure 4, faster rise of the lateral acceleration resulting from drivers steering motion, which is similar to the case on a dry road surface, is observed on a vehicle with 4WS. Furthermore, the vehicle attitude angle and yaw angular velocity are also reduced in the case of 4WS as compared to a vehicle with 2WS. This means that 4WS improves stability at a quick lane change by reducing excessive yaw motion which often observed in conventional (2WS) vehicles. This stability is more important on a slippery road surface where a vehicle tends to become divergently unstable due to lower adhesion coefficient between tires and a road surface.

Figure 5 shows comparison of variation of steering angle between 4WS and 2WS cars in several trials of a quick lane change maneuver on an icy road. Relatively smaller variation of steering angle time histories is observed in a 4WS car as compared to a 2WS car.

Regarding 4WS characteristics, the steering angle ratio between the rear and the front wheel is discussed here in after.

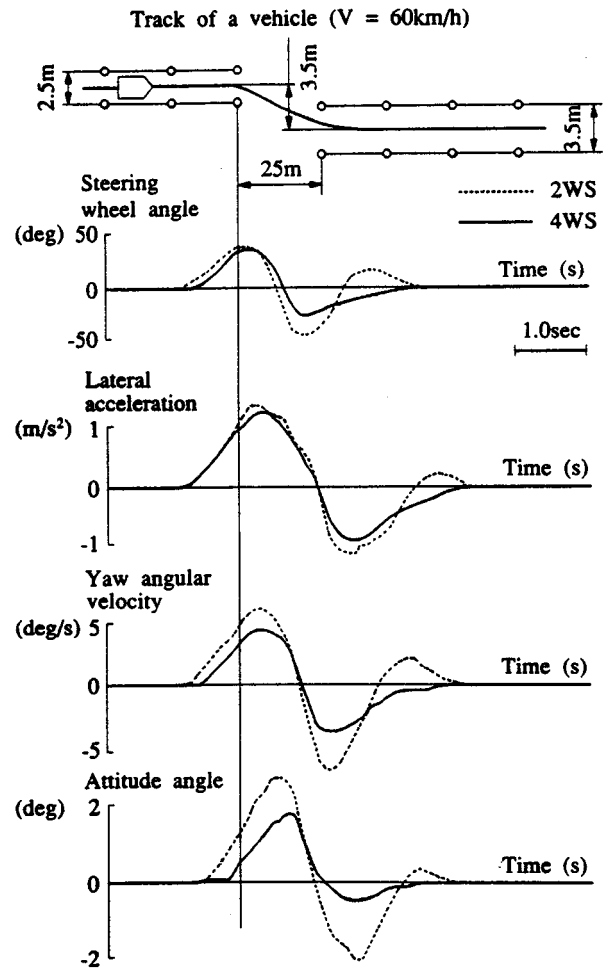


Figure 4. Lane change behavior on an icy road.

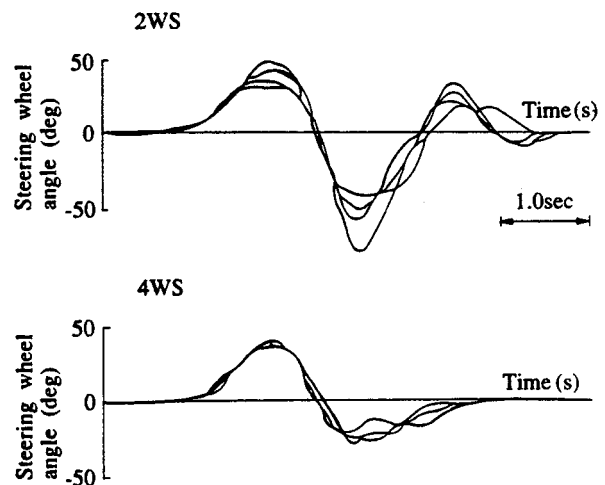


Figure 5. Comparison of variation of steering wheel angle at quick lane change on an icy road.

Figure 6 shows experimental results of the relationship between the cornering force and the slip angle of a tire for various road conditions. Cornering stiffness of a tire on a slippery road surface is smaller than that on a dry road surface. The vehicle attitude angle in a steady state cornering increases according to the decrease of the adhesion

coefficient between tires and a road surface as shown in figure 7.

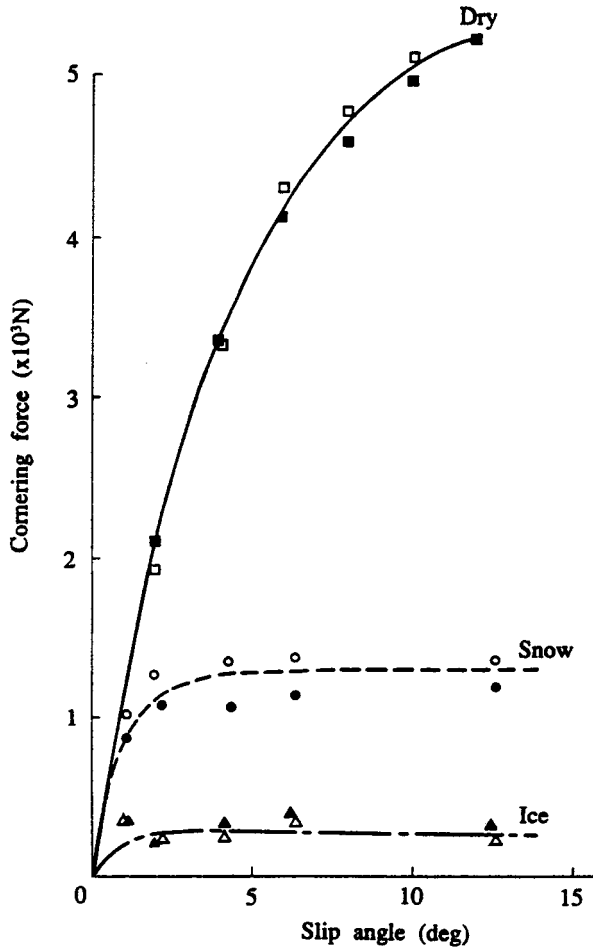


Figure 6. Tire cornering properties for various road conditions (experimental results).

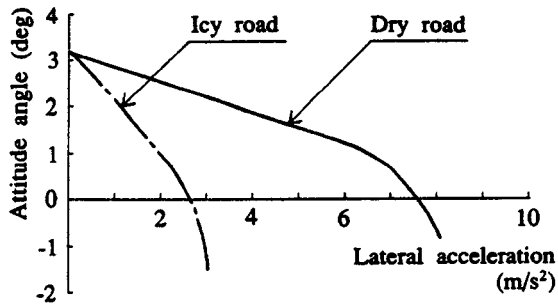


Figure 7. Vehicle attitude angle in a steady state cornering on an icy road.

The frequency response function between lateral acceleration and steering angle, which is calculated by the mathematical model with two degree of freedom and the experimentally obtained cornering stiffness, shows smaller gain and larger phase delay in the case of a 4WS car running on a slippery road surface than those on a dry road surface (figure 8).

Larger ratio of the rear steering angle to the front is expected in order to improve a lane change maneuverability on a slippery road surface. However, excessive steering

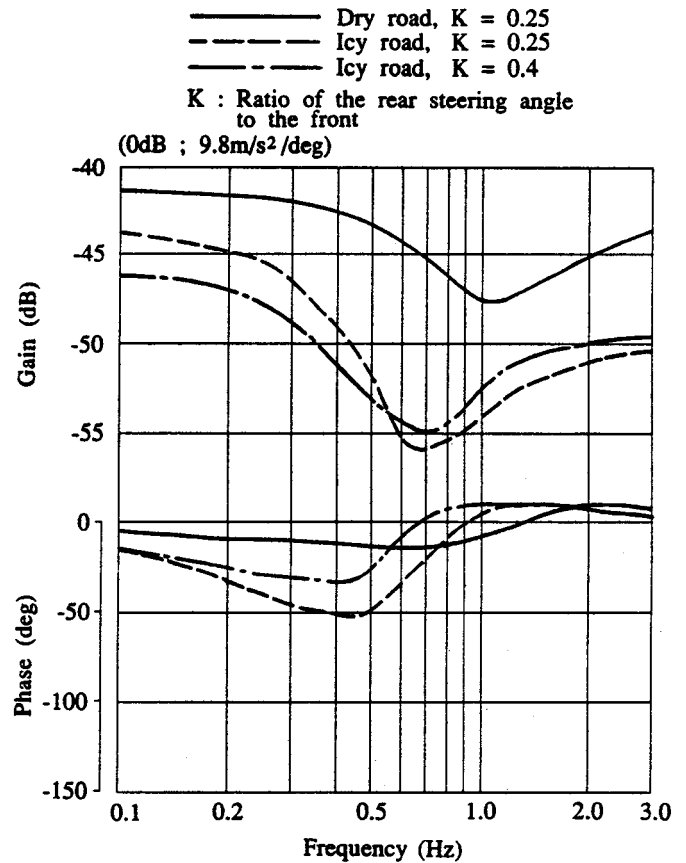


Figure 8. Frequency response of lateral acceleration to steering point.

angle ratio of the rear to the front causes the reduction of yaw angular velocity and leads a driver to excessive steering motion by which front wheels tend to lose the cornering stiffness. Therefore, steering angle ratio between the rear and the front of 4WS cars, should be kept in appropriate range by taking vehicle dynamics and human response into consideration.

As to the effect of traction force distribution and cornering force on vehicle dynamics, figure 9 shows the normalized relationship between traction force and cornering force on front and rear wheels. In case of a FWD car with 2WS, the front wheels tend to skid due to larger resultant force of traction and cornering force than the rear in lane change maneuver with acceleration on a slippery road surface. On the other hand, the lateral acceleration of a 4WS car is observed to be smaller than that of a 2WS car as shown in figure 4. Therefore, a 4WD car with 4WS has larger margin of tire adhesive property than other combinations of traction and steering control.

## Conclusions

In-phase 4WS was verified to be effective to improve vehicle accident avoidance maneuverability both on a dry and slippery road surface.

On an icy road surface, this effect was observed as reduction in variation of steering angle time histories in quick lane change.

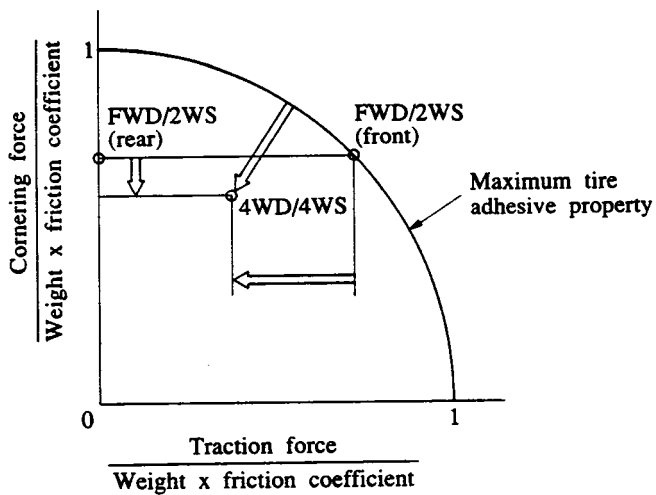


Figure 9. Normalized relationship between traction and cornering force.

Furthermore, the combination of 4WD and 4WS is more effective for accident avoidance maneuverability on a slippery road surface.

## References

- (1) Hiroaki Yoshida, Masayoski Nishimori, Takeshi Mitsui: Handling Characteristics of Four-Wheel-Steering Cars, JSAE Review, Vol. 9, No. 3, July 1988.
- (2) Rakuzou Mitamura: Future Prospect on Vehicle—New Technologies for Advanced Mobility, journal of the Japan Society of Mechanical Engineers (in Japanese), Vol. 83, No. 797, April 1985.
- (3) S. Sano, Y. Oguchi, Y. Furukawa, H. Nakaya: Influence of Vehicle Response Parameter on Driver Control Performance, 18th International Congress of FISITA, Hamburg, May 1980.
- (4) Tadao Tanaka, Masanori Tani, Hiroo Yuasa, Tetsushi Mimuro, Hiroaki Yoshida: Active Control Technology For Passenger Car, 22th International Congress of FISITA, Dearborn, No. 885105, Sep. 1988.
- (5) Rakuzou Mitamura, Masanari Tani, Tadao Tanaka, Hiroo Yuasa: System Integration for New Mobility, SAE Paper No. 881773, 1988.

# Technical Session 5A

## Side Impact Occupant Protection

Chairman: Prof. Dr. Bernd Friedel (Federal Republic of Germany)

### Side Impacts: Expected Benefits of Planned Standards

**Claude Henry, Christian Thomas,  
Gérard Faverjon, Claude Tarrière,  
Peugeot SA/Renault  
Claude Got, and Alain Patel,  
Orthopaedic Research Institute, France**

#### Abstract

It is clear that in terms of utility (cost/efficiency), the planned standards concerning protection from side impacts (the so-called global test procedure: collision between a mobile deformable barrier and a vehicle at 50 km/h, which can be replaced by a "composite test procedure" as at present under study by European car makers) appears of secondary importance by comparison with new initiatives which could be adopted concerning frontal impacts. (1)\*

What results can be expected from the planned "side impact" standards?

Based on the main characteristics of fatal accidents involving car occupants which occurred in France in the second quarter of 1980, and the accidentological data of the Laboratory of Physiology and Biomechanics associated with Peugeot SA/Renault, one observes that the planned impact speed, 50 km/h, which corresponds to a "mean" velocity change ( $\Delta V$ ) of 25 km/h for the impacted car, only covers approximately 10% of deaths and 30% of severe injuries in the category of occupants exposed to intrusion in car-to-car side collisions. As a consequence, the standard being prepared will no doubt lead to the adoption of provisions which will reduce the number of severe injuries, without having a very significant influence on the number of deaths.

Our evaluations show that the potential number of severe injuries concerned is less than 2.5% of all severe injuries (all types of impact taken together), the potential number of fatalities concerned being less than 1% of all fatal casualties.

#### Introduction

The combined analysis of data from the Peugeot SA/Renault survey (approximately 13,000 occupants involved in accidents causing bodily harm—Source 1) and the police reports on fatal accidents (2) which occurred in April, May and June 1980 on the entire French road network (1,400 motoring fatalities—Source 2) allows overall quantification of the risks to which occupants are exposed in the event of side impacts.

In 1987, 1,700 to 1,800 car occupants were killed and approximately 6,700 people were severely injured due to side impacts in France (table 1). In quantitative terms, side impacts come second after frontal impacts, which caused approximately 3,000 fatalities and approximately 20,000 severe injuries.

**Table 1. Relative importance of side impacts in France (all obstacles, all occupants).**

All occupants involved in accidents	16%	(Source 1)
Severely injured	21%	(Source 1)
Fatalities	29%	(Source 2)

Note: In 1987, 6,000 people were killed and 31,841 severely injured in passenger cars in France

Other studies carried out in Europe (3, 4) show that the proportion of severe casualties (persons killed and severely injured) due to side impacts is approximately 25%.

Part 1 of this study analyzes the main statistical data (obstacles encountered, occupants' position relative to the impacted area, risks for the occupant according to the point of impact).

Part 2 deals only with occupants involved in car-to-car side collisions who, being positioned on the impact side, were directly subjected to intrusion by the adjacent side panel. Standards for this very specific configuration are at present planned both in Europe (Composite Test Procedure or again the CEVE Procedure) and in the United States (NHTSA project). An estimate is given of the potential victims (severe injuries and fatalities) concerned by these projects.

#### Principal Characteristics of Side Impact Categories

This approach requires that a distinction first be made between two essential factors which, combined, provide a useful measure of the risk of injury to which an occupant is exposed in side impacts. These factors are:

- The type of obstacle impacted;
- The occupant's position relative to the impacted area.

The breakdown (by percentage) of all occupants involved, and those severely injured and killed in side

\*Numbers in parentheses designate references at end of paper.

impacts depending on the type of obstacle is given in table 2. Note, in particular, that car-to-car side collisions, which represent over two-thirds of side-impact collisions, cause less than one-third of fatalities.

**Table 2. Breakdown of 100 occupants according to type of obstacle and level of injury severity in side impacts.**

	OBSTACLES			TOTAL
	Fixed Objects	Utility Vehicles	Passenger Cars	
All occupants involved in accidents (Source 1)	21	11	68	100
Severely injured (Source 1)	35	14	51	100
Fatalities (Source 2)	46	26	28	100

Side impacts against rigid fixed obstacles such as trees, posts, walls, etc., or against utility vehicles (lorries, coaches) cause 50% of severe injuries and 72% of fatalities.

A knowledge of the occupants' position in the car relative to the impacted area is an essential item of information in understanding the causes of injuries. It is not sufficient to distinguish between occupants on the side opposite the impact and those on the impact side. In a single car, three radically different injury patterns can be observed, and a distinction must be made between:

- Occupants located on the impact side (nearside occupants) subjected to direct intrusion by the wall;
- Nearside occupants who are not affected by intrusion of the wall;
- Occupants located on the side opposite the impact (farside occupants).

Accident data shows that the risks differ greatly depending on the occupant's position, intrusion and the obstacle impacted (figure 1). On the whole, it appears that the risk is especially high when the occupant is "nearside with intrusion"; this group represents 48% of all severe injuries and 72% of all fatalities, although only one quarter of all those involved in accidents.

*"Nearside With Intrusion" Occupants* involved in car-to-car side collisions represent 16% of those involved in accidents, 25% of severe injuries and 21% of fatalities in side impact. This configuration is dealt with in part 2 of this study. We may specify here that for this group, the safety belt is quite effective (approximately 20%) in reducing the severity of injuries. This reduction, which is unbiased by differences of impact violence or age between those wearing seat belts and those not, may seem surprising. To the extent that the proportion of cases with an adjacent occupant is similar from one group to another, it can be assumed that the role played by the adjacent occupant with respect to an occupant located at the point of impact had more severe consequences for those not wearing seat belts,

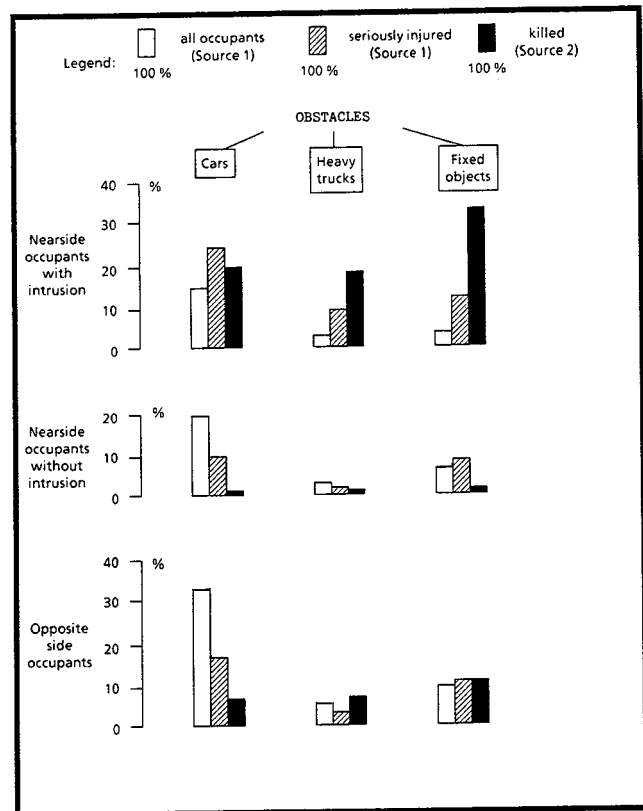


**Figure 1. Breakdown (%) by injury severity of occupants involved in side impacts according to types of obstacles, seat position and intrusion.**

the front occupants generally being both belted or both unbelted.

Nearside occupants subjected to direct intrusion by a utility vehicle or a fixed obstacle (approximately 7% of all those involved in side impacts) are especially exposed to risks of severe and fatal injuries, representing 23% of all severe injuries and 52% of fatalities respectively.

These victims, subjected to intrusion by a high, rigid obstacle show, among other things, craniofacial injuries due to direct impact of the head against the obstacle. Now, no realistic solution is at present in sight to reduce the severity of head injuries in the case of a direct side impact, and the potential for reducing severe casualties in this group is therefore very low. The percentage wearing seat belts for this group of casualties is very low (less than 20%). Given both the small numbers involved and the bias due to impact violence between those wearing and those not wearing seat belts, a valid evaluation of seat belt effectiveness cannot be made.

*"Nearside Without Intrusion" Occupants* (28% of occupants involved, with 20% of all severe injuries and less than 2% of fatalities) have little risk of being severely injured and still less of being killed by comparison with those exposed to intrusion. Since ejection is the cause of three quarters of fatalities and close on 30% of severe injuries in this impact configuration, it is clear that the seat belt is unquestionably effective by preventing ejection. The effectiveness in reducing the severity of injuries is calcu-

lated as 42% due to elimination of ejection and reduction of head impacts against rigid elements (A-Pillar in particular) by close on half in the case of very oblique impacts.

The occupants in this group are subjected to approximately the velocity change of the car, and the fact that the door unit can absorb energy during occupant/wall impact and that the wall can be deformed outwards all favour thoracic protection. For the rare cases of severe injuries recorded among non-ejected occupants, the head, due to impact against the frame (A-Pillar, B-Pillar, roof reinforcement) is the area most frequently affected, with the lower and upper members.

Non-ejected severe injury proportions according to various delta V levels for the impacted car are given in table 3. Since the occupants are not located directly at the obstacle impact point, we have grouped all occupants without taking into account the type of obstacle impacted. The planned standard covers only a small proportion of severe injuries (approximately 12% for these occupants). Not one fatality is covered by a delta V of 25 km/h.

**Table 3. Proportions of severe injuries and fatalities according to the delta V of the impacted vehicle for unejected nearside occupants without intrusion (all obstacles).**

Delta V of impacted vehicle (km/h)	Number of occupants	Proportions (%) of: severe injuries and fatalities	
		severe injuries and fatalities	fatalities
≤ 25	183	2.2%	0.0%
26-35	106	10.4%	0.0%
36-45	40	42.5%	2.5%
> 45	7	71.4%	28.6%
(Source 1)			
Note: There is no unejected fatality for a delta V of 25 km/h (Source 2)			

**Table 4. Proportions of severe injuries and fatalities according to the delta V of the impacted vehicle for unejected farside occupants (car-to-car collisions).**

Delta V of impacted vehicle (km/h)	Number of occupants, of whom: belted (1) unbelted (2)	Proportions (%) of: severe injuries and fatalities	
		severe injuries and fatalities	fatalities
≤ 25	227	0.9%	0.0%
	92 (1)	0.0%	0.0%
	135 (2)	1.5%	0.0%
26-35	144	8.3%	1.4%
	62 (1)	1.6%	0.0%
	82 (2)	13.4%	2.4%
36-45	64	26.6%	12.5%
	17 (1)	23.5%	17.6%
	47 (2)	27.7%	10.6%
> 45	21	76.2%	47.6%
	9 (1)	77.8%	33.3%
	12 (2)	75.0%	58.3%
(Source 1)			
Note: Only 4% of fatal casualties occur for a delta V of 25 km/h (Source 2)			

*Farside Occupants* (approximately 50% of occupants involved, for 32% of all severe injuries and 26% of

fatalities) are exposed to projection against the side panels, or even against the obstacle when it is high and located in the trajectory of the occupant. Here again, the obstacle has a significant influence on the severity of injuries; occupants involved in impacts against utility vehicles or fixed obstacles (16% of all casualties) are clearly more exposed to risks of severe and fatal injuries (15% of all severe injuries and 19% of fatalities respectively) than those involved in car-to-car collisions (33% of occupants involved in accidents, for 16% of severe injuries and 7% of fatalities).

Of all farside occupants (belted on the one hand, and unbelted, whether ejected or not, on the other hand), a 31% reduction in severity is observed due to the seat belt, by preventing projection against the walls and ejection. The effectiveness of the seat belt merely by preventing projection against the walls is far from insignificant up to an impacted car delta V of 35 km/h (tables 4 and 5).

**Table 5. Proportions of severe injuries and fatalities according to the delta V of the impacted vehicle for unejected farside occupants (car against fixed objects).**

Delta V of impacted vehicle (km/h)	Number of occupants, of whom: belted (1) unbelted (2)	Proportions (%) of: severe injuries and fatalities	
		severe injuries and fatalities	fatalities
≤ 25	35	2.9%	0.0%
	6 (1)	0.0%	0.0%
	29 (2)	3.4%	0.0%
26-35	40	22.5%	2.5%
	11 (1)	0.0%	0.0%
	29 (2)	31.0%	3.4%
36-45	19	26.3%	5.3%
	6 (1)	50.0%	16.7%
	13 (2)	15.4%	0.0%
> 45	9	66.7%	22.2%
	5 (1)	80.0%	20.0%
	4 (2)	50.0%	25.0%
(Source 1)			
Note: Only 4% of fatal casualties occur for a delta V of 25 km/h (Source 2)			

It is clear that a test involving an impacted car delta V of 25 km/h, irrespective of the type of obstacle impacted, causes only few severe injuries and fatalities. Clearly, the planned standard could cover only a minimum of severe injuries in the event of impacts against fixed obstacles or utility vehicles (generally high obstacles), since the head, which in many cases impacts the obstacle directly, is not protected.

## Sample of "Nearside Occupants with Intrusion" in Car-to-car Side Collisions

This very specific configuration, which, remember, represents 16% of all occupants involved in accidents, 25% of severe injuries and 21% of fatalities in side impacts, is at present the subject of planned standards both in Europe (Composite Test Procedure or again CEVE Procedure) and in the United States (NHTSA project).

On the basis of the data in the accidentological survey, a sample of 164 occupants was selected (57 belted and 107

unbelted), whose characteristics are given in figure 2, namely:

- The occupant, aged 10 or over, non-ejected, belted or unbelted, sitting in the front or rear seats, is positioned on the impact side and is subjected to intrusion of the side panel at the pelvic level. Cases where an adjacent occupant is present (side opposite the impact) are taken into account;
- The speed of the side-impacted car is zero or negligible;
- The speed of the impacting car is an estimated 20 km/h at least;
- The main direction of the forces (or resultant trajectory for the occupants) is in the range between 60° and 120°.

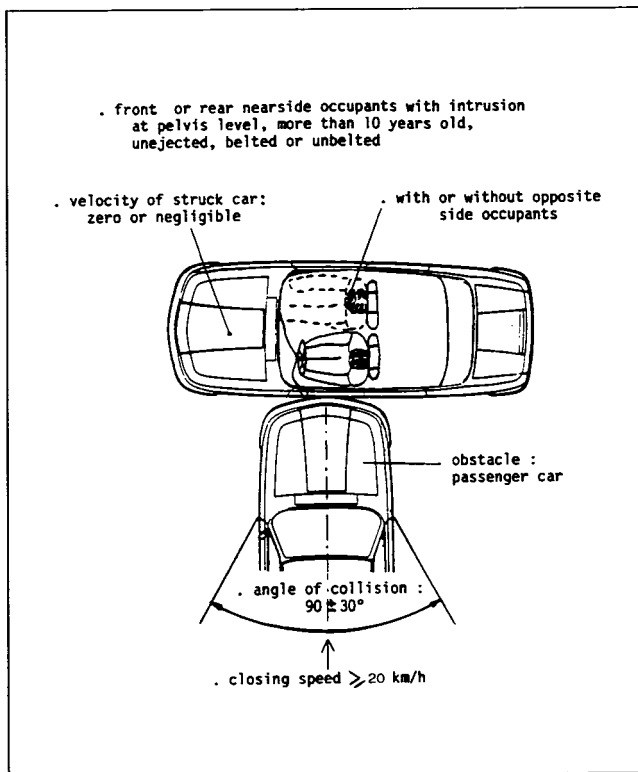


Figure 2. Description of criteria used to select the sample of nearside occupants with intrusion in car-to-car side collisions.

The study first deals mainly with a description of accidents in which the occupants were involved:

Impacted area and direction of forces;

Violence of impacts (in terms of delta V of the impacted vehicle and closing speed). For calculation of fatalities, the data from fatal accident police reports will be used.

An analysis is also made of the degree of severity of injuries by body area.

The second part evaluates the number of severe casualties (severe injuries + fatalities) concerned by current plans for this group of casualties.

## Sample Characteristics

### Impacted areas and main direction of forces (figure 3)

The classification of impacted areas on the body side panel shows that deformation is confined to the passenger compartment only (A- and C-Pillars not affected) in 45% of cases. The trajectory of the occupants is in 90% of cases perpendicular or slanting forward (slant of approximately 60° relative to the longitudinal axis of the impacted car).

Damage areas of impacted cars	Main direction of forces (C.D.C. - SAE J224)			Total
	2 or 10	3 or 9	4 or 8	
	24	13	3	(24.4 %) 40
	13	14	2	(17.7 %) 29
	4	2	3	(5.5 %) 9
	26	32	7	(39.6 %) 65
	9	7	1	(10.4 %) 17
	1	3	-	(2.4 %) 4
Total	77 (47.0 %)	71 (43.3 %)	16 (9.7 %)	164 (100 %)

Figure 3. Breakdown of damage areas of impacted cars according to main direction of forces for the sample of nearside occupants with intrusion (car-to-car side collisions).

### Violence of impacts and overall severity of injuries

The velocity change (delta V) of side-impacted cars is not the most relevant of impact violence parameters for occupants exposed to intrusion, any more than the closing speed. The main parameter characterizing the severity for occupants subjected to wall intrusion is the "occupant/side panel" impact velocity (5, 6), even if this is not sufficient to entirely explain the presence or absence of thoracic, abdominal or pelvic injuries in particular.

This being said, let us examine the violence of collisions in terms of delta V of the impacted car and the closing speed, for all occupants involved in accidents and for severe casualties.

The classification of injury severity levels (MAIS) according to impacted car delta V is given in table 6. The mean car delta V in this sample is 28 km/h for all occupants and 31 km/h for severe injuries (MAIS 3-4-5). For fatal casualties, 92% (Source 1) and 77% (Source 2) of them are involved in accidents with car delta V values greater than 30 km/h.

**Table 6. MAIS classification according to delta V of impacted car for nearside occupants with intrusion in car-to-car side collisions.**

MAIS	Delta V (km/h) of impacted car								TOTAL
	≤ 15	16-20	21-25	26-30	31-35	36-40	41-45	> 45	
0	4	9	5	2	-	-	-	-	20
1 - 2	8	20	22	21	9	5	-	-	85
3 - 4 - 5	-	2	8	6	6	8	4	-	34
Fatalities	-	-	-	2	3	5	7	8	25
Total (Source 1)	12	31	35	31	18	18	11	8	164
Fatalities (Source 2)	-	2	2	6	13	8	4	8	43
↑ "Mean delta V" of impacted car									

The 4 fatalities observed for a delta V of 25 km/h and less (Source 2) were aged 70 or more, and in each case the presence of an adjacent occupant is noted. Likewise, in the 26/30 km/h delta V class, 4 of the 6 fatal casualties were aged over 60. The effect of age on the risk of thoracic injuries in particular is perfectly evident for casualties (7), and it is clear that a large proportion of the fatal casualty population which could be covered by effective protective measures for car-to-car collisions has a low level of tolerance.

The classification of occupants, severe injuries and fatal casualties according to closing speed is given in table 7.

**Table 7. MAIS classification according to closing speed for nearside occupants with intrusion in car-to-car side collisions.**

MAIS	Closing Speed (km/h)									TOTAL
	≤ 30	31-40	41-45	46-50	51-55	56-60	61-70	71-80	> 80	
0	5	5	4	2	3	1	-	-	-	20 (12.2%)
1 - 2	8	16	15	14	10	14	7	1	-	85 (51.8%)
3-4-5	-	2	4	5	3	7	6	7	-	34 (20.7%)
Fatalities	-	-	-	1	-	-	7	3	14	25 (15.2%)
Total (Source 1)	13	23	23	22	16	22	20	11	14	164 (100%)
Fatalities (Source 2)	-	3	-	3	6	4	11	4	12	43
↑ Moving deformable barrier speed										

The mean closing speed is 55 km/h for all occupants and 59 km/h for severe injuries. For fatal casualties, 96% (Source 1) and 63% (Source 2) of them are involved in collisions at closing speeds greater than 60 km/h.

Here again, the potential fatality population concerned consists exclusively of elderly persons. The 6 fatalities observed at closing speeds of 50 km/h and less (Source 2) were aged over 55, while 4 of them were aged 70 or more. In all cases, the presence of an adjacent occupant is noted. The single fatality recorded in the accidentological sample was for a front female passenger aged 82.

### Occupant injuries

The classification of injury severity levels according to body area shows a predominance of severe injuries (AIS ≥ 3) to the thorax and the abdomen.

Of the 81 occupants involved in collisions in which the closing speed was estimated as at least 50 km/h (table 8a), the thorax is the main injury area (8.6% of cases of severe injury), followed by the abdomen (3.7%).

**Table 8a. AIS by body area for nearside occupants with intrusion in car-to-car side collisions (closing speed ≤ 50 km/h).**

Body Areas	AIS						Total	Proportions (%) of AIS ≥ 3
	0	1	2	3	4	5		
Head	34	28	18	1	-	-	81	1.2%
Neck	74	6	-	1	-	-	81	1.2%
Thorax	56	14	4	2	5	-	81	8.6%
Upper members	63	15	3	-	-	-	81	0.0%
Dorsolumbar spine	72	9	-	-	-	-	81	0.0%
Pelvis	58	15	7	1	-	-	81	1.2%
Abdomen	73	5	-	2	1	-	81	3.7%
Lower members	67	12	1	1	-	-	81	1.2%

In the most severe collisions (table 8b), the most vulnerable body areas are, in decreasing order:

The abdomen (29.2%);

The thorax (23.1%);

The pelvis (12.3%) and the head (10.8%).

**Table 8b. AIS by body area for nearside occupants with intrusion in car-to-car side collisions (closing speed > 50 km/h).**

Body Areas	AIS						Total (*)	Proportions (%) of AIS ≥ 3
	0	1	2	3	4	5		
Head	19	18	21	2	2	3	65	10.8%
Neck	59	5	1	-	-	-	65	0.0%
Thorax	28	14	8	3	10	2	65	23.1%
Upper members	45	12	7	1	-	-	65	1.5%
Dorsolumbar spine	58	5	2	-	-	-	65	0.0%
Pelvis	37	4	16	8	-	-	65	12.3%
Abdomen	41	3	2	6	8	5	65	29.2%
Lower members	49	9	6	1	-	-	65	1.5%

\* For 18 fatalities, no injury description is available

Severe craniofacial injuries are caused by impacts in the window frame area (4 cases out of 7) or against the bonnet of the impacting car (2 cases out of 7).

### Evaluation of the potential population of severe casualties covered by the planned standards

For only those occupants exposed to intrusion, we give here the rate of coverage of severe casualties (proportions of severe injuries and fatal casualties) involved in side collisions (car-to-car) similar to a test with a moving deformable barrier impacting at 50 km/h the passenger compartment of a car, which corresponds to a delta V value of 25 km/h when the weight ratio between the moving deformable barrier and the car is equal to 1. The potential populations of severe injuries and fatal casualties concerned by a delta V of 25 km/h are as follows:

MAIS 3-4-5: approximately 30% of cases;

Fatal casualties: approximately 10% of cases based on the analysis of fatal accident police reports. (This speed does not cover a single fatal casualty in the accidentological sample.)

A closing speed of 50 km/h gives a virtually equivalent proportion of severe casualties:

MAIS 3-4-5: approximately 32% of cases;

Fatal casualties: Approximately 14% of cases based on the analysis of fatal accident police reports. (In the accidentological sample, this speed covers only one fatal casualty out of 25.)

The slight deviations observed between the potential populations covered by a delta V of 25 km/h and by a closing speed of 50 km/h can be explained by the fact that the weight ratio between the cars is, on average, more favourable to the impacting car. The velocity change (delta V), taking into account the weight ratio, is in theory more relevant than the closing speed.

In the end, it appears that approximately 10% of fatal casualties and 30% of severe injuries (out of all severe casualties exposed to intrusion in a car-to-car collision) would be covered by a global side impact standard. In terms of statistics, this represents approximately 35 car occupants killed and 500 severely injured in France in 1987, or 0.6% and 1.6% respectively of all fatal casualties and all severe injuries.

To the extent that 60% of the occupants (Source 1) and 84% of fatal casualties (Source 2) exposed to intrusion had an adjacent occupant alongside them, these proportions probably represent maximum values, since the interaction between occupants is generally likely to increase the severity of injuries to occupants located on the impacted side.

### Discussion

Of the planned side-impact standards both in Europe and in America, none provides an effective answer to the

problem of protecting the occupants. The proposed standards involve major extra costs (structural improvement and padding on the side panel). The expected gains, in the most favourable case in which the standard could cover part of the "nearside without intrusion" and "farside" severe casualties, would be small.

For the latter two populations of casualties, the potential number of severe casualties concerned has been evaluated, namely:

For nearside occupants without intrusion: probably no fatal casualty, and from 100 to 150 severe injuries;

For farside occupants: approximately 5 fatal casualties and from 50 to 100 severe injuries in the best of cases.

The planned standards would therefore cover, at most, 40 fatal casualties and 750 severe injuries due to side impact, or less than 1% of all fatal casualties and less than 2.5% of all severe injuries. These results are summarized in figure 4.

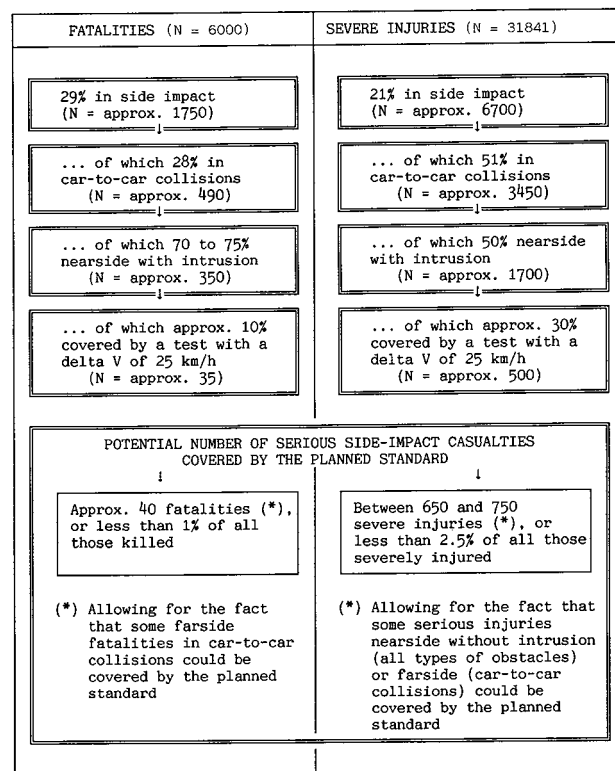


Figure 4. Probable effectiveness of the planned side-impact standard for motorists (reference year 1987, all of France).

It seems clear that side impacts cannot be easily solved by secondary safety measures. In the future, primary safety research (Prometheus and Drive programs) should in priority develop techniques aimed at reducing the risks of side collisions by developing effective driving aid systems.

Note that in France, "non-urban and non-intersection" side impacts cause close on half of the fatal casualties due to side impacts.

Improving the road infrastructure is also a way of reducing the risk of side impacts. The building of central

separating walls, protection by trees and also the replacement of country intersections with roundabouts are all essential possibilities which should not be overlooked given the difficulty of protecting against side impacts.

## Conclusions

Approximately a quarter of serious victims of car accidents (killed and severely injured) are involved in side impacts.

Car-to-car side collisions which, by themselves, account for two-thirds of occupants involved in side impacts, cause only 50% of severe injuries and slightly less than 30% of fatal casualties.

Side impacts against fixed obstacles (46% of fatal casualties) and collisions with utility vehicles (26% of fatal casualties) are especially murderous.

Nearside occupants subject to direct intrusion by the obstacle represent close on half of severe injuries and close on three quarters of fatal casualties due to side impacts. For fatal casualties, fixed obstacles and utility vehicles cause approximately 75% of deaths. No realistic solution is at present in sight to prevent side impacts in the event of direct impact by the occupant (and the head in particular) against high obstacles (trees, posts, walls, utility vehicles, etc.).

The planned standards would cover only a small proportion of all severe casualties (for all types of impact taken together) and would accordingly be of only very limited advantage.

Since the gains to be expected can only be slight, it is important that improvements to the side regions of cars with respect to secondary safety aspects should cover just what is necessary without involving unnecessary waste, if they are to be acceptable by all parties.

Gains concerning side impacts should be obtained by primary safety measures to avoid accidents. This is one of

the objectives of the European programmes Prometheus and Drive. Gains can also be obtained by improving the road infrastructure.

## References

(1) C. Thomas, S. Koltchakian, C. Tarrière, A. Patel and C. Got, "Inadequacy of 0 Degree Barrier Test with Frontal Real World Accidents", 12th International Technical Conference on Experimental Safety Vehicles.

(2) J.Y. Foret-Bruno, F. Hartemann, et al., "Principales caractéristiques des accidents mortels de voitures particulières survenus en France au cours du 2ème trimestre de 1980", Unpublished Report of the Laboratory of Physiology and Biomechanics Associated with Peugeot S.A./Renault.

(3) H. Norin, A. Nilsson-Ehle, C. Gustafsson, "Volvo Traffic Accident Research System as a Tool for Side Impact Protection Evaluation and Development", 9th International Technical Conference on Experimental Safety Vehicles.

(4) G.M. Mackay, D.K. Griffiths, J.M. Breen, P.D. Thomas, S.D. Lawson, "Investigation of a Representative Sample of Real World Side-Impacts to Cars", Contracts for EEC and TRRL, July 1983.

(5) B. Loyat, "Analyse des paramètres significatifs du choc latéral", Société des Ingénieurs de l'Automobile, March 1979.

(6) C. Thomas, C. Henry, F. Hartemann, F. Chamouard, C. Tarrière, A. Patel and C. Got, "Injury pattern and parameters to assess severity for occupants involved in car-to-car lateral impacts", 11th International Technical Conference on Experimental Safety Vehicles.

(7) J.Y. Foret-Bruno, F. Hartemann, C. Tarrière, C. Got and A. Patel, "Conditions Required to Avoid Being Killed in Cars in Side Impact", SAE Paper 830461.

## Side Impact Regulations—How do they relate to real world accidents?

**Pete Thomas and Mo Bradford,**

ICE Ergonomics

United Kingdom

### Introduction

In 1988 NHTSA published an Advance Notice Of Proposed Rulemaking (1)\* that described a test procedure and performance requirements to improve the protection available to car occupants in side impacts. The test configuration involves a mobile barrier with a mass of the median value of US cars and a stiffness similar to that of light trucks. This impacts the passenger compartment of the vehicle in a crabbed motion with an approach speed of 54 kph. The tested vehicle contains instrumented side impact dummies seated unrestrained in the front and rear struck side positions. Maximum levels of the Thoracic Trauma Index (TTI),

which is acceleration based, and pelvic acceleration are imposed to minimise torso and pelvis injury.

The corresponding European Experimental Vehicle Committee (EEVC) proposals (2) employ a softer mobile barrier, typical of the 'average' European car. The mass is lower and is based on the mass of production vehicles weighted by registration volume. The barrier strikes the passenger compartment of the tested car in a perpendicular configuration at an approach speed of 50 kph. A restrained, instrumented Eurosid dummy is seated in the front struck side seat. Maximum limits of the dummy transducer measurements are set to restrict head, chest, abdomen and pelvis injuries.

Both tests attempt to assess the severity of the impact perceived by a struck side occupant and these are viewed as the priority for improving side impact protection.

\*Numbers in parentheses designate references at end of paper.

A part of the development of any standard should be an appraisal of its likely effectiveness. Such an appraisal may fall into two stages; first an estimate of the numbers of car occupants who are in impacts that are similar to the test procedure, and second an estimate of the reduction of the levels of the injuries of those occupants. This analysis addresses the first stage of an appraisal and examines the similarity of the two test conditions to the data describing UK accidents.

## Accident Data

The field data used is that collected as part of the UK Cooperative Crash Injury Study and is based on cars that contain an injured occupant and that are towed away from the accident scene. The data collection procedures have been described previously (3, 4). An important characteristic of the study is that the relation between the sample of accidents and the population from which they are drawn is known (5). Analyses of the data therefore represent the local accident population and all accident numbers presented in this paper are weighted numbers unless explicitly stated.

Side impacted vehicles were defined as those struck on either the left or right sides of the vehicle with a principal direction of force between 1 and 5 o'clock or between 7 and 11 o'clock inclusive. There were 417 vehicles of this type in the sample and they represented 1830 in the original population. Within these vehicles there were 738 occupants representing 3250 when weighted. In the following analysis fatally injured occupants are defined as those who die within 30 days of the accident; those seriously injured have a maximum AIS of at least 3 but do not die within 30 days of the accident. Slightly injured occupants are the remaining occupants with injuries of some sort. An overview of this database has been published previously (6).

## Impact Configurations

A primary characteristic of both test procedures is the impact of the barrier at a point on the car side adjacent to the dummy. The EEVC test centres the barrier on the R-point whereas the NHTSA barrier has its most forward impact point 94 cm in front of the wheelbase centre.

The two test impact configurations involve dummies that are struck by the intruding car side structure. This side structure can be supported by the face of the impacting barrier so the effective stiffness becomes greater than that of the car side alone. This will only occur when the outer door panel is deformed to touch the inner panel. Occupants seated in positions where this may occur are classified here as being "potentially supported". In the real-world data car occupants may also be seated on the struck side and either be in front or behind the area directly struck by the bullet object but still strike an intruding car side. These were classified as striking an unsupported car side. Additionally they may contact an undamaged car side and be classified as having a non-intruding contact or they may be seated on the non-

struck side of the car. These definitions are shown in figure 1 and the distribution of the occupants in the accident population is shown in table 1.

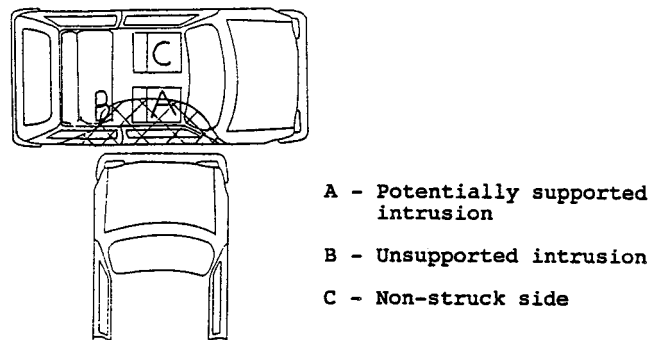


Figure 1. Classification of intruding contacts.

Table 1. Intrusion experience of occupants where known.

Intrusion experience	All severities	Serious Injuries	Fatal injuries
Struck side occupants			
No intrusion	565 (19%)	34 (14%)	3 (3%)
Unsupported	330 (11%)	38 (15%)	9 (10%)
Potentially supported	723 (25%)	108 (44%)	51 (55%)
Non-struck Side Occupants			
Restrained	934 (32%)	48 (19%)	19 (20%)
Unrestrained	370 (13%)	19 (8%)	11 (12%)
Total	2922 (100%)	247 (100%)	93 (100%)

The accident data revealed that 723 (25%) of the 2922 occupants of all severities of injury experienced supported intrusion patterns similar to the test conditions. 108 (44%) of the seriously injured occupants and 51 (55%) of those who died were also in cars with equivalent intrusion patterns to the test. It was not possible to discriminate between the incidence of the precise impact locations of the two tests but both simulate the intrusion patterns most frequently observed amongst the serious and fatally injured occupants. The EEVC barrier face has a central section that is stiffer than the outer sections to simulate the engine stiffness of bullet cars. Experimental collisions employing the barrier have suggested that this results in greater deformation of the central part of the door. Any contact from an adjacent occupant is therefore likely to be supported by the stiffer barrier face. The NHTSA barrier however has a constant stiffness across the barrier face. It tends to result in a constant deformation of the target car side structure that preserves the distance between the two door skins. There is therefore some potential ride-down space for an adjacent occupant. A further investigation of real-world accident data is required to examine the deformation patterns occurring in car to car side collisions and the effect.

Restrained occupants seated on the non-struck side of the car experienced quite different intrusion patterns. If restrained they rarely contacted an intruding car side. The changes in car design following adoption of either of the proposed test procedures will do little to reduce the injuries of these occupants. 48 (19%) of the seriously injured

occupants are restrained on the non-struck side of the car as are 19 (20%) of the fatally injured occupants.

Of the 30 fatal non-struck side occupants 14 (47%) were in impacts so severe that the intrusion extended into the non-struck side seat area and a further 6 (20%) were in cars that intruded above 45 cm but not as far as their own seat. Alternative methods of occupant protection such as improved seat belt systems or passive restraints for side impacts might be considered to reduce the injuries of the remaining 10 fatal non-struck side occupants. Such measures might also aid 28 (42%) of the 67 non-fatal seriously injured occupants seated on the non-struck side with low levels of intrusion to the vehicle. These casualties will be examined in more detail later in this paper.

The remaining occupants are those seated on the struck side either with no intrusion or with unsupported intrusion or unrestrained non-struck side occupants. The test proposals will have some effect on their injuries but any reductions may not be as great as for struck side occupants with supported intrusion.

### Pillar involvement

In experimental impacts involving the two barriers it has been observed that the A-pillars of smaller cars are frequently impacted, also the configurations are such that the B-pillars are always involved. Future designs of cars may have modified pillars that enable the loads in the test configuration to be more effectively distributed through the cars' structure. The involvement of the A and B-pillars was found to vary in the field data. This is shown in table 2 for the cars of all severities and those with serious and fatal injuries.

**Table 2. Involvement of pillars for the cars of struck side occupants.**

Pillars	All Severities	Seriously Injured	Fatally Injured
A-pillar involved	816 (45%)	135 (68%)	53 (71%)
B-pillar involved	667 (39%)	117 (60%)	52 (69%)
C-pillar involved	224 (13%)	52 (26%)	39 (52%)
A- and B-pillars	362 (21%)	86 (44%)	42 (56%)

The A-pillar often takes the impact loads of real world accidents; it does so more frequently than any other pillar. 53 (71%) of the 75 fatal struck side occupants had their adjacent A-pillar involved in the direct contact with 42 (56%) having both A- and B-pillars involved. The corollary is that 29% of all fatally injured struck side occupants do not have the adjacent A-pillar within the area of direct contact and 31% do not have the B-pillar involved. 22% of the seriously injured do not have the A-pillar involved and 40% do not have the B-pillar involved. When a pillar is struck by the bullet object it is usually loaded over a substantial part of its height, it is relatively easy for a strong pillar to spread loads to the rest of the car structure. If the pillar is loaded by an impact on the adjacent door the loads can only be transmitted through the hinges or the latch for most car designs; the effectiveness of a stronger door or pillars therefore becomes limited by the strength of these components. Table

2 suggests that this may currently occur in up to 30% of fatal side impacts.

### Direction of force

The barrier described in the US proposed regulation has a crabbed motion to simulate the forward trajectory of the tested car and loads are applied from a direction of 27 degrees forward of perpendicular. The EEVC proposals however assume the test vehicle is stationary and apply loads from a perpendicular direction. The real world data reveals that 36% of struck side occupants in side impacts are in cars with a purely perpendicular direction of force, while 41% have a force vector 30 degrees forward. Table 3 shows the clock directions of force for occupants with each level of injury.

**Table 3. Direction of principal force for all struck side occupants.**

Clock Direction of force	Fatal	Serious	Slight & uninjured	Total
1 & 11	10 (14%)	28 (14%)	109 (8%)	147 (9%)
2 & 10	39 (54%)	81 (41%)	565 (40%)	685 (41%)
3 & 9	19 (26%)	53 (27%)	520 (37%)	593 (36%)
4 & 8	4 (6%)	35 (18%)	207 (15%)	245 (15%)
<b>Total</b>	<b>72 (100%)</b>	<b>197 (100%)</b>	<b>1401 (100%)</b>	<b>1671 (100%)</b>

The proportion of occupants with a 30 degree forward component increases to 54% amongst the fatally injured occupants. The 2 o'clock and 10 o'clock impacts were more frequently associated with fatal injury impacts, of the 685 that occurred 6% were fatal compared to 3% of the 3 and 9 o'clock impacts. The direction of force distribution was found to vary with the nature of the striking object. The fatal 2 and 10 o'clock impacts occurred mainly when the bullet object was a truck or a pole. 66% of fatal pole impacts and 66% of fatal truck impacts were at 2 or 10 o'clock compared with only 31% of fatal car to car side impacts. The impact directions of fatal car to car impacts were more widely distributed, 31% were also at 4 and 8 o'clock.

In the accident population studied oblique impacts with poles were more often fatal than perpendicular impacts. There were 94 pole impacts with a force direction of 2 or 10 o'clock and 83 with perpendicular impacts. 20 (21%) of the oblique impacts were fatal compared with only 8 (10%) of the 3 and 9 o'clock impacts. A similar pattern existed for those occupants slightly injured.

Both sets of test proposals appear to simulate well the force directions applied in fatal side impacts with cars. The majority of fatal impacts were not with cars however and the more common, more often oblique, fatal impacts with poles and trucks were less well represented. The variation of the principle direction of force with striking object is believed to relate to the different accident circumstances involved. Car-to-car side impacts are often intersection collisions whereas car to pole impacts may more frequently be due to a loss of control.

## Barrier Characteristics

### Nature of bullet objects

The EEVC mobile barrier is designed to simulate a typical car in stiffness with a width of 158 cm and a mass of 950 kg. The US barrier is much stiffer with a mass of 1364 kg and a width of 168 cm and is more typical of a light truck. The ground clearance of the EEVC barrier is 30 cm while the NHTSA barrier is 2 cm lower.

No field data have been collected where the effective stiffness of the bullet object has been measured but the stiffness can be crudely classified according to the type of the bullet object. In general cars can be considered to be amongst the softest group of objects with trucks, utility poles and trees amongst the most stiff. The distribution of the bullet objects found amongst the field data is shown in table 4 for all struck side occupants, those seriously injured, and those killed.

**Table 4. Striking object distribution for struck side occupants and all fatally injured occupants.**

Striking Object	Struck Side Occupants			All fatally injured occupants
	All Severities	Seriously Injured	Fatally Injured	
Car	1026 (60%)	77 (39%)	23 (30%)	38 (36%)
Truck/Bus	216 (13%)	29 (15%)	16 (21%)	19 (18%)
LGV	96 (6%)	10 (5%)	2 (3%)	2 (1%)
Pole/tree	227 (13%)	62 (31%)	32 (43%)	43 (41%)
Other vehicle	7 (0.4%)	2 (1%)		
Other object	135 (8%)	18 (9%)	2 (3%)	3 (2%)
<b>Total</b>	<b>1707 (100%)</b>	<b>197 (100%)</b>	<b>75 (100%)</b>	<b>105 (100%)</b>

A car is by far the most common striking object, 1026 (60%) of all struck side occupants were in car to car collisions while poles and trucks were less common, representing about 13% of struck side occupants each. A different picture emerged amongst the seriously and fatally injured groups. 77 (39%) of the seriously injured and only 23 (30%) of the fatally injured struck side occupants were in cars struck by other cars. The most common object striking fatally injured occupants were trees or utility poles. Of the 227 struck side occupants in cars that struck poles or trees 32 (14%) died compared to only 23 (2%) of the 1026 that were struck by other cars. The death rate for impacts with trucks was 7%. Poles and trees are clearly particularly hazardous objects to collide with although impacts with cars are more common. This balance of injury risk and exposure results overall in similar numbers of fatalities due to each type of bullet object. Other studies have reported similar results. Hartemann (7) described a three month population of side impact fatalities in France where 30% of casualties were struck by a car, 45% against a tree or pole and 17% struck by a truck. FARS (8) data in the US described the involvement of cars, trucks and trees or poles as 31–33%, 27–36% and 31–42% respectively for fatal occupants in side collisions.

The effect of the height range of the fronts of the bullet cars was not determined within this analysis. It was therefore not possible to evaluate the relative consequences of the ground clearances of the two barriers.

The choice of a mobile barrier that has the characteristics of a car should result in new car designs that give optimum protection in car to car impacts. The level of protection in collisions with trucks and poles may be only slightly increased over current car designs. Therefore 60% of all side impact occupants and 30% of the fatal occupants would obtain maximum benefit from a car optimised for protection in car to car impacts. The group of struck side occupants in cars striking other objects and the unrestrained non-struck side occupants may well receive a lower level of protection. There were 1051 (32%) in the population of 3250 occupants in cars in side collisions. The 934 (29%) restrained non-struck side occupants are likely to receive only a minimal reduction in injuries.

The NHTSA test procedure would result in cars with protection optimised for impacts with objects with stiffness of light trucks. The test would be closely similar to the impact conditions of only 6% of struck side occupants in side collisions and 3% of the fatal occupants. However such a barrier would present a more severe impact to the test car than from a bullet vehicle of lower stiffness as the target cars' structure would be required to be more rigid. The ability of the NHTSA barrier to deform both A-pillar and B-pillar resulting in ride-down for struck side occupants appears to be an artificial benefit when car to car side impacts are examined.

If the barrier simulated a tree or pole only 13% of the whole population of struck side occupants would be represented as would 23% of those seriously injured. The proportion of fatal struck side occupants represented would rise to 43%.

Currently NHTSA is considering the retention of FMVSS 214 which incorporates a static test where a pole-like device is pushed into the side of the car. FMVSS 214 has been evaluated and has been shown to result in car designs that are effective in car to pole impacts (9). A test procedure that simulates car to car side impacts would seem to be less of a compromise when alongside an additional test examining the protection in pole impacts, particularly for the reduction of numbers of fatally injured occupants. The design of cars to protect occupants in side impacts with both cars and poles appears to be difficult although concept designs with external door beams have been discussed (10). There are no equivalent proposals for such a requirement in Europe. However the future addition of a supplementary pole-like test procedure to the mobile barrier tests proposed does appear to have the potential for a further reduction in fatalities. However there were still 11,100 single vehicle fatalities that occurred in the US (11) in 1987 and 2304 (21%) died in side impacts. FMVSS 214 is not completely effective and a significant constraint may be the numbers of fatal head injuries caused by striking the pole. The contact locations are examined in more detail later.

### Width

The diversity of the striking objects has consequences in terms of the width of the direct contact on the test vehicle—a

truck is likely to result in a wider contact area than a lamp-post. The median overlap for all severities and fatal occupants respectively was 149 cm and 180 cm. The complete distribution is shown in table 5 for struck side occupants.

**Table 5. Width of direct contact in cars of struck side occupants—median values and spread of values.**

Bullet Object	All Severities		Fatal Occupants	
	Median (cm)	25%-75%ile (cm)	Median (cm)	25%-75%ile (cm)
Cars	155	115 - 180	180	171 - 217
Truck/bus	175	150 - 185	313	216 - 395
Other vehicle	161	109 - 192	225	0
Tree/pole	45	30 - 75	60	30 - 202
All objects	149	92 - 178	180	130 - 256

The median width of direct contact for the cars of occupants of all severities was close to the 158 cm width of the European barrier. Truck impacts tended to result in wider overlaps but the spread of the measurements was large. Only pole impacts were significantly different with a median width of only 45 cm. All of the widths of overlap of the striking objects for the fatally injured occupants were wider, ranging from 60 cm for pole impacts to 313 cm for truck impacts—probably as a result of spreading of the bullet object under high loads. The spread of these measures was found to be relatively small for all striking objects in fatal collisions except for poles which had a spread of 172 cm between the 25%ile and the 75%ile. Trees surprisingly resulted in much wider direct contact than utility poles, the median values amongst the cars of fatal occupants were 30 cm for poles and 202 cm for trees. It was noted that 80% of the fatal tree impacts were either with a 2 or 10 o'clock direction of force. It appeared that the more glancing nature of these impacts was the cause of a relatively narrow striking object resulting in a wide area of direct contact.

Table 6 shows the percentile values that the two barrier widths represent. The EEVC barrier is close to the median value seen in the field data although it is too wide for the serious and fatally injured occupants. The NHTSA barrier, being 10 cm wider, is less typical of all severities of side impacts but more typical of the serious and fatal groups.

**Table 6. Percentile points of direct contact width distribution representing barriers.**

Test Proposal	All occupant severities	seriously injured	fatally injured
EEVC	52%ile	42%ile	32%ile
US	64%ile	46%ile	38%ile

## Mass

It was decided that the mass of the EEVC barrier would be 950 kg following examination of the characteristics of vehicles sold in 12 European countries in 1976, while the US barrier mass of 1360 kg was based on the fleet of vehicles sold in 1978. The UK field data used for this analysis has been collected in the years since 1984 and only a small part of the bullet car sample was built before 1976; this database can therefore be considered to be more up to date than the original CCMC (12) data.

The field data show that the median mass, including the occupants of all case cars in all types of impact in the area studied, was 992 kg and the EEVC barrier mass lies at the 39%ile while the NHTSA barrier represents the 94%ile. However the study population was not completely representative of the fleet of all cars on the road as all the case cars were aged below 6 years at the time of the accident. This difference from the study population may therefore be artificial. The median mass of the cars in the complete study population was not the same as that for the bullet cars in side impacts. The masses of these cars is significantly greater, both for all severities of impact as well as for serious impacts the median mass of the bullet cars was 1050 kg. The median for the bullet cars in fatal side impacts was heavier at 1150 kg. Table 7 shows the percentile point of the bullet car mass distribution that the two barriers represent.

**Table 7. Percentile point of masses of barriers.**

Test Proposal	All Occupant Severities	Seriously Injured	Fatally Injured
EEVC	24%ile	38%ile	below minimum
US	86%ile	95%ile	85%ile

As a representation of cars as the bullet vehicle in typical European side collisions, the EEVC barrier appears to be light. To be more representative of serious injury car collisions the mass should be raised by 100 kg to 1050 kg and by a further 100 kg to 1150 kg if the fatal conditions are to be reflected. It is of note that reference (2), citing a group of European field studies (13, 14, 15, 16) describes a typical car to car side collision and gives the bullet car mass as 1100 kg. The US barrier however appears to be heavier than necessary to reflect European conditions. It would be more typical if it were made 2-300 kg lighter. It is not possible to comment on its suitability for US conditions as no accident data is available to the authors.

## Impact speed

The EEVC proposed test procedure involves a barrier impact speed of 50 kph and the US proposes a 54 kph impact speed. The field data employs the CRASH3 computer program to estimate delta-v in a manner equivalent to its use within the US National Crash Severity Study. Table 8 shows the median values of delta-v for the cars of struck side occupants of each severity level in impacts with cars. CRASH3 does not estimate delta-v accurately for pole or truck impacts so the field data contains a high proportion of unknown values for these striking objects. Table 8 therefore only shows the values for car to car impacts. It was possible to estimate the delta-v of 491 vehicles, the remainder violated the assumptions of CRASH3. The use of CRASH3 provides an estimate of the impact severity to the target car as measured by delta-v. The computer algorithm incorporates a number of approximations in its implementation and its accuracy has been questioned particularly by those involved in accident reconstruction for litigation purposes. Smith (17) compares the true and predicted delta-v values of

30 staged side collisions using CRASH3 and shows that it tends to produce an underestimate. CRASH3 does not appear to be suitable for individual delta-v estimates and Smith states that it is best used in statistical studies where the under- and overestimates balance as much as possible. There is also no widely accepted alternative algorithm that is more capable of estimating the impact severity to a wide range of car models.

**Table 8. Median delta-v of struck side occupants when struck by cars.**

Injury severity	Median Delta-v Car to Car Impacts	Percentile Point of 25 kph
All injuries	24 kph	55%
Seriously injured	31 kph	24%
Fatally injured	43 kph	below lowest

The effect of the delta-v experienced in each of the test procedures will vary according to the mass ratio of the test. A car of the same mass as the barrier will have a delta-v of half the impact speed less the amount corresponding to the deformation energy. If the barrier is heavier the delta-v will be correspondingly greater due to momentum conservation. The assumption that the barrier mass represents the mass of a typical car infers that the median delta-v expected in the tests is 25 kph. The percentile point that a 25 kph delta-v represents is therefore shown in table 8. The median delta-v experienced by occupants of all injury severities is 24 kph so the severity of the EEVC test would represent these impacts well. The median delta-v of the seriously injured occupants in collisions with cars is 31 kph, above the nominal test delta-v as was that for the fatally injured casualties at 43 kph.

Rouhana (18) reports that NCSS data shows a median delta-v of 27 kph for serious injuries and 50 kph for fatal occupants. Cesari (19) found similar results in a small study of 39 car to car side impact collisions. He reported the mean delta-v for AIS 3 to 5 injuries to be 30 kph. Mackay (20) summarising other studies also describes the typical delta-v resulting in AIS 3+ injuries to be in the region of 30 kph with the 75%ile delta-v for these injuries at 38 kph.

The typical delta-v of 25 kph expected of the range of test impacts is therefore only close to the median value of car to car impacts of all injury severities. It is 6 kph too low for serious injury collisions and 18 kph too low to represent fatal collisions. The NHTSA barrier is heavier and will result in a median delta-v of 35 kph with the European car fleet. This value is between the median values for serious and fatal collisions and would appear to be a much closer compromise value than that obtained through use of the EEVC barrier.

It is of note that NHTSA in the Preliminary Regulatory Impact Analysis (21) states that NCSS data gives the median impact speed of serious injury accidents as 56 kph with an additional forward component of 28 kph. The US test speed therefore represents the lower threshold of serious injury and is inherently less severe than most serious and most fatal side collisions in the US.

When a test proposal is developed the injuries that are to be reduced first have to be defined. The impact severity of the test car can then be at the level by which 50% of these injuries have occurred. The effectiveness of the test is optimised when the acceptable dummy measurements represent the level where 50% of the population sustain the defined injuries. If the crash severity to the vehicle is below the level where 50% of injuries are sustained the acceptable dummy measurements have to be correspondingly reduced if the test is to be optimised for the population. The impact severity of the test cars resulting from the EEVC procedure are typically below the severity level where 50% of the population of struck side occupants sustain serious injuries. An equivalent situation exists comparing the NHTSA test to the US accident data. The permitted levels of dummy measurement in the EEVC test however are at the 50th percentile level although NHTSA is considering a range of levels.

The impact severity measures to the vehicle and to the occupant are not the same. The severity to the vehicle is usually measured by an estimate of delta-v; the velocity change of the target car during the time when the deformation is occurring. Experimental collisions however suggest that the impact severity to struck side occupants relates best to the travelling speed of the bullet car at the moment of impact. The link between the measures of impact severity to the vehicle and the occupant from field and experimental data is unclear.

Experimental collisions suggest that the test impact speed is at the level seen to result in severe injuries in cadaver tests while the field data from the UK, the US and France indicates it is not. Therefore there is a discrepancy between impact severity to the car measured in field data and the impact severity to the occupant measured in experimental data. It is recommended that a study be performed to examine this relationship between the two measures to clarify the situation.

## Occupants

NHTSA (21) have estimated the likely changes in injury levels following adoption of the proposed regulation. 78% of the reduction of fatalities is to struck side occupants as is 78% of the reduction of AIS 3-5 thorax injuries. The design improvements are expected to principally benefit struck side occupants and most of the serious and fatally injured occupants are in fact seated on the struck side in the front. The UK field data supports this distribution of seating positions. Table 9 shows the maximum injury severities of occupants and Table 10 the positions of fatalities. Tables 9 and 10 show the seating positions for each level of injury severity and for those that died.

55% of occupants were seated on the struck side of cars in which someone was injured representing 73% of all occupants with a maximum AIS of 3 or more and 71% of all fatally injured occupants. Only 59% of the occupants with injuries were seated on the struck side. It appears therefore that side impact protection that is intended for the struck-

**Table 9. Maximum AIS of occupants with known seating position.**

Maximum AIS	Struck Side	Non-struck Side	Row Totals
0	283 (17%)	452 (32%)	735 (24%)
1	760 (46%)	711 (51%)	1471 (24%)
2	358 (21%)	141 (10%)	499 (48%)
3	162 (10%)	50 (4%)	211 (7%)
4	32 (2%)	21 (2%)	53 (2%)
5	42 (3%)	23 (2%)	65 (2%)
6	34 (2%)	4 (-)	38 (1%)
<b>Total</b>	<b>1671 (54%)</b>	<b>1402 (46%)</b>	<b>3072 (100%)</b>

**Table 10. Survival rates of occupants.**

Survival	Struck Side	Non-struck Side	Row Totals
Fatal	75 (4%)	30 (2%)	105
Non-Fatal	1632 (96%)	1394 (98%)	3026
<b>Total</b>	<b>1707 (55%)</b>	<b>1424 (46%)</b>	<b>3131 (100%)</b>

side occupants with serious or fatal injuries is aimed at the occupants that most commonly sustain these injuries. If however such measures provide little benefit for non-struck side occupants then further methods of protection need to be developed to aid this significant group of casualties. Other field studies have observed similar frequencies of non-struck side occupants amongst fatal occupants in side impacts. Griffiths (22) found 28% of fatal occupants in side impacts were on the non-struck side and the rate reported in Peugeot-Renault (8) data is 26% while most recently Gloyns (23) reported the rate to be 36%.

### Occupant interaction

Neither the EVEC nor the NHTSA side impact proposals position a second test dummy on the front row of seats. The loading that the dummies receive in either test is applied from intruding side structures alone. Of the estimated 1707 struck side occupants in the population in the study area 739 (43%) were known to have a second occupant seated next to them. Additional loads from the adjacent occupant were observed to make the injuries of 134 (18%) more severe. Of the 75 struck side occupants who died 29 (39%) had this extra side loading as did 63 (24%) of the 267 that sustained a maximum AIS of 3 and above. Gloyns (23) reports a higher

incidence of side loading finding that over 50% of fatal struck side occupants experienced such loads. The proposed test procedures are therefore failing to reproduce the real side loading experience of 39% of all fatally injured occupants. Measures to protect struck side occupants might involve improved restraint systems for non-struck side occupants and would be an additional benefit of non-struck side occupant protection.

### Patterns of injury

The EVEC test proposals include an assessment of the level of head, chest, abdomen and pelvis injury while the proposed US test will measure the levels of injury to the rib cage and underlying organs and the pelvis. Much of the development of the proposed test procedures has centered around the reduction of torso injuries. In the field data it can be seen that injuries can be sustained by every body area of struck side occupants. The body areas normally associated with fatal injuries are the head, neck, chest and abdomen and these have been given the priority when developing improved side collision protection. The distribution of injuries amongst struck side occupants in the UK data is shown in table 11 for each severity group of occupants, the percentage of occupants with an injury to each body area is shown together with the percentage of occupants with an injury above a particular AIS level.

**Table 11. Struck side occupants—percentage with injuries to each body region and percentage with injuries above an AIS level.**

Body Area	Fatal Occupants		Serious Occupants		Slight Occupants	
	% with any Injury	% with AIS 4+ Injuries	% with any Injury	% with AIS 2+ Injuries	% with any Injury	% with AIS 2 Injuries
Head	92%	63%	55%	44%	52%	16%
Neck	22%	13%	8%	4%	13%	0%
Chest	94%	72%	43%	31%	21%	3%
Abdomen	77%	59%	22%	18%	7%	1%
Arms	65%	0%	51%	39%	37%	8%
Legs	82%	3%	60%	45%	36%	4%

Fatally injured occupants had an average of 1.5 injuries with a severity equal to the most severe injury. The multiplicity of injuries amongst the seriously injured was lower, there being an average of 1.1 injuries per person equal to the maximum AIS. Slightly injured occupants had an average of 2.5 per person reflecting the ease with which cuts and bruises are caused.

The chest, head and legs of fatally injured occupants were the most frequently injured; however not all of these injuries were highly life threatening. No occupant was found to die in a side impact with a maximum AIS below AIS 4 and the body areas where these injuries most frequently occur were the chest, head and abdomen. There was no AIS 4 arm injury defined. The priority attached to torso injuries is therefore justified by the field experience.

There was a different pattern amongst the survivors with a maximum AIS of 3 or more. The body areas most frequently injured were the legs, head, arms and then the chest; and a similar pattern exists for injuries of AIS 2 and above. Rib fractures or thoracic organ injuries rarely cause long term impairment except in the elderly whereas extremity

fractures, particularly when they involve a joint, may cause a significant reduction in the quality of life for survivors. The incidence of these injuries will not automatically decrease as a consequence of torso protection and the lack of protection criteria for extremity injuries appears to indicate an insufficiency in both sets of test proposals. A deeper analysis of the nature of these injuries is needed to evaluate the long term consequences and to establish the parameters for any future testing. Head injuries are seen to have a similar importance for the survivors. Rutherford (24) found that 10% of casualties with an AIS 2 head injury, representing a short period of unconsciousness, still had symptoms one year after the accident. Clearly the more severe head injuries have the potential for even greater lasting effect.

## Head contacts

The EEVC test proposals include measurements of the HIC values experienced by the dummy head aimed at limiting the likelihood of head injury. There is no equivalent within the US procedure. However NHTSA acknowledges the importance of head protection in reference (21) and suggests a future regulation requiring padding for the A-pillar, B-pillar and side header rail. Experimental car to car side collisions indicate that test dummies contact the side header only rarely although they may also pass through the side window aperture to strike the bonnet of the bullet car.

Struck side occupant trajectories in real world collisions are varied, even when restrained, as they reflect the wide range of impact directions to the vehicle. Within the group of accidents studied the most common contact material associated with injuries of any severity were side glazing materials. These were found to represent 41% of all head contacts. The B-pillar or seat belt swivel were associated with 11% of occupant injuries, the side header with 6% and the A-pillar with only 1% of injuries. The US suggestion of padding these areas would therefore influence a total of 19% of all head contacts in side impacts. The frequency of involvement of these structures reduces slightly when the more severe injuries are examined, amongst struck side occupants with a head injury of AIS 3 or more 16% of head contacts were within this area as were 16% of the head contacts of the fatally injured.

Objects outside the car were also found to be associated with head injuries particularly the more severe ones. Fatally injured occupants who had a head injury as their most severe had 59% of their head contacts outside the vehicle and 52% of all struck side occupants head injuries of AIS 3 and above were associated with head contacts outside the car. A similar pattern has been reported by Bradford (25) examining head injuries in all types of impact. She reports 64% of all head injuries above AIS 2 arise from a contact outside the vehicle. Some of these head injuries were known to be a result of partial ejection of the head beyond the plane of the vehicle but many were with objects that intruded into the survival space of the occupant. 50% of the head contacts of all fatally injured struck side occupants were with objects outside the car but only 13% followed partial or complete

ejection. It was not infrequent for a head injury to be associated with several contact points during the impact; such as the A-pillar and the bonnet of the striking vehicle. A deeper analysis is required to examine the relative influence of these contacts in more detail. It would appear that the NHTSA suggestions for a padding requirement could be expected to address the head injuries of a portion of injuries of all severities but would provide little benefit for the majority of occupants with serious or fatal head injuries. Griffiths reports similar results in reference (22) where 42% of the AIS head injuries of fatalities were found to arise from striking objects outside the car; 82% of these following partial ejection.

The EEVC test procedure too does not appear to address the problem of head injury causation sufficiently. The important sources of the head injuries of seriously and fatally injured occupants are glazing materials, objects outside the car and the A- and B-pillars. However the normal head contacts occurring during the EEVC tests are with glazing materials, which very seldom cause life-threatening injuries, and the B-pillar. The HIC measured when the dummy head strikes the top surface of a polyurethane foam barrier will be completely different to that measured from striking a tree. The test setup does not therefore seem likely to fully reflect the real-world circumstances in which serious head injuries are sustained and a headform impact test may be more appropriate.

It would appear to be difficult to protect a struck side car occupant from sustaining head injuries when the bullet object, for example a tree or a truck, is intruding heavily into the passenger compartment. Such impacts are probably unsurvivable with current technology, although other occupants in the same car but seated on the non-struck side or more distant from the area of supported intrusion may be more readily protected.

## Discussion

The development of test procedures has taken a pragmatic approach addressing the types of impact that are the most easily reduced in severity while being commonly associated with serious or fatal injuries. They necessarily represent a compromise of many parameters observed to influence injury outcome in field data. Hobbs (26) suggests that any test procedure should adequately represent the side impact injury process. This infers that the test should have the impact severity of a typical fatal collision and that the loads to the dummies should be transmitted in a reasonably realistic fashion if the numbers of fatalities are to be reduced.

There appear to be some significant differences between the test conditions and those in which many people die. Both test proposals simulate a car to car side impact but the field data suggest that only 36% of the fatally injured struck side occupants are in cars struck by other cars. More fatalities result from collisions with more hostile objects such as trees, trucks or lamp-posts. The proposed test conditions will have some effect on this group of casualties but levels

of protection will be optimised for a car to car side impact. The tests will however be a better simulation of non-fatal side impacts as collisions with cars form 39% of serious injury collisions and 60% of all side impacts. The NHTSA considerations for pole impact protection could provide an important degree of additional protection for car occupants. The introduction of an equivalent measure in Europe could help to address an important group of fatalities. However fatal head injuries from a contact directly on the pole are probably not preventable currently and are likely to be a limiting factor to the effectiveness of any regulation.

The mass of the EEVC barrier is 200 kg lighter than the median mass of bullet cars in fatal real world collisions while the NHTSA barrier is 200 kg heavier. If it were typical of non-fatal side impacts with cars it would be 100 kg heavier. The injury outcome in side collisions is related to the speed of the bullet car at impact and the stiffness of its front end, while the mass influences injuries to a lesser degree. However the EEVC barrier mass is 200 kg (21%) less than that seen in real-world collisions and is too different from real world fatal collisions. If the barrier mass were increased these collisions would be reproduced more realistically. The CCMC has proposed a harmonised barrier mass of 1100 kg and this represents a useful improvement in the severity of the test.

Both barriers have the front face parallel to the side of the test vehicle at impact although the NHTSA barrier has a crabbed motion simulating the forward velocity of the test car. The forces are applied with a clock direction of 9 and 10 o'clock for the EEVC and the NHTSA barrier respectively. The most common direction of force in the field data has a forward component and is at either 2 o'clock or 10 o'clock. This is particularly evident amongst fatal side impacts where 54% have one of these two directions of force. This trend mainly occurs in side impacts with poles and trucks. Fatal side impacts with cars have a fairly uniform spread of directions between 2 and 4 o'clock and 8 and 10 o'clock. Neither barrier is clearly more realistic than the other. A test to simulate pole impacts, however, would be more typical of real world serious and fatal pole impacts if it reflected the more frequent oblique impacts.

The impact speeds of the EEVC and NHTSA barriers are 50 kph and 54 kph respectively. If the test car mass is the same as the barrier the delta-v will be 25 kph, if the car mass is greater the delta-v will be lower. The field data has shown that the barrier mass is below the typical mass of bullet cars in the field and the range of delta-v when the current car population is tested is therefore below the range experienced in the field. A test delta-v of 25 kph is close to the median value for side impacts of all severities; 55% of car to car collisions are less severe. It is not close to the median of 31 kph for serious injury side collisions and is below the lowest value for fatal car to car impacts. Neither test reproduces the impact severity to the vehicle in impacts where the more serious or fatal injuries occur. If the test requirements are expected to address fatal car to car side impacts the delta-v should be 43 kph, if it is to address those

where serious injuries are sustained the test delta-v should be 31 kph. The experience in France and the US appears to be similar. Experimental collisions with cadavers and dummies suggest that the tests do reflect the impact severity to the occupant and that there is therefore a discrepancy between field data and experimental data. This difference needs to be resolved before the tests can be clearly seen to be sufficiently severe.

The benefits from the new designs of cars that pass either of the proposed regulations will apply mainly to struck side occupants. These occupants represent the majority of serious and fatally injured car occupants in side collisions. The reduction in the injuries of restrained non-struck side occupants will be less as they only contact the intruding side structures of cars in impacts with high intrusion. These casualties necessarily take a lower priority than struck side occupants but they still represent almost 30% of fatal and seriously injured casualties. There is a need for improved protection for these occupants, possibly using restraint systems that are more effective in perpendicular impacts.

Improved restraint systems that were worn would have an additional benefit for struck side occupants. The field data shows that it is common to find two occupants seated on the same row of seats and that they frequently interact during a side collision. The non-struck side occupant can apply additional loads to the adjacent occupant increasing the severity of the injuries of 18% of all occupants. Nearly 40% of fatal struck side occupants have this additional side loading applied to some part of their body aggravating their injuries. This analysis has not examined the body regions that experience additional loading nor the nature of the loads that are applied. These will depend on the principal direction of force and the restraint use of the non-struck side occupant. The field data shows that although this additional loading is common amongst fatally injured occupants neither test proposal attempts to simulate it. Neither uses non-struck side occupants and therefore both fail to reproduce a common situation where the severity of injuries is made worse. A deeper analysis is required to evaluate the degree of additional loading applied to struck side occupants, the body regions involved, and the conditions where it occurs.

The EEVC test proposal seeks to limit head, chest, pelvis and abdomen injuries while the NHTSA proposals only restrict the causes of chest and pelvis injuries. Both are based on the assumption that torso injuries are the priority and that reductions in chest injuries will result in a reduction in some abdomen injuries. Injuries to the chest and abdomen were both very common amongst fatal struck side occupants and they are frequently the most life threatening. The priority given to these proposals is therefore appropriate for fatally injured occupants. This is not the case for those sustaining serious injuries. The body regions that most often sustain injuries that have the potential for long term impairment are the head, arms and legs. These body areas were the most frequently injured amongst struck side occupants. The multiplicity of injuries amongst the

seriously injured was low so the reduction of just the most severe injury of each occupant could result in a significant improvement to the overall level of injuries of each occupant. Neither test proposal addresses extremity injuries and it is not evident that any dummy designed for side impact can measure forces to these areas. Without a suitable test requirement the injuries with the most potential for the disablement of survivors will not be reduced.

The limit on HIC imposed by the EEVC test shows a recognition of the importance of head injuries. However many of the most severe injuries are caused by contacts with an object outside the car. This may follow partial ejection of the head but is more frequently associated with a heavily intruding part of the bullet object. Apart from marginal cases it is difficult to envisage the severity of these contacts being reduced with current technology. Side window glazing that prevents partial ejection would aid some occupants although this could have other injurious consequences if it becomes difficult for occupants to escape from the car after the impact. While the EEVC test will measure head contact forces the only parts of the car likely to be contacted during such a collision will be the side glass, B-pillar and, in the more severe impacts, the top surface of the barrier. The test does not simulate the real world collisions that result in most serious head injuries. An improvement might be a headform impact of the type suggested in the NHTSA proposals; this does seem likely to address some but not most of the life threatening head injuries.

## Conclusions

- Most fatal impacts are a result of collisions with objects other than cars. Fatal tree and utility poles collisions are as common. A car-like barrier reproduces serious injury collisions better.
- The EEVC barrier mass is 200 kg lighter than the median bullet car mass in fatal impacts. The NHTSA mass is 200 kg lighter.
- The EEVC test procedure typically results in a target car delta-v that is lower than that of most serious and nearly all fatal collisions.
- Both tests apply the forces to the test car along a realistic direction. Fatal pole and truck accidents are more often oblique.
- The side strength of the test car may be limited by the performance of the door hinges and latch in at least 44% of fatal impacts on account of the impact location.
- The interaction with a non-struck side occupant appears to aggravate the injuries of 39% of all fatal struck side occupants.
- The torso and head are the most common sites of injuries of AIS 4 and above amongst fatal occupants. Seriously injured occupants have the legs, head and arms as their sites of severe injuries.
- Padding of the A-pillar, B-pillar and side header rail could influence 19% of the head injuries of all

severities of struck side occupants. 59% of the head injuries of fatally injured occupants were associated with contacts with objects outside the car.

Further investigations are necessary to examine the deformation profiles of doors, the discrepancy between vehicle and occupant severity measures and the mechanisms of side loading from non-struck side occupants.

## References

- (1) US DOT, NHTSA. Federal Motor Vehicle Safety Standards: Side Impact Protection. Notice of Proposed Rulemaking. Federal Register, Vol. 53, No. 17, Jan. 1988.
- (2) EEVC Working Group, Structures Improved Side Impact Protection in Europe, 9th ESV Conference. 1982.
- (3) Galer, M.D., Mackay, G., Clarke, S., Ashton, S., The causes of injury in car accidents—an overview of a major study currently underway in Britain. 10th ESV Conference, 1985.
- (4) Otubushin, A., Galer, M.D., Crashed vehicle examination techniques. SAE Congress, 1986.
- (5) Stearn, S., Sampling and weighting techniques for a large complex sample of accident data. IRCOBI Conference, 1988.
- (6) Harms, P., Thomas, P., Renouf, M., Bradford, M., Injuries to restrained car occupants—what are the outstanding problems. 11th Experimental Safety Vehicle Conference, 1987.
- (7) Hartemann, F. et al, Violence of fatal car-to-car side collisions and vulnerability of population at risk: a challenge of real-world accidents. 9th Experimental Safety Vehicle Conference 1982.
- (8) Association Peugeot-Renault, Report to ISO/TC 222/SC 10/GT 1 N 135.
- (9) Kahane, C.J., The effectiveness and performance of current door beams in side impact highway accidents in the US. 9th Experimental Safety Vehicle Conference, 1982.
- (10) Daniel, R., Biomechanical design considerations for side impact. Side impact: Injury causation and occupant protection. SAE SP 769.
- (11) NHTSA. Fatal accident reporting system 1987, Washington 1988.
- (12) CCMC. Development of the CCMC barrier for lateral collision testing. 1981.
- (13) Appel, H., Hoffman, J., Accident analysis of vehicle side collisions. 3rd IRCOBI Conference, 1977.
- (14) Hartemann, F., et al, Description of lateral impacts. 6th International Technical Conference on Experimental Safety Vehicles 1976.
- (15) Cesari, D., Ramet, M., Biomechanical study of side impact accidents. 5th Experimental Safety Vehicle Conference, 1974.
- (16) Langweider, K., Aspekte der fahrzeugsicherheit anhand einer untersuchung von realen unfallen. Technical University of Berlin, 1975.
- (17) Smith, R., Noga, J., Accuracy and sensitivity of

CRASH. 26th Stapp Car Crash Conference, 1982.

(18) Rouhana, S., Foster, M., Lateral Impact—An analysis of the statistics in the NCSS. 29th Stapp Car Crash Conference, 1985.

(19) Cesari, D., Dolivet, C., What can be expected from side impacts standards. Side Impact: Injury causation and occupant protection, SP 769, SAE Paper 890375.

(20) Mackay, G., The characteristics of lateral collisions and injuries, and the evolution of test requirements. Proceedings of legislative proposals for car occupant protection in lateral impact. I. Mech. E., 1989.

(21) NHTSA, Preliminary regulatory impact analysis: New requirements for passenger cars to meet a dynamic side impact test: FMVSS 214, Page IIIA-3, DOT HS 807 220, January 1988.

(22) Griffiths, D.K., Breen, J., Thomas, P., Lawson, S., Investigation of a representative sample of real world side impacts to cars. University of Birmingham, 1983.

(23) Gloyns, P., Rattenbury, S., Fatally Injured struck side occupants in side impacts. TRRL Contractors Report 113, 1989.

(24) Rutherford, W., et al, Symptoms are one year following concussion from minor head injuries. Injury, Vol. 10, pp. 225-230, 1978.

(25) Bradford, M., et al, Head and face injuries to car occupants in accidents—field data 1983-1985. IRCOBI Conference, 1986.

(26) Hobbs, C., Rationale and development of EEVC lateral impact test procedure. Legislative proposals for car occupant protection in lateral impact. I. Mech. E., London, 1989.

## Acknowledgements

In a study such as this which relies on the cooperation of many different organisations and individuals there are many people to acknowledge. The authors would like to thank all those who assist with the UK Accident Research Programme and who have made this study possible. In particular they would like to thank:

The sponsors for their financial support, namely: The Department of Transport's Transport and Road Research Laboratory; Vehicle Standards and Engineering Division; Vehicle Inspectorate Executive Agency; Ford Motor Company Ltd.; The Rover Group; Nissan UK Limited. In particular grateful thanks are extended to Gary Suthurst (Ford) and Doug Foot (VSE) for their helpful advice.

The Chief Constables and their officers in all the areas that the teams work in for allowing access to accident data.

The consultants and other staff at the many hospitals in the study areas for their assistance in providing injury data, especially Mr. G.G. Bodiwala of the Leicester Royal Infirmary for his valuable contribution.

The various coroners in the study areas for their cooperation in providing copies of post-mortem reports.

All members of the Accident Research Units at ICE Ergonomics and Birmingham University, and the Department of Transport District Office Teams.

The opinions expressed in this paper are those of the authors and are not necessarily those of the sponsors.

## Side Impacts: Test Crashes and Real-World Collisions

**Edwin S. Nowak, Alan German,  
Zygmunt M. Gorski, Robert N. Green,**  
The University of Western Ontario, Canada

### Abstract

The complexity of inter-related events occurring in injury-producing vehicle side impacts makes it necessary to validate controlled prospective crash studies with retrospective real-world investigations. Adequately detailed field investigation of side impact collisions is a necessary complement to controlled crash studies and other test procedures and modelling.

Over the past five years, the authors have collected a representative sample of over five hundred injury-producing crashes involving passenger cars in Southwestern Ontario, Canada. Case studies from this dataset have been selected which closely conform to the impact type, and collision severity, of the proposals for staged-collision testing with respect to side-impact protection standards. The implications for occupant protection are examined through

a review of the injuries sustained by the vehicle occupants in these real-world crashes.

### Introduction

The nature of current vehicle design leads to a significant safety problem with respect to side-impact collisions. Whereas it is possible to provide relatively extensive energy management zones at the front and rear of a vehicle, this is not the case for the side structure. Consequently, even moderate impacts to the side of the passenger compartment can lead to a significant measure of intrusion of the vehicle structure into the occupant space, and provide the potential for serious injury to the vehicle occupants.

The extent of the problem of side impacts is underscored by recent research conducted by the authors on injury-producing collisions involving passenger cars. Over the past five years a statistically-representative sample of such collisions has been drawn from a prescribed geographical area in Southwestern Ontario, Canada. This study forms part of a programme of in-depth investigations of real-world

crashes being conducted by the federal government for the purpose of identifying safety-related problems and determining effective countermeasures.

The details of the study methodology have been reported previously (1).<sup>\*</sup> Analysis of current study data shows that, whereas one third of passenger car occupants are located in side-impacted vehicles, this crash mode produces one half of the occupant fatalities.

## Staged-Collision Testing

The problem of side-impact protection for motor vehicle occupants is currently receiving much attention from governments and vehicle manufacturers on a worldwide basis. In particular, two testing methodologies have evolved, one in Europe, the other in North America. Both feature a staged collision of a moving barrier striking the side of the passenger compartment area in the motor vehicle under test with an impact speed of the order of 50 km/h (2).

The European test protocol specifies a moving barrier which has a lighter mass (950 kg), and has less stiffness (7.7 kN/cm) than is used in North America (1361 kg, 20 kN/cm). An impact speed of 50 km/h is used for the European barrier whereas the North American barrier is travelling at 54 km/h at impact. Furthermore, the European test involves the moving barrier impacting the test vehicle at 90 degrees, whereas the proposed North American test has the barrier crabbed such that the longitudinal axis of the barrier is angled at 27 degrees to the direction of motion of its centre of gravity. Finally, two different dummies, specifically designed to estimate the severity of side impacts to vehicle occupants, are used in the tests, EUROSID in Europe and SID in North America (3).

To some extent these staged collisions simulate the T-type collisions frequently observed in the real world; however, the problems inherent in using surrogates for human occupants remain. The biofidelity of the different dummies, and even the measured parameters which best describe the potential for injury to human occupants, remain the subject of debate (4).

The intent of the present paper is to provide a series of case studies of side-impact collisions which closely conform to the proposed test conditions. The crush resulting to the side-impacted vehicle, and the details of the injuries received by the vehicle occupants will be reviewed.

In Canada, a number of staged-collision tests have been performed using both the European and North-American test protocols. Both domestic and imported passenger cars have been used as target vehicles in the tests. A compilation of the resulting crush to the impacted vehicles shows that the deformation extends over approximately 190 cm of the side structure, with a maximum penetration of the order of 45 cm measured at the mid-door level (5).

The longitudinal extent of the damage patterns appears to be relatively consistent at between 180 and 200 cm along the struck surface. The degree of penetration to the side of the

struck vehicle is dependent on both the type of impacting barrier, and on the stiffness of the side structure which is contacted. It is evident that contact by the European barrier results in considerably less crush, than that resulting from the heavier, stiffer, and faster-moving, North-American barrier. The deflection of vehicle side structure observed in the staged collisions conducted to date has been of the order of 30 to 50 cm.

Since the case studies presented here are drawn from a sample of all collision types, rather than from a series of side-impact crashes, there are only a small number which closely conform to the test conditions. Because of this, no attempt has been made to differentiate collisions which are similar to the two different test methodologies. Rather, envelopes representing the minimum and maximum levels of side crush resulting from both test protocols were drawn, and crush profiles from real-world crash vehicles which fitted between these extremes were identified from the study data.

## Case Studies

The initial series of cases presented are those which most closely conform to the staged-collision test methodologies.

In these real-world crashes the vehicle crush has been determined by methods similar to those described by Tumbas (6). In all cases, the reported crush profile of the struck vehicle has been measured at the mid-door level which represents the approximate region of maximum deformation. Where available, the damage to each of the collision-involved vehicles is described using a Collision Deformation Classification (7). Occupant injury severity is reported using the Maximum Abbreviated Injury Scale (8).

### Case No. 1

V1: 1984 Oldsmobile Omega two-door sedan

V2: 1979 Mercury Capri two-door hatchback

Vehicle 2 was stopped facing south for a red traffic signal at an urban intersection. A vehicle to the driver's right commenced a right turn. Driver 2 proceeded across the intersection on the red light. Driver 1, travelling eastbound, braked hard but was unable to avoid a collision.

The front of Vehicle 1 struck the right side of Vehicle 2



Figure 1. Right-rear three-quarter view of Vehicle 2.

<sup>\*</sup>Numbers in parentheses designate references at end of paper.

(O3RZMW3). Damage was sustained across 160 cm of the passenger compartment, the maximum penetration being 40 cm (figure 1).

Driver 2, a 59-year-old male, was accompanied by his 60-year-old wife in the right-front seat. Both occupants were unrestrained at the time of the collision. The driver received no injuries.

The arm rest on the right-side door interior was distorted as a result of contact by the right-front passenger who complained of pain and tenderness to the chest. She also suffered strained neck muscles, received a contusion to the right thigh, and sprained two fingers in her right hand (MAIS 1).

### Case No. 2

V1: 1977 Chevrolet Impala two-door sedan

V2: 1980 Pontiac Firebird two-door sedan

Vehicle 2 was stopped, facing east, on an urban arterial roadway. Vehicle 1 was eastbound to the rear of the case vehicle. Driver 1 steered into the westbound lane, intending to pass the stationary vehicle. At this point, Driver 2 abruptly commenced a left turn, crossing in front of Vehicle 1. Driver 1 braked hard but the two vehicles collided.

The front of Vehicle 1 (12FZEW1) struck the left side of the case vehicle (09LPMW3). Crush across 149 cm of the left side of Vehicle 2 resulted from the impact (figure 2). A maximum penetration of 45 cm was located at the centre of the left-front door.

Driver 2, a fully-restrained, 25-year-old male, was reported by police to have sustained only minimal injuries and did not require any medical attention.



Figure 2. Left-side view of Vehicle 2.

### Case No. 3

V1: 1978 Chevrolet Camaro two-door sedan

V2: 1983 Plymouth Reliant four-door sedan

Vehicle 2 was travelling westbound, approaching a stop-sign-controlled intersection. Driver 2 failed to bring her vehicle to a halt and drove across the path of northbound Vehicle 1. Both drivers braked prior to their vehicles colliding.

The front of Vehicle 1 struck the left side of Vehicle 2 (10LPEW3). Crush extended across 169 cm of the passenger compartment of Vehicle 2 (figure 3), with the max-

imum penetration being 41 cm.

Driver 2, a fully-restrained, 20-year-old female, sustained strained muscles in her back and sought treatment from a chiropractor (MAIS 1).

The right-front passenger in Vehicle 2 was a fully-restrained, 20-year-old, female. She received a 10 cm laceration below the right knee anteriorly which required six sutures, and minor bruising to the upper left arm (MAIS 2).



Figure 3. Left-front three-quarter view of Vehicle 2.

### Case No. 4

V1: 1980 Volkswagen Scirocco two-door hatchback

V2: 1986 Plymouth Reliant four-door sedan

Vehicle 1 was travelling westbound along an urban arterial. Vehicle 2 was travelling northbound along an intersecting roadway. Driver 2 failed to stop at a red traffic light and entered the intersection. The front of Vehicle 2 impacted the left side of Vehicle 1 (10LPEW3).

There was a broad crush across 217 cm of the left side of the passenger compartment of Vehicle 1 (figure 4). The maximum penetration of 35 cm was located to the rear of the left B-pillar.

Driver 1, a 19-year-old male, was unrestrained. He sustained a contusion to the left side of his head as a result of contact with the window frame. He also received minor abrasions to a finger on his left hand, and to his right foot (MAIS 1).



Figure 6. Left-front three-quarter view of Vehicle 2.

## Case No. 5

V1: 1986 Chevrolet Chevy Van 20

V2: 1976 Chevrolet Impala four-door sedan

Driver 2 was travelling westbound along an urban arterial and made a left turn in traffic. Driver 1, travelling eastbound, braked hard; however, the front of Vehicle 1 (11FDEW4) struck the right side of Vehicle 2 (02RDAW4).

Crush to the right side of Vehicle 2 extended across 252 cm (figure 5). The maximum penetration was 54 cm at the mid-door level, located towards the rear edge of the right-front door.

Driver 2, a 66-year-old male, was accompanied by his 65-year-old wife who occupied the right-front seat. Both occupants of Vehicle 2 were fully restrained.

Contact by the right-front passenger was evident to the armrest and the side-door interior at the level of the base of the side window glass. This occupant sustained a fracture of the right pubic ramus, and of the inferior pubic ramus, and a fracture of the eighth rib posteriorly as a result of these contacts. She also received superficial lacerations and abrasions to the right side of the face from broken window glass (MAIS 2).



Figure 4. Left-front three-quarter view of Vehicle 1.

Driver 2 suffered fractures to ribs five and six on the right side from loading by the occupant restraint system, and a minor laceration to the scalp from contact by flying glass (MAIS 1).

## Case No. 6

V1: 1983 Ford Escort station wagon

V2: 1979 Pontiac Acadian four-door hatchback

Vehicle 1 was travelling southbound along an urban arterial. Vehicle 2 had been travelling eastbound and was stopped at an intersection with the arterial roadway. Driver

2 failed to observe any traffic and commenced a left turn directly across the path of Vehicle 1.

The front of Vehicle 1 (02FDEW1) struck the left side of Vehicle 2 (10LYEW3). There was a broad crush across 262 cm of the left side of Vehicle 2 (figure 6); the maximum penetration was measured at 41 cm in the region of the B-pillar.

Driver 2, a fully-restrained, 45-year-old female, was reported by police to have sustained minor injuries and did not receive hospital treatment.

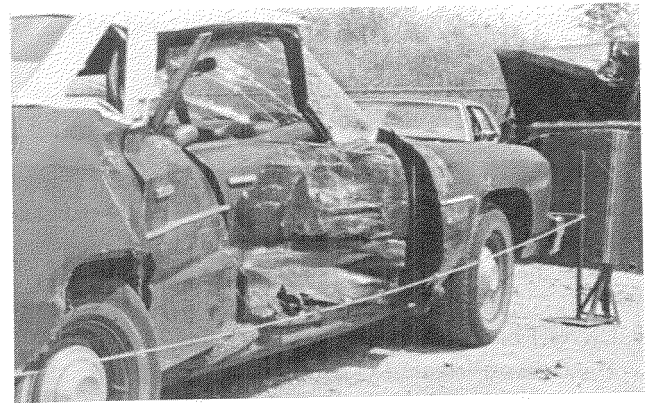


Figure 5. Right-rear three-quarter view of Vehicle 2.

## Case Studies with More Severe Intrusion

The above series of case studies, which closely conform to the proposed test configurations, indicate that in the real world one would not expect to see severe injuries to motor vehicle occupants resulting from such impacts. Many serious injuries, particularly fatal injuries to near side occupants, do however result from side-impact collisions.

Situations in which such fatal injuries are seen to occur include narrow impacts to the passenger compartment, adjacent to an occupied seating position, which result in extensive intrusion. Such cases arise for vehicles striking fixed objects such as trees, utility poles, and luminaires.

A second group of cases results from side impacts where the crush to the passenger compartment is of the order of that observed in the test collisions, but significant contact is made to one of the axles of the struck vehicles. Such collisions are often quite severe as a result of the inherent stiffness of the vehicle structure in the axle assembly region as compared to that in the area of the passenger compartment. The much greater energy transfer to the struck vehicle, and the greater lateral displacement of the impacted vehicle, compound the impact energy transmitted to the occupant who makes contact with the intruding side.

Additional cases result from high severity side impacts where the side intrusion extends beyond the levels observed in the staged collision tests. Whereas, some such collisions are extremely severe, a number of them result in side intrusion only marginally greater than that observed in the testing situation. The consequences of this greater intrusion are however considerable in relation to the injury potential

to the vehicle occupants. This latter scenario is illustrated by the following case studies.

### Case No. 7

V1: 1980 Chevrolet Citation four-door hatchback

V2: 1976 GMC Suburban utility vehicle

Vehicle 1 was travelling westbound, approaching an intersection. Driver 1 failed to observe a stop sign and drove into the intersection. Vehicle 2 was travelling northbound on the intersecting roadway. Driver 2 braked hard but the two vehicles collided.

The front of Vehicle 2 (01FDEW2) struck the left side of Vehicle 1 (09LZAW4). There was direct contact across 183 cm of the left side of Vehicle 1 with a maximum penetration of 61 cm (figure 7).

The only near-side occupant in Vehicle 1, the fully-restrained, 31-year-old, male driver, received fatal injuries. As a result of contact with the left-side door interior, he sustained fractures to the ribs number 1 through 11 on the left side, a fracture of the second rib on the right side, lacerations to the pleura, lungs, and pulmonary vessels, with haemopneumothorax and exsanguination (MAIS 5).

A 4-year-old male was restrained in a child seat in the right-front seating position. He received contusions to the shoulder and back from contact with the restraint system webbing and restraint shell (MAIS 1).

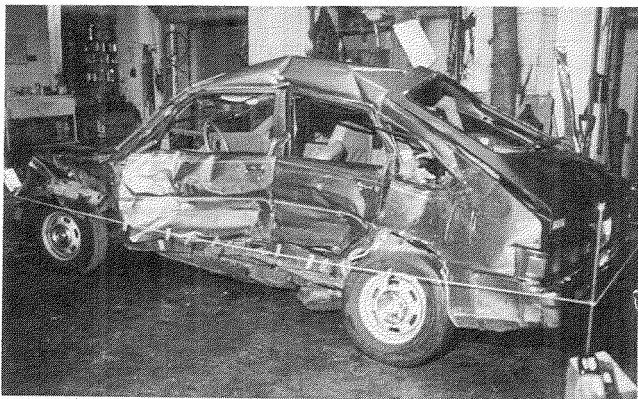


Figure 7. Left-rear three-quarter view of Vehicle 1.

A 30-year-old female occupied the right-rear seating position, and had a 1-year-old, male child on her lap. Both of these occupants were unrestrained. During the post-collision spin out of Vehicle 1 both rear-seat occupants were completely ejected. The female sustained a deep laceration to the left knee, a small laceration to the left eyelid, a bruise over the left eye, and abrasions to both feet (MAIS 2). The ejected child received fatal injuries, sustaining a fractured skull with a massive head injury, and multiple fractured ribs with haemothorax (MAIS 5).

### Case No. 8

V1: 1978 Pontiac Grand Prix two-door sedan

V2: 1980 Oldsmobile Cutlass four-door sedan

Vehicle 1 was travelling westbound along a rural arterial. Vehicle 2 was northbound on an intersecting concession.

Driver 2 failed to yield the right of way and Vehicle 2 travelled into the intersection. The front of Vehicle 2 (12FDEW2) impacted the left side of Vehicle 1 (09LYEW4).

The resulting damage extended along 347 cm of the left side of Vehicle 1 (figure 8). A maximum penetration of 72 cm was measured at the mid B-pillar.

Driver 1, a 38-year-old male, was unrestrained. He sustained a basal skull fracture with lacerations and contusions to the brain as a result of striking the edge of the hood of Vehicle 2. He also incurred a transection of his thoracic aorta, with exsanguination, from contact with the left-side door interior (MAIS 6).



Figure 8. Left-rear three-quarter view of Vehicle 1.

## Discussion and Conclusions

From an analysis of real-world, side-impact collisions involving intrusion into the occupant space and displacement of the struck vehicle, a number of factors contributing to occupant injury have been identified.

The pattern of side structure deflection was compared with the data generated in staged collision tests. Real-world collisions involving direct impact to the softer side structure between the wheel wells, with inward deflection of the order of 30–50 cm, resulted in very limited side displacement of the vehicle. These collisions generally involved minor injuries (MAIS 0–2) to the vehicle occupants.

Analysis of these collisions suggests that much of the collision energy was absorbed by the broad crush and deflection of the vehicle side structures, with minor energy transfer to vehicle occupants. This scenario is apparently close to the limit of occupant protection from severe injury in the standard North American passenger car. When side intrusion is at the upper limit, or beyond this range of intrusion, severe and fatal injury patterns are common.

Injury patterns to near side vehicle occupants are increased for a given degree of intrusion if the struck vehicle is also significantly displaced laterally as a result of the collision. This pattern is seen where some of the initial contact involves a stiff portion of the vehicle, usually the front axle.

For a given collision energy, side structure deflection and the degree of intrusion is increased when the impact takes

place across a narrow area such as side impact into trees and poles. These types of side impact often result in serious or fatal occupant injury in comparatively low speed collisions.

Current technology appears to provide adequate occupant protection from side impacts in the severity range associated with the proposed staged-collision testing. Our field studies suggest that this level of protection is close to a threshold above which serious injury is common. The design limits associated with the proposed staged collision testing must be extended to provide significant improvements for side impact protection if we are to prevent or mitigate the many serious injuries that continue to occur.

From our analysis of vehicle side impact collisions and the resultant occupant injury patterns, and relating these to data from staged collision tests, we highlight the following points for consideration in improving side impact protection for passenger cars:

1. Collision energy delivered to the side of a passenger vehicle must be dissipated by deflection of vehicle structures within the limits of intrusion described.
2. Structural changes to increase the capacity for energy dissipation should include a combination of increased side stiffness and mechanisms for promoting deformation across a broad area of vehicle structure.
3. A more forgiving dissipation of collision energy should include the frontal design of the striking vehicle.
4. The innermost layer of the vehicle side structure must be designed to cushion the occupant during inward deflection of the door due to intrusion and vehicle displacement.
5. The design limits associated with the proposed staged collision testing must be extended in order to provide significant improvements for side impact protection.

## References

- (1) German A, Gorski ZM, Green RN, and Nowak ES; PCS—The First Two Years of a Passenger Car Study in Southwestern Ontario; Proc. Canadian Multidisciplinary Road Safety Conference V; June 1–3, 1987; Calgary, Alberta; pp. 317–327.
- (2) Cesari D and Dolivet C; What Can be Expected from Side Impact Standards; SAE 890375; 1989.
- (3) Bendjellal F, Tarrière C, Brun-Cassan F, Forêt-Bruno JY, Caillibot P, and Gillet D; Comparative Evaluation of the Biofidelity of EUROSID and SID Side Impact Dummies; SAE 881717; 1988.
- (4) Viano DC; Evaluation of the SID Dummy and TTI Injury Criterion for Side Impact Testing; SAE 872208; 1987.
- (5) Dalmotas DJ; Road Safety and Motor Vehicle Regulation Directorate, Transport Canada (Private Communication).
- (6) Tumbas NS and Smith RA; Measuring Protocol for Quantifying Vehicle Damage from an Energy Basis Point of View; SAE 880072; 1988.
- (7) Collision Deformation Classification—SAE J224 MAR80; Society of Automotive Engineers, Warrendale PA; 1980.
- (8) The Abbreviated Injury Scale (1980 Revision); Association for the Advancement of Automotive Medicine, Des Plaines IL; 1980.

## Acknowledgements

The funding and support received from the Road Safety and Motor Vehicle Regulation Directorate of Transport Canada is warmly acknowledged. In particular, the contribution of Dainius Dalmotas in providing some results from the Canadian side-impact testing programme is greatly appreciated.

This type of field investigation programme would not be possible without the continued support of local police forces and medical personnel. Their efforts in support of our safety research activities are also warmly acknowledged.

## Upper Interior Head Protection: A Fleetwide Characterization

**Donald T. Wilke, Hampton C. Gabler,**  
National Highway Traffic Safety  
Administration,  
United States

### Abstract

Over 3000 fatalities and over 7000 serious head injuries result each year from occupants' heads striking various upper interior structures. The magnitude of this problem has prompted both government and industry to address the issue of reducing head injuries due to contact with these structures.

In a research project conducted by the National Highway Traffic Safety Administration (NHTSA) at the Vehicle Research and Test Center (VRTC), a component test approach was selected to evaluate the head injury causing potential of vehicle upper interior structures. Specifically, we chose a free-motion headform (FMH). The FMH can simulate the glancing and nonperpendicular head impacts experienced in real world accidents, and can measure head rotational motion.

For the purpose of validating the FMH results, 22 different head impact configurations were tested in 25 separate HYGES sled tests, using a full Hybrid III dummy. Also, 34 FMH tests were conducted under these same 22 configura-

tions. A regression analysis indicated the HIC response of a full Hybrid III dummy in a sled test can be estimated from the results of a similar FMH test.

FMH impact tests were conducted on the upper interior structures of twelve cars, which were selected to be representative of the passenger car fleet on U.S. roadways. An impact speed of 20 mph (32 kph) was used to test the A-pillars and front headers of these vehicles, while 15 mph (24 kph) was used on the side roof rails and B-pillars. HIC, peak resultant linear acceleration, and peak resultant rotational acceleration were measured in each test. In addition, the force/deflection characteristics of each structure were measured using a guided, rigid impactor.

## Problem Statement

In the United States, head impacts with the upper interior of vehicles are the leading cause of fatal crash victim head injury, for nonejected occupants. Estimates are that head/face to upper interior impacts result in over 3000 fatalities, and over 7000 serious head injuries (based on NASS 1979-1986). In terms of disability, approximately 50% of the medium term cognitive impairment in frontal crashes are due to contact with the A-pillars and roof rails (1).\*

To examine the severity of this problem from another perspective, we ranked the twenty leading injury producing contact zones, presented in figure 1, table 1, and table 2. The seriousness of head/face-upper interior impacts (3100 deaths/year, 10% harm) is second only to the severity of the chest-steering assembly impacts (5100 deaths/year, 12% of harm). Furthermore, as measured by the number of fatalities and harm, contact with the upper interior is the leading cause of head injury, followed by the windshield, and the roof. The period for which the accident data are currently available for analysis reflects a relatively low restraint usage. When additional years of NASS accident statistics become available, a shift in the distribution of injuries, as reported here, is expected. We anticipate that head impacts with upper interiors will continue to be a serious problem.

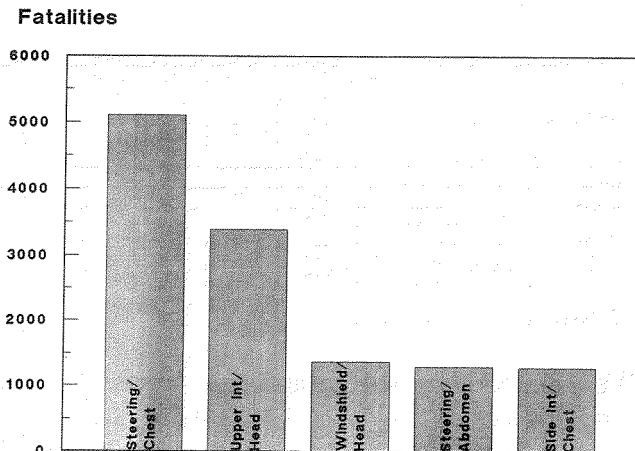


Figure 1. Comparing the components.

\*Numbers in parentheses designate references at end of paper.

Table 1. Ranking of occupant contact zones by number of fatalities.

Rank	Contact	Most Severely Injured Body Region	Number of Fatalities		
			all	cars	LTV's
1	Steering Assembly	Chest	5104	4176	927
2	Upper Interior	Head + Face	3385	2735	650
3	Windshield	Head + Face	1364	1188	176
4	Steering Assembly	Abdomen	1289	1123	166
5	Side Interior	Chest	1275	1269	7
6	Roof	Head + Face	1192	1105	87
7	Instrument Panel	Head + Face	886	710	176
8	Instrument Panel	Chest	881	793	88
9	Instrument Panel	Lower Extremities	896	785	111
10	Side Interior	Abdomen	762	723	40
11	Windshield	Neck	699	689	10
12	Roof	Neck	613	564	49
13	Interior	Abdomen	559	559	0
14	Upper Interior	Neck	444	315	130
15	Steering Assembly	Head + Face	419	419	0
16	Instrument Panel	Upper Extremities	265	153	109
17	Side Interior	Upper Extremities	221	133	88
18	Interior	Chest	242	242	0
19	Window Glass/Frame	Head + Face	198	23	175
20	Steering Assembly	Neck	192	192	0
All of the Above			20884	17896	2989
All Other Interior Contacts			2241	1604	637
All Noncontact			1624	1193	431
All Exterior Contacts			7251	5307	1943
All			32000	26000	6000

Table 2. Ranking of injury contact zones by harm.

Rank	Contact	Most Severely Injured Body Region	Percent Harm		
			all	cars	LTV's
1	Steering Assembly	Chest	12.15	11.90	13.45
2	Upper Interior	Head + Face	10.27	11.23	6.53
3	Windshield	Head + Face	8.93	9.71	5.88
4	Steering Assembly	Abdomen	5.36	4.56	8.60
5	Instrument Panel	Lower Extremities	3.69	3.86	3.06
6	Side Interior	Chest	3.16	3.58	1.36
7	Instrument Panel	Head + Face	2.95	2.18	5.95
8	Steering Assembly	Head + Face	2.85	3.20	1.47
9	Side Interior	Abdomen	2.02	2.42	0.36
10	Roof	Head + Face	1.81	2.01	1.04
11	Window Glass/Frame	Head + Face	1.80	1.59	2.59
12	Instrument Panel	Chest	1.69	1.79	1.29
13	Side Interior	Head + Face	1.61	1.85	0.68
14	Interior	Abdomen	1.51	1.81	0.26
15	Floor	Lower Extremities	1.51	1.44	1.78
16	Roof	Neck	1.35	1.00	2.58
17	Instrument Panel	Upper Extremities	1.30	1.11	2.00
18	Windshield	Neck	1.16	1.44	0.12
19	Steering Assembly	Upper Extremities	1.10	1.17	0.79
20	Interior	Chest	1.04	1.19	0.39
All of the Above			67.26	69.04	60.16
All Other Interior Contacts			10.76	11.44	8.18
All Noncontact			7.82	7.71	8.23
All Exterior Contacts			14.16	11.81	23.43
All			100.00	100.00	100.00

The upper interior, as defined in this paper, includes all components of the roof support structure. This grouping includes the A-pillar, the B-pillar, the C-pillar, the front roof rail, the side roof rails, the rear roof rail, and the side door window frames. The accident statistics include both passenger cars and light trucks/vans (under 10,000 pounds—4536 kg). When the paper refers to head hereafter, this term will refer to both the head and the face.

## Purpose

The objective of this program is to examine the degree of upper interior-head impact protection provided by the current production passenger car fleet. First, the paper contains a description of a promising technique for evaluating head injury potential using a component test. Secondly, it includes a discussion on the validation of this test procedure with respect to a series of full dummy sled tests. Finally, the results of a series of head-upper interior

impacts using twelve late model cars and the component test procedure are reported.

## Test Approach

Head impact testing of the upper interior requires a number of impact tests for each vehicle. A complete series of tests for a given vehicle would include tests of the A-pillar, the B-pillar, the side roof rails, and the front header. When compared with other head contact zones (e.g. the windshield), each of these components represents a relatively small target, requiring a very controlled test procedure to ensure consistent head strikes.

Test options for head impact testing included full-scale crash tests, sled tests with the vehicle body, and component tests. Our design objectives for the selected test approach were to accurately measure head impact responses, provide good control of head strike location, and minimize test expense. The full-scale crash testing option would require up to five crash tests to fully evaluate the upper interior. We did not pursue this option, because of both the expense and the lack of control over head strike location. Sled testing with a vehicle body has the advantage of more control and the realism of using a full dummy, but is considerably more expensive than the corresponding component test. While sled testing was not used to evaluate the fleet sample, heavy use of sled testing was made to validate the component test results.

Within the design objectives stated above, we chose to use the component test approach in this research program, to evaluate the head injury causing potential of production vehicle upper interiors.

## Component test description

The component headform test procedure selected for this program was based on a free-motion headform (FMH) which is launched into each component of interest. Impact velocities were derived from NASS, and vary with each upper interior component (2). For the A-pillars and front headers, the impact velocity is 20 mph (32 kph). For the side roof rails and B-pillars, the impact velocity is 15 mph (24 kph).

The FMH was developed from a Hybrid III head in an earlier project conducted by the NHTSA at the VRTC (3). As shown in figure 2, the headform is essentially a Hybrid

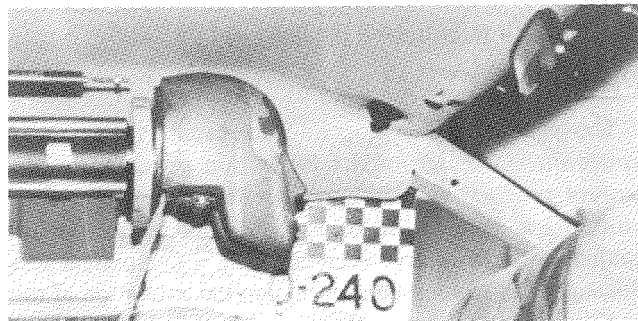


Figure 2. Free-motion headform impactor.

III head fitted with a specially designed mounting plate in place of the normal skull cap. For our experiments, the FMH is instrumented with a 9-accelerometer array which allows the calculation of both HIC and head rotational kinematics.

The FMH has two important advantages over more traditional, guided head impactors. First, since there is no guiding mechanism, the FMH can simulate the glancing and nonperpendicular impacts experienced in real world accidents. The second feature of the FMH is the ability to measure head rotational motion.

Excessive head rotational motion has been advanced as one of the leading explanations for some types of head injury (4). To date, however, biomechanics research in this area is still incomplete, and has yet to propose a widely accepted rotation injury criterion. However, it is anticipated that when such a criterion is developed, the FMH will have the potential for measuring the appropriate head rotational parameters which predict injury.

## Test procedure validation

Our primary objective during development of the FMH was to replicate the head responses of a full dummy in the crash environment. This section describes a battery of 59 validation tests in which the FMH test procedure was directly compared to the full Hybrid III dummy/sled test (5).

The 59 validation tests consisted of 34 FMH tests and 25 sled tests, simulating 22 different head impact configurations. Note that repeats of several FMH and sled tests were conducted. These tests consisted of impacts with actual and simulated vehicle upper interior structures, at a number of pitch angles, using both surrogates. Each was performed in baseline and padded configurations. Dytherm 4, manufactured by ARCO Chemical Company, was used as the padding for the A-pillar, side roof rail, and B-pillar tests, while Ethafoam 900, manufactured by Dow Chemical Company, was used on the front header tests. A matrix of these tests is shown in table 3. The numbers listed in the table indicate the number of tests performed under each configuration.

Table 3. Upper interior structure testing.

Vehicle	Component	angle*	Test Type			
			sled		FMH	
			base	pad	base	pad
Simulated	A-pillar	30°	1	1	3	3
		35°	1	1	1	1
		40°	1	1	1	1
		45°	1	1	2	3
		50°	1	1	2	2
Citation	A-pillar	47°	1	1	1	1
LTD	A-pillar	40°	2	3	2	3
Tempo	A-pillar	25°	1	1	1	1
	Front header	15°	1	1	1	1
	Side roof rail	35°	1	1	1	1
	B-pillar	70°	1	1	1	1

\* as measured from horizontal

## HYGE sled: the benchmark

Full dummy sled tests were conducted using four different sled bucks (5). The first, shown in figure 3, was the simulated A-pillar buck. This consisted of a fixture which held a length of steel tubing at any of the angles listed in table 3. The tubing was selected, in an earlier program (6),

to be roughly the same stiffness as a Chevrolet Citation A-pillar. The tubing was 1 inch square (254 mm<sup>2</sup>) by 18.75 inches (476 mm) long with a 0.11 inch (2.8 mm) wall thickness. The mounting was such that the ends were simply supported, not fixed or pinned.

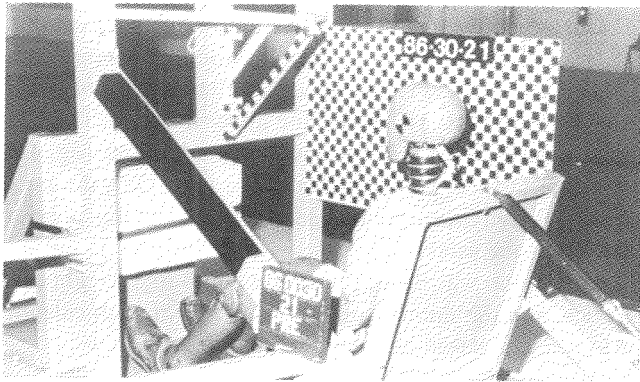


Figure 3. HYGE sled buck—simulated A-pillar.

A Hybrid III dummy, instrumented with a nine accelerometer array in the head, was used as the surrogate in these tests. The dummy was seated such that the forehead struck the steel tubing through the head's midsagittal plane, about 6 inches (152 mm) from the top end of the tube. An impact speed of 20 mph (32 kph), determined in an earlier phase of this program (2), was used for all simulated A-pillar tests. As indicated in table 3, ten tests were run, consisting of both baseline and padded tests at each of the five angles. The tubing was replaced prior to each test.

Similar sled tests were conducted on actual vehicle A-pillars, with sled bucks made from the bodies of a Chevrolet Citation and a Ford LTD. In each case, the car body was angled so that the head of the normally seated (per FMVSS 208) Hybrid III dummy would strike the A-pillar. Both the Citation and LTD sled bucks were used in baseline and padded A-pillar impacts, with a speed of 20 mph (32 kph).

A fourth sled buck was constructed from the body of a Ford Tempo. For this buck, the body could be positioned such that head impacts with the A-pillar, front header, side roof rail, and the B-pillar could be achieved. The Tempo sled buck is shown in figure 4, set up for a side roof rail test. An impact speed of 20 mph (32 kph) was used for the A-pillar and front header tests, while 15 mph (24 kph) was

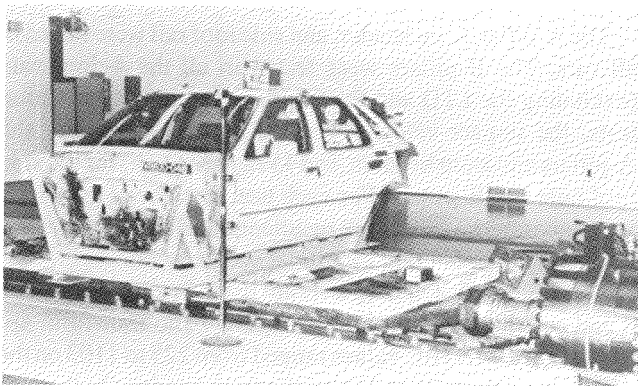


Figure 4. HYGE sled buck—Tempo side roof rail.

used for the side roof rail and B-pillar impacts (2). Both baseline and padded tests were conducted.

### Free-motion headform

As indicated in table 3, the FMH was used in simulated A-pillar tests as well as in Citation, LTD, and Tempo tests (5). The tubing and support used in these tests were identical to those used in the simulated A-pillar sled tests. The headform was positioned so that the forehead struck the tubing through the head's midsagittal plane, about 6 inches (152 mm) from the top of the tube. It was then fired horizontally into the tubing at a speed of 20 mph (32 kph). Again, the tests consisted of both baseline and padded tests at each of the five angles. The tubing was replaced prior to each test.

Similar tests were conducted on Citation and LTD A-pillars. In each case, the FMH was positioned to strike the A-pillar at the location determined from the occupant seated position. The FMH position was selected to coincide with that of a normally seated Hybrid III dummy. The FMH was placed at this position and horizontally aimed at the A-pillar, defining both the location of impact on the pillar and the angle of impact with respect to the longitudinal axis of the car. All A-pillars were tested in baseline and padded impacts, with a speed of 20 mph (32 kph). In figure 5, the set-up is shown for an FMH-to-LTD A-pillar test.



Figure 5. FMH test set-up—LTD A-pillar.

The FMH was also used on the Tempo upper interior structures. A-pillar impacts were performed following the same procedure as for the Citation and LTD A-pillars. Impact locations on the front header, side roof rail, and B-pillar were found based on the normally seated Hybrid III lateral, longitudinal, and vertical head positions, respectively. For each of these tests, the FMH was horizontally aimed at the structure from these positions. The A-pillar and front header were impacted at 20 mph (32 kph), while the side roof rail and B-pillar were struck at 15 mph (24 kph). Both baseline and padded tests were conducted.

### Test results and transform

For each Sled and FMH test indicated in table 3, the acceleration components of the head center of gravity were measured and the resultant calculated. The acceleration

components were filtered with an SAE Class 1000 analog filter prior to digitization and HIC values were calculated from the resultant (see table 4). If more than one test was conducted, the average of the HIC calculations was used for analysis, which is listed in the table. Individual responses are listed in the Appendix.

**Table 4. HIC values from upper interior testing.**

Vehicle	Component	angle*	Sled		FMH	
			base	pad	base	pad
Simulated	A-pillar	30°	626	343	477	192
		35°	1027	489	890	316
		40°	1096	629	1039	422
		45°	1552	836	1423	682
		60°	2169	1318	2320	1164
Citation	A-pillar	47°	1256	689	1058	496
LTD	A-pillar	40°	1287	661	1020	331
Tempo	A-pillar	25°	854	425	438	358
	Front header	15°	432	547	107	568
	Side roof rail	35°	535	171	351	226
	B-pillar	70°	792	555	1250	732

\* as measured from horizontal

A linear regression was performed in an attempt to correlate the FMH HIC results with those of the corresponding sled tests. The computation used FMH HIC and nominal impact velocity (15 or 20 mph, 24 or 32 kph) as the independent variables and sled HIC as the dependent variable. The relationship produced by the STEPWISE regression ( $r^2 = 0.93$ ) is presented below, and is plotted in figure 6:

$$HIC_{sled} = 0.81515 (HIC_{FMH}) + 61.58 (V_{nom}) - 932$$

In this equation, nominal velocity has the units of mph. For the 20 mph (32 kph) tests (empty symbols), this equation reduced to the following:

$$HIC_{sled} = 0.81515 (HIC_{FMH}) + 300$$

while for the 15 mph (24 kph) tests (solid symbols), it reduced as follows:

$$HIC_{sled} = 0.81515 (HIC_{FMH}) - 8$$

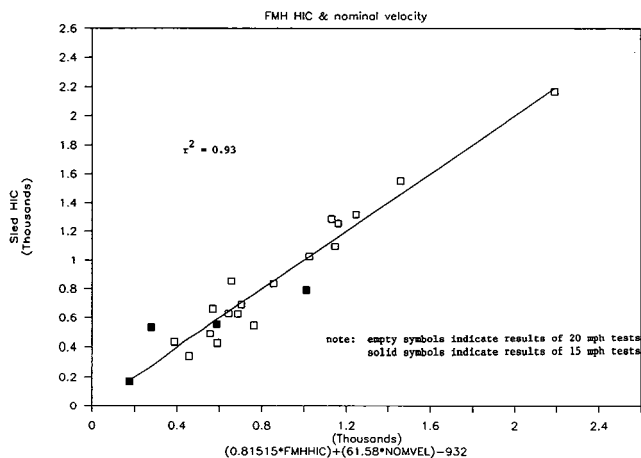


**Figure 6. Sled HIC versus FMH results.**

Using this transform, we can predict the HIC results from HYGE sled tests, with good confidence, from the HIC results of component level FMH tests, for both 15 and 20 mph (24 and 32 kph) nominal impact speeds.

## Production vehicle test results

Our next objective was to determine a fleetwide estimate of head injury potential in current production cars. Using 1987 sales figures (7), we selected a fleet sample of twelve cars for FMH testing of baseline upper interiors. The individual models were combined by body type (eg. GM A-body) and then ranked by body type sales. Only the top 40 selling body types were considered for use in this program (82% of total sales).

This group was then broken down into five weight categories, and the number of cars tested from each category was selected based on sales percentages as follows:

Weight Category	Curb Weight Range-lb (kg)	Percent of Sales*	Number Tested
1	0 - 2250 (0 - 1021)	21.6%	3
2	2250 - 2525 (1021 - 1145)	26.6%	3
3	2525 - 2750 (1145 - 1247)	17.3%	2
4	2750 - 3000 (1247 - 1361)	7.8%	1
5	over 3000 (over 1361)	26.7%	3
		100.0%*	12

\* percentage of top 40 selling body types only

The top 40 selling body types were then listed, in order of sales, for each weight category. From these lists, the appropriate number of body types from each category was selected for testing, based on their availability to the VRTC. The twelve models tested are listed below. The numbers in parentheses following each model are the body type overall sales rank and the body type sales rank within its weight category, respectively.

### weight category #1

2-door Ford Escort (2,1)  
2-door Nissan Sentra (13,3)  
2-door Mazda 323 (35,9)

### weight category #2

2-door Pontiac Sunbird (4,1)  
2-door Pontiac Grand Am (6,2)  
4-door Ford Tempo (9,4)

### weight category #3

4-door Chevrolet Celebrity (1,1)  
2-door Ford Mustang (21,3)

### weight category #4

4-door Ford Taurus (3,1)

### weight category #5

4-door Ford LTD (7,2)  
4-door Chevrolet Caprice (19,7)  
4-door Buick Electra (23,8)

## FMH responses

The A-pillar, front header, and side roof rail were tested in all cars. The B-pillars were tested in all the 4-door cars (excluding the LTD and the Caprice). As in the validation tests, the impact velocity was 20 mph (32 kph) for the A-pillars and front headers, and 15 mph (24 kph) for the side roof rails and B-pillars. For each test, three head responses were measured—HIC, peak resultant translational acceleration, and peak resultant rotational acceleration.

The HIC results of these tests are listed in tables 5 through 8 and are shown graphically in figure 7 (no transform applied). The FMH HIC values ranged from 225 to 1103 on the A-pillar and from 71 to 338 on the front header. On the side rail, the FMH HIC values ranged from 141 to 716 (exclud-

**Table 5. Results of production vehicle tests A-pillars—20 mph (32 kph).**

Vehicle	HIC		Peak Resultant Acceleration		Stiffness		Structure Angle (deg)
			Linear (g)	Rotational (rad/sec <sup>2</sup> )	lb/in (100%)	(kN/m) (95%)	
	Actual	Transformed					
Escort	253	506	90.3	7,786	1885 (330)	1994 (349)	35
Sentra	598	787	139.9	16,009	2630 (461)	2760 (483)	40
Mazda 323	669	845	138.4	14,407	2431 (426)	2569 (450)	40
Sunbird	1103	1199	200.4	28,122	2481 (435)	2769 (485)	24
Grand Am	721	888	156.0	18,936	2794 (489)	8092 (1417)	25
Tempo	438	657	123.6	12,750	3495 (612)	4513 (790)	25
Celebrity	579	772	141.7	15,140	3205 (561)	4779 (837)	24
Mustang	225	483	92.3	9,738	4049 (709)	5148 (902)	40
Taurus	290	536	104.3	13,643	2273 (398)	3023 (529)	38
LTD	1020*	1131*	181.1*	19,654*	2884 (505)	3309 (580)	40
Caprice	753	914	130.5	---- **	2897 (507)	2959 (518)	35
Electra	982	1100	173.3	16,427	2466 (432)	2628 (460)	40
average	636	818	139.1	15,692	2791 (489)	3712 (650)	34

\* average of two tests  
\*\* data anomalous

**Table 7. Results of production vehicle tests side roof rails—15 mph (24 kph).**

Vehicle	HIC		Peak Resultant Acceleration		Stiffness		Structure Angle (deg)
			Linear (g)	Rotational (rad/sec <sup>2</sup> )	lb/in (100%)	(kN/m) (95%)	
	Actual	Transformed					
Escort	442	352	115.3	9,421	1274 (223)	1429 (250)	46
Sentra	280	220	100.3	12,295	1457 (255)	1478 (259)	65
Mazda 323	178	137	79.8	11,914	1341 (235)	1385 (243)	65
Sunbird	419	334	115.7	14,557	2481 (435)	3891 (681)	63
Grand Am	210	163	84.2	11,541	1180 (207)	1321 (231)	59
Tempo	351	278	109.3	14,527	1854 (325)	1958 (343)	35
Celebrity	638	512	139.3	14,160	2097 (367)	2308 (404)	38
Mustang	408	325	120.7	14,562	2070 (363)	3411 (597)	50
Taurus	141	107	85.7	9,937	2368 (415)	2698 (473)	55
LTD	1876*	1829*	232.3	22,255*	2761 (484)	3961 (694)	42
Caprice	303	239	84.0	---- **	996 (174)	1063 (186)	37
Electra	716	576	141.4	14,211	1230 (215)	1469 (257)	50
average	371*	295*	106.8	12,713*	1759 (308)	2198 (385)	50

\* nominal impact speed was 20 mph (32 kph) for LTD test, not averaged  
\*\* data anomalous

**Table 6. Results of production vehicle tests front headers—20 mph (32 kph).**

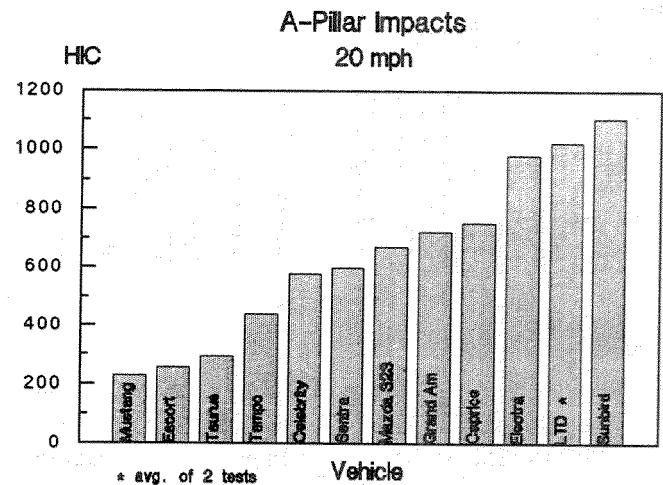
Vehicle	HIC		Peak Resultant Acceleration		Stiffness		Structure Angle (deg)
			Linear (g)	Rotational (rad/sec <sup>2</sup> )	lb/in (100%)	(kN/m) (95%)	
	Actual	Transformed					
Escort	115	394	59.4	7,951	1094 (192)	1056 (185)	19
Sentra	178	445	64.2	6,593	831 (146)	831 (146)	10
Mazda 323	71	358	50.8	5,980	410 (72)	387 (68)	18
Sunbird	192	457	67.5	10,357	703 (123)	960 (168)	20
Grand Am	164	434	72.7	11,735	1295 (227)	1340 (235)	19
Tempo	107	387	50.6	8,167	1202 (211)	1213 (212)	15
Celebrity	129	405	62.3	11,753	884 (155)	1062 (186)	15
Mustang	338	576	111.3	16,341	1279 (224)	1437 (252)	10
Taurus	125	402	70.6	11,059	1018 (178)	940 (165)	15
LTD	257	509	88.4	15,161	1063 (186)	1018 (178)	23
Caprice	194	458	78.4	---- *	776 (136)	901 (158)	16
Electra	99	381	55.0	8,028	1463 (256)	1662 (291)	18
average	164	434	69.3	10,284	1002 (175)	1067 (187)	17

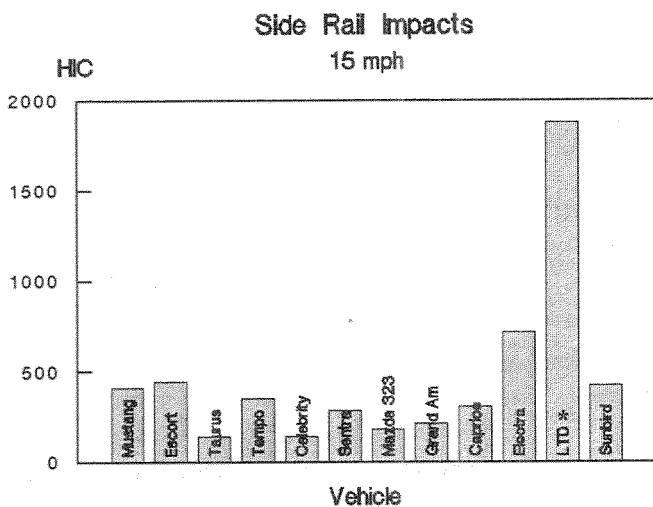
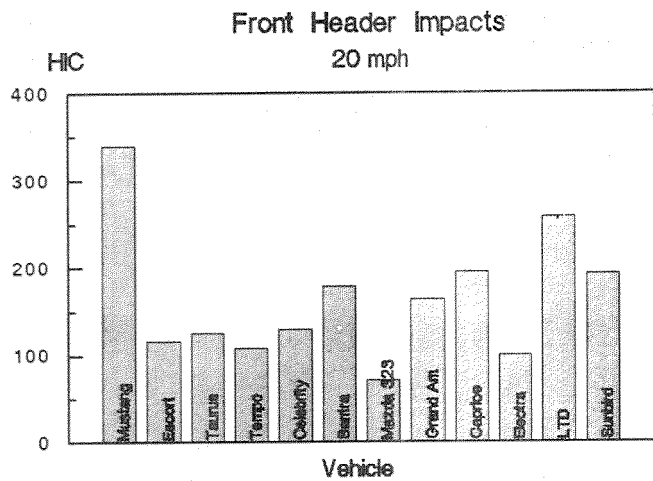
\* data anomalous

**Table 8. Results of production vehicle tests B-Pillars—15 mph (24 kph).**

Vehicle	HIC		Peak Resultant Acceleration		Stiffness		Structure Angle (deg)
			Linear (g)	Rotational (rad/sec <sup>2</sup> )	lb/in (100%)	(kN/m) (95%)	
	Actual	Transformed					
Tempo	1250	1011	179.6	14,135	3563 (624)	3545 (621)	70
Celebrity	1141	922	183.5	15,528	1821 (319)	1833 (321)	62
Taurus	944	762	158.7	12,735	4272 (748)	4647 (814)	55
Electra	587	470	118.4	---- *	520 (91)	586 (103)	67
average	981	791	160.1	14,133	2544 (446)	2653 (465)	64

\* data anomalous





\* nominal impact speed was 20 mph

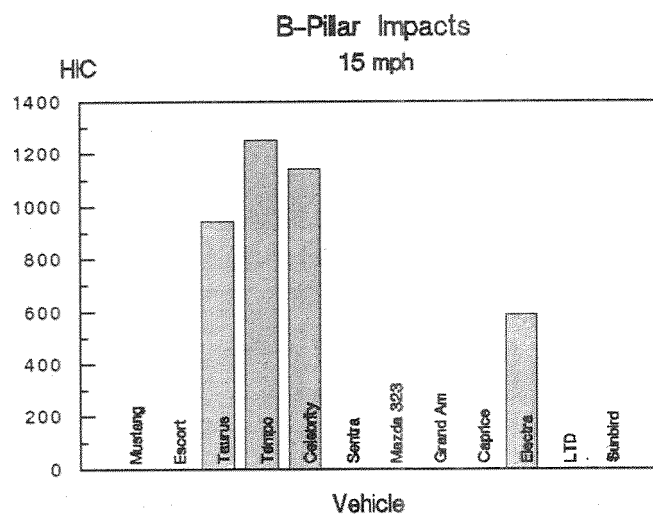


Figure 7.

ing the 20 mph—32 kph—LTD test), while they ranged from 587 to 1250 on the B-pillar. In general, the headform responses varied considerably among the vehicles, with the

B-pillar impacts producing the highest FMH HIC values and impacts on the front headers the lowest, on average.

The peak resultant linear acceleration and the peak resultant rotational acceleration for each test are also listed in tables 5 through 8. The resultant linear acceleration data were filtered with a nominal Class 180 digital filter (4-pole Butterworth filter with a cutoff frequency of 300 Hz). The peak resultant rotational acceleration data were obtained from the 9-accelerometer array mounted in the FMH and were filtered using a Class 1000 analog filter prior to digitization.

Earlier we stated that head contact with vehicle upper interiors is a significant safety problem. However, the majority of the HIC values calculated from our FMH tests are below the standard HIC-1000 threshold. We are currently reexamining these results. Our plans include conducting follow-up production car tests, using alternate test configurations with different impact angles and/or impact speeds, and considering other injury mechanisms.

### Structural responses

Structural stiffnesses were also measured for each structure in a separate series of tests using a guided, rigid headform (RHF), shown in figure 8. The RHF was developed by the General Motors Corporation (8) and has a hemispherical impact surface. All impacts were conducted perpendicular to the structure, at a nominal impact speed of 13.5 mph (21.7 kph). Linear headform accelerations and displacements were measured, thus providing force/deflection information for each structure.

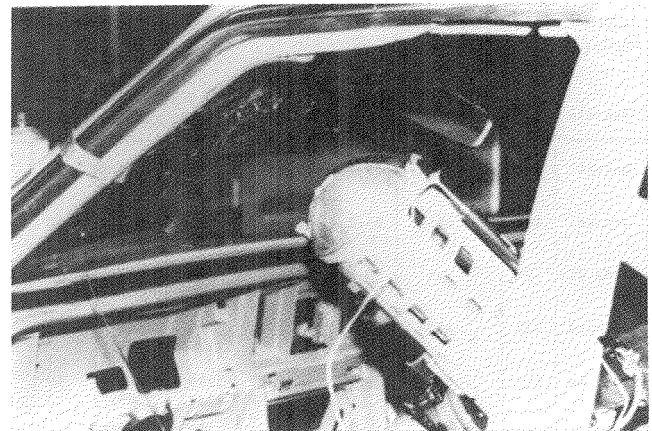


Figure 8. RHF test set-up—LTD A-pillar.

The stiffness values for each structure tested are listed in tables 5 through 8. Note that for each structure, two stiffnesses are listed, designated as 100% and 95%. The 100% stiffness is the slope of the force/deflection curve from the time of impact, as determined from the event switch, to the time of peak force. In some cases, the early portion of the curve was quite flat, rising more sharply after a significant amount of deflection. This flat portion may be due to a slight mispositioning of the event switch, thereby resulting in a premature time of impact, or due to some property of the structure which would serve to mitigate the impact.

Because of this uncertainty, a second stiffness was calculated in each case. We determined the point where the force level reached 5% of its peak and disregarded the portion of the force/deflection curve prior to this time. The stiffness designated as 95% in tables 5 through 8 was simply the slope of the remaining force/deflection curve. The cut-off level of 5% was chosen based on the review of a number of such curves.

Regardless of whether the 100% or the 95% stiffness was considered, the A-pillars were the stiffest structures, on average, followed by the B-pillars and then the side rails. The front headers were notably less stiff, on average, than the other structures.

We are currently conducting a detailed analysis in which we are examining the relationship between FMH responses and vehicle upper interior structural design parameters.

### Future work

The NHTSA is continuing to conduct research in the area of upper interior head protection. The testing of the twelve production vehicles presented in this text was recently completed and we are currently reexamining these results to determine how representative they are of real world head injuries. Our plans include conducting follow-up production car tests, using alternate test configurations with different impact angles and/or impact speeds.

In addition, we are analyzing these results to determine the relationship between structural design attributes and head impact severity. Candidate design attributes include, but are not limited to, structural stiffness, structural angle, hardpoints, and fabrication techniques. Once we better understand the effect that the design attributes have on head impact severity, our research will focus on determining practical methods for mitigating such impacts.

The Agency has also sponsored the development of a finite element model which simulates head impacts with vehicle upper interiors. The technique was recently validated in a series of simulations which model FMH impacts with Citation A-pillars, in both baseline and padded configurations. The model has produced results which predict those from actual FMH tests very closely. We expect that the finite element approach will improve our understanding of the interaction of occupant heads with upper interior structures and will aid in the development of injury countermeasures.

The tests reported in this paper have focused on protection of passenger car occupants. As noted in the accident statistics, head to upper interior impacts are also a serious problem for light truck and van (LTV) occupants. Research is currently underway to determine the injury causing potential of LTV upper interiors, and to explore the applicability of the FMH device to LTV testing.

### Summary

This paper has presented a fleetwide characterization of head to upper interior impact protection. The following is a

summary of our test results and analysis:

- In the United States, the seriousness of head/face-upper interior impacts (3100 deaths/year, 10% harm) is second only to the severity of the chest-steering assembly impacts (5100 deaths/year, 12% of harm).
- This project uses a component test approach to evaluate the head injury causing potential of production vehicle upper interiors. This approach was selected based on our design objectives, which were to accurately measure head impact responses, to provide good control of head strike location, and to minimize test expense.
- The FMH was selected as the component headform we will use to assess the head injury causing potential of vehicle upper interiors in passenger vehicles. We can estimate the HIC response of a full Hybrid III dummy in a sled test from the HIC results of a similar FMH test and the nominal impact velocity (in mph) using the following relationship:

$$HIC_{sled} = 0.81515 (HIC_{FMH}) + 61.58 (V_{nom}) - 932$$

$$r^2 = 0.93$$

- Since the FMH is a free-motion impactor and is capable of simulating glancing impacts, headform rotation occurs and can be measured. This allows for the possibility of using the FMH to predict head injury due to rotation, once such criterion is developed and accepted.
- Twelve production passenger cars were selected for use in this program, based on curb weight, sales, and availability. In each car, the A-pillar, front header, and side roof rail were tested to obtain headform impact responses, using the FMH. In four of the 4-door cars, the B-pillars were also tested. A nominal impact speed of 20 mph (32 kph) was used on the A-pillars and front headers, while 15 mph (24 kph) was used on the side rails and B-pillars (one exception—the LTD side rail was tested at 20 mph—32 kph).
- In general, FMH impacts with the different structures produced a relatively large range of HIC values. These FMH HIC ranges and averages were as follows (LTD results not included in the side rail range and average):

	<u>range</u>	<u>average</u>
<b>A-pillar</b>	- 225 to 1103	636
<b>Front Header</b>	- 71 to 338	164
<b>Side Rail</b>	- 141 to 716	371
<b>B-pillar</b>	- 587 to 1250	981

- For each structure of the twelve cars tested with the FMH, the stiffness was measured using a guided, rigid impactor. These tests were con-

ducted perpendicular to the structures, at 13.5 mph (21.7 kph), nominally.

- On average, the A-pillars were the stiffest structures, followed by the B-pillars, the side rails, and then the front headers. The average stiffnesses, in lb/in (kN/m), for these structures were as follows:

	100%	95%
A-pillar	2791 (489)	3712 (650)
Front Header	1002 (175)	1067 (187)
Side Rail	1759 (308)	2198 (385)
B-pillar	2544 (446)	2653 (465)

## References

(1) Jeffrey Marcus, Robert Blodgett; "Priorities of Automotive Crash Safety Based on Impairment;" Presented at the Eleventh International Technical Conference on Experimental Safety Vehicles; May 1987.

(2) M.W. Monk, H.C. Gabler, L.K. Sullivan; "Subsystem Testing For Head To Upper Interior Safety;" National Highway Traffic Safety Administration; Presented at the 11th International Technical Conference on Experimental Safety Vehicles; May 1987.

(3) R.A. Saul, M. Farson, D.A. Guenther; "Development of a Component Level Head Impact Test Device;" Presented at the 30th Stapp Car Crash Conference; SAE paper number 861889; October 1986.

(4) J.M. Abel, T.A. Gennarelli, H. Segawa; "Incidence and Severity of Cerebral Concussion in the Rhesus Monkey Following Sagittal Plane Angular Acceleration;" published in the proceedings of the 22nd Stapp Car Crash Conference; SAE paper number 780886; October 1978.

(5) D.T. Willke; "Selection of a Headform for Head/Upper Interior Testing;" Final report for project VRTC-86-0030; currently under internal NHTSA review for approval for publication.

(6) M.W. Monk, L.K. Sullivan; "Energy Absorption Material Selection Methodology for Head/A-Pillar;" National Highway Traffic Safety Administration; Presented at the 30th Stapp Car Crash Conference; SAE paper number 861887; October 1986.

(7) Automotive News; January 11, 1988 and January 18, 1988 issues.

(8) C.J. Griswold; "Side Impact Component Test Development;" Presented at the 9th International Technical Conference on Experimental Safety Vehicles; November 1982.

## Acknowledgements

The views and findings of this paper are those of the authors and do not necessarily represent the policy of the NHTSA. We are grateful to Michael Van Voorhis, Timothy Schock, and William Gwilliams for their efforts in the set-up and conduct of the tests, as well as to Claude Melton,

Stephen Elliott, and Roger Smart for their handling of the data.

We also wish to thank Thomas MacLaughlin, Thomas Hollowell, Michael Monk, and Lisa Sullivan for their assistance in formulating project objectives and for their efforts in the execution of these objectives.

Also, special thanks go to Susan Weiser for the preparation of the manuscript.

## FMH TESTING

### 30° Simulated A-Pillar

FMH HIC	baseline	padded
test #1	273	158
test #2	587	245
test #3	570	172
average	477	192

### 45° Simulated A-Pillar

FMH HIC	baseline	padded
test #1	1431	714
test #2	1415	672
test #3	xxxx	659
average	1423	682

### 60° Simulated A-Pillar

FMH HIC	baseline	padded
test #1	2112	1191
test #2	2528	1137
test #3	xxxx	xxxx
average	2320	1164

## LTD A-Pillar

FMH HIC	baseline	padded
test #1	975	295
test #2	1064	312
test #3	xxxx	385
average	1020	331

## SLED TESTING

### LTD A-Pillar

SLED HIC	baseline	padded
test #1	1267	500
test #2	1306	830
test #3	xxxx	652
average	1287	661

## Biomechanics of the Human Chest, Abdomen, and Pelvis in Lateral Impact

David C. Viano, Ian V. Lau, Corbin Asbury,  
General Motors Research Laboratories  
Albert I. King, Paul Begeman,  
Wayne State University

### Abstract

Fourteen unembalmed cadavers were subjected to forty-four blunt lateral impacts at velocities of approximately 4.5, 6.7, or 9.4 m/s with a 15 cm flat pendulum weighing 23.4 kg. Chest and abdominal injuries consisted primarily of rib fractures with a few cases of lung or liver laceration in the highest severity impacts. There were two cases of pubic ramus fracture in the pelvic impacts. Logist analysis of the biomechanical responses and serious injury, indicated that the maximum Viscous response had the best correlation with injury risk for chest and abdominal impacts. A tolerance level of VC = 1.5 m/s for the chest and VC = 2.0 m/s for the abdomen were determined for a 25% probability of serious injury. Maximum compression was similarly set at C = 38% for the chest and C = 44% for the abdomen. The experiments indicate that chest and abdominal injury can occur by a viscous mechanism during the rapid phase of body compression, and that the Viscous response is an effective measure of injury risk in side impacts. A compression tolerance is set to assess crushing injury risks. Pubic ramus fracture correlated with compression of the pelvis not impact force or acceleration. Pelvic tolerance was set at 27% compression.

## LTD Baseline A-Pillar

FMH	Peak Resultant Acceleration	
	Linear (g)	Rotational (rad/sec <sup>2</sup> )
test #1	177.5	20,866
test #2	184.6	18,441
average	181.1	19,654

The 1986 FARS indicates that 31.8% of passenger car fatalities occur in crashes with the principal direction of force lateral on the vehicle (figure 1). Two-thirds of the fatalities are in multi-vehicle accidents where the car is struck by a passenger car, truck, or other vehicle, while the other third involve single vehicle accidents into primarily fixed objects. Approximately an equal number of fatalities occur in driver side and passenger side lateral impact crashes, and the toll in human life is about 8,000 victims annually.

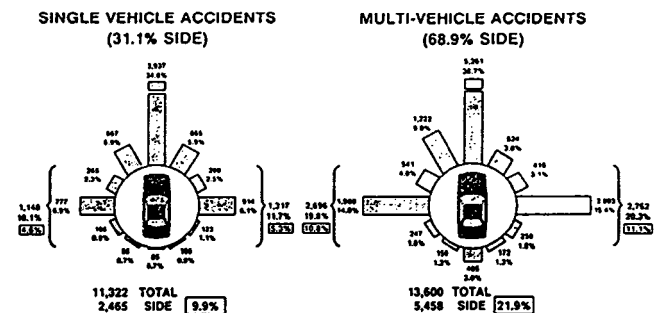


Figure 1. Distribution of impact by principle direction of force in 1986 FARS single and multi-vehicle fatal crashes.

A recent study (Viano 1989) of individual multi-vehicle side impact crashes indicates that a majority of the fatal crashes occur at an intersection and that the victim is primarily an older occupant. An evaluation of national statistics from NASS (table 1) indicates that when side and frontal impact crashes are compared, side impacts represent

about half of the crashes involving serious to fatal passenger car injury. When crashes are separated into multi-vehicle (car-car) or fixed object impacts, the age of the occupant emerges as an important factor in side impacts. In particular, multi-vehicle side impact crashes are a major cause (40–54%) of injury to occupants over the age of 40, whereas occupants of this age range are infrequently involved in side impact crashes into fixed objects.

**Table 1. Passenger car crashes from 1982–86 NASS with serious-fatal front seat occupant injuries.**

Age	Side Impact		Frontal Impact		Total
	Car-Car	Fixed Object	Car-Car	Fixed Object	
20–	2,840 (21%)	4,829 (36%)	3,536 (27%)	2,072 (16%)	13,277
20–40	8,068 (25%)	6,718 (20%)	10,971 (33%)	7,110 (22%)	32,867
40–60	5,004 (40%)	761 (6%)	5,466 (43%)	1,417 (11%)	12,648
60–80	5,010 (44%)	165 (1%)	4,123 (36%)	2,110 (18%)	11,408
80+	819 (54%)	46 (3%)	369 (25%)	270 (18%)	1,504
	21,741 (30%)	12,519 (17%)	24,465 (34%)	12,979 (18%)	71,704

The current study simulates the forces of contact on the chest, abdomen and pelvis in a side impact crash. A pendulum impact mass is used to load an unembalmed cadaver over a range of impact speeds and follows a protocol that has been used previously to study frontal impact responses (Kroell 1976). This allows direct comparison of the lateral impact responses to the frontal data, and takes advantage of a proven methodology for research on impact biomechanics.

The study also addresses a range of candidate mechanical responses for injury assessment. These include the Viscous (Viano 1988b, Lau 1986) and compression (Nahum 1970) responses for the chest and abdomen since they are an effective measure of injury risk by impact and crushing mechanisms, respectively. The Viscous response is evaluated since it is proven to be the underlying mechanism of soft tissue trauma to internal organs and vessels in blunt impact. It has also successfully pinpointed the time of greatest injury risk in an impact. This has helped focus efforts on vehicle design changes to improve product safety. The Viscous response has also been shown to accurately measure the risk of serious and life-threatening trauma in cadaver and animal studies.

Based on Cesari (1982), hip acceleration is investigated for pelvic fracture. Although response and injury will be compared with peak acceleration measurements, peak acceleration is an insufficient correlate and not a causal factor in soft tissue chest and abdominal injury (Brun-Cassan 1987). In addition, the recent acceleration formulation TTI, has been criticized by many in the scientific community (Tarriere 1988, Viano 1987b, Lau 1988). Although acceleration criteria have a rich history in product safety testing, our current understandings of human injury indicate that body deformations are the causal factor of soft tissue chest and abdominal injury and such deformation is not adequately assessed by acceleration measures.

A scientific understanding of frontal impact injury biomechanics has been developed by using the pendulum im-

pect methods of this study. This approach has successfully led to the development of human-like body deformation characteristics which include the force-deflection or compliance behavior of the chest and abdomen under impact loading. The data has enabled the development of the Hybrid III dummy which realistically simulates the human response in frontal impact, and enables a valid assessment of product safety improvements.

There has also been an advance in our understanding of the mechanisms of injury, and tolerance criteria of the human body to impact force. Much of this has been based on human cadaver tests, which help define body compliance and assess injury severity primarily based on skeletal trauma. Comparable research (Viano 1988b) has been conducted for frontal and lateral impacts with a physiological model to study life-threatening trauma, by laceration or rupture of internal organs and vessels or by interruption of normal cardiac or respiratory function. In frontal and lateral impact, the Viscous response has been shown to be the principal mechanical cause of soft tissue injury. This study aimed to assess its comparable tolerance level and risk function in lateral impacts of human cadavers.

## Materials and Methods

Unembalmed cadavers were provided through the Department of Anatomy at Wayne State University Medical School as part of a willed-body program.<sup>1</sup> They had an average age of  $53.8 \pm 13.9$  years and body weight of  $67.2 \pm 16.2$  kg.

### Specimen selection and handling

The specimen were selected on an age, condition, and cause of death criteria, which limited age to approximately 65 years unless the specimen was of good skeletal condition. All cadavers were tested after rigor mortis had passed. In some of the specimen, the average time lapsed between expiration and actual testing was one to two weeks. In other specimen, the time lapse was greater between the expiration and testing, so the specimen was frozen (4°F) for a period of time. Prior to testing, the specimen were refrigerated at 35°F.

### Instrumentation and preparation

The cadaver was instrumented with an array of accelerometers attached to the spine and pelvis. A triaxial accelerometer package was attached to the first, eighth and twelfth thoracic vertebrae and a similar package to the pelvic region at the second sacral vertebrae. Targets were attached to the triaxial clusters for photographic coverage and film analysis.

<sup>1</sup> The rationale and experimental protocol for use of human cadaver research subjects in this program have been reviewed by the Research Laboratories' Human Research Committee. The research complies with the provisions of the Uniform Anatomical Gift Act, follows guidelines established by the US Department of Transportation, National Highway Traffic Safety Administration and recommendations of the National Research Council of the National Academy of Sciences, and adheres to the provisions of The Declaration of Helsinki.

The cadaver's arterial system was pressurized by normal saline infused through a Foley catheter inserted in the aorta above the diaphragm. A vent tube was inserted in the brachial artery. Prior to an experiment, the catheter balloon was pressurized to block the flow below it and saline was pumped into the body until it flowed out of the vent tube. The vent was then clamped, ensuring pressure in the chest and upper abdominal organs. The lung was carefully drained of any fluid and then aerated repeatedly with room air prior to testing. The lung was pressurized.

## Necropsy

Autopsy was performed by a board certified pathologist, and special attention was paid to injury of the chest, abdomen, and pelvis.

## Data analysis

High speed movies of the impact were taken at 2,000 frames per second from the frontal and 500 frames per second from the posterior and overhead views. Frame-by-frame analysis of the impact event formed the basis for the instantaneous deflection data of the torso and hip. Deflection was processed to derive the compression and Viscous responses based on an established algorithm by Viano (1988a) and Lau (1986). The acceleration channels were processed by SAE or FIR filters.

## Injury functions

Viscous Response [VC(t)]—A time function produced by multiplying the instantaneous velocity of deformation and compression responses (units in m/s, derived from film data).

Compression Response [C(t)]—The instantaneous deformation divided by the initial torso thickness along the axis of the impact (dimensionless, derived from film data).

Spinal Acceleration Response [Gsp(t)]—Instantaneous lateral acceleration of the spine measured by an accelerometer on T1, T8, T12 or pelvis at S3 (units in g's derived from electronic data).

Force [F(t)]—Impact force resulting from pendulum contact (units in kN's, derived from acceleration of the pendulum from electronic data multiplied by the pendulum mass).

## Injury criteria

Viscous Criterion [VC]max—The peak Viscous response (Viano 1988a, Lau 1986).

Compression Criterion [C]max—The peak compression response.

Spinal Acceleration Criterion [Gsp]max—The peak lateral or resultant spinal acceleration response.

Force Criterion [F]max—The peak force acting on the body.

## Statistical methods

Injury risk functions were computed using the Logist function in the Statistical Analysis Package. This function

relates the probability of injury occurrence  $P(x)$  to the magnitude of a response parameter  $x$  based on a statistical fit to a sigmoidal function  $P(x) = [1 + \exp(\alpha - \beta x)]^{-1}$ . The goodness-of-fit of the statistic is quantified by the chi-squared ( $\chi^2$ ), p-value ( $p$ ) and correlation coefficient ( $R$ ).

## The impact

Experiments were conducted with a power-assisted pendulum impactor (figure 2). The 23.4 kg pendulum was freely suspended by guide wires and accelerated to impact speeds of approximately 4.5, 6.7 or 9.4 m/s in 5 cm by a pneumatically charged cylinder with thrust piston. The level of charge pressure determines the thrust velocity. The forward motion of the pendulum was abruptly stopped by a cable tether after 15 cm of contact.

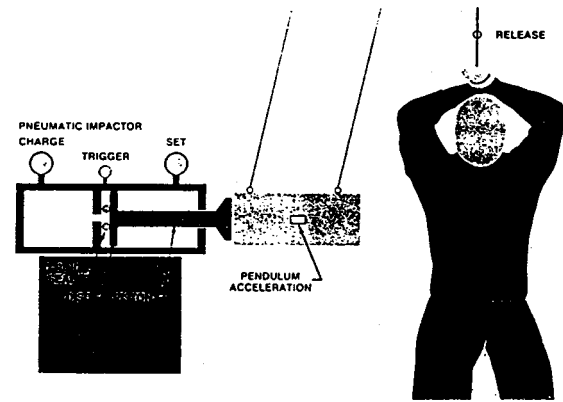


Figure 2. Experimental set-up with a pneumatic power-assisted pendulum and upright supported specimen.

The cadaver was suspended upright with hands and arms overhead. The specimen was rotated 30° so the point of pendulum contact was lateral on the thorax or abdomen. This protocol was used to assure that full lateral thoracic and abdominal impact occurred with the axis of force through the center of gravity of the torso. It resulted in controlled compression of the torso without coincident rotation of the body about the spine axis. The center of pendulum impact on the thorax was aligned with the xiphoid process (7.5 cm below midsternum). Abdominal impact was aligned 7.5 cm below the xiphoid (15 cm below midsternum). Pelvic impacts were conducted at 90° lateral with the impactor centered on the greater trochanter.

The pendulum interface was a smooth, flat, 15 cm diameter disc with the edges rounded. The axis of impact force was aligned through the center of gravity of the torso for chest and abdomen tests (approximately 2 cm anterior of the intrathoracic surface of the vertebrae). A uniaxial accelerometer was attached to the pendulum and its response was multiplied by the pendulum mass to give the force of impact. A suspension system released the arms at impact enabling a free torso response to impact. The off-side of impact was padded to gradually support the free body response.

Multiple tests were conducted on a specimen to increase biomechanical response data. This could include a low-

severity left abdominal impact, an injurious high-severity thoracic test and a lateral pelvic impact.

## Results

Three of six tests in the high velocity chest impact series resulted in lacerative injury of the lung, liver, diaphragm, kidney or spleen. In the high-velocity chest impact series, five of six specimen had flail chest with an average of 14 rib fractures. There were only two cases of severe upper abdominal injury in the high severity impacts and they consisted of laceration of the liver and diaphragm. In these impacts, only one of four specimen experienced more than eight rib fractures. There were six high velocity lateral impacts of the hip and, in spite of the high severity of loading, there were only two incidents of pubic ramus fracture. In terms of overall injury severity, each exposure was summarized by the number of rib fractures or skeletal injury, the maximum severity of skeletal trauma (SAIS),

**Table 2. Summary biomechanics and injury for lateral thoracic, abdominal and pelvic impact.**

Thorax Response	Test Speed (m/s)		
	4.42 ± 0.86	6.52 ± 0.32	9.33 ± 0.71
Force (kN)	2.67 ± 0.99	3.10 ± 0.48	6.30 ± 0.90
Deflection (cm)	8.40 ± 1.30	11.20 ± 1.35	14.18 ± 1.70
Compression (%)	28.1 ± 4.1	34.9 ± 4.5	43.2 ± 3.9
VC (m/s)	0.62 ± 0.23	1.10 ± 0.18	2.05 ± 0.41
C <sub>1-12</sub> -y	14.0 ± 6.0	46.1 ± 8.3	45.1 ± 8.3
C <sub>1-8</sub> -y	16.5 ± 6.5	33.6 ± 8.1	62.5 ± 20.4
C <sub>1-12</sub> -y	12.6 ± 8.5	25.4 ± 5.1	54.6 ± 25.3
MAIS	0.4 ± 0.9	2.8 ± 0.5	4.0 ± 0.6
SAIS	0.4 ± 0.9	2.8 ± 0.5	3.8 ± 0.4
Rib Fractures (#)	0.4 ± 0.9	5.2 ± 1.5	12.7 ± 4.5

Abdomen Response	Test Speed (m/s)		
	4.79 ± 0.77	6.83 ± 0.15	9.40 ± 0.87
Force (kN)	2.41 ± 0.49	3.71 ± 0.48	6.50 ± 1.10
Deflection (cm)	10.83 ± 2.30	11.43 ± 0.76	14.60 ± 2.36
Compression (%)	32.0 ± 6.6	36.2 ± 1.65	45.8 ± 3.1
VC (m/s)	0.77 ± 0.23	1.26 ± 0.12	2.22 ± 0.41
C <sub>1-12</sub> -y	6.9 ± 2.0	17.5 ± 1.9	37.5 ± 11.0
C <sub>1-8</sub> -y	10.8 ± 4.4	28.9 ± 7.1	29.1 ± 5.9
C <sub>1-12</sub> -y	11.6 ± 6.2	29.8 ± 12.4	44.3 ± 9.0
MAIS	0.7 ± 1.2	2.0 ± 1.4	2.0 ± 2.3
SAIS	0.7 ± 1.2	2.0 ± 1.4	1.8 ± 2.1
Rib Fractures (#)	0.8 ± 1.6	3.3 ± 3.0	3.8 ± 4.5

Pelvis Response	Test Speed (m/s)		
	4.83 ± 0.58	6.77 ± 0.10	9.65 ± 0.64
Force (kN)	5.45 ± 1.66	6.81 ± 1.60	11.20 ± 1.48
Deflection (cm)	4.90 ± 1.60	9.85 ± 1.34	7.83 ± 2.27
Compression (%)	13.5 ± 4.0	25.0 ± 0.3	22.9 ± 6.0
C <sub>1-8</sub> -y	7.7 ± 3.1	18.5 ± 3.9	31.6 ± 8.5
C <sub>1-12</sub> -y	15.0 ± 12.6	23.6 ± 3.6	39.9 ± 26.8
C <sub>3-3</sub> -y	34.4 ± 15.0		
MAIS	0	0	0.7 ± 1.0
SAIS	0	0	0.7 ± 1.0
Pelvic Fracture	0	0	0.3 ± 0.5

and the maximum overall severity of injury (MAIS).

The response and injury data were averaged in table 2 for the three pendulum impact speeds. Chest and abdominal impact responses increased as the severity of impact speed increased. The experimental protocol maximized the opportunity to define a correlation between injury and the measured response parameters but also set up the possibility that unrelated or weakly related parameters may also correlate with injury.

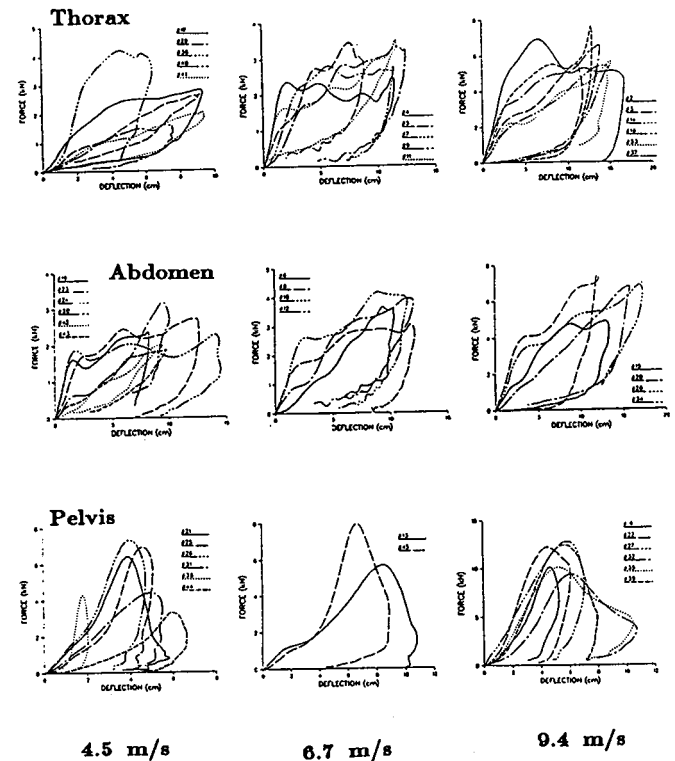


**Figure 3. Grouped dynamic responses for applied force and body deformation in 4.5, 6.7 and 9.4 m/s pendulum impacts of the thorax, abdomen and pelvis.**

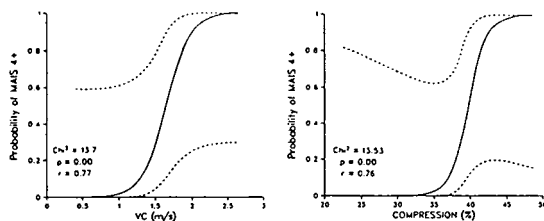
A comparison of the chest and abdominal impacts indicates a similar level of peak force, deflection, and compression for each level of impact severity. The Viscous response was higher in the abdominal impacts probably because of less skeletal structure resisting the low-deflection response. A lack of vitality in the upper abdominal organs may have led to a lower average severity of abdominal injury than occurred in chest impacts of comparable impact severity. Internal chest injury was frequently associated with multiple rib fractures indicative of flail chest. For the pelvic impacts, the force increased with the increasing severity of impact speed.

Figure 3 summarizes the force-deflection responses for the experiments at the low, middle, and high severity impact of the chest, abdomen, and pelvis. The force-deflection response defines the compliance of the torso or pelvis under

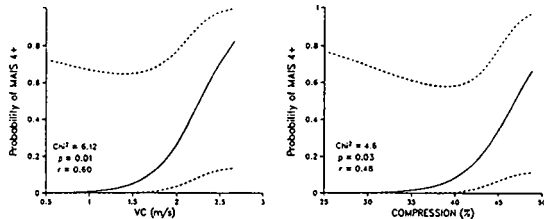
lateral impact and is a key biomechanical response of impact. The area under each curve represents the amount of energy absorbed by body deformation.

Logist analysis was applied to the biomechanical responses to identify risk functions for four or more rib fractures (MAIS 3+) or serious injury (MAIS 4+ or 9+ rib fractures). The Viscous response shows the strongest correlation with serious to critical injury for responses measured in the chest and abdominal impacts. Peak force had a higher correlation with serious injury but is an input parameter measured on the pendulum. Maximum chest compression was also a significant correlate with serious injury, whereas none of the responses correlated with the risk of moderate skeletal injury in the lateral abdominal impacts. Pelvic compression emerged as the only correlate with pubic ramus fracture.

### Thorax



### Abdomen



### Logist Statistics

Criteria/Severity/ED <sub>50</sub>	$\alpha$	$\beta$	$\chi^2$	p	R
<b>THORAX: 9+ Rib Fxs (MAIS 4+)</b>					
VC = 1.65 m/s	10.02	6.08	13.7	0.000	0.77
C = 39.8%	31.22	0.785	13.5	0.000	0.76
G <sub>T8-y</sub> = 49.5 g	12.95	0.262	10.2	0.000	0.75
<b>ABDOMEN: Critical Injury (MAIS 4+)</b>					
VC = 2.26 m/s	8.64	3.81	6.1	0.013	0.60
C = 48.8%	16.29	0.348	4.6	0.032	0.48
G <sub>T12-y</sub> = 45.6 g	7.73	0.169	4.9	0.027	0.53
<b>PELVIS: Pubic Ramus Fracture</b>					
C = 27.4%	84.02	3.07	11.48	0.001	0.908
d = 10.3 cm	16.91	1.64	6.64	0.010 (NS)	0.635
G <sub>S3-y</sub> = 142.7 g	3.16	0.022	0.34	0.561 (NS)	0.0

Figure 4. Logist functions and statistics for the probability of critical injury of the thorax and abdomen, and pubic ramus fracture of the pelvis.

The Viscous response emerged as the best and most descriptive measure of injury risk. Logist functions are plotted in figure 4 for the probability of serious injury as a function of the Viscous and compression response of the chest and abdomen. A 95% confidence interval is also given. The functions are sigmoidal in shape indicating three distinct regions. For low values of the response, there is a region of very low risk of injury. Similarly, for the very high values of the response, there is a flat high-risk of serious injury outcome. In-between is a region where injury risk is proportional to the associated response. The sigmoidal function is typical of a risk distribution with a biomechanical response from a population with weaker and stronger subjects.

Tolerance levels were determined for a 25% probability of serious injury in the chest, abdomen and pelvis. This probability level is consistent with previous studies of injury risk from human cadaver and animal impacts (Viano 1988a, 1988b, Lau 1986, 1987, 1988) and is at a risk level found in current crash protection standards. Tolerance to AIS 4+ injury is set at VC=1.5 m/s and C=38% for the chest and VC=2.0 m/s and C=44% for the abdomen. Pelvic tolerance is C=27%.

## Discussion

This study has shown that the Viscous response is the best biomechanical parameter to assess impact injury in lateral impact of the chest and abdomen. The finding is consistent with previous research by Viano (1988a) and Lau (1986) on impact injury in frontal loading of the chest and similar research by Lau (1987) on the abdomen. In those studies the Viscous response was found to be the causal mechanism and strongest correlate with injury. More recent experiments by Lau (1988) have shown that serious injury to soft tissues and organs occurs at the time of peak Viscous response, well before maximum deflection. We expect that serious abdominal and thoracic injury from high-speed lateral impact will be similarly associated with the rapid compression phase of loading.

Experiments by Viano (1988b) with anesthetized swine show also that lateral impact injury is associated with a viscous mechanism. Serious internal thoracic and abdominal injury occurred with minimal skeletal damage. The research confirms in a physiologic model with organ sizes and weights similar to that of man that the Viscous response is an effective measure of injury risk in lateral impact.

The correlation of maximum deflection or compression with injury is consistent with relationships found in previous studies on the frontal impact response of human cadavers and anesthetized swine. However, a relationship was not found between compression and injury in recent lateral chest impacts of anesthetized swine (Viano 1988b). In those tests, a relationship existed between low and middle severity impacts but was not found between the middle and high severity tests. Spinal acceleration was higher between the middle and high severity tests as well as

impact force, resulting in more whole-body displacement of the animal. The failure of maximum compression to correlate with an increased severity of injury is further evidence that soft tissue trauma may be more associated with the rapid-phase of body deformation during impact. However, in some circumstances injury may occur by a slow crushing load on the body, and maximum compression would be an important factor.

Although acceleration measures correlate with some types of injury in this study, they have been shown in other research to be unrelated when a range of test-types are merged. In two studies by Lau (1986, 1988), pendulum and sled tests could be independently shown to correlate body accelerations with injury; but, when the data were merged no relationship existed between peak accelerations and injury. This situation has been shown for frontal impact and is a result of acceleration being the sum of two independent components: one associated with deflection of the body, and the other with whole-body displacement in response to force. Our studies have shown that body deformation is the

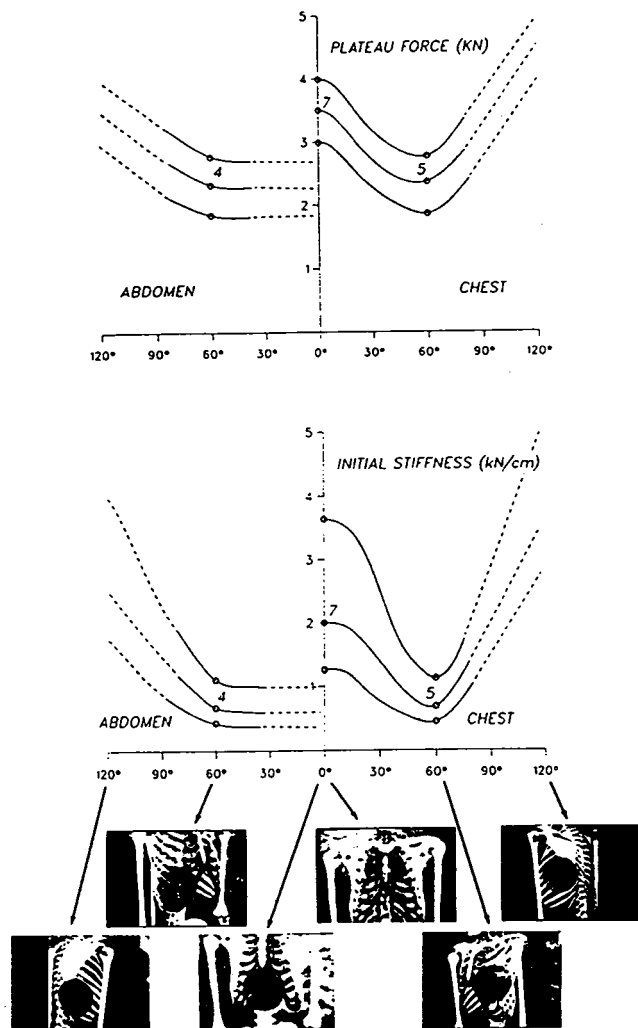


Figure 5. The global impact response of the human chest and abdomen is represented by the plateau force and initial stiffness (average  $\pm 1$  standard deviation). Solid lines connect known data and dotted lines represent estimates of the human response.

key factor in impact injury and that whole-body acceleration primarily brings the body to a common velocity with the impactor or sled.

Our work is part of an effort to define the global biomechanics of the human chest and abdomen. It is possible to characterize the force-deflection response by an initial stiffness, and average plateau force in the mid-deflection region. This was done for the frontal and lateral chest impacts and is plotted in figure 5 by orientation from frontal (0°) through 60° lateral to 120° lateral. Solid lines connect the regions where test data are available and the dotted lines represent an estimate of what the full global biomechanical response may be when a complete set of responses is collected for the 6.7 m/s blunt impact condition.

The force-deflection characteristics of the human chest are an important response for the development of anthro-

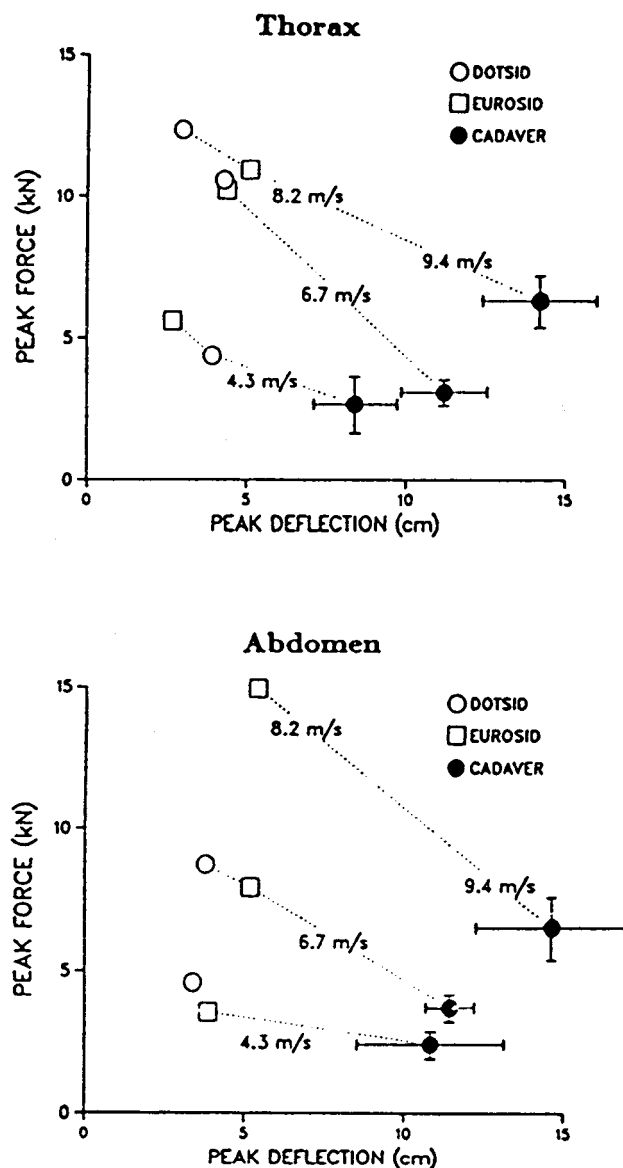


Figure 6. Peak force and deflection from blunt lateral impact of the human cadaver and current side impact test dummies at three levels of severity.

pometric test devices that simulate the human response to impact and assess injury risks. Figure 6 summarizes the peak force and deflection responses from lateral impacts of human cadavers at three test speeds as well as similar information from recent tests with the SID and EUROSID at similar speeds. These data indicate that current test devices develop significantly higher plateau forces and much lower deflections than the human cadaver and anesthetized swine. This lack of biofidelity in force-deflection response of the current side impact ATD's is a significant deficiency (Viano 1987a) in their ability to simulate the human response and injury in side impact tests.

Biofidelity is important because the design of side interior padding to optimize responses in the dummies will result in much stiffer materials to be compatible with the high force levels developed by the dummies. Stiff materials may essentially eliminate the safety potential for real occupants who develop much lower levels of force and thus need softer materials (Viano 1987b). The difference in compliance between current test dummies and the human will also result in significant differences in occupant kinematics during a side impact. In particular, the greater deflection experienced by the human chest and abdomen will allow the head to move more laterally with respect to the vehicle's side interior and will result in a significantly different trajectory of the head. This aspect is important to a system's engineering approach to improving side impact protection.

On the basis of this study and our previous research, we believe that the maximum Viscous response should be limited to protect against injury during the rapid phase of body deformation of the chest and abdomen during side impact loading. As shown in previous work by Viano (1988a) and Lau (1988), serious internal injury can occur without a significant number of rib fractures or rib cage injury at all. This evidence again supports the potential for the early occurrence of soft tissue injury at about the time of maximum Viscous response and where deflection or compression of the body has reached only about half of its maximum value. We also believe in the need to limit maximum chest compression during crash testing to protect against crushing injuries which may occur during slow or static deformation of the chest and abdomen. This is clearly a different mechanism of injury than the Viscous mechanism. Limiting the Viscous and compression response is a complementary approach to assessing safety systems (Viano 1988a, Lau 1986). Our data also indicate that compression of the pelvis may be a better predictor of hip fracture than pelvic acceleration.

## References

- (1) Brun-Cassan, F., Pincemaille, Y., Mack, P., Tarriere, C., "Contribution to the Evaluation of the Criteria Proposed for Thorax-Abdomen Protection in Lateral Impact." In *Proceedings of the 11th International ESV Conference*, Washington, DC, May, 1987.
- (2) Cesari, D., Ramet, M., "Pelvic Tolerance and Protection Criteria in Side Impact." In *Proceedings of the 26th Stapp Car Crash Conference*, Society of Automotive Engineers Technical Paper #821159, pp. 145-154, Warrendale, PA, 1982.
- (3) Kroell, C.K., "Thoracic Response to Blunt Frontal Loading." In *The Human Thorax-Anatomy, Injury and Biomechanics*. SAE Publication P-67, pp. 49-78, Warrendale, PA, Society of Automotive Engineers, 1976.
- (4) Lau, I.V., and Viano, D.C., "The Viscous Criterion: Bases and Applications of an Injury Severity Index for Soft Tissues," In *Proceedings of the 30th Stapp Car Crash Conference*, SAE Technical Paper #861882 pp. 123-142, October, 1986.
- (5) Lau, I.V., Horsch, J.D., Viano, D.C. and Andrzejak, D.V., "Biomechanics of Liver Injury by Steering Wheel Loading." *Journal of Trauma*, 27(3):225-235, April, 1987.
- (6) Lau, I.V. and Viano, D.C., "How and When Blunt Injury Occurs: Implications to Frontal and Side Impact Protection." In *Proceedings of the 32nd Stapp Car Crash Conference*, Society of Automotive Engineers Technical Paper #881714, Society of Automotive Engineers, Warrendale, PA, October, 1988.
- (7) Nahum, A.M., Gadd, C.W., Schneider, D.C., and Kroell, C.K., "Deflection of the Human Thorax Under Sternal Impact." SAE's International Automobile Safety Conference, Society of Automotive Engineers Technical Paper #700400, pp. 797-807, Detroit, MI, May 1970.
- (8) Tarriere, C., Brun-Cassan, F. and Thomas, C., "Specific Highlights Relative to Injury Parameters in Side Impacts Including Unanimous Opinions of ISO SC12 Working Groups 5 and C." ISO/TC22/SC12/-GTG, No. 256, 1988.
- (9) Viano, D.C., "Evaluation of the SID Dummy and TTI Injury Criterion for Side Impact Testing." In *Proceedings of the 31st Stapp Car Crash Conference*, SAE Technical Paper #872208, pp. 143-160, November, 1987a.
- (10) Viano, D.C., "Evaluation of the Benefit of Energy-Absorbing Material for Side Impact Protection: Part II." In *Proceedings of the 31st Stapp Car Crash Conference*, Society of Automotive Engineers Technical Paper #872213, pp. 205-224, Society of Automotive Engineers, Warrendale, PA, November, 1987b.
- (11) Viano, D.C. and Lau, I.V., "A Viscous Tolerance Criterion for Soft Tissue Injury Assessment." *J Biomech*, 21(5):387-399, 1988a.
- (12) Viano, D.C., Lau, I.V., Andrzejak, D.V., and Asbury, C., "Biomechanics of Injury in Lateral Chest Impact in Anesthetized Swine." General Motors Research Report, Appendix to the GM Response to the Side Impact Notice of Proposed Rulemaking, Federal Docket, 1988b.

# EEVC Working Group 9 Report on the EEVC Side Impact Test Procedure

R.W. Lowne,  
England

## Abstract

The EEVC first proposed a Test Procedure for Side Impact protection at the Fifth ESV Conference. Since that time the test procedure has been further developed, a specification for a mobile deformable barrier produced and a dummy specifically for use in lateral impacts has been developed. These have been reported at previous ESV Conferences. Over the last two years it has been possible to evaluate the test procedure because Production Prototypes of the dummy, EUROSID, and satisfactory examples of the deformable barrier face have been produced.

EEVC Working Group 9 has been created to support the development of the test procedure, including the dummy and MDB face and to consider the implications of the use of component test procedures and mathematical modelling in legislative testing. This report describes the current status of the test procedure, including some results of tests performed to this procedure using the new dummy and the MDB faces and draws conclusions from these tests and tests comparing the EEVC and NHTSA Barriers.

## Introduction

EEVC first proposed a procedure for the evaluation of the performance of vehicles in side impacts at the Fifth ESV Conference in 1974 (1).<sup>\*</sup> The proposals were in general terms but included the evaluation of the performance of the vehicle by the use of dummies.

The proposals were further developed at the Ninth ESV Conference (2). This revised procedure was to impact a stationary target car at 50 km per hour with a mobile barrier, to the front of which was attached a deformable face. The trajectory of the mobile barrier was to be perpendicular to the longitudinal axis of the target car and the centre of the barrier face was to be aligned with the R-point of this vehicle (figure 1). The deformable barrier face was intended to have crush characteristics based on test results with a number of European cars and was sub-divided into six blocks, each with its own force/deflection characteristics (figure 2). The performance of the car would be judged by the readings taken on a dummy. Since that time, the procedure has been further developed, three designs of Mobile Deformable Barrier faces have been produced and a dummy has been produced specifically for use in side impact tests (EUROSID).

A major review of the original proposal was made at the 11th Experimental Vehicles Conference, 1987 (3) following test experience with early versions of the Mobile Deformable Barriers (MDBs) and the Component Prototype version of EUROSID. The main parameters of

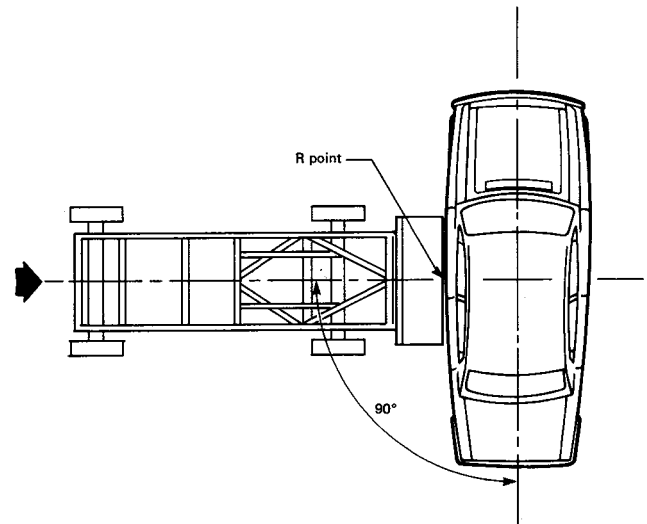


Figure 1. Configuration of the EEVC side impact test procedure.

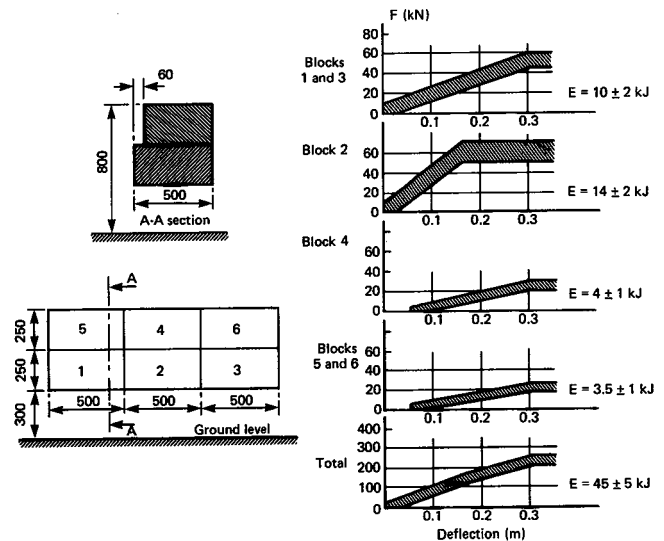


Figure 2. Main characteristics of the EEVC mobile deformable barrier.

the test procedure were confirmed with the exception that the height of the barrier face was raised from 250mm to 300mm and a proposal was made to permit excursions from the barrier force specification during the first 150mm of crush. Further testing to the EEVC procedure has followed using the Production Prototype EUROSID and later versions of the MDB faces.

EEVC Working Group 9 was created in 1988 to support the development of the test procedure, including the dummy and the MDB. The Working Group was also asked to examine the implications of the use of mathematical models in association with sub-systems or component tests for legislative testing and an assessment of the possibilities and difficulties of this approach is contained in section 5 below. This paper reports recent experience with side impact testing to the EEVC procedure.

<sup>\*</sup>Numbers in parentheses designate references at end of paper.

# EUROSID

Twenty four Production Prototype EUROSIDs have been produced for evaluation by a wide range of test institutes and the experience gained from this testing is being used to produce the specification and design of the first production version of the dummy. Some improvement has been made to the biofidelity of the dummy and problems with some of the instrumentation have now been eliminated. The details of the status of EUROSID are presented in another paper given at this Conference (4).

In the view of EEVC the production version of this dummy will provide an adequate tool for assessing the likelihood of injury from side impacts and is sufficiently reliable and consistent for use in the proposed side impact regulation dynamic test.

## Mobile Deformable Barrier Face

Mobile Deformable Barrier (MDB) faces constructed from rigid polyurethane foam and designed to meet the EEVC specification have been extensively tested by government and industry in both Europe and North America. Two designs have been developed within the EEVC, one manufactured by Fritzscheier GmbH and the other by Kenmont Ltd. A further design has been produced by UTAC in France. Although each appears to have satisfactory characteristics, none of them fully meets the original EEVC specifications (1). Further studies are planned to reconcile the performance of the barrier faces and the performance corridors.

Working Group 9 is considering the possible advantages of specifying the design of the barrier face in addition to a performance requirement.

## Experience With the Test Procedure

The EEVC Test Procedure specifies two side impact dummies; one in the front seat and one in the rear seat, both on the struck side. However, in order to improve photography of the inside of the vehicle, only the front dummy was used in these tests.

## Reproducibility

Side impact tests have been performed at three institutes on the same model of target vehicle; a small two door hatchback passenger car. The same make of MDB face was used for all tests.

Table 1 shows the results for these tests and table 2 presents the effect of applying the proposed EEVC Performance Criteria to the results. The main inconsistency is in the pubic symphysis force, but these tests were performed using a pubic symphysis transducer which is now known to produce erroneous results. A new force transducer is now specified for EUROSID (See Ref 4).

With the exception of the HIC values which are all well below the criterion level, it can be seen that the results are very consistent for full scale tests suggesting satisfactory reproducibility for the test procedure.

**Table 1. Test results on a small passenger car performed at three test institutes.**

Test Institute Parameter	BASt	BASt	TRRL	Ford
HEAD				
HIC	448	758	275	267
THORAX				
Peak Rib Deflection (mm.)	30.5	35.0	33.5	36.0
Peak Viscous Criterion (m/s)	0.6	0.7	0.5	0.7
Max. TTI	138	132	132	-
ABDOMEN				
Force > 4.5kN. @39mm. (Switch contact)	no	no	no	no
PELVIS				
Peak Ilium force (kN.)	1.9	2.7	2.5	2.6
Peak pubic symphysis force (kN)	7.3	8.1	11.2	10.3
MDB Peak longitudinal accel.(g)	14.2	14.3	15.3	15.5

**Table 2. Results of applying proposed EEVC test criteria to test results on a small car performed at three test institutes.**

Test Institute Parameter and Proposed Criterion	BASt	BASt	TRRL	Ford
HEAD				
HIC (1000)	pass	pass	pass	pass
THORAX				
Peak Rib Deflection (42mm)	pass	pass	pass	pass
Peak Viscous Criterion(1.0) (m/s)	pass	pass	pass	pass
ABDOMEN				
Force > 4.5kN. @39mm. (Switch contact)	pass	pass	pass	pass
PELVIS				
Peak Ilium force (10kN)	pass	pass	pass	pass
Peak pubic symphysis force (10 kN)	pass	pass	fail	fail
original transducer with known errors				

**Table 3. The effect of the impact speed of the mobile deformable barrier on the measured dummy parameters.**

Parameter		BASt	
Impactor speed (km/h)	45	50	55
HIC	167	265	-
Peak Chest Deflection (mm.)	30.0	38.5	44.5
Peak Pubic Symphysis Force (kN)	4.4	4.7	5.6
Peak Ilium Force (kN)	0.9	1.0	1.2
		TRRL	
Impactor Speed (km/h)	41	50	61
HIC	145	792	905
Peak Chest Deflection (mm.)	45.0	48.0	47.0
Peak Viscous Criterion (m/s)	1.0	1.3	1.4
Maximum TTI	135	169	218
Peak Pubic Symphysis Force (kN)	5.3	6.9	13.5
Peak Ilium Force (kN)	1.2	2.5	1.9

## Sensitivity

Tests to determine the effect of barrier impact speed have been performed at two Laboratories, BASt(5) and TRRL(6). The results are shown in table 3.

There is a general progression in the value of the parameters with increase in speed. This is more noticeable with the vehicle used in the BASt tests, which was a small hatchback car, than with the TRRL tests, which used a medium size hatchback.

TRRL has performed tests to investigate the effect of the mass of the Mobile Deformable Barrier on the injury parameters (6). The results of the tests, which were performed using a medium size hatchback car, are shown in table 4. The barrier masses selected are those proposed for the EEVC (950kg) and the NHTSA (1350kg) test procedures.

There do not appear to be any systematic differences between the results with the different barrier masses, at least with the vehicle model tested.

**Table 4. The effect of MDB mass on dummy transducer readings.**

Barrier Face Barrier Mass (kg) Dummy	EEVC 950 EUROSID	EEVC 1350 EUROSID
HIC	792	434
Peak Chest Deflection (mm.)	48.0	46.0
Peak Viscous Criterion (m/s)	1.3	1.3
Maximum TTI	169	167
Peak Pubic Symphysis Force (kN)	6.9	6.9
Peak Ilium Force (kN)	2.5	1.9

### Comparison of EEVC and NHTSA test procedures

BASt, TNO and TRRL have reported tests aimed at establishing the effects of the differences between the test procedures proposed by EEVC and NHTSA (5,7,6). These results are summarized in table 5. In all the tests quoted below, the dummy used was EUROSID to permit the effect of the test procedure, rather than the dummy, to be examined.

**Table 5. Comparison of EEVC and NHTSA test procedures.**

Test Procedure Barrier Face*	BASt		NHTSA NHTSA
	EEVC EEVC	NHTSA** EEVC	
HIC	265	160	
Peak Chest Deflection (mm.)	38.5	37.5	
Peak Pubic Symphysis Force (kN)	4.7	3.6	
Peak Ilium Force (kN)	1.0	0.7	
* 250mm ground clearance for both tests.			
** MDB mass 1100kg.			
Test Procedure Barrier Face	EEVC EEVC	TNO	NHTSA
		EEVC EEVC	NHTSA
HIC	115	240	611
Peak Chest Deflection (mm.)	40.0	39.5	27.5
Peak Viscous Criterion (m/s)	0.5	0.5	0.4
Max TTI	121	128	136
Abdomen Switch Contact	yes*	no	yes
Peak Pubic Symphysis Force (kN)	3.23	4.21	16.62
Peak Ilium Force (kN)	0.87	1.26	1.01
* switch contact force set at 4kN instead of 4.5kN			
Test Procedure Barrier Face	EEVC EEVC	TRRL	Car-Car
		NHTSA NHTSA	Car
HIC	792	-	254
Peak Chest Deflection (mm.)	48.0	30.0	53.0
Peak Viscous Criterion (m/s)	1.3	0.6	1.7
Max TTI	169	123	143
Abdomen Switch Contact	no	no	no
Peak Pubic Symphysis Force (kN)	6.9	15.8	6.6
Peak Ilium Force (kN)	2.5	-	1.3

The BASt tests, in which EEVC barrier faces were used for both tests, indicate that the crabbed test at 54km/h impact speed and 1100kg barrier mass is slightly less severe than the 50 km/h perpendicular impact with a barrier mass of 950kg but the differences are small.

The TNO and TRRL tests, which used different target car models, suggest that the NHTSA test procedure is likely to be less severe to the thorax area but more severe to the pelvis. The TRRL tests indicate that the EEVC test procedure gives closer results to the car to car test than does the NHTSA test procedure, at least for the models of target and bullet cars used.

## Mathematical Models for Side Impact Testing

WG9 is now currently evaluating proposals to use the prediction of mathematical models, usually supplemented by component tests to provide the input data, as an alternative to whole vehicle impact testing as a means of assessing the occupant safety of a vehicle. This would have advantages for the vehicle manufacturer if these predictions could be available at an early stage in the design process whereas full scale testing can only take place when prototypes are available. The advantage is somewhat less when component tests are required to provide input data since whole vehicle structures will be required.

The mathematical modelling approach also has the potential advantage that the evaluation of the vehicle for a range of occupant sizes, seat positions and impact speeds would be more practical than if whole vehicle tests were required each time. Depending on the technique used, a range of impacting objects such as trucks, rigid poles and rigid walls could be simulated in addition to simulating car to car impacts. The mathematical simulation part will, of course, be repeatable although any sub-systems testing will add variability.

However, the use of mathematical models is not straightforward and their ability to reproduce adequately the dynamics and reactions of a barrier impacting a car containing a dummy have yet to be demonstrated. Even if this approach is shown not to be sufficiently well developed to be applied in a legislative test to a new vehicle model, it might prove to be suitable for evaluating small design changes to approved models or to extend approval to a wider range of vehicle trim levels and specifications without the need for further dynamic tests.

The use of mathematical models to understand and reproduce the behaviour of vehicle in side impacts is still in its infancy but some lessons have been learnt from attempts to do so. CCMC have proposed a test procedure in which a vehicle bodysell and other necessary body and trim parts are loaded externally by a deformable face and internally by a rigid body block representing the occupant. A computer model uses these data as input to predict the behaviour in a dynamic test (8). This procedure is being modified to allow the computer to control continuously the rams for the deformable face and the dummy (computer in-the-loop). WG9 will be interested to consider this procedure when it is available and fully specified. Based on experience to date of mathematical models of side impact and the experience of full scale tests, WG9 have drawn the following interim conclusion:

1. The use of a mathematical model/subsystem test approach to vehicle side impact legislative testing would have the advantage of being able to approve a vehicle earlier on in the design stage than current whole vehicle tests on completed vehicle. The time advantage gained depends on the complexity of the mathematical model and on the

proportion of the vehicle necessary for the sub-system or component test.

2. A mathematical model approach would allow the performance of a vehicle to be assessed under a wider range of conditions than the single test condition of a full scale test.

3. The use of mathematical models is not straightforward and their ability to reproduce adequately the dynamics and reactions of a barrier impacting a car containing an occupant have yet to be demonstrated.

4. The model of the occupant must be sufficiently detailed to be able to predict likely modes of injury in lateral impacts and to give the correct load transfer between vehicle and occupant and between the major body parts of the occupant.

5. The sub-systems test procedure must be closely specified and must adequately represent the collapse of the vehicle under dynamic conditions.

6. The procedure for deriving the input data and for operating the model, including the dynamic correction factors, must be uniquely defined and must not rely on expert interpretation.

7. The procedure must be fully validated over a wide range of conditions which differ from those for which the model was calibrated.

8. The difference in the costs of testing a vehicle for final approval between full scale vehicle impacts and a mathematical model/subsystems test approach is not likely to be as great as might be supposed, although testing for development purposes could prove to be much less by using the latter approach.

9. Taking into account the present status of mathematical modelling and the time required to develop, validate and evaluate test procedures, WG9 considers that it will be 5 to 7 years before a mathematical model/sub-systems test approach could be considered seriously for legislative testing. It might prove practical for it to be used earlier for supplementary testing or Conformity of Production testing.

## Conclusions

1. The EEVC test procedure appears to give reproducible results; tests at three different laboratories gave similar results on one vehicle model.

2. The results are sensitive to impact speed of the mobile barrier but do not appear to be very sensitive to the barrier mass within the range tested (950–1350kg).

3. For the same barrier face, the perpendicular impact mode seems to be slightly more severe than the crabbed mode but the differences are small.

4. The NHTSA test procedure (using EUROSID) appears

to be slightly less severe to the thorax area but more severe to the pelvis. The test results with the EEVC procedure were closer to those of a car-to-car test than were the results using the NHTSA test procedure.

5. The EEVC Test Procedure appears to be able to discriminate between different models of vehicle and would encourage the design of vehicles with improved protection for occupants in side impacts.

6. Mathematical models for side impact simulation in association with sub-systems tests are not sufficiently well developed or proven for their use as the main legislative test in the near future.

## References

(1) European Experimental Vehicles Committee, *The Future of Car Safety in Europe*. Proceedings of the 5th ESV Conference, London, 1974.

(2) European Experimental Vehicles Committee Working Group No. 6, *Structures: Improved Side Impact Protection in Europe*, Proceedings of the Ninth ESV Conference, Kyoto, 1982.

(3) European Experimental Vehicles Committee on Side Impact (Cesari D. and I. Neilson), *Further Consideration of the European Side Impact Test Procedure*, Proceedings of the Eleventh ESV Conference, Washington, 1987.

(4) Roberts A.K., *Status Report of the EUROSID Dummy*. Proceedings of the 12th ESV Conference, Goteborg, Sweden, 1989.

(5) Glaeser K-P., *Results of Full Scale Tests with EUROSID under Different Test Conditions*. Proceedings of the 11th ESV Conference, Washington, 1987.

(6) Hobbs C.A., *The Influence of Car Structures and Padding on Side Impact Injuries*. Proceedings of the 12th ESV Conference, Goteborg, Sweden, 1989.

(7) DeCoo, P., A. Vermissen, E. Janssen, and J. Wisman, *Evaluation of European and USA Draft Regulations for Side Impact*. Preceding of the 11th ESV Conference, Washington, 1987.

(8) Richter R., H. Oehlschlaeger, R. Sinnhuber and R. Zobel, *Composite Test Procedure for Side Impact Protection*. SAE Paper 871117, SAE Govt./Industry Meeting, Washington, DC, May 1987.

## Appendix

Members participating in EEVC Working Group 9 meetings:

J. Bloch; D. Cesari; G. Ferrero; K-P. Glaeser; P. Hoekstra; C.A. Hobbs; E.G. Janssen; M.G. Langdon; R.W. Lowne (chairman); D. Matthes; A. Pastorino; E. Pullwitt; A.K. Roberts (secretary); W. Sievert; G.D. Suthurst.

# The Influence of Car Structures and Padding on Side Impact Injuries

C. A. Hobbs,  
Transport and Road Research Laboratory,  
United Kingdom

## Abstract

An analysis of over forty full scale impact tests has revealed much about the nature of side impacts and how improved protection can be achieved. Most of the tests have used the proposed EEVC Side Impact Test, which has been shown to be capable of distinguishing between current production cars which appear to offer different levels of protection. The most important factor identified as influencing protection is the vertical intrusion profile of the door. By separating the load path through the door from those into the car's structure, it has been possible to control door motion whilst at the same time increasing the rate of momentum transfer from the bullet vehicle to the target car. The increase in protection afforded by cars modified in this way has been substantial. The dynamic effects of transient door motion and structural failure have been seen to be important. It is not yet clear whether adequate account can be taken of them in computer simulation modelling.

## Introduction

Over the past three years, the Transport and Road Research Laboratory has carried out more than forty full scale side impact tests on cars. The data from these tests have been used: to validate the proposed EEVC (European Experimental Vehicles Committee) Side Impact Test Procedure (1),\* to aid the development of an EEVC MDB (Mobile Deformable Barrier) face (2,3,4) and the EUROSID side impact dummy, to provide an insight into the side impact injury process and to help indicate how improvements in car occupant protection may be achieved (5,6). The majority of these tests used the EEVC side impact test procedure but, for comparison purposes, some car to car impacts and some tests using the NHTSA (National Highway Traffic Safety Administration) MDB faces were also carried out.

A range of standard production cars, of different sizes, has been tested, as well as cars with modified structural characteristics and door padding. The way the cars were modified has developed as more has been learnt about the influence of structural characteristics on levels of protection.

Some tests have looked at the effect of virtually eliminating intrusion and of almost completely filling the gap between the door and occupant with padding. Although such modifications would be impractical for normal use, they have helped to give a better insight into the effects of intrusion and padding. Further tests have explored the effects of changing the trolley mass and impact speed.

So far, effort has been concentrated on studying protection of the thorax, pelvis and abdomen, performance being measured using the EUROSID dummy. To help in understanding the mechanisms of injury, this programme has closely interacted with work on computer simulation modelling and quasi-static testing of car structures (5,6,7).

## Side Impact Dynamics

### Mass and stiffness effects

During a side impact between a moving "bullet" vehicle and a stationary "target" vehicle, momentum is transferred from the bullet to the target. The rate of momentum transfer is dependent upon the effective stiffness of the numerous load paths between the bullet vehicle and the distributed mass of the target vehicle. In an impact, the effective stiffness of a car's structure is a combination of both its structural stiffness and inertial effects due to the mass of the individual parts of the structure. For a given target vehicle, the decelerating force acting on the bullet vehicle is directly related to this effective stiffness. With a soft target vehicle, the velocity difference between the bullet and target vehicles, during virtually all of the impact period, will be greater than with a stiff target vehicle. This relative velocity could be expected to determine side intrusion velocity which has been thought to be an important determinant of risk of injury.

Similarly, for target vehicles having the same effective stiffness but different masses, the velocity difference between the bullet and target during the impact will increase with mass. On this basis, to offer the same level of protection, heavy cars would require load paths with greater effective stiffness than light cars. At this stage, the extent of the inertial contribution to effective stiffness is not known. Nor is it known how this contribution varies with car size, mass and structural characteristics, except in very general terms. However if, as is thought likely, the effective stiffness of larger cars does not increase in line with the increase in mass, it could be expected that providing protection would be more difficult in heavier cars.

The stiffness characteristics of the bullet vehicle also have an important effect. Of particular importance is the way the strong and weak parts of the bullet and target vehicles line up in the impact. There is no guarantee that the stiff parts of the bullet vehicle will line up with the stiff parts on the target vehicle. It is much more likely that the few stiff areas on one vehicle will act against the greater area of weak structure on the other vehicle. As a result, the deflection of weak areas will be greater than the deflection of stiff areas. A deformable barrier face is able to take some account of this.

The argument presented above would appear to support the view that increasing the car's structural stiffness would reduce injury levels. However, there is evidence that other factors may be more important.

\*Numbers in parentheses designate references at end of paper.

## Timing of events in side impact

Although side impacts occur over a period of several seconds, the EUROSID performance parameters peak very early in the impact. Taking contact between the front of the mobile barrier and the car's side as time zero, typically: the door hits the dummy at 15–25 msec, maximum rib acceleration occurs at 25–30 msec, VC (Viscous Criterion) (8) is a maximum at 25–35 msec, maximum spine acceleration is achieved at 30–35 msec and maximum thorax compression occurs at 35–50 msec. Similar timings apply to the other body regions.

In most instances, all of the thorax and pelvis performance criteria have peaked by 50 msec, although this has extended to about 75 msec with some of the more extensively modified cars. By this time the centre of gravity of the target car has only moved about 80–130 mm, dependent upon its mass and structural characteristics. Intrusion of the door, relative to the car, is still increasing and the whole car, including the door, has still to make its major sideways movement.

As the performance parameters peak early in the impact, the dynamics of the door motion are important. On impact, the door rebounds off the incoming MDB and continues to bounce through the period when the performance parameters peak. Door velocities in excess of 65 km/h have been measured in 50 km/h impacts. At first contact of the door with the occupant, in this transient period, the effective stiffness and mass of the door can vary widely, depending on the car's structural design. Clearly the effective mass and stiffness of a door that is not in contact with the MDB face will be lower than the same door when it is being directly loaded by the incoming face.

## Side intrusion profile

At the start of the programme of tests, modifications to car structures were aimed at reducing intrusion. However, even though door padding was included, the reductions in measured performance parameters were small. It soon became clear that the vertical profile of the intruding door was having an important effect. Although in the tests only the final static intrusion profile could be measured, some information on the dynamics of the intrusion profile could be obtained from high speed cine film recordings.

The profile of the intruding door is controlled, to a great extent, by the characteristics of the "B post" and the "sill." The B post can be considered as a beam supported at its top and bottom. When loaded, it bends with the greatest deflection being near its centre, where the bending moment is greatest. This coincides with a change in cross-section at the car's waistline and results in the bottom half of the B post tilting inwards at the waistline.

The extent to which the door follows the motion of the B post is affected by the degree of interaction between the bottom of the door and the sill. If the sill prevents the bottom of the door from over-riding it, the degree of door tilt is increased (figure 1). If however, the door can easily ride

over the sill it may remain upright with little or no tilt (figure 2).

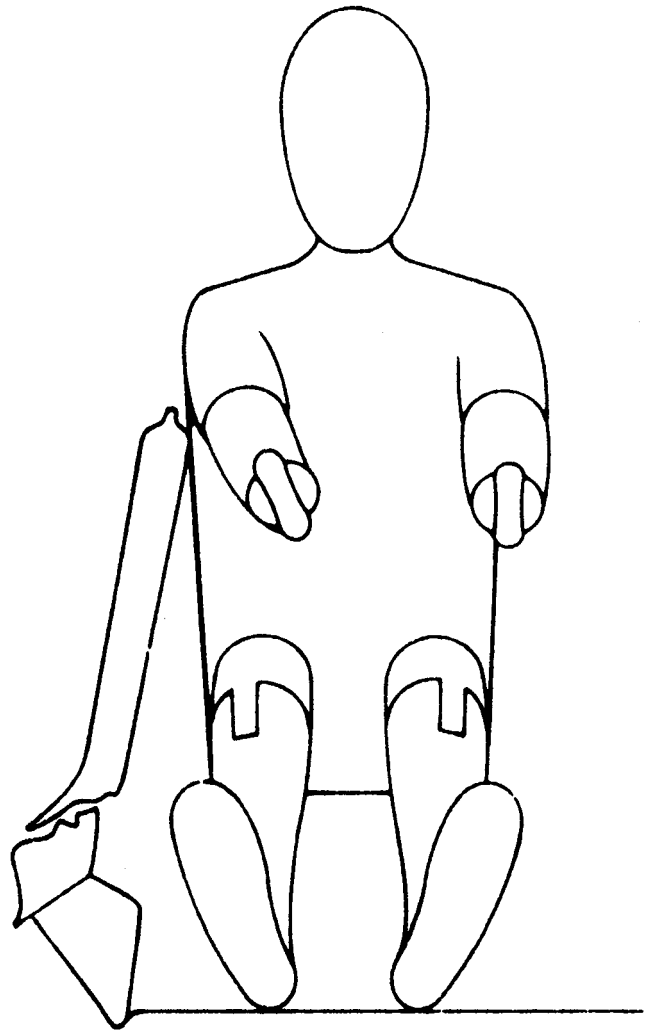


Figure 1. Car with significant door to sill interaction. Door tilts in at the waistline.

The degree of door tilt has been found to influence the way loads are transferred to the occupant. When the door tilts in at the top, loads are concentrated on the thorax. Where it remains upright, the loads are more evenly distributed and it may be that earlier loading of the pelvis reduces thoracic loading, by helping to accelerate the occupant sideways. The danger is that benefits for the thorax will be countered by increased risk of injury to the pelvis or abdomen.

Analysis of door motion is difficult. It has not been possible to fit transducers on those parts of the door adjacent to the EUROSID dummy, consequently motion has been measured some distance ahead of the dummy. The presence of the dummy has also prevented the measurement of door motion at different vertical locations. For these reasons, it has not yet been possible to study the dynamics of door tilt and to determine precisely how it affects the performance parameters measured by EUROSID. It is possible that the velocity profiles, rather than the displacement profiles, are important.

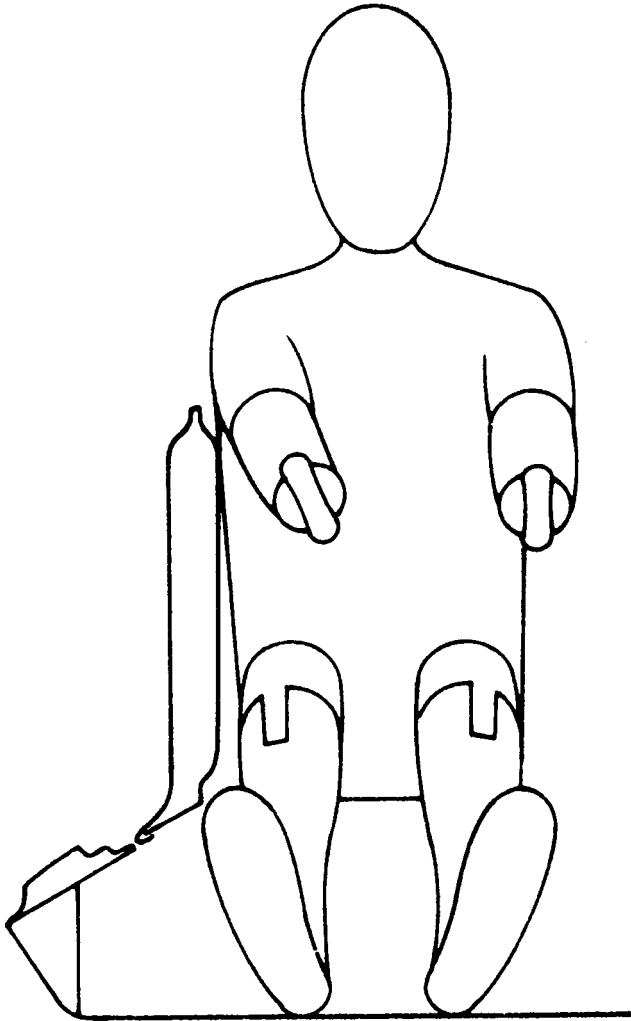


Figure 2. Car with little door to sill interaction. Door intrusion profile is vertical.

### The Development of Independent Door Motion

Although controlling the vertical intrusion profile and increasing the rate of transfer of momentum from the bullet vehicle would both appear important, it is not yet entirely clear what their relative importance is. Currently, improved control of the intrusion profile would appear to be more rewarding than increased momentum transfer. However the greatest improvements may be obtained by improving both aspects.

This can be achieved by further separating the load paths through the door into the occupant and through the car's structure to its distributed mass. This approach has been adopted in some of the most recent tests on modified cars at TRRL. Despite the fact that the modifications did not control the intrusion profile as well as had been intended, very significant improvements in the performance parameters were achieved.

### The importance of padding

Padding between the door and the occupant has the effect of attenuating the impulsive loading when contact occurs.

In addition, padding can alter the relative loading, and its timing, between different parts of the body. Our experience is that the optimum thoracic padding would appear to be much softer than had been expected. Somewhat stiffer padding has been used against the pelvis, where it has also been possible to increase the padding thickness. Thicker padding should be acceptable against the pelvis, as it does not get in the way of arm movement.

Of all the performance parameters measured, TTI (Thoracic Trauma Index) (9) is the most sensitive to the presence of padding. Padding significantly reduces peak rib acceleration which is one of the two parameters used in the calculation of TTI.

### Full Scale Side Impact Tests

The full scale side impact tests were performed in the open, on the TRRL test track. EEVC MDB faces, to the design used by Kenmont Ltd, were mounted on a mobile trolley which was towed to the impact point behind a powerful car. Additional guidance was provided by a channel mounted on the track surface. A single EUROSID dummy was seated in the front seat of the test car. In earlier tests, a second dummy had been placed in the rear seat but this had obscured the view from the rear "on board" camera. For these tests, no dummy was placed in the rear seat.

The arms of the dummy were positioned, as specified in the EUROSID Dummy User Manual, in a forward position so they could not protect the thorax. In order that the motion of the individual ribs could be observed, the dummy's suit was removed. To compensate for the suit's padding effect, a piece of the suit material was fitted to the impact side of the dummy's thorax. The dummy, the car and the trolley were extensively instrumented and high speed cine cameras recorded events in the vehicle as well as from outside.

The instrumentation on the dummy measured: head acceleration, rib acceleration and thorax compression at each rib, spine acceleration at three locations, pelvis lateral acceleration, pubic symphysis load, Ilium load and the operation of switch contacts in the abdomen. From these data, HIC (Head Injury Criterion), VC, TTI and spine translation and rotation about two axes were derived.

On the test car, the motion of the inner and outer skins of the door, just ahead of the dummy's thorax, was measured together with the motion of the car itself. In addition, final static intrusion of the car side was measured at a matrix of points. For the mobile trolley, its impact speed and post impact deceleration were measured.

A comprehensive record of the data from this programme of tests is given in Appendix I.

### Reproducibility tests with standard cars

The results from reproducibility tests on a small hatchback car (S1) have already been reported (5) and are repeated below (table 1). Further results can now be reported from a series of tests involving a medium sized hatchback car

(M1). Although the variation in the impact speed was a little greater than that specified for the proposed legislative test, the results obtained were fairly consistent (S1 and M1 in table 1). There was somewhat more variation in the parameters measured on the more lightly loaded ribs than for those most severely loaded. For the legislative test, it is proposed that only the maximum value be used. For both sizes of car, the maximum thorax compression and VC were maxima on the same rib in each test. However, maximum TTI was not always related to the same rib.

**Table 1. Side impact tests on production cars.**

Car Model	Test	Car Mass (kg)	Thorax			Lateral (G)	Pelvis	
			Comp. (mm)	VC	TTI		Symphysis (kN)	Ilium (kN)
S1	W1	980	54 M*	1.58 M	185 T	-	14.2	5.6
	W2	980	47 M	1.30 M	186 M	108	15.0	3.0
	W3	980	52 M	1.23 M	164 B	95	13.5	9.4
S2	X7	860	34 T	0.48 M	132 T	121	11.2	2.5
M1	W16	1053	48 B	1.35 B	169 B	137	6.9	2.5
	W18	1057	50 B	1.71 B	183 B	116	8.1	4.0
	W19	1044	55 B	1.88 B	215 T	133	6.5	2.6
L1	W20	1640	51 T	2.21 T	213 T	83	4.5	2.5
L2	X1	1553	55 B	1.94 B	181 B	95	5.3	3.8
L3	Y3	1280	31 B	0.60 B	145 M	79	5.6	1.9

\* T, M and B indicate which Rib - top, middle or bottom - gave the maximum value shown here.

### The effects of car size

In total, six different models of standard production car have been tested. Two were small hatchbacks (S1 and S2), one was a medium sized hatchback (M1), two were large saloons (L1 and L2) and one was a large estate (L3).

Although there was a size difference between the small and medium sized cars, there was not a great difference in their masses. However when the first two large cars (L1 and L2) were tested, the results did appear to confirm that protection of the thorax was likely to be more difficult with heavier cars (table 1). The pelvis parameters were better than with the lighter cars, but this may be because these larger cars were intended for sale in the U.S. market and were designed with strong sills to pass U.S. side strength tests.

Two of the cars tested, one small car (S2) and one large car (L3), were seen to perform much better than the other cars. All the thorax performance parameters were lower, although the load on the pelvis was quite high with the small car.

There was no evidence to suggest that these two cars had stiffer structures than the other cars tested. The rate of transfer of momentum was actually lower for this small car than for the other small car (S1). Comparing the large cars, the rate of momentum transfer was similar in all cases.

What was evident, was the difference in the vertical intrusion profiles. Cars S2 and L3 had much less interaction between the door and the sill and the doors had remained virtually upright. Examination of the B post of car L3 revealed that a double hinge had formed near its base allowing

its base to make a stepwise intrusion (figure 3). A further plastic hinge had formed some distance above the waistline, well above the thorax, but no hinge had formed at the waistline. Between these hinge formations, the B post had remained virtually upright. This had helped to ensure that the door also remained vertical.

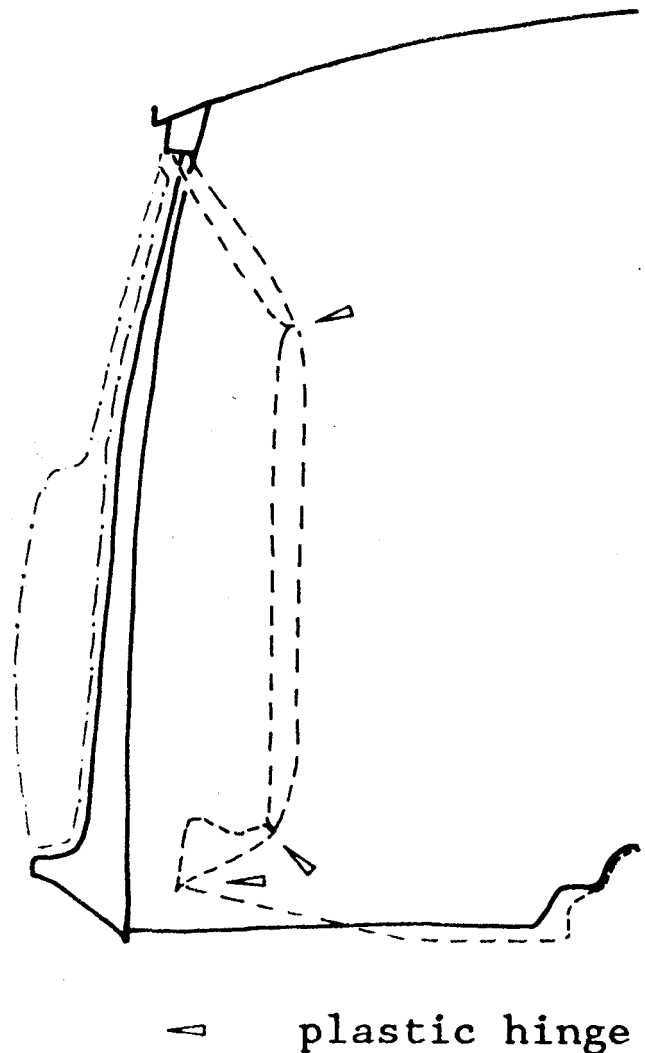


**Figure 3. B post with double hinge near base and single hinge above waistline.**

From these tests, it can be seen that both a small car and a large one have apparently been able to offer much better levels of protection, because their doors have remained upright.

### Influence of intrusion and padding

In an earlier French study (10), the effect of eliminating passenger compartment intrusion was reported. In this TRRL programme, tests have examined the effects of virtually eliminating intrusion, of almost completely filling the gap between the door and occupant with padding and of doing both together. Some problems were encountered in the test where padding alone was used and so some care has been needed in interpreting the results.

To minimise intrusion, a 6 mm steel plate was fitted to the

exterior of one of the small (S1) hatchbacks (figure 4). To examine the effects of padding alone, 100 mm of padding was fitted to the door adjacent to the dummy's thorax, abdomen and pelvis. To reduce its stiffness, adjacent to the thorax, the cross-sectional area of the foam was reduced by coring out holes. When tested in combination with the exterior plate, the padding thickness was increased to 150 mm.



Figure 4. Car fitted with an external steel plate to study the effects of reducing intrusion.

The presence of the external steel plate virtually eliminated intrusion but only produced a limited improvement in the performance parameters. Similarly, padding alone produced limited improvement (table 2). It was only when the two were combined that significant benefits were seen.

Table 2. Effects of padding and virtually eliminating intrusion.

Test	Thorax			Pelvis		
	Comp. (mm)	VC	TTI	Lateral (G)	Symphysis (kN)	Ilium (kN)
W1 standard	54 M*	1.58 M	185 T	-	14.2	5.6
W2 standard	47 M	1.30 M	186 M	108	15.0	3.0
W3 standard	52 M	1.23 M	164 B	95	13.5	9.4
W10 plate	48 M	0.86 M	139 M	39	3.7	-
W11 padding	49 T	1.05 T	-	-	8.5	2.6
W15 plate+padding	25 M	0.23 T	58 T	56	3.4	1.7

\* T, M and B indicate which Rib - top, middle or bottom - gave the maximum value shown here.

Clearly, with current technology, reducing intrusion to this extent would not be feasible for production cars and, even in these tests, dynamic intrusion was highest at the car's waistline. Almost comparable levels of improvement have subsequently been achieved by less drastic changes, as will be explained later in the paper.

### The effect of changing MDB impact speed

To examine the effects of changing impact speed, tests were carried out at impact speeds approximately 10 km/h

above and below the normal test speed. These tests were carried out using the medium sized cars (M1), although additional data was available from a test on a modified small car (S1). In this test the impact speed had been low because of a failure in the towing system. It has been possible to compare the results from this test with those from a similar car tested at the normal speed.

Comparing the low speed tests with those at the standard speed, it can be seen that, as expected, the performance parameters improved with reduction in impact speed (table 3). If however the results from the higher speed test are compared, the performance parameters did not all increase. Although pelvic loading and TTI increased, thorax compression and VC remained the same.

Table 3. Effects of changing MDB speed and mass.

Car Model	Test	Thorax			Lateral (G)	Pelvis	
		Comp. (mm)	VC	TTI		Symphysis (kN)	Ilium (kN)
M1	W16 normal	48 B*	1.35 M	169 B	137	6.9	2.5
	W18 normal	50 B	1.71 B	183 B	116	8.1	4.0
	W19 normal	55 B	1.88 B	215 T	133	6.5	2.6
	X17 fast MDB	47 B	1.38 B	218 M	155	13.5	1.9
	X18 slow MDB	45 B	0.98 B	135 B	111	5.3	1.2
	X16 heavy MDB	46 B	1.26 B	183 B	135	6.9	1.7
S1	X20 normal	39 B	0.60 B	86 T	96	5.5	2.9
	X19 slow MDB	33 T	0.30 B	57 M	72	3.5	1.7

\* T, M and B indicate which Rib - top, middle or bottom - gave the maximum value shown here.

The reason for this apparently anomalous result would appear to be due to a change in the way the car's structure failed in the impact. At the higher impact speed, collapse was more concentrated at sill level than had been the case in the lower speed impacts. As a result, the door remained more upright. In the 50 km/h impact, the B post tilted inwards at its waistline whereas, at 60 km/h, the tilt was outwards at the waistline.

As well as adding further confirmation of the importance of the vertical intrusion profile, this test had demonstrated the importance of dynamic effects in influencing the outcome of side impacts.

It is possible that the structural collapse changed because of a shift in the relative contributions from buckling and bending failure modes. Whereas bending increases in proportion to load, buckling failure is initiated when a threshold load is exceeded and collapse can then continue at lower load levels. In the case of side impacts, the car's side structure essentially fails in bending whereas the floor and its cross members fail in buckling.

The way in which impact speed changes the failure mode can be expected to vary with different structural design. Whether this effect can be adequately accommodated in computer simulation models is not yet clear.

It is interesting to note however, that the changes due to altering impact speed were in any case small compared with the differences between cars having different structural characteristics.

## The effect of changing MDB mass

In order to examine the effect of increasing the MDB mass a test (X16) was carried out with the trolley ballasted to 1350 kg. No deterioration in the performance parameters were seen from this change (table 3), and indeed the test results indicate that the thorax might have been more lightly loaded, as in the high speed test.

A study of the vehicles' motion showed that, with increased mass, the MDB decelerated more slowly. However, the increased mass had no detectable effect on the motion of the car's centre of gravity, over the first 100 msec of the impact. As far as the measured door velocity was concerned, no effect was seen in the first 50 msec. After 50 msec, the door velocity was increased but this was well after all the performance parameters had maximised.

## Car to car impact tests

To compare with the impacts using mobile barriers, a number of car to car side impact tests have also been carried out. These have used small and medium sized cars, S1 and M1, impacted by the same model of car. The medium sized car M1 was also impacted by another medium sized saloon car (M2) (table 4). Whereas both the small and medium sized hatchbacks (S1 and M1) had modern styling, with curved fronts and set back bonnet leading edges, the third car (M2) had a more prominent bonnet leading edge.

Table 4. Comparative car to car MDB tests.

Car Model	Test	Impactor	Thorax			Pelvis		
			Comp. (mm)	VC	TTI	Lateral (G)	Symphysis (kN)	Ilium (kN)
S1	W1	EEVC MDB	54 M*	1.58 M	185 T	-	14.2	5.6
	W2	EEVC MDB	47 M	1.30 M	186 M	108	15.0	3.0
	W3	EEVC MDB	52 M	1.23 M	164 B	95	13.5	9.4
	W13	Car S1	23 T	0.42 M	128 M	110	8.0	4.9
M1	W16	EEVC MDB	48 B	1.35 M	169 B	137	6.9	2.5
	W18	EEVC MDB	50 B	1.71 B	183 B	116	8.1	4.0
	W19	EEVC MDB	55 B	1.88 B	215 T	133	6.5	2.6
	X14	Car M1	40 M	0.93 B	137 M	96	9.8	0.3
X6	Car M2	53 B	1.66 M	172 B	119	6.6	1.3	
X12	NHTSA MDB	30 B	0.58 T	123 T	124	15.8	-	

\* T, M and B indicate which Rib - top, middle or bottom - gave the maximum value shown here.

In comparison with the EEVC MDB face, the small car (S1) produced better performance measurements for the thorax and at the pubic symphysis but similar pelvic acceleration. The medium sized hatchback (M1) also produced better measurements on the thorax but in this case pelvic acceleration and Ilium load, though broadly similar, were better and the pubic symphysis load was worse. When the medium sized hatchback (M1) was impacted by the medium sized saloon (M2), both thorax and pelvic parameters were of the same magnitude as those produced by the EEVC MDB face.

In each case, the EEVC MDB face was able to match the worst aspects of each of the different cars' features, without being excessively severe.

## Comparison between the EEVC MDB face and the NHTSA MDB face

Tests have compared the characteristics of the NHTSA MDB face with those of the EEVC MDB face and other cars. To simulate the "crabbing" of the NHTSA trolley, the NHTSA MDB faces were fitted, at the crabbed angle, to the front of the trolley which was also ballasted to the NHTSA mass. The dynamics of this arrangement are the same as for a crabbed trolley, except that the centre of gravity is effectively offset to one side. This is not thought to influence events during the important first 50 msec of the impact.

Analysis of the test results show that, unlike the EEVC MDB face, the NHTSA face did not produce performance measurements similar to those produced in the car to car impacts (table 4). The thorax measurements were much lower and the pubic symphysis load was much higher. Only the lateral acceleration of the pelvis was about the same.

## The development of intrusion resistance

At the beginning of the programme of work, the reduction of intrusion and increase in the rate of momentum transfer were major targets. The demonstration car ESV 87, which was presented at the 11th ESV Conference (5), was designed along these lines. In its side impact test, it showed improvements over the standard car, but the improvements were modest.

When it became clear that simple reinforcement was insufficient, a further aim of controlling the vertical intrusion profile of the door was added. To achieve this, B posts were strengthened, in an attempt to prevent them bending in the middle. At the same time, the doors were reinforced with door beams and the sills were strengthened. At the first attempt (W17), only limited control of the B post motion was achieved (table 5).

Table 5. Effects of reduced intrusion and padding.

Car Model	Test	Thorax			Pelvis		
		Comp. (mm)	VC	TTI	Lateral (G)	Symphysis (kN)	Ilium (kN)
M1	W16 standard	48 B*	1.35 M	169 B	137	6.9	2.5
	W18 standard	50 B	1.71 B	183 B	116	8.1	4.0
	W19 standard	55 B	1.88 B	215 T	133	6.5	2.6
	W17 modified**	36 T	0.56 M	121 M	66	2.9	1.6
	W23 modified	29 T	0.27 B	67 B	57	3.0	1.5
	X2 modified	41 M	0.73 T	104 T	45	3.5	2.0
S1	W1 standard	54 M	1.58 M	185 T	-	14.2	5.6
	W2 standard	47 M	1.30 M	186 M	108	15.0	3.0
	W3 standard	52 M	1.23 M	164 B	95	13.5	9.4
	X3 modified	50 M	0.94 T	124 T	71	6.5	3.5

\* T, M and B indicate which Rib - top, middle or bottom - gave the maximum value shown here.

\*\* Details of modification are given in the text and Appendix II

With the next car (W23), a complete tubular hoop was added around the interior of the car at the B post. This hoop was made from thick walled steel tube. In combination with the sill and door reinforcements and thick padding this gave quite good results. However, a repeat test with a more practical thickness of padding (X2) gave less satisfactory results. Furthermore when this type of tubing was used simply

as B post reinforcing, in a small car (X3), little benefit was seen. It was clear that a major contribution to its effectiveness, when used as a hoop, came from the resistive torque at the top and bottom which reduced deflection at the waistline. Designing a B post for production, with the capability to supply such resistive torques, is probably not feasible.

### The development of independent door motion and separate load paths

When it became apparent that the control of intrusion at door level seemed less important than control of the vertical intrusion profile, it became feasible to separate further the load paths through the door from those into the car's structure. To achieve this, a car (X20) was modified to incorporate tall stiff sills which would transfer the loads into the car. Above the sill level the B post was weakened to encourage it to intrude near its base. The aim was to make the B post rotate inwards, about its joint with the roof, with the minimum of bending. To prevent interaction between the door and the sill, a horizontal gap was left between them. In this way the door was controlled to intrude with a near vertical profile. The door itself had no reinforcement and was actually weakened at its waistline to prevent line loading from its stiff upper edge.

An inspection of the car after the test showed that the B post had still creased at the waistline. In an attempt to overcome this, a second car (Y4) was tested with the B post reinforced at its waistline (figure 5). This car is on display at the conference.



Figure 5. Car with independent door motion.

The results show that for both of these cars significant improvements were achieved compared with the standard production car (table 6). Although strengthening the B post at its waistline had been beneficial, neither of the cars' structures failed entirely as intended. It could be expected that better results would be obtained if the side structure

could be further developed so that it actually failed as intended.

Table 6. Effects of developing independent door motion.

Test	Thorax			Lateral (G)	Pelvis	
	Comp. (mm)	VC	TTI		Symphysis (kN)	Ilium (kN)
W1 standard	54 M*	1.58 M	185 T	-	14.2	5.6
W2 standard	47 M	1.30 M	186 M	108	15.0	3.0
W3 standard	52 M	1.23 M	164 B	95	13.5	9.4
X20 independent door	39 B	0.60 B	86 T	96	5.5	2.9
Y4 ind. door + B post	33 M	0.42 B	65 B	62	4.0	2.1

\* T, M and B indicate which Rib - top, middle or bottom - gave the maximum value shown here.

\*\* Details of modification are given in the text and Appendix II

Having said this, these cars have produced the best performance parameters of any tested, with the exception of those cars with extreme structural modifications and full gap filling padding (W15 and W23).

### Conclusions

Analysis of the data from a comprehensive series of car side impact tests has shown the importance of controlling the vertical intrusion profile of the incoming door. From this analysis, control of the vertical intrusion profile appears to be of greater importance than the prevention of intrusion. By separating the motion of the door from that of the load paths into the distributed mass of the car, it has been possible to achieve significant improvements in the performance parameters measured by the EUROSID dummy. Tests on standard production cars have shown that those for which door tilt is small have much better side impact performance than those where the door tilt is greater.

The EEVC test procedure has been shown to be capable of distinguishing between cars with different structural characteristics and would appear to be a good assessor of injury protection. The EEVC MDB face has been shown to reproduce the worst features of the bullet cars tested without being excessively severe. Its deformable nature has been shown to be capable of taking account of the stiffness variation across the impact area. Tests using the NHTSA MDB face showed that it did not reproduce the loading seen in car to car impacts. Despite its increased stiffness and mass, it presented a less severe impact for typical European cars than either the EEVC MDB or real cars.

Analysis of door motion and tests at different impact speeds have shown the importance of detailed dynamic effects. Firstly, the transient motion of the door following the initial impact has been seen to extend through the period when the performance parameters reach their maximum values. Secondly, the way a car's structure collapses has been seen to vary with speed, both because of inertial effects and because of possible changes in the relative contributions from buckling and bending failure modes. Whether these effects can be adequately accommodated in computer simulation models is not yet clear.

For the future, more detailed information on the motion of intruding side structures is required. The reason for the

importance of the intrusion profile needs exploring, to establish whether it is displacement, velocity or some other factor which is the major determinant of injury. Studying how separate load paths can be engineered into production cars, without the need for high sills, would ease the problem of providing increased protection.

Overall the outlook is promising. Much better side impact protection seems feasible and the proposed EEVC Side Impact Test Procedure would appear to be capable of distinguishing between good and bad cars.

## References

(1) European Experimental Vehicles Committee—Working Group No. 6, *Structures Improved Side Impact Protection in Europe*, Proceedings of the Ninth International Technical Conference on Experimental Safety Vehicles, Kyoto, 1982.

(2) Pullwitt, E., W. Sievert, D. Cesari, J. Bloch, R. Dargaud, I. D. Neilson and C. A. Hobbs, *Final Report of the First Phase*, EEC Contract No AO/83/394, 1984.

(3) Sievert, W., E. Pullwitt, C.A. Hobbs, J.A. Bloch and D. Cesari, *Validation of Mobile Deformable Barrier—Final Report*, EEC Contract No 84/7790/17, October 1985.

(4) Cesari, D., J. Bloch, W. Sievert, E. Pullwitt, I.D. Neilson and C.A. Hobbs, *Validation of the EEVC Mobile Deformable Barrier for Side Impact Testing*, Proceedings of the Tenth International Technical Conference on Experimental Safety Vehicles, Oxford 1985.

(5) Hobbs, C.A., M.G. Langdon, R.W. Lowne and S. Penoyre, *Development of the European Side Impact Test Procedure and Related Vehicle Improvements*, Proceedings of the Eleventh International Technical Conference on Experimental Safety Vehicles, Washington, 1987.

(6) Hobbs, C.A. and M.G. Langdon, *Thoracic Impact and Injury in Side Impact Accidents*, 1988 IRCOB Conference on the Biomechanics of Impact, Bergisch-Gladbach, 1988.

(7) Langdon, M.G., *Developments in the Simulation of Side Impact*, Proceedings of the Twelfth International Technical Conference on Experimental Safety Vehicles, Gothenburg, 1989.

(8) Lau, I.V., and D.C. Viano, *The Viscous Criterion—Bases and Applications of our Injury Severity Index for Soft Tissues*, Proceedings of the 30th Stapp Conference, 1986.

(9) Eppinger, R.H., J.H. Marcus and R.H. Morgan, *Development of Dummy and Injury Index for NHTSA's Thoracic Side Impact Protection Program*, SAE p840885, 1984.

(10) Cesari, D., M. Ramet and C. Cavallero, *Influence of Intrusion in Side Impact*, Proceedings of the Sixth International Technical Conference on Experimental Safety Vehicles, Washington, 1976.

Crown Copyright. The views expressed in this paper are not necessarily those of the Department of Transport. Extracts from the text may be reproduced, except for commercial purposes, provided the source is acknowledged.

## Appendix I

Model	Test Car		Impactor			Head HIC	Pelvis			
	Test No.	Mass (kg)	Type	Mass (kg)	Speed (km/h)		Lateral (max G)	Symphysis (max kN)	Ilium (max kN)	
S1	W1	980	EEVC MDB	950	52.2	782	-	14.2	5.6	
	W2	980	EEVC MDB	950	49.3	291	108	15.0	3.0	
	W3	980	EEVC MDB	950	51.1	863	95	13.5	9.4	
	W10	1040	EEVC MDB	950	48.6	473	39	3.7	-	
	W11	980	EEVC MDB	950	49.7	484	-	8.5	2.6	
	W15	1045	EEVC MDB	950	49.3	372	56	3.4	1.7	
	W13	980	Car S1	980	49.7	186	110	8.0	4.9	
	X3	860	EEVC MDB	950	50.4	500	71	6.5	3.5	
	X19	867	EEVC MDB	950	41.4	109	72	3.5	1.7	
	X20	867	EEVC MDB	950	51.5	204	96	5.5	2.9	
	Y4	918	EEVC MDB	950	51.5	257	62	4.0	2.1	
	M1	W16	1053	EEVC MDB	950	50.0	792	137	6.9	2.5
		W18	1057	EEVC MDB	950	53.3	260	116	8.1	4.0
		W19	1044	EEVC MDB	950	51.5	677	133	6.5	2.6
		W17	1180	EEVC MDB	950	50.4	152	66	2.9	1.6
		W23	1180	EEVC MDB	950	52.9	92	57	3.0	1.5
		X2	1115	EEVC MDB	950	49.0	113	45	3.5	2.0
		X6	1111	Car M2	1084	51.8	254	119	6.6	1.3
X12		1111	NHTSA MDB	1340	49.0	-	124	15.8	-	
X14		1053	Car M1	1050	51.1	510	96	9.8	0.3	
X16		1080	EEVC MDB	1350	50.4	434	135	6.9	1.7	
S2	X17	1106	EEVC MDB	950	61.2	905	155	13.5	1.9	
	X18	1100	EEVC MDB	950	40.7	145	111	5.3	1.2	
	X7	860	EEVC MDB	950	49.7	276	121	11.2	2.5	
	L1	W20	1640	EEVC MDB	950	53.3	572	83	4.5	2.5
	L2	X1	1553	EEVC MDB	950	49.7	445	95	5.3	3.8
	L3	Y3	1280	EEVC MDB	950	46.8	223	79	5.6	1.9

Details of impact and head and pelvis performance.

Test No.	Thorax Compression				Viscous Criterion				Thoracic Trauma Index				Max Rib		T12 Spine			
	Top	Mid	Bot	Max @msec	Top	Mid	Bot	Max @msec	Top	Mid	Bot	Max	maxG	@msec	maxG	@msec		
W1	46	54	48	54	41	1.20	1.58	1.20	1.58	29	185	171	178	185	214	27	157	30
W2	40	47	43	47	35	1.01	1.30	1.28	1.30	29	178	186	184	186	228	24	144	31
W3	36	52	45	52	44	0.68	1.23	1.15	1.23	30	157	161	164	164	185	25	142	31
W10	44	48	31	48	54	0.82	0.86	0.50	0.86	42	89	139	91	139	225	39	53	47
W11	49	45	43	49	-	1.05	0.71	0.60	1.05	25	-	-	-	-	96	21	-	-
W15	23	25	23	25	53	0.23	0.15	0.16	0.23	49	58	55	49	58	71	37	45	43
W13	23	21	17	23	58	0.26	0.42	0.27	0.42	38	110	128	124	128	159	35	98	41
X3	44	50	46	50	44	0.94	0.87	0.71	0.94	35	124	100	96	124	158	29	89	32
X19	33	31	29	33	74	1.82	1.83	1.88	1.88	29	55	57	53	57	58	53	55	38
X20	36	34	39	39	37	0.58	0.41	0.60	0.60	31	86	86	82	86	85	30	88	33
Y4	31	33	31	33	50	0.27	0.36	0.42	0.42	30	54	58	65	65	77	22	53	31
W16	36	40	48	48	39	1.04	1.02	1.35	1.35	31	164	162	169	169	232	28	106	36
W18	40	47	50	50	38	1.17	1.36	1.71	1.71	30	168	178	183	183	252	26	115	34
W19	49	53	55	55	35	1.82	1.83	1.88	1.88	29	215	206	205	215	300	27	129	33
W17	36	34	32	36	44	0.55	0.56	0.50	0.56	33	84	121	87	121	168	29	74	35
W23	29	26	29	29	59	0.15	0.24	0.27	0.27	33	44	49	67	67	91	29	42	43
X2	36	41	33	41	55	0.73	0.63	0.32	0.73	47	104	78	65	104	155	41	53	41
X6	50	52	53	53	41	1.39	1.66	1.46	1.66	35	143	169	172	172	248	31	95	39
X12	26	26	30	30	56	0.58	0.22	0.39	0.58	43	123	112	104	123	154	37	92	38
X14	34	37	40	40	50	0.70	0.77	0.93	0.93	43	127	137	133	137	190	38	84	45
X16	44	44	46	46	39	1.21	1.01	1.26	1.26	33	167	182	183	183	244	29	121	35
X17	45	46	47	47	34	1.30	1.27	1.38	1.38	29	203	218	210	218	277	25	159	31
X18	32	38	45	45	42	0.53	0.71	0.98	0.98	34	102	122	135	135	191	30	79	38
X7	34	31	28	34	55	0.46	0.48	0.47	0.48	33	132	130	123	132	151	31	114	34
W20	51	50	47	51	35	2.21	2.11	1.57	2.21	30	213	185	148	213	311	26	116	32
X1	49	47	55	55	33	1.52	1.52	1.94	1.94	27	180	177	181	181	233	23	129	30
Y3	28	27	31	31	39	0.51	0.42	0.60	0.60	32	143	145	144	145	205	31	84	35

Details of thorax performance.

## Appendix II

Car Model	Test	Modifications
S1	W10	6 mm External Steel Plate
	W11	Thorax Padding(1) - 100 mm Cored Urethane(2,3) Pelvis Padding - 100 mm Urethane
	W15	6 mm External Steel Plate Thorax Padding - 150 mm Cored Urethane Pelvis Padding - 150 mm Urethane
	X3	Reinforced floor, roof, sill and B post and tall door beam Thorax Padding - 75 mm Phenolic(4) Pelvis Padding - 100 mm Urethane
	X19	High, reinforced sill with weak independent door B post weakened at the bottom Thorax Padding - 50 mm Phenolic over 25 mm Urethane Pelvis Padding - 100 mm Urethane
	X20	High, reinforced sill with weak independent door B post weakened at the bottom Thorax Padding - 50 mm Phenolic over 25 mm Urethane Pelvis Padding - 100 mm Urethane
	Y4	High, reinforced sill with weak independent door B post weakened at the bottom and reinforced at the waistline Thorax Padding - 50 mm Phenolic over 25 mm Urethane Pelvis Padding - 100 mm Urethane

Car Model	Test	Modifications
M1	W17	Reinforced floor and sill and tall door beam B post supported at the waistline Thorax Padding - 100 mm Cored Urethane Pelvis Padding - 100 mm Urethane
	W23	Reinforced floor and sill, tall door beam and Steel tubular hoop fitted within the car at the B post Thorax Padding - 100 mm Cored Urethane Pelvis Padding - 100 mm Urethane
	X2	Reinforced floor and sill, tall door beam and Steel tubular hoop fitted within the car at the B post Thorax Padding - 75 mm Phenolic Pelvis Padding - 125 mm Urethane

1. All padding was wrapped in glass fibre netting
2. Cored to reduce stiffness, with 20 mm holes at 30 mm centres
3. 29 kg/m<sup>3</sup> Rigid Polyurethane foam (crush strength 170-200kN/m<sup>2</sup>)
4. 20 kg/m<sup>3</sup> Rigid Phenolic foam (crush strength approx 80 kN/m<sup>2</sup>)

Details of structural modifications and padding.

## Acknowledgements

The work described in this paper forms part of the programme of the Transport and Road Research Laboratory and the paper is published by permission of the Director.

# Effects of Belt Restraint Systems on Occupant Protection Performance in Side Impact Crashes

Nobuyoshi Shimoda, Yousuke Nishida,  
and Akihiko Akiyama,  
Honda R&D Co., Ltd.

## Abstract

Currently, belt restraint systems are among the most effective occupant protection devices now available and mandatory usage laws are spreading among the world's nations. Accordingly, the belt usage ratio is also increasing annually. Following the implementation of the FMVSS 208 Passive Restraint Regulation in the United States, a diversity of belt restraint systems has come to be offered on the automotive market.

This implies that an increasing number of belt-restrained occupants may be involved in side impact traffic accidents in the future.

Considering such a situation, in this paper, we focused attention on occupant head behavior in a side impact crash, and investigated the effects of several belt restraint systems on occupant head behavior and impact protection performance in side impact crashes.

For this purpose, we conducted 10 full-scale side impact crash tests according to the National Highway Traffic Safety Administration (NHTSA) test procedure using one model of a Honda subcompact car.

In half of these test cars, two '88 improved-type Side Impact Dummies (SID) were placed one behind the other on the near-side.

In the other half, two SID's were placed side by side in the front seats.

Five different restraint conditions were tested in both seating configurations, i.e., lap belts only, 2 point automatic shoulder belts (2P/A), 3 point automatic belts (3P/A), 3 point manual belts (3P/M) and no-restraints.

Based on these test results, we compared and analyzed whether SID head behavior and SID torso region accelerations were affected by differences of condition such as occupant restraints, seating positions and presence of a side occupant, and discussed the effectiveness of the belt restraint systems tested on side impact occupant protection.

## Introduction

The most popular belt restraint system now in use is 3P/M, a combination of lap and shoulder belts. But in a side impact crash, it has been argued, this belt system is mainly effective in protecting the far-side occupant and precluding the ejection of occupants. (1)\*

This lack of effectiveness for the near-side occupant may be because the effective buffer distance from the outmost side of the vehicle body to the near side occupant is so short, compared with the distance from the front end of the vehicle

to the occupant, that he may be more directly exposed to an impact from a striking car.

Nearly half the deaths in side impact crashes are related to head injuries. (2, 3 and 4) Yet, passenger car occupants, if in a proper seating position, seldom receive fatal head injuries from the initial direct impact in a car side crash. Presumably, the injuries are caused by the secondary contacts with the interior of their own car, or with outside objects during the moments immediately following the crash. Even if we exclude the consequences of occupants' ejection from the car, the incidence of head injuries in side impact crashes is by no means negligible. (5)

Ideally, it would be desirable if belt restraint systems offered occupant protection for secondary impacts in side crashes as well as in head-on collisions.

In this context, it can be argued that belt restraints are effective in mitigating injuries to near-side occupants.

But, in practice, experience shows that near-side occupants with 3P/M sometimes get serious head injuries in side impact crashes.

To date, the head injury mechanism of side-impact has not yet been fully clarified.

An analysis of traffic accident statistics indicates that in about half of all head injury cases, head contact points are "unknown". (3)

So, in order to provide satisfactory protection against head injuries in side-impact, it would be useful to clarify the behavior of the belt-restrained occupants' head.

As the first step in such research activities, this paper tries to find out how the heads of belt-restrained occupants behave, how they are affected by alternative belt restraints and conditions, and whether belt restraints can be used effectively for the occupants' head protection in side impact crashes.

A series of full-scale side impact tests were carried out according to the NHTSA test procedure (6) on 10 examples of sections of a generic model of a subcompact passenger car (Honda Quint Integra 3 door).

As shown in figure 1, each of 10 test cars had different SID seating configurations or restraint conditions.

During the tests, SID head behaviors and torso accelerations were observed to investigate the effects of the restraint systems in each SID seating position.

The NHTSA side impact test procedure has not yet been fully developed as a side impact test. Also the SID is not satisfactory with respect to some specific items to be measured nor do its responses have fully reliable biofidelity.

However, we decided to adopt the test procedure and the dummy as an interim means of comparison in this series of tests.

The occupant protection performance of each belt restraint system was measured at two different stages of side impact resulting in occupant injuries. One is the initial

\*Numbers in parentheses designate references at end of paper.

occupant impact stage (IOIS), a relatively early stage (within some 50 ms) of a crash in which the near-side occupant could be hit directly by the inside of the vehicle pressed inward by the striking car. The other is the secondary occupant impact stage (SOIS), in which the near-side occupant could be hurled by the rebound of IOIS or by the inertial force of the occupants' own body against the cabin interior, outside objects or another occupant.

## Test Procedure

Figure 1 provides an overview of the test vehicle conditions and number of tests.

Condition of Occupant Position	Impact Direction		Impact Direction	
	Near Side Front Occupant	Near Side Rear Occupant	Near Side Front Occupant	Far Side Front Occupant
No Restraint	1	2	1	1
Lap Belt	1	—	1	1
2P. Automatic Shoulder Belt	1	—	1	1
3P. Automatic Belt	1	—	1	1
3P. Manual Belt	1	3	1	1

Figure 1. Matrix of SID seating configurations and restraint conditions.

Ten full scale side impact tests according to NHTSA test procedures were conducted on these test vehicles to measure the accelerations of the SID torso regions and observe the SID head trajectories with two (or three) vehicle-mounted high speed cameras.

Figures 2 and 3 show the front and side views of a test vehicle before the test, and figure 4 shows the moving deformable barrier used in the tests.



Figure 2. The front view of a test vehicle before the test.



Figure 3. The side view of a test vehicle before the test.

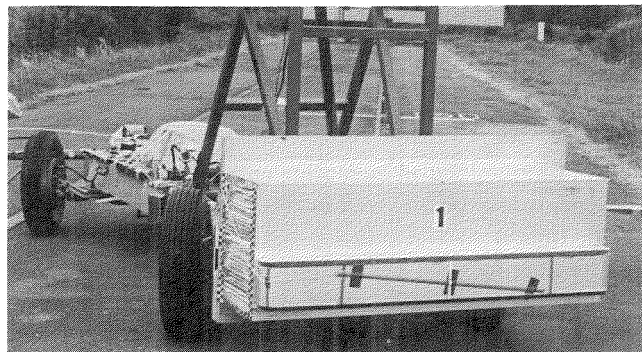


Figure 4. The moving deformable barrier.

## Test conditions

### NHTSA Prescribed Side Impact Test

- NHTSA-specified side impact moving barrier (1,360kg)
- Crab angle: 27°
- NHTSA-specified MDB
- Projected impact speed: 53.6 km/h

### Side Impact Dummy (SID)

- SID incorporated with 1988 retrofit kit. (Made by Alderson Research Laboratory).

(Measuring channels are filtered with SAE J 211 b for the head and SAE J 211 b + FIR for all other regions.)

### Belt restraint condition

Figure 5 provides the anchorage points of the belt restraint systems tested. Referenced to the SID hip point, each of the restraint system anchorage positions were set to reproduce the similar dimensions to the relating points of production cars.

## Test results

The SID head (the forehead center) trajectories for five different restraint conditions in three kinds of SID seating configurations, i.e., the front near-side (without far-side SID), the front near-side (with far-side SID) and the front far-side are shown in figures 6, 7 and 8. (Rear Seat SID head trajectories could not be observed.)

The acceleration time histories in three regions of the SID torso are shown in figures 9 through 16.

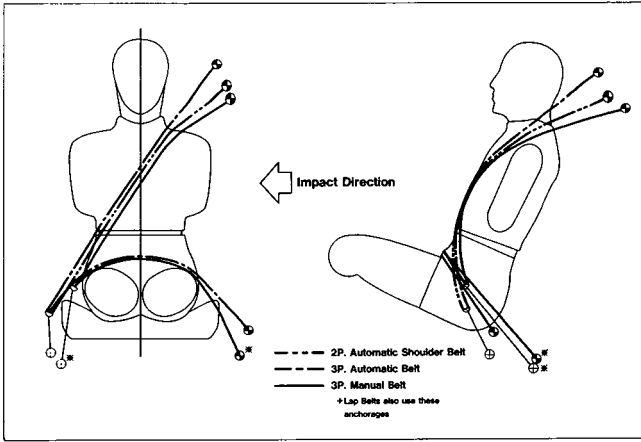


Figure 5. The anchorage positions of tested belt restraint systems.

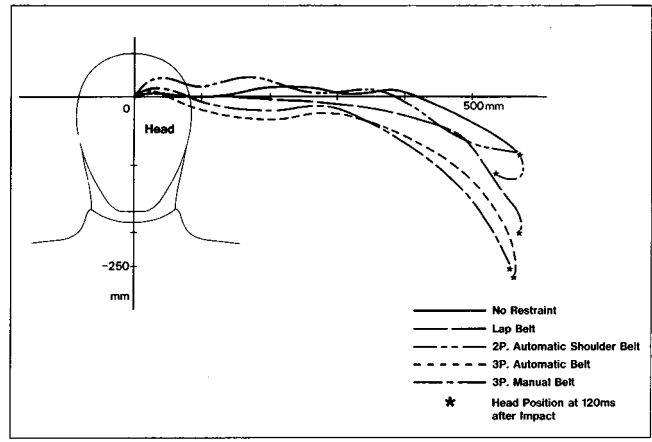


Figure 8. Head trajectories of front far-side SID (with near-side SID).

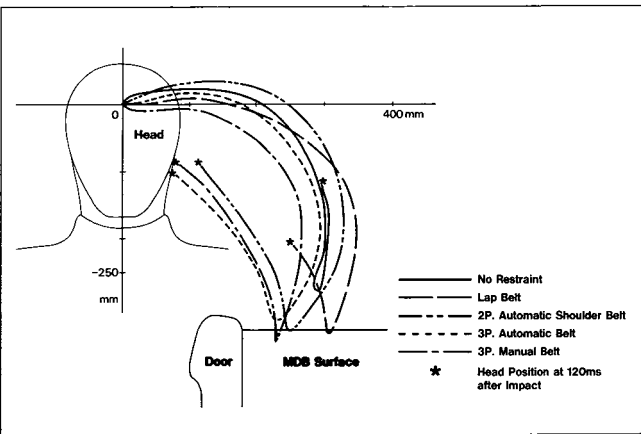


Figure 6. Head trajectories of front near-side SID (without far-side SID).

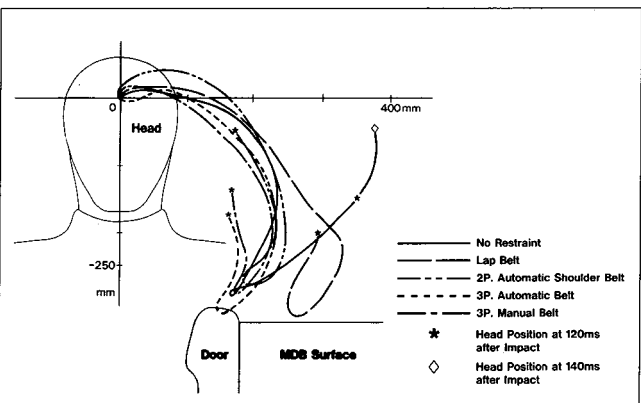


Figure 7. Head trajectories of front near-side SID (with far-side SID).

### Front near-side SID (without far-side SID)

*SID Acceleration (figures 9 and 10).*—The peak acceleration of the SID torso regions occurred within 50 ms during which the SID remained almost motionless. This suggests that belt restraints may not be so effective for occupant protection at the IOIS.

*Head Trajectory (figure 6).*—At around 80 ms after the MDB contacted the test vehicle, the head/face of the SID,

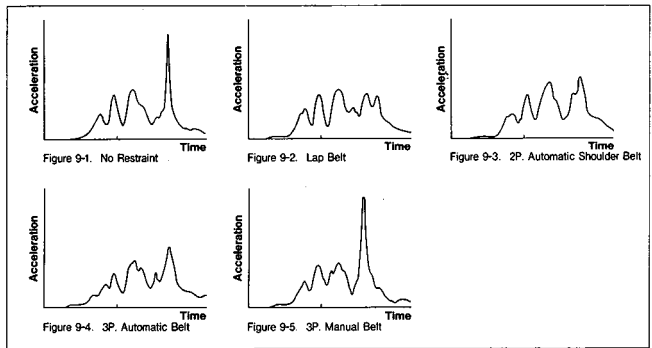


Figure 9. Head response of front near-side SID (without far-side SID) in five different restraint conditions (resultant acceleration).

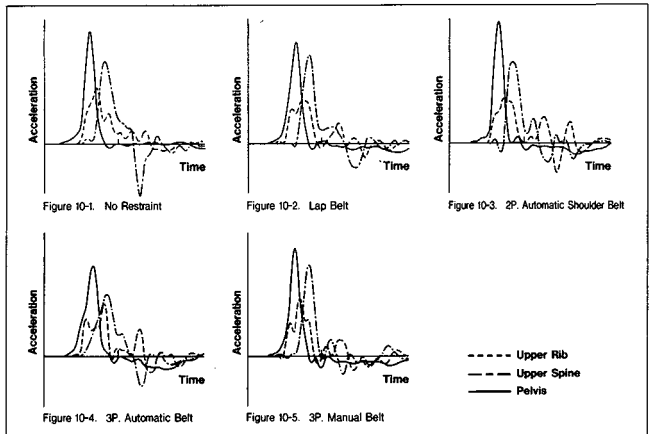
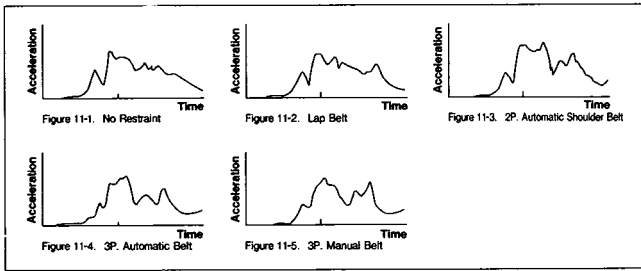


Figure 10. Torso response of front near-side SID (without far-side SID) in five different restraint conditions.

whether restrained or not, came in contact with the MDB or the upper edge of the vehicle door, and also the acceleration of the head reached its peak at this moment (figure 8). It may be argued from these findings and for the test conditions used that belt restraints provide not so effective occupant protection at the SOIS.

Note that all of the SID heads did not come in contact with any other part of the vehicle body.

As is apparent from the head trajectories in figure 6,



**Figure 11. Head response of front near-side SID (with far-side SID) in five different restraint conditions (resultant acceleration).**

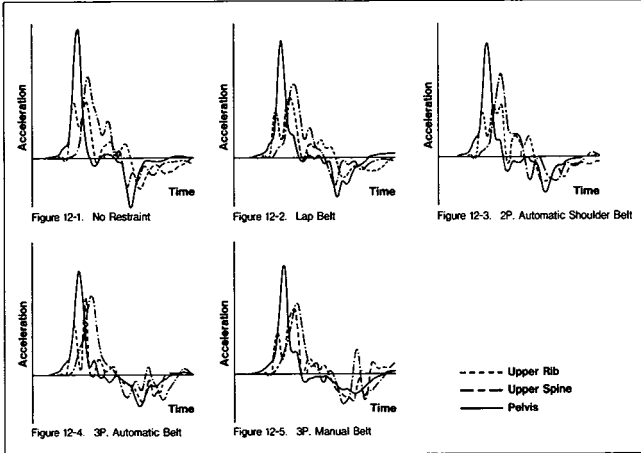


**Figure 12. Torso response of front near-side SID (with far-side SID) in five different restraint conditions.**

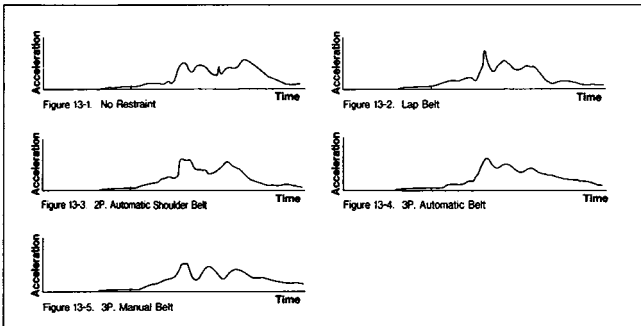


**Figure 13. Head response of front far-side SID (with near-side SID) in five different restraint conditions (resultant acceleration).**

however, the SID head, after hitting against the MDB, was pulled back toward the inside of the cabin by the restraint system, especially when it had a shoulder belt. This suggests that partial ejection of the near-side occupant's head at the SOIS may be mitigated with a belt restraint system.

Compared with the no restraint case, the head trajectory of the 2P/A restrained SID extended a little farther upward and outward, and that of the lap belt restrained SID, although staying below the unrestrained SID at the initial stage of impact, went farthest out at the latter stage.

These phenomena give a typical example of functional differences between the shoulder and lap belts during side impact. The 2P/A cannot effectively restrain the upward movement of the SID because it has no lap belt, but its

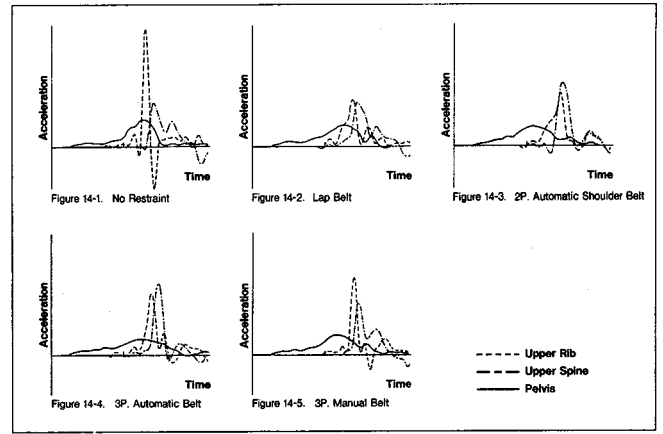


**Figure 14. Torso response of front far-side SID (with near-side SID) in five different restraint conditions.**

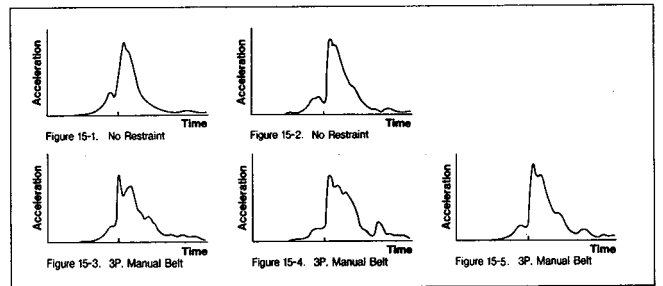


**Figure 15. Head response of rear near-side SID in two different restraint conditions (resultant acceleration).**

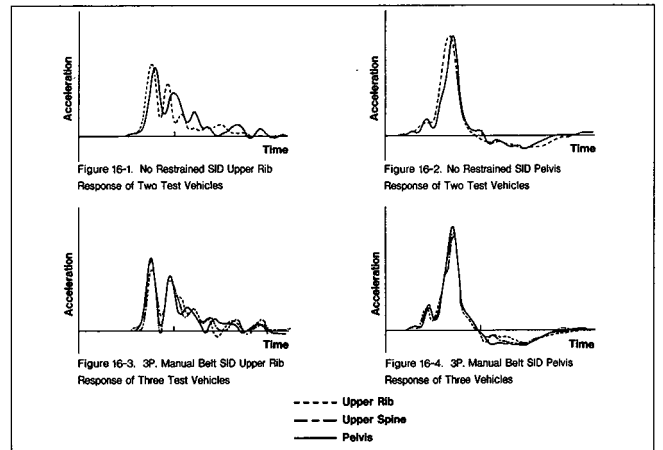


**Figure 16. Torso response of rear near-side SID in two different restraint conditions.**

shoulder belt checks the outward movement of the dummy. The lap belt, on the other hand, restrains the upward movement of the SID but fails to check its outward movement.

The head trajectory of the 2P/A restrained SID went farther outward than that of the no-restraint SID, probably because, at the IOIS, the pelvis of the latter moved away toward the far side of the vehicle and its torso was pulled back toward the inner part of the cabin, making the ejection of the head that much less. By comparison, the head of the 2P/A restrained SID moved farther outward in this example as its pelvis was restrained by the lower part of the shoulder belt from moving away toward the far side.

The head trajectories of both 3P/A and 3P/M restrained SIDs stayed within that of the no-restraint SID. This was probably because the lap and shoulder belts of these restraint systems checked the upward and outward movements of the SIDs.

Compared with the 3P/M, the 3P/A slackened somewhat, perhaps because the lap and shoulder ELRs, attached to the door, were displaced a little farther inward by the crash than the anchorage of the 3P/M which was attached to the side sill.

Apparently, this was why the head trajectory of the 3P/A restrained SID moved outside that of the 3P/M restrained SID.

### **Front near-side SID (with far-side SID)**

*SID Acceleration (figures 11 and 12).*—Up to about 50 ms after the MDB contacted the test vehicle, the accelerations of the front near-side SID with the far-side SID present were similar to those recorded without far-side SID present. Apparently, the presence of the far-side SID had little influence on the behavior of the near-side SID in this respect.

After more than 50 ms from the contact, the near-side SID contacted the far-side SID, but the torso acceleration of the former was significantly lower than the latter. This test result may be attributed to the asymmetric structure of the current SID design.

Accordingly, it would be desirable if a two directional SID were developed to facilitate research efforts in this area.

*Head Trajectory (figure 7).*—The head/face of the near-side SID, whether belt-restrained or not, hit against the MDB or the upper edge of the door with the far-side SID present. It did not come in contact with any other part of the vehicle body.

In all of the tests with the far-side SID present, the outward range of the head trajectories were shorter than those recorded without the far-side SID. This is probably due to the near-side SID coming in contact with the far-side one at an early stage of side impact, and its pelvis and upper torso were held between the collapsing door and the far-side SID, resulting in a head trajectory more closely centered on the neck.

The head trajectories of the lap belt-restrained and the no-restraint near-side SIDs moved farther outward when the far-side SID was present. In particular, the head of the no-restraint near-side SID jutted considerably out of the cabin in the later stages because its motion was left unchecked in these examples.

These findings suggest that belt restraints may influence the behavior of the near-side occupants in the SOIS.

But, in mitigating the partial ejection of the head, the shoulder belt is more effective than the lap belt.

### **Front far-side SID (with near-side SID)**

*SID Acceleration (figures 13 and 14).*—In all of the example restraint conditions examined, the far-side SID hit

against the near-side SID and the acceleration reached its peak more than 50 ms after the MDB Contact.

The peak acceleration of the unrestrained far-side SID was higher and occurred sooner than with any of the belt-restrained SIDs. This may have come from a combination of the near-side SID's rebound and the far-side SID's inertial motion.

Apparently, the effects of belt restraints were reflected in this phenomenon, indicating the potential usefulness of these restraint systems in protecting far-side occupants at the SOIS.

*Head Trajectory (figure 8).*—The amplitude of the head motion of the far-side SID remained virtually unchanged for all restraint conditions, because it contacted the near-side SIDs.

At an early stage of side impact, the head of a no-restraint far-side SID rotated almost horizontally, but after its torso hit against the near-side SID, its head trajectory shifted upward because its pelvis lifted slightly as it moved against the other dummy.

The common type of shoulder belt with its lower anchorage fixed on the cabin center was less effective in these tests in checking the upward motion of the far-side SID, as the belt tended to slip off the dummy shoulder at an early stage of side impact.

It was found that the head trajectory of the 2P/A restrained SID extended as far upward as that of the no-restraint SID.

The lowest head trajectories were achieved by the 3P/A and the 3P/M.

These findings illustrate differences among the belt systems in occupant restraint capability.

A combination of these observations and the SID acceleration data indicate that belt-restraint systems provide effective protection for far-side occupants at the SOIS.

### **Rear near-side SID**

The acceleration time responses for the rear near-side SIDs are shown in figures 15 and 16.

These SIDs, whether belt-restrained or not, showed roughly the same acceleration wave form. This indicates that for the particular impact used, and the resulting cabin and SID accelerations and other motions, the example belt restraints do not make a significant difference in the effective occupant motions at the IOIS. Of course other example impact trajectories, kinematics, and impact points may have produced different results.

These diagrams, also suggest that this series of tests had good reproducibility in the absence of configuration effects.

## **Summary and Conclusions**

A series of full-scale side impact tests were carried out according to NHTSA specified test procedure at a 27° crab angle, a crash speed of 53.6 km/h and with an NHTSA-specified MDB. Ten passenger car examples of one model were used, prepared in five different restraint configura-

rations, i.e., lap belt only, 2P/A, 3P/A, 3P/M and no-restraint. One test car from each of these five groups had two SIDs placed in tandem, one in the front seat and the other in the rear on the near-side, and the other car had two SIDs placed side by side in the front seats on the near and far-sides.

The head trajectories of the SIDs and their accelerations at several different regions were measured to examine the effects of varying seating positions and belt restraint systems. The findings for these examples may be summarized as follows:

1. In none of the restraint conditions, did the head of the front SID hit the upper part of the vehicle structure, such as the front pillar, center pillar or roof side rail, but instead the head, did strike the MDB or the upper edge of the vehicle door in some cases due to partial ejection of the SID.

If the biofidelity of the SID's sideways behavior can be relied upon, it can be assumed that head injuries of belt-restrained near-side occupants during side impact crashes are mostly caused by head partial ejection against the door upper edge or some external object. We believe occupants' heads seldom hit against any other structure in the car under these types of impact conditions.

2. At the IOIS, all of the belt-restraint systems used in the example tests were not so effective in protecting near-side occupants.

3. Belt restraints had some influence on the head trajectories of front near-side SIDs (without far-side SID) at the SOIS, but none of the restraint systems precluded the SID heads from hitting against the MDB or the vehicle door upper edge for the test conditions used.

4. The head trajectories at the SOIS of front near-side SIDs (with far-side SID present) differed significantly with belt-restraint configurations. It was found that the shoulder belt was more effective than the lap belt in mitigating the partial ejection of the head, but did not preclude the SID head from hitting against the door top in these example tests.

5. Belt restraints appeared to offer effective protection at the SOIS for the far-side SID (with near-side SID).

These findings indicate that the head trajectories of occupants, except in the case of near-side SIDs at the IOIS, are more or less influenced by belt restraints during side impact collisions. A possible way of reducing the incidence of head injuries due to partial head ejection could be to prevent the occupants' heads from translating out the side window during side impact.

However, there is no known side window that combines such occupant restraint capability with the function and performance of existing windows.

Further research efforts would have to be made on a technique to mitigate head partial ejection, possibly by restraining occupants' torsos more tightly.

Of course, the more firmly the torso is restrained, the greater the bending angle of the neck to the torso may become. Opinions (7 and 8) are divided on the subject and no definite assessment has yet been made on the effects of this phenomenon on the incidence of neck injuries in side impact.

These trade-offs must be borne in mind in developing any new restraint system to hold the torso more satisfactorily.

## References

(1) National Transportation Safety Board, Bureau of Safety Programs, "Performance of Lap/Shoulder Belts in 167 Motor Vehicle Crashes (Volume 1)", Report No. NTSB/SS-88/02 U.S. Department of Commerce PB88-917002, Mar. 1, 1988.

(2) Department of Transportation, National Highway Traffic Safety Administration, 49 CFR PART 571 (Docket No. 88-06, Notice 3), Federal Motor Vehicle Safety Standards; Side Impact Protection—Passenger Cars Federal Register/Vol. 53, No. 161/Friday, August 19, 1988/Proposed Rules.

(3) S.W. Rouhana, M.E. Foster, "Lateral Impact—An Analysis of The Statistics in The NCSS", SAE Technical Paper No. 851727, 1985.

(4) F. Hartemann, C. Thomas, J.Y. Foret-Bruno, C. Henry, A. Fayon, C. TARRIER, "Occupant Protection in Lateral Impacts", Proceedings of Twentieth Stapp Car Crash Conference, SAE Technical Paper No. 760806, 1976.

(5) S.C. Partyka, S.E. Rezabek, "Occupant Injury Patterns in Side Impacts—A Coordinated Industry/Government Accident Data Analysis" Proceedings of International Congress & Exposition, SAE Technical Paper No. 830459, 1983.

(6) Department of Transportation, National Highway Traffic Safety Administration, 49 CFR PART 571 (Docket No. 88-06, Notice 1) Federal Motor Vehicle Safety Standards; Side Impact Protection, Federal Register/Vol. 53, No. 17/Wednesday, January 27, 1988, Proposed Rule.

(7) F.H. Walz, P.F. Niederer, C. Thomas, F. Hartemann, "Frequency and Significance of Seat Belt Induced Neck Injuries in Lateral Collisions", Proceedings of The Twenty-Fifth Stapp Car Crash Conference; September 28-30, 1981.

(8) D.J. Dalmotas, "Injury Mechanisms to Occupants Restrained by Three-point Seat Belts in Side Impact", Proceedings of International Congress & Exposition 1983, SAE Technical Paper No. 830462 1983.

# Side Impact Protection System—A Description of the Technical Solutions and the Statistical and Experimental Tools

Hugo Mellander, Jan Ivarsson,  
Johnny Korner, S. Nilsson,  
Volvo Car Corporation

## Abstract

It is a well-known fact that injuries in side impact collisions constitute a large percentage of the injuries suffered by occupants of passenger cars.

A substantial amount of research has been conducted at Volvo during the last ten years in order to understand the mechanisms behind injuries in side impacts and to be able to introduce effective countermeasures in our cars.

Different technical solutions used to upgrade the occupant protection of passenger cars in car-to-car side impacts are presented. Specific features were built into a conventional uni-bodied passenger car and as a second step, engineering principles of a Side Impact Protection System were integrated into a prototype vehicle. The rationale behind these changes is described.

In a recently developed methodology, data from Volvo's Traffic Accident Research Team was analysed with statistical methods in order to set requirement targets for the product development.

The method makes it possible to infer expected injury reduction in real accidents from dummy measurements in laboratory tests.

The concept cars were evaluated in tests with a moving deformable barrier. The SID-dummy was used as the anthropomorphic measuring device.

The results show that a reduction of measured injury criteria can be achieved by introducing body side structures with optimized energy absorbing characteristics in car-to-car impacts. With a tuning of the mechanical properties of the door, where occupant contact may occur, the results can be improved even further.

## Introduction

Injuries in side impacts still constitute the second largest injury category in accident statistics after frontal impacts (1).<sup>\*</sup> The evolutionary process of vehicle design, where priority has been given to low air resistance and low weight in combination with compartment roominess and comfort, has so far given us a car shape with deformation zones in the front and rear but with a rather limited amount of body structure to absorb energy in side impacts.

Numerous attempts have been made to reinforce the body or pad the interior of passenger cars in order to show experimentally that it is possible to mitigate the effects of a side impact. The conclusions from this research have been obtuse, partly because the injury mechanism has been complex and difficult to understand and partly because

there has been a lack of good test methodology including dummy and injury criteria (2, 3, 4, 5).

Nevertheless, there is a common understanding today that structural reinforcement is needed to lower the velocity of the intruding side structure in car-to-car impacts, in order to create a basis on which an interior padding will work satisfactorily.

For side collisions with fixed, undeformable objects body stiffness and strength have less importance since the struck side will almost instantly be brought to a stop. Reasonable body characteristics are, however, required to ensure survival space after a collision. This is to some degree regulated in USA by FMVSS 214, where certain strength and stiffness requirements are imposed on the front doors.

However, interior padding is effective in smoothing out the contact phase between the occupant and the inside of the car.

This paper will give information on two successful research projects to improve the side impact crashworthiness of passenger cars.

The work has focused on the car-to-car crash configuration, since this is one of the most common injury producing types of accident and also a matter for a proposed legal requirement.

The authors of this paper are quite aware of the continuing controversy regarding the most suitable test methodology for side impacts. However, in order to bring forward feasible hardware solutions for consideration, and to expedite their incorporation in the ordinary passenger car, it has been necessary to choose one specific test method.

## Technical Solutions

### Improvements to a conventional uni-bodied car

*Structure.*—Neither the stiffness nor the strength of the side structure of uni-bodied cars have by tradition been optimized to take lateral forces under dynamic loading conditions. Door stiffness and strength were upgraded with the introduction of FMVSS 214 but this requirement only carries the deformation to a limited distance in a quasi-static test.

The objective was to come up with suggestions for required reinforcements or re-engineering of the body structure without causing severe penalties in terms of cost and increased weight.

A goal was set up to reduce the door intruding velocity at the time of dummy contact during dynamic loadings from a CCMC-barrier to <10 m/s in a 35 mph 90° side impact with the target car at rest. As a basis for the study, a midsize production car body was chosen.

The loading of a moving deformable barrier takes place over a large area of the impacted car and it is important to

<sup>\*</sup>Numbers in parentheses designate references at end of paper.

find the weak spots of the body. Once a failure has developed, as the cross section in a box section is destroyed by buckling, the structure collapses and the door velocity will increase.

The main load paths in a side impact are through the rocker panel, the cross member under the seat, and bending of the B-pillar supported by the roof beams.

In order to enhance the stiffness and strength of the side structure, a mathematical analysis was carried out at Cranfield Impact Centre in accordance with their in-house methodology (6).

Different quasi-static deformation tests were made on important elements and joints in order to map the characteristics of the body and obtain in-put data for the model.

A number of model runs on different solutions were tried, in an iterative process. It is beyond the scope of this paper to describe this work in detail, but briefly the following elements and joints were studied:

- A-pillar with door-hinges.
- Rocker panel and joint to B-pillar.
- B-pillar and joint to roof frame.
- Roof panel and influence of sunroof.
- Cross-member in the floor under seat.

The analysis pointed out the importance of having a stable cross-section of the rocker panel while bending of the B-pillar occurred. Consequently, five bulkheads were designed which improve the crushing resistance of the box-sectioned rocker panel considerably (see figure 1). Although it would have been desirable to improve the joint between the rocker panel and the B-pillar, it was impossible to find a suitable solution for this specific body.

The B-pillar was reinforced with an additional inner part to improve its bending characteristics. The joint between the B-pillar and the roof frame was re-engineered to improve bending resistance.

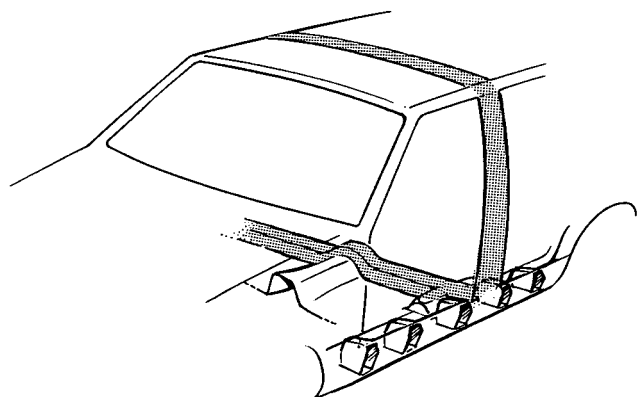


Figure 1. Improvements to a conventional uni-body. Shaded areas indicate reinforcements.

It was found that a roof with sun-roof had sufficient strength but that a specific roof strap (closed section, see figure 1) had to be fitted to cars without sun-roof. The cross-member between the rocker panel and the propeller shaft

tunnel had a geometry which initiated a bending collapse, and by changing the shape and adding material the performance could be considerably improved.

The suggested changes resulted in a stiffer and stronger side structure with better possibilities to remain energy absorbing during deformation without creation of collapse joints. For more specific information see reference (6).

*Interior.*—The existing door panel made of formed wood fibre was not changed and no extra padding was used between the panel and the inner door skin. The panel will crush during impact and dummy loading.

## Expanded and integrated improvements to a uni-bodied car

To further upgrade the side impact protection, a second project has been run. In this project, more extensive body changes were made and door panels with energy absorbing material was used.

The constraints were that the concept should be possible to apply on a modern 4/5-door midsize family car.

*Overall system description.*—In order to reduce the door intruding velocity the main principle has been to increase the lateral strength and stiffness of the car by using all the conventional elements such as the body, including the doors, the seats and the trim panels in a continuous load path.

In order to soften the occupant's contact with the door energy absorbing elements have been built into the doors between the inner door structure and the trim panel.

*Structural elements.*—In the very first phase of this project an in house lumped mass model was used to dimension the main load transferring structure.

The goal was to restrict the rate and depth of intrusion. As bullet vehicles, both a car and an MDB were analysed.

As a second step, a beam model was developed to enable a more detailed analysis. It was decided to try to avoid the initial peak and reduce the plateau of the velocity of the side frame and to keep the velocity at the time of occupant contact <10 m/s.

Important joints like B-pillar to upper roof rail have also been studied in finite element analysis.

In order to increase stiffness and strength at bumper height the body was equipped with a special concept which had been developed in several previous advanced engineering studies.

This concept consists of foam blocks inside the front doors and an enlarged lower joint of the B-pillar matching up with two thick-walled tubes in the front seats. Between the seats there is an energy absorbing box attached to the propeller shaft tunnel, (see figure 2).

The B-pillar has increased bending resistance and is supported at the lower level by substantial cross-members under the front and rear seat and also by the load transferring elements at bumper height.

At upper level the B-pillar is supported by an upgraded roof rail and a roof strap between the B-pillar (see figure 2).

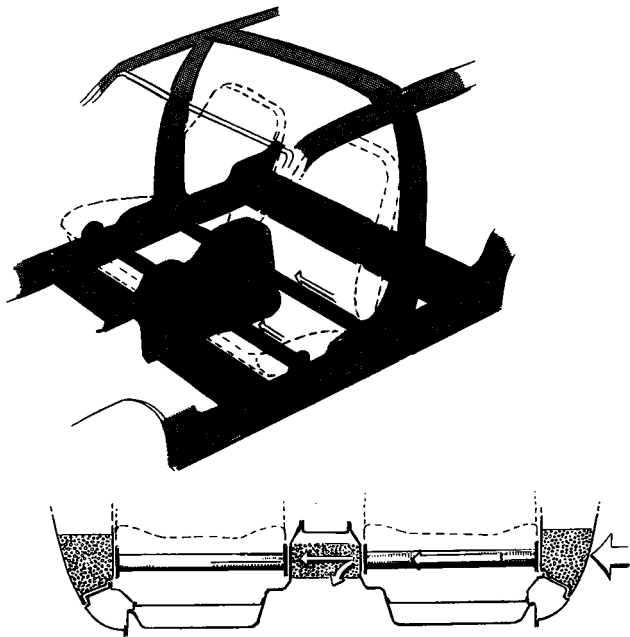


Figure 2. An integrated Side Impact Protection System. Shaded areas indicate load transferring elements. The arrows show major load paths.

All these elements have been carefully developed step by step both in mathematical analysis, component testing and full scale testing as mentioned above.

The guiding principle for crush energy management in this project has been the same as in the previous one. Special emphasis has been put on compatibility between structural elements and on prevention of failure buckling in the structure.

It is, for instance, critical that no bending collapse occurs in the B-pillar at chest height. The B-pillar, its upper and lower support and the door beams must therefore be carefully tuned in stiffness, strength and energy absorbing capacity.

The front doors have been specially engineered to carry an upper beam close to the outer panel enabling the inner panel to yield on occupant contact. The FMVSS 214 beam is placed at a low level where interaction with an occupant pelvis is avoided.

All hardware for operating windows and door locks has been omitted in the prototype. When incorporating these functions into a door it is essential that they are kept out of the way to avoid occupant contact.

*Interior.*—As mentioned earlier all clearances between doors, seats, and the tunnel box have been minimized, while still allowing space for seat adjustment.

The door panel has been designed to make room for a 100 mm thick layer of compliant tubes between the panel and the door at chest height. The doorpanel was flat with no armrest. At pelvic level the padding was 60 mm and consisted of thin-walled aluminum honeycomb.

The depth and characteristics of the padding have been developed in a mathematical model where the door and the padding interact with the US-SID dummy. The input door velocity profile has been taken from full-scale testing.

The critical points in such a simulation are the mechanical properties of the door during the dynamic crushing of the car.

In order to test a number of candidate materials and elements, quasi-static tests were performed. As the final step before full-scale testing, the chosen door padding was tested by impacting the dummy at rest with a moving barrier carrying the door panel with the underlying padding mounted on a support resembling the crushed door.

For the chest padding, a progressive (constant stiffness) characteristic was chosen to give protection in lower speeds and for the weaker portion of population. For the pelvis a square-wave characteristic was chosen.

## Statistical and Experimental Methodologies

In order to test the two prototypes, and to try to assess the achieved level of safety, the following methodology has been used.

### Procedure for evaluating occupant protection

As a first step in the research, a procedure for predicting the real-world effectiveness of different design approaches for side impact occupant protection was established (7). The method is summarized below.

The point of the procedure is the evaluation of real-world occupant protection over the whole range of crash severities where injuries occur, in contrast to the traditional single severity test.

By correlating real-world side impact accident data with laboratory test data for the same baseline design in equivalent crash configurations, it has been possible to develop chest and pelvis injury probability functions associated with dummy response amplitudes (see figure 3) where

$P(I|x)$  = injury risk (e.g. chest injuries AIS 3+) vs crash severity function obtained from real-world accident data,

$d(x)$  = dummy response vs crash severity function obtained from laboratory testing at different test speeds, and

$P(I|d)$  = injury risk vs dummy response function obtained by correlating  $P(I|x)$  with  $d(x)$ .

The baseline car used for developing  $P(I|d)$  was the Volvo 240. Provided that dummy response is measured by a parameter that fundamentally relates to the injury-producing mechanism, a given dummy response should correspond to the same injury risk, irrespective of in which car this response is measured. This means that the established injury risk vs dummy response function  $P(I|d)$  can be generally used for predicting the real-world injury risks in any car design that is tested in the laboratory—provided that the test procedure is kept the same.

The injury risk vs dummy response function  $P(I|d)$  can be employed in two ways: (1) for direct evaluation of a modified design, (2) for establishing a set of dummy re-

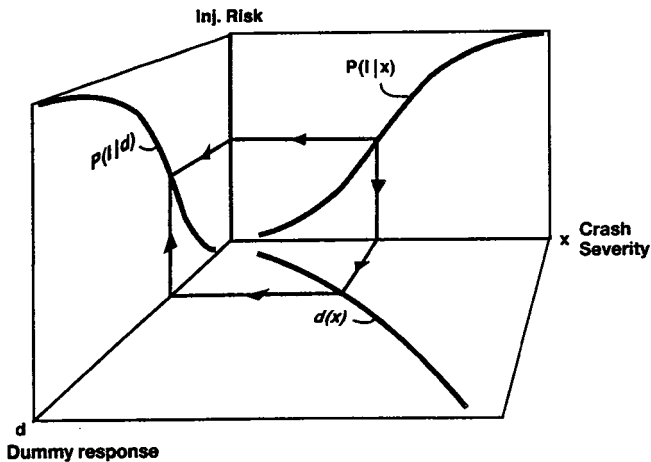


Figure 3. Converting injury risk versus crash severity  $P(I|x)$  into injury risk versus dummy response  $P(I|d)$ .

sponse reference curves that can be used as a guide in the design and evaluation process.

(1) *Direct evaluation of a modified design:*

Obtain the dummy response vs crash severity function  $d'(x)$  for the modified design by running crash tests at several different test speeds and use  $d'(x)$  for converting  $P(I|d)$  into a predicted real-world injury risk vs crash severity function  $P'(I|x)$  for the modified design (see figure 4).

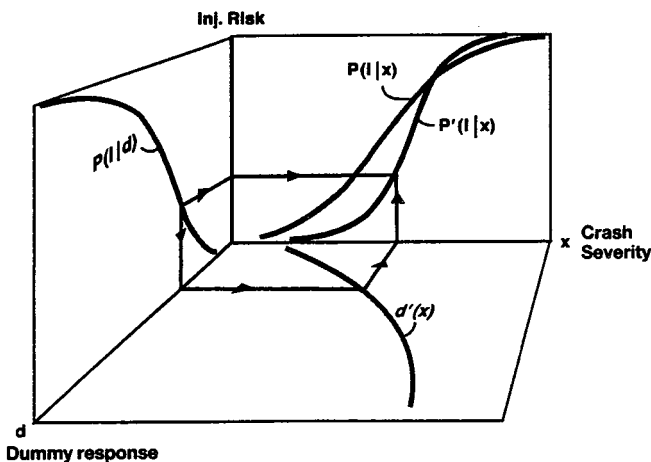


Figure 4. Converting injury risk versus dummy response  $P(I|d)$  into injury risk versus crash severity  $P'(I|x)$ .

When the crash severity distribution for real-world side impacts is known, the overall injury risk  $P'(I)$ , averaged over all crash severities, for the modified design can then be estimated by integrating the specific injury risk  $P'(I|x)$  over the range of crash severities and using the crash severity density at each crash severity level as a weight function.

The effectiveness of the modified design is the relative difference between the (known) overall injury risk  $P(I)$  for the baseline design and the predicted overall risk  $P'(I)$  for the modified design.

(2) *Establishing a set of dummy response reference curves:*

In this case, a set of conceivable injury probability vs crash severity functions  $P'(I|x)$  are obtained by shifting the baseline risk curve to the right. Corresponding overall injury risk reductions are calculated as above, using the known crash severity function as a weight function.

The established injury risk vs dummy response function  $P(I|d)$  is then used for converting the attempted set of real-world risk functions  $P'(I|x)$  into a set of dummy response reference curves  $d'(x)$ , corresponding to different degrees of overall real-world injury risk reduction, as described in figure 5.

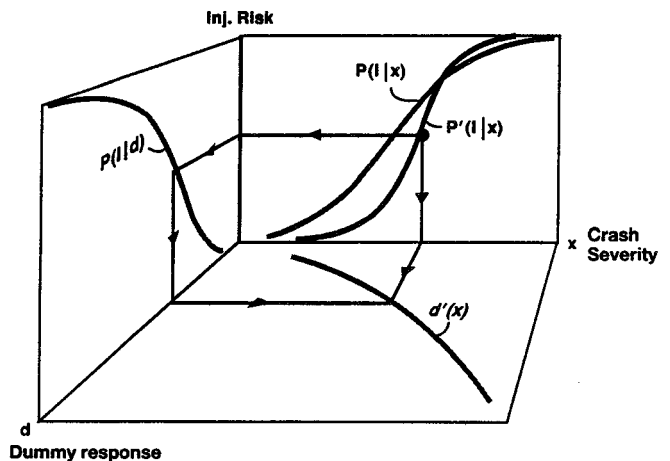


Figure 5. Converting a desired injury risk versus crash severity function  $P'(I|x)$  into a desired maximum dummy response versus crash severity curve  $d'(x)$ .

By comparing dummy response amplitudes for a modified design with the established set of response reference curves  $d'(x)$ , the overall real-world injury risk reduction for the given modified design can be approximately estimated by running laboratory tests at only a few different test speeds, provided that the test data variability is known.

In the side impact testing and development work currently in progress at Volvo, the latter evaluation strategy is employed, i.e., a set of dummy response reference curves has been developed that can be used as a guide when estimating the overall effectiveness of a modified design.

To be able to evaluate the overall effectiveness of the specific side impact protection projects described in this paper, crash tests will need to be run at different test speeds over the range of crash severities where injuries occur. This is to ensure good occupant protection even at the relatively more frequent, and thus very important, low crash severities.

The final product of these elaborations will be a diagram as shown in figures 6 and 7. From this diagram it is possible to approximately assess the overall injury reducing effect of a countermeasure by plotting the test data at different speeds.

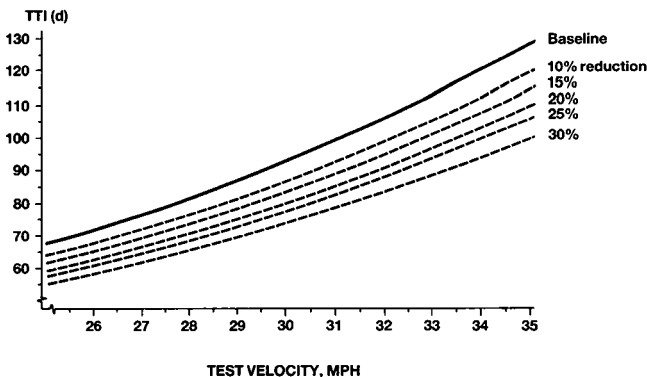


**Figure 6. Baseline data TTI(d) and a set of curves for different injury reduction.**

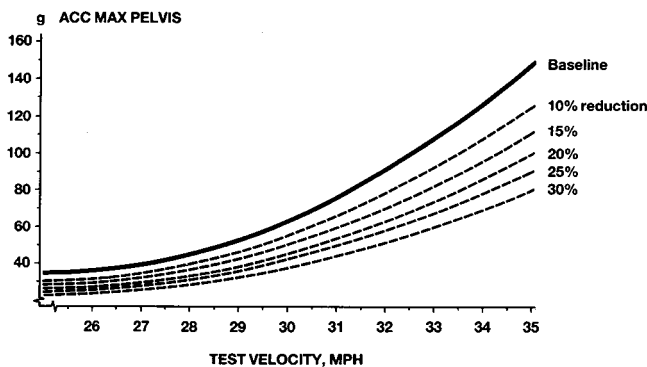


**Figure 7. Baseline data for pelvis and a set of curves for different injury reduction.**

To get an exact figure for the expected overall injury reducing effect the computations as described in (1) have to be performed.

## Laboratory experiments

As mentioned earlier, in-depth studies of side-impact accidents have been conducted by our accident research team. This knowledge is used to develop a laboratory procedure for side-impact testing. In this study the car-to-car accidents have been focused, although other areas also need to be considered in the future, i.e. fixed objects and collisions with heavy vehicles.

The full-scale performance test using a moving deformable barrier, and a side impact ATD and corresponding injury criteria have been used to assess the level of crash safety.

## Test configuration

Today, proposals from European and U.S. governments differ in terms of the approach for the barrier impact angle. The U.S. proposal (8) uses a "crabbed" configuration, 90/27 degrees, simulating an event where the struck and the striking vehicle are moving. The European configuration is a 90 degree impact with the target car at rest.

Although the crabbed configuration might be a more frequent situation in the real traffic environment, the differences in test results between the two methods are considered of minor significance. Because the "crabbed" impact is

considered less repeatable, the 90 degree impact has been chosen in our test matrix.

## Striking object barrier

Since the preference in this examination was to study the car-to-car impact, a moving deformable barrier (MDB) was used as the striking vehicle. This increases the repeatability compared with results obtained with a car as a bullet. Several barriers have been proposed over the years and the force-deflection characteristics differ significantly.

At present the CCMC and the EEVC MDBs are based on European cars. They present similar characteristics up to approximately 200 mm of deformation. For higher deformation, the EEVC barrier is softer while the CCMC barrier corresponds well with a Chevrolet Citation up to approximately 300 mm.

The aluminum honeycomb NHTSA barrier is much stiffer and does not represent the characteristics for most passenger cars.

Compared with the present car fleet, the CCMC barrier is the closest with respect to force characteristics, and it was chosen as the MDB in this study. The ground clearance was set to 250 mm.

## Test speed

Our accident data shows that 90% of all side impacts (irrespective of injury outcome) occur at impact speeds below 35 mph. Because of this, and since approximately half of the severe to fatal injuries are incurred below this speed, 35 mph was chosen as an appropriate single severity test speed for preliminary testing.

It must be emphasized again, that in order to assure that the safety design gives the desired level of protection over the whole velocity span, the final development testing must also be made at other speeds, especially in speeds lower than 35 mph.

## Anthropomorphic test device (ATD)

Today, there are basically two side impact dummies; the European Euro-SID and the American US-SID.

Both dummies have been subjected to various body and component testing to assess their biofidelity. This has been done by using the procedure recommended by ISO.

The results from these tests have shown that neither the Euro-SID nor the US-SID met these requirements. Although some projects have been undertaken to improve the biofidelity of these dummies, there is as yet no modified dummy that meets the ISO requirements.

The US-SID has been used for several years, and therefore the experience with it is greater than with the Euro-SID. The US-SID has also proved to be repeatable and able to discriminate between different levels of violence. It was therefore chosen to be used in this project.

## Injury criteria

Based on the frequencies and severity of injuries obtained

from our accident files, two body areas were chosen to be specially monitored in this study. These are the chest and the pelvis.

For the chest, the Thoracic Trauma Index (TTI(d)) was chosen as the criterion for chest injury. The TTI(d), proposed by NHTSA as injury predictor, is calculated from accelerations measured on the spine and the ribs on the impact side (8).

For the pelvis, peak acceleration was chosen.

## Test Results

### Test results—reinforced uni-body

As mentioned earlier, a number of tests with a deformable barrier were made until a satisfactory result was achieved.

*Structural results.*—In terms of permanent deformation, the reinforced car proved to be less deformed, (see figure 8).

The difference between the reinforced and the standard car, measured at the B-pillar, was approximately 100 mm.

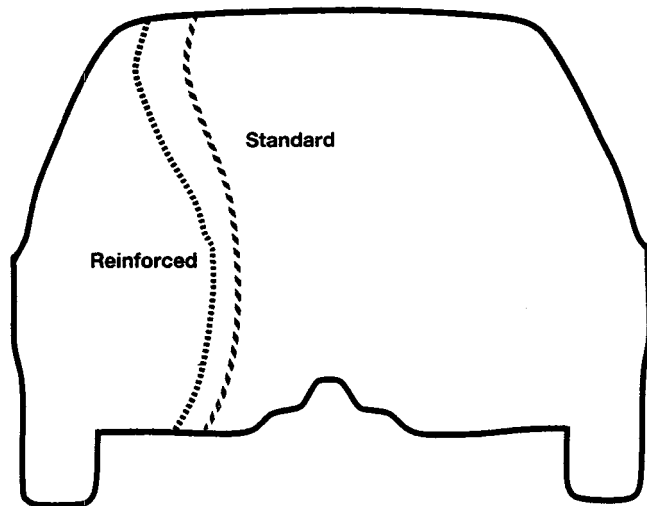


Figure 8. Permanent deformation at the B-pillar.

The door velocity profile was also lower than for the standard car (see figures 9 and 10). Somewhat disappointing, however, was the fact that the decrease in wall velocity at the moment of dummy contact was not as significant as first expected, but the velocity showed much more consistent behaviour during the first 25 msec when dummy contact is probable.

A positive effect of this is less sensitivity to the effect of distance between the occupant and the door.

### Dummy results

*Chest.*—The TTI(d) at 35 mph was 98 compared to 115 for the standard car. It should be noted that crushing of the door panel occurred and although the padding characteristics of the panel were not optimized, it is understood that it contributes significantly to the results.

*Pelvis.*—The pelvis maximum acceleration was 100 g for both the standard and reinforced car. No effect was measurable at pelvic level.

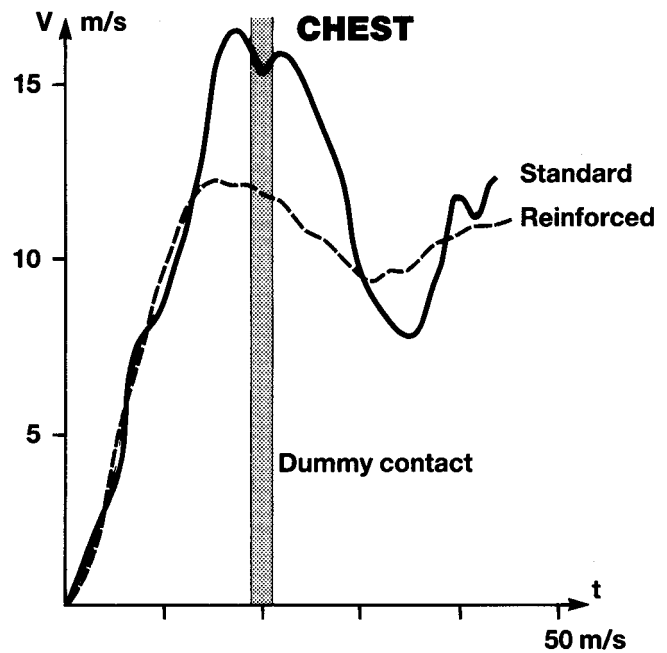


Figure 9. Door velocity time history at chest height.

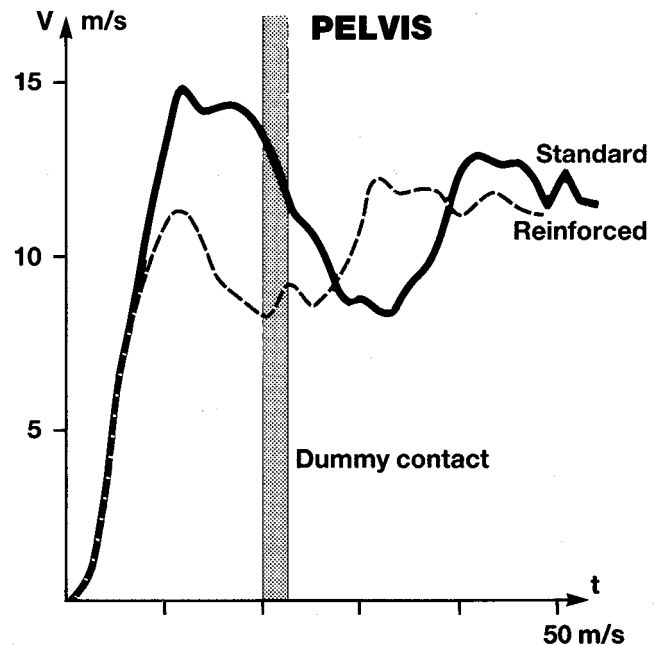


Figure 10. Door velocity time history at pelvis height.

### Test results—body with integrated side impact protection system

*Test with final prototype—structural results.*—The permanent deformation of the body is depicted in figure 11 in comparison to the standard car.

The tubes in the front seats limit the deformation and ensure that sufficient survival space is available after the collision.

The door velocity time history is shown in figures 12 and 13 for the chest and the pelvis height.

It has been found from mathematical simulation of the interaction between the door and the dummy that the most

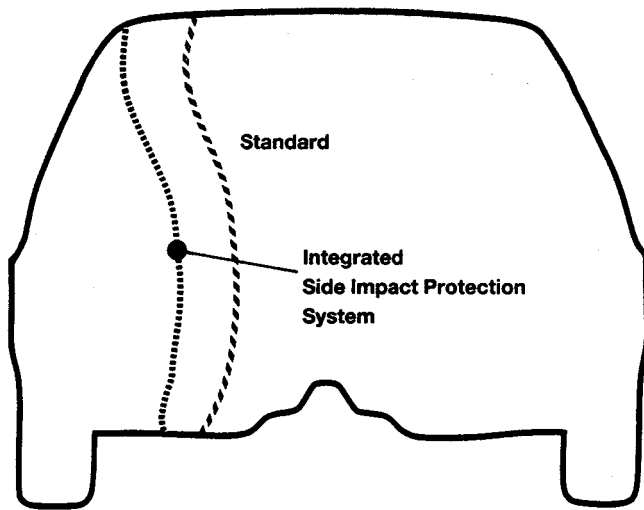


Figure 11. Permanent deformation at the B-pillar.

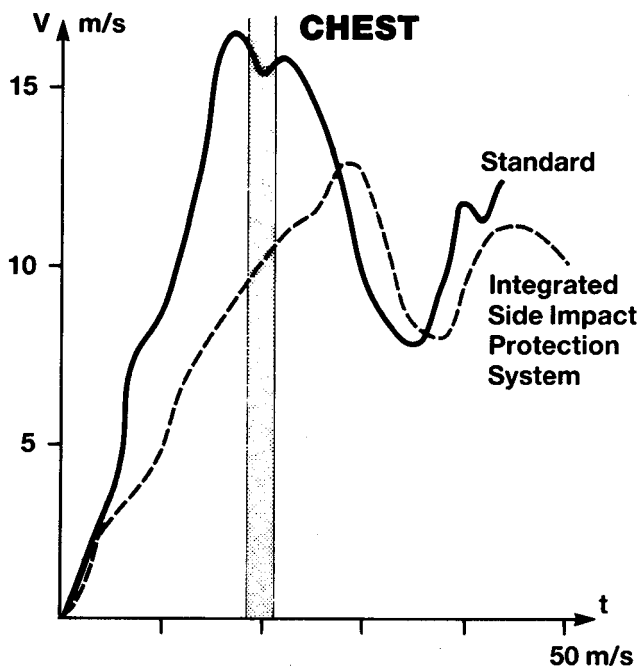


Figure 12. Wall velocity time history at chest height.

important parameter to reduce chest response is the door mean velocity during dummy contact. In the test with the prototype this mean velocity at chest height was 11 m/s.

Compared to tests with other cars this concept has shown a very repeatable door velocity time history throughout the project.

### Dummy results

*Chest.*—The TTI(d) was 80 compared to 115 for the standard car. The constant stiffness characteristic of the panel generates a peak of 65 g on the ribs. The spinal acceleration reaches its maximum of 95 g later in the phase when the door and the padding is more or less bottomed out.

*Pelvis.*—The maximum pelvis acceleration was 90 g compared with 100 g for the standard car. The constant

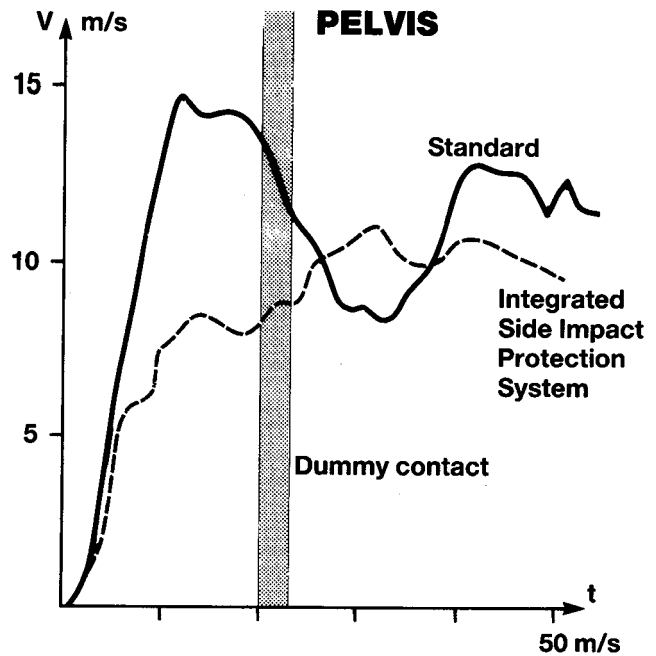


Figure 13. Wall velocity time history at pelvis height.

strength characteristic of the padding limits the peak acceleration.

### Discussion

Following the methodology described earlier in this paper, the single test speed results with the standard car and the two prototypes indicate the following reductions of severe to fatal injuries in chest and pelvis in car-to-car impacts (see figures 6 and 7). In relation to the baseline data, TTI(d) for the standard uni-bodied car suggests a ~15% reduction, the reinforced uni-bodied car a ~30% reduction and the uni-bodied car with the integrated side impact protection system a reduction in the region of 50%.

For the pelvis, the reduction was ~20% for the standard and the reinforced uni-bodied car. Consequently, no further improvement was seen in the pelvis region with the added reinforcements. In the car with the integrated side impact protection system the reduction was ~25% compared with baseline data.

However, it is necessary to continue the testing at other velocities and make repeated tests to assess the scatter before any final inference about the overall injury reduction can be made.

For the prototype with the integrated system, the detailed analysis of the test results from component and full-scale testing has given many important findings.

Interaction between the chassis of the seat and the metallic pelvis and spine skeleton may occur and create high peaks in accelerometer readings and by-pass the loading on the door padding. Stiff components in the door may cause localized loading on the dummy which may result in high injury criteria. The profile of the door panel will govern the deflection kinematics of the SID-chest. The existence of an armrest which catches the lower ribs will

cause large variations in dummy readings, other parameters being held constant.

The conflict between roominess and the desire to use a deeper door padding became very obvious in this project. Unless future consumers are willing to sacrifice some of the interior space, the only solution seems to be to make the padding expand when an impact occurs. This could be made, for instance, with a side airbag (12, 13).

It is also possible that the introduction of a new side impact dummy with better biofidelity will make it necessary to re-tune the padding force deflection characteristics of the door panel.

## Conclusions

In this project, it has been shown that a significant reduction of chest response [TTI(d)] can be achieved by careful engineering and reinforcement of a conventional uni-bodied car. Studies of the production feasibility of the changes are underway.

The prototype where structural and interior improvements are combined in an integrated, expanded solution improved the results even further and this suggests that a reduction of up to 50% for the chest and 25% for the pelvis of severe to fatal injuries in car-to-car impacts is a realistic goal. Further testing with an MDB at different impact velocities and with bullet cars with bumpers must be done before final conclusions can be made.

The conflict between compartment roominess and keeping the vehicle cross area small, and still being able to add sufficient depth of energy absorbing door padding, is obvious.

Ongoing research and innovations in this area, however, seem promising.

Redesign of the car door as a concept or the fitting of a side airbag could perhaps be solutions to this problem.

## References

- (1) Volvo Traffic Accident Research Systems as a Tool for Side Impact Protection and Development. H Norin, A Nilsson-Ehle, C Gustavsson, 9th ESV Conf. Kyoto 1982.
- (2) A Comparison Between Different Dummies in Car to

Car Side Impacts. Hugo Mellander, N Bohlin/Volvo Car Corporation. 8th ESV Conf. Wolfsburg, 1980.

- (3) Status of the Development of Improved Vehicle Side Structure for the Upgrade of FMVSS 214. William Thomas Hollowell/NHTSA, Michael Pavlick/The Budd Company. 8th ESV Conf. Wolfsburg, 1980.

- (4) Analytical Simulation of the Effect of Structural Parameters on Occupant Responses in Side Impacts of Passenger Cars. Thomas J Trella/Transportation Systems Centre, Joseph N Kianianthra/NHTSA, 11th ESV Conf. Washington D.C., 1987.

- (5) Legislative Proposals for Car Occupant Protection in Lateral Impact. Institution of Mechanical Engineers, April, 1989.

- (6) A Methodology for Enhancing Side Impact Crashworthiness. Roger Hardy, Cranfield Impact Centre, Hugo Mellander, Volvo Car Corp.

- (7) SAE 890747 A Method for Evaluation of Occupant Protection by Correlating Accident Data with Laboratory Test Data. Johnny Korner, Volvo Car Corp.

- (8) DOT/NHTSA, CFR Part 571, Docket No 88-06; Notice 1, NPRM FMVSS 214 Amendment Side Impact Protection. January 1988.

- (9) Injury and Intrusion in Side Impact and Rollovers. Charles E Strother, George C Smith, Michael B James, Charles Y Warner/SAE Febr 1984.

- (10) SAE 890881 Design of a Modified Chest for Eurosid Providing Biofidelity and Injury Assessment. Ian V Lau, David C Viano, Clyde C Culver and Edvard Jedrzejczak/Biomedical Science, dept. General Motors Research Labs.

- (11) SAE 890386 Biomechanical Design Considerations for Side Impact Roger P Daniel/Ford.

- (12) SAE 890602 Crash Protection in Nearside Impact—Advantages of a Supplemental Inflatable Restraint. Charles Y Warner, Charles E Strother, Michael B James, Donald E Shable and Timothy P Egbert/Collision Safety Engineering.

- (13) Airbag System for Side Impact Protection. Jan A Olsson, L-G Skötte, Electrolux Autoliv AB, S-E Svensson, Volvo Car Corporation. 12th ESV Conf. 1989.

## Air Bag System for Side Impact Protection

**Jan A. Olsson, Lars-Gunnar Skötte,**  
Electrolux Autoliv AB  
**Sven-Erik Svensson,**  
Volvo Car Corporation

### Abstract

It is difficult to install side impact padding of sufficient depth, due to the limited space inside conventional auto-

mobiles. A different approach is to use the air bag technique to provide sufficient energy absorption and softening of the occupant door impact.

Presented is an air bag system for side impact protection jointly developed by Volvo Car Corporation and Electrolux Autoliv AB.

The system uses pyrotechnical gasgenerators to deploy a side air bag hidden within the door structure.

A description of the function of the system is given to-

gether with a detailed description of the system components including the sensor and diagnostic unit, the gasgenerators and the side air bag.

Results from crash testing and computer simulation of the system will also be presented.

## Introduction

### Accident and legislative situation

Side impact is a severe type of traffic accident with a larger injury risk than other types of accidents.

The car accident situation is presented in the ESV paper "Volvo Traffic Accident Research Systems as a tool for side impact protection and development" by Hans Norin et al.

According to Norin approximately one-third of the accidents, resulting in injuries with an Abbreviated Injury Scale reading (AIS)  $\geq 2$  are side impact accidents. Injuries to the chest represent 34% and head 22% of the injuries to the various parts of the body. The proportion of injuries to the chest and head also increase when the crash severity increases.

This situation has also been observed by the legislative authorities in different countries.

One example of this is the notice of proposed rulemaking for side impact protection, NPRM, presented by DOT/NHTSA Docket 88-06 Notice 1. This NPRM is primarily focused on thoracic protection since the data indicates that contact between the thorax and the side interior is a major source of serious injuries and fatalities. A test method and the means to determine the injury criterion is also included.

DOT/NHTSA have also presented an advanced notice of proposed rulemaking, ANPRM, Docket 88-06, Notice 3, which specifically asks for information and discussion around the problem of head and neck injuries and ejections in side impacts. The ANPRM states that "several studies have shown that ejection increases the probability of an occupant fatality or serious injury by several times over that for non-ejection".

The conclusion of all this information is that an improved side impact protection level must be focused on injuries to the chest and head. The improvement for the head must be to reduce the ejection level.

### Technical alternatives

The ways to improve the protection level up to now have mainly been reinforcements of the side structure and/or the implementation of padding on doors, pillars and headers.

These modifications on the other hand have major drawbacks with increased weight, increased fuel consumption, reduced interior room, obstructed visibility etc. These properties are also important in a modern car and are therefore difficult to combine with improved side impact protection.

An alternative way to improve the side impact protection level could be the use of air bag technology. Air bags are widely used today and the technique has matured especially after the enforcement of FMVSS 208. However all air bag systems presently used are intended for occupant protection

in frontal crashes; could air bags be used in side crashes too?

A study to evaluate the feasibility of a side air bag system was therefore started between Volvo Car Corporation and Electrolux Autoliv AB.

The study included a preliminary design and evaluation of a complete system, including sensor, diagnostics, bag and gasgenerator.

## System Design

### System analysis

In the ESV report "Side impact protection system—a description of the technical solution and the statistical and experimental tools" by H. Mellander et al. the behavior of the side structure in a side impact was described. These results are used as input for this program. The tests performed show that the deformation zone is limited and there is contact between the dummy and the side structure after 18–20 ms.

An air bag system working under these conditions must therefore detect the crash and fill the bag considerably faster than a regular air bag system used for FMVSS 208 protection.

Another important difference compared to a regular air bag system is the distance between the occupant and the car structure. While the occupant in a normal passenger car compartment has a distance of 400–600 mm to the steering wheel or the instrument panel, he only has 150–200 mm to the side structure. A side air bag system must therefore be designed according to these conditions.

The height of the bag is dependant upon what parts of the occupant body the system is intended to protect. In our case, where the chest is considered most important, the height must be approximately 200–350 mm above the H-point.

In figures 1 and 2 it can be seen that the bag, in its deployed mode, is located close to the upper part of the door structure.

The bag must give protection over the whole chest width and the full seat track travel and it is therefore made in an ellipsoid tube shape. The main chest impact area in the vehicle is the upper rearward part of the door structure and the bag system was therefore located at this position.

With the seat track in the rearmost position the chest will impact against the B-pillar and the bag must therefore be designed in the asymmetric way shown in figure 2.

### Mathematical simulation

Mathematical models are useful especially in the early phases of projects because it is possible to study and sort out important parameters in a short time without extensive tests, even when no hardware is available. In this project a model was used to study the effect of using an air bag as protection in side impact.

The *mathematical model* used in this study is specially developed for simulations of side impacts and is designed as a one dimensional lumped mass model, shown in figure 3.

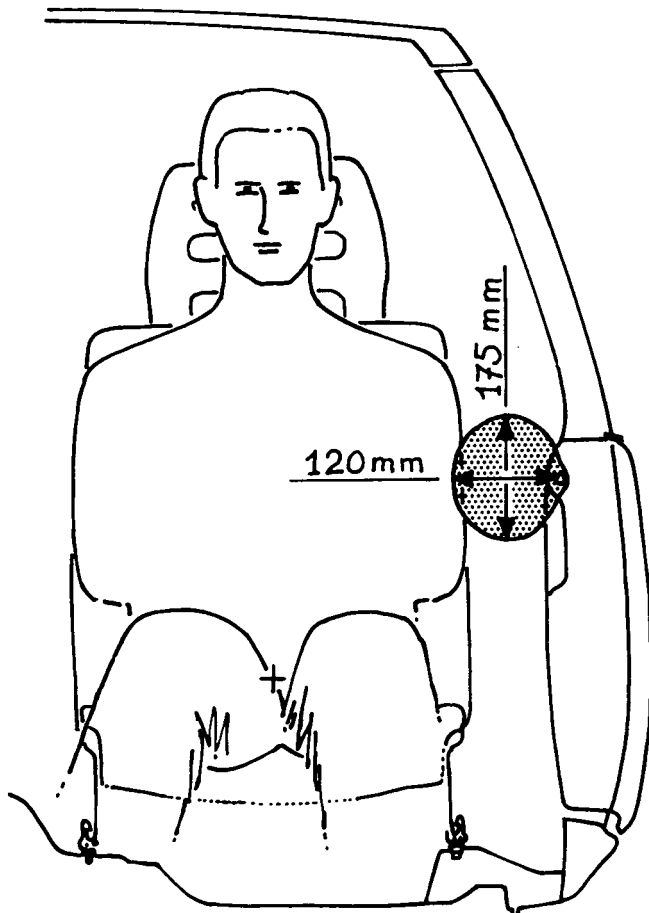


Figure 1. Frontal view of deployed side air bag.

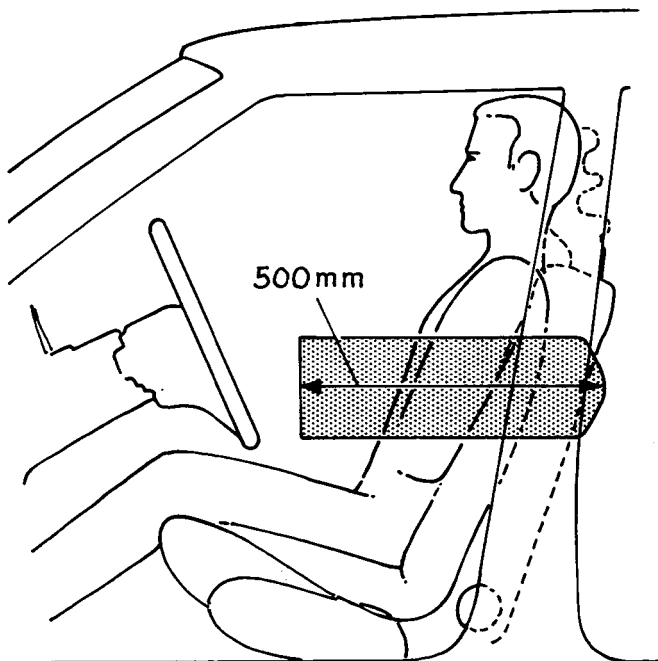


Figure 2. Side view of deployed side air bag.

The characteristics of springs and dampers are strongly nonlinear, and have been validated against dynamic experiments.

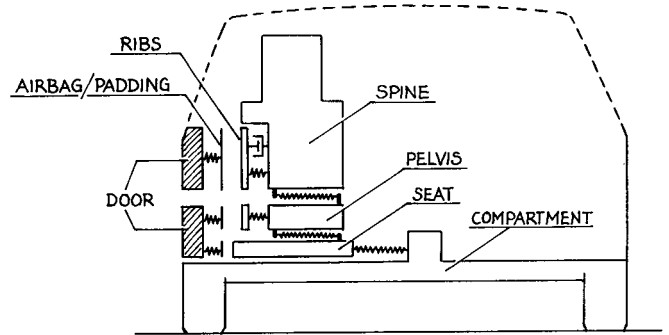


Figure 3. Mathematical model for side impact simulations.

The basic model has been used in several studies and is validated against sledtests as well as fullscale tests. An air bag system was implemented in the model as a separate unlinear spring characteristic.

*Simulation results.*—Simulations were made with different system configurations to define the bag system which gives an optimal system performance. The chosen system in this study was to use an 8 Litre bag filled to an over pressure of 1 Bar within 10 ms. With this system the improvement of occupant injury criteria was investigated at different door impact velocities.

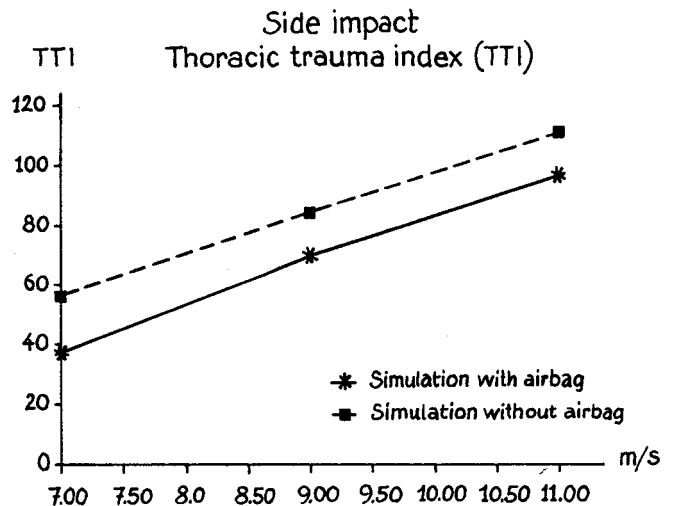


Figure 4. Simulation results with and without side air bag system at different door velocities.

In the initial simulations a constant door velocity was used corresponding to the sled test conditions. Simulations were also made with a realistic door velocity from a side impact test with complete vehicle. Door velocity according to figure 5 was used.

An improvement of the same magnitude can be seen also for the realistic door velocity.

Figure 6 also shows that the bottoming stiffness of the door structure has a great influence on the TTI value. TTI increases when stiffness increases. The reduction in injury index that is caused by the air bag system, does not decrease significantly if the bottoming stiffness decreases, which means that sledtests (with constant velocity and simulated door structure) could be used to reproduce a real side impact crash.

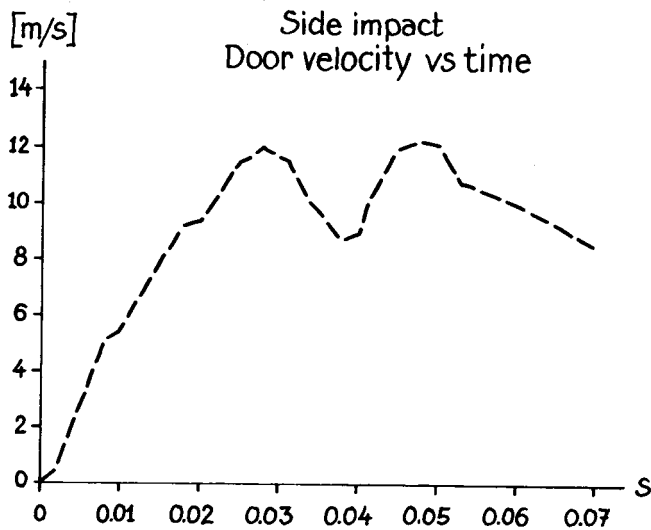


Figure 5. Side impact, door velocity versus time.

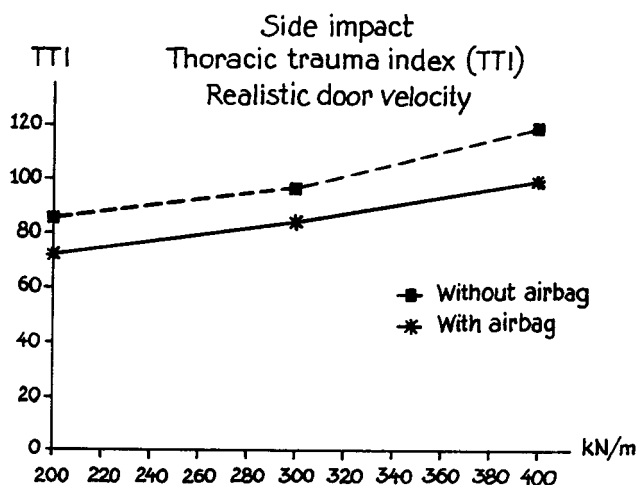


Figure 6. Thoracic trauma index (TTI) with realistic door velocity versus bottoming stiffness.

## Component design

To achieve the required system performance several alternatives were analysed. The best solution found was to use gasgenerators of a similar type to that used for pyrotechnical pretensioner retractors. For the side air bag application the generators must be loaded with 3–4 grams of propellant to meet the bag fill criteria.

The system is triggered by a deflection and force sensitive membrane switch located in the lower part of the door. The switch consists of eight segments. Segments one, three, five and seven close the circuit between the battery and the squib and segments two, four, six and eight close the circuit between the squib and the ground.

The intention is that two independent closures are required before the whole firing circuit is closed and the bagsystem is triggered. The project goal has been to have a closure of the complete firing circuit within 3 ms.

To meet this goal the sensor switch must be fixed to a rigid structure which gives a good reaction force. The switch was therefore fixed to the side impact bar in the lower part of the door, see figure 7.

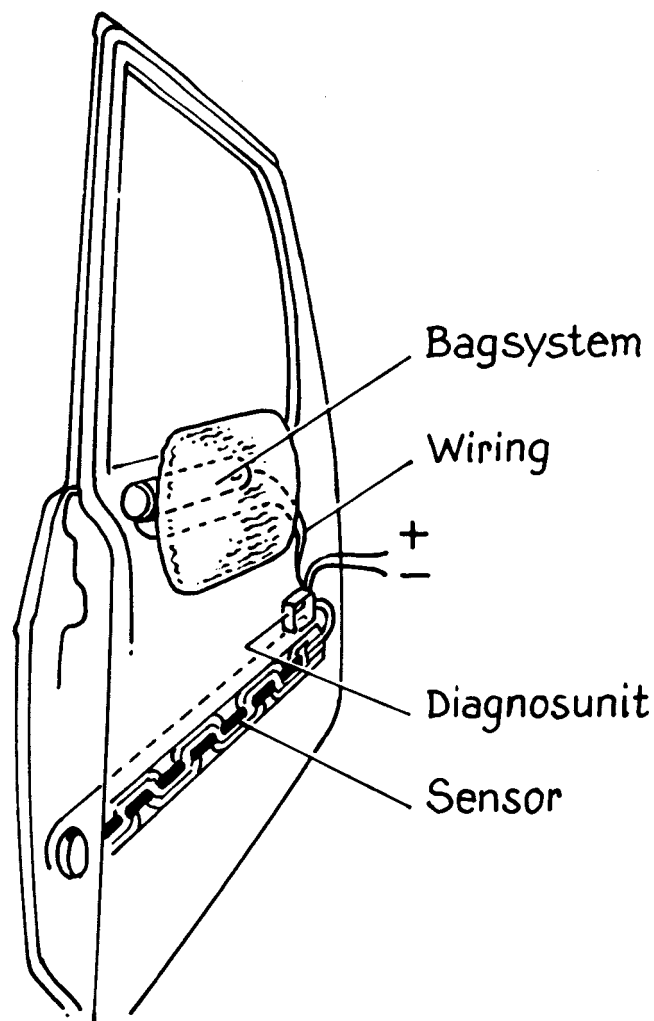


Figure 7. Complete side air bag system.

A diagnostic unit will also be fixed to the bar, controlling the system function.

The complete system including the bag system, the sensor and the diagnostic system will then be independent and selfcontained within the door with the only wiring connections being the battery voltage, ground and readiness indicator.

## Tests Performed

The bag system and the sensor system were tested separately to evaluate if an acceptable system performance could be reached.

### Bag system

Dynamic tests were made with a crash sled where the proposed type of side impact was simulated.

*Test conditions.*—A rigid door with a B-pillar was built from undeformable steel tubing and was fixed to the crash sled. A layer of padding, 25 mm thick, covered the rigid door with the intention of simulating the stiffness of a regular door. The alternative of using a regular door instead of the rigid one was found to give a softer impact structure than in a car crash test—because it is already deformed by the

barrier when the dummy is hit. It would also introduce an uncontrolled variation in the stiffness which could influence the results. It was therefore not chosen for the tests in this study.

A regular door panel and a B-pillar panel were fixed to the rigid door on the outside of the padding.

When an air bag system was used, a hole was cut in the upper rear part of the door panel. The airbag system was then fixed to the door with metal bands.

In the NPRM it is stated that the DOT-SID will be used for the determination of the side impact protection level. The acceleration in the chest rib, both upper and lower, the chest spine and the pelvis were measured and used for injury criteria calculation.

There was a difference compared with the proposed test procedure, in that the signals were not filtered in the required manner. Filtering according SAE CFC 180 was only used. This difference has an influence on the absolute values of the injury criteria and a direct comparison can not be made with other data. On the other hand a relative comparison can be made within this test series.

The dummy was placed on a styrofoam seat across the crash sled path. The position was aligned to give a chest impact in the centre of the deployed bag.

**Figure 8. Rigid door with dummy before test.**

The sled with the door and a B-pillar was then accelerated, and when a constant speed was reached at the end of the path, the side of the dummy was hit, as in a side impact.

The speed of the door at impact was lowered slightly to compensate for the stiffness of the rigid structure used in the door. Crash test results described in the ESV report "Side impact protection systems" by H. Mellander specify the impact speed to 11 m/s. In these tests the impact speed was reduced to 9 m/s.

During the sled tests with the air bag system, the deployment was initiated by an external timer. The triggering time was chosen by taking a sensor closure time of 3 ms into account. The triggering that initiated the bag deployment was therefore started 15 ms before the nominal contact between the door and the dummy chest.

While having contact door-chest the door and sled were not decelerated by any other means than the mass of the dummy. The intention was to have a constant door speed during the contact time. When the dummy started to separate from the door, at 350 mm after nominal contact between the door and the dummy, the sled was stopped mechanically.

*Test results.*—Several test series were performed and from the final series, the results with and without the side air bag system are presented.

**Figure 9. Bag deployment and influence on a dummy kinematics.**

Chest acceleration traces both with and without a side air bag can be seen in figures 10, 11 and 12 below.

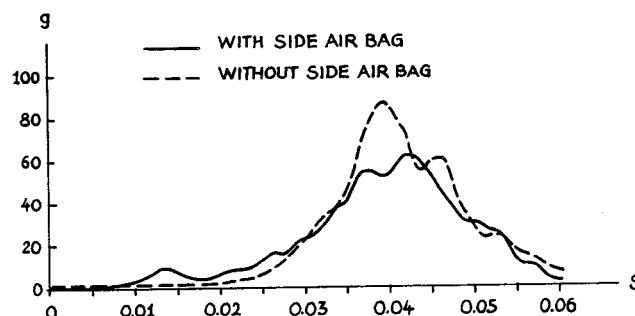


**Figure 10. Lower spine acceleration.**

Zero in the diagram time scales is at gasgenerator triggering, 15 ms before the nominal contact between the door and the dummy.

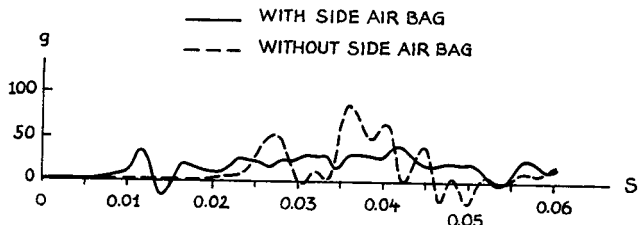


Figure 11. Upper rib acceleration.

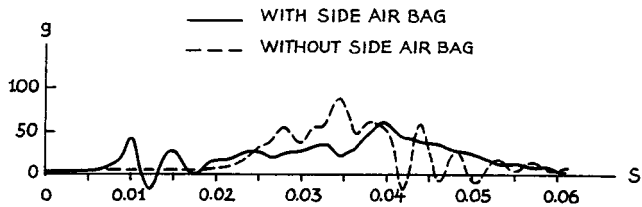


Figure 12. Lower rib acceleration.

In the lower spine diagram the influence of the air bag system can be seen as the bag accelerates the chest with approximately 5–10 G before there is contact between the door and the dummy. The severity of the impact when the door hits the chest is then reduced significantly.

In figure 11 and 12 the influence of the air bag system is seen on the rib accelerations. As for the lower spine the ribs are accelerated earlier and the maximum level is lowered when an air bag is used.

From high speed film analysis the head ejection can be studied. With the deployed bag the body movement is better controlled and retained in the compartment. The head ejection is also reduced which is shown in figure 13.

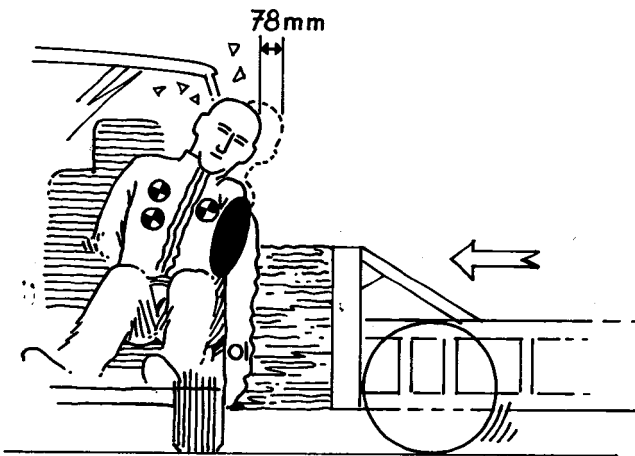


Figure 13. Head ejection.

In this final series of two tests, each test was done both with and without an air bag system. The injury criteria with equivalent systems shows good correlation and an average value is therefore calculated.

An improvement is also seen in the pelvis acceleration despite the fact that the bag is small and is not intended for a direct protection of the pelvis. An explanation is probably that when the bag starts to accelerate the chest, the pelvis also starts to move and the severity of the impact between the door and the pelvis is reduced.

*Mathematical simulation validation.*—The good correlation between sled test and simulations is shown in figure 15.

TEST No	SET UP	CHEST ACCELERATION				PELVIS ACC (g)	HEAD EJECTION (mm)
		LOWER SPINE (g)	UPPER RIB (g)	LOWER RIB (g)	TTI (g)		
9166	WITH SIDE AIR BAG	62.6	43.2	61.4	62.0	87.0	143
9172	—  —	65.8	40.9	68.6	67.1	102.0	127
AVERAGE	WITH SIDE AIR BAG	64.2	42.0	65.0	64.5	94.5	135
9170	WITHOUT SIDE AIR BAG	87.7	79.5	92.4	90.0	114.2	221
9171	—  —	86.2	91.5	88.5	87.4	123.6	208
AVERAGE	WITHOUT SIDE AIR BAG	87.0	85.5	90.4	88.7	118.9	214
IMPROVEMENT OF RESULTS		26%	51%	28%	27%	21%	79 mm

Figure 14. Summary of crash test results.

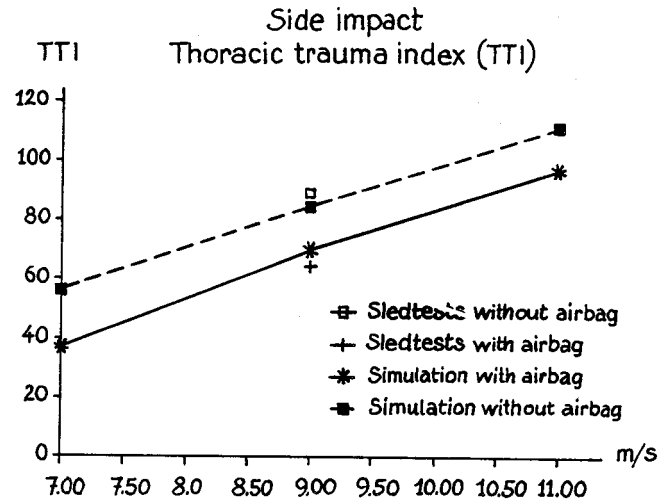


Figure 15. Simulation model validation.

The theoretical model of the air bag system shows a slightly less improvement than what has been measured in the sled tests. This could be explained by the fact that the model does not take any 3D effects into account.

### Sensor systems

Tests with the sensor system were made to evaluate the triggering performance and to analyse the “No fire” and “All fire” level.

*Test conditions.*—The tests with the sensor system were conducted in two basic situations:

- Pole impact against a fixed door.
- Side impact test in complete vehicle with moving barrier.

The pole impact tests were made with the door fixed to the ground, which was impacted by a rigid tube attached to a pendulum.

The simulated pole was designed to have approximately the same weight as a door ( $\approx 35$  kg). The impact velocity was decided after analysis of how fast a door could be opened. The impact velocity was then set at the maximum level 3 m/s.

This test was performed to study the resistance to unwanted sensor triggering in minor impact situations such as parking area accidents, door opening damages, etc. In these types of accident the door might be deformed but the sensor is not allowed to trigger.

Impacts were made at different places along the door and each impact place was tested once.

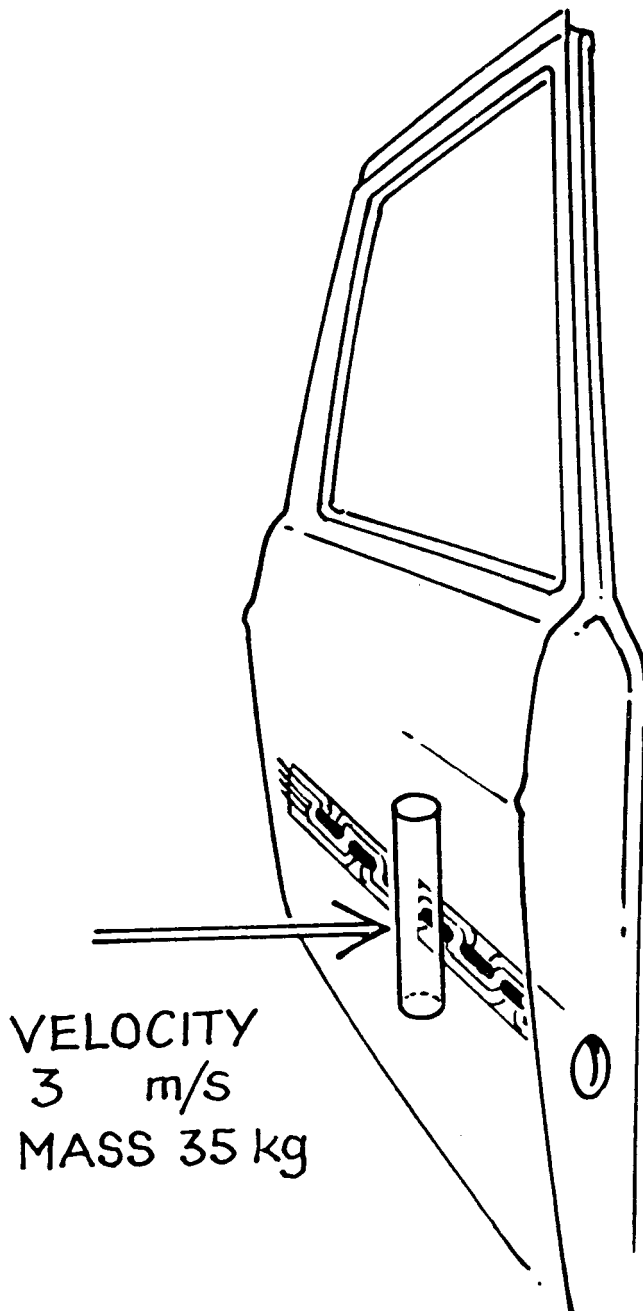


Figure 16. Pole impact.

The sensor system was also installed in a complete vehicle which was crashed in side impact with a moving barrier. Due to convenience and availability the crash was made according to the proposed European test standard with CCMC barrier and perpendicular impact configuration. This test was made to verify the triggering time in a crash where the side air bag must deploy.

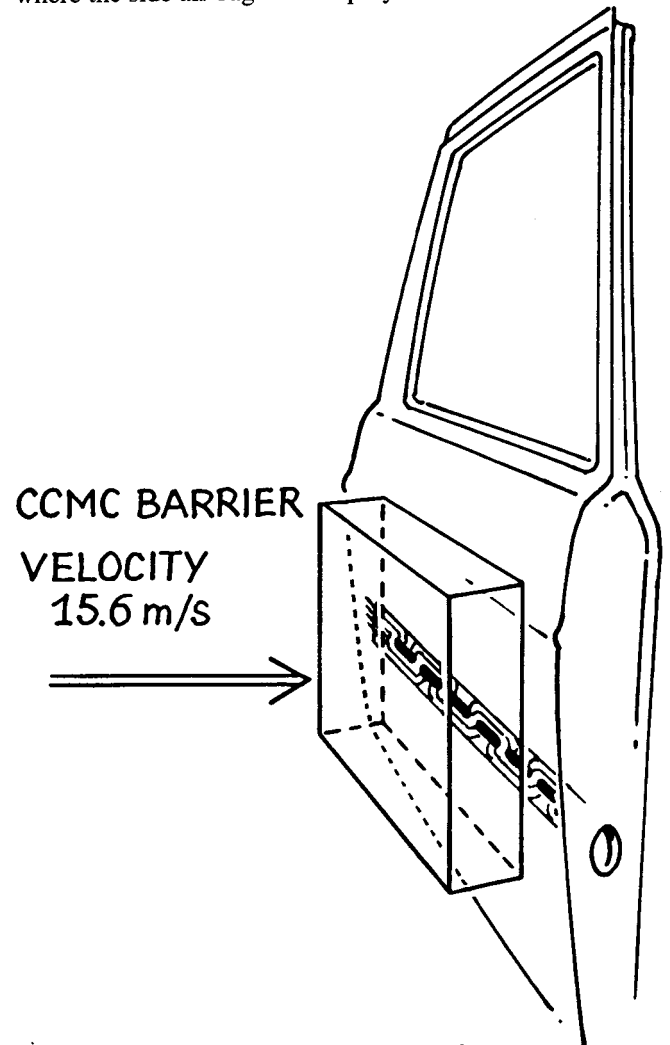


Figure 17. Side impact with a moving barrier.

*Test results.*—The sensor system has fulfilled the requirements in all crash situations. There was no triggering during pole impact. In the worst condition only one segment closed, which is insufficient for system triggering. The system will only trigger with two separate segment closures.

In the complete vehicle side impact crash the sensor triggered according to the requirement at 2–4 ms.

## Conclusion

It is possible to use air bag technology for side impact protection:

- With a deflection and force sensitive membrane switch the situations, where an air bag is needed, can be detected.

- A bag with a volume of 8 Litre can be filled quickly enough to cushion the occupant in a side impact.

A side air bag system can reduce the injury criteria by 20–30%:

- The chest acceleration levels are lowered for both ribs and spine, giving a reduction of TTI of approximately 27%.
- The head ejection is reduced by approximately 80 mm.
- The TTI value reduction is independent of door impact velocity between 7 and 11 m/s.

## References

(1) H. Norin, A. Nilsson-Ehle, C. Gustafsson. "Volvo Traffic Accident Research Systems as a tool for side impact

protection and development." IXth ESV CONFERENCE in Kyoto November 1982.

(2) DOT/NHTSA, CFR 49 Part 571. Docket No 88–06; Notice 1, NPRM FMVSS 214 amendment side impact protection. January 1988.

(3) DOT/NHTSA, CFR 49 Part 571. Docket No 88–06, Notice 3, ANPRM FMVSS 214 amendment side impact protection—passenger cars. August 1988.

(4) H. Mellander, J. Ivarsson, J. Korner. "Side impact protection system—a description of the technical solutions and the statistical and experimental tools." XIIth ESV CONFERENCE in Göteborg May 1989.

(5) C.Y. Warner, C.E. Strother, M.B. James, D.E. Struble, T.P. Egbert. "Crash protection in nearside impact—advantages of a supplemental inflatable restraint." SAE CONFERENCE in Detroit 1989.

## Study on Side Impact Test Methods

Analysis by Component Tests and Simulation

**M. Sakurai, T. Harigae, H. Ohmae,**  
Japan Automobile Research Institute, Inc.  
(JARI)

**Y. Nakamura, K. Watanabe**  
Japan Automobile Manufacturers Association,  
Inc. (JAMA)

### Abstract

In order to contribute to the worldwide discussions aimed at an improvement of the existing side impact test method, JARI and JAMA are engaged in a research project designed to provide a more realistic and effective test method in view of international harmonization.

The results of the full-scale tests by various research groups have shown that at least three problems exist: One, only a small amount of information on the vehicle characteristics can be obtained from full-scale tests. Two, it is difficult to relate the results of full-scale tests to the modification of vehicle designs. Three, it is even more difficult to apply the results of full-scale tests to vehicle design in progress.

To deal with these problems, JARI and JAMA have attempted to determine factors influencing the impact forces on vehicle occupants in a lateral collision, and have investigated the possibilities of a method combining component test procedures with a mass-spring simulation model. In this paper, factors influencing the severity of impact on the occupant were investigated by combining a component test with a simulation technique, and the results obtained were compared with those of a full-scale test, using structurally modified and padding-added vehicles.

It was found possible, by combining the component test and the simulation technique, to make a consistent predic-

tion of the influences of vehicle specification differences, to determine in detail the side impact behavior occurring in a full-scale test, and to use the calculated results for an improvement of vehicle design.

In addition, an attempt was made to evaluate the feasibility of the CCMC-proposed composite test procedure (CTP) as an alternative to the full-scale test. The results indicated that there is a more or less satisfactory correlation between the CTP and a full-scale test, and suggested that the CTP could be substituted for the full-scale test if the remaining problems found are to be solved.

### Introduction

The study on occupant protection in lateral collisions is a matter of worldwide importance nowadays. So far, full-scale tests (1, 2, 3, 4)\* and component tests (5, 6, 7, 8, 9, 10) have been proposed and studied in the United States and Europe.

Accordingly, in the interest of international harmonization, JARI and JAMA are carrying out a joint investigation of side impact procedures, to participate in the worldwide discussion for the development of a realistic and effective side impact test. As part of this investigation, we have already reported on the development of a new MDB (Moving Deformable Barrier) (11), a dummy evaluation test (12, 13, 14), and a full-scale test (15, 16, 17) at various international conferences.

Full-scale tests can provide only a small amount of information on vehicle characteristics, and that it is difficult to reflect the results directly on vehicle designs and to apply the results for modification of vehicle design underway.

We therefore studied a simulation technique combining a

\*Numbers in parentheses designate references at end of paper.

component test and a mass-spring simulation model and compared the results of this combined test with those of full-scale tests, attempting to discern the factors influencing the impact on occupants in lateral collisions and to develop a side impact test capable of analyzing the side impact behavior in a full-scale test and thus capable of modifying vehicle designs.

In addition, a CCMC-proposed composite test procedure (CTP) (18, 19) was examined, there is a view that the CTP has many advantages, including a satisfactory repeatability, an effective factor analysis, and a greater capability toward harmonization. This view also claims that, since the CTP could not only solve the aforementioned problems inherent in full-scale tests but also give a large amount of information on vehicle characteristics and side impact behavior, the CTP offers a possibility of a better clarification of vehicle performance for occupant protection.

To contribute to this worldwide discussion on CTP feasibility, this paper summarizes the results of our study combining component tests and simulation techniques, and also introduces the results obtained from our CTP tests performed in accordance with the proposed CTP outlines.

## Factors Influencing Occupant Impact Severity

To determine factors influencing the severity of a side impact on occupants, it is necessary to clarify the process in which the impact on the occupant is affected by the particular condition of a lateral collision.

Figure 1 outlines the time history of velocities and displacements of, the center of gravity of the striking vehicle, the struck vehicle, that of the struck door, and the occupant. Upon collision, the striking vehicle is gradually decelerated, but the struck vehicle is gradually accelerated. The struck door in particular is accelerated rapidly, resulting in an intrusion velocity equal to the differential between the velocity of the door and that of the center of gravity of the struck vehicle. The occupant remains in the same seating position until struck by the intruding interior surface of the struck door, and is then displaced from that position by further intrusion of the door surface. Consequently, the occupant receives an impact from the intruding door corresponding to the intrusion velocity of the door. The magnitude of impact is greatly influenced by the stiffness of the door.

When coming into collision with the occupant, the interior surface of the door has a specific velocity-time history including many factors such as the impacting velocity, the stiffness of vehicle side structure, and the vehicle weights. The occupant's response and point of contact with the intruding door are determined by the interior surface deformation mode and location relative to the occupant, and it is considered that the magnitude of the impact on the occupant varies with the stiffness of the interior surface in contact with the occupant.

Therefore, the main factors influencing the magnitude of

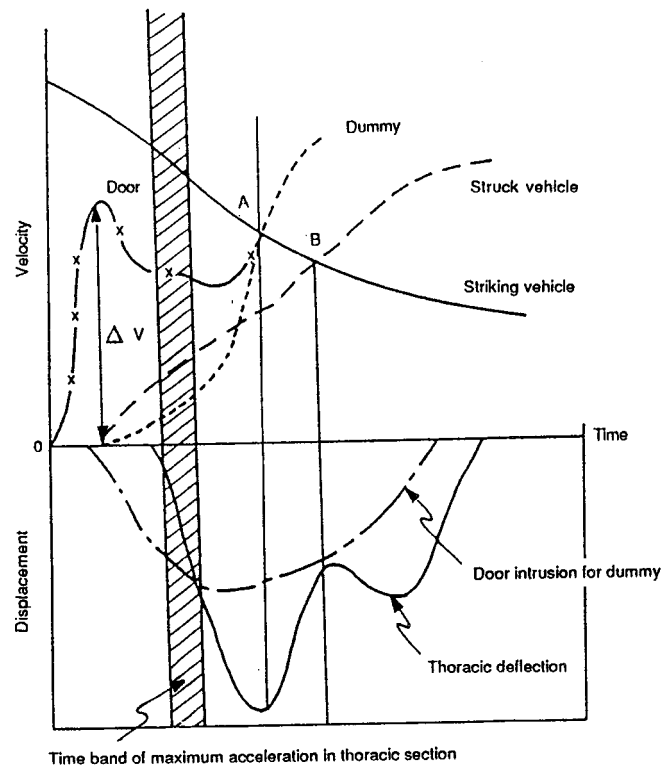


Figure 1. Summary of velocity-time history during side-impact.

impact on the occupant, from the standpoint of the struck vehicle, are as follows:

1. Velocity-time history of door intrusion.
2. Stiffness of door interior structure during intrusion.
3. Occupant's location, including the clearance between the occupant and the interior surface of the door.
4. Deformation mode of the door interior.

These factors must be fully taken into consideration in a study combining a component test with a simulation technique.

## Component Test

The component test carried out by JARI/JAMA focused on the stiffnesses of the vehicle side structure (exterior stiffness) and of the door interior structure, which are considered to be particularly large factors contributing to the intrusion velocity and interior stiffness. Specifically, attempts were made to determine how a modification of the side structure and the addition of pads inside the vehicle would affect the exterior stiffness and the door interior energy absorption characteristics of the test vehicle.

This JARI/JAMA-component test was composed of two parts: An exterior loading test designed to determine the strength of the vehicle side structure in terms of exterior stiffness, and an interior impact test aimed at determining interior characteristics. The test vehicles were unmodified models taken from the market and modified models with an additional side structure and padding.

## Test Condition

### Exterior loading test

The test conditions used in the exterior loading test are summarized in figure 2. Using the same MDB face as that used in full-scale tests, a static load with a loading velocity of 100 mm/min was applied on the side of a test vehicle fixed with wheel hubs, hitching hooks, and lower arms.

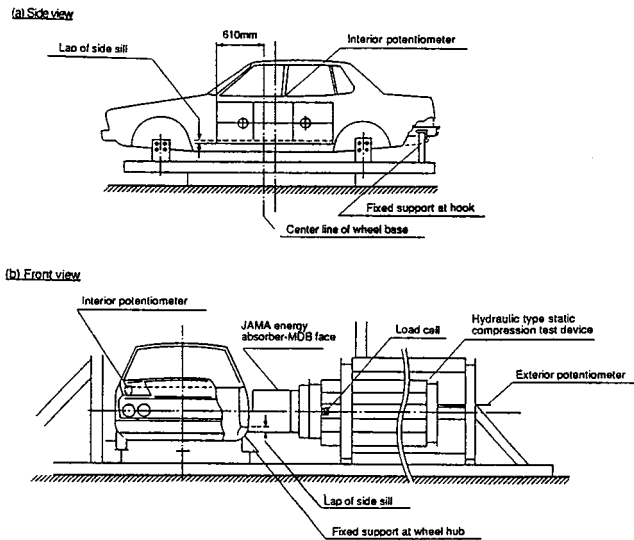


Figure 2. Summary drawing of exterior loading test layout.

The position of the MDB face against the test vehicle was identical to that used in the previous JARI-JAMA full scale tests based on actual accident data in Japan on lateral collisions, and thus the results of this exterior loading test were comparable with those of full-scale tests. Specifically, the MDB face was positioned in such a manner that a side edge of the MDB face was 610 mm in front of the wheelbase center of the test vehicle in the longitudinal direction and

that the lower edge of the MDB face overlapped the side sill by 35 mm in the vertical direction.

A JAMA MDB face (11) was employed, which has F/D characteristics and a shape (figure 3) virtually identical to those of the EEVC MDB face (20, 21) and is composed of polyethylene foams and rigid polyurethane foams.

The measurement points were set as follows:

(a) Load Measurement. Since the total load on the test vehicle must be measured, load cells were placed on the two hydraulic cylinders of the loading test device.

(b) Displacement Measurement. The loading device displacement (or loading device stroke), which includes the deformation of the vehicle exterior sheet metal and the MDB face deformation, were measured. Further, the amount of interior door intrusion in the thoracic area of the dummy at a full-scale test seating position was measured.

### Interior impact test

Figure 4 gives a summary of the interior impact test carried out to determine the energy absorbing characteristics of the door interior. After the completion of the exterior loading test, the vehicle was fixed with wheel hubs, and the door interior was struck from inside the vehicle by an impactor fitted with an impact face, while the impacted section of the door interior was supported from the outside. The exterior support was done by one block of MDB face in the same position and load with those in the exterior loading test of that vehicle. The vehicle exterior condition was not changed when the door was struck from inside by the impactor.

Figure 5 shows the shape of the impact face (22) and the location of the impact point. The impactor weighed 26 kg, including a built-in accelerometer. The impact point was set at the thoracic area of the dummy at a seating position as

Figure 3. Shape and F/D characteristic of JAMA MDB face.

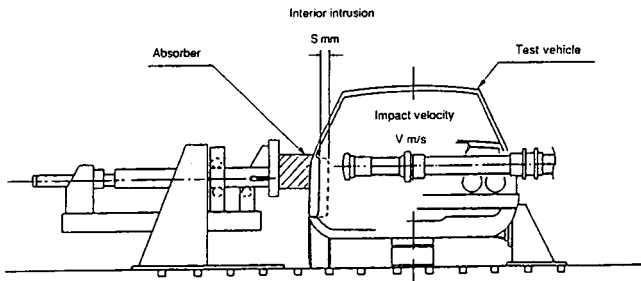
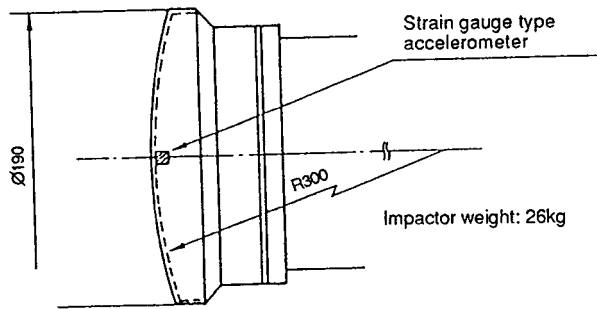
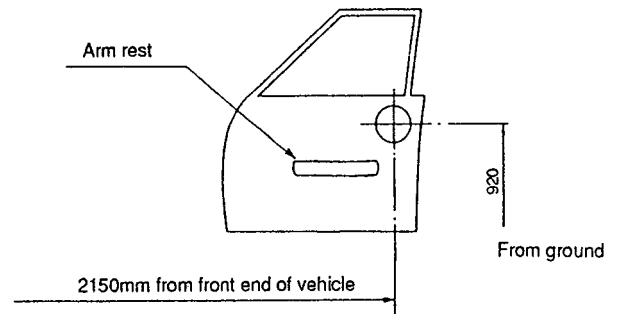


Figure 4. Summary drawing of interior impact test layout.

(a) Front shape of impactor



(b) Impact position of door



Unit: mm

Figure 5. Front shape of impactor and impact position.

Table 1. All test vehicles.

	Baseline vehicle (N)	Structurally modified vehicle (S-1)	Structurally modified vehicle (S-2)	Padding added vehicle (P-1)	Padding added vehicle (P-2)
Summary drawing of test vehicle					
Modification	Unmodified (four-door sedan)	Structurally modified exterior with 1.6mm steel plate	Structurally modified exterior with 3.2mm steel plate	Padding added interior (stiffness characteristics 2.5kg/cm <sup>2</sup> )	Padding added interior (stiffness characteristics 4.0kg/cm <sup>2</sup> )

vehicles are Japanese compact 4-door sedans. The unmodified baseline vehicle (N) was taken from the market, and the modified vehicles were two structurally modified vehicles (S-1 and S-2) and two padded vehicles (P-1 and P-2). Accordingly, there were a total of five test vehicles.

Details of the vehicle modifications are shown in figure 6. The side external sheet metals of the structurally modified vehicles were covered with a steel plate, those of the S-1 by a 1.6 mm thick steel plate and those of the S-2 by a 3.2 mm

used in a full-scale test, and the acceleration and displacement were measured by the following devices:

(a) Measurement of Acceleration. The acceleration of the impactor during the interior impact test was measured by an accelerometer fitted inside the impactor.

(b) Measurement of Displacement. The amount of interior deformation caused by the impactor was measured by a potentiometer placed on the impactor.

### Test vehicles

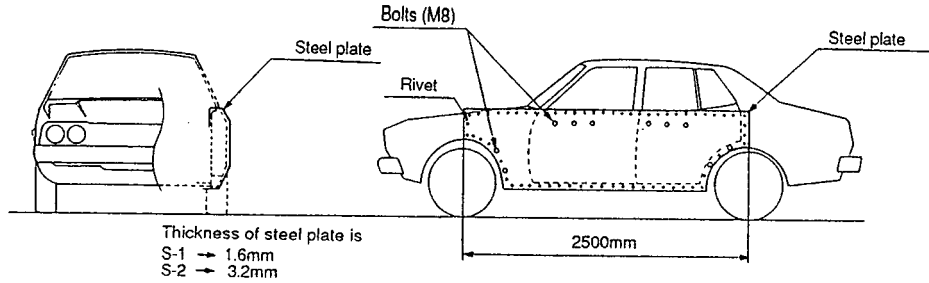
The test vehicles used are listed in table 1. All of the

thick steel plate. The door interiors of the padded vehicles were adhered with pads, those of the P-1 by a 2.5 kg/cm<sup>2</sup> padding and those of the P-2 by a 4.0 kg/cm<sup>2</sup> padding, in terms of compressive stress.

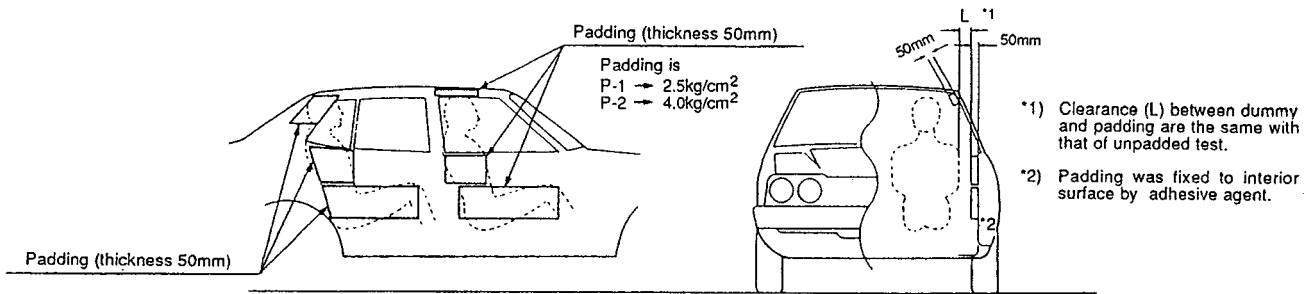
### Test results

Figure 7 shows the force-deflection characteristics of the baseline and modified vehicles obtained from each test. Figure (a) indicates the force-deflection characteristics with

(a) Structurally modified vehicle without padding  
(Structurally modified vehicle (S-1), (S-2))



(b) Padding added vehicle without structural modification  
(Padding added vehicle (P-1), (P-2))



**Figure 6. Modification of test vehicle.**

exterior deflection measured at a loading test device. Figure (b) shows the force-intrusion characteristics for the same load as for figure (a), but against interior intrusion.

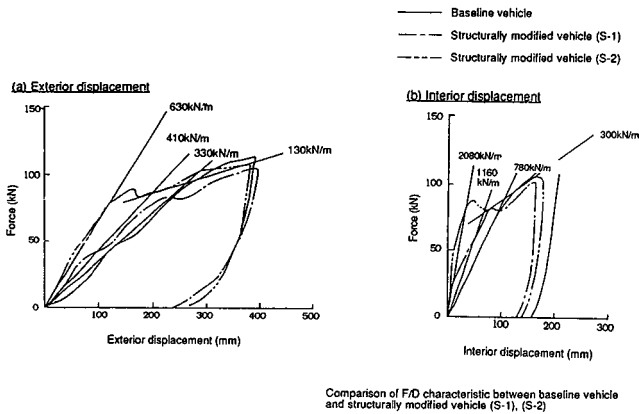


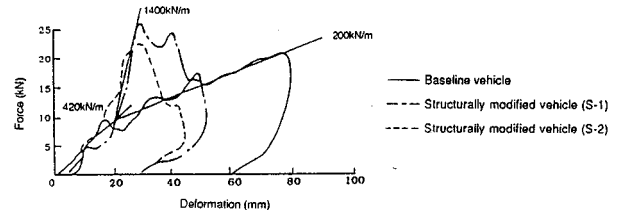
**Figure 7. Results of exterior loading test.**

The results showed that, within the indicated range of deformation, all vehicles recorded a two-stage slope as a side stiffness characteristic. Compared to the baseline vehicles, the structurally modified vehicles showed a larger spring constant in the first stage, thus indicating that the load was larger at an early stage of the deformation than at the later stages. With regard to the second-stage spring constant, however, there was no difference between the baseline and structurally modified vehicles.

The door interior stiffness test results for the baseline, structurally modified, and padded vehicles are compared in figure 8. The load values were determined on the basis of the

impactor weight and the acceleration data obtained by the accelerometer fitted inside the impactor.

(a) Comparison of F/D characteristic between baseline vehicle and structurally modified vehicles (S-1)&(S-2)



(b) Comparison of F/D characteristic between baseline vehicle and padding added vehicles (P-1)&(P-2)

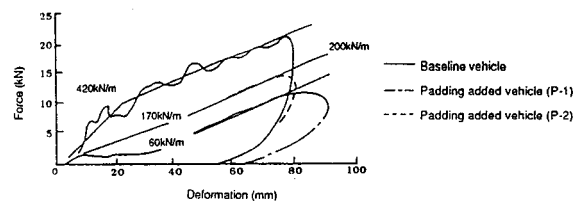


**Figure 8. Results of interior impact test.**

All vehicles showed an almost total loss of the hollow space inside the door due to a deformation of the exterior sheet metal. Under this condition, in the baseline vehicles, the force-deflection characteristics from inside out began to change when the deformation of door interior panel reached 20 mm, and the characteristics weakened as the deformation is increased. The padded vehicles showed a low level of stiffness as a whole. The structurally modified vehicles showed a sharp rise in the slope of the force-deflection characteristics after the deformation had reached 20 mm, and it was considered that this sharp rise occurred when the

deformation of the door interior panel reached the exterior sheet metal.

Accordingly, it was found that the deformation of the vehicle exterior sheet metal begin to influence the deformation of the door from the inside at its early stage, and that the interior stiffness is markedly increased by a strengthening of the exterior sheet metal. From these results, it was confirmed that, to understand the relationship between the interior stiffness of the door and the impact on the occupant, the conditions of the collision between the exterior sheet metal of the struck vehicle and the frontal structure (MDB face) of the striking vehicle must be reproduced.

## Simulation

Input data for a mass-spring model of the vehicle in the simulation was obtained from the exterior loading test and the interior impact test. The results of the simulation test were compared with the results of a full-scale test.

## Mass-spring model

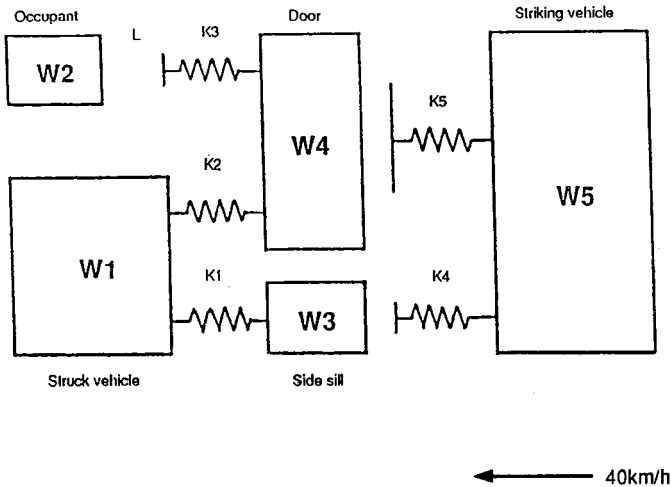


Figure 9. Mass-spring model.

The mass-spring model employed is shown in figure 9. The striking vehicle and the occupant of the struck vehicle are each composed of a single mass. On the other hand, the struck vehicle consists of three masses: a door, a side sill, and the remaining mass. Two spring systems were provided in each of the striking and struck vehicles, one corresponding to door movement, and the other corresponding to the side sill. (The door and side sill in this model do not exactly correspond to those of an actual vehicle.) The door interior was also furnished with a spring corresponding to the occupant-door system, with the clearance  $L$  to the occupant. The weight of the masses and the stiffnesses of the springs used in the simulation of a baseline vehicle are shown in table II and figure 10.

## Calculated results

The calculated results for the baseline vehicle, as shown in figure 11, suggest that the simulation using the mass-

Table II. Each weight value.

		Standard value
Struck vehicle weight	(W1)	975kg
Occupant weight (upper body)	(W2)	34kg
Side sill weight	(W3)	10kg
Door weight	(W4)	15kg
Striking vehicle weight	(W5)	1100kg

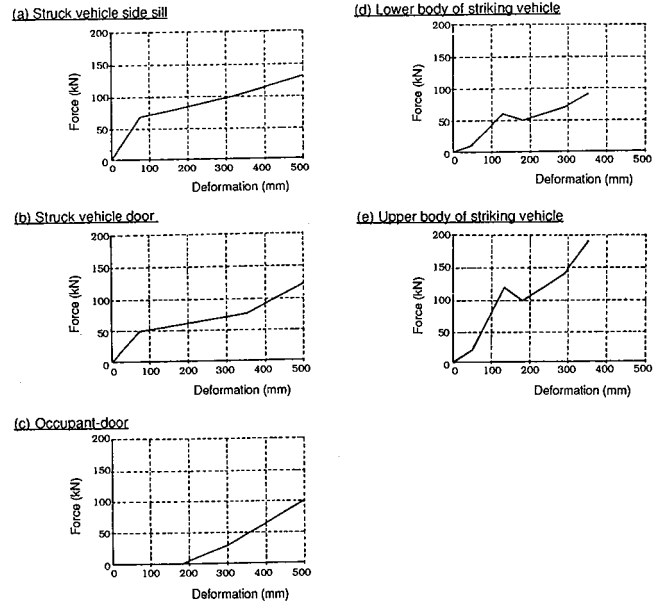


Figure 10. Input data of spring stiffness.

spring model is by and large capable of reproducing the side impact behavior. Figure 12 provides a comparison of the calculated results and the test results, and it is found from the figure that, although the absolute values are slightly

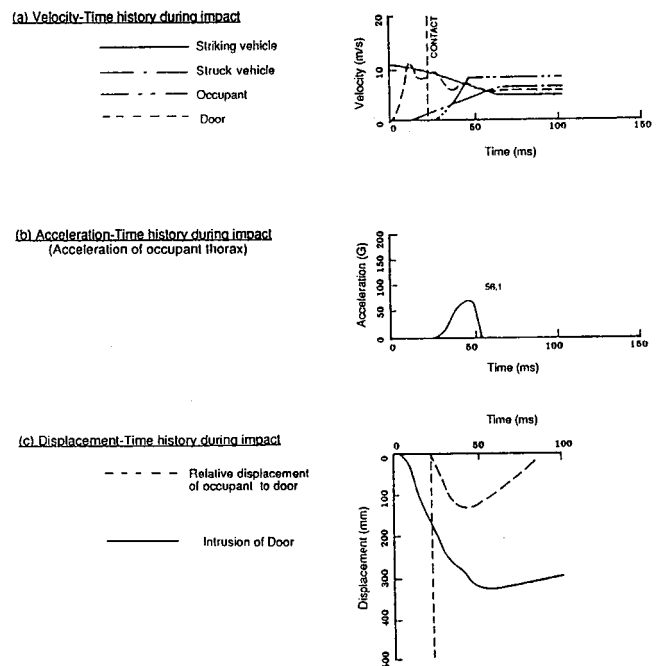


Figure 11. Calculation result for baseline vehicle.

different, the calculated results tend to conform with test results, and thus it was possible to predict the influence and effects of vehicle structural modification and padding by combining a component test with a simulation technique.

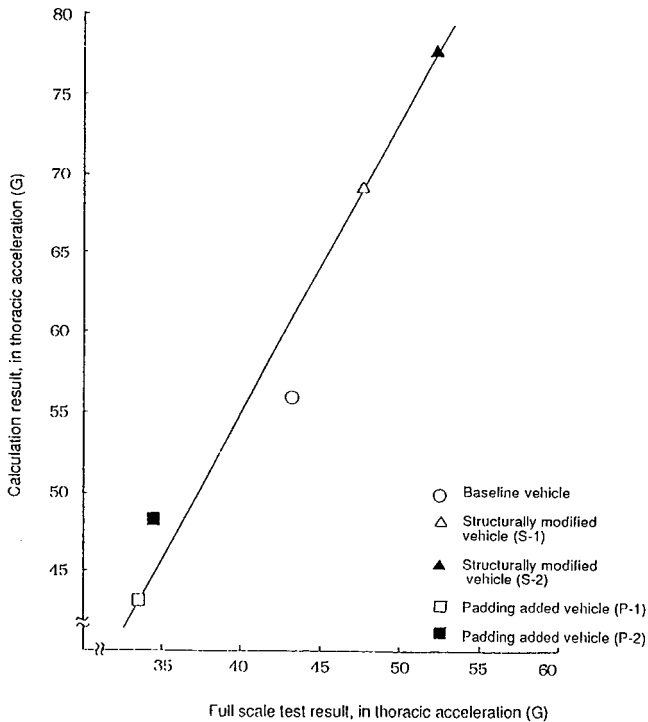


Figure 12. Comparison of results of simulation and full scale test at dummy thoracic acceleration.

## CTP Trial

A trial test was conducted to examine the possibility of using the CCMC-proposed CTP (18, 19) as an alternative to a full-scale test. Also, a trial calculation by a simulation technique was performed, using the Step I, II and III test results as input data for the model constants.

## Test condition

Comparisons of the CCMC-proposed test procedure and the test procedure used in this study are shown in table III. Although the procedures are virtually identical, the loading conditions (i.e., the values of the load and stroke serving as the criteria for determining the completion of each test step) of the two procedures differed due to the different capacities of the equipment used.

Further, the two test procedures differed in that, although the CCMC-proposed procedure required the maintenance of the exterior load during the transition to Step II, in the test procedure used in this test, this load was partially released in the transitional period. Another difference was the loading sequence being reversed between the thoracic and pelvic sections. The test conditions in this test conformed with those of an NHTSA full-scale test (1, 2).

## Test devices

Figure 13 gives the summaries of the devices used in this

Table III. Comparison of test method.

	CCMC	JARI/JAMA
<b>Step I</b> 	<ul style="list-style-type: none"> <li>Outside of test vehicle's structure is loaded until either interior door panel contacts driver's seat, or EDLD stroke is 200mm.</li> <li>Loading speed 4mm/s.</li> <li>EDLD force is held constant during Step I.</li> </ul>	<ul style="list-style-type: none"> <li>Outside of test vehicle's structure is loaded until interior door panel contacts driver's seat, being the aim of this test, hence until EDLD stroke is 120mm or intrusion at B-pillar is 60mm.</li> <li>Loading speed 3.3mm/s.</li> <li>EDLD is stopped at the end of Step I.</li> </ul>
<b>Step II</b> 	<ul style="list-style-type: none"> <li>Load first pelvic section with ILD until either ILD stroke is approx. 120mm or force is approx. 40kN.</li> <li>Unload pelvic section so that rebound characteristic can be determined.</li> <li>Load then thoracic section with ILD until either ILD stroke is approx. 120mm or force is approx. 40kN.</li> <li>Unload thoracic section so that rebound characteristic can be determined.</li> <li>Loading speed 4mm/s.</li> </ul>	<ul style="list-style-type: none"> <li>Load first thoracic section with ILD until either ILD stroke is approx. 120mm or force is approx. 20kN (being the capacity of ILD.)</li> <li>Load then pelvic section with ILD until either the ILD stroke is approx. 120mm or force is approx. 20kN.</li> <li>Loading speed 2mm/s.</li> </ul>
<b>Step III</b> 	<ul style="list-style-type: none"> <li>With pelvic (and thoracic, if separate loaded) section of interior door panel in contact with ILD force 100N.</li> <li>Load EDLD on the exterior until stroke of EDLD reaches 600mm or force of EDLD reached 200kN.</li> <li>Unload EDLD so that rebound characteristic can be determined.</li> <li>Loading speed 4mm/s.</li> </ul>	<ul style="list-style-type: none"> <li>Without pelvic and thoracic section in contact, EDLD operation continues until the limit of EDLD capacity. (160kN or 500mm)</li> <li>Loading speed 3.3mm/s.</li> </ul>

test. The loading test device A, used in Steps I and III, had a maximum loading capacity of 16 tons and an effective stroke of 500 mm. The front of the exterior loading device was fitted with an NHTSA-proposed aluminum honeycomb MDB face. The loading test device B, used in Step II, had a maximum loading capacity of 2 tons and an effective stroke of 150 mm.

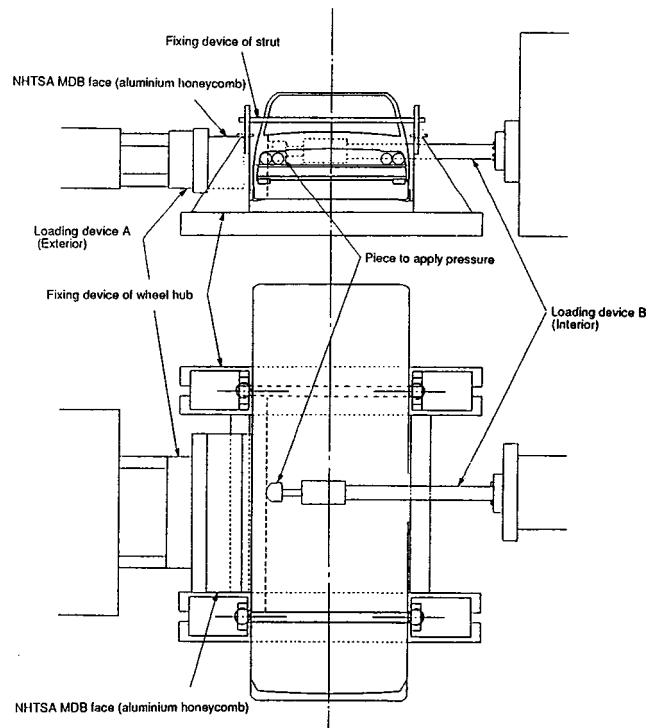


Figure 13. Summary drawing of test device.

Japanese one-ton class compact sedans were employed as test vehicles, comparable with the NHTSA full-scale test vehicles, but these sedans differed from those used in the aforementioned component test. The loading points of the loading test device in Steps I and III conformed with those used in the NHTSA method.

Figure 14 shows the shape and location of the interior loading device used in Step II. This device complies with the CCMC requirement in shape and aluminum material composition. Since the interior loading device used in this study was not capable of applying a load to both the thoracic and pelvic sections simultaneously, the same amount of load was first given to the thoracic section and then to the pelvic section. The loading was aimed at the dummy seating position where the seat was positioned at a point midway in the seat fore/aft adjustment travel and the seat back is placed in the manufacturer's stated nominal design position.

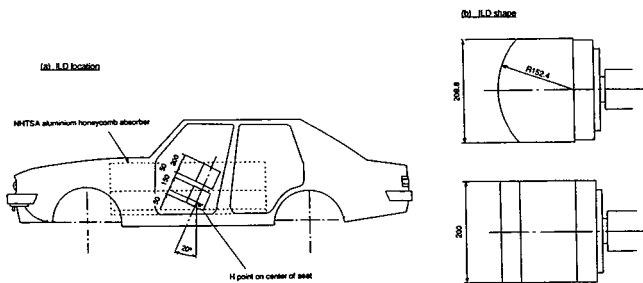


Figure 14. Shape and location of interior loading device.

## Fixing methods and measurement points

Figure 15 shows the method used to fix the test vehicle on the test device. The vehicle was supported at six points, i.e., at the wheel hubs of the four wheels and at the upper ends of the front wheel strut towers. To prevent vertical movement, the lower beam and the lower arm of the suspension of each wheel were welded together. The fixing jigs of the wheel hubs were vertically adjustable and were used to adjust the position of the vehicle against the MDB face.

Figure 16 shows the points at which the load and displacement were measured. Points 1 to 12 indicate points measured by a potentiometer and Points 13 and 14 those measured by a load cell. Point 11 inside the vehicle was not used to measure the displacement against the ground but the displacement between the right and left B-pillars. Except for the Point 12 displacement measurement and the Point 14 load measurement in Step II, all other parameters were measured throughout all steps in the test.

## Mathematical model simulation

Figure 17 shows the lumped mass model (18, 19) used in the simulation, and the weight of each mass part. This model basically complies with the CCMC, except for additional springs, dampers and some other items which are neglected due to an uncertainty in their values. Figure 18 presents the spring input data for the simulation: K1 being the MDB face

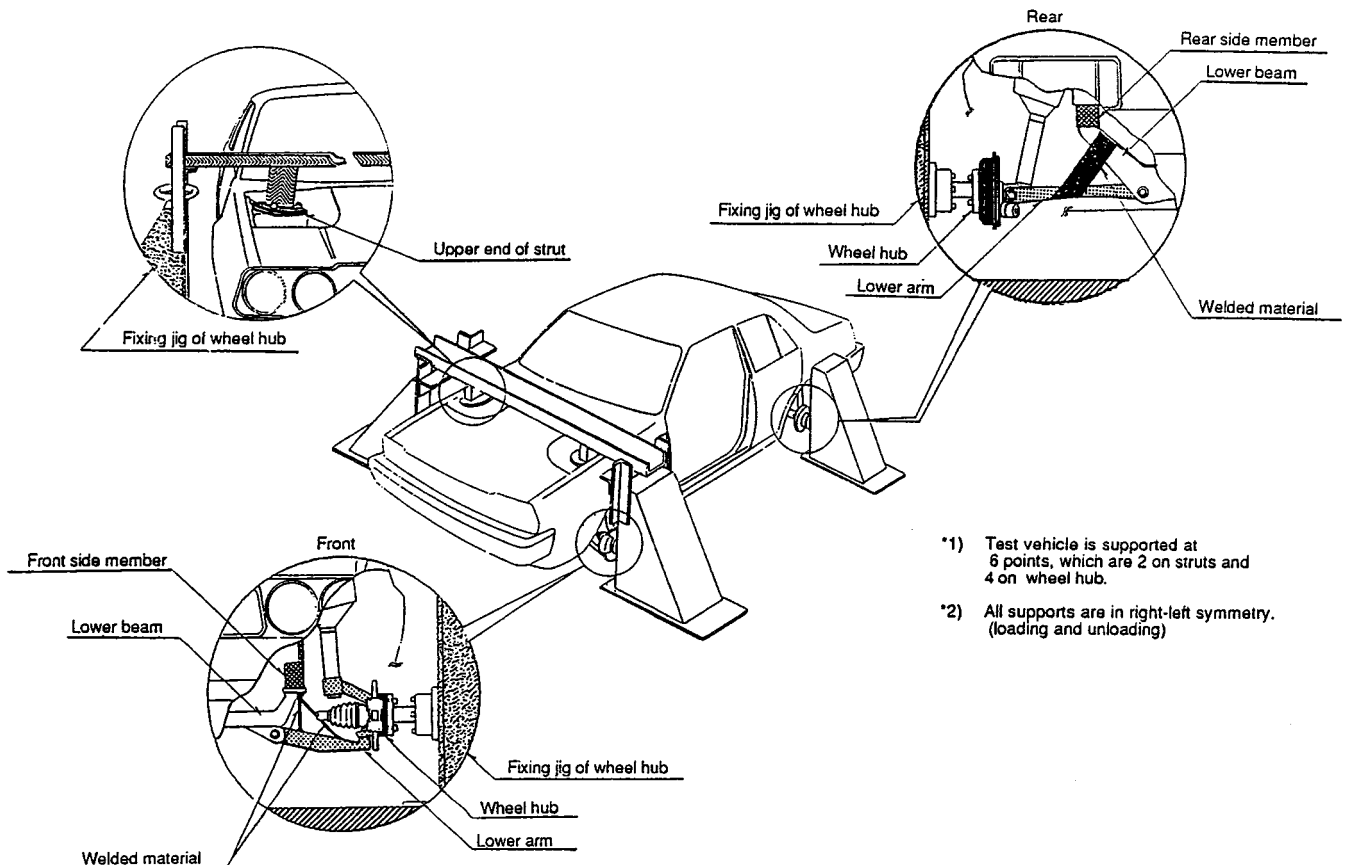
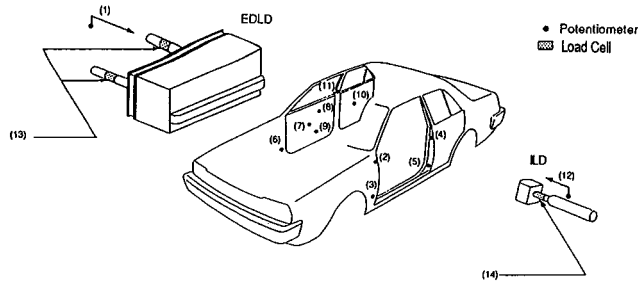


Figure 15. Condition of fixing supports of test vehicle.

(a) Locations of potentiometers and load cells

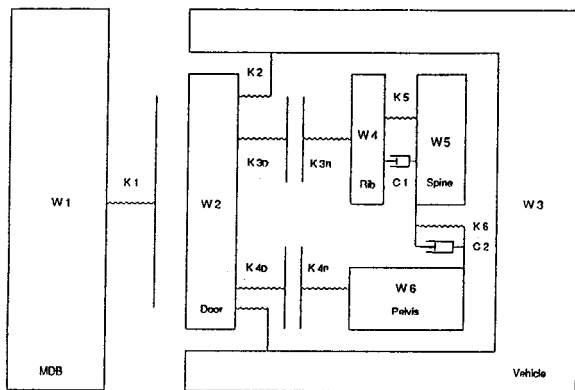


(b) Measured parameters

Measuring position	
Deformation	(1) Displacement of EDLD for ground.
	(2) Displacement of upper hinge at unloading side front door for ground.
	(3) Displacement of lower hinge at unloading side front door for ground.
	(4) Displacement of upper hinge at unloading side rear door for ground.
	(5) Displacement of lower hinge at unloading side rear door for ground.
	(6) Displacement of lower hinge at loading side front door for ground.
	(7) Displacement of center section at loading side front door for ground.
	(8) Displacement at a near point of thoracic section at loading side front door for ground.
	(9) Displacement at a near point of pelvis section at loading side front door for ground.
	(10) Displacement of center section in right rear door for ground.
	(11) Displacement of right pillar for left pillar.
	(12) Displacement of ILD for ground.
Load	(13) EDLD load
	(14) ILD load

Figure 16. Measurement of load and displacement.

(a) Lumped mass model



(b) Individual weight

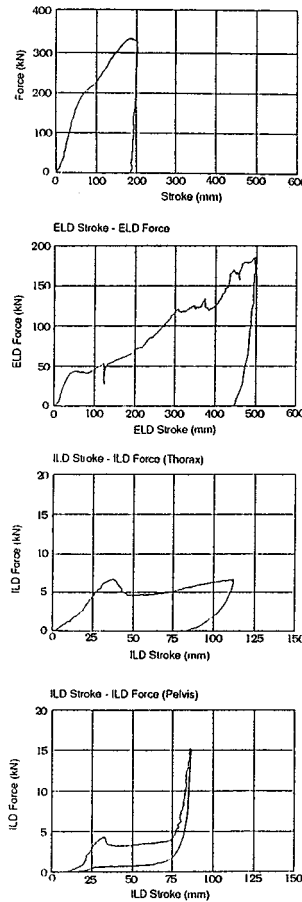
Subject	Weight (kg)
W1	1360
W2	40
W3	990
W4	6
W5	20
W6	15

Figure 17. Lumped mass model and individual weight.

input data, and K2, K3 and K4 being the input data on force-deflection characteristics obtained from the CTP test.

Figure 19 gives a comparison between the calculated results and the results of a test designed to obtain dummy input data (23), i.e., a SID dummy biofidelity drop test (13, 24) (drop height  $h = 1.0\text{m}$ ). Figures (a), (b) and (c) present

(a) Base data from test results.



(b) Input data

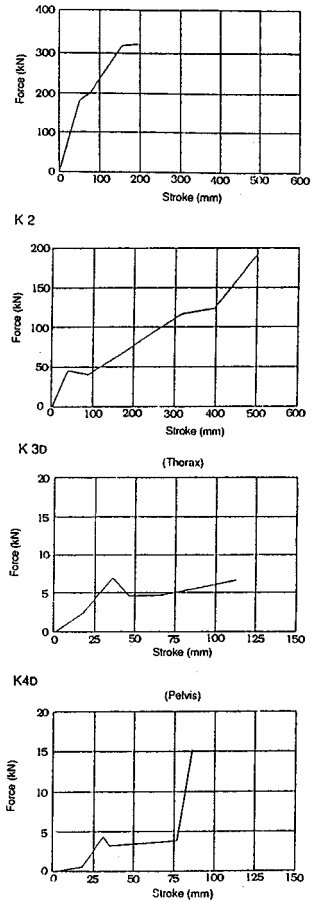
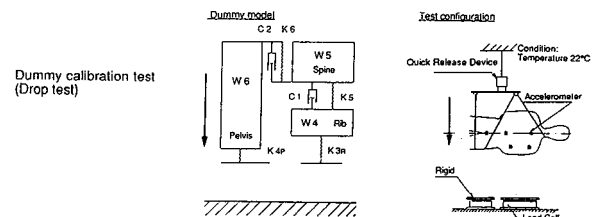
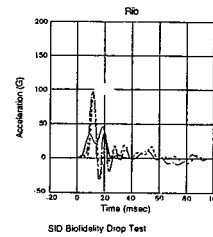


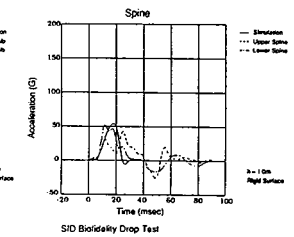
Figure 18. Base data and input data.



(a) Acceleration-Time curve Rib



(b) Acceleration-Time curve Spine



(c) Acceleration-Time curve Pelvis

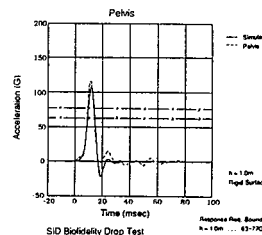


Figure 19. Comparison of results of simulation and test.

comparisons of the rib, spine and pelvis accelerations, respectively. The dummy input data was used after comparison and alignment with the calibration test results of the lumped mass model and the dummy.

### Calculated results

Figure 20 compares the calculated results and those of a full-scale test. Although the setting of the simulation model and the selection of the input data were not totally satisfactory, the calculated results and those of a full-scale test generally show a close correspondence. It would be possible to achieve an even closer correspondence by improving the simulation model and input data.

### Conclusion

Factors influencing the severity of impact on the occupant were investigated by combining a component test with a simulation technique, and the results obtained were compared with those of a full-scale test. The feasibility of the CTP was studied by a trial test. The findings made from these studies are summarized as follows:

1. It was possible to make a consistent prediction of full-scale test results by combining a component test with a mass-spring model simulation technique. Using this test-simulation method, the effects of an improvement made in the acceleration of the dummy thoracic section were reproduced, and the predicted results and actual tests results were found to be similar with respect to the influences of

differences in vehicle specifications. Accordingly, this test-simulation combination method is considered effective in analyzing collision behavior in full-scale tests and in improving vehicle designs for the protection of occupants.

2. The trial test of the CTP, which attempts to develop the concept of this test-simulation combination method as an alternative to the full-scale test, indicated a more or less satisfactory correspondence with full-scale test results. The accuracy of the CTP test could be improved by solving the following problems, so that it would be possible for the CTP to become an adequate alternative to the full-scale test.

(a) Vehicle Fixing Methods. If the test vehicle is fixed on the test device at the wheel hubs and the strut towers as in this study, it is difficult to reproduce the climbing of the MDB over the side sill of the struck vehicle and the bending of the whole struck vehicle in many lateral collisions. Accordingly, further studies are necessary to fully understand the influence of these types of collision behavior and to decide whether these more extensive deformations or only partial deformations should be reproduced by changing the method of support to obtain effective information on vehicle characteristics for occupant protection.

(b) Clarification of Differences Between Static and Dynamic Characteristics. Although interior and exterior stiffnesses can be determined by a static test, additional test data and improvements in the test method are required to include procedures to compare with dynamic character-

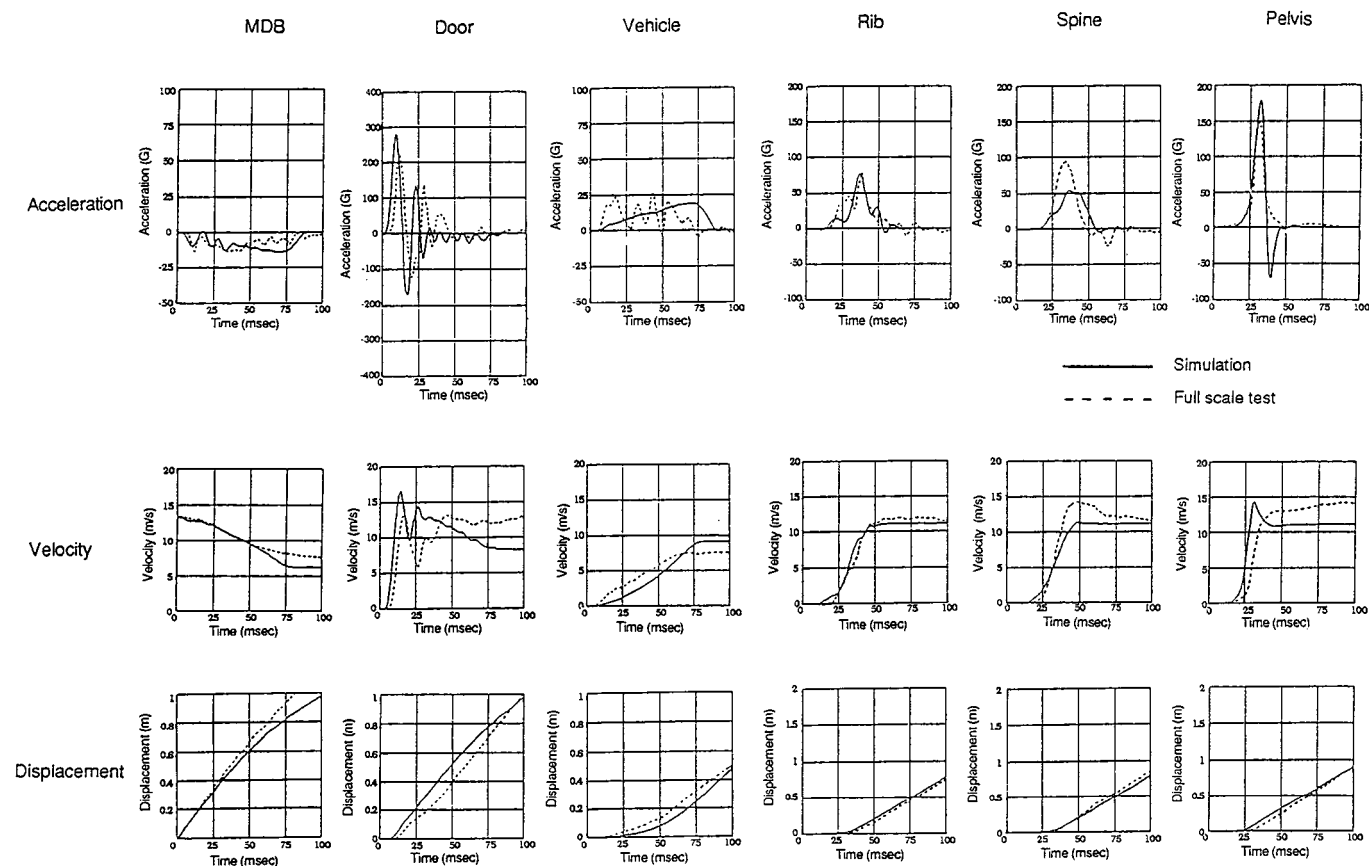


Figure 20. Comparison of the results at composite and full scale test.

istics such as one for converting static data into dynamic test data.

(c) **Methods of Determining Step I to III Transition.** It was insufficient in this study to clarify the optimal condition at which each step is to be started or ended, especially the transition from Step I to Step II involving a discontinuation of the exterior loading and the start of an interior loading. But this problem may be overcome when simulation is carried out in parallel with a series of tests to obtain effective data for such conditions.

(d) **Development of a Biofidelity Model.** Although the CTP mathematical model is currently dependent on anthropomorphic dummies, in the future it could be extended to a simulation model having a greater biofidelity than dummies, and hence should be effected in that direction. At the present stage, it is necessary to develop a mathematical model satisfying the DP9790-1 to DP9790-6 characteristics required for side impact dummies.

(e) **Setting of Measurement Points for Determining Vehicle Characteristics.** With the growing prospects of developing a test method with a high vehicle deformation behavior reproducibility and a simulation model with a high biofidelity, it will become necessary to reconsider measurement points to obtain the most useful force-deflection characteristics.

It is thought that the CTP can be used not only for evaluation purposes but also for a modification of vehicle designs. If the CTP would be established feasible, it could become more effective than the full-scale test. JARI/JAMA intend to continue their CTP studies using different models of vehicles in order to determine the effectiveness of the CTP, and to establish the CTP as a practical test method.

## References

(1) NHTSA; Federal Motor Vehicle Safety Standards; "Side Impact Protection", 49 CFR Part 571 [Docket No. 88-06, Notice 1] 1988.

(2) NHTSA; NHTSA Side Impact Testing Procedure. [Docket No. 79-04-GR-030] 1985.

(3) TRANS/SCI/WP29/GRCS/R58 (1985); Protection of the Occupants of a Passenger Car in the Event of a Lateral Collision.

(4) A. DeCoo and others; Evaluation of European and U.S.A. Draft Regulations for Side Impact Collisions, the 11th ESV International Technical Conference, (Washington, D.C.).

(5) J.R. Hackney and others; Results of the National Highway Traffic Safety Administration's Thoracic Side Impact Protection Research Program, SAE 840886.

(6) S.E. Henson; Status and Update of MVMA Component Testing, SAE 871116.

(7) C.J. Griswold; Side Impact Component Test Development, the 9th ESV International Technical Conference, 1982.

(8) C.J. Griswold; The Development and Application of Side Impact Component Test Methods, SAE 840887.

(9) T.F. MacLaughlin; Evaluation of Full Vehicle and Component Test Procedures for Improving Side Impact Crash-Survivability, SAE 830463.

(10) M.V. Monk; Sub-system and Full System Testing to Assess Side Impact Safety, SAE 830465.

(11) H. Ohmae and others; A Study on Energy Absorbing Units of MDB for Side Impact Test, the 11th ESV International Technical Conference, 1987.

(12) JAMA/JARI; Study on Side Impact Dummy by JAMA, ISO/TC22/SC12/WG5 N193, 1987.

(13) JAMA/JARI; The Biofidelity Test Results on SID and EUROSID, ISO/TC22/SC12/WG5 N213, 1988.

(14) JARI/JAMA; The Biofidelity Test Results on SID and EUROSID, IRCOBI, 1988.

(15) JAMA's Test Results and Comments on Side Impact Test Procedures, ISO/TC22/SC10/WG1 N145, 1988.

(16) JAMA/JARI; Study on Side Impact Test Method, ISO/TC22/SC10/WG1 N134.

(17) H. Ohmae and others; Analysis of the Influence of Various Side Impact Test Procedures, SAE 890378.

(18) R. Richter and others; Composite Test Procedure for Side Impact Protection, SAE 871117.

(19) ISO/TC22/SC10/WG1 DRAFT CCMC; Composite Test Procedure for Side Impact Protection, 1988.

(20) ISO/TC22/SC10/GT1, N90 (1985); Validation of the EEVC Mobile Barrier.

(21) D. Cesari and others; Validation of the EEVC Mobile Deformable Barrier for Side Impact Testing, the 10th ESV International Technical Conference, 1985.

(22) R.J. Wasko and others; Results of the Motor Vehicle Manufacturers Association Component Test Procedure Evaluation Program, the 10th ESV International Technical Conference, 1985.

(23) D.C. Viano; Evaluation of the SID Dummy and TTI Injury Criterion for Side Impact Testing, SAE 872208.

(24) ISO/TC22/SC12, DP9790-1-6; Road Vehicles—Anthropomorphic Side Impact Dummy.

# DEPTH: A Relationship Between Side Impact Thoracic Injury and Vehicle Design

Hampton C. Gabler, James R. Hackney,  
William T. Hollowell,  
National Highway Traffic Safety  
Administration,  
United States

## Abstract

In a previous NHTSA research program, the Door Effective Padding Thickness (DEPTH) was found to be highly correlated with side impact occupant protection. Using an expanded set of twenty-eight production car side impact tests and a series of modified vehicles side impact tests, this paper reexamines the question of how vehicle design influences side impact thoracic injury. The findings of this extended study confirm the conclusion of the earlier paper: Of the design variables investigated, DEPTH is the single design variable most strongly correlated with thoracic side impact injury potential.

## Introduction

The National Highway Traffic Safety Administration (NHTSA) has undertaken a research program to characterize the safety performance of the passenger car fleet in side impacts (1).<sup>\*</sup> As part of that study, twenty-eight (28) current production cars were tested in side impacts, and found to vary dramatically in their capability to provide occupant thoracic side impact protection.

In a NHTSA program using modified Volkswagen Rabbits, the influence of side impact design on thoracic injury was confirmed experimentally in a series of controlled side impact tests (2). Similar results were noted in a program conducted by MVMA in which a series of sixteen 1985 Ford LTDs, some with padding and structural modifications, were subjected to controlled side impacts (3).

The objective of this paper is to determine those vehicle design parameters which are key to thoracic side impact protection. A previous NHTSA research program, using a smaller set of crash tests, concluded that the Door Effective Padding Thickness (DEPTH) was strongly correlated with side impact occupant protection (4). This paper will revisit this conclusion using an expanded series of side impact tests, and will explore additional vehicle design parameters.

## Background

### Test procedure

Both the production car tests and the MVMA tests used the NHTSA proposed Side Impact Test Procedure to determine occupant side impact protection. The accident configuration for the NHTSA Side Impact Test Procedure is

a 90 degree impact to the occupant compartment of the target vehicle. The striking vehicle is a NHTSA Movable Deformable Barrier weighing nominally 3000 lbs and crabbed at 26 degrees. The initial velocity of the MDB is 33.5 mph. The struck vehicle is stationary. This accident configuration simulates a striking/struck velocity ratio of 30 mph/15 mph. The modified VW Rabbit test series used the basic NHTSA procedure, but selected two alternate test speeds: (1) 26/13 mph, and (2) 35/17.5 mph.

All impacts were delivered to the occupant compartment of the struck vehicle approximately 37 inches forward of the centerline of front and rear wheels. In the production car tests, the driver side of the struck vehicle was struck. In the MVMA tests, the right front passenger side of the struck vehicle was struck. The accident configuration of the production car tests is presented in figure 1.

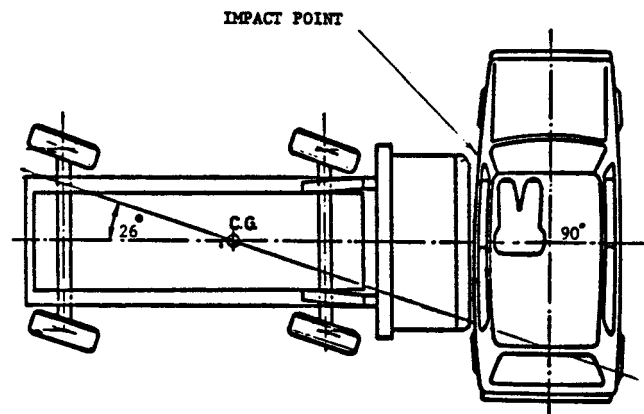


Figure 1. Side impact test configuration.

### Vehicle selection

A listing of the 28 production cars is presented in table 1. The set of production cars is composed of an earlier test sample of sixteen (16) cars from model years 1981-83, two cars from the 1985 model year, and an eight (8) car sample from model years 1987-88. Our earlier paper on the safety performance of cars in side impact was based on analysis of the first twelve crash tests presented in table 1.

To determine the influence of design on thoracic injury, NHTSA conducted a series of eight side impact tests using two door Volkswagen Rabbits as shown in table 3. Four of the tests were conducted with a velocity ratio of 26/13 mph, while the remaining four tests were conducted with a velocity ratio of 35/17.5 mph. For each speed, four vehicle configurations were considered:

### Modified VW Rabbit test matrix.

Vehicle	Striking/Struck Velocity (mph)	
	26/13	35/17.5
Baseline	X	X
Structural Mods	X	X

<sup>\*</sup>Numbers in parentheses designate references at end of paper.

Table 1. Production car tests: Side impact occupant responses (population-weighted).

Test no.	Stri/Stru Vehicle	Stri/Stru Velocity	Imp Ang	Occup Pos	Upper Rib G's		Lower Rib G's		Upper Spine G's		Lower Spine G's		Pelvis G's	Injury Name	Criterion Index (Age=0)	Probability AIS >= n		
					G's	G's	G's	G's	G's	G's	n=3	n=4				n=5		
675	MDB-to-Citation (baseline-4 DR)	30/15	90	LF	69.	77.	77.	90.	151.	TTI-86	83.5	45	12	1				
				LR	67.	111.	96.	86.	155.	TTI-86	98.5	62	21	2				
676	MDB-to-CITATION (baseline-4 DR)	30/15	90	LF	88.	86.	77.	103.	160.	TTI-86	95.5	59	19	2				
				LR	85.	120.	101.	88.	150.	TTI-86	104.0	68	26	3				
677	MDB-to-CITATION (baseline-2 DR)	30/15	90	LF	70.	72.	81.	114.	178.	TTI-86	93.0	56	17	2				
				LR	55.	72.	58.	58.	101.	TTI-86	65.0	23	5	0				
678	MDB-to-HORIZON (baseline-4 DR)	30/15	90	LF	124.	101.	79.	99.	170.	TTI-86	111.5	75	33	4				
				LR	86.	82.	56.	68.	106.	TTI-86	77.0	37	9	1				
679	MDB-to-OMNI (baseline-2 DR)	30/15	90	LF	130.	117.	104.	110.	171.	TTI-86	120.0	81	42	5				
				LR	100.	101.	74.	99.	107.	TTI-86	100.0	64	22	2				
683	MDB-to-GRANADA (baseline-2 DR)	30/15	90	LF	72.	90.	88.	115.	192.	TTI-86	102.5	66	24	3				
				LR	36.	45.	26.	42.	100.	TTI-86	43.5	10	1	0				
684	MDB-to-GRANADA (baseline-4 DR)	30/15	90	LF	95.	136.	87.	103.	165.	TTI-86	119.5	81	42	5				
				LR	37.	69.	44.	60.	162.	TTI-86	64.5	22	5	0				
702	MDB-to-CONCORD (baseline-4 DR)	30/15	90	LF	69.	58.	73.	76.	147.	TTI-86	72.5	31	7	1				
				LR	51.	53.	47.	55.	82.	TTI-86	54.0	15	2	0				
704	MDB-to-SENTRA (baseline-2 DR)	30/15	90	LF	122.	149.	109.	149.	213.	TTI-86	149.0	94	79	13				
				LR	57.	64.	75.	72.	132.	TTI-86	68.0	26	6	0				
710	MDB-to-RABBIT (baseline-2 DR)	30/15	90	LF	94.	112.	118.	119.	195.	TTI-86	115.5	78	37	4				
				LR	98.	104.	53.	79.	143.	TTI-86	91.5	54	16	2				
719	MDB-to-CIVIC (baseline-4 DR)	30/15	90	LF	63.	64.	92.	93.	138.	TTI-86	78.5	39	9	1				
				LR	81.	104.	83.	79.	148.	TTI-86	91.5	54	16	2				
744	MDB-to-Dodge 400 (Baseline)	30/15	90	LF	88.	123.	110.	114.	193.	TTI-86	118.5	80	41	5				
				LR	96.	131.	91.	93.	148.	TTI-86	112.0	75	33	4				
811	MDB-to-Civic (baseline-4 DR)	30/15	90	LF	71.	80.	113.	118.	107.	TTI-86	99.0	63	21	2				
				LR	122.	122.	103.	78.	122.	TTI-86	100.0	64	22	2				
820	MDB-to-Sentra (baseline-2 DR)	30/15	90	LF	104.	108.	148.	115.	205.	TTI-86	111.5	75	33	4				
				LR	91.	103.	74.	57.	146.	TTI-86	80.0	40	10	1				

Table 1. (continued). Production car tests: Side impact occupant responses (population-weighted).

Test no.	Str1/Stru Vehicle	Str1/Stru Velocity	Imp Ang	Occup Pos	Upper Rib G's		Lower Rib G's		Upper Spine G's	Lower Spine G's	Pelvis G's	Injury Name	Criterion Index (Age=0)	Probability AIS $\geq$ n		
					G's	G's	G's	G's						n=3	n=4	n=5
855	MDB-to-Mazada (baseline-4 DR)	30/15	90	LF	98.	97.	125.	113.	164.			TTI-86	105.5	69	27	3
				LR	128.	90.	124.	91.	183.			TTI-86	109.5	73	31	3
856	MDB-to-Sentra (baseline-2 DR)	30/15	90	LF	150.	151.	143.	112.	183.			TTI-86	131.5	88	57	7
				LR	63.	71.	60.	53.	136.			TTI-86	62.0	20	4	0
863	MDB-to-Civic (baseline-4 DR)	30/15	90	LF	79.	59.	125.	136.	147.			TTI-86	107.5	71	29	3
				LR	111.	123.	107.	71.	140.			TTI-86	97.0	61	20	2
879	MDB-to-Spectrum (baseline-2 DR)	30/15	90	LF	94.	85.	111.	73.	145.			TTI-86	83.5	45	12	1
				LR	97.	129.	70.	78.	101.			TTI-86	103.5	67	25	3
887	MDB-to-Celebrity (baseline-4 DR)	30/15	90	LF	75.	68.	69.	83.	na			TTI-86	79.0	39	9	1
				LR	110.	104.	56.	77.	99.			TTI-86	93.5	57	17	2
1145	MDB-to-Sentra - 87 (baseline-2 DR)	30/15	90	LF	91.	78.	122.	107.	169.			TTI-86	99.0	63	21	2
				LR	102.	121.	107.	80.	132.			TTI-86	100.5	64	23	2
1210	MDB-to-Tercel (baseline-4 DR)	30/15	90	LF	76.	65.	na	87.	101.			TTI-86	81.5	42	11	1
				LR	75.	96.	na	62.	93.			TTI-86	79.0	39	9	1
1222	MDB-to-Cavalier (baseline-4 DR)	30/15	90	LF	79.	85.	60.	84.	86.			TTI-86	84.5	46	12	1
				LR	93.	99.	72.	75.	123.			TTI-86	87.0	49	13	1
1256	MDB-to-Bonneville (baseline-4 DR)	30/15	90	LF	77.	61.	60.	81.	76.			TTI-86	79.0	39	9	1
				LR	75.	79.	96.	68.	108.			TTI-86	73.5	32	7	1
1257	MDB-to-Taurus (baseline-4 DR)	30/15	90	LF	86.	68.	55.	86.	105.			TTI-86	86.0	48	13	1
				LR	91.	87.	50.	46.	91.			TTI-86	68.5	27	6	0
1263	MDB-to-Sprint (baseline-2 DR)	30/15	90	LF	87.	70.	99.	133.	169.			TTI-86	110.0	73	31	3
				LR	63.	69.	67.	75.	99.			TTI-86	72.0	31	7	1
1264	MDB-to-Excel (baseline-4 DR)	30/15	90	LF	73.	73.	77.	103.	105.			TTI-86	88.0	50	14	1
				LR	79.	92.	71.	88.	145.			TTI-86	90.0	53	15	1
1269	MDB-to-Caprice (baseline-4 DR)	30/15	90	LF	39.	66.	28.	49.	60.			TTI-86	57.5	17	3	0
				LR	60.	66.	32.	38.	55.			TTI-86	52.0	14	2	0
1272	MDB-to-Golf (baseline-2 DR)	30/15	90	LF	101.	101.	117.	113.	155.			TTI-86	107.0	71	28	3
				LR	114.	125.	87.	96.	115.			TTI-86	110.5	74	32	4

Note: na = not available

### Modified VW Rabbit test matrix—(continued)

Vehicle	Striking/Struck Velocity (mph)	
	26/13	35/17.5
Padding Only	x	x
Padding + Mods	x	x

The MVMA conducted a program which parallels the NHTSA side impact investigation as shown in table 2. In the MVMA test series, sixteen 1985 Ford LTDs, some with padding and structural modifications, were subjected to controlled side impacts. Four vehicle configurations were examined:

### MVMA Ford LTD test matrix

Vehicle	Arm-to-Door Distance	
	0"	5"
Baseline	2	2
Structural Mods	2	2
Padding Only	2	2
Padding + Mods	2	2

### Occupant responses

The occupant responses for each test were measured using a NHTSA Side Impact Dummy (SID) as a human surrogate. For the production car tests and modified VW Rabbit tests, one SID was seated in the driver's seat and the second SID was seated in the left rear passenger's seat. In the MVMA Ford LTD tests, a single SID dummy was positioned in the right front passenger's seat.

For both sets of tests, the acceleration of the lower rib, upper rib, lower spine, upper spine, pelvis, and head were measured for each SID. The peak occupant thoracic and pelvic responses are tabulated in tables 1, 2, and 3. The Thoracic Trauma Index (TTI) was computed using the peak rib and spine accelerations. TTI is defined as follows for a 50-percentile human:

$$TTI = 1.4 \text{ Age} + 0.5(\max(\text{urg}, \text{lrg}) + \text{t}12\text{g})$$

where

Age = age of the occupant

urg = upper nearside rib peak acceleration

Table 2. MVMA Ford LTD tests: Side impact occupant responses (population-weighted).

Test no.	Stri/Stru Vehicle	Stri/Stru Velocity	Imp Ang	Occup Pos	Upper Rib G's	Lower Rib G's	Upper Spine G's	Lower Spine G's	Pelvis G's	Injury Name	Criterion Index (Age=0)	Probability AIS $\geq$ n		
												n=3	n=4	n=5
849	MDB-to-LTD (base-nopad-0in.)	30/15	90	RF	89.	100.	105.	102.	150.	TTI-86	101.0	65	23	2
850	MDB-to-LTD (base-nopad-0in.)	30/15	90	RF	95.	112.	105.	104.	137.	TTI-86	108.0	72	29	3
851	MDB-to-LTD (base-nopad-5in.)	30/15	90	RF	68.	74.	64.	96.	154.	TTI-86	85.0	47	12	1
852	MDB-to-LTD (base-nopad-5in.)	30/15	90	RF	50.	73.	80.	119.	144.	TTI-86	96.0	60	19	2
853	MDB-to-LTD (base-w/pad-0in.)	30/15	90	RF	43.	39.	47.	69.	51.	TTI-86	56.0	16	3	0
869	MDB-to-LTD (base-w/pad-0in.)	30/15	90	RF	51.	50.	60.	72.	59.	TTI-86	61.5	20	4	0
854	MDB-to-LTD (base-w/pad-5in.)	30/15	90	RF	62.	46.	52.	70.	54.	TTI-86	66.0	24	5	0
868	MDB-to-LTD (base-w/pad-5in.)	30/15	90	RF	57.	45.	51.	61.	51.	TTI-86	59.0	18	3	0
885	MDB-to-LTD (mod-nopad-0in.)	30/15	90	RF	67.	51.	60.	94.	91.	TTI-86	80.5	41	10	1
886	MDB-to-LTD (mod-nopad-0in.)	30/15	90	RF	56.	58.	62.	95.	93.	TTI-86	76.5	36	8	1
870	MDB-to-LTD (mod-nopad-5in.)	30/15	90	RF	54.	61.	65.	100.	115.	TTI-86	80.5	41	10	1
882	MDB-to-LTD (mod-nopad-5in.)	30/15	90	RF	57.	59.	71.	117.	139.	TTI-86	88.0	50	14	1
880	MDB-to-LTD (mod-w/pad-0in.)	30/15	90	RF	49.	43.	47.	54.	44.	TTI-86	51.5	13	2	0
881	MDB-to-LTD (mod-w/pad-0in.)	30/15	90	RF	50.	48.	48.	59.	48.	TTI-86	54.5	15	3	0
883	MDB-to-LTD (mod-w/pad-5in.)	30/15	90	RF	52.	41.	47.	62.	38.	TTI-86	57.0	16	3	0
884	MDB-to-LTD (mod-w/pad-5in.)	30/15	90	RF	48.	49.	52.	63.	42.	TTI-86	56.0	16	3	0

lrg = lower nearside rib peak  
acceleration  
t12g = lower spine peak  
acceleration

Using the thoracic impact risk functions recommended by Morgan et al (5), TTI was used to predict the probability of injury at AIS levels 3, 4, and 5. Note that the probability of injury presented in tables 1 and 2 have been population-weighted using the distribution of ages of occupants in the National Crash Severity Study (NCSS) (1). Figure 2 presents the relationship between the Thoracic Trauma Index and the age-weighted probability of thoracic side impact injury.

As shown in table 1, the probability of injury varies widely among the tested production vehicles. In our earlier

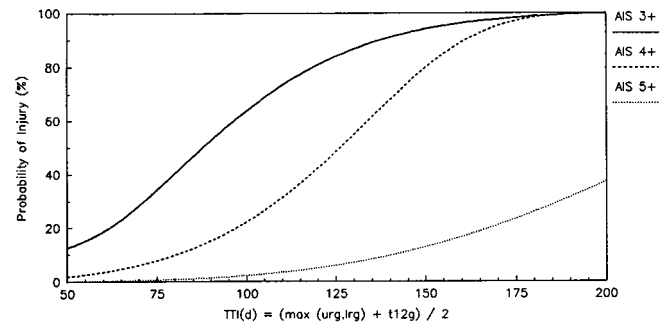


Figure 2. Probability of thoracic side impact injury—age weighted over population at risk.

set of production cars, the probability of serious thoracic injury (AIS = 3) ranged from a low of 31% for the AMC Concord, to a high of 94% for the 1982 Nissan Sentra. In our

Table 3. Modified Volkswagen tests: Side impact occupant responses (population-weighted).

Test no.	Stri/Stru Vehicle	Stri/Stru Velocity	Imp Ang	Occup Pos	Upper Rib G's	Lower Rib G's	Upper Spine G's	Lower Spine G's	Pelvis G's	Injury Name	Criterion Index (Age=0)	Probability AIS $\geq$ n		
												n=3	n=4	n=5
512	MDB-to-V.W. Rabbit	26/13	90	LF	74.	88.	87.	106.	177.	TTI-86	97.0	61	20	2
					105.	112.	72.	70.	120.			91.0	54	16
623	MDB-to-V.W. Rabbit (opt.mod.—unpadded)	26/13	90	LF	73.	68.	59.	74.	140.	TTI-86	73.5	32	7	1
					45.	63.	56.	57.	122.			60.0	19	4
603	MDB-to-V.W. Rabbit (baseline—padded)	26/13	90	LF	65.	62.	57.	80.	90.	TTI-86	72.5	31	7	1
					39.	46.	32.	47.	58.			48.5	11	2
596	MDB-to-V.W. Rabbit (opt. mod.—padded)	26/13	90	LF	58.	60.	59.	72.	69.	TTI-86	66.0	24	5	0
					42.	49.	27.	54.	111.			51.5	13	2
513	MDB-to-V.W. Rabbit	35/17.5	90	LF	178.	172.	153.	138.	221.	TTI-86	158.0	98	88	16
					127.	184.	77.	96.	131.			140.0	91	68
621	MDB-to-V.W. Rabbit (opt.mod.—unpadded)	35/17.5	90	LF	115.	231.	90.	163.	200.	TTI-86	197.0	100	100	36
					59.	72.	73.	93.	164.			82.5	44	11
604	MDB-to-V.W. Rabbit (baseline—padded)	35/17.5	90	LF	100.	110.	114.	135.	167.	TTI-86	122.5	83	45	6
					56.	68.	56.	85.	137.			76.5	36	8
587	MDB-to-V.W. Rabbit (opt. mod.—padded)	35/17.5	90	LF	69.	79.	109.	115.	123.	TTI-86	97.0	61	20	2
					60.	60.	58.	87.	159.			73.5	32	7

latest set of eight 1987–88 cars, the probability of serious thoracic injury (AIS = 3) ranged from a low of 17% for the Chevrolet Caprice, to a high of 71% for the Volkswagen Golf.

Comparison of the 1981–83 tests and the 1987–88 tests suggests that side impact designs have improved since the initial set of tests with 1981–83 model cars. The Nissan Sentra is a case in point: TTI has dropped dramatically from TTI = 149.5 for the 1982 Sentra to TTI = 99.5 for the 1987 Sentra. This represents a 33% decrease in the span of five model years.

## Methodology

### Occupant responses vs. vehicle design

In this paper, we will mathematically search for the relationship between occupant impact responses and vehicle design parameters. First, we will characterize the design and response of each vehicle as a set of discrete parameters. Second, we will use a step-wise regression technique to determine occupant response as a function of

the vehicle response. Finally, we will examine the results of the regression analysis to identify those design parameters most crucial to occupant protection in side impacts.

In this study, the struck vehicle was characterized by the geometry and mass parameters tabulated in tables 4a, 4b, and 4c. Occupant seating position is defined by four parameters: arm-door distance, hip-door distance, head-window distance, and head-side rail distance. Struck Vehicle Impact Response for each test is presented in tables 5a, 5b, and 5c. Static crush in this table was measured at the axle height and the h-point height, and was averaged over a range of 30 inches and 42 inches from the nominal impact point. This area, on the side of the car, encompasses the location of the struck front seat occupant.

Door impact responses were described by the parameters tabulated in tables 6a, 6b, and 6c. Chief among these parameters is the Door Effective Padding Thickness as measured at the upper rib, the lower rib, the pelvis, and as averaged across all three sensor locations. An earlier NHTSA study using twelve production cars concluded that the DEPTH design variable was highly correlated with TTI.

Table 4a. Production cars: Struck vehicle description.

Test No.	Vehicle Model	Number Doors	Total Weight (lbs.)	Wheel Base (in.)	Vehicle Length (in.)	Vehicle Width (in.)	Vehicle C.G. (in.)	Arm-Door (in.)	Hip-Door (in.)	Head-Door (in.)	Head-S.Rail (in.)
675	Citation	4	3045	104.8	176.8	68.8	46.0	4.9	6.7	9.4	6.5
676	Citation	4	3060	105.0	176.5	69.1	46.3	4.3	6.3	8.1	5.8
677	Citation	2	3100	104.9	176.7	68.1	43.3	5.4	7.1	9.4	6.6
678	Horizon	4	2600	99.1	162.5	66.5	45.8	3.6	5.5	8.9	5.9
679	Omni	2	2680	96.8	173.9	66.1	44.1	4.1	6.4	8.9	6.2
683	Granada	2	3380	105.4	195.3	71.1	49.3	4.8	7.3	9.3	6.4
684	Granada	4	3415	105.6	197.5	71.2	49.0	4.9	7.3	9.1	7.1
702	Concord	4	3555	108.5	180.0	70.4	53.7	3.2	6.4	7.7	4.9
704	Sentra	2	2340	94.6	167.1	63.9	44.5	3.9	6.2	7.3	5.1
710	Rabbit	2	2403	94.9	154.4	63.0	44.7	3.5	4.9	7.9	6.5
719	Civic	4	2488	91.3	161.4	62.2	43.8	3.4	5.8	6.9	5.0
744	Dodge400	2	3028	100.0	180.8	68.6	41.3	4.5	5.7	8.2	5.8
811	Civic	4	2468	91.3	161.5	62.6	44.2	3.0	5.3	5.8	3.5
820	Sentra	2	2377	95.0	167.0	64.5	45.1	3.8	6.6	8.9	7.0
855	Mazda626	4	2827	99.5	178.1	66.6	45.4	5.2	7.3	9.9	7.6
856	Sentra	2	2382	94.5	166.5	64.0	43.2	3.8	6.2	8.9	6.3
863	Civic	4	2453	91.4	161.4	62.3	45.4	4.3	7.1	8.6	6.3
879	Spectrum	2	2365	94.0	156.1	63.4	44.3	4.2	6.3	8.5	6.5
887	Celebrit	4	3374	104.9	188.3	67.8	45.4	5.1	7.1	9.8	6.3
1145	Sentra87	2	2510	95.5	168.8	64.9	47.3	4.1	6.8	8.0	6.4
1210	Tercel	4	2550	93.4	157.5	64.5	41.4	3.7	5.5	7.3	5.0
1222	Cavalier	4	2940	101.3	174.1	65.5	43.4	3.8	6.0	8.4	5.7
1256	Bonnevil	4	3820	111.0	198.6	72.6	45.6	4.8	7.3	11.3	7.7
1257	Taurus	4	3690	105.6	188.3	71.6	46.1	4.4	7.7	10.6	6.6
1263	Sprint	2	2100	88.5	144.7	60.5	41.7	3.1	5.6	8.6	6.2
1264	Excel	4	2700	93.6	167.5	63.7	43.7	3.7	6.3	7.2	5.1
1269	Caprice	4	4030	115.0	212.0	75.5	57.2	5.8	7.9	11.0	7.8
1272	Golf	2	2660	97.6	157.9	65.0	40.7	3.8	5.7	8.5	5.5

Table 4b. MVMA Ford LTD tests: Struck vehicle description.

Test No.	Vehicle Model	Number Doors	Mod Pad	Total Weight (lbs.)	Wheel Base (in.)	Vehicle Length (in.)	Vehicle Width (in.)	Vehicle C.G. (in.)	Arm-Door (in.)	Hip-Door (in.)	Head-Door (in.)	Head-S.Rail (in.)
849	LTD	4	N N	3247	106.0	195.5	70.0	52.3	0.0	1.0	4.8	4.4
850	LTD	4	N N	3239	106.5	196.5	68.6	53.9	0.0	1.0	4.8	4.3
852	LTD	4	N N	3234	106.2	195.6	70.6	52.1	5.0	6.1	9.2	6.9
851	LTD	4	N N	3261	105.5	195.9	70.4	52.9	5.1	6.0	9.3	6.9
853	LTD	4	N Y	3216	106.2	195.6	70.6	51.4	0.0	0.1	8.9	6.8
869	LTD	4	N Y	3205	106.0	197.6	70.0	53.1	0.0	0.0	9.2	6.7
854	LTD	4	N Y	3214	106.0	196.0	70.0	53.1	5.0	6.0	14.9	11.5
868	LTD	4	N Y	3215	106.0	196.6	69.9	52.6	5.0	5.9	14.9	18.8
885	LTD	4	Y N	3263	105.5	196.4	70.1	51.8	0.0	1.0	4.5	4.4
886	LTD	4	Y N	3240	105.5	196.0	70.3	52.2	0.0	0.8	4.0	4.1
870	LTD	4	Y N	3262	105.8	196.4	70.5	52.0	5.0	6.1	9.2	7.0
882	LTD	4	Y N	3242	105.5	196.2	69.9	52.1	5.0	6.5	9.2	7.6
880	LTD	4	Y Y	3249	105.5	196.4	69.6	52.0	0.0	0.2	9.5	7.2
881	LTD	4	Y Y	3253	106.0	196.2	69.0	53.1	0.0	0.5	9.3	7.4
883	LTD	4	Y Y	3238	105.5	196.2	69.2	52.5	5.0	5.7	14.3	10.8
884	LTD	4	Y Y	3204	105.5	196.4	70.1	52.4	5.0	6.2	14.5	10.6

Table 4c. Modified VW Rabbit tests: Struck vehicle description.

Test No.	Vehicle Model	Number Doors	Mod Pad	Total Weight (lbs.)	Wheel Base (in.)	Vehicle Length (in.)	Vehicle Width (in.)	Vehicle C.G. (in.)	Arm-Door (in.)	Hip-Door (in.)	Head-Door (in.)	Head-S.Rail (in.)
512	Rabbit	2	N N	2447	95.5	154.5	61.0	42.3	3.5	6.1	8.0	7.3
603	Rabbit	2	N Y	2546	94.0	154.6	63.8	41.9	0.0	5.2	7.5	6.0
623	Rabbit	2	Y N	2460	94.8	154.7	63.0	42.8	3.3	5.3	8.3	6.1
596	Rabbit	2	Y Y	2395	95.0	154.0	63.5	42.1	0.1	2.5	8.8	6.4
513	Rabbit	2	N N	2472	94.5	154.5	61.0	42.0	3.3	6.0	8.4	8.0
604	Rabbit	2	N Y	2485	94.8	154.5	63.8	42.6	0.0	2.4	7.6	5.9
621	Rabbit	2	Y N	2340	94.8	153.8	63.6	42.1	3.1	5.3	7.6	5.5
597	Rabbit	2	Y Y	2380	94.9	155.6	63.5	43.1	0.0	2.3	8.8	6.7

Table 5a. Production cars: Struck vehicle impact responses.

Test No.	Vehicle Model	Number Doors	Impact Point (in.)	Max Static Crush (in.)	Static Crush		Average (in.)
					● Axle (in.)	● H-Point (in.)	
675	Citation	4	37.5	17.7	11.3	15.1	13.2
676	Citation	4	38.0	16.9	11.2	13.1	12.2
677	Citation	2	37.0	18.7	10.3	15.7	13.0
678	Horizon	4	38.0	14.5	13.4	13.5	13.5
679	Omni	2	37.0	15.9	11.0	14.2	12.6
683	Granada	2	38.5	18.4	11.9	16.6	14.3
684	Granada	4	37.5	21.5	10.7	17.9	14.3
702	Concord	4	38.5	17.0	9.1	15.4	12.3
704	Sentra	2	37.0	18.2	14.6	18.0	16.3
710	Rabbit	2	37.9	18.5	na	na	na
719	Civic	4	38.0	16.5	11.0	15.6	13.3
744	Dodge400	2	36.5	20.7	15.5	20.0	17.8
811	Civic	4	34.5	15.6	10.1	15.2	12.7
820	Sentra	2	37.0	18.6	12.3	18.5	15.4
855	Mazda626	4	35.5	22.3	12.3	20.1	16.2
856	Sentra	2	38.0	23.4	12.2	17.9	15.1
863	Civic	4	37.5	17.4	11.8	16.9	14.4
879	Spectrum	2	36.5	15.7	8.9	14.8	11.9
887	Celebrit	4	38.0	15.4	10.0	13.3	11.7
1145	Sentra87	2	33.2	18.2	11.1	16.8	14.0
1210	Tercel	4	36.0	12.0	5.7	11.1	8.4
1222	Cavalier	4	36.5	14.6	8.9	14.4	11.7
1256	Bonnevil	4	37.0	18.3	12.4	17.8	15.1
1257	Taurus	4	35.8	14.2	8.6	14.0	11.3
1263	Sprint	2	37.1	14.4	8.1	13.4	10.8
1264	Excel	4	37.0	17.4	12.8	17.1	15.0
1269	Caprice	4	36.6	15.2	10.7	14.2	12.5
1272	Golf	2	36.7	13.9	7.7	13.8	10.8

Table 5b. MVMA Ford LTD tests: Struck vehicle impact responses.

Test No.	Vehicle Model	Mod	Pad	Arm-Door (in.)	Impact Point (in.)	Max Static Crush (in.)	Static Crush		Average (in.)
							● Axle (in.)	● H-Point (in.)	
849	LTD	N	N	0.0	34.2	16.3	10.9	14.6	12.8
850	LTD	N	N	0.0	36.2	19.9	11.7	16.1	13.9
852	LTD	N	N	5.0	37.0	20.0	12.6	17.0	14.8
851	LTD	N	N	5.1	36.6	19.8	12.8	16.7	14.8
853	LTD	N	Y	0.0	32.0	17.7	10.7	15.9	13.3
869	LTD	N	Y	0.0	39.0	22.1	13.7	18.1	15.9
854	LTD	N	Y	5.0	35.0	21.3	12.7	17.5	15.1
868	LTD	N	Y	5.0	36.0	22.3	11.4	18.3	14.9
885	LTD	Y	N	0.0	36.3	12.7	5.5	9.6	7.6
886	LTD	Y	N	0.0	37.2	14.0	5.5	9.9	7.7
870	LTD	Y	N	5.0	38.1	14.3	6.1	10.9	8.5
882	LTD	Y	N	5.0	37.0	14.7	7.5	12.6	10.1
880	LTD	Y	Y	0.0	37.1	14.4	7.0	9.8	8.4
881	LTD	Y	Y	0.0	38.8	13.2	7.2	11.8	9.5
883	LTD	Y	Y	5.0	38.0	15.9	9.5	13.6	11.6
884	LTD	Y	Y	5.0	38.0	13.8	7.0	12.1	9.6

Table 5c. Modified VW Rabbit tests: Struck vehicle impact responses.

Test No.	Vehicle Model	Mod	Pad	Impactor Init. Vel (mph)	Arm-Door (in.)	Impact Point (in.)	Max Static Crush (in.)	Static Crush		Average (in.)
								● Axle (in.)	● H-Point (in.)	
512	Rabbit	N	N	25.6	3.5	37.0	13.0	5.4	10.8	8.1
603	Rabbit	N	Y	26.1	0.0	37.5	12.7	5.8	11.6	8.7
623	Rabbit	Y	N	26.1	3.3	38.0	8.5	2.5	8.0	5.3
596	Rabbit	Y	Y	26.2	0.1	37.0	10.2	4.1	9.3	6.7
513	Rabbit	N	N	35.4	3.3	37.0	16.4	11.0	15.3	13.2
604	Rabbit	N	Y	35.1	0.0	36.0	17.4	11.0	17.2	14.1
621	Rabbit	Y	N	35.1	3.1	38.0	14.9	8.0	13.9	11.0
597	Rabbit	Y	Y	35.1	0.0	37.0	14.1	na	na	na

Table 6a. Production cars: Door impact responses.

Test Vehicle No.	Model	Number Doors	Arm-Door (in.)	Impactor Init.Vel (mph)	Contact Vel			Common Vel			DEPTH			Avg (in.)
					U.Rib (mph)	L.Rib (mph)	Pelv (mph)	U.Rib (mph)	L.Rib (mph)	Pelv (mph)	U.Rib (in.)	L.Rib (in.)	Pelv (in.)	
675	Citation	4	4.9	30.1	26.0	26.5	27.9	19.7	20.4	22.8	5.3	6.0	7.1	6.1
676	Citation	4	4.3	30.1	26.0	26.6	27.6	19.6	20.5	22.5	5.4	5.9	6.8	6.0
677	Citation	2	5.4	30.1	25.3	25.9	27.1	20.0	20.2	22.8	4.3	4.9	5.7	5.0
678	Horizon	4	3.6	30.1	26.1	26.3	28.2	20.0	20.6	23.8	5.3	5.1	5.7	5.4
679	Omni	2	4.1	30.1	26.2	26.6	28.3	20.8	21.0	23.6	4.4	4.5	6.9	5.3
683	Granada	2	4.8	30.1	24.9	25.9	27.4	18.2	19.8	23.1	4.3	5.2	5.8	5.1
684	Granada	4	4.9	30.1	25.9	25.6	27.8	19.2	19.2	22.7	6.1	4.8	6.8	5.9
702	Concord	4	3.2	30.1	27.8	25.9	27.2	18.3	17.8	21.2	9.5	6.1	6.7	7.4
704	Sentra	2	3.9	30.1	26.6	26.9	28.3	22.1	22.3	25.2	4.2	4.1	5.0	4.4
710	Rabbit	2	3.5	30.1	na	na	na	na	na	na	na	na	na	na
719	Civic	4	3.4	30.0	26.7	27.0	28.4	20.0	20.4	23.1	5.5	5.9	7.2	6.2
744	Dodge400	2	4.5	30.1	25.9	25.1	27.7	19.0	20.6	23.6	5.7	3.6	5.1	4.8
811	Civic	4	3.0	30.1	27.9	28.1	29.4	20.9	21.0	24.1	6.3	6.3	7.8	6.8
820	Sentra	2	3.8	30.0	26.6	27.7	29.0	22.5	22.3	25.4	4.2	5.9	6.7	5.6
855	Mazda626	4	5.2	30.0	26.9	27.0	27.3	20.5	20.9	23.8	6.4	6.3	4.2	5.6
856	Sentra	2	3.8	30.0	26.2	27.0	28.5	22.7	22.1	25.3	3.6	4.5	5.3	4.5
863	Civic	4	4.3	30.0	27.6	27.8	26.7	19.8	20.4	23.0	6.8	6.9	3.8	5.8
879	Spectrum	2	4.2	30.2	26.1	26.9	28.6	20.0	20.3	23.8	4.5	5.8	6.4	5.6
887	Celebrit	4	5.1	30.2	26.7	26.7	28.3	18.1	18.3	24.5	8.0	7.8	6.1	7.3
1145	Sentra87	2	4.1	30.1	27.7	27.1	27.6	20.6	21.2	24.1	7.6	6.2	4.4	6.1
1210	Tercel	4	3.7	30.3	26.9	26.2	28.0	18.4	18.3	21.8	7.3	6.2	6.9	6.8
1222	Cavalier	4	3.8	30.4	28.7	27.1	28.6	19.7	20.4	22.9	9.2	5.3	6.5	7.0
1256	Bonnevil	4	4.8	30.5	25.7	26.6	28.3	18.5	19.7	21.4	4.9	6.2	8.2	6.4
1257	Taurus	4	4.4	30.0	25.0	25.2	27.5	17.1	17.7	21.6	4.8	5.0	6.6	5.5
1263	Sprint	2	3.1	30.3	25.8	26.8	29.2	19.8	21.0	24.2	4.1	4.6	7.4	5.4
1264	Excel	4	3.7	30.5	26.6	26.8	28.4	18.5	20.5	23.3	5.8	5.6	6.4	5.9
1269	Caprice	4	5.8	30.1	24.2	24.6	27.3	15.0	17.0	17.8	7.6	5.7	9.1	7.5
1272	Golf	2	3.8	30.4	27.1	28.0	29.2	19.4	19.5	22.9	6.0	7.4	8.7	7.4

Table 6b. MVMA Ford LTD tests: Door impact responses.

Test Vehicle No.	Model	Mod Pad	Arm-Door (in.)	Impactor Init.Vel (mph)	Contact Vel			Common Vel			DEPTH			Avg (in.)	
					U.Rib (mph)	L.Rib (mph)	Pelv (mph)	U.Rib (mph)	L.Rib (mph)	Pelv (mph)	U.Rib (in.)	L.Rib (in.)	Pelv (in.)		
849	LTD	N	N	0.0	30.2	27.5	28.1	28.5	18.6	20.8	23.9	5.1	5.3	4.3	4.9
850	LTD	N	N	0.0	29.9	28.7	28.3	28.5	19.9	20.2	23.5	8.9	5.4	5.5	6.6
852	LTD	N	N	5.0	30.0	24.8	24.8	28.3	17.1	19.1	22.4	4.8	4.1	7.4	5.4
851	LTD	N	N	5.1	30.0	24.6	23.6	27.4	18.2	14.3	22.0	4.1	5.7	5.9	5.2
853	LTD	N	Y	0.0	30.2	29.4	28.8	28.8	19.2	19.7	21.4	11.4	10.0	8.1	9.8
869	LTD	N	Y	0.0	30.1	29.6	29.2	28.8	20.0	20.9	22.0	12.2	10.2	8.0	10.1
854	LTD	N	Y	5.0	30.1	24.8	24.6	28.4	18.0	17.8	18.7	5.7	5.6	12.2	7.8
868	LTD	N	Y	5.0	30.2	25.3	25.2	28.5	18.0	18.2	19.0	6.5	6.2	11.9	8.2
885	LTD	Y	N	0.0	30.2	27.1	26.3	28.6	17.2	18.3	21.6	6.3	4.9	7.0	6.1
886	LTD	Y	N	0.0	30.2	26.4	27.9	28.4	17.8	19.6	21.9	5.4	7.0	6.3	6.2
870	LTD	Y	N	5.0	30.1	22.9	23.6	26.4	15.3	16.1	18.2	4.5	5.1	7.6	5.7
882	LTD	Y	N	5.0	30.1	23.7	24.8	26.3	14.4	17.1	19.5	4.7	5.5	7.0	5.7
880	LTD	Y	Y	0.0	30.2	28.5	26.3	28.3	17.0	17.4	19.1	9.5	5.7	8.0	7.7
881	LTD	Y	Y	0.0	30.1	27.8	26.0	28.4	16.5	17.0	18.9	8.1	5.5	8.4	7.3
883	LTD	Y	Y	5.0	30.1	29.8	23.3	27.7	15.5	15.9	16.8	16.3	4.9	10.5	10.6
884	LTD	Y	Y	5.0	30.1	23.6	29.1	26.5	14.9	15.4	16.5	5.2	14.4	8.4	9.3

Table 6c. Modified VW Rabbit tests: Door impact responses.

Test Vehicle No.	Model	Mod Pad	Arm-Door (in.)	Impactor Init.Vel (mph)	Contact Vel			Common Vel			DEPTH			Avg (in.)	
					U.Rib (mph)	L.Rib (mph)	Pelv (mph)	U.Rib (mph)	L.Rib (mph)	Pelv (mph)	U.Rib (in.)	L.Rib (in.)	Pelv (in.)		
512	Rabbit	N	N	3.5	25.6	21.5	21.5	24.8	16.7	17.2	19.9	3.5	3.4	8.8	5.2
603	Rabbit	N	Y	0.0	26.1	24.0	24.3	25.0	17.4	18.0	20.7	5.1	5.1	4.9	5.0
623	Rabbit	Y	N	3.3	26.1	21.2	20.7	22.3	14.2	15.1	18.5	4.7	3.8	3.5	4.0
596	Rabbit	Y	Y	0.1	26.2	23.3	23.7	24.4	16.8	17.5	20.1	5.5	5.5	4.4	5.1
513	Rabbit	N	N	3.3	35.4	31.4	33.9	33.6	25.4	26.4	29.1	4.5	9.0	5.7	6.4
604	Rabbit	N	Y	0.0	35.1	32.2	32.7	33.8	25.8	26.7	29.4	5.2	5.1	5.6	5.3
621	Rabbit	Y	N	3.1	35.1	31.3	30.4	32.2	23.3	24.3	28.2	7.4	3.7	4.3	5.1
597	Rabbit	Y	Y	0.0	35.1	32.2	32.3	33.4	24.6	25.3	28.1	6.7	6.4	5.6	6.2

## Definition of DEPTH

DEPTH is defined as the relative displacement between the door and occupant from the time of occupant-door contact until the time of occupant-door separation. From the crash observer's perspective, DEPTH is the amount which the occupant crushes the door.

DEPTH is the maximum deflection measured between the occupant accelerometer and the door accelerometer. Depending on the location of occupant instrumentation, this will include a portion of the dummy compression as well as the crush of the door. As measured by the rib accelerometers, DEPTH includes compression of the dummy skin between the ribs and door surface. The effect of skin compression is considered to be negligible. Likewise, compression of the dummy at the pelvis contact point is considered insignificant as the pelvis is rigid.

## Door kinematic parameters

For our study, struck door contact with the occupant is defined to have taken place once the occupant velocity exceeds a threshold velocity of 0.2 mph. The door is assumed to have reached the impactor velocity prior to contacting the occupant. Door contact velocity is then equal to the impactor velocity at the time of contact.

This method avoids having to rely on struck door accelerometers to determine door contact velocity. Struck door accelerometers are subjected to very severe impact loads, and measurements from these instruments frequently contain anomalies (6). Our method received a measure of ex-

perimental confirmation in a recent NHTSA side impact test using a specially instrumented Chevrolet Celebrity (7). Based on direct measurements of struck door displacement, door contact velocity at the H-point was estimated to be approximately 25 mph. Using the same model car in NHTSA Test No. 887, our method estimated door contact velocity to range between 26.7 mph and 28.3 mph.

The time of door-occupant common velocity is defined to be that instant when the occupant reaches the same velocity as the intruding door. Tables 7a, 7b, and 7c present the door contact velocity, the time of contact, the common velocity, and the time of common velocity, as measured at the struck upper rib, the struck lower rib, and the pelvis.

## Occupant Responses Versus Vehicle Design: Regression Analysis

To statistically determine the relationship between the vehicle design and occupant injury, the vehicle structural characteristics and occupant impact responses were combined and examined with a stepwise regression technique. The production vehicles were analyzed separately from the MVMA test series.

The computed linear fits for the production vehicles are shown below and presented in figures 3, 4, 5, and 6.

$$\begin{aligned} \text{TTI} &= 195.6 + -16.3 * \text{Davg} & R^2 &= 0.521 \\ \text{Llrg} &= 88.1 + -12.2 * \text{DlIr} + 4.1 * \text{Maxcrush} & R^2 &= 0.470 \\ \text{T12g} &= 220.4 + -10.5 * \text{Davg} + -0.019 * \text{Vehtwt} & R^2 &= 0.549 \\ \text{Pelg} &= 307.2 + -13.1 * \text{Dpel} + -23.5 * \text{Ndoor} & R^2 &= 0.627 \end{aligned}$$

Table 7a. Production cars: Door impact time history.

Test No.	Vehicle Model	Number Doors	Time of Contact			Time of Common Vel		
			U.Rib (msec)	L.Rib (msec)	Pelv (msec)	U.Rib (msec)	L.Rib (msec)	Pelv (msec)
675	Citation	4	22.125	20.000	13.750	44.750	41.875	33.875
676	Citation	4	21.000	18.750	13.875	42.500	39.125	33.250
677	Citation	2	25.875	23.750	18.000	45.125	44.375	34.500
678	Horizon	4	22.375	21.375	14.125	44.250	42.125	30.750
679	Omni	2	24.250	23.125	15.000	42.875	42.250	33.875
683	Granada	2	29.375	25.750	19.750	54.625	47.500	35.875
684	Granada	4	23.750	25.125	16.000	47.875	48.000	35.125
702	Concord	4	14.375	22.000	17.000	46.375	47.750	36.625
704	Sentra	2	24.500	23.125	16.250	41.875	41.125	30.000
710	Rabbit	2	na	na	na	na	na	na
719	Civic	4	20.750	19.125	13.000	44.750	43.000	33.375
744	Dodge400	2	25.000	28.250	19.000	53.125	45.000	33.750
811	Civic	4	18.500	17.625	9.625	43.250	42.750	31.500
820	Sentra	2	25.250	21.125	12.375	40.750	41.375	30.000
855	Mazda626	4	22.625	21.750	20.375	47.375	45.500	33.875
856	Sentra	2	25.375	22.750	14.500	38.500	40.500	29.375
863	Civic	4	18.375	17.875	20.750	44.750	42.875	34.000
879	Spectrum	2	25.375	22.375	13.250	45.625	45.125	32.750
887	Celebrit	4	20.375	20.375	13.125	50.875	50.000	29.250
1145	Sentra87	2	17.625	20.125	18.250	43.500	41.750	31.625
1210	Tercel	4	17.250	19.425	12.300	42.825	43.125	33.225
1222	Cavalier	4	9.825	17.325	10.050	40.050	38.175	30.975
1256	Bonnevil	4	22.950	19.725	12.000	47.775	43.275	37.950
1257	Taurus	4	24.000	23.325	13.875	49.650	46.950	34.275
1263	Sprint	2	23.400	19.950	8.925	45.450	40.275	28.500
1264	Excel	4	19.800	19.200	12.300	52.500	42.150	31.950
1269	Caprice	4	22.575	21.525	13.200	57.375	47.400	43.875
1272	Golf	2	19.050	15.600	9.600	42.150	42.000	32.550

Table 7b. MVMA Ford LTD tests: Door impact time history.

Test No.	Vehicle Model	Mod	Pad	Arm-Door (in.)	Time of Contact			Time of Common Vel		
					U.Rib (msec)	L.Rib (msec)	Pelv (msec)	U.Rib (msec)	L.Rib (msec)	Pelv (msec)
849	LTD	N	N	0.0	16.750	14.875	12.000	44.750	36.250	27.625
850	LTD	N	N	0.0	9.375	16.000	10.375	39.125	38.375	28.250
852	LTD	N	N	5.0	28.000	28.250	14.875	58.375	48.625	35.250
851	LTD	N	N	5.1	27.875	30.750	18.125	47.750	69.500	35.500
853	LTD	N	Y	0.0	8.375	10.625	11.375	46.250	44.625	38.625
869	LTD	N	Y	0.0	5.875	8.875	11.500	43.750	42.125	37.750
854	LTD	N	Y	5.0	27.625	28.250	12.875	53.500	54.375	50.875
868	LTD	N	Y	5.0	26.625	27.250	14.250	55.375	55.125	51.750
885	LTD	Y	N	0.0	16.750	19.000	10.000	45.750	41.625	32.625
886	LTD	Y	N	0.0	18.750	14.250	11.375	46.000	39.875	32.625
870	LTD	Y	N	5.0	28.500	26.625	17.875	51.250	48.250	41.250
882	LTD	Y	N	5.0	26.750	23.875	17.500	56.500	45.750	38.500
880	LTD	Y	Y	0.0	11.125	18.625	11.375	45.625	44.125	39.500
881	LTD	Y	Y	0.0	14.000	19.500	10.375	45.375	44.250	38.500
883	LTD	Y	Y	5.0	5.000	29.500	14.875	55.625	54.375	50.250
884	LTD	Y	Y	5.0	28.625	7.375	18.875	54.375	52.125	48.625

Table 7c. Modified VW Rabbit tests: Door impact time history.

Test No.	Vehicle Model	Mod	Pad	Impactor Init.Vel (mph)	Arm-Door (in.)	Time of Contact			Time of Common Vel		
						Up.Rib (msec)	Lo.Rib (msec)	Pelvis (msec)	U.Rib (msec)	L.Rib (msec)	Pelv (msec)
512	Rabbit	N	N	25.6	3.5	30.625	30.000	10.250	47.875	46.250	35.375
603	Rabbit	N	Y	26.1	0.0	21.375	19.750	16.000	44.000	42.125	33.875
623	Rabbit	Y	N	26.1	3.3	24.375	26.250	20.250	48.750	45.000	33.875
596	Rabbit	Y	Y	26.2	0.1	17.750	16.125	13.250	42.500	40.375	31.125
513	Rabbit	N	N	35.4	3.3	22.500	13.625	15.125	39.750	36.750	29.375
604	Rabbit	N	Y	35.1	0.0	16.375	15.000	10.500	35.500	33.125	25.375
621	Rabbit	Y	N	35.1	3.1	17.875	21.375	14.750	43.375	40.000	28.625
597	Rabbit	Y	Y	35.1	0.0	14.250	13.750	10.250	37.250	35.375	27.500

where

- TTI =Thoracic Trauma Index
- T12g =Lower Spine G's
- Llrg =Lower Rib G's
- Pelg =Pelvic Peak Acceleration
- Davg =Average DEPTH
- Dlir =DEPTH at the Lower Rib
- Dpel =DEPTH at the Pelvis

Vehtwt =Total Vehicle Weight with Passengers (pounds)

Maxcrush=Maximum Residual External Side Structure Crush (in.)

Because only four tests were available for each speed, a stepwise regression was not run on the modified VW test results. To some extent however, increasing TTI appears to

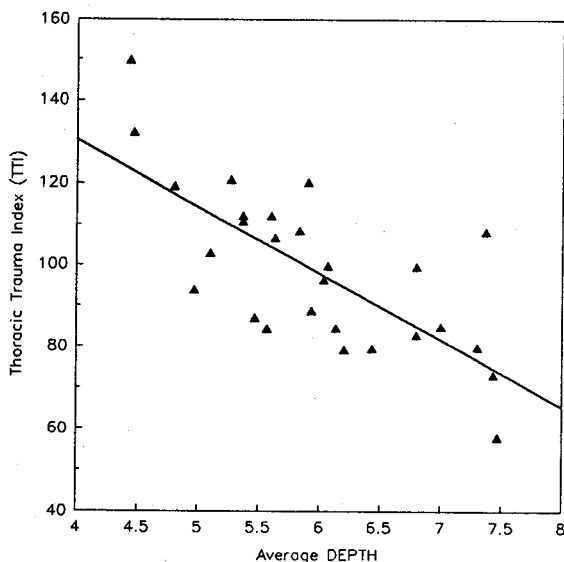


Figure 3. TTI versus average DEPTH for production cars.

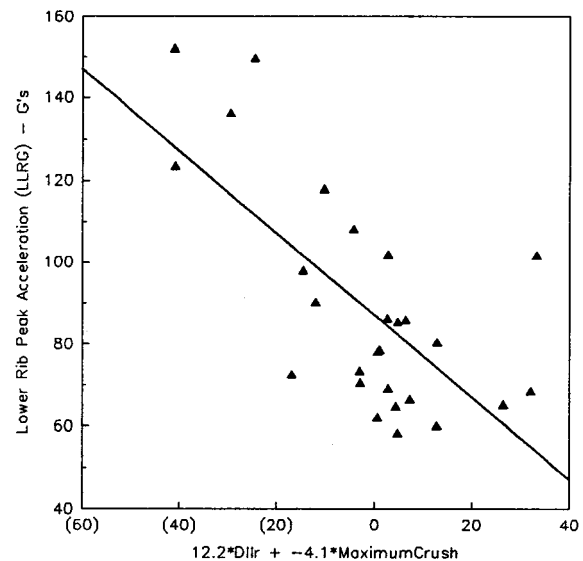


Figure 4. Lower rib peak acceleration versus vehicle design for production cars.

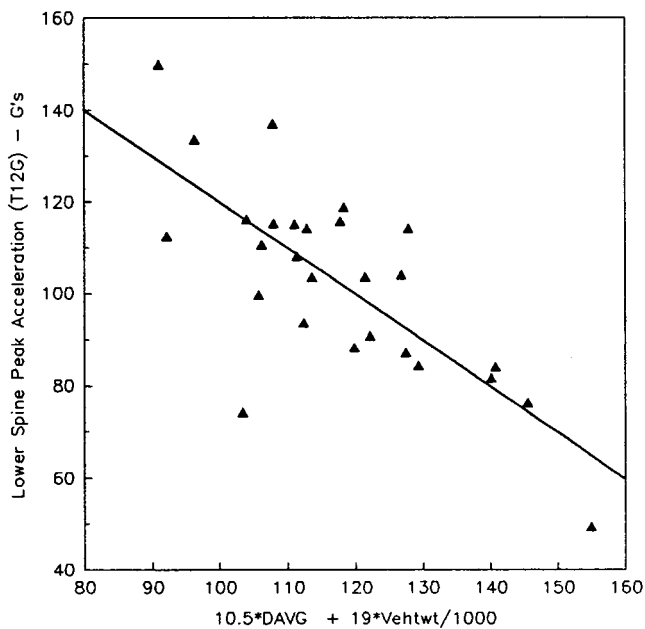


Figure 5. Lower spine peak acceleration versus vehicle design for production cars.

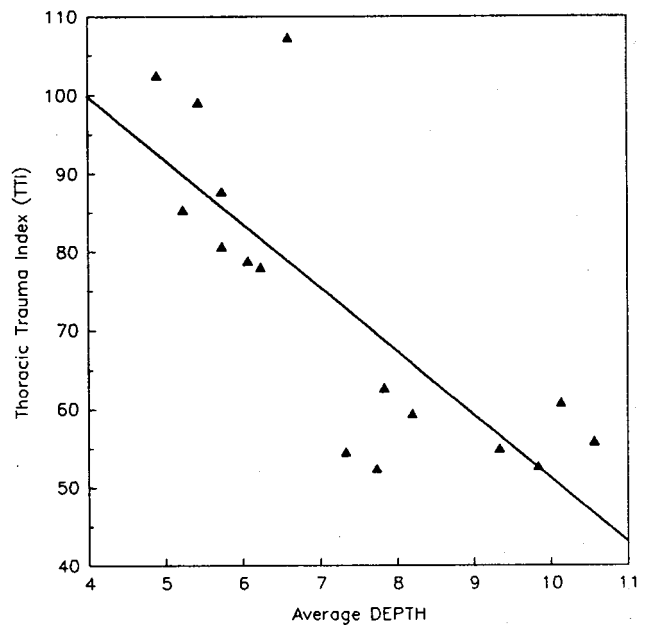


Figure 7. TTI versus average DEPTH for MVMA tests.

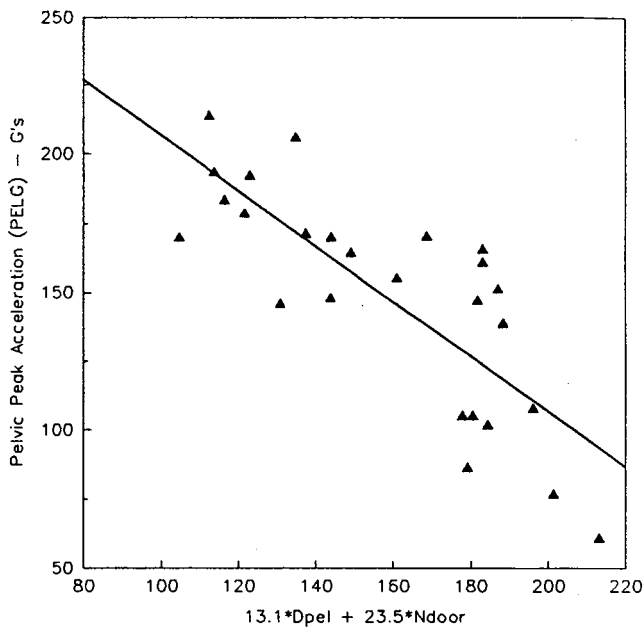


Figure 6. Pelvic peak acceleration versus vehicle design for production cars.

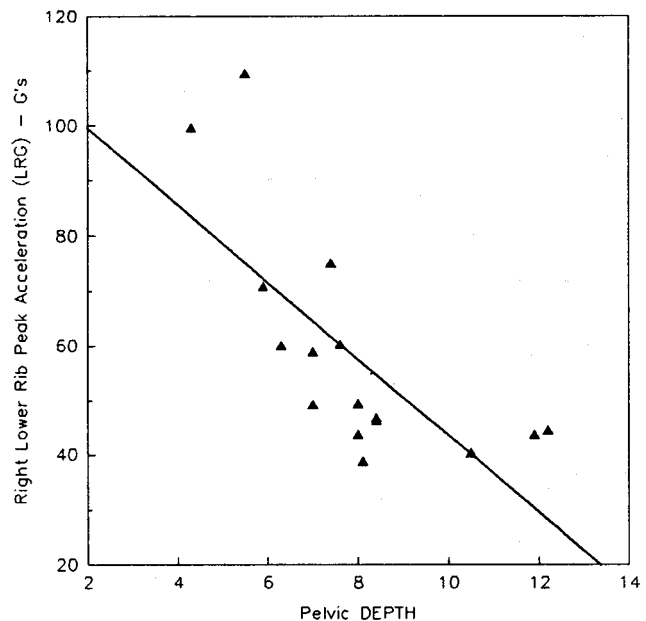


Figure 8. Lower rib peak acceleration versus pelvic DEPTH for MVMA tests.

be related to decreasing DEPTH in these tests. The one exception is the set of baseline tests which have a high TTI and a high DEPTH. The high DEPTH for these cases, due to an unusually early time of door contact, appears to be an artifact of the DEPTH algorithm rather than a physical attribute of the actual door.

The computed linear fits for the MVMA Ford LTD test series are shown below and presented in figures, 7, 8, 9, and 10.

$$\begin{aligned}
 \text{TTI} &= 132.3 + -8.1 * \text{Davg} & R^2 &= 0.629 \\
 \text{Llrg} &= 113.7 + -7.0 * \text{Dpel} & R^2 &= 0.519 \\
 \text{T12g} &= 156.2 + -9.9 * \text{Davg} & R^2 &= 0.643 \\
 \text{Pelg} &= 236.3 + -20.2 * \text{Davg} & R^2 &= 0.715
 \end{aligned}$$

## Discussion of Results

### Importance of DEPTH

These mathematical fits indicate the important influence which DEPTH has on occupant impact responses. Peak occupant responses are strongly correlated with DEPTH. For the production vehicles, three other structural design parameters, the number of doors, the vehicle weight, and the maximum external crush, are also correlated with occupant impact responses. Pelvic acceleration is, in general, lower for four door cars than for two door cars. Lower rib acceleration is proportional to the maximum external structural crush.

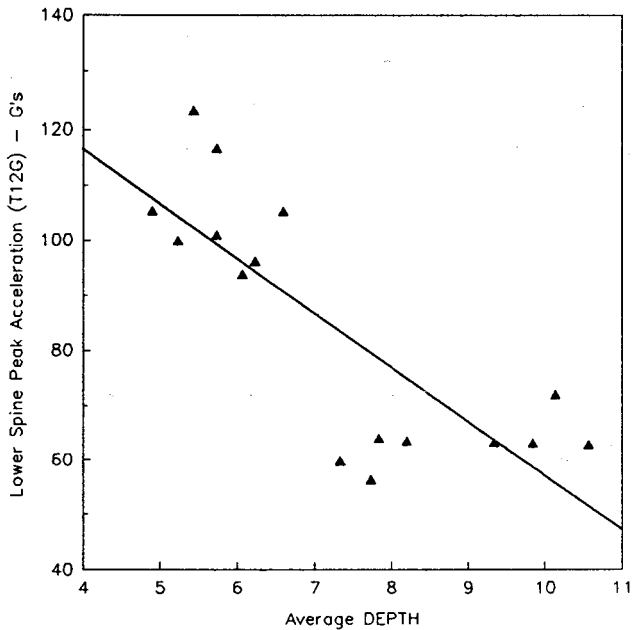


Figure 9. Lower spine peak acceleration versus average DEPTH for MVMA tests.

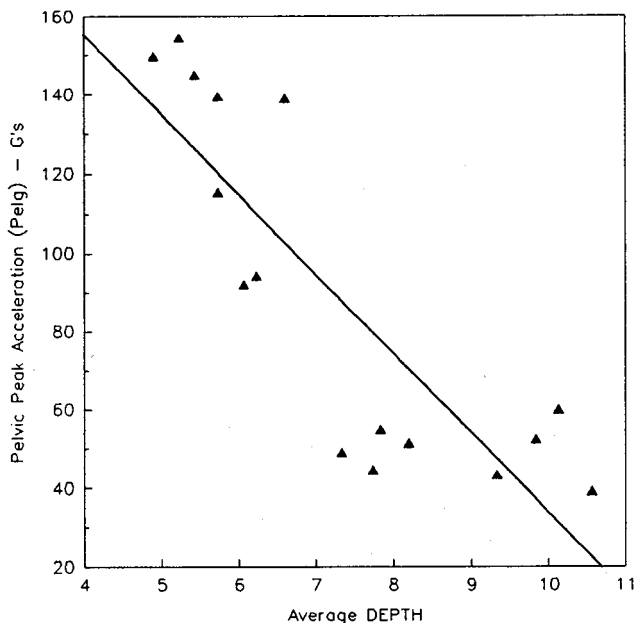


Figure 10. Pelvic peak acceleration versus average DEPTH for MVMA tests.

Lower spine peak acceleration is, in general, lower for heavier cars.

### DEPTH versus vehicle design parameters

The statistical analysis of occupant responses versus vehicle design parameters indicate that decreasing values of TTI are highly correlated with increasing DEPTH. The vehicle design parameters which affect DEPTH remain to be determined. Among the candidate design variables are vehicle geometry and weight, external static crush, the number of doors, and occupant spacing with respect to the door. Using the production vehicle test sample, another stepwise

regression was run using these variables as independent variables and DEPTH as the dependent variable. The computer mathematical fit between average DEPTH and two of these parameters is shown below:

$$D_{avg} = 6.75 + 0.436 * N_{door} - 0.2 * AxleCrush$$

$$R^2 = 0.542$$

where

$D_{avg}$  = average DEPTH =  $(D_{pel} + D_{llr} + D_{lur}/3)$

$N_{door}$  = Number of Car Doors (2 or 4)

$AxleCrush$  = Static External Crush at the axle height

This paper has found a good relationship between DEPTH and two elements of vehicle design, i.e. number of doors and the static external crush of the struck car. Note that other design parameters, not investigated here, may also have an influence on DEPTH. These parameters, many of which have been examined by Kaniyanthra et al (8) for a subset of the cars reported here, would include door thickness and width, inner and outer design stiffness, pillar/roof/floor stiffness, lateral strength of the driver's seat, seat design, and dash board design.

### Comparison of the 1982 Sentra and the 1987 Sentra

The Nissan Sentra is an interesting example of the effect of design enhancement in a particular vehicle. The two door 1982 Nissan Sentra was found to have the highest Thoracic Trauma Index (TTI = 149.5) and the highest pelvic acceleration (Pelg = 213.5 G's) of any production vehicle in our test sample. Two repeats of this test gave similar results.

After receiving indications from Nissan that side impact improvements had been made in the process of redesigning the Sentra for the 1987 model year, the Nissan Sentra was again tested. The test of two door 1987 Nissan Sentra revealed a dramatic improvement in occupant protection. The Thoracic Trauma Index dropped to 99.5 while the peak pelvic lateral acceleration was reduced to 169.5 G's.

An examination of average DEPTH for the two models suggests the design improvements which Nissan made to affect this improvement: average DEPTH was increased by 38% from 1982 to 1987, from 4.4 inches for the 1982 Sentra to 6.1 inches for the 1987 Sentra. How was this increase in DEPTH achieved? Our regression analysis suggests that increased DEPTH is correlated with lower amounts of external crush. The two tests of the Sentra further confirm this relationship: external crush at axle height at the location of the driver dropped by 24%, from 14.6 inches for the 1982 Sentra to 11.1 inches in the 1987 Sentra.

### Effect of structural stiffening

Our statistical fits indicate that larger DEPTHS (and lower TTI's) are associated with cars that limit the amount of external crush of the side structure. Given the goal of increasing DEPTH, the most obvious design option would be

to preserve the integrity of the door by stiffening the side structure. The MVMA Ford LTD tests provide an experimental test of this design concept.

Four of the MVMA tests were conducted with modified LTDs in which the A-pillars and B-pillars had been stiffened without alteration (e.g. padding) to the door interior surface. Comparing these tests with the four baseline LTD tests suggests that to some degree structural stiffening does increase DEPTH—although the improvement is modest. The mean Average DEPTH for the baseline cars was 5.5 inches while the mean Average DEPTH for the modified cars with no padding was 5.9 inches. Structural modification produced a 17% drop in TTI from a mean TTI of 98.4 for the baseline LTD's to a mean TTI of 81.1 for the modified LTD's.

### Effect of padding on DEPTH

The MVMA test series also shows how the presence of padding influences DEPTH and TTI. Three inches of padding was added to four of the LTDs. No structural modifications were made to these cars. Padding without structural modification decreased TTI by 40%, from a mean TTI of 98.4 for the baseline LTD's to a mean TTI of 58.7 for the padded LTD's.

The DEPTH parameter also detected the presence of padding. The mean Average DEPTH for the baseline cars was 5.5 inches as compared with a mean Average DEPTH for the padded cars of 8.9 inches. Note that three inches of padding added an almost equal amount of 3.4 inches to average DEPTH.

A similar relationship is observed when structurally modified cars without padding are compared to structurally modified cars with padding. The mean Average DEPTH for the modified/unpadded cars was 5.9 inches as compared with a mean Average DEPTH for the modified/padded cars of 8.7 inches. Note that three inches of padding added an almost equal amount of 2.8 inches to average DEPTH.

Based on only sixteen tests of one car and one padding design, it is unclear whether this correspondence between padding thickness and incremental DEPTH should be viewed as a design guideline or as merely a coincidence. However, we *can* conclude that padding decreases TTI and increases average DEPTH.

### Future Work

Several activities are planned by NHTSA to further evaluate the safety performance parameters of production vehicles in side impacts. These activities include continued full systems testing of production vehicles which will be used to supplement the above studies and more fully evaluate the importance of DEPTH across the complete vehicle fleet.

A recent NHTSA task force developed recommendations for side impact crashworthiness research for the mid-nineties. These task force recommendations were presented at the 1989 SAE Government/Industry Meeting in Wash-

ington, D.C. The brief descriptions of possible side impact crashworthiness activities presented below are based on these recommendations. (Note: these descriptions are very general, and are presented only as potential guidelines of some of the research activities that NHTSA may pursue in the future).

- *Light trucks and vans.*—NHTSA has begun a research program to test the safety performance of light trucks and vans in side impacts. Currently, work is focusing on the adaptation of the NHTSA Side Impact Test Procedure suited to this category vehicle.
- *Increased crash severity.*—A research program is currently being formulated to investigate the side impact safety performance of production vehicles at higher speeds and non-perpendicular impact angles.

### Conclusions

This paper has examined the results of 28 side impact tests using current production cars, and 16 side impact tests using baseline and modified Ford LTDs. The objective has been to determine the effect of vehicle design on the response of side-struck occupants. Our conclusions are:

- Current production cars vary widely in their capability to protect the side-struck occupant. The Thoracic Trauma Index varies from a low of 57.7 for the 1988 Chevrolet Caprice to 149.5 for the 1982 Nissan Sentra. Peak Pelvic acceleration ranges from a low of 60.8 G's for the Caprice to a high of 213.7 G's for the 1982 Sentra.
- Of the design attributes investigated for the vehicles tested, Door Effective Padding Thickness (DEPTH) is the single design parameter most strongly correlated with TTI. Lower values of average DEPTH are associated with higher TTI's.
- Design enhancement can dramatically drop TTI as witnessed by comparison of the crash tests of the 1982 Sentra and the 1987 Sentra. After design modifications between the two model years, TTI dropped from 149.5 in 1982 to 99.5 in 1987. The design modifications appear to be reflected in DEPTH: average DEPTH increased by 38% from 1982 to 1987.
- DEPTH is highly correlated with the number of doors and residual external door crush.
- The structural stiffening performed on the modified MVMA Ford LTDs was reflected to some degree in increased DEPTH. DEPTH was also able to detect the presence of padding in the MVMA tests.

### References

- (1) Hackney, J.R., H.C. Gabler, J.N. Kaniyanthra, and D.S.

Cohen. "Update of the NHTSA Research Activity in Thoracic Side Impact Protection for the Front Seat Occupant". *Proceedings of the 31st Stapp Car Crash Conference*. SAE Paper 872207. New Orleans, Louisiana, November 1987.

(2) Gabler, H.C., K.P. White and W.D. Pilkey, "Thoracic Side Impact Protection Program: Countermeasure Effectiveness", University of Virginia Letter Report, September 1984.

(3) Preuss, C.A. and R.J. Wasko, "Status and Update of MVMA Full Vehicle Testing," SAE Paper 8711155, May 1987.

(4) Gabler, H.C. and J.R. Hackney, "The Safety Performance of Production Vehicles in Side Impact," *Proceedings of the Tenth International Technical Conference on Experimental Safety Vehicles*. Oxford, England, July 1985.

(5) Morgan, R.M., J.H. Marcus, and R.H. Eppinger, "The Biofidelity of NHTSA's Proposed ATD and Efficacy of TTI," *Proceedings of the 30th Stapp Car Crash Conference*, San Diego, California, October 1986.

(6) Willke, D.T., M.W. Monk, and J.N. Kianianthra; "Side Impact Subsystem Thoracic Impactor Evaluation," *Proceedings of the 12th International Technical Conference on Experimental Safety Vehicles*. Gothenburg, Sweden, May 1989.

(7) Willke, D.T. "Side Impact Door Velocity Measurement," NHTSA Project VRTC-87-0056 Final Report. April 1989.

(8) Kianianthra, J.N., Trella, T.J., and Edwards, S.P., "Safety Performance Evaluation of Production Vehicles in Side Impacts using the Modeling Approach," *Proceedings of the 12th International Technical Conference on Experimental Safety Vehicles*. Gothenburg, Sweden, May 1989.

## Variability of Results of the Same Test Conducted in Three Different Laboratories

---

**Bloch J., Cesari D.,**  
Inrets—LCB, France  
**Pullwitt E., Sievert W.,**  
BAST, Federal Republic of Germany  
**Lowne R., Robert A.,**  
TRRL, United Kingdom

### Abstract

Passenger protection in a side collision was investigated in numerous tests in different Laboratories. As for other studies and researches involving an international cooperation, results of tests are compared. The aim of this presentation is to investigate the validity of the result exchanges and in other words to look at the reproducibility of the same test conducted in different Laboratories.

INRETS, BAST and TRRL decided to conduct the same test in the same conditions and to compare the results. As these three Laboratories are involved in side impact protection research, this study was based on a full-scale side impact test against a Ford Fiesta according to ERGA conditions.

As a result of the investigation, it can be stated that some differences occurred because of the accumulation of differences between the technical parameters required for the test performance.

Nevertheless, the main conclusion is that the protection criteria were not exceeded in the three Laboratories.

### Introduction

The protection of passengers in private vehicles involved in a side collision is an important aspect of vehicle safety

research. A directive which will establish a test procedure for vehicles to be licensed in Europe is at present being drafted by the ERGA SAFETY GROUP of the European Community. The principal marginal conditions of this test were considered as early as 1982 by the Working Group 6 of the EEVC (1).\*

Numerous vehicle and barrier tests were carried out in order to test these parameters. Representative smaller vehicles as well as vehicles from the upper medium class were used in test series conducted by the BAST, INRETS, TRRL and by other Laboratories, especially the car manufacturers. These tests were particularly conducted for developing the structure of the deformable barrier front and the EUROSID (EUROpean Side Impact Dummy).

The aim of this work is to investigate the importance on the results of the technical differences for conducting tests in different Laboratories. To carry out this investigation, the BAST, the INRETS and the TRRL decided to conduct the same full-scale side impact test in the same conditions and to compare their results.

### Test Conditions

For these tests, one popular vehicle type has been chosen, namely the Ford Fiesta.

The vehicle was subjected to a side impact test (only full vehicle test) according to the ERGA Safety draft directive (Document ERGA S65 Amendment 1) as shown on figure 1.

Two tests were carried out by the BAST (tests SKW 1, SKW 3), one by INRETS (test BFL 01) and one by TRRL (test X 7).

\*Numbers in parentheses designate references at end of paper.

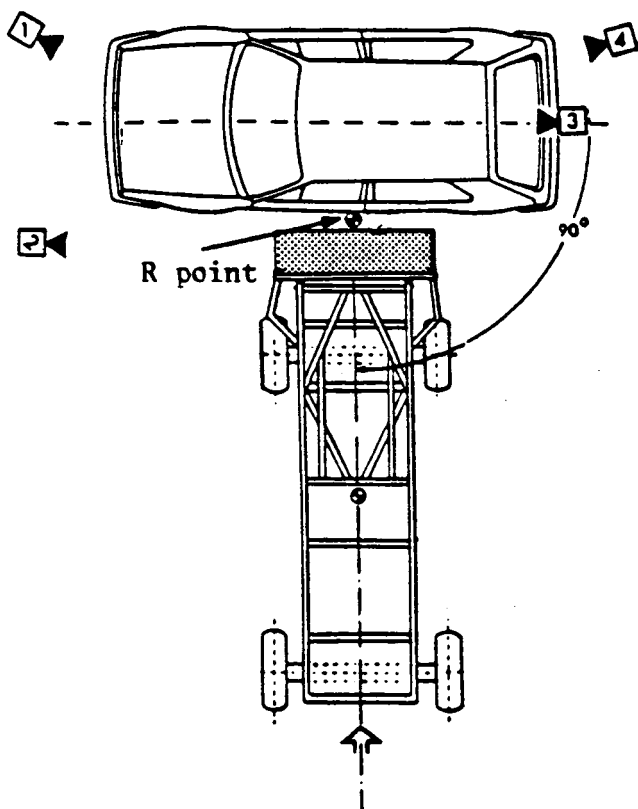


Figure 1. Test configuration according to the ERGA directive.

The test conditions were:

- The vehicle to be tested was stationary and was hit on the left at an angle of 90° by a movable deformable barrier travelling at a speed of 50 km/h.
- The impact point in relation to the longitudinal centre plane of the barrier was the R-point of the test vehicle.
- The mass of the vehicle to be tested corresponded to the unladen weight plus dummy weight.
- The deformable front face of this barrier was 500 mm high, 1500 mm wide, and had a ground clearance of 300 mm. The elements manufactured by Kenmont (GB) corresponded to the stiffness and energy dissipation requirement laid down in the above-mentioned ERGA document.
- A dummy was placed only in the driving seat.
- As measurements were a little different from one laboratory to the others. In table 1 are summarized these measurements on the test vehicles and in table 2, the measurements on the dummy.
- On the Ford Fiesta, the residual deformations are measured along three lines drawn on the external side panels as mentioned in figure 2.

## Acquisition and recording of measured values

Certain parameters for the measuring of dynamic processes in the field of impact test measuring techniques

Table 1. Measurements on the vehicles in the three laboratories.

	BASt	TRRL	INRETS
triaxial acceleration at centre of gravity	X		X
two door accelerations in impact direction	X		X
non impacted side accelerations			
- base of A post		X	
- base of B post		X	
- top of B post		X	
inner lateral deformation			
dynamic	X	X	
static		X	
outer lateral deformation			
dynamic		X	
static	X		X

Table 2. Measurements on the dummy in the three laboratories.

	BASt	TRRL	INRETS
triaxial head acceleration	X	X	X
triaxial thorax acceleration - T1	X		X
uniaxial thorax acceleration - T1		X	
uniaxial thorax acceleration - T12	X	X	X
rib acceleration in three ribs	X	X	X
deflection of three ribs	X	X	X
abdomen contact switches	X	X	X
triaxial pelvic acceleration	X		X
uniaxial pelvic acceleration		X	
forces on ilium - right	X	X	
left	X	X	X
force pubic symphysis	X	X	X

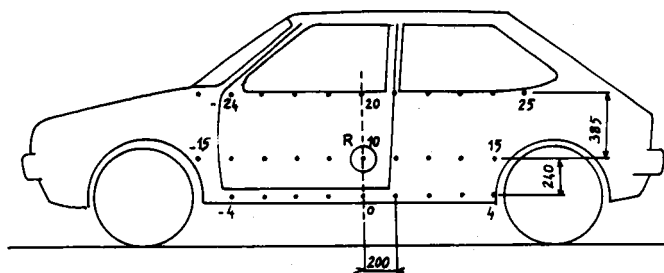


Figure 2. Position of the measuring points to establish residual lateral deformation.

are laid down in the ISO 6487 (1980), e.g., filtering (CFC—Channel Filter Class) and signal magnitude (CAC—Channel Amplitude Class). No such regulations exist for the sort of acquisition technique to be used (e.g., whether piezoresistive or piezoelectric transducer) nor for the means of data transfer and recording.

Caused by the minimal number of fixed parameters in this ISO-regulation, different characteristics of transducers and the use of differing measuring chains could lead to different progressions in case of rapid events.

Since protection criteria mentioned below allow a comparison between different Laboratories, some relevant

data concerning the measuring and evaluation techniques used must be considered:

- The type of transducers for forces and acceleration.
- Filtering and sampling of individual measured values depending on measuring position.
- The data transfer techniques.

## Test Results

The front structure of the barrier demonstrated good deformation behaviour, with no large undeformed pieces detaching themselves. The deformation of both the vehicles and the barriers front faces were very similar in all tests.

## Vehicles behaviour

All Ford Fiestas suffered severe deformation on the left side which consisted of a deep intrusion into the A-pillar and wind-screen frame, side door and B-pillar and into the rear third of the wheel house. The deformation at the three measurement planes, seen in figure 3 make this clear.

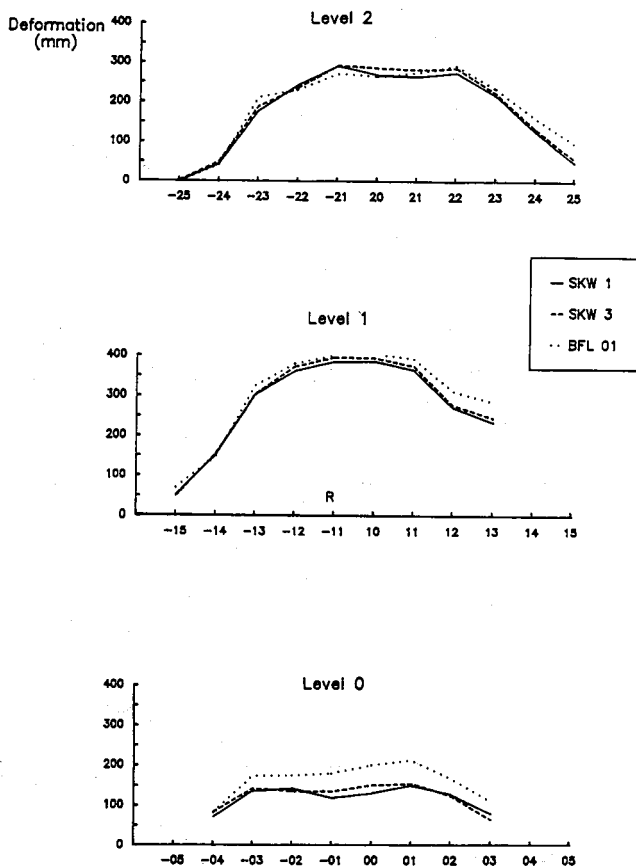


Figure 3. Residual vehicles deformations in the three measuring planes for the two tests conducted by the BAST (SKW 1 and SKW 3) and the one conducted by INRETS (BFL 01).

Graphic representation also shows that in these tests the reproducibility of the deformation by the deformable barrier face was very good, even if we can note a difference on level 0 between the BAST tests and the INRETS one. This

difference may be due to a light offset in the relative positions between the front face of the barrier and the side door-sill of the vehicle.

In addition to the known negative effects for the passenger of the deep deformation in the passenger cell, additional dangers were presented in the form of sharp edges, resulting from the displacement and breakage of interior fittings, e.g., steering wheel, dashboard and seats, and jammed safety belts, hindering escape from the vehicle.

In a further comparison of the behaviour of the vehicles in an impact situation, figure 4 shows the speed progressions of the barrier, the Ford Fiesta and its left side door. The measurement of acceleration at the door was taken approximately in the dummy's thorax impact area.

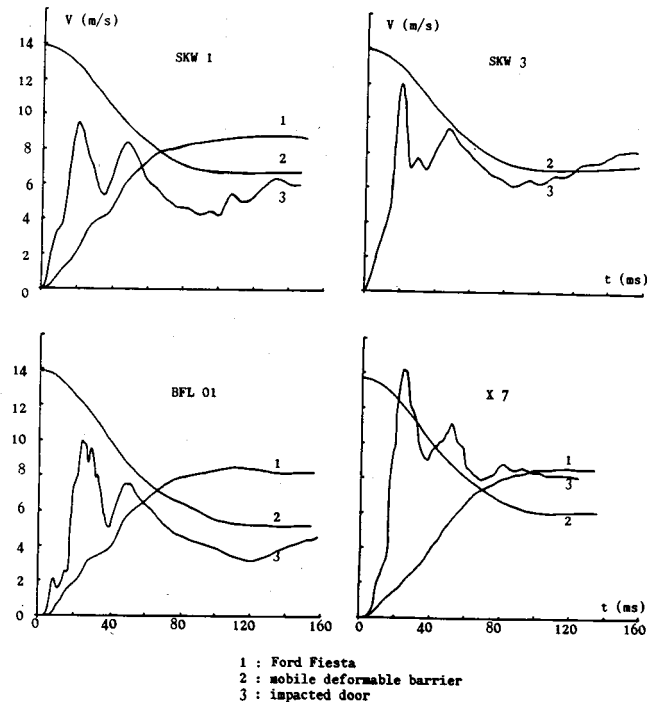


Figure 4. Speed variations during the four tests.

A comparison of these curves shows that, with the same test parameters and very similar vehicle damage, different speed changes can be measured at the vehicle door. One reason is that the acceleration measured in the door of the test vehicle is dependent on the impact of the barrier outside and the dummy inside. Since the outside impact was similar in the tests, the different rate of door acceleration in two tests must have been the result of a slight deviation in the dummy's positioning and seat height above the ground. Despite these clear differences in door acceleration, there were no significant differences in the dummy loads.

The load values measured on the cars are presented in table 3.

## Dummy loads

The measured values of dummy loads and the protection criteria deduced from these loads are listed in table 4.

Beside the observance of protection criteria following the

**Table 3. Vehicle load values in the four tests.**

VEHICLE LOAD	BAST		TRRL	INRETS
	SKW 01	SKW 03	X 7	BFL 01
<b>BARRIER</b>				
a <sub>max</sub> (g)	14.2	14.3	15.3	17.9
a <sub>(0-50 ms)</sub> (g)	7.4	7.1	-	10.0
V <sub>(t=100ms)</sub> (m/s)	7.2	6.7	9.3	10.2
<b>FIESTA</b>				
a <sub>max</sub> (g)	26.8	-	-	32.5
a <sub>(0-50 ms)</sub> (g)	12.5	-	-	11.4
V <sub>(t=100ms)</sub> (m/s)	8.4	-	-	8.4
Door :				
a <sub>max</sub> Door (g)	111.0	171.5	215.6	150.0
a <sub>(0-50 ms)</sub> Door (g)	16.6	10.6	21.8	15.5
V <sub>max</sub> Door (m/s)	9.6	12.1	14.1	10.0

**Table 4. Dummy load parameters in the four tests.**

DUMMY LOADS	BAST		TRRL	INRETS
	SKW 01	SKW 03	X 7	BFL 01
<b>HEAD</b>				
a <sub>y</sub> / a <sub>y3ms</sub> (g)	70/48	69/54	-	38/34
a <sub>res</sub> / a <sub>res3ms</sub> (g)	91/64	82/64	- /81	42/40
HIC	448	758	275	247
<b>THORAX</b>				
T1: a <sub>y</sub> / a <sub>y3ms</sub> (g)	93/83	85/75	80/	57/53
a <sub>res</sub> / a <sub>res3ms</sub> (g)	94/84	87/76	-	58/54
SI	740	744	-	333
<b>RIBS: a<sub>y</sub>max (g)</b>				
upper (g)	145	126	150	93
mid (g)	186	163	145	101
lower (g)	178	171	132	82
T12: a <sub>y</sub> max (g)	126	117	114	92
<b>Thoracic Trauma Index (TTI)</b>				
upper rib (g)	134	121	132	93
mid rib (g)	156	140	130	97
lower rib (g)	152	144	123	87
<b>RIB DEFLECTION</b>				
upper rib (mm)	28.0	35.0	33.5	30.5
mid rib (mm)	30.5	33.5	31.0	35.5
lower rib (mm)	30.5	32.5	28.0	26.5
<b>Viscous Criterion (VC)</b>				
upper RIB (m/s)	0.51	0.71	0.46	0.54
mid RIB (m/s)	0.54	0.63	0.48	0.65
lower RIB (m/s)	0.64	0.72	0.47	0.39
<b>ABDOMEN</b>				
Force > 4.5 kN	no	no	no	no
<b>PELVIS</b>				
a <sub>y</sub> / a <sub>y3ms</sub> (g)	99/91	104/97	121/114	120/113
a <sub>res</sub> / a <sub>res3ms</sub> (g)	101/92	107/99	-	121/115
illum crest				
left (kN)	1.9	2.7	2.5	2.0
right (kN)	0.6	0.6	-	-
pubis symphysis (kN)	7.3	8.1	11.2	-

EC draft directive other values used for determining the protection criteria are also considered here.

The protection criteria to be measured on EUROSID are as follows:

(Draft directive ERGA side impact documents S 65 Rev. 2a.)

- Head protection criterion (HPC)

HIC ≤ 1000, this value is only used as a criterion in the case of head contact with a part of the vehicle.

- Thorax protection criterion (TPC)

None of EUROSID's three sets of ribs may suffer deflection greater than or equal to 42 mm, and the Viscous Criterion based on the chronology of the deflection progress must be ≤ 1.0 m/s.

- Protection criterion for the abdomen

In this area, the force from an impact must be ≤ 4.5 kN, i.e., the switches with a switching threshold of > 4.5 kN must not respond. At the same time, the maximal crushing must be maximum to 30 mm.

- Protection criterion for the pelvis

Forces were measured at three points of the pelvis: at the left and right ilium and at the pubic symphysis. Forces must be maximum 10 kN;

As was expected, the dummy loads resulting from this crash behaviour were overall very similar.

Unlike the loads on the thorax and pelvis, the head load in the side collision test is highly dependent on the position of the dummy. The position laid down for the tests rarely resulted in the head hitting the rigid B-pillar. In the case of the vehicles tested here (figure 5), it was generally the glancing impact against the roof which led to notable head acceleration. The dummy kinetics and the relatively late contact meant the impact was no longer as powerful as in the lower parts of the body fixed in the seat. In no test the limit value of the head protection criterion (HIC 1000) was exceeded.

Concerning the thorax load, the protection criteria (deflection ≤ 42 mm and VC ≤ 1 m/s) were fulfilled in both tests. If we look at the rib deflections, the maximum values are very close. The major difference which is only 7 mm is observed at the upper rib between tests SKW 1 and SKW 2. If we consider the VC values we can note some differences from one test to another but overall the limit of 1.0 m/s were fulfilled in the four tests.

At the pelvis level, the load values on the left iliac wing are very similar as the whole shape of the curves whereas the force on the pubic symphysis is over the limit of 10 kN in the TRRL test. This is in the four tests the only value which is over the protection criteria limits proposed by the ERGA directive but we know the pubic force transducer is now subject to modifications in order to improve its signal reproducibility.

Beside the protection criteria of the EC draft directive, the values for the thorax area include the acceleration of the thoracic vertebra, measured in the upper and lower sections (T1 and T12), and the acceleration of the ribs. The mean values of rib and lower thoracic vertebra accelerations from the thorax load criterion favoured by the NHTSA, the Thoracic Trauma Index (TTI). If the TTI protection criterion was used to judge the results of these tests, except in the INRETS test, the values exceed the limit. This value, in-

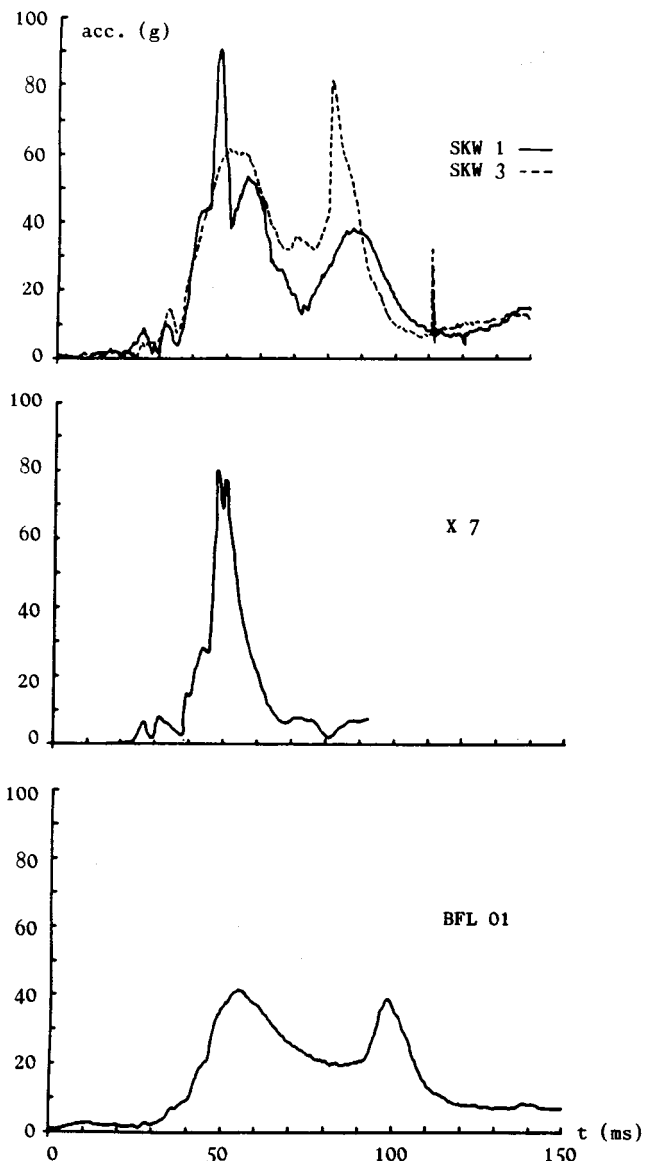


Figure 5. Resulting head accelerations in the four tests.

tended to prevent injuries greater than AIS 3, is quoted in (2) as 80–115 g.

For the pelvis the acceleration measured at the centre of gravity may be used as a protection criterion, too. In the US proposal (2) a protection criterion is quoted for the pelvis which considers the maximum acceleration. The range of limit values there is given as 130–190 g. The pelvis loads in the tested small cars were lower.

## Conclusion

Passenger protection in a side collision was investigated in four experiments with a Ford Fiesta in three different Laboratories.

The results of the measurements taken on the vehicles and dummies have been presented, and the damage and load mechanics explained.

As a result of the investigation, it can be stated that even if we observed some variations in the results, the small vehicle selected comply with the specifications of the directive drafted by the ERGA-S working group, except for one pubic symphysis force. This fact that all three Laboratories observed the same tendencies about the overall behaviour of the vehicle is the most important result.

Nevertheless, it can be stated that differences were observed and we have to try to explain the reasons of this. These reasons can be classified in six categories: the laboratory parameters, the vehicles structures, the relative positions of vehicles, the position of the dummy, the reproducibility of the dummy behaviour, the transducers and measures recording techniques.

By laboratory parameters, we consider especially the ground surface aspect which can influence the vehicles kinematics. On another hand, even if the definition of vehicles is the same in all Laboratories, the vehicles can be not exactly identical. This is true for the mobile barrier but especially for the impacted vehicle; if the model is the same, the "histories" are different and it is difficult to evaluate the influence of the age and of the servicing on the structure. The condition of tires is also an important parameter for the car kinematic.

Concerning the dummy, its position on the driver seat depending of the seat itself and of the installation procedure can be origin of variations when measures are compared because the interior deformations on the whole lateral intrusion area are very localized and contacts points with the dummy can vary from one test to the other. Moreover, as the EUROSID is still in an improvement phasis, the three dummy used in the four experiments described in this paper were a little different and we know, for example, that the pubic force transducers had a non satisfactory behaviour. This can explain on one hand the deflection of the measurement in the INRETS test and on the other hand the overpassing of the limit in the TRRL test.

Finally, the results are very dependent on the transducers and on the measures recording techniques and we can recommend Laboratories to precise it when comparing the results.

In conclusion, it can be stated that comparisons of test results between different Laboratories are valid but that a maximum of parameters described above must be explicit especially when results are near the criteria limits.

## References

- (1) European Experimental Vehicles Committee (EEVC). Structures Improved Side Impact Protection in Europe 9th ESV—Conference, Kyoto, Nov. 1982.
- (2) Department of Transportation—NHTSA. Notice of Proposed Rulemaking on Side Impact Protection Federal Register, Vol. 53, N° 17, Jan. 1988.

# Influence of Driving Speed of Side Impacted Vehicle on Dummy Loading

Eberhard Faerber,  
Bundesanstalt für Strassenwesen

## Abstract

Nine side impact tests with two moving subcompact cars (Volkswagen Rabbit) were conducted. The speed of the impacting vehicle was always 50 km/h. The speed of the impacted vehicle was set to 20, 30 and 40 km/h—each configuration was tested three times. The impact point was as defined in NHTSA NPRM on side impact. On the driver seat an US-SID and on the rear seat an Hybrid II dummy were positioned.

## Introduction, Aim of the Study

In the United States as well as in Europe in recent years side impact fatalities account for about 30 percent of all occupant fatalities (1, 2). About two thirds of all side impact fatalities are due to vehicle-to-vehicle side impacts. Because of the large number of fatalities and injuries which continue to result from side impact crashes NHTSA published (January 21, 1988) a Notice of Proposed Rulemaking (NPRM) on side impact protection (2) to amend to FMVSS 214 (Side Door Strength). The proposed amendments require an additional test in which the car is struck in either side by a moving deformable barrier simulating another vehicle. The moving deformable barrier is a steel structure with a 259 cm wheelbase, with 160 cm track width, and has two aluminum honeycomb blocks on the front to simulate the energy absorption characteristics of a striking automobile.

By using the National Crash Severity Study (NCSS) data, NHTSA determined the median speed of all side impact accidents (42 km/h striker/ 21 km/h struck), and the median speed of the serious injury accidents (56/28 km/h). Based on its analysis of accident data and its judgement about the threshold speed of serious injury accidents, NHTSA tentatively decided that the threshold speed of serious injury (48,3/24,1 km/h  $\hat{=}$  30/15 mph) is the most appropriate test speed to be simulated.

In Europe namely by the Committee of Common Market Automobile Constructors (CCMC) and by the European Experimental Vehicles Committee (EEVC) standard side impact test procedures with moving deformable barriers were developed too. The proposed speed configuration of the European draft regulations is 50 km/h for the impacting car while the struck vehicle is at rest.

Two competitive regulation proposals differ among other items in an essential parameter: the driving speed of the struck vehicle whose safety performance has to be examined in a legal test. To clarify the effect of this discrepancy the aim of this study was to investigate the influence of driving speed of the side impacted vehicle on vehicle and dummy loadings.

## Test Method

The BAST is participating in the work of EEVC to develop a standardized side impact test procedure. Many different test series were carried out to assess and decide on specific test parameters. Some exemplary studies shall be mentioned: side impact dummy comparison (3), influence of impactor shape, stiffness and mass (4) and testing and assessing the EEVC deformable element (5). Depending on the goal of the investigation always different test procedures had to be applied. Because there could not be kept a global concept for the main test parameters, it was decided to establish the test configuration for the presented study close to the procedure of NPRM on side impact.

The left front edge of the striking vehicle impacted the struck automobile 940 mm (37 in) forward of the center of its wheel base. Both test vehicles were Volkswagen Golf Rabbit. Because there is no information available about the behaviour of existing deformable elements under lateral loading, for the striking object an automobile of the same type as the struck car was selected.

The impact speed of the striking vehicle was always 50 (–0,8) km/h. The driving speed of the target vehicle was 20, 30 and 40 km/h at the moment of impact. The longitudinal centerlines of the test cars were perpendicular to each other. The test weight of the automobiles was their curb weight (795  $\pm$  5 kg). The car's own brakes were activated at the instant of impact.

As the height of the middle of the bumper of the striking car was 485 ( $\pm$ 10) mm and the ground clearance of the left side of the struck vehicle was 210 ( $\pm$ 15) mm, the bumper and the longitudinal frontal beams of the striking car could override the left side sill of the target car.

In the target vehicle two dummies were seated: on the driver seat an US-SID and on the rear seat behind the driver a Hybrid II dummy were positioned. The front seat was moved 50 mm forward from the rearmost position. Front seat back angle was adjusted at 25°. Distances between the dummies and the car interior were kept constant. The main distances were measured to:

shoulder/side structure		pelvis/side structure
driver dummy	95 $\pm$ 5 mm	150 $\pm$ 10 mm
passenger dummy	95 $\pm$ 5 mm	160 $\pm$ 10 mm

The front seat dummy was belted. The dummies were equipped with the provided transducers.

The standard crash test propulsion system of the BAST consists of a regulated engine which drives an endless cable. For the impact tests with two moving cars a second propulsion system was coupled to the endless cable, see figure 1. At the endless cable section moving to the collision point the striking vehicle was coupled. At the cable section moving in the other direction a second cable was coupled. The second cable was pulled from a cable drum on which a sufficient length of cable was wound up. A gear with

adjustable transmission ratios (2:5, 3:5 and 4:5) was connected with the first and a second cable drum. On the second cable drum a third cable was wound up which towed the target vehicle to the collision point.

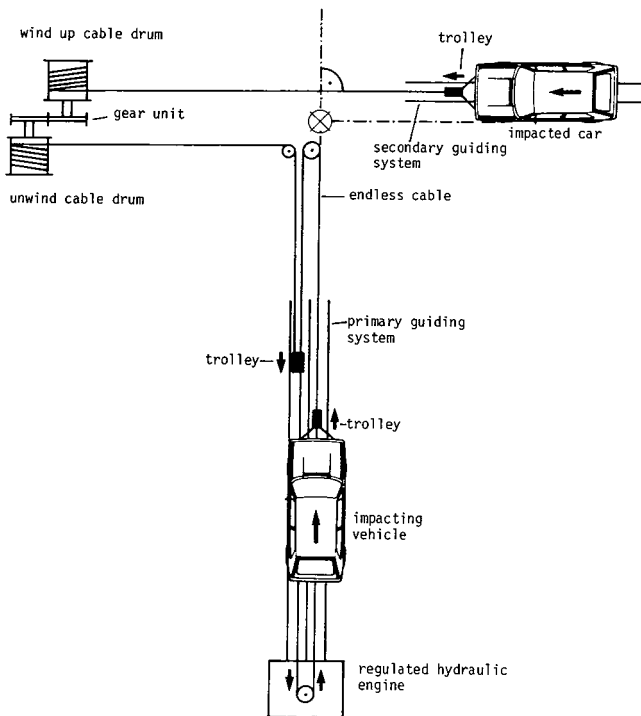


Figure 1. Propulsion system for the test vehicles.

## Test Results

In the following tables the test data are summarized. Mostly 3 ms accelerations were analysed because other characteristic values as peak acceleration, pulse duration, average acceleration and instants of special events showed a higher scatter or lower tendencies with the different test configurations. Overlooking the figures even for the 3 ms values the high scatter of results is evident. For some parameters there seems to be an in- or a decrease of measuring values with increasing collision speed for most of the other not. For statistical analysis of the test data the Spearman ranking correlation method (6) was applied and the Spearman correlation coefficients ( $r_s$ ) with ties and their significance values (SIG) were calculated.

The Spearman coefficients can lie between  $-1$  and  $+1$ :  $-1$  means full degressive (negative) and  $+1$  means full progressive (positive) correlation. Coefficients higher than a value of about  $|0,6|$  (depending on the number of tests) indicate a statistical correlation between the dependent (dummy loading) and the independent (target vehicle speed) parameter of the 5% error probability level (SIG < 0,05). Only some parameter showed a more or less weak positive or negative correlation with the driving speed of the impacted vehicle.

To evaluate the effect of the increase of this driving speed from 20 to 40 km/h linear and non linear regression analysis were performed.

But due to the low number of test results per parameter and the high scatter of the data, the calculated factors of quality of regression were poor. Furthermore the influence of driving speed of the target vehicle on the dummy loadings was very low, usually substantially lower than the scatter of measuring data at a certain test speed configuration.

Therefore, it is not useful or should be done with great care to apply the evaluated regression equations to predict dummy loadings for a specific test configuration from dummy loadings which were measured in different test configurations.

## Vehicle measurements

At the vehicles accelerations and residual deformations were measured. The desired impact point was met with greater accuracy at lower speeds of the struck car (from 0,0 to + 6 [+forward] cm at 20 km/h, from  $-1,5$  [-rearward] to 14,0 cm at 30 km/h and from  $-9,5$  to 19,5 cm at 40 km/h).

The most essential vehicle related test results are summarized in table 1. The location of the target points at the struck car, whose intrusions were measured are defined in figure 2.

For the striking vehicle the scatter of measuring values was considerably higher. With increasing speed of the struck vehicle the front of the striking car was bent further to the left (4–6 cm). The mean longitudinal deformation of the striking car was nearly unchanged in all test configurations.

Concerning the lateral residual intrusions (depth and shape) of the impacted automobile no tendencies could be found. The presented data are restricted to the target points close to the driver dummy. In figure 3 the intrusions at levels 1 and 2 are illustrated. There was no influence of driving speed on velocity as well as duration of intrusion of the side structure.

For the accelerations of the impacted car, correlations and linear regressions (see table 1A) were calculated. Regarding longitudinal accelerations weak, regarding lateral accelerations, practically no correlations were found.

The presented data and the observed car rotations during the collision as well as the final car position lead to the conclusion that the increasing speed of the struck vehicle is preferably transduced into skid (rotatory, translatory) motion and to a lesser extent transduced into deformation forces.

## Dummy loadings

For all presented data correlation and linear regression analysis were performed.

Again it shall be emphasized that the statistical calculation procedures were formally applied although the number of tests is very low and the applicability on crash test data cannot be tested and proven.

## Head

In side impacts head accelerations, summarized in tables 2 and 2A, are of less importance. The very low HIC-values support this statement. Except for the x- and y-components of passenger head no influence of the speed of the struck

Table 1. Measurements on the impacted car.

Test Nr.	Velocity (km/h)	Car accelerations		Car Intrusions at target point					
				level 1			level 2		
		$a_x/3ms$ (g)	$a_y/3ms$ (g)	- 11	10	11	- 21	20	21
1	20	- 5,3	- 12,6	303	329	353	209	238	264
2	20	- 5,8	- 11,9	372	398	421	258	280	300
3	20	- 4,2	- 11,5	269	285	306	198	217	250
4	30	- 4,9	- 14,3	317	309	318	259	264	239
5	30	- 4,7	- 11,0	317	318	311	195	200	203
6	30	- 4,9	- 10,3	296	295	298	200	211	225
7	40	- 6,2	- 14,2	287	294	298	190	204	198
9	40	- 6,1	- 15,7	288	294	289	186	188	185
11	40	- 6,3	- 13,2	267	280	254	243	214	181
$r_s$		0,6351	0,5270						
SIG		0,033	0,072						

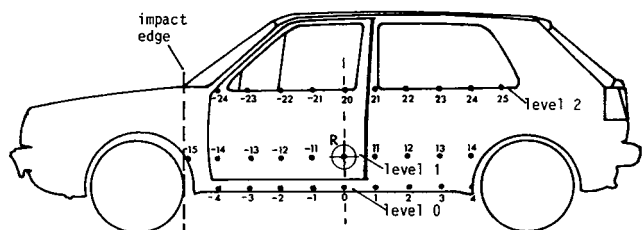


Figure 2. Location of target points to measure the residual intrusion of the struck car.

vehicle was found. In x-direction there is an increase in y-direction there is a decrease in the 3 ms values. For the resultant accelerations these effects neutralized each other.

### Thorax

In all tests summarized in tables 3 and 3A the 3 ms-accelerations were close to but remained below the 60 g/3 ms limit. A very weak progressive influence of speed can be observed in c.g. x-acceleration of the US-SID on the driver seat. Surprisingly a degressive effect on LURI (left upper rib)-acceleration can be observed, which however is nearly completely vanished in the TTI (thoracic traumatic index). The interpretation of this result might be found in the construction of the thorax of the SID.

The statistical analysis of the rear passenger dummy data indicates a progressive correlation between struck car speed and thoracic accelerations, but the variances in the different parameters are very high. It should be remembered that the rear seat dummy was a Hybrid II type.

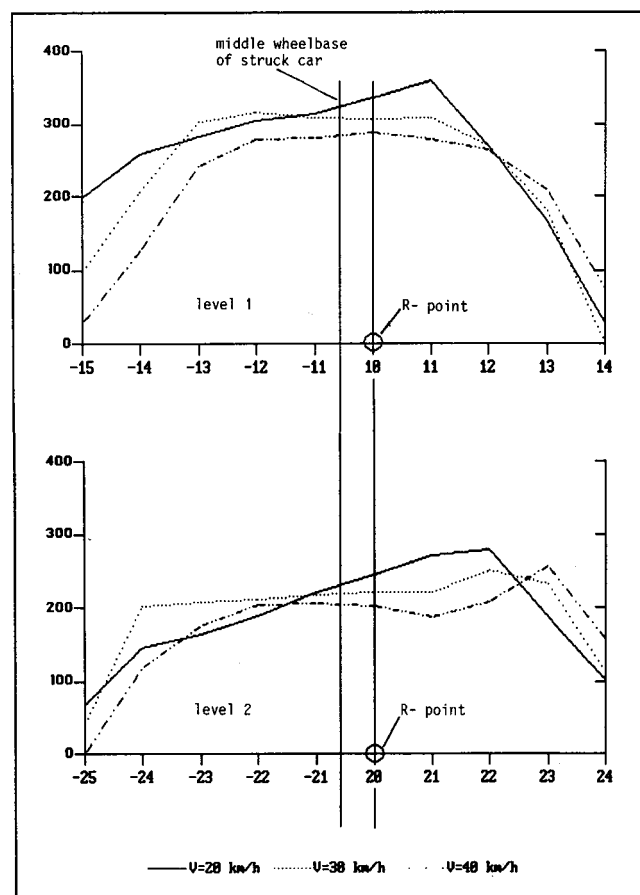


Figure 3. Residual intrusion of struck car at two levels: level 1—dummy pelvis, level 2—dummy thorax.

Table 1A. Linear regression equations of side impacted car 3ms-accelerations.

Parameter	Constant (SD)*	Slope (SD)	· v*	r <sup>2</sup>
Driver a <sub>x</sub>	= 3,7 (12,5)	+ 0,06 (0,03)	· v	0,40
ay	= 9,2 ( 1,9)	+ 0,12 (0,06)	· v	0,34
Pass. a <sub>x</sub>	= 3,7 ( 0,8)	+ 0,06 (0,03)	· v	0,40
ay	= 9,2 ( 1,9)	+ 0,12 (0,06)	· v	0,34

\* dimensions: (g), v in (km/h), SD = Standard Deviation

Table 2. Head accelerations.

Test Nr.	Velocity (km/h)	Head, Driver				Head, Rear Passenger			
		a <sub>x</sub> /3ms (g)	a <sub>y</sub> /3ms (g)	a <sub>res</sub> /3ms (g)	HIC	a <sub>x</sub> /3ms (g)	a <sub>y</sub> /3ms (g)	a <sub>res</sub> /3ms (g)	HIC
1	20	- 9,1	-20,4	27,3	140	- 4,4	- 39,1	41,5	75
2	20	-10,1	-21,9	29,4	171	- 5,0	- 58,1	58,5	155
3	20	- 8,7	-22,3	31,8	155	- 6,0	- 43,2	44,3	102
4	30	-14,6	-16,6	29,8	136	- 20,3	- 28,4	39,1	91
5	30	-30,9	-35,5	48,3	214	- 10,6	- 36,3	38,7	69
6	30	-14,6	-21,5	30,2	161	- 16,7	- 26,5	34,0	65
7	40	-14,3	-17,8	27,9	145	- 50,6	- 9,1	50,1	103
9	40	-19,8	-18,3	31,5	184	- 27,4	- 13,0	35,0	98
11	40	-15,4	-23,0	28,5	170	- 31,0	- 34,0	48,1	255
	r <sub>s</sub>	0,6880	-0,2108	-0,0572	-	0,9487	-0,8433	- 0,1581	-
	SIG	0,020	0,293	0,446	-	0,001	0,002	0,342	-

Table 2A. Linear regression equations of head 3ms-accelerations.

Parameter	Constant (SD)*	Slope (SD)	· v*	r <sup>2</sup>
Driver a <sub>x</sub>	= 4,5 ( 8,3)	+ 0,36 (0,27)	· v	0,21
ay	= 24,7 ( 7,5)	- 0,09 (0,24)	· v	0,02
a <sub>res</sub>	= 31,9 ( 8,7)	- 0,01 (0,28)	· v	0,0002
Pass. a <sub>x</sub>	= -27,7 ( 9,7)	+ 1,6 (0,31)	· v	0,78
ay	= 74,1 (12,0)	- 1,4 (1,39)	· v	0,66
a <sub>res</sub>	= 48,8 (10,5)	- 0,19 (0,34)	· v	0,04

\* dimensions: (g), v in (km/h), SD = Standard Deviation

Table 3. Thorax accelerations.

Test Nr.	Velocity (km/h)	Thorax, Driver						Thorax, Rear Passenger		
		$a_x/3ms$ (g)	$a_y/3ms$ (g)	$a_{res}/3ms$ (g)	LURI/3ms (g)	RURI/3ms (g)	TTI*	$a_x/3ms$ (g)	$a_y/3ms$ (g)	$a_{res}/3ms$ (g)
1	20	-15,7	-47,7	49,4	-70,3	-50,7	61,9	-6,3	-17,3	18,8
2	20	-9,4	-43,1	44,3	-60,9	-58,4	40,2	-8,1	-9,9	9,9
3	20	-13,3	-47,0	50,1	-58,8	-51,3	57,7	-5,6	-18,3	19,0
4	30	-7,5	-48,5	49,3	-37,1	-39,9	41,8	-6,7	-27,0	29,8
5	30	-11,3	-55,9	57,2	-52,8	-52,5	57,4	-11,1	-**	-
6	30	-12,3	-**	-	-43,5	-48,6	-	-30,1	-22,0	30,7
7	40	-38,3	-12,0	38,9	-49,4	-50,0	33,4	-22,8	-27,7	28,2
9	40	-25,0	-47,6	49,3	-48,2	-59,2	52,2	-22,5	-34,0	40,3
11	40	-19,0	-55,4	58,8	-50,5	-67,5	59,3	-15,1	-23,3	32,0
	$r_s$	0,5798	0,1260	-0,0317	-0,6325	0,2108	-0,2520	0,7379	0,8819	0,8189
	SIG	0,051	0,383	0,470	0,034	0,293	0,274	0,012	0,002	0,006

\*  $TTI = 0,5 \cdot (LURI + TH12Y)$ , FIR-Filter 100 Hz

\*\* defect

Table 3A. Linear regression equations of thorax 3ms-accelerations.

Parameter	Constant (SD)*	Slope (SD)	$\cdot v^*$	$r^2$
Driver $a_x$	= - 5,1 ( 9,8)	+ 0,73 (0,32)	$\cdot v$	0,43
$a_y$	= 56,1 (18,5)	- 0,38 (0,59)	$\cdot v$	0,06
$a_{res}$	= 48,1 ( 8,8)	+ 0,05 (0,28)	$\cdot v$	0,009
LURI	= 73,3 (10,6)	+ 0,70 (0,34)	$\cdot v$	0,38
TTI	= 57,9 (14,2)	- 0,25 (0,46)	$\cdot v$	0,05
Pass. $a_x$	= - 5,9 ( 9,2)	+ 1,67 (0,29)	$\cdot v$	0,43
$a_y$	= 2,7 ( 5,8)	+ 0,66 (0,19)	$\cdot v$	0,68
$a_{res}$	= - 0,31 ( 6,9)	+ 0,88 (0,22)	$\cdot v$	0,72

\* dimensions: (g), v in (km/h), SD = Standard Deviation

### Pelvis

The highest loadings were observed in this dummy region. Very weak correlations exist between driving speed of struck car and pelvis x-accelerations of both the driver and the passenger dummy. Again the high scatter of test data is obvious.

### Summary and Conclusions

Nine side impact tests with two moving automobiles (Volkswagen Golf Rabbit) were performed. The impact speed of the striking car was always 50 km/h. The struck car was moving in perpendicular direction at 20, 30 and 40 km/h.

h. Each test configuration was repeated three times. Impact configuration was similar to NHTSA New Proposed Rulemaking for side impact testing.

The increasing speed of the struck car is predominantly transduced into rotatory and translatory motions of the involved vehicles and to a lesser extent transduced into deflection forces.

Although the resulting speed of the test configuration was increased from about 54 (50/20-configuration) to 64 km/h (50/40-configuration—energy plus 41%) and the angle of the speed vector of the side impacted vehicle shifted from about 22 to 39 degrees, there was no influence of the driving

Table 4. Pelvis accelerations.

Test Nr.	Velocity (km/h)	Pelvis, Driver			Pelvis, Rear Passenger		
		$a_x/3ms$ (g)	$a_y/3ms$ (g)	$a_{res}/3ms$ (g)	$a_x/3ms$ (g)	$a_y/3ms$ (g)	$a_{res}/3ms$ (g)
1	20	- 8,2	-86,7	88,6	- 9,4	- 35,9	36,1
2	20	- 9,3	-103,5	104,2	- 5,9	- 39,0	40,1
3	20	-11,2	-82,1	82,6	- 17,0	- 53,2	55,1
4	30	-25,8	-83,2	88,8	- 25,6	-103,8	119,5
5	30	-21,3	-98,6	101,3	- 20,4	-*	-
6	30	-11,2	-83,3	84,5	- 18,7	- 89,0	89,6
7	40	- 9,8	-84,3	85,1	- 27,0	- 78,0	84,7
9	40	-25,9	-87,7	93,9	- 20,7	- 74,3	81,4
11	40	-12,5	-103,9	104,2	- 16,4	- 24,0	41,9
	$r_s$	0,5557	0,2117	0,2117	0,6325	0,1890	0,4410
	SIG	0,060	0,292	0,292	0,034	0,327	0,137

\* defect

Table 4A. Linear regression equations of pelvis 3ms-accelerations.

Parameter	Constant (SD)*	Slope (SD)	$\cdot v^*$	$r^2$
Driver $a_x$	= 88,7 (12,5)	+ 0,05 (0,4)	$\cdot v$	0,003
$a_y$	= 5,3 ( 9,0)	+ 0,33 (0,29)	$\cdot v$	0,15
$a_{res}$	= 88,7 (11,6)	+ 0,13 (0,37)	$\cdot v$	0,02
Pass. $a_x$	= 2,0 ( 6,9)	+ 0,53 (0,22)	$\cdot v$	0,45
$a_y$	= 38,0 (37,6)	+ 0,80 (1,21)	$\cdot v$	0,07
$a_{res}$	= 30,2 (37,7)	+ 1,28 (1,21)	$\cdot v$	0,16

\* dimensions: (g), v in (km/h), SD = Standard Deviation

speed of the side impacted vehicle on the loadings of the driver dummy (US-SID). For the rear seat dummy (Hybrid II) in some parameters there was a significant tendency of increasing dummy loadings with increasing driving speed. In all test configurations the pelvis accelerations were high. All other dummy loadings remained well below the known performance criteria limits.

## References

- (1) D. Otte, et al.: Erhebungen am Unfallort Unfall- und Sicherheitsforschung Straßenverkehr BMV/BAST, Band 37, 1982.
- (2) National Highway Traffic Safety Administration, 49 CFR PART 571, Docket No. 88-06, Side Impact Protection Notice of Proposed Rulemaking.

(3) Glaeser, K.-P.: Lateral Dummy Comparison Testing 9th International Technical Conference on Experimental Safety Vehicles (ESV), Kyoto, 11/1982.

(4) Sievert, W., Pullwitt, E.: Lateral Protection of Passenger Cars Comparison Tests by Means of Different Barrier Configurations Proc. of the 27th Stapp Car Crash

Conference San Diego, 1983.

(5) Sievert, W., Pullwitt, E.: Movable Deformable EEVC-barrier for Side Impact 11th ESV Conference 1987, Washington, D.C.

(6) L. Sachs: Angewandte Statistik 6. Auflage, Springer Verlag, Berlin, Heidelberg, New York, Tokyo, 1984.

## Developments in the Simulation of Side Impact

---

**M.G. Langdon,**  
Transport and Road Research Laboratory,  
United Kingdom

### Abstract

Simulation models of side impact have been developed as part of the basic research aimed at understanding the mechanisms by which injuries are caused, and the methods by which car design can be improved to minimise injuries. Early simulation models were based on experimental tests in which cars were hit by rigid impactors. These models represented the side structure of the target car by a single mass/spring element. However, analysis of tests, using both mobile deformable barriers and cars as impactors, have shown that this simple model provides a poor representation of reality. When a car side is hit by a non-rigid impactor, there is considerable relative movement of the different structural components, such as the sill, the A and B posts, and the door. The way in which this relative motion occurs, particularly between the door and the sill, can have a considerable effect on occupant injuries. It is essential that these motions are properly represented if a simulation is to be effective. The paper discusses ways in which a simulation can model these complex motions, both in terms of the car structure and of its interaction with the occupant. The paper also describes some of the difficulties in obtaining adequate calibration data for the dynamic model from quasi-static tests. The present stage of development of simulation at TRRL is described, together with results from a set of quasi-static crush tests on one car model. It concludes that much has been learnt from using simulation models as a complement to dynamic tests, but that current models are far from being able to provide a complete substitute for full scale impact tests.

### Introduction

Since the early 1970s there has been an increasing interest in the development and use of computer simulation models to investigate various problems relating to occupant injury in side impact accidents (1, 2, 3, 4, 5, 6)\*. Three main objectives can be identified: basic research to complement results from full scale impact tests, design aid for manu-

facturers to help develop better car structures, and most recently as a possible regulatory test to replace full scale impact testing (7).

Most of the models use simple lumped component systems (masses, springs, dampers) to represent the complex structures of real car bodies. Models of this type were originally developed for the simulation of frontal impact, where it is much easier to identify the significant components involved in the structural response to the impact. The dynamics of side impact are more complex, and in the development of models to represent the problem there has been a continuing conflict between the desirability to simplify as much as possible, and the necessity of adding further components to the model to give a sufficiently complete representation of the real world phenomena. Simplification has been most apparent in the representation of the occupant, which has frequently consisted of a one-dimensional thorax only, either completely rigid, or possibly with a single mass/spring/damper system to represent a rib. However, some recent models have added a pelvic section to give a more complete representation. It is possible to use a complex linked rigid body model to represent an occupant, as with the Calspan CVS (8) and Madymo (9) programs, but there are problems in linking such models to the vehicle sub-model, and such linkage has been rare.

The development of adequate side-impact models must at present be regarded as incomplete, and much work remains to be done before they can be regarded as standard development tools, rather than as research undertakings in their own right. This paper reviews some aspects of the present state of the art in model development, with particular reference to current work at the Transport and Road Research Laboratory (TRRL). The paper first sets out the requirements of models developed for different objectives. The structural system to be modelled is next described, with particular emphasis on aspects which it is felt important to include in a model. A section on methods available for simulation is followed by a discussion of the problems of data collection for model calibration, including a description of recent quasi-static crush tests carried out by TRRL. Finally there is a description of the present stage of development of models at TRRL, and a discussion of the

problems encountered in trying to correlate the model with the results from full scale impact tests (10, 11).

## **Objectives of Simulation**

### **Research**

The most fruitful use of side impact simulation so far has been as a research tool to improve understanding of the mechanisms of injury causation. A side impact on to a vehicle structure, which intrudes inwards and injures an occupant, is an extremely complicated process, much of which is not open to observation in a full scale impact experiment. The use of simulation enables data to be obtained on the motion of any part of the structure which is represented in the computer model. Furthermore, it is possible to repeat simulation experiments with controlled alterations in any desired parameters (e.g. input speed, initial gap between occupant and door, stiffness of the sill structure) without the confounding effects of inevitable small variations in results between supposedly identical full scale tests. Such additional tests are also, of course, far cheaper than additional full scale tests. At TRRL the use of simulation has helped in understanding various effects seen in full scale tests, even though the absolute values of some of the simulation outputs has differed from the full scale test results. (Such differences in turn have suggested inadequacies in the simple simulation model.)

Simulation of the occupant has also improved understanding of some of the mechanisms of injury within the body, and in the future might help to decide which injury criteria are most relevant to the prediction of injuries of people in real accidents.

### **Design**

There are at present no "obvious" ways of designing cars to meet the requirements for side impact protection in tests of the type being proposed by the European Experimental Vehicles Committee (EEVC) (12) and the National Highway Traffic Safety Administration (NHTSA) (13). Past attempts to improve side impact safety in research vehicles by overall strengthening of the structure have usually not been very successful. It appears that a rather sophisticated approach to improvement is necessary, with the emphasis being on obtaining the correct relationship between the stiffnesses of various parts of the structure, rather than just on the absolute level of stiffness.

With the impending introduction of side impact test regulations, manufacturers need to be able to predict the side impact performance of a new vehicle at a relatively early stage of manufacture, so that major changes are unlikely to be required when a complete vehicle is finally tested. Probably the best way in which such predictions can be made is by computer simulation. The stiffness data required for input to such a simulation could be obtained either from component tests, or possibly by some form of finite element analysis of the body structure. The latter poses difficulties, as the analysis has to remain valid whilst the materials are deforming

plastically rather than elastically, and elements undergo changes in orientation during folding of the collapsing structure.

It may not be necessary for such design purposes that the simulation should give results which agree exactly with those from full scale impact tests, as engineering judgement could be used to "adjust" results in the light of previous experience. However, the car would still have to pass a regulatory test before being marketed; the objective of the "design aid" simulation is to minimise the probability that it would fail such a test.

### **Regulatory tests**

A recent development has been the proposal that a simulation model could be used as a regulatory test, in place of a full scale impact test. The input data describing the car structure would be obtained by a quasi-static crush test on a complete car body (14). The proposal could have considerable advantages for a manufacturer, if a body-in-white for the crush test were adequate and could be provided at an earlier stage of development than the complete car necessary for a full scale impact test. In this case more time would be available to overcome problems. The principal requirements for use in regulatory testing are that the method of collecting input data should be well defined and straightforward, and that the model output should have been shown to be an accurate representation of full scale impact test results for a wide range of verification tests. This poses severe problems for simulation modelling in comparison with its use for research or as a design aid, since on the one hand more consistently accurate output results are required, while on the other hand the acquisition of data for input needs to be simpler, with no scope for the use of "engineering judgement".

An open question, not yet resolved, is whether validation of such a test procedure would require the results to provide a good fit to full scale impact results for a wide range of car and occupant parameters, or only in terms of criteria which are used to judge whether the vehicle has passed or failed the test, such as peak values of injury criteria. Unless the model can show agreement with full scale tests over a wide range of parameters, and with reasonable correspondence of event times, it is difficult to see how it can be extrapolated with confidence to test new car types for which there is no previous experience of the results of dynamic impact. Impact tests of previously untried car types at TRRL have frequently produced surprises of some sort, which could only have been predicted by a very sophisticated model.

## **The System to be Modelled**

### **Interactions between structure and occupant**

The effects of a frontal impact on a car occupant are simpler to simulate, as the occupant is fairly remote from the direct effects of the impact on the car structure. The main loadings on the occupant are through the seat and harness (and/or airbag) systems which are attached to relatively

undistorted parts of the structure, although some account has to be taken of intrusion into the passenger compartment of objects affecting occupant contact. Moreover, the motion of the occupant within the passenger compartment has only a small effect on the overall motion of that part of the car structure, so for many purposes the occupant simulation can be completely decoupled from the vehicle simulation. In the use of Calspan CVS or Madymo simulations it is common to assume a "vehicle deceleration" pulse, which is completely independent of occupant motion, to describe the motion of the passenger compartment.

In side impact the situation is completely different. The occupant is in close contact with the part of the car structure which is directly involved in the impact. The main loadings on the occupant are from the door, and possibly from the B-pillar in some cars. These components have a rather complex motion relative to the rest of the car structure, and are themselves likely to be deforming whilst in contact with the occupant, so that different parts of the structure loading the occupant can have significantly different motions. These relative motions between different parts of the intruding structure are thought to have a significant effect on occupant injuries.

The door inner skin and B-post are relatively light, and can under some circumstances strike the occupant when they have no large mass behind them (e.g. if there is a "bounce" away from the impacting object after the initial impact). In such a case the mass of the occupant is comparable with that of the intruding car structure and can have a significant effect on its motion. The dynamic systems of the car structure and the occupant are therefore closely coupled.

If the simulation is to give an accurate picture of the effect on occupant motion (and hence on injury) of various differences between car structures, it is necessary to model all these interactions in some detail.

## Contact points

In full scale side impact tests, contact between the occupant and the vehicle structure is observed for the head, thorax, abdomen, and pelvis. Contact also occurs on the thigh, and injury to the femur is a factor in real accidents, but there is little knowledge of the loading involved as a suitable load measuring dummy leg has not yet been developed.

Arms are not a major cause of injury in real accidents (though the struck-side arm can provide useful padding for the chest if it happens to be interposed between the chest and the door). In side impact tests using the European Side Impact Dummy (EUROSID) the arms are extended and kept high (hands on the steering wheel) and are thought to play little significant part in the impact dynamics. They are not included in most side impact simulations.

The head is not normally involved in the initial impact, though serious injuries can occur when its subsequent motion causes it to strike the header rail, or some other part of the car side. Its precise motion is rather unpredictable, and although measurements of head acceleration are always

taken in side-impact tests, these should be supplemented in regulatory tests by impacts with a special headform on a range of possible areas of contact. It appears that reduction of head injuries will depend largely on the provision of suitable padding in possible contact areas, and it seems unlikely that changes in the design of car side structures will by themselves have much influence on head injuries. Head contact and motion has therefore been omitted from current side impact simulation models.

This leaves the current areas of interest for contact as the thorax, abdomen and pelvis (with the thigh as a possible area of interest for loading the pelvis).

Early side impact models have concentrated on the thorax since, together with the head, this is the most important area of injury in accidents. Most models have considered the thorax in terms of a single point contact, with one-dimensional motion of the thorax masses. In models of the Calspan CVS and Madymo types, contact between the car structure and occupant thorax can be represented in terms of the intersection between a plane (door) and ellipse or ellipsoid (thorax), with the contact force determined by the amount of overlap. This does not provide a very good representation of the rather complex dynamics of thoracic rib structures, and most models use more detailed mass/spring/damper systems for this purpose. These have normally included two masses, a light one to represent the ribs and a larger one to represent the spine; it is generally assumed that most of the soft tissue mass in the thorax is concentrated at the spine. Connection between rib and spine is through a spring and viscous damper, though the TRRL models use a second spring in series with the damper to give viscoelastic damping, as in the actual EUROSID dummy (15, 16). For simplicity it is usual to include only one rib in the simulation, with the mass, spring, and damper parameters factored to represent all the ribs in a dummy (or human occupant). This may be too much of an oversimplification, as it is known that in full scale impact tests injury parameters can differ significantly between top, middle and bottom ribs of the dummy. However, the inclusion of additional ribs to provide two or three contact points on the thorax would also require further sophistication in the vehicle structure model.

The abdomen has been largely ignored in simulation, as it has normally been assumed that sufficient information can be obtained by studying the thorax and pelvis. This might be plausible if the only part of the abdomen to be considered were the relatively thin segment of the "soft abdomen" between the bottom floating rib and the pelvis. The "thorax" of a side impact dummy like EUROSID, however, only represents the upper ribs which encase the lungs and heart. The "abdomen" represents the part of the body containing the liver and spleen, most of which is enclosed by the lower ribs and is quite stiff. It is therefore able to transmit significant force from the impacted surface to the spine. A model representation of EUROSID which only includes the upper thorax (EUROSID rib structure) and pelvis is unable to transmit sufficient force to the thoracic spine to generate the magnitude of spinal acceleration observed in full scale im-

pact tests. An adequate representation of a dummy occupant may therefore have to include the abdomen as a contact point with the vehicle. This raises questions about the effect on bending and rotation of the dummy torso by these multiple contact points; this problem is discussed later in the paper.

Pelvic injuries, although not as frequent a cause of fatality as thoracic injuries, are important. It is therefore desirable that a simulation should include the pelvis and estimate the magnitude of suitable pelvic injury parameters. Recent work at TRRL (10) has also suggested that the magnitude and timing of impact loads on the pelvic area can have a significant effect on the value of thoracic injury parameters, giving further reason for including pelvic contact in the model. The pelvis itself is a fairly rigid structure, apart from the padding provided by skin and subcutaneous tissue over the bony protrusions. Pelvic contact is included in most recent simulations. It can be modelled in terms of a direct force to the spine, without the complications required for modelling the thorax. However the form of connection that should be included between the pelvic spine and the thoracic spine is not yet clear. The simple shear connection included in some models may not be sufficient to show the correct interactions between pelvic and thoracic motion.

It is possible that in some side impact situations there may be significant direct loading into the spine by the seat back. The magnitude of such loading has not been established, and seat/spine contact is not yet included in any simulation models.

### **Door tilt and structural interactions**

If a sophisticated occupant model with multiple contact points is necessary to simulate all the relevant phenomena observed in full scale tests, it is necessary to provide an equally sophisticated model of the car structure to interact with that occupant model. The most obvious aspect visible in a crashed vehicle is the tilt of the door in a vertical plane, with intrusion frequently being greater at the waistline than lower down. Results of full scale crash tests at TRRL suggest that there is a correlation between the final tilt angle of the door (variation of intrusion with height) and the severity of occupant injury; a vertical door indicates lower injury than a tilted door. This can be partially explained in terms of load spreading; a vertical door loads all the contact points evenly, while a tilted door concentrates the load on one contact point, producing severe injuries at that point. However, this does not necessarily describe the whole story, as final tilt angle does not necessarily correlate exactly with tilt angle in the early stages of impact when the occupant injuries occur. It is an unfortunate fact that there is at present very little knowledge of just how a door intrudes into the passenger compartment during side impact, as it is not currently possible to instrument a door in the places where it interacts with the dummy occupant. The present limited measurements which have been made are at a point ahead of the occupant, where the motion may be rather different. It is hoped to carry out tests at TRRL in the near future with an

unoccupied car, in which the door can be more fully instrumented. Although the motion in the absence of the occupant will not be quite the same as when an occupant interacts with the door, the experiment should throw some light on the complexities of door motion.

A fact which has been established is that at the door centre (in front of the occupant) there are major oscillations when there is side impact by a deformable barrier. After the initial impact the door "bounces" off the barrier, and can attain a speed significantly higher than the impact speed. In one car type impacts at 13.9 m/s (50 km/hr) have produced peak inner door speeds of over 18 m/s. As the door loses contact with the barrier face it is pulled back by the rest of the car structure, which has not reached this high speed, and decelerates down to quite a low speed. Typically this could be 6 m/s or less, reached at between 28 and 38 msec after the initial impact. The speed then rises again, and may oscillate several more times; the details can be very different for different types of car, or for different types of impactor. Although details of the door motion at the points of contact with the occupant are probably a little different, the broad picture is likely to be similar.

It has still not been possible to elucidate the exact connection between details of the door motion and the injury parameters measured by the dummy. However, factors which seem to be relevant include:

- (i) The door velocity at the first contact time.
- (ii) The effective mass behind the door in the early stages of contact. A high velocity contact by a light door is much less serious if the door is not in contact with the impactor, and is decelerating, than if it has the full mass of the impactor behind it.
- (iii) The amount the door has crushed at the moment of contact. In some cases it appears that the door was already fully crushed, with the outer and inner door skins in close contact, before contact with the occupant. In other cases there was still a gap between inner and outer skins, which effectively acted as padding, at the time of contact with the occupant. In these cases an imprint of the dummy was left in the inner door skin. Injury parameters were lower than would otherwise have been expected.

It appears from these observations that the motion of the door is rather complex, and that its relative motion compared with the motion of other parts of the car structure is an important factor in determining occupant injuries. For these reasons it was decided that the simulation model at TRRL should consider the sill, the A-pillar, the B-pillar, the door, and the "rest of the car", as separate components which can move relative to each other. This leads to considerable complications in the model formulation, and particularly in the difficult practical problem of obtaining the relevant "spring" stiffnesses between the various components. When a model has been developed which can accurately reproduce all the phenomena which are relevant to occupant injury, for a wide range of types of car structure, it may be

possible to simplify the model somewhat. However, any simplification made before all the implications are fully understood would be premature, and potentially dangerous if the model were subsequently to be used as a substitute for full scale dynamic testing.

It may be noted that if a rigid (or very stiff) barrier is used as the impactor, the whole side of the car tends to be constrained to move inwards as a single unit, with all components having a common velocity. In this case a simpler model could well be adequate to represent such an impact, but a rigid barrier would not provide a good representation of impact by another vehicle.

## Simulation Methods

### Lumped mass/spring systems

A car consists mainly of a fabrication of shaped steel pressings, with the mass and stiffness distributed throughout the structure. It also contains a few lumped masses, such as the engine, transmission, and suspension/wheels. An impact (i.e. a sudden change of velocity applied to one part of the structure) is propagated into the structure as a wave, or set of waves, which progress with finite velocity. (The propagation velocity, which determines how long it takes for a disturbance to reach distant parts of the structure, must not be confused with the velocity change which is transmitted. In an analogy with sound transmission, the propagation speed is the "wave velocity", while the actual velocity change which occurs in the structure is the "particle velocity".) In a real car structure propagation can be both by longitudinal waves, transmitted by compression of the material, and by transverse waves, transmitted by bending and shear. The wave velocity of the compression waves is so fast in metallic materials that for many purposes it can be considered as instantaneous, and so the effects of wave speed can be ignored, but the finite propagation time of the transverse waves can be significant in the context of impacts on cars.

It may be noted that by the use of Fourier transforms, the propagation of small amplitude waves through the structure can also be described in terms of a frequency response, called the Frequency Transfer Function. If the structure were different in that the mass was concentrated at a few points, instead of being distributed continuously, the higher frequencies would be considerably attenuated in the transfer function. This would alter the impulse response, and hence the response to an impact. However, the behaviour in quasi-static experiments is determined only by the very low frequencies in the transfer function, which would remain virtually unaltered by any change in mass distribution.

It would be difficult to model the transmission of impulse waves through something as complicated as a car body structure, even if the material behaved in a linear fashion (i.e. elastically, with no plastic deformation), and the disturbances were small (i.e. without significant buckling). In side impact accidents neither condition is satisfied, and

so a wave transmission model of the problem (using finite element techniques), though feasible in principle, would be excessively costly and time consuming and is not at present a practicable possibility. It is therefore necessary to develop a simpler model which can give an approximate solution to the problem at reasonable cost.

Finite element modelling divides the structure up into a large number of small elements, each of which is defined by its mass, and by the way in which it is connected to the neighbouring elements. Simplifying the simulation consists of enlarging the elements and reducing the complexity of connections, so that the end result is a model with a few large masses, interconnected by a small number of (usually non-linear) spring/damper systems. With proper design of the (non-linear) spring elements, such a model can still give an accurate representation of the transmission of forces between two points in the structure, provided the forces are applied slowly, as in quasi-static crushing experiments. However, the transfer function of such a model (to use the linear analogy) is deficient in terms of high-frequency response, and so the model becomes steadily less accurate in its representation of reality when the applied impulses become larger in amplitude and shorter in duration, as in a side impact crash. The art of simulation is to use the smallest number of discrete elements which give an adequate representation of reality for the particular purpose required.

The TRRL simulation includes a module which represents the response of a distributed parameter system, without the use of finite elements, by a direct representation of impulse waves within the module. This is only valid when the material is behaving linearly, and so can be used to represent (approximately) soft tissues within the occupant model, but is inappropriate for representing any parts of the car structure.

### Linked rigid body models

The lumped element models discussed above assume that the elements consist of point masses, which do not accommodate rotation. Although point mass models can have more than one dimension, only translational interactions can be represented, with no account being taken of rotation. In modelling the car occupant in side impacts, consideration of rotation is important because of the way in which rotational torques, as well as translational forces, control the interaction between the pelvis and thorax.

Acceleration measurements made at two different points on the spine (T1 and T12) sometimes show substantial differences, due to rotation of the thorax around the roll axis. This is not surprising, as force is applied to the thorax at a number of different locations. External forces are applied to the three separate ribs of the EUROSID dummy and to the abdomen. In addition there are reaction forces from the neck (connected to the head mass) and the lumbar spine (connected to the pelvis). The sum of the moments from all these forces around the centre of gravity of the thorax is unlikely to be zero. The effect of this rotation is to modify the lateral

motion of the spine at the level of the ribs, and hence to modify the injury parameters shown by those ribs.

Experience at TRRL suggests that a one-dimensional dummy model, using separate thorax and pelvis elements linked by a spring/damper shear element, may not be adequate to estimate injury parameters in the simulation. The TRRL model is currently being modified to include a two-dimensional simulation of the dummy, with linked segments to represent the pelvis, lumbar spine, thorax/abdomen (these are rigidly connected in EUROSID), neck and head. When the new model is developed, it will be possible to compare results obtained from it with those from the original one-dimensional model, and also with those from models with various intermediate levels of sophistication. It should then be possible to determine the form of the least complicated model which gives an adequate representation of real world tests.

The dynamics of the linked segments and their connecting joints are similar to those used in the two-dimensional versions of Calspan CVS or Madymo, but the contact points of the thorax will be represented by the same sprung rib with viscoelastic damping that is used in the current model, rather than by the intersecting ellipse/plane formulation available in the other linked segment simulation models.

It is possible that a full two-dimensional model may also be required to represent the rotation of the door in the vehicle sub-model, but this part of the model has not yet been fully developed.

### **Program organisation**

A simulation program is an exact mathematical analogue of a simplified physical system, which in turn is an approximate representation of the real world system which is being modelled. There are two main ways in which a program can be matched to a simplified physical system.

One is to write a general program which, in any particular case, is adjusted to conform to a particular physical configuration by the provision of a suitable set of data in a control file. This is the approach adopted by Calspan CVS and Madymo. Such a program is fairly flexible, in that it can easily be modified if changes are required in the underlying model, provided that such changes do not require programming facilities beyond those envisaged by the original program designer. They should be "transparent" in use, as although the actual programs are extremely complicated, all the data describing the system being modelled is clearly exposed in the data file. Disadvantages are that such programs require a lot of computer storage, and possibly running time, as they provide a lot of facilities which are not regularly required. They are useful for research purposes, but would be an unlikely choice for a simulation to be used for a regulatory test.

The alternative is to tailor a program precisely to fit a particular problem; i.e. the program is "hard wired". The disadvantage is that the program is inflexible, and has to be re-written by a specialist if any changes are required in the

underlying physical system. Such programs may, in practice, be rather "non-transparent". Unless a program has been written in terms of clearly defined modules, it can be difficult to see the correspondence between the coding and the problem being solved. However, they are economical in storage and running time requirements, since they should contain no unnecessary coding which is not used for the particular problem being studied. Such a program might be less useful as a research tool, but ideal for regulatory testing.

The simulation program suite being developed at TRRL is rather different from either of these alternatives. The basic programs are tailor made for each problem, and to simplify program writing and operation use the ACSL (Advanced Continuous Simulation Language) high level language. This provides a step-by-step integration facility, using either fixed length or variable length steps, and automatically carries out most of the organisation required for manipulation of the differential equations and initial conditions. It also provides powerful on-line facilities for repeating runs with modified values for any constants. A particular advantage is the provision of facilities for including user-written Macros and Fortran subroutines. The result is that it is possible to set up program modules, common to many programs, which can represent any particular building blocks in the overall simulation. These modules are stored in Macro and subroutine libraries remote from the actual program. They can be nested, so that it is possible to build up complex dynamic systems which require only a very limited amount of coding in the main program. For example, a single call statement could reference a Macro describing the EUROSID dummy, which in turn would reference modules describing the thorax, a single rib system, a spring with viscoelastic damping, and the skin covering the rib. Different versions of the dummy macro with different degrees of sophistication in the dynamic modelling are available in the library, and any one can be chosen simply by changing a single line of code in the main program. The main programs are relatively short, and are "transparent" to the user because of their basic simplicity. It is very easy to add modules to the library when new facilities are required. The whole system is versatile in use, and provides a useful research tool. Its very versatility, and the current need to use the ACSL Translator, would make it unsuitable as a simulation for regulatory purposes as it stands. However, it would not be difficult to "freeze" any particular model, and rewrite it as a Fortran program with the required subroutines and macros included in a single program unit.

### **The current stage of development of the TRRL model**

The TRRL simulation models are derived from an early side impact simulation developed at British Leyland (now Rover Group), for impact by a rigid impactor. This model was modified for use with a deformable barrier by adding a (non-linear) spring to the front of the original impactor (17). Although this program gave a useful insight into details of

the dynamics of side impact, it became apparent that it was not able to reproduce all the phenomena which full scale tests had shown to be important in determining injuries, and it was not giving correct results. The program has therefore been modified to include more detail of the dynamic processes, and further modifications are in progress to take account of results from quasi-static and dynamic impact tests. The intention is to continue modifications (mostly requiring increasing sophistication) until the simulation results give adequate agreement with full scale test results. When this has been achieved, further work will investigate what (if any) simplifications to the program are possible without seriously degrading the performance, in terms of agreement with full scale tests.

The current system reproduced by the simulation is shown in figure 1. The most significant improvement over the original version is the division of the barrier face into several areas with different stiffnesses, which contact different parts of the car structure. The specification for the EEVC barrier (12) defines six areas (figure 2), with four different stiffnesses. The current assumption in the model is that the three bottom barrier segments 1, 2, 3 all contact the sill, which is rigid so that all three segments compress together as a single unit, for which a combined force/deflection characteristic is applicable. It is assumed that the top side segments, 5 and 6, contact the A and B posts respectively, and the centre top segment contacts the door. This is an oversimplification, as in practice segments 5 and 6 will also contact the edge of the door, as will the top of segment 2, so further adjustment of the model may be required. The deformable elements in the barrier are represented in the simulation by "springs". As with most other non-linear springs for the model, these are defined by a table of force/deflection characteristics, which includes loading and unloading segments so that the relevant hysteresis characteristics can be provided. ACSL provides a standard routine for linear interpolation from these tables. The front of the deformable barrier face consists of an alloy sheet of low, but not negligible mass. This is included as a separate element only for the top centre segment 4, where a single mass represents the barrier front and the outer door skin (after contact). The initial gaps between the barrier front and the car structure can be set independently for the top and bottom of the barrier.

The sill is connected to the main mass of the car through a spring (deformable massless element) which represents the sill and floor pan structures, together with any relevant cross stiffening. Comparison between quasi-static and dynamic full scale tests suggests that the dynamic stiffness of the sill is considerably greater than the quasi-static stiffness, so this spring incorporates a dynamic magnification factor in the model, of the form:

$$F_D = F_S (1 + kV/V_R)$$

where:

$F_D$  = dynamic force of spring between sill and "rest of car".

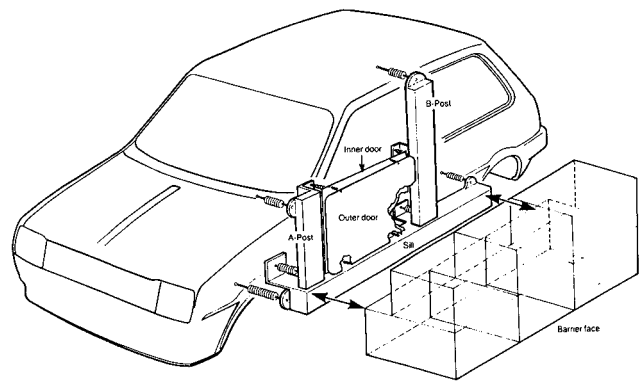


Figure 1. Car model for simulation.

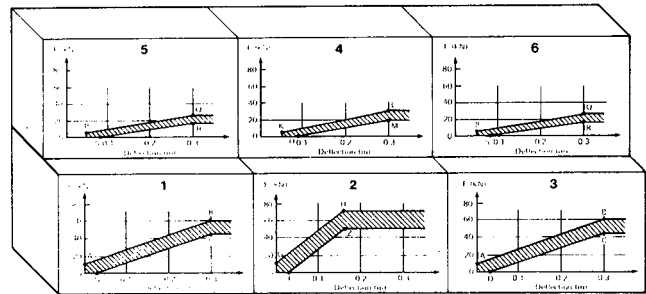


Figure 2. Segmentation of EEVC barrier, showing different stiffnesses.

- $F_S$  = static force estimated from force/deflection curve.
- $k$  = dynamic magnification factor.
- $V$  = compression speed of "spring".
- $V_R$  = reference speed (50 km/hr in this simulation)

In the current version of the model, which does not yet include a tilting door, the A and B posts are each represented by point masses connected by "springs" to both the sill and the rest of the car structure. Quasi-static crush tests, in which car bodies were loaded separately (in different tests) on the sill and on the mid points of the A and B posts, showed that the post forces and/or deflections could not be related solely to the relative motion with the sill. The A-post has a stiff connection to the rest of the car structure through the firewall and dash, while the B-post is less stiffly connected through the roof. The bending of the B-post is a complicating factor in this case. The next version of the model will probably have to include separate motions at two levels of the A and B posts, to provide an input for door tilting.

The "door" in the model represents the inner door structure of a real car, and is not directly impacted by the barrier front. Impact occurs on the outer door, from which loads are transmitted to the rest of the car structure through a spring connection to the inner door. This in turn transmits loads through springs to the sill, A-post, and B-post. In the next version of the model there will probably be connections to the A and B posts at two heights, to provide an adequate description of door tilt.

There is provision for dynamic magnification in all the springs connecting to the A and B posts and the inner and

outer doors, but it is thought that the need for them is likely to be much less here than for the sill-body connection, as deformation is mainly through bending rather than buckling. The magnifiers are therefore currently set to zero.

Loads are transmitted from the inner door to the dummy through two pads, which contact the thorax and pelvis. The load/deflection characteristics of the pads can be set to have any characteristics required by the user. The initial gap between the door pads and the occupant can also be set independently for thorax and pelvis.

The dummy thorax consists of a single rib structure, with spring/mass/damper parameters factored to represent the three ribs of EUROSID. The rib is covered by a pad representing the skin and subcutaneous tissue (represented by a covering of Sorbothane in EUROSID). In the present version the rib system is connected to the pelvis by a rigid spine, which can move laterally and rotate, but which does not include a shear element. This will soon be replaced by a more elaborate version which will have separate two-dimensional segments for the pelvis, thorax, and head connected by elements representing the lumbar spine and neck, with appropriate hinges at the joints.

The simulation can include the effects of tyre loads on the vehicle as it is propelled sideways, and of lateral belt loads on the occupant (using a very simple formulation), but it has been found that neither of these has much effect on the overall results.

## Data Input for Simulation

### Requirements

The main data inputs required for a dynamic simulation are the masses of each component which is separately represented, and the force/deflection characteristics of each "spring" which connects components. A two-dimensional simulation would also require the moment of inertia of any component which has rotational freedom, and a geometric description of the points of application of all forces, and their directions.

### Masses

It is very difficult to estimate the effective masses of the various "lumped" components within the car, defined in the simulation model. A real car body has a continuous structure without well defined boundaries between different regions, so any division in the model into separate lumped masses is artificial, and it is unclear where the boundaries should be placed. It is possible to estimate the actual masses of parts such as the door, but in practice some of the door mass may effectively be carried by adjacent structures, such as the B-post. As has been stated by Richter et al (7), it may be that the results are not very sensitive to variations in the mass of some components, since their motion is largely determined by effects from extraneous masses. So it may well not be necessary to attempt much precision in estimating masses, other than those for the large components such as the impacting mobile barrier (or car) and the main mass

of the impacted car. Probably the best way of estimating masses is to work back from the observed dynamic responses in one full scale test to estimate component masses under those test conditions, and assume that the equivalent component masses will be similar for other test conditions. It should also be possible to use such previous experience to derive factors for estimating the effective component masses for other car types. Similar comments apply to estimates of moments of inertia, where these are required.

Estimating the mass of dummy components is a great deal easier, as in this case most of the components can be dismantled and weighed.

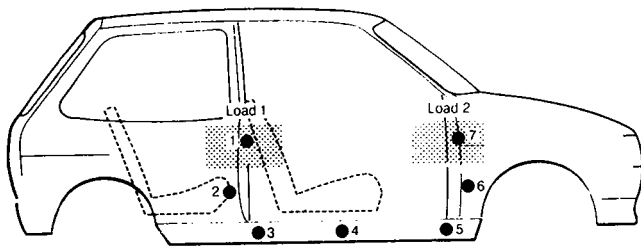
### Quasi-static crush experiments

The force/deflection characteristics of the various elements ("springs") connecting masses within the car structure have to be estimated by means of a "quasi-static" crush experiment. This requires the car body shell to be held stationary in a suitable rig, while loads are applied to various parts of the structure, and the corresponding deflections are measured at a number of points. The problem of holding the car stationary is not trivial, as it is important to do this in a way which does not significantly change any of the stiffnesses which are to be measured. This is much more difficult than for experiments relating to frontal impact. The solution adopted for tests carried out by TRRL was to support the full length of the sill structure on the "non-struck" side of the car by a pre-shaped block. The "non-struck" side suspension pick-up points were also held rigidly. The "struck" side suspension points were constrained vertically, to prevent any roll motion of the car, but in a way which applied no forces in a horizontal plane.

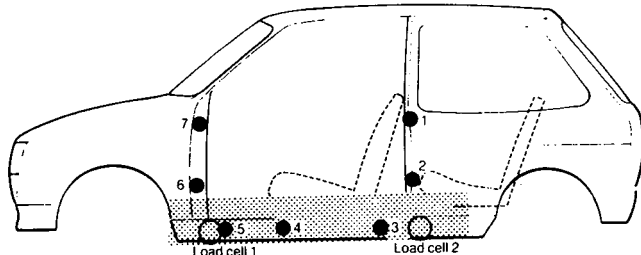
Loads were applied to the body through compliant blocks, to avoid local stress concentrations. The blocks were made of a similar material to that used for the deformable front of the EEVC barrier. Loading was applied by a hydraulic ram, which was controlled to produce a constant rate of movement, rather than an increasing force. Four separate tests were carried out in the TRRL experiments, to try to assess the relative stiffness of different parts of the structure. The location of the loading points is shown in figure 3.

Test 1 was intended to assess the stiffness of the A and B posts without a door, at the level of the upper part of the door. It had initially been assumed that the effect on each post could be considered independently of the loading on the other. This was found not to be strictly true, but the error is not serious. Deflections were measured at a number of heights on the A and B posts, and at several points on the sill (figure 3a). Deflections were also measured at corresponding points on the "non-struck" side. There was very little deflection on the non-struck sill, but rather more at the top points on the A and B posts on the non-struck side due to "lozenging" of the structure.

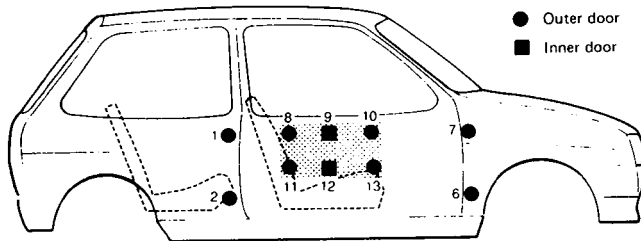
Test 2 (figure 3b) applied a load to the sill only, again without a door, and deflections were measured at the same points as in test 1. The deformable impactor was loaded at



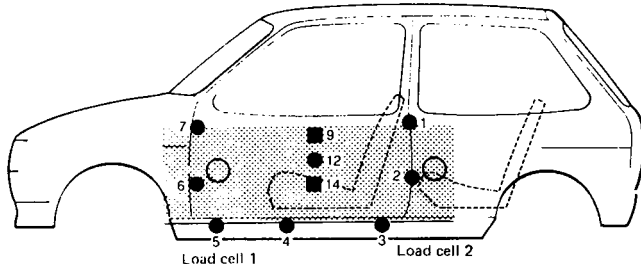
(3a) Test 1 - Load applied to A and B posts



(3b) Test 2 - Load applied to sill



(3c) Test 3 - Load applied to centre of door



(3d) Test 4 - Load applied through EEVC deformable barrier

**Figure 3. Quasi-static crush tests, showing area of indentors and location of deformation measuring points.**

two points, driven by the same hydraulic ram so that movement was the same, but with separate load measurements at each point.

Test 3 (figure 3c) applied a load to the centre of the door only. In this case the door deflection was measured at four points on the outer skin and two on the inner. Deflections were also measured on the A and B posts, but not on the sill.

Test 4 (figure 3d) used a complete EEVC deformable barrier face to load the whole side of the car. Deflection measurements were made on the A and B posts, the sill, and the door inner and outer skins. Two loading points were used, as for test 2.

No measurements were made of the deflection caused by loading the door from the inside, as in the CCMC composite test procedure. This would have been difficult in the test rig

used, and was not at the time expected to yield any additional information relevant to the development of the simulation model.

During the course of each test the load was periodically reduced to zero, so that deflection measurements could be made for an unload/reload cycle. This data was required in order that hysteresis cycles could be correctly modelled in the simulation. (This is necessary to provide adequate damping.) It was found that after the load had been re-applied the force/deflection curve followed on very closely from where it had been broken by the unloading phase. There is no reason to suppose that the overall force/deflection curve was any different from the one that would have been obtained if loading had been continuous. The slope of the force/deflection curve while unloading was very similar, for any particular measuring point, regardless of the amount of deflection before the load was removed. This suggests that a fairly simple model can be used to represent a hysteresis cycle.

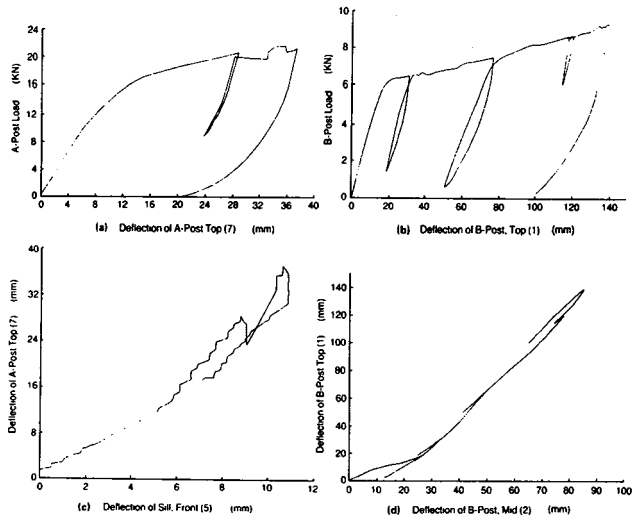
### Quasi-static test results

Some typical results from quasi-static crush tests are shown in figures 4-7. These are the raw results taken directly from the experimental data, apart from the corrections necessary to allow for the small whole-body motion measured on the non-struck side. This was measured, either at the centre of the sill when measurements were available (tests 1 and 2), or at the bottom of the A-post (test 3), or at the bottom of the B-post (test 4). The maximum corrections were less than 10 mm for tests 1, 2, and 3, and less than 20 mm for test 4. All the unload/reload cycles are shown.

The crush tests were essentially force driven, although in practice the large mass of the crush rig gave a reasonably steady strain rate. In the plots of force against displacement force is therefore actually the independent variable, and the various displacement measurements are the dependent variables. However, to conform with the usual method of displaying such data, displacement is shown on the horizontal axis and force on the vertical axis.

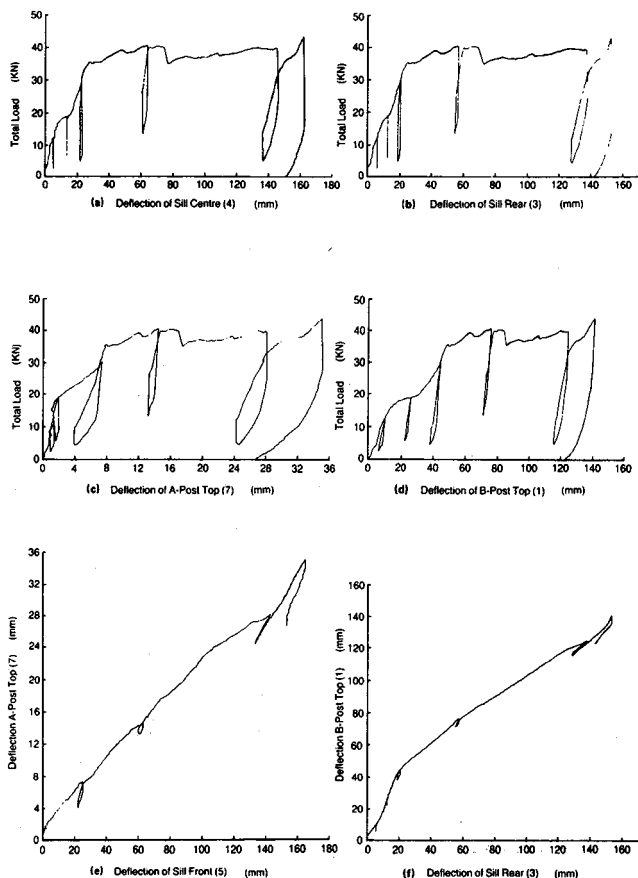
Figure 4 shows the force/deflection characteristics for the top (waistline level) of the A and B posts (figures 4a and 4b). The A-post is much stiffer as would be expected. When loads are applied to the top (waistline) of the A and B posts, there is also some deformation lower down, right down to sill level. There was some difficulty in interpreting the results, as in this experiment the A and B posts were loaded simultaneously, but it seems likely that almost all the sill deformation was due to the load on the A-post. The B-post is relatively so weak that it supports much less load, and all the deformation is taken up in the B-post itself rather than by the sill. Figure 4c shows the relationship between deformation in the A-post and in the sill, due to loading on the A-post at the waistline. Figure 4d shows the corresponding relationship between deformation at the B-post waistline, and half-way down to the sill.

Figure 5 shows the effects of loading the sill in test 2. Figures 5a and 5b show the relationship between total load



**Figure 4. Quasi-static test results—Test 1 (load on A and B posts). (Adjusted for motion of sill on non-struck side.)**

and deflections at the front and rear of the sill respectively. The curves are very similar, but there is slightly more deflection at the front. Figures 5c and 5d show the corresponding relationships between total sill load and deflections at the top (waistline) of the A and B posts respectively. Figures 5e and 5f show the relationships between deflection at the waistline and at the sill for the A and B posts respectively. This relationship is approximately linear for the A-post, but has a very pronounced change of slope for the B-post.



**Figure 5. Quasi-static test results—Test 2 (load on sill). (Adjusted for motion of sill on non-struck side.)**

Figures 6a and 6c show the relationship between load and deflection of the outer and inner doors respectively, when the door is loaded centrally (Test 3). These figures refer to the top of the door. Figure 6e shows the corresponding deflection at a lower point of the inner door; it is significantly less than for the top. Figure 6b shows the relationship between upper door compression and load, with compression being estimated by the difference between outer and inner door deflections. In the test it was not possible to measure inner and outer deflections at quite the same place (see figure 3c), so the difference in deflections is not quite the true compression. It will be seen that in this car the door is essentially squeezed flat at a compression of about 80 mm, so that even high loads can cause no further compression.

Figure 6d shows the relationship between deflection of the outer door and of the B-post at waistline level. Figures 6f and 6h show the relationship between load on the door and deflections of the B and A posts respectively. Figure 6g shows the relationship between load on the door and the difference between the inner door and B-post deflection. This curve was used to estimate the force/deflection characteristics of the door to B-post “spring” in the simulation model. A corresponding curve was derived for the A-post. This was of similar shape, but stiffer.

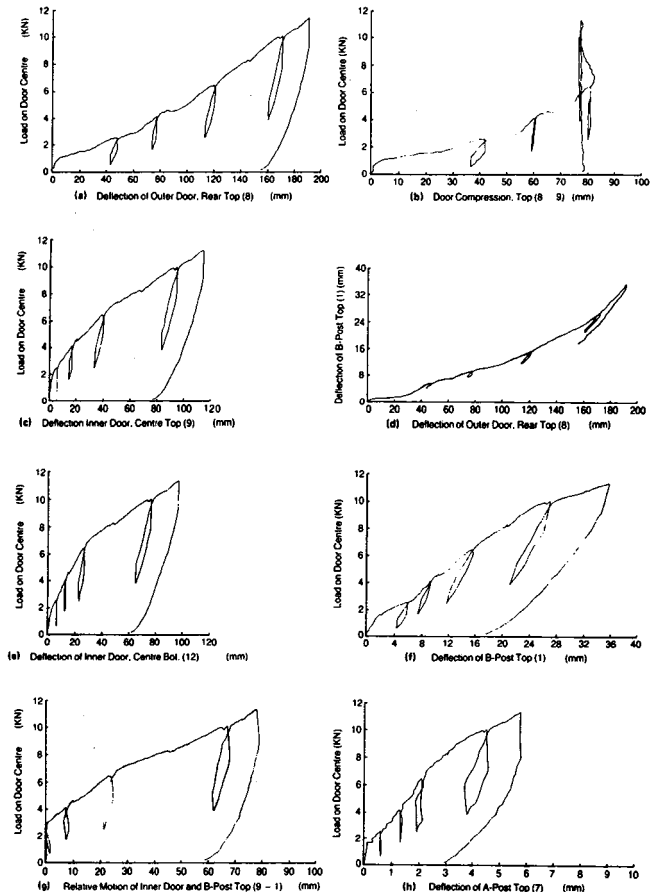


**Figure 6. Quasi-static test results—Test 3 (load on door). (Adjusted for motion of bottom of A-Post.)**

Figure 7 shows the effects of loading the car side with an EEVC deformable barrier face (Test 4). Figures 7a and 7c show the (total) force/deflection relationships for the outer and inner doors. Figure 7b shows the force/compression relationship for the upper part of the door, using deflection measurements for the centre outer door minus the upper inner door (see figure 3d). Figure 7d is the corresponding figure using the deflection of the lower inner door, showing a higher effective stiffness.

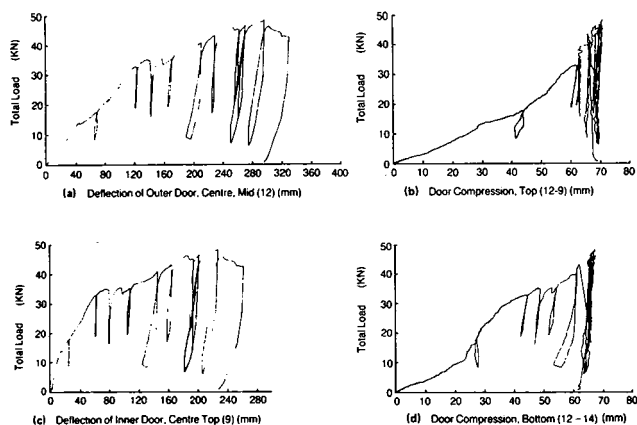


Figure 7. Quasi-static test results—Test 4 (EEVC barrier face). (Adjusted for motion of bottom of B-Post.)

### Interpretation of quasi-static crush data

In order to run a side impact simulation program it is necessary to be able to calculate the force on each mass element, knowing the relative displacements of all the relevant elements. If all the force/deflection characteristics were linear over the whole range of interest, this would best be done by the use of influence coefficients. In this case the force on each element is calculated as the sum of the products of each displacement with the relevant influence coefficient.

$$F_i = \sum_{j=1}^n k_{ij} u_j$$

where:

$F_i$  = Force on the  $i$ -th element

$\sum$  = Summation symbol

$k_{ij}$  = Influence coefficient on the  $i$ -th force by the displacement of the  $j$ -th element

$u_j$  = Displacement of the  $j$ -th element

Unfortunately, as has been shown in figures 4–7, the force/deflection characteristics are very non-linear, and the influence coefficient approach is not valid. An attempt has been made to estimate the force/deflection characteristics for the set of “springs” shown in figure 1. The sill spring characteristics were found directly from the results of test 2 using the sill centre deflections (intermediate between figure 5a and figure 5b). The A and B post spring characteristics were then estimated from test 1, and the door characteristics from the results of test 3. This produced enough data to set up a working simulation model, which is a good

enough approximation to reality to provide a useful research tool.

Interpretation has been complicated by the use of force as the driving factor in the crush tests, rather than displacement. This was necessary in the type of rig which was available, but in future tests it would be desirable to provide more loading points. These should be controlled directly in terms of displacement, with force (measured at the various loading points) being regarded as the dependent variable.

The current simulation model assumes that the characteristics of each spring depend on the deflection of that spring, and are independent of deflections elsewhere in the system. This may not be true in a complex non-linear system such as the side structure of a car, and further work is required to improve the force estimation sub-model. However, it may prove unnecessary to map the force/deflection characteristics for any arbitrary distribution of deflections across the structure, as data is only required for sets of deflections likely to be encountered in a side impact. This set must, however, embrace the conditions of a dynamic side impact. Because of inertia and rebound effects, this will not usually correspond closely with the sets of deflection measurements recorded in the whole barrier front quasi-static crush experiment of test 4. A developed version of the computer controlled composite test procedure (CTP) (14) might provide suitable data, using a number of rams, controlled for displacement, to load different parts of the structure.

### Dynamic stiffness effects

As explained above, the simulation model allows the inclusion of an empirically determined “dynamic magnification factor” to allow for the different stiffnesses observed in static and dynamic tests. The increase in stiffness under dynamic loading has several causes:

(i) The stress/strain relationship of most materials changes with different strain rates.

(ii) Structures are stiffened against buckling by “lateral inertia”. In order for buckling to occur, part of the structure has to move transversely to the direction of compression; at high strain rates this transverse motion is opposed by the inertia of this part of the structure.

(iii) The mode of buckling may itself change at high strain rates, again due to inertial effects.

A classic case of mode change occurs in the floor structure of a car. In a quasi-static crush, the floor tends to buckle over its entire width. However in a dynamic impact most of the buckling occurs between the struck side of the car and the tunnel, as the tunnel is constrained by its inertia so that the compression load is higher on the struck side than on the non-struck side of the floor (see figure 8). If the structure were being modelled in more detail, the floor structure should be shown as two springs, separated by a mass representing the tunnel.

An entirely different effect occurs in the deformable barrier front. In this case the foam plastic material is stiffer under quasi-static loading conditions than under dynamic

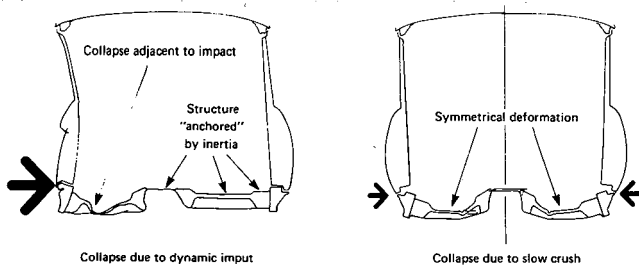


**Figure 8. Comparison of floor buckling under quasi-static loading and dynamic input.**

loading. The barrier front is designed to have the correct (specified) stiffnesses for its various segments under the conditions of dynamic loading at an initial speed of 50 km/hr. The material is not very speed sensitive in the range of speeds likely to be encountered in impact tests; it is in fact fairly uniform within a range of a decade either side of the test impact speed. The TRRL simulation uses the specified stiffnesses rather than any directly measured quantities, so the simulation should be a good representation of reality in this respect. However, there would be a potential problem if the stiffness of the barrier front were measured directly in a quasi-static test, and the result were then used, without correction, in an impact simulation. There may also be an effect on the distribution of loading across the car side in the quasi-static test, as the barrier face will be less compliant than under impact conditions.

## Results from Simulation

### Relationship to full scale impact tests

The development of simulation at TRRL has been very closely linked with work on full scale impact tests, and to date has been mainly used to improve understanding of details of the impact dynamics. There has been a clear symbiosis between simulation and full scale testing, with an information flow in both directions.

The simulation has indicated the likelihood of occurrence of various phenomena, which have then been investigated and found to occur in full scale tests. For example, the importance of door rebound, and subsequent velocity oscillations, was first observed in simulation, before suitable instrumentation had been developed for use in car impact tests. Simulation also highlighted the relative importance of structural modifications and padding, and was able to suggest suitable values of stiffness for the door padding.

These results were mainly qualitative rather than quantitative. There have been many discrepancies between simulation and full scale results when exact quantitative comparisons were made. These have been due to various inadequacies in the simulation modelling. Finding the cause of the discrepancies has invariably led to a better understanding of what really happens in full scale impacts. The representation of the car side structure by a number of separate mass elements was the first result of such observations. Other significant observations have concerned the

whole-car motion after impact, and spinal accelerations in the dummy.

### Car body motion—mass and dynamic magnification effects

The initial comparison between simulation and reality was made for the overall motion of the body shell, measured in impact tests by an accelerometer at the bottom of the B-post on the non-struck side of the car. The force on the body shell (i.e. the “rest-of-car” not directly involved in the impact) is largely determined by the motion and stiffness of the sill. This stiffness (sill to body) is probably the easiest to measure accurately in the quasi-static crush test, so if the simulation is to give any reasonable representation of reality, it should be able to make a good prediction of this motion.

The results of a full scale crash test were analysed to estimate the equivalent mass of the car, by assuming that all the mass was concentrated at the bottom of the non-struck side B-post, and applying the laws of conservation of momentum to the car and the impacting trolley. The analysis showed that, in the first 100 msec of the crash, this equivalent mass was consistently lower than the real mass, probably due mainly to the way the car bends and leaves the ends behind while the centre is pushed away by the impactor (“banana-ing”). There may also be some effect from the resilient mounting of heavy components such as the engine and suspension, and from the effect of roll. The actual mass of the car was about 920 kg (without the dummy). The effective mass rose from 450 kg at 10 msec after impact to 840 kg at 31 msec, averaged about 750 kg, with small fluctuations, until about 65 msec, and then rose slowly with increasing time. An average effective mass of 750 kg was selected for the simulation.

It was thought likely that the dynamic stiffness of the sill structure would be greater than the measured quasi-static stiffness, so the simulation was run with values of the dynamic magnification factor varying between 0 and 1.0. Figure 9 shows the value of car body acceleration produced by the simulation, with three different values of the dynamic magnification factor  $k$ . It will be seen that increasing the factor increases the magnitude of acceleration soon after the impact, and shortens the period before acceleration is reduced to zero. Figure 10 shows a comparison between the “best” simulation result (with  $k = 1$ ), and the result recorded in a full scale impact test. The full scale test result shows a lot of oscillation, even after filtering at 100 Hz. The oscillation is due to the complexity of force transmission through the distributed structure of the car body. This cannot be reproduced by the simulation, which represents the whole floor structure by a single (non-linear) spring, with no distributed masses.

Fortunately, these oscillations are unlikely to be relevant to the problem of occupant injury, and the important factor for the simulation to reproduce is the component velocities. Figure 11 compares the velocity of the car body measured in

a crash test with the velocity estimated by simulation, using no dynamic magnifier for the sill spring force. The curves are comparable, but the simulation shows a noticeable lag. Figure 12 is similar, except that the simulation uses a dynamic magnification of 1.0. With this change the two curves really are very similar, and the use of this value of dynamic magnification appears to be justified. It may be noted that in this simulation the changes made to match the simulation to the car body motion had relatively little effect on the injury parameters measured on the dummy model. The change from the real car body mass of 950 kg to the effective mass of 750 kg had a negligible effect, and the addition of the dynamic magnification factor for the sill stiffness decreased the principal injury parameters (peak rib compression, viscous injury, TTI) by less than 5%. However the smallness of the effects in this example does not necessarily imply that they would be so small in other simulations.

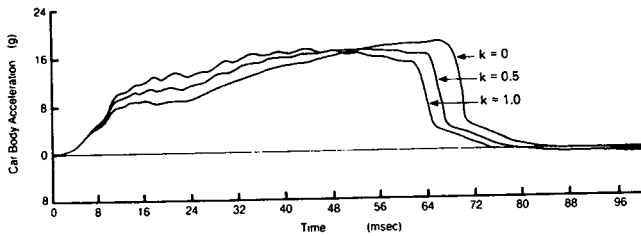


Figure 9. Car body acceleration—comparison of simulations with three values of dynamic magnification factor  $k$ .

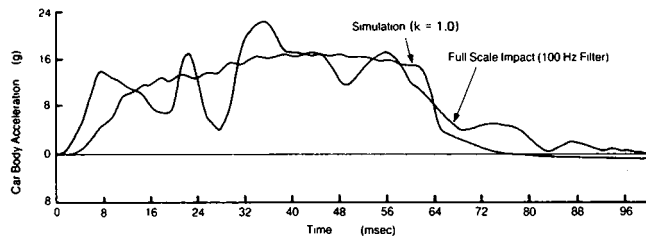


Figure 10. Car body acceleration—comparison of simulation with results from a full scale impact test.

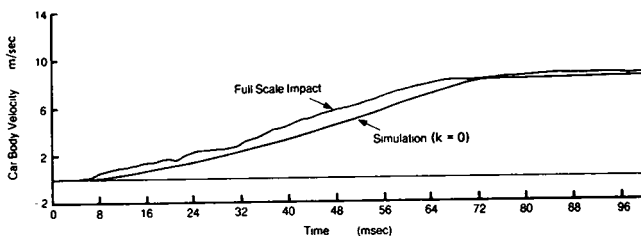


Figure 11. Car body velocity—comparison of simulation ( $k = 0$ ) with results from a full scale impact test.

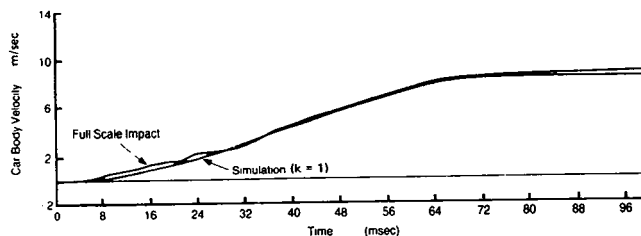


Figure 12. Car body velocity—comparison of simulation ( $k = 1$ ) with results from a full scale impact test.

For further comparison figures 13 and 14 show the acceleration and velocity of the car body estimated by a simplified simulation in which the whole side of the car (sill, A and B posts, and inner door) is treated as a single mass element. The stiffness was derived from quasi-static test 4, in which the whole side of the car was crushed by an EEVC deformable barrier face. The deflection was measured on the inner door (figure 7c). A dynamic magnification factor of 1.0 was used, but as can be seen there is a considerable difference between the full scale and simulation results. Figures 15 and 16 show the effect of increasing the dynamic magnification factor to the improbably high value of 4.0 in the simplified simulation. This gives quite a good fit between reality and simulation for times greater than about 30 msec after impact, but the initial differences are still much greater than with the more sophisticated multiple element simulation. With this simulation model changing the effective body mass again had a minimal effect on injury parameters, but changing the dynamic magnification factor (for the side to body stiffness) had major effects. For example, raising  $k$  from 0 to 1.0 reduced the major injury parameters by about 20%. Raising  $k$  further to 4.0 reduced rib compression by a further 5%, but again reduced viscous criterion and TTI by about 20%.

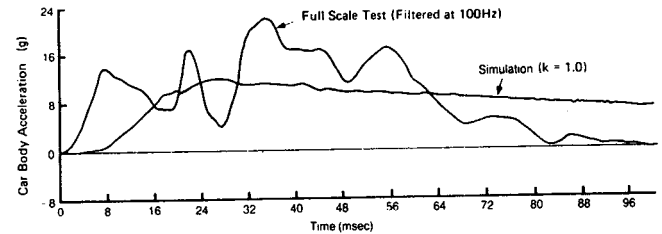


Figure 13. Car body acceleration—comparison of result from simplified simulation ( $k = 1$ ) with result from a full scale side impact test.

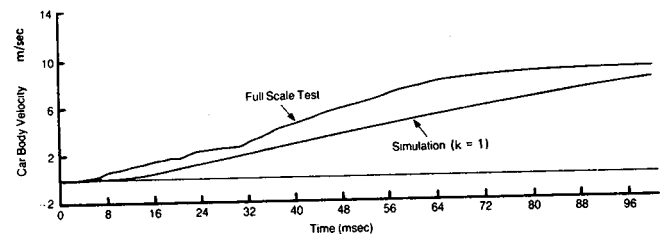


Figure 14. Car body velocity—comparison of result from simplified simulation ( $k = 1$ ) with result from a full scale side impact test.

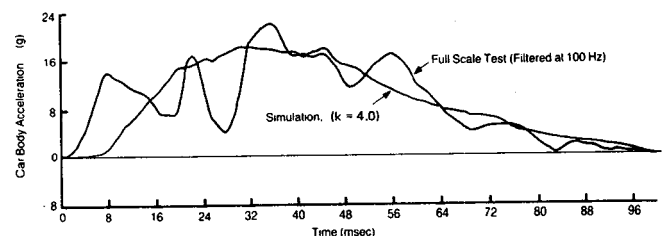


Figure 15. Car body acceleration—comparison of result from simplified simulation ( $k = 4$ ) with result from a full scale side impact test.

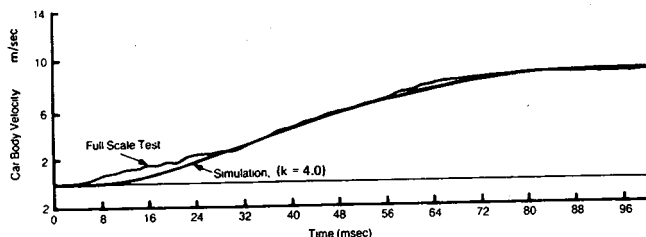


Figure 16. Car body velocity—comparison of result from simplified simulation ( $k = 4$ ) with result from a full scale side impact test.

## Dummy spine accelerations

It has not yet been possible to compare simulation results for dummy injury parameters directly with those from full scale impact tests, as the simulation model for the door and B-post area is still under development. The simpler model with a single mass to represent the side structure of the car had given dummy injury parameters which were clearly too high compared with reality, and it was this observation which gave much of the impetus for the development of the more sophisticated model.

However, comparison of rib and spine accelerations showed a clear discrepancy between the dummy simulation and EUROSID, even though care had been taken to provide an accurate model of the rib structure. The peak spine accelerations were much lower, relative to the rib acceleration, than the values observed in full scale impact tests. Further examination of the dynamics of the EUROSID rib system showed that, on its own, it was incapable of transmitting sufficient force to give the observed spine accelerations. The additional force required to produce these observed thoracic spine accelerations can only be transmitted through the pelvis, the abdomen, or directly into the spine from the seat back. No attempt has yet been made to model direct interaction with the seat back, since at present this is thought unlikely to be a major factor determining spine acceleration.

As a temporary expedient, it was possible to obtain spine accelerations of the right order of magnitude by appropriate factoring of the rib spring and damper parameters, so that the rib system could generate larger forces. This is unsatisfactory as a long term solution, and cannot be regarded as providing a proper representation of either EUROSID or a human occupant.

It is clearly necessary to model the additional load paths into the thoracic spine which must exist, according to the results of both dummy and cadaveric experiments. However, the modelling of load paths from the pelvis and abdomen presents problems, quite apart from the difficulty of determining appropriate stiffness parameters. It is not sufficient to provide simple translational links between the thorax and pelvis (and abdomen), since significant torques are generated as well as the translational forces. These can only be modelled by a full two-dimensional simulation, which is currently under development. When this is available, it will be possible to carry out a proper study of the possible load paths into the spine, using data from full scale tests to match

the rotation of the dummy. This should eventually lead to a better understanding of the way in which the car structure interacts with the occupant, and causes injury.

## Conclusions

Mathematical modelling of side impact on car structures has proved to be a very useful research tool, and has given considerable insight into the complicated dynamics of the impact process. Knowledge gained by the development and use of simulation models is likely to lead to the design of safer cars.

Useful progress has been made towards the design of a simulation model which can reproduce the dynamics of side impact on a car and its occupant with sufficient accuracy for most purposes, and it is reasonable to expect the goal of an adequate simulation to be reached within the next year or two.

However, it appears that such a simulation model will have to be fairly complex, and contain a number of separate mass elements if it is to reproduce all the factors known to be important in determining injury in side impact. Furthermore the model will require knowledge about certain factors such as the equivalent masses of different parts of the structure, and the relationship between static and dynamic stiffnesses for certain structural elements. These can at present only be determined by dynamic experiments on a structure which is at least similar, if not necessarily identical, to the one being simulated. Although in some cases it appears that values of injury parameters may not be significantly affected by moderate variations in the values of these factors, it cannot be assumed that this is universally true. For example, it was not true for the effect of dynamic magnification factors in the simplified model in which the whole side structure was represented by one mass. Considerable caution is therefore necessary about proposals to use simulation as a complete substitute for full scale tests. The reliable use of mathematical modelling for this purpose is likely to be some way in the future.

## References

- (1) Emmerson, W.C. and J.E. Fowler, *The Application of Computer Simulation in Vehicle Safety*, Fifth International Technical Conference on Experimental Safety Vehicles, London 1974. pp 712–720.
- (2) Schmid, W., *Mathematical Modelling of Occupant Biomechanical Stress Occurring During a Side Impact*, SAE Passenger Car Meeting, Troy, MI., 1978. SAE Paper 780670.
- (3) Hofmann, J. and H. Appel, *Mathematical Simulation of Side Impact—A Contribution to the Problem of Rigid/Deformable Barriers*. Proceedings of the Eighth International Conference on Experimental Safety Vehicles, Wolfsburg, 1980. pp 637–646.
- (4) Padgaonkar, A.J. and P. Prasad, *A Mathematical Analysis of Side Impact Using the CAL3D Simulation Model*, Proceedings of the Ninth International Technical

Conference on Experimental Safety Vehicles, Oxford, 1985. pp 578–585.

(5) Trella, T.J. and J.N. Kianianthra, *Occupant Response Sensitivity Analyses Using a Lumped Mass Model in Simulation of Car to Car Side Impacts*, Proceedings of the Tenth International Technical Conference on Experimental Safety Vehicles, Oxford, 1985. pp 755–771.

(6) Trella, T.J. and J.N. Kianianthra, *Analytical Simulation of the Effects of Structural Parameters on Occupant Responses in Side Impacts of Passenger Cars*, Proceedings of the Eleventh International Technical Conference on Experimental Safety Vehicles, Washington 1987. pp 62–76.

(7) Richter, R., H. Oehlschlaeger, R. Sinnhuber and R. Zobel, *Composite Test Procedure for Side Impact Protection*, SAE Paper 871117, SAE Govt./Industry Meeting, Washington, DC, May 1987.

(8) Massing, D.E., G.W. Kostyniuk and S.M. Pugliese, *Crash Victim Simulation—A Tool to Aid Vehicle Restraint System Design and Development*, Proceedings of the Sixth International Technical Conference on Experimental Safety Vehicles, Washington DC., 1976. pp 363–381.

(9) Wismans, J., T. Hoen and L. Wittebrod, *Status of the MADYMO Crash Victim Simulation Package 1985*, Proceedings of the Tenth International Technical Conference on Experimental Safety Vehicles, Oxford, 1985. pp 784–794.

(10) Hobbs C.A. and M.G. Langdon, *Thoracic Impact and Injury in Side Impact Accidents*, Proceedings of the International IRCOBI Conference on the Biomechanics of Impacts, Bergisch-Gladbach, 1988. pp 345–360.

(11) Hobbs C.A., *The Influence of Car Structures and Padding on Side Impact Injuries*, Paper to be presented to the Twelfth International Technical Conference on

Experimental Safety Vehicles, Gothenburg, 1989.

(12) EEVC Working Group No. 6., *Structures Improved Side Impact Protection in Europe*, Ninth International Technical Conference on Experimental Safety Vehicles, Kyoto, 1982. pp 396–409.

(13) NHTSA—US Department of Transportation, *Federal Motor Vehicle Safety Standards—Side Impact Protection*. 49CFR Part 571 Docket No. 88–06 Notice 1 Federal Register/Vol. 53 No. 17 Jan. 1988.

(14) Volvo Car B.V., *The Volvo Car B.V. Composite Test Rig*, Presentation at the Volvo Car B.V., Helmond, The Netherlands, 9 March 1989.

(15) The EEVC Ad Hoc Group on Dummies, *The EUROSID Side Impact Dummy*, Proceedings of the Tenth International Technical Conference on Experimental Safety Vehicles, Oxford, 1985. pp 153–165.

(16) Langdon, M.G., *Modelling the Lateral Impact of the Thorax in Car Side Impact Accidents*, Proceedings of the Tenth International Safety Conference on Experimental Safety Vehicles, Oxford, 1985. pp 114–124.

(17) Hobbs, C.A., M.G. Langdon, R.W. Lowne and S. Penoyre, *Development of the European Side Impact Test Procedure and Related Vehicle Improvements*, Proceedings of the Eleventh International Technical Conference on Experimental Safety Vehicles, Washington DC, 1987. pp 92–103.

Crown Copyright. The views expressed in this paper are not necessarily those of the Department of Transport. Extracts from the text may be reproduced, except for commercial purposes, provided the source is acknowledged.

## Acknowledgements

The work described in this paper forms part of the programme of the Transport and Road Research Laboratory and the paper is published by permission of the Director.

## Mathematical Modelisation of Side Collisions

**C. Steyer, P. Mack, P. DuBois, Regie Renault, Renault, France**

### Abstract

Numerical simulation can be very useful in the study of side impact both for a better understanding of the structural behaviour and to provide more representative human body characterisations.

In the first part of this paper, a complete structural model using the Finite-Element method and running on a supercomputer simulates the impact of a deformable barrier ( C. E. V. E. ) on a vehicle. This modelisation takes into account the very complex deformations and interactions inside the structure and between the car and the barrier. The comparison with the experiment is very satisfactory and the model can be considered as validated.

As for the modelisation of the occupant, the recent eval-

uations of SID and EUROSID dummies in lateral impact showed their poor biofidelity and also their important differences of conception as regards human being. For those reasons, it is necessary to have recourse directly to the human being. A simple modelisation was developed by the LPB-APR on the basis of cadaver tests and integrated in the model of structural deformation described above. Then, the data provided by this model were used with Prakimod to simulate the behaviour of the human being under lateral impact with a given structural deformation.

### Introduction

Several regulation projects are studied to improve the protection of the occupants in case of a side impact. A lot of experimental analysis has been done at Renault over the last years and not less than 150 crash tests have been performed.

Even with such a great volume of data, it is sometimes

difficult to get a clear insight into the fundamental phenomena occurring during the impact. Several plastic hinges appear on the side frame, the floor or the roof. It is very difficult for instance, to predict what would happen if the structure was modified in a way such as one of those hinges disappeared.

The interaction between the occupant and the structure is also quite complicated. Some structural changes may decrease the final deformation but have negative effects on the impacting speed of the dummy and on injury criterions. The same thing can occur with some door-reinforcements which increase the local stiffness of the structure.

Those reasons justify the use of numerical simulations to shorten and improve the conception of a new car as concerns side-impact. Once the necessary experimental validations of such tools are done they provide very accurate and reliable tendencies on the physical behaviour of the various elements.

Two numerical approaches are presented in this paper. In this first part, the simulation possibilities of the finite element method for side-impact are illustrated. The covered field concerns both the behaviour of the structure and a first step toward the introduction of an occupant model.

The second part deals with semi-empirical models. An analysis of the behaviour of the human body has led to a physically equivalent system composed of masses, springs and viscous dampers. This characterisation has been associated with the structural deformation inside the software Prakimod in order to study a two-dimension interaction between the structure and the occupant.

## Experimental Conditions

The chosen test is in agreement with the C.E.V.E. regulation project. The studied vehicle is impacted orthogonally by a deformable barrier at a speed of 50 km per hour. The weight of the impacting charriot is 950 kg. The deformable element is divided into 6 geometrical areas (figure 1). Each of those 6 contact areas and the whole barrier has to stay within prescribed force vs deflection curves of a calibration test against a rigid wall.

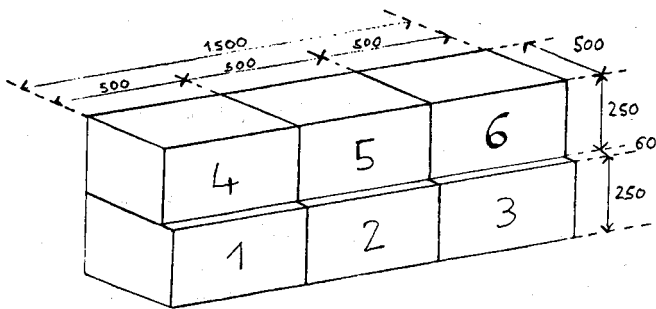


Figure 1. View and dimensions of the used barrier (dimensions in mm).

A few manufacturers propose such barriers realised with different technologies and materials. The one we used is a crushable foam version. The impact with the structure

occurs through two aluminum plates located in the frontal part. Several foam blocs ensure the right stiffness distribution.

We would like to emphasize that very special care has been taken for the definition of the impacted vehicle. As we wanted to validate the modelisation of the structural behaviour, the main purpose was to reduce as much as possible the origins of differences between test and simulation. In this first step no dummy was placed inside the car. We also took away most equipment of the passenger space especially the seats whose influence may be important. They would require some further characterisation tests because a predictive modelisation of the seat under those loading conditions seemed quite hazardous. At last, all the important masses have been connected rigidly to the structure which is the easiest to reproduce in the simulation.

## Calculation Method

Automotive crash in general and side impact in particular is a highly non-linear short duration phenomenon. Indeed, the maximum deformations are reached in only one tenth of a second and within this very short time span a multitude of physical events take place. These events include metal sheet buckling, plastification of the steel, complicated contacts but rarely rupture so that classical continuum formulation can be applied. The features of the numerical techniques used to simulate such a process are the following:

Spatial discretisation using 3-Dimensional shell finite elements. In the RADIOSS code a 3 or 4 noded bilinear shell is used in a so called global formulation based upon curvatures and bending moments rather than strains and stresses.

Two different algorithms designed to simulate either folding of one sheet upon itself or contact of two shells, for both a penalty method is used to evaluate contact forces as a function of the detected penetration.

Time integration of the conservation of momentum equations using an explicit integrator (in this case the central difference scheme). This is the main specific feature of crashworthiness analysis.

Such simulation programs have been used for several years in the field of frontal crash analysis. Their application for side impact is more recent. (I)\*

## Simulation Model

As the impacting barrier is deformable, a specific modelisation of this part had to be done. Several kind of finite element and material laws have been tried until we could obtain a reasonably representative behaviour of the barrier.

The results obtained with two modelisations are presented later in the paper. Barrier number one has force vs deflection characteristics that fit to the average values of the C.E.V.E. prescriptions. Barrier number two has been

\*Numbers in parentheses designate references at end of paper.

recalibrated very precisely on an actual test against a rigid wall and accounts better for the actual behaviour during the impact of the car which is an even more complex phenomenon.

The structural modelisation itself was more classical. We kept the model used for static or dynamical analysis on the non-impacted side whereas the side of impact was remeshed finer especially on the side frame and the floor. A model of both doors was also introduced on this side.

Several contact definitions have been introduced in the model. The first series concern the interaction between the barrier and the structure. Some other contact areas were defined inside each door because the outer skin transmits efforts to the inner parts once the doors get deformed. At last some localised contacts have been foreseen between the doors and their environment.

No special boundary conditions have been introduced on the structure. The friction effect of the wheels on the ground was compared to the average force of the barrier on the vehicle and appeared to be of a smaller order of magnitude. In the same way the vertical reaction of the suspension was checked to remain small compared with the inertial forces.

The total number of elements, not including the barrier, is 14,700 (picture of the complete model in figure 2) and the computer time required for a 60 millisecond simulation is 14 hours of C.P.U. time on a Cray XMP14 computer.

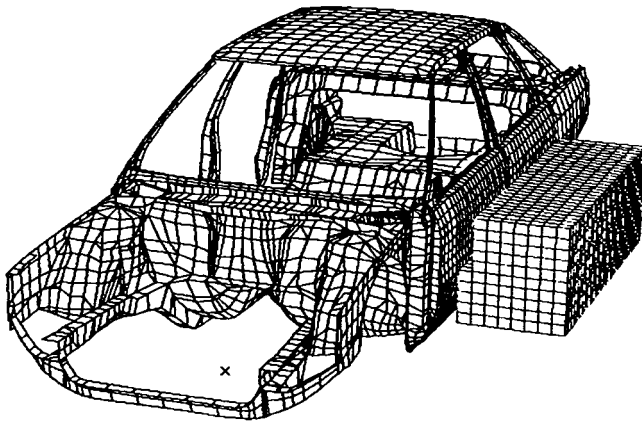


Figure 2. View of the complete simulation model.

## Results and Comparison With Experiment

As we have seen before, in the field of crash analysis, the cooperation between the testing and calculation team is fundamental. This has to be done through physical modelisation assumptions that are to be validated by experimental observations.

For this simulation, we could get quite good results before any correlation of that kind (Model 1). Figure 3 represents the relative deformation measured between two points on each side of the car. The first couple of points is located in the lower part of the B-pillar (about 350 mm above the floor). The second points (figure 4) are at the front door about 100 mm in front of the B-pillar and 50 mm under

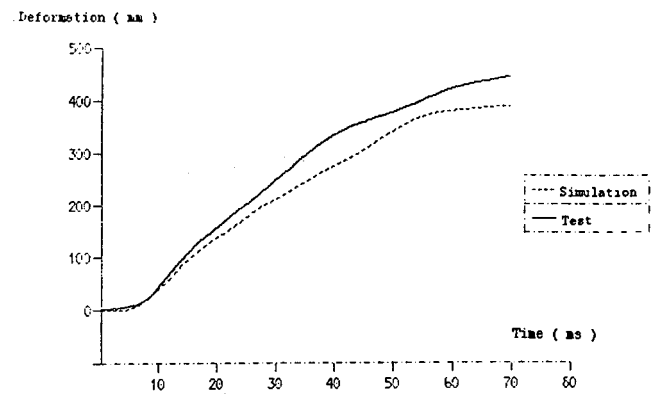


Figure 3. Comparison of the relative deformation on the lower B-pillar between test and simulation for Model 1.

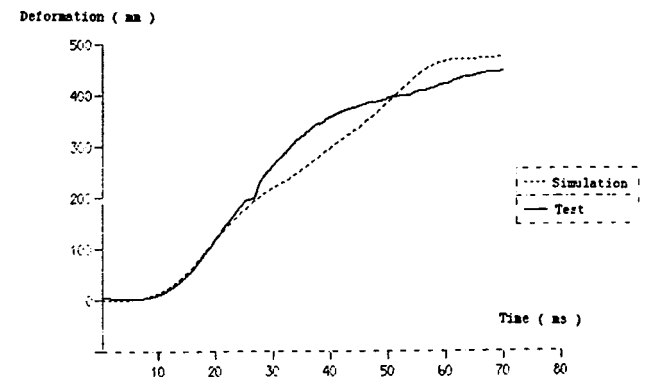


Figure 4. Comparison of the relative deformation on the front door between test and simulation for Model 1.

the top of the door body. Those points give a good representation of the side frame deformations. The differences between test and simulation are in both cases already fairly acceptable.

Several checks have to be done on the numerical behaviour of the model itself. The main source of errors comes from uncomplete contact definition. The potential contacts must all be defined at the beginning. During the simulation, the structural deformation may induce some new interactions that are quite difficult to foresee considering the initial shapes.

Figure 5 illustrates those problems: it is the deformation of one section in the front door. The deformed shape of the door, for instance, has not much in common with the initial shape. The C.P.U. time used for the computation of those contacts becoming quite important, we could not afford to have too much contact definitions that were not actually useful.

We have improved the barrier model as explained before, and completed the contact definition in the structural model until the physical behaviour was entirely satisfactory. (Model 2) We are now going to analyse in a more detailed way the results of that last simulation.

The first interesting information is the comparison between the speed of the barrier and the impacted car's center of gravity. (figure 6 and 7) According to those curves, the impact ends at 75 millisecond when both the chariot and the car reach the same speed of 8 meters per second.

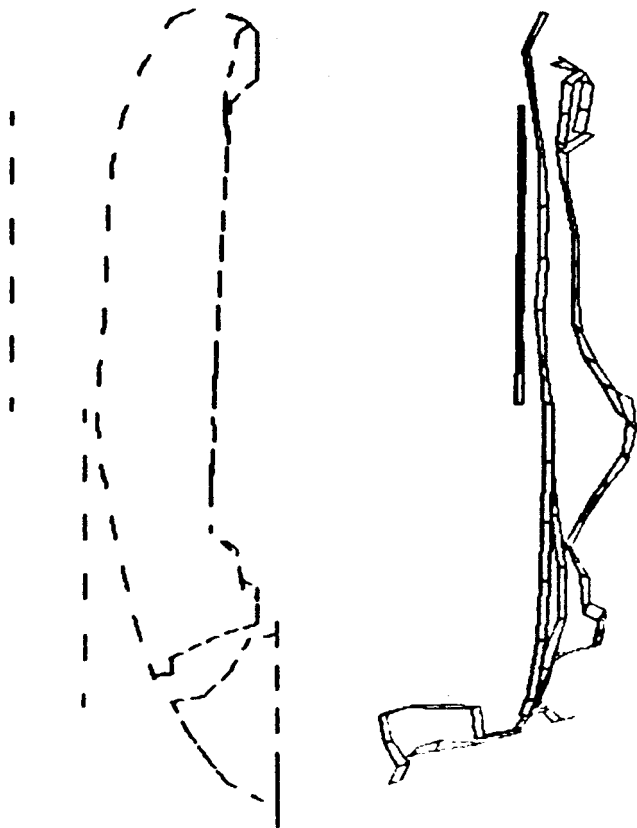


Figure 5. Initial shape and deformed shape at 40 ms of a front door section.

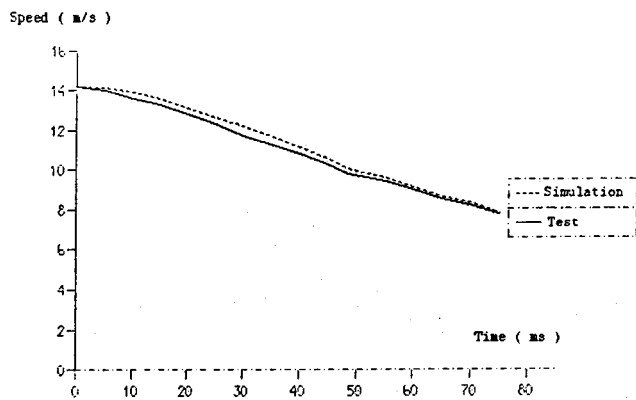


Figure 6. Comparison of the barrier speed between experiment and simulation.

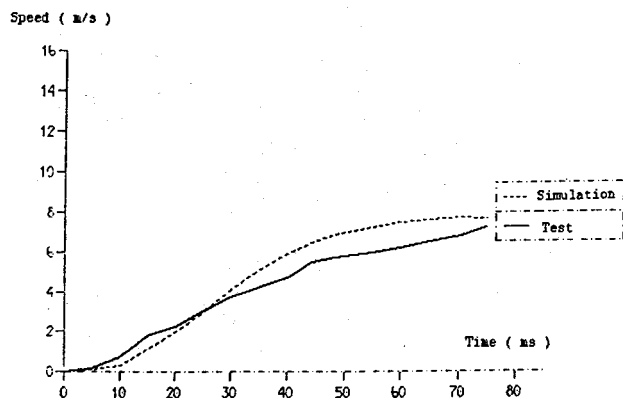


Figure 7. Comparison of the car center of gravity speed between experiment and simulation.

A second important element of comparison is the position and shape of the main plastic deformation areas in the structure. The four main features of this impact are the following:

- The V-shape deformation of the B-pillar.
- The deformation of the floor.
- The collapse of the roof.
- The crushing and bending of the doors.

On all those points, the numerical simulation is found to be in very good agreement with experimental observations. Figure 8 shows a side view of both deformed shapes.

The relative deformations are, as expected, better than for Model 1 (figure 9 and 10). But what is more interesting is the comparison of the relative deformation speeds (figure 11 and 12). The maximum value and shape of the curves are now very close to the experiment. It is obviously more difficult to obtain similar deformation speeds than just similar deformations.

## Modelisation of the Occupant

As mentioned in the introduction, the interaction between the structure and occupant is very important in the case of side impact. The results presented in this part are the result of a cooperation with the Laboratory of Physiology and Biomechanics that provided us the required data for the representation of the human body as exposed in the second part of this paper.

The model we used is very near in its philosophy to the one developed in the context of the Composite Test Procedure. The body is represented by two segments one for the thorax and one for the pelvis. Each of those segments consists of an undeformable interface element connected to a simple physical model composed of one mass, two springs and one damper. The shape of the undeformable element is a portion of cylinder standing for the volume of the occupant. Besides, another physical system couples the masses of the thorax and pelvis. At last the system is fully guided in the transverse direction.

In the case we studied, the occupant model can be considered in almost direct contact with the structure (figure 13). That means that the inner door plastic parts have not to be taken into account in the simulation. Any padding with a given deformation law could be integrated easily in this modelisation if necessary.

Such a simulation is quite expensive in terms of computing time and is not suited for a general parametric study on the occupant model and interface conditions. This is the field of the semi-empirical models developed in the second part of the paper. The simplifications introduced in those last models can be studied and validated with the help of our complete finite-element simulation.

The results of the simulation are consistent with the calibration information available for the occupant model considering the average speed of the interfaces during the contact of the occupant and the structure. The maximum

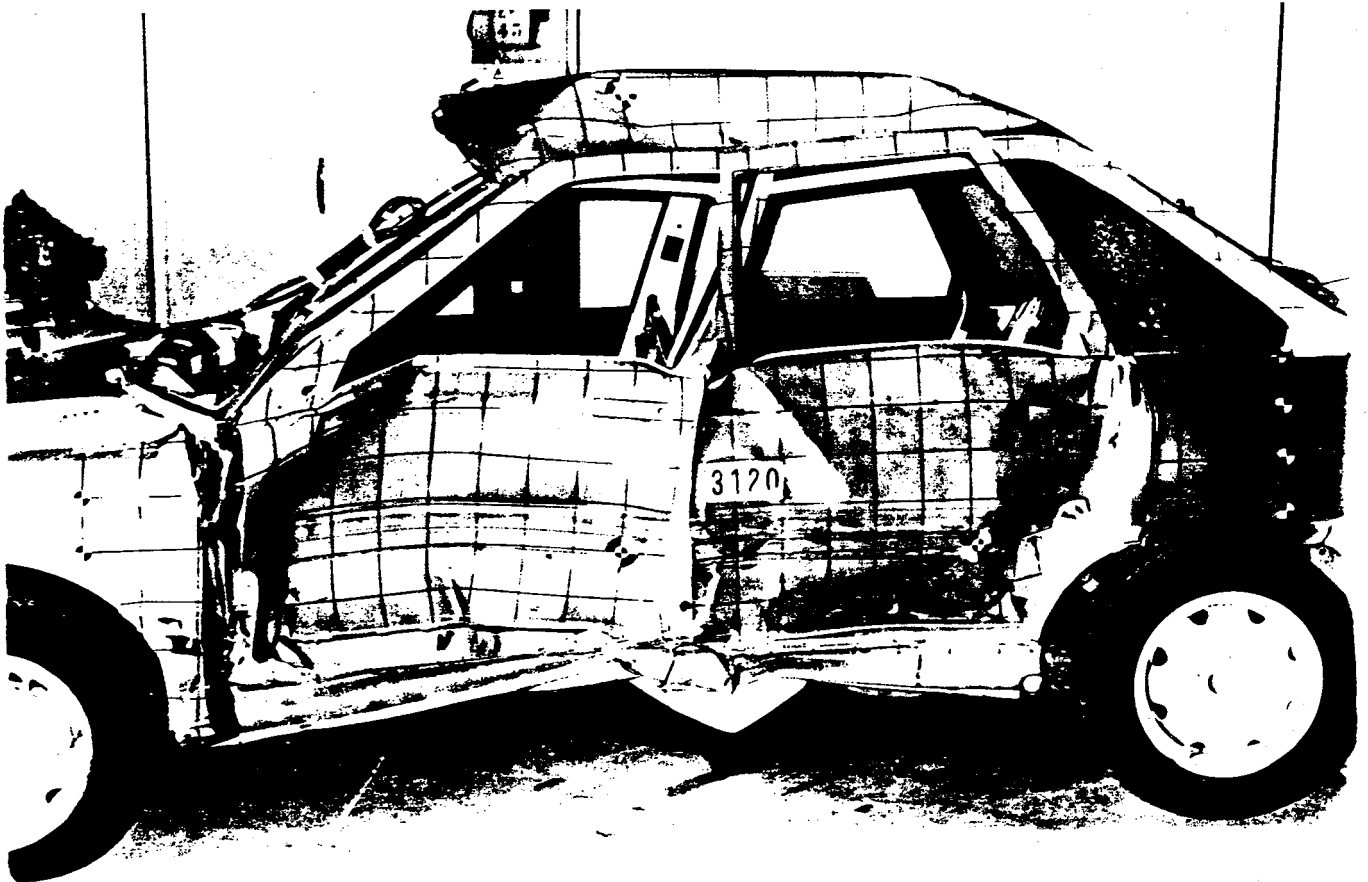
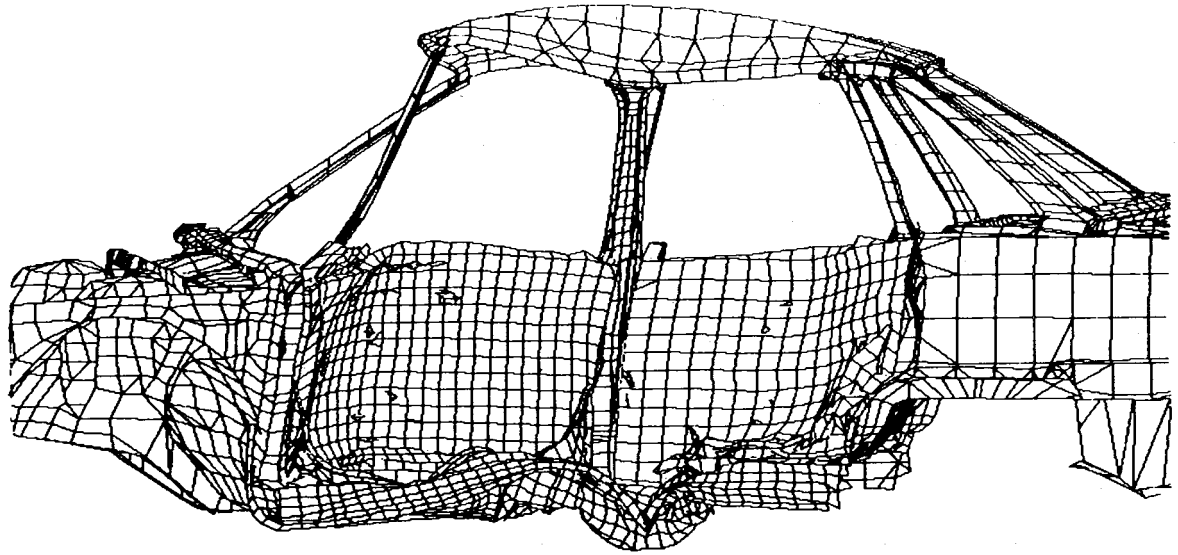


Figure 8. Final structural deformation of the experiment and simulation.

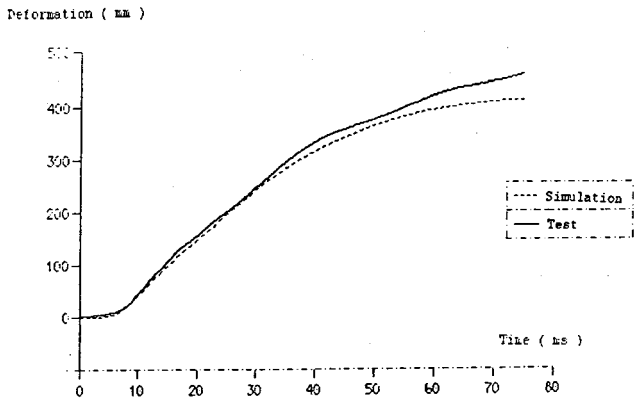


Figure 9. Comparison of the relative deformation on the lower B-pillar between test and simulation for Model 2.

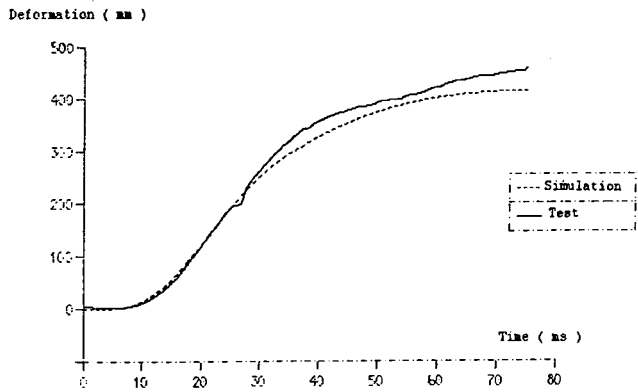


Figure 10. Comparison of the relative deformation on the front door between test and simulation for Model 2.

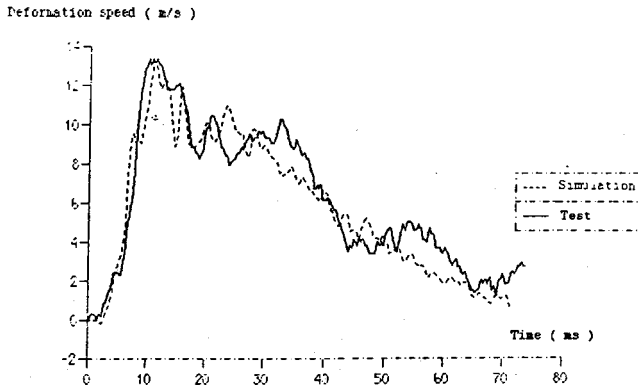


Figure 11. Comparison of the relative deformation speed on the lower B-pillar between test and simulation for Model 2.

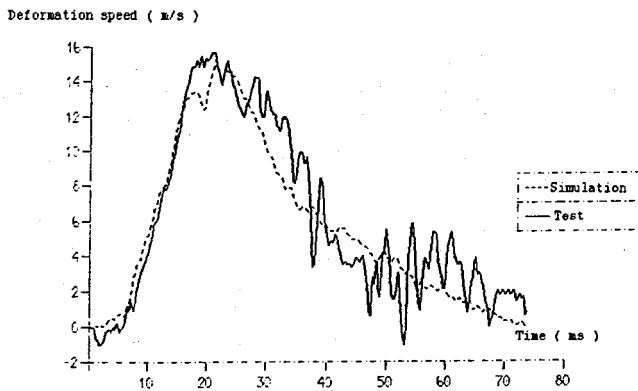


Figure 12. Comparison of the relative deformation speed on the front door between test and simulation for Model 2.

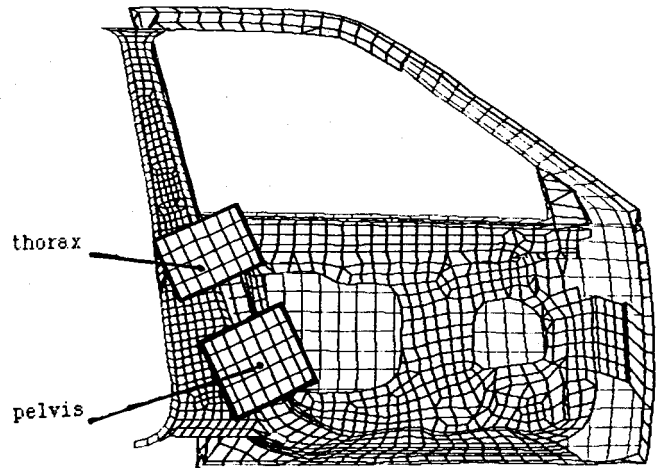


Figure 13. Side-view of the occupant model placed inside the structure.

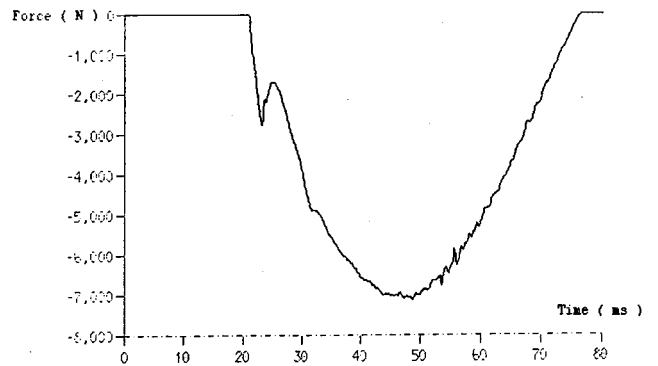


Figure 14. Contact force between the thorax and the structure.

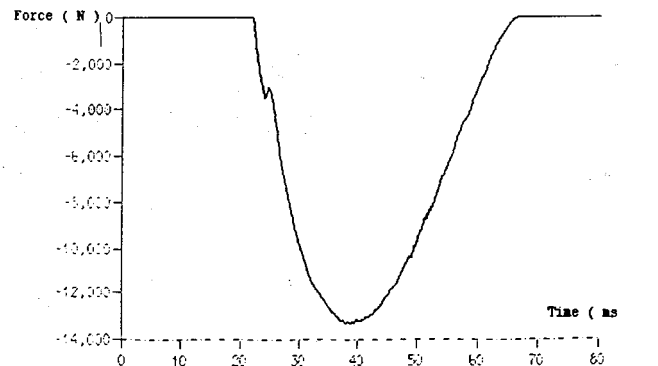


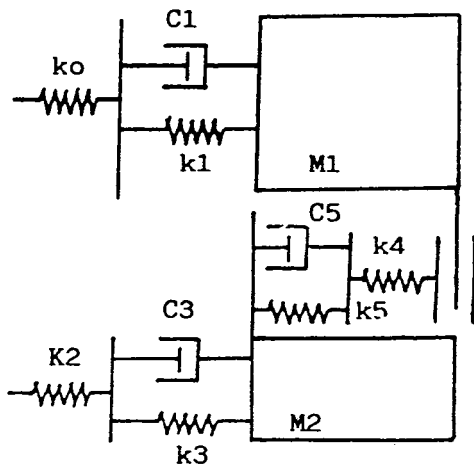
Figure 15. Contact force between the pelvis and the structure.

force is 7 KNewton for the thorax and 13 KNewton for the pelvis and is reached first on the pelvis. (figure 14 and 15)

### Simple physical model of the human being

One of the major advantages of mathematical modelization is the capability of immediately integrating all the new data produced by the biomechanical experiments. Similarly and instantaneously, the validation of the model can be checked out by simulating biomechanical tests with human subjects, selected as being the best references available. This is what has been performed by the Laboratory of Physiology and Biomechanics associated with Peugeot S.A./Renault:

1. By performing special tests with human subjects, to obtain the necessary data which do not exist in bibliography world-wide. The characteristics of the coupling function between the thorax and the pelvis, for the essential provided by the spinal column, were obtained by these new APR experiments. The model issued from these experiments is shown below:



2. By validating the mathematical model of the human being thus obtained, with reference to highly conventional available data, such as those obtained from already old experiments such as those of the HSRI (7) for the thorax, and INRETS for the pelvis (8), or very recent experiments performed by G.M. (1).

The mathematical modelization can be used to simulate various occupant configurations. For example, the thorax can be covered or uncovered by the arm, the mass of the occupant can vary, the skeletal resistance, which depends on the age and activity of the users can also vary.

The model presented herein represents the configuration for which the existing data are the most numerous, i.e. the "uncovered thorax". A complementary experimental program is now in course to enable the CCMC to modelize the "thorax covered by the arm" configuration. Further details can be found in reference (5).

### Modelling of the human being in side impacts with Prakimod

The object of this study is an initial modelling of the human being in side impacts, by means of the 2-dimensional model Prakimod (Peugeot Renault Accident Kinematics Model (4)).

This model will first be validated on the basis of the impactor tests by Mr. Viano (1) performed on cadavers at different speeds.

Following this, mathematical simulation of the structure in side impacts will be adopted as input data.

This will allow complete simulation of a global impact, from the car structure to the human being.

### Construction of the model

To construct the model of the human being, we have used the study by Robbins (2) on driving posture and the image of a 50-percentile human being scanned by a MRI system.<sup>1</sup>

#### Construction of the skeleton

The skeleton consists of the following 6 segments:

- C.G. head—Occipital condyles
- Occipital condyles—C6/T1
- C6/T1—T8/T9
- T8/T9—T12/L1
- T12/L1—Sacrum
- Sacrum—Point H

The mass and centre of gravity for each segment is defined on the basis of the work by McConville (3).

### Definition of ellipses

Prakimod is a simple global behaviour model, and for each contact with an ellipse there is only one possible deformation.

This being so, it is preferable to increase the number of ellipses to refine the model's behaviour.

We therefore defined the following ellipses:

Ellipse	Center (transverse axis)
Shoulder	T3
Arm	
Hard upper thorax	T6/T5
Hard middle thorax	T8/T9
Hard lower thorax	T10
Soft thorax	T11/T12
Upper abdomen	L2
Lower abdomen	L5
Pelvis	
Iliac wing	Iliac wing
Ischium	Ischium

Since the human being scanned by RMI is in reclining position, we used the work by Robbins (1) to apply a rotation movement to each segment of the spinal column corresponding to the sitting position (figure 16).

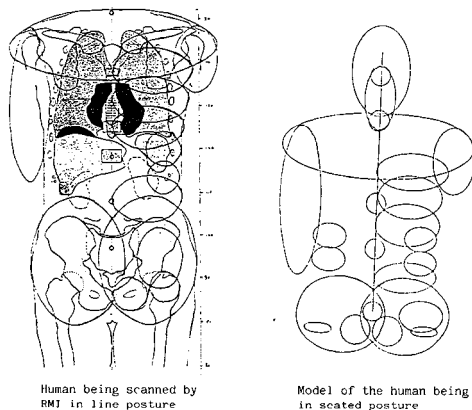


Figure 16. Construction of the model.

<sup>1</sup> MRI: Magnetic Resonance Imaging

## Validation

Validation will allow definition of the behaviour of the thorax, abdomen and pelvis, by means of Viano impactor tests (1).

No data is at present available for characterization of the shoulder and arm behaviour, so that only the behaviour of the thorax will be modelled.

Three curves were selected according to Viano parameters to validate the model response to: deflection versus time; V.C. versus time; Load versus time.

## Simulation of the thorax (figures 17, 18, 19)

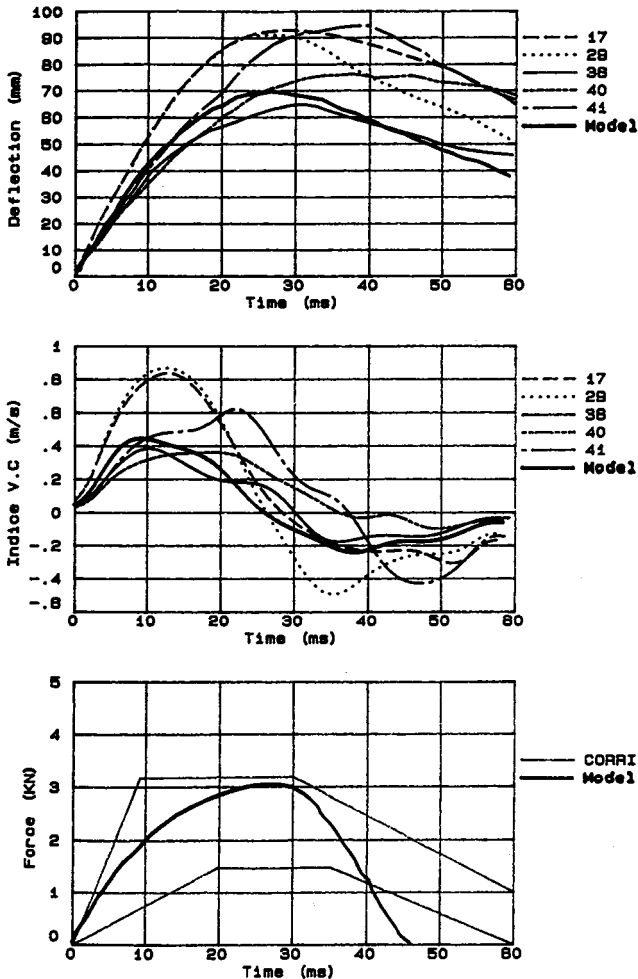


Figure 17. Dynamic response of the thorax for lateral impacts at 4.42 m/s. Comparison of model with Viano data.

Information is available from impactor tests performed in the "driver" position, i.e., without interposed arm. The impactor is centred on a 7.5 cm axis under the middle of the sternum. The impactor diameter is 150 mm and it weighs 23.4 kg.

Three impact velocities are available, 4.5, 6.7 and 9.4 m/s, with five tests for each velocity.

For thoracic deflection and V.C., the model behaves very well for all three velocities.

On the other hand, for load versus time, the model goes slightly beyond the corridor for all velocities.

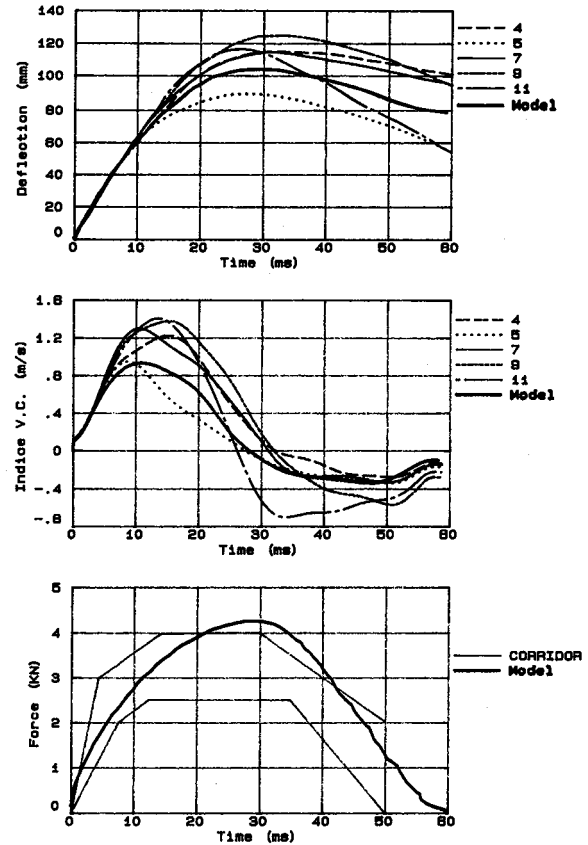


Figure 18. Dynamic response of the thorax for lateral impacts at 6.7 m/s. Comparison of model with Viano data.

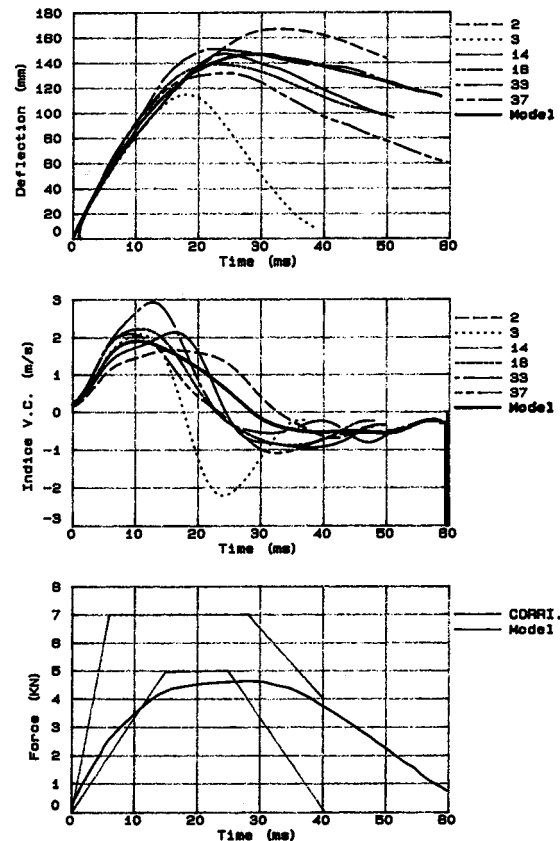


Figure 19. Dynamic response of the thorax for lateral impacts at 9.4 m/s. Comparison of model with Viano data.

## Simulation of the abdomen (figures 20, 21, 22)

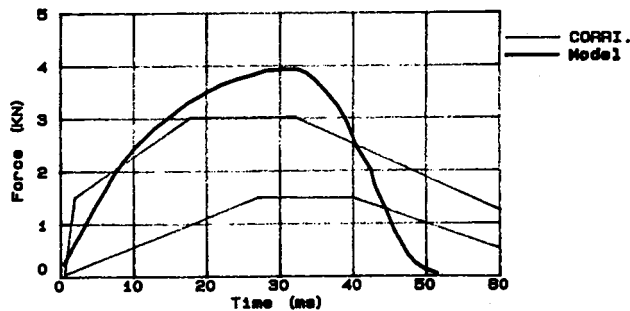
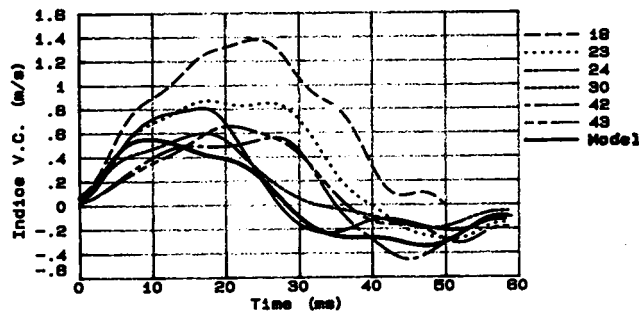
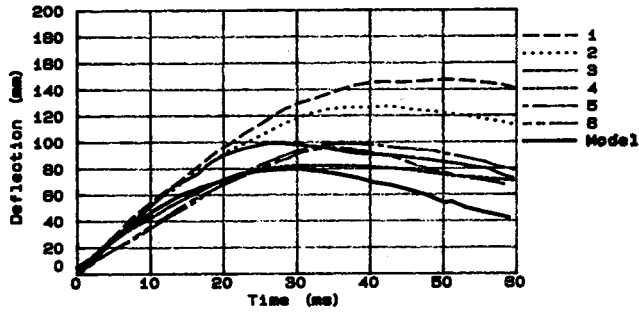


Figure 20. Dynamic response of the abdomen at 4.8 m/s. Comparison of model with Viano data.

The test conditions are identical to those for the thorax except that the impactor is located on an axis 15 cm below the middle of the sternum.

Three impactor velocities are available, 4.8, 6.8 and 9.4 m/s.

In terms of deflection and V.C., the model performs well by comparison with real tests, but in terms of load it goes beyond the corridors for the velocities of 4.8 and 6.8 m/s, and on the other hand is slightly below the corridors for the 9.4 m/s velocity.

## Simulation of the pelvis (figures 23, 24)

Same impactor configuration as for the previous tests, with the impactor centred on the greater trochanter.

Two impact velocities are available, 5.2 and 9.8 m/s.

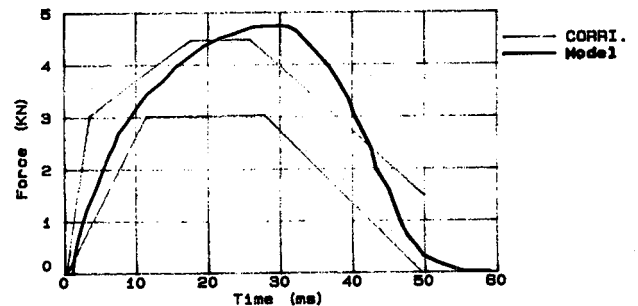
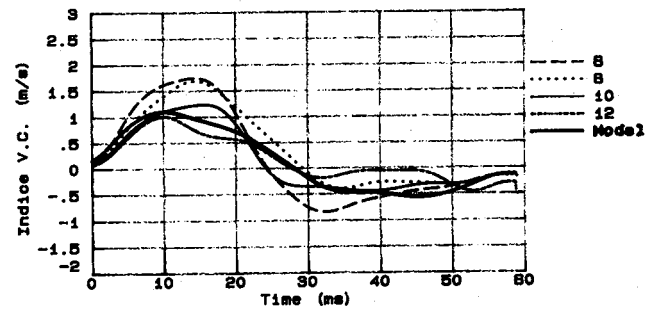
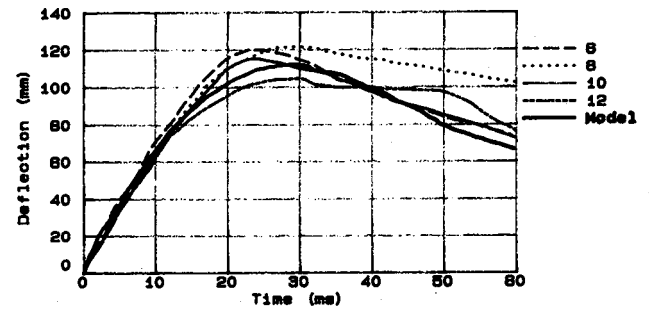


Figure 21. Dynamic response of the abdomen for lateral impacts at 6.8 m/s. Comparison of model with Viano data.

The model performs well in deflection, but under load, on the other hand, it exceeds the two corridors.

## Validation conclusions

For the thorax, the abdomen and the pelvis, the Prakimod model behaves well in terms of deflection and V.C., and although the responses for load versus time are less satisfactory they are nevertheless not too far from the corridors.

With reference to the work by Viano (1), V.C. is one of the best injury criteria for side impacts, and in this case the model is biologically faithful in terms of deflection and V.C. However, if we want perfectly to simulate the human being, other tests would have to be performed to understand the more complex mechanisms of behaviour of the human being's body areas.

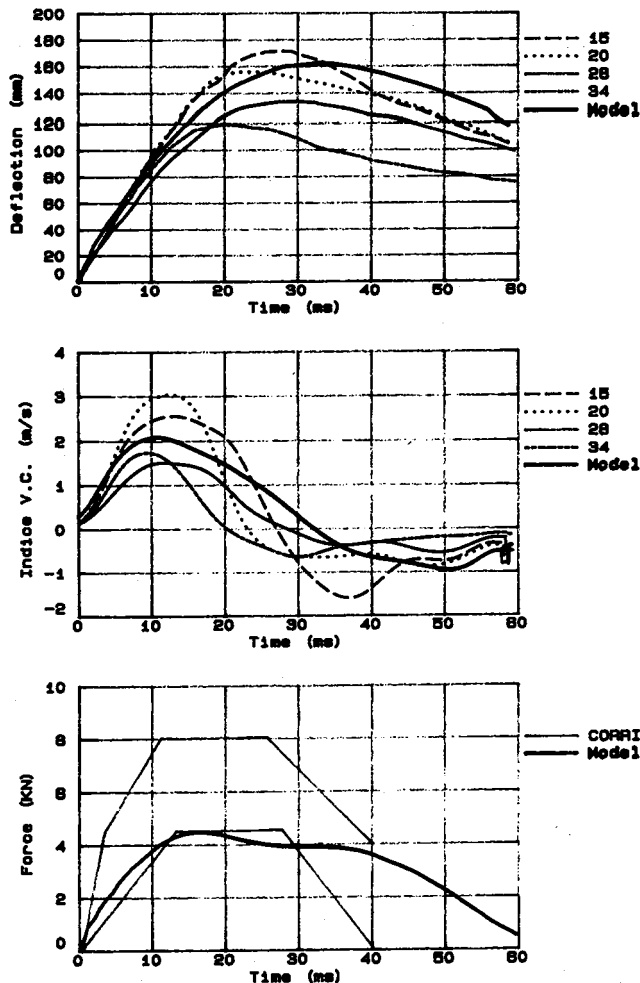


Figure 22. Dynamic response of the abdomen for lateral impacts at 9.4 m/s. Comparison of model with Viano data.

On the other hand, to characterize the whole human being, we lack data concerning the behaviour of the shoulder and interposed arm, at different velocities.

### Simulation of a global side impact

The input data for this modelling exercise are as follows:

- Transverse acceleration of the car body;
- Deformation of the car door versus time in the dummy plane.

This data is obtained directly from the structural simulation performed using a 1-dimensional dummy. Since the dummy used has 2 parts, the surface-indeformable thorax and pelvis, and knowing that the Prakimod model covers the whole human being, by an initial approximation we can adopt a deformation point for the thorax and a point for the pelvis and we can liken the car door to a straight line between those two points.

### Results (figures 25, 26, 27)

The results of this simulation in terms of deflection seem to be high, approximately 200 mm for the thorax and 180 mm for the pelvis. This can be explained by the Viano reference impactor test configuration, using a cylinder of

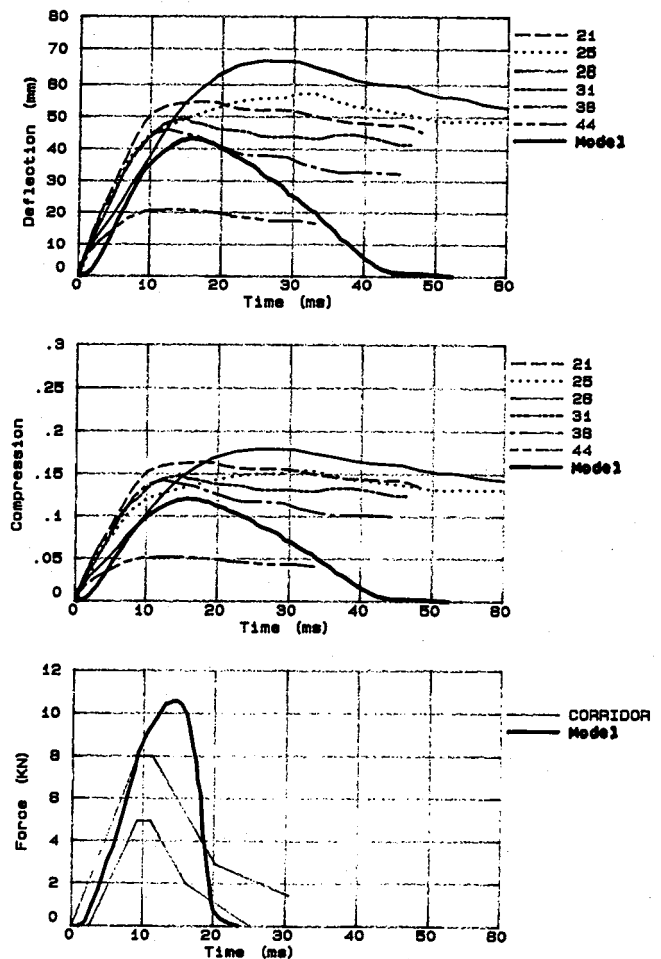


Figure 23. Dynamic response of the pelvis for lateral impacts at 9.2 m/s. Comparison of the model with Viano data.

diameter 150 mm. Such tests seem unsuitable in terms of impacting area in relation to the deformed car door area. It seems probably that tests performed by a larger impactor would be more representative of a car door impact.

## General Conclusions for Mathematical Modelling

This study enabled an initial complete simulation of a side impact, with first a simulation of the structure and second a simulation of the human being.

Note that the dummy used for structural simulation is greatly simplified in shape and behaviour (1 dimension) and that validation of the 2-dimensional Prakimod model is based on tests performed on an impactor which has an apparently small surface area by comparison with the area of the impacting car door. However, this study shows the feasibility of mathematical models as a tool for research and development work in the study of side impacts.

To continue this work, structural simulation should be performed directly on a dummy defined along three dimensions, but at present insufficient data is available concerning these three dimensions for the human being.

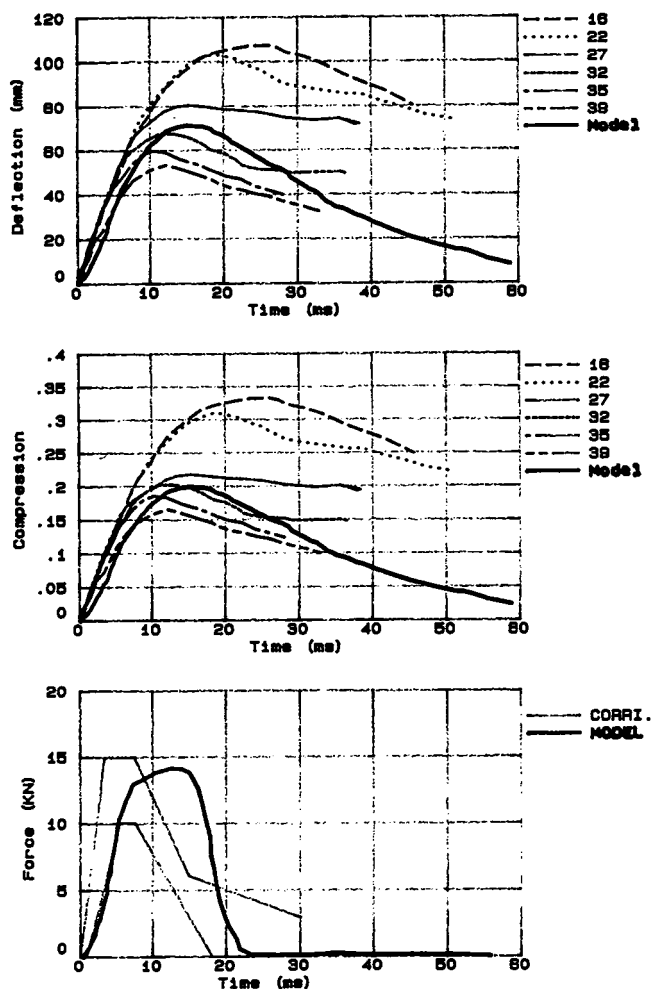


Figure 24. Dynamic response of the pelvis for lateral impacts at 4.8 m/s. Comparison of model with Viano data.

## References

(I) A Numerical Simulation of the Proposed European Side Impact Test Procedure. Stanger, J., Hatch, T., Du Bois, P., (1988). Second International Conference on Supercomputing Applications in the Automotive Industry, Seville, Spain.

(II) Draft Regulation From Economic Commission For Europe, Trans. SC1-WP29-6RCS-R58.

(III) RADIOSS<sup>2</sup> user Manual.

(1) "Biomechanics of the human chest, abdomen, and pelvis in lateral impact", D.C. Viano, I.V. Lau, C. Asbury, General Motors Research Laboratories, IMechE Conference 28/04/89.

(2) "Seated posture of vehicle occupants", Robbins et al., 27th Stapp Car Crash Conference, SAE Paper 831617.

(3) "Anthropometric relationship of body and body segment moments of inertia", McConville et al., Aerospace Medical Research Laboratory, December 1980. AFAMRL-TR-80-119.

(4) "PRAKIMOD": Peugeot Renault Accident Kinematics Model; Theory, Validation and Application. F.

<sup>2</sup> RADIOSS is a trademark of MECALOG S.A. Paris, France

## Results (figures 25, 26, 27)

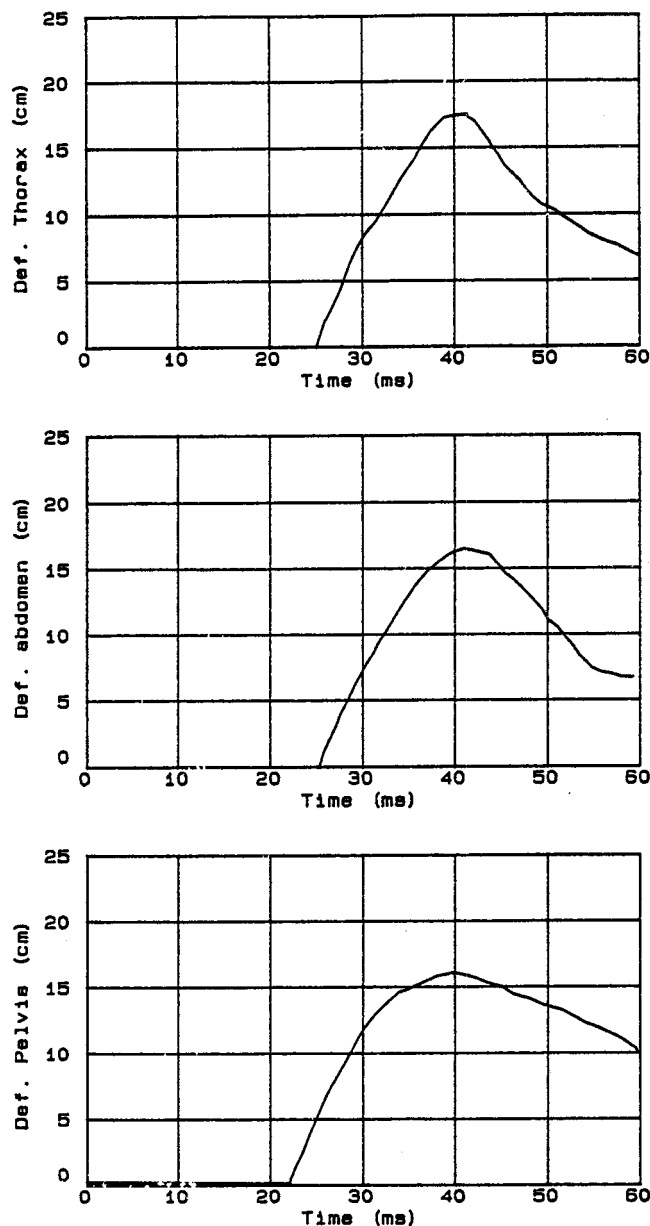


Figure 25. Results of the global simulations in terms of deflection.

Schuller, P. Mack, F. Brun Cassan, C. TARRIERE, LPB-APR-IRCOBI Conference September 1988.

(5) "Mathematical modelization of human beings in lateral impact", Dr. C. TARRIERE-CCMC IMechE Conference 28/04/89.

(6) Composite Test Procedure for Lateral Impact, Dr. Richter-CCMC IMechE Conference 28/04/89.

(7) "Development of a Promising Universal Thoracic Trauma Prediction Methodology", R.H. Eppinger, K. Augustyn and D.H. Robbins; Twenty-Second Stapp Car Crash Conference, SAE 780891, October 1978.

(8) "Caractéristiques de réponse à un choc latéral permettant d'évaluer la biofidélité d'un mannequin", Documents ISO/DP 9790-1 à 6.

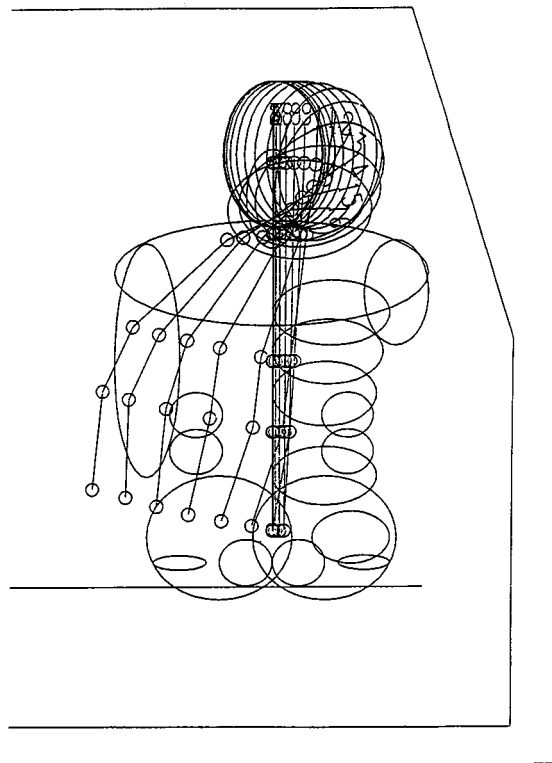


Figure 26. Segments kinematics of the global simulation.

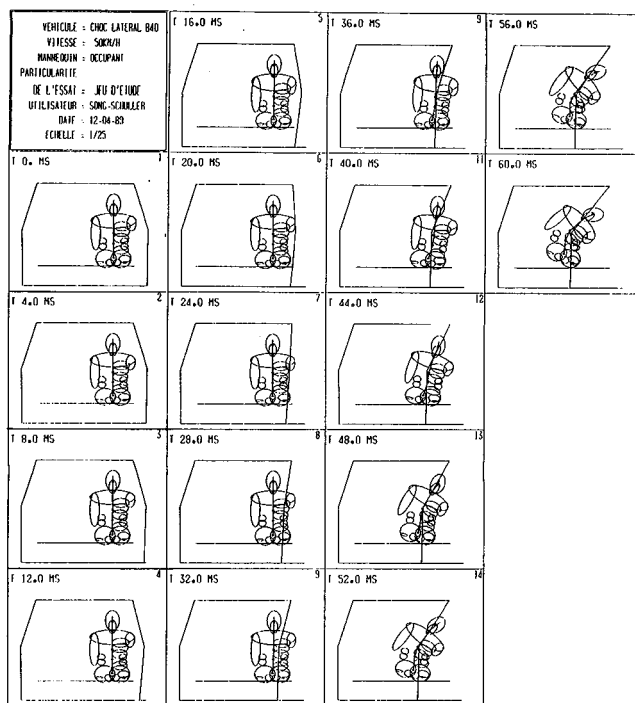


Figure 27. Kinematics of the global simulation.

## Side Impact Subsystem Thoracic Impactor Evaluation

Donald T. Wilke, Michael W. Monk,  
Joseph N. Kanianthra,  
National Highway Traffic Safety Administration,  
United States

### Abstract

In January, 1988, the National Highway Traffic Safety Administration (NHTSA) issued a Notice of Proposed Rulemaking (NPRM) for side impact protection. In this notice, the Agency proposed that the level of side impact protection in passenger cars be assessed through full-scale crash testing. The NHTSA has conducted extensive research, as has the vehicle safety community in the U.S.A. and in Europe, to explore the use of subsystem testing for assessing side protection in passenger cars.

This paper presents the findings from a study conducted to evaluate the thoracic subsystem test device and associated test procedures, developed by the Motor Vehicle Manufacturers Association of America (MVMA), for use in assessing side impact protection in vehicles. In the tests conducted by the NHTSA's Vehicle Research and Test Center (VRTC), the MVMA thoracic impactor was tested for its ability to produce thoracic responses for injury assessment and for its capability to differentiate between padded and unpadded doors. These tests included testing of cars fixed to the floor as well as testing of doors in a frame.

Three series of tests were performed using the device on nine vehicle models that were previously crash tested. The data from these tests were analyzed to determine the device's capability to distinguish between padded and unpadded doors, and to distinguish performance differences in car/door/side structure designs. Subsystem test results were also compared to full-scale side impact crash test results.

### Introduction

The topic of testing to assess thoracic injury in side impacts has received a great deal of interest in the last several years. An earlier study performed at the National Highway Traffic Safety Administration (NHTSA), Vehicle Research and Test Center (VRTC), investigated the feasibility of performing subsystem, or component, level tests for this purpose (1).<sup>\*</sup> Upon comparison, it was found that the component test results indicated the same benefit from added padding to the inner door as crash tests, but were different from full-scale crash test results in discrimination among production vehicles.

During fiscal year 1985, the Motor Vehicle Manufacturer's Association (MVMA) sponsored the development of a thoracic subsystem test device and its associated test procedures. For the study of this paper, this device was borrowed and installed at the VRTC. An

<sup>\*</sup>Numbers in parentheses designate references at end of paper.

evaluation of the device and test procedures has subsequently been completed (2).

This paper reviews the test procedure developed at the VRTC for this program. This includes outlining the test objectives, defining test parameters to meet these objectives, and presenting the matrix of tests conducted. Also included is a comparison of the results from tests performed using different test methodologies.

## Objective

The objective of this study was to evaluate the MVMA Thoracic Impactor and its associated procedures. This required the development of additional test procedures and parameters by the VRTC. It included an evaluation of the impactor on its ability to produce responses that could be used in thoracic injury assessment.

## Test Procedure Development

### Test objectives

In order to develop a test procedure and a matrix of tests, it was necessary to establish the goals of the testing. First, a test device and procedure should be capable of distinguishing between padded and unpadded door conditions. In addition, they should be able to differentiate among various cars and between good and poor door/side structure designs. A test matrix was developed to determine how well the MVMA device and procedures could accomplish these functions.

Another test objective was to compare the results of the subsystem tests with those of full-scale crash tests. This involved defining subsystem test parameters to simulate the crash environment as nearly as possible. This objective also made it necessary to select vehicles for testing which had previously been crash tested.

The suggested MVMA subsystem test procedure called for mounting the door in a rigid frame. Previous subsystem test programs done at the VRTC utilized the full body of the vehicle, thereby testing not only the door but the surrounding side structure. A comparison of these methods was of interest. Therefore, tests were planned to make this comparison.

Finally, door-to-occupant contact velocities in crash tests may relate to some door/side structure property, such as stiffness. If this is true, then the impact velocities used for the subsystem tests should be dependent upon this property. Therefore, force/deflection data from exterior static crush tests were collected for all doors tested, whether mounted in the vehicle body or in the frame.

### Testing

To achieve the objectives outlined in the previous section, three series of tests were conducted. Test Series Number 1 utilized the full body of each vehicle tested. These tests included fixturing the cars to the floor, performing an exterior pre-crush on each door/side structure, and impacting the

interior of all of the doors at the same pre-determined speed. For one vehicle, the door was replaced following an unpadded test, and a padded test was conducted. From these tests, the ability of the device to distinguish between padded and unpadded doors, and to distinguish between different vehicles when tested at the same speed was determined. In addition, exterior crush force/deflection data were collected for each vehicle. These were used in developing a velocity adjustment procedure based upon the side structural strength of a vehicle.

Test Series Number 2, similar to the first series, also used the full body of the vehicles. The impact velocity was determined separately for each car, using the velocity adjustment procedure developed from the exterior crush data obtained in the first series of tests. From these tests, the ability of the subsystem approach to distinguish between good and poor door/side structure designs were determined. Also, a comparison of these test results to those of the corresponding crash tests was made.

Finally, a third series of tests was done which essentially followed the subsystem test procedure suggested by the MVMA. This included mounting the doors in a rigid frame, performing a pre-crush on each, and impacting them at the same pre-determined velocity as in series 1. With these tests, a comparison of the door-in-frame and the full-body subsystem approaches was made.

The vehicles selected for testing were those for which the Agency has crash test data. Several vehicle models had been tested, both by the NHTSA and the MVMA, under the same conditions (as specified in the NPRM for Side Impact Protection, issued January 1988). From these, the cars selected for subsystem testing were as follows:

- 4-door Chevrolet Celebrity
- 4-door Chevrolet Citation
- 2-door Dodge 400
- 2-door Ford Granada
- 4-door Plymouth Horizon
- 4-door Ford LTD
- 4-door structurally modified Ford LTD
- 2-door Volkswagen Rabbit
- 2-door Chevrolet Spectrum

### Impact and pre-crush location

For each vehicle in each series of tests, it was necessary to determine certain test parameters. These include the impact location on the interior of the door, the location of the exterior pre-crush, and the extent of this pre-crush. The impact velocities used were also determined. This included determining the velocity for the first and third series of tests, as well as developing a velocity adjustment procedure for determining the individual velocities for the second test series.

Since the full-body tests were to be compared to the crash tests, the impact location on the inner door for each of these tests should match that impacted by the SID in the corresponding crash test, as determined from crash test photogra-

phy. The vertical line containing the center of the SID ribcage was located from each crash test. The impact for the corresponding subsystem test was centered on this line (see table 1) and located such that the impactor face hit just below the window opening of the door.

**Table 1. Impact and pre-crush locations.**

Vehicle	Horizontal Impact Locations*			Vertical Pre-Crush Locations # - All Tests
	Impact	Pre-Crush	Door-In-Frame Impact & Pre-Crush	
Celebrity	7"	9.5"	8.5"	4.5"
Citation	6"	8.5"	7.8"	4.8"
Dodge 400	21"	23.6"	22.5"	5.6"
Granada	18.5"	21"	22.5"	4.5"
Horizon	7.5"	10"	11.3"	5.2"
LTD	5.5"	8"	11.5"	5.9"
Rabbit	11.5"	14"	15.5"	5.7"
Spectrum	10.8"	13.2"	17.3"	5.8"

\* distance forward of the lower rear corner of the window opening  
# distance from bottom edge of crusher face above lower rear corner of closed front door

It was also necessary to specify the location of the pre-crush for each car. Normally, the pre-crush would be centered on the same vertical line as the impact. In the first series of tests, several additional tests were conducted (not reported here) in which impacts were centered farther forward on the same door, for the same pre-crush. This required that the pre-crush be centered 2.5" (64 mm) forward of the impact centerline (see table 1). The one padded test performed on the replaced door used the same pre-crush and impact locations as the corresponding unpadded test. In order to allow for comparisons, the pre-crush location used for each car in the first series of full-body tests was also used in the second series of full-body tests.

The vertical location of the crusher face was determined using the suggested MVMA procedure. The bottom edge of this face was positioned 15.7" (400 mm) above the ground surface reference plane for the vehicle being tested. Using the lower rear corner of the closed front door as a reference, this position was found from the standard MVMA specifications for each vehicle (see table 1).

The longitudinal interior impact and exterior pre-crush locations for the door-in-frame tests were found differently than for the full-body tests. Since only one test was done per door, the impactor was centered on the vertical centerline of the crusher face. As in the suggested MVMA procedure, the crusher face was positioned such that its vertical centerline passed through the mid-seat H-point. In cases where the crusher face was within 3" (75 mm) of the door opening, the crusher face was moved to achieve this minimum clearance (see table 1). The vertical pre-crush and impact locations were determined in the same manner as for the full-body tests.

The extent of the pre-crush was determined from the MVMA proposed subsystem test procedure. An exterior crush of 9.1" (230 mm) was applied to all doors/side structures. Once extended, the crusher face was held in this extended position throughout the conduct of the dynamic test. Inner panel displacements were also monitored for all tests.

## Impact Velocity

One of the potentially critical test parameters to be determined was impact velocity. In crash tests, the moving barrier velocity was the same for each test. The actual contact velocity between the door and the occupant may be a function of the moving barrier velocity and the integrity of the struck vehicle's side structure. A good design appears to reduce this contact velocity more than a poor design, thereby offering a greater degree of occupant protection.

In a subsystem test, however, the impact velocity must be determined prior to testing. If all vehicles are tested at the same speed, benefits from superior door design may not be evident. Ideally, the impact velocity in a subsystem test would vary from vehicle to vehicle, being representative of the actual contact velocity that would occur in a crash test of the particular vehicle. Determining these contact velocities is not trivial.

Nine vehicles, listed previously, that had been crash tested were selected for subsystem testing with the MVMA thoracic impactor. An attempt was made to determine the door-to-occupant contact velocity for each test. Dummy rib and spinal acceleration data from the crash tests were used to determine the time of door-to-occupant contact. Struck door accelerations were used to determine door velocities at contact. The struck door accelerometers were placed in a very severe environment in the crash tests, so it was not unusual for the data from these instruments to contain anomalies. Since the use of these data was rather subjective, and since the results were scattered, the door accelerometer information was not used to determine contact speeds for individual cars, but was only used to determine a general range and overall average for contact velocities. This average contact velocity was found to be 18 mph (29 km/h), and was used as the impact velocity for the first series of full-body tests and the series of door-in-frame tests.

For the second series of full-body tests, it was still necessary to derive an individual contact speed for each of the cars, for use in a correlation with exterior crush properties. Peak rib and spinal velocities from the crash tests were more reliable and more consistent than the door velocities. Unfortunately, these velocities differ from the actual contact velocities by rebound velocities and variations in the velocity during the loading on the dummy that are not easily determined. The rebound velocities are probably not constant from one vehicle to the next, although assuming them to be so may lead to predicting reasonable contact velocities.

Dummy rib and spinal peak velocities from each crash test were used as possible independent variables in the STEPWISE routine of the Statistical Analysis System (SAS). These are listed in table 2 and were defined as follows:

RIBV—peak average rib velocity

SPINEV—peak average spinal velocity

The dependent variables for these regressions were taken from the static force/deflection data obtained from the exte-

rior pre-crush performed on each vehicle in the first full-body test series. These were the stiffness (average slope of the rising portion of the force/deflection curve), peak force, and static crush energy from each car (area under the rising portion of the static force/deflection curve, ie. not the dynamic crush energy seen in a crash test). These are also listed in table 2.

**Table 2. Crash test velocities and exterior crush results SAS variables.**

Vehicle	Independent Variables		Dependent Variables		
	RIBV (mph)	SPINEV (mph)	Stiffness (lb/in)	Peak Force (lb)	Crush Energy (ft-lb)
Celebrity	22.4	25.7	920	7580	3252
Citation	24.7	27.1	904	7744	3624
Dodge 400	25.3	26.1	777	6793	3228
Granada	23.6	26.7	947	7606	3245
Horizon	24.6	27.1	690	6962	3516
bas LTD	22.5	26.0	774	6548	2911
mod LTD	19.5	21.6	1770	13,382	5308
Rabbit	25.5	27.2	666	6119	2903
Spectrum	24.8	29.6	633	5768	2956

STEPWISE was run using the data described above. Only one variable model was considered since there were a relatively small number of data points. When stiffness (STIFF) and peak force (FORCE) were used as dependent variables, the highest correlations existed with peak spinal velocities. Although stiffness and peak force produced the same coefficient of determination when correlated with peak spinal velocity ( $r^2 = 0.81$ ), stiffness was chosen as being more representative of the entire exterior crush event than peak force. Thus, spinal velocities could be predicted from the stiffness of a vehicle's door/side structure by the following relationship:

$$SPINEV = 31.28 - 0.00549(STIFF)$$

where STIFF is in lb/in and SPINEV is in mph.

The line predicted by this relationship is shown in figure 1, along with the actual data points from the nine cars tested. Note that this regression was heavily influenced by the rightmost data point (modified LTD). Using this equation, a predicted spinal velocity was calculated for each car (see table 3). As mentioned previously, spinal velocity differs from the actual contact velocity by some rebound velocity. Based on the approximation that rebound velocity was a constant percentage of the spinal velocity, contact velocities were estimated by normalizing the predicted spinal velocities to the average contact velocity of 18 mph (29 km/h). These predicted contact velocities, also listed in table 3, were used as the impact speeds for the second series of full-body tests. [Crash test data obtained since the completion of this study indicated that an impact velocity of 22 to 25 mph (35 to 40 kph) may have been more appropriate (3). While this would have increased the response levels, the relative difference between the cars would not necessarily change.]

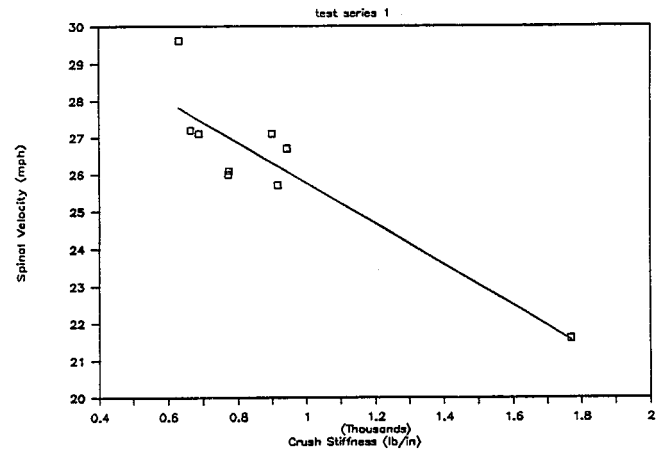


**Figure 1. Stiffness/velocity regression.**

**Table 3. Adjusted velocities—regression results.**

Vehicle	Stiffness (lb/in)	Actual Spinal Velocity (mph)	Predicted Spinal Velocity (mph)	Predicted Contact Velocity (mph)
Celebrity	920	25.7	26.2	17.9
Citation	904	27.1	26.3	18.0
Dodge 400	777	26.1	27.0	18.5
Granada	947	26.7	26.1	17.9
Horizon	690	27.1	27.5	18.8
bas LTD	774	26.0	27.0	18.5
mod LTD	1770	21.6	21.6	14.8
Rabbit	666	27.2	27.6	18.9
Spectrum	633	29.6	27.8	19.0
average	XXX	26.3	26.3	18.0

## Padding

The MVMA thoracic impactor was evaluated to determine its ability to distinguish between padded and unpadded door conditions. The padding selected for use was that used in the MVMA MDB-to-Ford LTD crash tests (4). This was ArCel padding, manufactured by the ARCO Chemical Company, and had a nominal density of 2lb/in<sup>3</sup> (32 kg/m<sup>3</sup>).

The results of the crash tests of Reference 4 indicated that this padding was too stiff, thereby not offering as much protection to the occupant as was possible. Softening the padding, to a point, would reduce the impact severity. Beyond that point, when the padding becomes too soft, impact severity increases. A limited attempt was then made to determine this "optimum" stiffness.

First, an 18 mph (29 km/h) test was done into a rigid surface, recording both small and large mass accelerations, as well as the relative deflection between the two masses. A second test, also at 18 mph (29 km/h), was done into a 3" (76 mm) thick piece of 8" X 12" (203 X 305 mm) ArCel padding. The peak accelerations and relative deflections from these tests are compared in table 4. The padding produced a

significant decrease in the small and large mass peak accelerations, as well as in the relative deflection, over the rigid impact (41%, 44%, and 9%, respectively).

Table 4. Padding stiffness results 18 mph.

Impact Surface	Acceleration (g)		Relative Deflection (inches)
	small mass	large mass	
Rigid	171.4	83.6	2.97
Padding	101.3	47.1	2.70
Padding With Holes	66.4	45.3	2.67

A second piece of ArCel padding was also tested at 18 mph (29 km/h). It had the same exterior dimensions as the first, but had nine  $\frac{7}{8}$ " (22 mm) holes drilled through it vertically. These holes were intended to reduce the effective stiffness of the padding. The results of this test are also listed in table 4. The large mass peak acceleration and relative deflection remained essentially unchanged from the previous padding test, but the small mass response showed another sizable decrease (34%).

Because the small mass acceleration decreased, this reduced stiffness padding represented an improvement over the original padding. It was recognized that an even softer padding might be closer to the "optimum" stiffness when mounted to an actual door since the door acts as a spring in series with the padding. However, this was intended to be a limited investigation, so the reduced stiffness padding described above was selected for use in the padded full-body test.

## Hardware

In order to perform the required tests, support hardware for the impactor was needed. This included a frame to support the impactor, a pre-crush device, a means to secure the car to the ground in the full-body tests, and a frame to mount the doors for the door-in-frame tests.

Figure 2 gives an overview of the hardware. The vehicles were positioned between parallel I-beams which were bolted to the floor. Raised off of their suspension, the cars attached to cross-horses at both the front and rear bumper mount locations. These cross-horses fastened to the I-beams. To further reduce body movement, chains were added in line with the direction of crush. Early tests indicated that this method of securing the vehicles results in essentially no general body movement during the pre-crush phase of testing.

The pre-crushes were accomplished with the apparatus shown to the right in figure 2. Powered by a servo-controlled hydraulic pump, a 4" diameter piston pushed the crush plate into the side of the vehicle being tested. This was a cast aluminum plate identical to the one used in the sub-

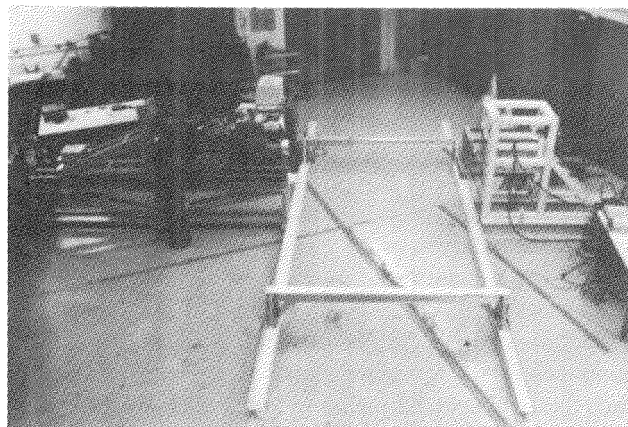


Figure 2. Overview of test hardware.

system tests performed for the MVMA (5). This device was adjustable to achieve the desired vertical position for the crush plate. The entire pre-crush apparatus could also be adjusted laterally relative to the car (left to right in the photo).

A frame was built to support and position the impactor itself, shown in the left side of figure 2. The frame allowed the impactor to reach into and across the width of the tested car and be easily moved out of the way to allow vehicle installation. The impactor was mounted on a triangular frame and was adjustable vertically. The triangular frame was attached to a rectangular sub-frame by means of linear bearings, which permitted movement of the impactor into and out of the vehicle being tested. The triangular frame and impactor were secured prior to performing a test. The rectangular sub-frame was also capable of limited adjustment in the longitudinal direction relative to the car (in and out of the page).

Finally, a frame was built for mounting the doors tested (see figure 3). The doors mounted to two posts by their hinges and latches/striker pins. The periphery of the doors was also supported along the bottom and sides by means of bars mounted in a backup frame. These supports simulated the door opening of the vehicle, except that they were rigid.

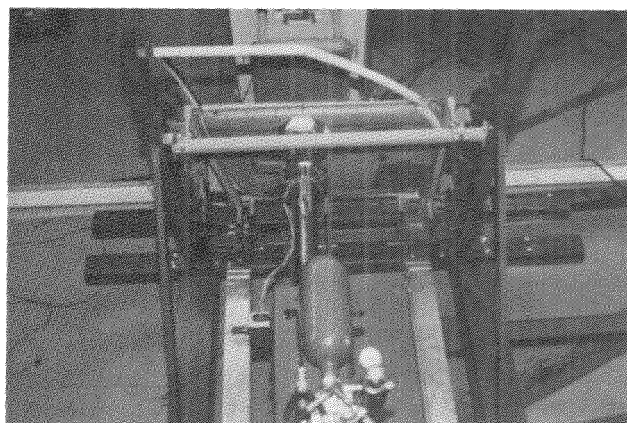


Figure 3. Door frame fixture.

## Impactor Calibration

The MVMA Thoracic Impactor was a two mass system connected by a spring/damper element. A schematic view of the impactor is shown in figure 4. The spring/damper element was actually composed of two parts, a cylindrical Urethane main "spring" between the two masses and a conical secondary "spring". Upon impact, the small mass moved toward the large mass, thereby compressing the Urethane spring. After about 1 inch (25 mm) of relative deflection, compression of the conical spring began. This continued for the rest of the stroke between the two masses, for a total of about 3.2 inches (81 mm). These springs were a major factor in determining the dynamic response characteristics of the impactor.

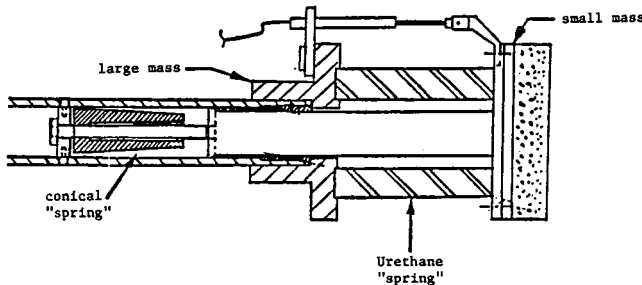


Figure 4. MVMA thoracic impactor.

The impactor was to meet the force/time and peak relative deflection corridors established from the one and two meter cadaver drop tests performed by Association Peugeot-Renault (APR) (6), and normalized by Krause (7). Therefore, calibration impacts were performed into a rigid surface at both the 1 and 2 meter drop speeds (9.91 and 14.01 mph—15.95 and 22.55 km/h, respectively). The force/time histories from these calibration tests, as compared to the APR corridors, are shown in figures 5 and 6. At the lower speed, the resulting force curve followed the corridor fairly well during the loading portion, but reached a peak about 350 lbs (159 kg) above the upper limit of the corridor. At the 2 meter drop speed, the resulting force curve stayed within the corridor for essentially the entire event. These results were similar to those obtained by the MVMA from earlier testing.

The peak relative deflections measured for these tests were 1.40" and 2.43" (35.6 and 61.7 mm), respectively. The calibration ranges for these values were as follows:

- 1 meter—1.06 to 1.30" (26.9 to 33.0 mm)
- 2 meter—1.54 to 1.85" (39.1 to 47.0 mm)

As can be seen, the device did not meet the peak deflection criterion established.

After the previously described tests were performed, as well as many others, the impactor was disassembled and inspected. It was found that the conical spring was torn nearly in half at its mid-length. This spring was replaced and the calibration tests were repeated. The 1 meter drop speed test produced a force versus time trace very similar to that

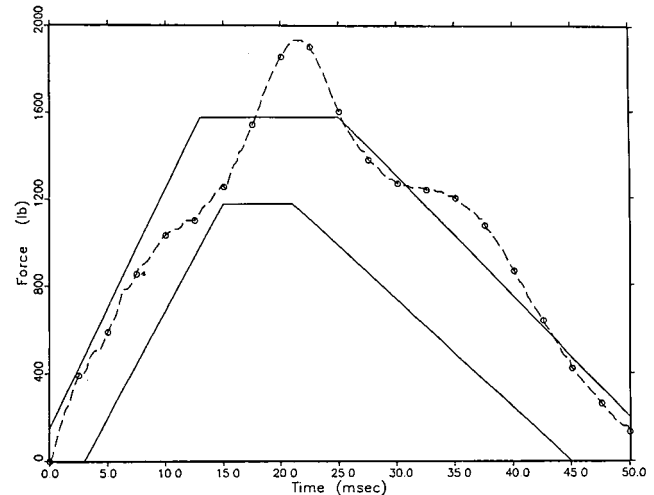


Figure 5. 1 m calibration—urethane spring system.

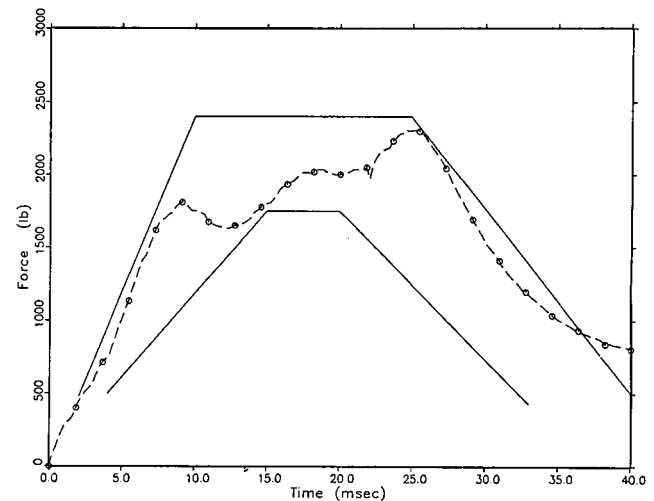


Figure 6. 2 m calibration—urethane spring system.

done previously (see figure 7). The peak relative deflection for this test was 1.37" (34.8 mm), which was closer to the desired range, but still high. The 2 meter drop speed test resulted in the force versus time curve shown in figure 8. There was quite a difference from the original curve, with an exaggerated center hump, peaking about 300 lbs (136 kg) higher than the original. Peak relative deflection for this test was 2.39" (60.7 mm), slightly lower than the original, but still half an inch over the specification.

Throughout all testing, two conical springs were torn, and a third damaged. A brief investigation led to the finding that the cone would deteriorate gradually from the inside surface. This degradation would become evident, if inspected, after very few impacts, but many were required to actually tear the cone. The severity of the impacts would determine the actual number it could withstand.

## Test Methodology Comparison

### Test results

The most crucial aspect of this program was to evaluate the ability of the device and its associated procedures to assess

the thoracic injury potential of vehicles. This included performing three series of tests, two using the full body of the vehicles, the third testing the doors mounted in a fixture. In addition, one padded test was done to estimate the benefit from 3" (76 mm) of ArCel padding, using the impactor. The results from the three series of tests are listed in tables 5 through 7.

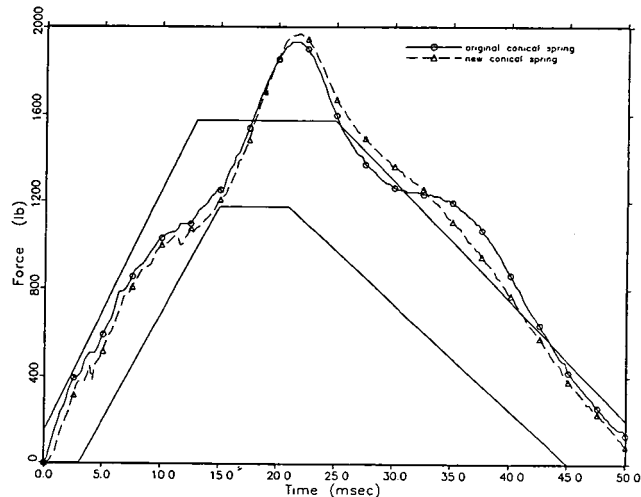


Figure 7. 1 m calibration—urethane spring system.

Note the relative deflection between the large and small masses as shown in figure 9. Frequently, this deflection flattened near the peak. Since this happened at various levels of deflection, it was not due to overscaling the instruments or data acquisition components. Both peak accelerations and peak velocity occur prior to this flattening.

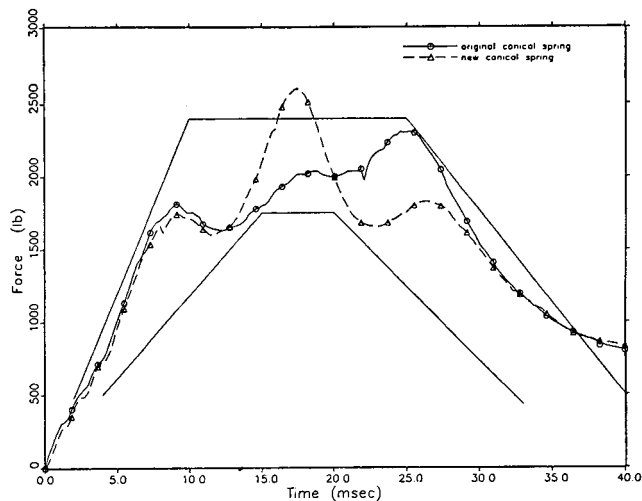


Figure 8. 2 m calibration—urethane spring system.

### Comparison of Results

*Padding effects.*—Baseline and padded Granada tests were conducted. The purpose of these was to estimate the benefit from 3" (76 mm) of ArCel padding, using the impactor. The peak accelerations, peak relative deflections, and peak Viscous Criterion (8), or V\*C, for these two tests are compared in table 5. Overlay plots of these responses for the two tests are shown in figures 10 through 13. Note that the largest peak of the baseline small mass acceleration occurred at about 60 msec. This was due to the small mass rebounding into the large mass and was therefore not considered to be the peak small mass response. In summary, 3" (76 mm) of ArCel padding had the following effect on the

Table 5. MVMA thoracic impactor test results full-body test series No. 1—18 mph.

Vehicle	Test Number	Actual Impact Velocity (mph)	Peak Acceleration (g)		TTI			Peak Relative Deflection		VC(max)	
			sm mass (rib)	lg mass (T12)	age 0	age 23	age 41	(in)	(msec)	(m/sec)	(msec)
Celebrity	P25018	18.0	118.6	44.4	81.5	113.7	138.9	2.48	27.000	1.035	22.625
Citation	P25001	17.7	94.2	41.4	67.8	100.0	125.2	2.35	30.625	0.747	15.375
Dodge 400	P25006	17.9	55.2	48.8	52.0	84.2	109.4	2.58	34.250	0.871	24.250
Granada (baseline)	P25013	18.0	71.7	51.3	61.5	93.7	118.9	2.60	35.125	0.973	20.625
Granada (padded)*	P25017	18.0	43.0	31.2	37.1	69.3	94.5	2.18	39.250	0.426	32.375
Horizon	P25011	18.0	92.8	35.7	64.3	96.5	121.7	2.22	32.500	0.763	27.875
bas LTD	P25019	17.9	72.5	50.6	61.6	93.8	119.0	2.63	32.125	1.279	19.875
mod LTD	P25020	17.8	73.7	53.3	63.5	95.7	120.9	2.67	29.625	1.307	17.625
Rabbit	P25021	18.0	77.3	59.2	68.3	100.5	125.7	2.67	30.750	1.237	18.250

\* Granada padded test was done on a new door and at the same location as Granada unpadded test.

Table 6. MVMA thoracic impactor test results fixtured door tests—18 mph.

Vehicle	Test Number	Actual Impact Velocity (mph)	Peak Acceleration (g)		TTI			Peak Relative Deflection		VC(max)	
			sm mass (rib)	lg mass (T12)	age 0	age 23	age 41	(in)	(msec)	(m/sec)	(msec)
Celebrity	P25036	18.1	113.9	50.5	82.2	114.4	139.6	2.83	26.750	1.202	20.625
Citation	P25038	18.0	116.1	46.0	81.1	113.3	138.5	2.88	22.875	1.361	17.500
Dodge 400	P25030	17.7	53.2	35.6	44.4	76.6	101.8	1.66	38.750	0.384	15.250
Granada	P25028	17.7	48.2	33.2	40.7	72.9	98.1	1.38	36.250	0.250	14.000
Horizon	P25039	18.0	96.0	44.8	70.4	102.6	127.8	2.51	33.000	0.733	15.000
LTD	P25040	18.0	83.0	41.3	62.2	94.4	119.6	2.21	32.625	0.533	13.500
Rabbit	P25031	18.0	127.2	63.4	95.3	127.5	152.7	2.81	22.250	1.292	16.000
Spectrum	P25035	18.1	73.9	40.4	57.2	89.4	114.6	1.94	34.500	0.524	14.000

Table 7. MVMA thoracic impactor test results full-body test series No. 2—adjusted velocities.

Vehicle	Test Number	Impact Velocity (mph)		Peak Acceleration (g)		TTI			Peak Relative Deflection		VC(max)		Crash Tests TTI age=0
		intended	actual	sm mass (rib)	lg mass (T12)	age 0	age 23	age 41	(in)	(msec)	(m/sec)	(msec)	
Celebrity	P25045	17.9	17.86	111.9	39.9	75.9	108.1	133.3	2.40	30.625	0.827	26.625	79.0
Citation	P25044	18.0	17.97	80.9	43.8	62.4	94.6	119.8	2.70	32.750	0.875	23.125	89.5
Dodge 400	P25046	18.5	18.36	90.4	42.7	66.6	98.8	124.0	2.51	36.375	0.867	27.375	118.5
Granada	P25051	17.9*	22.63*	119.4	92.4	105.9	138.1	163.3	2.92	23.000	1.733	19.875	102.5
Horizon	P25049	18.8	18.97	100.9	41.7	71.3	103.5	128.7	2.66	30.125	1.094	25.250	111.5
bas LTD	P25050	18.5	18.40	66.8	54.5	60.7	92.9	118.1	2.77	24.125	1.287	19.000	98.5
mod LTD	P25054	14.8	14.78	56.2	38.5	47.4	79.6	104.8	2.28	32.625	0.613	27.000	83.5
Rabbit	P25047	18.9	18.74	68.5	61.9	65.2	97.4	122.6	2.73	25.375	1.242	19.875	115.5
Spectrum	P25048	19.0	19.07	74.2	61.5	67.9	100.1	125.3	2.84	24.375	1.350	19.125	83.5

\* test intentionally conducted at a higher speed, as discussed in the 'Comparison of Full- and Sub-System Approaches' section.

responses measured by the impactor: peak small mass and large mass accelerations were reduced by 40% and 39%, respectively, resulting in a 40% reduction of TTI (age=0), and peak relative deflection and peak V\*C decreased 16% and 56%, respectively.

*Comparison of subsystem approaches.*—Another aspect of this study was to compare two different subsystem test procedures. This was done using the results of the full-body tests performed in test series 1 and those of the fixtured door tests, since both were conducted using a nominal impact speed of 18 mph (29.0 km/h). Comparisons were made between peak accelerations, peak relative deflections, peak

V\*C, static crush curves, and overall deformation of the doors.

In many cases, the crush pattern on the fixtured door was very different from that mounted in the body. Overhead views of the crushed doors from the full-body (a) and fixtured door (b) baseline LTD tests are shown in figure 14. Note that the full-body door followed the contour of the crush plate reasonably well, while the fixtured door creased in the center, causing it to bend away from the crush plate. This left a large gap between the plate and the exterior surface of the door. As evidenced in the figure, the pre-crush locations for the fixtured door tests were determined differ-

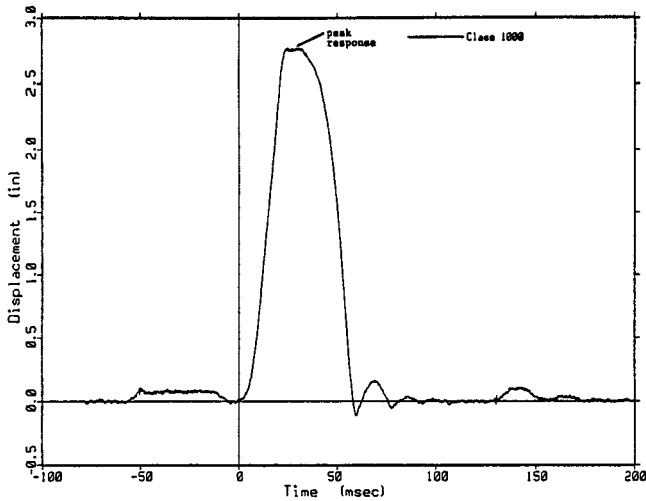


Figure 9. Baseline LTD—relative deflection.

ently from those of the full-body tests. One of the reasons for this was the proximity of the rigid fixturing.

Overlays of the force vs. exterior crush and inner panel displacement vs. exterior crush curves for the baseline LTD full-body and fixtured door tests are shown in figures 15 and 16. The force curves are similar for the first 4 1/2" (115 mm) or so, but then separate. As indicated in figure 16, about 3 1/2" (90 mm) more exterior crush was required to produce inner panel displacement on the fixtured door than on the body mounted door. The main reason for these differences, as well as those of the crush patterns shown in figure 14, was that the door fixture had a rigid "B-pillar" while that of the car body was not. The B-pillar of a car has a large effect on the side strength of a vehicle. Mounting a door in a rigid frame changed the crush characteristics significantly.

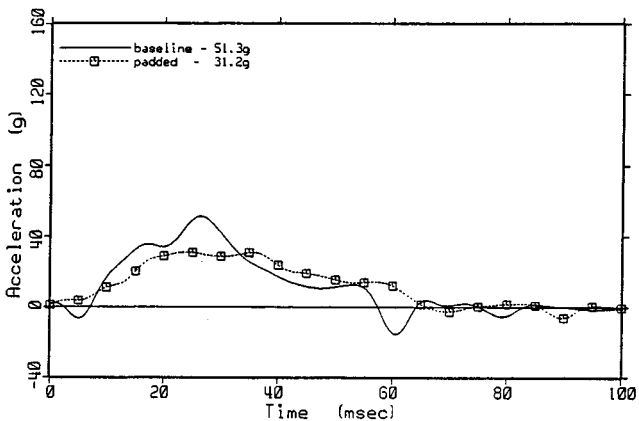


Figure 10. Granada—large mass—HSRI filter.

The results of the dynamic tests (listed in tables 5 and 6) were also used to compare the two subsystem approaches. Three response measurements were used: TTI (age=0), peak relative deflection, and peak V\*C. These are compared in figures 17 through 19 for each door, with the full-body test results in increasing order. Linear correlations were done to compare the full-body test results with those of the fixtured door tests. The regressions produced coefficients of deter-

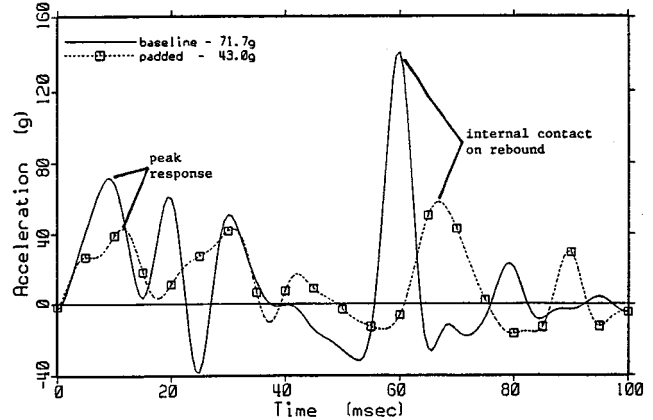


Figure 11. Granada—small mass—HSRI filter.

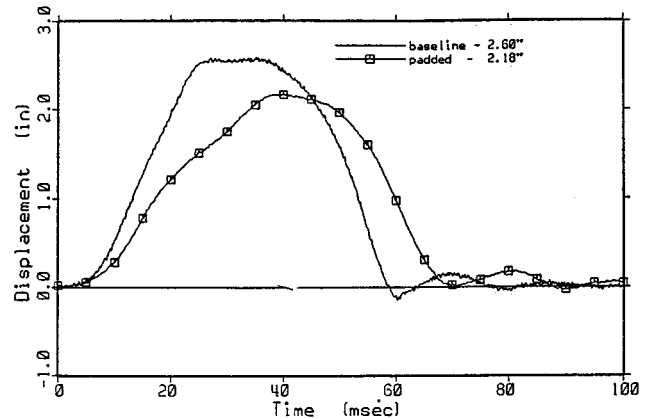


Figure 12. Granada—relative deflection.

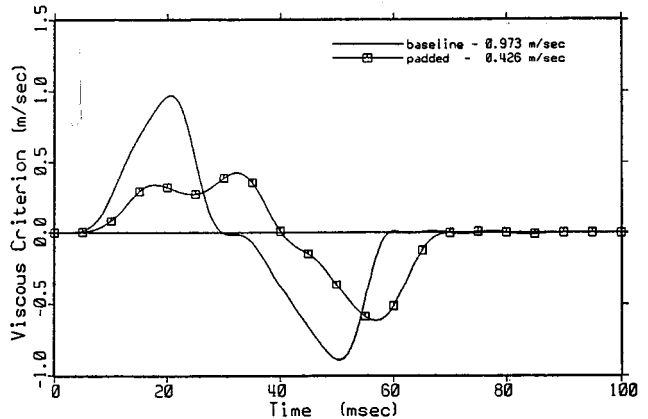
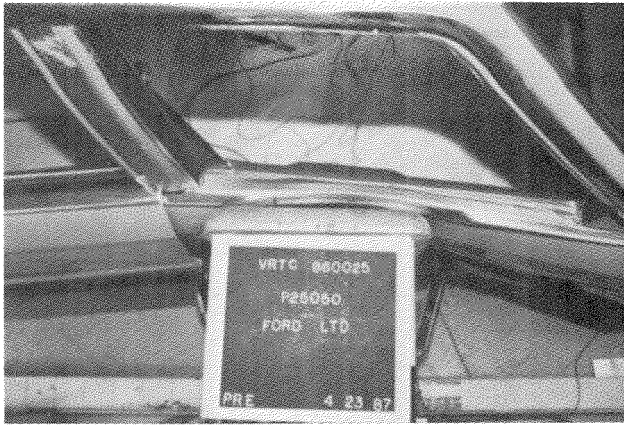


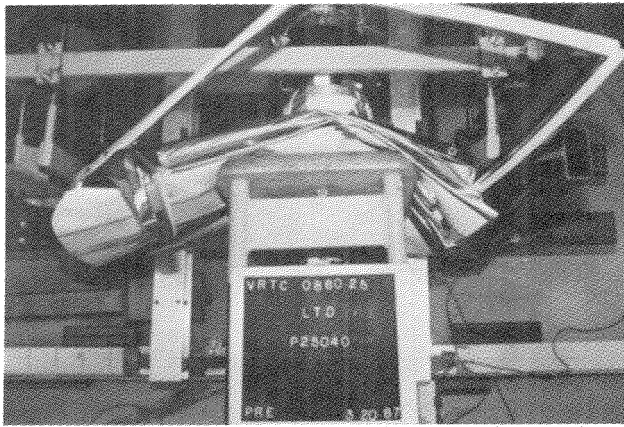
Figure 13. Granada—viscous criterion.

mination ( $r^2$ ) for TTI (age=0), peak relative deflection, and peak V\*C of 0.51, 0.14, and 0.00, respectively.

The number of tests that produced essentially the same results ( $|\Delta| < 10\%$ ), the number in which the full-body test produced higher results, and the number in which the fixtured door test produced higher results are summarized in table 8. These figures and table indicate that one approach did not consistently give the same or higher results than the other, but that they varied considerably. Overall, there was a mild correlation of TTI values between the two approaches, and no significant correlation based upon deflection or V\*C.



a. Full-body pre-crush.



b. Fixtured door pre-crush.

Figure 14. Baseline LTD pre-crush comparison.

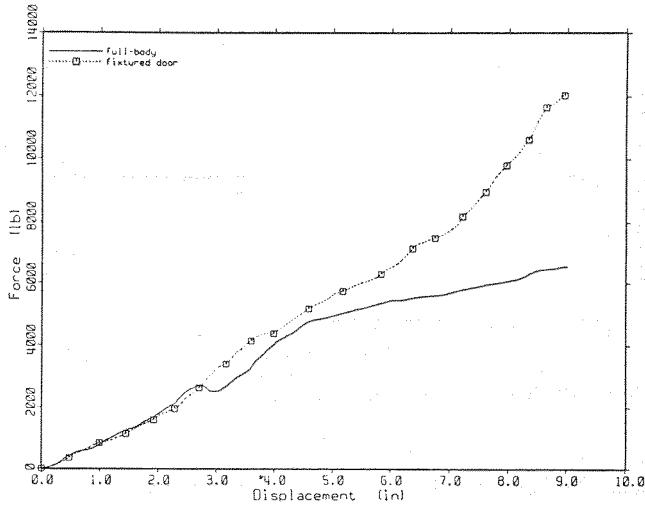


Figure 15. Baseline LTD—exterior crushes.

Comparison of full- and subsystem approaches.—A second series of full-body tests were conducted using various impact speeds. These speeds were determined as described previously, and each was intended to be representative of the door-to-occupant contact velocity that occurred in the full-system crash test performed on that particular vehicle. The results of these tests (listed in table 7) were compared to those from the crash tests. Comparisons were made based

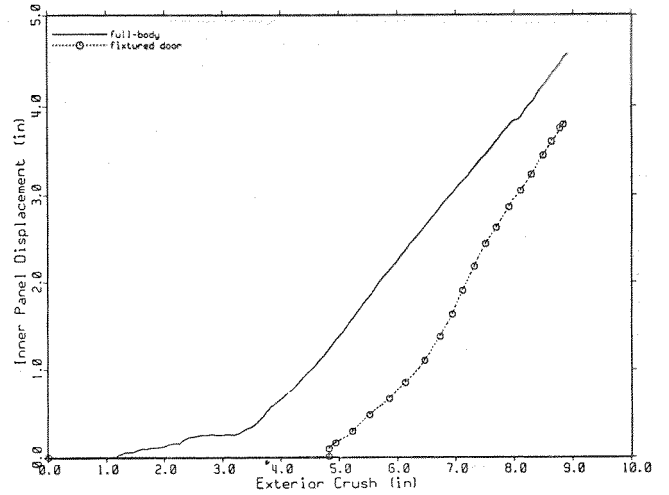


Figure 16. Baseline LTD—Inner panel displacement.

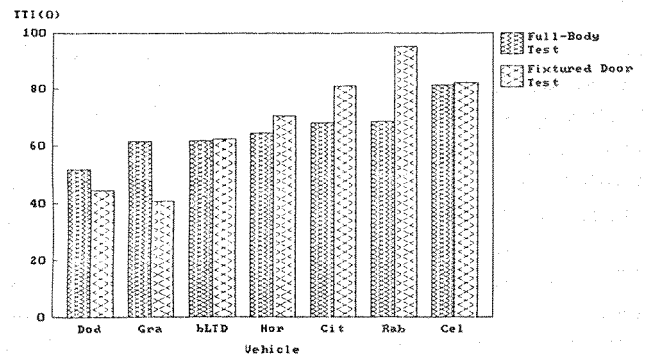


Figure 17. Full-body/fixtured door test comparison TTI (age=0).

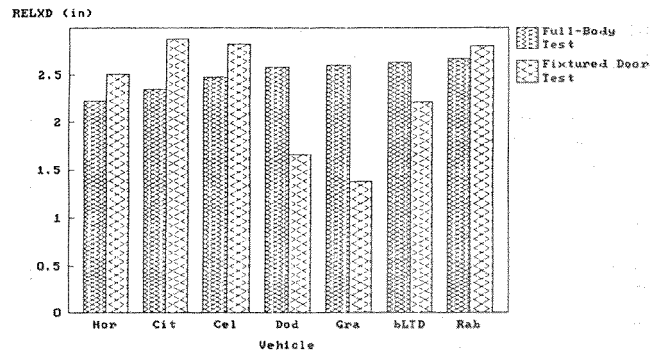


Figure 18. Full-body/fixtured door test comparison—peak relative deflection.

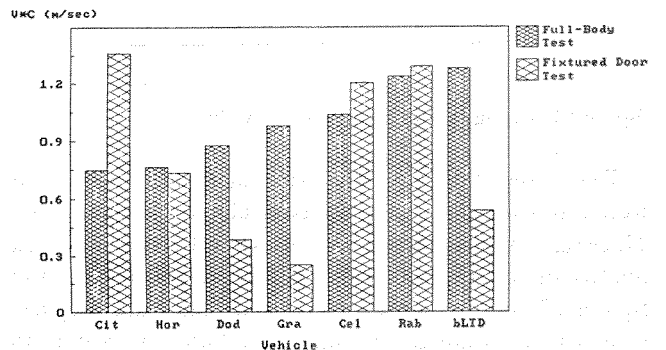


Figure 19. Full-body/fixtured door test comparison peak Viscous Criterion.

**Table 8. Full-body versus fixtured door test results frequency summary.**

	TTI(0)	Relative Deflection	Peak V*C	average
same $ \Delta  \leq 10\%$	3	1	2	2
full body higher	2	3	3	2 2/3
fixtured higher	2	3	2	2 1/3
total	7	7	7	7

on TTI (age = 0) only, since comparative relative deflections and V\*C's were not available for the crash tests.

A comparison of the TTI (age = 0) values for the crash tests (in increasing order) and for the second series of full-body subsystem tests is shown in figure 20. Note that the baseline Granada test results from the first series of tests were used here rather than those from the second. The reason for this was that impact velocity found for this vehicle to simulate the crash test contact velocity was 17.9 mph (28.8 km/h), which was very close to the 18.0 mph (29.0 km/h) used in the first series of tests. Instead of repeating that condition, the second test was done using a higher speed.

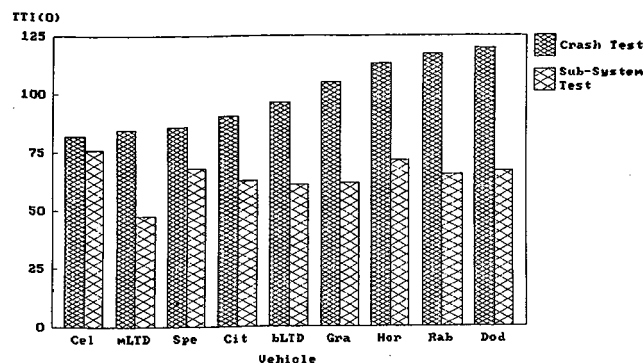


**Figure 20. Crash test/subsystem test comparison TTI (age=0)**

Two things stood out when the results were compared. First, the subsystem tests produced less severe impacts than the crash tests in every case, with an average decrease in TTI (age = 0) of 34.4%. This may simply indicate that the impact velocities chosen for the subsystem tests were not high enough to produce similar injury levels at the crash tests. [Crash test data obtained since the completion of this study indicated that an impact velocity of 22 to 25 mph may have been more appropriate (3)]. Second, the injury levels predicted by the impactor showed little variation among the production vehicles. Excluding the modified LTD test, the average TTI (0) was 66.4, with a coefficient of variation of 7.9%. This compares to a coefficient of variation on the crash test TTI (age = 0) values for the same eight vehicle models of 14.9% (see table 7). A linear regression was performed to compare the TTI (age = 0) values of the subsystem tests with those of the crash tests. The resulting  $r^2$  value was 0.02, indicating that no significant correlation existed. Overall, for the test procedures used in this study,

the impactor and crash test results did not follow similar patterns and the results from one type of test could not be predicted by the results of the other.

Although comparisons with crash test results could not be made, two other response measurements were estimated from the impactor test results. As shown in figure 21, the peak relative deflections from the second series of full-body tests, like the TTI (age = 0) values, showed little variation among the production vehicles. Excluding the modified LTD, the average peak relative deflection was 2.65" (67.3 mm), with a coefficient of variation of 5.4%. The peak V\*C values, on the other hand, showed a higher level of variation (see figure 22). Excluding the modified LTD, the average peak V\*C was 1.064 m/sec, with a coefficient of variation of 19.5%.

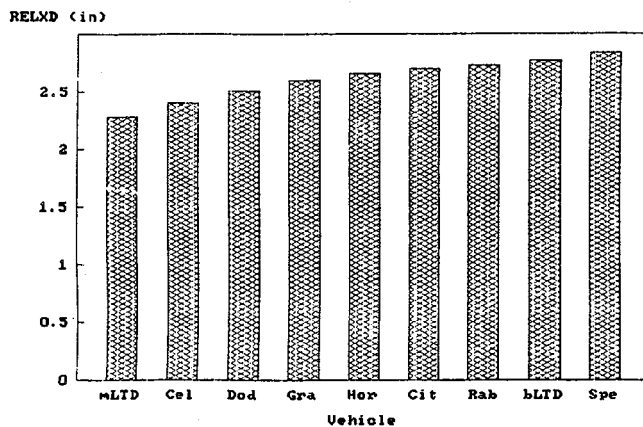


**Figure 21. Full-body subsystem tests: adjusted velocities—peak relative deflection.**

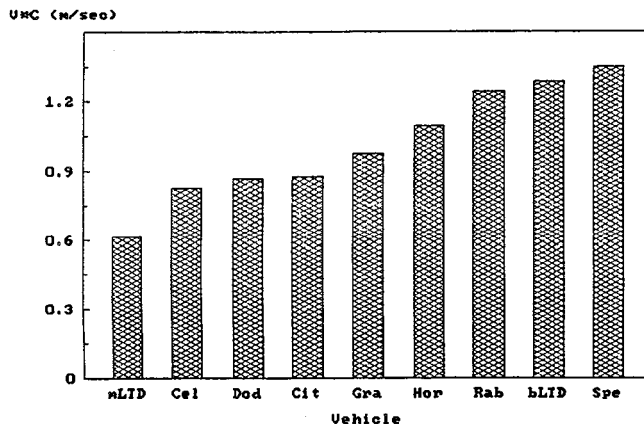


**Figure 22. Full-body subsystem tests: adjusted velocities—peak Viscous Criterion.**

It was also possible to distinguish between the baseline and structurally modified vehicles, using the impactor and this test procedure. The results of the LTD's tested in the second series of full-body tests are contained in table 7. All three response measurements decreased in the modified vehicle test. TTI (0) decreased 21.9%, peak relative deflection decreased 17.7%, and VC (max) decreased 52.5%. This was expected since the impact speed predicted from the study described previously and used for testing for the mod-

ified LTD was 20% lower than that for the baseline vehicle (14.8 and 18.5 mph—23.8 and 29.8 km/h, respectively). Note in table 5, that when these two vehicles were tested at the same impact speed, the results were nearly identical.

## Conclusions

Based on the results and observations of this study, the following conclusions were made:

1. For the subsystem test procedures used in this study, the MVMA Thoracic Impactor and the full-body crash test results were essentially unrelated. The TTI (age = 0) values from the second series of full-body subsystem tests were 34.4% lower, on average, than the crash test values. A linear regression comparing the two sets of values produced a coefficient of determination,  $r^2$ , of only 0.02.

2. The ability to show variation among the production vehicles tested using the thoracic impactor and the procedures of this study was dependent upon the response measurement considered. The coefficients of variation for the second series of full-body subsystem tests were as follows:

- TTI (age = 0)—7.9%
- peak relative deflection—5.4%
- peak Viscous Criterion (V\*C)—19.5%

The coefficient of variation for the TTI (age = 0) values from the crash tests on the same eight vehicle models was 14.9%

3. The 3" (76 mm) ArCel padding sample used on the Granada door resulted in substantial response reductions. In full-body tests, with an impact speed of 18.0 mph (29.0 km/h), the padded test responses were reduced as follows:

- TTI (age = 0)—40%
- peak relative deflection—16%
- peak Viscous Criterion—56%

4. Using the thoracic impactor and the full-body test procedures of this study, it was possible to distinguish between baseline and structurally modified vehicles only if an impact velocity adjustment procedure was applied. When both were tested at a nominal speed of 18 mph (29 km/h), the structurally modified vehicle produced the following response changes:

- TTI (age = 0)—3.1% increase
- peak relative deflection—1.5% increase
- peak Viscous Criterion—2.2% increase

Using the adjusted impact speeds of 18.4 and 14.8 mph (29.6 and 23.8 km/h) for the baseline and modified vehicle tests, respectively, the modified vehicle responses were reduced as follows:

- TTI (age = 0)—21.9%
- peak relative deflection—17.7%

peak Viscous Criterion—52.4%

5. Using a nominal impact speed of 18 mph (29 km/h) for all tests, a slight correlation was found between the TTI results of the full-body subsystem tests and the fixtured door subsystem tests. No significant correlation was found using other response measurements. Linear regressions performed to compare the two subsystem test approaches produced the following coefficients of determination,  $r^2$ :

- TTI (age = 0)—0.51
- peak relative deflection—0.14
- peak Viscous Criterion—0.00

6. Many of the peak relative deflections measured in this study flattened near the peak. Peak accelerations and peak V\*C occur prior to this flattening.

7. The thoracic impactor did not meet the calibration corridors as well as desired, but its calibration performance was judged to be acceptable. The original 1 meter drop speed calibration test done on the impactor produced a force/time history that stayed within the corridor during most of the loading phase, but peaked about 350 lb (159 kg) above the corridor. Peak relative deflection for this test was 1.40" (35.6 mm), which was 0.10" (2.5 mm) above the corridor. The original 2 meter drop speed calibration test produced a force/time history that matched the corridor very well. Peak relative deflection for this test was 2.43" (61.7 mm) which was 0.58" (14.7 mm) above the corridor.

8. The durability of the conical secondary spring used in the thoracic impactor was not good. During the course of testing, two were torn and replaced, one was damaged. It was determined that deterioration occurred gradually from the inside surface.

9. The response of the thoracic impactor was somewhat sensitive to the condition of the conical secondary spring. Calibration tests done following the replacement of the torn conical spring with a new one produced different results. The 1 meter drop speed test showed very little change from the corresponding original test, with a peak relative deflection of 1.37" (34.8 mm). The 2 meter drop speed calibration test produced a different force/time history than that of the corresponding original test, peaking about 300 lb (136 kg) higher than the first test. The peak relative deflection was 2.39" (60.7 mm).

## References

- (1) Donald T. Willke, Michael W. Monk; "Side Interior Stiffness Measurement"; Final report for project SRL-66, report number DOT-HS-806-708; September 1984.
- (2) Donald T. Willke, Michael W. Monk; "Side Impact Subsystem Development: MVMA Thoracic Impactor Test Procedure and Evaluation"; Final Report for project

VRTC-86-0025, report number DOT-HS-807-373; November 1988.

(3) Donald T. Willke; "Side Impact Door Velocity Measurement;" final report for project VRTC-87-0056; April 1989.

(4) Patrick M. Miller, Leonard R. Kamholz; "Analysis of MVMA 16 Car Crash Test Data"; Final report for MGA Agreement No. MGA 8621-C6135-SI, MGA File No. C86R-04; June 1986.

(5) Leonard R. Kamholz, Patrick M. Miller; "Subsystem Testing and Evaluation of MVMA Thorax Impactor"; Final Report for MGA Agreement No. MGA 8626-C6137C, MGA File No. C86R-06; November 1986.

(6) Tarriere, C., et al.; "Synthesis of Human Tolerances Obtained from Lateral Impact Simulations;" Seventh International Technical Conference on Experimental Safety Vehicles; June, 1979.

(7) Krause, P.L.; "Normalization of Side Impact Cadaver Dynamic Response Data Utilizing Regression Techniques;" paper number 840883 presented at the SAE Government/Industry Meeting; May 1984.

(8) Lau, Ian V. and Viano, David C.; "The Viscous

Criterion-Bases and Applications of an Injury Severity Index for Soft Tissues;" paper number 861882 presented at the Thirtieth Stapp Car Crash Conference; October, 1986.

## Acknowledgements

The views and findings of this paper are those of the authors and do not necessarily represent the policy of the NHTSA. The authors are grateful to Rodney Herriott and Glenn Wagoner for their efforts in the set-up and conduct of the tests, as well as to Claude Melton for his help in the procurement of the vehicles and doors.

The authors also wish to thank Thomas MacLaughlin and James Hackney for their assistance in formulating project objectives and for their efforts in the execution of these objectives.

The authors are also grateful to the Motor Vehicle Manufacturers Association for its cooperation in loaning the impactor to the NHTSA for this program, and to the MGA Corporation for their assistance and instruction on operating the device.

Also, special thanks go to Susan Weiser for the preparation of the manuscript.

## Safety Performance Evaluation of Production Vehicles in Side Impacts Using the Modeling Approach

**Joseph N. Kianthra,**  
National Highway Traffic Safety Administration  
**Thomas J. Trella,**  
Transportation Systems Center  
**Stephen P. Edwards,**  
Automated Sciences Group Inc.,  
United States

### Abstract

For the past several years, the National Highway Traffic Safety Administration (NHTSA), has conducted research on thoracic protection in side impacts. As part of this research a lumped mass computer model was developed for simulating side crashes. This model has been exercised extensively to simulate the interaction of the struck car door and the occupant in side impacts. Simulation studies were also undertaken to investigate the effects of various vehicle design parameters on occupant responses.

This paper analyzes the performance differences seen in eight production vehicles tested with the NHTSA side impact test procedure, with the aid of this model. The energy absorption in various parts of the side structure of the struck car, the striking barrier and the occupant represented in the model were computed for the passenger car tests simulated. The results showed that increased energy dissipation in the struck vehicles generally yielded lower Thoracic Trauma.

Index (TTI). Viscous Criterion (VC) showed a similar trend for absorbed energy in the door core due to thorax contact. However, such energy dissipation in certain components alone does not assure that the desired vehicle or occupant response to effectively reduce the TTI measured on the dummy (TTI(d)). Instead, the appropriate sharing of the energy in an optimum manner among the various interacting components is essential to achieve the lowest possible TTI(d).

A mathematical relationship between the energy dissipated in three of the major structural components in the model and the TTI(d) has been derived knowing the energy dissipation distribution for the eight vehicle tests simulated. This relationship is utilized to present a set of useful curves which will enable the user to select energy absorption levels for various components of the side structure when TTI(d) level desired for a particular vehicle design is known.

### Introduction

Thoracic injuries constitute a very large portion of the serious to fatal injuries among occupants involved in car-to-car side impact accidents. The NHTSA has issued a Notice of Proposed Rulemaking (NPRM) (1)\* proposing to amend FMVSS 214 (2), "Side Door Strength", to establish its test procedures and performance requirements for passenger cars in side impacts. As a prelude to this activity the NHTSA

\*Numbers in parentheses designate references at end of paper.

has conducted numerous research projects on side impact protection in passenger cars for the past several years, including side impact tests of production cars between 1983 and 1985 (3, 4, 5, 6).

One research effort that was undertaken looked at the effects of various vehicle design parameters on occupant response with the aid of a lumped mass computer model (7) specifically developed for simulating side impacts. This model has been successfully used in evaluating various injury mitigation concepts for passenger car designs and to identify the most significant parameters that affect occupant responses. The sensitivity of some of those parameters in producing different levels of thoracic response measurements have also been investigated. Using the model, many side impact tests of production passenger cars conducted by NHTSA have been simulated. The model has shown close correlation to vehicle test results (7) and is considered suitable for analytical investigation of the influence of certain structural components in crash performance of cars in side impacts.

This paper analyzes the safety performance differences, as measured by the TTI(d) (8) and the VC (9), seen in the production vehicles simulated in terms of the structural behavior of the various vehicle components represented in the model. We begin with a brief description of the model. A

detailed description of the model is given in (7). Next we describe the test conditions and the occupant and vehicle structural characteristics that are likely to affect the safety performance of vehicles. Finally we present a detailed discussion of the methodology used in analyzing the simulation results and provide findings and conclusions.

## Side Impact Crash Model

Figures 1 through 2a show the mathematical model that simulates the responses of the Moving Deformable Barrier (MDB), the struck car and an unrestrained occupant, the Side Impact Dummy (SID), seated in the front seat on the struck side.

The struck car is characterized by nine masses and twenty one non-linear energy absorbing elements (EA's) that interconnect the various masses representing the different components of the struck vehicle. Four masses are used to model the response of the upper and lower, inner and outer sections of the door. The upper and lower sections of the A and B pillars are represented by an additional four masses. The remaining masses of the struck vehicle components are lumped with the rear seat occupant and is represented by a single mass designated as the passenger compartment. The

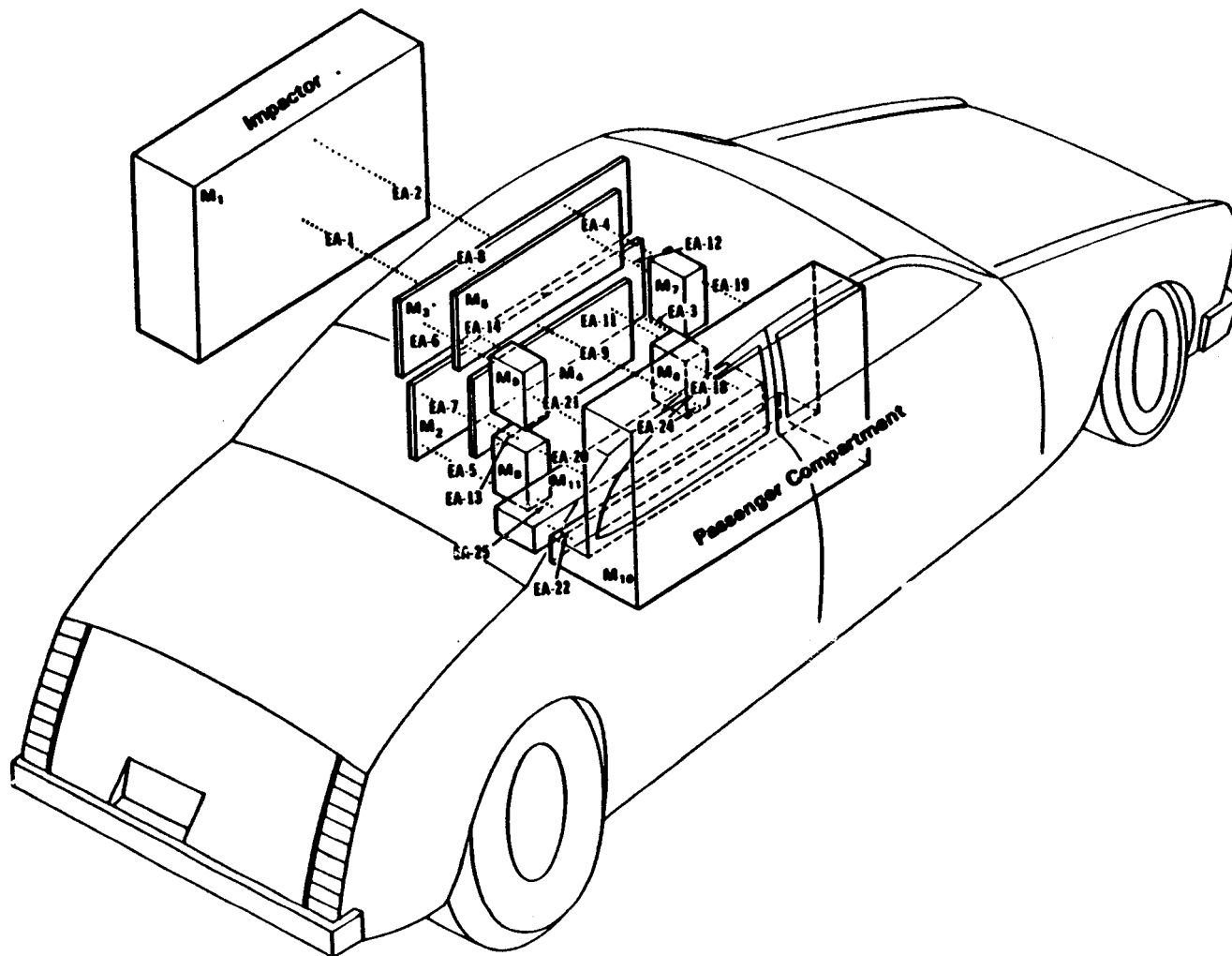


Figure 1. Lumped spring mass model for impacting vehicles.

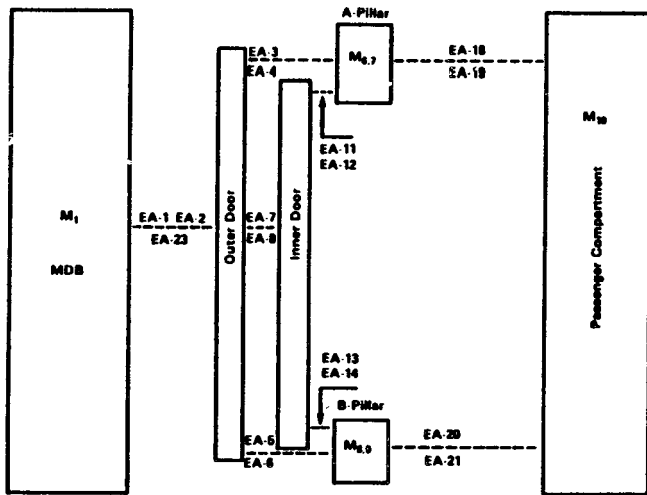


Figure 1a. Top view of the impacting vehicle model.

pillar sections and the door masses are interconnected by non-linear energy absorbers. Similarly the passenger compartment is also connected to the pillars. The energy absorbers in this model can be grouped to represent the following attachments:

- Group A: Outer Door to Pillar (EA-3, 4, 5, 6)
- Group B: Inner Door to Outer Door (EA-7, 8)
- Group C: Pillar to Passenger Compartment (EA-18, 19, 20, 21)
- Group D: Inner Door to Pillar (EA-11, 12, 13, 14)
- Group E: Upper Door to Lower Door (EA-10, 15)
- Group F: Upper Pillars to Lower Pillars (EA-16, 17)

The MDB is characterized by a single mass and two non-linear energy absorbing elements that represent the softer face and stiffer bumper sections of the front of the MDB.

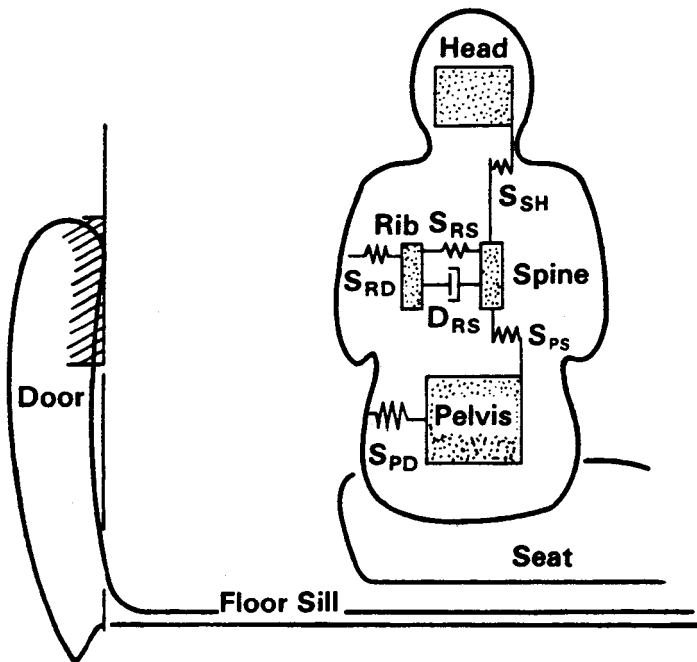


Figure 2. Lumped spring mass model of occupant.

- $M_H$  Head Mass
- $M_P$  Pelvis Mass
- $M_R$  Rib Mass
- $M_S$  Spine Mass

- $S_{RD}$  Rib-to-Door Energy Absorber
- $S_{PD}$  Pelvis-to-Door Energy Absorber
- $S_{RS}$  Rib-to-Spine Energy Absorber
- $S_{SH}$  Spine-to-Head Energy Absorber
- $S_{PS}$  Pelvis-to-Spine Energy Absorber
- $D_{RS}$  Rib-to-Spine Damper

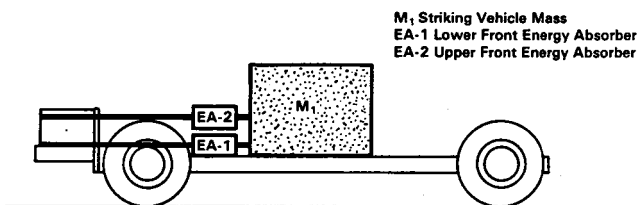


Figure 2a. Schematic of the moving deformable barrier.

Impact energy from the MDB is transferred to the struck vehicle through the pillars and the door sections. The occupant comes in contact with the inner door mass. The occupant response due to its interaction with the door is used in calculating the TTI(d).

The SID is modeled by four masses and six non-linear energy absorbers. Two of the masses represent the thorax, one representing the equivalent mass that interacts with the

impacting surface of the car door and the other representing the remaining equivalent mass of the thorax. These two masses are inter-connected by an energy absorbing non-linear spring and a viscous damper in parallel. The pelvis and the head are also included in the dummy model, with the door interacting with the pelvis and the pelvis connected to the spine as shown in figure 2. The model assumes that the energy from the impact is transferred to the SID directly by the door. The interaction between the dummy and the seat is neglected. Even though the head responses can be obtained from the one dimensional model, no interactions of the head with the side structure is considered in this simulation study.

## Vehicles Simulated

In an effort to establish the validity of the test procedures and test conditions in discriminating side impact safety

performance of vehicles, NHTSA conducted twenty side impact tests of production cars between 1983 and 1985 (3, 4, 5, 6). The primary objective of the test program was to determine the safety performance level of selected production cars in side crashes, while fine tuning the test devices and test procedures used. Since the issuance of the NPRM that proposes to amend FMVSS 214, NHTSA has conducted eight additional tests of production cars in 1988 (10) primarily to expand the existing side impact data base. Motor Vehicle Manufacturers Association (MVMA) (11) also conducted tests of Ford LTD cars, using the NHTSA test procedures and the SID to evaluate the repeatability of the test results.

In all of the tests above, the test condition simulated a 90 degree intersection collision with the striking vehicle moving at 30 mph (48 Km/hr) and the struck car at 15 mph (24 Km/hr). The impact point was 37 inches (92.5 cm) forward of the centerline of the wheel base. The struck vehicle remained stationary and the striking vehicle was towed at the closing velocity of approximately 33.5 mph (54 Km/hr) at a crab angle of 26 degrees. A MDB weighing 3000 lbs and having a 45 psi hexcel honeycomb face and 245 psi hexcel honeycomb bumper is used as the striking vehicle. A SID placed in the driver seat measures upper and lower rib and spine accelerations as well as the pelvis and head accelerations in the lateral direction. The thoracic injury potential is indicated by the TTI. TTI(d) as measured by the dummy is computed by averaging the Finite Impulse Response (FIR) filtered maximum rib acceleration and the peak lower spine acceleration.

The mathematical model mentioned earlier has been used to simulate eight of the vehicles tested. Out of these, five tests were from the earlier series of twenty tests, one from the MVMA series and two from the latest series of eight

tests. The vehicle makes and models included in the simulation are given below:

1. 1982 Honda Civic 4 door, weight 2488 lbs.
2. 1982 Nissan Sentra 2 door, weight 2340 lbs.
3. 1981 VW Rabbit, 4 door, weight 2465 lbs.
4. 1984 Chevrolet Celebrity 4 door, weight 3374 lbs.
5. 1985 Chevrolet Spectrum 2 door, weight 2488 lbs.
6. 1985 Ford LTD 4 door, weight 3239 lbs.
7. 1988 Toyota Tercel 5 door, weight 2550 lbs.
8. 1988 Chevrolet Sprint 2 door, weight 2100 lbs.

Figure 3 displays a ranking of these vehicles, based on the TTI(d) determined from the tests and by model simulations. Note that the simulation results are based on averaging the maximum rib and peak lower spine response from the model without any filtering of the model response. Also, given in figure 4 is the ranking on the basis of VC obtained from simulations of these tests. Since the vehicle and occupant are modeled as lumped masses and non-linear energy absorbers, it is envisioned that the safety performance, as measured by TTI(d), can be directly correlated to the physical characteristics assigned to the various vehicle components and their behavior in the model.

### Safety Performance Parameters

In a majority of side impact accidents, thoracic injuries of occupants may be caused mainly by the occupants' impact against the door interior and other intruding structures. A secondary impact can also occur due to velocity change of the struck vehicle. Even though it is difficult to determine the thoracic impact velocity of the door interior, it could be surmised that the primary impact velocity for the occupant could be as high as the impact speed of the striking vehicle.

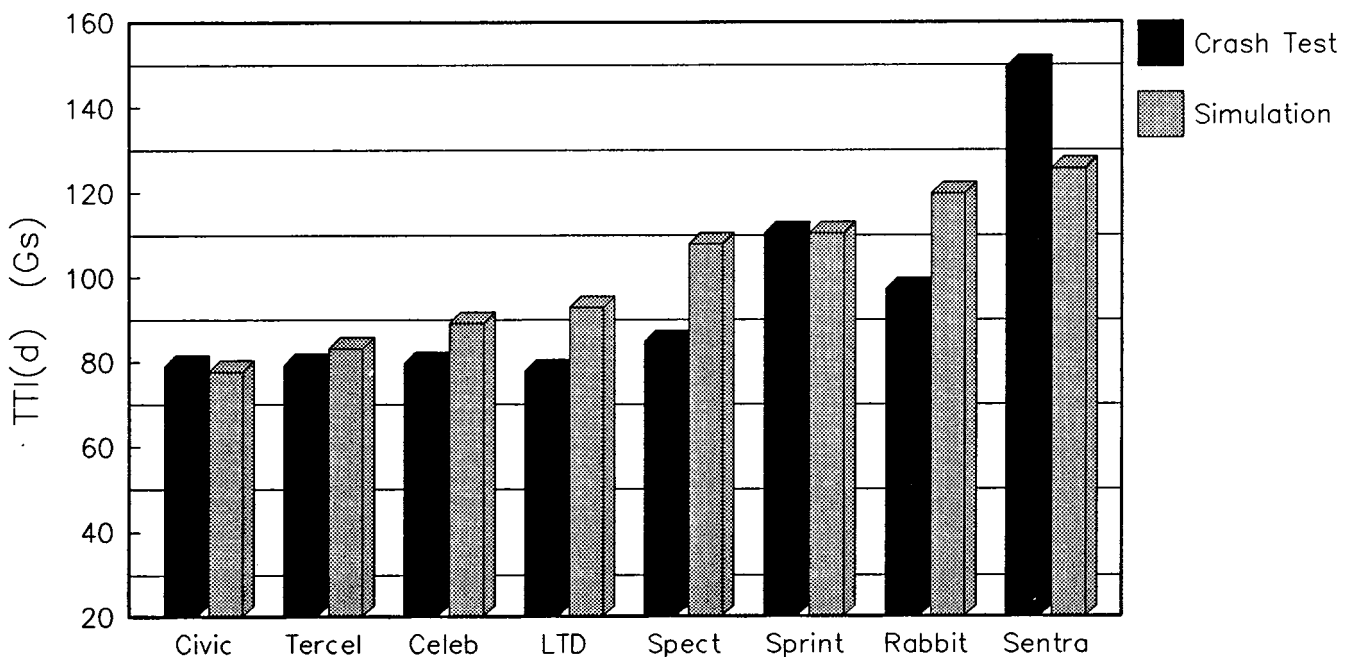


Figure 3. Vehicle rankings: thoracic trauma index.

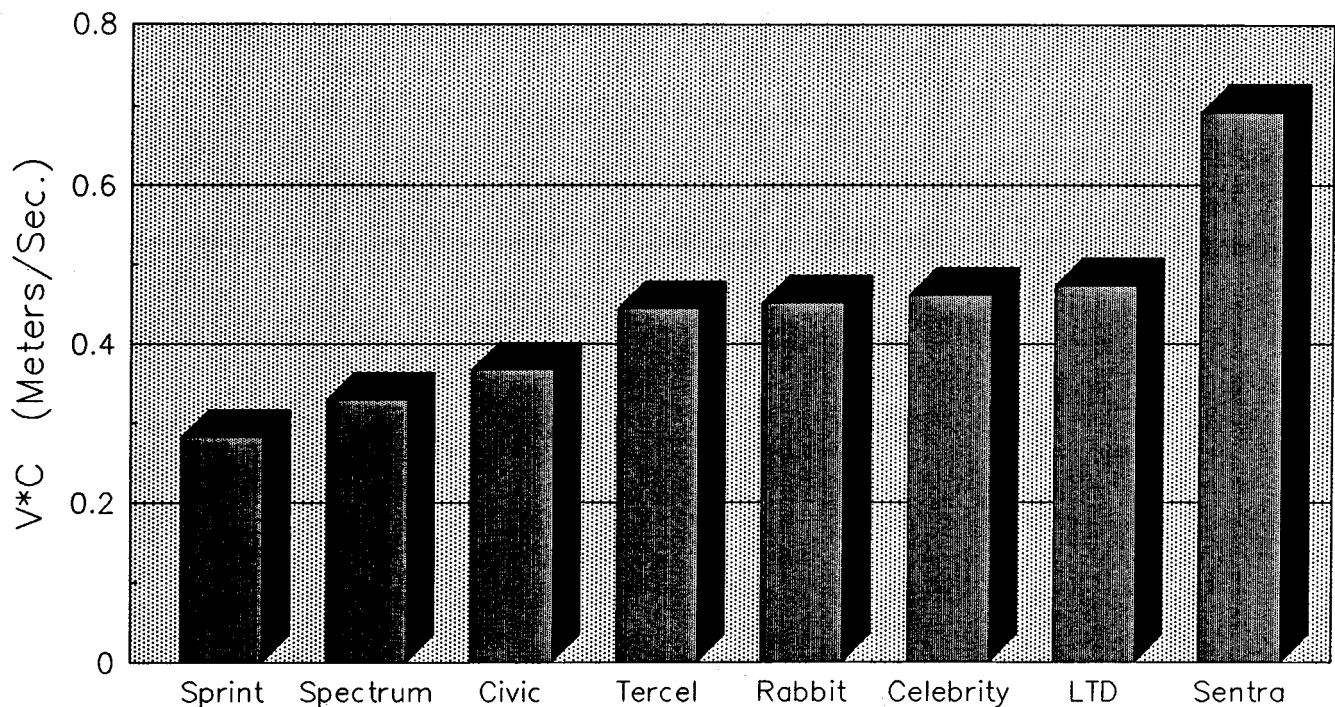


Figure 4. Vehicle rankings: modeled viscous criterion.

This could occur when the side structure of the impacted car has low side strength and it easily deforms. On the other hand, for extremely high strength side structures, the occupant impact velocity may be the same as the velocity change of the struck car, or even higher. In a real situation, neither of these theoretical conditions occur. The occupant impact velocity in real world accidents will, in all probability, lie between the velocity of the striking vehicle and the velocity change of the struck vehicle.

The occupant interior impact velocity is only one aspect of the overall injury causing parameter. Sudden collapse of the door structure, reducing the available space for the occupant, is equally unacceptable for the occupant. This requires that the structural integrity of the vehicle be maintained at least for some period of time during the crash. Also, any "hard" points on the door interior surface should be limited to areas where the occupant is least likely to contact.

The engineering challenge facing the designer is to select the appropriate design characteristics so as to minimize the occupant contact velocity while maintaining the compartment integrity. Thus the overall response of the struck vehicle is an important factor which affects the injury measurements obtained in tests of vehicles. For example, in some of the side impact tests conducted by NHTSA, it was observed that buckling and tear failure of the pillar and floor structure occur very early during the crash event and that the occupant injuries indicated by TTI(d) were severe. When such dramatic failures do not occur, the thoracic injury measurements tend to be low. Similarly, in some vehicles, the collapsed door appears to have no energy absorption capabilities remaining after the test while others indicate otherwise.

It is therefore conceivable that a number of vehicle design characteristics such as door thickness at the occupant contact areas, pillar design, pillar/floor/roof and pillar/door attachments, the seat and dash board design, the door width, and the car weight, all have important influence on the dummy injury measurements obtained in vehicle tests. Further, vehicle structural characteristics; such as the pillar strength, door strength, energy dissipation capability of side structures, and lateral resistance offered by the seat and seat attachment to the floor; also have an important bearing on the response characteristics of the struck vehicle. In addition to all of the above, occupant seating, occupant/vehicle contact area, impacting vehicle characteristics, impact point and the principal direction of applied force during the crash etc., also have equally important influence on the severity of the crash. Thus it is clear that the severity of the injuries an occupant receives in side crashes depend upon many factors such as the structural characteristics and masses of the striking and struck vehicles, the impact point and impact angle, the position of the occupant with respect to the intruding structures, the impact velocity and the capability of the occupant to withstand the crash loading.

As a designer of a vehicle, one may have control of a few of the parameters mentioned above. As an occupant, a person totally relies on the protection capability of the vehicle to reduce the severity of the injuries he or she may receive. Even though it is difficult to design a vehicle to perform safely at all possible impact conditions and speeds, the most logical approach is to make the vehicles perform satisfactorily at least at the most prevalent accident conditions. In proposing the 30/15 mph impact condition in the NPRM, NHTSA had concluded, on the basis of the U.S. accident statistics, that side impacts producing moderate to

severe injuries and fatalities in side crashes occurred at that speed and at an impact angle of 90 degrees (12). In defining the test barrier, the agency considered it necessary to use a barrier that is consistent in its loading behavior and that is capable of discriminating struck car safety performance. Even though the NHTSA MDB is heavier and stiffer than the other barriers used in Europe and Japan, the test configuration is considered to be representative of the impacting vehicle in injury producing crashes in the U.S. fleet.

The simulation studies described in this paper are based on test conditions and test devices described in the NHTSA proposed side impact test procedure. As such all the baseline results pertain to side impact tests of production vehicles using the 3000 lb NHTSA MDB striking a point 37 inches forward of the center line of the wheel base and using the unrestrained SID placed in the driver seating position. The purpose of this paper is to analyse the influence of as many of the struck vehicle design and structural characteristics as possible on the occupant response measurements indicated in the tests by using the mathematical model described earlier. This model is not comprehensive enough or even suitable for a complete analysis of the implications of vehicle structural characteristics. Nevertheless, it is possible to examine the effect of energy absorption capabilities of certain components of the vehicle structure, component stiffness characteristics, and their strength on the occupant responses and the resulting TTI(d) as determined with this model.

For the purpose of this paper, crash energy is defined as the overall energy input into the struck vehicle that is equivalent to the initial kinetic energy of the striking vehicle less the final kinetic energy at the striking vehicle at the end of the crash. Since the energy in each of the components of the interacting vehicle/barrier/dummy system are varying with respect to time, it is essential to compare these energies at a prescribed time when all the energy transfer would have been completed. For the analyses of the eight vehicles simulated, 75 milliseconds was considered to be sufficient for the energy transfers to have been completed in these tests. Also, since the occupant has left the contact with the door at about 45 milliseconds, this is sufficient time for the structure to reach a steady state. We also assumed that no secondary impacts of the dummy occur after 75 milliseconds. Therefore, all the analyses presented will be based on this period of time.

It is also assumed that in all of the tests simulated, the barrier impact velocity, the crab angle, the barrier weight, the effects of barrier braking etc. are similar. The occupant kinematic differences seen in the tests like dummy rotation are not considered in this analysis which uses the one dimensional model. Further, the terms dissipated, absorbed, expended, and consumed have been used throughout this paper interchangeably to describe energy dissipated in various components of the vehicle model.

## Analysis and Discussion

Energy from the moving barrier is in part transferred to the struck vehicle, which is initially stationary. Since the MDB is considered to be moving in the lateral direction at 30 mph (48 Km/hr), the total energy to be distributed in the system is approximately 90 K ft-lbs (122 K Newton-meters). Out of this, the kinetic energy retained by the barrier at the end of 75 milliseconds in the eight car tests simulated ranged from 15 K ft-lbs to about 28 K ft-lbs (20 to 38 K Newton-meters). The energy thus transferred to the struck vehicle together with that dissipated in the barrier face, ranged from 62 to 75 K ft-lbs (84 to 102 K Newton-meters) (table 1). The simulation of these tests showed that the barrier face absorbed from 3.3% of the crash energy in the Chevrolet Sprint crash event to about 5.7% in the Chevrolet Celebrity crash event. For a majority of the vehicles, the energy dissipated in the barrier is consistently about 4%.

The exact breakdown of the total crash energy into energy dissipated in the impactor and that which is transformed into kinetic energy of the vehicle, along with the remaining energy transferred to the dummy in these simulations are presented in table 1. The crash test TTI(d) and the model TTI(d) are also given in table 1. The energy absorbed (AE) in various components of the struck vehicle is presented in table 2. As seen in table 2, the model results indicate that maximum dissipation of energy occurs in the structural components attaching the pillar to the passenger compartment, followed by the outer door-to-pillar attachments and the door inner core structure. About 62 to 80% of the energy is absorbed in the pillar-to-vehicle compartment structural elements (Group C EA's) for the eight vehicles simulated while only 11 to 29% is consumed in the outer door-to-pillar connections (Group A EA's). The door inner core (Group B EA's) accounts for only about 4 to 8%. The remaining energy is dissipated in the inner door-to-pillar attachments (Group D EA's) and the pillar structure itself.

Figure 5 shows the total energy absorbed in the struck vehicle from table 2 plotted against the TTI(d) for the eight vehicles simulated. The data show that the higher the energy dissipated in the struck vehicle, the lower the TTI(d). However, it is not apparent from the data in this figure the importance of sharing of this total energy among the various structural components of the car. This will be illustrated in the subsequent analysis.

The data in table 2 show that the TTI(d) correlates well with the energy dissipated in both groups A and B energy absorbers and to a lesser extent, the energy absorbed in group C elements. The differences in the energy dissipation among the various structural components in the worst and best performing vehicles, indicated by their TTI(d), are presented in graphical form in figures 6 and 7. In these figures, the complete distribution of the crash energy is shown. Along with this, the distribution of the energy absorbed in the struck vehicle components are also indicated.

**Table 1. Modeled vehicle results.**

	Crash Test TTI(d)	Modeled TTI(d)	Crash Energy	KE Rise of Vehicle	Absorbed in Impactor	Delivered to Dummy
Rabbit	97	120	68,242	22,802	2,702	7,001
Sentra	149	126	66,330	22,390	3,096	6,619
Civic	79	78	66,962	22,690	2,795	5,025
Spectrum	85	108	68,920	24,789	3,665	5,118
LTD	78	93	84,661	25,093	3,669	4,285
Celebrity	80	89	75,601	24,831	4,295	3,800
Tercel	79	83	66,189	22,929	2,532	3,364
Sprint	110	110	62,610	21,590	2,101	5,792

\* Energy in Ft-Lbf

TTI(d) in G's

**Table 2. Absorbed energy in modeled vehicles.**

	Modeled TTI(d)	Total EA in Vehicle	Out Door-Pill Group A	Door Core Group B+E	In Door-Pill Group D	Up-Lo Pill Group F	Pillars-PXC Group C
Rabbit	120	35,737	4,183	1,289	130	620	29,515
Sentra	126	34,225	4,640	1,324	96	619	27,546
Civic	78	36,452	9,190	2,467	10	310	24,475
Spectrum	108	35,348	8,126	2,671	5	1,345	23,201
LTD	93	41,614	12,002	2,825	59	575	26,153
Celebrity	89	42,675	9,977	2,849	15	206	29,628
Tercel	83	37,364	9,120	1,548	10	454	26,232
Sprint	110	33,127	7,006	1,939	34	857	23,291

\* Energy in Ft-Lbf

TTI(d) in G's

### Structural Stiffness Relationship

The choice of equivalent stiffness as a parameter to characterize the safety performance of cars was attempted

in this study. Other parameters such as equivalent strength could have been used in place of stiffness since both parameters indicate similar trends. Equivalent stiffness is

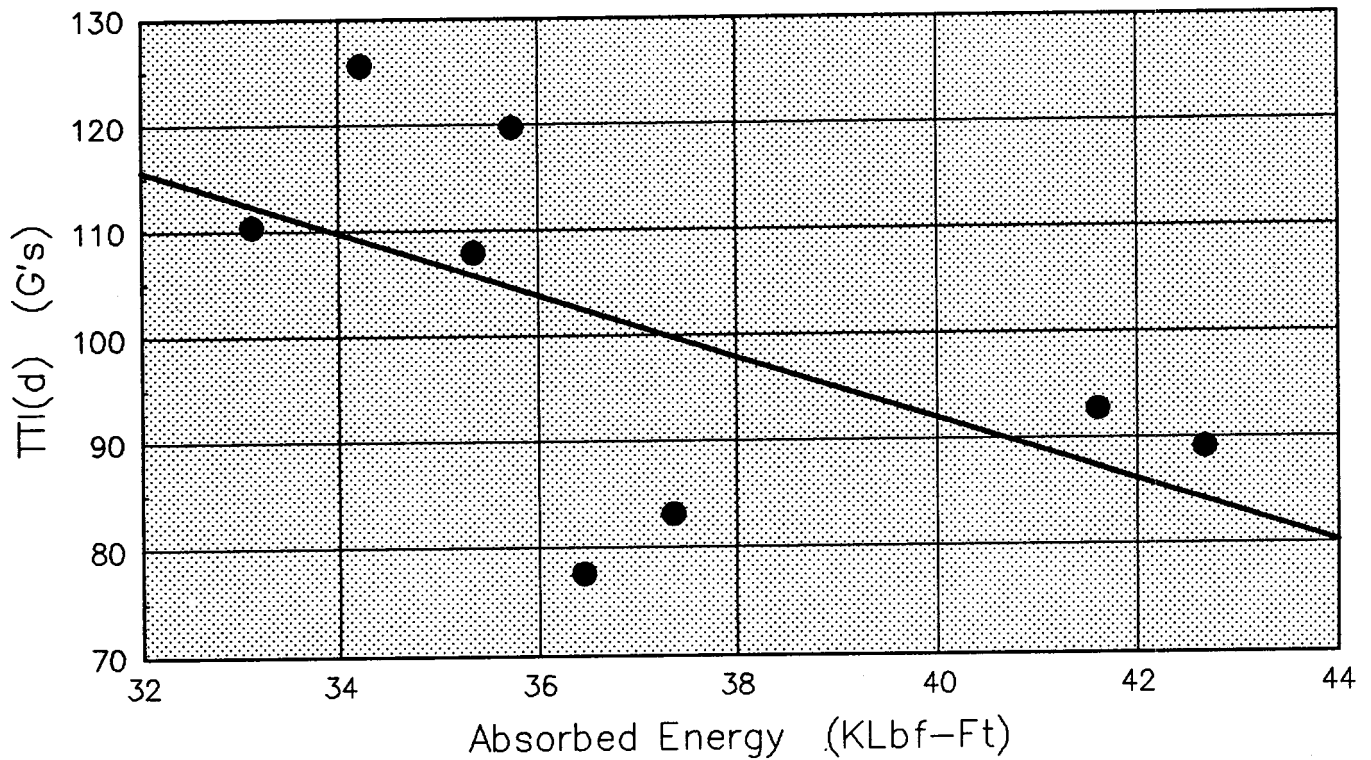


Figure 5. Modeled total absorbed energy in struck vehicle.

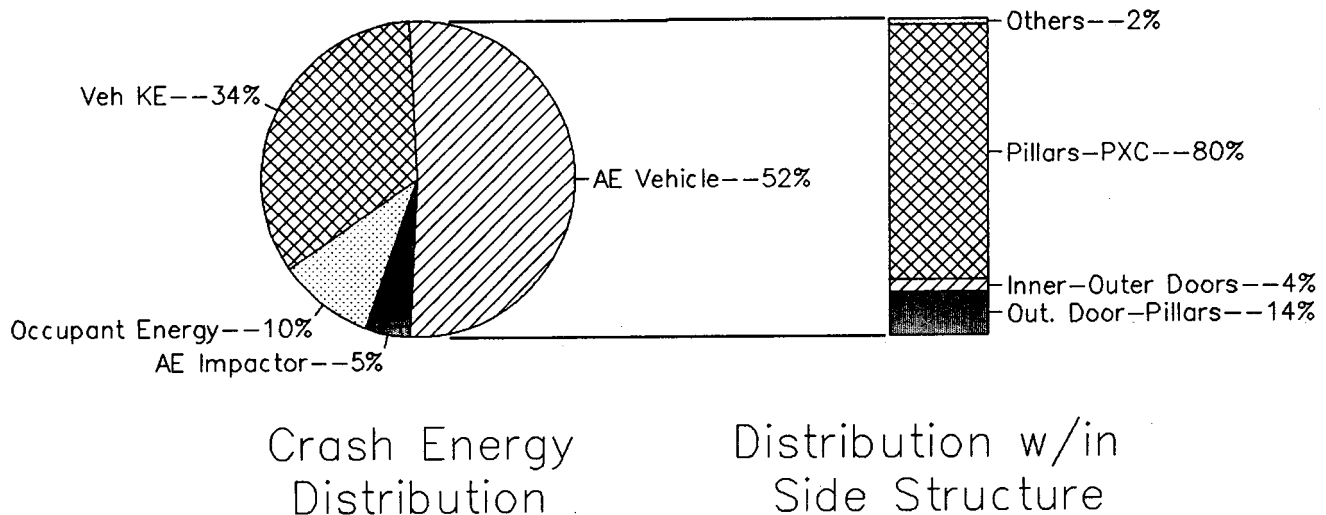
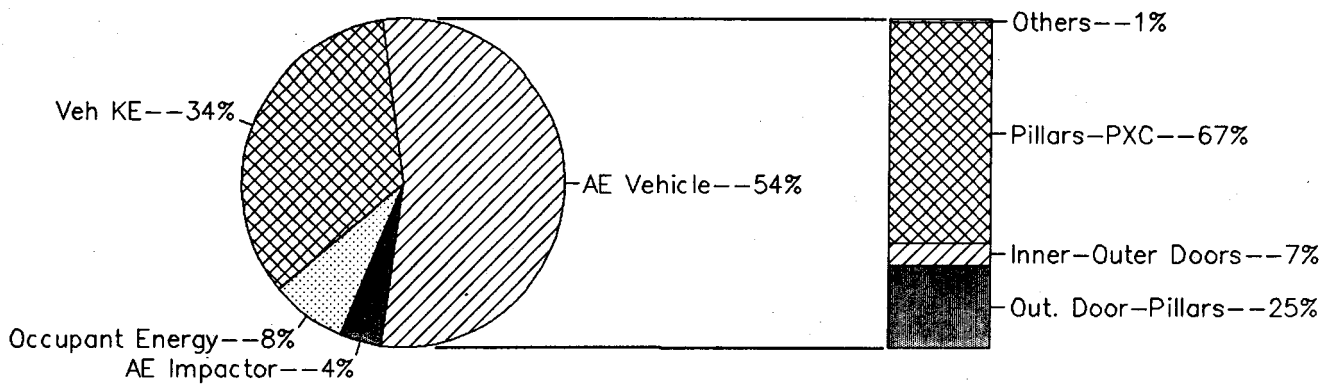


Figure 6. Crash energy and side structure energy distribution (1982 Nissan Sentra).

defined in this paper as the energy absorbed in a component divided by the square of the total crush of that component. The stiffness values for the three major groups of side structure elements, namely groups A, B and C, were calculated. The results are tabulated in table 3. It shows that the outer door-to-pillar structures are the stiffest followed by the pillar-to-compartment elements and the inner door core components.

The pillar-to-compartment structural stiffness (Group C EA's) as well as door-to-pillar (Group A EA's) and TTI(d) correlations are shown in figure 8 for the eight vehicles simulated. This figure shows that generally, the higher the equivalent stiffness of pillar-to-compartment (Group C

EA's) and door-to-pillar (Group A EA's) structural elements, the lower was the TTI(d) in the cars simulated, with the exception of the Ford LTD for Group A and Honda Civic for Group C. Ford LTD tests conducted by MVMA were different from the other tests conducted by NHTSA as the Ford LTD's were impacted on the right side. However, it is not known whether this caused any deviation from the general trend observed in the other vehicles. It should be noted that the Celebrity, Ford-LTD and Tercel vehicles' pillar-to-passenger compartment structure showed the highest equivalent stiffness. Of these three vehicles, the Celebrity and Tercel also revealed higher values for the outer door-to-pillar equivalent stiffness and lower values



Crash Energy Distribution

Distribution w/in Side Structure

Figure 7. Crash energy and side structure energy distribution (1982 Honda Civic).

Table 3. Modeled equivalent stiffness.

	Modeled TTI(d)	Out Door-Pill Group A	Upper Door Core (EA-8)	Pillars-PXC Group C
Rabbit	120	51,044	15,682	48,136
Sentra	126	57,113	16,645	52,378
Civic	78	119,875	10,106	56,453
Spectrum	108	85,402	9,906	63,163
LTD	93	58,381	8,356	79,901
Celebrity	89	100,107	9,432	69,899
Tercel	83	101,154	10,338	81,284
Sprint	110	94,708	17,013	63,488

\* Stiffness in Lbf/Ft

TTI(d) in G's

for the equivalent stiffness for the outer-to-inner door energy absorber. These vehicles had TTI(d)'s ranging between 80 and 90 Gs.

The authors believe that the TTI(d) correlated well with these stiffness parameters because the energy absorber groups selected to define these equivalent stiffnesses represent distinct zones of the vehicle which are generally affected in a crash. Therefore, the energy imparted by the MDB is mostly absorbed in these groups of side structural elements represented in the model.

### Optimized Struck Car Stiffness

With the aid of this model, the lowest achievable TTI(d) in the Nissan Sentra was investigated by varying the stiffness levels of the different side structure energy absorbing elements depicted in the model. Stiffness changes are defined as multiplication factors for the baseline vehicle force levels in the force-deflection characteristic traces. Their corresponding energy absorption levels due to these stiffness changes were used to evaluate the TTI(d).

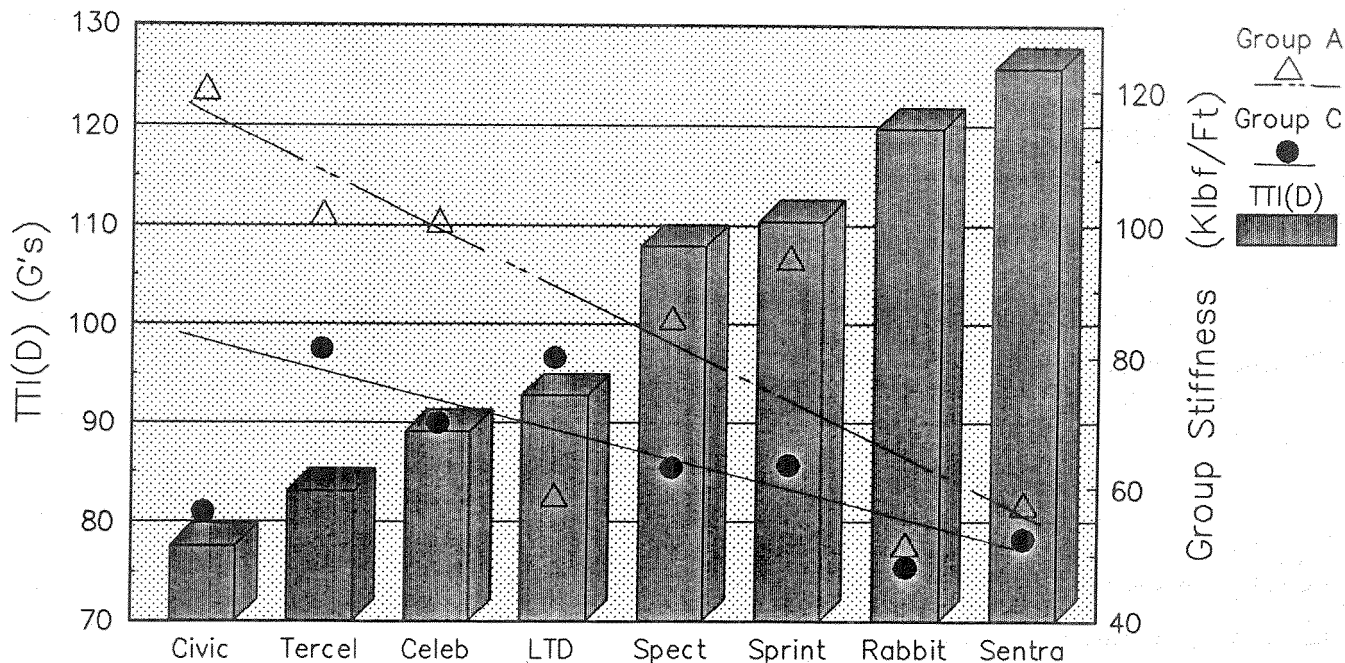


Figure 8. Side structure equivalent stiffness (ranking of modeled vehicles).

Since the energy absorbers in Groups A and C absorb most of the impact energy from the MDB, the energy absorbers contained in these two groups were subjected to the following stiffness changes:

Level 1—EA-18, -19, -20 and -21 (Group C) varied from 0.2 thru 2.5 nominal stiffness with EA-3, -4, -5, -6 (Group A) maintained at their nominal stiffness value,

Level 2—EA-3, -4, -5, -6 and EA-18, -19, -20, -21 (Groups A and C) simultaneously varied from 0.2 thru 2.5 nominal stiffness, and

Level 3—EA-18, -19, -20, -21 (Group C) varied between 0.2 thru 2.5 nominal stiffness with EA-3, -4, -5, -6 (Group A) stiffness factor based on the maximum amount of energy absorbed by the EA-3, -4, -5 and -6 (Group A) elements. The stiffness factor for Group A elements ranged from 0.5 to 2.9 in this case.

The stiffnesses of the remaining EAs were maintained at their baseline values.

Figure 9 shows that the TTI(d) decreased as stiffnesses were increased for all the three levels of variations in the Nissan Sentra. The increase in side structure stiffness decreased the total absorbed energy of the struck car as well as the TTI(d). On the surface, this may appear to contradict what was indicated earlier that total absorbed energy has an inverse relationship to TTI(d). However, it will become apparent in the subsequent discussion that not only the total absorbed energy, but also how this energy is shared by various elements of the side structure is equally important. The lowest TTI(d) levels were achieved when the outer door-to-pillar (Group A EA's-3, -4, -5 and -6) were chosen to yield the maximum amount of absorbed energy (Level 3).

Figure 10 shows the relationship between VC and three levels of stiffness variations. As mentioned before, increase

in side structure stiffness resulted in a decrease in car absorbed energy. VC also showed the same decreasing trend as TTI(d) for all the three levels of stiffness increases. However, the reduction achieved in TTI(d) for increase in stiffnesses (Level 3) was much more than what was observed in VC. For both the injury measures, increase in stiffness was found to be effective only up to about 1.5 nominal stiffness. As before, the lower VC levels were achieved by the variations where the outer door-to-pillar (Group A EA-3, -4, -5, and -6) were chosen to yield the maximum amount of absorbed energy.

Figure 11 shows that the TTI(d) vary over a large range of values for the same amount of total energy absorbed by the vehicle when the side structure is optimized to yield the maximum amount of energy absorbed in EA-3, -4, -5, and -6 (Group A, outer door-to-pillar) for the different levels of the pillar-to-compartment, EA-18, -19, -20 and -21, stiffnesses (Level 3). However, the amount of energy absorbed by the various interconnecting EAs differs for approximately the same total energy absorbed by the entire car. Level 3 indicates that it is important to absorb as much of the crash energy as possible in EA-3, -4, -5, and -6 (Group A, outer door-to-pillar) energy absorbers.

It is also observed that the decreased total absorbed energy in the car at large stiffness values for Group A and Group C energy absorbers, results in lower TTI(d) and is also accompanied by an increase in the absorbed energy by the MDB.

The foregoing discussion makes it clear that arbitrarily increasing the overall side stiffness is not necessarily going to achieve the desired reduction in TTI(d). Instead, it is necessary to make a judicious selection of stiffnesses for the various structural components so that the crash energy is shared in an optimal way to reduce the TTI(d) to the lowest possible level.

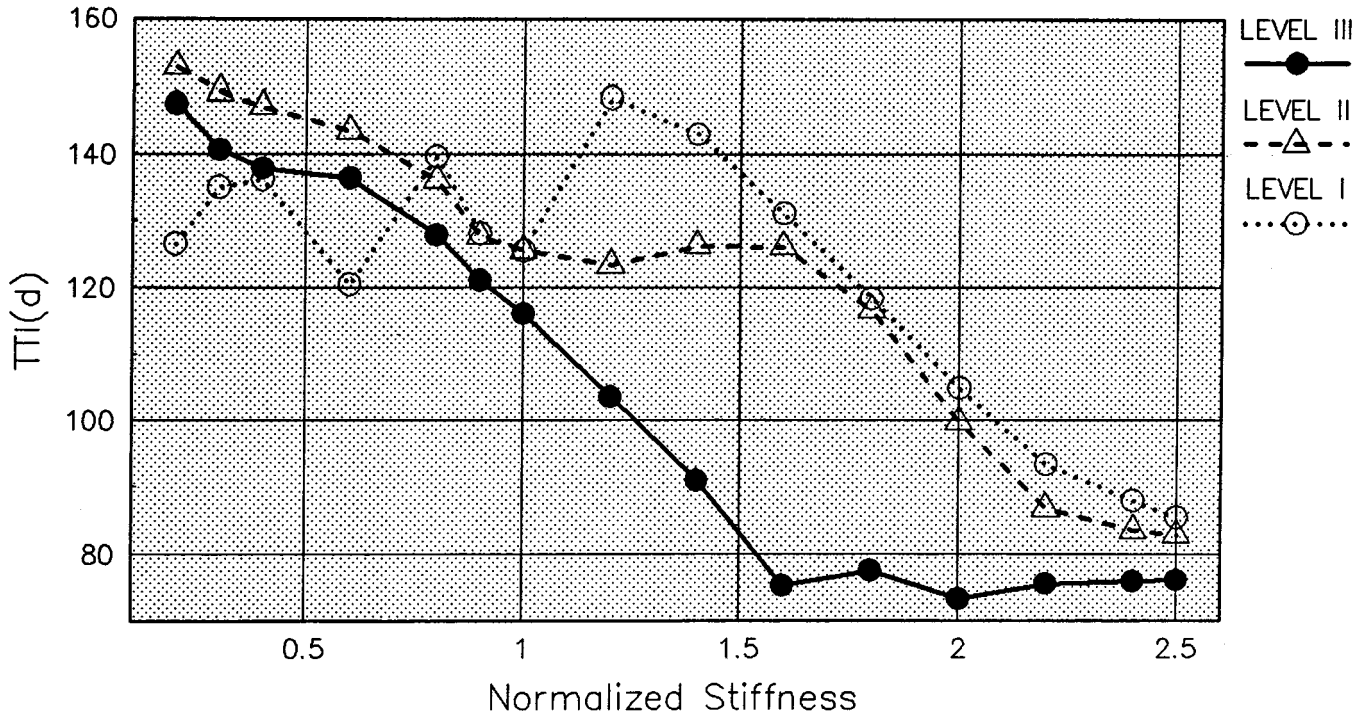


Figure 9. TTI(d) vs normalized stiffness.

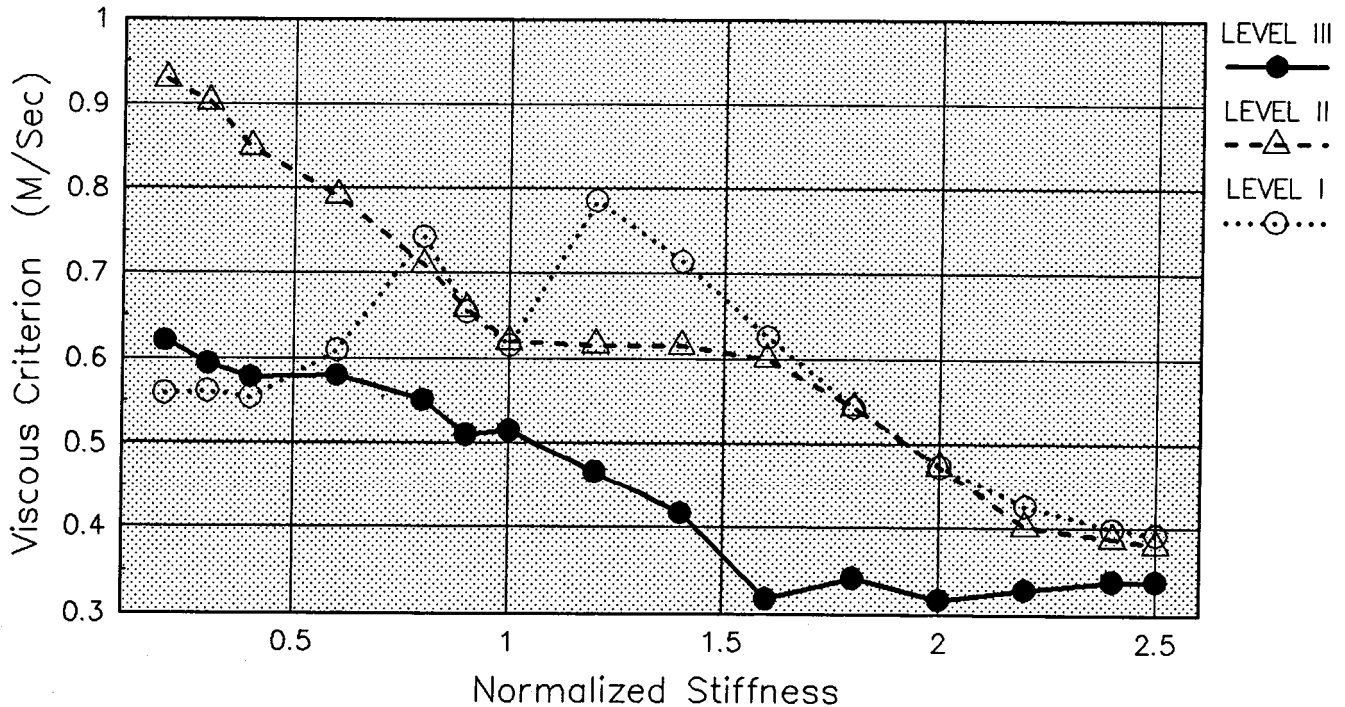


Figure 10. V\*C vs normalized stiffness.

To illustrate this point, refer back to figures 6 and 7 to compare the crash energy dissipation that occurs in the Nissan Sentra and the Honda Civic cars. In the Nissan Sentra, approximately 52% of the crash energy is dissipated by the vehicle side structure while about 54% of the energy is dissipated in the Honda Civic. The energy absorbed in the side structure is broken-down into that dissipated in different components of the vehicle structure represented in the model. The pillar-to-passenger compartment energy

absorbers use most of this energy followed by the outer door-to-pillar structures. The third most important energy absorbing element in the system is the inner-outer door core elements while the other components such as the upper-to-lower pillar and inner door-to-pillar attachments use only a small fraction of the energy dissipated in the struck vehicle, totalling less than 2% of the energy dissipated in the vehicle, for most of the cars simulated. When the energy dissipated in the three major energy absorbing components of the

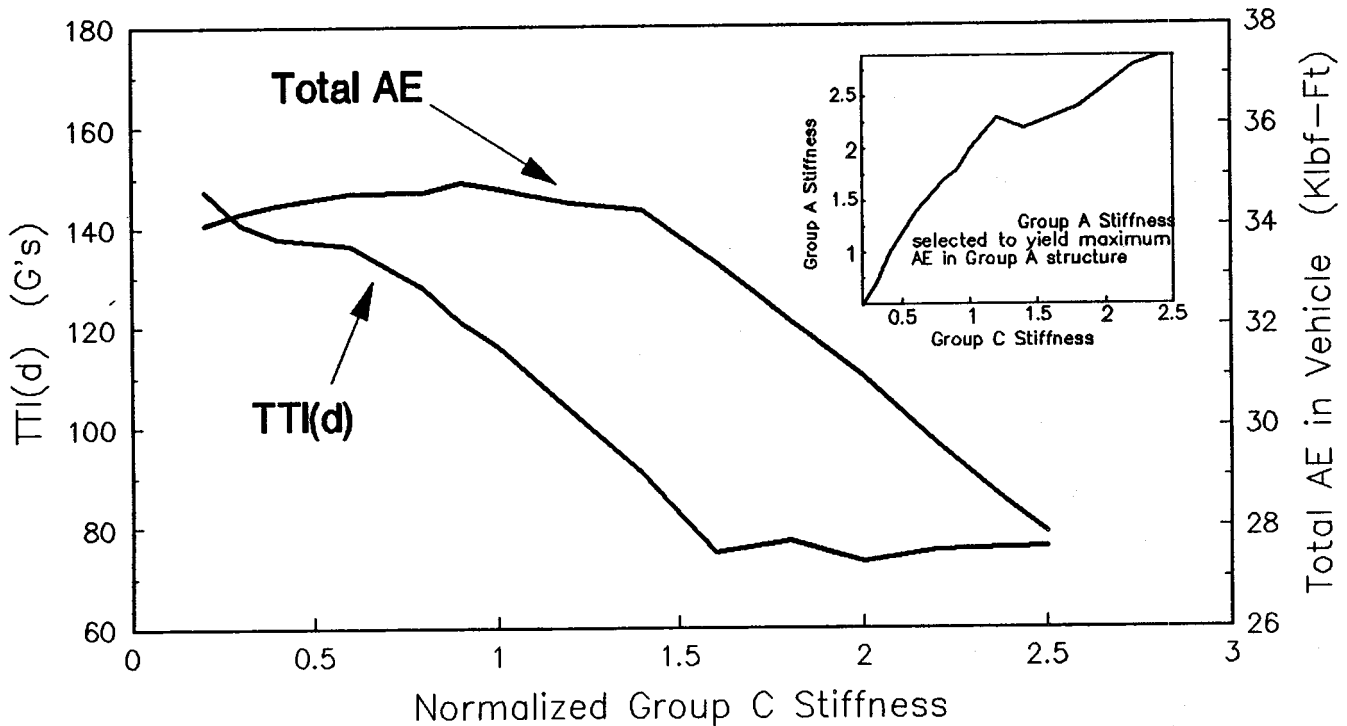


Figure 11. Side structure stiffness analysis (Nissan Sentra trials).

Nissan Sentra and the Honda Civic are compared, it is seen that there are appreciable differences in the amount of energy being shared by these components of the two vehicles. When the two vehicles are compared, it is observed that more energy is absorbed in the outer door-to-pillar, pillar-to-passenger compartment and door inner core elements of the structure for the Honda Civic than in the Nissan Sentra car.

Since the occupant response shows a general trend of reduced TTI(d) with increased energy absorption in the components of the side structure modeled, it is assumed possible to select a mathematical model that results in a functional relationship between TTI(d) and the energy dissipated in these components. For this relationship, the small amount of energy dissipation that occurs in all except the three major components of the side structure simulated are neglected. If the energy dissipated in the outer door-to-pillar, outer door-to-inner door core, and the pillar-to-compartment are expressed as a fraction of the total energy dissipated in the side structure, designated here as  $r_1$ ,  $r_2$  and  $r_3$  respectively, then  $\sum r_i < 1$ . The mathematical relationship of the following form was then chosen to relate the TTI(d) and the variables  $r_1$ ,  $r_2$  and  $r_3$ :

$$TTI(d) = \{ e^{(ar_1 + br_2 + cr_3 + d)} \} \dots \dots \dots (1)$$

where  $a$ ,  $b$ ,  $c$ , and  $d$  are constants.

The energy absorbed in the three major structural component groups (table 2) were expressed as fractions of the total absorbed energy in the struck cars for the eight vehicles simulated. TTI(d) and the values of  $r_1$ ,  $r_2$  and  $r_3$  obtained from the simulations of the eight vehicles were used to determine the coefficients  $a$ ,  $b$ ,  $c$ , and  $d$  in equation (1) utilizing the Statistical Analysis System (SAS) GLM

procedure. The coefficients  $a$ ,  $b$ ,  $c$ ,  $d$  and the correlation coefficient ( $r^{*2}$ ) obtained through this procedure are given below:

$$a = -9.88, \quad b = -7.261, \quad c = -7.776, \\ d = 12.653 \quad \text{and} \quad r^{*2} = 0.846$$

Though the selected function is not unique, it is useful in developing a family of curves relating the TTI(d) and  $r_1$ ,  $r_2$ , and  $r_3$  that will give a better understanding of the interaction between the major components of the side structure modeled.

As stated before, when some energy dissipation occurs in other components of the side structure than its three major elements, the  $\sum r_i < 1$ . The limiting case is when  $\sum r_i = 1$ . A series of curves relating the TTI(d) and  $r_1$ ,  $r_2$ , and  $r_3$  for the limiting case is shown in figure 12. This figure shows lines of constant  $r_1$  and  $r_2$  for values between 0.0 and 0.75 for both the variables. The range of TTI(d) for this case is between 16 g's and 220 g's.

The maximum TTI(d) occurs when  $r_2 = 1$  and  $r_1$  and  $r_3$  are both zero. Similarly, the TTI(d) is a minimum when  $r_1 = 1$ , and  $r_2$  and  $r_3$  are both zero. When  $r_1$  and  $r_2$  are both zero and  $r_3 = 1$ , the TTI(d) is 131 g's. It is thus clear from figure 12 that the theoretically achievable TTI(d) is bounded by the two lines for  $r_1 = 0$  and  $r_2 = 0$  for the case  $\sum r_i = 1$ .

When  $\sum r_i < 1$ , the TTI(d) is again bounded by the conditions  $r_1 = 0$  and  $r_2 = 0$  as before. However, the maximum and minimum TTI(d) shifts upward from the limiting case  $\sum r_i = 1$ . For example, using equation (1), when  $\sum r_i = 0.9$ , TTI(d) max. = 454 g's when  $r_1$  and  $r_3$  are zero and  $r_2 = 0.9$ . Similarly TTI(d) min. = 43 g's when  $r_2$  and  $r_3$  are zero and  $r_1 = 0.9$ .

The values of  $r_1$ ,  $r_2$  and  $r_3$  for baseline vehicles modeled

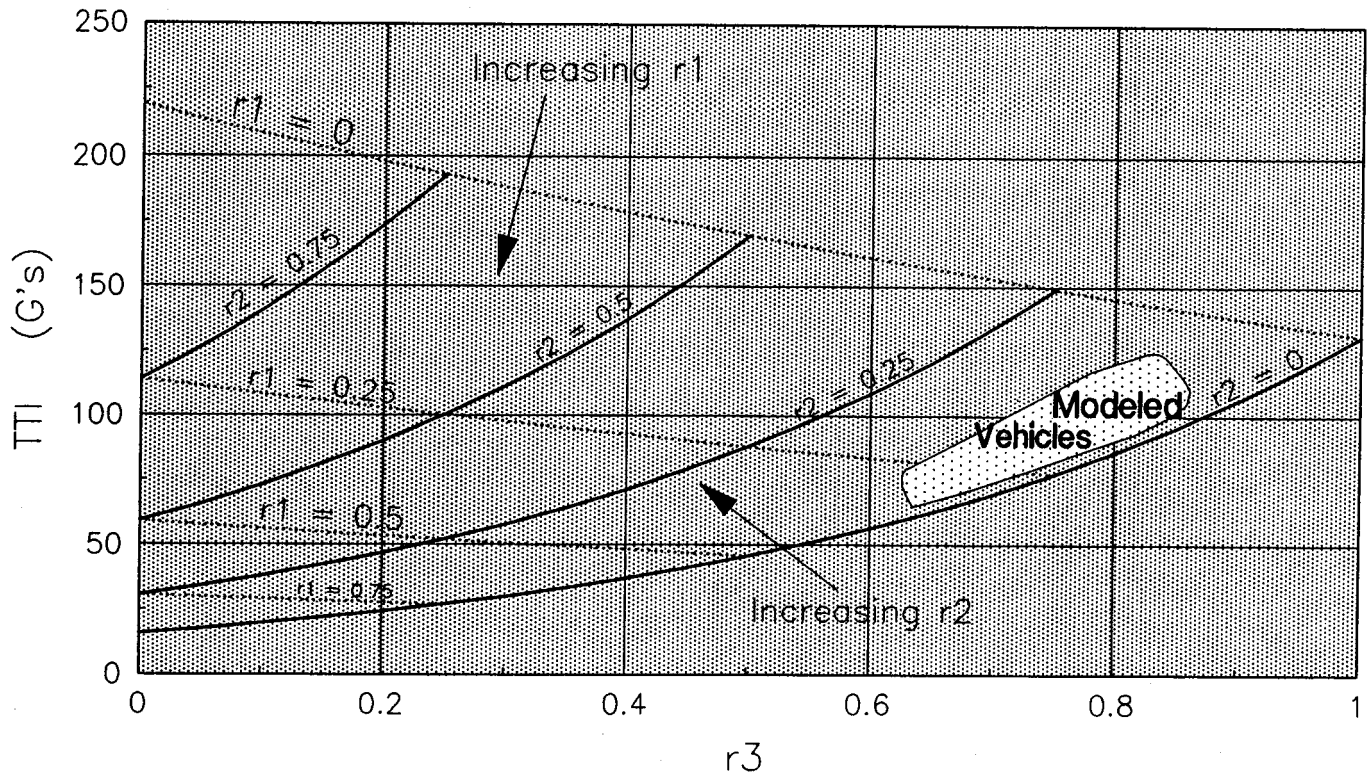


Figure 12. TTI(d)/side structure energy (sum Ri = 1.00).

are around 0.2, 0.05 and 0.73 respectively. Therefore, the region of interest is for values of r1, r2 and r3 in that proximity. This region for the vehicles modeled is indicated in figure 12. Figure 13 shows the relationship between TTI(d), r1, r2, and r3 values in the range of interest for the limiting case when  $\sum Ri = 1$ . For each value of r1, the

minimum achievable TTI(d) lies along the line of constant r2=0. For example, when r1=0.2 and r2=0, the minimum TTI(d) achievable is about 86 g's for r3=0.8.

It is recognized that the data used in developing the mathematical relationship between the TTI(d) and the absorbed energy is from simulations of tests of baseline cars

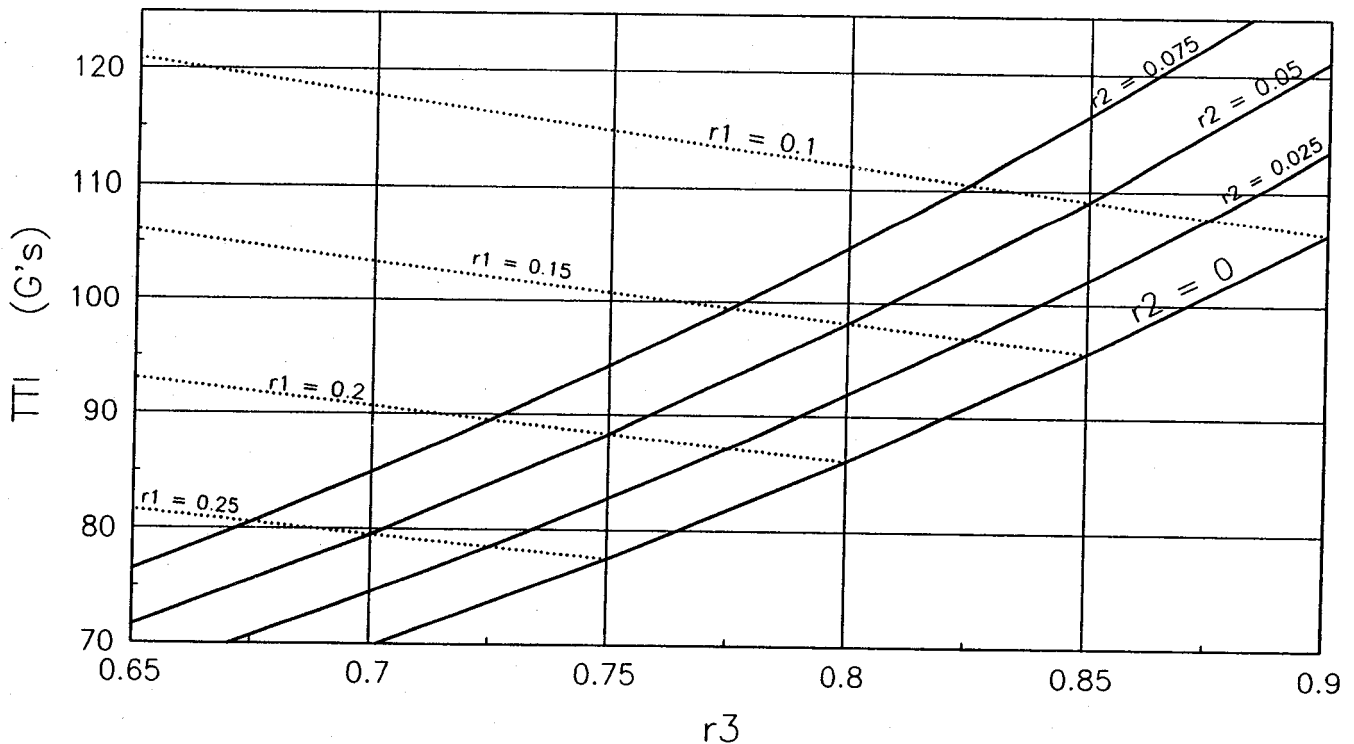


Figure 13. TTI(d)/side structure energy (region containing modeled vehicles sum Ri = 1.00)

which use current design technology. The methodology in no way implies that the relationship indicated in the family of curves shown in figure 12 will always be valid when side structure designs change or when new materials or padding is used in vehicles. All the same, the concept is useful to investigate the effects of varying energy dissipation characteristics in different parts of the side structure.

This is a very useful concept. It is easy to see the trade-off the engineer has to make between the three major groups of structures to achieve a certain level of TTI(d) performance. Also, the cost and feasibility of choosing a particular force-deflection characteristic for achieving a certain level of energy dissipation may be difficult. In order to achieve the desired TTI(d) level, it may be necessary to make a trade-off between all of the side structure components, and if necessary decide on adding other energy absorption materials to the door, such as padding. The minimum TTI(d)

for any pair of  $r_1$  and  $r_2$  for a given  $\sum r_i$  is indicated by the intersection of the  $r_1$  and  $r_2$  lines. TTI(d) decreases as  $r_2$  and  $r_3$  decreases and  $r_1$  increases.

## Door Crush and Absorbed Energy Due to Occupant Contact

The ability of the door to retain as much of its original thickness during a crash and at the same time maintain the ability to absorb energy due to occupant contact is a desirable design feature. This is brought out in figure 14 where the model shows that of the eight vehicles considered in this study, the vehicles with the least amount of door gap available to cushion the occupant from the impact also yielded the highest TTI(d). The general trend showed that, the more the door crush due to thorax contact, the less was the TTI(d).

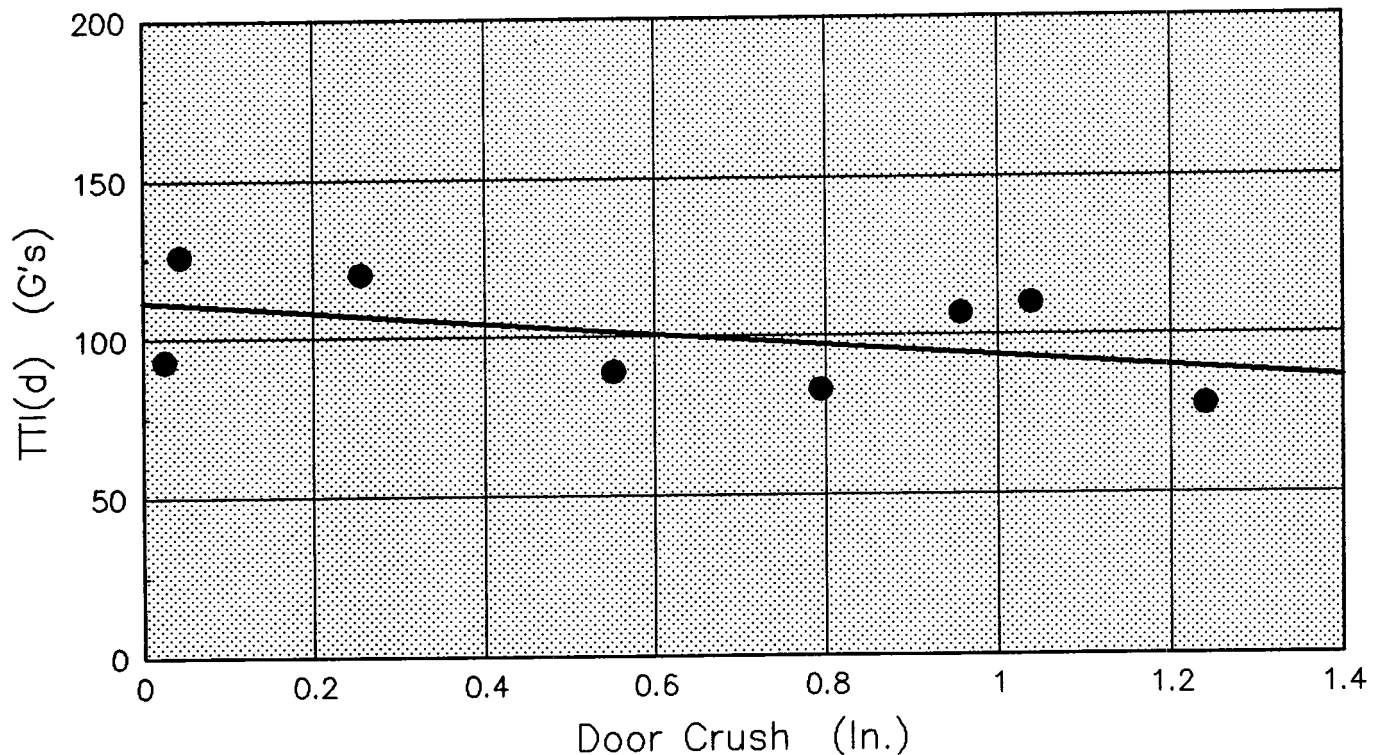


Figure 14. Door crush due to occupant contact.

Figure 15 shows for these same vehicles, the general trend which was observed between the TTI(d) and the energy absorbed by the door caused by thoracic contact. The absorbed energy was computed in the simulations by computing the total energy absorbed in the EA-8 energy absorber at the end of the simulation minus the total energy absorbed in the EA-8 energy absorber when the pelvis alone impacted the door in a separate run of the simulation. These results showed that the occupant TTI(d) generally reduced with increased levels of absorbed energy in the door core. Interestingly, the higher absorbed energy levels shown in this figure are in the range of energy levels which have been calculated with the model for a 3 inch thick GTR-pad

material (13) placed on the inner surface of the door in order to reduce the TTI(d)'s.

Figure 16 shows the same general trend for VC as observed in figure 15 for TTI(d).

## Effect of Door Contact Velocity

The door-occupant contact velocities for the upper and lower masses of the door were obtained using the simulations for the eight vehicles. The results showed that the contact velocities calculated in these simulations are much higher than have generally been estimated from side impact test data. For the vehicles simulated, the velocities ranged from 22 mph (35.2 km/hr) to 28 mph (44.8 km/hr) for the upper door-occupant thorax contact.

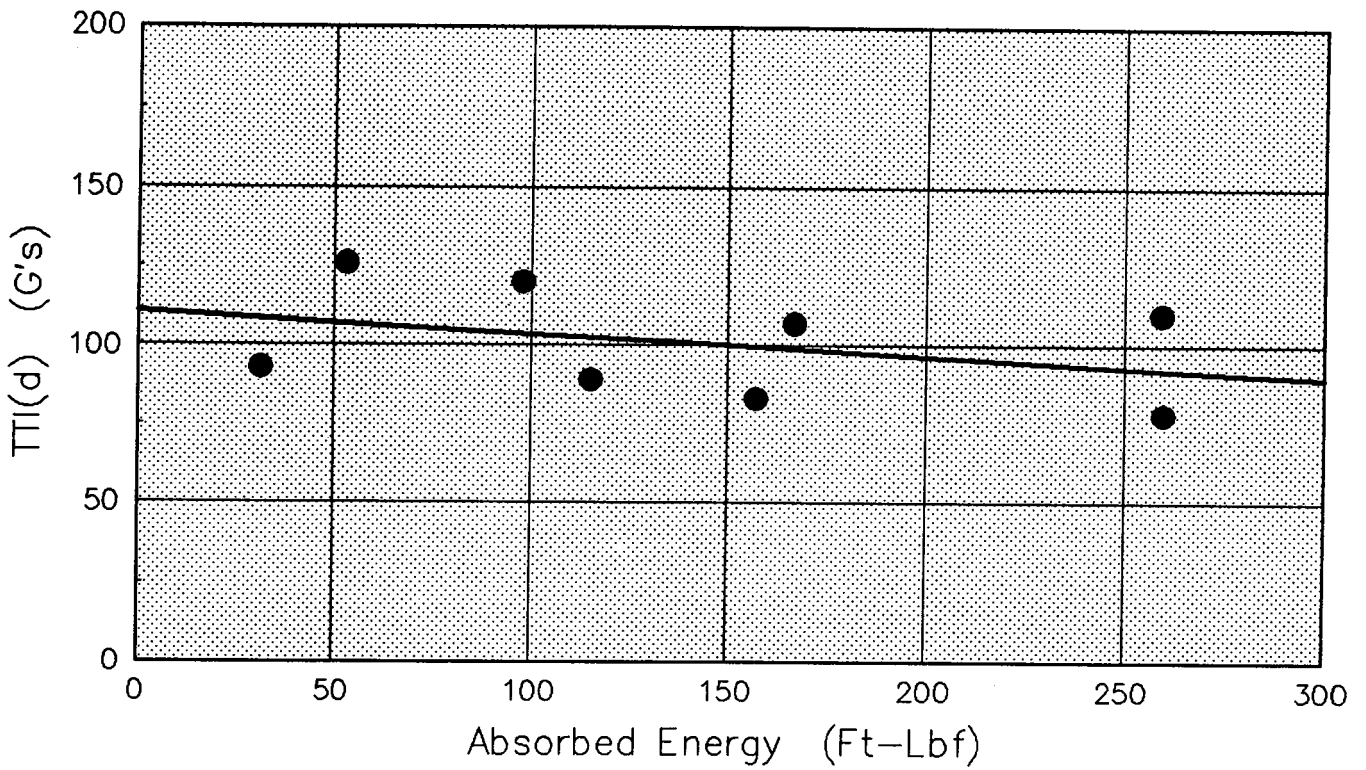


Figure 15. TTI(d) .vs. absorbed energy in door core due to occupant contact.

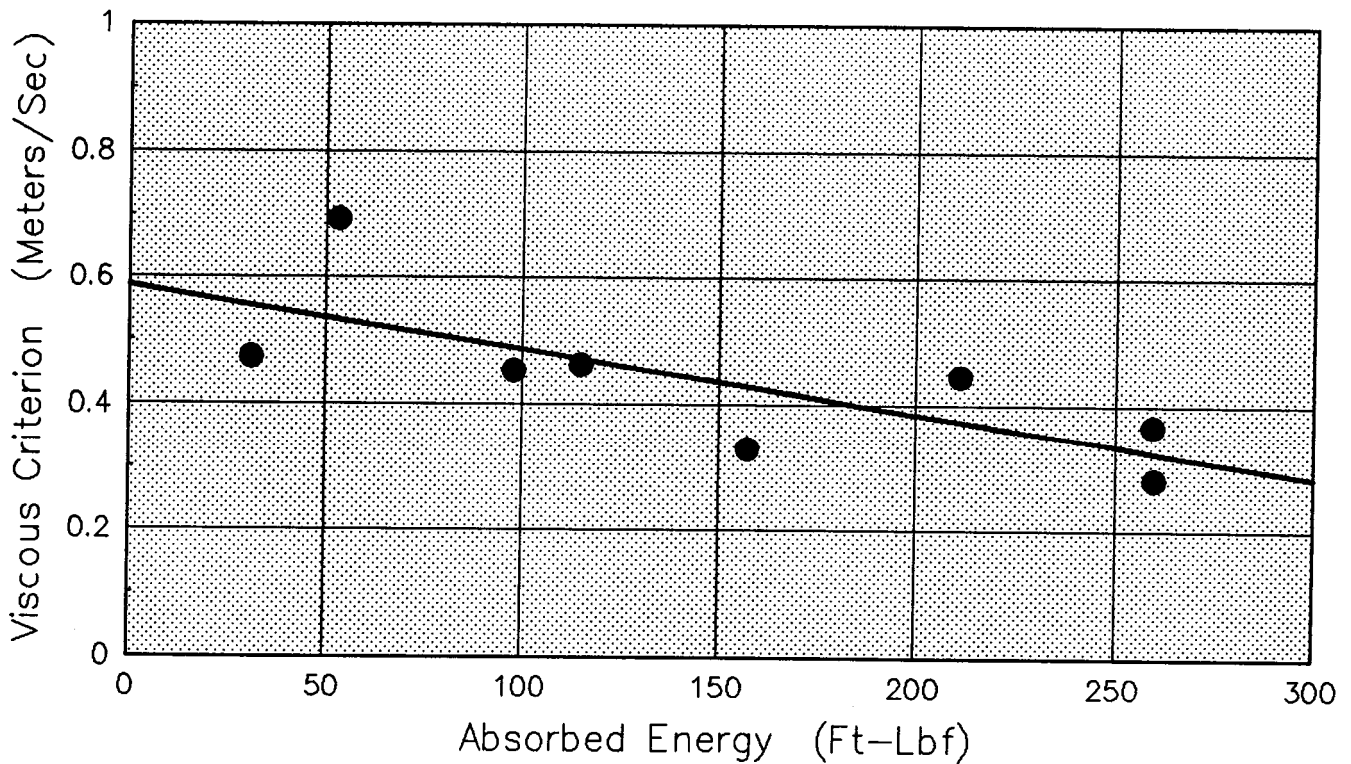


Figure 16. V\*C .vs. absorbed energy in door core due to occupant contact.

An independent estimate of the door-dummy contact velocities for production car side impacts is reported in reference (4). Those estimates are of the same magnitude as presented in this analysis and tend to confirm the estimates obtained in these simulations. The lower door-pelvis

contact velocities were slightly lower than the contact velocity for the thorax and were in the range of 20.5 mph (32.8 km/hr) to 28 mph (44.8 km/hr). Figure 17 shows the trend that the higher contact velocities at the thorax resulted in higher TTI(d)'s.

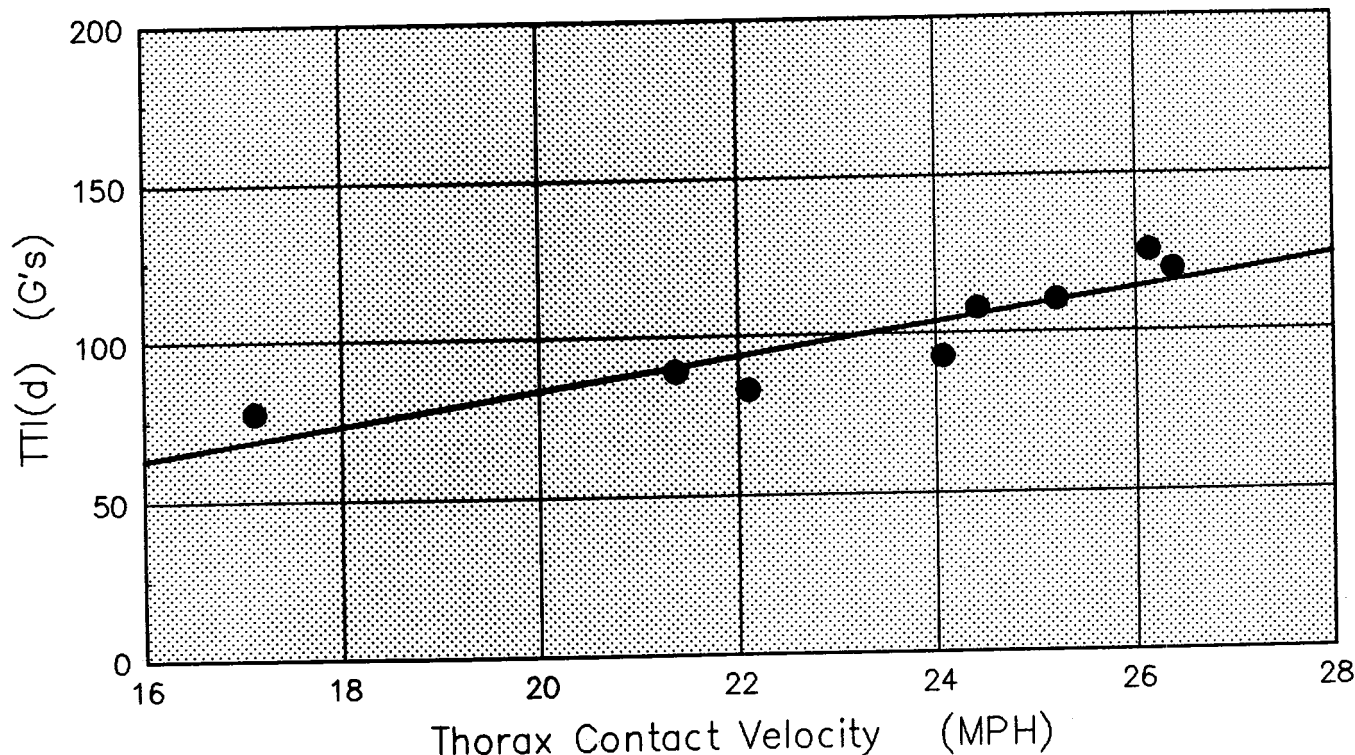


Figure 17. Modeled door contact velocity upper door to thorax.

## Summary and Conclusions

The safety performance differences as measured by TTI(d) in eight production passenger cars tested by NHTSA were analysed using a lumped mass model developed for side impact simulation and reported in reference (7). The structural behavior differences seen in various components of the side structure modeled were analysed in terms of the energy dissipated by different structural elements represented in the model. Analysis showed that, in general, an increase in absorbed energy in the side structure resulted in lower TTI(d). While increase in the total absorbed energy in the struck vehicle is deemed desirable, it has been established that such an increase achieved through reduction of stiffness of the major structural components represented in the model, may result in higher TTI(d). It is important that the energy dissipation occur in a manner so as to reduce the TTI(d), thus indicating the importance of sharing of energy between the various structural components.

A new concept for selecting side structural elements for optimum TTI(d) on the basis of fractional energy dissipated in the three major components of the modeled structure has been introduced as design curves relating the TTI(d) to the three variables. These variables represent the fraction of energy dissipated in the outer door-to-pillar, outer door-to-inner door core, and the pillar-to-compartment components of the side structure designated as the variables  $r_1$ ,  $r_2$  and  $r_3$  respectively.

As expected, contact velocity has been shown to be an important parameter affecting TTI(d). The analysis

presented in this paper is based on modeling only eight vehicles tested. Therefore, the results discussed are preliminary. Additional vehicles will have to be modeled to confirm some of the conclusions reached in this analysis.

Data from about fifty side impact tests of passenger cars using the NHTSA MDB and the SID are available in the NHTSA crash test data base. It is our plan at this time to model as many of the tests as necessary to confirm the findings reported here. Also, a relationship between TTI(d) and equivalent stiffnesses of the various components represented in the model similar to the one described in this paper will be attempted. Since energy absorption correlates well with TTI(d), it is possible that the DEPTH (4,14) parameter may also correlate with absorbed energy. This will also be investigated in future analyses. The energy dissipation due to pelvic contact and its relation to pelvic g's obtained will also be examined.

The analyses presented here confirm the suitability of the model for such analyses as well as parametric studies to investigate the effects of various vehicle design parameters on TTI(d) and VC.

The discussion and conclusions in this paper represent the opinions of the authors and not necessarily those of the NHTSA. The United States Government does not endorse products or manufacturers. Trade or manufacturers' names appear herein solely because they are essential to the object of the paper. This document is disseminated under the sponsorship of the Department of Transportation in the interest of information exchange. The United States Government assumes no liability for the contents or use thereof.

## References

- (1) Federal Register, 53 FR 2239, January 27, 1988.
- (2) Code of Federal Regulations: 49 CFR, Parts 400 to 999, 571.214, Side Door Strength, October 1987.
- (3) Hackney, J.R., et al., "Results of the National Highway Traffic Safety Administration's Thoracic Side Impact Protection Research Program," SAE Paper 840886.
- (4) Gabler, H.C.III., and Hackney, J.R., "The Safety Performance of Production Vehicles in Side Impacts," Proceedings, Tenth International Technical Conference on Experimental Safety Vehicles, Oxford, England, July 1985.
- (5) Monk, M.W., and Willke, D.T., "Side Aggressiveness Attributes," Proceedings, Tenth International Technical Conference on Experimental Safety Vehicles, Oxford, England, July 1985.
- (6) Hackney, J.R., Gabler, H.C., Kianianthra, J.N., and Cohen, D.S., "Update of the NHTSA Research Activity in Thoracic Side Impact Protection for the Front Seat Occupant". Proceedings of the 31st Stapp Car Conference. SAE Paper 872207, New Orleans, Louisiana, November 1987.
- (7) Trella, T.J., and Kianianthra, J.N., "Analytical Simulations of the Effect of Structural Parameters on Occupant Responses in Side Impacts of Passenger Cars," Proceedings, Eleventh International Technical Conference on Experimental Safety Vehicles, Washington, D.C., May 1987.
- (8) Morgan, R.M., Marcus, J.H., and Eppinger, R.H., "The Biofidelity of NHTSA's Proposed ATD and Efficacy of TTI," Proceedings, 30th Stapp Car Crash Conference, October 1986.
- (9) Viano, D.C., and Lau, I.V., "Thoracic Impact: A Viscous Tolerance Criterion," Proceedings Tenth International Technical Conference on Experimental Safety Vehicles, Oxford, England, July 1985.
- (10) "Side Impact Tests," Contract Number DTRS-57-87-00047, TTD #5.
- (11) Preuss, C.A., and Wasko, R.J., "Motor Vehicle Manufacturers Association Subsystem and Full Vehicle Side Impact Test Procedure Development Program," Proceedings, Eleventh International Technical Conference on Experimental Safety Vehicles, Washington, D.C., May 1987.
- (12) "Fatal Accident Reporting System 1985: A Review of Information on Fatal Traffic Accidents in the U.S. in 1985," U.S. Department of Transportation, National Highway Traffic Safety Administration.
- (13) Monk, M., and Sullivan, L., "Side Impact Padding Integration Study," NHTSA—Vehicle Research and Test Center, East Liberty, Ohio, NHTSA DOT HS-805-957, March 1981.
- (14) Gabler, H.C., Hackney, J.R., Hollowell, W.T., "DEPTH: A Relationship between Side Impact Thoracic Injury and Vehicle Design," Proceedings Twelfth International Technical Conference On Experimental Safety Vehicles, Gothenburg, Sweden, May 1989.
- (15) "The European Side—Impact Dummy: Eurosid," Proceedings of the seminar held in Brussels, December, 1986.
- (16) DeCoo, P.A., et al., "Evaluation of European and USA Draft Regulations for Side-Impact Collisions," Proceedings, Eleventh International Technical Conference on Experimental Safety Vehicles, Washington, D.C., May 1987.
- (17) Willke, Donald T., Monk, M. and Kianianthra J.N., "Side Impact Sub-System Thoracic Impactor Evaluation," Proceedings, Twelfth International Technical Conference on Experimental Safety Vehicles, Gothenburg, Sweden, May 1989.

## Acknowledgements

The authors wish to express their sincere appreciation for the many suggestions offered throughout the course of this work to Mr. James R. Hackney, (DOT-NHTSA/NRD-11), Dr. Tom Hollowell (DOT-NHTSA/NRD-11), Mr. Bill Brubaker (DOT-NHTSA/NRM-12) and Mr. Herbert H. Gould (DOT-RSPA/TSC).

## Side Impact Simulation Analysis Using an Improved Occupant Model

J. Hasewaga, T. Fukatsu, T. Katsumata,  
Toyota Motor Corporation

### Abstract

Various simulation models have been proposed so far as a means of the analysis on side impact phenomena. However, it was difficult to simulate actual occupant behaviors in impact accidents and the complex thoracic response in particular, since most of those models have been derived from the simple one-dimensional spring-mass model approach.

The authors, therefore, analyzed DOTSID thoracic

responses through dummy impacts tests using a rigid surface impactor, and improved the previous occupant model developed by Toyota, taking account of dummy rotational motions as well. For the verification of the validity of this new model, predictions made by this model were compared with actual dummy behaviors determined by a padded impact tester which simulated the full-scale vehicle impact. As a result, it has been verified that the accuracy of the new model for the prediction of dummy behaviors is higher than the previous model.

The new model was also used in parametric studies to

evaluate potential injury reduction measures in side impacts.

## Introduction

The occupant energy absorption space in car-to-car side impact accidents is relatively small compared with that of frontal or rear-end accidents, and for the occupant injury reduction measures, it is found to be generally more difficult in side impact accidents.

In this regard, manufacturers and research laboratories have been carrying out extensive side impact tests on actual vehicles, and evaluations and reviews on technologies for the development of countermeasures have conducted in energetic manners.

Side impact phenomena, however, involve various factors, such as (1)\* the stiffness of the front portion of striking vehicle, (2) the stiffness of side portions of struck vehicle, (3) behaviors of occupants, etc. The development of countermeasures was thus considered as a cost and time consuming process.

Under such circumstances, a variety of numerical simulations (references 1-3) by modelling said factors have been conducted, in order to determine the mechanism which causes occupant injuries. Results of such studies have been used in extensive parameter studies, taking account of the impact speed, the weight of the striking car and so on, to find a proper guideline for the establishment of injury reduction measures.

The authors have been also carrying out such simulations, using a simple spring-mass model as a means of analysis on side impact phenomena. The previous occupant model has been thus improved based on the DOTSID model, with a higher accuracy in the prediction of occupant injuries. Details of this new model will be reported in the following.

## Previous Occupant Model

The previous occupant model used in past is shown in figure 1. It was designed to simulate the DOTSID, with each of the rib and spine considered as a single mass, and a simple linear viscous damper and a non-linear spring located between the rib and the spine to connect them. Only one degree of freedom was provided with this model to allow lateral linear motions of the occupant in the direction of impact alone.

Simulation results using the previous model are shown in figure 2. While the results of pelvis accelerations agree fairly well with the test data, thoracic accelerations show some significant difference. A conflict also occurred in efforts to provide good correlation between simulation data and test data. That is, when an attempt was made to adjust characteristics of the model to provide a better correlation in rib behavior with the test data, the spine response deviated further from the test data and vice versa.

It was thus recognized that the conventional spring-viscous damper model would have to be modified in order to

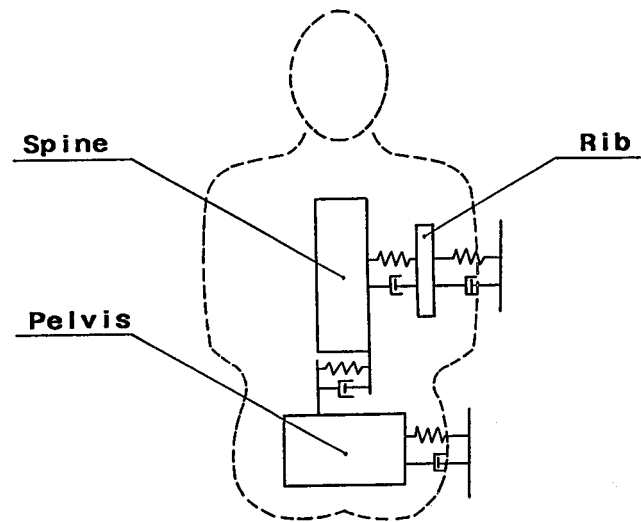


Figure 1. Previous model (DOTSID).

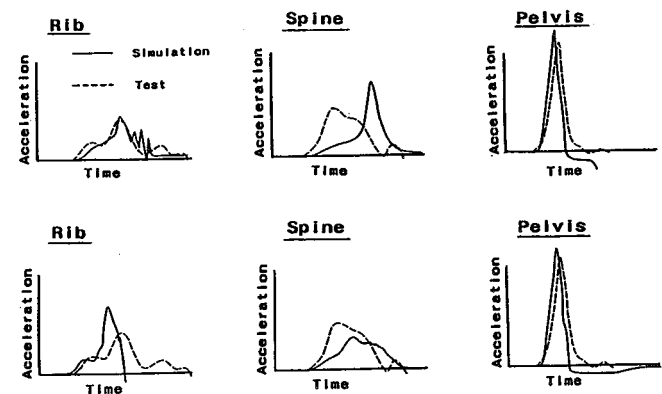


Figure 2. Comparison between test data and simulation results.

upgrade the accuracy in predicting thoracic injuries.

Figure 3 shows typical dummy motions in actual vehicle tests. Acceleration waveforms are sometimes different between spine positions of T1 and T12, presumably due to the difference in spine rotation. The previous model has the problem of incapability to reproduce the spine rotation, since such a rotation is not taken into account.

## Improvements of the DOTSID Model

### Improvement of thoracic damper

There are three types of load transmission paths during thoracic impacts as given below:

- (1) Rib attaching hinge
- (2) Interference between the rib ballast and antibottoming pad
- (3) Damper

The previous model was characterized by the simple thoracic damper which acted as the linear viscous damper. Three kinds of steps have been taken to improve the damping characteristics.

First, the structure of the damper was reconsidered.

Figure 4 shows the cross-section of the damper. This

\*Numbers in parentheses designate references at end of paper.

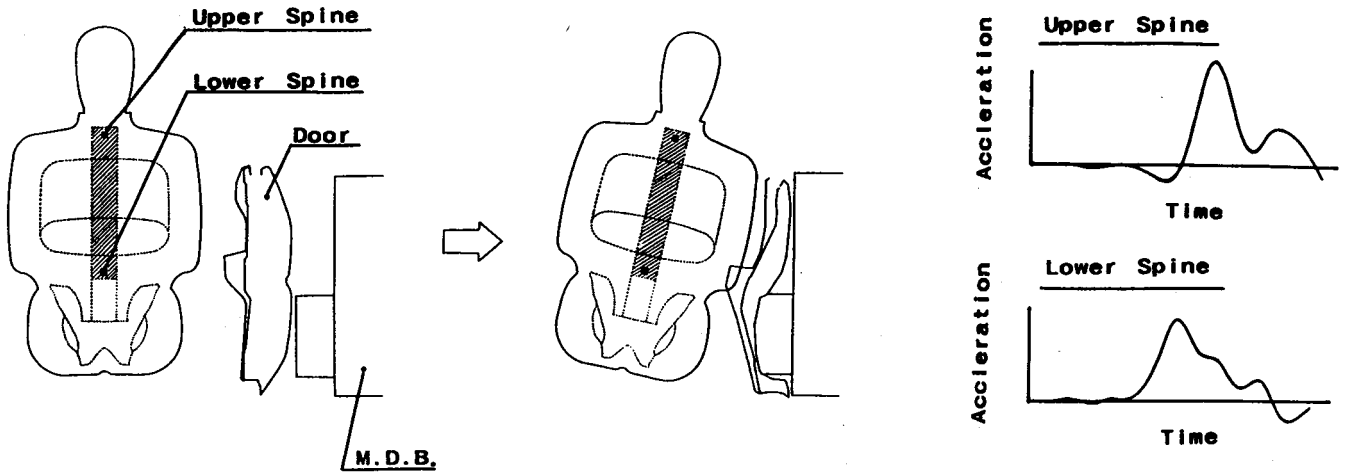


Figure 3. Dummy response in side impact.

damper had four orifices on the cylinder wall, and it was considered that the damping force would occur in the damper by the oil flowing out of the orifices, and the oil flow velocity would change according to the number.

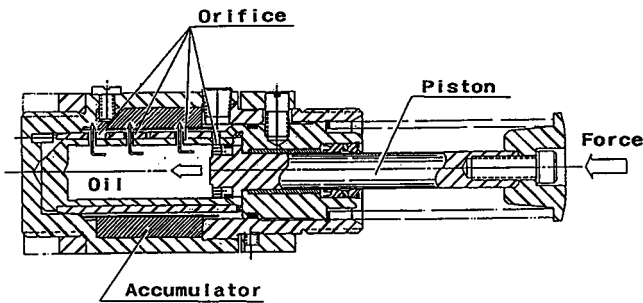


Figure 4. Cross-section of damper.

The second step, therefore, was to characterize the damper by means of fluid mechanism as shown below. Employing the law of continuity, the oil flow velocity gives:

$$V_o = \frac{S_o}{n \cdot S_p} * V_p \quad (1)$$

where

- $V_o$  : velocity at orifice
- $V_p$  : piston velocity
- $S_p$  : area of piston
- $S_o$  : area of orifice (Each orifice has same area.)
- $n$  : number of orifices available for the oil flow

In general, the damping force generated by orifice is

$$F = C * V_o \quad (2)$$

where

- $F$  : damping force
- $C$  : constant value

The third step was the implementation of a series of damper impact tests for the verification of the validity of the new model. Impact velocities were varied in the range of 16

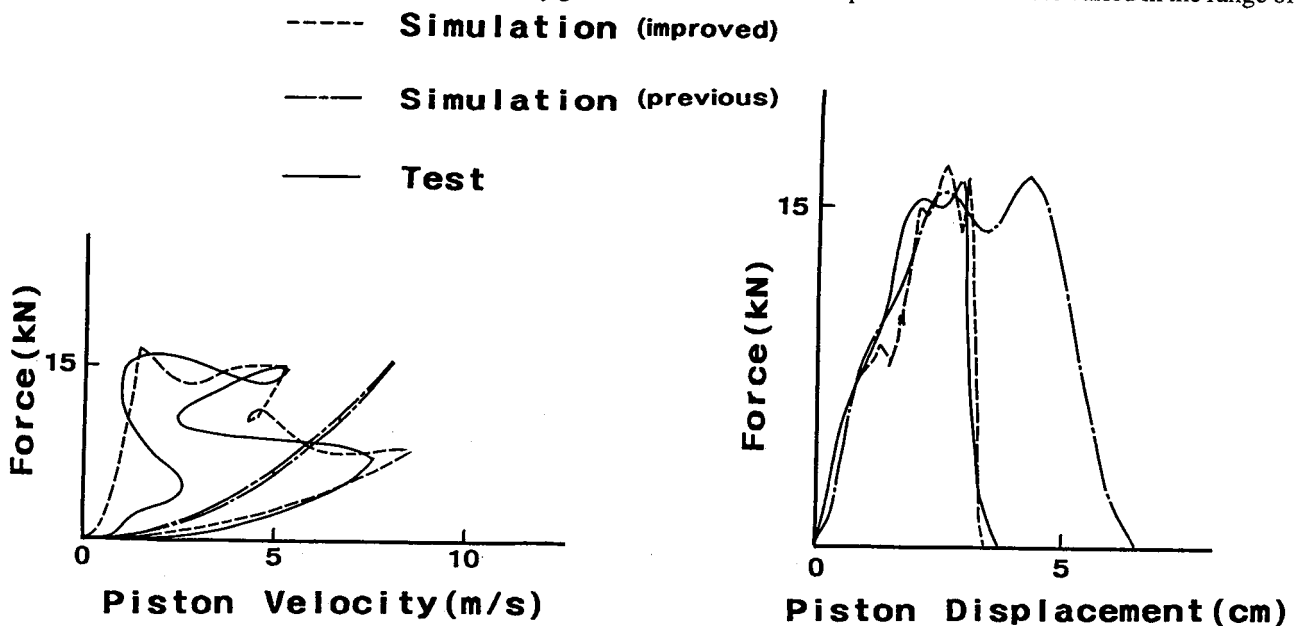


Figure 5. Comparison of force-displacement and velocity characteristics with test data.

to 44 km/h. Figure 5 shows the force-displacement and velocity characteristics at the impact velocity of 29 km/h.

It has been verified by the test data that the improved model is capable of a faithful simulation of the characteristic phenomenon of the increased damping force despite the reduced velocity of the damper piston. It has been also found that the previous model is incapable of simulating this phenomenon.

### Spine and other elements

The previous model took no account of the rotational motion of the spine as stated earlier. The spine of the improved model, on the other hand, is provided with two degrees of freedom—that is, it is capable of turning around the longitudinal axis of the chest rotation, in addition to the single degree of freedom given in the previous model. The head motion, which presumably affects the chest rotation, is also incorporated in the new model. Moreover, three non-linear springs are incorporated as couplings of the impactor-to-rib and the rib-to-spine, in order to represent the load transmission in chest rotation more faithfully. Figure 6 shows the improved model.

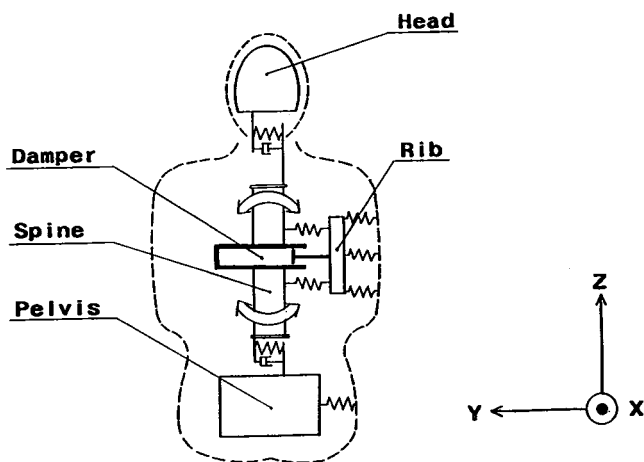


Figure 6. Improved model.

### Equations of motions

Equations of motions for the new model are as follows.

$$\text{Impactor} : M_i \cdot \ddot{Y}_i = -\sum_{j=1}^3 (F_{IR})_j \cdot \cos(\Theta_s) - F_{IP}$$

$$\text{Rib} : M_R \cdot \ddot{Y}_R = \left\{ \sum_{j=1}^3 (F_{IR})_j - \sum_{j=1}^3 (F_{RS})_j - F_D \right\} \cdot \cos(\Theta_s)$$

$$M_R \cdot \ddot{Z}_R = \left\{ \sum_{j=1}^3 (F_{IR})_j - \sum_{j=1}^3 (F_{RS})_j - F_D \right\} \cdot \sin(\Theta_s)$$

$$I_R \cdot \ddot{\Theta}_R = \sum_{j=1}^3 (F_{IR})_j \cdot (L_{IR})_j - \sum_{j=1}^3 (F_{RS})_j \cdot (L_{RS})_j$$

$$\text{Spine} : M_S \cdot \ddot{Y}_S = \left\{ \sum_{j=1}^3 (F_{RS})_j + F_D - F_{SP} - F_{SH} \right\} \cdot \cos(\Theta_s)$$

$$M_S \cdot \ddot{Z}_S = \left\{ \sum_{j=1}^3 (F_{RS})_j + F_D - F_{SP} - F_{SH} \right\} \cdot \sin(\Theta_s)$$

$$I_S \cdot \ddot{\Theta}_S = \sum_{j=1}^3 (F_{RS})_j \cdot (L_{RS})_j - F_D \cdot L_D - F_{SH} \cdot L_{SH} - F_{SP} \cdot L_{SP}$$

$$\text{Head} : M_H \cdot \ddot{Y}_H = F_{SH} \cdot \cos(\Theta_s + \Theta_H)$$

$$M_H \cdot \ddot{Z}_H = F_{SH} \cdot \sin(\Theta_s + \Theta_H)$$

$$I_H \cdot \ddot{\Theta}_H = F_{SH} \cdot L_H$$

$$\text{Pelvis} : M_p \cdot \ddot{Y}_p = F_{SP} \cdot \cos(\Theta_s + \Theta_p) + F_{IP}$$

$$M_p \cdot \ddot{Z}_p = F_{SP} \cdot \sin(\Theta_s + \Theta_p)$$

$$I_p \cdot \ddot{\Theta}_p = F_{SP} \cdot L_p \quad (3)$$

where

$F_{IR}$  : impactor-to-rib force

$F_{RS}$  : rib-to-spine force

$F_D$  : impactor-to-spine damper force

$F_{IP}$  : impactor-to-pelvis force

$F_{SP}$  : spine-to-pelvis force

$F_{SH}$  : spine-to-head force

$M$  : concentrated mass

$I$  : product of inertia on the longitudinal (X) axis

$\Theta$  : turning angle

$L$  : length of arm for the moment of rotation

R as subscript; rib

S as subscript; spine

H as subscript; head

P as subscript; pelvis

j as subscript; the number of impactor-to-rib and rib-to-spine couplings

Geometrical dimensions and inertial properties are shown in tables 1 and 2.

Symbol	Length of Moment-Arm(cm)
$(L_{IR})_1$	7.6
$(L_{IR})_2$	0.0
$(L_{IR})_3$	7.0
$(L_{RS})_1$	6.4
$(L_{RS})_2$	0.0
$(L_{RS})_3$	6.4
$L_D$	0.0
$L_{SH}$	17.4
$L_H$	2.5
$L_{SP}$	14.2
$L_P$	9.2

Table 1. Geometrical dimensions.

Segment	Mass(kg)	X-Moment of Inertia ( $\text{kg} \cdot \text{m}^2$ )
HEAD	5.3	0.024
RIB	7.3	0.053
SPINE	17.1	0.053
PELVIS	16.1	0.120

Table 2. Inertial properties.

### Characteristics of elements

Figure 7 shows force-displacement characteristics of the improved DOTSID model. The data have been obtained

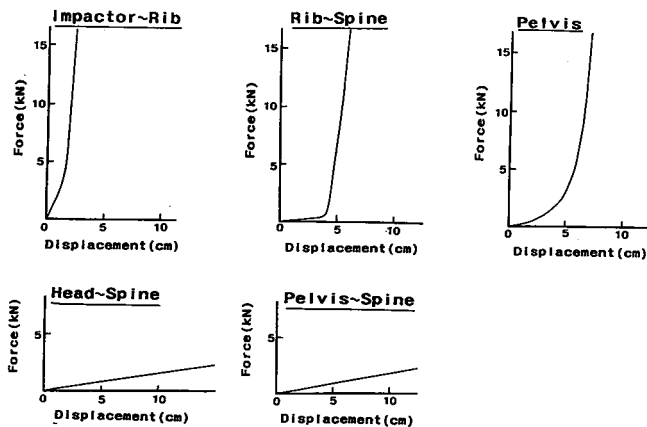


Figure 7. Force-displacement characteristics of improved model.

through quasi-static compression tests and bending tests carried out so far. The rib-spine data show a sharp rise by the displacement of 40 mm or so, as the rib ballast starts contacting the antibottoming stopper made of a rubber pad.

### Verification of New Model

Three types of case studies have been conducted for the verification of the validity of the entire new model, as shown in figure 8.

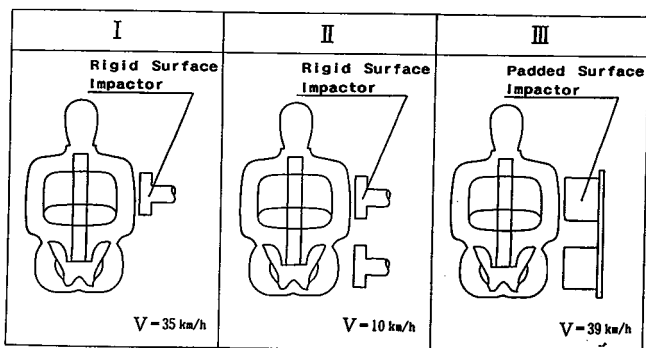


Figure 8. Impact test conditions for validation of improved model.

(I) The kinematic comparison of accelerations of upper and lower ribs between the test data and the model is shown in figure 9. The correlation between the two is qualitatively satisfactory except for the difference in peak acceleration. The effect of spine rotation is small in this case, as the impact speed was high (Case I).

(II) Figure 10 shows results of the Case II study on the chest and the pelvis impact tests using a rigid impactor. Similar to the Case I, the qualitative correlation between the model and test data is satisfactory. The effect of the direct pelvis impact is particularly significant on spine acceleration.

(III) Comparative results of Case III study using a padded impactor simulating the full-scale test are shown in figure 11. In this case, each one of ribs shows a wavy mode with two peaks in the acceleration-time

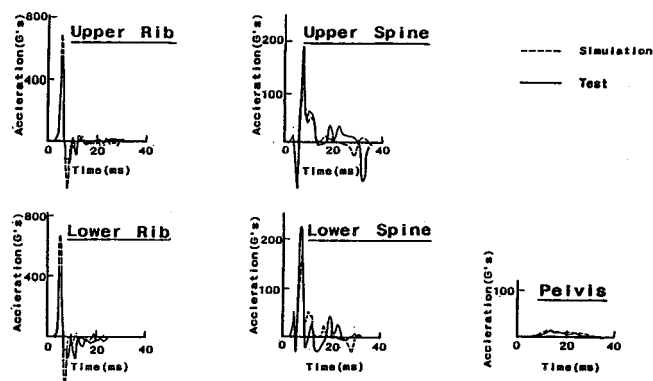


Figure 9. Comparison between test data and simulation results (Case I).

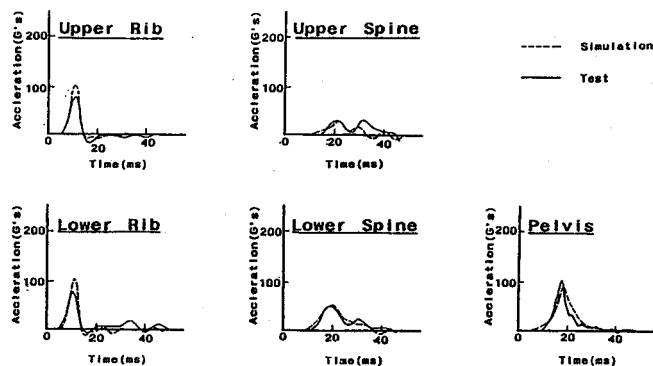


Figure 10. Comparison between test data and simulation results (Case II).

history. Differences in acceleration wave-forms of spines T1 and T12 are more obvious than the Case II because of a more significant deformation of the damping pad.

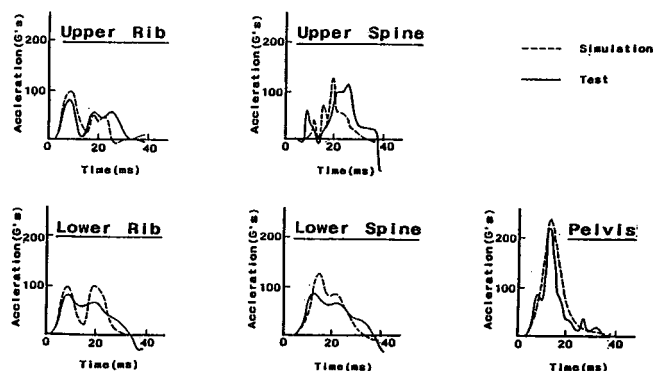


Figure 11. Comparison between test data and simulation results (Case III).

Figure 12 illustrates the top view of the DOTSID's rib cage. Figure 13 shows rib and spine acceleration-time histories and force-time histories of impactor-to-rib and rib-to-spine forces. Each of the rib and spine response was calculated at its center of gravity. Spine acceleration waveforms and the rib-to-spine force-time history are quite similar, with two sharp peaks of rib accelerations. This means that the padding force increases the rib accelerations against the damping force due to the following mechanism.

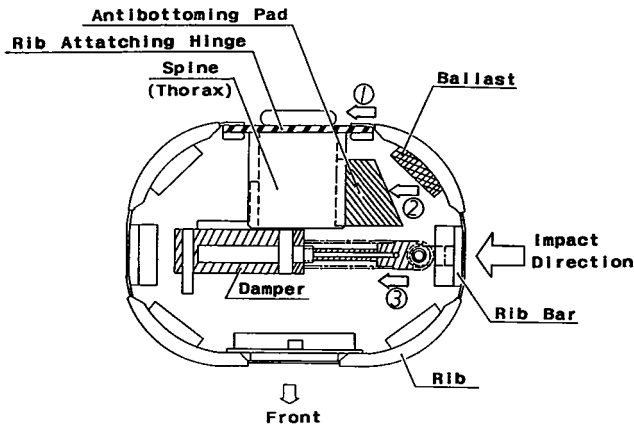


Figure 12. Thoracic structure.

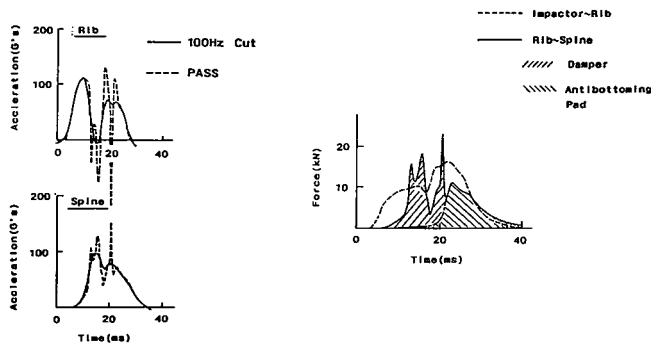


Figure 13. Relation between thoracic acceleration and force.

The rib-to-spine force consists mainly of the damper force and the contact force between the rib ballast and the antibottoming pad. The damper force becomes higher than the impactor-to-rib force in the phase of 12 msec to 16 msec after the collision of the padded impactor. In this phase, the damper force reduces the rib acceleration against the impactor-to-rib force. Because of this mechanism, the rib response shows a wavy mode with two peaks in the acceleration-time history.

As described in the foregoing, it has been verified that the new model is capable of predicting the DOTSID chest acceleration accurately in various forms of impacts, and useful for the reduction of occupant injuries in side impacts.

## Parametric Studies

Based on the improved model, parametric investigations were carried out for the padded impact condition as shown in figure 11. This study is on the parameter variations of the chest padding characteristics. The DOTSID response to the parameter variation has been also evaluated with the TTI (d) and Viscous Criterion ( $V \times C$ ) (reference 4). For the assessment of the padding characteristics, two schemes were used in the simulations. The force-deflection characteristics of the padding used in the study are shown in figure 14.

The first variation scheme, Case A, involves the change of padding stiffness as shown in the left half of figure 14. The second variation scheme, Case B, involves the change of padding crush strength as shown in the right half of figure

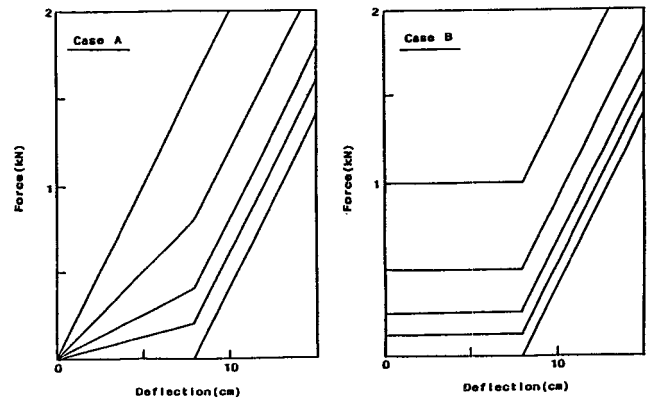


Figure 14. Force-deflection characteristics of padding.

14. In both cases, the padding thickness is fixed at 8 cm, and the hard contact of the padding is represented by the steep slope in the second portion of each curve.

Other parameters, i.e., the pelvic padding, impact speed (39 km/g) and impact weight (1726 kg) have been kept constant throughout the studies.

Figure 15 shows the simulation results. In the case A, there is a significant difference between the TTI (d) and the  $V \times C$  in the lower stiffness area. TTI (d) seems to indicate the optimal stiffness for a lower injury. On the other hand, the  $V \times C$  indicates diminution below the TTI (d) optimal stiffness. In the case B, the TTI (d) and the  $V \times C$  seem to have a similar tendency. TTI (d) may have the optimal padding crush strength around 0.5 kN for a lower injury. It is around 0.25 kN the optimal padding crush strength of the  $V \times C$ .

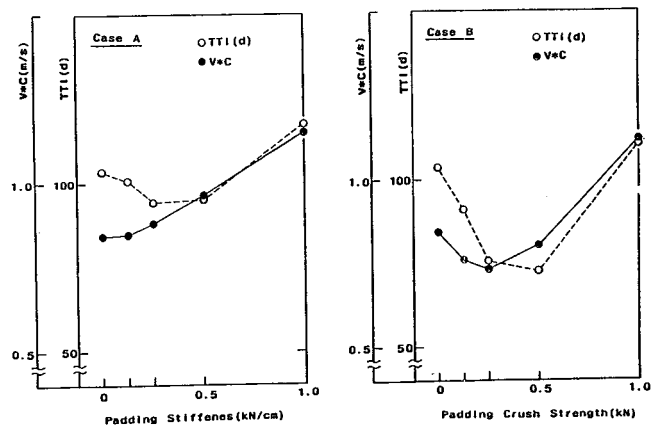


Figure 15. Relation between thoracic injury and padding variation by simulation.

## Conclusions

(1) The thoracic injury prediction accuracy was particularly poor in the previous DOTSID model using the spring-mass approach. Thus, the thoracic model has been improved by means of the following:

- modeling approach based on the mechanism of occurrence of damper force; and
- modeling approach taking account of the spine

rotation based on actual thoracic behaviours of occupants in side impact accidents.

It has been verified by the comparison of simulation results of this model with dummy test data that this model is capable of improving the injury prediction accuracy.

(2) Complex mechanism of the occurrence of chest accelerations has been clarified owing to the in-depth analysis of simulation results.

(3) Using this improved model, parametric studies have been carried out to relate the thoracic injury severity to the struck vehicle side stiffness. As a result, it is found that the optimum value of the vehicle side structure stiffness for the injury reduction differs according to the kind of injury criterion applied—i.e., the difference between the TTI (d) and the viscous criterion.

More extensive parameter studies are intended for the development of proper injury reduction measures, and

efforts will be continued for further improvements of the impact model in order to simulate human characteristics as closely as possible.

## References

(1) Thomas, J. T., Joseph, N. K., "Application of Derived Characteristics from Dynamic Test Data for Simulation of car-to-car Side Impacts Using a Lumped Mass Approach", SAE Paper 851187, 1985.

(2) P. Zimmermann, B. Richter, H.-ch, Wille, "IMPACT—Integrated Multiple Program for Accident Crash Trauma", SAE Paper 840868, 1984.

(3) Arvind J, Padgaonkar, Priyaranjan Prasad, "Simulation of Side Impact Using the CAL3D Occupant Simulation Model", SAE Paper 791007, 1979.

(4) Viano, D. C., Lau, I. V., "Thoracic Impact: A Viscous Tolerance Criterion", 10th Experimental Safety Vehicle Conference, 1985.

## The Composite Test Procedure (CTP)—State of the Art

**B. Richter,**  
CCMC, Belgium

### Abstract

In 1988, the European car manufacturers represented by the CCMC, decided to promote an alternative method to full-scale side impact testing. Since this alternative method is a combination of testing and computer evaluation, it is called Composite Test Procedure (CTP). It was presented at the meeting with the EC Commission and Government representatives and the CCMC Car Technical Commission in Brussels on 28 April 1988.

A major advantage of the CTP over the current full-scale tests is that with the CTP there is no need for a mechanical dummy. In the CTP, occupant loading is evaluated by means of a mathematical "dummy". Since the properties of a mathematical dummy are free of scatter, the repeatability of the CTP promises to be superior to that of the full-scale test.

Mechanical dummies considered thus far for use in full-scale tests have proved unsatisfactory in terms of bio-mechanical response. CCMC therefore believes that a mathematical occupant is better suited to provide human-like behaviour. In order to achieve this goal, a more sophisticated occupant model is being implemented in the CTP.

Although the CTP's ultimate goal is humanlike response, it has to be demonstrated that the CTP can produce results equivalent to those obtained in dynamic tests with a physical dummy. This can be done by comparing the full-scale test results to the equivalent CTP results.

A very recent development of the CTP is the Computer Controlled CTP (CC-CTP). This approach not only represents the full-scale test better but also simplifies the whole

test procedure. This paper describes the CTP's state of advancement and how the CC-CTP works.

### Introduction

Developments in the field of safety legislation over the past few years have caused great debate among motor vehicle manufacturers and regulatory authorities. A characteristic of this development is the proliferation of anthropomorphic test dummies required for full-scale tests.

Currently, only one single dummy, the Hybrid II, is required to comply with safety standards for frontal collision. As this dummy is scheduled to be replaced by Hybrid III at the beginning of the 1990s, motor vehicle manufacturers will have to work with both dummies for a transition period.

If one considers the outlay involved in the procurement, maintenance and calibration of one single family of dummies (approx. 30–40 examples of the 50% type), an estimate can be made as to the increase in costs which will be brought about by the multiplication of dummy types. The crucial point however is the much larger number of full-scale tests required because of the proliferation of dummies and the resultant increase in vehicle development time.

These concerns have led to the development of various methods to simplify and improve the accuracy of side impact test procedures. One such method that shows high potential for producing meaningful countermeasures and improving test accuracy is termed the Composite Test Procedure (CTP) and is being developed in a joint effort by the major world motor vehicle manufacturers represented in CCMC, JAMA and MVMA.

In order to coordinate the research activities of these three

associations in the most efficient way possible, a CTP Steering Committee has been set up. The Committee, equally composed of experts from CCMC, JAMA and MVMA, meets on a regular basis. One of the Committee's major tasks is to ensure the CTP meets the particular safety conditions prevailing in all the regulatory jurisdictions, making it a potential candidate for an international harmonized regulatory requirement.

Following a brief review of the various test methods available for side impact evaluations, a description and progress report of the Composite Test Procedure will be given as well as a description of future projects scheduled to finalize development of this test procedure.

## Side Impact Test Methods

Various test methods designed to evaluate improvements in side impact protection have been investigated. These methods range from simple laboratory tests of vehicle components such as doors, A- and B-pillars, to full-scale tests using instrumented anthropomorphic test dummies. The full-scale test is currently the most popular.

## Full-scale Tests

The full-scale tests for side impact proposed in the U.S. and in Europe are different. The most important difference lies in the dummy used. The SID (HSRI-SID) is proposed to be used in the U.S., whereas Europeans propose to use the EUROSID.

All attempts to date to harmonize the specifications of these two test procedures have failed. The chances that a common procedure will be agreed upon appear to be minimal. Consequently, if these two test procedures are eventually adopted by the U.S. and European governments, it will result in a further proliferation of test dummies and additional testing requirements. There is serious concern that the duplication of efforts will not result in improved side impact protection for vehicle occupants contrary to what would happen if a single, meaningful test procedure were to be adopted.

Full-scale tests, however, indubitably offer individual vehicle manufacturers the opportunity of selecting a combination of various measures appropriate to obtain specific dummy loading levels. This fact has led to the opinion in some quarters that the full-scale test is the only means to evaluate vehicle safety and to the belief that the test results are much more accurate than they really are. The points discussed below will attempt to show how imprecise and limited the safety data produced by dynamic side impact tests are because of the inherent nature of the test configuration.

## Test speed

The full-scale test is only performed at a single test speed whereas the speeds occurring in real accidents cover a wide spectrum. It is not clear whether measures for the specified

test speed used in a full-scale test have an optimum effect considering the speed spectrum.

## Mass and rigidity of the movable barriers

It is claimed that the full-scale test can provide an evaluation of the side impact protection of a vehicle based on a collision with a barrier of specific mass and rigidity. Realistically however, the vehicle under examination is subjected to a much broader spectrum of masses and rigidities corresponding to the wide variety of vehicles on the road.

## Dummy characteristics and seating position

The full-scale test requires the dummy to correspond to the so-called 50% male with regard to its mass distribution and size. In addition, a precisely defined seating position is specified. Even if the biomechanical characteristics of the dummy were to correspond to those of the 50% male, the problem would still remain—as described in the sections above—of transposing the results of one “representative” person to the entire population of vehicle occupants.

## Conclusion

In summary, it can be said that all of the above full-scale test parameters describe an accident in such detail that the probability of precisely that accident occurring in real life is practically nil. This means that the full-scale test can at best provide a rough forecast of what would happen in a real accident. This fact expresses itself concretely in the lack of success in harmonization negotiations between the relevant authorities in Europe and the U.S. Although both propose a full-scale test, each side is reluctant to accept that the other party's proposal can provide an adequate evaluation because of the specific test requirements.

The most serious disadvantage of current full-scale tests, however, can be attributed to the shortcomings of the test dummies. The dummies provide scattered results on account of the complexity related to the biomechanical requirements and, therefore, a large number of tests are required to provide a reliable evaluation of a vehicle model. In addition, neither the U.S. SID or the European EUROSID has successfully demonstrated the biomechanical characteristics that fall within the loading corridors specified in ISO/TC22/SC12, document DP 9790.

It would be reasonable to assume that compliance of currently available dummies with the biomechanical specifications conflicts with the requirements for a durable, reliable measuring instrument. For the sake of completeness, it should be noted that a committee set up by the Society of Automotive Engineers is developing a new dummy that shows promise of exhibiting more humanlike behaviour (i.e. ISO corridor responses) in side impacts. Nevertheless, doubts persist as to whether any future mechanical dummy will be apt to resolve the intrinsic conflict between the demands for biofidelity and durability, for example.

## Component Tests

The component test, pursued for a time by the American automobile manufacturers, avoids the use of an anthropomorphic test dummy. The component test is based on the fundamental idea that protection for occupants in a side impact can be verified entirely by the energy absorption characteristics of the inner door. Side structure components are simply pre-deformed from the exterior by a rigid ram at a constant stroke depth so that the surface shape is more or less realistic for the subsequent deformation of the door inner panel by the dynamic double-mass impactor.

The weakness of this method is that the designer is completely deprived of the freedom to choose whether he would like to obtain the required occupant protection level by means of padding, structural improvements or both. Accordingly, it is not possible to design a vehicle with an optimum combination of structural elements and padding when using the component test approach.

## The Composite Test Procedure (CTP)

The weaknesses of the full-scale test and the deficiencies of the component test methods have led motor vehicle manufacturers to look for new procedures.

In April 1988, European motor vehicle manufacturers represented by the CCMC proposed a COMPOSITE TEST PROCEDURE (CTP).<sup>1</sup> This test procedure combines testing and calculation, thus providing dynamic outputs (accelerations, velocities) just as the full-scale test, but offers a number of advantages over the full-scale test. These advantages can be summarized as follows:

a. A fully equipped vehicle or body-in-white, with all necessary components for lateral impacts, can be used in the test, allowing the safety characteristics of the vehicle to be evaluated at an early stage.

b. The CTP does not use a mechanical dummy. The loads to which occupants are subjected are calculated with the help of a mathematical occupant. As the characteristics of a mathematical occupant are not subject to scatter, the CTP offers superior overall test repeatability.

c. Everything indicates that a mathematical occupant is better suited than a mechanical dummy to simulate human behaviour. In addition, less time and money is required to modify a mathematical occupant as new biomechanical findings emerge, which is not the case for a mechanical dummy. A first proposal for a mathematical occupant was presented on 28 April 1989, together with this status report.

d. Although the CTP results are developed from a specified collision speed and vehicle/barrier mass, results for other speeds and masses can, within certain limits, be derived from the same test. Thus, other accident situations can be evaluated from a single test which is not possible using a full-scale test.

e. The CTP offers deeper insight into the collision

process. It is therefore not only suitable as a test procedure, but can also be used as a development tool. It goes without saying that, as in the case of full-scale tests, the designer is free to select the countermeasures he wants. He can exploit the options both in terms of structure and padding to protect the occupants.

## Current Status of the CTP

### The test procedure

To illustrate the changes that have been brought to the CTP since it was first presented by CCMC in April 1988, we have reproduced in figure 1 the original single piece interior loading device (ILD) which was used at that time, and which represented the torso of a 50th percentile dummy. The mathematical model corresponding to this single piece ILD is given in figure 2.

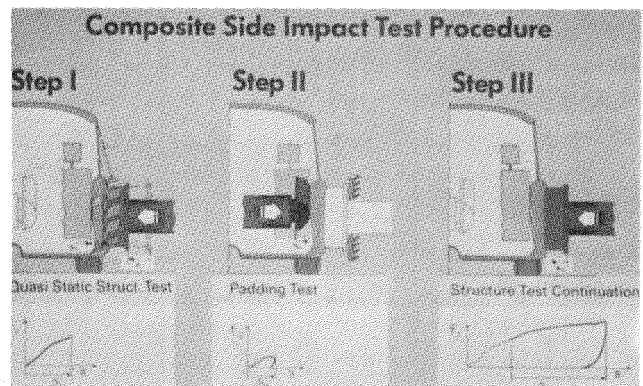


Figure 1. Original CTP, using single piece ILD.

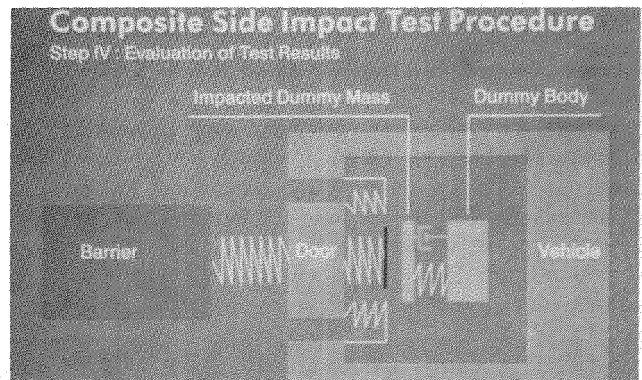


Figure 2. Mathematical model corresponding to the single piece ILD.

Although this rather simple design and its corresponding mathematical model already gave satisfactory results in comparison to the full-scale tests, CCMC decided to introduce separate ILDs for the thorax and pelvis, with an additional load cell included in the thoracic ILD to identify possible load concentrations at abdominal level (figure 3). The final shapes of the ILD sections for the humanlike occupant will be defined by CCMC, JAMA and MVMA in the near future.

The lack of provisions in the original CTP version to detect load concentrations at abdominal level had been one

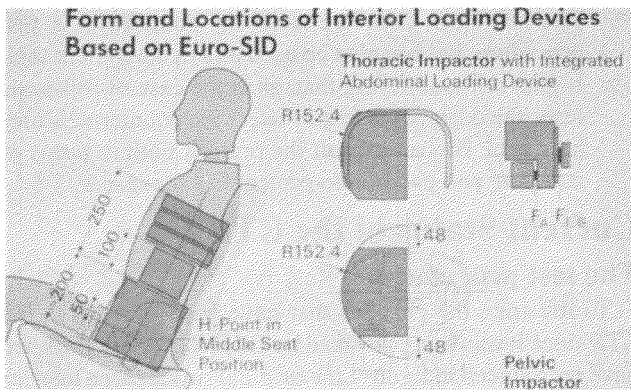


Figure 3. Dimensions of the ILD based on the EUROSID.

of the major causes for concern in certain quarters, e.g. government experts critical of CCMC's new approach. A similar design, without abdominal force measurement however, has been adopted for the ILDs corresponding to the US-SID, taking into account that this dummy's abdomen is not equipped with any switches or other load sensing devices (figure 4).

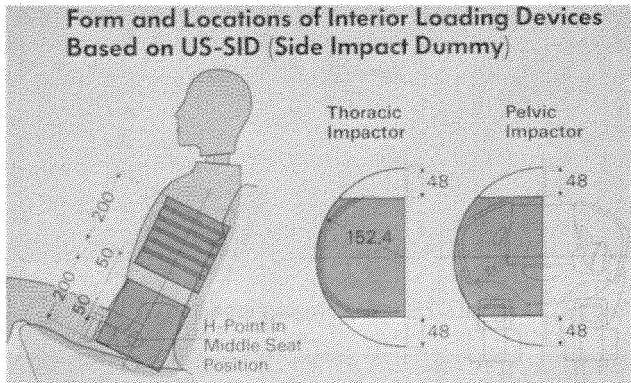


Figure 4. Dimensions of the ILD, based on the US-SID.

Despite these changes to the ILD design, the current CTP version remains based on a step-by-step approach, consisting in a sequence of quasi-static force/deflection measurements followed by a calculation which provides dynamic results of the barrier, vehicle and occupant. As shown in figure 5, a body-in-white or full vehicle with the equipment required for side protection (seats, padding) is fixed in position.

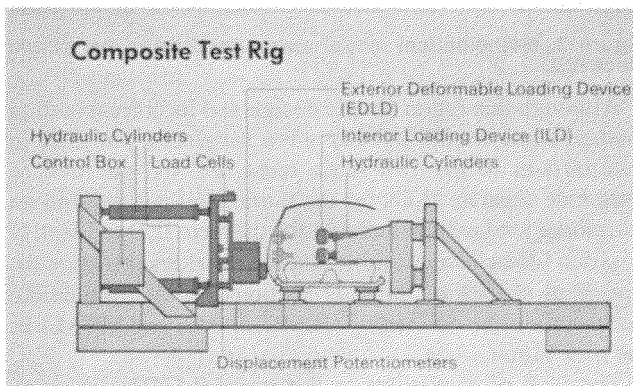


Figure 5. Composite test rig.

A loading device with a deformation element representing another vehicle or a deformable barrier is used to deform the exterior. The interior loading devices represent the occupant. Figure 6 shows the test set-up.

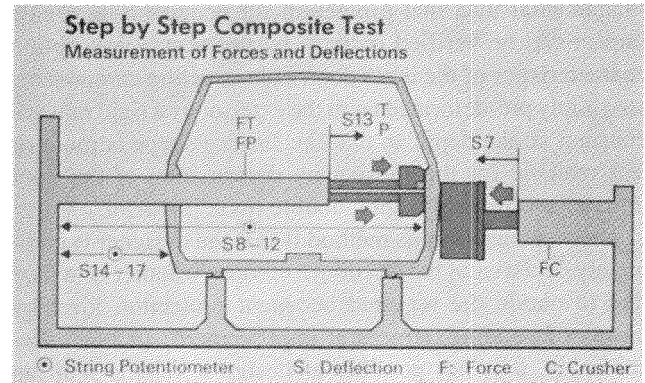


Figure 6. Composite test set-up.

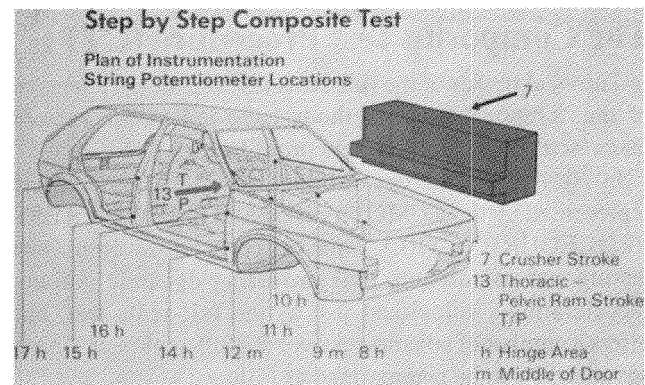


Figure 7. Measurement of ram strokes and vehicle deformation.

By measuring the forces applied and the resultant deformation (figures 6 and 7), all the important vehicle characteristics for side impact can be calculated. The test procedure is performed according to the step-by-step procedure shown in figure 8 and explained as follows.

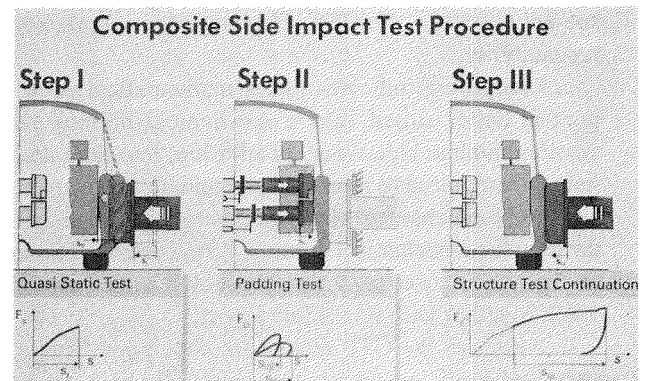


Figure 8. Test procedure for step-by-step method for composite test.

First the exterior loading device deforms the side of the vehicle and is stopped when the inside of the door makes contact with the seat. This is Step I. The end of Step I

corresponds approximately to the point at which the occupant makes contact and is accelerated by the door. The force of the exterior loading device is then kept constant.

In Step II, the interior loading device deforms the inner panel of the door. This produces the force/displacement characteristics for thoracic and pelvic loading. The dimensions of the (rigid) interior loading device representing both the thorax and pelvis are shown in figure 4.

The end of Step II is determined by a certain energy absorption of the vehicle door during occupant contact. Step III is a continuation of Step I. The exterior loading element continues to deform the side of the vehicle until all the deformation energy of the side impact has been absorbed.

In Step IV, the dynamic process is then calculated using the measurements recorded during Steps I, II, and III.

Figure 9 shows the basic mathematical model used in the dynamic process. The characteristics of the mathematical dummy, represented by the masses  $m_4$ ,  $m_5$ ,  $m_6$  and by the groups of characteristics  $F_4$ ,  $F_5$ ,  $F_6$ ,  $F_7$  are not a part of the test procedures and must be specified beforehand. These parameters can be defined to represent a mechanical dummy such as SID or EUROSID, or a human as specified in ISO/TC22/SC12-DP 9790.

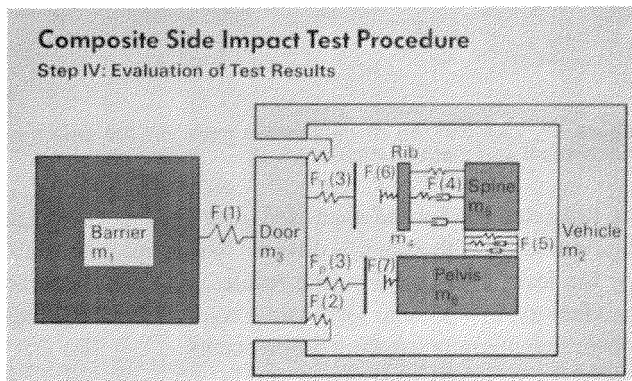


Figure 9. Model for the calculation of dynamic processes.

## Test results

One of the goals of the CTP is to provide the mathematical dummy with characteristics which are more representative of human behaviour than is possible with existing mechanical dummies (example in figure 10).<sup>2</sup> As sufficient information on human biomechanical characteristics is not presently available, the practicability of the CTP can only be demonstrated in comparison with tests using mechanical dummies. Accordingly, a series of tests were required where results were available from full-scale tests with differing vehicle configurations. This requirement was satisfied by a series of tests conducted by MVMA using various modifications to the American passenger car of the type Ford LTD.

With the same modifications used in the MVMA tests, tests were performed (at MGA Corporation in Akron, N.Y. USA) using the CTP method. The four vehicle configurations considered were:

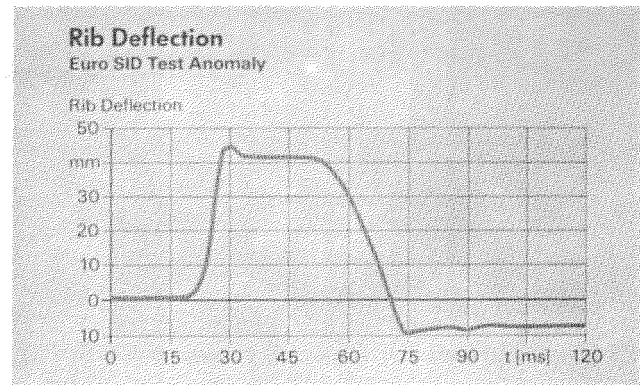


Figure 10. Anomalies in recording measurements at ribs of EUROSID in FST.

HN: unpadded door, no space between dummy and door.

HF: unpadded door, space between dummy and door.

PN: padded door, no space between dummy and door.

PF: padded door, space between dummy and door.

Figures 11 and 12 show one of the vehicles used in the CTP tests as well as the deformation element (NHTSA element) used as the exterior loading device.

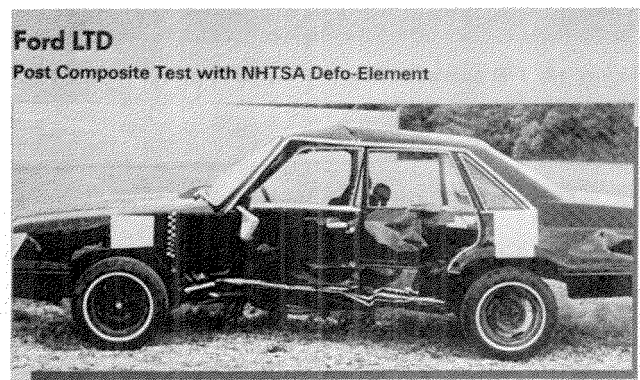


Figure 11. Deformed Ford LTD after composite test with NHTSA deformation element.

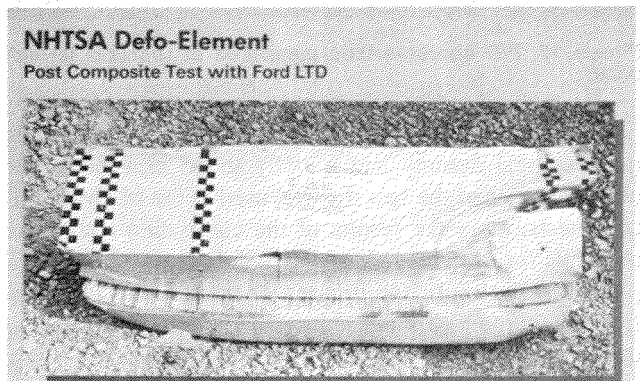


Figure 12. Deformed NHTSA deformation element after composite test with Ford LTD.

The test results of Steps I and III are shown together in figure 13 and the results of Step II are shown in figures 14 and 15.

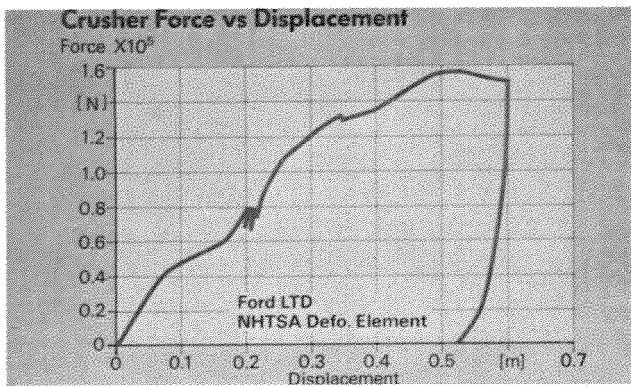


Figure 13. F/D characteristic measured at exterior ram.

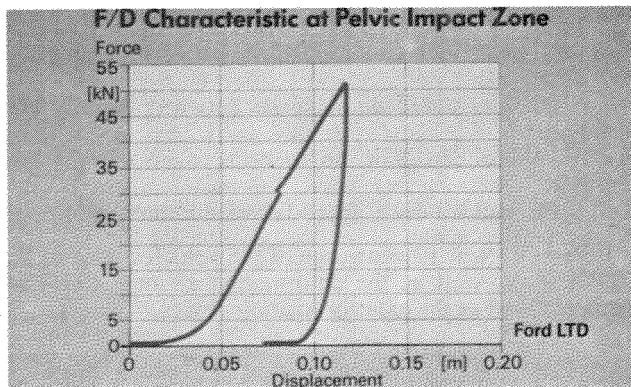


Figure 14. F/D characteristic measured at pelvic impact zone.

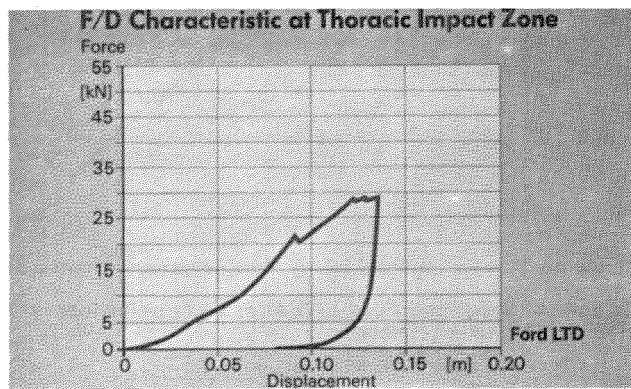


Figure 15. F/D characteristic measured at thoracic impact zone.

Before performing Step IV, the model parameters of the mathematical dummy had initially to be adjusted to the characteristics of the specific SID used in the MVMA full-scale tests. Only the results of the calibration tests were available for this and unfortunately did not provide a complete description of the dummy characteristics. Missing from the dummy calibration information was the coupling of the thorax and spine as shown as F5 in figure 9.

Figures 16 and 17 show a comparison between the SID calibration measurement and the CTP calibration results. Using the characteristics of the mathematical dummy established in this manner, the results could then be calculated within the framework of the CTP.

Figures 18 to 23 show a comparison between the CTP and

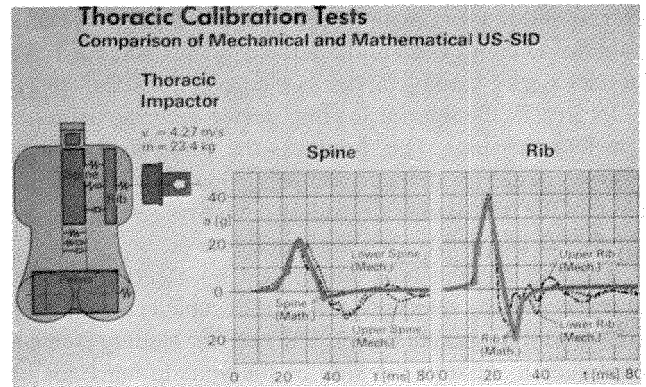


Figure 16. Comparison of calibration tests on the thorax of mechanical and mathematical US-SID.

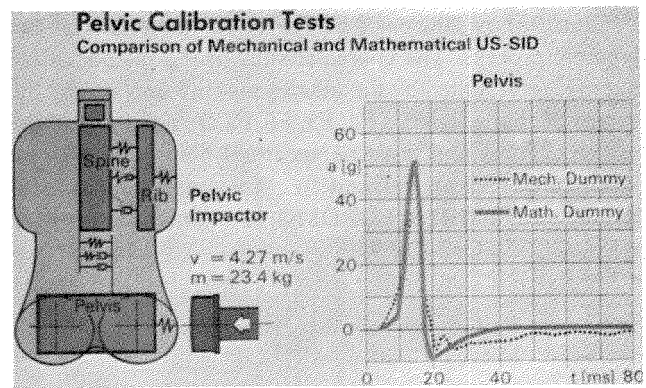


Figure 17. Comparison of calibration tests on the pelvis of mechanical and mathematical US-SID.

the full-scale test for the unpadded, near spacing (HN) test configuration. Although it is difficult to indicate a standard for the level of agreement, the results can be considered satisfactory, in particular for the time below 30 milliseconds where maximum occupant loading occurs.

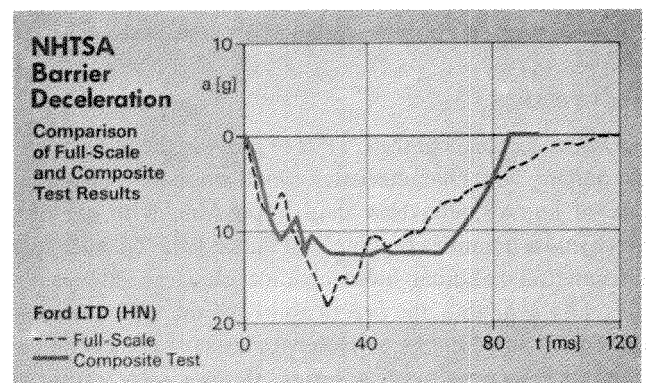


Figure 18. Comparison of barrier deceleration in FST and CTP.

The tables in figures 24 and 25 provide an overview of all tests. It can be seen that there is agreement in important trends. This applies in particular to the effectiveness of the space between the occupants and the door in the case of unpadded doors and to the value of padding in general for occupant rib loading. The comparison will have to be made again once the results of the computer controlled CTP (See

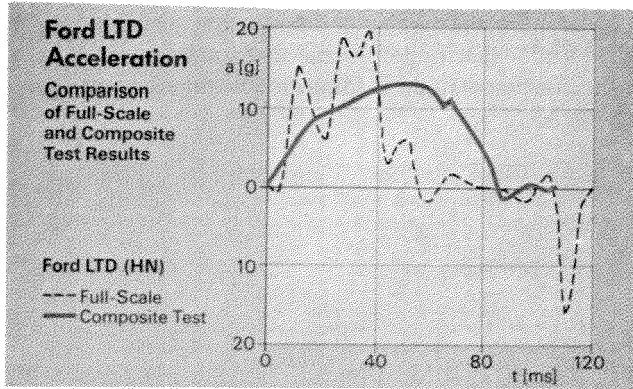


Figure 19. Comparison of Ford LTD acceleration in FST and CTP.

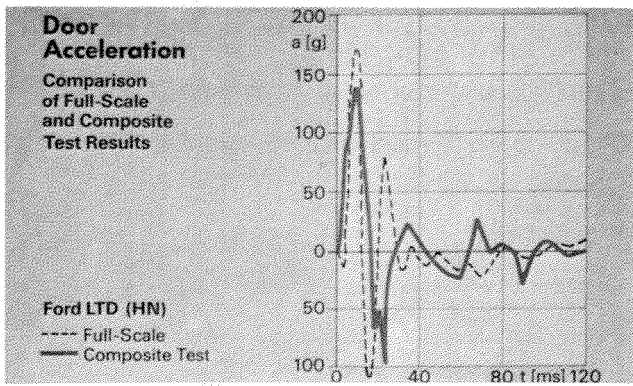


Figure 20. Comparison of door acceleration in FST and CTP.

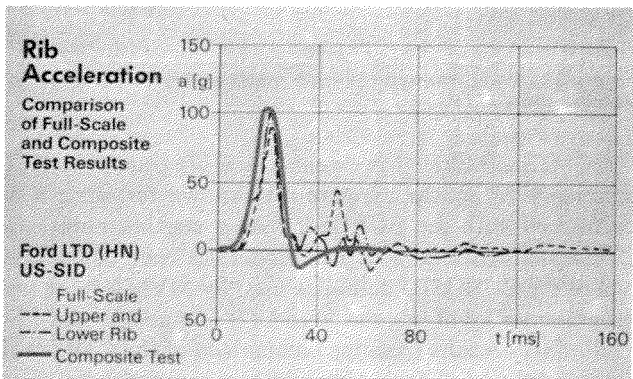


Figure 21. Comparison of rib acceleration in FST and CTP.

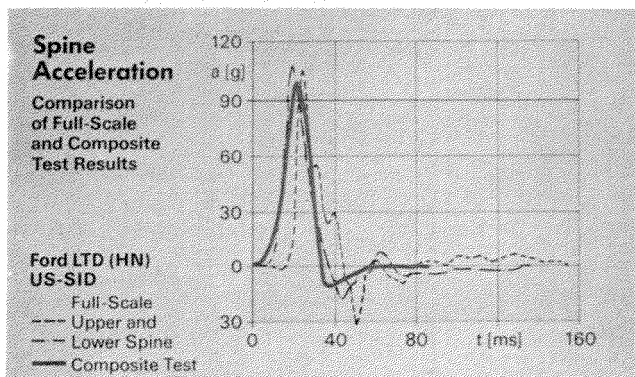


Figure 22. Comparison of spine acceleration in FST and CTP.

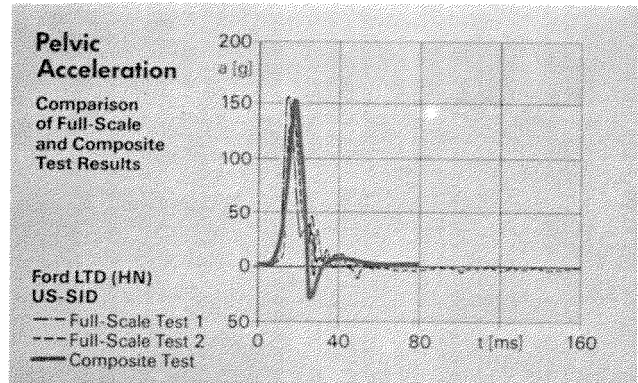


Figure 23. Comparison of pelvic acceleration in FST and CTP.

below "Further Development of the CTP") are available and the mathematical dummies are finally validated.

**Ford LTD Driver Dummy Loads**  
Comparison of Full-Scale and Composite Test Results

Method I Dynamic Factor = 0.0	HN			HF		
	Full-Scale 1	Full-Scale 2	Com- posite	Full-Scale 1	Full-Scale 2	Com- posite
Rib [g]	Upper	90	95	68	50	
	Average	98	105	66		61
	Lower	99	109	70	74	
Spine [g]	Upper	105	107	64	80	
	Average	108	100	92		59
	Lower	105	105	99	123	
Pelvis [g]	Average	156	131	157	143	
	Average	143	155	150		109
TTI	Average	102	107	84.5	98.5	
	Average	105	104	92		61

HN: Baseline Structure, Hardboard Door, Dummy Near Seated (0.0 m)  
HF: Baseline Structure, Hardboard Door, Dummy Far Seated (0.13 m)

Figure 24. Comparison of US-SID loads in FST and CTP for Ford LTD HN and HF.

**Ford LTD Driver Dummy Loads**  
Comparison of Full-Scale and Composite Test Results

Method I Dynamic Factor = 0.0	PN			PF		
	Full-Scale 1	Full-Scale 2	Com- posite	Full-Scale 1	Full-Scale 2	Com- posite
Rib [g]	Upper	42	49	55	61	
	Average	45	45	51		33.5
	Lower	38	49	43	44	
Spine [g]	Upper	51	61	51	53	
	Average	62	59	58		44
	Lower	63	71	63	63	
Pelvis [g]	Average	52	62	52	60	
	Average	57	56	61		44
TTI	Average	52	60	59	62	
	Average	56	52	61		38

PN: Baseline Structure, Padded Door (0.13 m), Dummy Near Seated (0.0 m)  
PF: Baseline Structure, Padded Door (0.13 m), Dummy Far Seated (0.13 m)

Figure 25. Comparison of US-SID loads in FST and CTP for Ford LTD PN and PF.

The quantitative differences which occur in individual cases—such as for spine acceleration—require careful analysis. They cannot automatically be considered as pointing to a deficiency in the CTP—as can be seen from the examples in figures 26 and 27. Here, it would seem that the problem results from anomalies that occurred in the full-scale test.

### Further development of the CTP

Fundamental considerations and practical experience would indicate that dynamic effects of the structure and

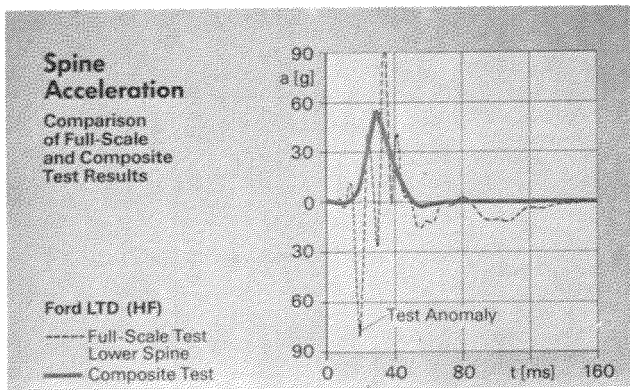


Figure 26. Anomalies in recording measurements at lower spine in FST.

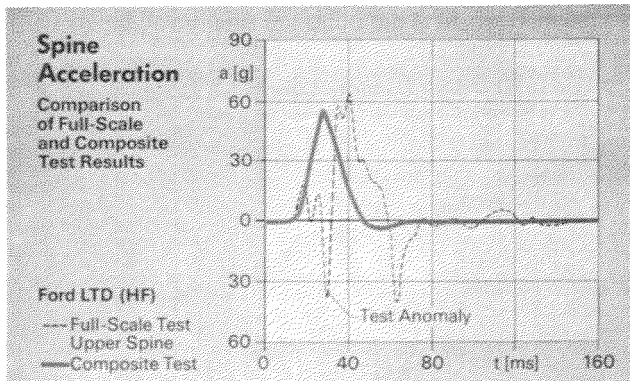


Figure 27. Anomalies in recording measurements at upper spine in FST.

padding are of secondary importance in the event of a side impact collision. However, this point is being considered for further development within the framework of the joint CCMC, JAMA and MVMA activities.

Another area of investigation is the replacement of the current step-by-step procedure with a computer controlled method. This method is called Computer Controlled Composite Test Procedure (CC-CTP) and is currently undergoing development. The CC-CTP combines measurements and calculations in a single laboratory test controlled by one computer (figure 28). Here the calculation determines which data is required at any particular moment and controls the test rig accordingly.

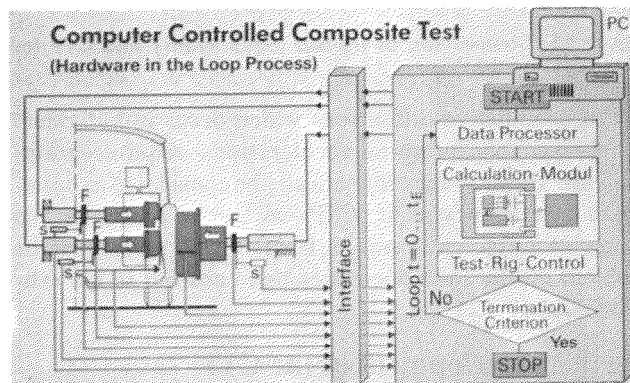


Figure 28. Computer controlled composite test procedure (CC-CTP).

In addition, the number of deformation measuring points is reduced so that the deformation measurements are limited to the movement of the loading devices themselves (figures 29 and 30).

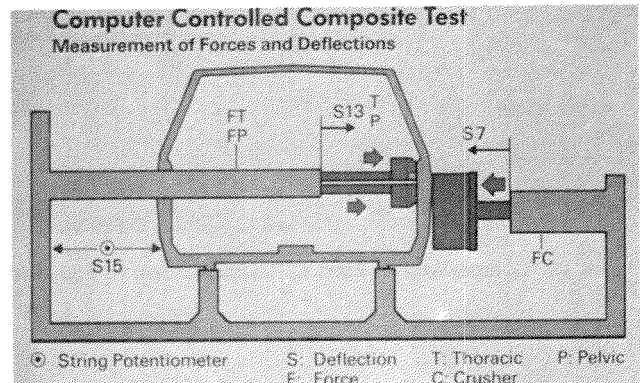


Figure 29. Reduction of measuring points in CC-CTP.

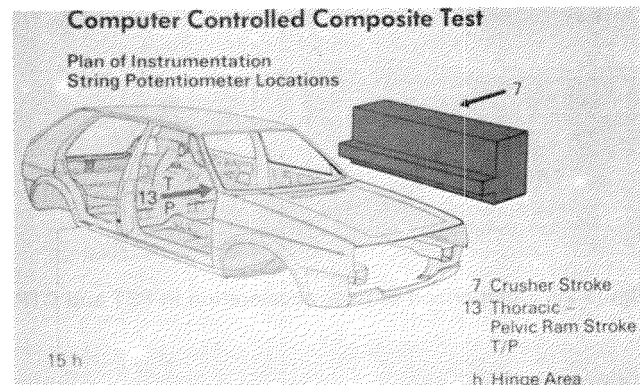


Figure 30. Measurement of ram strokes and body-in-white deflection in CC-CTP.

CCMC has initiated an extensive test programme to evaluate the CTP and to compare it to known full-scale tests performed with the EUROSID. As a starting point, the CTP's mathematical occupant model has been adjusted to one of the EUROSID dummies used by MVMA in its test programmes involving the Ford LTD (figures 31 and 32). Preliminary results from the comparison of the CTP to the corresponding full-scale tests with that car model are given in figures 33 to 35.

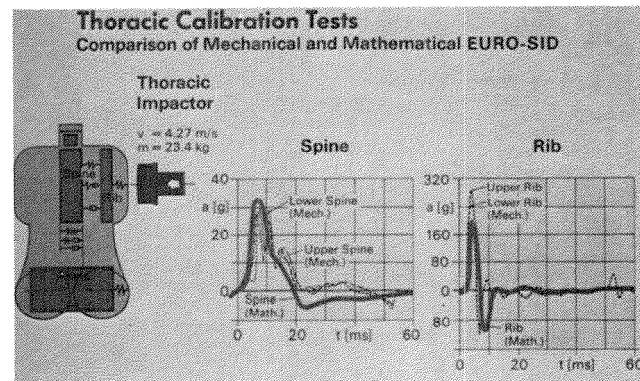


Figure 31. Comparison of calibration tests on the thorax of mechanical and mathematical EUROSID.

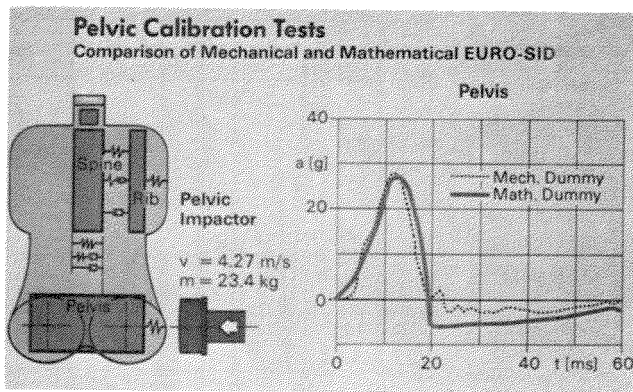


Figure 32. Comparison of calibration tests on the pelvis of mechanical and mathematical EUROSID.

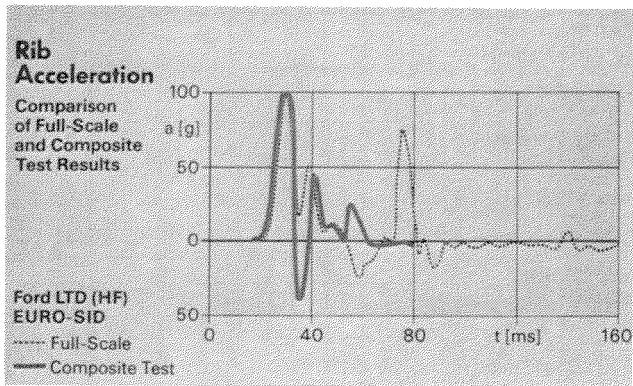


Figure 33. Comparison of rib acceleration in FST and CTP with EUROSID.

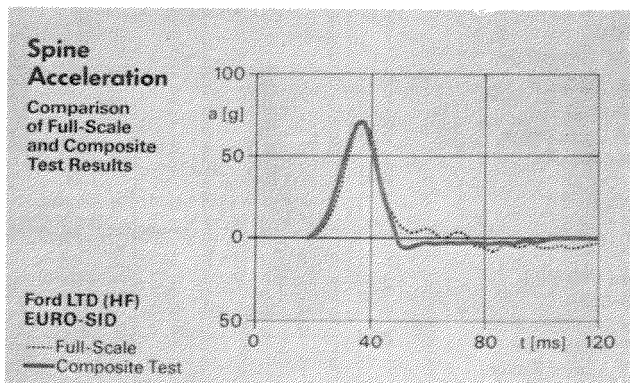


Figure 34. Comparison of spine acceleration in FST and CTP with EUROSID.

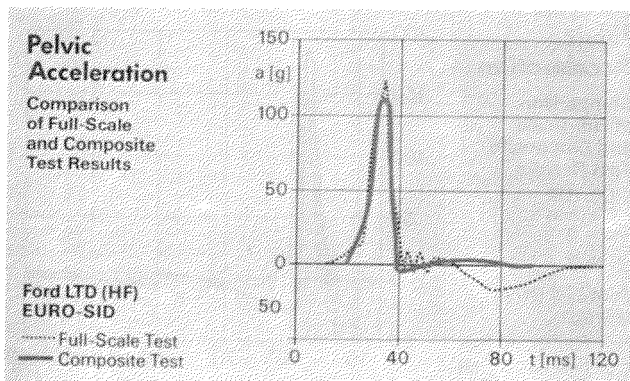


Figure 35. Comparison of pelvic acceleration in FST and CTP with EUROSID.

The CTP mathematical model may have to be adjusted to the specific EUROSID examples that were used in the various tests that have been performed in Europe. Obviously, in order for CCMC to demonstrate that the CTP leads to results at least similar to those obtained in full-scale tests, the known deficiencies of individual EUROSIDs will also have to be included in the CTP mathematical dummy. One may therefore expect the calibration test graphs reproduced in figures 31 and 32 to differ according to the particular production batch and EUROSID model that was used in a given full-scale test.

Related to CCMC's criticism of current physical dummies and their deficiencies in representing humans in biomechanical terms, CCMC has launched a research programme aiming to provide the data necessary to implement a mathematical occupant model of the human occupant. This will then be introduced into the final version of the CC-CTP.

## Summary

Of the various test procedures available for evaluation of side impact protection, the Composite Test Procedure offers greater potential for providing optimum and meaningful countermeasures. Compared to full-scale testing, the following advantages of the CTP are evident:

- It is easier to perform.
- It provides results which are easier to reproduce.
- It makes it easier to incorporate new biomechanical findings.
- It can be applied from an earlier stage of vehicle development.
- It offers a new approach towards harmonizing legislation on side impact collisions.
- It allows a wider approach to vehicle designs, resulting in solutions which are more robust.

## References

(1) CCMC booklet: "Composite Test Procedure for Side Impact Protection—an Alternative Approach"; exchange of views between EC Commission and Government representatives and the CCMC Car Technical Commission, Brussels, 28 April 1988.

(2) Publication by the Association of Automotive FAT Research on EUROSID: "Analysis of the EUROSID in 21 Full-Scale Side Impact Tests"; IRCOBI/EEVC Workshop on the Evaluation of Side Impact Dummies, Bergisch-Gladbach, 13 September 1988.

## Appendix

### The Computer Controlled Composite Test Procedure (CC-CTP)

### Progress achieved after the IMECHE seminar

CCMC's progress report published at the seminar

organized by the Institution of Mechanical Engineers in London aimed at illustrating the changes that have been brought to the CTP since its first presentation. At the same time, the report described the research projects underway to further develop the procedure.

One essential element of CCMC's work programme has been successfully completed only a few days ago: under contract with CCMC, MGA performed two computer controlled CTP tests, one in "NHTSA configuration", the other one in "EEVC configuration" together with the respective barrier faces. The initial, very promising results were presented by MGA in a meeting of the CCMC ad hoc working group AHC on May 11, 1989 in Brussels.

The most important characteristic of the CC-CTP is that, after the test vehicle and the MDB face have been set in accordance with the test conditions, it runs automatically once initiated, without any further intervention by the test operator. Since the strokes of the hydraulic cylinders are automatically controlled by the computer under "real time" conditions and as a function of the momentary force/deflection characteristics of the barrier face, the vehicle side structure, and the padding, the deformation patterns of the vehicle correspond more closely to those observed under dynamic test conditions.

Figures i to v show a sample of CC-CTP test results in comparison with two full scale tests (FST) on the Ford LTD under identical test conditions. In both FSTs, the NHTSA barrier was run into the vehicle in "crabbed" configuration, and space was provided between the US-SID and the unpadding interior panel ("HF" configuration).

### Rib Acceleration

Comparison of Full-Scale and Composite Test Results  
 - CC-CTP  
 - Method II  
 -  $\alpha = 0$   
 - FST 1

Ford LTD (HF) US-SID

Full-Scale  
 --- Upper and  
 --- Lower Rib  
 — Composite Test

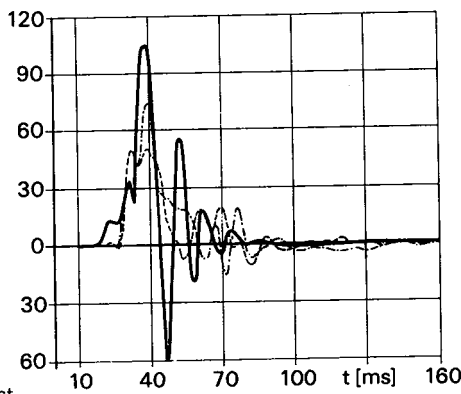


Figure i. Rib acceleration in CC-CTP versus FST 1.

Test anomalies and significant scatter could be noted during those two full scale tests. Most probably, these anomalies are related mainly to the dummy, and are very unlikely to ever manifest themselves in tests using the CTP dummy model.

With one exception, the CTP dummy produced higher loads than could be observed in the two full scale tests. This indicates that both the existing CTP dummy and its underlying interior loading devices need further development. On the other hand, the acceleration/time histories

### Rib Acceleration

Comparison of Full-Scale and Composite Test Results  
 - CC-CTP  
 - Method II  
 -  $\alpha = 0$   
 - FST 2

Ford LTD (HF) US-SID

Full-Scale  
 --- Upper and  
 --- Lower Rib  
 — Composite Test

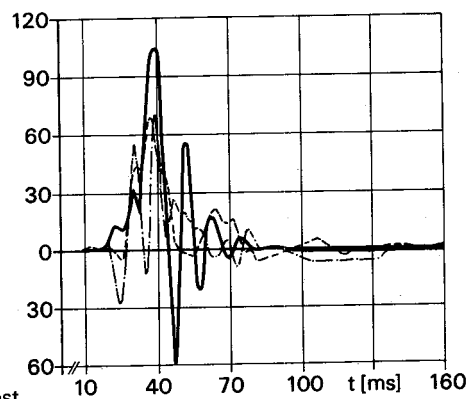


Figure ii. Rib acceleration in CC-CTP versus FST 2.

### Spine Acceleration

Comparison of Full-Scale and Composite Test Results  
 - CC-CTP  
 - Method II  
 -  $\alpha = 0$   
 - FST 1

Ford LTD (HF) US-SID

Full-Scale  
 --- Upper and  
 --- Lower Spine  
 — Composite Test

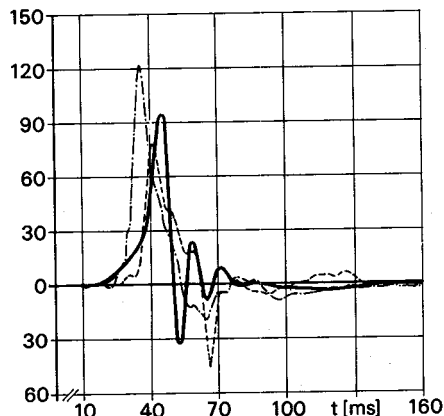


Figure iii. Spine acceleration in CC-CTP versus FST 1.

### Spine Acceleration

Comparison of Full-Scale and Composite Test Results  
 - CC-CTP  
 - Method II  
 -  $\alpha = 0$   
 - FST 2

Ford LTD (HF) US-SID

Full-Scale  
 --- Upper and  
 --- Lower Spine  
 — Composite Test

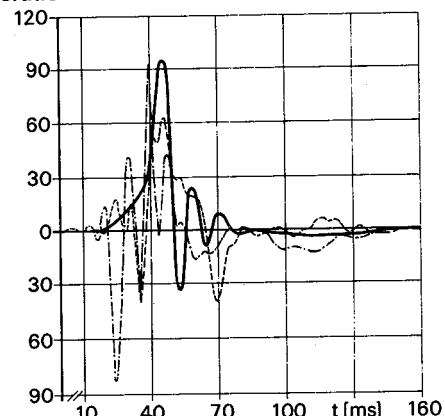


Figure iv. Spine acceleration in CC-CTP versus FST 2.

### Pelvic Acceleration

Comparison of Full-Scale and Composite Test Results  
 - CC-CTP  
 - Method II  
 -  $\alpha = 0$

Ford LTD (HF) US-SID

Full-Scale Test 1  
 --- Full-Scale Test 2  
 — Composite Test

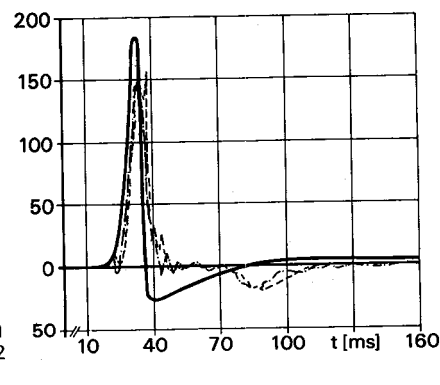


Figure v. Pelvic acceleration in CC-CTP versus FST 1 and 2.

of both the FST and the CTP tests are satisfactorily inphase. As can be observed in FSTs, contact of the pelvis with the door occurs earlier than with the ribs.

Further research aimed at validating the CTP dummies, on the basis of human beings and existing dummies (US-SID and EUROSID) is underway at APR, under contract for CCMC. Another goal of this research is the definition of the

final shape of the interior loading devices corresponding to the CTP occupant model.

After the final CTP dummy and occupant models and their corresponding ILDs are available, an extensive evaluation test programme will be launched, coordinated by the CTP Steering Committee which is equally composed of representatives from CCMC, JAMA, and MVMA.

## **An Assessment of a Composite Test Procedure for Side Impact**

**J.A. Bennett, K.H. Lin, Y.-C. Deng,**  
General Motors Research Laboratories

**J. Stocke,**  
General Motors Current Product Engineering

### **Abstract**

A composite test procedure for side impact evaluation has been proposed by Volkswagen as an alternative to full scale dynamic test procedures for side impact compliance. Alternative procedures such as this approach could offer increased customer benefit due to lower testing costs and perhaps ultimately increased side impact safety. The Volkswagen procedure utilizes a three-step static crush of door inner and outer structures and then uses this data in a lumped mass computer model to simulate the full scale crush. The fundamental assumptions of this procedure, such as dynamic rate effects and alternative load path assumptions are evaluated. The bulk of the report is devoted to a comparison of results from the alternative test procedure with full scale dynamic moving barrier tests. Results are shown for a full sized four door vehicle and a two and four door intermediate vehicle. The sensitivities of the results to several parameters such as door mass and strain rate were evaluated. It was found that the portion of the static test associated with the inner panel was probably the most critical part of the alternative procedure. If this test is not controlled accurately, the simulation results may differ significantly from the results of a full scale dynamic test. Although there is still relatively little data available, significant differences between the alternative protocol and the dynamic test were observed. Some of these differences may be difficult to resolve within the proposed protocol. Several other alternative procedures also based on computer simulation are suggested.

### **Introduction**

Currently, both the National Highway Traffic Safety Administration (NHTSA) in the U.S. and the European Economic Community (EEC) have proposed full-scale dynamic test procedures as compliance measures for passenger vehicles for side impact. Although there exist significant differences in details between these two tests, the concept is essentially similar. The vehicle will be impacted on its side by a deformable moving barrier and

tolerance levels will be specified on anthropomorphic dummies placed in the impacted vehicle. These test procedures have been under development since the 1970's and there still remains significant disagreement within the technical community about their efficacy as an assessment technique for side impact injury mitigation. In order to resolve some of these difficulties, Volkswagen (1),\* has proposed an alternative procedure using static component tests and a mathematical system simulation using this static data. We believe there is merit in examining alternative compliance procedures to full scale dynamic tests for side impact. However, it is imperative that this alternative procedure be a system evaluation procedure and this implies that the alternative procedure probably will involve some type of computer simulation.

Modeling simulations are commonly used as tools for automobile crash development, and are routinely accepted in other disciplines when it is difficult, impractical or impossible to perform full scale tests. For example, wind gust loading during a space vehicle launch is estimated using probability based processes to determine both the vehicle structure design and whether it is safe to launch the particular vehicle. Also, in the nuclear power industry computer simulations of a large number of catastrophic events are used to certify the design of the power plant. Furthermore, although it is not a certification process, the NHTSA specifies the use of a simulation program, CRASH3, to generate accident data for the NASS file. The data in this file is in use to develop their side impact compliance process.

Although it is possible to construct several alternative compliance procedures which meet the goal of a computer based system evaluation, the Volkswagen composite test procedure (CTP) merits consideration. An extensive evaluation of this procedure serves two important purposes. First, it will allow us to determine the merits of the CTP as an alternative test procedure. Secondly, the process of carrying out this evaluation can develop a methodology for evaluating other alternative compliance processes.

As pointed out earlier, a considerable amount of effort has gone into developing the dynamic full scale test procedures that are currently under discussion. In addition, there is a

\*Numbers in parentheses designate references at end of paper.

significant uncertainty as to whether these dynamic procedures are the correct assessment technique of side impact injury mitigation. To attempt to establish an alternative procedure to serve as a correct assessment technique is probably inappropriate at this time. However, any such technique must ultimately be related to full-scale dynamic impact. Therefore, a possible methodology for evaluation is to assume that the NHTSA (or EEC) dynamic procedure is a correct assessment technique for side impact injury mitigation. Now the only question that remains to be addressed is what margin of difference must be imposed on an alternative procedure such that it will remain conservative with respect to the full scale dynamic impact. This separation of issues will then allow us to examine the crucial aspects of the alternative procedure. Two areas need to be investigated in some detail. First, any inherent limitations imposed by the alternative procedure which may ultimately limit its practicality as a compliance procedure must be determined. Secondly, an objective assessment can then be made of a comparison of the alternative procedure with respect to a full-scale dynamic test applied to a number of vehicles.

## Fundamental Concerns in Lumped Mass Modeling

The composite side impact test procedure as proposed by Volkswagen is essentially a lumped mass modeling approach. This approach was initially developed by Kamal, et al. (2, 3) as a technique for modeling of frontal impact behavior. As such it is one of the most used techniques in the automotive industry for development purposes for frontal and rear impact behavior, and its strengths and weaknesses are well known. The Volkswagen implementation of this procedure for side impact is shown in figures 1a and 1b. Two versions are shown here, an initial one which they applied to a Volkswagen Golf and a second version which they later applied to a Ford LTD (4). The major differences are in their representations of the dummy and the interior surface of the vehicle. The force-deflection curves of the various springs are obtained by statistically crushing a full vehicle in a pre-determined sequence. The sequence is described in the Volkswagen report (1). There are three fundamental concerns in lumped mass modeling that need to be addressed: the variability associated with the modeling, rate dependency, and path dependency.

In comparing a dynamic test procedure with an alternative procedure, there are two types of variability that need to be discussed. The first is the variability in the full scale dynamic procedure itself. The most extensive data currently available on the subject is the sequence of tests performed by the U.S. Motor Vehicle Manufacturers Association (MVMA), in which they tested a sequence of Ford LTD's in a number of configurations, but in each configuration they performed two identical tests. The results of these tests are available in (5). Figure 2 shows a summary of some of the tests using the NHTSA SID dummy. These results are

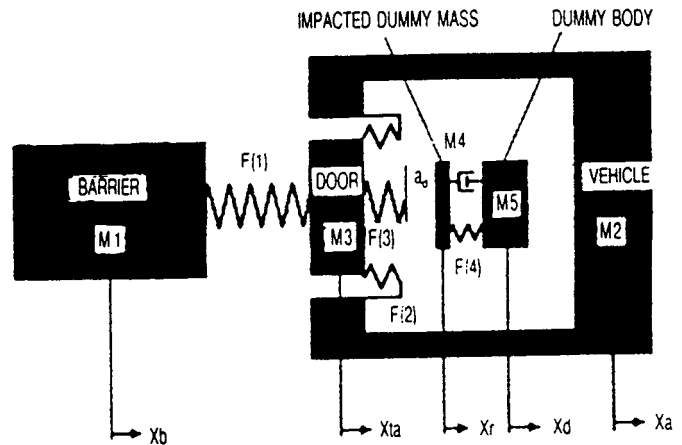


Figure 1a. Model 1—A mathematical model proposed by Volkswagen to evaluate the CTP test results (reference 1).

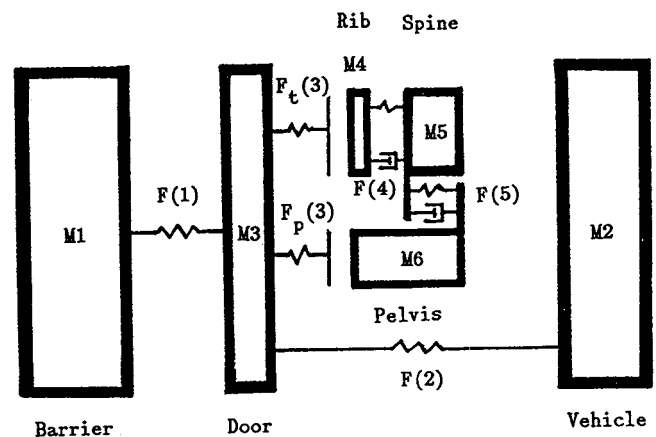


Figure 1b. Model 2—A mathematical model proposed by Volkswagen to evaluate the CTP test results (reference 4).

typical of the entire test series and indicate that in terms of dummy measures, the test to test variability was generally low with the worst variability being of the order of less than 20%. There is relatively little data available on the variability of static test of major structural components that are used in lumped mass simulations. Some typical data from identical specimens of front rail components is shown in figure 3. Typically, this type of variability may result in a 5–10% variability in the response in a lumped mass simulation. It is clear that additional work will be needed to generate data associated with static test variability in side impact simulation.

The second area of rate dependency has been an issue since the introduction of the lumped mass modeling technique (2). It is well understood that some materials perform differently from a structural standpoint as the impact speed increases. Since the component tests for lumped mass simulation are conducted statically, this phenomenon is typically handled by including a rate dependency parameter in the computer model such that the force-deflection curves are modified by this parameter as a function of the instantaneous rate of deflection. Because this parameter is a component parameter as opposed to a material parameter, it becomes very difficult to specify one number that can be used in all situations, and different

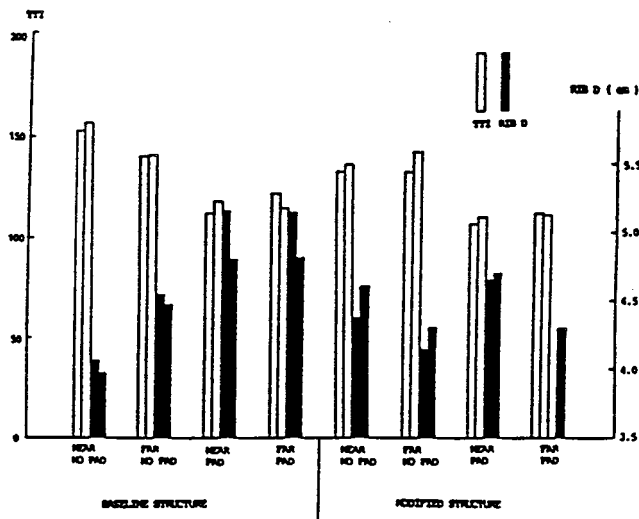


Figure 2. MVMA side impact test results.

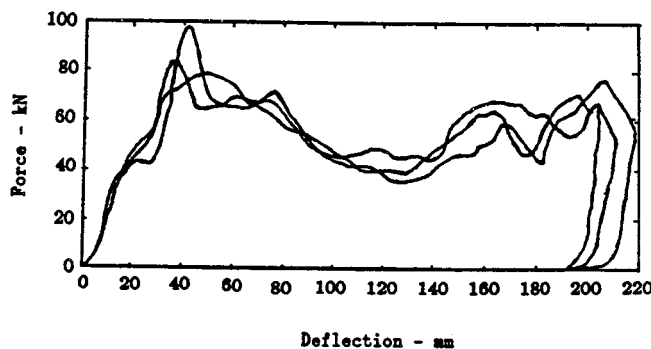


Figure 3. Variability of front rail drop-tower test data.

groups have developed different methodologies to determine an appropriate parameter. At GM we have traditionally used 1% per mile per hour to represent mild steel components in frontal impacts, whereas high strength steel and aluminum components have essentially a zero strain rate effect. Very little rate information is available on polymeric materials that are traditionally used for padding. It is known that these materials may be highly variable in their rate sensitivity, and this is clearly an additional area that will require further research in order to quantify these numbers. However, the dilemma this phenomenon presents to an alternative certification procedure is obvious. A most desirable side impact structure would be one which is soft at low speeds and stiffer at high speeds, and therefore, any alternative compliance procedure must develop some way of incorporating any type of rate dependent structure that might be invented in the future.

The third area of concern is path dependency. Unlike linear elastic structures, in nonlinear problems the final result is dependent upon the loading sequence involved. As a simple example, consider a tube loaded both axially and in bending. If the tube is first bent, and then crushed, the final response will be much different than if it is first crushed and then bent. This problem is well understood by practitioners of lumped mass modeling and they are aware that the failure mode in the component test must match the failure mode in

the dynamic test in order to get correct results. This fundamental limitation of lumped mass modeling has essentially precluded its use in full three-dimensional simulations, although mathematically there are no limitations to constructing such a simulation. Similar problems arise in trying to develop a complex multiple load path simulation model, and therefore it is difficult to conceive of an effective compliance procedure built around a multiple load path model. For this reason, a lumped mass alternative compliance procedure will probably be not much more complex than the first model (figure 1a) proposed by Volkswagen. The second model (figure 1b) in fact introduces a multiple load path by using two springs to represent the interactions between the occupant and the interior.

As a result of our discussion of inherent limitations with the lumped mass modeling approach, the following tentative conclusions can be drawn. Although more data needs to be generated, the variability probably will not be a major factor. On the other hand, some method must be developed to handle the rate dependency problem. The material factor approach, although simple, requires that these factors be developed for all materials that might be used in future vehicles, or that some standard test procedure be developed to ascertain these factors. A second alternative that has been proposed is to use a dynamic test on the interior portion of the component test protocol. Finally, because of the fundamental path dependency problems the complexity of the model should not be significantly extended beyond that already proposed.

## Results From Evaluation of the Composite Test Procedures

Volkswagen has presented the results from two series of tests. The first of these was the Volkswagen Golf (1) and used the model shown in figure 1a. The test procedure used the CCMC barrier, crabbed to the vehicle, and the SID dummy. The second series of tests was conducted on the Ford LTD (4) according to the NHTSA test protocol and used the SID dummy. The simulation model shown in figure 1b was applied in this case. GM has just completed an additional series of tests. Three vehicles were tested. A full size 4-door vehicle (identified in the figures as F4), an intermediate 4-door vehicle (I4), and an intermediate 2-door vehicle of the same body style (I2). Two dynamic tests were performed for each vehicle style using the NHTSA barrier protocol, but one using the SID dummy and the other the EUROSID dummy. These dynamic tests were performed at the GM Proving Ground. The static tests were performed by MGA Corporation, Buffalo, New York, and were tested according to the Volkswagen double ram protocol for the model in figure 1b. This is the same protocol as used on the Ford LTD tests which were also conducted by MGA. The static test results for the three components are shown in figures 4 through 6. One surprising result in the test data needs to be pointed out at this time. The thorax

interior spring force-deflection curve in figure 6 for the intermediate 4-door vehicle never shows an increasing force level of the magnitude exhibited by the other vehicles. This is clearly unrealistic because at some point all of the door inner material must be crushed and the stiffness of the barrier should dictate the stiffness of the interior spring.

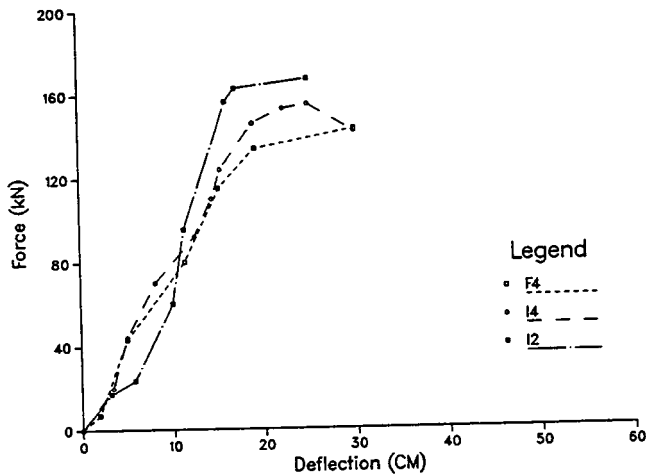


Figure 4. Force-deflection curves for F(1).

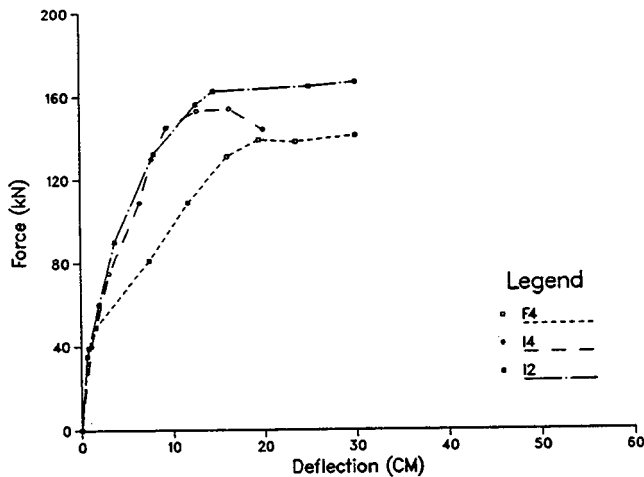


Figure 5. Force-deflection curves for F(2).

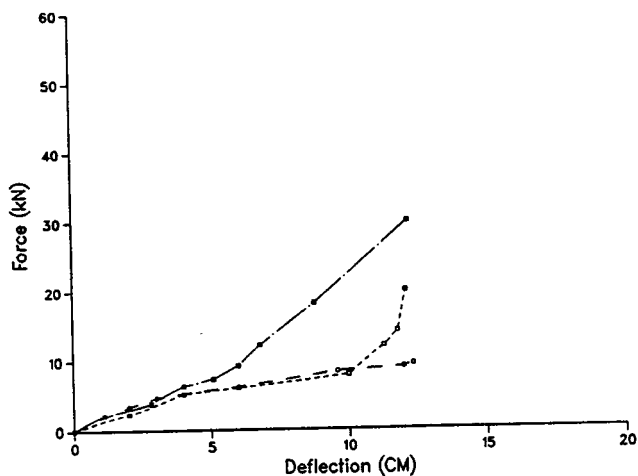


Figure 6a. Force-deflection curves for F(3) thorax.

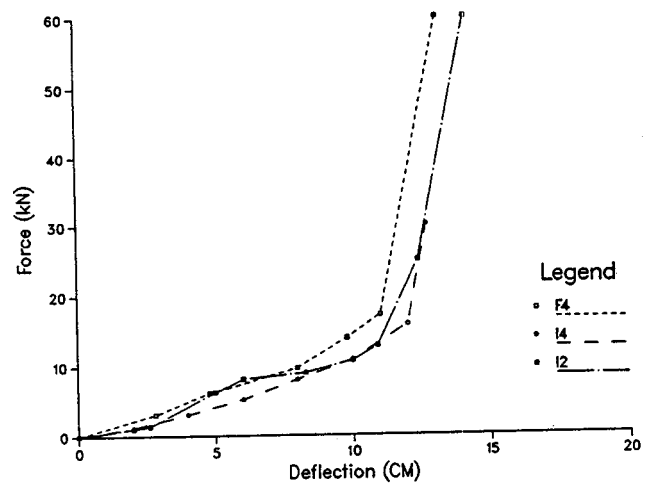


Figure 6b. Force-deflection curves for F(3) pelvis.

Since the dynamic tests were run at an angle of 27 degrees at a speed of approximately 54 km/hr and the simulation does not directly comprehend the angled impacts, the normal velocity was used in the simulations. A summary of accelerations and displacements of the dummy responses in the composite test procedure as compared to similar responses in the dynamic full scale test is shown in figure 7. The Model 1 results are calculated assuming that F(3) is composed of the thorax force only. For comparison, results from the Volkswagen Golf and the Ford LTD are also shown in this figure as obtained from (1, 4). Differences for the GM vehicles range from +3% to -72% for model 2. If we neglect the results from the intermediate 4-door for which the interior static test is somewhat suspect, the differences range from +3% to -52%. A full set of results for all three vehicles for the model 2 dummy are shown in figures 8 through 12. In general, the responses for the structural behavior are fairly good, whereas the responses for the occupant model are somewhat erratic with the responses for the intermediate 4-door vehicle extremely low. In particular the responses for both the peak door velocity and the time of peak door velocity are quite good and are within 20% and 10% respectively. These results are generally consistent with the expectations from lumped mass models in that the responses of the major masses are usually more accurate and displacements and velocities tend to be more accurate than do accelerations.

Another interesting summary of the results is shown in figure 13, in which for each of the dummy measures, spine acceleration, rib acceleration, and rib deflection, each series is ranked as best, middle, and worst for both the tests and the model. On looking at the model results, in none of the three cases does the model predict the same ranking as does the test. However, if the suspect 4-door intermediate data is removed, the model gives the same ranking in one of the three cases.

## Discussion of Results

There are several things that might contribute to the differences between the composite test procedure results

Spine A Rib A Rib D

F4	Test	66	66	26
	Model 1	83(+26%)	140(+112%)	32(+23%)
	Model 2	68(+ 3%)	65(- 2%)	13(-50%)
I4	Test	76	70	29
	Model 1	18(-76%)	22(-69%)	13(-55%)
	Model 2	25(-67%)	22(-69%)	8(-72%)
I2	Test	124	108	30
	Model 1	54(-56%)	56(-48%)	25(-17%)
	Model 2	60(-52%)	63(-42%)	20(-33%)
Golf	Test	72	70	27
	Model 1	67(- 7%)	90(+29%)	34(+26%)
	Model 2			
LTD(HN)	Test	104	102	
	Model 2	95(- 9%)	113(+11%)	
LTD(HF)	Test	96	68	
	Model 2	56(-42%)	75(+10%)	
LTD(PN)	Test	63	47	
	Model 2	38(-40%)	40(-15%)	
LTD(PF)	Test	59	54	
	Model 2	38(-36%)	40(-26%)	

Figure 7. Summary of SID test and simulation results.

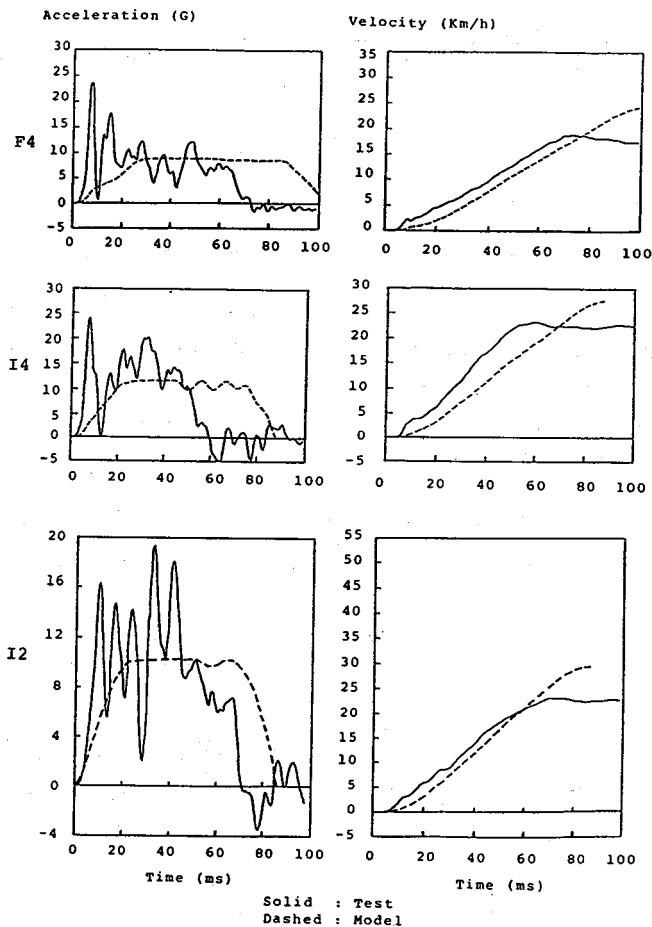


Figure 8. Struck car acceleration and velocity.

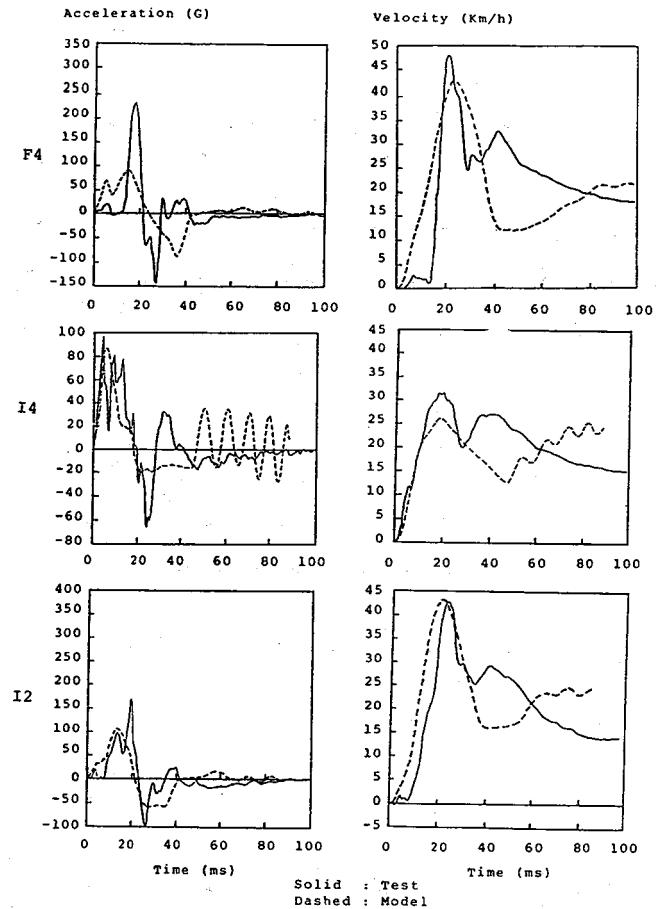


Figure 9. Door acceleration and velocity.

and the full scale dynamic test procedure results. For example, one of the causes of the discrepancy could be the simulation itself. Although Volkswagen communicated to us a copy of the computer program that they used to run their simulations, an implementation of the same technology that is available within GM was used. This was convenient because of the postprocessing capabilities that were in place within GM for this code. In order to establish that the GM implementation produced the same results as the Volkswagen, the available parameters for the Golf and LTD simulations were input into our code. Simulations were run and virtually identical results were produced. One such example is shown in figure 14. A second possible cause of discrepancy is in the full scale test procedure used. These tests were run with the NHTSA test protocol at the GM Proving Ground. Since two identical tests were run on each vehicle with different dummies in the vehicle, a comparison of the door velocities from each of these tests will indicate at least the variability inherent in the tests. Figure 15 indicates that there was no significant variability in the door velocity for identical vehicles. The tangential effect was clearly not addressed in the simulation, however since no consistent differences were observed, this effect is difficult to assess. A third possibility is with the static tests that were run. As stated previously, these tests were conducted by MGA who had previously conducted the Ford LTD test for Volkswagen, and therefore, the protocol is at least consistent

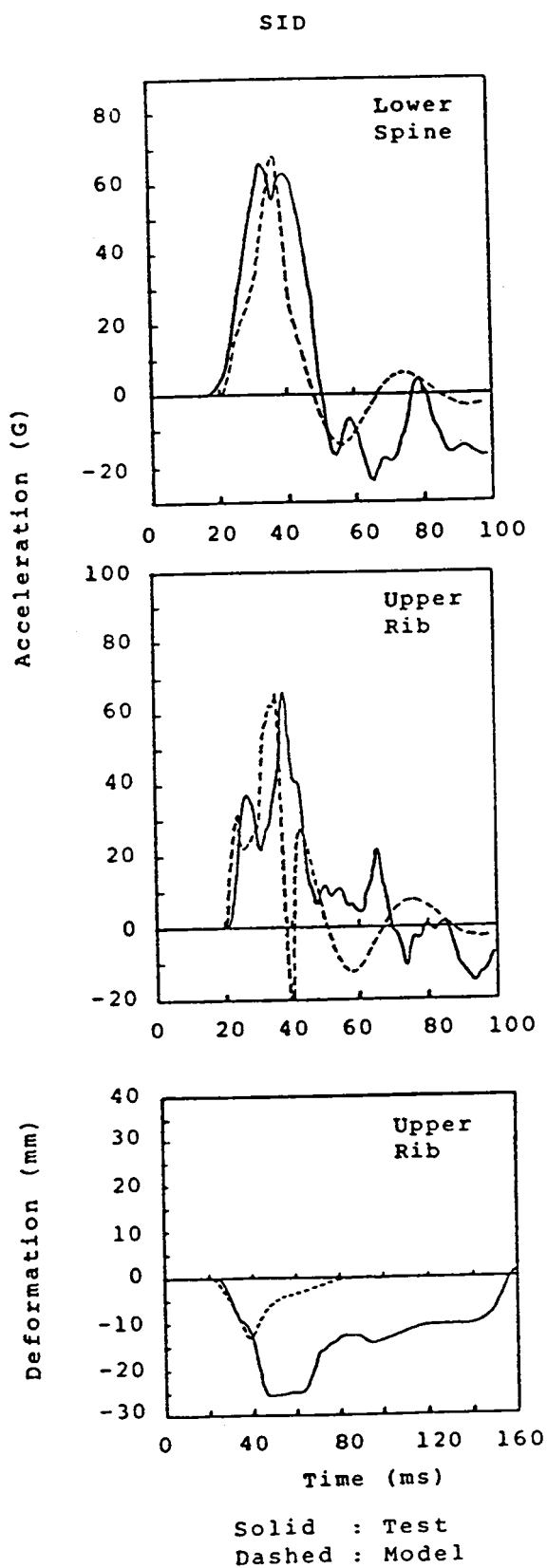


Figure 10. Dummy response for vehicle F4.

among the various tests that have been run. The force-deflection curves for spring F(1) which represents the barrier and some portion of the door response are shown in figure 4. These curves show an initial consistency of slope

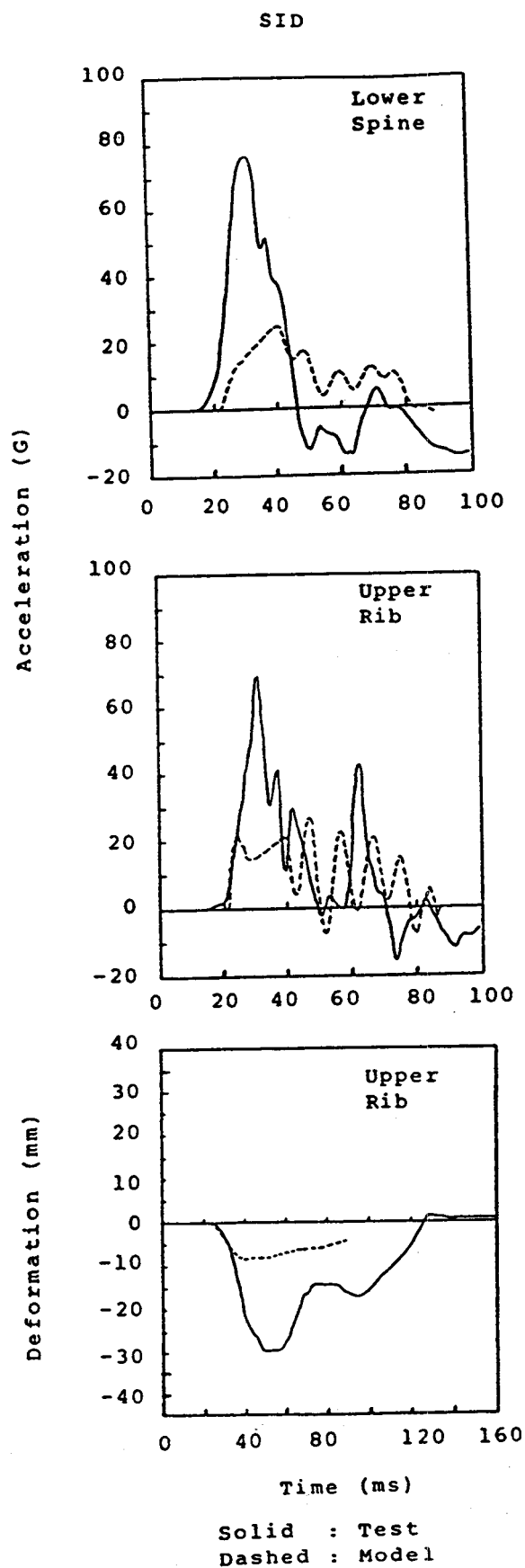


Figure 11. Dummy response for vehicle I4.

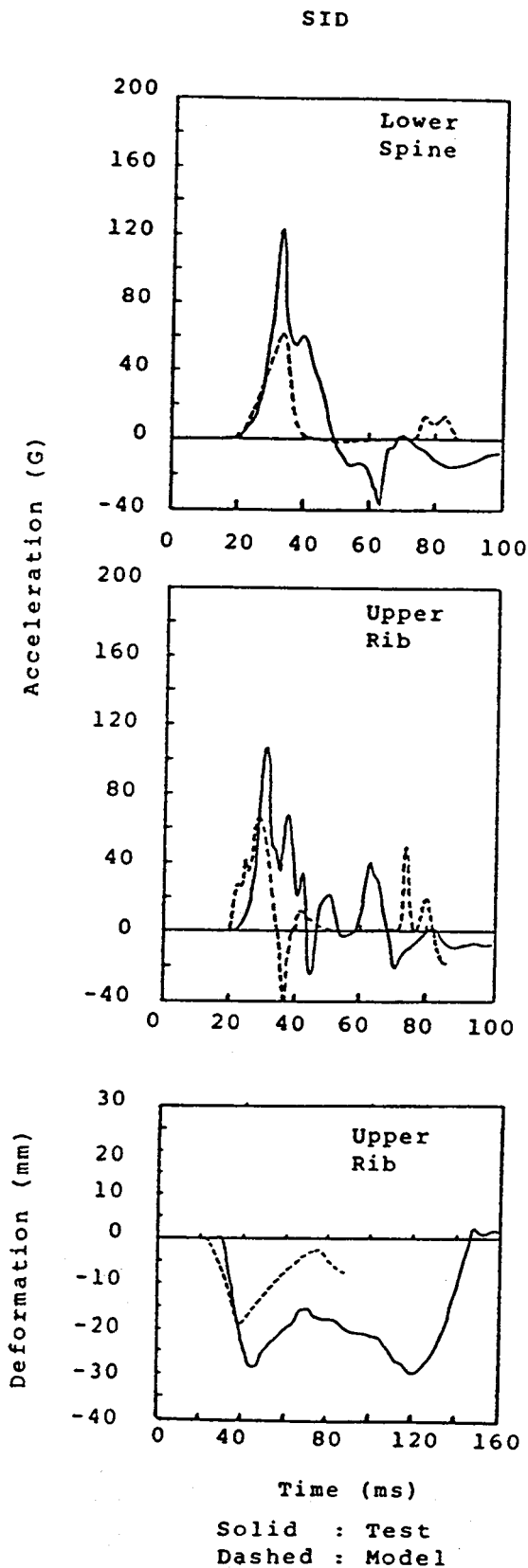


Figure 12. Dummy response for vehicle I2.

followed by differing points at which the curve becomes extremely soft which probably represents the different deformation levels of some part of the side structure. The

Criterion	Method	Best	Middle	Worst
Spine A	Test	F4	I4	I2
	Model	I4	I2	F4
Rib A	Test	F4	I4	I2
	Model	I4	I2	F4
Rib D	Test	F4	I4	I2
	Model	I4	F4	I2

Figure 13. Ranking of the test vehicles.

force-deflection curves for spring F(2) are shown in figure 5 and represent the deformation of the remaining vehicle structure. This is essentially the deflection of the A- and B-pillars relative to the undeformed part of the vehicle. In this case we see differences in the curves occurring very early in the deformation process. The remaining spring F(3) is shown in figure 6. This spring is intended to represent the interior of the vehicle as seen by the occupant. Under the current protocol, the ram pushing the exterior of the vehicle is stopped when the interior touches the seat and the interior is then crushed. As shown in figure 6, there are significant differences among the thorax curves. As pointed out previously, the 4-door intermediate shows no hardening behavior at all, and this clearly must exist at some point in time. This behavior is shown by the 4-door full sized vehicle. It was observed during the test of this vehicle that the exterior ram was allowed to push approximately 5 cm further into the vehicle than was specified by the test protocol. So, although the results generated for this vehicle compare somewhat favorably with the dynamic test results, it was not tested exactly as specified as in the protocol. As discussed previously, the 4-door intermediate vehicle produced occupant measures that were significantly below the dynamic test results. As can be seen, the spring representing the interior of the vehicle essentially acted as an extremely soft interior interface which is consistent with the static force-deflection curve in figure 6. It appears that the most sensitive part of the simulation is the interaction of the occupant with the interior spring, and in order to get comparable results with the dynamic test the occupant must interact with the stiffer portion of the curve. It is our belief that correctly specifying the protocol for spring F(3) is critical in producing results that are similar to the full scale dynamic test.

Finally, we would like to comment on some specific studies of the CTP mathematical model itself. From the structural standpoint, the selection of the equivalent door mass was thought possibly to be a key issue. For the full size vehicle the mass was taken to be 60 kg and for the intermediate vehicles it was taken to be 50 kg. These were chosen to roughly represent the same percentage of vehicle mass as did the Golf and LTD simulations. In order to investigate the effect of reasonable changes in the door mass, the mass in the Volkswagen Golf simulation was changed by  $\pm 7.8\%$  and the simulations were rerun. As shown in figure 16 this resulted in a change of approximately  $\pm 3.5\%$  in the chest

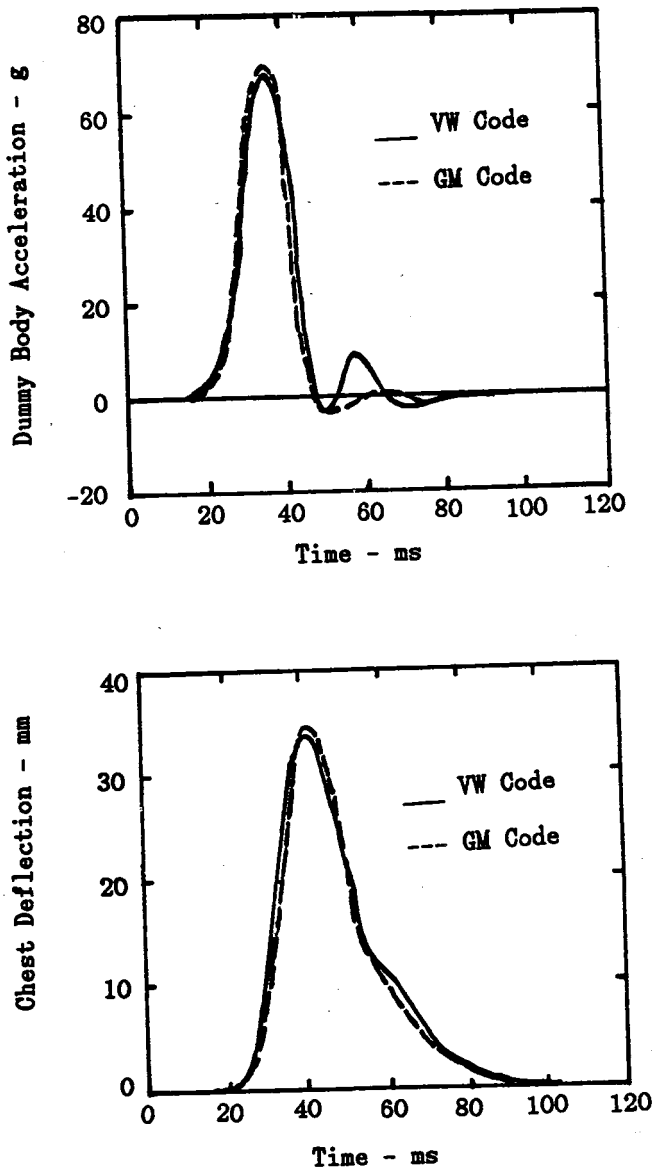


Figure 14. Comparison of simulation results from GM code and VW code based on the VW Golf/Model 1 input data (reference 1).

deflection. Other similarly small changes were also observed. This suggests that precise determination of the door mass is not a critical issue, and that once a reasonable formula for computing an equivalent door mass has been agreed upon, the errors contributed by this approximation are relatively small.

The next area investigated was that of the strain rate effect. Because of the large components in this model it is very difficult to identify a rigorous selection for the strain rate parameter. In both the Volkswagen and the Ford LTD simulations a strain rate parameter of 0 was used. This is also true of the results that are shown in all previous figures, since we were attempting to replicate the CTP protocol. For our experiments, we selected the strain rate parameter of all springs (except in the occupant) to be 1% per mile per hour assuming that this represented mild steel behavior. The entire group of simulations were then rerun using this set of

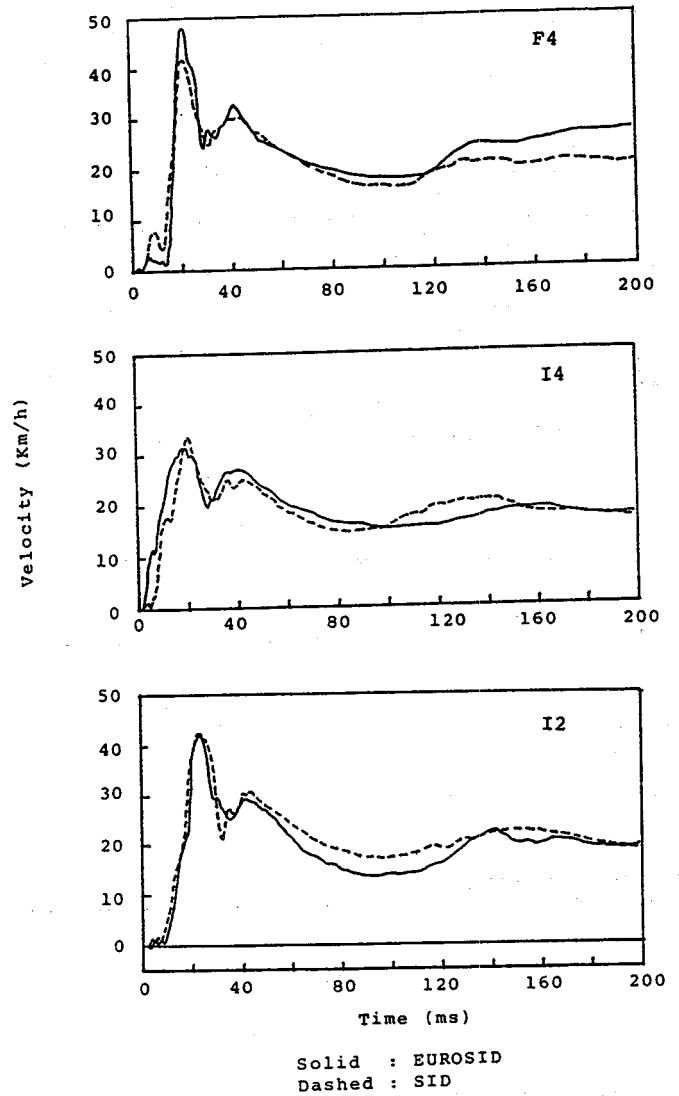


Figure 15. Door velocity in full-scale tests.

DOOR MASS SENSITIVITY

% Vehicle Mass	DOOR MASS		CHEST DEFLECTION	
	Door Mass	% Change	Deflection	% Change
4.15%	43.16kg	+7.8%	36.23mm	+3.34%
3.85%	40.04kg	--	35.06mm	--
3.55%	36.92kg	-7.8%	33.84mm	-3.48%

Figure 16. The effect of door mass variation on chest deflection in simulation based on the Volkswagen Golf/Model 1 data.

parameters. Only selected results will be discussed. Figure 17 shows the response of the velocity of the door mass both with and without strain rate effects for the full sized vehicle. As one might expect, strain rate reduces the peak door velocity. In figure 18 the response for the dummy is shown. Here we see significantly higher levels for the occupant responses. This can be explained by looking at figure 19 which shows the force-deflection curves actually experienced during the simulation for the response with and without strain rate effect. In the case with strain rate effect, sufficient energy was absorbed in other parts of the structure

such that the response never got into the stiffening portion of the curve. However, when the strain rate effect was inactive, the response encountered the stiffening portion of the curve and significantly increased the force levels on the occupant. As a result, no conclusion could be drawn as to the improved quality of results using the strain rate effects and therefore, the results reported in figure 7 do not contain any strain rate effects. It is conceivable that a strain rate effect parameter could be determined for each component for each vehicle which would produce high quality results, but clearly, this is inconsistent with the concept of a compliance procedure.

Finally, let us examine the models of the dummies, Model

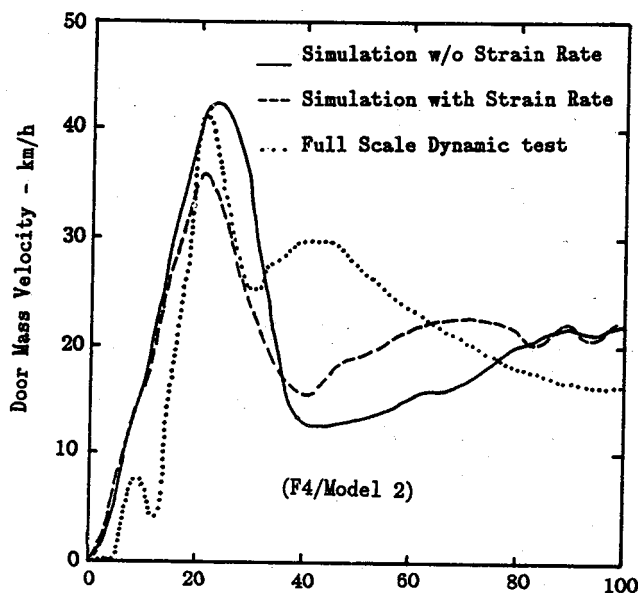


Figure 17. The effect of strain rate on door mass velocity.

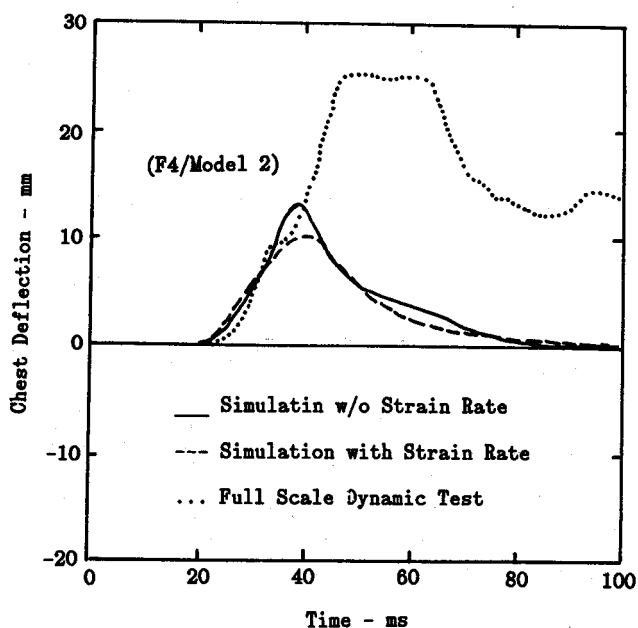


Figure 18. The effect of strain rate on chest deflection.

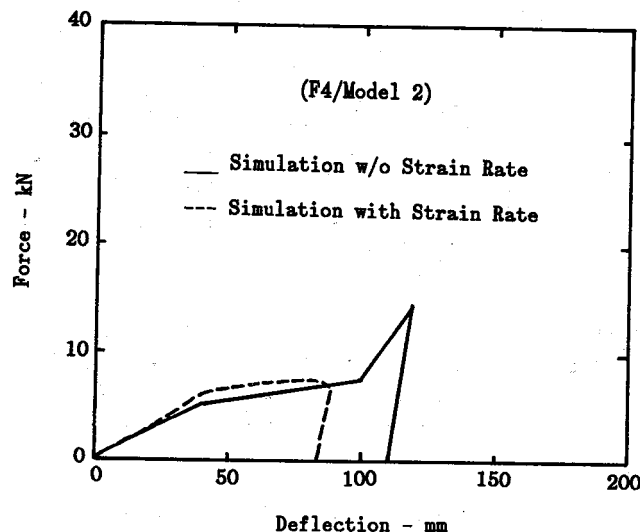


Figure 19. Force-deflection curves of  $F_1(3)$  from simulations reflecting the effect of strain rate.

1 and Model 2, as implied by figures 1a and 1b which are replicated complete with force specifications and mass specifications in figure 20. These are the forces and masses selected by Volkswagen based on their ability to replicate the response of a pendulum test. In general, this selection is not unique and other combinations of springs and masses could produce similar correlations with pendulum tests but perhaps different results in the dynamic simulation. The significant change in rib mass (Model 2 is approximately  $1/3$  of Model 1) is most curious. The results in figure 7 do not seem to clearly favor either of the models. As pointed out earlier, we are reluctant to recommend a more complex model of any part of the CTP because it introduces problems of insuring that the tests constructed to determine the component behavior resolve any anticipated path dependency problems. Perhaps the best approach might be to select some small model such as the Model 1 and then use a regression analysis to obtain the best fit to the dynamic test data of the full vehicle tests.

In conclusion, the specification of the dummy and the interior component test appear to be the major contributors to the differences between the CTP response and the full scale dynamic test response. Although some improvements may be made to these parts of the CTP to reduce these discrepancies, the existing somewhat limited data and the inherent limitations suggest that we will require a margin of difference of the order of 25 to 50% in order to insure conservativeness with respect to the dynamic test environment.

## Other Alternative Procedures

As we indicated previously, the CTP is just one of a number of alternative procedures that might be proposed. One of these proposed by Volkswagen is to modify the CTP to include what they call "computer in the loop" (6). This process would run the dynamic simulation simultaneously with the component tests. In this scenario the simulation

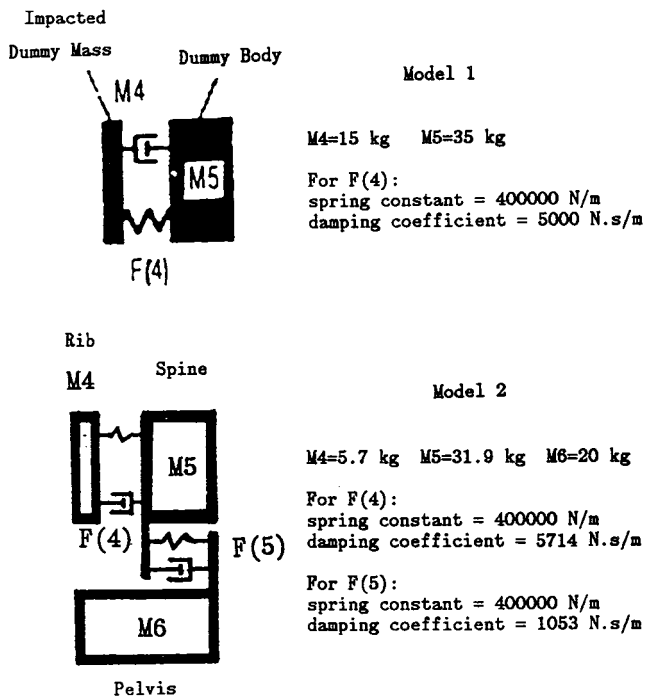


Figure 20. Dummy parameters for Model 1 and Model 2 as proposed by Volkswagen (references 1, 2).

would indicate when the occupant contacted the interior surface. At that point, the exterior ram would be held and the interior ram would start to deform the interior surface. This could resolve many of the difficulties associated with insuring that the simulation is on the correct portion of the interior response curve. Conceivably, this process could be broken down into fine enough steps such that many of the problems associated with path dependency could in fact be resolved. On the other hand, if it were necessary to go to a dynamic impact for the interior component test, the 'computer in the loop' approach could only be used to indicate when the dynamic test should be started.

Another approach would be to investigate more sophisticated simulation techniques. A number of these have been discussed at one time or another in the literature in terms of side impact modeling. The next step in simulation sophistication would essentially involve the CVS/CAL3D, or MADYMO methods of occupant simulation such as described in (7). This approach would allow a better simulation of the occupant's three-dimensional motion within the vehicle. The force interactions however, are predicated on the same assumptions that are included in the lumped mass modeling, and as a result, does not allow for more sophisticated modeling of the structural details. In (7), the structural response was modeled by selecting springs connecting the ellipsoids representing the side structure such that the static and dynamic test behavior of the structure was captured. A more sophisticated level of structural modeling for side impact has been proposed in (8, 9). Although slightly different in details, they are conceptually quite similar. The major structural failure mechanism in side impact is essentially a hinging mechanism,

and these approaches rely on a component test of these key hinging mechanisms. As a result, it may be possible to specify a small number of component hinge tests that need to be conducted such as the B-pillar to rocker, and B-pillar to roof rail, etc., and perhaps components such as door latches. These tests could be conducted in a less costly manner than the full vehicle test as envisioned in the CTP, and could be potentially easier to specify. A third alternative is to use full non-linear finite element modeling. This is a technology that has been emerging during the past three to five years, and has the potential to resolve virtually all the difficulties associated with the lumped mass type of methods. One such example is given in (10). The rate dependency can be handled at the material level, and therefore material tests can be specified. The remaining test information that is required is essentially material properties for which existing test procedures are in place. It is entirely conceivable that a full finite element model of the dummy or occupant could also be constructed using this technology. However, we are some years away from realizing the full potential of this approach. Each of the last three modeling approaches has shown excellent agreement with test data (of 5 to 10%) as indicated by the references. It should be cautioned that these were isolated instances in which careful efforts were made to correlate to one particular test. However, they do indicate the possibilities for resolving the many difficulties associated with the simpler CTP simulation.

## Concluding Remarks

A methodology which involves assessing the inherent limitations as well as comparing results to full scale tests has been proposed for initially investigating alternative procedures to full scale dynamic test for side impact compliance. This approach has been followed in making an initial evaluation of the Volkswagen CTP proposal. Although there is clearly promise in using the CTP as a compliance procedure, work needs to be done to develop protocols that will decrease the confidence factor that will be needed to insure that the results are conservative with respect to the dynamic tests. Several other alternative computer based systems compliance processes were suggested.

## References

- (1) Richter, R., Oehischlaeger H., Sinnhuber, R., and Zobel, R. "Composite Test Procedure for Side Impact Protection," SAE Paper 871117, May 1987.
- (2) Kamal, M. M. "Analysis and Simulation of Vehicle to Barrier Impact," SAE Transactions, Vol. 79, pp. 1498-1503, 1970.
- (3) Kamal, M. M. and Lin, K.-H. "Collision Simulation," in *Modern Automotive Structural Analysis*, M. M. Kamal and J. A. Wolf eds. VanNostrand Reinhold, New York, 1982.
- (4) Volkswagen, personal communication.
- (5) U. S. Motor Vehicle Manufacturers Association,

"MDB to Car Side Impact Tests of a 26 Degree Crabbed Moving Barrier into a 1985 Ford LTD at 33.5 Miles per Hour," NHTSA Docket Number 86-06-N01-32.

(6) CCMC, "Composite Test Procedure for Side Impact Protection," Draft 15, April, 1988.

(7) Deng, Y.-C., "Design Considerations for Occupant Protection in Side Impact—A Modeling Approach," SAE Paper 881713, Proceedings of the 32nd Stapp Crash Conference, Atlanta, 1988.

(8) Ni, C.-M., "Vehicle Side Impact Structural Analysis," Proceedings of the 9th Experimental Safety Vehicle

Conference, Kyoto, Japan, Nov 3, 1982.

(9) Ng, P. and Tidbury, G. H., "The Development of a Vehicle Angled Side Collision Computer Simulation Program," Proceedings of SAE 6th Vehicle Structural Mechanics Conference, Paper 860822, April 22-24, 1986, pp. 199-208.

(10) Vander Lugt, D. A., Chen, R. J., and Deshpande, A. S., "Passenger Car Frontal Barrier Simulation Using Nonlinear Finite Element Methods," Proceedings of SAE 7th Vehicle Structural Mechanics Conference, Paper 871958, April 11-13, 1988, pp 277-281.

## Application of Finite Element Method to the Design of a Light Weight Composite Passenger Car Door

Dr. Mostafa Rashidy, Dr. Majid M. Sadeghi,  
Cranfield Impact Centre Ltd., England

### Abstract

The paper describes the development of a finite element model to predict the deformation values of a passenger car door under lateral loading. This correlated closely to those of the measured deflections from a test on an actual door. The model has proved to be valuable for investigating the behaviour of the door under static loading conditions. The paper then discusses the application of the techniques for designing a light weight composite car door.

One aspect of the research was concerned with occupant safety during side impact. Hence, an anti-intrusion door beam was designed and incorporated into the model to satisfy the Federal Motor Vehicle Safety Standard (FMVSS214) requirement. The initial crush resistance was obtained by using a composite tube. The combined effect of the tube and the reinforcing ribs of the inner panel of the composite door satisfied the intermediate and peak crushing resistance requirements of the FMVSS214.

The material used for the composite door design was a glass mat reinforced thermoplastic. The properties of this material were used in a plastic analysis which predicted the deformation and the failure load with acceptable accuracy. The composite door resulted in a 36.9% reduction in weight and a 33.6% reduction in material cost. The technique provides significant savings in prototype testing and enables efficient use of the material.

### Introduction

Man's search for some form of motive power goes back over 300 years. It was the advent of the bicycle in 1860s which revived touring by road. As the decade wore on, more features were designed to motor car to make motoring more comfortable and safer. The need to save energy has forced the automotive industry to concern itself with factors such as vehicle weight, aerodynamic, transmission design and

friction losses. Weight and aerodynamic shape became the key factors in reducing fuel consumption and it is the area of weight where composites make a decisive contribution.

It is true to say that plastics, as engineering materials, could not compare favourably with the metallic materials. However, the development of first generation thermoplastics based composites has resulted in the introduction of toughened, filled and reinforced grades of polypropylene and polyamide for more critical under-bonnet and exterior body panel application.

The use of reinforced plastic is also far from restricted to the simpler less critically loaded components. The application will extend from body panels to areas such as suspension units, chassis and support framework where high strength and fatigue loading resistance are essential.

The replacement of steel structures by composite materials has been practised for many years. The development of a novel concept requires massive investments in design and prototype manufacturing and testing. In order to select the best concept, the designer must obtain the cost/performance relationship of the new design. Most car components have complicated geometry and design constraints. Therefore, a quick tool is required to evaluate the design parameters. One such tool is the Finite Element Method of structural analysis.

The door is the most complicated component of a car with all kinds of reinforcements to take the forces exerted in the hinges and latch areas plus supporting the window lift mechanism and maintaining a perfect seal between the door and the body shell at high speeds. The door is chosen because it is an independent component and also contributes towards the strength of the side structure especially during side impact.

In view of the fact that the car door is subjected to considerable stresses, comprehensive analysis and testing were carried out on the steel door to establish the design requirements for the concept composite door design. Based on these criteria, various materials and their processing techniques were considered to obtain the optimum design.

The concept composite door design was based on the innovative use of glass mat reinforced polypropylene thermoplastic.

### Development of a finite element model for the steel door

Structural problems encountered in engineering design tend to be complex. Establishing the structural idealization which approximates the true behaviour of the structure is a prime problem. Finite Element Structural Analysis leads to better results than the classical approximating method. To model the steel door the engineering drawings and manufacturing specifications such as tolerances, the relationship of hardware attachment, door assembly and the location of the local reinforcements were studied.

The main factor which influences the generation of an approximate mesh configuration are the displacement interpolation functions used in the formulation of the selected elements, the number of the nodes on the element and the number of the integration points on the element. The idea of predicting the overall behaviour of the structure is essential in order to avoid unnecessary fine mesh generation which increases the cost of analysis.

In the door model the inner panel was approximated to a flat rectangular plate with the access holes included. The outer panel was represented by a curved panel and the front, rear and lower shut faces were modelled as flat panels ignoring the recesses at hinges and latch areas. The window aperture, the window corner panels and the door overlap panels were discarded because they had no great effect on the behaviour of the model. The analysis is limited to the main body of the door. Figure 1 shows a simple representation of the door using eight noded isoparametric shell elements. The model was analysed for various load cases using the ABAQUS finite element code which provided an under-

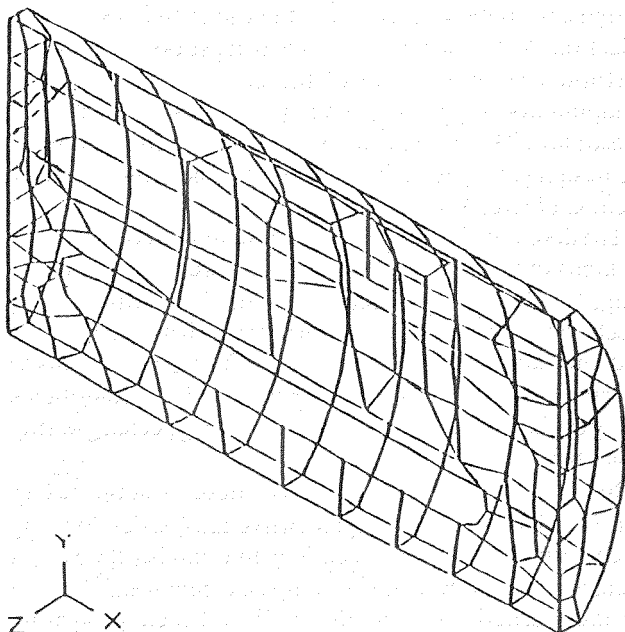


Figure 1. Finite element model of the steel door.

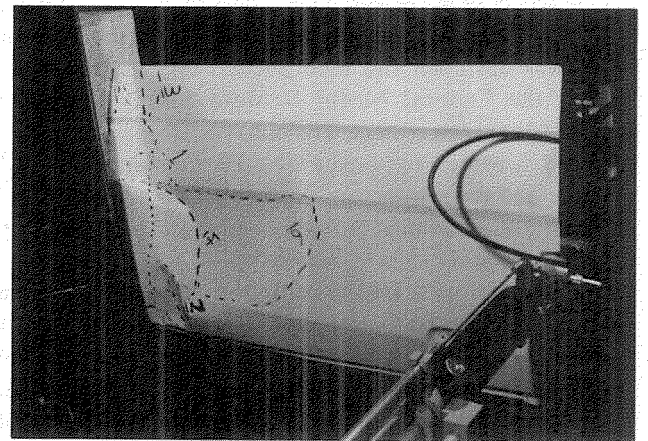
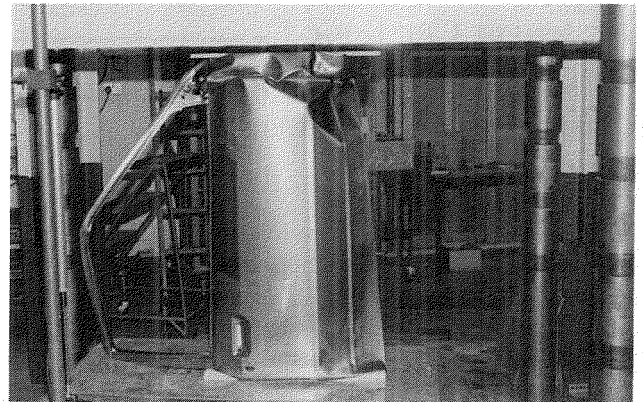
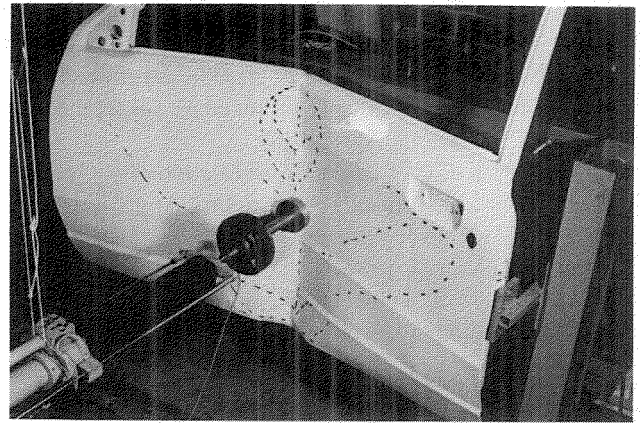


Figure 2. Intrusion, compression and bending tests on the steel door.

standing of the structural behaviour and the load path for the steel door. Laboratory testing of the steel door was carried out to provide data for comparison with the finite element analysis results, figure 2. The coarse mesh model provided an acceptable result with respect to the analysis CPU time and cost.

Study of the steel door behaviour (1)\* indicated that an

\*Numbers in parentheses designate references at end of paper.

optimal composite door would require a mechanism to provide the required torsional and bending stiffnesses. Also a better transition of the load flow from the hinge attachments to the latch area was essential. Based on the results of these analyses many concepts were considered for maximizing the door weight/cost performance tradeoffs. The composite door concept was developed around fixed constraint points such as hinge attachments, latch position, overall dimensions, test and finite element analyses results of the steel door and the properties of the composite material.

### Selection of material

There are a wide range of materials to choose from but it is important to realize that although a material may be chosen mainly because it is able to satisfy a required property, it must always possess in addition certain back-up properties. These may be categorized as mechanical, chemical, physical properties and economic factors. Typical desirable properties for each category are strength, toughness and stiffness for mechanical properties, oxidation and degradation resistance for chemical properties, density for physical property and finally material and manufacturing costs for economic consideration (1).

Composites, however, are difficult to fit into the steel-oriented assembly environment of the motor industry. In contrast, new materials require new processing methods and equipment and also require proper training of the work force. To speed up the transition from steel to composite, the new materials should be designed such that they can be processed using existing tools and manufacturing plant, thereby reducing the capital investment cost.

The most ideal plastic materials are the stampable thermoplastic sheets (2). These materials are commercially available under different names and grades, depending on the type of reinforcement. The well known stampable thermoplastic with polypropylene as the matrix material is glass mat reinforced thermoplastic (GMT), manufactured by Symalit AG. The data sheet supplied by the material manufacturer (3) refers to GMT as an isotropic, tough and light material with good energy absorption characteristics both at high and low temperatures. To verify the properties of 40% glass content grade of GMT, a series of tests were carried out to check the values of the flexural strength, flexural modulus, tensile strength, tensile modulus, compression strength and impact strength. These tests indicated that there exist a slight variation of the properties at various material orientation as shown in table 1. However, it can be assumed that the material is isotropic in the plane of the laminate.

Due to the fact that the material will be exposed to high and subzero temperatures and various impact velocities, a series of impact tests were carried out. The results of these tests are summarized in table 2. The comparison between several candidate materials to replace steel in the automotive industry, table 3, suggests that the glass mat reinforced polypropylene composite is most suitable material for load bearing application.

Table 1. Mechanical properties of the GM40PP composite.

Test No.	Sample Orientation								
	90			0			45		
	1	2	3	4	5	6	7	8	9
Tensile Strength N/mm <sup>2</sup>	51.6	67.7	54.4	63.3	69.6	70.3	72.2	81.0	76.6
Average Value N/mm <sup>2</sup>	57.9			67.7			76.6		
Elastic Modulus N/mm <sup>2</sup>	4559	7598	6784	6332	6332	7306	7149	7915	7915
Average Value N/mm <sup>2</sup>	6314			6656			6759		
Shear Strength N/mm <sup>2</sup>	50.5	53.9	56.6	56.2	56.9	54.3	45.9	44.8	43.6
Average Value N/mm <sup>2</sup>	55.8			53.6			44.8		
Comp. Strength N/mm <sup>2</sup>	64.0	60.5	63.3	68.3	64.0	-	68.3	81.1	76.9
Average Value N/mm <sup>2</sup>	62.6			66.2			75.4		

Table 2. Tabulated results of impact tests on GM40PP composite.

TEST NO.	PRESSURE (PSI)	SPEED M. P. H.	TEMPERATURE (C°)	MAXIMUM STRENGTH (KN)	MAX. DEFL. (MM)	ENERGY ABSORBED (J)	STATUS
1	0	8.53	AMBIENT	14.79	32.3	108.05	*
2	10	11.8	AMBIENT	11.58	40.2	225.96	** , ***
3	15	15.24	AMBIENT	20.02	46.7	380.51	** , ***
4	25	18.91	AMBIENT	14.99	43.5	702.52	****
5	0	8.601	80	14.77	34.5	108.9	*
6	15	14.56	80	22.84	44.7	411.9	****
7	10	11.59	80	19.84	41.6	207.2	** , ***
8	0	8.62	-30	14.92	32.6	111.73	*
9	15	14.97	-30	24.89	43.8	351.3	**
10	25	19.03	-30	29.19	44.7	706	****

\* No visible damage  
 \*\* Surface crack  
 \*\*\* Dent visible  
 \*\*\*\* Fracture  
 \*\*\*\*\* Total separation  
 Maximum deflection is measured at maximum strength.

Table 3. Comparison of several requirements criteria for possible material variants.

Material Variant	Requirement Criteria						
	Mechanical Properties	Impact Strength	Chemical Resistance	Temperature Resistance	Design Freedom	Weight	Cost
Sheet Metal	*****	*****	*	*****	***	*	**
SNC	****	**	*****	****	*****	**	***
Thermo-plastics	**	****	*****	**	*****	*****	**
GMT	****	*****	*****	****	*****	*****	****

\* Very Poor  
 \*\* Poor  
 \*\*\* Moderate  
 \*\*\*\* Good  
 \*\*\*\*\* Very Good

## Composite door design

Based on the tests, analysis and the overall geometry of the steel door, the composite door model was created, figure 3. The two piece composite door concept was designed with the inner panel and its reinforcing ribs, figure 4, as the main load bearing component. The ribs on the inner panel also contributed towards the side intrusion protection behaviour of the door. High stresses around the hinge and latch areas and the cut-outs in the inner panel were reduced with the design of a rib structure. This allowed the inner panel to act as a monocoque structure.

The use of lower bound mechanical properties of the selected composite material in a plastic collapse analysis predicted failure forces and deformation patterns which were in good agreement with the steel door test results, figures 5 to 8, respectively. The weight comparison between the steel door model and the composite door model showed that a weight reduction of 36.9 percent was achieved with a 33.6 percent reduction in material cost.

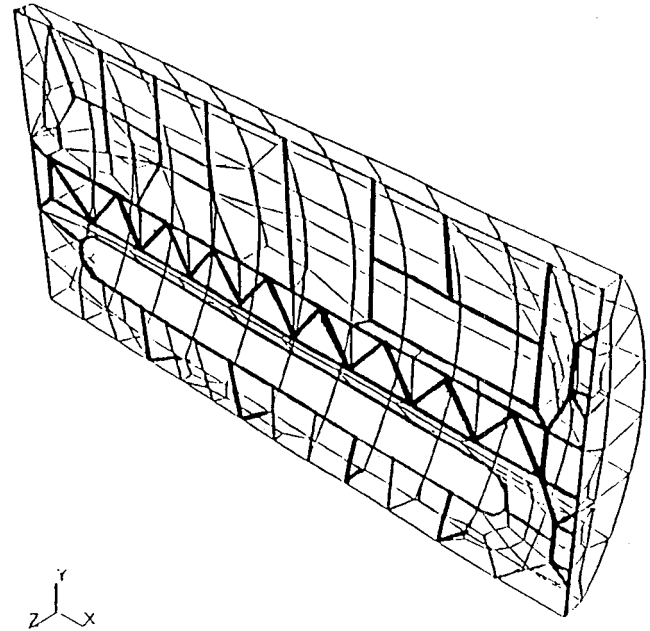


Figure 3. Finite element model of the composite door.

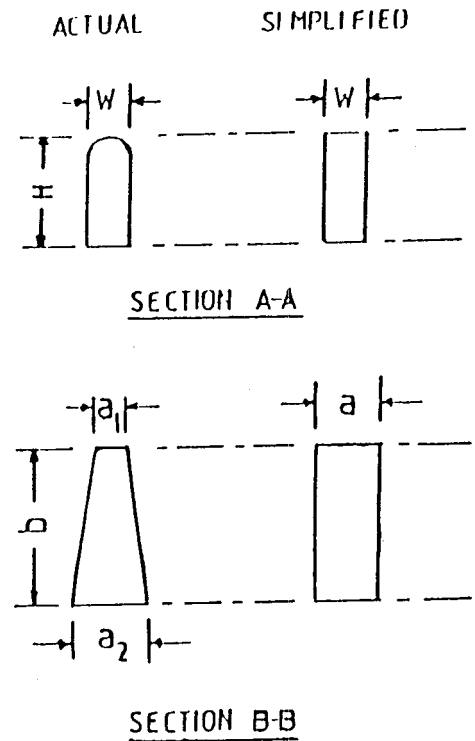
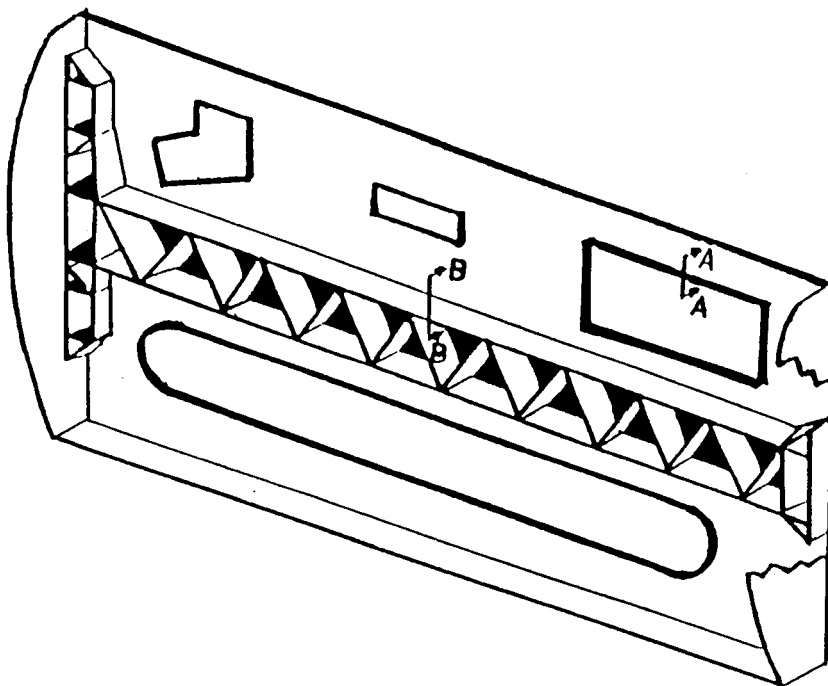


Figure 4. The inner panel of the composite door.

## Door anti-intrusion beam design

The occupant safety in the event of vehicle side impact has caused concern within the motor industry. In order to provide an added occupant protection a composite anti-intrusion beam was included in the concept door design. The FMVSS 214 legislation specifies a strength requirement for motor car door to minimize the injuries caused by

intrusion into the passenger compartment in a side impact.

The design strategy was based on the available space inside the door and accounted for fittings and required clearances for various attachments. In order to establish a suitable finite element idealization, the boundary conditions as well as the general characteristics of the door had to be analysed.

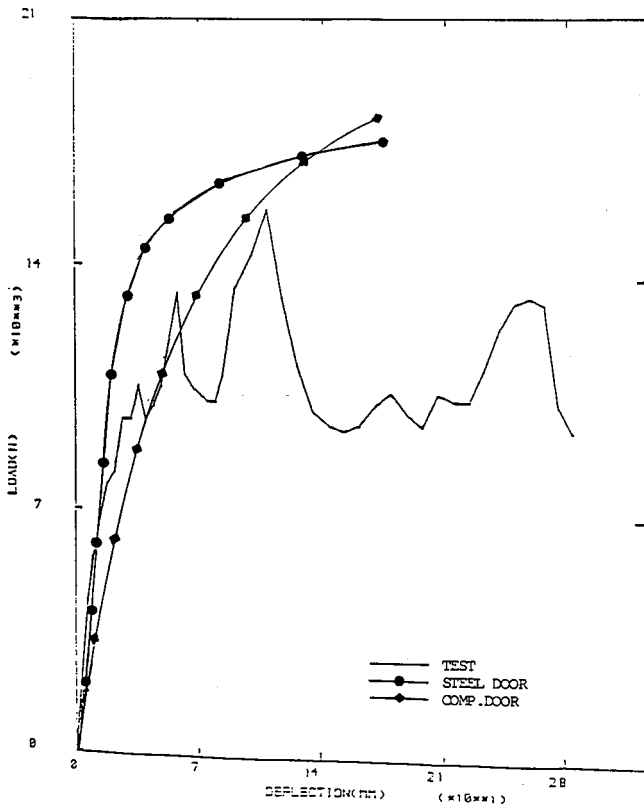


Figure 5. Comparison of load/deflection curves for axial collapse load case.

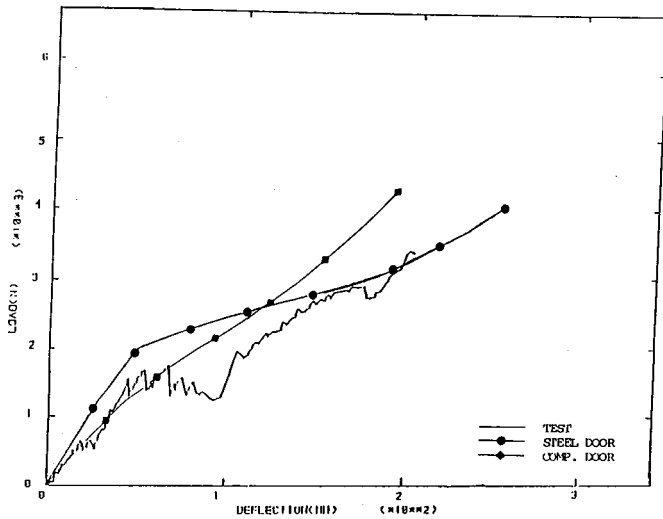


Figure 6. Comparison of load/deflection curves for outer panel deflection load case.

The anti-intrusion beam worked in two stages in order to satisfy the initial, intermediate and peak crush resistance. The initial resistance to the intrusion was achieved by catenary action of the door beam during the first 100 mm intrusion, figure 9. The door beam is a circular tube made of laminated glass reinforced polypropylene. The lamination was designed such that the random strand mat layer provided the rigidity and the unidirectional layer the bending stiffness.

For the remaining intrusion, the outer door beam started to fracture due to large deflection but the ribs on the inner

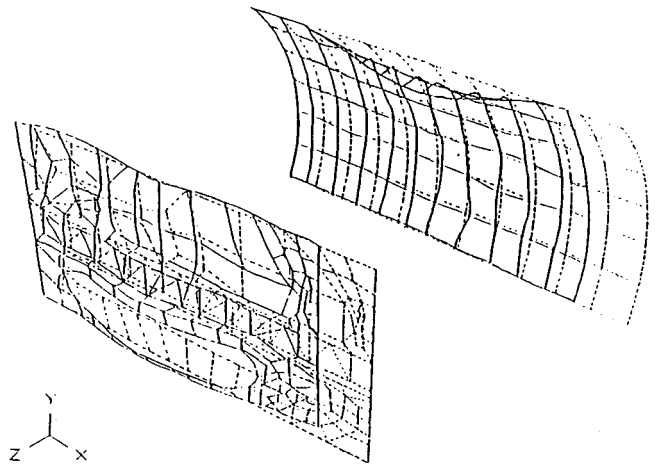


Figure 7. Deformed geometry of composite door, axial collapse load case.

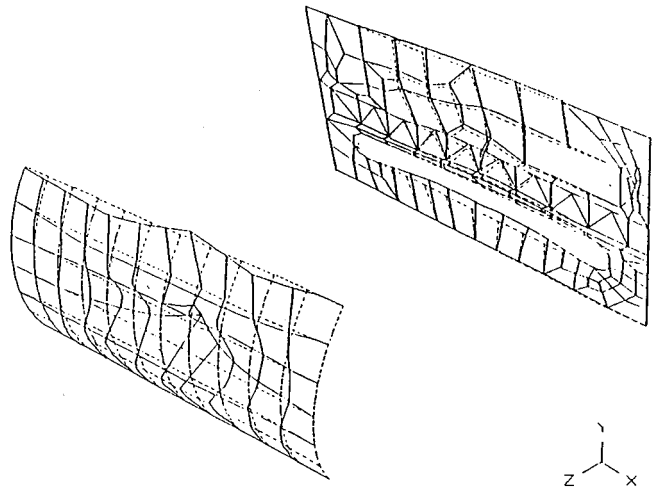


Figure 8. Deformed geometry of composite door, outer panel deflection load case.

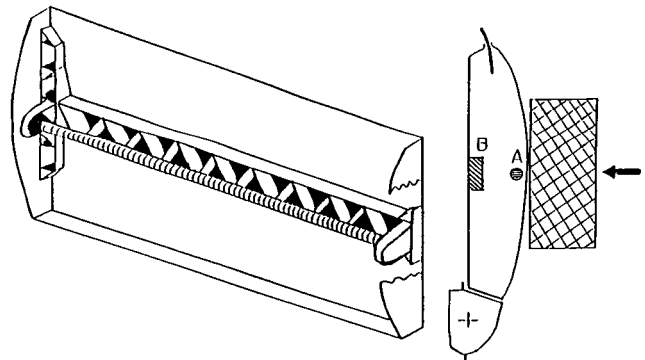


Figure 9. The anti-intrusion door beam.

panel interacted with the door beam, allowing the door to resist the intrusion. At 263 mm intrusion the ribs on the inner panel of the door started to fail sequentially due to their geometry configuration, causing a gradual decrease of the load, figure 10. This analysis was carried out using the Cranfield Structural High Deformation program (CRASH-D) which predicted the collapse modes, figure 11. The achieved initial, intermediate and peak crush resistance of the anti-intrusion device indicated that the level of occupant

protection during side impact can be improved, provided the side structure of the car is sufficiently strong to resist the loads transmitted through the door hinges and the latch. To validate the beam idealization of the door, a finite element beam model was developed which followed the characteristics of the test data of an intruded steel door, figure 12.

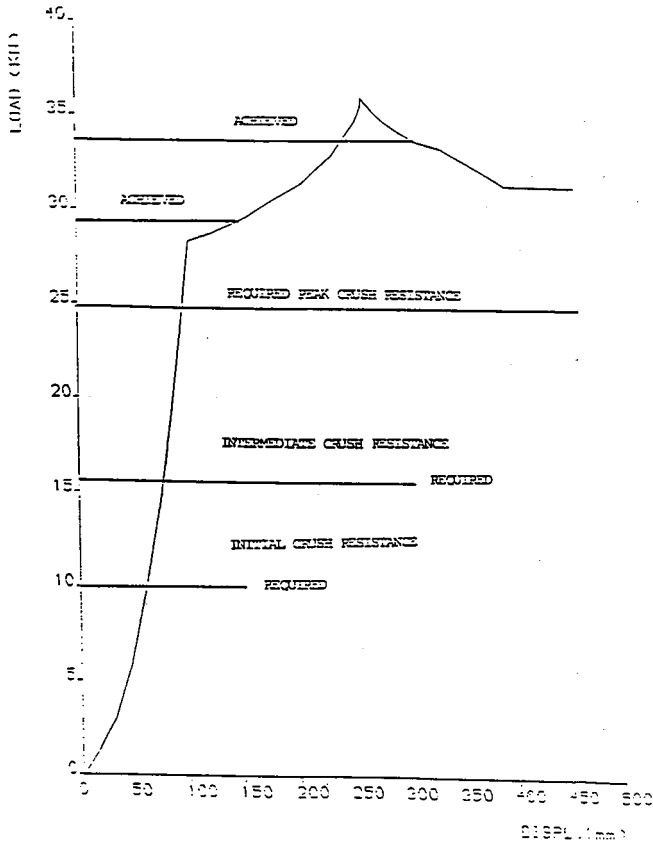


Figure 10. Load/deflection characteristic of the composite door beam.

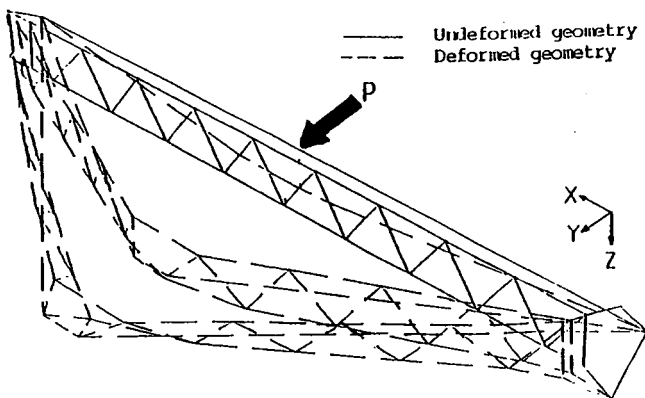


Figure 11. Deformed geometry of the door beam.

Cranfield Impact Centre have developed a beam idealization method (4, 5, 6, 7) using a hybrid approach, combining component testing and analysis, for simulating the behaviour of side structures during side impact, figure 13. This approach quickly and cost effectively predicts the behaviour of the side structure with reasonable accuracy. The dynamic behaviour, (i.e. the velocity and deformation of the

side structure and the kinematics of the occupant subjected to various impact speed), can be evaluated. Figures 14 to 15 represent typical results for a 4-door vehicle using the above approach.

Improving the intrusion resistance of the side structure and designing doors to provide the maximum available compliance will improve both acceleration and deformation response of the occupant. The concept of clean door design, (i.e. no hard objects between the occupant and the outer panel of the door), will generate low acceleration pulses for the occupant. However, the rib deformation criteria will depend on the gap between the occupant shoulder and the inner trim panel of the door, the thickness of the padding and the stiffnesses of the padding and the inner panel of the door. Also, the position of the door beam and interaction between the doors and the side structure, (i.e. the use of inter-lock mechanism between the door and the rocker), can affect both the structure and occupant responses.

## Conclusion

The trend towards lightweight construction in the motor industry will continue through the use of plastics and suitable light alloys. It must still be determined to what extent conventional materials can be superseded by fibre reinforced plastics in load-bearing applications. A suitable design method and composite material can provide a low cost method of reducing component weight. The main conclusions of this research are summarised below:

1. The steel door test and analysis results indicated that a mechanism was required in composite door design to provide sufficient torsional and bending stiffnesses. Also a better transition of load from the hinges to the latch was essential in order to use the whole of side structure effectively. The finite element method proved to be an extremely valuable tool for providing better and quicker design decisions.

2. The selection of a suitable composite material with reasonable mechanical and chemical properties and good fabrication characteristics at low cost was a difficult task. The motor industry has its own requirement which makes this task even harder. To make the new design attractive to the industry, the concept must be economically acceptable. Hence, it should take into account the material cost, capital investment and ease of fabrication. The selected material for the concept door has the above characteristics.

3. The use of data applicable to a random-in-the-plane fibre orientation distribution in isotropic plastic collapse analysis gave acceptable deformation results. However, less favourable fibre orientation could occur during the production process. Therefore, a lower bound mechanical properties data should be used in the analysis using such materials.

4. The composite door analysis predicted failure forces which were in good agreement with the steel door test results. The weight comparison between the steel and composite door models showed that a weight reduction of

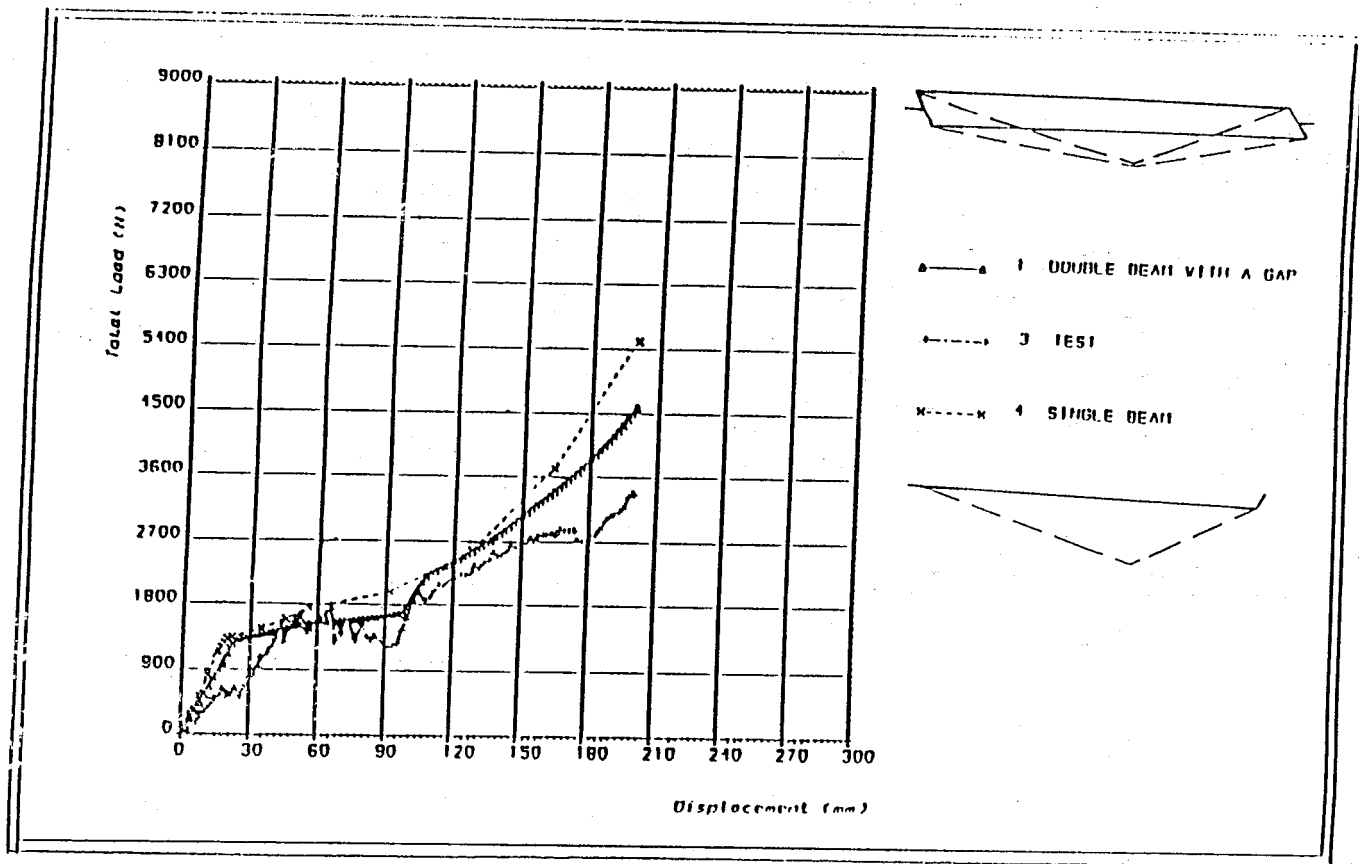


Figure 12. Comparison of load/deflection curves for side intrusion analyses.

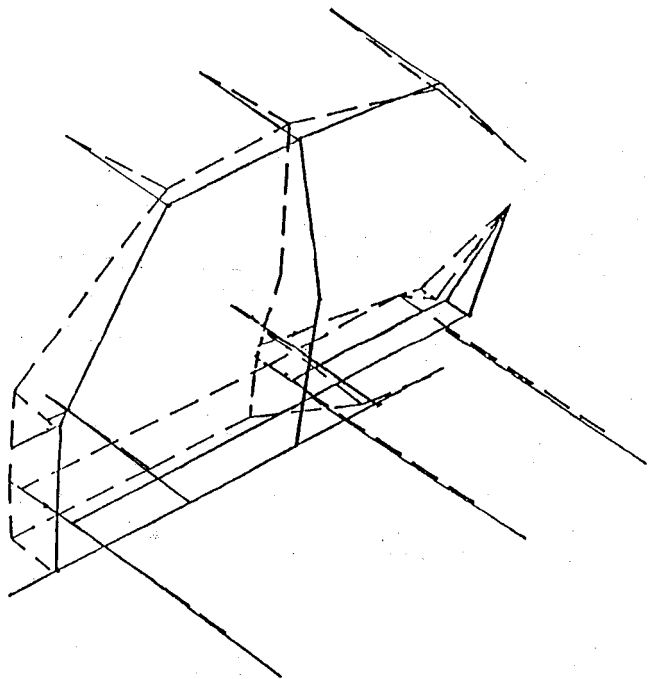


Figure 13. Beam idealization of a 4-door car side structure.

36.9 percent was achieved with a 33.6 percent reduction in material cost. However, different materials require completely different design methods to maximize the weight/cost ratio.

5. The design and analysis of an anti-intrusion door beam

showed that the FMVSS 214 requirement concerning the occupant protection during side impact was achieved.

6. Improving the intrusion resistance of the side structure and maximizing the door compliance and introduction of a clean door concept reduces the occupant injury levels.

Finally it should be noted that the design concept described in this paper is based only on finite element analysis results. Therefore, further prototype manufacturing and testing are needed to enhance the method and applicability of composite material.

## References

- (1) Rashidy, M., "Design and Analysis of a Cost and Weight Efficient Load Bearing Composite Passenger Car Door", Ph.D Thesis, Cranfield Institute of Technology, 1988.
- (2) Six, J.R., "High Performance Safety Parts From Stampable Thermoplastic Sheets", SAE Paper No. 860276.
- (3) Symalit, "Data Sheet Issued by symalit", Symalit AG, Switzerland.
- (4) Miles, J.C., "The Application of Finite Element Method to Vehicle Collapse Analysis", Ph.D Thesis, Cranfield Institute of Technology, 1977.
- (5) Kecman, D., Miles, J.C., "Application of Finite Element Method to the Door Intrusion and Roof Crush Analysis of a Passenger Car", III-rd Int. Conf. on Vehicle Structural Mechanics, 1979.
- (6) Sadeghi, M.M., "Test Analysis Interaction in Crash

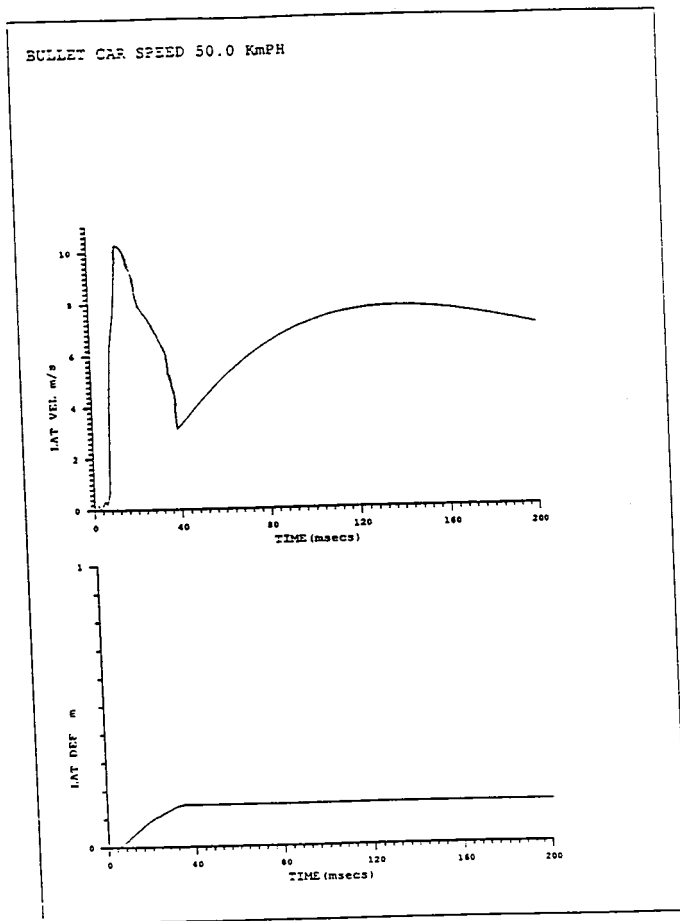


Figure 14. Side frame lateral deflection and velocity.

Simulation of Automobile Structures", Int. Conf. on Modern Vehicle Design Analysis, 1983.

(7) Hardy, R.N., "Towards Optimised Side-Impact Vehicle Structures", 11 Int. Technical Conf. on Experimental Safety Vehicle, 1987.

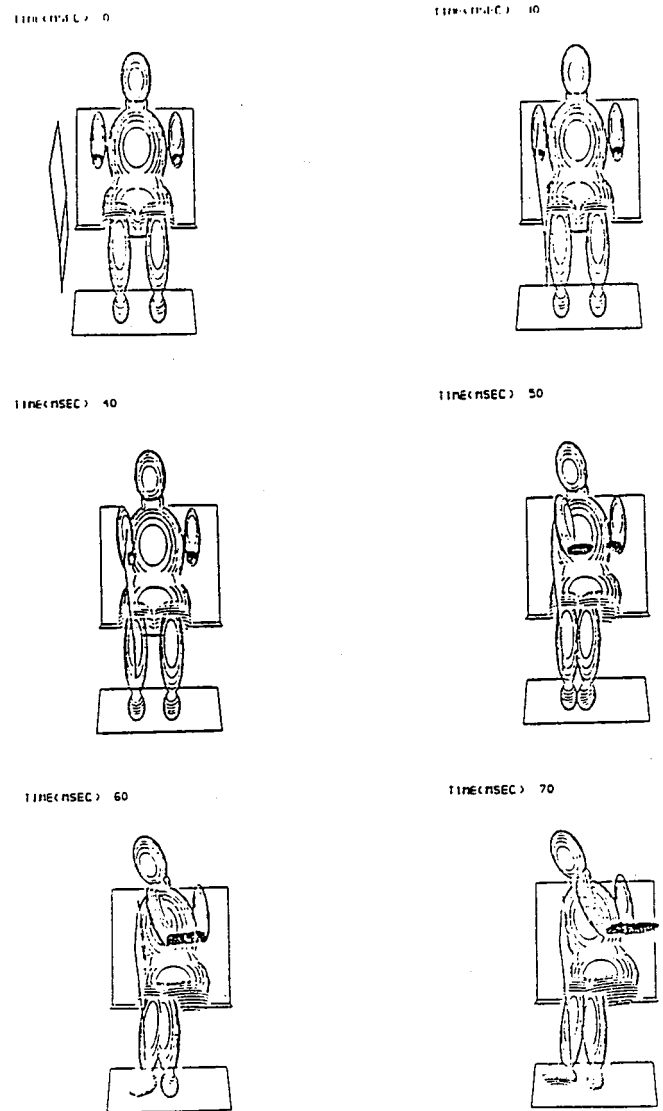


Figure 15. Occupant behaviour during side impact.

## Analysis of Factors Affecting Dummy Readings in Side Impact Tests

K. Watanabe and T. Yamaguchi,  
Nissan Motor Co., Ltd.

### Abstract

The assurance of adequate occupant protection in side impact accidents is an issue of worldwide significance. In January 1988, the National Highway Traffic Safety Administration in the United States issued a Notice of Proposed Rule Making in which a side impact test procedure is proposed. Studies are also under way in Europe concerning other procedures for conducting side impact tests.

In this work, an analysis was made of the effects of various vehicle component parameters on dummy readings obtained in full-scale tests. The component parameters examined included a time history of door velocity into the

passenger compartment, crash force of the vehicle, door padding hardness and thickness and dummy seating position, among others. The analytical results clarified which vehicle factors have a pronounced effect on dummy readings.

An analysis was also made of the effects of the test procedure differences on dummy readings. Experiments were carried out to make clear the influence that the crabbed angle and barrier stiffness exert on dummy readings. Based on the experimental results, a study was made of the necessity of applying a crabbed angle and of the possibility of devising a test procedure using a rigid barrier.

### Introduction

Full-scale test results were analyzed to examine the

effects that various vehicle component parameters have on dummy readings. The full-scale tests were conducted according to the procedure (figure 1) proposed by the National Highway Traffic Safety Administration (NHTSA) in its Notice of Proposed Rule Making issued in January 1988 (1).\* The side impact dummies used in the full-scale tests were SID (2).

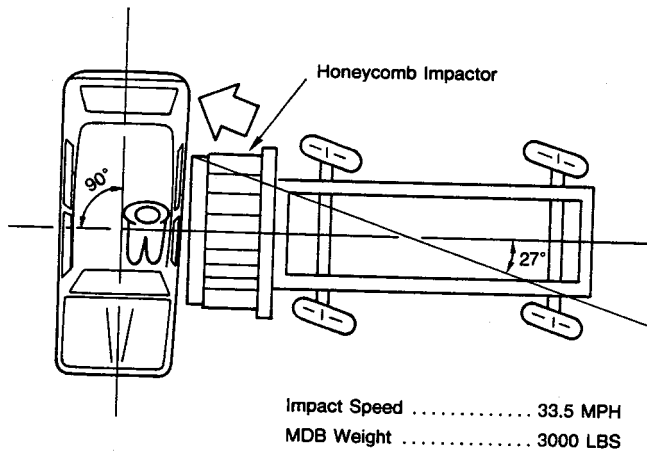


Figure 1. Test configuration.

The test vehicles were partially modified so as to make it easier to identify and analyze the effects of the vehicle component parameters. The pillars, side sills, floor panels and other parts were reinforced and paddings were added to the doors. The following factors were chosen to represent the component parameters and the effect of each factor on the dummy readings was analyzed:

- Impact velocity between door and dummy.
- Reduction in door velocity during impact with dummy.
- Crash force of the vehicle.
- Amount of vehicle deformation.
- Door padding thickness.
- Door padding hardness.
- Vehicle weight.
- Dummy seating position.

The dummy readings selected for analysis included the thoracic trauma index (TTI) (3) and rib deflection for the chest region, the head injury criteria (HIC) for the head, and peak acceleration of the pelvis for the pelvic region (figure 2). The SID was not originally developed for the purpose of measuring rib deflection. Therefore, in this work, rib deflection was examined only for the sake of comparison, since the object of this study was to identify quantitative trends in the effects of the component parameters on dummy readings.

The rib deflection and head acceleration data used in calculating HIC were obtained by filter processing in accordance with the SAE J-211b specification. Rib acceleration and spine acceleration data for calculating TTI and

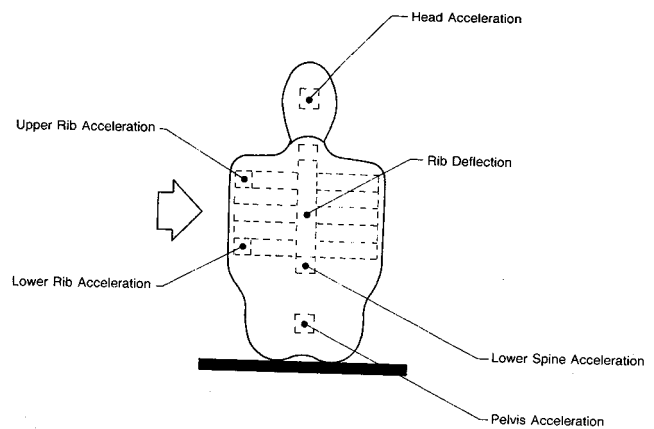


Figure 2. Measurement on the dummy.

pelvis acceleration data were obtained by filter processing according to the following steps (3):

- (1) Filtering with a 300 Hz SAE Class 180 filter.
- (2) Subsampling at a 1600 Hz sampling rate.
- (3) Filtering with a finite impulse response (FIR) filter.

A study was also carried out to examine the effects of test procedure differences on dummy readings. To clarify the influence of the crabbed angle, the following three types of tests were conducted using a test vehicle having the same specifications:

- Side impact test between a moving barrier and a moving test vehicle.
- Side impact test with a stationary vehicle and non-crabbed moving barrier
- Side impact test with a stationary vehicle and a crabbed moving barrier

The effect of the stiffness of the moving deformable barrier (MDB) on dummy readings was also investigated. A rigid barrier having the same dimensions and weight as the MDB (4) proposed by the NHTSA was manufactured and a comparison was made between the test results obtained with it and with the MDB.

## Effects of Vehicle Component Parameters

Velocity-time data for the MDB, struck vehicle, door and dummy obtained in a side impact test with vehicle A are shown in figure 3. The phenomena that occurred in each time step are described below:

- $T_0-T_1$  : Following the impact, the door is accelerated and reaches the same velocity as the MDB.
- $T_2$  : The door impacts the dummy. During the interval of  $T_0-T_1$ , the vehicle has moved in the direction of movement of the MDB, but the dummy remains in a stationary position relative to the ground.
- $T_3$  : The dummy reaches the same velocity as the door and separates from the door.

\*Numbers in parentheses designate references at end of paper.

$T_4$  : The vehicle and the MDB reach the same velocity, and the body deformation stops.

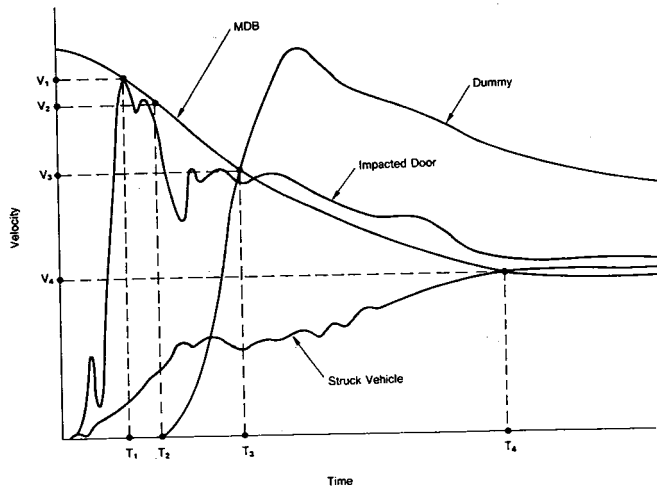


Figure 3. Velocity-time data for the MDB, struck vehicle, impacted door and dummy in side impact test.

It is seen that the dummy is in contact with the door only in the interval between  $T_2$  and  $T_3$ . Therefore, the following two factors can be considered as vehicle parameters having an effect on dummy readings:

- Time history of door velocity between  $T_2$  and  $T_3$
- Energy absorption properties of the door

Here, the energy absorption properties of the door refers to the capacity of the door to absorb impact energy at the moment of impact between the dummy and the door.

### Effects of Time History of Door Velocity

In considering the correlation between the time history of the door velocity in the interval of  $T_2$ - $T_3$  and dummy readings, the time history can be divided into two stages:

- $V_2$  : Door velocity at the moment of impact between the door and the dummy ( $T_2$ )
- $\Delta V$  : Reduction in door velocity ( $V_2$ - $V_3$ ) during the impact ( $T_2$ - $T_3$ )

The results obtained in an analysis of the effects of these two factors are as follows. The correlation found in full-scale tests between TTI and  $V_2$  is shown in figure 4 and that between TTI and  $\Delta V$  is given in figure 5. An attempt was made in the tests to measure the velocity history of the door using an accelerometer. However, deformation of the door panel where the accelerometer was attached caused the axis of the accelerometer to shift, making it impossible to obtain accurate values. Therefore, in the subsequent analysis the values used for  $V_2$  and  $\Delta V$  were calculated from MDB velocity histories.

It was seen in figure 3 that at time  $T_1$ , prior to impact between the door and the MDB, the door reached the velocity of the MDB. Subsequent to that point, the door penetrated the passenger compartment while still in contact with the MDB. Consequently, it can be assumed that the velocity

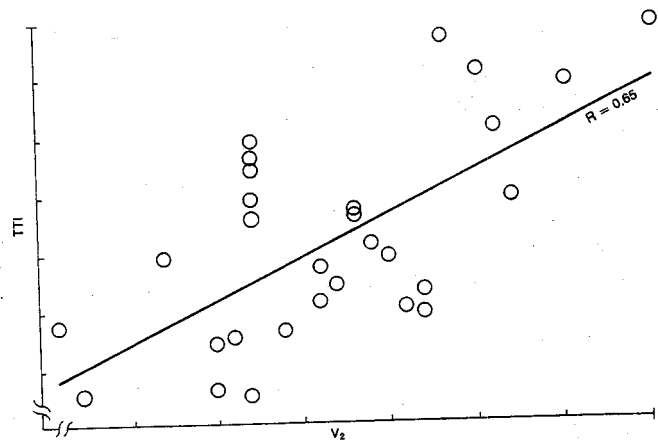


Figure 4. Relationship between  $V_2$  and TTI.

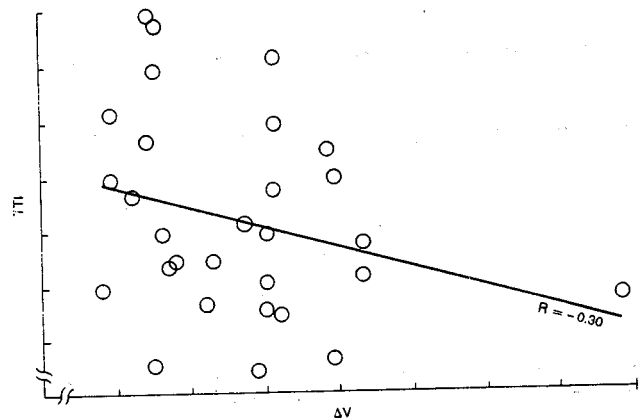


Figure 5. Relationship between  $\Delta V$  and TTI.

time history of the MDB after  $T_1$  is virtually the same as that of the door.

It is seen in figure 4 that TTI becomes smaller as the impact velocity of the door and dummy,  $V_2$ , decreases. Considering that other factors, such as the door padding thickness and dummy seating position, were not the same, because these full-scale tests were carried out using various vehicles, it can be concluded that the correlation coefficient noted in the figure of 0.65 shows a high degree of correlation.

Figure 5 indicates that TTI tends to become smaller with a larger reduction in the door velocity,  $\Delta V$ , during its impact with the dummy. However, the correlation coefficient is smaller than that calculated for  $V_2$ .

From these results it can be seen that TTI is affected more by the velocity of the impact between the door and the dummy than by the reduction in door velocity during the impact. If we consider this in terms of the crash force of the vehicle, it can be concluded that TTI is greatly affected by the crash force of the vehicle in an extremely early stage of the side impact (i.e., 0 to 20 msec) prior to the contact between the dummy and the door.

The correlation between rib deflection and  $V_2$  is shown in figure 6 and that between rib deflection and  $\Delta V$  is given in figure 7. It is seen that both  $V_2$  and  $\Delta V$  have virtually no correlation with rib deflection, which is completely different from the tendency observed for TTI.

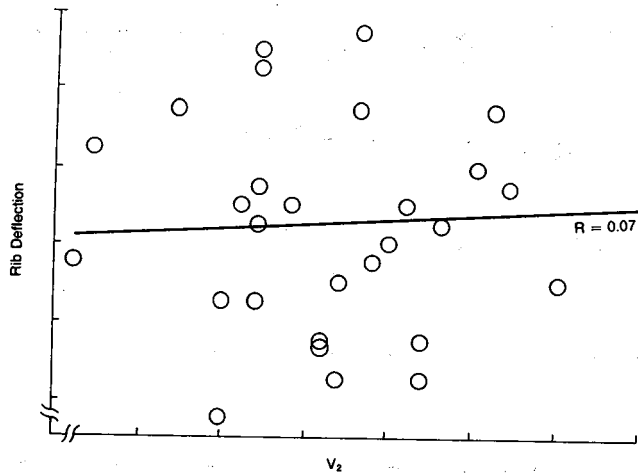


Figure 6. Relationship between  $V_2$  and rib deflection.

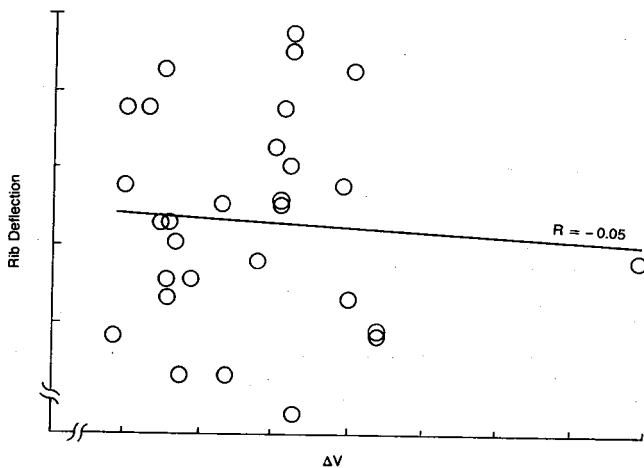


Figure 7. Relationship between  $\Delta V$  and rib deflection.

The correlation between HIC and  $V_2$  is presented in figure 8 while figure 9 shows the correlation with  $\Delta V$ . Also, the correlation between pelvis acceleration and  $V_2$  and  $\Delta V$  is given in figures 10 and 11, respectively. Both HIC and pelvis acceleration tend to decrease as  $V_2$  increases and as  $\Delta V$  becomes smaller. In addition, both of these dummy readings show a higher correlation with  $V_2$  than with  $\Delta V$ .

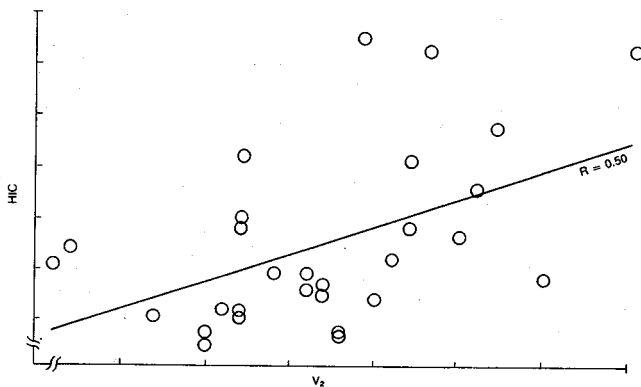


Figure 8. Relationship between  $V_2$  and HIC.

This result seems suitable for pelvis acceleration since it receives a direct impact from the door. However, since head

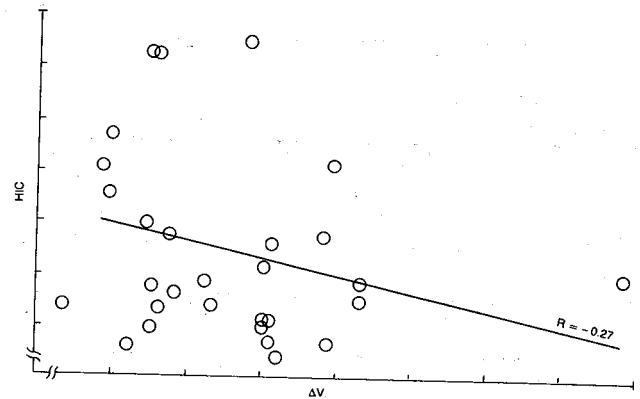


Figure 9. Relationship between  $\Delta V$  and HIC.

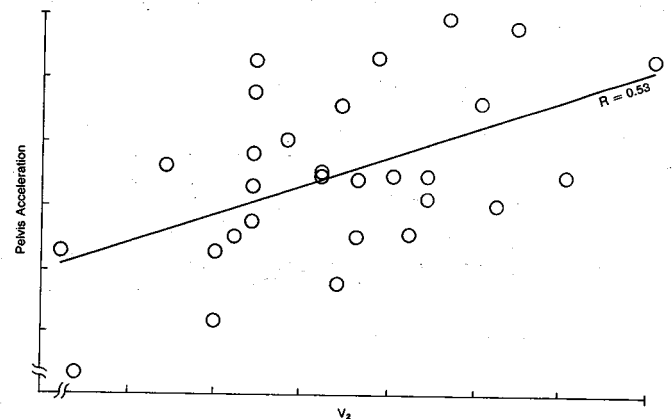


Figure 10. Relationship between  $V_2$  and pelvis acceleration.

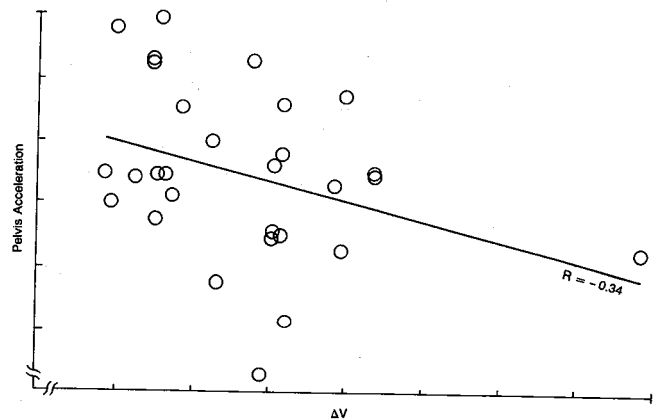


Figure 11. Relationship between  $\Delta V$  and pelvis acceleration.

does not receive such a direct impact from the door, its high correlation with  $V_2$  is thought to be attributable to the following reason. In many cases when side impact tests are carried out according to the NHTSA procedure, the head of the dummy does not strike the vehicle frame and only receives a force input from the chest region. Consequently, as  $V_2$  decreases, the force transmitted from the chest to the head also decreases, resulting in a lower HIC value.

However, an analysis of NHTSA's Preliminary Regulatory Impact Analysis (PRIA) data (5) indicates that the causes of head injuries in real-world accidents are extremely diverse. Comparative data on places of head contact with different parts of the vehicle are given in figure 12. One

set of data was taken from an analysis in PRIA of actual accidents resulting in AIS 3 or greater head injuries. The other set was obtained in side impact tests conducted by the authors.

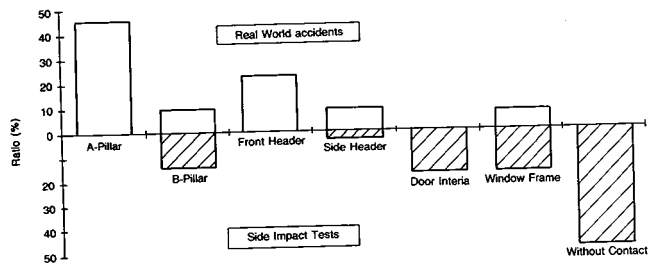


Figure 12. Ratio of head contact area in real world accidents and side impact tests.

The figure shows considerable difference in how the places of contact are distributed. For instance, in the full-scale tests conducted by the authors, there was no instance of contact between the head and the A-pillar, whereas it accounted for as much as 46% of all the places of contact in the real-world accident analysis. It would appear that evaluations of places of head contact in full-scale tests using the NHTSA procedure do not correlate directly with the distribution patterns seen analyses of real-world accidents.

Next, an analysis was made of the correlation between dummy readings and the crash force of the vehicle and degree of body deformation, two factors that are strongly related to the door velocity time history. The crash force of the vehicle,  $F$ , was calculated using Eq. (1), in which the energy absorbed by the vehicle during a side impact test,  $\Delta E$ , is divided by the amount of dynamic body deformation,  $S_D$ . The formulas for calculating  $\Delta E$  and  $S_D$  are shown below. Equation (2) was derived from the law of conservation of momentum before and after an impact, assuming that the velocity of the MDB and that of the vehicle are the same after an impact.

$$F = \Delta E / S_D \quad (1)$$

$$\Delta E = M * m * v^2 / 2 (M + m) * \quad (2)$$

where,  $M$  is the MDB mass,  $m$  the weight of the vehicle,  $v$  the impact velocity of the MDB and  $\alpha$  a coefficient for the energy lost on account of the turning of the vehicle.

$$S_D = S_S * \beta \quad (3)$$

where,  $S_S$  is the amount of static body deformation and  $\beta$  is the ratio of static to dynamic deformation. The correlation between the crash force of the vehicle and TTI is shown in figure 13 while that between the degree of body deformation and TTI is presented in figure 14. It is seen that TTI tends to decrease with higher crash force levels, indicating there is a strong relationship between TTI and the crash force of the vehicle. This is attributed to the fact that the velocity at which the door impacts the dummy,  $V_2$ , is reduced in the case of a vehicle having a higher level of crash force.

Since the degree of body deformation is influenced by the

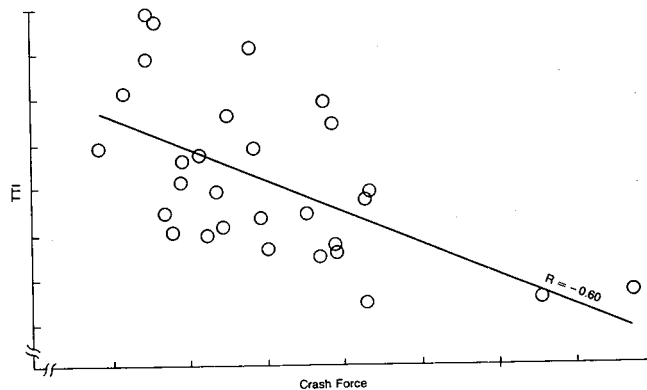


Figure 13. Relationship between crash force of the vehicle and TTI.

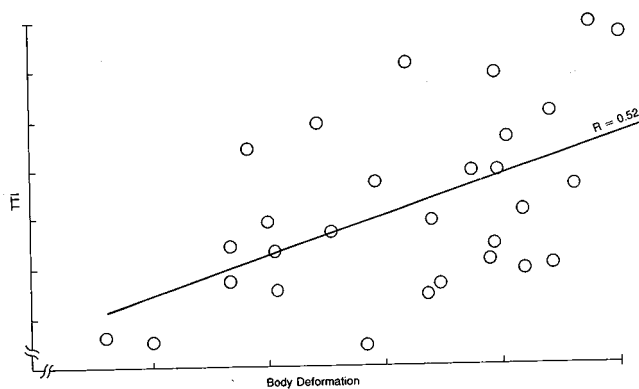


Figure 14. Relationship between degree of body deformation and TTI.

vehicle weight, as was indicated in Equation (2), body deformation does not show as strong a correlation with TTI as the crash force of the vehicle. Nonetheless, TTI still tends to be lower when there is less body deformation.

The results discussed so far in this section can be summarized as follows:

(1) TTI shows a stronger correlation with the impact velocity between the door and the dummy,  $V_2$ , than with the reduction in door velocity,  $\Delta V$ , during the impact between the two, and it tends to become smaller as  $V_2$  decreases. A higher level of crash force of the vehicle reduces TTI, as does a reduction in the degree of body deformation.

(2) However, there is no correlation between rib deflection and  $\Delta V$  or  $V_2$ , and it tends to show a different result relative to the time history of the door velocity than TTI.

(3) Similar to TTI, HIC and pelvis acceleration show a stronger correlation with  $V_2$  than with  $\Delta V$ .

(4) The locations of head contact are clearly different between the distribution seen in real-world accidents and that observed in side impact tests.

### Effects of energy absorption properties of the door

Among the energy absorption properties of the door that can influence dummy readings, one typical factor is the door

padding. The effects of the door padding could not be analyzed accurately in the full-scale tests because there were too few vehicles to which door padding had been added for analytical purposes. Consequently, sled tests were carried out in order to make an accurate assessment of the effects of the padding thickness and hardness. An outline of the test procedure is given in figure 15. In figure 16, TTI, rib deflection and pelvis acceleration are shown as a function of the padding thickness. It is seen that TTI and pelvis acceleration show a marked tendency to decrease with increasing padding thickness, but rib deflection does not show any sensitivity to padding thickness.

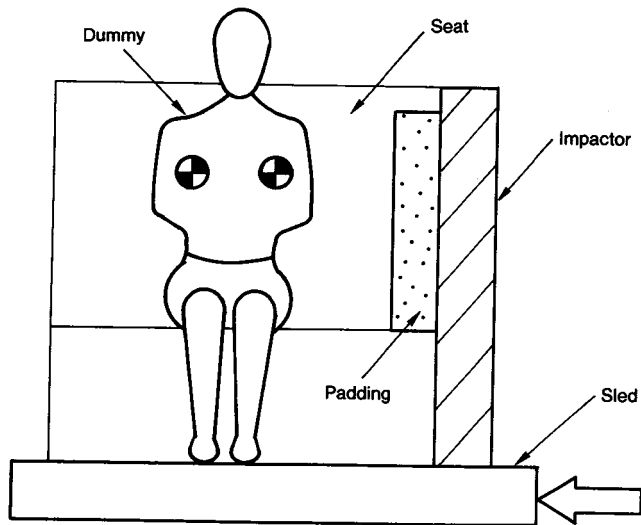


Figure 15. Outline of test equipment.

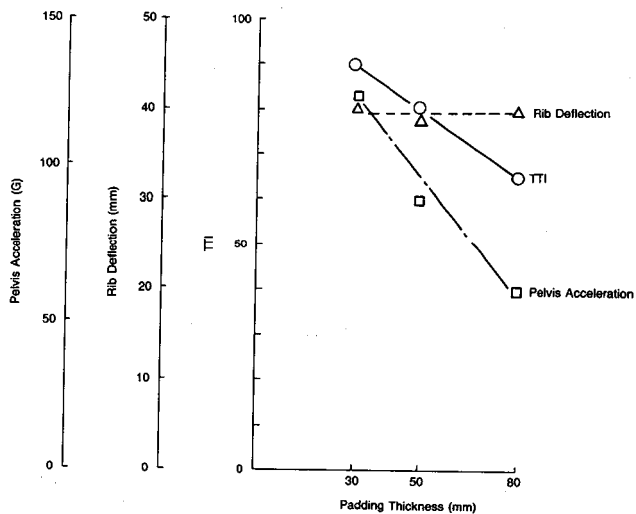


Figure 16. Relationship between padding thickness and dummy readings.

Sled tests were carried out with three types of door paddings (figure 17) in order to examine the relationships between door padding hardness and TTI and rib deflection. Typical test results are shown in figure 18. It is seen that TTI is more markedly affected by door padding hardness than rib deflection. In addition, the door padding hardness that

minimizes TTI differs from the hardness that minimizes rib deflection. Padding B is the best for reducing TTI while padding C is the best for reducing rib deflection. The results indicate that a softer door padding is better for minimizing TTI than for minimizing rib deflection.

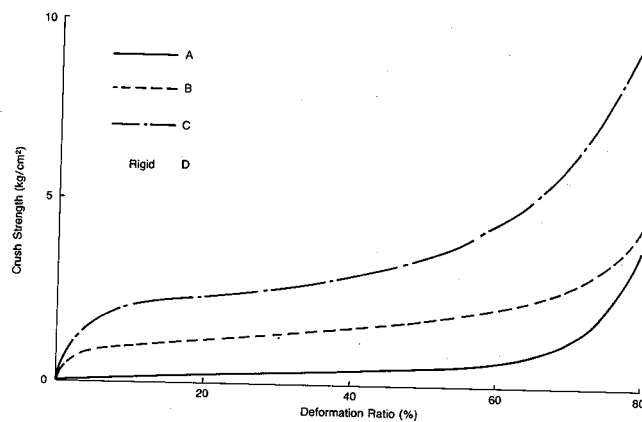


Figure 17. Static crush characteristics of paddings.

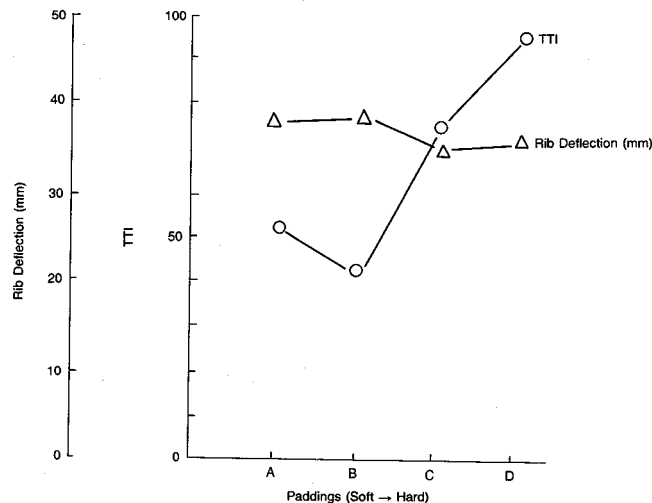


Figure 18. Relationship between padding hardness and dummy readings.

The results presented in this section can be summarized as follows:

- (1) Both TTI and pelvis acceleration show marked sensitivity to the door padding.
- (2) Rib deflection is little affected by the door padding.
- (3) TTI and rib deflection show different tendencies in relation to door padding hardness.

### Effects of other factors

The foregoing sections have described the effects on dummy readings of the time history of the door velocity and the energy absorption properties of the door. Two other factors related to these vehicle parameters are the seating position of the dummy and the vehicle weight. An analysis was also made of the effects that these two factors have on dummy readings.

The correlation between vehicle weight and TTI is shown in figure 19. It is seen that TTI decreases with increasing vehicle weight. This is attributed to the fact that a heavier vehicle has a slower velocity change after an impact, which works to reduce the impact velocity between the door and the dummy,  $V_2$ . However, in comparison with the crash force of the vehicle, the correlation coefficient between the vehicle weight and TTI is smaller and the effect of the vehicle weight is not so large.

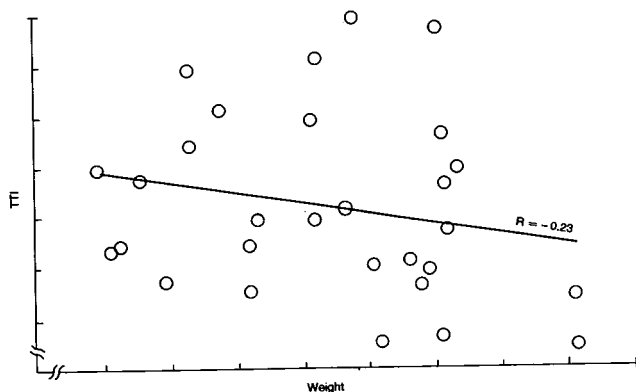


Figure 19. Relationship between vehicle weight and TTI.

Figure 20 outlines the investigation made of the correlation between the seating position of the dummy and dummy readings. As shown in this figure two distances, dimension A and dimension B, were chosen as factors that were thought to influence the impact velocity between the dummy and the door. Dimension A is the distance between the dummy's chest and the door interior trim while dimension B is the distance from the dummy's pelvis and to the same door part. The correlation between dimension A and TTI and rib deflection is shown in figures 21 and 22, and that between dimension B and pelvis acceleration is presented in figure 23. As the distance to the door interior trim increases, TTI and pelvis acceleration tend to decrease. Still, the correlation coefficient is small, which suggests that the distance between the dummy and the door interior trim has little effect on these dummy readings. Rib deflection, on the other hand, shows a higher correlation with this distance than TTI. As the distance to the door interior trim increases, rib deflection tends to decrease.

The results of this section can be summarized as follows:

- (1) As the vehicle weight increases, TTI tends to decrease, but the effect of the vehicle weight is small.
- (2) Rib deflection tends to decrease with increasing distance between the dummy and the door interior trim, but TTI and pelvis acceleration are little affected by this distance factor.

## Effects of Differences in Test Procedures

The test procedure proposed by the NHTSA in the Notice mentioned earlier calls for the use of a deformable and

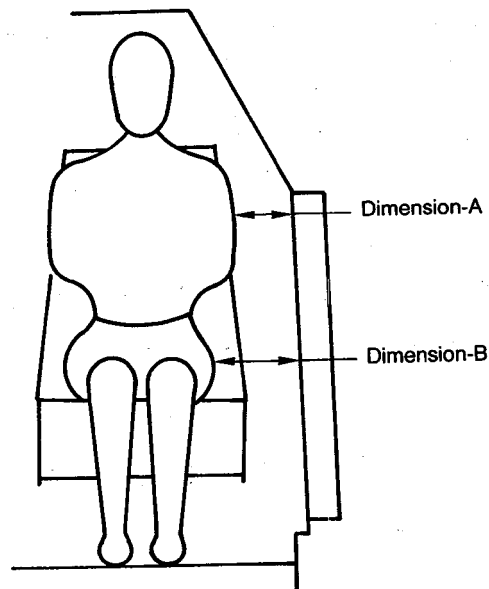


Figure 20. Lateral clearance dimensions.

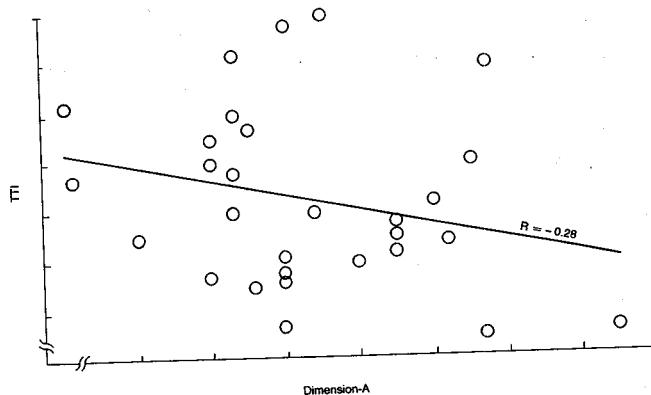


Figure 21. Relationship between dimension-A and TTI.

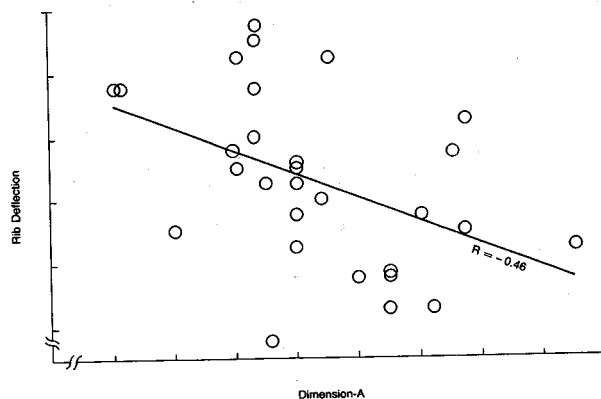


Figure 22. Relationship between dimension-A and rib deflection.

crabbed barrier for the purpose of simulating a car-to-car impact, which results in an extremely complex impact test configuration. Provided that identical results can be obtained, it is felt that a simpler test procedure is preferable. A study was made as to whether identical dummy readings could be obtained with a simpler test procedure using a rigid barrier with and without a crabbed angle. As the first step of

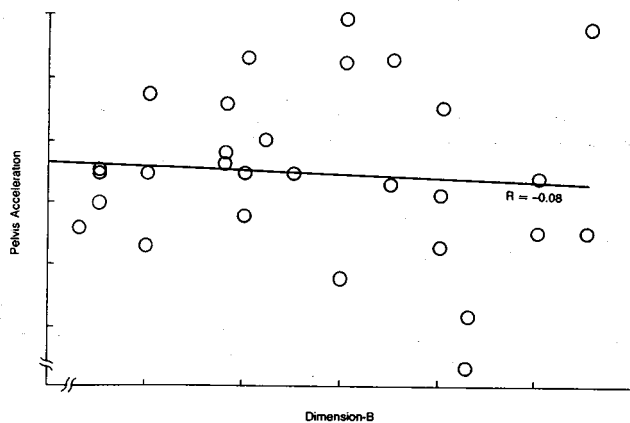


Figure 23. Relationship between dimension-B and pelvis acceleration.

the study, an experiment was carried out to clarify the effects of different crabbed angles and barrier rigidity levels on dummy readings.

### Effects of crabbed angle

In order to examine the effects of the crabbed angle on dummy readings, three types of tests were carried out as shown in figure 24, using three four-door sedan models having the same specifications.

- Test A

The deformable barrier impacted the test vehicle at a right angle at a velocity of 30 mph. The struck vehicle was moving at a velocity of 15 mph at the time of the impact.

- Test B

The deformable barrier traveling at a velocity of 30 mph struck a stationary test vehicle at a right angle. In this test procedure, the velocity component of the struck vehicle in test A was ignored.

- Test C

The deformable barrier traveling at a velocity of 33.5 mph struck a stationary test vehicle at a crabbed angle of 27 degrees. In this procedure, the velocity component of the struck vehicle in test A was expressed by the crabbed angle and impact velocity.

Typical test results are shown in figure 25. The values obtained for TTI and pelvis acceleration are very similar in all three types of tests. It is seen that there is no pronounced difference between the crabbed and non-crabbed test results. These results suggest that the velocity component of the struck vehicle has little effect on dummy readings and can therefore be ignored. Consequently, the non-crabbed test procedure would be a more desirable method to use from the standpoint of its simplicity.

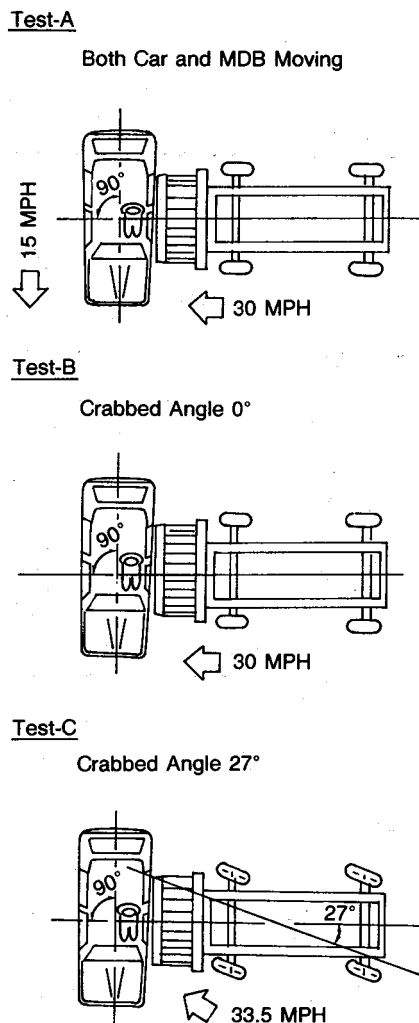


Figure 24. Test configuration.

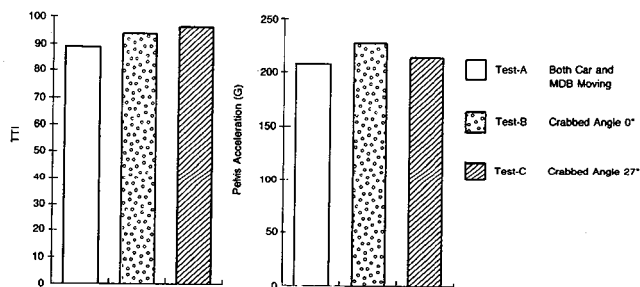


Figure 25. Comparison between crabbed and non-crabbed test results.

### Investigation of a test procedure using a rigid barrier

The variability in the dynamic characteristics of the MDB could have the effect of influencing the variability of the test results. Two series of tests were carried out with a rigid barrier in order to examine the possibility of devising a test procedure without using the MDB. The rigid barrier used in these tests had the same configuration and weight as the MDB proposed by the NHTSA.

The first series of tests with the rigid barrier were carried

out using the same impact velocities as in the tests conducted with the MDB. The dummy readings obtained are shown in figure 26 and the static deformation of the body outer panels measured at the center of the door is given in figure 27.

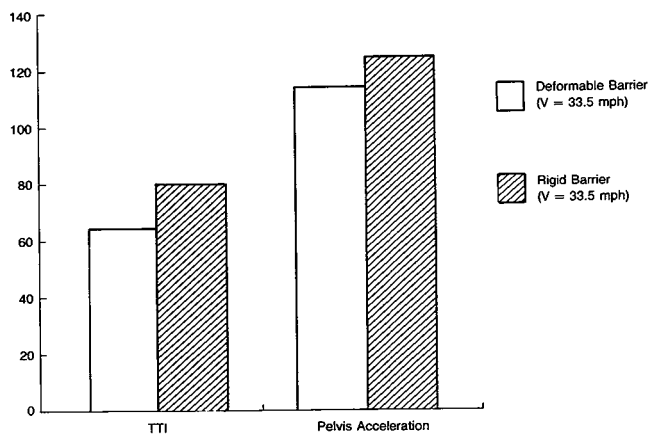


Figure 26. Comparison of dummy readings in the tests with deformable and rigid barrier.

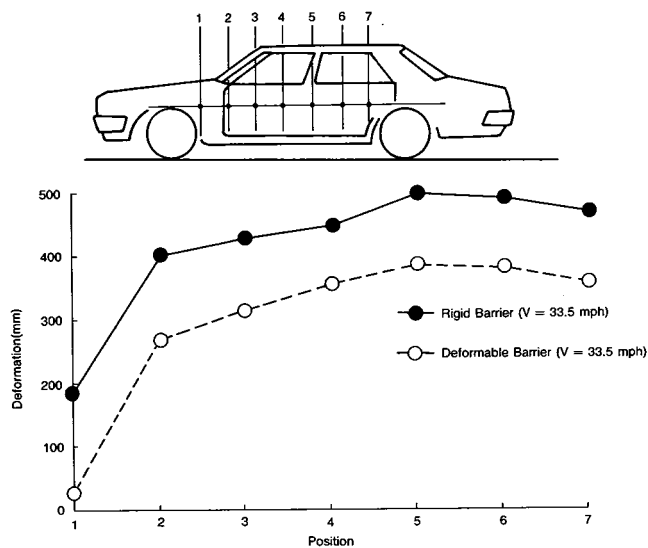


Figure 27. Comparison of body deformation in the tests with deformable and rigid barrier.

In the tests conducted with the MDB, the aluminum honeycomb structure of the barrier face absorbed a certain portion of the impact energy. Since all that energy was absorbed by the vehicle in the tests conducted with the rigid barrier, a greater degree of body deformation naturally occurred and, as a result, the values for TTI and pelvis acceleration were larger.

In the second series of tests, an effort was made to achieve the same level of absorbed energy by the test vehicle. The amount of energy absorbed by the honeycomb structure of the MDB was calculated from the degree of deformation it showed and from its dynamic force-deformation characteristics data. The result was approximately 700 kgf-m. In the second test series, the impact velocity was lowered from 33.5 mph to 31.7 mph so as to reduce the amount of energy

absorbed by the vehicle by 700 kgf-m. The dummy readings obtained are shown in figure 28 and the degree of body deformation is presented in figure 29. It is seen that the degree of body deformation corresponds very well with the result obtained in the MDB test. As a result, the values for TTI and pelvis acceleration are also very similar.

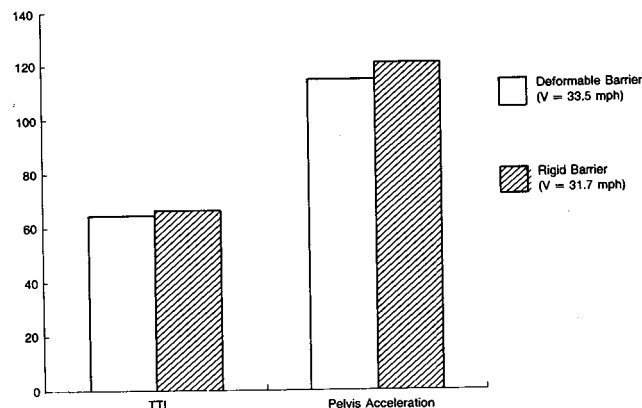


Figure 28. Comparison of dummy readings in the tests with deformable and rigid barrier.

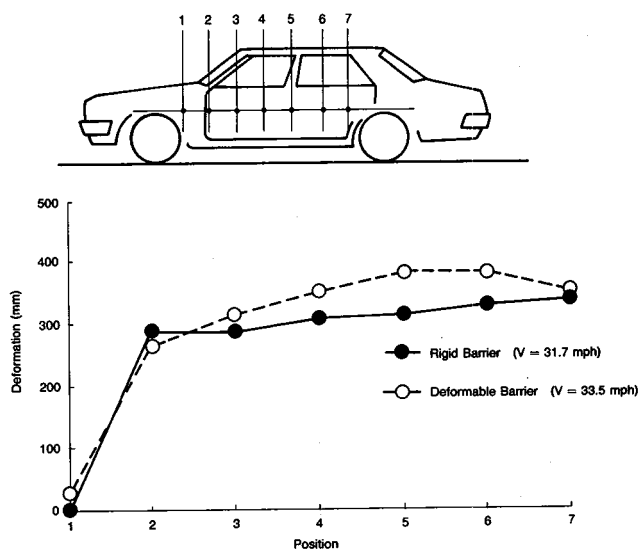


Figure 29. Comparison of body deformation in the tests with deformable and rigid barrier.

Although only one vehicle body style was used in these tests, it is thought that by expanding the test vehicle samples, a rigid barrier test procedure could be developed that would yield the same results as obtained with the MDB.

## Conclusion

Full-scale test results and sled test results were analyzed to examine the effects on dummy readings of various vehicle parameters. It should be noted that the purpose of this work was to analyze experimentally the correlation between different vehicle parameters and dummy readings. Consequently, before the results of this work can be incorporated in production vehicles, there are issues

relating to passenger compartment comfort, vehicle weight increases and other factors that must be resolved. The major results of this study are summed up in table 1, and the following conclusions can be drawn from the analytical results:

**Table 1. Correlation between vehicle component parameters and dummy readings.**

Parameters	TTI	Rib Deflection	Pelvis G	HIC
Impact Velocity Between the Door and the Dummy	⊙	×	○	○
Reduction in Door Velocity during the impact between the Door and the Dummy	△	×	△	×
Crash Force of the Vehicle	○	×	○	○
Vehicle Deformation	○	×	△	○
Padding Thickness	⊙	△	⊙	-
Padding Hardness	⊙	△	⊙	-
Vehicle Weight	×	×	×	×
Clearance between the Dummy and Door Trim	×	○	×	×

Correlation ⊙ Very good ○ Good △ Moderate × Poor

(1) TTI shows a higher correlation with the impact velocity between the door and the dummy,  $V_2$ , than with the reduction in door velocity,  $\Delta V$ , that occurs during the impact between the two. This indicates that TTI is greatly affected by the crash force of the vehicle at the initial stage of the impact. TTI is also markedly influenced by the thickness and hardness of the door padding.

(2) The rib deflection findings can only be regarded as reference data because of the poor biofidelity of the SID. Still, a strong correlation is seen between rib deflection and the distance between the dummy's chest and the door interior trim. Rib deflection is little affected by the time history of the door velocity and the door padding, unlike TTI which tends to be strongly influenced by these factors. Even though TTI and rib deflection are dummy readings for the same chest region, they correlate differently with the vehicle component parameters.

(3) Like TTI, pelvis acceleration is greatly affected by the impact velocity between the door and the dummy and by the door padding. Pelvis acceleration and TTI show similar correlation with vehicle parameters. These similarities are thought to be caused by the fact that both of these dummy readings are based on acceleration data.

(4) As the foregoing results indicate, dummy readings show different correlation with vehicle component parameters depending on whether they are based on acceleration data or on deflection data. Consequently, in making assessments of vehicle

performance based on dummy injury levels, the use of the inadequate injury criteria could result in vehicle modifications which are ineffective in improving occupant safety under actual field conditions. Because of this possibility, injury criteria should be determined on the basis of carefully conducted studies.

(5) The HIC value tends to decrease with a decreasing impact velocity between the door and the dummy. However, the locations of head contact seen in the results of side impact tests carried out according to the NHTSA's procedure differ from the places of contact found in an analysis of actual accidents. This discrepancy indicates that the procedure for assessing head injuries in full-scale tests requires careful examination.

In an effort to simplify the side impact test procedure, an analysis was made of the effects of the crabbed angle and barrier stiffness on dummy readings. The following conclusions can be drawn from the analysis:

(1) Three types of tests were conducted: one involving a right-angle impact with both the vehicle and barrier moving, one involving a crabbed impact between the moving barrier and a stationary vehicle and one involving a non-crabbed impact between the moving barrier and a stationary vehicle. Both the crabbed and non-crabbed impact tests showed TTI and pelvis acceleration values that were similar to the results of the test in which the vehicle and barrier were moving. These results indicate that there is no need to go so far as to apply a crabbed angle. Consequently, the non-crabbed test procedure is regarded as being preferable because of its simplicity.

(2) Tests were conducted with a rigid barrier in which the impact velocity was lowered so that the amount of energy absorbed by the vehicle upon impact would be the same as in a MDB test. The TTI and pelvis acceleration values obtained were virtually identical to the results found in MDB tests. The variability in the dynamic characteristics of the MDB could increase the degree of variability in the test results. Studies should be carried out to examine the possibility of designing a test procedure using a moving rigid barrier.

## References

- (1) "Federal Motor Vehicle Safety Standards; Side Impact Protection", NHTSA 49 CFR Part 571, Docket No. 88-06, Notice 1, 1988.
- (2) "Side Impact Anthropomorphic Test Dummy", NHTSA 49 CFR Part 572, Docket No. 88-07, Notice 1, 1988.
- (3) Richard M. Morgan, Jeffery M. Marcus and Rolf H. Eppinger, "Side Impact—The Biofidelity of NHTSA's Proposed ATD and Efficacy of TTI", SAE 861877, 1987.

(4) "Set of Drawings for the NHTSA Side Impactor Prepared by Dynamic Science Inc.", NHTSA, Docket No. 79-04 GR.

(5) "Preliminary Regulatory Impact Analysis on the

ANPRM's for Side Impact Protection Upgrade", NHTSA, Docket No. 88-06, Notice 3, 1988.

(6) "Protection of the Occupants of a Lateral Collision", TRANS/SC1/WP29/GRCS/R58, 1985.

## Reconstitution With Partial Testing of a Full-Scale Side Impact Test Severity

**J. Bloch, D. Cesari, R. Biard,**  
INRETS / LCB,  
France

### Abstract

All studies undertaken to analyse phenomena occurring in lateral collision accidents are based on two types of experimental collisions—global collisions and "sub-system" collisions.

This latter type is designed to reproduce the component variables of global lateral collisions in a simplified form with the aim of evaluating how a given vehicle performs.

Simplification usually means selection. For this reason the INRETS Laboratoire de Chocs et de Biomécanique (LCB) decided to simulate the severity of global lateral collisions as accurately as possible using a partial test which nevertheless considers all the parameters.

Attempts to simulate collisions involving 2 different vehicles require data from global reference tests and are obligatorily complex as they involve a large number of variables. This situation is made even more difficult by a certain number of experimental problems which were also investigated.

Even if the low number of tests implemented so far have not yet enabled the accurate reproduction of the severity of the global collisions used for reference purposes, they have enabled the evaluation of the impact on severity of various parameters which could be very useful in the context of the preparation of a definitive simplified sub-system experimental protocol.

### Introduction

Research carried out over the last few years into secondary vehicle security and concerning both frontal and lateral collisions basically used global type experimental procedures. Recently, another type of approach has been introduced which involves analysing the performances of a given vehicle using a sub-system experimental protocol.

The benefits of this simplified approach include lower costs per experiment which means that more tests can be carried out. As simplification is the main objective sought by the architects of this new approach, the proposals and the research findings presented in this field may appear to be somewhat unrelated to global collision simulation. One example of this was the fact that, according to the methods presented, deformation of the vehicle subjected to impact

could be induced statically as the measurement of internal vehicle rigidity, and that the evaluation of collision severity on an occupant could be made using simplified dummies, by the use of specifically designed impacters or by mathematical simulation techniques.

Such simplifications, the basis of all sub-system trials, beg the question as to whether they give results as accurate as global experimental collisions. To try and reply to this question, it was essential to understand the influence of the main parameters used for the overall protocol. These were the aims of the research programme presented in this document: to make an accurate evaluation of a specific global lateral collision and then to attempt to reconstruct a collision of similar severity using partial tests in a stepwise manner. This research was also interesting for French manufacturers within the general framework of sub-system procedures.

The study used two widely distributed vehicles with different structures to create the experimental global lateral collision used as a reference. Vehicle A was a 3-door model and vehicle B had 4 doors. The two main steps comprising the reconstitution work were (a) a pre-deformation of the vehicle body shells and (b) the reproduction of the contact between the lateral structure of the vehicle and the occupant.

### The Reference Tests

The sub-system experimental protocols shown elsewhere must use a configuration defined at the outset to enable the reproduction of the phenomena which contribute to injuries. For this reason we have used a specific lateral collision configuration which was representative of the majority of vehicle/vehicle impacts—the ERGA group European configuration.

With the purpose of making the most accurate possible analysis of the phenomena occurring during the collision we implemented a large number of measurements during experiments A & B, both on the vehicle and on the EUROSID dummy installed in the driving seat.

Eight (8) accelerations to the structure (figure 1) were measured on the impacted vehicle in a direction on the following locations:

- The base of the left and right A pillars (1 & 2)
- The base of the left and right B pillars (3 & 4)
- Mid-height of the left and right B pillars (5 & 6)

Two penetration measurements on the left front door were made at the thorax (T) and pelvis (P) levels.

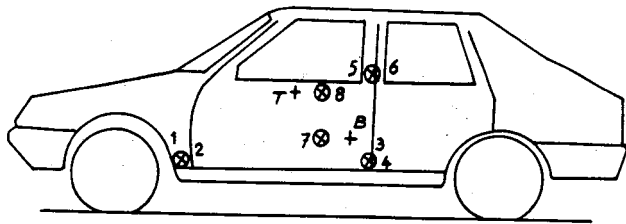


Figure 1. Localization of transducers on tested vehicles.

The following measurements were made on the EUROSID dummy in the driving seat:

- Head : 3 accelerations (x, y, z)
- Thorax : 3 rib deflections  
1 spinal acceleration (y)  
2 rib accelerations (y)
- Pelvis : 1 sacral acceleration  
1 pubic force  
1 iliac wing stress
- Abdomen : 3 contacts

These measurements and the resulting biomechanical parameters were used as references for the severity reconstitution experiments described below.

In addition to these measurements made during the collision, residual deformation of the impacted vehicles was also evaluated.

## Static Crushing of Vehicle Body Shells

It is known that when a lateral collision occurs the most seriously injured passengers are located on the collision side, directly in front of the intrusion area. The intrusion phenomenon was most naturally observable on the driver in the experiments described above and was used as reference data in this research programme. Examination of previous research aiming to define lateral collision sub-system experimental protocols shows that all include an initial phase which consists in deforming the lateral structure used. As our purpose was to reconstitute phenomena occurring during lateral collisions in the fullest possible way, we also pre-deformed the side of the body shells of the two vehicles being investigated.

In parallel, and to try to evaluate pre-deformation significance, we also carried out reconstitution experiments on the occupant/lateral panel impact using non-deformed structures.

This work was implemented using body-in-white shells and thus crushing could not be dynamic. A static test consisting in crushing the front side of a European deformable mobile barrier made of polyurethane foam against a dynamometric wall showed that deformation occurred with energy levels close to those recommended for dynamic tests in the CEVE specifications (figure 2). This observation led us to think that it was possible to deform body shells statically using the front side of this mobile barrier.

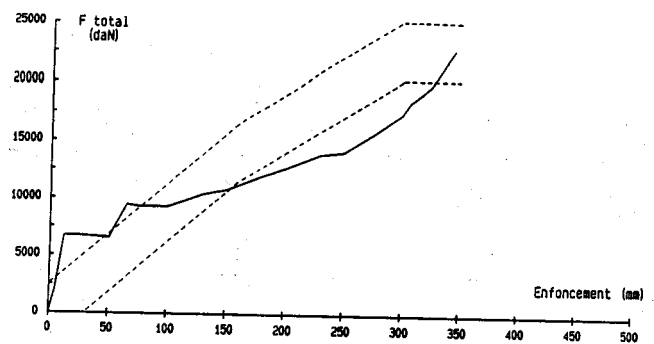


Figure 2. Static crushing force of the european front face compared with the dynamic corridor.

## Determination of the depth of penetration to be obtained

The decision to pre-deform one side of the vehicle body shell implies the definition of the final shape of the crushed panel. Crushing the body shell with the front side of a deformable mobile barrier means that one does not control the overall shape of the final profile. The best one could do was to produce a deformation in a specific point of the body shell side panel, the remainder of the impactation being generated by the process itself.

Because of this factor, it was decided to enhance the reproduction of the phenomena intervening in a true collision at the thorax level as this is the part of the body which is the most seriously and the most commonly affected in this type of accident.

Given the decision to induce an impact at a point coming into contact with the thorax, how deep should the deformation thus caused be? The principle retained was that induced lateral panel deformation at the thorax level should be the same as that measured during the reference experiments at the instant at which the biomechanical criteria recorded on the thorax of the EUROSID dummies attained maximum values.

The use of the films and of door deformation measurements during global collision experiments gave these values as 330mm for vehicle A and 300mm for vehicle B.

## Description of the pre-deformation procedures

Figure 3 shows the results of tests run in the PSA Automobile Safety Laboratory. Front panel /1/ was fixed and guided at the end of an ram /2/. Dynamometric pads /3/ were inserted to record energy consumption during crushing. Vehicle body panels were attached to the ground by the wheel hubs and the body was supported on the opposite side by a rigid longitudinal beam /4/. During crushing, ram motion was measured /5/ as was thorax level /6/ (figure obtained from the collision data) and pelvic level /7/ impaction.

In every test, each of the deformation penetration values aimed at the thorax was exceeded by 55mm to take account of restitution from the residual elasticity of the deformed panel.

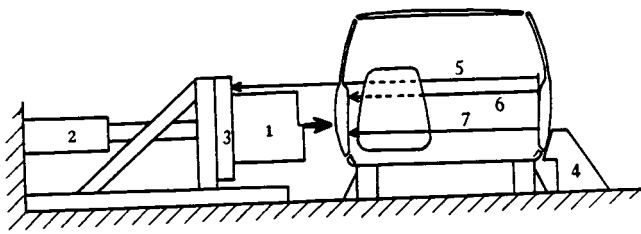


Figure 3. Configuration of car body-in-white static crushing tests.

In comparison with the shape of vehicles impacted dynamically during the reference experiments, lateral deformation of one of the two vehicles appeared to be satisfactory whereas the bottom of the door was excessively deformed in the other.

To conclude discussion of this initial pre-deformation phase, the main findings concern the possibility of crushing vehicle body panels using European mobile barriers with polyurethane foam front faces. It is also interesting to note the importance of the relative positions of the front face and the vehicle body shell as well as the method used to attach the shell to the ground. During our experimental programme the shell was firmly fastened to the ground whereas it seems preferable to allow the deformation side to move to some extent.

## Contact Between the Passenger and the Deformed Lateral Panel

As our initial intentions were to use a sub-system experiment to reproduce the shock severity of a global test on a EUROSID dummy, it seemed simpler to reuse the dummy as a measuring device latterly too.

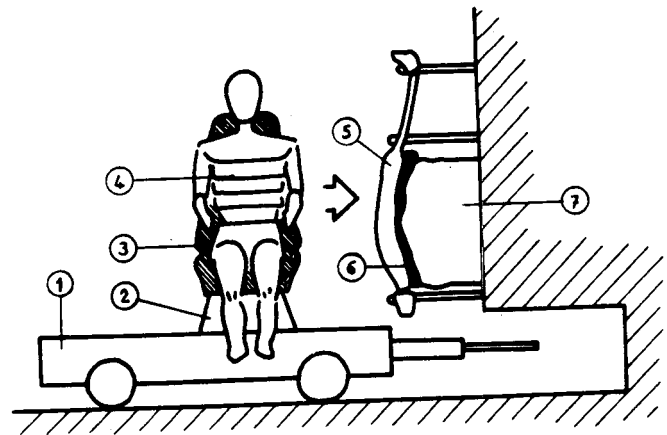
The inclusion of the greatest possible number of parameters coming into play during a global shock is complicated and for this reason we decided to define the simplest possible experimental protocol to simulate the shock between the dummy and the lateral panel. This protocol is described in figure 4. The dummy is installed in the same seat as used in the test vehicle attached to a mobile trolley. In the conditions defined below the trolley + seat assembly moves towards the lateral structure which has previously been cut out of the vehicle's body shell and which is pressed up against the foam front face used to deform it. There is an interface between the panel and the foam to fill the residual empty spaces.

### Selection of impact speed

Several calculations can be used to consider the speed at which the trolley and dummy should approach the structure attached to the shock wall:

1. One can consider the complete system as shown in figure 4, (i.e. 1 + 2 + 3 + 4).

In this case, link 2 is rigid or least similar to the seat/floor attachment used in the vehicle itself. Thus trolley 1 speed variation relative to the ground from the moment of contact between the EUROSID dummy and



1. Trolley
2. Trolley/seat interface
3. Seat of the vehicle (A or B)
4. EUROSID
5. Side structure
6. Deformable pad
7. Front face of european MDB

Figure 4. Test configuration to simulate the occupant/side structure impact.

the panel must be similar to the speed variation of the door panel relative to the floor of the vehicle during an authentic global shock. This implies the choice of a contact speed and the deceleration of the trolley over a very short distance.

As we know that the attachment between the dummy and the seat is weak, the added complication of imposing a deceleration law after contact does not appear to be justified.

2. One can only consider system 3 + 4 in figure 4.

In this case link 2 slides (double trolley system) or is very fragile. Thus only the speed at the EUROSID/panel contact needs to be imposed.

As the non-attachment of the dummy on the seat is accounted for, and thus, a fortiori, that of the dummy on the chariot as well, it was this second system which was used. This means determining the speed of the trolley at the moment of contact between the dummy and the panel.

As we had chosen to enhance the severity of the shock at the thorax level, determination of the speed at the moment of contact between the dummy and the isolated panel had to be based on the observation of the speed at which the door panel was deformed at the thorax level during the global shock reference tests.

Our initial hypothesis led us to choose as the impact speed the instantaneous speed measured during the reference tests at the moment at which the biomechanical criteria recorded on the thorax were at their maximum values. This is why the speeds used in the first trials were respectively fixed for vehicles A and B at 30 and 33 k.p.h.

A second hypothesis which seems more realistic was to decide that the reference tests should have also considered the speed of the panel at the instant it came into contact with

the driver's thorax. These speeds were respectively 42 and 38 k.p.h.

As the question of the merits of pre-deforming the side of the body panel was also under review, a total of 6 reconstitution tests were made. The main features are given in the table below.

Vehicle	Trial	Body Panel	Speed (k.p.h.)
A	A	Deformed	30
A	A2	Not deformed	30
A	A3	Not deformed	42
B	B1	Deformed	33
B	B2	Not deformed	33
B	B3	Not deformed	38

Generally speaking, the true speeds observed in the tests were very close to the theoretical speeds given above except for the third test on vehicle A (test A3) in which the speed was 37.8 k.p.h. instead of the 42 k.p.h. specified due to a technical error when setting up the test rig.

## Results and Comments

As stated above, test results were obtained from instruments attached to the EUROSID dummy and the consequent biomechanical criteria.

Overall, results obtained from these initial tests were disappointing for both vehicles. If the results for vehicle A show that we can hope to reach our objective by introducing a few improvements, results from vehicle B contain several aberrations which show how difficult it is to succeed in this endeavour.

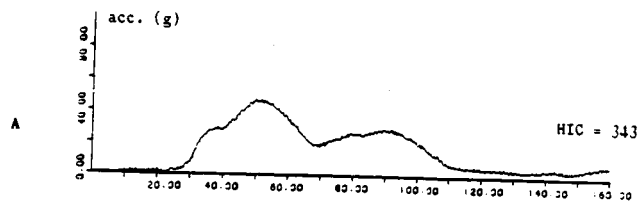
There are many reasons why such difficulties arise and seeking their causes could be profitable providing that it is possible to define the significance of the various parameters coming into play when a collision occurs and also the defects inherent in the experimental protocol used.

As an initial approach, let us review the principle features of the results obtained from studying the head, thorax and pelvis of the EUROSID dummy.

### The head of the EUROSID dummy

Measures are taken of 3-axis accelerations and the relevant HICs. Figure 5 gives resultants of accelerations for vehicle A and shows that if the lateral panel of the vehicle (trial A2) is not deformed, the kinematic described by the dummy is different, provoking a contact between the head and the longitudinal lateral roof panel beam. If this beam is removed there is obviously no contact, and it is possible to reproduce approximately the same shock severity as can be seen from the third reconstitution test. The same observations can be made about vehicle B.

### REFERENCE



### RECONSTITUTIONS

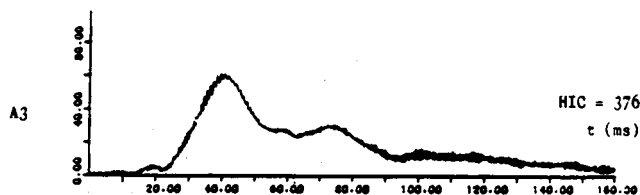
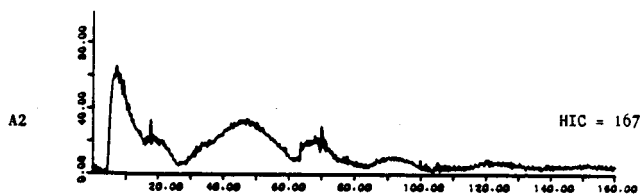
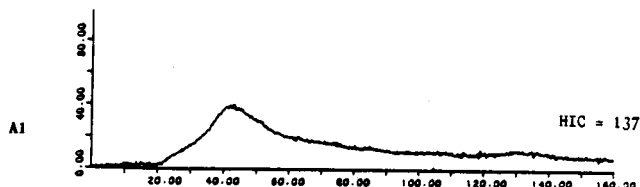


Figure 5. Resulting head accelerations concerning the vehicle A tests.

### The thorax of the EUROSID dummy

Interpretation is much more complex for this part of the body. Maximal transversal values for spinal acceleration are as follows:

Test N°	A	A1	A2	A3
Maximum acceleration (g)	79.6	55.7	54.9	69.6
Test N°	B	B1	B2	B3
Maximum acceleration (g)	90.4	58.2	62.6	61.9

When A1/A2 and B1/B2 test result values are compared, predeformation does not seem to make any significant contribution. The result obtained at 38 k.p.h. in test A3 is close to the reference value. However, for vehicle B, the value obtained at 38 k.p.h. is slightly below that obtained in test B2, which appears to be an anomaly. The same phenomenon is observable in the rib deflection measurements.

The results for vehicle A rib deflection measurements (figure 6) are more satisfactory as far as maximum values are concerned but it was observed during the reconstitution

tests that the speed at which the ribs were penetrated (the positive slopes of the graphs) was lower.

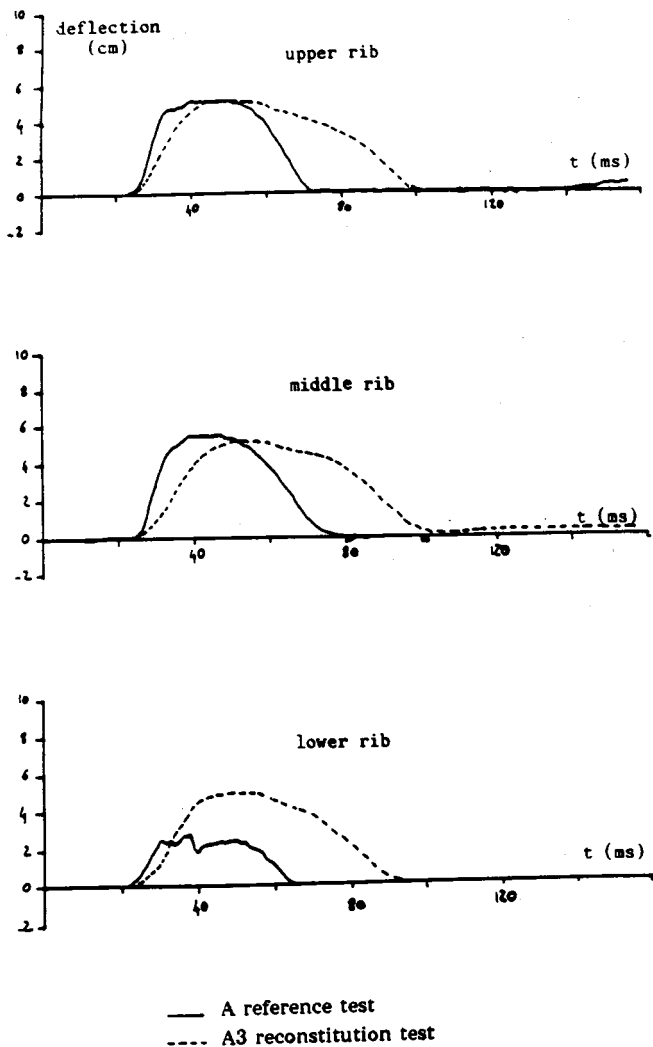


Figure 6. Comparison of the EUROSID rib deflections.

An initial explanation of this lesser severity is that, for vehicle A, the true speed of the final reconstitution test was lower than that defined using data from the reference test.

A second explanation which concerns both vehicles appears from the films. They show that the lateral panel support made up of the mobile european barrier front face and an interface mat (figure 4) deforms under the shock and one can imagine that the rigidity of this support is not correctly reproducible nor in conformity with the rigidity of the front face when it collapses during a global shock.

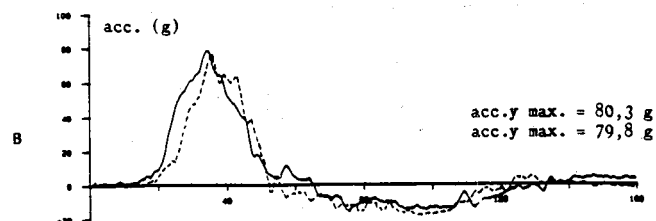
### The pelvis of the EUROSID dummy

As for the thorax, the severity of shocks reconstituted at the pelvic level is lower than the reference shocks for both transversal sacral acceleration and for the stresses recorded in the iliac wings and the pubis.

For vehicle B, the results closest to the reference values for both transversal sacral acceleration and pubic strain

were obtained when the lateral structure of the vehicle was pre-deformed (figures 7 and 8).

### REFERENCE



### RECONSTITUTIONS

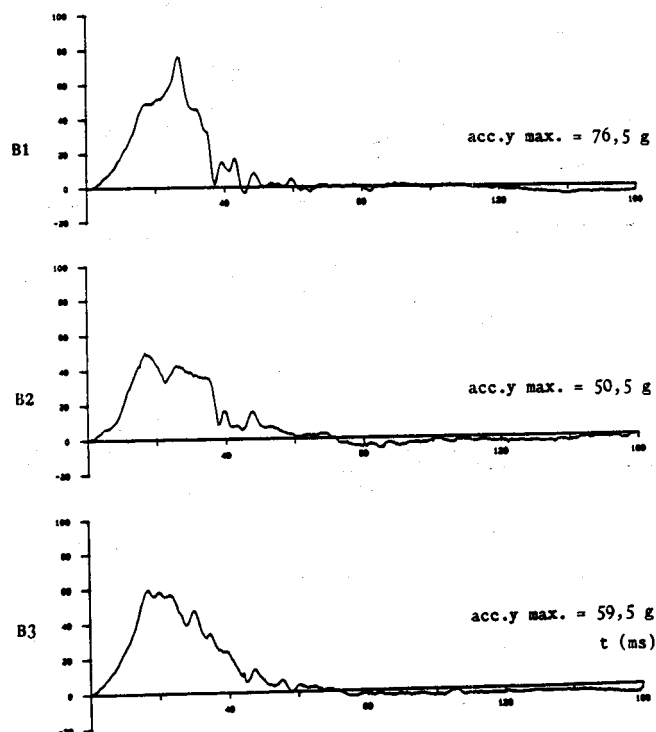


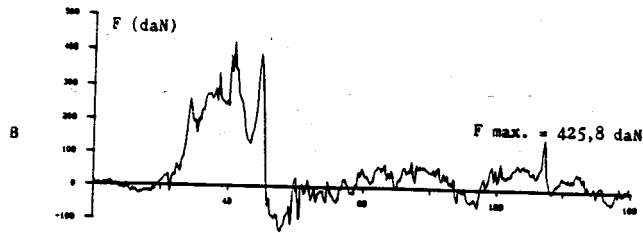
Figure 7. Transversal pelvis accelerations concerning vehicle B.

## Conclusion and Propositions for the Elaboration of Sub-system Tests

As stated above, these initial trials, designed to reconstitute the severity of global lateral collisions, have enabled the significance of some of the shock parameters to be determined and the importance of some aspects of the experimental protocol to be revealed. These parameters include:

- The importance of pre-deformation of the lateral structure of the impacted vehicle. The degree of pre-deformation must fall within the limits of the deformation observed at the instant of contact with the occupant and maximum deformation.
- The importance of global rigidity of the lateral panel. Rigidity stems both from the deformed panel itself but also, and essentially, from the

#### REFERENCE



#### RECONSTITUTIONS

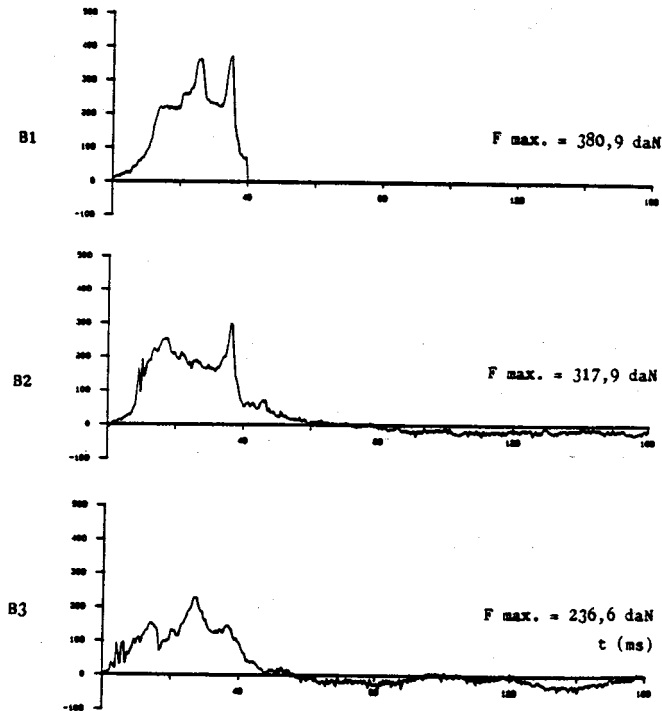


Figure 8. Pubic forces concerning vehicle B.

panel support assembly which was imperfect in the research programme described above.

If a dynamic test method is used to study passenger/body panel contact, the following points should be considered:

**Contact speed choice.** In our case we carried out a reconstitution from a base provided by a global reference test during which we measured the lateral structure penetration speed in the passenger cell at the moment at which contact was made with the occupant. However, a reference of this nature cannot exist when one wants to design a sub-system test procedure to predict the structural performance of a vehicle in the design phase.

One way of getting round this difficulty would be to use static panel/occupant contact tests as in the Composite Test Procedure supported by the CCMC but it would be essential in this case to ensure the rigorous evaluation of a dynamic contact severity, both in terms of measuring the rigidity of the lateral structure which can vary with respect to speed and in terms of the occupant simulation device which must integrate its own rigidity and which must, in every case, give the best possible simulation of the characteristics of the human body in both the static and the dynamic mode.

In conclusion, even if the research described above did not enable full global shock severity reconstitution through partial testing, we did acquire beneficial experience in the detailed analysis of lateral impact which will be extremely useful in the preparation of a simple, reliable and repeatable test procedure which will not require the prior implementation of global dynamic reference tests.

## A Methodology For Enhancing Side Impact Crashworthiness

Written Only Paper

**R. N. Hardy,**  
Cranfield Impact Centre,  
United Kingdom  
**H. Mellander,**  
Volvo Car Corporation,  
Sweden

### Abstract

The world-wide vehicle community has for the last five years focused its attention on side impact crashworthiness. Now, NHTSA has published a prospective timetable for the introduction of side impact legislation—revised FMVSS 214. Although it is essential for a vehicle to pass a legislative test it must also perform well during real-life accidents.

Volvo has developed an in-house test method in which good resemblance to real-life accidents is achieved. It was

against the background of this in-house test procedure that Cranfield Impact Centre investigated the potential for enhancing the performance of a conventional production car during side impacts.

The methodology uses a hybrid technique for evaluating side impact crashworthiness. Iteration with the technique enables identification of compatible component properties and hence to enhanced side impact crashworthiness. The methodology is described, discussed and demonstrated in this paper.

### Introduction

Accident statistics relating to side impact accidents are well documented in many countries (1, 2, 3).\* In the U.K.

\*Numbers in parentheses designate references at end of paper.

data shows that in general 74% of side impacts occur at junctions, when vehicle speeds are unlikely to be high. However, when side impacts occur they tend to generate more injuries than other types of collisions. A comparison of U.K. data, using the U.K. definitions of slight, serious and fatal injuries shows the following:

	slight	serious	fatal	sample
Side impacts	67%	29%	4%	466
Non-side impacts	77%	22%	1%	3270

Further, during a side impact with another car it is not uncommon for the nearside occupant to experience a velocity change greater than the velocity change of the car in which he is sitting (4).

The main cause of injuries to an occupant is the change in velocity which he experiences (4). Intrusion on its own does not necessarily cause injuries, although gross intrusion of the inner door panel/side structure may eventually become important as a cause of injuries.

Methods of reducing or minimising the velocity change of the occupant generally revolve around two parameters:

- (i) Side structure characteristics.
- (ii) Padding characteristics.

Neither of these, on their own, will provide the total solution to reducing the level of occupant injuries, but each will play its part. How then to assess the benefits each can offer? A methodology which includes a capability for the rapid and cost effective assessment of various options is clearly needed. Just such a methodology, which includes both component testing and computer simulations, is described here.

## The Methodology

The methodology uses a hybrid technique (figure 1). The structural and energy absorbing elements and joints of the side structure are first tested to determine their non-linear behaviour. A data file is then constructed which includes this non-linear behaviour together with a coarse finite element mesh of the side structure. This is analysed with the CRASH-D computer program to determine the structural characteristics of the side structure. The motion characteristics of the side structure and car centre of gravity are then determined. The kinematics of the occupant and his likely level of injuries are predicted with an occupant simulation program—e.g. Madymo or Calspan.

Once the basic simulation models have been constructed they can be used to enhance the structural performance of the car during side impacts. Now a series of computer simulations are performed with variations in the characteristics of the elements and joints of the side structure. This process identifies the areas of the structure where revised component properties would maximise the enhancement of side impact crashworthiness. The designs for components having the characteristics identified in the computer simulations can be finalised after a component test programme. Final computer simulations are then

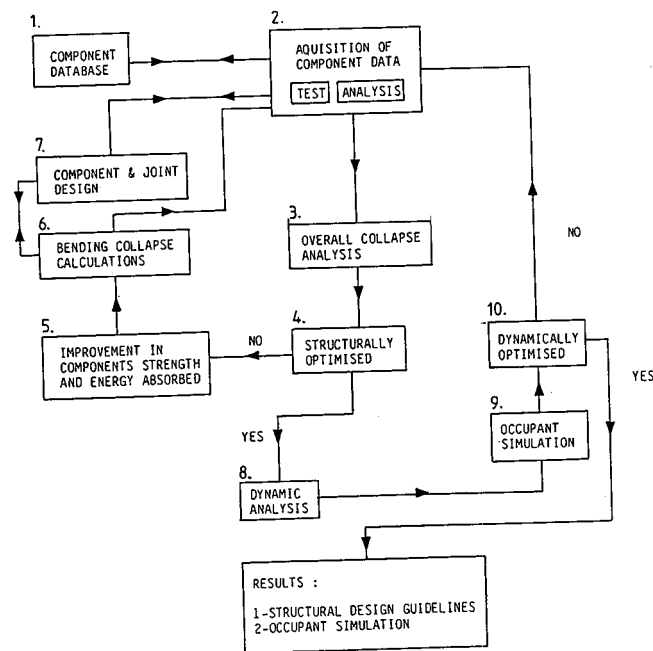


Figure 1. Flowchart of the methodology.

conducted using the component properties from the tests to confirm the likely improvement in side impact performance of the car.

## The place of the methodology in the development of passenger cars

Although the methodology requires the input of component non-linear properties, this does not restrict its use to the improvement of crashworthiness of current production or prototype cars. Once a number of a manufacturers' cars have been tested to obtain a likely range of component properties a database can be established. This database can be used as a springboard in the design process of a new or concept car. Revised component properties can be introduced until the desired side impact performance is achieved. Thus the methodology can be used to:

- (i) Investigate the means by which the crashworthiness of a current production vehicle could be improved (5).
- (ii) Steer the design process during the concept stage (6).
- (iii) Interact with the development programme of a car at the prototype and pre-production stages in a timescale helpful to the programme.

This methodology does not preclude the use of the Composite Test Procedure (7) or even full scale testing from being used in the design and development of a car or for that matter any other vehicle.

The methodology offers important advantages over these other two methods, not least because it can be used from the concept design stage, in terms of timing and costs. In addition, these methods do not provide information on the relative contribution of the various structural components to the overall collapse performance of the car side structure. Thus,

actual sources of strength or weakness cannot be readily or reliably classified and, therefore, any suggested design alterations may not improve the structure in the most direct and rational manner.

### Use of the methodology

The methodology was used on a conventional production car. The objective was to reduce the intrusion velocity of the door/side structure at the time of dummy contact to less than 10m/s. The impact conditions were a stationary target car struck by a CCMC mobile deformable barrier travelling perpendicular to the longitudinal axis of the struck car at 56km/h. (It was felt that an APROD dummy occupant would experience reduced accelerations and impact forces under these conditions.)

In addition, the Impact Centre were given limits for the weight which could be added to the car. Also a list of those components which could not be changed, those which could have some changes and those which, if necessary, could be completely redesigned.

Initially, simple bending, torsion, shear and compression tests were carried out on the elements and joints of the car which would contribute to its side impact crashworthiness. The moment and energy absorption capabilities of the components were thus evaluated and could be compared by means of tables and bar charts (figure 2a).

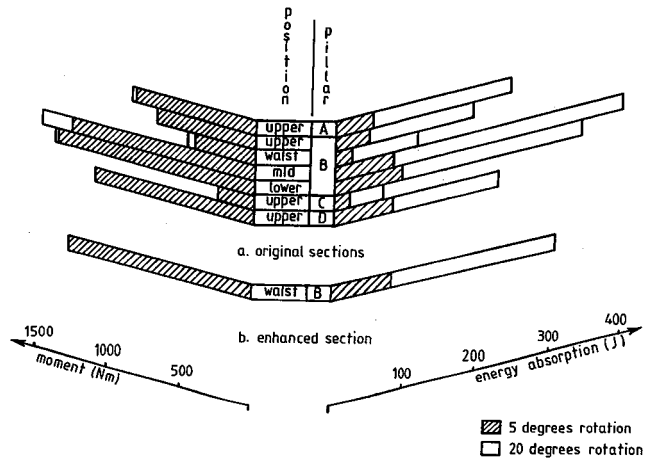


Figure 2. Moment and energy absorption capabilities of cross-sections from bending tests about a longitudinal axis.

A data file incorporating these properties, a coarse F.E. mesh (figure 3) and other information were analysed with the CRASH-D program to determine the force-deflection characteristics of the car side (figure 4) and the likely collapse mechanism (figure 5).

The velocity of the front door at chest height (figure 6) and pelvis height were calculated with a spring-mass model. Finally, these velocities, the properties of the inner door panel including padding and the characteristics of an APROD dummy were input to the Calspan CVS program to determine the kinematics and accelerations of a car occupant (figures 7 and 8).

The characteristics of the production car were thus evalu-

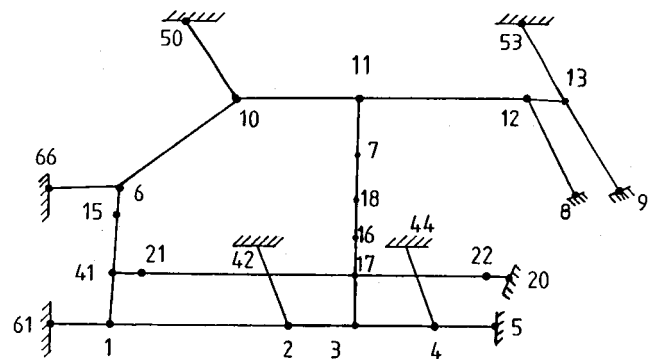


Figure 3. F. E. mesh.

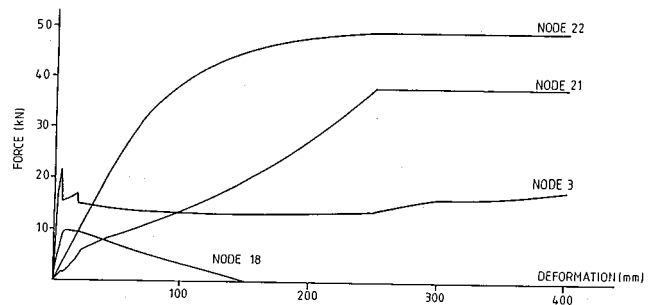


Figure 4. Force-deflection characteristics for side structure.

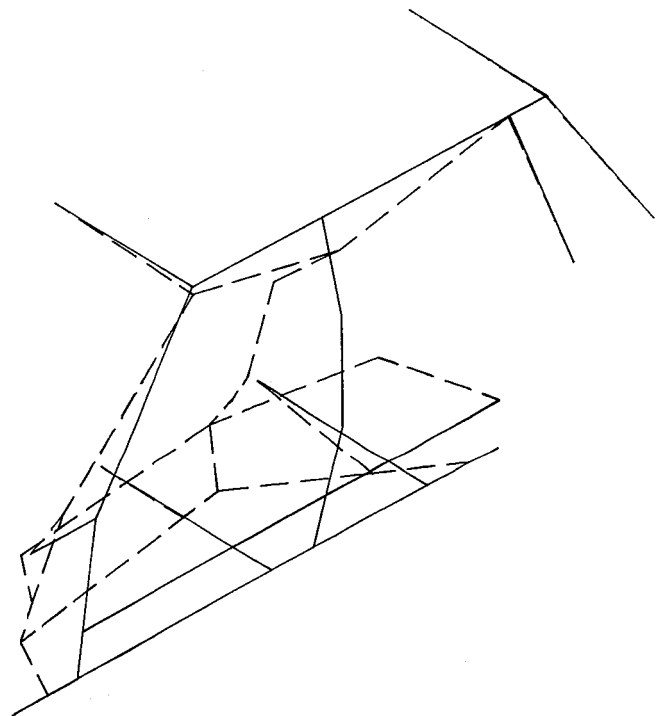


Figure 5. Collapse mechanism.

ated and could be compared with results from a full size test.

A series of parametric investigations were then undertaken to determine the structural properties which would enable the 10m/s velocity target to be achieved.

Five major components were eventually identified, which with modifications or redesigns could potentially give the required improvement in crashworthiness (8).

Designs for new or revised components were undertaken

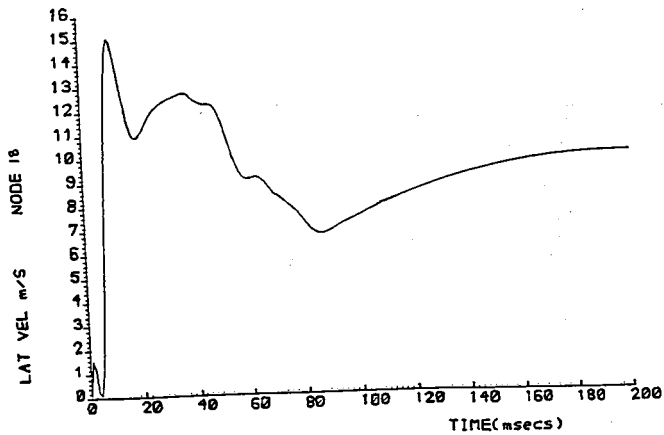


Figure 6. Door velocity at chest height.

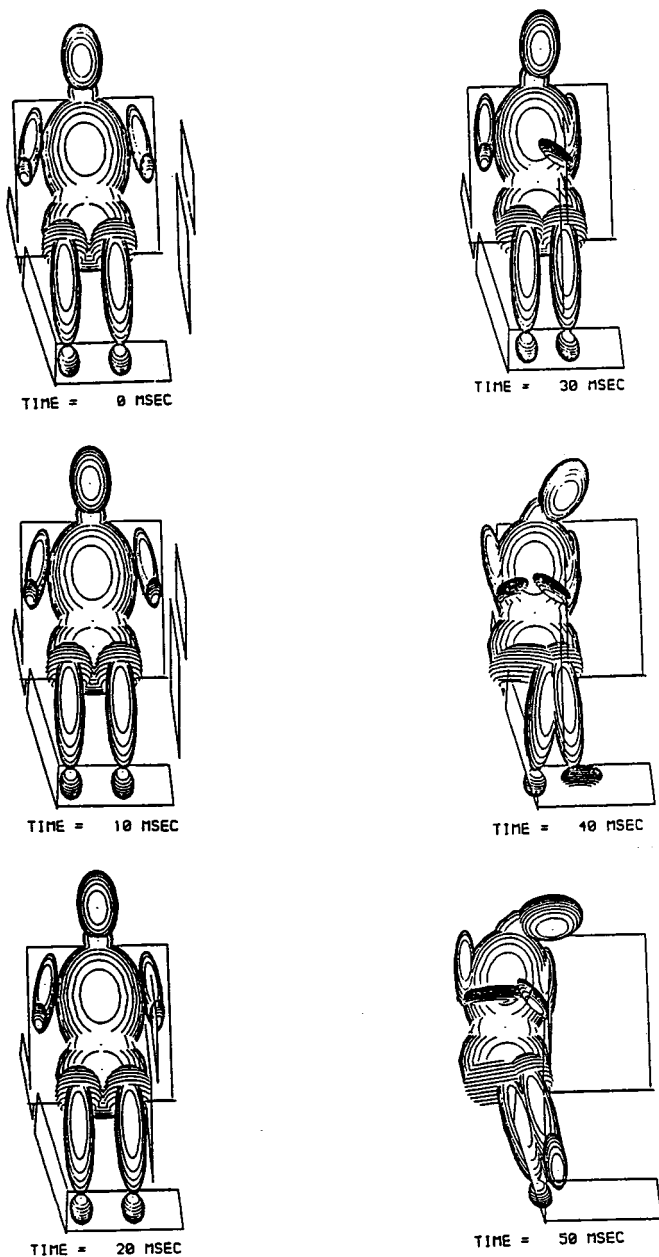


Figure 7. Occupant kinematics.

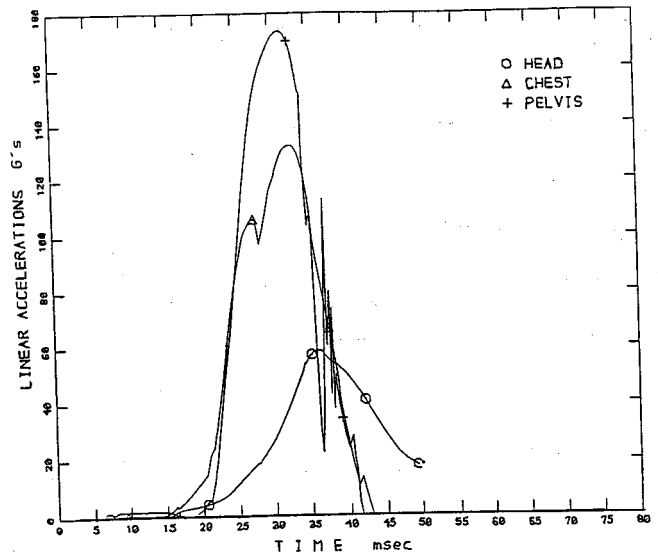


Figure 8. Occupant accelerations.

to achieve the properties needed. Components to these designs were then constructed, assembled with the necessary surrounding structure, if any, and tested.

Further computer simulations were then undertaken to determine if the properties from the component test results were sufficient to achieve the required structural crash-worthiness target.

If the target had not been achieved, components were modified or completely redesigned, constructed and tested again.

The test result for a redesigned B pillar section showed a significant improvement (figure 2b).

The final computer simulations showed improved force-deflection characteristics for the car side (figure 9) and the achievement of the 10m/s velocity target (figure 10). The occupant kinematics and accelerations were also much improved (figures 11 and 12).

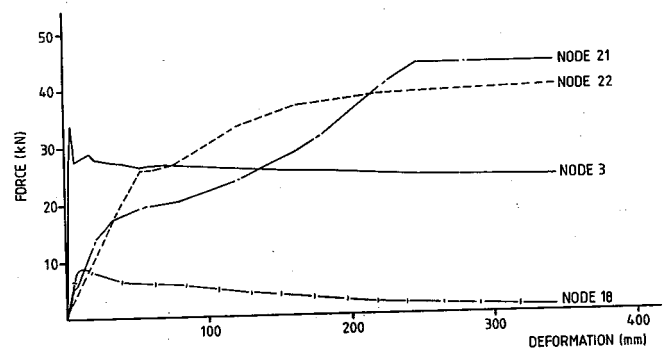


Figure 9. Enhanced force-deflection characteristics for side structure.

## Productionisation

The simulation results and design information concerning the new and revised components were passed to Volvo. If incorporated into a current production car these changes should enable it to demonstrate compliance with the 10m/s velocity target.

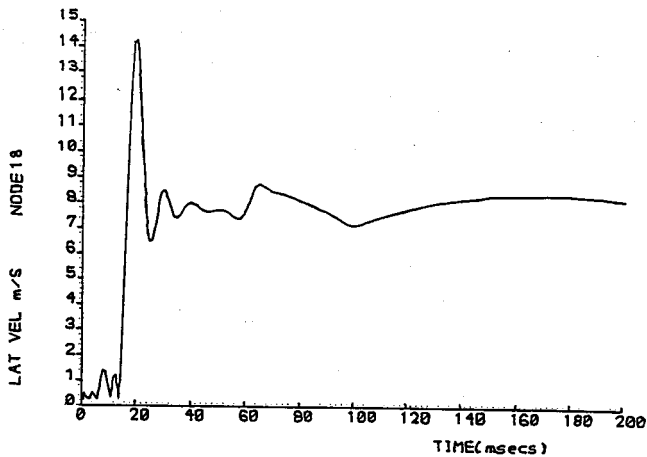


Figure 10. Enhanced door velocity at chest height.

During the course of the work reported here, the Impact Centre strived to ensure the new and revised components could be incorporated into a production car on an assembly

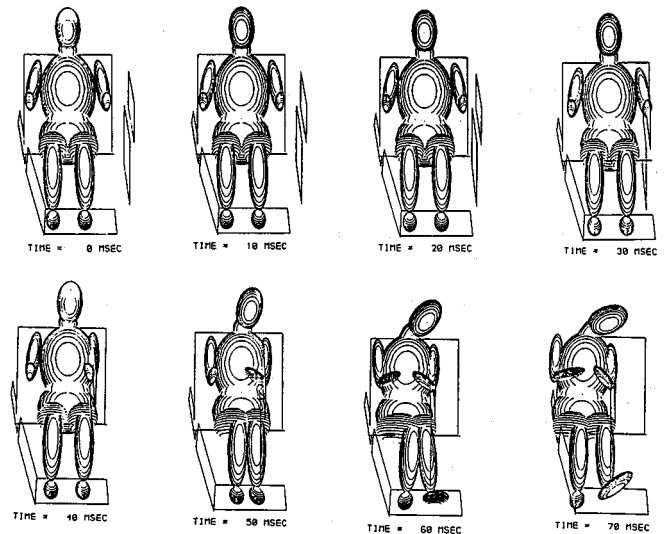


Figure 11. Enhanced occupant kinematics.

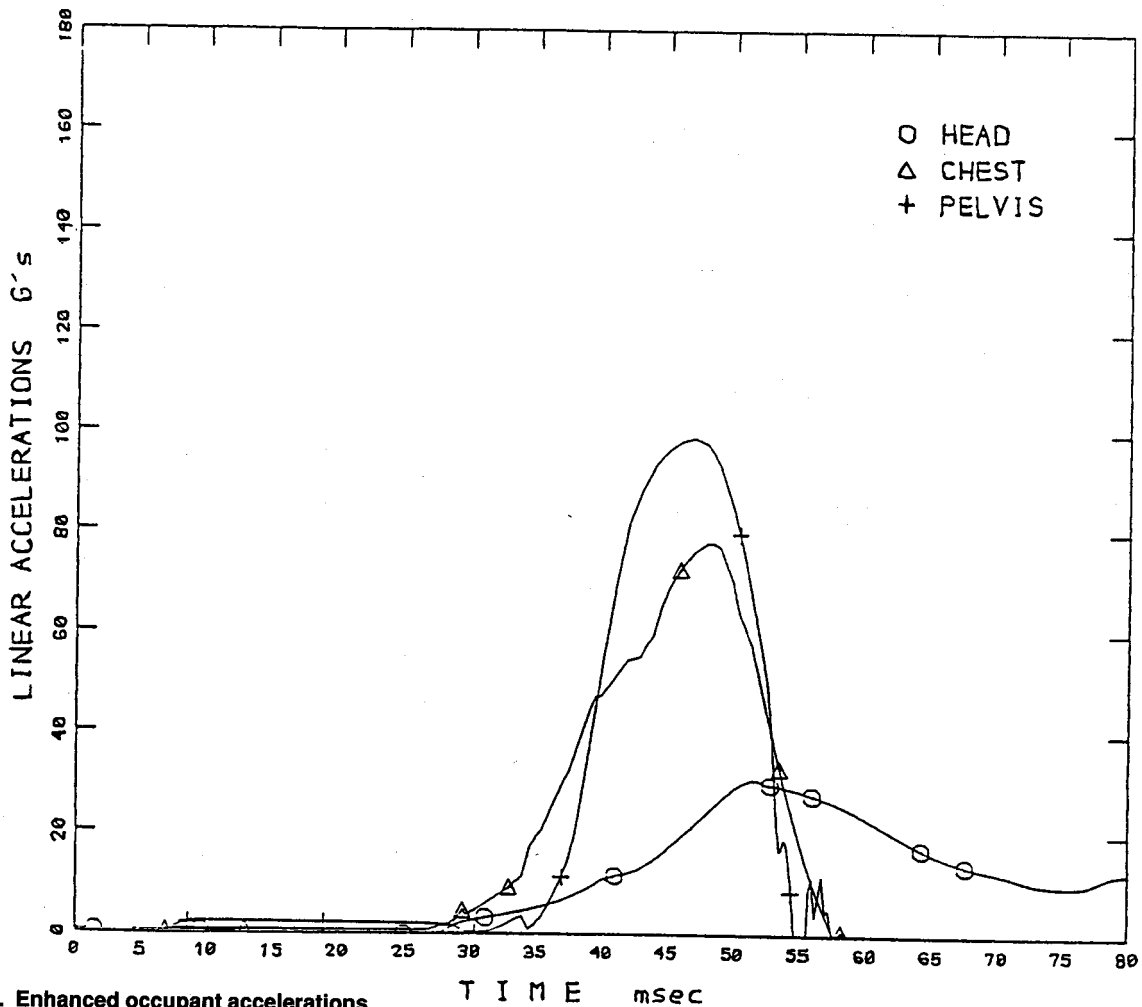


Figure 12. Enhanced occupant accelerations.

line. Nevertheless, it should be pointed out that the final decision concerning the feasibility of these changes must be Volvo's.

The technical solutions, as they were built into a prototype car and later evaluated in a full scale test, are

described in another paper at this 12th International Technical Conference on Experimental Safety Vehicles (8).

## References

- (1) Griffiths, D.K., et al. An Investigation of a Repr-

sentative Sample of Side Impacts to Cars. Accident Research Unit Report No. 23, University of Birmingham, 1983.

(2) Cesari, D. and Ramet, M. Biomechanical Study of Side Impact Accidents. Proc. 5th ESV Conf., p. 511-520, London, 1974.

(3) Viano, D.C., et al. Involvement of Older Drivers in Multi-vehicle Side Impact Crashes. Proc. 23rd Conf. Assoc. for the Advancement of Automotive Medicine, October 1988.

(4) Mackay, G.M. The Characteristics of Lateral Collisions and Injuries and the Evolution of Test Requirements. Proc. of Int. Seminar on Legislative Proposals for Car Occupant Protection in Lateral Impact, Instn. Mech. Engrs., London, April 1989.

(5) Hardy, R.N. and Suthurst, G.D. Simulations to Assess the Influence of Car Lateral Impact Characteristics on Occupant Kinematics. Proc. Instn. Mech. Engrs., Vol. 199 No. D2, 1985.

(6) Suthurst, G.D., Ng, P. and Sadeghi, M.M. Inclusion of Crashworthiness in Concept Design. Proc. 10th ESV Conf. p. 772-779, Oxford, 1985.

(7) Committee of Common Market Automobile Constructors (CCMC) Composite Test Procedure for Side Impact Protection System—An Alternative Approach. Progress Report, 28 April 1989.

(8) Mellander, H., Ivarsson, J., Korner, J. and Nilsson, S. Side Impact Protection System—a description of the technical solutions and the statistical and experimental tools. Proc. 12th ESV Conf., Gothenburg, 1989.

# Technical Session 5B

## Evaluation and Assessment

Chairman: Gunnar Carlsson, Sweden

### A Mechanical Buckle Pretensioner to Improve a Three Point Seat Belt

Yngve Håland and Torbjörn Skånberg,  
Electrolux Autoliv AB,  
Sweden

#### Abstract

The occupant protection in a car can be improved by supplementing the three point seat belt with an efficient pretensioner. This is of special importance if there is a lot of slack in the belt caused by e.g. thick clothes.

This paper describes a mechanical pretensioner which has been in production since January 1989. It acts on the seat belt buckle. At the very beginning of a crash the buckle is rapidly pulled down, thereby pretensioning both the lap- and chest belt parts.

The pretensioner comprises a preloaded torsional spring, which acts upon the buckle and a sensor mechanism for triggering. The design, performance and effectiveness of the buckle pretensioner in a three point belt system with and without slack is presented. The main advantages are reduction of occupant forward displacement, lower impact speed into the steering wheel, less head injury criteria (HIC) and less risk of submarining.

#### Introduction

The three point seat belt is an efficient restraint system in cars. There are however means to further improve it. One problem is that excessive belt slack can cause unnecessary injuries to the head, chest and abdomen. A pretensioning device which acts very early in a crash, before an unrestrained mass has moved more than 20 mm, and that is strong enough (1000 N), will reduce the risk of these injuries.

Our company, a manufacturer of seat belts, has developed a low cost mechanical pretensioner which works by rapidly pulling down the seat belt buckle. The pretensioner has been in production since January 1989.

This paper gives a description of the buckle pretensioner, how the triggering is set and results from 35 mph tests.

#### Background

During the initial phase of an impact, when the front zone of the car is being deformed, a person restrained by a standard belt system initially continues at an unchanged speed. The distance the person travels before the belt starts to absorb energy and decelerates him depends partly on the locking distance of the retractor and the so called film spool effect, but is mainly dependent on the slack of the belt. The

amount of slack depends on several factors, for example the type of clothing worn by the person, the belt geometry and seat position. A way of eliminating slack is to equip the belt with a pretensioner. There are different ways of pretensioning. You can for example retract the belt webbing by rewinding the retractor. This is often done by pyrotechnical means. An other way is to pull the buckle downwards towards the buckle attachment point. The advantage of pretensioning at the buckle is that you simultaneously pull in the diagonal and the lap part of the belt.

#### Description of the Buckle Pretensioner

The buckle pretensioner is an all mechanical solution bolted into the seat at the standard buckle attachment point. The pretensioner assembly is shown in figure 1. It consists of three main parts, namely the sensor, the pulling and the locking parts. They are separately described below.

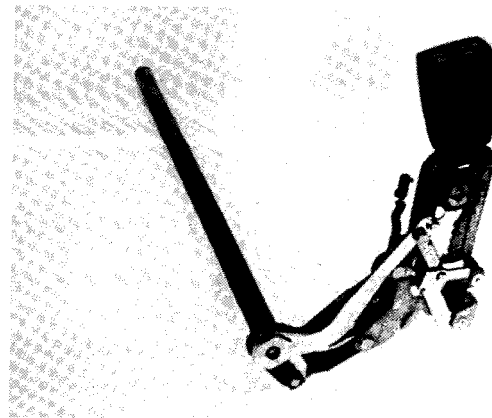
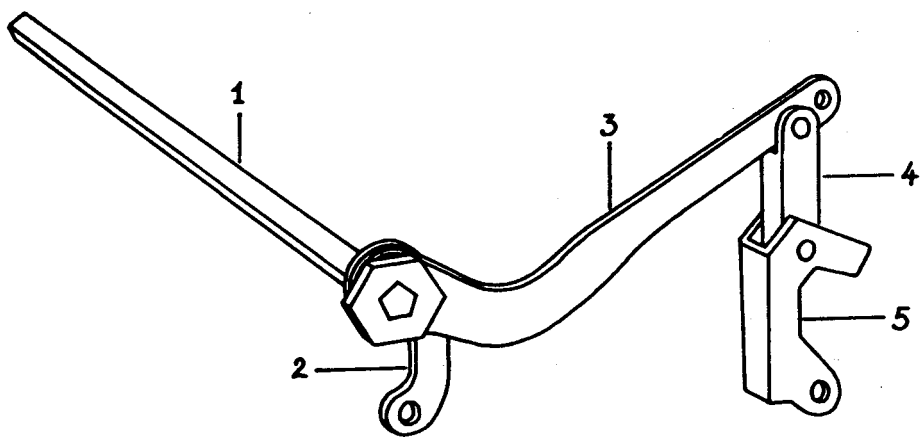


Figure 1. Mechanical buckle pretensioner.

#### Sensor part

The sensor is fully mechanical and is integrated with the mechanism that makes the pulling. It consists of five parts.

The different parts are configured in a way that the torque from the tensioned torsion bar spring creates the following arrangement of reaction forces acting upon the lever.



- 1. spring
- 2. rear leg
- 3. lever arm
- 4. upper leg
- 5. lower leg

Figure 2. Sensor part.

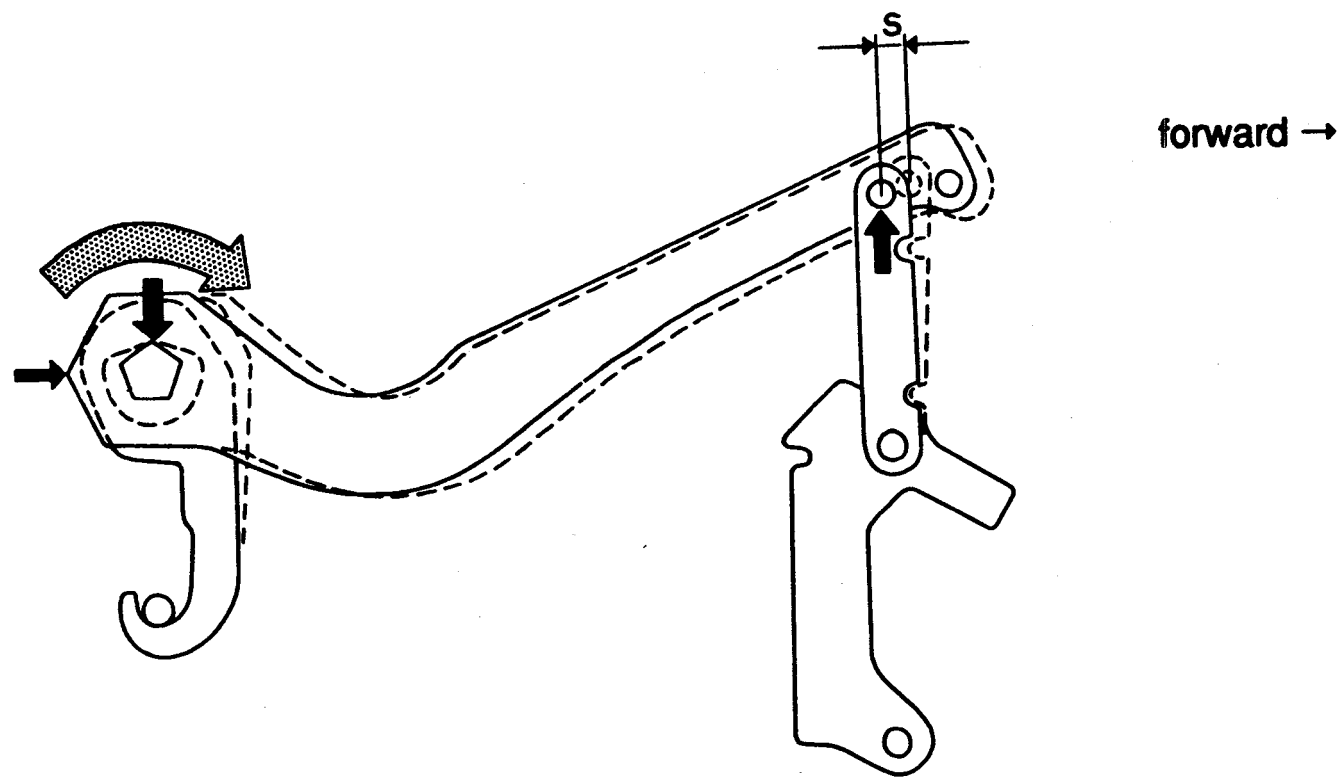


Figure 3. Reaction forces.

The lever arm is striving to move backwards but is prevented from doing so and is only allowed to move forward. The force needed to move the lever arm forward is in theory constant, but taking into account the bending of the torsion bar and some friction the force actually increases slightly. If the lever arm is moved forward a distance  $S$  mm the two legs, upper and lower, are positioned in a straight line and for an additional motion they will collapse. The pretensioner has then triggered and the pretensioning force is released to pull the buckle downwards. The sensor characteristics can easily be altered to suit various carpulses, only by changing the geometry of the legs.

A typical sensor force characteristic is shown in figure 4. The characteristic is chosen so that pretensioning will take place only when needed avoiding inadvertant triggering. A complete pretensioning has to be completed before the person (dummy) has moved 20 mm forward relative to the car during the impact. The low speed impact behaviour is shown by the two figures 5a and 5b. By following the full drawn line it can be seen that for a 9.3 km/h impact speed the lever arm doesn't reach the collapsing distance. It only moves 0.9 mm whilst at 12.3 km/h it collapses after 16 ms. The dummy (an unrestrained mass) has by this time moved only 3.2 mm. Thus it is evident that the sensor characteristic

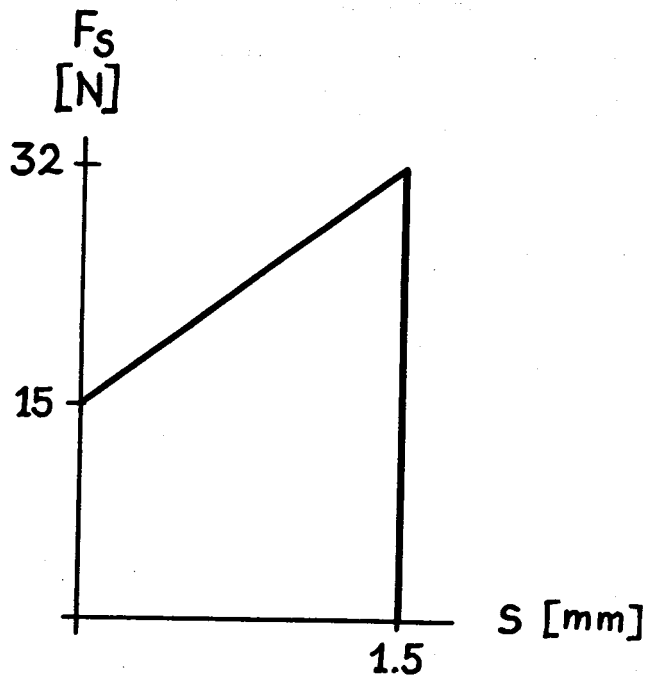


Figure 4. Sensor force characteristic.

“swallows” low energy/low speed pulses and triggers above a certain level. When you take into account that the pulling action takes a maximum of 10 ms, the pretensioning

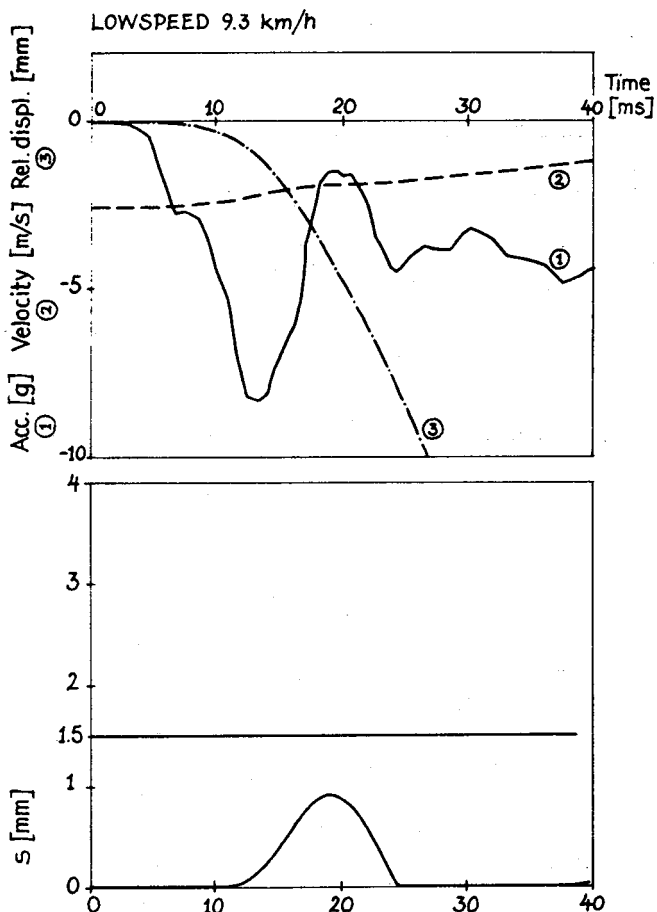


Figure 5a. 9.3 km/h impact.

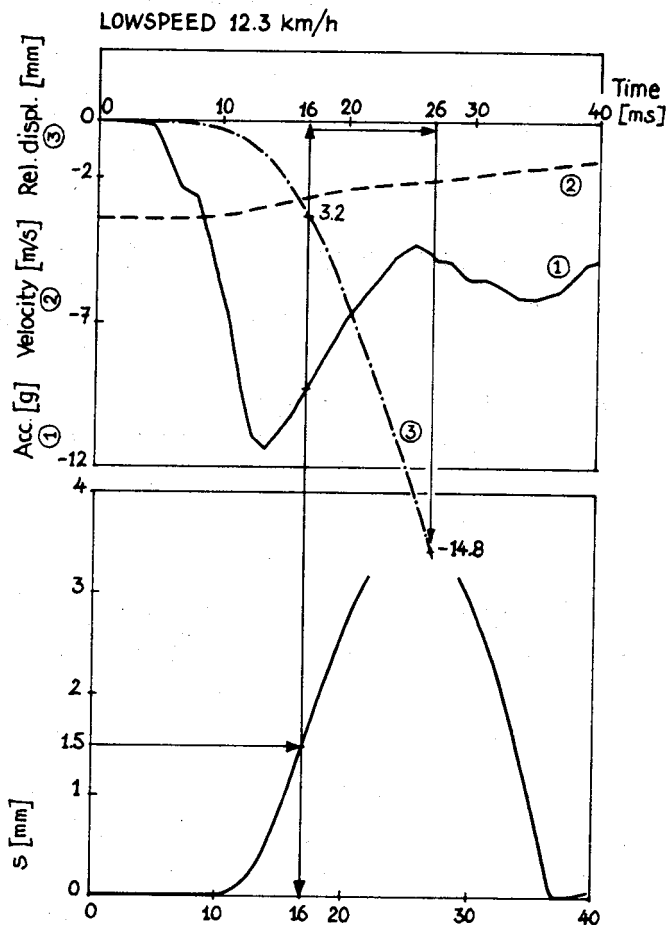


Figure 5b. 12.3 km/h impact.

in this case is completed after 26 ms. The dummy has moved 14.8 mm—this is well below the allowable 20 mm. The minimum triggering pulse for this setting was around 10 g.

The behaviour in high speed crashes is shown in figure 6a. The lever arm collapsing distance is reached after 4.8 ms—and full pretensioning is completed after 14.8 ms. By this time the dummy has moved 16.5 mm.

In an oblique crash the sensor only senses the frontal axis component of the deceleration. A comparison between a 0° and a 30° impact at 30 mph can be found in table 1. See also figures 6a and 6b respectively.

Table 1. Comparison of triggering in 0° and 30° frontal 30 mph impact.

	Triggering Time (ms)	Time to full Pretensioning (ms)	Dummy Motion (mm)
0°	5	15	17
30°	19	29	18

### Pulling part

The pulling part consists of a spring and a lever arm.

When the sensor part has collapsed the spring is free to pull the buckle downwards. The nominal torque of the

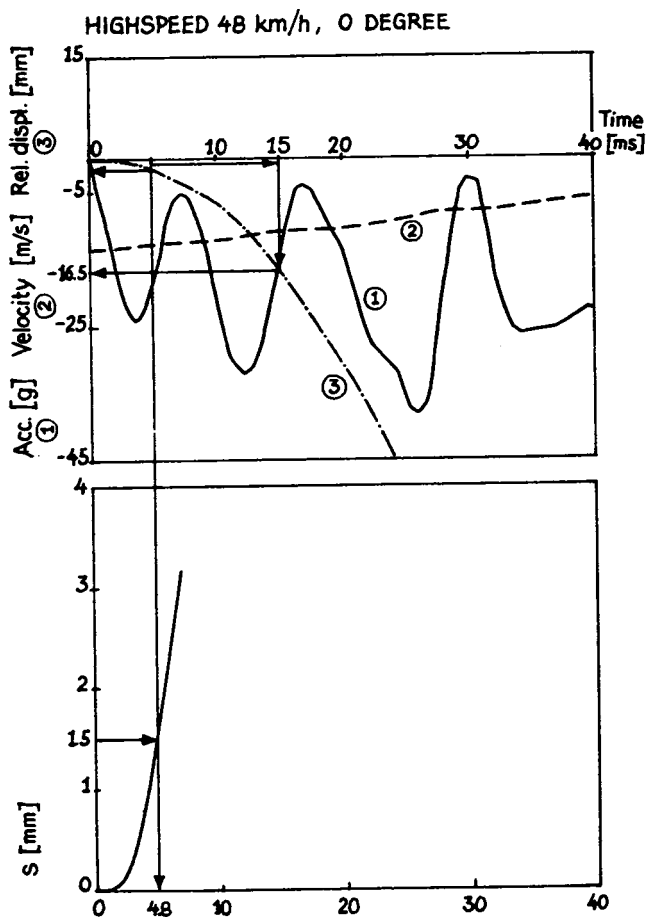


Figure 6a. 48.4 km/h 0° impact.

spring is 150Nm and the pulling force 1000 N. This force decreases to 40% when the pulling operation is complete. The force vs time characteristic is shown below.

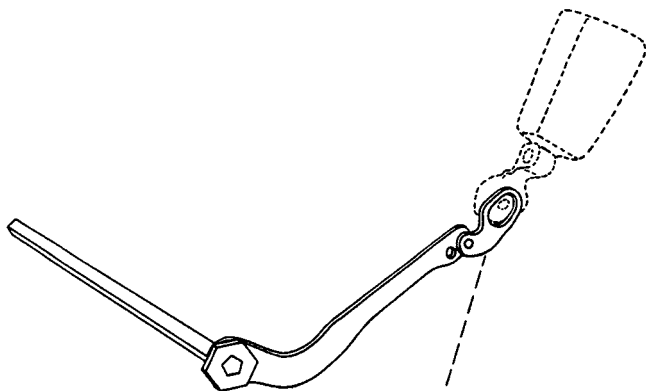


Figure 7. Pulling part.

### Locking part

The occupant restraint load is taken by the locking plate, which has a toothed element. It must be able to take the load imparted by a Hybrid II 95th percentile male dummy in a 40 mph impact. The locking plate is directly bolted into the seat. The load is thereby transferred to the normal seat attachment point.

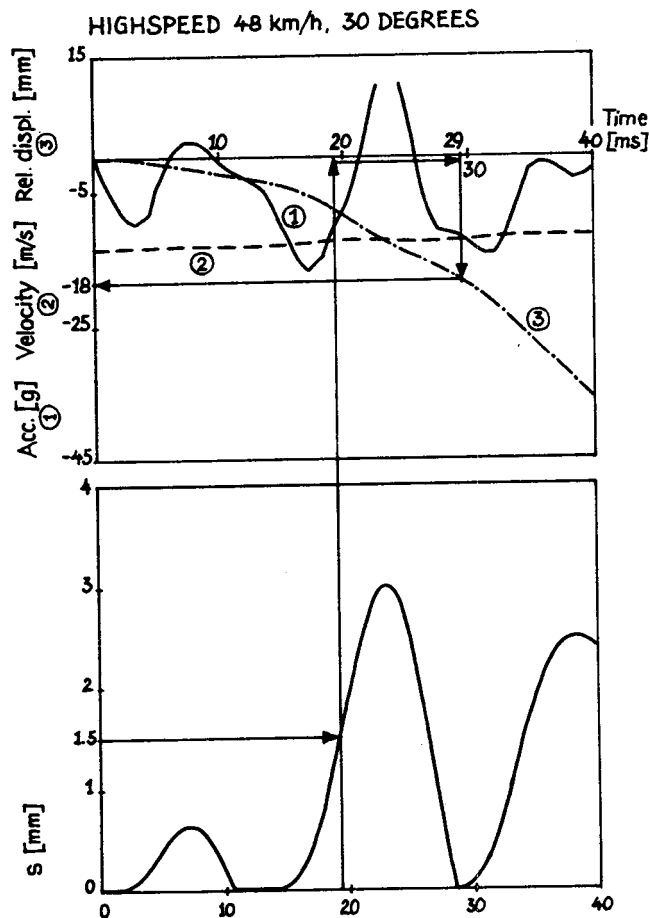


Figure 6b. 48.7 km/h 30° impact.

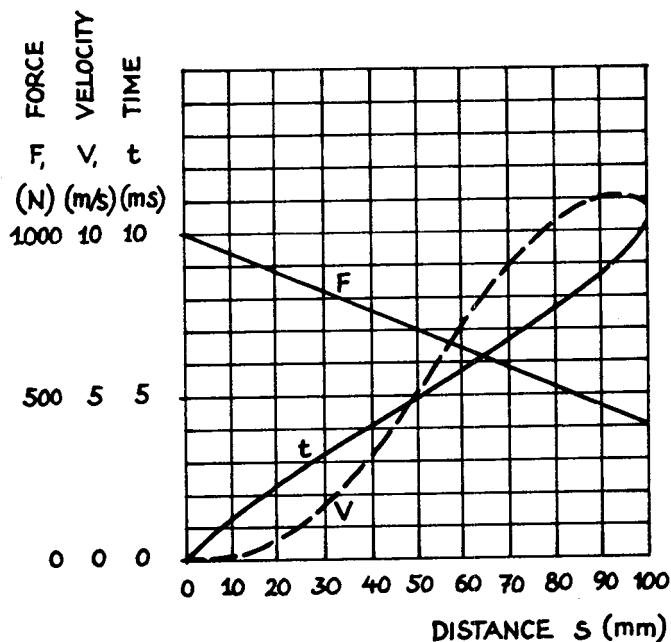


Figure 8. Force and torque characteristics.

### Test Equipment

The sled crash track facility at the Electrolux Autoliv R&D centre in Vågård Sweden uses a hydraulic

transmission system. The sled is accelerated over a 40 m distance. The maximum possible speed of the sled is 50

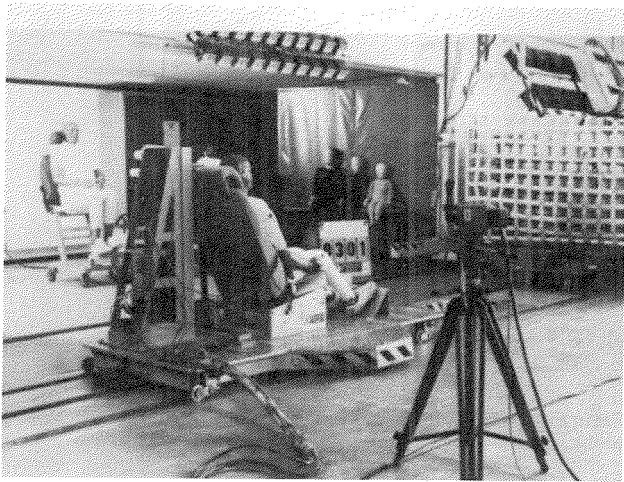


Figure 9. The Electrolux Autoliv crashtrack in Vårgårda, Sweden.

mph. Max weights that can be pulled are 1 ton at 50 mph and 2 ton at 40 mph.

The braking of the sled is achieved by the deformation of steel plates of different lengths and cross sections at different positions. Any carpulse can be accurately simulated by this brake arrangement. The sled data acquisition system consists of onboard amplifiers (max 54 channels possible) as well as an onboard data memory. The data are transferred after the test to a mini computer for processing. The amplifiers have a basic filtering of CFC 1000 and additional filtering is made numerically by the computer.

High speed cameras (max 3) are used for recording of for example dummy motion, webbing extraction and pretensioning action. Evaluation of the high speed films is undertaken using a filmscreen with a digitizer coupled to a personal computer. The software permits calculation of displacements, velocities and accelerations.

## Test Configuration and Test Parameters

A standard vehicle seat with a reinforced substructure able to withstand repeated dynamic tests was attached to the sled.

The belt geometry was equivalent to the front installation of a four door sedan car. See figures 10 and 11. The tests were run without dashboard or steering wheel.

The impact speed was  $35 \text{ mph (56,3 km/h)} \pm 0,2 \text{ mph}$  and the stopping distance  $585 \pm 20 \text{ mm}$ . The deceleration pulse was acc. to figure 12. An antropomorphic dummy, Hybrid II 50th percentile male, was used. The evaluation of test data was made in accordance with FMVSS 208.

To simulate belt slack a foam material of 30 mm thickness was inserted between the webbing and the dummy in the chest area and with two layers (60 mm) in the pelvis/abdomen area. The characteristic of the 30 mm foam was a

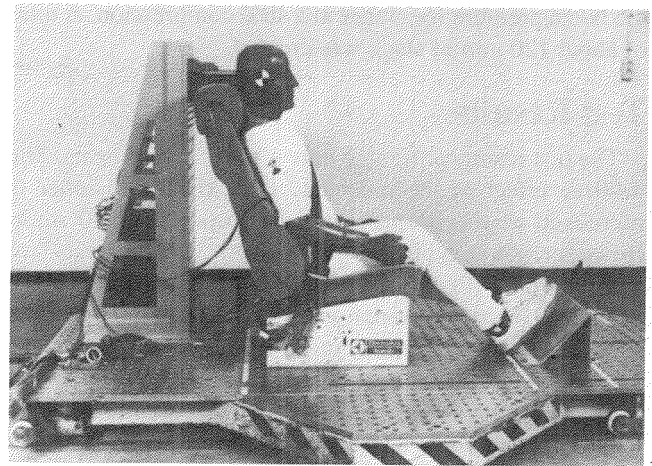


Figure 10. Side view.

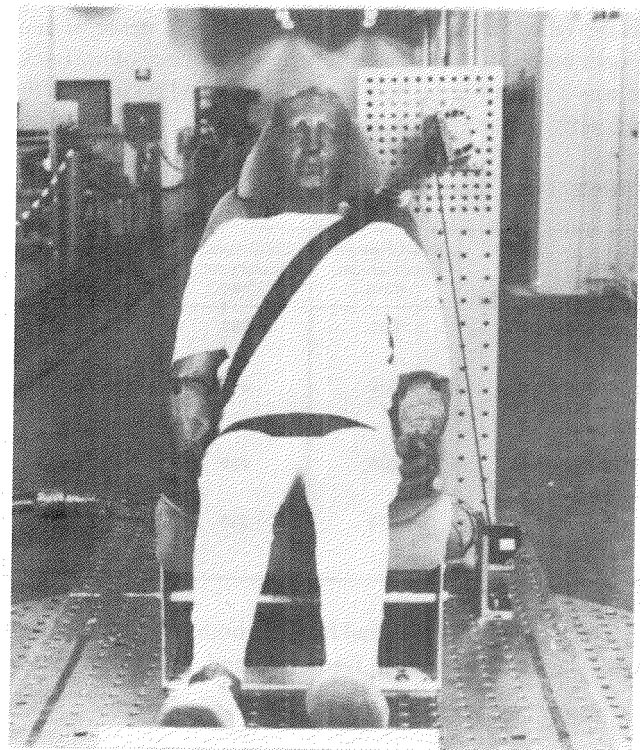


Figure 11. Front view.

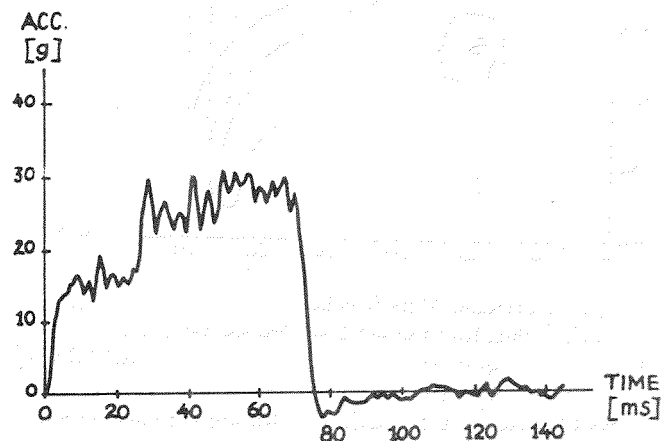


Figure 12. Sled deceleration pulse.

4.6 N/cm pressure resistance at a 40% compression. A total of about 120 mm of slack was created.

## Test Results

The test results presented here are for 35 mph tests. The positive effect of the mechanical buckle pretensioner is increased at this impact speed compared to 30 mph. However some typical figures from 30 mph tests are mentioned. With the same seat configuration and belt geometry as in the 35 mph tests the use of a pretensioner resulted in a typical reduction of HIC of about 25%. This was applicable to belts both with (120 mm) slack and without. The reduction of maximum chest acceleration (>3 ms) was about 4 g in both cases.

## Forward displacement

The displacements of head, chest and pelvis can be seen in the table below. The time to trigger the buckle pretensioner was 9–10 ms. The pulling down distance of the buckle was 35 mm for the belt with no slack and 65 mm for the belt with 120 mm slack.

Table 2. Head, chest and pelvis displacement.

	Head Forward Displacement (mm)	Chest Forward Displacement (mm)	Pelvis Forward Displacement (mm)
Std. three point belt. No slack.	600	350	265
Three point belt with buckle pret. No slack.	570	315	180
Std three point belt. 120 mm slack.	630	400	310
Three point belt with buckle pret. 120 mm slack.	590	325	220

The trajectory of the head for belts both without slack and with slack can be seen in figures 13 and 14.

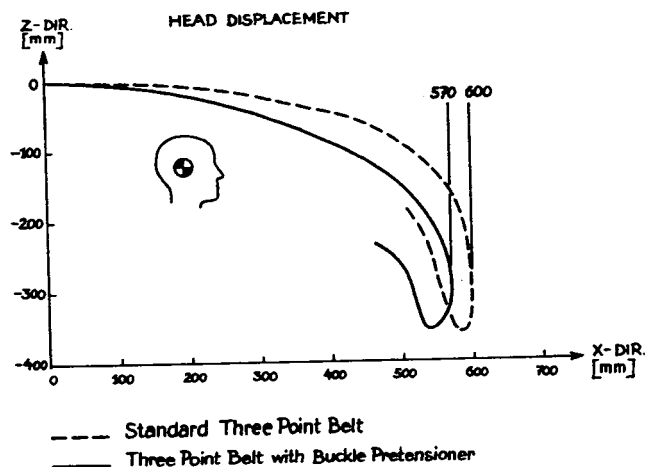


Figure 13. Head displacement. Three point belt without slack.

As expected the reduction in forward displacement is larger for a belt system with slack than for a corresponding

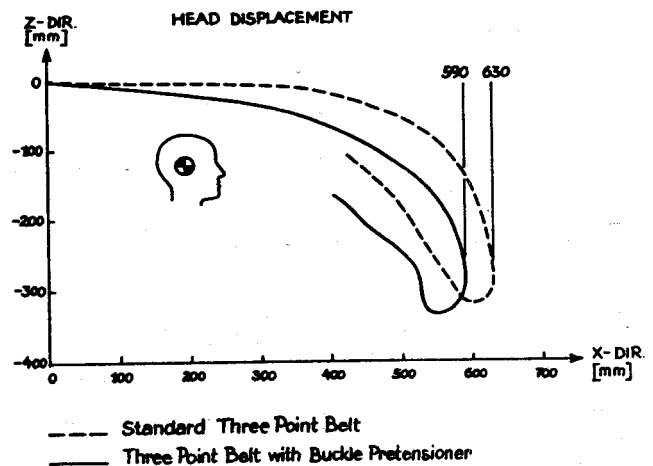


Figure 14. Head displacement. Three point belt with 120 mm slack.

one without slack. The reduction is also larger for the pelvis than for the head. For belts with 120mm slack the head forward displacement is reduced by 40mm from 630 to 590 mm and the pelvis forward displacement by 90 mm from 310 to 220 mm. This latter figure indicates how effective the buckle pretensioner is in preventing submarining.

As far as the head is concerned it is not only the forward displacement that is of interest but also the speed when for instance impacting the upper rim of the steering wheel. Figures 15 and 16 show the velocity of the head versus forward displacement.

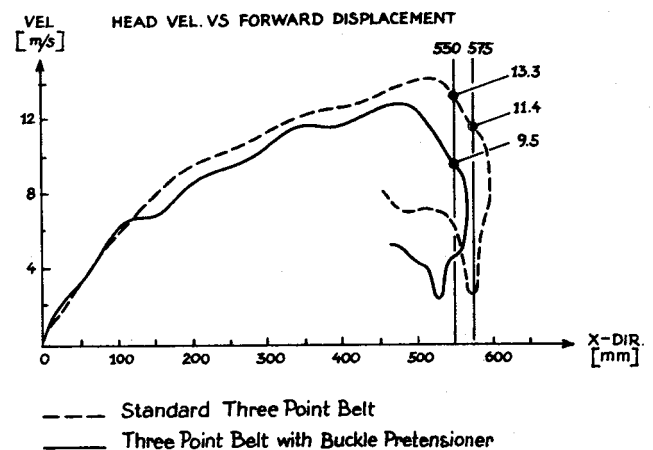


Figure 15. Head velocity versus head forward displacement. Belts without slack.

If the head impacts the steering wheel after a 550 mm forward movement the velocity is 13.3 m/s for the standard three point belt with no slack and only 9.5 m/s for the belt with a buckle pretensioner. If the steering wheel is another 25 mm forward (at 575 mm) the impacting velocity is 11.4 m/s for the standard belt whilst head contact will not occur in the case of a belt with a pretensioner. The test results for belts with slack show the same effect. The buckle pretensioner is therefore effective in reducing the impact of the head into the steering wheel.

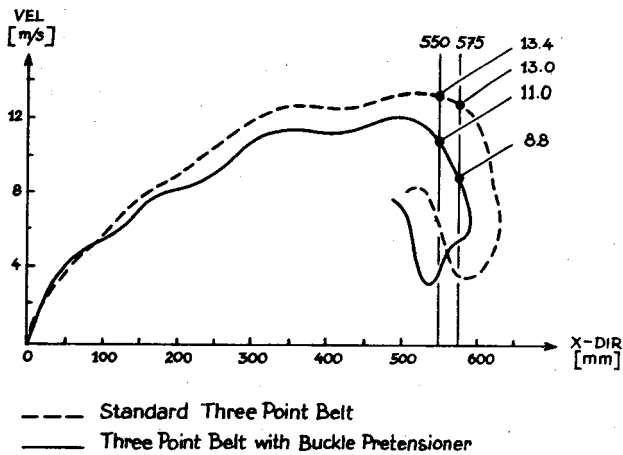


Figure 16. Head velocity versus head forward displacement. Belts with 120 mm slack.

### Head injury criteria and chest acceleration

Figures 17 and 18 show values for head injury criteria (both HIC and HIC<sub>36</sub>) and chest acceleration for the different cases.

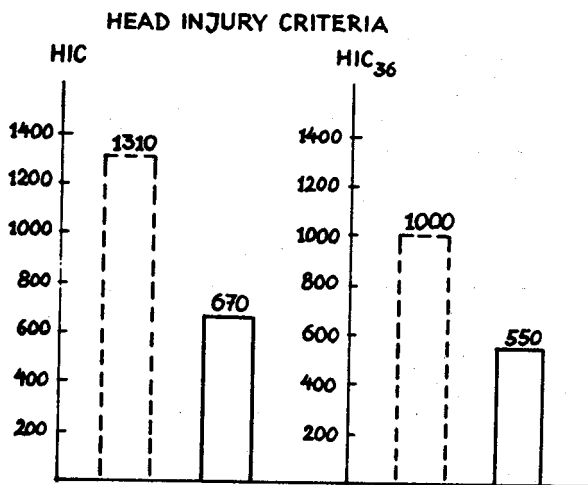


Figure 17. HIC and chest acceleration. Belts without slack.

The reduction of HIC is considerable—about 50% in all four cases. The largest reduction, from HIC 1880 to 870 (-54%), was achieved with the belt with 120 mm slack. The corresponding figures for HIC<sub>36</sub> were 1220 and 670 respectively.

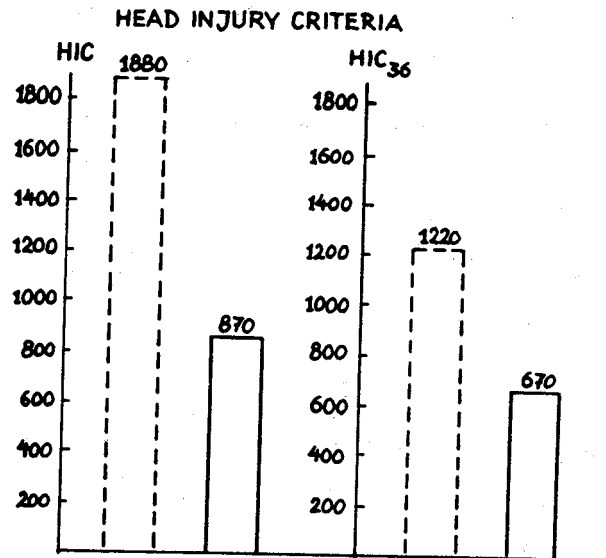


Figure 18. HIC and chest acceleration. Belts with 120 mm slack.

There is also a significant reduction of max chest acceleration (>3 ms). The reduction was from 49 g to 43 g for belts with no slack and from 55 g to 51 g for belts with slack.

### Chest belt force

The curves for the chest belt forces in figures 19 and 20 show that the dummy is arrested earlier (about 8–10 ms) in

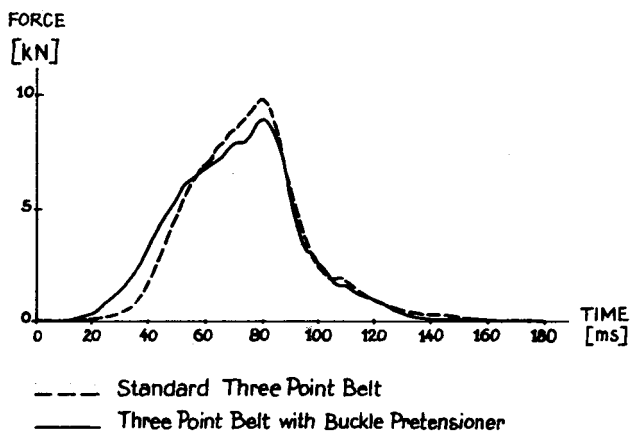
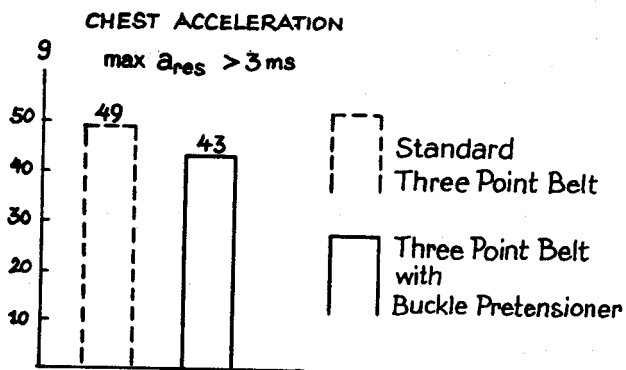


Figure 19. Chest belt force. Belt without slack.

belts where the buckle pretensioner has worked. The slope of the curves are lower and there is a reduction in peak values.

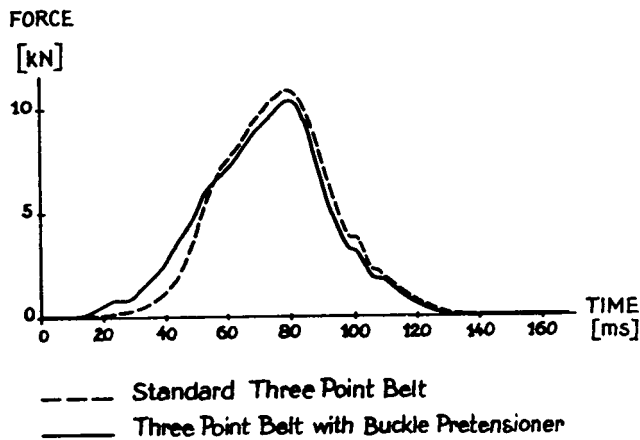


Figure 20. Chest belt force. Belts with 120 mm slack.

## Summary and Conclusions

The mechanical buckle pretensioner acts with a high initial spring force of 1000 N. It can trigger and complete the pretensioning operation before an unrestrained mass has moved 20 mm forward. The sensor threshold level can be set so that inadvertant triggering can be avoided.

Test result show that the use of a buckle pretensioner will mean a less severe head impact with the steering wheel.

The HIC value can be reduced significantly. In 35 mph barrier tests a reduction of HIC by 50% to less than 1000 was achieved with 120 mm of initial slack in the belt.

The pelvis displacement was decreased by up to 90 mm, thereby reducing the risk of submarining.

The belt with a pretensioner is loaded quicker (about 10 ms). This means lower peakloads and reduced maximum chest accelerations.

It can be concluded that the mechanical buckle pretensioner is a cost effective device to supplement the standard three point belt.

## Estimating Effectiveness of Increased Seat Belt Usage on the Number of Fatalities

F. Wegman, J. Bos and F. Bijleveld,  
SWOV Institute for Road Safety Research,  
The Netherlands

### Abstract

Research results indicate a wide variation in belt use effectiveness (reduction of the number of casualties in percents of belt use increases from 0% to 100%). Results are reported from an increase to a decrease of more than 50%.

Accepting some variation in different countries due to different accident circumstances, weakness in research designs could form a part of the explanation of this variation.

Analyses have been made of trends in fatality rates of car occupants in three European countries: the Netherlands, the Federal Republic of Germany and Great Britain. The aim was to assess seat belt use effectiveness using common, plausible assumptions.

It turned out that is not recommendable to use the before and after comparison, because it is hard to assume that there are no other influences than changes in seat belt use. Before and after comparison with a control group is a—methodologically seen—strong design but its application could be unnoticed weak, despite “plausible” assumptions. So a dangerous design. The use of time series analysis is recommended but the nature of the seat belt intervention and other influences and their course in time have to be known. Specific and careful research and good data are needed.

On the basis of the actual knowledge we think that the best estimation of belt use effectiveness is 35–40%.

### Introduction

The Dutch government decided in 1986 to strive for 25% less casualties in the year 2000 than in 1985. To arrive at this quantitative aim, a policy was formulated in which some “profitable priorities” are the central themes. One of these priorities is the promotion of seat belt use. In figure 1 the development is given of belt use in the Netherlands. In June 1975 it became mandatory for front seat occupants to use the belt in cars built after 1970. Between 1975 and 1979 the presence of belts increased from 70% to 100%.

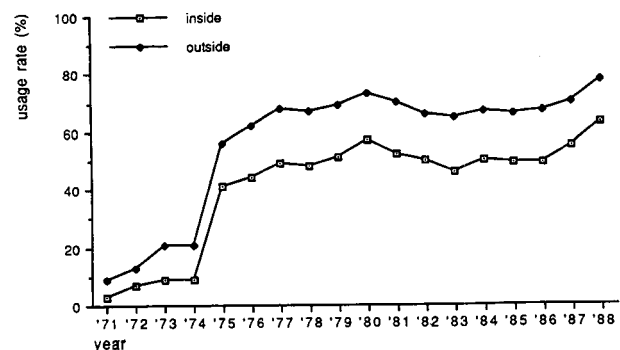


Figure 1. Usage rates of seat belts in the Netherlands inside and outside built-up areas.

Before mandatory use the users' percentage was 13% inside and 28% outside built-up areas. Within one year the

percentages increased to 49% respectively to 67%. Until 1986 the use remained on the same level, but since 1987 it has increased. There are clear indications that this increase is due to (regional) policy in the fields of information campaigns and police enforcement (Gundy 1988, and Varkevisser & Arnoldus 1989). The users' percentages were 63% inside and 77% outside built-up areas in 1988. The percentages are still considerably below those of Great Britain and the Federal Republic of Germany (see figure 2).

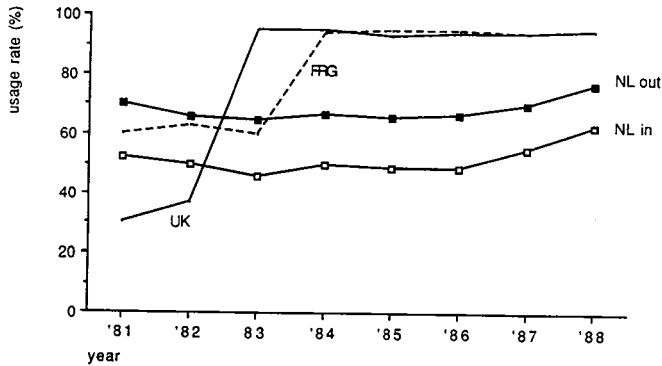


Figure 2. Usage rate (%) of seat belts in the Netherlands, the Federal Republic of Germany and Great Britain.

Belts reduce the risk and the severity of injuries for car occupants in accidents. Based on theoretical considerations this has been proven by laboratory tests and by in-depth studies. Belts prevent the ejection of car occupant and diminish the risk of being harmed by the car's interior. The possibility of a belt causing severe injuries is extremely small. An individual occupant thus runs less risk to get (severely) injured in an accident, but it is still a question how much the number of killed and severely injured occupants would decrease if more of the drivers and passengers would use the belt. This is specially interesting when introducing mandatory belt use. We define effectiveness of belt use as the reduction of the number of casualties in percents if belt use increases from 0% to 100%.

It remains a question how much the increase of belt use has contributed and will contribute to the arrival at the goal of -25% by 2000 in the Netherlands. How many casualties are prevented if belt use rises by 1%? Some researchers have indicated that seat belts are not that effective, and Janssen recently (1989) drew the conclusion that belt use laws have not been proven to be effective. The study was based on a time series analysis of the numbers of killed car occupants per kilometre driven from eight Western European countries.

Bos's study of literature (1989) on the belt use effectiveness led to three conclusions:

- effectiveness is reported from an increase of casualties to a decrease of more than 50%, so a wide range;
- sometimes the research methodology was not quite impeccable;
- most researchers seem to wrestle with the

problem of an "effectiveness below expectation".

The aim of this contribution is to search for the explanation(s) of the great differences in belt effectiveness, shown in the various reports.

### Decrease of the number of casualties by belt use

Set the number of casualties at 0% use at  $No$ . Set the percentage of belt use at  $Ub$  and the number of casualties at  $Cb$ . If the belt use effectiveness is  $e$  the relationship between these quantities is:

$$Cb = (1 - Ub) No + Ub (1 - e) No \quad (1)$$

or the number of casualties in a before period  $Cb$  is the sum of the number of casualties not using the belt and that of using it. Equation (1) can be rewritten:

$$Cb = (1 - Ub.e) No \quad (2)$$

If belt use would increase later to  $Ua$ :

$$Ca = (1 - Ua.e) No \quad (3)$$

The expected reduction of casualties is then:

$$Rc = \frac{Cb - Ca}{Cb} \quad (4)$$

This equation can be transformed to:

$$Rc = \frac{(Ua - Ub)e}{1 - e.Ub} \quad (5)$$

The relationship between  $e$  and  $Ua$ , so the relationship between belt use effectiveness and users' percentage in the "after period" can be rendered on the basis of equation (5):

$$e = 1/(Ub - (Ub - Ua)/Rc) \quad (6)$$

In figure 3, where  $e$  and  $Ua$  from several studies are compared, a great variation is shown. It is possible of course

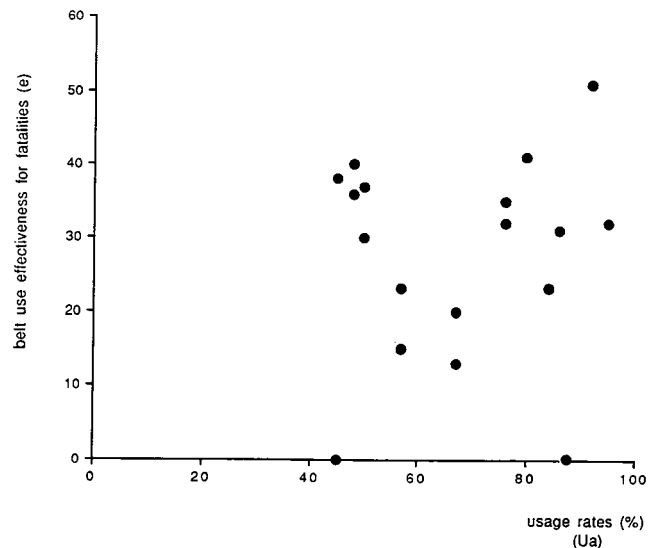


Figure 3. Belt use effectiveness for fatalities (e) and usage rates (Ua) reported in different studies.

that seat belt use laws in different countries have a different effect because circumstances and types of accidents vary between countries. It is known e.g. that belts are more effective in head-on collisions than in head-tail or side collisions. If a truck enters the car compartment the belt is hardly effective. If the distribution of the different types of accidents vary, the effectiveness of the belt will vary too. But before conclusions are drawn the validity of the results has to be studied.

### Surveys on belt use

Nearly all studies on the effectiveness of belt usage use sample data of belt use among traffic participants, not of injured road users. Dutch accident registration does not have data on belt use among casualties, a problem of many more countries. Then it is known how many car occupants after belt use became mandatory, use the belt (direct aim of the law!) and this number may be compared to the number of the before period, but often it is not known how many of the involved car occupants really used the belt and consequently are not or less severe, injured (indirect aim of the law!).

An important question is how the sample was made among road users. It is important because it is a known fact that not all drivers use the belt everywhere, always and on all roads. In the Netherlands this has been established as well (Varkevisser & Arnoldus, 1989). The belt appears to be less used at night than by day (Noordzij, 1988). This fact is not taken into consideration in the yearly national samples on belt usage (Varkevisser & Arnoldus, 1989). It might mean a slight (there is little traffic at night) overestimation of belt use and consequently under-estimation of the belt effectiveness. The sample must also be representative for traffic on the different kinds of roads, an indication of which was produced only recently in the Netherlands, though observations have been made for years.

Another important point is the development of belt use in time. If there is an obvious development it must be possible to observe it like that, which means regular sampling, e.g. every month. If these data are not known interpolation is necessary, with all its uncertain consequences. The importance may be shown by data from 4 US states (Lund et al., 1987). They show that belt use decreased strongly in one year, but it is not known whether this was gradually or immediately after the introduction of mandatory use.

Monthly sampling proves that belt use increases, even before it is mandatory. The increase in belt use before the introduction of the mandatory use and the decrease after a period of great use immediately after it has become mandatory have to be known to prevent over- or under-estimation of the effect. It appears not to be usual to report on the details of observations of belt use, even though it is necessary if only to avoid too precise estimations of belt effectiveness.

### Methodology

To determine the reduction of the number of casualties due to the increase of belt use some usual problems have to

be solved with the research design: the number of casualties has to be determined after the increase of belt use and this number has to be compared to the estimated number if belt use would not have changed. Besides it has to be shown that this change is caused by the increase of belt use and cannot be otherwise explained.

Mandatory belt use offers profitable possibilities from the research viewpoint because it has always caused a considerable increase of belt use in a short period of time (Vaaje, 1986). This situation enhances the possibilities to find a significant effect and reduces effects of other (disturbing) influencing factors.

A number of possible research designs:

1. A comparison is made between numbers of casualties where the belt can be effective and where it can not. It means a comparison of numbers of casualties of front seat occupants of cars before and after the introduction of the belt use law.

2. The number of casualties among front seat occupants of cars before and after the introduction of mandatory use is compared to a control group. This is to correct for other developments between the before and after study periods. There are two possibilities for the composition of the control group: the number of car occupants in a comparable area where the law was not changed or the number of casualties not influenced by the mandatory use.

3. A more differentiated following (than just before and after) of the development in time of numbers of casualties among front-seat car occupants and a looking for a trend breach—after a sudden strong rise of belt use—in the numbers of casualties. Here too a control group may be used.

In all three designs it is recommendable to not use the absolute numbers of casualties as a criterion, but to relate them to driving distances to make it possible to correct for changes.

Recently a number of overviews was made of research on the effectiveness of safety belt use laws (e.g. Hedlund, 1986; and Campbell & Campbell, 1986). In Bos' (1989) study the strong and the weak methodological aspects of the various research designs are given.

The methodological aspects of the various designs will be discussed here on the basis of data from three European countries: the Federal Republic of Germany, Great Britain, and the Netherlands. These countries were selected because they all have mandatory belt use laws and good and ready information.

The development of the fatality rates (number of fatalities in cars per kilometre driven) is given in figure 4 for the three countries. It would have been better to use kilometre travelled, but these data are not available in a good enough quality. In the Netherlands the seat belt use law became effective in June 1975. In the Federal Republic of Germany two dates are important: from 1 January 1976, safety belt use is mandatory and from 1 August 1984, non-use is

punishable. In Great Britain belt use became mandatory in February 1983, after some earlier efforts.

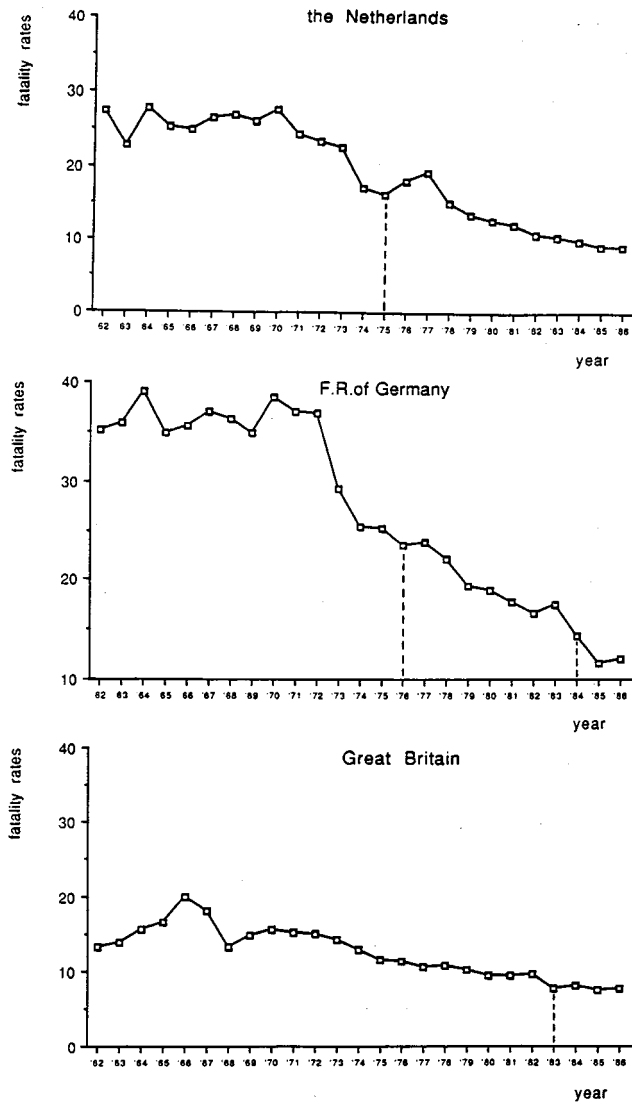


Figure 4. Fatality rates for car occupants in The Netherlands, Federal Republic of Germany and Great Britain and indicating introduction of mandatory seat belt usage.

### Before and after comparison

In the three countries it is easily possible to compare the fatality rates before and after the introduction of the law. If these rates would not be influenced by other factors the comparison gives the effect of the law. First an estimation has been made assuming a linear trend in the before and after period. Analysis of variance turned out this was a wrong assumption. The results given in table 1 are based on comparisons of the mean values. The variation in the results per country if longer or shorter before and after periods are taken into account, and compared between the countries shows the unlikelihood of the results. The Dutch data make it reasonable to suppose that there were more influencing factors, specially the decrease from 1973 to 1974 which will have been influenced by the energy crisis: speed limits were introduced on the Dutch roads as a consequence of the crisis

and by the end of 1973 a law became effective on drunk driving. The conclusion may thus be drawn that it is impossible to assess this result to the belt use law in the Netherlands, a control group is needed.

Table 1. Effects of seat belt usage increase from  $U_b$  to  $U_a$  on a reduction of fatalities (Rf) and seat belt effectiveness (e) in The Netherlands, the Federal Republic of Germany and Great Britain based on before and after comparison (n.s., not significant, \*significant at 95%-level).

in %	NL		FRG		UK	
	1 year	4 years	1 year	4/2 years	1 year	4 years
Belt usage before ( $U_b$ )	15	11	60	60	40	40
Belt usage after ( $U_a$ )	53	55	95	95	95	95
Reduction of fatalities (Rf)	+5	-25	-33	-34	-20	-20
Belt use effectiveness (e)	+13	-53*	-60*	-62*	-32*	-32*
	n.s					

The German data show a reasonably stable situation in the period of the introduction of the "Verwarnungsgeld" in 1984. The length of the period considered hardly influences the calculated effect. If the belt use law were the only influencing factor the effectiveness would be ca. 60%.

In Great Britain also the introduction of the belt use law took place in a relatively quiet period. If no other influences were to be found, which seems to be indicated by the overview of measures/influences a reasonable estimation of the belt use law effectiveness is found here: -32%.

If we assume the safety belt use effectiveness to be comparable in all three countries and see the results, we have to conclude that other factors have influenced the results. The uncertainty cannot be eliminated in this research design. In general this design must be called methodologically weak, because it is hard to assume that there are no other influences than safety belt use. Because we often cannot "explain" developments in numbers of fatalities (related or not related to exposure) it is not recommendable to use this design in research on effects of measures.

### Before and after comparison with a control group

The first possibility is to find a control group within the country where the law became effective. We compare e.g. the number of casualties on the front seat of cars to the total number of casualties. In the year the law became effective this ratio has to go down, a continuing trend if belt use does not change.

For the three countries the ratio of fatalities in cars compared to the total number was calculated on the basis of an estimation from the past. For the Netherlands a backward estimation was made as well. This estimation is compared to the actual number and then it is determined whether there was a significant difference. For all three countries the results indicate that in this way no significant differences have been found.

With this method the chance seems to be very small to find any significant difference.

An other drawback of this method could be the idea that belt users behave more dangerously, which may cause more casualties among the "third party". Theoretically this phenomenon (an example of the risk compensation theory) cannot be discarded, but practically little evidence was found in the framework of belt use (Evans et al., 1982; Lund & Zador, 1984; O'Neill et al., 1985; OECD, 1989).

A second possibility in this design is to compare fatality rates before and after the introduction in countries to other countries with the same trend in fatality rates. This method can be used for the three countries involved, i.e. the third country can be compared with the other two separately or on average. The results of this calculation are given in table 2.

**Table 2. Fatality rates after the introduction of the seat belt laws (observed) compared with fatality rates using trend in other countries as control (estimated) (n.s. not significant, \*significant at 95%-level).**

	Observed	NL	FRG	UK	Comb.	Rf	e
		Estimated					
The Netherlands	16.4	-	15.1	16.3	15.5	+ 6%	+13% n.s
F.R. of Germany	11.8	14.4	-	14.8	14.6	-19%	-42%*
Great Britain	7.7	7.5	7.3	-	7.4	+ 4%	+ 7% n.s

It would mean for the Netherlands and Great Britain that introduction of mandatory belt use would have ended in an increase of the fatality rate, and for the Federal Republic in a significant reduction of ca. 20%, realizing the introduction date in the second half of the year.

Summarizing we conclude that though the research design—before and after comparison to a control group—is a strong design theoretically seen, its application has practical problems asks sometimes for unverifiable assumptions and leads to such results that the method must not be recommended for this use.

### Time series analysis

In literature many research reports appear to have used time series analyses. This design is particularly indicated if:

- The (after) period is (too) short; seasonal effects e.g. then have to be admitted and estimates in this respect necessitate assumptions;
- Within the (after) period other interventions take place at different moments; through time series analyses the various effects may be determined, but assumptions have to be made on the nature of the interventions and on their course in time; simultaneous interventions need a control group.

On the basis of Bos's literature study we conclude that two researchers—from a methodological viewpoint—may be called very strong. They report on the reduction of the number of casualties in Great Britain after the introduction of the belt use law as of 1 February 1983, using time series analyses. Scott & Willis (1985) report on the effects in the first year, and Harvey & Durbin (1986) have studied almost

two years. Safety belt use rose from 40% by the end of 1982 to 95% from February 1983. Monthly data show that this percentage remained at this high level. Scott & Willis use a log-linear regression, in which influences of trend and seasons are admitted. The method assumes that the linear series has the same trend in the before and in the after period. When the error plot is inspected—with differences between observed figures and numbers fitted by the model—the opposite of this assumption would not appear. A dummy variable is used, being 0 in the before and 1 in the after period: intervention. Changes in the numbers of casualties are determined for various categories of road users. Scott & Willis conclude that the number of fatal casualties among drivers decreased by some 20% and among other car front seat occupants by 30% thanks to belt use. An average reduction of 25% means a belt effectiveness of 38%. Scott & Willis cannot exclude the possibility that part of this reduction is due to another method of testing on drunken driving, introduced in 1983.

Harvey & Durbin execute a time series analysis, structuring time series modelling, provided with the possibility of an intervention analysis. The trends before and after do not have to be the same now, as they have to be for Scott & Willis.

Harvey & Durbin conclude that the number of casualties (fatalities and severely injured) was reduced by 25% for all car front seat occupants. After introduction of the seat belt law, the number for other road users did not change. The results of the two researchers agree very well and make us conclude that an estimation of a belt use effectiveness of ca. 35–40% at this moment is the best to be made. This conclusion is supported by a report from the USA, where Evans determined belt use effectiveness in his own elegant way. He did not use time series analysis.

Evans developed a method, the "double pair comparison method", to determine the effectiveness of belts for an accident population of a jurisdiction where it is known whether a belt was used in an accident. This possibility is offered by FARS (Fatal Accident Reporting System). Accidents with at least one fatality are studied here. In Evans' method the criterion is used of the number of killed drivers with belt related to the number of killed passengers without belt. This ratio is related to the reference proportion of numbers of killed drivers and killed passengers, when none of them used the belt.

Evans concludes that if all car front seat occupants not using a belt would start using one and they would not otherwise change their behaviour the number of fatalities would decrease by ca. 43% (Evans 1986, 1988).

A research design using a time series analysis seems to offer most possibilities to determine the effects of the interventions. In the British circumstances this possibility was enhanced by the high rise of belt use in a short period of time (in one month) in an otherwise quiet period regarding accident development. This situation was not so in the middle of the seventies when a number of European countries introduced mandatory belt use. It is a question whether a time

series analysis then also can detect effects of measures.

### State-space model description

On the data bases of car occupants fatalities of the Netherlands, Great Britain, and the Federal Republic of Germany a number of analyses was executed with a model that may be described as:

Set the fatality rate in one year at  $y_t$ . This number is equal to the number of the year before that,  $y_{t-1}$ , plus a certain trend in that year ( $a_t$ ), in a formula:

$$y_t = y_{t-1} + a_t$$

The model used now tries to estimate value for  $a_t$ . Taken into account are the development of the expectation error of  $y_t$  from  $y_{t-1} + a_t$  and the observation error in  $y_t$ . The estimates for  $y_t$  together results in a filtered estimation for  $y_t$ , which together with the trend at time  $t + 1$  is used to estimate  $y_{t+1}$ . For time  $t = 0$  all available information is used, i.e. the observed value of that year only, to determine the filtered value.

In the analysis the presence of two effects is assumed. First an effect to be indicated as "energy crisis effect" from 1974, though it is not clear which caused the sudden steep decrease of the number of casualties per kilometre driven. The analysis resulted in the description of the observed values with the following model: before 1974 the development was linear, in 1974 a trend breach took place, and after that there was another linear trend. To compensate for belt use a second intervention was added, in which it was assumed that a second breach occurred in the year mandatory belt use was introduced. They result in value  $b_t$ , in a formula:

$$y_t = y_{t-1} + b_t$$

For the combined interventions:

$$y_t = y_{t-1} + a_t + b_t$$

Because it is not well known in which way the energy crisis effect influenced the development of traffic safety we checked what the effects would be with two assumptions, giving the extremes. The first assumption is that the effect would lead to a one-year decrease of fatality rates, and in the other to a permanent one. The effect of increased belt use on the development of the number of casualties was calculated in either case. The results are given in figure 5. The model estimates the most suitable intervention on the basis of the assumptions used. The results of the three countries show that belt use would result in a decrease of casualties, depending on the assumption, (in a one-year effect) or in an increase in case of a permanent effect of the energy crisis (figure 5).

Reality will be in between but the variation of the results and the uncertainty on the nature of the effect of the energy crisis is so high that this method cannot indicate the effectiveness of safety belt use laws, especially not if both interventions happen to coincide like they did in the Netherlands.

The Netherlands: number of killed car occupants per traffic volume

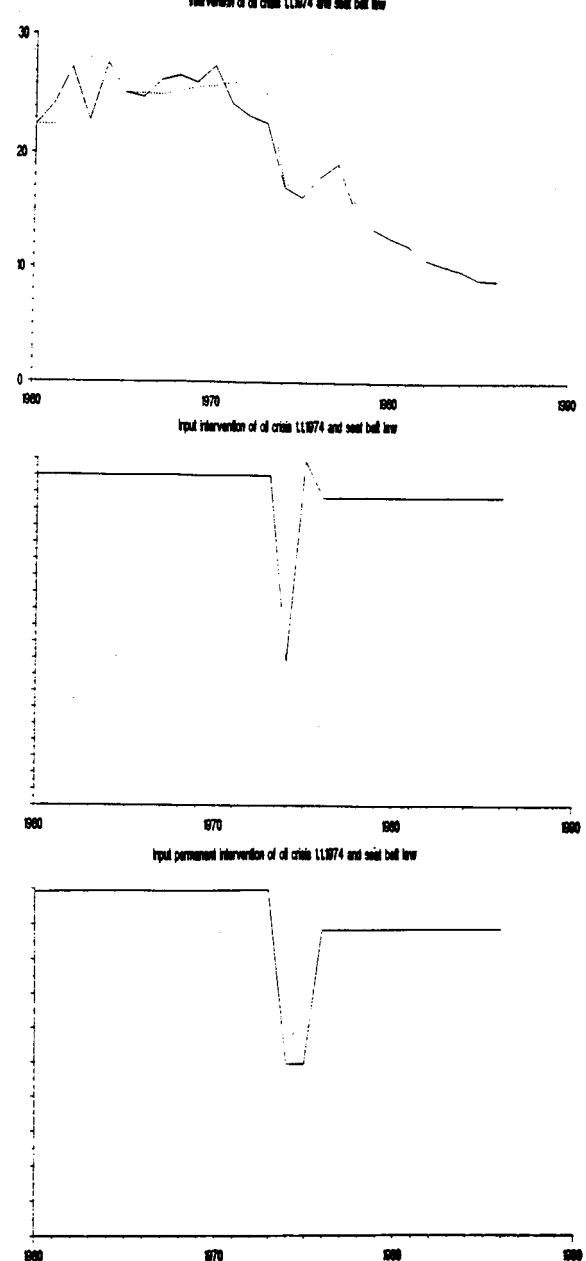


Figure 5. Normation of the derivative of the model estimation of the fatality rate, given an one year or permanent intervention of the energy crisis and an introduction of a seat belt law intervention.

### Conclusions and recommendations

(1) Safety belts reduce the risk and the severity of injuries in collisions. If an individual runs less risk of (severe) injuries in a collision it still is a question how much the number of casualties is reduced if more car occupants use the belt. Study of the literature shows that the dispersion in effectiveness is enormous. The research designs and the assumptions used therein are questionable. They seem to not be taken too lightly.

(2) Research on the effectiveness of belt use can be done with the following designs: before and after comparison;

before and after comparison with control groups, and with time series analysis. To illustrate our warning not to take the assumptions too lightly three designs were applied on the data of the Federal Republic, Great Britain, and the Netherlands.

(3) Before and after study is a weak design from the methodological viewpoint, because it must be assumed that no other influences play a role but changes in seat belt use. The results show an enormous spread. It is recommended not to use this design.

(4) Before and after comparison with control groups is a strong design. The selection of the control group is essential. The results show that seemingly plausible assumptions regarding the control group result in different output. Therefore this is a dangerous design.

(5) With time series analyses effects of measures may well be determined, if the nature of the interventions and their course in time can be determined. Specific and careful research on process variables (belt wearing rates) and the availability of accident data of good quality are needed.

(6) On the basis of the actual knowledge we think that the best estimation of belt use effectiveness is 35–40%.

## References

- Bos, J. (1989). Effektiviteit van autogordels. Een literatuurstudie. SWOV, Leidschendam, 1989.
- Campbell, B.J. & Campbell, F.A. (1986). Seat belt law experience in four foreign countries compared to the United States. University of North Carolina, Chapel Hill, 1986.
- Evans, L., Wasielewski, P. & Von Buseck, C.R. (1982). Compulsory seat belt usage and driver risk-taking behavior. *Human Factors* 24 (1), 1982.
- Evans, L. (1986). The effectiveness of safety belts in preventing fatalities. *Accid. Anal. & Prev.* 18 (1986) 3.
- Evans, L. (1988). Examination of some possible biases in double pair comparison estimates of safety belt effectiveness. *Accid. Anal. & Prev.* 20 (1988) 3.
- Gundy, C.M. (1988). The effectiveness of a combination of police enforcement and public information for improving seat-belt use. In: Rothengatter, J.A. & De Bruin, R.A. (eds). *Road user behaviour, Theory and research*. Van Gorcum,

1988.

Harvey, A.C. & Durbin, J. (1986). The effects of seat belt legislation on British road casualties: A case study in structural time series modelling. *Journal of Royal Statistical Society* 149, Part 3, 1986.

Hedlund, J. (1986). Casualty reductions resulting from safety belt use laws. In: *Effectiveness of safety belt use laws: A multinational examination*. National Highway Traffic Safety Administration, 1986.

Janssen, W.H. (1989). Het effect van gordelwetgeving op slachtofferaantallen in een aantal West-europese landen. IZF 1989–13. Instituut voor Zintuigfysiologie TNO, Soesterberg, 1989.

Lund, A.K. & Zador, P. (1984). Mandatory belt use and driver risk taking. *Risk Analysis* 4 (1984) 1.

Lund, A.K.; Zador, P. & Pollner, J. (1987). Motor vehicle occupant fatalities in four states with seat belt use laws. In: *Restraint technology: Front seat occupant protection SP-690*. Warrendale, 1987.

OECD (1989). Road user capacities and behavioural adaptations in adjusting to changing traffic tasks and accidents risks. (Draft final report). OECD, Paris, 1989.

O'Neill, B.; Lund, A.K.; Zador, P. & Ashton, S. (1985). Mandatory belt use and driver risk taking: An empirical evaluation of the risk-compensation hypothesis. In: Evans, L. & Schwing, R.C. *Human behavior and traffic safety*. Plenum Press, 1985.

Noordzij, P.C.; Meester, A.C. & Verschuur, W.L.G. (1988). Night-time driving: the use of seat belts and alcohol. *Ergonomics* 31 (1988) 4.

Scott, P.P. & Willis, P.A. (1985). Road casualties in Great Britain during the first year with seat belt legislation. Research report 9. Transport and Road Research Laboratory, Crowthorne, 1985.

Vaaje, T. (1986). Safety belt usage laws in various countries. In: *Effectiveness of safety belt use laws: A multinational examination*. National Highway Traffic Safety Administration, 1986.

Varkevisser, G.A. & Arnoldus, J.G. (1989). *Aanwezigheid en gebruik van autogordels 1988*. SWOV, Leidschendam, 1989.

## The Effect of Fully Seat-Integrated Front Seat Belt Systems on Vehicle Occupants in Frontal Crashes

J. Harberl, F. Ritzl, S. Eichinger,  
Bayerische Motoren Werke AG,  
Fahrzeug-Sicherheit

### Abstract

For years, the entire worldwide production of BMW passenger cars has been equipped with 3-point belts installed in the front seats. It has been proven, through many

theoretical and experimental investigations, that the ideal location for the lower seat belt anchorage points, is the seat frame itself rather than the conventional mounting to the chassis. In the case of seat frame mounting, the lower belt portion stays fixed in relation to the occupant in all seat adjustment positions, and accordingly provides optimum comfort and protection to the occupant. Additionally, a lap belt angle of approximately 60° from the horizontal has been proven to be the most effective.

This technical paper describes BMW's research of an alternative installation location for the upper shoulder belt anchorage point and its influence on occupant protection and comfort. The first part of the investigation reviews the results of theoretical examinations, taking well known parameters into account. As a result of theory, in the second part an anchorage point in the upper seat back was further examined, using computer simulation models as well as a series of experimental frontal impact tests. The corresponding dummy load data are compared with those of conventional belt geometry. Finally, a short overview of additional safety features of a seat integrated belt system in the overall crash scenario is presented.

## Introduction

Seat belts designed as 3-point retractor belt systems have demonstrated their high protective effect for vehicle occupants (1, 2, 3)\*. The design of such a restraint system is subject to an extensive range of international regulations with regard to construction and effectiveness, so that a minimum level of protection is always guaranteed.

However, several particularly safety-conscious automobile manufacturers have gone beyond these legal requirements and introduced a series of improvements to the standard 3-point automatic seat belt system on their own initiative.

The following list contains examples which are now installed by a number of manufactures either as optimal or standard equipment:

- 3-point retractor belt with anchorage points for the buckle and the belt end directly on the seat. Advantage: steep lap belt angle for optimum pelvis restraint in all seat positions.
- Shoulder belt attached to the car body by an adjustable height anchorage, some with automatic adjustment device. Advantage: belt geometry is adaptable to the size of the occupant, resulting in increased safety and comfort.
- Belt clamping device integrated into the retractor. Advantage: no "film spool effect", so that occupants are not displaced as far forward in an emergency situation.
- Belt tensioner system integrated into the retractor. Advantage: elimination of belt slack, reducing forward displacement of occupants.
- Belt tensioning/clamping retractor: a combination of the two above mentioned versions. Advantage: the effects of both systems are combined to minimize forward displacement of occupants.
- Improved rear seat belt systems, e.g. with optimized belt geometry and seat-integrated buckles in an outside position. Advantage: high acceptance due to easy handling and optimum

comfort as well as improved protection in all accident situations (even in lateral impacts) (4).

All these effective measures, however, cannot overcome one remaining disadvantage of almost all current seat belt systems: the diagonal belt run, which significantly influences the level of comfort and protection, still depends to a large extent on the position of the seat, since the upper point of the diagonal belt is attached firmly to the car body. Even with the height adjustment capability, a uniformly effective seat belt run cannot be achieved for every occupant position. This shortcoming becomes particularly evident on vehicles which have no B-pillars due to their basic design concept, such as convertibles and coupes.

In view of these facts, we made it our objective to develop a belt restraint system which eliminates these disadvantages: a system which guarantees optimum occupant restraint for all conceivable body sizes and at the same time is exceptionally easy to use and more comfortable to wear than ever before.

## System development and test results

It was clear right from the beginning that new paths would have to be explored in order to meet these requirements. The most obvious starting point was to move the upper belt point towards the occupant, in other words to integrate it into the seat back itself. Not only would belt location no longer be influenced by seat position, but advantages with regard to restraint effectiveness were also expected in view of the shorter belt and more favourable belt angle at the first belt/shoulder contact point (5). In addition, a belt tongue installed closer to the occupant is easier to reach and the reduced belt length and belt friction reduce retraction forces, improving comfort and convenience still further.

Of course, the introduction of a seat-integrated belt system of this kind also necessitates extremely robust seats and seat mountings. Because of the anticipated problems, the additional safety potential of this system was first established by means of theoretical investigations.

The accuracy of the findings then had to be proven in a computer simulation model for predicting the forces exerted on vehicle occupants. Following this, prototype seats of the required strength were constructed and examined in sled tests. The interaction between the seat and a vehicle was then investigated in crash tests with modified production cars.

## Theoretical investigations

Compared to the standard belt geometry with B-pillar anchorage point, the seat integrated belt system (SBS) shows three main advantages concerning restraint effectiveness:

- Shorter belt length. (Forward displacement of occupants is decreased since the amount of belt which can be stretched is reduced, especially with

\*Numbers in parentheses designate references at end of paper.

the use of a belt clamping device at the upper shoulder point.)

- Almost horizontal belt run on to the shoulder. (Restraint forces are built up earlier, so that the occupant's body is coupled more rapidly to the passenger compartment of the vehicle and is participating in the crash event as early as possible.)
- The belt wraps well around the body. (This brings extensive benefits in a number of load situations occurring in actual crashes, keeping the occupant's torso position right in front of the seat back without rotating out of the belt.)

Two of these three claims, which are logical even if they require confirmation, are also borne out by theoretical analysis, the optimization objective of which is the familiar requirement for the occupants to participate at the earliest possible moment in the vehicle deceleration process. This can be described mathematically by the following simple equation:

$$\frac{\Delta F}{\Delta x} \Rightarrow \text{maximum}$$

where  $\Delta F$  = variation in belt force per unit of occupant forward displacement  $\Delta x$ .

From this, the following formula was derived in (6):

$$\frac{\Delta F}{\Delta x} = K (x^2/l^3)$$

This describes in a simple manner the relationship between shoulder belt run angle and belt length with the force built up in the diagonal belt per occupant forward displacement (see figure 1 and 2).

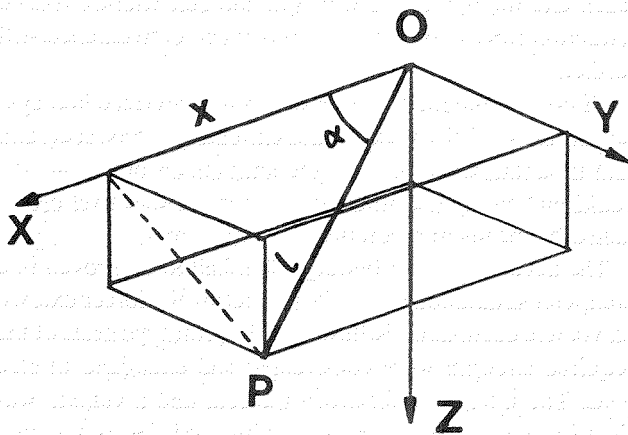


Figure 1. 3-dimensional correlation.

- K = spring constant of seat belt
- P = idealized fixed belt contact point on occupant (= first point of contact between belt and shoulder)
- O = upper belt anchorage point
- l = belt length between points P and O
- x = component of l in vehicle longitudinal axis
- $\alpha$  = angle between belt and vehicle longitudinal axis

The quotient  $(x^2/l^3)$  is referred to as the anchorage coefficient C, and is dependent only on the geometrical pattern of

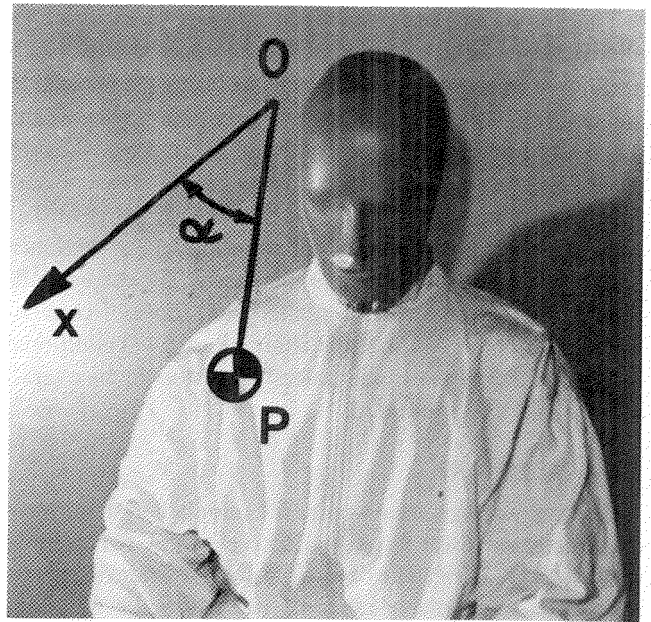


Figure 2. Schematic geometry of shoulder belt.

the belt location. According to the above equation the value of C is an important factor in the assessment of occupant safety:

$$\text{From } X = l \cos \alpha \text{ we obtain} \\ C = (\cos \alpha)^2/l$$

This shows that a reduction of l and  $\alpha$  towards zero, both leads to an increased C. The reduction in occupant load as C increases was already confirmed by sled tests in (6).

If we now examine a geometry representing the integration of the upper belt point into the seat back, we can clearly see that the distance l is much shorter than with conventional belt systems. Also the angle  $\alpha$  is greatly reduced by moving the horizontal belt run on to the shoulder.

In a simple example calculation of C the difference between conventional belt geometry and the seat integrated belt system (SBS) is shown:

Conventional geometry:

$$\alpha = 55 \text{ degrees}$$

$$l = 0,30 \text{ m}$$

$$C = 1,0 \text{ m}^{-1}$$

SBS:

$$\alpha = 29 \text{ degrees}$$

$$l = 0,25 \text{ m}$$

$$C = 3,0 \text{ m}^{-1}$$

### Computer simulation

The advantages of SBS derived from theoretical analysis were achieved subject to the upper point of the diagonal belt participating rigidly in the vehicle deceleration process. The seat back would therefore have to possess an infinitely high level of stiffness. This degree of rigidity is neither attainable nor desirable on an actual seat. With a specific rigidity rating, the shoulder belt force pattern can be influenced, so that the maximum force in the shoulder belt and

therefore the acceleration load on the chest is limited. In this way, the seat back also acts to a certain extent as a force-limiting element.

In analyses of standard belt systems, the Madymo computer simulation model correlates well with the results from sled tests. Therefore this model was also used to calculate the dummy response when integrating the upper diagonal belt anchorage into the seat in conjunction with force limitation by the seat back. When designing the model, a belt clamping device at the belt outlet in the seat was included.

To simplify the calculation, the rigidity characteristics of an actual floor pan assembly, which certainly exerts an influence on the results by way of its elastic and plastic deformability, were not taken into account in the arithmetic model. The calculation was based on a sled impulse which corresponds with a rigid barrier collision at 35 mph.

Figures 3 and 4 show the computer modelling with dummy positions at different times.

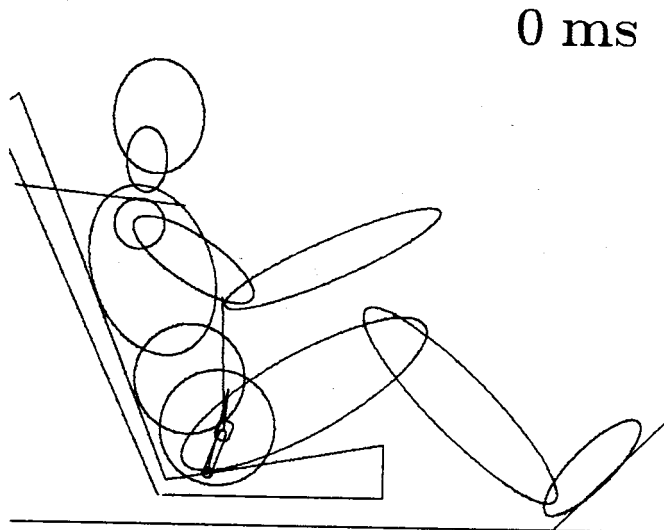


Figure 3. Computer model: occupant position at  $t = 0$  ms.

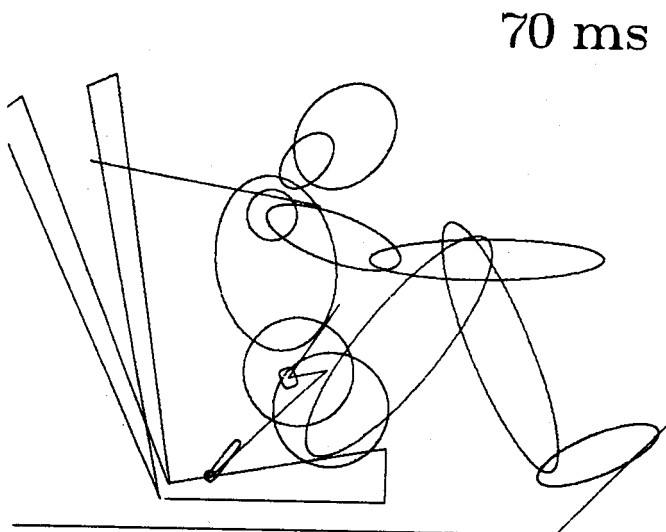


Figure 4. Computer model: occupant position at  $t = 70$  ms.

Figure 4 shows occupant kinematics at the moment of maximum belt force  $t = 70$  ms. The defined forward displacement of the seat back is easy to discern here.

The calculation results indicate the advantages of SBS. The expected earlier belt force increase in comparison with conventional belt geometry is immediately recognizable in the belt force time diagram (figure 5). The force-limiting effect of the seat back is also clearly reflected by the path of the curve. It is expressed by the qualitatively more rectangular shape in comparison with the more triangular shape of conventional systems.

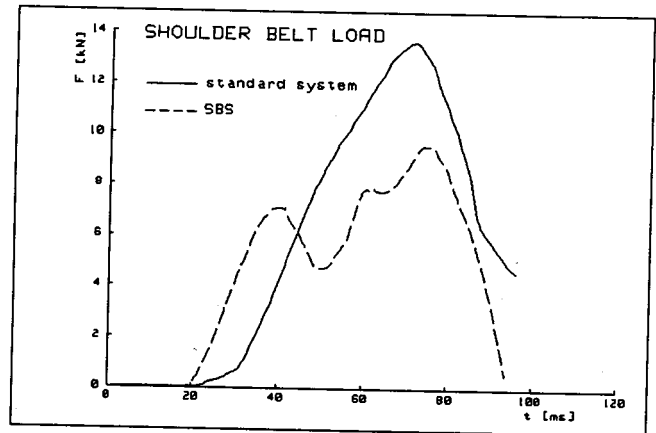


Figure 5. Calculated shoulder belt load.

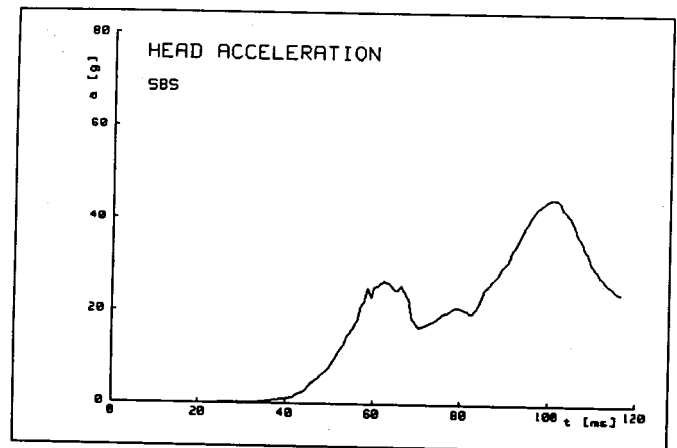


Figure 6. Calculated restraint head acceleration.

The computer results for head and chest loads also confirm the increased safety potential of the SBS (figures 6 and 7). The peak values of both curves stay far below the biomechanical limits. The calculation of the head acceleration curve for example produced an extremely low HIC value of only 264.

### SBS prototypes in accident simulation

In the next phase, prototype seats with integrated seat belt systems were constructed on the basis of theoretical findings. These were put through sled tests and crash tests with modified production cars in order to provide the first empirical results. A short description of the principal design fea-

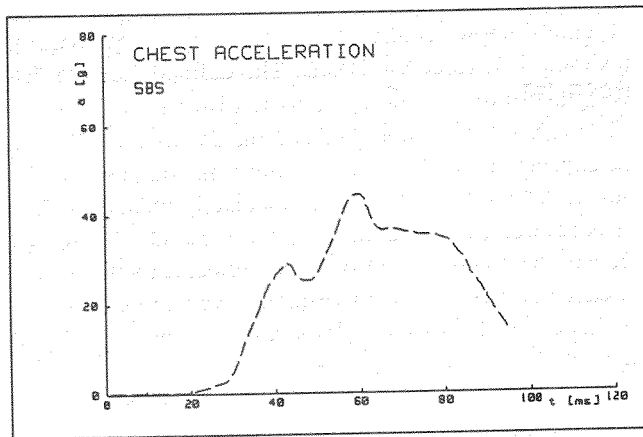


Figure 7. Calculated resultant chest acceleration.

tures which have a direct influence on occupant restraint is given below:

- Buckle and belt end are anchored to the seat frame with short connecting fittings so that an optimum lap belt angle of approximately 60° is achieved and both anchorages move correspondingly with every adjustment of the seat base.
- The upper belt point which is integrated into the head restraint arm of the seat back, is adjustable in height. The height is adjusted automatically by an electromotor drive according to the seat base height setting. As figure 8 shows, this results in a consistently good, relatively flat belt run angle on to the shoulder, even for extreme body sizes.

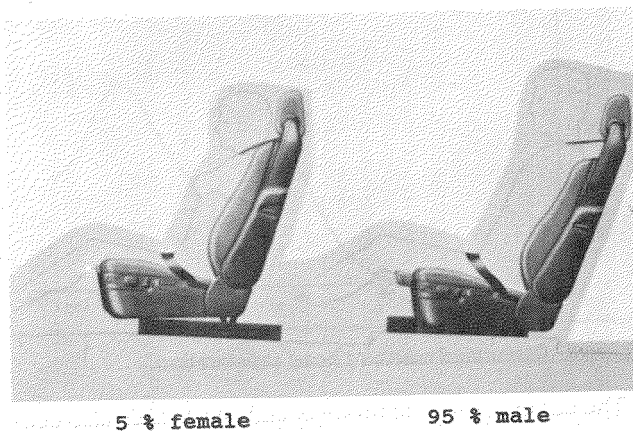


Figure 8. Shoulder belt run for extreme body sizes.

- A belt clamping device is integrated to avoid the “film spool effect”. For practical reason, it is located directly at the belt outlet of the seat, reducing the stretchable length of the belt to a minimum.
- The load-sustaining seat elements are extremely rigid and have a well-defined deformation characteristic to guarantee a specific force-limiting effect in extreme load situations without fracturing individual elements.

- A ramp integrated into the seat shell combined with a rigid seat base provides excellent pelvic support and greatly reduces the likelihood of “submarining”.

### SBS in sled tests

The following test parameters were selected for the first series of crash simulation tests with SBS.

- Test carried out on a Bendix Hyge-sled (see figure 9)
- Rigid sled construction for the seat anchorage points
- Acceleration pulse according to regulation ECE R 16
- Simulated rigid barrier impact speed of 50 km/h
- Dummy according to Part 572, Hybrid II

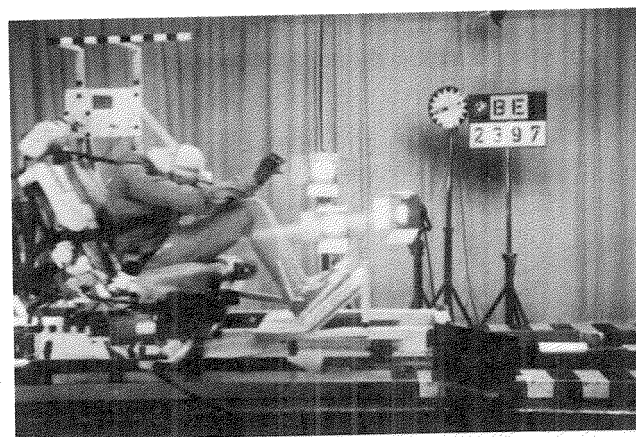


Figure 9. Experimental sled test set-up.

Since this test method with the absolutely rigid anchorage of the seat to the sled does not take into account the capacity of the actual floor assembly to deform a certain degree, correspondingly high loads are exerted on the seat. However, this test procedure with such restricted parameters is particularly well suited for a comparative analysis of seat and belt characteristics. Biomechanical safety evaluation of the SBS was based on the generally accepted criteria. In addition to the dummy size and seat position required by FMVSS 208 (“50% male” in middle sitting position), dum-

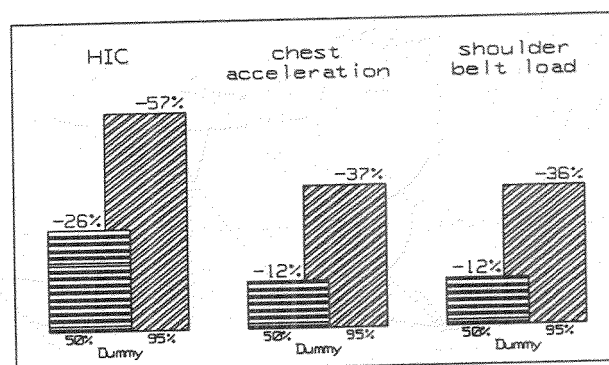


Figure 10. Reduced occupant load on 50% and 95% male dummy in sled tests with SBS.

mies of other sizes and in different seat positions were also used (95% male, 5% female). The results for a "50% male" dummy in the standard seat position and a "95% male" dummy with the seat adjusted correspondingly rearward are compared below with the results for conventional seat belt geometry (figure 10).

Figures 11–13 show the corresponding load/time curves for:

- Resultant head acceleration,
- Resultant chest acceleration and the
- Shoulder belt force

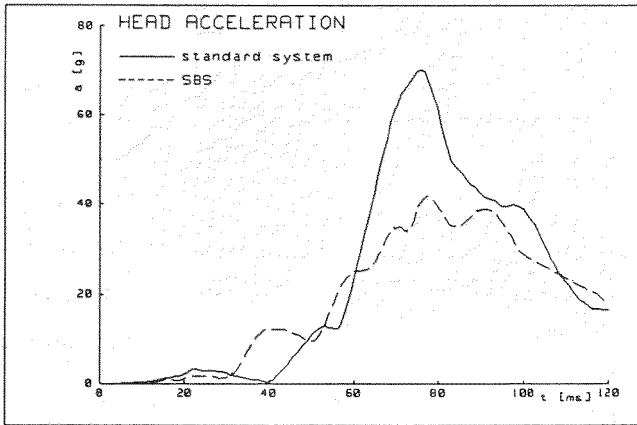


Figure 11. Head acceleration—"95% male."

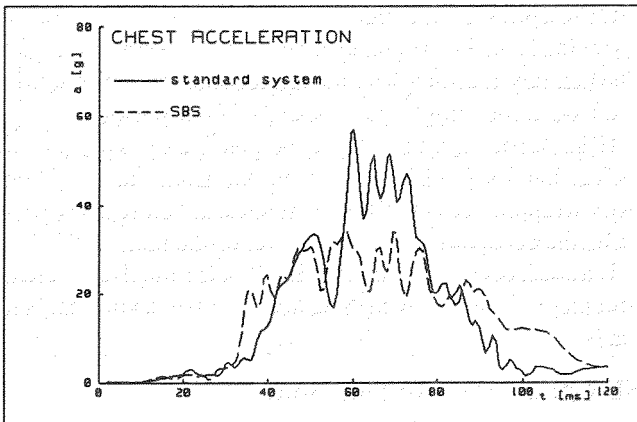


Figure 12. Chest acceleration—"95% male."

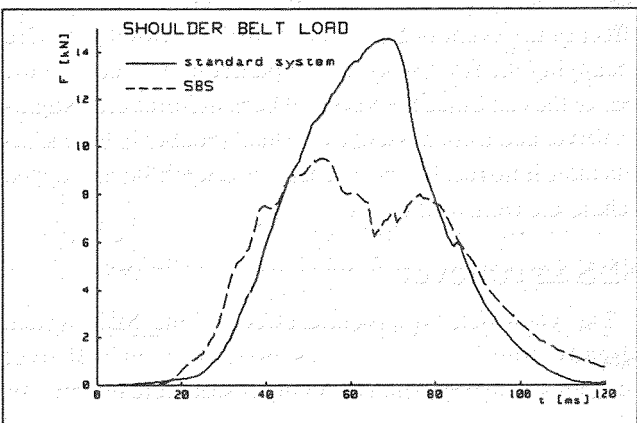


Figure 13. Shoulder belt load—"95% male."

of the SBS compared with the conventional seat belt system in tests with a "95% male" dummy.

This confirms the results predicted in section 2.2 by the calculation both qualitatively and quantitatively to a very high degree:

The SBS enables an earlier load increase together with a load limiting effect resulting in remarkable improvements in occupant protection.

### SBS in real car crash tests

The positive results of the crash simulation tests under idealized conditions with absolutely rigid seat mountings were next checked in an actual car with a modified floor



Figure 14. Dummy restraint with SBS.



Figure 15. Crash car with SBS.

assembly. In other words, the interaction between SBS and a feasible floor assembly concept and the effects of a specific car crash pulse had to be tested. For this purpose, a series of production car was prepared and its floor pan reinforced to meet SBS requirements. Figure 14 and 15 show the test car equipped with SBS.

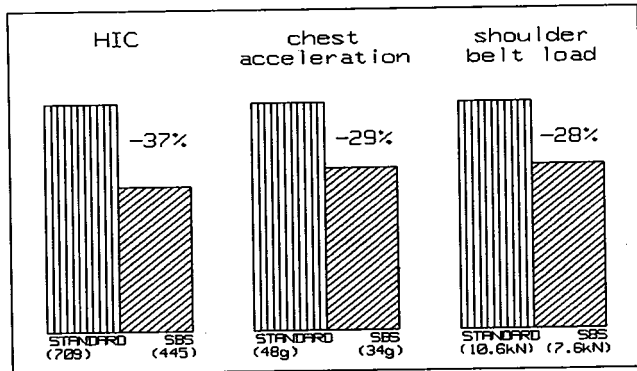


Figure 16. Reduced occupant load on 50% male dummy in real car crash test with SBS.

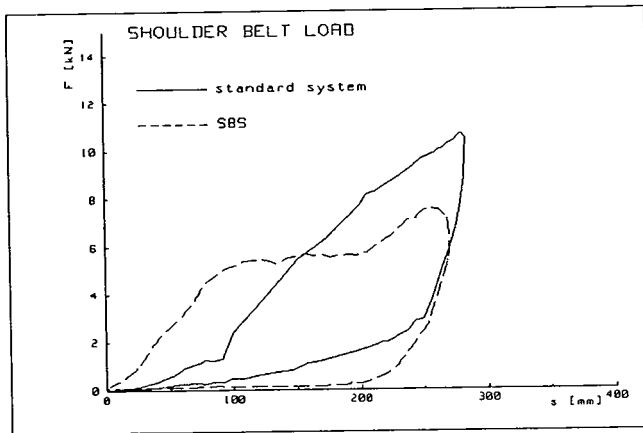


Figure 17. Shoulder belt load as a function of relative dummy forward displacement.

Crash test configuration according to FMVSS 208 (Part 572 dummy; 30 mph/0° rigid barrier impact).

The considerably reduced occupant load values measured in this crash test are shown in figure 16, compared with a conventional belt restraint system.

The best explanation for this remarkable reduction in load values is provided by figure 17, which shows the correlation between shoulder belt load and dummy forward displacement relative to the car. Again the high energy efficiency of the SBS is demonstrated.

### SBS in other crash scenarios

In addition to the advantages in frontal accident events which have already been described, SBS also offers benefits in terms of safety and convenience in almost all other forms of vehicle crash.

### SBS in side impacts

As already mentioned, the system has an exceptionally rigid seat frame in both the longitudinal and lateral direc-

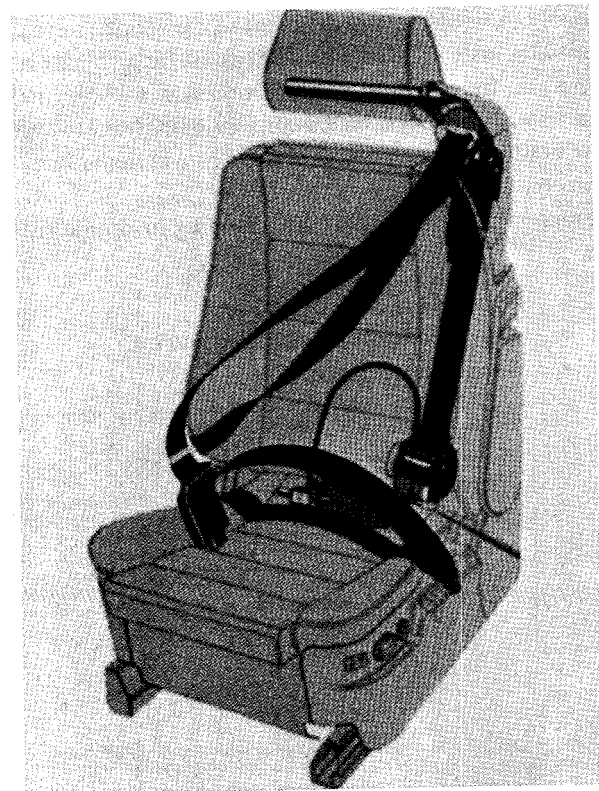


Figure 18. SBS safety features.

tions. These characteristics, combined with the essential extra stiffness of the floor pan, results in demonstrably lower loads on the occupants in the event of a side collision. The primary reason for this is reduced lateral deformation and a correspondingly lower speed of door penetration.

If the impact is not absolutely perpendicular to the side of the car but comes diagonally from the front, the excellent body wrapping effect of the diagonal seat belt reliably prevents the occupant from rotating out of the belt.

If a crash occurs in which the B-pillar is forced rearwards, occupants protected by SBS do not incur any additional belt loads.

### SBS in a rear-end collision

The high stiffness of the seat back and connections to the seat frame by the SBS increase the occupant protection effect in the event of a rear-end collision as well for those occupying the front seats, but in particular for those in the rear of the car. Since the SBS seat back deforms only slightly, driver and front passenger are held reliably in their seats and there is no risk for the rear seat passengers being trapped behind the front seat backs.

### SBS in rollover

The good belt wraparound effect of the SBS system already mentioned improves protection in roll over accidents. The occupant is held in his seat more effectively. The risk of contact injuries, particularly as a result of head contact with parts of the roof frame, is further reduced.

## Conclusion

Integration of all 3-point belt anchorages into the seat permits a further improvement in both user convenience and the safety to be achieved. Loads on the occupants are significantly reduced in the event of a frontal collision, but in all other accident situations as well, SBS increases the level of occupant protection.

The decisive advantage of SBS is however that it provides equally effective protection for persons of all sizes and therefore represents a major step forward for tall persons in particular.

Figure 18 shows a driver's seat with fully integrated belt system, with references to the principal safety features.

All belt anchorage points move with the seat—optimum belt geometry in all seat positions.

Automatic height adjustment of head restraint and seat belt outlet—eliminates incorrect adjustment.

Clamping device at belt outlet—reduces occupant forward displacement.

Defined energy absorption—minimizes occupant load.

High-strength frame structure—improves protection in side impacts and rear end collisions.

Seat shell with integrated ramp—prevents “submarining”.

## References

(1) Bolin, N.J., “A Statistical Analysis of 28.000 Accident Cases with Emphasis on Occupant Restraint Value.” SAE Paper 670925.

(2) HUK-Verband, “Fakten zu Unfallgeschehen und Fahrzeugsicherheit.” Büro für Kfz-Technik. München 1977.

(3) Langwieder, Klaus, “Aspekt der Fahrzeugsicherheit anhand einer Untersuchung von realen Unfällen.” Dissertation. Berlin 1975.

(4) Haberl, J.; Eichinger, S.; Winterschoff, W.; “New Rear Safety Belt Geometry—A Contribution to Increase Belt Usage and Restraint Effectiveness.” SAE Paper 870488.

(5) Hotnschik, H.; Müller, E.; Ruter, G.; “Necessities and Possibilities of Improving the Protective Effects of Three Point Seat Belts.” Battelle-Institut. 1976.

(6) Nakahama, R.; Katoh, H.; “Study on the Relationship Between Seat Belt Anchorage Location and Occupant.” ESV 1987.

## Rear seat occupant protection. A study of children and adults in the rear seat of cars in relation to restraint use and car characteristics.

Krafft M, Nygren C, Tingvall C.,

Karolinska Hospital  
dep of ENT and Folksam Ins Co  
Stockholm.

### Abstract

The rear seat of passenger cars has not been studied to any degree compared with the front seat. The use of restraints among rear seat passenger is also lower for rear seat passenger.

In this study the rear seat occupant protection was analyzed by using a material with both damage only as well as injury producing accidents. All injuries were coded according to AIS. The effectiveness of restraint use among children and adults as well as the influence of car size and type was investigated. The difference between front and rear seat occupants was also studied regarding injury risk and pattern.

### Background

Restraining of car occupants has been used as a safety measure in road traffic for the past forty years. The standard of safety belts has been raised considerably both in safety and comfort since then. These efforts have been mainly concentrated to the adult front seat occupants, while occupants in the rear seat and children only partly have benefitted from the increased knowledge and technique. To be able to transport a child in a car the car has to be equipped especially for this purpose.

The use of restraints for children and adults in the rear seat is lower than occupants in the front seat (1).\* It is therefore important to study the benefits from restraining also rear seat occupants in order to get a better knowledge from which incitements for better technique and increased use can be taken.

The objectives of the present study were to:

1. Study the risk relation between the front and the rear

seat for restrained occupants.

2. Study the effectiveness of restraint use for children and adults in the rear seat.

3. Study the influence of vehicle weight on injury risk for rear seat occupants.

## Material and Methods

A prospective study was conducted on children and adults in the rear seat travelling in private passenger cars involved in accidents that occurred in Sweden during the period 1st June 1983 to 31st December 1984. All cases of car damage, both damage-only and injury-producing and reported to the Folksam Insurance Company, were filed and a questionnaire was sent to the driver, if possible, in all cases (approximately 80,000). The questionnaire was to be returned if at least one occupant, either adult in the rear seat or a child, has been present in the car in question during the accident.

The questionnaire contained questions about the travel occasion, the accident, car damage, the age, sex and size of all occupants, available restraints, used restraints, and injuries. If any of the occupants had been injured, medical data such as hospital records and doctor's certificates were collected from the insurance files.

From the registration number of the car, the car make and model were identified and information was thereby obtained about the seat belt system, interior dimensions, service weight and type of head rest etc.

Personal injuries were coded according to the Abbreviated Injury Scale (AIS) (1980 version) (2). All injuries are classified into one of six levels, where AIS 1 is a very minor injury in terms of the death risk and AIS 6 is an unsurvivable injury. The Injury Severity Score (ISS) (3), where the highest AIS values for up to three body areas are squared and summed. Both AIS and ISS are ordinal scales.

ISS and AIS for body regions were used to predict the outcome in terms of death or permanent medical disability by a method called Rating system for Serious Consequences (RSC) (4). Values for young car occupants (0-30 years) (see appendix) were used. RSC has a range from 0 to 1, and is calculated from the formula:

$$RSC = r_f + ((1 - r_f) * (1 - \pi(1 - r_{id})))$$

where  $r_f$  is the risk of dying based on the ISS value and  $r_{id}$  is the risk of receiving a permanent medical disability of at least 10% due to an injury to one out of the body regions coded according to AIS.

The average RSC,  $mrsc$ , defined as sum of RSC/number of injured, was assumed to be approximately normally distributed for large  $n$ . For this reason only  $mrsc$  and the standard deviation of  $mrsc$  are given when  $n$  was at least 20, although this limit was set arbitrarily. In some cases the limit was ignored.

Restraint effectiveness was calculated in the usual way from the formula:

$$e = (P_u - P_r) / P_u$$

Where  $P_u$  and  $P_r$  are the proportions of injured among unrestrained and restrained children. The sample variance for  $e$  was calculated from the formula:

$$S^2 = P_r / P_u * (((1 - P_r) / X_1) + ((1 - P_u) / X_2))$$

where  $X_1$  and  $X_2$  are the numbers of injured restrained and unrestrained children, respectively.

Two-tailed t-tests were used for comparisons of two proportions and averages. \*, \*\* and \*\*\* denote the level of significance (0.05, 0.01 and 0.001, respectively).

The quality of the data was assessed on the basis of a random sample of 100 accidents for which a questionnaire should be sent back. It was found that 78 returned the questionnaire and 22 did not. Among those cases where at least one occupant was injured (16), 14 answered the questionnaire.

## Results

A total of 10 118 occupants were involved in the accidents studied. Their distribution can be seen in table 1.

**Table 1. The number of occupants on different positions in the car.**

	Number of occupants	restraint use	children
Drivers	2911	94.8%	-
Front seat passengers	2407*	94.1%	(19.2%)
Rear seat passengers outboard positions	3970	42.1%	49.2%
Rear seat passengers middle position	830	20.0%	57.7%

\*Rearward facing seat were excluded.

It can be seen in table 1 that the restraint use differed substantially between the front and the rear seat. In the front seat, almost 95% of the occupants used seat belts, while in the rear seat, less than 40% (38.3%) were restrained. There was a big difference between the outboard positions and the mid position.

It can also be seen from table 1, that the proportion of children in the rear seat is high. More than 50% of the rear seat passengers were children. The mid rear position is relatively more often used by children than the outboard positions as compared to adults.

The mid rear position is used by almost 18% of the rear seat occupants.

In table 2 the proportion of injured on different seating positions is showed. The occupants are also divided into age groups.

**Table 2. Risk of injury in the front and rear seat for restrained occupants.**

Age	n.	Drivers	Front seat occupants (forward facing systems)	Rear seat occupants outboard pos.
0-14	-	-	266	12.8*
15-30	982	12.4	826	11.6
31-50	1396	13.2	645	15.0
51-	365	16.7	344	19.5
all.	2743	15.4	2081	14.1

\*Corresponding figure for rearward facing systems is 1.2%.

\*Numbers in parentheses designate references at end of paper.

It can be seen in table 2, that for restrained occupants there is a correlation between injury risk and age. In the front seat older occupants have a higher injury proportion. The distribution of age on different seating positions therefore influences the total injury proportion when comparing i.e. the front and the rear seat. It can be seen in the table that the rear seat occupants were generally younger compared to the occupants in the front seat. The high injury risk in the front seat among the oldest occupants is explained by the fact that the very old occupants were more frequently in the front seat than in the rear seat proportionally.

It shall also be noted, that the injury proportion for rearward facing child seats in the front seat, is lower than for any other group.

**Table 3. Risk of injury in the front and rear seat in cars of different weight. (15 years and older) restrained occupants.**

Car weights	Drivers		Front seat pass.		Rear seat pass.	
	No	% inj	No	% inj	No	% inj
-950 kg	365	17.3	223	14.4	78	15.4
951-1250 kg	1253	14.1	822	16.9	301	13.0
1251 kg-	1126	11.2	770	11.6	280	10.4

From table 3, it can be seen that there is a strong relationship between injury risk and weight of the car. It can also be seen that there were fewer rear seat occupants in the small cars compared to the large ones. This fact also influences the total injury risk when comparing the front and the rear seat.

In small cars, the injury risk was approx. 50% higher than in large ones.

**Table 4. Risk of injury in the rear seat for restrained and unrestrained occupants.**

Age	Forward facing child restraint		Adult seat belt 3p.		Adult seat belt 2 p. (mid seat)		No restraint	
	No	% inj	No	% inj	No	% inj	No	% inj
-14	556	6.5	425	9.2	85	7.1	1274	17.0
15-	-	-	613	11.6	60	15.0	1690	18.9

In table 4, the injury proportion for restrained and unrestrained occupants is shown. The figures in the table can be used for calculation of restraint use effectiveness. For adults, the reduction of the injury risk was 38.6% (22.0-55.2%, 95% confidence limits). For children, the effectiveness is higher, around 55%, while for children sitting in a forward facing restraint the effectiveness was even higher.

**Table 5. Injury severity in ISS-groups for rear seat occupants.**

Age	ISS 1-3	4-10	11-	killed	n
-14					
Restraint used	85.2	14.8	0.0	0.0	81
No restraint	67.7	28.6	3.2	0.5	217
-15					
Seat belt	76.0	22.5	1.4	0.0	71
No seat belt	65.9	26.6	5.3	2.2	320

In table 5, the injury severity is presented. It can be seen that the severity, expressed in ISS is different for restrained and unrestrained occupants. While among unrestrained adults, more than 7% of the injured were either seriously or

fatally injured, this was true for only 1.4% of the restrained. The differences between the restrained and unrestrained were significant (\*\*\*).

In table 6, the injury severity, as measured by RSC, risk of serious consequences, is presented. Also by using this technique, there is a clear and significant difference between restrained and unrestrained for adults, while for children, there was no such difference.

**Table 6. The mean risk of serious consequences (mrsc) and the standard deviation for mrsc associated with restraint use. Note mrsc is differently calculated for adults and children.**

Age	mrsc	Std. mrsc	n	95% confidence limits
-14				
Restrain used	0.0188	0.0365	81	1.8-2.0%
Restrain not used	0.0238	0.077	217	1.4-3.4%
15-				
Restrain used	0.0433	0.047	71	4.2-5.4%
Restrain not used	0.0711	0.133	320	6.0-7.2%

It can also be seen from table 6, that the risk of serious consequences is lower for children than adults. The reduction in mrsc for adults was 39%.

**Table 7. Injury pattern for rear seat occupants and drivers.**

	-14		15-		(Driver, restr.)
	restrained	not restrained	restrained	not restrained	
Skull/brain	30.7	39.1	21.1	22.5	21.3
Neck	7.3	6.9	42.3	17.2	42.1
Face	26.0	40.2	12.7	25.3	14.2
Extremities	16.5	29.1	35.2	37.5	38.3
Chest	9.1	6.9	22.5	11.6	19.9
Abdomen	17.0	6.3	18.3	19.4	17.2
External	2.2	2.1	8.4	4.1	3.8

In table 7, the injury pattern is seen for restrained and unrestrained occupants. Among children, injuries to the skull, face and extremities were highly reduced, while injuries to the abdomen increased relatively. In absolute risks, there was however no injury type or localisation that increased.

Among adults, especially injuries to the neck were both relatively and absolute more common among restrained. This was true also for chest injuries. Injuries to the face were highly reduced while other injuries were reduced to the same amount as the total number of injuries.

Compared to drivers, the injury pattern among adult rear seat occupants similar with a high proportion of neck injuries.

Comparing restrained children and adults, children still have more injuries to the head and face.

**Table 8. The risk of injury and the mean risk of permanent disability for unrestrained rear seat occupant on the mid rear and outboard rear positions.**

		no.	% inj	mrsc
-14	mid	374	13.1	0.0188
	outboard	900	18.7	0.0245
15-	mid	290	18.3	0.0970
	outboard	1400	19.1	0.0605

In table 8, the different positions of the rear seat are compared. It can be seen that while there was a large and

significant difference for children between the mid and outboard positions, no such difference was present for adults. For children the injury severity was similar irrespective of position, while for adults, the injuries were more severe on the mid position.

## Discussion

In this paper, several parameters affecting the injury risk for rear seat passengers were presented. Although rear seat occupants is a smaller group compared to front seat occupants comprising 10–15% of all occupants (1, 7, 8) it is essential that also subsets of the population can be described adequately concerning risk and potential protection. The willingness and possibility to protect car occupants can be related to the risk and potential risk reduction and the background for decisions should therefore be described with sufficient precision and methods.

In the present study, a material with both injury producing and damage only accidents was used. This kind of material gives the possibility to estimate risks and risk reduction with a better precision than materials based on injuries only due to the fact that the exposure is known. The exposure in terms of accident severity was however not known. In a technique used by Evans' (5), this can be done, but the size of the material will then decrease.

The material was carefully coded concerning the medical data thus giving the possibility to assess also injury severity and pattern. This is important as restraint effectiveness should not be measured only in reduced injury risk but also injury severity (10).

It was shown in the present study, that consideration must be taken to age as a factor influencing the risk of injury. The age distribution in the front and the rear seat differs. Rear seat passengers are younger, and the proportion of children is higher. Children and younger occupants have a lower injury risk than older occupants and can therefore give a biased estimate of the front and rear seat injury risk. The effects of separating the occupants due to age has been demonstrated also by Norin et al (9) as well as Huelke and Lawson (6).

Another factor that influences the risk relation between the front and the rear seat was the size of the car. Rear seat occupants were less frequent in small cars where the injury risk is higher. In the present study the injury risk was 50% higher in cars weighing up to 950 kg compared to cars weighing more than 1250 kg for restrained rear seat occupants.

It seems to be a fair assumption that by taking age and car size into consideration, the risk of injury in the front and the rear seat is so homogeneous that they can be analyzed together and not separately in the field of crash protection.

It has been shown earlier that the injury severity for unrestrained occupants in the front and the rear seat is similar (8, 9).

The risk reduction due to restraint use in the rear seat was obvious. For children, the effectiveness was more than 50%,

while for adults, the effectiveness estimation was 22–55%. In all, the effectiveness was over 50%. Evans estimated the fatality reduction to 9–27% which must be considered to be lower than in the present study. The lower effects in the study by Evans can be explained by the fact that the belt system most common was lap belts, while in the present study, most cars had three-point belts (5).

In another Swedish study the effectiveness was estimated at 52% for children and 28% for adults (9).

In the present study, the injury severity was shown to be affected by restraint use. When measured by mrcs, mean risk of being either killed or disabled, the risk decreased by 39%.

Injuries that were mostly affected by restraint use were injuries to the head and face. Neck injuries increased as a result of restraint use.

The high risk of being injured in the rear seat and the high effectiveness of restraint use in the rear seat for both children and adults leads to the conclusion that the restraint standard in the rear seat must be high. The big proportion of children also focuses on the need for integrated child restraints (10).

It is also of importance to increase belt use in the rear seat. It seems from most countries that the belt use in the rear seat is lower than in the front seat, even when there is a legislation (1). This implies that the comfort and other factors related to belt use is increased in the rear seat. The possibility to install automatic crash protection ought to be investigated. The fact that an unrestrained rear seat occupant is a risk to a front seat occupant in case of a frontal collision also leads to that the use of seat belts in the rear seat must increase (8).

## Conclusions

The risk of injury to restrained front and rear seat occupants is similar when taking age and car size into account.

The effectiveness of restraint use in the rear seat is higher for children compared to adults.

The weight of the car influences the risk of injury in the rear seat for both children and adults.

## References

- (1) Effectiveness of safety belt use laws: A multinational examination DOT HS 807018. Washington D.C. 1986.
- (2) Abbreviated Injury Scale, 1980 revision. AAAM. Morton Grove 1980.
- (3) Baker SP, O'Neill B, Haddon W Jr, Long WB. The Injury Severity Score: A method for describing patients with multiple injuries and evaluating emergency care. *The Journal of Trauma*, Vol. 14. No. 3 1974: 1887–196.
- (4) Gustafsson H, Nygren Å, Tingvall C. Rating system for serious consequences (RSC) due to traffic accidents. Risk of death or permanent disability. In: Proc. 10th Int. Conf. on Experiments Safety Vehicles 1985. Oxford 1985: 556–560.
- (5) Evans L. Rear seat restraint system effectiveness in

preventing fatalities. *Accid, Analysis and Prevention* Vol 20, No 2, 1988: 129-136.

(6) Huelke DF, Lawson TE. Injuries to rear-seat passengers in frontal automotive crashes. *HSRI Res Rev* vol 9 no 1 1978: 11-14.

(7) Langwieder K. Risk of injury for the back seat passengers in road accidents. Effectiveness of safety belts. Manuscript 1986.

(8) Nygren Å, Aldman B, Gustaffsson H, Tingvall C, Wersäll J. The use of an insurance material to study traffic safety. In: *Proc. 9th Int. Conf. on ESV*. 1982.

(9) Norin H, Nilsson, Ehle A, Sareton E, Tingvall C. The injury-reducing effect of seat belt use on rear seat passengers. *Volvo-TSV report* 1980.

(10) Tingvall C, Children in cars. Some aspects of the safety of children as car passengers in road traffic accidents. *Suppl. 339. Acta Paediatrica Scandinavia*. 1987.

## Appendix

ISS values and mortality risks ( $r_i$ ) used in the RSC scale.

ISS	Mortality risk
1-3	0.000
4-8	0.001
9-14	0.005
15-19	0.040
20-24	0.080
25-24	0.080
25-29	0.160
30-34	0.260
35-39	0.370
49-44	0.500
45-49	0.650
50-54	0.650
55-	1.000

If at least one AIS 5 is present, the mortality risk ( $r_i$ ) is set at least 0.5. An AIS 6 is set at 1.0.

In this example ISS had to be based on the highest AIS for only two body regions, as the skull, brain and neck are treated as one body region in ISS and out of the two lower extremity injuries the one with the highest AIS was chosen. For the disability risk calculations, three values were used, as in this case the skull/brain injury and neck injury are separated, while only lower extremity injury is included.

In the example, the injured child received injuries that

were not likely to lead to death, while the disability risk was high, 22.6%. The most probable disabling injury was the fractured patellae (19.0% risk) followed by the neck injury (4.0% risk).

If RSC is treated as a random variable, the density function is probably very skew. The minimum number of observations that have to be available to consider the mean RSC (mrsc) as approximately normally distributed is therefore 25.

$r_{id}$  values for permanent medical disability for different body regions and AIS levels, used in the RSC scale.

Body region	AIS 1	AIS 2	AIS 3	AIS 4	AIS 5
Skull/brain	0.01	0.02	0.15	0.25	0.50
Neck	*	0.10	0.50	0.50	0.75
Face	0.0001	0.005	0.10	0.10	
Arm	0.0005	0.035	0.15	0.60	
Leg	0.0005	0.15	0.25	0.60	
Chest	0.0001	0.0005	0.01	0.03	0.05
Abdomen	0.0001	0.001	0.001	0.01	0.01
Pelvis	0.0001	0.075	0.075	0.075	
Back	0.001	0.05	0.20	0.75	
External	0.001	0.05	0.05	0.05	

\* 0.10 if rear-end collision, 0.04 if other direction.

$r_{ia}$  values for permanent medical disability for different body regions and AIS used in the RSC scale for young car occupants aged 0-30 years.

Body region	AIS 1	AIS 2	AIS 3	AIS 4	AIS 5
Skull/brain	0.002	0.004	0.15	0.25	0.50
Neck	0.04	0.10	0.27	0.50	0.75
Face	0.0001	0.005	0.05	0.10	
Arm	0.0005	0.035	0.15	0.60	
Leg	0.0005	0.10	0.19	0.60	
Chest	0.0001	0.0005	0.01	0.03	0.05
Abdomen	0.0001	0.0001	0.0001	0.01	0.01
Pelvis	0.0001	0.075	0.075	0.075	
Back	0.0001	0.05	0.12	0.75	
External	0.0001	0.05	0.05	0.05	

Assessment of the injury severity of an injured child in terms of AIS, HAIS, ISS, and RSC.

Injury description	AIS	HAIS	HAIS <sup>2</sup>	$r_{id}$	$1-r_{id}$
Cerebral concussion					
Unconsciousness 1 - 15	2	2	4	0.004	0.996
Neck pain	1			0.04	0.96
Fractured patella, complicated	3	3	9	0.19	0.81
Fractured tibia	2				
ISS				13	
$r_i$				0.005	
$1 - \pi(1 - r_{id})$					0.226
$RSC = 0.005 + (1 - 0.005) * 0.226 = 0.230$					

## Passive Compared to Active Approaches to Reducing Occupant Fatalities

Leonard Evans,  
General Motors Research Laboratories

### Abstract

The results of a recent study which estimated the effectiveness of airbags in reducing driver and right-front-passenger fatalities are summarized. In addition, the effectiveness of various other active and passive approaches to occupant crash protection are also discussed. Passive

approaches include energy absorbing steering columns, instrument panel padding, and increasing car mass. Active approaches include lap/shoulder belts in the front seats of cars, lap-only belts in the rear seats of cars, motorcycle helmets, car passengers transferring from front to rear seats, and crash avoidance. It is concluded that many disparate approaches can generate important reductions in occupant fatalities (a one percent reduction in occupant fatalities saves about 200 lives per year). The most commonly discussed active protection device (the lap/shoulder belt) is

substantially more effective at reducing driver fatalities than is the most commonly discussed passive device (the airbag). A 54% use rate of lap/shoulder belts generates the same fatality reduction as universal use of airbags (without other restraints). It is recommended that discussions of occupant protection should include all measures which reduce occupant harm. For example, of the various passive approaches reviewed, increasing car mass generates the largest occupant fatality reductions.

## Introduction

In recent years the effectiveness of a variety of occupant protection devices in reducing fatalities to occupants of motor vehicles has been determined quantitatively using fatal crash data. Some of these determinations are reviewed and summarized in the present paper, which has two main purposes. First, to compare the effectiveness of passive and active approaches to occupant protection, and second, to suggest that all approaches which reduce harm to occupants of vehicles should be included when the term occupant protection is used.

Passive protection refers to protection incorporated directly into the engineering of the transportation system in such a way that no user action is required each trip. The most discussed passive protection device has been the airbag. A recent determination of the effectiveness of this device in preventing fatalities is summarized in this paper. The effectiveness of other forms of passive protection, such as energy absorbing steering columns and increased vehicle mass, are also discussed.

Active protection requires action, such as fastening a safety belt, by the driver, or other occupant, each trip. Here we summarize effectiveness estimates for lap/shoulder safety belts in car front seats, switching from front to rear seat, lap-only belts in rear seats, and helmets for motorcyclists. Crash avoidance as another approach to active occupant protection is also discussed.

## Results

### Effectiveness of airbags in reducing driver fatalities

In a recent study (1)\* airbag effectiveness in preventing fatalities was inferred by applying a number of assumptions to empirically determined results for fatality reductions provided by lap/shoulder belts. Here we provide a brief review of that study; for discussion of the rationale behind the assumptions and details of the calculation, the reader is referred to the original paper (1). The main assumptions were that airbags did not affect ejection probability, were deployed only in frontal, or near frontal, crashes, and in such crashes they provided the same interior impact reducing effectiveness as lap/shoulder belts. The airbag effectiveness calculation therefore requires the distribution of occupant deaths by direction of impact, and lap/shoulder belt effectiveness by direction of impact and ejection contribution.

Impact directions for fatally injured unrestrained car drivers

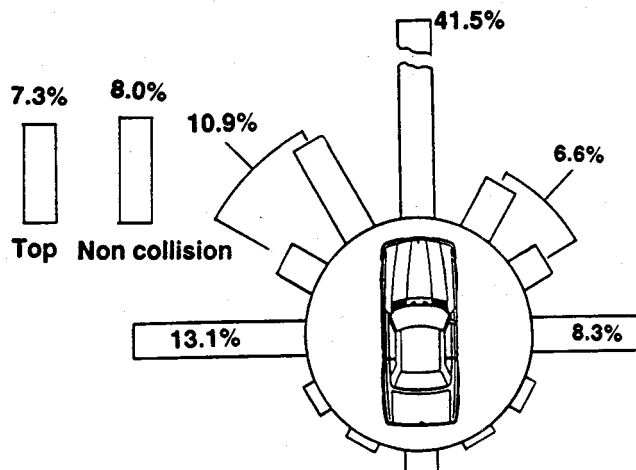


Figure 1. Distribution of driver deaths by principal impact point, from (1).

Figure 1 shows driver fatalities by principal impact point, defined as the impact judged to have produced the greatest personal injury or property damage for a particular vehicle. All fatal crash data in this paper are from the Fatal Accident Reporting System (FARS), a computerized data file maintained by the National Highway Traffic Safety Administration containing detailed information on all traffic crashes occurring in the United States since January 1, 1975 in which anyone was killed (2). Figure 2 shows lap/shoulder belt effectiveness versus principal impact point, with the component of this effectiveness which is due to eliminating ejection (3) shaded. The remaining unshaded portion is the component of lap/shoulder belt effectiveness which is due to reducing occupant impact, and is the effectiveness we assume for airbags. It is apparent from

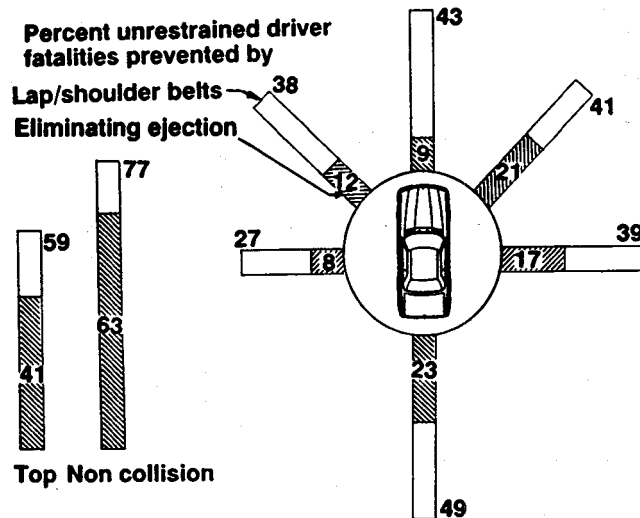


Figure 2. Effectiveness of lap/shoulder belts in preventing driver fatalities, and the fraction of fatalities prevented by eliminated ejection according to impact direction. For example, in frontal (12 o'clock) crashes, lap/shoulder belts prevent 43% of driver fatalities; 9% of this is due to eliminating ejection, so that 34% is due to interior impact reduction; from (1).

\*Numbers in parentheses designate references at end of paper.

figure 2 that lap/shoulder belts reduce fatalities for all principal impact points, and that much of this effectiveness is due to ejection prevention; even for rear impacts, lap/shoulder belts substantially reduce fatalities. Lap/shoulder belts are (77 ± 6)% effective in preventing driver fatalities in "non-collisions", most typically rollovers; 63% of this effectiveness is due to ejection prevention, compared to 14% from reducing interior impact.

By assuming that frontal, and near frontal, crashes include those with principal impact points at 10, 11, 12, 1 or 2 o'clock, airbag effectiveness for drivers is calculated from the information in figures 1 and 2 as  $0.415 \times 34 + 0.175 \times 24 = 18.3$ , with a standard error of 4.2; that is, we find that airbags are (18 ± 4)% effective in reducing driver fatalities. In (1) it is similarly calculated that airbags are (13 ± 4)% effective in reducing right-front passenger fatalities. These estimates assume non-use of safety belts. In conjunction with a lap-only belt, the airbag has been estimated in the literature to have effectiveness similar to that of the lap/shoulder belt (4); if used in conjunction with a lap/shoulder belt, overall effectiveness has been estimated by NHTSA (4) to be about five percentage points higher than for the lap/shoulder belt alone.

The fatality reducing effectiveness found is of the magnitude expected, based on a number of prior estimates (4, 5, 6) discussed in (1) and listed in table 1.

Table 1. Estimates of airbag effectiveness.

Method and Reference	Effectiveness estimate
Fatality reductions inferred by estimating reductions in occupant impact with the vehicle's interior[1].	18% driver 13% psngr
Experts judged the fatality prevention potential of various protection devices for 706 actual fatalities[5].	18%
Serious injuries (AIS ≥ 3) to occupants protected by airbag compared to unprotected occupants in matched crash[6].	9%
Fatality reductions estimated from national accident data files and other information[4].	20% - 40%

### Comparison with other passive devices

Table 2 shows the airbag effectiveness estimates discussed above, together with estimates of fatality reducing effectiveness of other passive and active approaches to reducing occupant fatalities. Most of the remainder of the paper focuses on describing and discussing the entries in table 2.

Table 2. Estimates of effectiveness of various approaches to reducing occupant fatalities.

Protection approach	Persons protected	Fatality reducing effectiveness
<b>PASSIVE</b>		
Airbag	Car drivers	(18 ± 4)%
Airbag	Car right-front seat passengers	(13 ± 4)%
Energy absorbing steering column, etc.	Car drivers	(6 ± 3)%
Improved instrument panel padding, etc.	Car right-front seat passengers	about 6%
Double car's mass	All occupants of car	about 65%
<b>ACTIVE</b>		
Front seat lap/shoulder belt	Car drivers	(42 ± 4)%
Front seat lap/shoulder belt	Car right-front seat passengers	(39 ± 4)%
Change from unbelted front to unbelted rear passenger	Car right-front seat passengers	(26 ± 2)%
Rear seat lap-only belt	Car outboard rear passengers	(18 ± 9)%
Motorcycle helmet	M <sup>o</sup> cycle drivers and passengers	(28 ± 8)%
Crash avoidance -- if it occurs	All road users	100%

### The energy absorbing steering column, etc.

The "energy absorbing steering column, etc." entry in table 2 refers to the combined effects attributed to the introduction of two Federal Motor Vehicle Safety Standards (FMVSS), namely, FMVSS 203, which required energy absorbing steering columns designed to cushion the driver's chest impact and a frontal crash, and FMVSS 204, which limited the rearward displacement of the steering wheel towards the driver. These standards, which became effective in January 1968, were both aimed at reducing driver injury risk in frontal crashes. Kahane (7, 8) used FARS data from 1975 through 1979 to estimate the influence of these standards on fatalities by two different methods; each method provided consistent estimates, leading to a composite estimate (7, 8) of effectiveness in reducing driver fatalities in frontal crashes (12 ± 5)%. A separate analysis suggests that the performance on impact. Kahane finds that the fatality reducing effectiveness is similar to that of FMVSS 203 plus FMVSS 204, which is the basis of the entry in table 2.

### Increasing car mass

The entry for "doubling car mass" arises from relationships between car mass and occupant fatality risk summarized in table 3. The car mass effect for two-car crashes is based on (11). The car mass effect for all other crashes is from (12), and replaces a slightly different earlier estimate (13) based on fewer data; this effect should be essentially independent of the mix of cars on the road because it is mainly due to single-car crashes (which account for almost

half of all driver fatalities). Although the fatality risk a driver in a specific car faces in a two-car crash increases as the mass of other increases, it is far from intuitively obvious how the reduction in fatality risk to a driver switching to a heavier car is influenced by the mix of other cars. Indeed, one cannot infer even the sign of the change without knowledge of many details. The simple weighted average in table 3 does not take into account any specific mix of cars, nor does it reflect many details such as different involvement rates in two-car crashes as a function of car mass (14). Any calculation incorporating all known relevant effects in a mathematically rigorous manner would be complex beyond what is required here; there is no reason to expect that such a calculation could give a materially different answer.

**Table 3. Comparison of fatality risk in 900 kg car to that in 1800 kg car.**

Crash type	Fraction of all driver fatalities	Fatality risk in 900 kg car Fatality risk in 1800 kg car
Two car crashes	about 25%	4
All other crashes	about 75%	2.4
Weighted average		2.8

In order to reflect the above and other uncertainties, the entry in table 2, which is nominally one minus the reciprocal of  $2.8 = 64.3\%$ , is given as an approximate rounded value. This risk reduction is compatible with insurance industry injury claim data. For example, for two-door models, large cars were found to have injury claim frequencies 47% lower than those for small cars; the corresponding difference for four-door models was 44% (15). The mass of the large cars (the categories are based on wheelbase) is less than double the mass of the small cars.

The comparison in table 3 of doubling the car mass from 900 kg to 1800 kg follows the example in the original papers cited (11-14). More generally, the percent fatality risk reduction for any mass increase,  $\Delta m$ , can be expressed as  $100 [1 - \exp(\beta \Delta m)]$ , where  $\beta = -0.00114$  for  $\Delta m$  in kg, or  $\beta = -0.00052$  for  $\Delta m$  in pounds. Thus, the calculation indicates that increasing the mass of a car by 174 kg (384 pounds) generates an 18% reduction in fatality risk for all occupants in the car, the same risk reduction that a driver airbag provides for the driver. It is not strictly correct that mass increases generate the same fatality risk reduction for all car occupants. Applying the same procedures as in (16) to FARS data stratified by car mass and principal impact point shows that the risk of fatality in the rear to that in the front increases with car mass in non-frontal crashes, so that an increase in car mass therefore generates a somewhat smaller fractional reduction in fatality risk to rear than to front seat occupants.

It should be stressed that the above discussion focused on an individual switching to a car of a different mass. If all cars increased in mass, fatality risk reductions would be smaller, but still large (recall that almost half of all occupant fatalities involve only one car). Also, when cars of similar mass crash into each other, fatality risk is still less for two

large cars crashing into each other than for two small cars crashing into each other (17).

### Active occupant protection

The most basic difference between active and passive protection is that the active protection is available only on occasions when the device is used. The values in table 2 are estimates of the effectiveness of the device if it is used. Overall fatality reductions depend not only on the effectiveness of the device when used, but on the use rate. For devices such as safety belts there is convincing evidence that users are safer drivers than non-users, so that benefits are less than proportional to use rates (18,19).

### Lap-shoulder belts

The most widely discussed active occupant protection device is the manual lap/shoulder belt which has been available to drivers and right-front passengers in essentially all cars in the U.S. since model year 1974. We do not address the various forms of automatic belts that have appeared in recent years because no satisfactory estimates of effectiveness are yet available. The estimates shown in table 2 for active, or manual, lap/shoulder belts are from (20). These, as well as the effectiveness estimates for lap-only belts in rear seats (21) and motorcycle helmets (22), were determined by applying the double pair comparison method (23) to FARS data. A summary of all these estimates is given in (24).

The values in table 2 suggest weakly that effectiveness of lap/shoulder belts may be somewhat higher for drivers than for right-front passengers. Other studies (25,26) have found larger differences in the same direction. There does not appear to be any obvious explanation of this difference. The higher fraction of passengers compared to drivers who are female, and thereby more likely to die from the same impact (27), is unlikely to influence effectiveness much because the greater fatality risk is present whether the female occupant is belted or unbelted. Although lap/shoulder belt and airbag effectiveness are each higher for drivers than for right-front passengers, the difference has different causes in each case. The airbag difference arises, in part, because cars with only one occupant have a different distribution of fatal crashes by impact direction than cars containing a driver and a right-front passenger; in particular, a larger fraction of frontal crashes (1). A calculation using the variation of safety belt effectiveness with impact direction (1) shows that differences in the distribution of impact directions between lone and accompanied drivers generate no appreciable (less than 0.1%) difference in overall belt effectiveness. The additional indication in (1) that belt effectiveness is higher for drivers than for right-front passengers in frontal crashes suggests that factors such as the presence of the steering wheel may be relevant.

### Choice of front or rear seat

The choice of whether to sit in a front or rear seat is not usually thought of as part of active occupant protection.

However, when there is only one non-belt-wearing passenger accompanying the driver, that passenger forgoes a 26% fatality risk reduction (16) by making the usual choice of sitting in the front rather than the rear outboard seat. Opting for the less safe alternative in this, and in other situations (such as forward-facing seats in airlines, trains and busses) are other obvious examples of the general principle that safety is one of many often competing goals sought in transportation systems (28). If the passenger is a belt user, and uses the restraint system available in most cars until recently (lap/shoulder belts in the front seat, lap belts in the rear), then the fatality risks in front and rear become indistinguishable (16). Although we do not yet have estimates of the effectiveness of the now widely installed lap/shoulder belts in rear outboard seats, it seems likely that passengers using such systems would have lower fatality risks than belted front seat passengers; even if the front seat were equipped with an airbag, it seems likely that a lap/shoulder belted rear seat occupant might still have lower fatality risk than a lap/shoulder belted front seat passenger.

### Other active protection approaches

The effectiveness lap-only safety belts to prevent fatalities to adult rear outboard-seat occupants shown in table 2 is from (21); Kahane (29) reports an effectiveness of 17%. Motorcycle helmets (22) are included because they relate to many of the matters we explore, and are one of only a small number of devices with fairly well known effectiveness. Although crash avoidance is not normally considered in the context of occupant protection, we include it for the reasons given in the discussion section.

### Protection provided to different occupants, and in different types of crashes

Here we address the question of whether the devices in table 2 protect all occupants equally, or whether some favor occupants of a particular type (for example, younger drivers, intoxicated drivers, etc). Such a concern arises because, for example, older occupants fatalities are more likely to be the result of side impact than those of younger occupants (30,31). As some of the devices in table 2 (airbags, energy absorbing steering column, improved instrument panel padding) protect mainly in frontal crashes, this suggests that they might offer younger (or drunker) occupants more protection than older (or more sober) occupants.

Figure 3 shows the fraction of all driver fatalities that resulted from frontal impact versus driver age for single-car crashes, two-car crashes, and for all crashes (32). For all crashes, there is a remarkable lack of any dependence on driver age. This arises despite important changes in crash types with age. Younger drivers are more likely to be involved in rollover crashes, while a larger fraction of older driver fatalities result from side impact. A similar lack of dependence of the fraction of all fatal crashes that are frontal was found for alcohol use (32), the explanation being similarly that drunk drivers were more likely to be involved in rollover crashes, whereas a larger fraction of all fatalities to

sober drivers resulted from side impact. The relative absence of any dependence on driver age implies that the airbag, and the energy absorbing steering column provide similar fatality reducing effectiveness for drivers of all ages, and all levels of alcohol use.

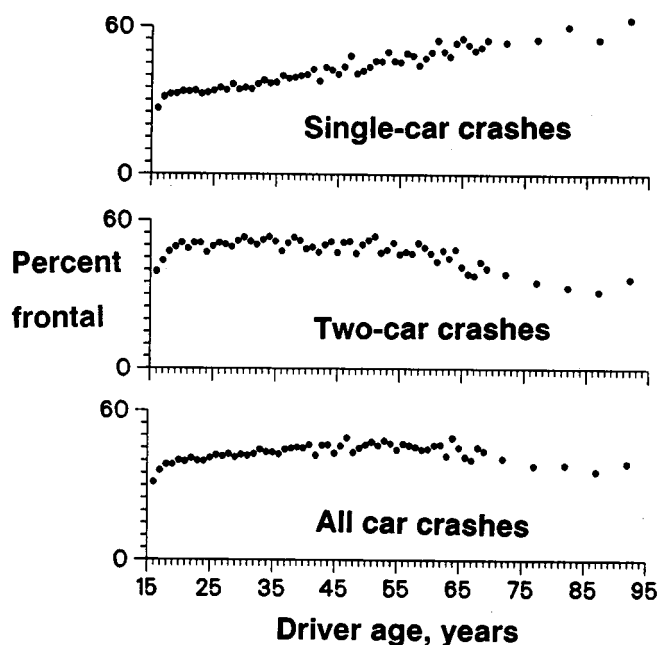


Figure 3. The percent of driver fatalities that are frontal (principal impact point at 12 o'clock) for single-car crashes, two-car crashes and all crashes; from (32).

The generally higher fraction of all crashes that are frontal in two-car crashes compared to in one-car crashes leads to the somewhat surprising result that devices designed to protect only in frontal crashes are in fact more effective in two-car crashes than in one-car crashes.

Unlike the airbag, the effectiveness of lap/shoulder belts does appear to depend on driver age. Almost half of its effectiveness flows from preventing ejection (1). The effective-

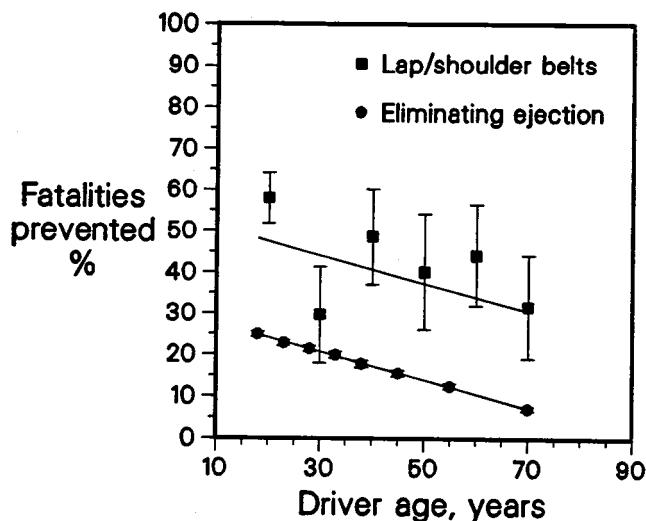


Figure 4. The effectiveness of lap/shoulder belts in reducing fatalities (upper data) and the percent fatalities preventable by eliminating ejection (lower data) versus driver age. The lower line is a weighted least squares fit to the lower data; the upper line is parallel to the lower; from (32).

tiveness of lap/shoulder belts and the fraction of fatalities preventable by eliminating ejection are shown in figure 4. The fit to the safety belt data is a line parallel to the fit to the ejection data, as described in (1). Hence the finding in (1) that front-seat lap/shoulder belt effectiveness is higher at younger adult ages.

## Discussion

The entries in table 2 with the largest effectiveness estimates for both passive and active protection are for approaches not normally even considered in the context of occupant protection. The omission of car mass from most discussions of passive protection seems difficult to understand given that increasing car mass appears to satisfy every definition of passive protection. The omission of crash avoidance is perhaps more understandable, as discussed below.

Although avoiding the crash altogether clearly reduces occupant harm by 100%, such a countermeasure is not traditionally considered in the context of occupant protection. Traditional determinations of occupant fatality reductions intrinsically require knowledge of the number of occupants in each of four categories; those killed using and not using the device, and those not killed using and not using the device. Drivers avoiding crashes usually leave no evidence. If an intervention or device reduces crash risk, it is still unlikely to provide specific unharmed occupants that one could be confident would have been harmed but for the intervention. Yet various policy and other interventions can lead to reductions in fatalities (33). A 34% drop in the number of traffic fatalities per unit distance of driving on the U.S. rural Interstate system followed the Arab oil embargo begun in October 1973 (34). A 66% reduction in serious injuries and fatalities during weekend drinking hours has been associated with the period immediately following the introduction of the 1967 British Road Safety Act (35, page 66). It is extremely unlikely that we will ever see even one of the large number of people whose lives are saved by such interventions explain to a television audience that, but for the intervention, they would be dead.

Even more difficult than determining the influence of specific interventions on occupant harm is the question of long term evolutionary changes. This is particularly true for the sort of slow evolution towards safer driving practices related to changing social norms (34,36). Although difficult to quantify, such effects clearly contribute a large proportion of the reductions in fatality risk to occupants which have occurred over the decades. For example, the fatality rate in the U.S. in 1986 was 2.63 deaths per hundred million miles driven, compared to 21.86 in 1923. That is, the fatality rate (all traffic fatalities) declined by 88% from 1923 to 1986 (37, page 70-71). Current U.S. fatality rates (deaths per unit distance of travel and deaths per registered vehicle) are more than 95% below current rates in many less economically developed countries (38, page 12; 39, page 111-119; see also 40-41). Clearly, the more traditional occupant protection devices (even if augmented by the

others not listed table 2) cannot collectively generate changes of such magnitude. Behavioral factors necessarily play an important role.

The other item not normally considered part of occupant protection is car mass. This is more surprising, because it has been long ago firmly established that increasing car mass decreases occupant injury risk (42-44).

One characteristic in which increasing car mass differs from the other forms of occupant protection in table 2 is that, while decreasing risk to occupants in the car in question, it increases risks to other road users, especially occupants of other cars into which it crashes. If one car in a two car crash were to have its mass increased, while the other one remained unchanged, there would be a net reduction in fatality risks (44). This is because the decrease in fatality risk in the heavier car would be larger than the increase in the smaller car. While such effects are important and interesting, it should be recalled that about 75% of fatally injured car occupants do not die in two car crashes. Another way the larger car imposes increased risk on others is its increased size as such. Other factors being equal, it is more likely to strike another vehicle or pedestrian.

Another feature of increasing car mass which makes it different from most of the other items in table 2 is that its effect appears to be relatively independent of other effects. This is not so for occupant protection devices in general. For example, because lap/shoulder belts and airbags both reduce driver impact with interior structure, their combined effectiveness is *not* given by  $1 - (1 - 0.42)(1 - 0.18) = 52\%$ , as would be the case if they were independent effects; as noted earlier, an airbag in conjunction with a lap/shoulder belt is estimated in the literature (3) to increase the lap/shoulder belt effectiveness by 5 percentage points (say, from 42% to 47%). As the estimates in (3) tend to be higher than values obtained later, I believe that the 5 percentage point estimate is also likely to be high. The combined effects of airbag and energy absorbing column are unlikely to be much different than those of the airbag alone; similar comments apply to any combination of occupant protection devices with overlapping functions. In contrast, increasing car mass appears to operate independently of other occupant protection devices. This is suggested by two studies (12,45) which examined the dependence of lap/shoulder belt effectiveness on car mass. The absence of any systematic effects in either study suggests that using a lap/shoulder belt in a large car reduces fatality risk by a similar proportion to using it in a small car. Such a result, which is reasonable on intuitive grounds, suggests that the effectiveness of airbags, energy absorbing steering columns, and improved instrument padding would be likewise relatively independent of car mass. Thus, the combined effects of increased mass and use of any one of these devices could be calculated by assuming that their effects operated independently. For example, doubling car mass and using an airbag (compared to no restraint) is calculated to reduce fatality occupant risk by  $1 - (1 - 0.65)(1 - 0.18) = 71\%$ .

The finding that large and small cars are driven dif-

ferently (46,47) is not related to passive protection, but is an aspect of crash avoidance. Engineering features which users perceive are, in general, likely to influence driver behavior; the extent to which they do so should, ideally, be determined empirically (48). There is little convincing evidence that wearing lap/shoulder belts produce observable driver behavior changes, and convincing evidence that if there are any such effects, they could not be large (49,50). It seems unlikely that the installation of airbags would lead to important modifications in driver behavior.

The question of car mass raises the even broader question of the choice of vehicle. An unhelmeted motorcyclist reduces his fatality risk by 28% by wearing a helmet. He can reduce it by 95% by travelling by car rather than motorcycle (37, page 60); the risk reduction would be smaller, but still large, even if motorcyclists are associated with higher than average levels of risk taking behavior (51). By transferring from the motorcycle to the car, he of course imposes a greater risk on other road users, but with a substantial net reduction in overall risk.

If attention is narrowed to include only the traditional occupant protection devices, then we find that the effectiveness of the most commonly discussed active device, the lap/shoulder belt, exceeds that of the most commonly discussed passive device, the airbag. Indeed, it is estimated that a driver who (despite all advice to not do so) switches from lap/shoulder belt use to airbag-only use increases his fatality risk by 41% (1). The lap/shoulder belt of course protects only if worn, so that the overall system effectiveness depends on use rates. Eqn 25 of (49) indicates that a use rate of 54% leads to a system wide driver fatality reduction of 18%. That is, 54% of drivers wearing lap/shoulder belts generates the same fatality reduction as all drivers being protected by airbags only. Although US rates are currently below 54% (recent data (52) indicates 42%), many other countries have much higher rates (53).

The question of what emphasis should be placed on the various approaches to occupant protection is of a quite different nature than the exclusively technical question of effectiveness. Most approaches involve costs of various types. It appears to be universally recognized that, although increasing car mass increases safety, such increased safety is purchased with a variety of economic and other costs. Essentially similar trade-offs are an intrinsic feature of all safety interventions (54). The cost need not necessarily be economic—it could be in terms of reduced mobility (for example, lower speed limits, older ages for driving licensure, increased legal restrictions on the mobility of older drivers beyond those they voluntarily chose in response to declining abilities (55), etc.) or increased restrictions on alcohol consumption, a single factor which is responsible for 47% of traffic fatalities (56). Even if prohibiting motorcycles would reduce U.S. traffic fatalities by about 4,000 per year, most would consider such a measure an unacceptable reduction in personal freedom.

## Conclusions

Many approaches to occupant crash protection can be identified which have the potential to make important contributions to reducing occupant fatalities. Although the effectiveness of the approaches reviewed varied over a wide range, it should be remembered that a one percent reduction in car occupant fatalities represents 200 fewer deaths annually in the United States. Any method which can make reductions of such magnitude makes a claim for serious evaluation in terms of economy, practicality and other costs. However, in addition to focusing on specific devices we should also keep in mind the potential harm reductions which might be available from more general considerations such as vehicle choice, car mass, and crash avoidance.

## References

- (1) L. Evans, Restraint effectiveness, occupant ejection from cars, and fatality reductions, General Motors Research Publication GMR-6398, September 1, 1988.
- (2) National Highway Traffic Safety Administration: *Fatal Accident Reporting System 1987*, Document DOT HS 807 360, December 1988.
- (3) L. Evans and M.C. Frick, Potential fatality reductions through eliminating occupant ejection from cars, *Accident Analysis and Prevention*, (in press), 1989.
- (4) National Highway Traffic Safety Administration, Final regulatory impact analysis, amendment of FMVSS 208, passenger car front seat occupant protection, Washington, July 11, 1984.
- (5) R.A. Wilson and C.M. Savage, Restraint system effectiveness—a study of fatal accidents, Proceedings of automotive safety engineering seminar, sponsored by Automotive Safety Engineering, Environmental Activities Staff, General Motors Corporation, June 20-21, 1973.
- (6) H.D. Pursel, R.W. Bryant, J.W. Scheel and A.J. Yanik, Matched case methodology for measuring restraint effectiveness, Society of Automotive Engineers, SAE paper 780415; included in SAE Transaction for 1978, 1965-1994.
- (7) C.J. Kahane, An evaluation of Federal Motor Vehicle Safety Standards for passenger car steering assemblies: Standard 203—Impact protection for the driver; Standard 204—Rearward column displacement, National Technical Information Service, Report No. DOT HS-805, 705, 1981.
- (8) C.J. Kahane, Evaluation of current energy-absorbing steering assemblies, Society of Automotive Engineers, SAE paper 820473; contained in SAE Special Publication SP-507, *Occupant Crash Interaction with the Steering System*, 45-49, Detroit, February 1982.
- (9) L. Evans and M.C. Frick, Relative fatality risk in different seating positions versus car model year, Proceedings of the 32nd Annual Meeting of the American Association for Automotive Medicine, Seattle, Washington, September, 1988, pages 1-13.
- (10) C.J. Kahane, An evaluation of occupant protection in frontal interior impact for unrestrained front seat occupants of cars and light trucks, Report No. DOT HS 807 203, January 1988.

- (11) L. Evans, Car size and safety: results from analyzing U.S. accident data, Proceedings of the Tenth International Technical Conference on Experimental Safety Vehicles, Oxford, England, July 1-4, 1985; US Department of Transportation, National Highway Traffic Safety Administration, DOT HS 806 916, pp 548-556, February 1986.
- (12) L. Evans, Fatality risk for belted drivers versus car mass, *Accident Analysis and Prevention*, 17, 251-271, 1985.
- (13) L. Evans, Driver fatalities versus car mass using a new exposure approach, *Accident Analysis and Prevention*, 16, 19-36, 1984.
- (14) L. Evans, Involvement rate in two-car crashes versus driver age and car mass of each involved car, *Accident Analysis and Prevention*, 17, 155-170, 1985.
- (15) Highway Data Loss Institute, Insurance injury report—passenger cars, vans, pickups, and utility vehicles—1984-1986 models, HLDI Reports 186-1, August 1987.
- (16) L. Evans and M.C. Frick, Seating position in cars and fatality risk, *The American Journal of Public Health*, 78, 1456-1458, November 1988.
- (17) L. Evans and P.F. Wasielewski, Serious or fatal driver injury rates versus car mass in head-on crashes between cars of similar mass, *Accident Analysis and Prevention*, 19, 119-131, 1987.
- (18) W.H. Hunter, R.J. Stewart, J.C. Stutts and E.A. Rodgman, Overrepresentation of non-belt users in traffic crashes, 32nd Proceedings of the Association for the Advancement of Automotive Medicine, 237-256, 1988.
- (19) L. Evans, Belted and unbelted driver accident involvement rates compared, *Journal of Safety Research*, 18, 57-64, 1987.
- (20) L. Evans, The effectiveness of safety belts in preventing fatalities, *Accident Analysis and Prevention*, 18, 229-241, 1986.
- (21) L. Evans, Rear seat restraint system effectiveness in preventing fatalities, *Accident Analysis and Prevention*, 20, 129-136, 1988. Also see, L. Evans, Rear compared to front seat restraint system effectiveness in preventing fatalities, Society of Automotive Engineers, SAE paper 870485; contained in SAE Special Publication SP-691 *Restraint Technologies—Rear Seat Occupant Protection*, 39-43, Detroit, February 1987.
- (22) L. Evans and M.C. Frick, Helmet effectiveness in preventing motorcycle driver and passenger fatalities, *Accident Analysis and Prevention*, 20, 447-458, 1988.
- (23) L. Evans, Double pair comparison—a new method to determine how occupant characteristics affect fatality risk in traffic crashes, *Accident Analysis and Prevention*, 18, 217-227, 1986.
- (24) L. Evans, Occupant protection device effectiveness in preventing fatalities, Proceedings of the Eleventh International Technical Conference on Experimental Safety Vehicles, Washington, D.C., May 12-15, 1987; U.S. Department of Transportation, National Highway Traffic Safety Administration, DOT HS 807 233, pp 220-227, November 1988.
- (25) B.J. Campbell, Safety belt injury reduction related to crash severity and front seated position, University of North Carolina Highway Safety Research Center, March 1984.
- (26) A.C. Malliaris and K. Diggs, Crash protection offered by safety belts, Proceedings of the Eleventh International Technical Conference on Experimental Safety Vehicles, Washington, D.C., May 12-15, 1987; U.S. Department of Transportation, National Highway Traffic Safety Administration, DOT HS 807 233, pp 242-252, November 1988.
- (27) L. Evans, Risk of fatality from physical trauma versus sex and age, *The Journal of Trauma*, 28, 368-378, 1988.
- (28) F.A. Haight, The place of safety research in transportation research, *Transportation Research*, 19A, 373-376, 1985.
- (29) C.J. Kahane, Fatality and injury reducing effectiveness of lap belts for back seat occupants, Society of Automotive Engineers, SAE paper 870486; contained in SAE Special Publication SP-691 *Restraint Technologies—Rear Seat Occupant Protection*, 45-63, Detroit, February 1987.
- (30) Viano, D.C., Culver, C.C., Evans, L., Frick, M.C., and Scott R., Involvement of older drivers in multi-vehicle side impact crashes, GM Research Laboratories Research Publication GMR-6607, March 17, 1989. For presentation to the 33rd Annual Meeting of the Association for the Advancement of Automotive Medicine, October 2-4, 1989, Baltimore, MD, and publication in proceedings of the meeting.
- (31) P.K. Verhaegen, K.L. Toebat and L.L. Delbeke, Safety of older drivers: a study of their over involvement ratio, Proceedings of the Human Factors Society, 32nd Annual Meeting, Anaheim, CA, 1988.
- (32) L. Evans, Airbag effectiveness in preventing fatalities estimated according to type of crash, driver age, and blood alcohol concentration, General Motors Research Laboratories Publication GMR-6594, March 8, 1989. For presentation to the 33rd Annual Meeting of the Association for the Advancement of Automotive Medicine, October 2-4, 1989, Baltimore, MD, and publication in proceedings of the meeting.
- (33) J.D. Graham (ed), *Preventing Automobile Injury—New Findings from Evaluation Research*, Auburn House, Dover, MA, 1988.
- (34) L. Evans, Factors controlling traffic crashes, *Journal of Applied Behavioral Science*, 23, 201-218, 1987.
- (35) H.L. Ross, Deterrence-based policies in Britain, Canada and Australia, in *Social Control of the Drinking Driver*, M.D. Laurence, J.R. Snortum and F.E. Zimring (eds), The University of Chicago Press, 1988.
- (36) L. Evans, Young driver involvement in severe car crashes, *Alcohol, Drugs and Driving*, 3, 63-78, 1987.

- (37) National Safety Council, *Accident Facts*, Chicago, 1988 Edition.
- (38) G.W. Trinka, I.R. Johnson, B.J. Campbell, F.A. Haight, P.R. Knight, G.M. Mackay, A.J. McLean and E. Petrucelli, *Reducing Traffic Injury—A Global Challenge*, A.H. Massina & Co., Melbourne, Australia, 1988.
- (39) International Road Federation, *World Road Statistics 1980–1984*, 1985 Edition.
- (40) G.D. Jacobs and I. Sayer, Road accidents in developing countries, *Accident Analysis and Prevention*, 15, 337–353, 1983.
- (41) G.D. Jacobs and C.A. Cutting, Further research on accident rates in developing countries, *Accident Analysis and Prevention*, 18, 119–127, 1986.
- (42) B.J. Campbell and D.W. Reinfurt, The relationship between driver crash injury and passenger car weight, Highway safety research center, University of North Carolina, Chapel Hill, NC, 1973.
- (43) D.F. Mela, How safe can we be in a small car?, Proceedings of the Third International Conference on Automotive Safety, San Francisco, July 15–17, 1974.
- (44) H.C. Joksch, Analysis of the future effects of fuel shortage and increased small car usage upon traffic deaths and injuries, Report number DOT–TSC–OST–75–21, January 1976.
- (45) L. Evans and M.C. Frick, Safety belt effectiveness in preventing driver fatalities versus a number of vehicular, accident, roadway and environmental factors, *Journal of Safety Research*, 17, 143–154, 1986.
- (46) P.F. Wasielewski and L. Evans, Do drivers of small cars take less risk in everyday driving?, *Risk Analysis*, 5, 25–32, 1985.
- (47) L. Evans, Human behavior feedback and traffic safety, *Human Factors*, 27, 555–576, 1985.
- (48) L. Evans, Driver behavior revealed in relations involving car mass, in *Human Behavior and Traffic Safety*, L. Evans and R.C. Schwing (eds), Plenum Press, pp 337–352, 1985.
- (49) L. Evans, Estimating fatality reductions from increased safety belt use, *Risk Analysis*, 7, 49–57, 1987.
- (50) L. Evans, Comments (on two papers on mandatory safety belt use laws, and reflections on broader issues), in, *Preventing Automobile Injury—New Findings from Evaluation Research*, J.D. Graham (ed), Auburn House, Dover, MA, pp 73–83, 1988.
- (51) J.G.U. Adams, *Risk and freedom—the record of safety regulation*, Transport Publishing Projects, London and Cardiff, 1985.
- (52) National Highway Traffic Safety Administration: 19-city safety belt and child safety seat use observation survey (for 4th quarter of 1987), Washington, DC, Feb. 1988.
- (53) B.J. Campbell and F.A. Campbell, Casualty reduction and belt use associated with occupant restraint laws. Contained in *Preventing Automobile Injury—New Findings from Evaluation Research*, J. Graham (ed), Auburn House, Dover MA, pp 24–50, 1988.
- (54) R.C. Schwing, Trade-offs, in *Societal Risk Assessment—How Safe is Safe Enough*, R.C. Schwing and W.A. Albers, Jr. (eds), Plenum Press, pp 129–145, 1980.
- (55) L. Evans, Older driver involvement in fatal and severe traffic crashes, *The Journal of Gerontology: Social Sciences*, 43, S186–S193, 1988.
- (56) L. Evans, The fraction of traffic fatalities attributable to alcohol, General Motors Research Publication GMR–6636, March 30, 1989.

## Impairment Resulting From Motor Vehicle Crashes

**Stephen Luchter,**  
National Highway Traffic Safety  
Administration,  
United States

### Abstract

Motor vehicle crashes are a major cause of death and injury in the United States. Quantifying the enormous impacts on society resulting from these deaths and injuries has been the subject of numerous studies. This paper discusses the present state of knowledge of an approach to quantifying societal impacts, called impairment, in which the parameter of interest is the time injured persons are unable to function at their pre-injury level. In this approach, a “whole body impairment factor” for each specific injury is multiplied by the life expectancy of the injured person, resulting in “person-years of impairment”. The duration of the impairment for less than lifetime, and any reduction in life expectancy as a result of the injury are accounted for in

the methodology. Topics of particular emphasis in the paper are the definition of impairment, the attributes that comprise impairment, and comparisons with other concepts that have been developed to quantify health status and the impact of injuries on society.

### Introduction

Motor vehicle crashes reported to the police in the United States result in injuries to about three and a half million persons each year (1),\* about forty-six thousand of whom die (2). A means of allocating the limited resources available to attack such a vast problem is needed which will result in the greatest reduction in the impact of these injuries and fatalities on society. This paper is concerned with measuring societal impact, and particularly with the current status of the method called Impairment.

\*Numbers in parentheses designate references at end of paper.

Table 1. Incidence of motor vehicle occupant injuries in the United States in 1986.

AGE	AIS 1	AIS 2	AIS 3	AIS 4	AIS 5	FATAL
0-4	69347	6623	1287	149	97	954
5-9	78479	6716	3045	133	313	1005
10-14	78859	9076	2747	302	38	1201
15-19	578131	62091	18305	3662	2353	6839
20-24	568676	71022	22888	3048	1646	7970
25-29	451448	50835	15294	2627	1822	5932
30-34	298239	38297	10195	893	556	4215
35-39	257933	27093	7870	1024	328	3203
40-44	175326	18424	5642	641	404	2186
45-49	105315	13588	4711	278	356	1700
50-54	102213	13135	3499	360	21	1575
55-59	110180	12208	6369	394	142	1563
60-64	82258	10001	3168	1128	33	1564
65-69	54136	7930	1728	251	162	1458
70+	116400	13461	4431	1221	496	4437
Unknown	142106	2543	291	39	20	254
Total	3269046	363043	111470	16150	8787	46056

Source: Injury data from the National Accident Sampling System, Fatality data from the Fatal Accident Reporting System [4]

## Measures of Societal Impact

Until recently, there have been two ways to estimate the societal impact resulting from motor vehicle crashes, by the number of persons affected (incidence), or by the economic impacts. With the increasing use of occupant restraints and advances in trauma medicine saving many lives that would have been lost in the past, the interest in accurately measuring the long term impacts on survivors has increased. A method has been developed to measure these long term impacts by measuring the time lost as a result of the injury. This method, called impairment, focuses on the impact the injury has on the individual. The effect the individual's injuries have on society is then the sum of the time lost by each injured person. Note that each of these methods provides a different insight into societal impacts, and they should be considered as complementary to each other.

## Incidence

Probably the simplest way of measuring the societal impact is by counting the number of persons injured or killed. With currently available data, injury incidence can be disaggregated by age, sex, body region injured, injury severity using the Abbreviated Injury Scale (AIS) (3), and other factors. (The AIS has been shown to be a good indicator of threat to life.)

An example of incidence in 1986 is shown in table 1, where the number of injured survivors of motor vehicle crashes at AIS levels from 1 to 5 and the number of fatalities

are shown for each five year age bracket through 65 and for those 70 and older (4). For all severity levels, injuries to persons under 15 are low, peak in either the 15-19 or 20-24 cohort and trend downward after that, with fatalities dropping more slowly than serious injuries. Note that the 70+ cohort includes persons injured or killed up to about 90.

Using incidence as a measure of societal impact has the advantage of being a direct measure of the number of persons actually injured or killed. However, there is concern over the accuracy of the injury data, as the data shown here are based on an estimate developed from a sample of police reports. The AIS 1, 2 and 3 values can be considered reasonably accurate, as they are based on large numbers of persons in the initial sample. The AIS 4 and 5 values have much smaller sample size and cannot be treated with the same level of confidence. The fatality data are based on a census of all motor vehicle related fatalities in the United States and can be considered quite accurate. A concern with the fatality data is that there is a cutoff of 30 days after the crash, and some persons, especially older persons, may die after 30 days as a result of the injuries received in a crash.

Another disadvantage of using incidence as a measure of societal impact, which recently has been confirmed by a careful study, is that it is difficult to compare injuries at the same severity to different body regions (5). The fatality rates and the long term consequences are different for the same AIS level for different body regions. Or, stated in another way, the AIS does not appear to be a good indicator of the long-term effects of trauma on survivors. Thus, even

Table 2A. Summary of human capital costs.

COST CATEGORY	\$, Billion	Percent
Property Losses	27.37	36.9
Insurance Expense	20.86	28.1
Productivity Losses	16.38	22.1
Legal and Court Costs	4.32	5.8
Medical Costs	4.12	5.6
Emergency Costs	0.70	0.9
Other Costs	0.45	0.6
Total	74.20	100.0

Injury or Accident Severity	\$, Billion	Percent
AIS 1	9.39	12.7
AIS 2	2.47	3.3
AIS 3	1.88	2.5
AIS 4	1.01	1.4
AIS 5	2.71	3.7
Fatality	16.50	22.2
Property Damage Only	29.59	39.9
Uninvolved	10.64	14.3
Total	74.19	100.0

Table 2B. Distribution of unit societal costs, percent.

Cost Category	AIS 1	AIS 2	AIS 3	AIS 4	AIS 5	FATAL
Medical Costs	8.4	33.6	34.8	24.1	55.5	0.6
Productivity Loss	4.0	10.9	14.0	26.2	31.9	86.9
Property Damage	33.2	27.0	19.1	5.9	1.3	1.3
Legal/Court	21.8	11.6	24.1	10.6	3.7	5.0
Emergency Costs	2.5	2.3	1.1	0.4	0.1	0.1
Insurance Admin.	24.8	12.0	5.5	31.7	7.2	5.7
Public Assistance	0.2	0.1	0.1	0.8	0.2	0.2
Insurance U/write	2.2	1.1	0.5	0.1	0.0	0.0
Gvt. Programs	2.9	1.4	0.7	0.1	0.0	0.0
Total Cost, \$	3,245	6,245	14,742	64,812	284,752	358,310

Source for both tables - Reference 9

Note: Table 2B totals do not add to 100% in all cases due to rounding.

if we knew how many AIS 4 head injuries and how many AIS 4 thorax injuries resulted from crashes, there is no way to determine if either has a greater impact, because a greater number of thorax injuries do not necessarily have a greater impact than a lesser number of head injuries. To measure the long term effects requires some factor that either directly measures the long term effects or is a surrogate for a direct measure.

## Economic Impacts

One weighting factor that has been applied to incidence to provide an indication of the impact injuries have on society is to use the cost to society. Techniques have been developed to estimate the direct and indirect monetary costs to society, and to monetize otherwise intangible impacts such as pain, suffering, grief, "willingness to pay", etc.

## Human capital

The human capital approach, initially developed in the 1960's (6), has become widely accepted as the method of estimating the societal cost of motor vehicle crashes. As applied at the National Highway Traffic Safety Administration (NHTSA), this accounting of the costs resulting from motor vehicle crashes sums the medical, property damage, insurance overhead, legal and court, emergency, and public assistance overhead costs, as well as the cost of government programs to reduce crashes and the resulting fatalities and injuries, and of particular importance in fatalities and the more serious injuries, lost productivity (7, 8). Future costs such as long term medical expenses and lost productivity are discounted back to their present value.

An estimate of societal costs of motor vehicle crashes in 1986, using NHTSA's human capital methodology, is shown in table 2A (9). These data are based on motor vehicle injury incidence during 1986 from NHTSA's National Accident Sampling System (NASS) (4), the number of fatalities from NHTSA's Fatal Accident Reporting System (FARS) (4), and an indexing of the unit human capital cost values developed in (8). In developing the basic cost estimates in (8), a 7% discount rate and a 1.5% productivity growth factor were used. Note that the cost for those injured relate to injured survivors.

The percent distribution of the unit human capital costs by severity level and cost category is shown in table 2B. Note that the costs due to lost productivity increases significantly as the injury severity increases. The medical costs at the AIS 4 and 5 levels include more than one year's costs and the amounts shown include the discounted value of the future costs.

Recent results of research in human capital costs are included in references 10, 11, 12, and 13.

Although the human capital method is currently the most accurate approach to measuring the costs to society, it has certain limitations when estimating societal impacts. Primarily, it does not count persons equally. It effectively downgrades the importance of children, young adults, homemakers, the unemployed and older persons, with greater weight given to persons in their peak earning years. This is a particularly important bias when considering the effects of motor vehicle crashes, where the injury incidence is highly skewed toward the young adult. Note however that this is not an inaccuracy in the human capital methodology, only a limitation in how the results should be applied.

The total economic impact depends on the age distribution of the incidence. Especially for serious injuries with long term effects and for fatalities, the lost productivity and the medical costs after the first year make up a major part of the total. Unfortunately, both the earnings and the discounted earnings are highly non-linear functions of age.

A qualitative illustration of the problem at the AIS 1, 2, and 3 levels is shown in figure 1, where the normalized incidence for injured survivors at the AIS 1, 2, and 3 severity levels is shown as a function of age, along with the normalized average earnings. (For the AIS 1, 2, and 3 sever-

ity levels, discounting has not been used in the NHTSA analysis because costs were assumed to not occur after one year). In this figure, each vertical bar represents the percentage of the maximum incidence for that age cohort. For example, the largest incidence of AIS 1 injuries occurs in the 15 to 19 year old cohort. The 0 to 4 age cohort experiences about twelve percent of the incidence as the 15 to 19 year olds. Similarly, for the earnings, the curve shows the percentage of the maximum earnings. At age 45 to 49, the average person achieves peak earnings. At age 30 to 34, the average person achieves about 80 percent of their peak earnings.

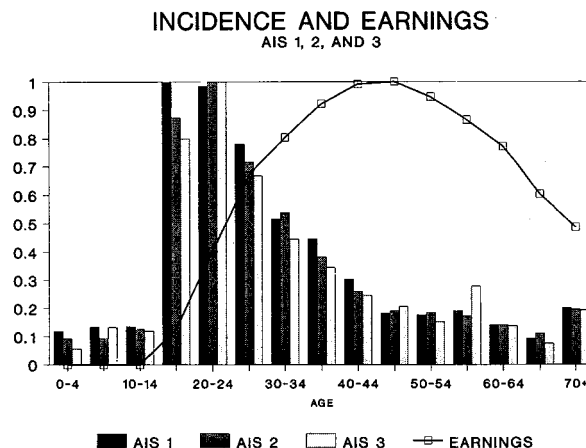


Figure 1. Incidence and earnings.

The age/earnings distribution differs significantly from the age/incidence distribution. Whereas the AIS 1, 2, and 3 incidence peaks in either the 15 to 19 or the 20 to 24 age cohort, earnings do not peak until 45 to 49 years. This results in the productivity of the 0-15 year old portion of the population not counting at all, the higher incidence cohorts counting little, and the low incidence middle age group counting a lot. However, since lost productivity is 4.0, 10.9, and 14 percent respectively of the total unit cost for the AIS 1, 2, and 3 levels respectively (see table 2B), this overall undercounting cannot be considered a serious problem, given all of the other potential errors.

The situation is more significant for the AIS 4, 5, and Fatal injuries. This is illustrated qualitatively in figure 2,

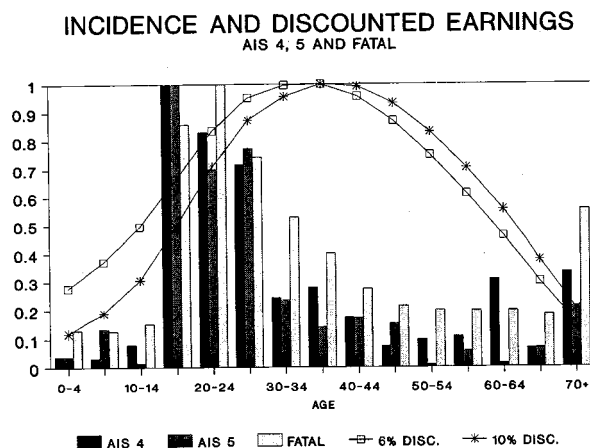


Figure 2. Incidence and discounted earnings.

where the normalized incidence is shown along with the discounted average earnings at both 6% and 10% discount rates (not including the effect of possible future changes in productivity). The range of 6 to 10 percent is considered a reasonable bound for the discount rates that may be applied to this type of analysis.

For the AIS 4 and 5 injuries, where discounting affects about 40% to 50% of the total (lost productivity and some part of the medical costs from table 2B), a large error is introduced. For illustrative purposes, assume that half of the total costs at the AIS 4 and 5 levels are affected by discounting. Thus, persons under age 15 are counted at between 60 and 75 percent as much as a person unaffected by discounting. This range of percentages is based on the half unaffected by discounting (50%), plus 20 to 30 percent of the remaining half that is affected by discounting. The 20 to 35 percent can be seen from figure 2. Similarly, persons in the 15 to 19 and 20 to 24 cohorts, with by far the largest part of the total incidence, count about 80 percent as much as a person in peak earning years (half plus 60 to 70% times the other half), persons in the age cohorts between 25 and 49 count for about 95% of a person in the peak earning years (half plus about 90% of the other half), after which the percentage declines to about 60 percent at the older age brackets (half plus 20% of the other half).

The error introduced into the calculation for the economic effect of fatalities on societal impact is larger than the effect of the AIS 4 and 5 injured survivors, because 87% of the total cost of fatalities is based on lost productivity. For example, persons in the peak incidence cohort for fatalities, 20 to 24, would count for 80% as much as a person in their peak earning years, (13% not discounted plus about 75% of the remaining 87%), while older age cohorts, with much smaller incidence, would be counted nearly at full value.

Although the human capital cost is widely accepted as the most accurate measure of what society pays as a result of injuries, it does not reflect the overall societal impact. The primary problem is that it counts individuals differently, due to the differences in earnings as a function of age, the effect of discounting, and the male/female differences in work force participation and earnings.

### Willingness to pay

The human capital approach is based on the identifiable costs to society as the result of a crash. Although experts differ on some details, the general outline of the human capital approach and its derivatives is reasonably well defined. An alternative approach to estimating the economic impacts on society of motor vehicle related injuries is based on the concept that people are willing to pay more than the identifiable costs in order to avoid being injured or killed (13). This approach has been advocated by some economists as the correct measure of benefits for use in cost/benefit analyses, however not all authors agree on the details of the methodology (14). Work is still underway to develop the willingness to pay concept, including an exten-

sion of the concept to injuries (10, 13). For additional discussion of this topic see (12).

### Harm

The human capital and willingness to pay methods are generally applicable to determining the overall economic impacts on society. Neither method is well adapted to determine the societal impacts of specific injuries. The "harm" concept was developed to allow consideration of the effects of individual injuries (15). It normalized the human capital societal costs of each injury severity level using the Abbreviated Injury Scale (AIS) (3), including the relative percentage of those killed at that injury severity level. The main shortcoming of harm was found to be that by considering only the threat to life, that is the AIS level of the injury, important relative effects were neglected. As noted earlier, a recent study showed that injuries at the same AIS level to different body regions have different relative frequency of fatality, and different long term effects (5). Theoretically at least, this shortcoming could be overcome if costs were available for each body region/severity level.

### Impairment

Another weighting factor that can be applied to incidence to estimate the societal impact is called Impairment. A discussion of Impairment and its current status is the primary topic of this paper. In this approach, a "whole body impairment factor" is applied to the most serious injury, and multiplied by the remaining life expectancy of the injured individual. The whole body impairment factor is intended to portray the degree to which the person is functionally impaired. It is based upon the composite decrement in functional performance of a series of attributes that persons in society exhibit. The product of the impairment factor and the life expectancy is then the amount of time the person will not be functioning at full capacity over the remainder of their lifetime. The Impairment concept was developed as a means of eliminating some of the biases introduced when economic costs are used as a measure of societal impacts. In the Impairment concept, a person's worth is not based on their earning ability. Rather, life itself is considered as having its own inherent value.

INJURIES, FATALITIES, EXPECTANCY  
NORMALIZED WITH RESPECT TO MAX VALUES

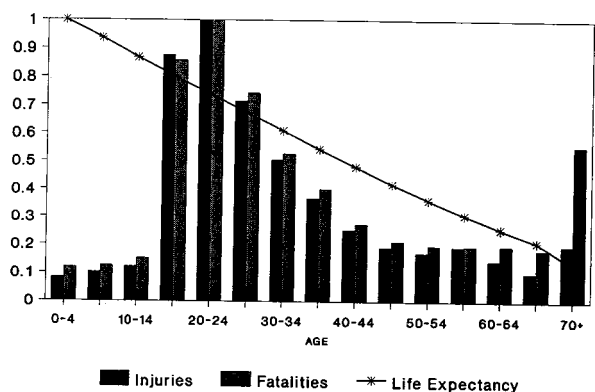


Figure 3. Incidence and life expectancy.

A qualitative illustration of the match between injury and fatality incidence and life expectancy is shown in figure 3. Here the age/expectancy distribution does not differ as widely from the age/incidence distribution as in the economic models. If there is any overcounting it occurs at the youngest ages, which generally reflects the cultural characteristic of western industrial society to highly value its children.

This paper describes the current state of the effort to develop the Impairment concept to the point where it can be widely applied to measure the societal impact of motor vehicle crashes, and discusses the additional work that needs to be done in order to achieve that goal.

## Evolution of the Impairment Concept

The initial effort to develop impairment as an alternative to economic measures of societal impact of motor vehicle injuries considered the effects of specific injuries rather than the effects at the AIS level (16). The impairment resulting from each injury included in the AIS manual (3), the Occupant Injury Code (OIC), was estimated for each of six impairment attributes: mobility, cognitive, sensory, pain, cosmetic, and daily living. A physician, expert in a particular medical specialty (neurology, orthopedics, plastic surgery, general surgery), judged which of four levels of impairment (minor through maximum) would result for each injury, and the duration of that impairment. Three time frames were considered: less than a year, a year to five years, and five years and beyond. In addition, differences in impairment for four age categories were considered, as was any reduction in life span as a result of the particular injury. The result of this effort was a listing of the impairment estimates, disaggregated by the categories noted above. Although this was a monumental undertaking, the results were difficult to use, and thus were not widely applied.

A further step in the evolution of Impairment was the development of the Injury Priority Rating, (IPR) (17). Like harm, the IPR represented the normalized cost of an injury, but used costs appropriate for each injury at the OIC level. It also considered survivors and fatalities separately. Most important to the development of the Impairment concept was the idea of collapsing the factors in (16) to a "whole body impairment factor", similar to those developed by the American Medical Association (18).

Another key to the development of the impairment concept, the idea of using time as a measure of impairment, came from two NHTSA in-house efforts. One estimated the duration of short term impairments lasting less than one year by collapsing the time values for each of the six categories of impairment in (16) into an equivalent single time period (19). The other, (20), estimated the long term impairment (greater than one year) for each injury using the whole body impairment factors developed in (17). These factors were multiplied by the life expectancy of persons injured in motor vehicle crashes at the AIS 2 and above level, taken from the 1982-1984 National Accident Sampling System data base. This resulted in "person-years of impairment".

The duration of the impairment for less than lifetime, and any reduction in life expectancy as a result of the injury also were accounted for. The study found that about 0.7 million person-years are lost each year in the United States to survivors of motor vehicle injuries, and, taking death as 100% impairment, 1.7 million person-years are lost to fatalities. These papers also demonstrated how impairment could be used to solve a variety of practical problems. In addition, the papers identified further work needed before Impairment could be widely applied—the development of a comprehensive definition of impairment, the development of a consensus on the impairment resulting from each injury, how best to combine the impairment factors into an equivalent whole body factor, and the development of an approach to quantifying the impairment of AIS 1 injuries.

## Comprehensive Definition of Impairment

Being impaired means that in some way a person cannot function "normally". In the same way as being healthy includes physical, mental, and social health, a person may be physically, mentally, or socially impaired. All of these factors must be considered in developing a comprehensive definition of impairment that can be used operationally.

In every-day speech impairment, disability, and handicap often are used interchangeably, however, these words do have different meanings. Impairment means lessening in value or strength, disability means being incapable of normal physical activity, and handicap means a person has a hindrance or disadvantage. In this paper, these dictionary definitions are modified and narrowed so that they can be used as the basis for developing quantitative estimates. Overall, the definitions follow those of the American Medical Association (AMA) (18) and the Association for the Advancement of Automotive Medicine (AAAM) (21), and in part the World Health Organization (WHO) (22). At times the distinctions between these definitions are subtle, and must be considered in the context of the application.

"Impairment" is defined here as a functional loss resulting from an injury, the "loss" being describeable in medical terms, such as found in the Abbreviated Injury Scale (3), or the International Classification of Diseases (22). For example, amputation of an arm, having a disfiguring scar, or suffering from depression, etc., would be typical impairments. Impairment is independent of the person's age, sex, occupation, or socio-economic status, (except where the impairment is unique to persons of a particular age, or sex).

"Disability" is defined here as a reduction in one's ability to participate actively in society in a manner appropriate to the person's age, sex, socio-economic status and relationship status prior to the injury. For example, as a result of the loss of an arm, a young, single, fashion model with adequate prosthesis might no longer be able to engage in his former occupation, and his social life might be affected if his

**Table 3. Comparison of definitions.**

<u>AMERICAN MEDICAL ASSOCIATION</u>	<u>WORLD HEALTH ORGANIZATION</u>	<u>ASSOCIATION FOR THE ADVANCEMENT OF AUTOMOTIVE MEDICINE</u>	<u>THIS PAPER</u>
<u>IMPAIRMENT</u>			
"the loss of, loss of use of, or derangement of any body part, system or function", based on "an assessment of data collected during a clinical evaluation"	"any loss or abnormality of psychological, physiological, or anatomical structure or function"	"the loss of function or abnormal function of an organ, tissue, or organ system resulting from an injury and remaining after healing has occurred"	the loss of physical, mental, or social function resulting from an injury
<u>DISABILITY</u>			
"the limiting loss or absence of the capacity of an individual to meet personal, social, or occupational requirements" based on a nonmedical assessment	"any restriction or lack (resulting from an impairment) of ability to perform an activity in the manner or within the range considered normal for a human being"	"the effect or consequence of an impairment or multiple impairments on the whole person as a member of society"	a reduction in one's ability to actively participate in society in a manner appropriate to one's age, sex, socio-economic and relationship status

HANDICAP

"a disadvantage for a given individual, resulting from an impairment or a disability, that limits or prevents the fulfilment of a role that is normal (depending on age, sex, and social and cultural factors) for that individual"	"the loss of function, the abnormal appearance, or the abnormal behavior caused by an impairment which is evident to the public"	society's view of the functional loss resulting from an impairment
---	--	--

friends and companions were not particularly supportive, whereas a bank teller with a spouse and children, suffering the same impairment, might be able to return to her job and largely continue her earlier social life. The model would be considered disabled, the bank teller not disabled, even though they both had the same impairment.

One reason for the importance of the distinction between the definitions of impairment and disability is that data are available describing injuries people receive, from which impairment can be estimated. These data are applicable to the general population. Data are not always available to describe the social or economic situation of the injured person, and thus disability may be unknown. If it is known, it is not likely to be applicable to the general population. Care must be taken in reading the literature, however, as these definitions are not universally accepted, and some authors use "disability" as "impairment" as defined here.

"Handicap" is defined here as society's view of the functional loss resulting from an impairment. For example, a wheelchair-bound paraplegic would be impaired, might be

**Table 4. Some functional status factors by author and intended application.**

Hirsch et al	Carsten & O'Day	States & Viano	MacKenzie et al	Torrence
Impairment Rating	Injury Priority Disability Scale	Impairment & Survivors	Trauma	Genl. Population
Mobility	Mobility	Mobility	Mobility	
Cognitive	Cognitive System	Central Nervous		
Sensory	Sensory	Sensory		
Pain	Pain	Pain		
Cosmetic	Cosmetic Disfigurement	Cosmetic/		
Daily Living		Daily Living	Self Care Activity	Self Care & Role
	Sexuality/ Reproduction			
		Physical Capabilities	Physical Function	
			Social/Emotional Function	
			Health Problem	

disabled, but if there were access ramps at sidewalk crossings, and facilities for use of a wheelchair in public accommodations, probably would not be considered handicapped by these definitions.

A comparison of these definitions with those of the AMA, AAAM, and the WHO is shown in table 3. All of the

definitions of impairment include the concept of loss of function, and are in reasonably close agreement. The definitions of disability are not in close agreement, with the AMA and AAAM definitions including the concept that disability is the result of the outcome of an impairment related to the particular individual, while the WHO definition is closer to

**Table 4 (continued). Some functional status factors by author and intended application.**

Kaplan	Wood-Dauphinee et al	Stewart et al	Jacobs	Wolfson et al
Genl. Use	Reintegration of Patients	Patients & Genl. Population	Head Injury	Stroke Victim
Mobility	Mobility		Mobility	Transfer, Ambulation, Wheelchair
			Cognition	Understanding
		Pain		
	Self Care		Self Care	Dressing, bathing, continence, eating
Physical Activity	Daily Activities	Physical Function		
Social Activity	Recreational & Social Activity	Social Functioning	Social & Adaptive Living Skills	
Symptom		Health Perception		
	General Coping Skills	Mental Health, Role Function	Behavior/Emotional Problems	Mental Status
	Personal Relationships			
	Presentation of Self to Others			
			Communications	Speech
			Household Business & Housework	
			Child Care	
			Employment	
			Community Skills	
			Education	
			Seeking Employment	

**Table 4 (concluded). Some functional status factors by author and intended application.**

Rosser	Sintonen
Inpatients	General Public
	Moving
	Seeing, Hearing
Distress	
	Sleeping, Eating, incontinence
	Social Participation
	Perceived Health
	Communicating
	Working
Disability	

what the other two would consider impairment. The WHO definition of handicap is close to the AMA definition of disability. The AAAM definition of handicap introduces the concept of public perception.

### **Functional Status Scales—A Review of the Literature**

Having defined impairment as a functional loss, it is next necessary to consider just what is meant by function. This complex subject has been the subject of considerable research, undertaken for a variety of reasons, and based upon a variety of theoretical approaches. A small sample of these research results are summarized in table 4. This table is not intended to be comprehensive, as the literature on functional status, indices related to a specific injury or disease, and quality of life indices, etc. is quite extensive.

Each column in table 4 is a list of functional attributes described by the cited author. These are grouped so that similar functions are on the same row. Note that not all of the definitions of terms are in total agreement. What to some authors is daily living is to others self care, and to still others physical functioning. Additional details on most of these scales are included in the Appendix.

The first three entries in table 4 (Hirsch et. al. (16), Carsten and O'Day (17), and States and Viano (21), were developed to describe impairment resulting from injuries sustained in motor vehicle crashes. Although these lists of attributes cover a wide variety of human functions, there is no factor concerned with the use of the upper limbs (except indirectly through daily living), or of impairment to internal organs. Only the States and Viano set of attributes in table 4 includes sexuality and reproduction.

MacKenzie et. al. (23) used a three attribute scale to describe functioning of trauma survivors: self care, (feeding, bathing, dressing, toileting, and bed transfer), mobility (getting around own home, the neighborhood, and the ability to use public transportation) and physical capabilities (walking a quarter of mile, walking up and down stairs without resting, using fingers to grasp and handle as major functions, and standing for long periods of time, bending down, and light lifting as minor functions). Even though MacKnezie uses only three attributes, her work covered the physical functions in a thorough manner. However, this listing does not include factors relative to emotional or social functioning.

Torrance and his colleagues have written extensively about the application of multi-attribute utility theory to scaling health status. Their scale uses three major attributes: physical function (mobility and physical activity), role function (self-care and role activity), and social-emotional function (emotional well being and social activity), plus a category called health problem, (a diversity of factors such as vision, scars, pain etc.) (24). A more recent publication cited by Torrance indicates that cognitive, sensory, and pain attributes should be included in a comprehensive scale (25).

Kaplan (26) also uses a three factor scale, mobility, physical activity, and social activity. This scale is typical of the

psychometrically derived scale of health status. In addition, Kaplan developed a "correction factor" to be applied to the health status depending on symptom or health problem.

A scale developed to assist in determining how well a person reintegrates into society was developed by Wood-Dauphinee et. al. (27), who take the view that the person's roles in family, community, or work settings are more important than their physical capabilities. Thus, the use of adaptive equipment, supervision or assistance in order to accomplish the tasks is not considered a reduction in function. This scale includes three mobility factors, plus self care, daily activities, recreational activity, social activity, general coping skills, personal relationship, and presentation of self to others.

The scale developed by Stewart et. al. is based on the six "health concepts" of pain, physical function, social function, health perception, mental health, and role function (28). This scale was developed to provide a short form useful for general health surveys. One of the physical functions pertains to what other authors have called self care (eating, dressing, bathing, or using the toilet).

Jacobs developed a very comprehensive scale of 700 discrete daily behaviors in twelve "major life areas", to describe the functional status of survivors of severe traumatic head injury (29). Excluded are those who are comatose, and those with mild long term impairment. The major life areas are shown in the table. Several of the factors would be in what this paper would call disability, such as household business, employment, seeking employment, etc.

The final three columns represent scales reported elsewhere in the literature but not reviewed in the original (30, 31, 32). Note that Rosser's Disability includes mobility, social disability and work performance.

Examining the results in table 4 as a whole, it is surprising that there is as much commonality as there is, since these scales were developed for different purposes. Almost all of the scales include some factor for mobility, and most include attributes relating to cognitive impairment, pain, and daily living functions. Several include attributes relating to mental health and social functioning. Unfortunately, however, there is not enough commonality that an inclusive scale can be synthesized. Thus it became necessary to develop a set of attributes and the interrelationship between them based on an analysis of how people in society actually function.

## Functional Status—A Systems Engineering Approach

A typical engineering approach to solving a complex problem is to break it down into manageable parts. It is often helpful to develop a model describing the total entity and its major systems, and then break these major systems into sub-systems and components. This method was applied to develop a comprehensive list of the attributes of human functioning.

## The model

A model of the attributes of a healthy person in a "normal" setting was conceived. The attributes for persons in a hospital or extended care facility are then subsumed into the basic definitions. Any decrement from the healthy conditions will then describe impairment.

The model identifies four levels of human functioning: fundamental functions necessary to be alive (primitive functions), functions to allow operation as an independent being (mechanical functions), functions related to emotional well-being and higher level thinking (thinking-feeling functions), and functions related to interaction with others (interactive functions). The model is represented in figure 4 as a series of concentric circles. In some ways this concept is similar to the Maslow concept of hierarchy of needs found in the psychology literature. Here however it is not fully necessary for attributes at a lower level to take precedence over higher level attributes.

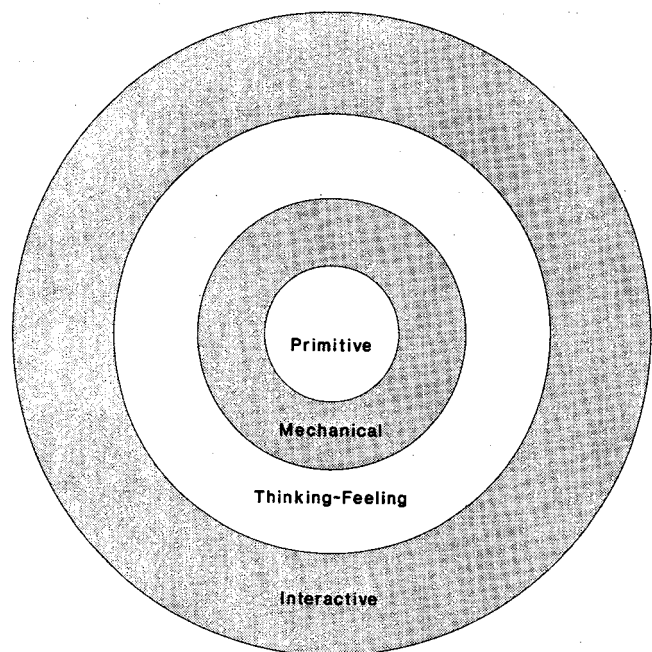


Figure 4. Pictorial representation of human functioning.

At the most primitive level, such as if a person were in hibernation, the body can be thought of as functioning as if it were a chemical plant. Raw materials (air, water, food) enter the "plant", a variety of chemical processes occur, and products (body heat, waste) leave the plant. A variety of "pumps", "heat exchangers", "pipes", and "reactors", have to operate properly. The "control system" is simple, and not particularly adaptive. There is no interaction with others, and interactions with the environment occur only to the extent that the inputs and outputs come from and go to the environment. Impairment at this level includes loss of or improper functioning of the body's internal organs, a reduction in the ability to eat or drink, and any difficulties with elimination.

At the next level, the body can be thought of as functioning as an adaptive mechanical device, not just like a robot, but aware of what is going on, initiating and controlling its motions, but without feelings. The senses provide information about the environment, the brain processes the information, and directs some part of the body to do something. Impairment at this level would include sensory impairment, (such as blindness, deafness, lack of tactile sensation, lack of smell, lack of taste, and pain); simple cognitive impairment resulting from lack of ability to translate sensory information into physical action, given that the senses are functioning, and the body parts are capable of normal motion; and impairment due to inability or restriction in movement of body parts, such as a "frozen" joint, amputation of a limb, etc.

It is necessary to depart from the mechanical analogies at the next level, because the person now loses any robot-like qualities. He is able to think creatively so as to change his situation, and has feelings such as happiness or sadness.

**Table 5. Impairment attributes derived from systems analysis.**

Type/Level	Primitive	Mechanical	Thinking-Feeling	Interactive
Basic Bodily Functions	breathing eating drinking digesting eliminating circulating (blood) sleeping			
Sensory		seeing hearing touching smelling tasting feeling pain		
Motion of body parts		walking grasping speaking		
Cognitive		controlling body motions	reasoning logically having judgement thinking creatively	
Emotional			feelings of self worth	interacting with others having appropriate sexual drive

Impairment in this case would include reduction in reasoning ability and judgement, and psychological impairment (emotional well being).

The model takes into account the innately gregarious nature of humans at the highest level of functioning. At this level, a person interacts with others by sharing both things and ideas, negotiating, recognizing the needs of others, etc. Impairment at this level would include a reduced ability to interact with others. Sexuality is included in this level rather than in the mechanical level, recognizing that sexuality includes not only lust but intimacy as well.

## Results

Based on this model, the attributes of a "whole person" in society are shown in table 5. Excluded from the list is reproduction, as lack of ability to reproduce is not considered to be an impairment. Some persons do not want to reproduce, and others may be infertile due to age or illness. Also excluded is what may be a significant category, the

effect of an injury or fatality on other persons. For example, it has been indicated that persons in a vehicle in which someone was killed in a crash may suffer from post traumatic shock syndrome. If these survivors were not otherwise injured, their impairment would not likely be found by current data collection techniques. Another exclusion is being disfigured. This is a matter of definition. Disfigurement is included in two places, lack of ability to move body parts, or in feelings of self worth as a result of unsightly scars, etc.

Note that all of the entries in table 5 are stated in the form of a verb. This is to recognize that these attributes imply action or state of being, not static description. A rigorous definition for each attribute remains an area for further research.

## Attribute Severity

The method of quantifying impairment described in this paper requires that severity levels be defined for each attribute. For example, slight, moderate, and maximum could be considered as levels of severity. Each attribute will have some level or range of performance where there is no impairment. As performance degrades, impairment increases. For example, visual acuity of between 20/20 and 20/40 might be considered as unimpaired vision, and visual acuity of 20/400 or worse might be considered as total visual impairment. Visual acuity between these values would represent an intermediate level of impairment.

As shown in the Appendix, each author has their own idea on the number of severity levels appropriate for a particular attribute. Hirsch et. al. utilized the same four levels for each attribute: slight, moderate, severe, and maximum (16). A separate definition for each attribute/severity level combination was developed by an expert in the field. For example, moderate cognitive/psychological impairment was defined as "Often disoriented, loss of ability to do simple arithmetic, slight impairment of language or memory, may be psychotic but not committable". States and Viano defined six severity levels for mobility, central nervous system impairment, pain, and activities of daily living; four for cosmetic/disfigurement and sensory; and three for sexuality and reproduction (21). Kaplan utilized five levels for mobility and social activity and four for physical activity (26).

A different approach is taken by the American Medical Association (18). They define numerical values for impairments found in twelve body systems: the extremities, spine and pelvis; the nervous system; the respiratory system; the cardiovascular system; the hematopoietic system; the visual system; ear, nose, throat and related structures; the digestive system; the reproductive and urinary systems; the endocrine system; the skin; and mental and behavioral disorders. For example, amputation of the thumb at the interphalangeal joint is considered as 75% impairment of the thumb.

In Carsten and O'Day's work (17), the percent impairments for each attribute were taken from AMA values (18) for a typical injury related to each definition. For example,

maximum mobility impairment was taken as 85%, the value shown in the AMA publication for "Cannot use upper extremities". These values were roughly confirmed by a forced choice ranking by a small group. The forced choice indicated higher numerical impairment values than the AMA for the less severe levels of impairment.

Another approach to measuring severity level avoids the need to define attributes, and places each injury onto an arbitrary impairment scale. A recent TRRL report used a five level scale: nil, slight, moderate, severe, and very severe (33). (See Appendix for further details). Here, too, the authors defined this scale as related to disability, rather than impairment, however it appears from the context that it is appropriate to consider it as an impairment scale.

The Japanese insurance industry also has a "disability" scale that appears to be related to impairment as defined in this paper (34). "Injuries which fail to heal completely and continue to affect the body to some extent are recognized as disabilities even if the resulting disorders do not continue throughout a person's lifetime." In this listing, long term effects are divided into 14 classes. A typical impairment in Class 1 is total loss of function of both upper limbs. A typical impairment in Class 14 is being disabled in the functions of the little finger of one hand. A complete listing is shown in the Appendix. An analysis of this table shows that the body regions/functions included are eyes, ears, nose, mastication and speech, teeth, nervous system or psyche, spinal column, thorax and abdominal organs, upper limbs, lower limbs, hands and fingers, feet and toes, deformities, and genitals. Classes 1, 2, and 3 impairments generally last a lifetime. About 97% of disabilities are in classes 7-14. In addition to the scale listing, a "Rate of Loss of Working Capacity" for each Class is identified, as follows: 1, 2, 3 = 100%, 4 = 92%, 5 = 79%, 6 = 67%, 7 = 56%, 8 = 45%, 9 = 35%, 10 = 27%, 11 = 20%, 12 = 14%, 13 = 9%, 14 = 5%. If one assumes that the loss of working capacity can be considered as impairment, it is possible to use the scale quantitatively. For example, "disabled in the function of all fingers of both hands" is in Class 4, and would with this assumption be considered 92% impairment. A monetary amount also is applied, ranging from Y25 million for grade 1 to Y75 thousand for grade 14. The relative monetary scale does not follow the relative loss of working capacity scale.

Another approach to defining severity level is to apply utility theory (24). In the utility approach each health state (attribute/severity level combination in the jargon of this paper) has a value between 0 and 1.0, where 0 is dead and 1 is healthy. When considering impairment, disutility is the parameter of interest, where 1 implies total impairment and 0 none. Utility (and disutility) generally is measured by survey techniques. A sample of persons is shown the descriptions of several health states, and they determine their relative preferences for these different states using any of several techniques, such as:

- *Rating scale.*—subjects define where a particular health state falls between a most desired and a

- least desired state;
- *Standard gamble*.—subjects choose between two alternatives, certainty of a particular health state for life or some treatment what will result in either a probability of being healthy for life, or immediate death. The probability is varied until the subject is indifferent to the outcome;
- *Time trade-off*.—two alternatives are presented—some health state for the remaining life expectancy, and healthy for a variable time less than the remaining life expectancy, followed by death. (Note however that the time trade off technique is not universally accepted (35).)

One difficulty with applying the utility approach to a particular person's situation is that a person's preference for health states varies with their risk propensity. A person with high risk tolerance may have a lower disutility for a particular health state than a risk averse person.

Determining the appropriate number of severity levels for each attribute, developing rigorous definitions for each attribute/severity level combination, and quantifying the impairment resulting from each attribute/severity level combination remain as areas for further research. Research is also needed to apply these attributes/severity level combinations to the injuries resulting from motor vehicle crashes.

## Whole Body Impairment

As used in this paper, the whole body impairment factor is a number between 0 and 1 which indicates the overall degree to which an injured person functions at less than a normal level. In order to develop these factors it is necessary to quantify each attribute/severity level combination, and then to combine the applicable factors into a single factor relating to the whole body.

The AMA approach identifies a percent impairment for individual body functions and then combines the individual factors according to the formula

$$C = A + B(1 - A) \quad (1)$$

where C is the combined value, A is the decimal rating of one impairment, and B is the decimal rating of another (18). For example, if a person had two impairments that individually had 35% and 20% whole body impairment, the combined value would be

$$C = .35 + .20(1 - .35) = .35 + .13 = .48$$

Carsten and O'Day [17] also used the AMA method to determine whole body impairment values from the individual attributes.

Multi-attribute utility theory also has approaches to combining attributes. A discussion of this complex subject is beyond the scope of this paper. The reader is referred to the literature, particularly (36).

## Discussion

The feasibility of the impairment concept as a measure of the societal impact of injuries has been demonstrated (16,

19, 20). The analysis of the current state-of-knowledge concerning impairment presented in this paper identified further research needed to develop the method to a point where it can be widely accepted and applied as a measure of societal impact, and brought some inherent shortcomings into focus. These are summarized in this discussion.

## Advantages and limitations

Probably the most important advantage of the impairment method of measuring the societal impact of injuries is that it counts persons more nearly equal than the economic methods. Persons of the same age and sex receiving the same injury are by definition counted as equals in the impairment method. An unemployed person doesn't count for zero as in the economic methods. Also, males and females are counted as equals except for the differences in their life expectancy. Thus persons in the workforce or at home are counted equally, eliminating the need for elaborate methods to estimate the monetary contribution to society of home-makers. Another advantage is that the method allows a highly disaggregated analysis, as the whole body impairment factors are applied to specific injuries rather than to broad classes of injuries. Also, impairment can account for different long term effects for the same injury as a function of age, and can include any reduction in life expectancy as a result of a particular injury. Although it is theoretically possible to do a similarly disaggregated analysis with the economic methods, it is not practical, as the costs of individual injuries are not available, whereas impairment estimates are feasible at the injury level.

One factor that should be recognized when applying impairment is that the basic value to society is taken to be the fact that a person is alive. Also, the variation of life expectancy with age is a quite smooth, nearly monotonic relationship rather than the highly non-linear age/earnings function. Since younger persons are expected to live longer, they are counted more heavily than older persons. However, as shown earlier in this paper, in the impairment method, persons in the highest incidence category (15 to 24 years old) are counted more nearly equal to their incidence, older persons are counted about the same as in the economic methods, and the very young are counted much more highly than they are in the economic methods, where often they are counted as zero. This set of biases is more nearly in line with the cultural values of Western Industrialized Society, where considerable efforts are expended for the very young.

## Need for Further Research

The work to date has been based upon one approach to defining impairment, the attributes that should be included, the severity levels that should be associated with each attribute and their definitions, how the various factors could be combined into composite whole body impairment factors, and the application to injuries (16, 17, 19, 20). Although this work has demonstrated the value of the impairment concept as a measure of societal impact, and provided considerable insight into its application, the

factors were developed by one physician in each of four specialties, which did not include specialists in rehabilitation medicine or allied health professionals who have contact with injured persons over the longer term. Also several additional attributes have been identified in the literature and appear to be important. In order to bring the concept to a point where it can be widely applied in the safety community, further development in several areas is needed.

## Definition

One issue that needs to be settled is the development of a consensus definition of impairment that would be broadly accepted by the safety and medical communities, meeting the needs of the various disciplines involved. A comprehensive definition would include a generic statement of what impairment is, the attributes that should be included, and the related severity levels and their definitions. This paper has offered a generic definition of impairment and has presented a list of attributes based upon a comprehensive systems approach. These can serve as a starting point for further discussion, and once agreement is reached, the severity levels appropriate for each impairment attribute need to be identified and defined so that they could be used operationally.

## Application to injuries

Once a consensus of the attribute/severity level definitions have been agreed to, these factors must be applied to the injuries expected in motor vehicle crashes. The earlier results (16, 17, 19, 20) are based primarily on the injuries shown in AIS 80 (3). (Certain additional injuries also were used). The AIS 80 scale has been supplanted by the AIS 85 scale in many applications (3). Several of the injury definitions and severity levels have been changed between these two versions of the AIS. Another scale that is becoming more widely used is the ICD scale (22). Any application of the attribute/severity level definitions must consider each of these scales in order to make the results applicable to currently available data, to data now being collected, and to possible future applications.

## Whole body impairment factors

Two problems that need to be resolved in order to complete the development of the whole body impairment factors have been identified.

A numerical value of impairment must be developed for each attribute/severity level combination. For example, what is the impairment resulting from a severe cognitive impairment? To be most useful, these values should reflect society's view of the relative importance of the different attributes. In order to do this, an approach is necessary that will capture a broad cross section of societal views. In addition, it is necessary to know the medical practitioner's view on the value of these factors in order to have some idea of any differences in viewpoint between the medical professionals and the general population.

The second problem is how to combine the individual values into a single overall whole body impairment factor. This paper has defined a set of twenty three attributes, which would likely have an average of four or five severity levels. As noted above, the American Medical Association has a method of combining any number of factors. Also multi-attribute theory has developed techniques to combine a large number of factors. These approaches need to be examined and decisions made on how best to accomplish this combination.

## Conclusion

The changing safety environment in the United States as a result of greater use of occupant protection systems and the advances in trauma medicine have brought about an increased interest in the long term effects of injuries resulting from motor vehicle crashes. Various measures of these effects have been developed, including sophisticated approaches to measure injury incidence, economic impacts applying a number of approaches based on a variety of economic theories, and more recently, measures of the integrated lifetime loss of time. This latter approach is being called Impairment.

Basically, impairment is defined as a loss of function and is quantified by multiplying a whole body impairment factor for a particular injury by the injured person's remaining life expectancy. The whole body impairment factor is based on a combination of the impairments resulting from a set of attributes and severity levels. For example, one impairment attribute may be mobility, and it might have three severity levels, mild, moderate, and severe. Each of these would have a numerical value.

To determine what attributes are needed to describe impairment, a model of human functioning was developed, which considered human functioning at four levels: primitive, mechanical, thinking-feeling, and interacting. Twenty three attributes were identified. Further work is needed to develop a consensus on these attributes and to develop rigorous definitions for each at appropriate severity levels. Also remaining to be accomplished is the relating of these attributes to all known injuries, and the development of a societally based judgement on the numerical value of impairment for each attribute/severity level combination.

The advantages of impairment are at the philosophical as well as the practical level. Each person of a particular age and sex counts the same, with life itself as the measure of intrinsic worth. There is no need to be concerned with averaging income, or calculating equivalent homemaker's contributions to society.

## References

- (1) Based on an average of 1982-1984 data developed by the National Accident Sampling System. See "Traffic Related Disabilities and Impairments and Their Economic Consequences", Stephen Luchter, SAE 860505, appearing in "Crash Injury Impairment and Disability: Long Term Effects", SAE SP-61.

- (2) Based on data in the National Highway Traffic Safety Administration's Fatal Accident Reporting System, FARS, for the past few years. The FARS totals are based on a census of all deaths in the United States resulting from motor vehicle crashes within thirty days of the crash.
- (3) "The Abbreviated Injury Scale, 1980 Revision", American Association for Automotive Medicine, Morton Grove, IL, 1980, "The Abbreviated Injury Scale, 1985 Revision", American Association for Automotive Medicine, Morton Grove, IL 1985. This organization is now known as the Association for the Advancement of Automotive Medicine. They are currently working on a 1990 revision of the AIS.
- (4) The injury data is from "National Accident Sampling System 1986, A Report on Traffic Crashes and Injuries in the United States", and the fatality data is from "Fatal Accident Reporting System 1986, A Review of Information on Fatal Traffic Accidents in the United States in 1986", both published by the National Highway Traffic Safety Administration.
- (5) "On the Examination of Biases in the Abbreviated Scale", R. Eppinger, 11th International Technical Conference on Experimental Safety Vehicles, Washington, DC, May 1987.
- (6) "Estimating the Cost of Illness", Dorothy P. Rice, Health Economic Series, No. 6, U.S. Dept. of Health and Human Services, 1966.
- (7) "The Economic Costs to Society of Motor Vehicle Accidents", Lawrence J. Blincoe and Stephen Luchter, SAE 830614.
- (8) "The Economic Cost to Society of Motor Vehicle Accidents", DOT HS 806 342, January, 1983.
- (9) "The Economic Cost to Society of Motor Vehicle Accidents, 1986 Addendum", National Highway Traffic Safety Administration, September, 1987.
- (10) "The Socio-Economic Impacts of Injuries Resulting From Motor Vehicle Crashes", Ted R. Miller and Stephen Luchter, FISITA 885162, Presented at the FISITA Conference, September, 1988, Washington DC.
- (11) "The Lifetime Economic Costs of Injury", Wendy Max et. al., Presented at the American Economics Association Annual Meeting, December 1988, New York.
- (12) "Status of Cost of Injury Research in the U.S.", Stephen Lucher, Barbara Faigin, Daniel Cohen, Louis Lombardo, For Presentation at the Experimental Safety Vehicle Conference, Gothenburg, June, 1989.
- (13) "Crash Costs and Safety Investment", Ted R. Miller, Stephen Luchter, and C. Philip Brinkman, Presented at the Association for the Advancement of Automotive Medicine Annual Meeting, September, 1988, Seattle, Washington.
- (14) "Federal Agency Valuations of Human Life", Clayton P. Gillette and Thomas D. Hopkins, Report to the Administrative Conference of the United States, July, 1988.
- (15) "A Search for Priorities in Crash Protection", A. C. Malliaris, Ralph Hitchcock, and James Hedlund, SAE 820242 and "Harm Causation and Ranking in Car Crashes", A. C. Milliaris, Ralph Hitchcock, and Marie Hansen, SAE 850090.
- (16) "Impairment Scaling from the Abbreviated Injury Scale", A. Hirsch et al., DOT HS-06 648, June 1983.
- (17) "Injury Priority Analysis", Oliver Carsten and James O'Day, UMTRI 84-24, October 1984 and "Relationship of Accident Type to Occupant Injuries", Oliver Carsten, UMTRI 86-15, April 1986.
- (18) "Guides to the Evaluation of Permanent Impairment, 2nd Edition", American Medical Association, Chicago, 1984.
- (19) "Priorities in Automotive Crash Safety Based on Impairment", J. Marcus, R. Blodgett, 11th International Technical Conference on Experimental Safety Vehicles, May, 1987, Washington, DC.
- (20) "The Use of Impairment for Establishing Accident Injury Research Priorities", Stephen Luchter, SAE 871078.
- (21) Personal communication, John D. States, in his capacity as chair of an Association for the Advancement of Automotive Medicine committee considering impairment scaling. "Proposed Impairment Scale (IS) and Disability Scale (DS)", John D. States, and David C. Viano, June 29, 1987.
- (22) "International Classification of Impairments, Disabilities, and Handicaps", World Health Organization, Geneva, 1980.
- (23) "Predicting Posttrauma Functional Disability for Individuals Without Severe Brain Injury", Ellen J. MacKenzie, et. al., Medical Care v 24 n 5 May 1988 and "Functional Recovery and Medical Costs of Trauma: An Analysis by Type and Severity of Injury", Ellen. J. MacKenzie et. al., The Journal of Trauma v 28 n 3 March 1988.
- (24) "Application of Multi-Attribute Utility Theory to Measure Social Preferences for Health States", George W. Torrance, Michael H. Boyle and Sargent P. Horwood, Operations Research, v 30, n 6 Nov. Dec. 1982.
- (25) "Health Status Index for Children in Ontario", D. T. Cadman, et. al., Ontario Ministry of Health Research Grant DM 648. McMaster University, Department of Pediatrics, 1985, referenced in "Utility Approach to Measuring Health-Related Quality of Life" George W. Torrance, Journal of Chronic Disability, Vol. 40, No. 6, pp 593-600, 1987, Permagon Journals Ltd.
- (26) "Health Preference Measurements for Health Decisions and the Evaluation of Long-Term Care", Robert M. Kaplan, in Values and Long Term Care, edited by Kane and Kane, Lexington Books, 1982.
- (27) "Assessment of Global Function: The Reintegration to Normal Living Index", Sharon L. Wood-Dauphinee et. al., Arch Phys Med Rehabil v 69, August 1988.
- (28) "The MOS Short-form General Health Survey", Rita L. Stewart, Ron D. Hays, and John E. Ware, Jr., Medical Care, July 1988 v 26 n 7.
- (29) "The Los Angeles Head Injury Survey: Procedures and Initial Findings Harry E. Jacobs", Arch Phys Med Rehabil v 69 p425-431, June 1988.

(30) "Preference Measurement for Functional Status in Stroke Patients: Inter-Rater and Inter-Technique Comparisons", Wolfson et al., in Value and Long Term Care, Robert L. Kane and Rosalie A. Kane ed., Lexington Books, 1982.

(31) "Recent Studies Using a Global Approach to Measuring Illness", Rachel M. Rosser, Medical Care v XIV, n 5, supplement, May 1976, as referenced in "Multiattribute Utility Theory as a Method of Measuring Social Preferences for Health States in Long Term Care", George W. Torrance, in Values and Long-Term Care, Robert L. Kane and Rosalie A. Kane, Editors, Lexington Books, 1982.

(32), Sintonen 1982, as referenced in "Estimates of Willingness to Pay for Pollution-Induced Changes in Morbidity: A Critique for Benefit-Cost Analysis of Pollution Regulation", Lauraine G. Chestnut & Deniel M. Violette, EPA 230-07-85-008, Sept 1984.

(33) This severity level approach was used in "Permanent Disability in Road Traffic Accident Casualties", E. Grattan and J A Hobbs, TRRL Laboratory Report 924, 1980, and "Long-term Disability Following Road Traffic Accidents", C S B Galasko, P Murray, M Hodson, R J Tunbridge, J T Everest, TRRL Research Report 59, 1986. It was attributed to "The Injury Severity Score of Road Traffic Casualties in Relation to Mortality, Time of Death, Hospital Treatment Time and Disabilities", J P Bull, Accident Analysis and Prevention, 1975, 7.

(34) "Social and Economic Losses from Road Accidents", The Japan Research Center for Transport Policy, June, 1986.

(35) "Optimizing Patient and Societal Decision Making by the Incorporation of Individual Values", Barbara J. McNeil and Stephen G. Pauker, in Values and Long-Term Care, edited by Kane and Kane, Lexington Books, 1982.

(36) George W. Torrance has written extensively on the development of a health scale based upon the application of utility theory. In addition to those already cited, his publications include: "The Utility of Different Health States as Perceived by the General Public", David L. Sackett and George W. Torrance, J Chron Dis 1978 vol 31, pp 697-704, Permagon Press Ltd.; "Multiattribute Utility Theory as a Method of Measuring Social Preferences for Health States in Long Term Care", George W. Torrance, in Values and Long-Term Care, Robert L. Kane and Rosalie A. Kane, Editors, Lexington Books, 1982; "Economic Evaluation of Neonatal Intensive Care of Very-Low Birth-Weight Infants", Boyle, Torrance, Sinclair, & Horwood, New England Journal of Medicine, v 308, n 22, June 2, 1983; "Health States Worse Than Death" G. W. Torrance, 3rd International Conference on System Science in Health Care, W. v Eimeren, R. Engelbrecht, Ch. D Flagle, Eds., Springer Verlag, Berlin 1984; "Measurement of Health State Utilities for Economic Appraisal, A review", George W. Torrance, Journal of Health Economics 5 (1986) 1-30, North Holland.

(37) "Parameter Estimates for a QALY Utility Model", John M. Miyamoto, and Stephen A. Eraker, Medical Decision Making vol 5 no 2 pp 191-213 1985.

From: "Impairment Scaling from the Abbreviated Injury Scale", Aurther E. Hirsch et. al., Final Report, DOT Contract Number DTNH22-80-C-07455, June 1983

### Mobility

Minor	Impaired mobility with intact functional ability.
Moderate	Impaired mobility with mildly abnormal function. Partially dependent on mechanical assistance. Unable to lift reasonable size objects (needs crutches, walker).
Severe	Severely impaired mobility with abnormal function. Dependent on mechanical assistance and wheel chair, occasionally needs attendant.
Maximum	Entirely dependent on attendant otherwise confined to bed.

### Cognitive/Psychological

Slight	Mild inappropriate behavior, neurotic, increased irritability, intermittent confusion, occasional swings into elation-depression, increased errors in language and mental arithmetic.
Moderate	Often disoriented, loss of ability to do simple arithmetic, slight impairment of language or memory, may be psychotic but not committable.
Severe	Severe memory impairment, severe impairment of language processing and/or psychotic committable behavior.
Maximum	Vegetative, total amnesia, no purposeful response to stimuli.

### Disfigurement/Cosmetic

Slight	Normally covered, amenable to cosmetic cover-up. Readily covered orthosis.
Moderate	Can be effectively covered by cosmetics and/or forces a change in dress habits, may require orthosis but does not require prosthesis.
Severe	Prosthesis or cover-up required.
Maximum	Severe, readily observable, not amenable to cosmetic, prosthetic, or clothing cover-up.

### Sensory

Slight	10 to 25 percent loss to special senses or limbs.
Moderate	26 to 50 percent loss to special senses or limbs.
Severe	Greater than 50 percent loss to special senses or limbs.
Maximum	Total loss to special senses or limbs.

### Pain

Slight	Normal function with no or occasional non-narcotic drugs and/or other non-invasive therapy.
Moderate	Normal function only with the use of non-narcotic drugs and/or other non-invasive therapy.
Severe	Can function normally only with narcotic drugs and/or invasive therapy.
Maximum	Cannot function normally even with narcotic drugs and/or invasive therapy.

### Daily Living

Slight	Inability to do some normal non-essential activities.
Moderate	Inability to do most non-essential and/or some essential activities.
Severe	Partially dependent on assistance for essential functions.
Maximum	Totally dependent on assistance for most activities and functions.

From "Proposed Impairment Scale (IS) and Disability Scale (DS)", John D. States, and David C. Viano, June 29, 1987

### Mobility

Minor	Detectable impairment of mobility but with intact functional ability; i.e. minor limp due to knee with degenerative arthritis.
Moderate	Walking distance limited to less than 1/4 mile. Uses cane occasionally. Can use stairs.
Serious	Cane, crutches, prosthesis and/or walker are necessary for walking except in dwelling. Stairs are difficult, railing is essential.
Severe	Wheelchair is used by choice but patient can stand and walk with apparatus; i.e. crutches or walker.
Very Severe	Wheelchair is required for ambulation although patient can stand and walk short distances with crutches or walker.
Totally Immobile	Requires hoist for transfer, cannot stand, requires aide for activities of daily living.

Central Nervous System Impairment - Cognition, Psychological Functions, Speech, and Motor Deficits

Minor	Mild inappropriate behavior, occasional errors in language and arithmetic.
Moderate	Noticeable memory loss, difficulties with simple arithmetic, difficulty in self expression, infrequent disorientation, dizziness, difficulty in balance.
Serious	Occasional disorientation, significant memory loss or language impairment, occasional signs of psychosis, motor deficit impairment of hands, extremities. ADL detectably limited.
Severe	No memory for recent events; disoriented, psychotic, requires sheltered home, speech unintelligible, severe motor weakness, incoordination or spasticity, self feeding slow and uncertain. ADL severely limited.
Very Severe	No memory, total loss of speech, psychotic, usually requires institutional care, virtual complete motor paralysis. No ADL.
Coma	Vegetative, no purposeful response to stimuli, brain dead.

Cosmetic/Disfigurement

Minor	Normally covered, amenable to cosmetic makeup. Readily covered orthosis.
Moderate	Can be covered by cosmetics and/or forces change in dress, may require orthosis but not prothesis.
Serious	Prosthesis or coverup required.
Severe	Readily observable, not amenable to cosmetic, prosthetic, or clothing coverup.

Sensory

	Vision	Hearing	Sensation	Taste and Smell
Minor	Minor loss but does not interfere with usual activities, correctable with readily available aids such as glasses, hearing aids.			
Moderate	Correctable to 20/100 in best eye	Hearing loss not fully correctable with aid	26 to 50% loss to special senses or limbs	Complete loss of taste or smell
Serious	Complete loss of one, partial loss of vision in other eye	Total hearing loss	Greater than 50% to total loss	Complete loss of both taste and smell
Severe	Legally blind			

Pain

Minor	Occasional pain, analgesics not required nor used, no interference with sleep, normal ADL, work, recreational and social abilities.
Moderate	Occasional pain, more frequent, occasional use of non-narcotic analgesics.
Serious	Constant or occasional severe pain, non-narcotic analgesics required for sleep, work. Recreation restricted by time and/or intensity. Narcotic analgesics occasionally required.
Severe	Constant or severe occasional pain requiring narcotics or invasive therapy. Sleep poor, unable to work. Recreation and socialization severely limited. ADL limited.
Very Severe	Constant or severe occasional pain requiring narcotics or invasive therapy. Sleep poor, unable to work. Recreation and socialization severely limited. ADL limited.
Total	Constant and/or occasional pain uncontrolled except with large doses of narcotics

which effect CNS. Incomplete control with invasive therapy. ADL severely limited.

### Activities of Daily Living

Minor	Detectable limitation of ADL but limitation does not interfere with work nor with most recreational activities.
Moderate	Requires occasional assistance and/or use of special equipment of devices, able to work and manage home.
Serious	Requires assistance several times a day; i.e. dressing and undressing, can do own toilet, manages at work with occasional assistance, uses special equipment such as wheelchair, specially equipped automobile.
Severe	Requires frequent assistance but not full time, uses highly specialized equipment to operate car. Home and workplace modified with ramps, elevators, hoists.
Very Severe	Completely dependent, requires aid for bathing, feeding, dressing, turning pages of reading material, requires assistance to move in bed.
No ADL	Unresponsive, in coma, requires total care.

### Sexuality/Reproduction

Minor	Decreased frequency of intercourse because of occasional pain or decreased libido.
Moderate	Inability to have satisfactory erection, loss of libido. Pain with intercourse. Reduced fertility.
Serious	Complete loss of capability for an erection. Pain precluding intercourse. Reduced fertility.

From "Functional Recovery and Medical Costs of Trauma: An Analysis by Type and Severity of Injury", Ellen J. MacKenzie et. al., The Journal of Trauma v 28 n 3 March 1988

### Self care

feeding, bathing, dressing, toileting, and bed transfer.

### Mobility

getting around own home, the neighborhood, and the ability to use public transportation.

### Physical capabilities

(major) walking a quarter of mile, walking up and downstairs without resting, using fingers to grasp and handle

(minor) standing for long periods of time, bending down, and light lifting.

From "Application of Multi-Attribute Utility Theory to Measure Social Preferences for Health States", George W. Torrance, Michael H. Boyle and Sargent P. Horwood, Operations Research, v 30, n 6 Nov. Dec 1982

### Health State Classification System

Level	Description
-------	-------------

Physical Function: Mobility and Physical Activity

1	Being able to get around the house, yard, neighborhood or community WITHOUT HELP from another person; AND having NO limitations in physical ability to lift, walk, run, jump, or bend.
---	--

- 2 Being able to get around the house, yard, neighborhood or community WITHOUT HELP from another person; AND having SOME limitations in physical ability to lift, walk, run, jump, or bend.
- 3 Being able to get around the house, yard, neighborhood or community WITHOUT HELP from another person; AND NEEDING mechanical aids to walk or get around.
- 4 NEEDING HELP from another person in order to get around the house, yard, neighborhood or community; AND having SOME limitations in physical ability to lift, walk, run, jump or bend.
- 5 NEEDING HELP from another person in order to get around the house, yard, neighborhood or community; AND NEEDING mechanical aids to walk or get around.
- 6 NEEDING HELP from another person in order to get around the house, yard, neighborhood or community; AND NOT being able to use or control the arms and legs.

Role Function: Self-care and Role Activity

- 1 Being able to eat, dress, bathe and go to the toilet WITHOUT HELP; AND having NO limitations when playing, going to school, working or in other activities.
- 2 Being able to eat, dress, bathe and go to the toilet WITHOUT HELP; AND having SOME limitations when playing, going to school, working or in other activities.
- 3 Being able to eat, dress, bathe and go to the toilet WITHOUT HELP; AND NOT being able to play, attend school or work.
- 4 NEEDING HELP to eat, dress, bathe and go to the toilet AND having SOME limitations when playing, going to school, working or in other activities.
- 5 NEEDING HELP to eat, dress, bathe and go to the toilet AND NOT being able to play, attend school or work.

Social-Emotional Function: Emotional Well Being and Social Activity

- 1 Being happy and relaxed most or all of the time, AND having an average number of friends and contacts with others.
- 2 Being happy and relaxed most or all of the time, AND having very few friends and little contacts with others.
- 3 Being anxious or depressed some or a good bit of the time, AND having an average number of friends and contacts.
- 4 Being anxious or depressed some or a good bit of the time, AND having very few friends and little contact with others.

Health Problem

- 1 Having no health problem.
- 2 Having a minor physical deformity or disfigurement such as scars on the face.
- 3 Needing a hearing aid.
- 4 Having a medical problem with causes pain or discomfort for a few days in a row every two months.
- 5 Needing to go to a special school because of trouble learning or remembering things.
- 6 Having trouble seeing even when wearing glasses.
- 7 Having trouble being understood by other.
- 8 Being blind OR deaf OR not able to speak.

From "Health Preference Measurements for Health Decisions and the Evaluation of Long-Term Care", Robert M. Kaplan, in Values and Long Term Care, edited by Kane and Kane, Lexington Books, 1982

Function Levels: Combinations of Steps on Mobility, Physical Activity, and Social Activity Scales, and Associated Levels of Well-being (Social Preference Weights)

MOBILITY	PHYSICAL ACTIVITY	SOCIAL ACTIVITY	LEVEL OF WELLBEING
NO SYMPTOM PROBLEM COMPLEX			
Drove car and used bus or train without help (5)	Walked without physical problems (4)	Did work, school, or housework and other activities (5)	1.000
SYMPTOM/PROBLEM COMPLEX PRESENT			
Drove car and used bus or train without help (5)	Walked without physical problems (4)	Did work, school, or housework and other activities (5)	0.7433
Drove car and used bus or train without help (5)	Walked without physical problems (4)	Did work, school, or housework but other activities limited (4)	0.6855
Drove car and used bus or train without help (5)	Walked without physical problems (4)	Limited in amount or kind of work, school or housework (3)	0.6683
Drove car and used bus or train without help (5)	Walked without physical problems (4)	Performed self-care, but not work school or housework (2)	0.6955
Drove car and used bus or train without help (5)	Walked without physical problems (4)	Had help with self-care activities (1)	0.6370
Drove car and used bus or train without help (5)	Walked with physical limitations (3)	Did work, school, or housework and other activities (5)	0.6769
Drove car and used bus or train without help (5)	Walked with physical limitations (3)	Did work, school, or housework but other activities limited (4)	0.6172
Drove car and used bus or train without help (5)	Walked with physical limitations (3)	Limited in amount or kind of work, school or housework (3)	0.6020
Drove car and used bus or train without help (5)	Walked with physical limitations (3)	Performed self-care, but not work school or housework (2)	0.6292
Drove car and used bus or train without help (5)	Walked with physical limitations (3)	Had help with self-care activities (1)	0.5707
Did not drive or had help to use bus or train (4)	Walked without physical problems (4)	Did work, school, or housework but other activities limited (4)	0.6065
Did not drive or had help to use bus or train (4)	Walked without physical problems (4)	Limited in amount or kind of work, school or housework (3)	0.5913
Did not drive or had help to use bus or train (4)	Walked without physical problems (4)	Performed self-care but not work school or housework (2)	0.6185
Did not drive or had help to use bus or train (4)	Walked without physical problems (4)	Had help with self-care activities (1)	0.5600
Did not drive or had help to use bus or train (4)	Walked with physical limitations (3)	Did work, school, or housework but other activities limited (4)	0.5402

MOBILITY	PHYSICAL ACTIVITY	SOCIAL ACTIVITY	LEVEL OF WELLBEING
Did not drive or had help to use bus or train (4)	Walked with physical limitations (3)	Limited in amount or kind of work, school or housework (3)	0.5250
Did not drive or had help to use bus or train (4)	Walked with physical limitations (3)	Performed self-care but not work, school or housework (2)	0.5523
Did not drive or had help to use bus or train (4)	Moved own wheelchair without help (2)	Limited in amount or kind of work, school or housework (3)	0.5367
Did not drive or had help to use bus or train (4)	Moved own wheelchair without help (2)	Performed self-care but not work school or housework (2)	0.5649
In house (3)	Walked without physical problems (4)	Performed self-care but not work school or housework (2)	0.6488
In house (3)	Walked without physical problems (4)	Had help with self-care activities (1)	0.5902
In house (3)	Walked with physical limitations (3)	Did work, school, or housework but other activities limited (4)	0.5704
In house (3)	Walked with physical limitations (3)	Limited in amount or kind of work, school or housework (3)	0.5552
In house (3)	Walked with physical limitations (3)	Performed self-care but not work school or housework (2)	0.5824
In house (3)	Walked with physical limitations (3)	Had help with self-care activities (1)	0.5239
In house (3)	Moved own wheelchair without help (2)	Performed self-care but not work school or housework (2)	0.5950
In house (3)	Moved own wheelchair without help (2)	Had help with self-care activities (1)	0.5364
In house (3)	In bed or chair (1)	Performed self-care but not work school or housework (2)	0.5715
In house (3)	In bed or chair (1)	Had help with self-care activities (1)	0.5129
In hospital (2)	Walked without physical problems (4)	Performed self-care but not work school or housework (2)	0.6057
In hospital (2)	Walked without physical problems (4)	Had help with self-care activities (1)	0.5471
In hospital (2)	Walked with physical limitations (3)	Performed self-care but not work school or housework (2)	0.5394
In hospital (2)	Walked with physical limitations (3)	Had help with self-care activities (1)	0.4808
In hospital (2)	Moved own wheelchair without help (2)	Performed self-care but not work school or housework (2)	0.5520
In hospital (2)	Moved own wheelchair without help (2)	Had help with self-care activities (1)	0.4934
In hospital (2)	In bed or chair (1)	Performed self-care but not work school or housework (2)	0.5284
In hospital (2)	In bed or chair (1)	Had help with self-care activities (1)	0.4699
In special care unit (1)	Walked without physical problems (4)	Performed self-care but not work school or housework (2)	0.5732

MOBILITY	PHYSICAL ACTIVITY	SOCIAL ACTIVITY	LEVEL OF WELLBEING
In special care unit (1)	Walked without physical problems (4)	Had help with self-care activities (1)	0.5147
In special care unit (1)	Walked with physical limitations (3)	Performed self-care but not work school or housework (2)	0.5070
In special care unit (1)	Walked with physical limitations (3)	Had help with self-care activities (1)	0.4483
In special care unit (1)	In bed or chair (1)	Had help with self-care activities (1)	0.4374
Dead (0)	Dead (0)	Dead (0)	0.0000

Symptom-Problem Complexes and Linear Adjustments for Level-of-Well-being Scores

Trouble seeing (includes wearing glasses or contacts)	.01898
Pain or discomfort in one or both eyes, such as burning or itching	.03370
Trouble hearing (includes wearing hearing aid)	.08338
Earache, toothache, or pain in jaw	.09779
Sore throat, lips, tongue, gums or stuffy, runny nose	.09332
Several or all permanent teeth missing or crooked	.07154
Pain, bleeding, itching, or discharge (drainage) from sexual organs (excludes normal menstruation)	-.09202
Itching, bleeding or pain in rectum	-.03795
Pain in chest, stomach, side, back or hips	-.03824
Cough and fever or chills	.00775
Cough, wheezing, or shortness of breath	-.00752
Sick or upset stomach, vomiting, or diarrhea (watery bowel movements)	.00655
Fever or chills with aching all over and vomiting or diarrhea (watery bowel movements)	-.07216
Hernia or rupture of abdomen (stomach)	-.05008
Painful, burning, or frequent urination (passing water)	-.03271
Headache, dizziness, or ringing in ears	.01308
Spells of feeling hot, nervous or shaky	.01288
Weak or deformed (crooked) back	-.04743
Pain, stiffness, numbness, or discomfort of neck, hands, feet, arms, legs, or several joints	-.03439
One arm and one leg deformed (crooked), paralyzed (unable to move), or broken (includes wearing artificial limbs or braces)	-.06814
One hand or arm missing, deformed (crooked), paralyzed (unable to move) or broken (includes wearing artificial limbs or braces)	-.06087
One foot or leg missing, deformed (crooked), paralyzed (unable to move), or broken (includes wearing artificial limbs or braces)	-.06304
Two legs deformed (crooked), paralyzed (unable to move) or broken (includes wearing artificial limbs or braces)	-.08806
Two legs missing (includes wearing artificial limbs or braces)	-.10270
Skin defect of face, body, arms or legs, such as scars, pimples, warts, bruises or changes in color	.06331
Burning or itching rash on large areas of face, body, arms, or legs	.01706
Burn over large areas of face, body, arms, or legs	-.11004
Overweight for age and height	.07848
General tiredness, weakness, or weight loss	-.00270
Trouble talking, such as lisp, stuttering, hoarseness, or being unable to speak	.01936
Trouble learning, remembering, or thinking clearly	-.08298
Loss of consciousness such as seizures (fits), fainting, or coma (out cold or knocked out)	-.15066
Taking medication or staying on prescribed diet for health reasons	.11238
Breathing smog or unpleasant air	.15553
No symptoms or problems	.25672
Spells of feeling upset, depressed or crying [Note: The reference showed the factor for this symptom/problem as blank]	

From "Assessment of Global Function: The Reintegration to Normal Living Index", Sharon L. Wood-Dauphinee et. al., Arch Phys Med Rehabil v 69, August 1988

Patient version of the RNL

1. I move around my living quarters as I feel is necessary (Wheelchairs, other equipment or resources may be used).
2. I move around my community as I feel is necessary (Wheelchairs, other equipment or resources may be used).
3. I am able to take trips out of town as I feel are necessary (Wheelchairs, other equipment or resources may be used).
4. I am comfortable with how my self-cares needs (dressing, feeding, toileting, bathing) are met. (Adaptive equipment, supervision, and/or assistance may be used).
5. I spend most of my days occupied in a work activity that is necessary or important to me (Work activity could be paid employment, housework, volunteer work, school, etc. Adaptive equipment, supervision, and/or assistance may be used).
6. I am able to participate in recreational activities (hobbies, crafts, sports, reading, television, games, computers, etc.) as I want to. (Adaptive equipment supervision and/or assistance may be used.)
7. I participate in social activities with family, friends, and/or business acquaintances as is necessary or desirable to me. (Adaptive equipment, supervision, and/or assistance may be used.)
8. I assume a role in my family which meets my needs and those of other family members. (Family means people with whom you live and/or relatives with whom you don't live but see on a regular basis. Adaptive equipment, supervision, and/or assistance may be used.)
9. In general, I am comfortable with my personal relationships.
10. In general, I am comfortable with myself when I am in the company of others.
11. I feel that I can deal with life events as they happen.

From "Permanent disability in road traffic accident casualties", E. Grattan and J A Hobbs, TRRL Laboratory Report 924, TRRL, 1980

Disability Level	Definition	Example
Nil	no residual incapacity	
Slight	full range of activities possible, individual not quite returned to complete normality	slight, occasional headaches or minimal or painless loss of movement in a joint
Moderate	no interference with normal activities might interfere with "special" activities such as sports	some instability of joint, or shortening of lower limb by 2 cm deafness in one ear, loss of smell
Severe	interfered, to a variable extent with normal activities and limited or precluded "special" activities	loss of or loss of function of an eye, a major part of a limb
Very Severe	mainly or totally incapable of normal activities	substantial and irreversible brain damage or spinal cord damage with paraplegia

From "Rationalization of the Payment of Medical Expense Under Japanese Compulsory Automobile Liability Insurance (CALI) and Voluntary Bodily Injury Liability Insurance; and the Method of Awarding Grade of Permanent Disability under CALI", Medical Research Department, Automobile Insurance Rating Association of Japan, October, 1988

Grade	Amount K Yen	Description
1	25,000	<ol style="list-style-type: none"> <li>1. Those who have been blind in both eyes.</li> <li>2. Those who are disabled in the functions of mastication and speech.</li> <li>3. Those who have the heavy impediments or disturbances left in the functions of the nervous system or in the psyche and require care and protection at all times.</li> </ol>

4. Those who have the heavy impediments left in functions of the thorax and abdominal organs and require care and protection at all times.
  5. Those who have lost both upper limbs upward of the elbow joint.
  6. Those who have been totally disabled in the functions of both upper limbs.
  7. Those who have lost both lower limbs upward of the knee joint.
  8. Those who have been totally disabled in the function of both lower limbs.
- 2      21,860
1. Those who have been blind in one eye, and have the other eye, the vision of which has become 0.02 or less.
  2. Those the vision of both of whose eyes has become 0.02 or less.
  3. Those who have the heavy impediments or disturbances left in the functions of the nervous system or in the psyche and require care and protection as occasion demands.
  4. Those who have the heavy impediments left in the functions of the thorax and abdominal organs and require care and protection as occasion demands.
  5. Those who have lost both upper limbs upward of the wrist joint.
  6. Those who have lost both lower limbs upward of the foot joint.
- 3      18,980
1. Those who have been blind in one eye and have the other eye, the vision of which has become 0.06 or less.
  2. Those who have been disabled in the functions of mastication or speech.
  3. Those who have the heavy impediments or disturbances left in the functions of the nervous system or in the psyche and cannot labour for life.
  4. Those who have the heavy impediments left in the functions of the thorax and abdominal organs and can not labour for life.
  5. Those who have lost all fingers of both hands.
- 4      16,370
1. Those the vision of both of whose eyes has become 0.06 or less.
  2. Those who have the heavy impediments left in the functions of mastication and speech.
  3. Those who have totally lost the audition of both ears.
  4. Those who have lost one upper limb upward of the elbow joint.
  5. Those who have lost one lower limb upward of the knee joint.
  6. Those who have been disabled in the functions of all fingers of both hands.
  7. Those who have lost both legs upward of the Lisfranc's joint.
- 5      13,830
1. Those who have been blind in one eye and have the other eye, but vision of which has become 0.1 or less.
  2. Those who have the heavy impediments or disturbances left in the functions of the nervous system or in the psyche and cannot serve in any labour but the specially light one.
  3. Those who have the heavy impediments left in the functions of the thorax and abdominal organs and cannot serve in any labour but the specially light one.
  4. Those who have lost one upper limb upward of the elbow joint.
  5. Those who have lost one lower limb upward of the knee joint.
  6. Those who have been totally disabled in the functions of one upper limb.
  7. Those who have been totally disabled in the functions of one lower limb.
  8. Those who have lost all toes of both feet.
- 6      11,540
1. Those the vision of both of whose eyes has become 0.01 or less.
  2. Those who have the heavy impediments left in the functions of mastication or speech.
  3. Those, the audition of both of whose ears can not catch a loud voice, unless it is uttered close by the auricles.
  4. Those who have totally lost the audition of one ear and the audition of the other ear can not catch an ordinary voice, when it is uttered at a distance of more than 40 cm from them.
  5. Those who have the heavy deformity or motorial impediment left in the spinal column.
  6. Those who have been disabled in the functions of two of the three greater joints in one upper limb.
  7. Those who have been disabled in the functions of two of the three greater joints in one lower limb.
  8. Those who have lost the five fingers of one hand or four fingers of it including the thumb and the second finger.

- 7 9,490
1. Those who have been blind in one eye and have the other eye, the vision of which has become 0.6 or less.
  2. Those, the audition of both of whose ears can not catch an ordinary voice, when it is uttered at a distance of more than 40 cm from them.
  3. Those who have totally lost the audition of one ear and the audition of the other ear can not catch an ordinary voice, when it is uttered at a distance of more than 1 m from them.
  4. Those who have the impediments or disturbances left in the functions of the nervous system or in the psyche and can not serve in any labour but the light one.
- 7 contd
5. Those who have the impediments left in the functions of the thorax and abdominal organs and can not serve in any labour but the light one.
  6. Those who have lost the thumb and the second finger of one hand or three fingers or more if it including either the thumb or the second finger.
  7. Those who have been disabled in the functions of five fingers of one hand or four fingers of it including the thumb and the second finger.
  8. Those who have lost one leg upward of the Lisfranc's joint.
  9. Those who have a residual pseudo-joint on one upper limb have a heavy impediment of movement left.
  10. Those who have a residual pseudo-joint on one lower limb have a heavy impediment of movement left.
  11. Those who have been disabled in the functions of all toes of both feet.
  12. Those females who have the remarkable deformities left on their external appearances.
  13. Those who have lost both testicles.
- 8 7,500
1. Those who have been blind in one eye, or have one eye, the vision of which has become 0.02 or less.
  2. Those who have the motorial impediment left in the spinal column.
  3. Those who have lost two fingers of one hand including the thumb.
  4. Those who have been disabled in the function of the thumb and the second finger of one hand or three fingers or more of it including the thumb or the second finger.
  5. Those who have one lower limb shortened by 5 cm or more.
  6. Those who have been disabled in the functions of one of the three greater joints in one upper limb.
  7. Those who have been disabled in the functions of one of the three greater joints in the lower limb.
  8. Those who have the false joint left in one upper limb.
  9. Those who have the false joint left in one lower limb.
  10. Those who have lost all toes on one foot.
  11. Those who have lost the spleen or the kidney on one side.
- 9 5,720
1. Those, the vision of both of whose eyes has become 0.6 or less.
  2. Those, the vision of one of whose eyes has become 0.06 or less.
  3. Those who have the hemianopsia, the contraction of the field of vision, or the distortion of the field of vision left in both eyes.
  4. Those who have the heavy losses left in both eyelids.
  5. Those who have lost their noses and have the heavy impediments left in the functions of them.
  6. Those who have the impediments left in the functions of mastication and speech.
  7. Those, the audition of both of whose ears cannot catch an ordinary voice when it is uttered at a distance of more than 1 m from them.
  8. Those, the audition of one of whose ears cannot catch a loud voice, unless it is uttered close by the auricles and the audition of the other ear has difficulty in catching an ordinary voice, when it is uttered at a distance of more than 1 m from them.
  9. Those who have totally lost the audition of one ear.
  10. Those who have the impediments or disturbances left in the function of the nervous system or in the psyche and have labour to be engaged in limited to a considerable extent.
  11. Those who have lost the thumb of one hand, those who have lost two fingers including the thumb, or those who have lost three fingers except the thumb and the second finger.
  12. Those who have been disabled in the functions of two fingers of one hand including the thumb.
  13. Those who have lost two toes or more of one foot including the first toe.

14. Those who have been disabled in the functions of all toes of one foot.
15. Those who have the heavy impediments left in the genital organs.

10 4,340

1. Those, the vision of one of whose eyes has become 0.1 or less.
2. Those who have the impediments left in the functions of mastication or speech.
3. Those who have 14 teeth or more repaired dentally.
4. Those, the audition of both of whose ears has difficulty in catching an ordinary voice, when it is uttered at a distance of more than 1 m from them.
5. Those, the audition of one of whose ears can not catch a loud voice, unless it is uttered close by the auricle.
6. Those who have lost the second finger of one hand or two fingers of it except the thumb and the second finger.
7. Those who have been disabled in the functions of the thumb of one hand, those who have been disabled in the functions of two fingers including the second finger, or those who have been disabled in the functions of three fingers except the thumb and the second finger.
8. Those who have one lower limb shortened by 3 cm or more.
9. Those who have lost the first two or the other four toes of one foot.
10. Those who have the heavy impediments left in the functions of one of the three greater joints of one upper limb.
11. Those who have the heavy impediments left in the functions of one of the three greater joints of one lower limb.

11 3,160

1. Those who have the heavy functional impediments in accomodation or motorial impediments left in both eyeballs.
2. Those who have the heavy motorial impediments left in both eyelids.
3. Those who have the heavy damage left in one eyelid.
4. Those who have 10 teeth or more repaired dentally.
5. Those, the audition of both of whose ears cannot catch a low voice, when it is uttered at a distance of more than 1 m from them.
6. Those, the audition of one of whose ears can not catch an ordinary voice, when it is uttered at a distance of more than 40 cm from them.
7. Those who have the deformity left in the spinal column.
8. Those who have lost the third or fourth finger of one hand.
9. Those who have been disabled in the functions of the second finger of one hand, or those who have been disabled in the functions of two fingers of it except the thumb and the second finger.
10. Those who have been disabled in the functions of two toes or more of one foot including the first toe.
11. Those who have the impediments left in the thorax and abdominal organs.

12 2,170

1. Those who have the heavy functional impediments in accomodation or motorial impediments left in one eyeball.
2. Those who have the heavy motorial impediment in one eyelid.
3. Those who have 7 teeth or more repaired dentally
4. Those who have lost the major part of the auricle of one ear.
5. Those who have the heavy deformity left in the collar-bone, the breastbone, the rib, the shoulder blade or the pelvis.
6. Those who have the impediments left in the functions of one of the three greater joints of one upper limb.
7. Those who have the impediments left in the functions of one of the three greter joints of one lower limb.
8. Those who have the deformity left in the long pipe bone.
9. Those who have been disabled in the functions of the third finger or the fourth finger of one hand.
10. Those who have lost the second toe of one foot, those who have lost 2 toes including the second toe, or those who have lost 3 toes except the first and second toes.
11. Those who have been disabled in the functions of the first toe or the other 4 toes of one foot.
12. Those who have the obstinate nervous symptoms left in the affected parts.
13. Those males who have the remarkable deformities left on the external appearances.
14. Those females who have the deformities left on the external appearances.

13 137

1. Those, the vision of one of whose eyes has become 0.6 or less.
2. Those who have the hemianopsia, the contraction of the field of vision,

- or the distortion of the field of vision left in one eye.
3. Those who have the damage left in parts of both eyelids, or have the eyelash baldness left on them.
  4. Those who have 5 teeth or more repaired dentally.
  5. Those who have lost the little finger of one hand.
  6. Those who have lost a part of the finger bones of the thumb of one hand.
  7. Those who have lost a part of the finger bones of the second finger of one hand.
  8. Those who have become unable to extend and contract the last joint of the second finger of one hand.
  9. Those who have one lower limb shortened by 1 cm or more.
  10. Those who have lost 1 or 2 toes of one foot except the first and second toes.
  11. Those who have been disabled in the functions of the second toe of one foot, those who have been disabled in the functions of 2 toes including the second toe, or those who have been disabled in the functions of 3 toes except the first and second toes.

14

75

1. Those who have the damage left in a part of one eyelid, or have the eyelash baldness left on it.
2. Those who have 3 teeth or more repaired dentally.
3. Those, the audition of one of whose ears cannot catch a low voice, when it is uttered at a distance of more than 1 m from them.
4. Those who have the deformed scars of the size of the palm left on the exposed sides of the upper limbs.
5. Those who have the deformed scars of the size of the palm left on the exposed sides of the lower limbs.
6. Those who have been disabled in the functions of the little finger of one hand.
7. Those who have lost a part of the finger bones of the finger of one hand except the thumb and the second finger.
8. Those who have become unable to extend and contract the last joints of the fingers of one hand except the thumb and the second finger.
9. Those who have been disabled in the function of 1 or 2 toes of one foot except the first and second toes.
10. Those who have the nervous symptoms left in the affected parts.
11. Those males who have the deformities left on the external appearances.

## Status of Costs of Injury Research in the United States

---

**Stephen Luchter, Barbara Faigin,  
Daniel Cohen, Louis Lombardo,**  
National Highway Traffic Safety Administration

### Abstract

Understanding the composition and magnitude of the enormous economic burden injuries place on society remains a research issue, even though this subject has been under study for several decades. The human capital approach to measuring economic costs has evolved to the point where the methodology is widely accepted and many practical applications have been demonstrated. Most of the gaps in the state-of-knowledge of the human capital methodology concern problems of measurement, including estimating several sub-sets of the incidence, and problems in estimating the magnitude of some costs which are not collected routinely. The human capital method and certain of its derivatives are the primary method now used by the National Highway Traffic Safety Administration for determining economic costs resulting from injuries.

Another approach to measuring the economic impact of injuries, called willingness to pay, is being developed. This approach is concerned with value rather than cost, and is more directly applicable to cost/benefit analysis than is human capital. Significant measurement problems remain to be solved for the willingness to pay method. This method is not widely applied within the National Highway Traffic Safety Administration because this agency does not perform strict cost benefit analyses in its formal decision making process.

Neither the human capital nor the willingness to pay methods of economic analysis provide a measure of the overall impact to society resulting from injuries, which is a broader, inter-disciplinary problem, requiring considerably more development.

### Introduction

Injuries place an enormous burden on society, economically, socially, and emotionally. This paper reviews the current status of research completed and

underway in the United States to determine the composition and magnitude of the economic costs resulting from injuries, primarily injuries resulting from motor vehicle crashes. It describes the methodologies now in use to estimate costs, presents recent research results, identifies other research currently underway, and discusses the unsolved problems that should be considered for further research. It also emphasizes that since economic costs do not measure the social or emotional burden resulting from injuries they are not a comprehensive measure of total societal impact.

## Human capital

The principal method now being used for estimating the costs of injuries is called the Human Capital method, which measures the cost of resources used or lost as the result of an injury, such as medical costs, legal costs, earnings lost as a result of an injury, etc. All future costs are discounted to the present.

Even though it has certain shortcomings the human capital method is the most accurate method yet devised to determine the societal costs in monetary terms as a result of injuries. Note, however, that this method does not identify the total societal impact of injuries, which includes several non-monetary aspects, nor does it fully capture the costs from the individual's point of view.

## Evolution of the human capital methodology

Before there was an interest in costs of injuries, attempts were made to estimate the costs of illness in order to develop national priorities for allocation of health care resources. These studies were based on various methods ranging from gross estimates to detailed analyses. Productivity losses were calculated for morbidity and mortality but often age, sex, labor force participation rates, and other factors were not included. These were added to medical and other costs, but in some cases, transfer payments were incorrectly added into the totals.

In 1966, Dorothy Rice precisely structured the human capital methodology and authored what is considered by many to be the landmark work on the application of the human capital approach to the measurement of the cost of illness (1).<sup>\*</sup> In her report she referenced work by Rashi Fein (2), Burton Weisbrod (3), Herbert Klarman (4), and Selma Mushkin (5) in the late 1950's and early 1960's which focussed on developing costs for application to benefit-cost analysis of investments in public health. Her study developed and applied a framework for calculating the costs of illness in the U.S. for 1963. Costs were developed according to two components: direct costs, which are the actual dollar expenditures related to the illness or injury, and indirect costs, which measure the value of lost output due to reduced productivity. These estimates, and subsequent work by Rice on the cost of illness were based on prevalence (i.e. costs associated with all illnesses or injuries for a given year whether or not the onset was in that year) as opposed to

incidence (present and future costs for those individuals contracting the illness in that year). This work was updated in 1972 and again in 1980 (6).

A significant contribution to the costs of injury literature, by Hartunian et al., was published in 1981. It described both methodology and results of a calculation of incidence-based costs of coronary heart disease, cancer, stroke, and motor vehicle injuries (7). The results were disaggregated by age and sex, and for the costs of motor vehicle injuries, by severity using the Abbreviated Injury Scale (AIS). The results show that the cost to society, in 1975, using a discount rate of 6%, was \$23.1 billion for cancer, \$14.4 billion for motor vehicle injuries, \$13.7 billion for coronary heart disease, and \$4.6 billion for stroke.

A compendium of data on deaths resulting from injuries by Baker et al. was published in 1984 (8). In this study the data were disaggregated by various demographic and socioeconomic variables. Injury types included were non-motor vehicle transportation, machinery, falls, firearms, burns and fire, drowning, choking and suffocation, poisoning, motor vehicle occupants, pedestrians, motorcyclists and bicyclists. Although the focus of this book was on incidence, especially for non-motor vehicle injuries, it was an important contribution to the problem of costs of injuries as it included data on the distribution of injuries across the socioeconomic spectrum of the population.

## Application of human capital costing at NHTSA

In 1971 work was begun at NHTSA to evaluate the costs of motor vehicle injuries. In the spring of 1972, an internal working paper by Yasnowsky and Faigin (9) on the application of the Dorothy Rice methodology to incidence data from 1971 motor vehicle accidents indicated a fatality cost of \$200,000 and an average cost per non-fatal injury of \$7,300. Though an assessment of disability status was made for the determination of non-fatal injury costs, the available data precluded any detailed analysis of costs by injury severity at that time.

Three years later, a more detailed analysis by Barbara Faigin utilized the basic methodology of the earlier NHTSA work with a modified list of costs (10). Data on costs and injury severity by AIS were available and were incorporated into the fatal and non-fatal injury cost estimates. In addition, data from a DOT study of the economic impact of auto accidents was utilized (11). Average costs for 1975 fatal and AIS 5 through 1 level non-fatal injuries were estimated at \$287,175; \$192,240; \$86,955; \$8,085; \$4,350; and \$2,190 respectively.

In 1983, NHTSA revised its 1976 estimates (12). The methods developed in 1976 work were expanded, and use was made of the data in the National Accident Sampling System. In the 1983 study, the estimated total economic cost to society of motor vehicle crashes included medical costs, productivity losses, property damage, legal and court costs,

<sup>\*</sup>Numbers in parentheses designate references at end of paper.

insurance administration and underwriting, emergency service costs, coroner and medical examiner costs, public assistance administration, and government programs.

**Table 1. Summary of aggregate societal costs of motor vehicle crashes in 1986 dollars.**

COST CATEGORY	\$, Billion	Percent
Property Losses	27.37	36.9
Insurance Expense	20.86	28.1
Productivity Losses	16.38	22.1
Legal and Court Costs	4.32	5.8
Medical Costs	4.12	5.6
Emergency Costs	0.70	0.9
Other Costs	0.45	0.6
Total	74.20	100.0

Injury or Accident Severity	\$, Billion	Percent
AIS 1	9.39	12.7
AIS 2	2.47	3.3
AIS 3	1.88	2.5
AIS 4	1.01	1.4
AIS 5	2.71	3.7
Fatality	16.50	22.2
Property Damage Only	29.59	39.9
Uninvolved	10.64	14.3
Total	74.19	100.0

**Table 2. Summary of unit societal costs of motor vehicle crashes in 1986 percent.**

Cost Category	AIS 1	AIS 2	AIS 3	AIS 4	AIS 5	FATAL
Medical Costs	8.4	33.6	34.8	24.1	55.5	0.6
Productivity Loss	4.0	10.9	14.0	26.2	31.9	86.9
Property Damage	33.2	27.0	19.1	5.9	1.3	1.3
Legal/Court	21.8	11.6	24.1	10.6	3.7	5.0
Emergency Costs	2.5	2.3	1.1	0.4	0.1	0.1
Insurance Admin.	24.8	12.0	5.5	31.7	7.2	5.7
Public Assistance	0.2	0.1	0.1	0.8	0.2	0.2
Insurance U/write	2.2	1.1	0.5	0.1	0.0	0.0
Gvt. Programs	2.9	1.4	0.7	0.1	0.0	0.0
Total %*	100	100	100	100	100	100
Total Unit Cost, \$	3,245	6,245	14,742	64,812	284,752	358,310

Source for both tables - Reference 13  
 \*Note: Totals do not add to 100% in all cases due to rounding.

A 1986 update of these costs estimated a total economic cost of \$74.2 billion resulting from motor vehicle crashes, based on a seven percent discount rate (13). Note that this total includes property damage, and thus not all of the costs are specifically injury related. Rather, this total should be viewed as accident related. These costs are based upon an estimated incidence representative of the early 1980's, 3.4 million injuries, over 46,000 deaths, and 45 million damaged vehicles. Tables 1 and 2 summarize these 1986 estimates.

Roughly \$60 billion of the overall cost represents losses that could be reduced in a roughly proportionate manner if crashes, injuries, and fatalities were to decrease. The remaining portion, totalling \$14.5 billion, represents costs which are relatively fixed, i.e., that will not change in direct response to foreseeable changes in the crash or injury rate. This latter category of costs include primarily insurance underwriting costs, which are the administrative costs of writing and maintaining insurance policies, and the cost of government agencies that were established to improve vehicle or highway safety.

In 1988, NHTSA published three reports concerning applications of human capital costs. These reports provided

"cookbook" approaches to determine the savings that could be achieved by increased use of motorcycle helmets (14), increased use of safety belts (15), and estimating the costs of motor vehicle crashes in state and local jurisdictions (16). These reports made use of the 1986 updates of the agency's estimates of human capital costs noted above, and appropriate formulae for effectiveness, usage, and factors for estimating local incidence.

## Application of costs of injury data in setting research priorities

Costs of injury data are applied for a number of different purposes. These applications define the type of data and the degree of resolution required to solve practical problems. One such application has been conducted at NHTSA, utilizing costs of injury data to help establish priorities for future research efforts directed at enhanced crash protection.

To determine relative societal costs, weighting parameters based on human capital costs can be applied. One such parameter that has been widely used at NHTSA has been the "harm" concept. This concept, introduced in 1982 and upgraded in 1985, attempts to relate the relative costs of injuries for each injury severity level using the Abbreviated Injury Scale (AIS) of injury severity (17, 18). Harm is defined as "the sum of injuries of crash victims, with each injury weighted in proportion to the economic cost of the outcome of such injury whether fatal or not". In addition to harm, other parameters that could be used in estimating priorities have been developed. Concepts that consider impairment consequences in addition to threat to life have been discussed in the literature. Hirsch, et. al. developed a system for evaluating the impairment consequences of an injury (19). This system considers the specific injury and its severity and the victim's age. This system has been utilized by Carsten and O'Day (20) and Marcus and Blodgett (21) in examining crashworthiness priorities. The current state-of-knowledge of the impairment concept has been described by Luchter (22, 23).

The following discussion is not intended as a comprehensive discussion of crashworthiness priority development, but rather as an illustration of how the approaches applied in the past can vary with different cost assumptions. Specific analyses are presented. NHTSA's National Accident Sampling System (NASS) 1986 files, a nationally representative sample of crashes occurring within the United States was utilized in these analyses. This file contains information on the six most serious injuries resulting from a crash (24). Harm was applied to the maximum injury received by an occupant. Note that other algorithms could have been used, such as applying harm to all injuries received.

The harm weighting factors associated with each AIS value, called the "base" weights here, are based on the injury costs presented by Miller, Luchter, and Brinkman, adjusted by subtracting the property damage costs (25).

They are shown in table 3, which also summarizes the other approaches used in the analysis. In the "head" mod, the weighting factor is doubled from that of the "base" harm for the AIS 2 thru 5 severity level injuries. The weightings remain the same to the other body regions. Likewise, for the "neck" mod, it is assumed that low severity neck injuries are more serious than other body regions at similar severities. For neck injuries at the AIS 1 and 2 level the weighting factor is doubled from that of the baseline while all other body regions injured continue to use the "base" weightings.

**Table 3. Examples of different injury cost weightings.**

AIS LEVEL	AIS 3+ INJURIES	BASE WEIGHTS	HEAD INJ MOD	NECK INJ MOD
			AIS 2-5	AIS 1,2
AIS 1	0	1.6	1.6	3.2
AIS 2	0	5.0	10.0	10.0
AIS 3	1	15.0	30.0	15.0
AIS 4	1	150.0	300.0	150.0
AIS 5	1	386.0	770.0	386.0
FATAL	1	418.0	418.0	418.0

The results of the analysis are shown in figure 1. As can be seen, no matter which analytical approach is used, the most significant body region appears to be the head, followed by the chest, even though the absolute values differ depending on which method was used. When counting AIS 3+ injuries, the head, chest, and lower extremity body regions each account for approximately the same amount of harm. In applying the "base" weights, the head and chest are the dominant body regions. For the "head" mod weighting factors, the harm attributed to the head body region increases from 37% to 45%. For the "neck" mod weighting factors, the harm attributed to the neck almost doubles from 7% to 12%. Based on this analysis, it can be seen how differences in "harm" between different body regions can result in fairly substantial differences in priority ratings.

Focusing on head injuries, figure 2, shows that although there is a very high incidence of low severity head injuries, the bulk of the harm is associated with the more serious AIS 4 though fatal injuries. Focusing on neck injuries, figure 3, both incidence and harm are seen to be high for the low severity (AIS 1) injuries, and the small number of fatal neck injuries account for most of the remaining harm.

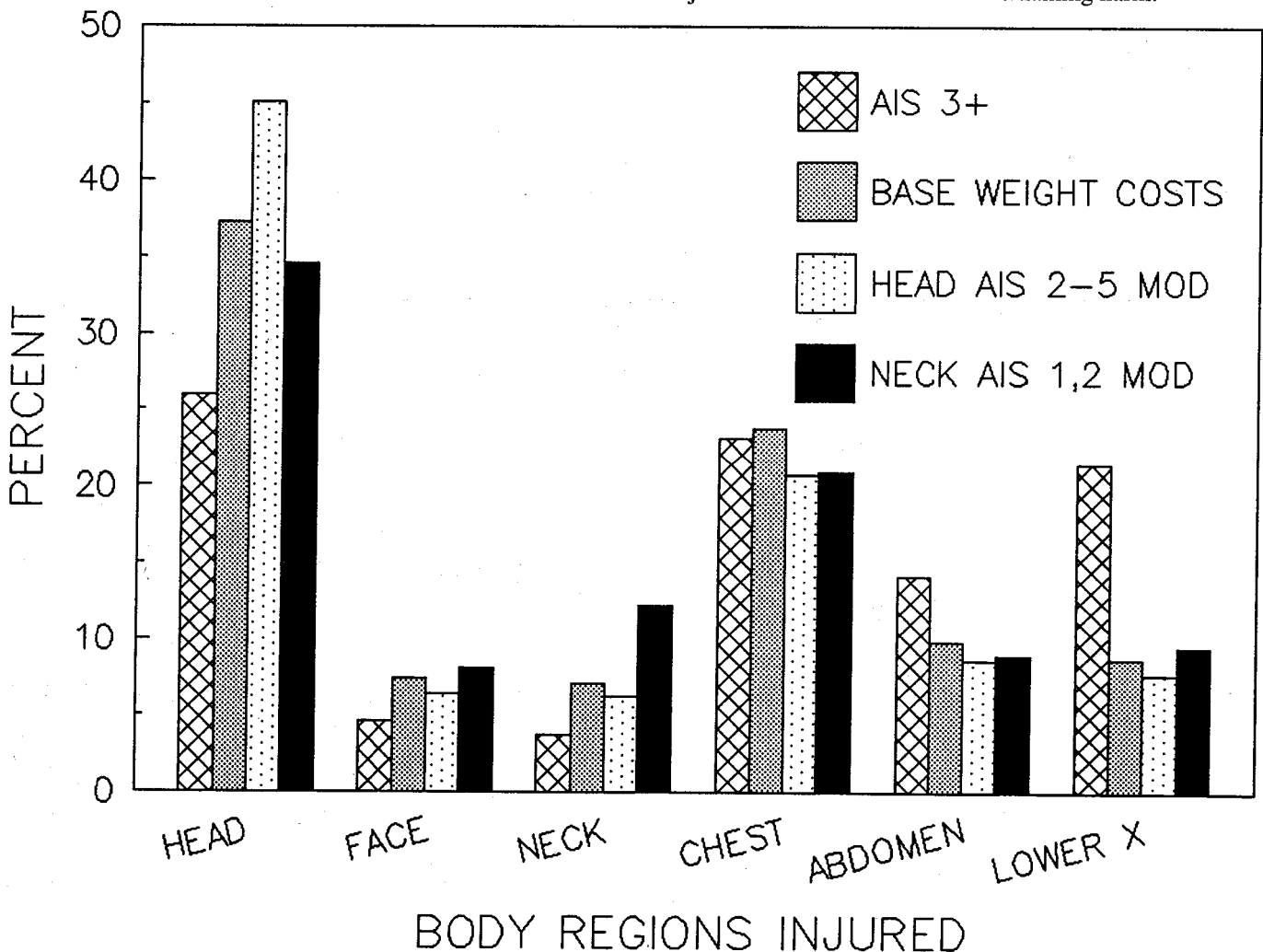


**Figure 1. Distribution of body regions injured 1986 NASS files for passenger car occupants.**

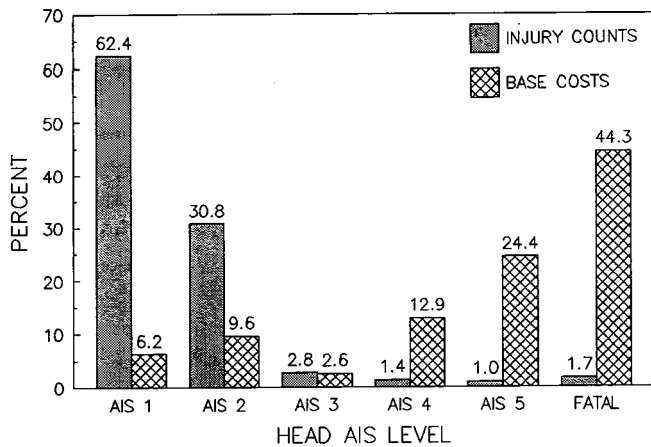


**Figure 2. Head injury distribution by injury severity. Application of different weightings 1986 NASS file for passenger cars.**

Although this discussion was not intended to be comprehensive, nor to define priorities, it demonstrates that injury costs should be known with reasonable resolution, as their values can affect practical application of the data.

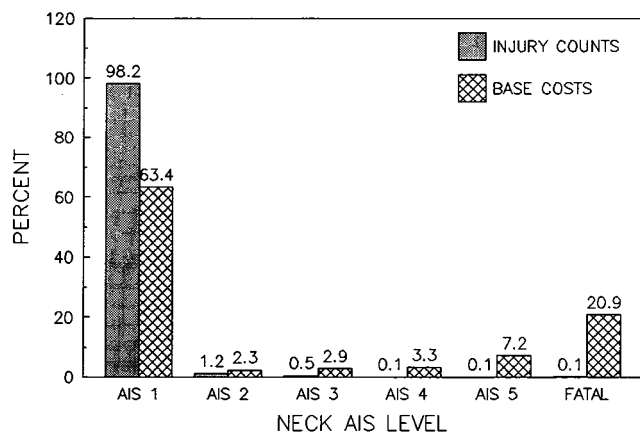


**Figure 3. Neck injury distribution by injury severity. Applications of different weightings 1986 NASS file for passenger cars.**

### Application of human capital in NHTSA regulatory actions

NHTSA analyzes both costs and benefits in connection with most rulemaking actions in compliance with the requirements of either the Office of Management and Budget (Executive Order 12291), or the Department of Transportation (DOT Order 2100.5). However, the agency does not conduct strict cost/benefit analyses for its regulatory actions primarily because the governing statutes do not require safety decisions to be based upon strict cost/benefit considerations. Rather, the agency measures safety benefits in terms of lives saved and injuries avoided. It should be noted that current Department of Transportation policy is that where cost/benefit analysis is done, a value of at least \$1 million per life saved must be used. Higher values may be used if justified.

### Application of human capital costing to developing national level priorities

A 1985 report by the National Academy of Sciences (NAS), "Injury in America", found that Federal funding of research on injury control was disproportionately low when compared with (a) the high costs of injury, (b) the research expenditures on other public health programs such as cancer, heart disease and stroke, and (c) the likelihood of success as a result of the available "Exciting opportunities to understand and prevent injuries" (26). The report contrasted the total Federal research expenditures on injuries, heart disease, and cancer with the respective number of pre-retirement years of life lost, as shown in figure 4. This figure shows millions of life years lost and millions of dollars of federal research. It is plotted on a logarithmic scale, and shows that although injuries have twice the life years lost as cancer and stroke, the disease research is from six to ten

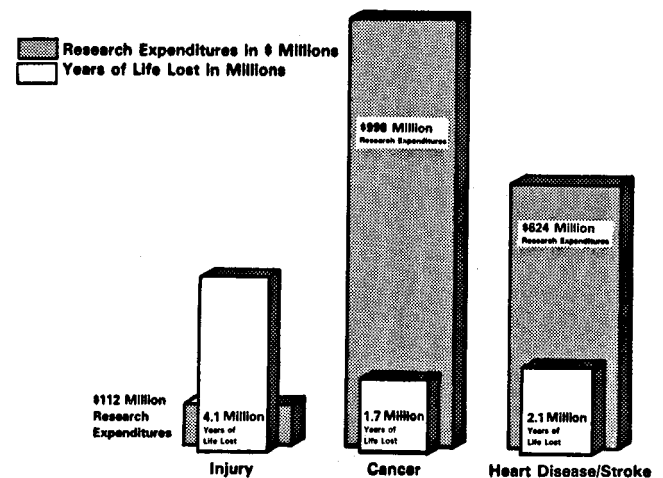


**Figure 4. Comparative magnitudes of health and safety problems and the resources devoted to their solution.**

times greater. The report helped the Congress to conclude that additional resources devoted to injury programs would be in the nation's interest. As a result, a national program has been established in injury control, a Division of Injury Epidemiology and Control was established at the Centers for Disease Control, within the Center for Environmental Health and Injury Control, five Injury Prevention Research Centers have been funded, and an extensive research program in injuries is underway. About 55 percent of these monies are being used to support motor vehicle and highway safety related injury research. Another feature of the program is the holding of national conferences to facilitate the exchange of research results.

Costs of injuries was one of the topics covered at the 1987 Injury Control Conference. An overview of the subject of estimating injury costs, "The National Safety Council's Estimates of Injury Costs", was presented by I. B. Etter of the National Safety Council (27). The conclusion of the

paper was that “there is much work still to be done in this field”. A paper presented by Carol MacLennon of Michigan Technological University, “The Unmeasured Costs of Injury”, reviewed much of the research on the limitations of economic approaches to valuing the costs of injuries and called for research on a broader “social consequences” model of costs of injuries (28). Such a model would include many far reaching costs that are not included in current costs of injuries studies. In addition, a “Topical Table” open discussion by a panel of experts on motor vehicle injury costs covered the human capital methodology, the willingness to pay methodology, unmeasured costs, and alcohol related costs.

The 1988 Injury Control Conference also included a “Topical Table” on injury costs. In these sessions, informal presentations of current research results were followed by questions from potential users. A number of issues were uncovered:

- Accurate measurement of injury incidence continues to be a problem, especially concerning injuries not treated at a hospital. As a result more people are injured than most data bases indicate. There is some evidence that even serious injuries may be included in this missing incidence data.
- Most of the data on costs is really data on paid charges. Since not all charges are paid, the actual costs of injuries are greater than shown in the data.
- Cost data from Trauma Centers, where patients with more severe injuries are treated, underrepresent actual costs of care because trauma centers are allowed the same charges as the average facility, whereas their costs are higher due to special facilities and expertise.
- There is evidence that persons in lower socio-economic groups receive different, lower cost, treatment than persons with greater ability to pay. This may skew the total cost estimates downward.
- There may be some overreporting for minor injuries treated in emergency rooms. Physicians may report some kind of injury so that the person can receive payment from their insurance—“multiple contusions” is a diagnosis often used for persons not seriously injured.
- Most cost estimates do not include the costs resulting from secondary illness, that is, problems that arise as a result of an injury, such as urinary problems for persons confined to wheel chairs.
- Data are sparse on the behavioral or psychological impacts on injured persons and how this relates to their return to their former lifestyle. These non-physical impacts are thought to be significant.
- Standard definitions for impairment and disability do not exist. U.S. practice differs from that established by the World Health Organization.

- There is a great need for long-term cost data for injuries. Many researchers believe that the long term costs of minor to moderate, as well as serious injuries may be significantly undercounted.

## Recent Results

### NHTSA grant studies

In the summer of 1987, NHTSA undertook a study of the economic costs and other impacts of injuries on individuals, families, communities, and society. Grants were awarded to the University of California, San Francisco, Institute for Health and Aging, and The Johns Hopkins University, School of Hygiene and Public Health to study the economic costs, public program impacts, and long-term impacts resulting from injuries of all types, and the potential cost savings of injury prevention strategies. The grants were conducted as part of the NHTSA/Centers for Disease Control Trauma Research Program. A Report to Congress is in preparation which will describe the research and findings.

In these studies, the human capital approach to injury cost measurement was applied using secondary data sources to determine cost estimates for the population of injuries occurring in 1985. One of the most significant contributions of this work was the development of injury incidence estimates by cause, by age, and by severity. Table 4

**Table 4. 1985 injury incidence rates and totals by cause, intent and severity level.**

Cause	Fatalities		Hospitalized Injuries		Non-Hospitalized Injuries	
	Rate	Total	Rate	Total	Rate	Total
Motor Vehicle	19.4	45,923	220.6	523,028	2,026.1	4,803,000
Falls	5.4	12,866	330.5	783,357	4,848.3	11,493,000
Firearms	13.3	31,556	27.5	65,129	72.1	171,000
Fire/Burns	2.4	5,671	22.9	54,397	591.4	1,403,000
Drownings*	2.6	6,171	2.3	5,564	11.0	26,000
Poisonings	5.0	11,894	92.2	218,554	620.5	1,472,000
Other**	12.0	28,487	293.9	696,707	14,764.9	35,001,000
Total		142,568		2,346,735		54,369,000
Cause by Intentionality						
Unintentional	38.2	90,469	834.6	1,978,518		NA
Intentional	20.8	49,276	110.4	261,738		NA
Intent Unknown	1.2	2,823	44.9	106,479		NA
Total		142,568		2,346,735		54,369,000

\* Includes near-drownings

\*\* Includes work related, sports and recreation related, other transportation, and all other sources of injury.

indicates these incidence findings. Data from the National Hospital Discharge Survey, the National Health Interview Survey, and Mortality Statistics of the U.S., along with cause-specific data bases, were carefully evaluated to produce these estimates.

The research indicated that the total cost of injuries occurring in 1985 was \$160 billion. Table 5 indicates the cost findings by cause and severity on a unit and total basis.

The study found that additional data was needed for a comprehensive evaluation of the incidence and costs of injuries. Such data might be gathered by a Supplement to the National Health Interview Survey on Injuries, Accidents

**Table 5. Lifetime costs of injuries and fatalities, 1985 by cause and severity, dollars in millions.**

Cause	Total	Fatalities	Hospitalized Injuries	Non-Hospitalized Injuries
Motor Vehicle*	51,142	18,897	23,515	8,730
Falls	37,280	1,642	29,904	5,734
Firearms	14,410	12,172	2,160	78
Burns	3,831	1,424	1,920	487
Drowning**	2,453	2,278	175	-
Poisoning	8,537	4,433	3,853	251
All other	42,422	8,989	19,347	13,086
Total	160,075	49,835	80,874	29,366

\* Authors have included legal and court costs for motor vehicle which are not included in the other categories.

\*\* Includes near drownings

and Rehabilitation, together with a follow-up for long-term costs and consequences, and a series of well-designed, coordinated studies of the long-term consequences for patients treated at trauma centers. The study also found the need for universal use of nature and cause of injury coding (ICD-N and ICD-E) to provide national estimates of injuries.

### Rand study

Currently underway at the Rand Corporation, Institute for Civil Justice, is a study to determine the economic losses that households suffer as a result of injury, the sources of reimbursement and compensation that Americans use to cover these losses, and the role of the tort liability legal system in providing compensation. The study is designed in part to replicate a major study of accidental injury loss and compensation in England, which was conducted by the Oxford University Centre for Socio-Legal Studies.

The RAND study includes a large-scale telephone survey of more than 25,000 households to identify households with injured individuals and tort liability claimants, and to estimate national rates of different forms of economic loss, compensation and legal claiming; a follow-up (baseline) telephone survey of a subset of about 3,000 individuals to collect detailed information about their injury, the circumstances of their accident, economic losses over the past 12 months as a result of the injury, benefits, reimbursement and compensation received from various sources to cover these losses, attitudes towards the injury, injurer, and accident, and experiences seeking compensation through the tort liability system; a re-interview of a small number of respondents who will be empanelled to study longer-term claiming behavior; and the use of additional data sets, such as the Survey of Income and Program Participation (SIPP), to impute expenditure values that individuals do not report reliably.

### Costs of spinal cord injuries

For the past several years Monroe Berkowitz at Rutgers University has conducted research for the Paralyzed Veterans of America Spinal Cord Research Foundation on the costs of spinal cord injury and severe disability. In a February, 1985 study he presented a review of existing data sources and previous studies on spinal cord injury incidence and cost and the results of his evaluation of costs based on the Survey of Disability and Work compiled by the Social

Security Administration of the Department of Health and Human Services (HHS, SSA) (29). Using the 1985 study as a point of departure, he conducted an additional investigation published in February, 1986, which utilized data from the Survey of Income and Program Participation and the National Medical Care Utilization and Expenditure Survey (30).

Both of these efforts applied a human capital methodology for measuring costs. Based on the data deficiencies determined in these studies, Berkowitz is currently engaged in a new study to measure the economic consequences of traumatic spinal cord injuries. Data collected through 800 personal interviews will be used to produce a national estimate of the number of spinal cord injured persons and the costs of SCI to individuals, families and society. Incidence will be measured for the number of new cases in 1985, 1986, and 1987 and a prevalence estimate will be made of the total number of spinal cord cases in existence in the U.S. on January 1, 1985. Another goal of the study is to establish a permanent computerized database on the economic consequences of spinal cord injury.

### Costs of injuries to belted and unbelted occupants

A recently completed study compared hospital costs of belted and unbelted victims of motor vehicle crashes in Iowa (31). The results included an age and sex distribution of those injured, injury severity levels by body region, hospital charges, disposition from emergency departments, and payment status. Statistically significant higher risk of injury for unbelted persons was demonstrated in all comparisons except for those whose most severe injury was at the AIS 1 level. Not included were charges for physicians, emergency medical services, and rehabilitation. The average hospital charges for injured persons who were unbelted were \$2,462, 3.3 times as high as the hospital charges of \$753 for injured persons who were belted.

Another recent study of the hospital and emergency room costs associated with persons injured in motor vehicle crashes was performed in Chicago from January to June, 1986 (32). The main purpose of the study was to determine any differences between these costs for persons who were restrained and those who were not. The study results showed mean charges of \$583 for persons injured while restrained, and \$1,583 for unrestrained persons. The report also included data on injury severity scores, payment, and the demographics of the injured population.

An automobile crash study currently being conducted by the Maryland Institute for Emergency Medical Services Systems (MEIMSS) is examining restraint usage, acute and long-term costs of injuries sustained in the sample of crashes, and many other crash variables (33).

### Other sources of cost data

Theoretical work in this decade by Broome, Marshall, Arthur, Berger, and others has made notable contributions to the methodology for measuring of costs of injuries (34).

In addition, several other data sets and special studies have produced injury cost data.

A number of studies on the impact of motorcycle helmet use have been published. Notable among these are work by Rivara, Bergman, and associates at the Harborview (Washington) Injury Prevention and Research Center (35), measurement of the costs of unhelmeted motorcyclists in Texas (36), a study on the effects of re-enacting state helmet use laws (37), and a study by Bray and associates at the University of California, Davis on the cost of orthopedic injuries (38). Also on the subject of motorcycle injuries, data is being collected on costs as part of a Maryland Department of Transportation study (33).

The National Spinal Cord Injury Data Base, funded by the National Institute on Disability and Rehabilitation Research (NIDRR) and maintained at the University of Alabama, Birmingham, contains medical cost and rehabilitation data for spinal cord injuries occurring as far back as 1972. A Head Injury Data Base, also funded by NIDRR, is in its initial phases and will contain longitudinal cost data on head injuries similar to that in the Spinal Cord Injury Data Base.

Trauma Centers' Annual Reports contain some injury cost data, specifically on charges for acute trauma care (39). In addition, individual researchers have published papers which included injury cost data. Ellen MacKenzie and associates at The Johns Hopkins University have undertaken significant research on the treatment related costs of traumatic injuries (40). Julian Waller at the University of Vermont also has done research on the costs of certain types of injuries (41). Data on severe injury costs by type of injury are available from the Michigan Catastrophic Claims Association (42).

### **Willingness to Pay**

Another approach to economic analysis of injuries is called Willingness to Pay. Instead of seeking to estimate the costs of injury, it attempts to estimate the "value" of the lives lost or the injuries sustained. A recent report by the Rand Institute for Civil Justice found that "most economists would agree that willingness to pay is the most conceptually appropriate criterion for establishing the value of life" (43). Another recent report to the Administrative Conference of the United States cited a number of different Federal agency applications of costs derived by a willingness to pay approach (44).

Willingness to Pay estimates are based on quantifying the incremental risks persons are willing to take in order to achieve some desired end, that is the "small change in their probability of continued safe and healthy living" (45). For example, some persons are willing to take greater risks in their jobs in return for higher pay. The application of this concept to highway safety was undertaken by the Federal Highway Administration (FHWA) in 1982, when it initiated research to review and study the basis of accident costs to assist highway officials in their efforts to allocate program resources for highway safety improvements.

In January, 1984, the FHWA published a report based on the work of Miller, Reinert, and Whiting titled "Alternate Approaches to Accident Cost Concepts" (46). FHWA characterized the report as presenting "state-of-the-art methods for deriving highway accident cost estimates essential in evaluating highway safety countermeasures." The report concluded that "Estimates of willingness to pay for life and safety would be theoretically superior to human capital costs for use in benefit-cost analyses. Empirical studies of willingness to pay offer widely divergent value of life estimates, and most are based on questionable data, assumptions, or estimation procedures".

A succinct summary of interim results of additional FHWA sponsored research concluded in 1986 that willingness to pay values of life of about \$1.1 million should be recommended as consistent with current economic thought even though these values were considerably higher than values currently used by some highway agencies (47). Further results have been reported recently (25, 45).

The current best estimate of the Willingness to Pay value of life in the United States is \$2 million (45).

Willingness to Pay theory has been accepted by some economists as the proper approach for cost/benefit analyses. However, as stated in the Administrative Conference report, "While willingness-to-pay provides the most inclusive analysis currently available for evaluating the benefits derived from regulatory reduction of fatalities, it falls far short of an ideal process and can produce results that are misleading for failure to consider all variables relevant to an inclusive valuation process" (44). The authors have a concern that when willingness to pay is applied outside of the strict cost/benefit context it can be easily misinterpreted.

It should be noted that there is active interest in the willingness to pay concept outside the United States. For example, the UK Ministry of Transport has recently revised its estimate of Willingness to Pay to avoid a fatality from £283,000 to £500,000 in 1987 prices (48). (At the current exchange rate of \$1.65/£, this would equal an increase from \$467,000 to \$825,000.) A recent Australian study considered willingness to pay and its relationship to human capital (49), and a recent New Zealand study included estimates of willingness to pay to avoid a fatality in that country (50).

### **Unresolved Issues in the Measurement and Application of Injury Costs**

No matter what approach is taken to estimate injury costs, the quality of the estimate and the confidence that can be placed on it depend to a large degree on the comprehensiveness and completeness of the underlying data used in developing the estimate. Other problems arise in the application of the results to questions of societal impact, where the social or emotional aspects of the problem, such as pain and suffering, are not amenable to economic analysis and have not been included in the total. Certain of these problems merit further study.

## **Incidence**

It is difficult to define incidence due to limitations in sources of data. For example, differences between data derived from sampling techniques and from epidemiological data show factors of three to five in the number of persons seriously injured in certain categories (51). Another recent report showed that the numbers of brain injured and spinal cord injured persons does not agree with the values derived by sampling techniques (52). Also, the data reported here as part of the NHTSA Grant Studies, using incidence based on public health records and personal reporting, differ from some specific data bases such as NASS. There is a strong likelihood that the number of injured persons is much larger than the presently available data suggest.

## **Multiple injuries**

Most often an injured person has more than one injury, especially for those with the more serious injuries. For example, a person with a moderate brain injury also may have an open fracture of the femur. Both of these injuries may have long-range cost implications; however, with current data collection schemes it is not possible to disaggregate the costs. This creates a number of problems if one is interested in determining the cost resulting from a particular injury, which is often the case in applications of cost data relating to vehicle countermeasure development. At present the data are typically treated for the most serious injury, as shown in the example above concerned with methods of establishing research priorities.

## **Uncounted and undercounted costs**

The magnitudes of some cost categories are not well known, and are believed to be undercounted. For example, in the medical cost area, there is considerable data on hospital and emergency room charges; however, data on physicians' charges is not widely available, and there is limited knowledge of rehabilitation costs. There is also some evidence that costs often go far beyond costs to the injured person and extend to the family and community as well. In the productivity area, there have been some attempts to include the costs of lost productivity as a result of the time spent by significant others in caring for injured persons; however, further work is needed. Investigation also is warranted into measurement of the costs that might be incurred by persons who are not physically injured but who may have serious emotional reactions to the injury or death of someone else, such as when someone else is killed in a crash but the individual is not hurt at all. Also, related to this, is the evidence of increased mortality following bereavement, and the consequences of serious injuries that can extend across generations as families are affected by the death of a parent or child (53). Another important aspect of the uncounted cost problem is the fact that the available data generally reflects charges, not costs, and costs are believed to be generally higher than the charges.

## **Unmet needs**

One concern with the Human Capital methodology is that although it attempts to measure the actual costs to society, it does not attempt to determine what it would cost if all of the needs were being met. That is, some persons do not have their injuries treated, or do not receive rehabilitation care (which could return them to productive lives) because they cannot afford to. A rigorous application of Human Capital says these costs were not incurred thus they need not be measured. It appears, however, that there is a societal cost here that is not being counted.

## **Who pays and transfer payments**

Knowledge of the sources of payment for the direct costs of injury can yield important information, especially in the public program context. Similarly, transfer payments for both direct and indirect costs provide important information, as long as they are not added to total costs, which would result in double counting. Knowledge in these areas could be strengthened.

## **Use of economic costs as measures of societal impact**

An additional problem with costs developed under the human capital methodology, of particular significance when considering the effects of injuries and fatalities resulting from motor vehicle crashes, is the undercounting of the significance of the injuries for certain age groups due to the application of discounting. Although discounting normalizes future costs to the present year, injuries of the very young and very old essentially do not count, and injuries to late teens, the largest category in the incidence of motor vehicle injuries, count for less than injuries to persons in their peak earning years. Thus, using the human capital cost estimates for purposes other than estimating the resources used and lost resulting from injuries, such as a measure of societal impact, results in answers that are contrary to some highly developed cultural attitudes. As an alternative measure, evaluation of life years lost may be more reflective of basic societal attitudes, such as the importance society places on the development of the very young.

## **Willingness to pay**

There are several unresolved issues remaining with the willingness to pay methodology. They include:

- The best estimates have a range of over a factor of about 2 to 1. This is hardly encouraging as an accurate estimate, especially considering the concerns with any societal measure mentioned above, such as incidence errors, etc.
- The estimates are based on a variety of studies reported in the literature. Certain assumptions are implicit in these analyses, such as that there is a free labor market, that persons have full information, etc. These assumptions often are unrealistic.
- Extension of the willingness to pay concept to

injuries is at an early stage. Some questions remain about the appropriate methodological base to use for such estimates.

- Little work has been done on the difficult problem of determining what the public at large believes the value of life to be. Included here are some definitional problems that must be addressed, such as is the value to be considered as the difference between life and death, or is it the difference between life as it normally would have progressed and life as a quadriplegic or brain damaged person dependent on family, friends and society? Clearly, how the question is asked will influence the value chosen by the answerer.

At the base of many of the concerns with Willingness to Pay is that it attempts to value life. There is a "moral" concern here which goes beyond any methodological concern. Willingness to Pay presumes to arrive at monetary values for such human values as love, hope, aspirations, grief, pain, and suffering. The authors contend that these are priceless, and can not be expressed in monetary terms.

## **Beyond Human Capital and Willingness to Pay**

Even with its shortcomings, Human Capital is a highly developed economic methodology. Willingness to Pay, though not as fully developed, also meets a need in certain economic analyses. The principal problem, as the authors see it, is that these economic estimating tools are often used in non-economic settings. Many decisions include consideration of factors which do not fit in the economist's model, such as attitudes, social and cultural values, and political considerations. For those cases where non-economic considerations are important it is desirable to go beyond the constructs of the Human Capital and the Willingness to Pay theories to an approach that would include these other concerns.

One such approach, called the Rational Investment Decision, was an attempt to go beyond the narrow Willingness to Pay concept and include the concept that society may find it worthwhile to develop a methodology that would allow decisions to be made on a societal investment basis (43).

Another concept would add to estimates derived from the Human Capital and Willingness to Pay economic approaches those costs that an informed society would want to take into account in any carefully considered decision on health and safety. This is being called here the Wise Investment Decision Estimate (WIDE). Some of the costs of injuries that may be included in a WIDE methodology are costs that presently are unmeasured, or poorly measured, such as loss of parental support, nurturing and guidance. These costs are often borne by individuals, families, friends and neighbors for many years subsequent to the injury. The value to society of reducing or eliminating a public health problem for future generations would also be included. The

need for a "social consequences" model of loss that might include sociomedical indicators was raised in the discussion by MacLennan (28). Obviously, there is a need for additional research in order to develop and test these concepts.

## **Conclusions**

Two methods of economic analysis of the impacts of injuries have been developed, called the Human Capital and Willingness to Pay methods, and additional conceptual and methodological approaches have been explored by researchers. The Human Capital methodology attempts to measure costs. The Willingness to Pay approach attempts to measure value. The latest estimated cost for a motor vehicle fatality is \$400,000 using the Human Capital method, and the value of a life is estimated at \$2 million using the Willingness to Pay method.

Research results are now available on both an individual incident and a national level, for a variety of injuries occurring as a result of a number of causes. Detailed data are available for certain particular injury types, such as spinal cord injuries, or injuries resulting from particular causes, such as motor vehicle crashes for unrestrained occupants. Several methods have been demonstrated using costs of injuries and related data in making decisions at both very detailed and broad levels.

Using either economic cost or economic value for decision-making leaves out several critical elements, such as social and cultural concerns, and political considerations. These frequently are given great weight in making decisions, especially policy decisions, even though they can not be expressed quantitatively. This speaks for the need for further development at the conceptual level.

Although important decisions cannot be made based solely on costs, these data can be valuable as part of the process. For example, the costs to local jurisdictions of having to treat uninsured, unbelted motor vehicle crash victims can influence the decision to require occupant protection.

Further work is needed in the development of cost estimates. Measurement of incidence has several gaps. Many injured persons do not end up in any data base, and there is some evidence that there may be seriously injured persons in this uncounted incidence. Several categories of costs are not counted at present, and they could have major effects on the total. These include persons who are injured but who cannot afford medical care, or who receive minimal care; the costs borne by the family or household in lost work caring for an injured person; the costs to community organizations that respond to injured people in time and resources; costs related to uninjured persons who are affected emotionally; and the costs borne by the hospital or trauma center who are reimbursed by formula rather than for total charges and which are ultimately borne by society at large through higher medical charges in general; etc. Another concern is that costs of rehabilitation may be grossly underestimated.

Additional conceptual work is needed on developing a methodology for assessing costs from the individual's point of view. The perspective of human capital cost measurement is primarily societal. Willingness to pay attempts to measure costs to the individual by determining the amount that individuals who are alive and well are willing to pay for reductions in injury or fatality risk. Neither of these methodologies comprehensively measures the costs from the viewpoint of the injured or dead person. A new methodology for cost measurement from the individual perspective could focus on information gathered from injured persons and their families and attempt to place a value on what has been lost.

The economic analysis methods discussed in this paper have validity when properly applied, however neither Human Capital nor Willingness to Pay fully measures the societal impact of injuries and fatalities. Difficulties arise when these methods are used beyond their limits of validity. However, it is apparent that there is a need for a measure of the total impact on society resulting from injuries, to include not only the economic, but the social and emotional impacts as well.

This review of the current state-of-knowledge of costs of injuries indicates that unanswered questions remain in both the conceptual framework and measurement capabilities concerning costs of injuries. Research leading to greater knowledge of costs of injuries should prove valuable in improving the decisions made by society to reduce the impacts of injuries.

## Disclaimer

The opinions expressed in this paper are those of the authors, and do not necessarily reflect the position of the National Highway Traffic Safety Administration.

## References

- (1) "Estimating the Cost of Illness", Dorothy Rice, U.S. Department of Health, Education and Welfare, U.S. Public Health Service, 1966.
- (2) "Economics of Mental Illness", Rashi Fein, Basic Books, New York, 1958.
- (3) "Economics of Public Health", Burton Weisbrod, University of Pennsylvania Press, Philadelphia, 1961.
- (4) "Syphilis Control Programs", Herbert Klarman, in *Measuring Benefits of Government Investments*, The Brookings Institution, Washington, D.C., 1964.
- (5) "Health as an Investment" Selma Mushkin, *Journal of Political Economy*, Vol. 70, No. 5, Oct. 1962.
- (6) "The Economic Costs of Illness: A Replication and Update", Dorothy Rice et al., in *Health Care Financing Review*, Vol. 7, No. 1, Fall 1985.
- (7) "The Incidence and Economic Costs of Major Health Impairments", by Nelson Hartunian, Charles N. Smart, and Mark S. Thompson, Lexington Books, 1981.
- (8) "The Injury Fact Book", Susan P. Baker, Brian

O'Neill, and Ronald S. Karpf, Lexington Books, 1984.

(9) "Societal Costs of Motor Vehicle Accidents", John Yasnowsky and Barbara Faigin, U.S. Department of Transportation, National Highway Traffic Safety Administration, May 1972.

(10) "The Societal Costs of Motor Vehicle Accidents, 1975", Barbara Faigin, U.S. Department of Transportation, DOT-HS 802 119, December 1976.

(11) "Economic Consequences of Automobile Accident Injuries", in *Automobile Insurance and Compensation Study*, U.S. Department of Transportation, 1970.

(12) "The Economic Cost to Society of Motor Vehicle Accidents", U.S. Dept. of Transportation, DOT HS 806 342, January, 1983; "The Economic Costs to Society of Motor Vehicle Accidents", L. J. Blincoc and S. Luchter, SAE 830614.

(13) "The Economic Cost to Society of Motor Vehicle Accidents, 1986 Addendum", National Highway Traffic Safety Administration, September, 1987.

(14) "A Model for Estimating the Economic Savings from Increased Motorcycle Helmet Use", DOT HS-807 251, March, 1988.

(15) "A Model for Estimating the Economic Savings from Increased Safety Belt Use", DOT HS-807 252, March 1988.

(16) "A Model for Estimating Economic Costs from Motor Vehicle Crashes in State and Local Jurisdictions", DOT HS-807 253, March 1988.

(17) "A Search for Priorities in Crash Protection", A. C. Malliaris, Ralph Hitchcock, and James Hedlund, SAE 820242.

(18) "Harm Causation and Ranking in Car Crashes", A. C. Milliaris, Ralph Hitchcock, and Marie Hansen, SAE 850090.

(19) "Impairment Scaling from the Abbreviated Injury Scale", A. Hirsch et. al., DOT HS-06 648, June 1983.

(20) "Injury Priority Analysis", Oliver Carsten and James O'Day, UMTRI 84-24, October 1984 and "Relationship of Accident Type to Occupant Injuries", Oliver Carsten, UMTRI 86-15, April 1986.

(21) "Priorities in Automotive Crash Safety Based on Impairment", J. Marcus, R. Blodgett, 11th International Technical Conference on Experimental Safety Vehicles, May, 1987, Washington, DC.

(22) "The Use of Impairment for Establishing Accident Injury Research Priorities", Stephen Luchter, SAE 871078.

(23) "Impairment Resulting from Motor Vehicle Crashes", Stephen Luchter, for presentation at the Experimental Safety Vehicle Conference, Gothenburg Sweden, June, 1989.

(24) "National Accident Sampling System 1986, A Report on Traffic Crashes and Injuries in the United States", National Highway Traffic Safety Administration, 1986.

(25) "Crash Costs and Safety Investment", Ted. R. Miller, Stephen Luchter, and C. Philip Brinkman, Presented at the Association for the Advancement of Automotive

Medicine Annual Meeting, September, 1988, Seattle, Washington.

(26) "Injury in America", Committee on Trauma Research, National Academy of Sciences, Washington DC 1985.

(27) "The National Safety Council's Estimates of Injury Costs", I. B. Etter, Public Health Reports, Nov-Dec 1987, vol 102, no 6, Public Health Service, U.S. Department of Health and Human Services.

(28) "The Unmeasured Costs of Injury", Carol MacLennon, Public Health Reports, Nov-Dec 1987, vol 102, no 6, Public Health Service, U.S. Department of Health and Human Services.

(29) "Economic Consequences of Spinal Cord Injury", Monroe Berkowitz, Bureau of Economic Research, Rutgers University, for the Spinal Cord Research Foundation, Paralyzed Veterans of America, Feb. 1985.

(30) "Economic Consequences of Severe Disability", Monroe Berkowitz, Bureau of Economic Research, Rutgers University, for the SCRC/PVA, Feb. 1986.

(31) "Iowa Safety Restraint Assessment, I.S.R.A., A study of motor vehicle crash injuries and hospital charges in belted and unbelted victims, November 1987-March 1988", Iowa Methodist Medical Center, December, 1988, also see "Trauma Prevention from the Use of Seat Belts", Timothy D. Peterson, Iowa Medicine, Des Moines IA, May 1987.

(32) "Prospective Study of the Effect of Safety Belts on Morbidity and Health Care Costs in Motor-Vehicle Accidents", Elizabeth M. Orsay et. al., JAMA, December 23/30 1988, vol 260 n 24.

(33) "Automobile Crash Trauma Study", University of Maryland at Baltimore, Maryland Institute for Emergency Medical Services Systems (MIEMSS), ongoing. "Motorcycle Accidents in Maryland, A Study Linking Police, Ambulance, Hospital, Cost Review Commission and Death Certificate Data", Maryland Department of Transportation, Office of Transportation Planning, ongoing.

(34) "Costs of Illness Studies—An Annotated Bibliography", Dorothy Rice and Sander Kelman, University of California, San Francisco, Institute for Health and Aging, 1988.

(35) "Motorcycle Injuries: What are the Costs and Who Pays?", Rivera et. al., Harborview Injury Prevention and Research Center and the Departments of Pediatrics, Epidemiology, and Neurological Surgery, University of Washington, Seattle, Washington, 1988; also reported in "The Public Cost of Motorcycle Trauma", Journal of the American Medical Association, Vol. 260, No. 2, July 8, 1988.

(36) "The Costs of Treating Head Injured Unhelmeted Motorcyclists in Texas", Texas Department of Public Safety, unpublished, March, 1989; based in part on Lloyd, et.al., "A Comparison of Helmeted and Unhelmeted Motorcyclists Admitted to a Community Trauma Center", Texas Department of Health/CDC funded, 1988.

(37) "Impact of the Re-Enactment of the Motorcycle Helmet Law in Louisiana", Norman McSwain, and Anita Willey, Tulane University School of Medicine, December, 1984.

(38) "The Cost of Orthopedic Injuries Sustained in Motorcycle Accidents", Bray, et.al., University of California, Davis, Medical Center, in JAMA, Vol. 254, No. 17, Nov. 1, 1985.

(39) One Example: "County of San Diego Annual Trauma System Report", Department of Health Services, Division of Emergency Medical Services, Annual (March).

(40) "Functional Recovery and Medical Costs of Trauma: An Analysis by Type and Severity of Injury", MacKenzie, et.al., Journal of Trauma, Vol. 28, No. 3, March, 1988; and "The Economic Impact of Traumatic Injuries—One Year Treatment Related Expenditures", MacKenzie, et.al., JAMA, Vol. 260, No. 22, Dec. 9, 1988.

(41) "Disability, Direct Cost, and Payment Issues in Injuries Involving Woodworking and Wood Related Construction", Julian A. Waller, Stephen R. Payne, and Joan M. Skelly, to appear in Accident Analysis and Prevention.

(42) Michigan Catastrophic Claims Association, Livonia, Michigan 48154.

(43) "Computing Economic Loss in Cases of Wrongful Death", E. M. King and J. P. Smith, The Institute for Civil Justice, The Rand Corporation, Report Number RAND/R-3549-ICJ, 1988.

(44) "Federal Agency Valuations of Human Life", Clay Gillette and Thomas Hopkins, Report to the Administrative Conference of the United States, July 7, 1988.

(45) "The Socio-Economic Impacts of Injuries Resulting From Motor Vehicle Crashes", Ted. R. Miller and Stephen Luchter, FISITA 885162, Presented at the FISITA Conference, September, 1988, Washington DC.

(46) "Alternate Approaches to Accident Cost Concepts", T. R. Miller, K. A. Reinert, and B. E. Whitning, Report no FHWA/RD-83/079, Federal Highway Administration, Washington DC January 1984.

(47) "Accident Costs for Highway Safety Decision", by Brenda C. Kragh, Ted. R. Miller, Public Roads, June 1986, vol 50 no 1, Federal Highway Administration, U.S. Department of Transportation.

(48) Infonet, Issue No. 2, March 1989, Published by the International Driver's Behavior Research Association, Paris.

(49) "Cost of Road Accidents in Australia", L. A. Steadman and R. J. Bryan, Bureau of Transport and Communications Economics, Occasional Paper 91, Australian Government Publishing Service, Canberra, 1988.

(50) "A Review of Research on Unintentional Injury, A Report to the Medical Research Council of New Zealand", John Langley and Elizabeth McLoughlin, Special Report Series No. 10, Medical Research Council of New Zealand, Auckland, August 1987.

(51) "Traffic Related Disabilities and Impairments and

Their Economic Consequences”, Stephen Luchter, SAE 860505.

(52) “Estimated United States Incidence of Disabling and Fatal Central Nervous System Traumas: A Need to Re-Evaluate Priorities”, Thomas E. Anderson and David C.

Viano, presented at the 1986 IRCOBI Conference.

(53) “Bereavement”, Committee for the Study of Health Consequences of the Stress of Bereavement, Institute of Medicine, National Academy of Sciences, Washington, DC 1984.

## Proposal of a Motor Vehicle Safety Assessment

H. Appel, W. Glatz, F. Kramer,  
Technical University of Berlin

### Abstract

A means of assessing the passive safety of passenger motor vehicles would represent a desirable instrument for the legislator, the automobile industry and the consumer. In contrast to the dominating criteria of assessment for vehicles such as, amongst other features, the engine power, the economy of interior utilization, the aerodynamics and the consumption of resources, no clear and generally accepted assessment standards are available for the field of passive safety.

The proposed method of assessment combines the results of experimental safety tests which are carried out in accordance with existing mandatory test conditions or test conditions which are under discussion, with biomechanical validation of load values measured in tests.

The assessment is made by means of risk functions defined for individual parts of the body, these functions being compiled by correlation of the results of accident analysis with results obtained from computed simulation.

The degree of fulfillment of the particular protection criterion thus arrived at is weighted by factors which take into account the frequency of occurrence and the severity of the accident in relation to cost.

The test program comprises in each case at least one safety test for head-on and side-on collisions against a rigid or deformable barrier as well as a side-on collision test between two vehicles of the type being examined in the particular case. Computer-aided analysis and assessment of the simulation results permit determination and graphic representation of an overall safety index referred to the vehicle as well as partial and individual safety grades.

The passive safety offered by the vehicle being tested in each case can be quoted for individual seating positions, a specific accident constellation or individual endangered regions of the body.

### Introduction and Problems

Among the complex spectrum of demands placed on a passenger motor vehicle, a dominating position is occupied by the function of the vehicle as a means of transport, the economical implementation of this—meaning economical utilization for the user and the economic implications of the consumption of resources (production and operation)—and

the ecological stress imposed on the environment (pollution and noise).

To this must be added criteria which are specific to motor vehicles, e.g. the engine power, economy of space and aerodynamics.

If these criteria are used for comparison of different vehicles, clear, generally accepted and quantifiable physical assessment parameters are available.

From the point of view of society in general, assessment of the consequences of the technology employed is also necessary, i.e. in particular the detrimental ecological consequences.

Thus it cannot be disputed that high demands must be placed on the safety of the vehicle. However at the present time no assessment criteria and standards are available which would do justice to the importance of the issue and which differentiate between active safety and passive safety.

A method of assessment of the passive safety of passenger vehicles would, all in all, appear both necessary and desirable from the point of view of the legislative authorities, automobile manufacturers and not least the consumer.

Such a means of assessing safety can serve the legislative authorities for effective and purpose-oriented influence on road safety as well as for reconsideration of measures already taken and can also be incorporated in the work of drawing up and debating new regulations and guidelines.

For vehicle manufacturers, there is an incentive to increase the level of safety of their products even further and to gain a competitive edge among customers who have become increasingly sensitive to such issues.

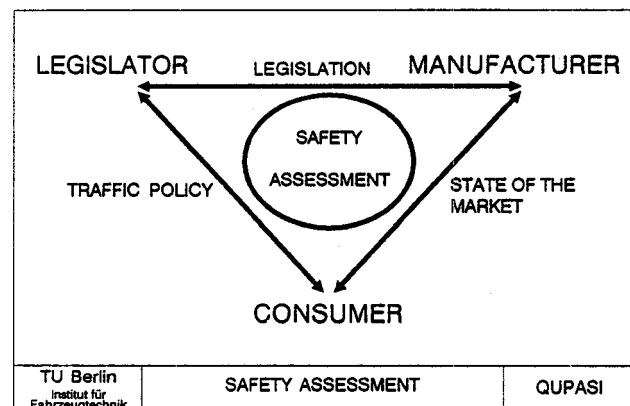


Figure 1. Effects of safety assessment.

On the other hand there may be a necessity for manufacturers to have to react to a conceivable change in the demand situation. For the consumer a transparent assessment of safety offers an additional, objective decisionmaking criterion for the purchase of a vehicle and, assuming that public relations work is increased, may awaken and promote safety consciousness.

For the assessment of passive safety, the main means at present available involves statistical analyses (1,2,3)\* which, by comparison of accident-dependent follow-up parameters such as property damage and personal injury quantifiable in terms of money, supply a means of assessment with retrospective validity.

Other procedural proposals are experimentally oriented (4,5,6) and use the results of individual safety tests as assessment parameters.

Since there was a lack of a consistent and practicable method of validating the safety level of individual types or categories of cars, the possibilities and the problems involved in safety assessment were analyzed within the scope of a research project with the title "Quantification of Passive Safety of Passenger Motor Vehicles" (7) commissioned by the Federal Highway Research Institute.

The assessment method proposed attempts to combine the various approaches and provides for incorporation of the biomechanics of the passengers and the economic accident consequences in an experimental analytical procedure.

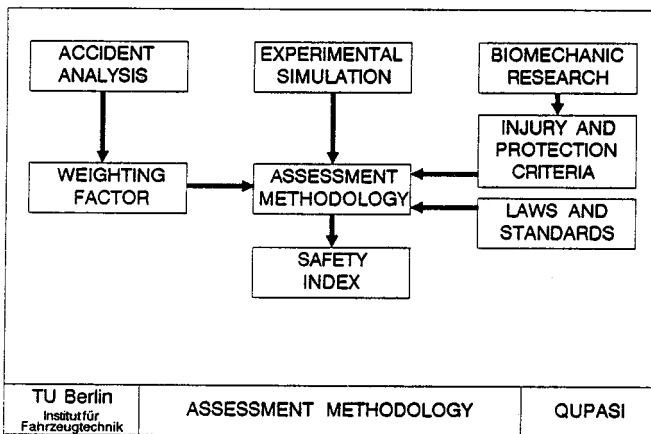


Figure 2. Input parameters for assessment algorithm.

## Accident Analysis

The analysis of the real sequence of events of an accident is of decisive importance for compiling the boundary conditions for experimental simulation.

Basing considerations on accident data collected by the Accident Research Department of the Technical University of Berlin and the Medical Highschool Hannover for the Federal Highway Research Institute (8), a statistical evaluation was carried out with the aim of obtaining a detailed insight into all the parameters defining the reality of an accident.

\*Numbers in parentheses designate references at end of paper.

These include the various types and sorts of collisions, the position of the occupants in the car involved in the accident, the injured regions of the body and the injury causing areas within the car as well as vehicle-specific parameters such as the crash weight, type and use of a restraint system and the damage sustained to the vehicle.

The relevance of individual accident constellations and the resulting injuries to passengers arises from the determined frequency of occurrence and the economic losses arising which are taken into account via the costs caused by the injuries. Assuming that a relationship is established between each dummy measuring point and the body part of the passenger, further systematic analysis of the data provides what are termed relevance factors which in the procedure of assessment serve for weighting the loading parameters determined by technical tests.

## Experimental Simulation

For the purpose of laying down the test conditions for the experimental part of the safety assessment procedure, considerations are based on the mandatory safety test, a head-on collision with a rigid barrier and the proposal for a European side-on collision test with a mobile, deformable barrier. In addition a side-on collision test between two vehicles of the type under investigation serves to take into account the degree of comparability.

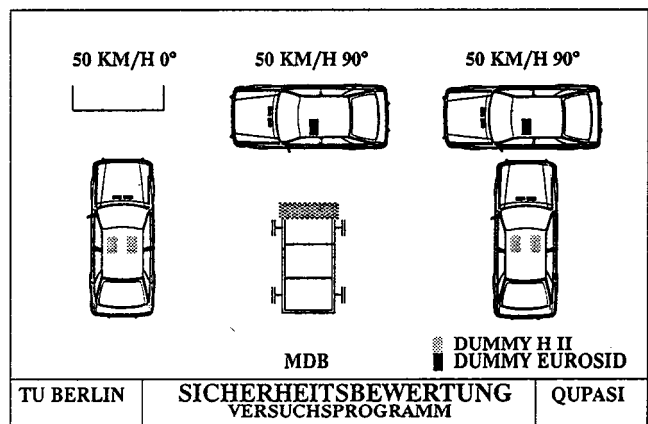


Figure 3. Test program for safety assessment.

The instrumentation and the occupation of the vehicle correspond to FMVSS 208 as well as the European draft for a side-on collision test procedure. The collision speed for all tests amounts to 50 km/h at an angle of 0° respectively 90°. The loadings on the occupants are measured using dummies of types Hybrid II and Eurosid. The use of new dummy types and extension of the technical methods of measurements is also possible if required.

## Procedural Directive

To obtain statistically reliable test results, a finite number of safety tests is necessary. However, for the field of vehicle compliance tests only one single test is provided, which means that the value measured will with a certain degree of probability deviate from the true value.

To reduce the expenditure required for the procedure, account is taken of this deviation of the measured values in a procedure directive.

This directive defines a Minimum Demand  $MA =$  protection criterion level minus variance and an Upper Tolerance Limit  $TG =$  protection criterion level plus variance of the measurement.

The level of the particular load value in relation to these parameters decides on whether the result can be admitted for assessment, whether a single repeat test and an assessment of the mean values is necessary or whether the result must possibly be excluded from the procedure.

## Risk Function

The results of a minimum of three and a maximum of six full-scale safety tests obtained from the proposed procedure can now be incorporated in the actual assessment procedure.

The determined physical loading parameters are first related to the protection criterion level defined for the particular measuring point, i.e. the tolerance limit for the loading on the relevant part of the body. These standardized values are the input variables for the risk functions referred to body parts.

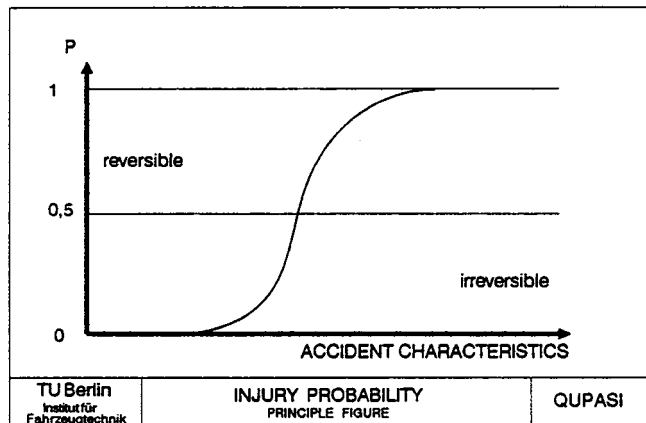


Figure 4. Probability function for occupant injury.

By combining accident analysis with computed simulation, the functions establish a relationship between the real consequences of an accident (occupant injuries) and the experimentally determined load values (physical loadings).

Analogous to the sensors in the head, chest, pelvis and femurs of the dummy, the AIS-coded classes of injury severity are represented in the statistical analysis as a function of the accident parameters in relation to the speed and mass classes for head-on and side-on collisions.

The result is a distribution function for the probability of occurrence of reversible and irreversible injuries for each part of the body sustained in the head-on or side-on crash direction considered in each case.

Taking this statistical analysis of the sequence of events of the accident as a point of departure, boundary values are determined to define the input parameters for computed simulation.

These boundary conditions being such that they should secure the same frequency distribution define the number of computer runs.

The implementation of the procedure in a computer program permits output of an overall safety index both for the whole vehicle as well as a partial safety index for the level of the passive safety of the test vehicle in the event of head-on or side-on collisions and safety ratings referred to seating places and to the occupants' body parts.

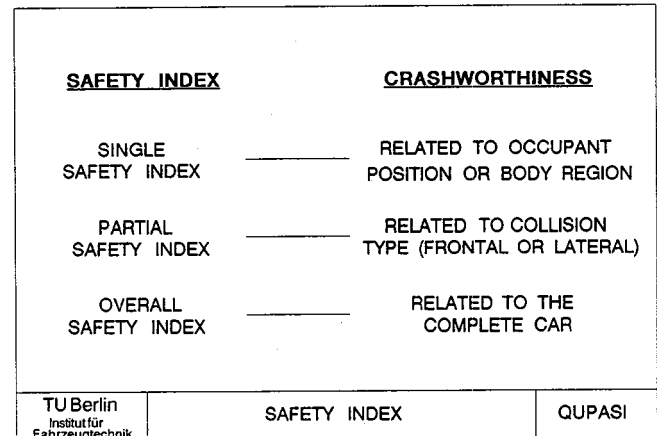


Figure 5. Assessment algorithm.

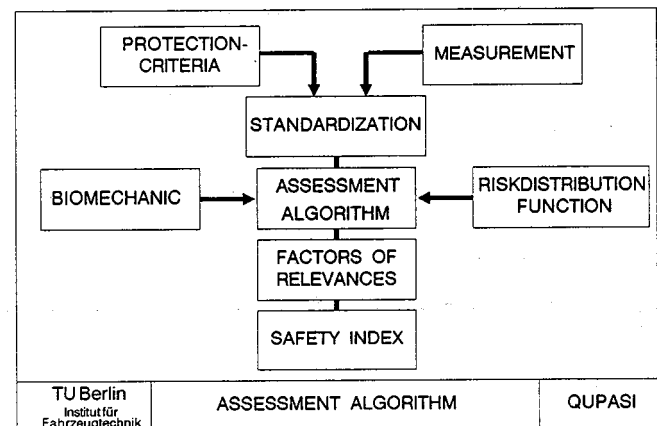


Figure 6. Indices for vehicle safety assessment.

## Application

Fields of application for the above-developed assessment procedure include comparative tests to establish technical safety within one class of vehicle, a longitudinal section comparison between relevant vehicles of successive series of models as well as an estimate of the increase in passive safety after modification of a vehicle.

## References

- (1) Folksam Insurance Company, Säkra och farliga bilar, Viking Books 1984.
- (2) Vehicle Safety Consultants Ltd., Car Safety Rating Scheme.
- (3) TÜV Autoreport 1986, "Nicht in allen Autos gute Überlebenschancen."

(4) Penoyre, S., Transport and Road Research Laboratory, A Crashworthiness Rating System for Cars, 9th ESV-Conference Kyoto.

(5) Miller, Patrick, Rydznski, Analysis of Frontal Impact Test Data—New Car Assessment Program—DOT—HS—395, February 1984.

(6) ADAC, ADAC-Motorwelt Heft 11/88, "Der große Crash Test."

(7) Appel, H., Kramer, F., Glatz, W., Lutter, G., "Quantifizierung der Passiven Sicherheit von Personenkraftwagen," Forschungsprojekt FP 8517/2 im Auftrage der Bundesanstalt für Strassenwesen, Abschlussbericht 1989.

(8) Otte, D., Erehbungen am Unfallort MHH/TUB, Projekt FP 7263/7506/7813-4/8200-1 BAST.

(9) Kramer, F., Insassen-Crashmechanik-Rechenmodell für Frontalkollisionen Programmbeschreibung, Verifikation und Validierung. Forschungsbericht 324/88 TU-Berlin 1988.

(10) Hofmann, J., Rechnerische Untersuchung zur optimalen Seitenstruktur von Personenkraftwagen, Dissertation 1980 TU-Berlin.

(11) Kramer, F., Schutzkriterien für den Fahrzeug-Insassen im Falle sagittaler Belastung TU Berlin, 1989.

## Low Speed Rear Impacts and the Elastic Properties of Automobiles

**D.P. Romilly, R.W. Thomson,**  
Department of Mechanical Engineering  
**F.P.D. Navin, M.J. Macnabb,**  
Department of Civil Engineering,  
University of British Columbia

### Abstract

Many low speed, rear impact accidents produce occupant neck injuries which have become a concern to the insurance industry and the medical profession. The authors, with the cooperation of the Insurance Corporation of British Columbia (ICBC), conducted approximately 30 low speed pendulum tests to measure the elastic and plastic properties of selected vehicles in rear end collisions. Displacement/time traces were generated from high speed video recordings of selected points on the vehicle and an anthropometric dummy occupant. The authors noted that a high impact speed was required to produce perceptible damage to the test vehicle. This speed caused violent movement to the test dummy neck. Discussion of these results with insurers indicates there is a conflict between bumper stiffness (required for the Canadian 8 km/h bumper standard) desired by the material damage section of the insurance industry, and the need for vehicle compliance for occupant protection. Investigation into the vehicle's elastic and plastic properties will also aid in the design of Civil Engineering roadside structures and provide a better understanding of injury causation at low impact speeds.

### Introduction

Sprains to the neck and back occur in more than half of all casualty producing accidents. Associated insurance injury claims are estimated at over \$100M (Cdn.) for the province of British Columbia, Canada annually. A recent provincial publication indicates that whiplash reports in B.C. increased approximately 30% from 1986 to 1987 (1).<sup>\*</sup> The report also noted that damage to these cars was typically less than damage occurring in other casualty producing accidents.

A litigious syndrome does not appear to be the sole reason for the increasing numbers of injury claims. Whiplash or neck hyper-extension is, in many cases, symptomatic and subjective in its diagnosis as existing evaluation techniques are unable to identify soft tissue injuries (2,3). Assuming that genuine injuries are reported for accidents where vehicles show little or no damage, the authors have initiated an investigation into the dynamic response of the vehicle and its occupant to low speed impacts.

The mechanics of a high speed collision are relatively well documented. The vehicle structure deforms, converting the system's kinetic energy into sound, thermal and strain energies. The rate of deformation is a result of the vehicle's stiffness characteristics while the amount of recoverable deformation is a function of its elastic properties. At high impact speeds, very little elastic recovery occurs and the vehicle generally behaves as a plastic body. At low impact speeds, however, plastic behaviour may be absent allowing most of the total impact energy to be recovered in elastic rebound. For the occupant, the best ride down profile occurs when the vehicle behaves as a plastic body with large deformations to reduce the overall acceleration. This creates a major dilemma for the manufacturer, occupant and insurer. Each would like the vehicle to provide the maximum protection for the occupant with the minimum material damage to the vehicle during a collision. As the vehicle becomes stiffer, the vehicle damage costs are reduced as less permanent deformation takes place. However, the occupant experiences a more violent ride down which increases the potential for injury. This implies that vehicles which do not sustain permanent damage in low speed impacts produce correspondingly higher dynamic loadings on their occupants than those which deform plastically under the same or possibly more severe impact conditions. It is this premise which is under investigation in this research project.

Much of the existing literature has addressed vehicle and occupant dynamics in the moderate to high speed range (greater than 50 km/h). This is due to many countries setting

<sup>\*</sup>Numbers in parentheses designate references at end of paper.

vehicle performance standards based on occupant survival of 50 km/h barrier impacts. However, it should be noted that the majority of accidents occur below this speed. Injury costs from these low speed accidents are not insignificant, especially in neck injuries from rear impacts.

Based on the experience derived from the development of an earlier low speed crash barrier (4), the researchers initiated a project to study both vehicle and occupant response using a more accurately controlled, and repeatable, low speed impact facility. A pendulum style impactor was developed permitting preselected impact conditions in a controlled test environment. This allowed a systematic study to determine the vehicle and occupant responses as functions of the impact parameters (i.e. mass, velocity, impact energy, impact geometry, etc.).

This paper presents the first phase of work completed with the new impact facility. Impact tests were conducted to investigate the dynamic response of a vehicle and driver to known rear-end impacts. The results of these tests are presented and discussed with respect to quantifying the relative motion between the vehicle and occupant for low impact speeds and the crash performance of the vehicle.

## Low Speed Impact Test Facility

### Impact pendulum design

In order to provide controlled impacts in the low speed range, the pendulum style impact facility shown in figure 1 was designed and constructed. The facility is capable of impact speeds up to 20 km/h with a swung mass selectively variable from 300 to 2000 kg. It has been designed to be recognized as a valid information source based on the Canadian Motor Vehicle Safety Standards (CMVSS 215) (5) and the Society of Automotive Engineers (SAE J980a) (6) guidelines. The pendulum impactor faces prescribed in these guidelines were modified to provide a surface profile more representative of a vehicle front end. This facility is located at the ICBC Research and Training Center in Burnaby, B.C. and is portable, having a relatively quickly assembly/disassembly time. Manual set-up and operation

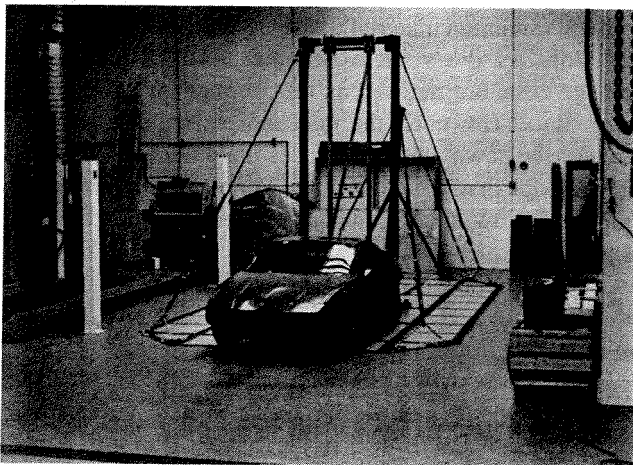


Figure 1. Low speed impact test facility.

were used to maintain simplicity which is reflected by the low material cost of \$1300 Cdn. and the relatively short construction time of six man-weeks.

### Instrumentation

The occupant, vehicle, and pendulum motions were recorded using a Kodak Ekta-Pro 1000 high speed video system with a maximum sampling rate of 1000 full frames/second. Video images of the occupant and vehicle (benchmarked with targets as in figure 2) were recorded throughout the test and post-processed to yield displacement histories for subsequent analysis and modelling. This proved to be a simple, flexible, data acquisition system which also provided qualitative information beyond the recording capabilities of a sensor based system.

The pendulum velocity was measured by a speed trap consisting of three equidistant mechanical switches mounted such that the last switch was tripped by the pendulum just prior to impact.



Figure 2. High speed video image of occupant and car.

### Test vehicles and crash dummy

The vehicles tested in this project were two and four-door Volkswagen Rabbit hatchbacks. These models were chosen because they are representative of compact cars currently on the road and have been extensively tested by UBC in previous research studies (7). All of the test vehicles were insurance "write-offs" supplied through ICBC. Each vehicle was free of damage in the rear portion and free rolling. This ensured that the test vehicles were representative of functional cars. Due to accessibility, a Hybrid II anthropometric dummy was used to represent the occupant and was made available to us courtesy of the Transport Canada Test Centre in Blainville, P.Q. A comparison, provided by Foster et al (8) of the Hybrid II neck performance, relative to the criteria put forth by Mertz and Patrick (9) is shown in figure 3. The results suggest the Hybrid II has limited use in whiplash testing because of an overly stiff neck arrangement. With this performance noted, it was expected that the dummy would yield conservative head-neck deflections. Interpretation

tions of the results is based on the relative neck response to different test conditions and avoids direct inference of possible human injury. Although this may be unsatisfactory, it is necessary due to the lack of available human neck response data.

### Testing procedures

Prior to each test the vehicle mass was determined and matched by the pendulum. Test vehicle specifications (model, year, seatback type, occupant safety system, etc.) and information relating to any pre-existing damage was logged. The car was positioned in line with the pendulum, the parking brake engaged and the transmission placed in gear. The crash dummy was then positioned in the seat and the distance between the mounted targets (as in figure 2) were recorded. Triggering of the camera preceded the release of the pendulum by 2.5 seconds to provide the necessary lead time for initializing the recording process.

After each test, a general vehicle inspection was performed by the researchers and the Material Damage staff at ICBC to locate any damage resulting from the impact. The dummy was also examined for final position, signs of interior contact, etc.

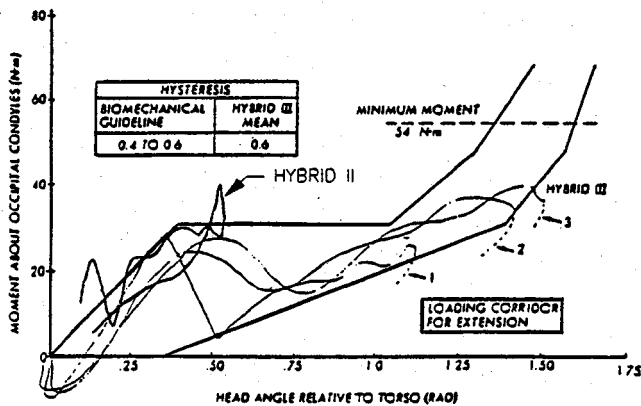


Figure 3. Performance of Hybrid II neck against Mertz-Patrick criteria (from reference 8).

To utilize the vehicles in the most effective manner, six were impacted three times each, at increasing speeds from 8 to 20 km/h (it should be noted that the first two lower speed impacts did not produce any detectable residual deformation). Two additional vehicles were tested to study the effect of variation in occupant posture (head inclination angle) and the presence of a head restraint system on occupant response at impact speeds of 8 km/h.

All of the tests which employed head restraints had the restraint adjusted to the lowest position. This reflected trends reported by States et al (10) and MacKay (11) where adjustable head restraints were found to be in the lowest position in 70-90% of the vehicles surveyed.

### Kinematic Data Analysis

To obtain the required kinematic information, the video images were digitized to give displacement information for both the occupant and the vehicle. Benchmark points were

digitized frame by frame, producing displacement versus time curves which were corrected for projection distortion and depth effects. Data smoothing was performed by obtaining a least squares fit to the data. The software provided time rate of change values of the displacement data which was used to generate velocity and acceleration curves.

### Impact Test Results

For the Volkswagen Rabbit, limited damage to the vehicle was found for speeds under 15 km/h. Only a 5 mm movement of the bumper isolator mounting bolt within its adjustment slot was detected. Above 15 km/h, crush was found to begin developing in the rear fenders and trunk area floor panels. For impact velocities below this threshold, only cosmetic damage to the bumper itself was found. A slight curvature initially present in the bumper was removed as a result of the impacts, however, the amount of energy absorbed during this process was minimal compared to the total elastic energy. Some fluid leakage from the bumper isolators also occurred, but did not have any significant effect on the isolator performance during subsequent higher speed impacts. The full stroke length of the isolators appeared consistent at 5 cm. The 15 km/h damage threshold also supports the value presented in (8) where interpolation from barrier crush values indicated a damage threshold of 13.7 km/h. Figure 4 shows the impact pendulum, bumper and rear fender displacements versus time for a 14 km/h impact. The envelope between the bumper and vehicle (rear axle) displacements is representative of the energy absorbed by the bumper system.

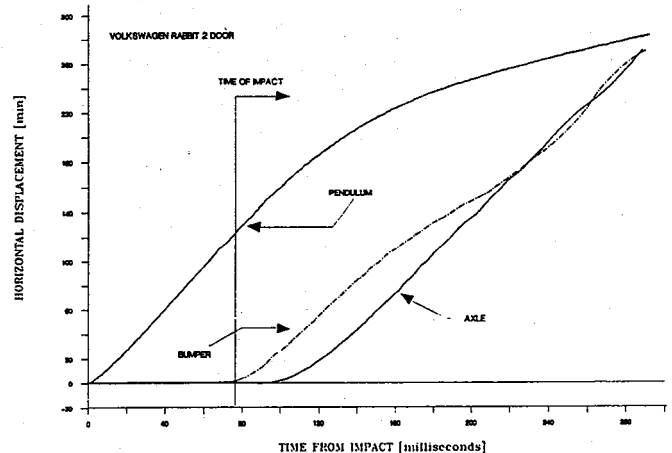


Figure 4. Displacement of bumper, vehicle and pendulum for a 14 km/h impact.

Whiplash or hyper-extension is generally related to the rearward deflection of the head relative to the body. Figure 5 shows the relative displacement and acceleration of the head's center of gravity, relative to the shoulder. The results shown were produced by a 9.2 km/h impact. As indicated, the maximum horizontal deflection and accelerations occur at approximately 120 ms. The rotational deflections of the head, figure 6, also reach maximum values at this time. The positive rotation and velocity in this diagram signify the

extension movement (head rotating rearwards). It is also evident from these figures that the head continues to move rearward while the shoulders rebound off the seat and move forward (shown at 108 ms on figures 5 and 6). This differential motion between the head and shoulders will result in increased neck loading especially as the inertial forces developed by the head grow larger at higher collision speeds. The presence of whiplash in cars with head restraints was recognized by States (10) where differential rebounds, from the seatback and head restraint, may produce increased rearward deflections of the head, relative to the shoulder. The shoulder was found to rebound before the head in all the tests analyzed in this study. To further investigate this effect, the acceleration and displacements (relative to the car) for the shoulder and head are plotted in figure 7 for cases with and without head restraint. These plots are the results of 8 km/h pendulum impacts. Figure 7 provides a seatback "stiffness" performance indicator. The curves already show that the shoulder moves through a smaller range of motion than the head. States' suggestion for a tuned seating system stiffness may require a similar "stiffness" approach to properly match the seatback and head restraint response.

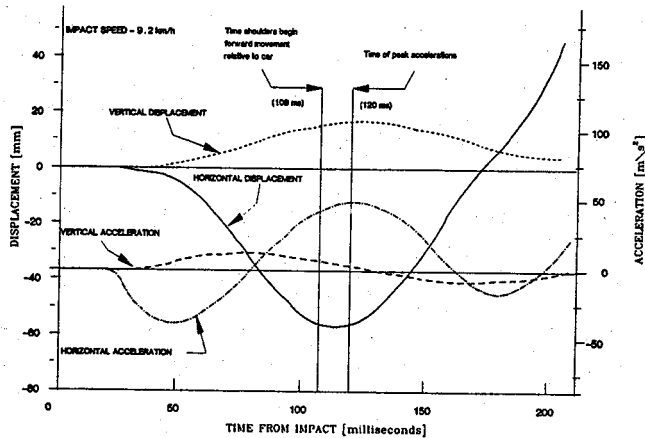


Figure 5. Relative motion of head to shoulder for a 9.2 km/h impact.

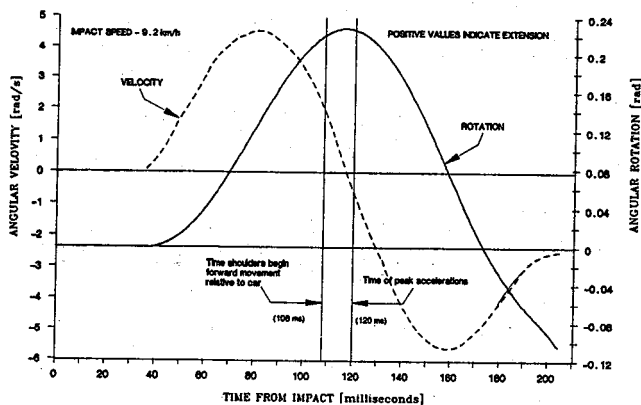


Figure 6. Rotational motion of the head (pitch).

From figure 7, one can see that the shoulders exhibit smaller deflections with higher accelerations in the presence of a head restraint than without a head restraint.

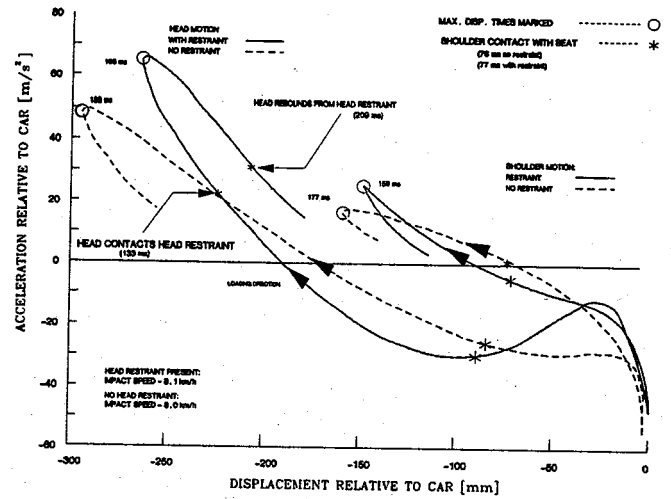


Figure 7. Effect of head restraint on occupant displacement and acceleration.

For the head, higher accelerations are encountered after rebound than before headrest contact (for the same displacement) because of the spring effect of the restraint. The converse is true without the headrest because there is no reloading of the neck from the seat structure. These trends also appear in the angular motion plots of the head depicted in figure 8 for the same tests. A higher peak angular velocity is experienced with smaller rearward rotations of the head with the use of a headrest (0.62 rad) compared with lower peak angular velocity and larger rearward rotations without the use of a headrest (0.7 rad). This resulted in an increase in positive differential acceleration of the head of approximately 25% with the introduction of an improperly adjusted head restraint. This suggests that injury severity may be a function of both displacement and dynamic loading.

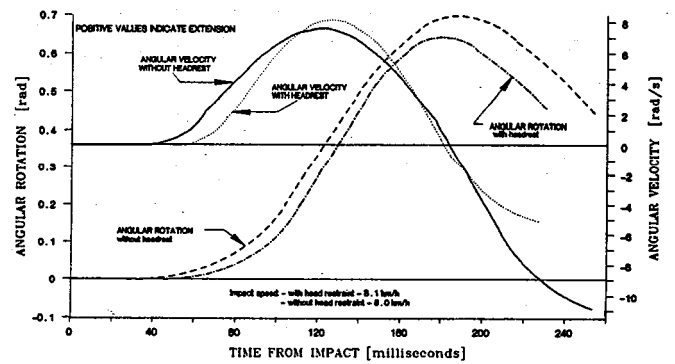


Figure 8. Effect of head restraint on angular motion of the head.

Figure 9 shows a set of vehicle and occupant response curves for an 18.4 km/h impact with a normally positioned dummy. The influence of initial posture can be observed from figure 10. This test was conducted with a 20° forward leaning head position at an 8.1 km/h impact speed. The initial rearward velocity of the head (ear) in the 18.4 km/h impact is less than that found at half the collision speed, with the occupant head forward. This is because the head has less time to rotate rearward before contacting the head restraint and indicates that small changes in head position can

markedly effect head velocities encountered during an impact. Figure 11 shows the relative displacement between the head and the shoulder for these two tests. The displacements are of the same magnitude, indicating that a forward leaning occupant could increase their chance of injury to levels found at much higher impact speeds. As noted on the diagrams, again the shoulder rebounds to a forward velocity relative to the car before the head. The corresponding occupant head deflections at 9.2 km/h (figure 5) show a normally placed dummy moves less than the inclined occupant shown in figure 11, even though the latter experienced a slightly lower impact speed. All the impacts recorded suggest that the elastic effects of the seat allow the vehicle to almost reach its maximum forward speed as the occupant's head reaches its maximum rearward speed. This increases the rearward displacements encountered which increases the propensity for a whiplash injury. Decreasing the rearward deflection of the head would reduce this velocity disparity and the attending neck loadings. It is felt that a human neck would allow a much greater relative displacement between the head and shoulders than shown with the Hybrid II. However, it is also felt that the same trends can be expected in a human subject for the same conditions albeit at different magnitudes.

The elastic behaviour of the seat is a critical factor as evidenced by the magnitude in which it catapults (in the order of 150% of the original impact velocity) the occupant forward after reaching a maximum rearward deflection. Reducing this forward acceleration would both lower the seat loading on the neck structure and reduce the likelihood of interior impacts. One method to control the seatback influence on the occupant would be to use the seat to absorb energy in some non-recoverable manner; through frictional or damping dissipators. Alternatively, a rigid seat and headrest coupled with a non-rebounding surface may be a means to limit the relative head-shoulder motion by forcing the head and shoulders to move as a unit. Deployable head restraints were researched by Melvin et al (12) and were found to be promising, but no additional work in this area has been found in the literature.

Noting the vehicle velocity curves (figures 9 and 10), there is a difference between the vehicle velocity attained and the original impact velocity. This reduction is 38% at the higher speed where structural crush takes place and 22% at the lower speed where a greater portion of the energy is elastic and is translated to the occupant compartment. At lower speeds, losses through the sliding wheels and compliance of the bumper and suspension systems become increasingly important as dissipation mechanisms during impact.

Visually noted from the video recording was the ramping displacement of the occupant up the seat back, even at the lower (8 km/h) speeds. Also detected from the video was the slack which developed between the seatbelt and the dummy's chest at the higher impact speeds. This identifies the inability of the retractor to spool up the free play of the seat belt. The use of a faster seatbelt retractor to control

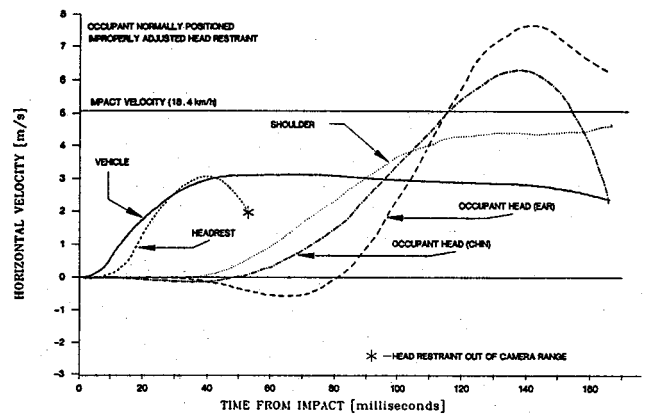


Figure 9. Vehicle and occupant velocity trends for an 18.4 km/h impact.

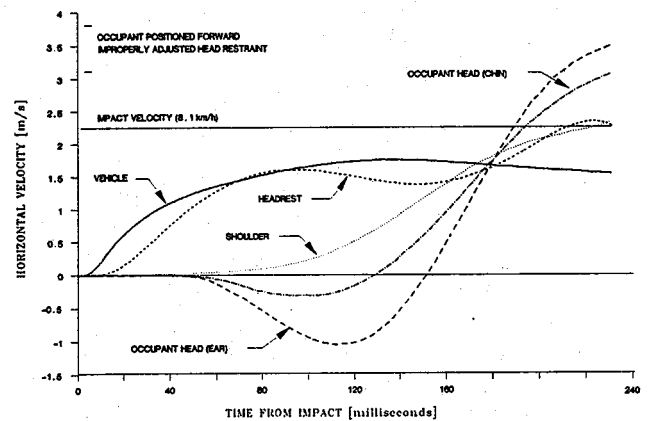


Figure 10. Vehicle and occupant velocity trends for 8.1 km/h impact.

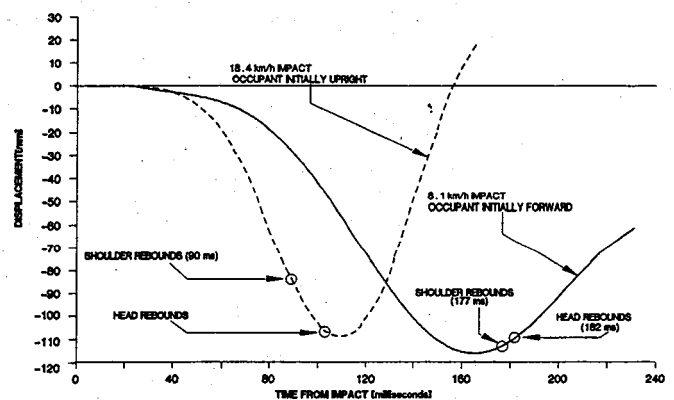


Figure 11. Effect of impact speed on relative displacement of occupant head to the shoulder.

shoulder rebound is another possible solution for reducing the whiplash injury potential. Should the belt spool in and lock in the rearmost position as the occupant moved back, the differential velocity between head and shoulder would be reduced.

## Conclusions of Preliminary Testing Phase

A brief description of the low speed, rear impact test program at UBC has been presented. The developed

pendulum impact facility performed reliably, providing controlled and repeatable impacts throughout the initial testing phase of this project. The video recording system employed in these tests provided useful information for understanding the collision kinematics of both the vehicle and occupant. Of interest to researchers is the lack of, or minimal, structural damage resulting from impact speeds below 15 km/h, and the increase of personal injury claims associated with these impacts. The absence of structural damage indicates that the bumper isolator system and retardation forces at the tire/ground interface are the predominant mechanisms of energy absorption by the vehicle during impact.

It was observed that the resulting deflection of the seatback with subsequent rebound, tends to pitch the occupant forward during impact with the shoulder displacement leading the head. This relative head to shoulder motion is the likely source of whiplash injury. The spring rate effects for the seat back and the head restraint have been presented in a quantifiable form in figure 7. Since the stiffer neck of the Hybrid II is more resistant to the loadings experienced in this testing, the limited neck rotations recorded with the Hybrid II suggest that higher rotations can be expected by humans in similar loading situations and that an increased potential for neck injury will occur.

The effect of an improperly positioned head restraint and initial occupant posture was shown to affect the maximum deflections of the head. The occupant experienced lower accelerations with increased deflections when the headrest is not present. The head also experienced larger deflections relative to the shoulder when the occupant's initial position was moved farther from the seat. This latter effect was seen to produce effects comparable to responses at twice the impact speeds with a normally seated occupant.

The present compliance standards in Canada for head restraint employ a "best case" scenario. The tests are conducted for a 95 percentile male with a fully upright adjusted head restraint (CMVSS 202). As mentioned before, the majority of drivers do not properly adjust the head rests. The presence of ramping in the 50 percentile occupant used in this research suggests that a large portion of the population will not receive all the protection that is provided to them. The standards set by the government are met by the manufacturer, but unfortunately the occupant is not responding by using the existing head restraints properly.

Future work includes more full scale vehicle impact testing planned for the summer of 1989. During these tests the vehicles will be instrumented (accelerometers and strain gauges) to provide accelerations and frame deformations (unavailable from video recording) needed to fully develop

and quantify elastic body stiffness. Of specific interest is an attempt to reduce occupant compartment loading through an improved energy absorbing bumper system.

## References

- (1) Mercer, G.W., "Whiplash Producing Casualty Traffic Accidents: Trends, Characteristics, Persons Involved, and Consequences, British Columbia, 1987", Counter Attack Program, Ministry of Labour and Consumer Services, British Columbia, Canada, 1988.
- (2) Mulligan, G.W.N., Thom, R., Dyck, K., Sobie, C., "Whiplash Injuries to the Neck: Acute Cervical Sprain, Hyperextension Injury; A Continuing Enigma for Clinicians and a Frequent Dilemma for Litigants", Canadian Association of Road Safety Professionals; Blainville, P.Q., Canada, June, 1988.
- (3) Mertz, H.J., "Neck Injury", SAE Conference Proceedings, P49, Human Tolerances to Biomechanics, Impact and its Application to Automotive Design, 1973.
- (4) Miyasaki, G.W., Navin, F., Macnabb, M., "A Crash Test Facility to Determine Automobile Crush Coefficients", SAE Paper 880224, 1988.
- (5) "Motor Vehicle Safety Test Methods", Transport Canada, TP 3666-E.
- (6) "On Highway Vehicles and Off Highway Machinery", SAE Handbook Volume 4, 1984.
- (7) Navin, F., Macnabb, M., Miyasaki, G.W., "Elastic Properties of Selected Vehicles", SAE Paper 880223, 1988.
- (8) Foster, J.F., Kortge, J.O., Wolanin, M.J., "Hybrid III—A Biomechanically Based Crash Dummy", SAE Paper 770938, Proceedings of Twenty-First Stapp Car Crash Conference, October, 1977, New Orleans, USA.
- (9) Mertz, H.J., Patrick, L.M., "Strength and Response of the Human Neck", SAE Paper 710855, Proceedings of Fifteenth Stapp Car Crash Conference, November, 1977, Coronado, Calif., USA.
- (10) States, J.D., Balcerak, J.C., Williams, J.S., Morris, A., Babcock, W., Polvino, R., Riger, P., Dawley, R.E., "Injury Frequency and Head Restraint Effectiveness in Rear-End Impact Accidents", SAE Paper 720967, Proceedings of Sixteenth Stapp Car Crash Conference, November, 1972, Detroit, Mich., USA.
- (11) MacKay, M., "Occupant Protection and Vehicle Design", Proceedings of Crash Performance Standards and the Biomechanics of Impact: What are the Relationships, AAAM, IRCOBI, February, 1989, San Antonio, Tex., USA.
- (12) Melvin, J.W., McElhaney, J.H., Roberts, V.L., Portnoy, H.D., "Deployable Head Restraints—A Feasibility Study", SAE Paper 710853, Proceedings of Fifteenth Stapp Car Crash Conference, November, 1971, Coronado, Calif., USA.

## Aknowledgements

This project would not have been possible without assistance from the following organizations:

National Science and Engineering Research Council;

Transport Canada, Road Safety Directorate (Chris Wilson, Director General);

ICBC Material Damage Division (John Gane, Manager)

UBC Accident Research Team (F.P.D. Navin and G.R. Brown, Coordinators)

## Effect of Internal Fittings on Injury Value of Unrestrained Occupant

Written Only Paper

Koichi Oho, Isao Sugamori and Kazuhisa Yamasaki

### Abstract

An overall improvement in the crash characteristics of vehicle body, occupant restraint devices (seat belt and air bag etc.) and energy absorption characteristics of the secondary impact objects (steering and instrument panels etc.) is essential for minimizing injuries to occupants when a vehicle gets involved in an accident. It is needless to say that striking proper balance among these is the main crux in designing. For this, it is necessary to analyze the behavior of occupants at the time of accident and the state of injuries they sustain so that the contribution of each factor to the injuries can be pinpointed.

This paper discusses the investigations carried out by the authors on the effects of crash characteristics of the vehicle body, position of the windshield glass and instrument panel and the rigidity of instrument panel and cross beam etc. on the injury values of the dummy, after analyzing the behavior of unrestrained dummy in the passenger seat during frontal collision at 30 MPH and 15 MPH by carrying out simulation with MVMA-2D program and by sled test.

This study enabled the authors to gain some significant information on the effects of internal fittings on the injury values of the dummy. Sled test carried out with vehicle modified on the basis of these data confirmed the validity of the findings.

### Method of Investigation

#### Simulation calculation model

The program MVMA-2D developed at Michigan University for analyzing the behavior of occupant was used in calculation. As shown in figure 1, a two dimensional model with 9 concentrated masses and 10 links was used for the dummy. Elliptical bodies were provided to each link to represent the body outline and to produce contact reaction force.

#### Sled test

The behavior of unrestrained dummy was studied by 30 MPH (48 km/h) and 15 MPH (24 km/h) sled tests. Figure 2 shows the vehicle acceleration curves of the sled tests. A Hybrid III type dummy was used. The sitting posture of the dummy was decided on the basis of the method specified in

FMVSS 208. The seat position was set almost at the center. As the secondary impact objects like the instrument panel etc., get pushed towards the rear due to backward movement of the engine and the dashboard during barrier test, these were fixed after making proper allowance for the amount of displacement toward rear.

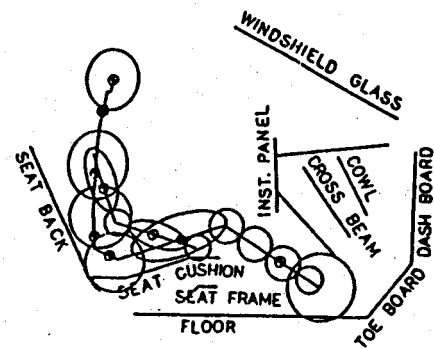


Figure 1. Calculation model.

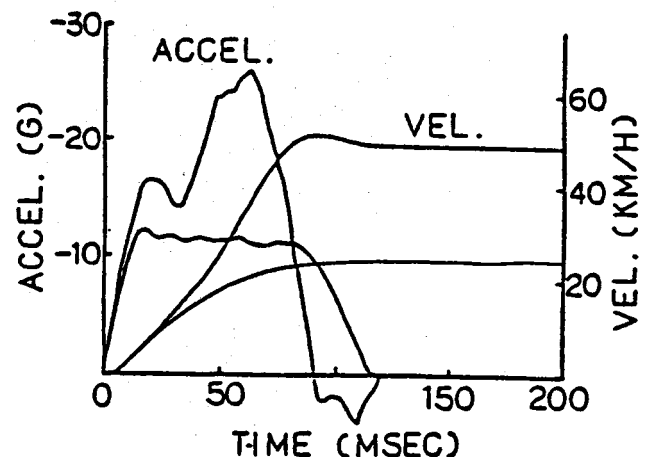


Figure 2. Acceleration curves for sled test.

### Behavior of Unrestrained Occupant and Verification of Accuracy of Calculation Model

Simulation model was prepared after studying the behavior of unrestrained occupant by sled test. For verifying the accuracy of calculation model, it is necessary to investigate the degree of accuracy by which the behavior of the dummy and the acceleration curves for each section of the dummy determined in the calculation model correlate

(4) Penoyre, S., Transport and Road Research Laboratory, A Crashworthiness Rating System for Cars, 9th ESV-Conference Kyoto.

(5) Miller, Patrick, Rydznski, Analysis of Frontal Impact Test Data—New Car Assessment Program—DOT-HS-395, February 1984.

(6) ADAC, ADAC-Motorwelt Heft 11/88, "Der große Crash Test."

(7) Appel, H., Kramer, F., Glatz, W., Lutter, G., "Quantifizierung der Passiven Sicherheit von Personenkraftwagen," Forschungsprojekt FP 8517/2 im Auftrage der Bundesanstalt für Strassenwesen, Abschlussbericht 1989.

(8) Otte, D., Erhebungen am Unfallort MHH/TUB, Projekt FP 7263/7506/7813-4/8200-1 BAST.

(9) Kramer, F., Insassen-Crashmechanik-Rechenmodell für Frontalkollisionen Programmbeschreibung, Verifikation und Validierung. Forschungsbericht 324/88 TU-Berlin 1988.

(10) Hofmann, J., Rechnerische Untersuchung zur optimalen Seitenstruktur von Personenkraftwagen, Dissertation 1980 TU-Berlin.

(11) Kramer, F., Schutzkriterien für den Fahrzeug-Insassen im Falle sagittaler Belastung TU Berlin, 1989.

## Low Speed Rear Impacts and the Elastic Properties of Automobiles

**D.P. Romilly, R.W. Thomson,**  
Department of Mechanical Engineering  
**F.P.D. Navin, M.J. Macnabb,**  
Department of Civil Engineering,  
University of British Columbia

### Abstract

Many low speed, rear impact accidents produce occupant neck injuries which have become a concern to the insurance industry and the medical profession. The authors, with the cooperation of the Insurance Corporation of British Columbia (ICBC), conducted approximately 30 low speed pendulum tests to measure the elastic and plastic properties of selected vehicles in rear end collisions. Displacement/time traces were generated from high speed video recordings of selected points on the vehicle and an anthropometric dummy occupant. The authors noted that a high impact speed was required to produce perceptible damage to the test vehicle. This speed caused violent movement to the test dummy neck. Discussion of these results with insurers indicates there is a conflict between bumper stiffness (required for the Canadian 8 km/h bumper standard) desired by the material damage section of the insurance industry, and the need for vehicle compliance for occupant protection. Investigation into the vehicle's elastic and plastic properties will also aid in the design of Civil Engineering roadside structures and provide a better understanding of injury causation at low impact speeds.

### Introduction

Sprains to the neck and back occur in more than half of all casualty producing accidents. Associated insurance injury claims are estimated at over \$100M (Cdn.) for the province of British Columbia, Canada annually. A recent provincial publication indicates that whiplash reports in B.C. increased approximately 30% from 1986 to 1987 (1).\* The report also noted that damage to these cars was typically less than damage occurring in other casualty producing accidents.

A litigious syndrome does not appear to be the sole reason for the increasing numbers of injury claims. Whiplash or neck hyper-extension is, in many cases, symptomatic and subjective in its diagnosis as existing evaluation techniques are unable to identify soft tissue injuries (2,3). Assuming that genuine injuries are reported for accidents where vehicles show little or no damage, the authors have initiated an investigation into the dynamic response of the vehicle and its occupant to low speed impacts.

The mechanics of a high speed collision are relatively well documented. The vehicle structure deforms, converting the system's kinetic energy into sound, thermal and strain energies. The rate of deformation is a result of the vehicle's stiffness characteristics while the amount of recoverable deformation is a function of its elastic properties. At high impact speeds, very little elastic recovery occurs and the vehicle generally behaves as a plastic body. At low impact speeds, however, plastic behaviour may be absent allowing most of the total impact energy to be recovered in elastic rebound. For the occupant, the best ride down profile occurs when the vehicle behaves as a plastic body with large deformations to reduce the overall acceleration. This creates a major dilemma for the manufacturer, occupant and insurer. Each would like the vehicle to provide the maximum protection for the occupant with the minimum material damage to the vehicle during a collision. As the vehicle becomes stiffer, the vehicle damage costs are reduced as less permanent deformation takes place. However, the occupant experiences a more violent ride down which increases the potential for injury. This implies that vehicles which do not sustain permanent damage in low speed impacts produce correspondingly higher dynamic loadings on their occupants than those which deform plastically under the same or possibly more severe impact conditions. It is this premise which is under investigation in this research project.

Much of the existing literature has addressed vehicle and occupant dynamics in the moderate to high speed range (greater than 50 km/h). This is due to many countries setting

\*Numbers in parentheses designate references at end of paper.

vehicle performance standards based on occupant survival of 50 km/h barrier impacts. However, it should be noted that the majority of accidents occur below this speed. Injury costs from these low speed accidents are not insignificant, especially in neck injuries from rear impacts.

Based on the experience derived from the development of an earlier low speed crash barrier (4), the researchers initiated a project to study both vehicle and occupant response using a more accurately controlled, and repeatable, low speed impact facility. A pendulum style impactor was developed permitting preselected impact conditions in a controlled test environment. This allowed a systematic study to determine the vehicle and occupant responses as functions of the impact parameters (i.e. mass, velocity, impact energy, impact geometry, etc.).

This paper presents the first phase of work completed with the new impact facility. Impact tests were conducted to investigate the dynamic response of a vehicle and driver to known rear-end impacts. The results of these tests are presented and discussed with respect to quantifying the relative motion between the vehicle and occupant for low impact speeds and the crash performance of the vehicle.

## Low Speed Impact Test Facility

### Impact pendulum design

In order to provide controlled impacts in the low speed range, the pendulum style impact facility shown in figure 1 was designed and constructed. The facility is capable of impact speeds up to 20 km/h with a swung mass selectively variable from 300 to 2000 kg. It has been designed to be recognized as a valid information source based on the Canadian Motor Vehicle Safety Standards (CMVSS 215) (5) and the Society of Automotive Engineers (SAE J980a) (6) guidelines. The pendulum impactor faces prescribed in these guidelines were modified to provide a surface profile more representative of a vehicle front end. This facility is located at the ICBC Research and Training Center in Burnaby, B.C. and is portable, having a relatively quickly assembly/disassembly time. Manual set-up and operation

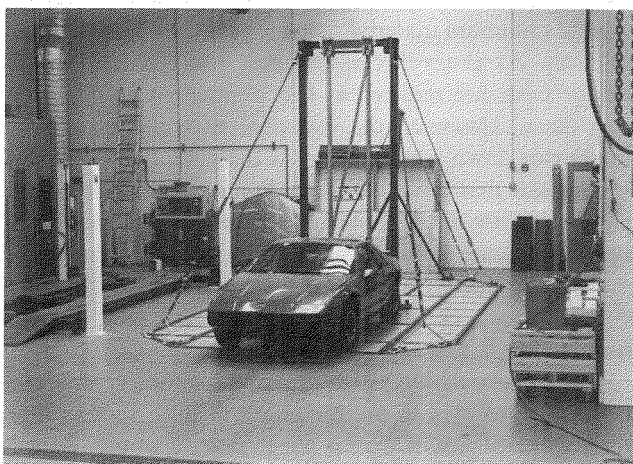


Figure 1. Low speed impact test facility.

were used to maintain simplicity which is reflected by the low material cost of \$1300 Cdn. and the relatively short construction time of six man-weeks.

### Instrumentation

The occupant, vehicle, and pendulum motions were recorded using a Kodak Ekta-Pro 1000 high speed video system with a maximum sampling rate of 1000 full frames/second. Video images of the occupant and vehicle (benchmarked with targets as in figure 2) were recorded throughout the test and post-processed to yield displacement histories for subsequent analysis and modelling. This proved to be a simple, flexible, data acquisition system which also provided qualitative information beyond the recording capabilities of a sensor based system.

The pendulum velocity was measured by a speed trap consisting of three equidistant mechanical switches mounted such that the last switch was tripped by the pendulum just prior to impact.

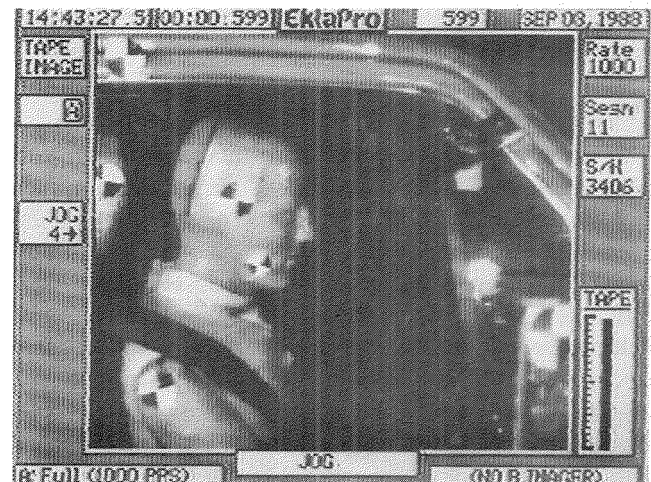


Figure 2. High speed video image of occupant and car.

### Test vehicles and crash dummy

The vehicles tested in this project were two and four-door Volkswagen Rabbit hatchbacks. These models were chosen because they are representative of compact cars currently on the road and have been extensively tested by UBC in previous research studies (7). All of the test vehicles were insurance "write-offs" supplied through ICBC. Each vehicle was free of damage in the rear portion and free rolling. This ensured that the test vehicles were representative of functional cars. Due to accessibility, a Hybrid II anthropometric dummy was used to represent the occupant and was made available to us courtesy of the Transport Canada Test Centre in Blainville, P.Q. A comparison, provided by Foster et al (8) of the Hybrid II neck performance, relative to the criteria put forth by Mertz and Patrick (9) is shown in figure 3. The results suggest the Hybrid II has limited use in whiplash testing because of an overly stiff neck arrangement. With this performance noted, it was expected that the dummy would yield conservative head-neck deflections. Interpreta-

tions of the results is based on the relative neck response to different test conditions and avoids direct inference of possible human injury. Although this may be unsatisfactory, it is necessary due to the lack of available human neck response data.

### Testing procedures

Prior to each test the vehicle mass was determined and matched by the pendulum. Test vehicle specifications (model, year, seatback type, occupant safety system, etc.) and information relating to any pre-existing damage was logged. The car was positioned in line with the pendulum, the parking brake engaged and the transmission placed in gear. The crash dummy was then positioned in the seat and the distance between the mounted targets (as in figure 2) were recorded. Triggering of the camera preceded the release of the pendulum by 2.5 seconds to provide the necessary lead time for initializing the recording process.

After each test, a general vehicle inspection was performed by the researchers and the Material Damage staff at ICBC to locate any damage resulting from the impact. The dummy was also examined for final position, signs of interior contact, etc.

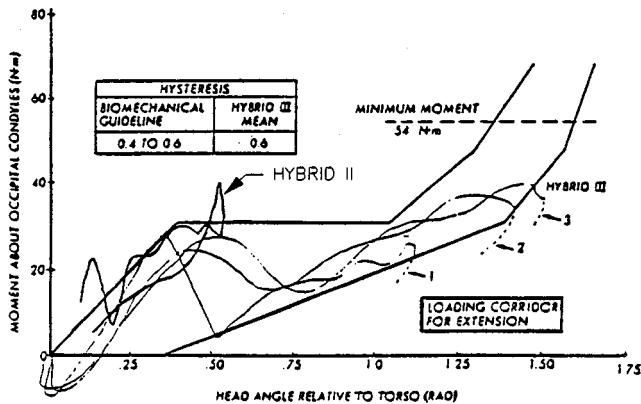


Figure 3. Performance of Hybrid II neck against Mertz-Patrick criteria (from reference 8).

To utilize the vehicles in the most effective manner, six were impacted three times each, at increasing speeds from 8 to 20 km/h (it should be noted that the first two lower speed impacts did not produce any detectable residual deformation). Two additional vehicles were tested to study the effect of variation in occupant posture (head inclination angle) and the presence of a head restraint system on occupant response at impact speeds of 8 km/h.

All of the tests which employed head restraints had the restraint adjusted to the lowest position. This reflected trends reported by States et al (10) and MacKay (11) where adjustable head restraints were found to be in the lowest position in 70–90% of the vehicles surveyed.

### Kinematic Data Analysis

To obtain the required kinematic information, the video images were digitized to give displacement information for both the occupant and the vehicle. Benchmark points were

digitized frame by frame, producing displacement versus time curves which were corrected for projection distortion and depth effects. Data smoothing was performed by obtaining a least squares fit to the data. The software provided time rate of change values of the displacement data which was used to generate velocity and acceleration curves.

### Impact Test Results

For the Volkswagen Rabbit, limited damage to the vehicle was found for speeds under 15 km/h. Only a 5 mm movement of the bumper isolator mounting bolt within its adjustment slot was detected. Above 15 km/h, crush was found to begin developing in the rear fenders and trunk area floor panels. For impact velocities below this threshold, only cosmetic damage to the bumper itself was found. A slight curvature initially present in the bumper was removed as a result of the impacts, however, the amount of energy absorbed during this process was minimal compared to the total elastic energy. Some fluid leakage from the bumper isolators also occurred, but did not have any significant effect on the isolator performance during subsequent higher speed impacts. The full stroke length of the isolators appeared consistent at 5 cm. The 15 km/h damage threshold also supports the value presented in (8) where interpolation from barrier crush values indicated a damage threshold of 13.7 km/h. Figure 4 shows the impact pendulum, bumper and rear fender displacements versus time for a 14 km/h impact. The envelope between the bumper and vehicle (rear axle) displacements is representative of the energy absorbed by the bumper system.

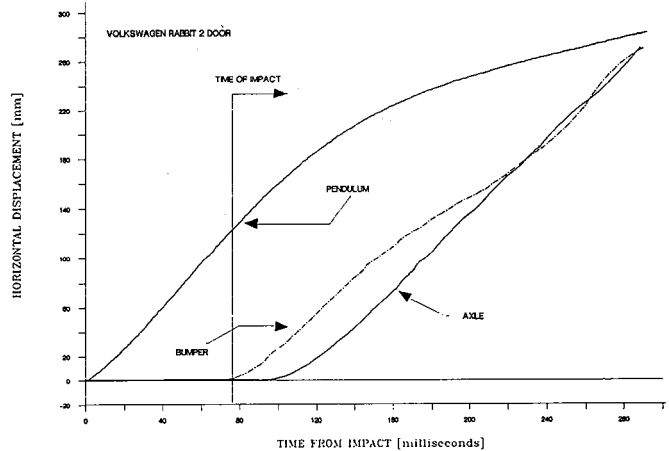


Figure 4. Displacement of bumper, vehicle and pendulum for a 14 km/h impact.

Whiplash or hyper-extension is generally related to the rearward deflection of the head relative to the body. Figure 5 shows the relative displacement and acceleration of the head's center of gravity, relative to the shoulder. The results shown were produced by a 9.2 km/h impact. As indicated, the maximum horizontal deflection and accelerations occur at approximately 120 ms. The rotational deflections of the head, figure 6, also reach maximum values at this time. The positive rotation and velocity in this diagram signify the

extension movement (head rotating rearwards). It is also evident from these figures that the head continues to move rearward while the shoulders rebound off the seat and move forward (shown at 108 ms on figures 5 and 6). This differential motion between the head and shoulders will result in increased neck loading especially as the inertial forces developed by the head grow larger at higher collision speeds. The presence of whiplash in cars with head restraints was recognized by States (10) where differential rebounds, from the seatback and head restraint, may produce increased rearward deflections of the head, relative to the shoulder. The shoulder was found to rebound before the head in all the tests analyzed in this study. To further investigate this effect, the acceleration and displacements (relative to the car) for the shoulder and head are plotted in figure 7 for cases with and without head restraint. These plots are the results of 8 km/h pendulum impacts. Figure 7 provides a seatback "stiffness" performance indicator. The curves already show that the shoulder moves through a smaller range of motion than the head. States' suggestion for a tuned seating system stiffness may require a similar "stiffness" approach to properly match the seatback and head restraint response.

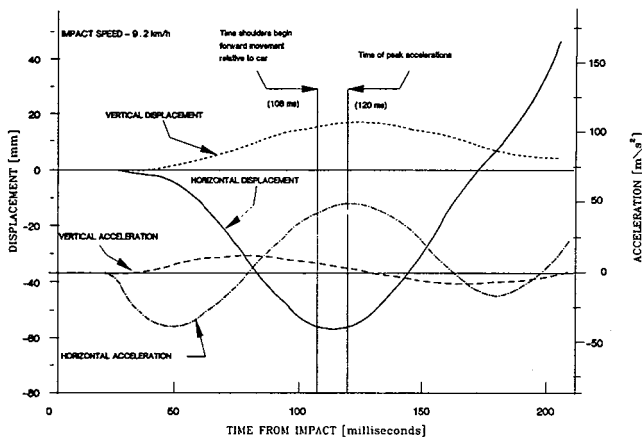


Figure 5. Relative motion of head to shoulder for a 9.2 km/h impact.

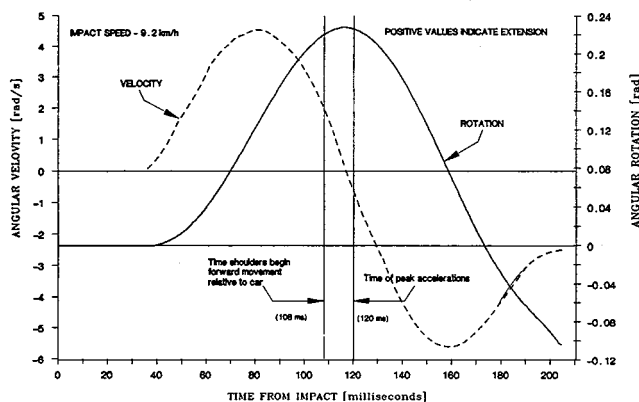


Figure 6. Rotational motion of the head (pitch).

From figure 7, one can see that the shoulders exhibit smaller deflections with higher accelerations in the presence of a head restraint than without a head restraint.

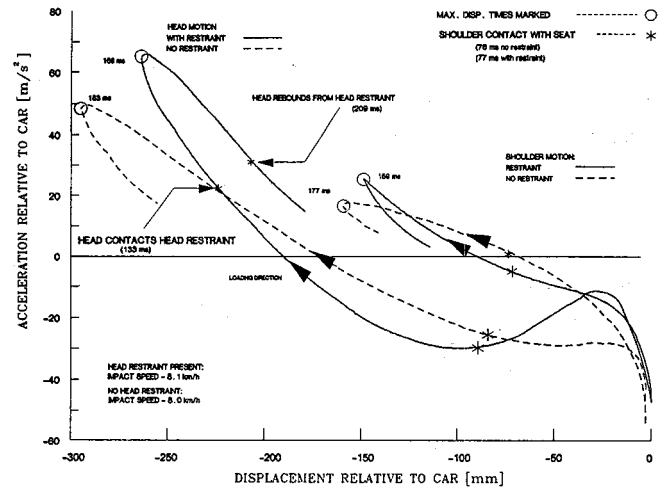


Figure 7. Effect of head restraint on occupant displacement and acceleration.

For the head, higher accelerations are encountered after rebound than before headrest contact (for the same displacement) because of the spring effect of the restraint. The converse is true without the headrest because there is no reloading of the neck from the seat structure. These trends also appear in the angular motion plots of the head depicted in figure 8 for the same tests. A higher peak angular velocity is experienced with smaller rearward rotations of the head with the use of a headrest (0.62 rad) compared with lower peak angular velocity and larger rearward rotations without the use of a headrest (0.7 rad). This resulted in an increase in positive differential acceleration of the head of approximately 25% with the introduction of an improperly adjusted head restraint. This suggests that injury severity may be a function of both displacement and dynamic loading.

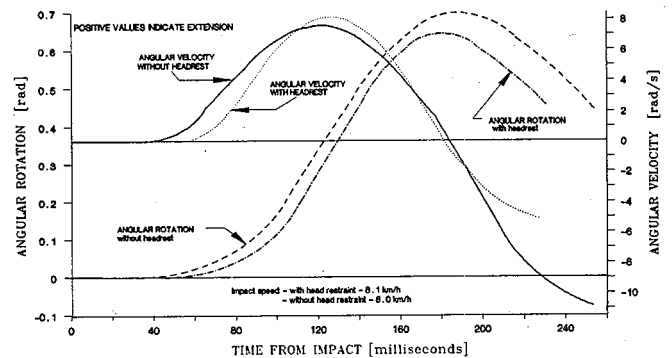


Figure 8. Effect of head restraint on angular motion of the head.

Figure 9 shows a set of vehicle and occupant response curves for an 18.4 km/h impact with a normally positioned dummy. The influence of initial posture can be observed from figure 10. This test was conducted with a 20° forward leaning head position at an 8.1 km/h impact speed. The initial rearward velocity of the head (ear) in the 18.4 km/h impact is less than that found at half the collision speed, with the occupant head forward. This is because the head has less time to rotate rearward before contacting the head restraint and indicates that small changes in head position can

markedly effect head velocities encountered during an impact. Figure 11 shows the relative displacement between the head and the shoulder for these two tests. The displacements are of the same magnitude, indicating that a forward leaning occupant could increase their chance of injury to levels found at much higher impact speeds. As noted on the diagrams, again the shoulder rebounds to a forward velocity relative to the car before the head. The corresponding occupant head deflections at 9.2 km/h (figure 5) show a normally placed dummy moves less than the inclined occupant shown in figure 11, even though the latter experienced a slightly lower impact speed. All the impacts recorded suggest that the elastic effects of the seat allow the vehicle to almost reach its maximum forward speed as the occupant's head reaches its maximum rearward speed. This increases the rearward displacements encountered which increases the propensity for a whiplash injury. Decreasing the rearward deflection of the head would reduce this velocity disparity and the attending neck loadings. It is felt that a human neck would allow a much greater relative displacement between the head and shoulders than shown with the Hybrid II. However, it is also felt that the same trends can be expected in a human subject for the same conditions albeit at different magnitudes.

The elastic behaviour of the seat is a critical factor as evidenced by the magnitude in which it catapults (in the order of 150% of the original impact velocity) the occupant forward after reaching a maximum rearward deflection. Reducing this forward acceleration would both lower the seat loading on the neck structure and reduce the likelihood of interior impacts. One method to control the seatback influence on the occupant would be to use the seat to absorb energy in some non-recoverable manner; through frictional or damping dissipators. Alternatively, a rigid seat and headrest coupled with a non-rebounding surface may be a means to limit the relative head-shoulder motion by forcing the head and shoulders to move as a unit. Deployable head restraints were researched by Melvin et al (12) and were found to be promising, but no additional work in this area has been found in the literature.

Noting the vehicle velocity curves (figures 9 and 10), there is a difference between the vehicle velocity attained and the original impact velocity. This reduction is 38% at the higher speed where structural crush takes place and 22% at the lower speed where a greater portion of the energy is elastic and is translated to the occupant compartment. At lower speeds, losses through the sliding wheels and compliance of the bumper and suspension systems become increasingly important as dissipation mechanisms during impact.

Visually noted from the video recording was the ramping displacement of the occupant up the seat back, even at the lower (8 km/h) speeds. Also detected from the video was the slack which developed between the seatbelt and the dummy's chest at the higher impact speeds. This identifies the inability of the retractor to spool up the free play of the seat belt. The use of a faster seatbelt retractor to control

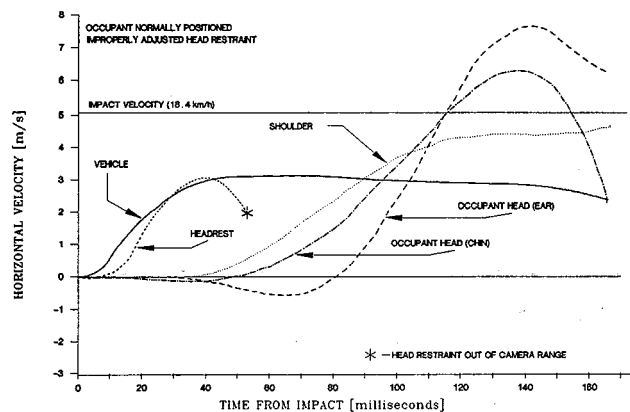


Figure 9. Vehicle and occupant velocity trends for an 18.4 km/h impact.

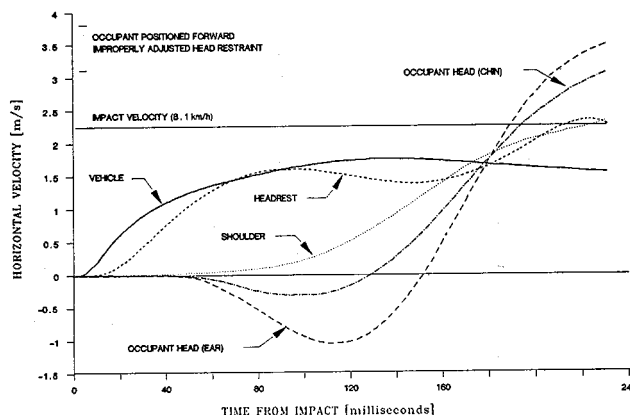


Figure 10. Vehicle and occupant velocity trends for 8.1 km/h impact.

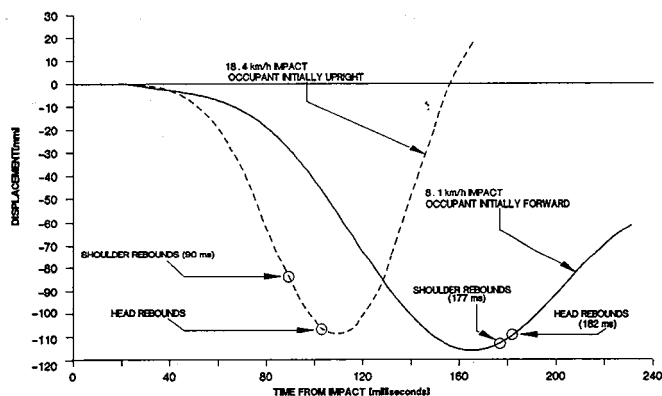


Figure 11. Effect of impact speed on relative displacement of occupant head to the shoulder.

shoulder rebound is another possible solution for reducing the whiplash injury potential. Should the belt spool in and lock in the rearmost position as the occupant moved back, the differential velocity between head and shoulder would be reduced.

## Conclusions of Preliminary Testing Phase

A brief description of the low speed, rear impact test program at UBC has been presented. The developed

pendulum impact facility performed reliably, providing controlled and repeatable impacts throughout the initial testing phase of this project. The video recording system employed in these tests provided useful information for understanding the collision kinematics of both the vehicle and occupant. Of interest to researchers is the lack of, or minimal, structural damage resulting from impact speeds below 15 km/h, and the increase of personal injury claims associated with these impacts. The absence of structural damage indicates that the bumper isolator system and retardation forces at the tire/ground interface are the predominant mechanisms of energy absorption by the vehicle during impact.

It was observed that the resulting deflection of the seatback with subsequent rebound, tends to pitch the occupant forward during impact with the shoulder displacement leading the head. This relative head to shoulder motion is the likely source of whiplash injury. The spring rate effects for the seat back and the head restraint have been presented in a quantifiable form in figure 7. Since the stiffer neck of the Hybrid II is more resistant to the loadings experienced in this testing, the limited neck rotations recorded with the Hybrid II suggest that higher rotations can be expected by humans in similar loading situations and that an increased potential for neck injury will occur.

The effect of an improperly positioned head restraint and initial occupant posture was shown to affect the maximum deflections of the head. The occupant experienced lower accelerations with increased deflections when the headrest is not present. The head also experienced larger deflections relative to the shoulder when the occupant's initial position was moved farther from the seat. This latter effect was seen to produce effects comparable to responses at twice the impact speeds with a normally seated occupant.

The present compliance standards in Canada for head restraint employ a "best case" scenario. The tests are conducted for a 95 percentile male with a fully upright adjusted head restraint (CMVSS 202). As mentioned before, the majority of drivers do not properly adjust the head rests. The presence of ramping in the 50 percentile occupant used in this research suggests that a large portion of the population will not receive all the protection that is provided to them. The standards set by the government are met by the manufacturer, but unfortunately the occupant is not responding by using the existing head restraints properly.

Future work includes more full scale vehicle impact testing planned for the summer of 1989. During these tests the vehicles will be instrumented (accelerometers and strain gauges) to provide accelerations and frame deformations (unavailable from video recording) needed to fully develop

and quantify elastic body stiffness. Of specific interest is an attempt to reduce occupant compartment loading through an improved energy absorbing bumper system.

## References

- (1) Mercer, G.W., "Whiplash Producing Casualty Traffic Accidents: Trends, Characteristics, Persons Involved, and Consequences, British Columbia, 1987", Counter Attack Program, Ministry of Labour and Consumer Services, British Columbia, Canada, 1988.
- (2) Mulligan, G.W.N., Thom, R., Dyck, K., Sobie, C., "Whiplash Injuries to the Neck: Acute Cervical Sprain, Hyperextension Injury; A Continuing Enigma for Clinicians and a Frequent Dilemma for Litigants", Canadian Association of Road Safety Professionals; Blainville, P.Q., Canada, June, 1988.
- (3) Mertz, H.J., "Neck Injury", SAE Conference Proceedings, P49, Human Tolerances to Biomechanics, Impact and its Application to Automotive Design, 1973.
- (4) Miyasaki, G.W., Navin, F., Macnabb, M., "A Crash Test Facility to Determine Automobile Crush Coefficients", SAE Paper 880224, 1988.
- (5) "Motor Vehicle Safety Test Methods", Transport Canada, TP 3666-E.
- (6) "On Highway Vehicles and Off Highway Machinery", SAE Handbook Volume 4, 1984.
- (7) Navin, F., Macnabb, M., Miyasaki, G.W., "Elastic Properties of Selected Vehicles", SAE Paper 880223, 1988.
- (8) Foster, J.F., Kortge, J.O., Wolanin, M.J., "Hybrid III—A Biomechanically Based Crash Dummy", SAE Paper 770938, Proceedings of Twenty-First Stapp Car Crash Conference, October, 1977, New Orleans, USA.
- (9) Mertz, H.J., Patrick, L.M., "Strength and Response of the Human Neck", SAE Paper 710855, Proceedings of Fifteenth Stapp Car Crash Conference, November, 1977, Coronado, Calif., USA.
- (10) States, J.D., Balcerak, J.C., Williams, J.S., Morris, A., Babcock, W., Polvino, R., Riger, P., Dawley, R.E., "Injury Frequency and Head Restraint Effectiveness in Rear-End Impact Accidents", SAE Paper 720967, Proceedings of Sixteenth Stapp Car Crash Conference, November, 1972, Detroit, Mich., USA.
- (11) MacKay, M., "Occupant Protection and Vehicle Design", Proceedings of Crash Performance Standards and the Biomechanics of Impact: What are the Relationships, AAAM, IRCOBI, February, 1989, San Antonio, Tex., USA.
- (12) Melvin, J.W., McElhaney, J.H., Roberts, V.L., Portnoy, H.D., "Deployable Head Restraints—A Feasibility Study", SAE Paper 710853, Proceedings of Fifteenth Stapp Car Crash Conference, November, 1971, Coronado, Calif., USA.

## Acknowledgements

This project would not have been possible without assistance from the following organizations:

National Science and Engineering Research Council;

Transport Canada, Road Safety Directorate (Chris Wilson, Director General);

ICBC Material Damage Division (John Gane, Manager)

UBC Accident Research Team (F.P.D. Navin and G.R. Brown, Coordinators)

## Effect of Internal Fittings on Injury Value of Unrestrained Occupant

Written Only Paper

Koichi Oho, Isao Sugamori and Kazuhisa Yamasaki

### Abstract

An overall improvement in the crash characteristics of vehicle body, occupant restraint devices (seat belt and air bag etc.) and energy absorption characteristics of the secondary impact objects (steering and instrument panels etc.) is essential for minimizing injuries to occupants when a vehicle gets involved in an accident. It is needless to say that striking proper balance among these is the main crux in designing. For this, it is necessary to analyze the behavior of occupants at the time of accident and the state of injuries they sustain so that the contribution of each factor to the injuries can be pinpointed.

This paper discusses the investigations carried out by the authors on the effects of crash characteristics of the vehicle body, position of the windshield glass and instrument panel and the rigidity of instrument panel and cross beam etc. on the injury values of the dummy, after analyzing the behavior of unrestrained dummy in the passenger seat during frontal collision at 30 MPH and 15 MPH by carrying out simulation with MVMA-2D program and by sled test.

This study enabled the authors to gain some significant information on the effects of internal fittings on the injury values of the dummy. Sled test carried out with vehicle modified on the basis of these data confirmed the validity of the findings.

### Method of Investigation

#### Simulation calculation model

The program MVMA-2D developed at Michigan University for analyzing the behavior of occupant was used in calculation. As shown in figure 1, a two dimensional model with 9 concentrated masses and 10 links was used for the dummy. Elliptical bodies were provided to each link to represent the body outline and to produce contact reaction force.

#### Sled test

The behavior of unrestrained dummy was studied by 30 MPH (48 km/h) and 15 MPH (24 km/h) sled tests. Figure 2 shows the vehicle acceleration curves of the sled tests. A Hybrid III type dummy was used. The sitting posture of the dummy was decided on the basis of the method specified in

FMVSS 208. The seat position was set almost at the center. As the secondary impact objects like the instrument panel etc., get pushed towards the rear due to backward movement of the engine and the dashboard during barrier test, these were fixed after making proper allowance for the amount of displacement toward rear.

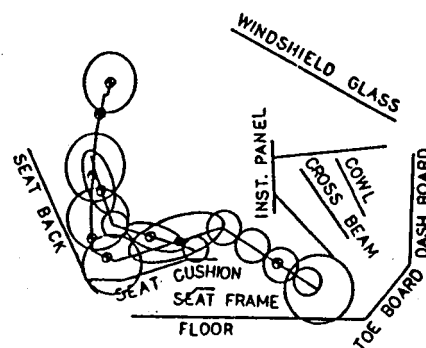


Figure 1. Calculation model.

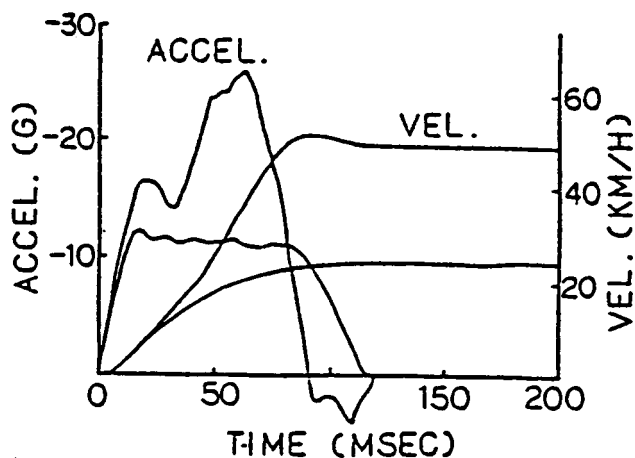


Figure 2. Acceleration curves for sled test.

### Behavior of Unrestrained Occupant and Verification of Accuracy of Calculation Model

Simulation model was prepared after studying the behavior of unrestrained occupant by sled test. For verifying the accuracy of calculation model, it is necessary to investigate the degree of accuracy by which the behavior of the dummy and the acceleration curves for each section of the dummy determined in the calculation model correlate

with the test results. The behavior of the dummy and the acceleration curves found during sled test as well as the results of accuracy verification carried out with the base model will be described below.

(1) Behavior of Dummy:

Figure 3 shows the calculation results and the test results of the initial posture of the dummy (t = 0 sec) and its posture at the time of collision (t = 110 msec). A comparison of the amounts of displacement of the head position and of the hip point has been shown in figure 4. These results show that the head of the dummy in the passenger seat dashes against the glass, the chest against the instrument panel and the knee against the lower part of the instrument panel. At 15 MPH, the head strikes against the upper part of the instrument panel. From these findings, the authors concluded that as far as the behavior of the dummy is concerned, the calculation model correlated very well with the test results.

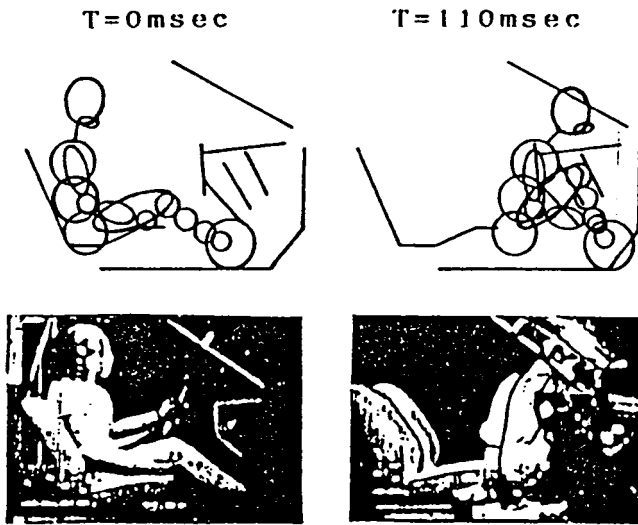


Figure 3. Dummy behavior (for 30 MPH).

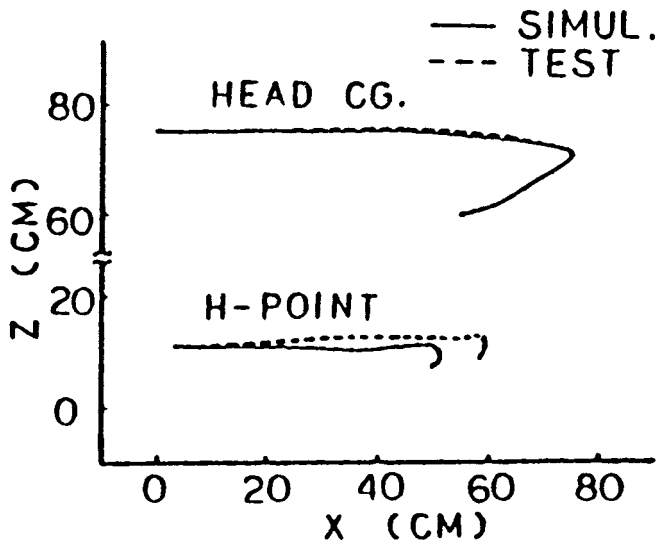


Figure 4. Amounts of head and hip displacement in dummy (for 30 MPH).

(2) Acceleration Curves of Dummy:

A comparison of the acceleration curves for head and chest and of load curve for femur obtained by testing and by simulation has been shown in figure 5. From the figures it will be seen that there is more or less good correspondence in the timings of ascent, peak and descent as well as in the values at these timings in the

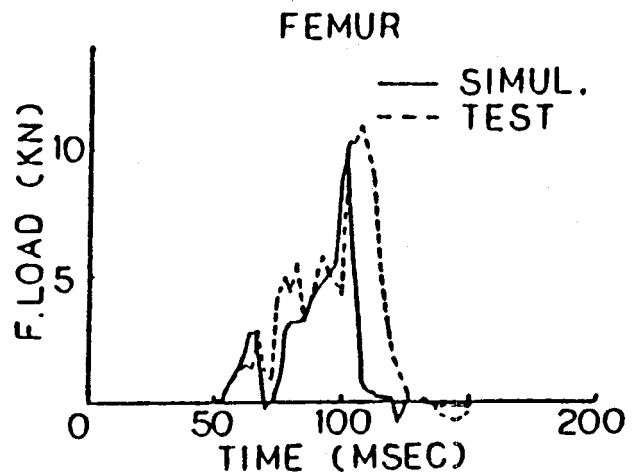
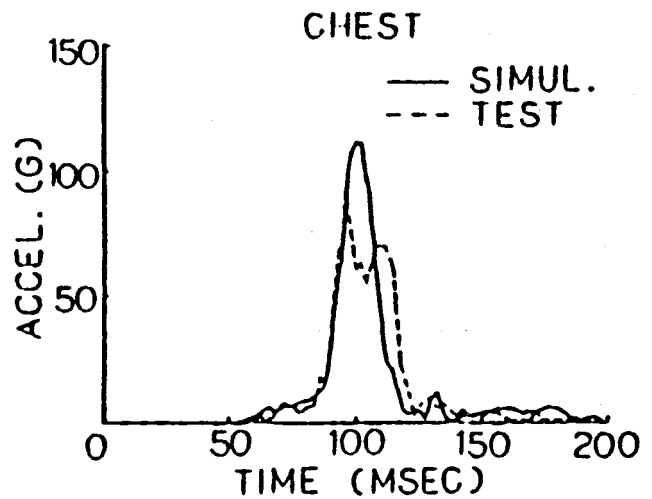
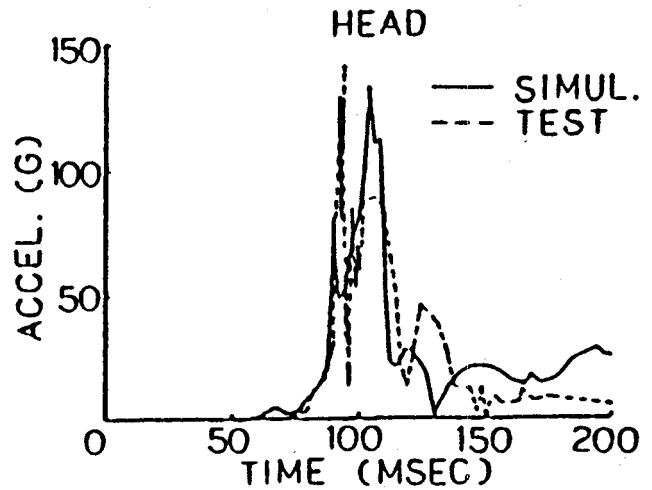


Figure 5. Acceleration and load curves of dummy.

two sets of curves. From this the authors concluded that simulation gave the timing of contact of the dummy with the secondary impact objects like the instrument panel accurately. This shows that simulation correctly predicted the distribution of contact reaction force (external force) acting on various parts of the dummy.

(3) Face Injury in the Dummy:

When collision takes place at 30 MPH, the face of the dummy crashes against the windshield glass. The glass breaks causing injury to the face.

## Results of Parameter Study

### Effects of vehicle body crash characteristics

The following two cases will be considered by idealizing the crash characteristics (acceleration curves) of vehicle body shown in figure 2 into triangular shape.

#### (1) Effect of Ascent Time (30 MPH Collision):

Calculations were carried out by varying the time  $t_1$  (ascent time) at which acceleration became maximum as has been shown in figure 6, and the effects of ascent time on injury value were investigated. The results have been shown in figure 7. From the figures it will be seen that the injury value shows a trend of slight decline when  $t_1$  is small. Here the maximum acceleration has been taken to be  $-26\text{ G}$ , which is the same as the peak value in the acceleration curve of

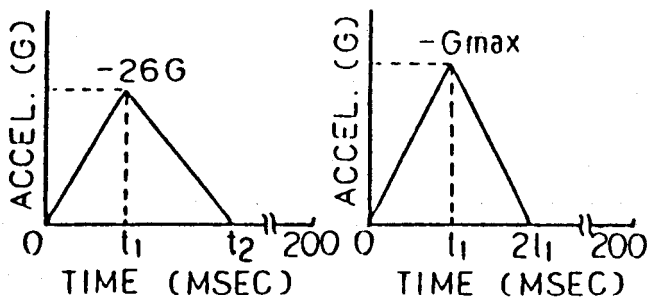


Figure 6. Idealized vehicle body acceleration curve.

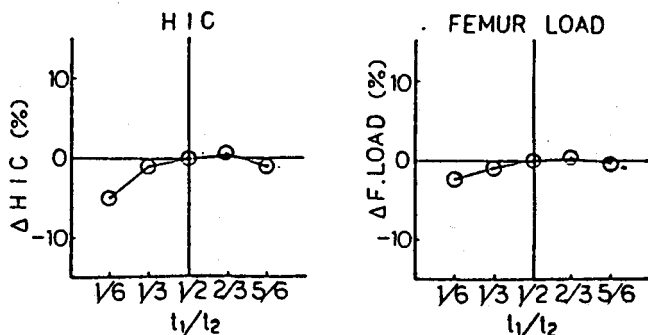


Figure 7. Effect of ascent time (for 30 MPH).

figure 2. The time  $t_2$  (time at which acceleration ended) here is 104.6 msec.

#### (2) Effect of Maximum Acceleration:

Calculations were carried out by varying the maximum acceleration  $-G_{max}$  as has been shown in the figure 6, and the effects of maximum acceleration on injury value were investigated. The results have been shown in figure 8. The figures show strong positive correlation between maximum acceleration and injury value. It shows that the injuries get reduced drastically with the decrease of maximum acceleration. On the other hand, for the same impact speed, the maximum acceleration bears the relation of inverse proportionally with the crash value of vehicle body. This shows that to take as large a crash distance as possible is advantageous for reducing the injury value.

### Effects of the position of instrument panel and glass

The position of the front section of the instrument panel with which the chest of the dummy makes contact was moved forward and backward for investigating the effect of instrument panel position on injury. The results have been shown in figure 9. From the figure it will be seen that the HIC and the chest G decrease with the shifting of the instru-

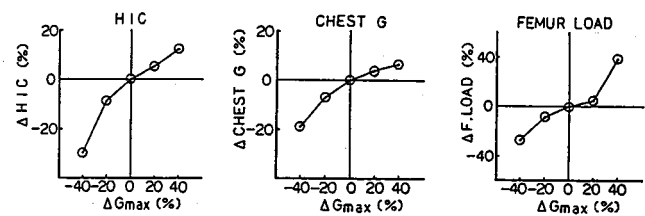


Figure 8. Effect of maximum acceleration (30 MPH).

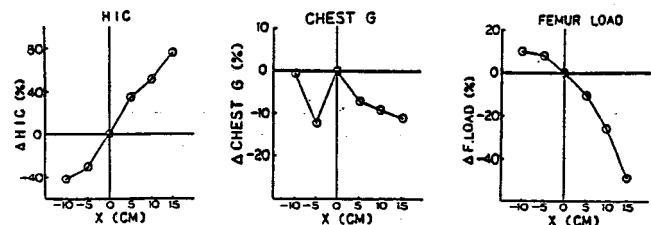


Figure 9. Effect of instrument panel position.

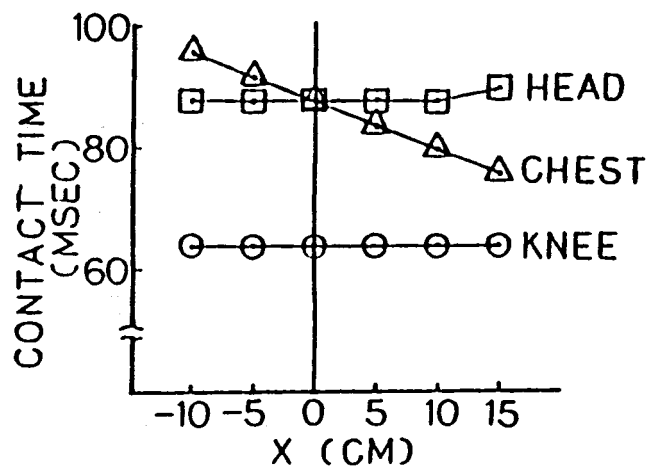


Figure 10. Contact time of dummy.

ment panel in the forward direction. The femur load on the other hand increases. The proportion of decrease in HIC is about 4 times larger than the proportion of increase in the femur load. Again, the figure 10 shows that the time of impact of the chest get delayed, but there is almost no change in the time of impact of head and knee. On the other hand, the reverse trend is noticed when the instrument panel is shifted backward.

### Effect of rigidity of instrument panel

The effect of varying the mechanical characteristics (the load-displacement curve) of the front section of the instrument panel with which the chest makes contact was studied. Here, the load was increased or decreased at a certain fixed proportion for a certain displacement. The results have been shown in figure 11. From the figure it will be seen that the HIC and chest G decrease with the softening of the instrument panel. The femur load increases on the other hand in this case. The proportion of decrease in HIC is about 4 times higher than the proportion of increase in femur load. The trend reverse with the hardening of the instrument panel.

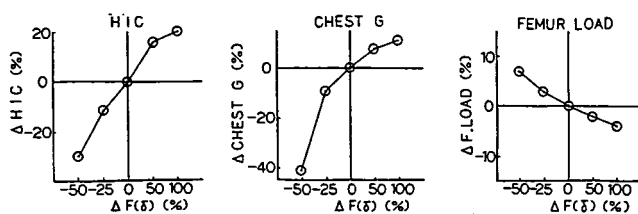


Figure 11. Effect of rigidity of instrument panel.

### Effect of cross beam rigidity

The effect of varying the load-displacement curve of the metallic cross beam located inside the instrument panel with which the knee of the dummy makes contact was studied. The mode of variation was similar to that employed in the case of instrument panel. As shown in figure 12, both HIC and femur load decrease largely with the hardening of cross beam. The femur load decreases here because with the hardening of cross beam it no longer remains in contact with the high rigidity section (cowl) of the vehicle body.]

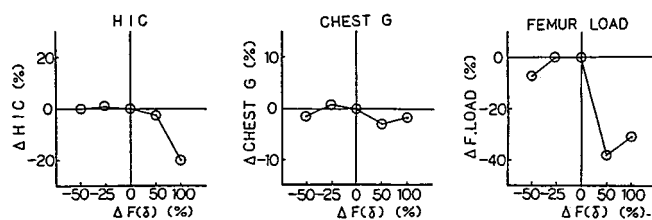


Figure 12. Effects of mechanical characteristics of cross beam.

### Effects of countermeasures

HIC and the femur load measured with base model fabricated according to pre-countermeasure specifications was

pretty high. Hence the following countermeasures were adopted on the basis of the results of parameter study.

Proposed countermeasures:

- (1) Softening the front section of the instrument panel with which the chest of dummy makes contact by 25%.
- (2) Hardening of the cross beam with which the knee of dummy makes contact by 200%.
- (3) Adjusting the instrument panel position in such a way that the head and chest of the dummy will make contact with the instrument panel simultaneously.

Calculations carried out to verify the effects of the countermeasures proposed above showed that HIC and femur load would get reduced by 26% and 34% respectively. Sled test carried out with vehicle modified by incorporating the above countermeasures showed 25% decrease in HIC, 48% decrease in right femur load and 10% increase in left femur load. This proves the soundness of the proposed countermeasures. Again, the moment of the head section and the cuts in the face could also be restricted to the minimum. The left femur load increased because the cross beam touched the vehicle body as the distance between the cross beam and vehicle body was too small. The authors will take up this question at some convenient later date.

### Conclusion

- (1) The way the crash characteristics of vehicle body, the location of instrument panel, mechanical characteristics of instrument panel and cross beam and positioning of seat frame effect the injury values was investigated by means of parameter study.
- (2) Accuracy of the base model was verified. It was found to have possessed a high degree of accuracy that can be supported by parameter study.
- (3) Countermeasures were evolved to reduce the injury values largely on the basis of the results of parameter study, and the soundness of the countermeasures was verified by carrying out tests.

### References

- (1) B.N. Bowman, R.O. Bennett and D.H. Robbins, "MVMA Two-Dimensional Crash Victim Simulation, Version 3, Volume 1-3", Final Report, UMTRI-85-24-1, 2, 3, June 29, 1985, The University of Michigan, Transportation Research Institute.
- (2) Oho, Uchiyama, Yamasaki and Tanaka, "Shin FMVSS 208 Hyoka ni kansuru Mondaiten (Problems in New FMVSS 208 Assessment)", Isuzu Giho, No. 76, p. 113-120.
- (3) J. Wismans, J.H.A. Hermans, "MADIMO 3D Simulations of Hybrid III Dummy Sled Tests", SAE Paper No. 880645 (1988).

# Consideration of Potential Safety Effects for a New Vehicle-based Roadway Illumination Specification

Written Only Paper

**Gerald Stewart and August Burgett,**  
National Highway Traffic Safety  
Administration,  
United States

## Abstract

This paper describes how accident data and travel data can be combined to provide a basis for setting priorities and evaluating safety effects of new vehicle-based roadway illumination specifications.

Methods for making distinctions between daylight and darkness are applied to both accident tabulations and vehicle miles of travel tabulations. Exposure-based accident rates are calculated for several types of accidents and roadways.

Measures for improvements in safety are discussed in terms of reductions in nighttime exposure-based rates as related to improvements in visibility of signs, road markings and general aspects of the roadway environment.

## Introduction

Illumination performance of headlamps are specified as part of Standard No. 108 of the NHTSA Federal Motor Vehicle Safety Standards. The purpose of this standard is to reduce accidents and deaths and injuries by providing adequate illumination of the roadway and by enhancing the conspicuity of motor vehicles on public roads so that their presence is perceived and their signals understood, both in daylight and in darkness or other conditions of reduced visibility.

New vehicle-based roadway illumination performance specifications are being developed. These new specifications are being developed in response to the need for standards which are more performance oriented and less design restrictive. The approach to developing new standards is to require the vehicles to provide certain illumination on the roadway.

This paper describes how accident data and travel data can be combined to provide a basis for setting priorities and examining effects on safety. Methods for making distinctions between daylight and darkness are presented and applied to both accident tabulations and corresponding tabulations of vehicle miles of travel to establish exposure-based accident rates for several types of accidents and roadways. These exposure-based rates are used for setting priorities.

The paper also discusses possible approaches to examination of the effects of improved roadway illumination. In general, these approaches provide the initial step for consideration of potential safety effects which can result from implementation of the new safety-oriented vehicle-based illumination specifications.

## Relating Night-to-Day Accident Rates

Relating night-to-day accident rates involves both accident counts and vehicle miles of travel. Also an important component of the relationship is the percentage of nighttime vehicle miles of travel. Calculation procedures are as follows:

- A(d) = number of day accidents
- A(n) = number of night accidents
- M(d) = vehicle miles of day travel in 100 millions
- M(n) = vehicle miles of night travel in 100 millions
- T = total vehicle miles of travel
- P = night percentage of travel
- R(d) = rate of day accidents per 100 million vehicle miles
- R(n) = rate of night accidents per 100 million vehicle miles
- R = ratio of night-to-day rates

$$R(d) = A(d)/M(d) ; R(n) = A(n)/M(n) ; R = R(n)/R(d)$$

$$M(n) = T \times P ; M(d) = T \times (1 - P) ;$$

$$R = \frac{A(n) (T) (1 - P)}{A(d) (T) (P)} \quad (\text{Eq. 1})$$

The most important component of the relationship formula is the distinction between day and night conditions. The tabulation of accidents must accurately separate accidents into day and night categories and the corresponding travel information must be treated in a similar manner to determine accurately the percent of nighttime travel.

Clear distinctions between daylight and darkness conditions can be based on the astronomical event called "civil twilight". Civil twilight begins in the morning and ends at sunrise or begins at sunset and ends in the evening when the Sun is geometrically six degrees below the local horizon. Before morning civil twilight and after evening civil twilight, artificial illumination is ordinarily required. Twilight periods, the times when ambient light conditions change from darkness to daylight (morning) or from daylight to darkness (evening) last about 30 minutes.

Thus, by using ambient light conditions it is possible to define nighttime as the time between the ending of evening civil twilight and the beginning of morning civil twilight. The lengths of these periods of darkness for a given location vary according to the longitude and latitude of the location and time of year. Daylight periods consist of the times between the beginning of dawn and the end of dusk as determined by the onset of civil twilight.

This definition of nighttime may give a conservative estimate of times when motor vehicle lighting should be used. For example some accident files include a variable in which the accident investigator directly codes the ambient

light condition using subjective judgement. In periods of inclement weather this latter variable might indicate that the ambient conditions were dark even though the civil twilight algorithm indicates a lighter condition. However, the files of travel information do not have this additional variable. Because data from these two types of files are combined in these analyses it is necessary to use information that is common to both types of files for coding the ambient light level. This led to use of the civil twilight algorithm.

## Tabulations of Accidents by Daylight and Darkness

Accidents can be classified according to the type of area (Urban or Rural), by type of roadway (Interstate, Arterial, or Local, Minor, and Collectors), and by type of accident (Pedestrian, Offroad, Roadside, or Overturn). Single-vehicle accidents provide the best basis for study of possible effects of changes in roadway illumination by motor vehicles. Tabulations of single-vehicle fatal accidents are shown in table 1.

**Table 1. Single-vehicle fatal accidents (1982-1986) from NHTSA FARS (Fatal Accident Reporting System). Alaska excluded—ambient light algorithm used. See pages B5-B7 of reference 3 for algorithm.**

Roadway Type	Pedestrian		Offroad		Roadside		Overturn	
	Day	Night	Day	Night	Day	Night	Day	Night
Urban Interstate	383	1213	273	417	795	1475	266	420
Urban Arterials	4428	8046	1625	3609	1709	4227	517	897
Urban Local	3338	3101	1645	3301	1081	2336	415	713
Rural Interstate	205	690	544	478	902	1056	1154	785
Rural Arterials	1117	3236	2593	3868	1389	2473	1973	2194
Rural Local	1967	2902	6134	9695	2011	3650	3570	4173
All Types	11438	19188	12814	21368	7887	15271	7895	9182

## Tabulations of Vehicle Miles of Travel

Vehicle miles of travel for the same 5-year period from 1982 to 1986 can be summarized according to type of area and type of roadway. Total vehicle miles of travel are obtained from State summary files. Percent of travel for nighttime (darkness) hours are estimated by using the civil twilight criterion discussed earlier. Tabulations of vehicle miles of travel and percentage of nighttime travel are shown in table 2.

**Table 2. Vehicle miles of travel and estimated percentage of nighttime travel for 5-year period 1982-1986, excluding Alaska.**

Roadway Type	Total Miles (Millions)	Percent in Darkness
Urban Interstate	1,006,687	19.43
Urban Arterials	2,641,644	16.88
Urban Local	1,307,319	14.51
Rural Interstate	742,522	22.52
Rural Arterials	1,371,407	20.08
Rural Local	1,034,034	16.35
All Types	8,103,613	19.51

Calculations of exposure-based rates can now be performed using the tabulated results in tables 1 and 2. The calculated rates reflect the definition of darkness conditions

as determined by the ambient light algorithm which was used on both the accident tabulation and on the estimation of percentage of nighttime travel. The results computed here are for single-vehicle fatal accidents only because this class of accidents gives the best comparative basis for consideration of potential effects of roadway illumination improvements. Results for exposure-based rates are shown in table 3.

**Table 3. Exposure-based rates for single vehicle fatal accidents per 100 million miles of travel.**

Roadway Type	Pedestrian		Offroad		Roadside		Overturn	
	Day	Night	Day	Night	Day	Night	Day	Night
Urban Interstate	.05	.62	.03	.21	.10	.75	.03	.21
Urban Arterials	.20	1.80	.07	.81	.08	.95	.02	.20
Urban Local	.30	1.63	.15	1.74	.10	1.23	.04	.38
Rural Interstate	.04	.41	.09	.29	.16	.63	.20	.47
Rural Arterial	.10	1.18	.24	1.40	.13	.90	.18	.80
Rural Local	.23	1.72	.71	5.73	.23	2.16	.41	2.47
All Types	.18	1.21	.20	1.35	.12	.97	.12	.58

**Table 4. Night-to-day rate ratios for selected single-vehicle fatal accidents.**

Roadway Types	Pedestrian	Offroad	Roadside	Overturns
Urban Interstate	12.40	7.00	7.50	7.00
Urban Arterials	9.00	11.57	11.88	10.00
Urban Locals	5.43	11.60	12.30	9.50
Rural Interstate	10.25	3.22	3.94	2.35
Rural Arterials	11.80	5.83	6.92	4.44
Rural Locals	7.48	8.07	9.39	6.02
All Types	6.72	6.75	8.08	4.83

**Table 5. Priority order for single vehicle fatal accident rates (\*) for selected accident types in darkness by type of roadway.**

Priority	Accident Type and Roadway Type	Exposure-Based Rates (*)
1	OFFROAD/RURAL - LOCAL	5.73
2	OVERTURN/RURAL -LOCAL	2.47
3	ROADSIDE/RURAL - LOCAL	2.16
4	PEDESTRIAN/URBAN - ARTERIAL	1.80
5	OFFROAD/URBAN - LOCAL	1.74
6	PEDESTRIAN/RURAL - LOCAL	1.72
7	PEDESTRIAN/URBAN - LOCAL	1.63
8	OFFROAD/RURAL - ARTERIAL	1.40
9	ROADSIDE/URBAN -LOCAL	1.23
10	PEDESTRIAN/RURAL - ARTERIAL	1.18
11	ROADSIDE/URBAN - ARTERIAL	.95
12	ROADSIDE/RURAL - ARTERIAL	.90
13	OFFROAD/URBAN - ARTERIAL	.81
14	OVERTURN/RURAL - ARTERIAL	.80
15	ROADSIDE/URBAN - INTERSTATE	.75
16	ROADSIDE/RURAL -INTERSTATE	.63
17	PEDESTRIAN/URBAN - INTERSTATE	.62
18	OVERTURN/RURAL - INTERSTATE	.47
19	PEDESTRIAN/RURAL - INTERSTATE	.41
20	OVERTURN/URBAN - LOCAL	.38
21	OFFROAD/RURAL - INTERSTATE	.29
22	OVERTURN/URBAN - INTERSTATE	.21
23	OFFROAD/URBAN - INTERSTATE	.21
24	OVERTURN/URBAN - ARTERIAL	.20

(\*) NOTE: Accident Rate = Number of Accidents per 100 Million Vehicle Miles of Travel

Ratios of night-to-day rates can also be computed as a basis for further work on estimating or projecting effects of

improved roadway illumination. Table 4 presents the rate ratios calculated from Equation 1.

The primary use of exposure-based rates is to establish the priority rankings of accident types and roadway types. Table 5 shows the priority order for accident and roadway types based on descending order of exposure-based rates for darkness conditions. Absolute counts can also be used as a basis for setting priorities; however, exposure-based rates are generally best for the overall rank ordering of accident situations.

The priorities in table 5 have been used in support of a companion project which focuses on the relationship between visibility needs and vehicle-based roadway illumination (6).<sup>\*</sup> The companion project includes computer modelling of nighttime driving conditions. The conditions include the presence of either an approaching or a following glare-producing vehicle on various types of roads such as straight, curved or hilly.

## Approaches to Consideration of Potential Reductions

The development of new vehicle-based performance provides for specifications that can have an effect on safety. This section reviews an approach that might be used to examine the effect on safety of new lighting specifications. This approach can be used for estimating benefits that will result from implementation of new specifications or for evaluating safety effects after implementing new specifications.

This section also discusses an approach for calculating the sizes of the changes in safety that would be necessary to distinguish the effect of new lighting specifications from changes that occur due to chance alone.

For single-vehicle accidents, headlighting is directly involved in the ability of the driver to see the road and roadway features and obstacles. Thus, lack of proper roadway illumination can contribute to a driver failing to stay on the road or to a vehicle hitting a person or other object on or near the road. The accident types presented in table 1 thus become the accidents which are most likely to be affected by improvements in vehicle roadway illumination.

## Reductions in Nighttime Rates

Improvements in safety can be measured in a variety of ways. One measure of safety improvement is the amount that nighttime driving becomes more like daytime driving. Application of this measure would utilize tables such as table 3 and estimates of changes in the values of the nighttime entries in this table. The premise for this approach is that when roadway features are more visible less accidents occur.

At this time no data on before-after effectiveness are available for vehicle roadway illumination improvements; however, it is helpful to examine other situations where

roadway illumination was evaluated. For example the relationship between the presence of fixed illumination on freeways and accidents has been studied with the result of an average reduction of 40 percent in night accidents as a result of the addition of fixed lighting (1). Improvements in visibility of roadway signs and markings have also shown significant reduction in accidents as a result of better illumination of roadway features (11).

One approach to evaluating the effect of new lighting specifications is to estimate the change in the difference between nighttime and daytime accident rates. A perfect nighttime system would provide the same visibility as is available during daytime, and, the ratios in table 4 would all be unity. In general, if we assume that future daytime rates are the same, the new ratios in table 4 would be given by:

$$R(\text{new}) = (1 - f)R + f \quad (\text{Eq. 2})$$

where  $f$  = effectiveness factor  
and  $R = R(n)/R(d)$  (See Eq. 1)

Future daytime rates can be the same although vehicle miles of travel may be slightly different for two different 5-year periods. Assuming no change for daytime rates, a reduction in future nighttime exposure-based rates is computed from the difference in day and night rates. For example a reduction of 10 percent of the difference between current night and day rates would produce the results shown in table 6.

A general formula for this type of calculation is as follows:

$$\text{NEW NIGHTTIME RATE} = (1 - f)R(n) + fR(d) \quad (\text{Eq. 3})$$

where  
 $f$  = effectiveness factor  
 $R(n)$  = current nighttime exposure-based rate  
 $R(d)$  = current daytime exposure-based rate

The results in table 6 correspond to an overall 8.6 percent reduction in fatal accidents. With this approach the cases with the larger day-night rate differences have the larger benefits in terms of accident reductions. Future work will be necessary to determine the appropriate factor, i.e. "f", to be used for the percent reduction based on the current difference in nighttime and daytime rates.

**Table 6. New nighttime rates after reductions based on current day-night rate difference—10% reduction—assuming no change in vehicle miles.**

Roadway Type	Accident Type							
	Pedestrian		Offroad		Roadside		Overturn	
	Old	New	Old	New	Old	New	Old	New
Urban	.62	.56	.21	.19	.75	.69	.21	.19
Interstate								
Urban	1.80	1.64	.81	.74	.95	.86	.20	.18
Arterial								
Urban	1.63	1.50	1.74	1.58	1.23	1.12	.38	.35
Local								
Rural	.41	.37	.29	.27	.63	.58	.47	.44
Interstate								
Rural	1.18	1.07	1.40	1.28	.90	.82	.80	.74
Arterial								
Rural	1.72	1.57	5.73	5.23	2.16	1.97	2.47	2.26
Local								
All Types	1.21	1.11	1.35	1.24	.97	.89	.58	.53

<sup>\*</sup>Numbers in parentheses designate references at end of paper.

Another extension of Equation 1 can be used to estimate the effects on safety for changes in exposure-based rates. This extension is obtained by rearranging Equation 1 and replacing the known value of nighttime accidents by an estimate of future nighttime accidents. The resulting equation is:

$$E(n) = \frac{R [A(d)] P}{(1 - P)} \quad (\text{Eq. 4})$$

where

- E(n) = number of expected accidents at night
- R = ratio of night to day rates
- P = percentage of night travel

Thus, changes in values of R that are different than those in table 4 can be the basis for estimates of the effect.

## Statistically Significant Reductions

A practical formula for determining the percent change necessary for a statistically significant change in a count such as number of accidents is as follows:

$$\text{PERCENT REQUIRED} = \frac{\chi_a^2}{2b} \left( \sqrt{1 + \frac{8b}{\chi_a^2}} - 1 \right) \quad (\text{Eq. 5})$$

- $b$  = number of accidents in the before period
- $\chi_a^2$  = the Chi-Square Value with 1 degree of freedom

Application of Equation 5 to the accident counts in table 1 produces the results shown in table 7. These results represent the required changes in fatal accidents for a future 5-year period in order to attribute the changes to improved vehicle roadway illumination specifications rather than to chance.

**Table 7. Percent reduction required for statistically significant changes in fatal accident counts.**

Roadway Type	Pedestrian		Offroad		Roadside		Overturn	
	%	Number	%	Number	%	Number	%	Number
Urban	6.57	80	11.51	48	5.97	88	11.04	46
Interstate								
Urban	2.58	207	3.84	139	3.55	150	7.62	68
Arterial								
Urban	4.14	128	4.01	132	4.76	111	8.53	61
Local								
Rural	8.67	60	10.37	50	7.04	74	8.14	64
Interstate								
Rural	4.05	131	3.71	143	4.63	114	4.91	108
Arterial								
Rural	4.27	124	2.35	228	3.82	139	3.57	149
Local								
Total Reductions	730		740		676		496	

## Closure

Tables 1 to 7 have all been produced using the number of fatal accidents in the selected types of single vehicle accidents. Similar tables can be produced for non-fatal accidents or for fatalities and injuries in fatal accidents.

## Effectiveness Considerations

Exposure-based rates can be used to make comparisons between rates such as those presented here and the exposure-based rates which exist after the new specifications are in use.

In general, the effectiveness of new forward illumination is expected to vary for the different accident and roadway types. Statistical considerations provide insight on accident reduction levels which can be attributed to improved illumination rather than to chance. The approach based on differences in daytime and nighttime rates reflects the desire to develop roadway illumination specifications which address the worst nighttime driving situations first.

At the present time there are no quantitative facts available upon which to develop effectiveness measures for improved forward illumination systems. However, past studies of visibility-accident correlations and effectiveness of fixed lighting give evidence that reductions in fatal accidents may be feasible as a benefit from improved forward lighting practices which eliminate problems of glare and low contrasts, and low contrasts and brightness.

The search for insights relating to effectiveness of new vehicle-based roadway illumination standards should be continued. Special studies are being performed which may provide new insights on some of the nighttime accidents which can be characterized by a likelihood of poor driver visibility for the nighttime conditions. For example, rollover (i.e. overturn) accidents for the State of Maryland are being studied carefully with respect to vehicle design features (7). The rollover data that are being collected provide an opportunity to examine the characteristics of nighttime accidents with respect to driver visibility factors as those factors are represented in the new specifications and modelling efforts used to develop them. Insights resulting from investigation of rollover accidents may also apply to some of the other accident types such as offroad and roadside fatal accidents. The process of determining which accidents may have been avoided in the context of better vehicle roadway illumination must be developed in terms of the modelling efforts used to establish the new specifications and in terms of characteristics of accidents either from national files such as FARS, NASS and CARD or from special studies such as the Rollover study.

## Conclusions

This paper describes the use of accident data for two purposes. The first purpose is to help establish driving conditions which should receive priority consideration in the development of new vehicle specifications for roadway illumination. For example offroad accidents on rural local roads were found to have the highest nighttime accident rate. The second purpose is to explore approaches that may be meaningful for evaluation of the effect on safety of changes in roadway illumination specifications. For example, it was found that on the average, there must be at least a 4.1 percent reduction in nighttime single-vehicle fatal accidents to be able to attribute the reduction to a change in headlighting rather than to pure chance.

## References

- (1) "Relationship Between Illumination and Freeway Accidents", Paul C. Box, IERI Report Project 85-67,

Illuminating Engineering, (May/June 1971).

(2) United States Naval Observatory Circular No. 171, Computer Programs for Sun and Moon Illuminance With Contingent Tables, P.M. Janiczek and J.A. DeYoung.

(3) The Almanac for Computers 1987, U.S. Naval Observatory, Nautical Almanac Office.

(4) "We Drive By Night", Hershchel W. Leibowitz and D. Alfred Owens, Psychology Today, January 1986.

(5) "Nighttime's Fatal Vision", Linda Wasmer Smith, Friendly Exchange, August 1987—NHTSA press clips 10/02/87.

(6) "Relationship Between Visibility Needs and Vehicle-Based Roadway Illumination", Paper #89-4B-0-001, 12th International Technical Conference on Experimental Safety Vehicles, Burgett, Ulman, VanInderstine, May 1989.

(7) "The Crash Avoidance Rollover Study: A Database for the Investigation of Single Vehicle Rollover Crashes, Paper

#89-2B-0-003, 12th International Technical Conference on Experimental Safety Vehicles, Harwin-Emery, May 89.

(8) Highway Safety Performance (1982-1986) Fatal and Injury Accident Rates on Public Roads in the United States—Report of the Secretary of Transportation to the United States Congress—Prepared by the Offices of Highway Safety and Highway Planning—U.S. Department of Transportation, Federal Highway Administration.

(9) Highway Statistics (1982-1986)—Prepared by the Office of Highway Information Management, Federal Highway Administration, U.S. Department of Transportation.

(10) Computer Tapes of Hourly Traffic Counts by Highway Class, Information received from States by the Federal Highway Administration Office of Highway Information Management.

(11) "The Nighttime Accident Problem, Phil Hirsch, Pageant Press, Inc. New York 1957.

## **The Effect of Occupant Restraints on Children and the Elderly in Motor Vehicle Crashes**

Written Only Paper

**Elizabeth Mueller Orsay, M.D.,**

University of Illinois

Lutheran General Hospital

**Timothy L. Turnbull, M.D.,**

University of Illinois

Mercy Hospital and Medical Center

**Mary Dunne, M.D.,**

University of Illinois

Illinois Masonic Medical Center

**John A. Barrett, M.D.,**

University of Illinois

Cook County Hospital

**Patricia Langenberg, Ph.D.,**

University of Illinois

School of Public Health

**Charles P. Orsay, M.D.,**

University of Illinois

Cook County Hospital

### **Introduction**

Trauma resulting from motor vehicle accidents (MVA) is currently the leading cause of death in young people and the seventh leading cause of death overall in the United States. Statistically Americans can expect to be involved in an MVA every 10 years and has a 33% chance of sustaining a disabling injury during a lifetime of driving. (1)\* 1.3 million years of potential life before age 65 years were lost in 1984 as a result of MVA associated injuries. (2) The overall economic loss to the U.S. attributable to MVA's in 1980 has

been estimated to be \$57.2 billion. (3) The following prospective study was undertaken to evaluate the effects of safetybelt use in injuries and health care costs, specifically in pediatric and elderly population.

### **Materials and Methods**

During the period of January 1, 1986 to July 1, 1986, data were collected on patients who presented after an MVA to the emergency department or trauma unit of four Chicago area hospitals. All patients presenting with complaints referable to an MVA that had taken place within the previous 24 hours were eligible for inclusion. Pedestrians, bicyclists, motorcyclists, bus passengers and those in trucks with more than two axles were excluded.

Initial data were collected prospectively for all study subjects by the examining physician. The physician administered a structured questionnaire which included the following data: 1. determination of safety belt usage; 2. position of subject in vehicle; 3. mechanism of injury (front-end, rear end, or broadside collision). For all subjective data collected, independent confirmation was sought from paramedics, police or others, whenever possible.

The medical records (emergency and inpatient, if applicable) of all subjects were subsequently reviewed by a member of the research team. An Injury Severity Score (ISS) was calculated based upon the Abbreviated Injury Scale Manual (1985 edition). (4) This score is obtained by assigning a numerical score (1-5) to the severity of injury in each region.

The squares of the three highest scores are then summated to obtain the ISS. Financial records were analyzed to determine the total hospital (exclusive of physician fees)

\*Numbers in parentheses designate references at end of paper.

and emergency department charges generated as a direct result of the MVA for each subject. Cost of consultants, admitting physicians, repeat hospitalizations and rehabilitation were not included.

Study subjects were divided into two groups (restrained and unrestrained by safety belts) for purposes of data analysis. Preliminary power calculations were made for an alpha of .05 and a power of .90 to detect a difference in ISS score of at least 0.5. The principal statistical tests used were t-tests for comparisons of means of continuous variables, and Chi-square tests for drawing inferences concerning proportions.

## Results

A total 1,364 patients were enrolled into the study. Seven hundred and ninety one patients (58%) were wearing a safety belt, whereas 573 (42%) were not. 45.2% of pediatric patients (defined as  $\leq 18$  years of age) were restrained and 61.6% of elderly patients (defined as  $\geq 65$  years of age) were restrained. The injury severity score for safety belt wearers was  $1.8 \pm 0.07$  (standard error of mean) as opposed to non-safety belt wearers who had a mean injury severity score of  $4.51 \pm 0.31$  ( $p < 0.001$ ), (two tailed t-test) a 60% reduction of injury. Restrained pediatric patients as well as restrained elderly patients had significantly lower injuries severity scores than the unrestrained (table 1). Restraint systems were most beneficial in reducing injuries to the head and face in both the pediatric and elderly patients. Of the total 179 head and facial injuries that occurred, 132 (73.7%) occurred in unrestrained pediatric and elderly patients (98 in pediatric patients, 34 in elderly patients).

**Table 1. Mean Injury Severity Score (ISS) and costs in restrained versus unrestrained pediatric and elderly patients.**

		Restrained	Unrestrained	% Reduction	p value
Pediatric Patients	ISS	$1.25 \pm 0.19$	$3.03 \pm 0.48$	58.7%	0.002
	Cost (n=76)	$\$226 \pm 59$	$\$1389 \pm 723$ (n=92)	83.7%	0.141
Elderly Patients	ISS	$2.71 \pm 0.58$	$7.68 \pm 1.40$	64.7%	0.002
	Cost (n=45)	$\$1474 \pm 508$	$\$3280 \pm 822$ (n=28)	55.1%	0.052

Regardless of the patients position in the vehicle, restrained patients consistently had lower injury severity scores than unrestrained patients (table 2). Front seat passengers (driver and front seat passengers) had significantly lower scores in the restrained group than the unrestrained group for both pediatric and elderly patients. A trend for lower injury severity scores in restrained patients is also noted in back seat passengers in both pediatric and elderly patients. Statistical significance was not reached in this group, although it should be noted that the samples sizes were small. Overall, restrained occupants incurred mean costs of \$543 versus unrestrained occupants who incurred costs of \$1,583 an almost three fold increase. ( $p < .001$ ). Again, costs on the pediatric patients and the elderly

patients were considerably higher in the non-seatbelt wearers compared to the seatbelt wearers (table 1).

**Table 2. Mean Injury Severity Scores in restrained versus unrestrained patients according to position in vehicle.**

		Restrained	Unrestrained	% Reduct.	p value
Pediatric Patients	Front seat (n=103)	$1.56 \pm 0.27$	$3.51 \pm 0.59$	55.6%	0.003
	Back seat (n=57)	$0.59 \pm 0.14$	$2.57 \pm 0.89$	77%	0.092
Elderly Patients	Front seat (n=62)	$2.77 \pm 0.60$	$7.95 \pm 1.94$	65.2%	0.002
	Back seat (n=11)	$1.50 \pm 0.50$	$7.4 \pm 1.67$	79.7%	0.161

## Discussion

Despite passage of child passenger restraint laws in all 50 states and seat belt laws in 31 states and the District of Columbia, motor vehicle trauma remains a significant cause of morbidity and mortality in the pediatric and elderly populations. This study clearly demonstrates the benefit of seat belt use in reducing injury and health care costs in both populations.

Though the effects of child safety seats for younger children (newborns to age four) are well documented (5-7), this study evaluated the pediatric age group from newborn to age 18 years. To our knowledge, this is the first study to evaluate the effects of seat belts in elderly patients involved in motor vehicle trauma.

The effect of motor vehicle trauma in each of these two populations is significant. In pediatric patients, motor vehicle accidents remains the leading cause of death, despite passage of mandatory seat belt legislation across much of the country. The death or disability of a young person is always tragedy, especially one that could have been avoided. Seat belts can and do reduce injury and death resulting from auto accidents.

Elderly patients are more vulnerable to the effects of motor vehicle trauma, as reflected by their higher injury severity scores. The older patient suffers an increase in the incidence and severity of injury from similar traumatic forces as compared to younger patients. In addition, recovery from these injuries take much longer and patients stand a greater chance of permanent impairment or disability. The economic impact of caring for injured pediatric and elderly patients is tremendous. Decker et al estimated a savings of \$8.4 million for universal use of child safety seats in Tennessee in 1982 and 1983. (5) The costs required to care for a permanently disabled child over a lifetime is staggering. In addition, society loses the potential productivity of a child who is disabled or killed in an auto accident. Above all, the human suffering that results from such injury or death is appalling.

The elderly incur far greater health care costs than their younger counterparts. In this series the costs to care for the injured older patient was more than double that of the group

overall, for both the restrained and unrestrained patients. Older patients suffer more severe injuries from relatively minor trauma compared to younger auto accident victims. Again, society bears the burden of increased health care costs for these patients as most of them are receiving medicare.

In conclusion, this study demonstrated the medical benefit in reducing morbidity as well as the social benefit in reducing health care costs in seat belt users in both pediatric and elderly patients.

## References

(1) Sleet DA: "Motor Vehicle Trauma and Safety Belt Use in the Context of Public Priorities", *J Trauma*, 1987; 27: 695-702.

(2) Seat Belt Use: United States. *MMWR*, 1986; 35: 301-304.

(3) The Economic Cost to Society of Motor Vehicle Accidents, US Dept. of Transportation publication (HS) 806-342. National Highway Traffic Safety Administration, 1985.

(4) Committee on Injury Scaling: The Abbreviated Injury Scale, 1985 revision. Arlington Heights, IL, American Association for Automotive Medicine, 1985.

(5) Decker MD et al: "The Use and Efficacy of Child Restraint Devices", *JAMA*, 1984; 252: 2571-2575.

(6) Wagenaar AC and Webster DW: "Preventing Injuries to Children Through Compulsory Automobile Safety Seat Use", *Pediatrics*, 1986; 78: 662-672.

(7) Guerin D and MacKinnon DP: "An Assessment of the California Child Passenger Restraint Requirement", *Am J Public Health*, 1985; 75: 142-144.

# Technical Session 6A

## Pedestrian Impact Protection

Chairman: Dominique Cesari, France

### A Study of Test Methods to Evaluate Pedestrian Protection for Cars

---

**J. Harris,**  
EEVC Working Group 10

#### Abstract

The European Experimental Vehicles Committee has set up a Working Group to assess and develop test methods for evaluating pedestrian protection for passenger cars. This work is scheduled to be completed by March 1990.

The methods to be considered are sub-systems tests to the bumper, the bonnet leading edge and the bonnet top. Test conditions appropriate for vehicle to pedestrian impacts of upto 40 km/h, will be considered, with adjustments made to the test requirements to allow for the influence of the vehicles' frontal shape.

This report prepared by the Group gives the basic requirement of each sub-systems test, the test methods and the proposed development programmes.

The role of mathematical computer simulation in this work is described and also an outline of compatibility studies to assess any conflict between proposals for pedestrian safety and operational requirements or the requirements of current regulations.

#### Summary

The development programme of EEVC Working Group 10 to assess and develop test methods for evaluating pedestrian protection for passenger cars will be based on the following basic conditions and development programme.

#### Basic conditions

(1) Three separate tests will be developed to evaluate the pedestrian protection at the bumper, the bonnet leading edge and the bonnet top of cars.

(2) The bumper test will include the air dam, when fitted; the bonnet leading edge test will include headlight surround and the leading edge of the wings; the test to the bonnet top will include the scuttle, the lower edge of the windscreen frame and the top of the wings.

(3) The assessment methods will be sub-systems tests to each of these three locations. The basic requirements of sub-systems tests are that they represent the important interactions between the vehicle structure that is under assessment and the corresponding body regions that are liable to suffer serious injury from striking it.

It is necessary that sufficient of the vehicle structure is included in the test to demonstrate the performance and interactions of all the contributing vehicle components.

(4) Test methods will be considered that evaluate the performance of each part of the vehicle structure with respect to both child and adult pedestrians, at impact speeds up to 40 km/h.

(5) Acceptance levels will be proposed that aim to represent injury severities of AIS 2 to the joints of the legs and AIS 3 to other body regions. For the legs the main objective is to reduce the risk of permanent disability, particularly to the knee joint. Permanent disability is difficult to isolate by the AIS scale and an acceptance level of AIS 2 is necessary at the joints to reduce this risk. Injury to the long bone however, is less likely to result in permanent disability and in these cases acceptance levels of AIS 2 would be difficult to achieve and predict.

(6) The severity of the impacts to some locations of a car, are partly dependent on the general frontal car shape. These variations in impact severity will be allowed for by adjusting the total impact momentum of the test.

#### Detailed objectives of the study

The items that will be considered in developing each of the sub-systems tests are:

(1) The mechanism of injury to each of the body regions that suffers injury from vehicle impact.

(2) The shape, stiffness, mass, mass moment of inertia of the impactors and the test velocity, particularly with respect to the different shapes and styles of cars.

(3) The degrees of freedom of the impactor—rigidly mounted to the propulsion system, mounted through a torque loaded hinge or free flight.

(4) The relationship of the transducer outputs on the impactors with respect to the injury severities and tolerance values of children and aged adults.

(5) Assess the compatibility of the developing pedestrian safety proposals with existing vehicle regulations, other safety features for vehicle occupants, or basic operational requirements of cars.

(6) Assess the performance of some typical current designs of car against the proposed tests.

(7) Give precise definitions of each of the three vehicle locations to be tested (bumper, bonnet leading edge and bonnet top).

(8) Comment on the suitability of the different propulsion systems studied, for each test method.

#### Development studies

(1) Studies to develop test methods will be based on full

scale dummy tests, computer simulations, cadaver tests and accident data. Full use will be made of existing data, supplemented where necessary by additional testing to obtain an understanding of the characteristics of each phase of a pedestrian impact.

(2) Accident data and cadaver test data will be used to identify the regions of a body most at risk, the mechanisms of injury and also to give a better understanding of tolerance values.

(3) Impacts to pedestrians by cars representing a wide range of frontal shapes, will be simulated on a computer for comparison with existing data to give a more strongly supported and broader based data set.

(4) Impactor devices will be developed from the results of full scale dummy tests, computer simulations or cadaver tests as appropriate and variations in test requirements will be determined to reflect the influence of vehicle shape.

(5) The outputs of transducers, fitted to the test impactors will be calibrated for acceptance levels, by comparison with the results of full scale tests, cadaver data and accident data.

(6) The finally developed tests proposals will be tested against representative cars of current designs to determine, the feasibility of the proposals and their compatibility with existing regulations and normal operating requirements.

## Introduction

An EEVC Working Group has been set up to assess and develop test methods for evaluating pedestrian protection for passenger cars. Both industry and research institutes are represented on the Group, with the research and development programme undertaken by five organisations: BAST, INRETS, Laboratoire de Physiologie et de Biomecanique APR, TNO and TRRL. The study was requested by ERGA-S the adhoc passive safety advisory Group of the European Commission and the Commission is providing financial support. The work is scheduled to take two years with completion by March 1990.

Accident data (1)\* have shown that the regions of a car most frequently causing serious pedestrian accident injury are:

The leading edge of the bonnet and wings, the top of the bonnet and wings, including the scuttle and lower edge of the windscreen, the bumper and the A post.

Research has shown that acceptable levels of safety may be given to all of these areas (2, 3, 4) except the "A post" which requires further work to develop practical and effective improvements.

## Possible test methods

Various outline proposals for test methods to evaluate pedestrian protection have been discussed in the literature (5, 6, 7, 8) which include full scale dummy tests, sub-systems testing and mathematical computer simulations. All of these proposals considered the important influences of vehicle speed, the height of the pedestrian victim and the

overall frontal shape of the car on the severity of each phase of an impact.

*Full scale dummy tests* require a sophisticated dummy that is robust and has stiffness characteristics that represent a human frame. A dummy automatically responds to, and takes account of the shape of the vehicle under test, but it will only evaluate a narrow strip of bonnet top across the width of a car for each size of dummy used. The dummy is liable to be damaged in the tests and assessment of each phase of the impact is difficult. Repeatability is uncertain.

*Sub-systems tests* may be to any precise location on a car using robust impactors. Evaluation of each impact is simpler than for dummy tests, with good repeatability and a more rigorous examination of the vehicle structure.

The design of the impactors must reflect the important characteristics of pedestrians body regions that may make contact with the vehicle structure under test.

The variations on the severity of pedestrian impact, resulting from the influence of different frontal car shapes, may be allowed for, by corresponding pre-determined variations of the impactor momentum for the tests.

*Mathematical computer simulations* are a more complex method of determining the test requirements of sub-systems tests.

The simulation model must be validated over the full range of the vehicle shapes that are to be tested. The data set of the pedestrian must represent human stiffness and response characteristics. Each car has its own unique data set, describing the shape and the dynamic crush characteristics of the different vehicle structures under test.

The crush characteristics would be determined by progressive sub-systems tests starting with the bumper. The impact data from leg to bumper sub-systems tests would be fed into the simulation model, so that it may progress to and define the requirements of the bonnet leading edge sub-systems test. The result of the bonnet edge test would similarly be fed back into the simulation model, so that it may progress to and define the requirements of the bonnet top sub-system test.

This method would be more precise than using pre-determined typical values for the test conditions, but the increased precision is not important when providing safety for a potentially wide mix of pedestrian accident victims.

## Proposed Test Method

Of these options the Group has been given the objective of developing sub-system tests to assess the safety performance of the bumper, the bonnet leading edge and the bonnet top. The impact requirements of the sub-systems tests are to be based on pre-determined typical values relating to salient structural dimensions that describes the general frontal car shape.

This method avoids the difficulties and variables of dummy testing. It also avoids the need to develop and approve computer simulation programs and data sets representing pedestrians for inclusion in a regulation.

\*Numbers in parentheses designate references at end of paper.

Determination of the appropriate impact test condition would also be simplified.

This paper describes the objectives and the methods that will be adopted in developing the test proposals.

## Mathematical Computer Simulations

### The role of computer simulation

In previous EEVC reports dealing with pedestrian safety (1, 5) the values of mathematical models especially in combination with component or sub-systems testing has been well recognised.

Computer simulation models have been extensively used to obtain a better understanding of the interactions in an impact between a pedestrian and a vehicle and of the influence that changes in a cars frontal shape would have on these interactions (9).

Based on the results of these simulations, a set of guide lines were proposed specifying the depth and stiffness of protection required to be built into the components of the fronts of cars for the safety of pedestrians as well as suggestions for sub-systems testing (7).

The use of a simulation to obtain the basic data, allowed a wide range of idealistic vehicle shapes to be studied and parameters calculated, that would be difficult to obtain from any full scale dummy or cadaver tests.

### Validation

To justify using simulation data of this type as a basis for determining test requirements, it is essential that the model used for simulations has been fully validated and shown to give a correct interpretation of the impact conditions.

The series of simulations outlined above was validated against a series of full scale dummy tests for the parameters that could be directly compared.

To support this existing data, further simulations will be undertaken using a different model to give a broader set of data and a more comprehensive validation, particularly in the areas that are difficult to measure by full scale tests.

### Proposed simulation model

This additional validation will be done by TNO using a Madymo model. A review of existing models (10) showed that they varied considerably in their complexity. The simpler 2 dimensional models with a limited number of segments can offer satisfactory results, but the reliability improves slightly as the number of segments defining the dummy is increased and also if a 3 dimensional version is used (11).

To obtain the best use of computing time and accuracy of complex models, the 2 dimensional version will be used for the parametric study of this work and the 3 dimensional model will be used to analyse the influence of leg position on impact characteristics. Both models have previously been validated for pedestrians and cyclists (12, 13).

## Contact model

One of the most important aspects concerning the simulation of pedestrian accidents is the representation of the contacts between vehicle and pedestrian, especially for the edge contacts.

The research mentioned above leading to safety guidelines used a Calspan 3D CVS program that had been modified to give an improved contact model (9). In this model the vehicle contact surface consisted of up to 30 rectangular plane panels (figure 1).

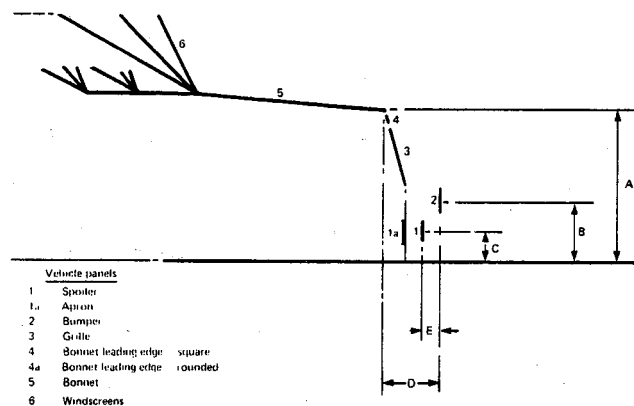


Figure 1. Vehicle simulation panels Calspan 3D program.

In the Madymo pedestrian models the external geometrics of pedestrians and vehicles are simulated by hyper-ellipses and planes (figure 2). This use of a different type of model should reduce the risk of the two models containing similar basic weaknesses.

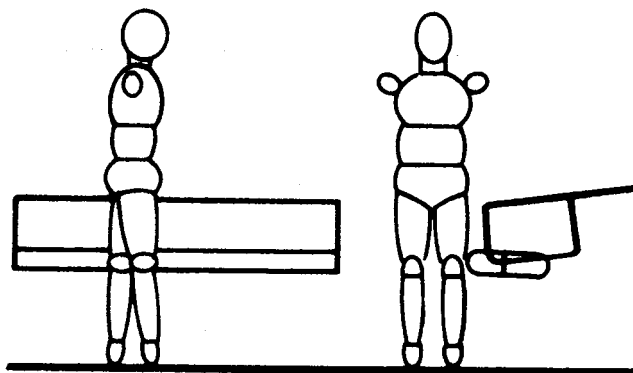


Figure 2. Madymo pedestrian simulation.

## Dummies simulated

To make the validation of existing data as comprehensive as possible the dummy that is modelled in this study will be different to the Ogle dummy simulated in the Calspan programme. In this exercise the model will simulate a TNO 6 years old child dummy and a Part #572, 50th percentile dummy that has improved neck and knee joints.

## Research programme

The schedule of the simulations undertaken will be based on the following conditions and requirements:

(1) The vehicle impact speed simulated will be 40 km/h.

(2) The output data will include the impact locations of the different segments of the pedestrian model to the vehicle, as well as the effective masses of these segments. The impact forces and penetrations will be calculated as well as the lateral bending angle of the knee.

(3) The influence of vehicle shape will be studied for the range of vehicle dimensions shown below. These will include current styles of cars and possible future trends (figure 3).

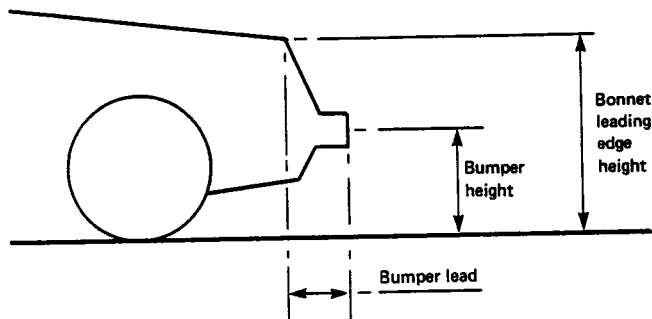


Figure 3. Definition of vehicle dimensions.

Bonnet Leading Edge Heights—from 600 to 800 mm

Bumper Leads—from 100 to 350 mm

Bumper Vertical Depth—100 mm minimum

Bumper centre height—330–450 mm.

(4) The choice of the range of vehicle shapes simulated, will be developed as the work progresses, so that the study concentrates on the areas of significant change in pedestrian impact severity.

(5) The influence of vehicle stiffness will be studied. The strengths simulated will range between the minimum required to give a durable and viable structure for normal use and the maximum stiffness that gives reasonable penetration and safe loadings for the pedestrian.

## Bonnet Top—Sub-system Test

Head injuries are the most frequent cause of pedestrian fatalities and these often result from striking the top of the bonnet (1).

Head impact may be to any part of the structures adjacent to the bonnet top and all of these elements are included in the following studies by BAST to develop a bonnet top sub-systems test (14).

### Test method

The objective is to develop a test procedure in which impactors are propelled into the tops of bonnets, wings scuttle and windscreen lower frames to assess the safety potential of the structure.

The impactors will represent child and adult headforms,

for tests to the forward and rearward sections of the bonnet respectively.

Headform impact conditions appropriate for vehicle to pedestrian impact velocities of up to 40 km/h will be considered with adjustments made to the test conditions to allow for the influence of the vehicles frontal shape.

The test methods will only assess injury potential resulting from linear accelerations. The group acknowledge that rotational acceleration may be an important feature of head injury; we believe however that there is insufficient information currently available to justify introducing rotational acceleration measurements into a proposal for test methods.

## Accident data

Accident data (1) reported that head injuries were more frequently caused by impact with the vehicle rather than with the ground.

A recent indepth study of 529 pedestrian accidents (15) reported that for impacts in the speed range 30 to 50 km/h, 87 per cent of the pedestrians suffered head injury.

Brain injury was reported in 25 per cent of the child and 20 per cent of the adult cases at speeds below 30 km/h. These values increased to 45 and 52 per cent respectively in the speed range 30 to 50 km/h and to 68 and 63 per cent respectively for speeds between 50 and 70 km/h.

Fractures of skull or facial bones were found to occur infrequently at low speeds and were reported in only 5 per cent of the child and 15 per cent of the adult cases for speeds of 30 to 50 km/h. These values increased to 18 per cent and 32 per cent respectively in the speed range 50 to 70 km/h. When fractures occurred they were often associated with brain injuries. For accidents at less than 70 km/h, more than 50 per cent of severe head injuries (without soft tissue injuries) were combined brain injury and facial or skull bone fractures.

Soft tissue injuries occurred frequently at any impact speed, but they were of minor severity. In the speed range of 30 to 50 km/h nearly 80 per cent of the pedestrians suffered soft tissue injuries, mostly to the forehead.

## Full scale tests and simulations

The results from full scale impact tests with pedestrian dummies and cadavers and also of computer simulations have shown the overall kinematics of head impact (9, 16, 17, 18).

These showed that the head of an adult most frequently strikes the rearward part of the bonnet top, the windscreen frame or the windscreen itself. The head impacts of children are more frequently to the frontal part of the bonnet top.

The results also showed the variation of velocity and direction of motion at impact and an indication of the average effective mass.

## Test equipment

To study these impact conditions a special hydraulic impactor has been developed for BAST which is able to propel dummy parts at velocities up to 50 km/h against the

outer surfaces of a test car (figure 4). This device will be used for the development of the headform test methods to achieve the necessary headform velocities and impact directions.

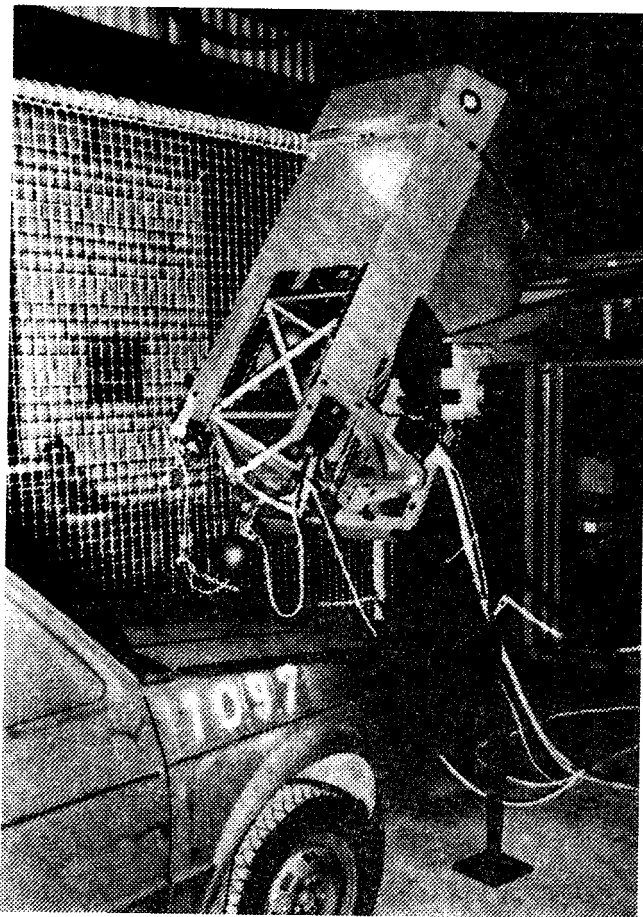


Figure 4. Hydraulic gun for head impact tests.

### Headform impactor

The child and adult headforms will be spheres of different sizes, weights and materials. Their weights will be 6.8 kg for the adult headform and 2.5 kg for the child headform; the diameters will be 165 mm and 130 mm respectively.

This specification was proposed in the original TRRL guide lines ERGA Doc/S60 but if necessary, changes will be made to the headforms as the work progresses.

Skin coverings of silicone material have been developed and fitted to both headforms.

### Instrumentation

The headforms are instrumented with one set of triaxial accelerometers at the centre of mass of the headforms. Measurements are also taken of impact velocity and structural deformations of the test car. Load measuring foils (Fuji foil) are used in the development programme to give an indication of surface pressure during impact. This will help to assess whether further work will be necessary to evaluate the risk of skull fracture from impact with a bonnet top that

has been designed to give acceptable headform accelerations.

Head injury criterion (HIC) will be calculated from the accelerometer time histories.

### Development programme

The headforms have been calibrated and some pre test runs completed.

The continuing programme will include the following stages:

(1) The influence of shape will be studied with respect to the results of simulation and full scale tests.

(2) The resulting head accelerations and dents in the bonnets from the sub systems tests, based on the findings of (1) above will be compared with those obtained in full scale tests.

The adult sub-systems tests will be validated by comparisons with car/cadaver tests previously conducted by INRETS.

For child headform validation, only dummy tests are available. The tests of BAST, INRETS and TNO in the frame of the Biomechanics programme (19) using a dummy representing a six year old child will be utilised for these comparisons.

(3) Protection criterion will be determined based on maximum acceleration for a given time, or by HIC.

(4) If further studies of accident investigations show the necessity for frangible headforms, these will be considered later in the project.

### Bonnet Leading Edge Sub-Systems Test

In a pedestrian accident the severity of the impacts with the leading edge of the bonnet vary widely with respect to the bonnet's location relative to the bumper and to the ground. Also the body regions that are most frequently injured range from the femur and pelvis of adults to the abdomen of young children.

The following studies by TRRL will take into account, these aspects, to develop a sub-systems test to assess the injury potential of the bonnet leading edge.

### Requirement of test method

The objective is to develop a test procedure in which impactors are propelled into the leading edges of the bonnet and wings and to the headlight surround, as necessary, to assess the safety potential of the structure.

The safety requirements of the aged adult pelvis and femur and the child upper abdomen will be studied and suitable impactors developed.

Impact test conditions appropriate for vehicle to pedestrian impact velocities of up to 40 km/h, will be considered with adjustments made to the test conditions to allow for the influence of the vehicles' frontal shape.

## Accident data

Accident data (1) shows that the aged adult femur and pelvis are most frequently at risk from bonnet edge impacts. These injuries although serious are rarely life threatening.

This data also suggests that the child and adult abdomen followed by the child thorax although less frequently involved are most at risk from life threatening injuries. A USA sample (20) based on the concept of HARM (21) showed for the child the thorax to be much more at risk than the abdomen, but these differences could probably be attributed to different definitions of the composition of the thorax and abdomen.

To obtain a clearer understanding of the abdominal, thoracic injuries, data has been extracted from the Scottish Hospitals In Patients Statistics (SHIPS) data source (22) which combines in-patient data for Scotland with police accident data. This data gives the injury and severity without attributing the cause.

The sample contained 5298 pedestrians aged 0-14 years and 7255 over 15 years old who received in patient treatment.

The frequency and the severity of injuries to each body region have been weighted by a HARM factor based on reported injury costs (21) using the scale shown in table 2 and the percentage of total injury and HARM weighted injury for each body region are shown in table 3.

AIS	1	2	3	4	5	6
HARM WEIGHTING	.7	3.0	9.2	56.7	232.2	264.9

**Table 2. Relationships between AIS and HARM weighting factor based on injury costs.**

BODY REGION	All injuries to each body region as percentage of total injury count			
	Based on frequency		Based on HARM	
	0-14 YEARS	15-99 YEARS	0-14 YEARS	15-99 YEARS
Lower Limb	53.5	37	34.5	34
Lower Abdomen	.3	.6	.9	2.1
Abdomen unspecified	1.0	.4	2	2
Upper Abdomen	.8	.3	17.4	7
Thorax	1	5	4.5	7
Spine	.4	2	.4	4.0
Head	35	41.7	36	35.7
Upper limbs	8	13	4.2	8.2
Total	100	100	100	100

**Table 3. Percentage distribution of injury by body region based on frequency and HARM for Scottish Hospitals (SHIPS) pedestrian accident data.**

The abdominal data is shown divided into three sections. The lower abdomen includes all of the organs of the lower trunk up to the bottom of the rib cage. The upper abdomen consists of the portion of the abdomen inside the rib cage

and below the diaphragm and includes the liver spleen and kidneys.

These results show that all of the abdomen suffers less than 2 percent of the total number of injuries suffered by all body regions. On the basis of HARM however the child upper abdomen suffers 17.4 percent of all injury and the adult upper abdomen 7 percent.

## Full scale tests and simulations

Reported impact tests on different simulated shapes of cars (18, 23) gave details of the energy absorbed in the front structure, the impulse of the impact (momentum change) and the mean effective mass of the contact.

These show that both the severity and the direction of impact to the bonnet leading edge vary in a regular pattern with respect to the overall shape of the front of a car. Typically each impact consisted of two separate phases. The initial part of the impact which accelerates the struck body region of the dummy up to the speed of the vehicle. This was followed by a period of more variable duration when force was transmitted through the impacted body region to the more remote segments of the dummy.

## Test equipment

To study those variations in test conditions a small trolley has been built to propel impactors into the fronts of cars at speeds up to 40 km/h.

The impactors will be mounted on a ram and just prior to impact the trolley will be stopped allowing the ram guided impactor to run freely into the test car.

The first tests will be with an impactor representing a femur (figure 5), later tests will include an impactor representing a child's upper abdomen. The femur impactor will in the research stage, include measurements of bending moment, force, acceleration and impact velocity. Measurements of panel deformation will also be obtained.

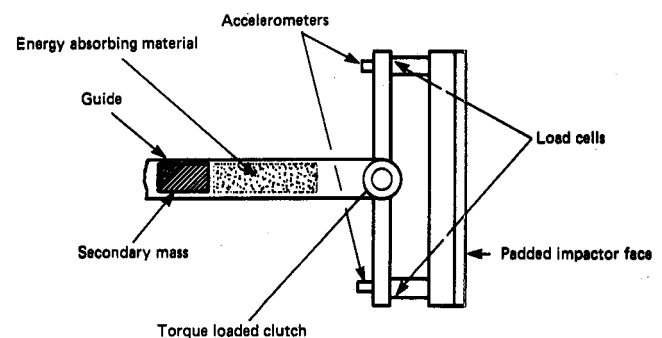


**Figure 5. Femur impactor.**

The femur impactor is mounted via a torque loaded pin joint so that, if necessary, the action of a pedestrian pivoting around the bonnet leading edge may be reproduced.

A test trolley has been used for the development stage of this work to allow the choice of a wide range of impacts and mounting conditions which can be changed rapidly. Alternative forms of propulsion system will be considered as the work progresses and the final requirements become more firmly established.

## Development programme

The programme to develop the test methods will include the following stages:

(1) Mathematical computer simulation comparing dummy and impactor tests to identify the principal design requirements of an impactor guidance system.

(2) Conduct impactor tests against a range of simulated car shapes and develop the impactor as necessary to reproduce reported variations in impact severity.

(3) Validate the test method by comparing resulting impactor accelerations and dents in the bonnet leading edges from the sub-systems tests with results from full scale dummy tests. The vehicles damage will also be compared with the existing results of cadaver tests conducted by INRETS and adjustments to the test method will be made as necessary.

(4) Conduct repeatability tests on the finalised system.

## Bumper sub-systems test

The bumper is one of the most frequently involved parts of a car in pedestrian accidents. The body regions that are most likely to be injured are the upper or lower legs, or the knee joint, depending upon the relative heights of the bumper and of the pedestrian. Although the resulting injuries are rarely life threatening they can have long term consequences, such as permanent disability, particularly for the knee joint (24).

These variations of impact conditions will be included in research by INRETS to develop a sub-systems test to evaluate the protection afforded by bumpers.

## Requirements of test method

The objectives of the following research are to develop a test method in which an impactor is propelled into a bumper (and if appropriate the air dam) to assess the safety potential of the structure.

The tests will be conducted at velocities up to 40 km/h and the impactors to be developed, will reflect the mass and size variations of the legs of children and adults.

## Accident data

Published data (25, 26) report that between 70 and 85 percent of pedestrians involved in an accident, sustain a leg injury. In the SHIPS data table 3, 53 per cent of all child injuries and 37 percent of all adult injuries were to the legs.

## Full scale tests and simulations

Research using cadavers has been performed in recent years to obtain a better understanding of the detailed mechanism of leg injury in pedestrian accidents (27, 28). The conclusions from these studies are:

(1) Pedestrian leg injuries may occur either at knee level (ligament/joint injuries) or to the long bone (tibia fibula) fractures.

(2) The knee joint injuries are related to bending moments applied to the knee.

(3) The long bone fractures appear to be related to shearing forces at the impact point.

(4) The shape of the striking surfaces, (Bumper/front face) and their stiffness distribution, has a clear influence on the frequency and severity of leg injuries.

(5) There is less probability of a knee joint injury resulting from an impact by a low mounted bumper (380 mm above the ground).

(6) With present designs of cars and bumpers, leg injuries can occur at impact speeds of 20/25 km/h or more.

Computer simulation (9) has predicted that when a pedestrian is struck by a car, the magnitude of the impact energy of the bumper, is not dependent on the frontal shape of the car, except for designs with a short bumper lead.

## Test equipment

A propulsion system will be developed to guide the impactors, horizontally into the bumper.

Two impactors will be developed. One will represent an adult leg and the second a child leg.

Each impactor will consist of two segments representing the upper and lower legs with an articulated joint representing the knee. Two types of joint will be considered; a deformable steel bar and a torque controlled hinge joint.

The designs will reflect the experience gained with a symmetrical pedestrian dummy developed by Chambers University and INRETS (29).

In the experimental stages strain gauges and transducers will be fitted to the impactors to measure bending moments at the knee and shear forces in the lower leg at the point of impact.

## Development programme

A series of impacts of a trolley mounted bumper into the legs of cadavers have been completed by INRETS prior to the start of this project.

The programme to develop this test method will include:

(1) An analysis of these tests and other existing cadaver test data, to determine the apparent mass and the stiffness (force deformation characteristics) of the body parts in contact with the bumper.

(2) The information determined in (1) above will be used to develop, two, double segment impactors. One impactor to represent a child leg the other an adult. The size of the impactors will represent the anthropometry of the pedestrians that are shown by statistics to be most frequently involved in accidents.

(3) The development of the knee joint will compare the performances of the torque controlled hinge and a flexible bar system. The use of strain gauges to measure knee bending moment will also be compared with the direct measurement of flexion angle.

(4) The determination of the shear force in the long

bone is more complex, because the maximum force occurs at the impact point on the leg, and this may vary according to the geometry of the car front to be tested.

Methods to be considered include an adjustable shear force transducer which can be pre-positioned according to the geometry of the car front to be tested.

(5) Tolerance values for the adult, will be developed from the results of cadaver work. For the child, relevant biomechanical data is not available and published results of animal tests and scaled down adult values will be considered as a guide to develop tolerance values.

(6) The test procedures and the impactors will be validated by two series of tests. One by comparison with cadaver pedestrian tests performed with the same type of car. In a second series different types of car will be used to test the effectiveness of the procedure against a range of car shapes.

## Compatibility

When test methods and safety requirements are proposed, it is not sufficient to just demonstrate that the proposals are possible, it is also necessary that they are seen to be practical from an operational, an engineering and a cost viewpoint.

With respect to pedestrian protection requirements, there are several important, compatibility aspects to be considered and this work will primarily be undertaken by Laboratoire de Physiologie et de Biomecanique APR. Guidance on the requirements for structural deformation, with respect to vehicle shape will be derived from the simulation work by TNO.

## Objectives

The programme of work for this section of the project may be modified as the requirements of the proposals become more firmly established, but the principal objectives are as follows:

(i) Determine the magnitude of any conflict between proposals for pedestrian safety and current regulations or possible future requirements.

Areas of possible conflict that will require particular attention are:

The bumper requirement for exterior protection. Engine compartment and emission control requirements. Changing aerodynamic shape to reduce fuel consumption. The requirements of sensors for air bags and seat belt tensioners.

The introduction of new materials.

(ii) Obtain an estimate of the extent to which current designs of popular cars meet the safety proposals. Identify the areas where for some types of car it will be difficult to meet the standards proposed.

(iii) Quantify the penalties that may result from introducing the proposed standard.

## Conclusions

A programme of research has been described to develop sub-systems tests, that evaluates the protection offered to pedestrians by passenger cars. Test methods will be developed by BAST.INRETS and TRRL to assess the protection at three discrete areas of the front of cars: the bumper, the bonnet leading edge and the bonnet top.

The test methods will be based on vehicle impact speeds of up to 40 km/h and will consider the requirements of both child and adult pedestrians. The bonnet leading edge and bonnet top test conditions will reflect the changes, resulting from the influence of the general shape of the front of the car.

Base line data for the studies will be drawn wherever possible from existing research, but further computer simulations by TNO will be included to obtain further evidence of the influence of vehicle shape and structural stiffness or impact severity.

Studies by APR to show if these proposals are practical supported by the results of simulations by TNO, will assess their compatibility with current regulations, operational requirements or possible future development.

The extent to which some typical current designs of popular cars meet the safety proposals, will be assessed, together with the cost and the penalties that may result from meeting them.

## References

- (1) EEVC Committee "Pedestrian Injury Accidents". Proceedings Ninth International Technical Conference on Experimental Safety Vehicles Kyoto Japan, November 1982.
- (2) Wollert, W. et al., "Realisation of Pedestrian Protection Measures on Cars." Proceedings Pedestrian Impact and Injury Assessment, SAE Detroit USA March 1983.
- (3) Kessler, J.W., "Development of Countermeasures to reduce pedestrian head injury." Proceedings Eleventh International Technical Conference on Experimental Safety Vehicles, Washington USA May 1987.
- (4) Hobbs, C.A. et al. "PSCI—Demonstration Car With Improvements for Pedestrian Protection." Proceedings Tenth International Technical Conference on Experimental Safety Vehicles, Oxford, Great Britain. July 1985.
- (5) EEVC Committee. "Pedestrian Injury Protection by Car Design". Tenth International Technical Conference on Experimental Safety Vehicles, Oxford, Great Britain. July 1985.
- (6) Stuertz, G., "Experimental Simulation of the Pedestrian Impact." Tenth International Technical Conference on Experimental Safety Vehicles, Oxford, Great Britain. July 1985.
- (7) Harris, J., "Simplified Test Recommendations for Pedestrian Protection" Proceedings Tenth International Technical Conference on Experimental Safety Vehicles. Oxford, Great Britain. July 1985.

- (8) Hamilton, M.N., "Experimental Study of Thoracic Injury in Child Pedestrians." Proceedings Eleventh International Technical Conference on Experimental Safety Vehicles, Washington USA May 1987.
- (9) Harris, J. N.D. Grew, "The Influence of Car Design on Pedestrian Protection." Proceedings Tenth International Technical Conference on Experimental Safety Vehicles Oxford, Great Britain. July 1985.
- (10) Wismans, J., J. Van Wijk, "Mathematical Models for the Assessment of Pedestrian Protection Provided by a Car Contour." Proceedings Ninth International Technical Conference in Experimental Safety Vehicles. Kyoto Japan, November 1982.
- (11) Wijk J. van, et al., "Madymo Pedestrian Simulations." Proceedings Pedestrian Impact and Injury Assessment, SAE Detroit USA March 1983.
- (12) Janssen, E.G., J. Wismans, "Experimental and Mathematical Simulation of Pedestrian—Vehicle and Cyclist—Vehicle Accidents." Proceedings Tenth International Technical Conference on Experimental Safety Vehicles, Oxford, Great Britain, July 1985.
- (13) Janssen, E.G., J. Wismans, "Evaluation of Vehicle—Cyclist Impacts Through Dummy and Human Cadaver Tests." Proceedings Eleventh International Technical Conference on Experimental Safety Vehicles. Washington USA May 1987.
- (14) Lestrelin, D. et al., "Vehicle Pedestrian Head Impacts—a Computer Method for Rating a Profile Without Previous Mathematical Modelization." Proceedings Tenth International Technical Conference on Experimental Safety Vehicles, Oxford, Great Britain July 1985.
- (15) Otte, D.: Einfluss der Fahrzeugfrontgeometrie auf die Verletzungssituation von verunfallten Fussgaegern, Studie der Unfallforschung der MHH im Auftrag der BAST, 4/88.
- (16) Brun-Cassan, F. et al, "Reconstruction of Actual Car—Pedestrian Collisions with Dummy and Cadavers." Proceedings Pedestrian Impact and Injury Assessment. SAE Detroit USA March 1983.
- (17) Cavallero, C. et al., "Improvement of Pedestrian Safety: Influence of Shape of Passenger Car-front Structures Upon Pedestrian Kinematics and Injuries: Evaluation Based on 50 Cadaver Tests." Proceedings Pedestrian Impact and Injury Assessment SAE Detroit USA March 1983.
- (18) Lawrence, G.J.L., J. Harris, "Car to Pedestrian Impact Energies and Their Application to Sub-system Testing." Proceedings Eleventh International Technical Conference on Experimental Safety Vehicles, Washington, USA. May 1987.
- (19) Faerber, E., "Synthesis Report of Phase 3, Project G6 Proposed Standardized Pedestrian Test Methodology." Proceedings Biomechanics of Impacts in Road Accidents, Brussels, Belgium. March 1983.
- (20) MacLaughlin, T.F., et al, "NHTSA's Advanced Pedestrian Protection Program." Proceedings Eleventh International Technical Conference on Experimental Safety Vehicles. Washington USA May 1987.
- (21) Malliaris, A.C. et al., "Harm Causation and Ranking in Crashes." SAE Paper 850090 February 1985.
- (22) Stone, R.D., "Computer Linkage of Transport and Health Data." Department of the Environment. Department of Transport TRRL Report LR 1130. Crowthorne 1984 (Transport and Road Research Laboratory).
- (23) Lawrence, G.J.L., "The Influence of Car Shape on Pedestrian Impact Energies and Its Application to Sub-system tests." Proceedings Twelfth International Technical Conference on Experimental Safety Vehicles, Gothenburg, Sweden, May 1989.
- (24) Bunkertorp, O., et al., "Clinical Studies on Leg Injuries in Car Pedestrian Accidents." Proceedings 1981 IRCOBI Conference Salon de Provence, France. September 1981.
- (25) Ashton, S.J., et al., "Pedestrian Injuries and the Car Exterior." Society of Automotive Engineers Transactions Paper 770092 Warrendale: Society of Automotive Engineers, 1977.
- (26) Garret, J.W., et al., "Pedestrian Injury Causation Parameters.: U.S. Contract DOT-HS-7-01579. Report No. DOT-HS-806-148 October 1981.
- (27) Bunkertorp, O., et al., "Experimental Studies on Leg Injuries in Car to Pedestrian Accidents." Proceedings 1981 IRCOBI Conference. Salon de Provence France, September 1981.
- (28) Cesari, D., et al., "Interaction Between Human Leg and Car Bumper in Pedestrian Tests." Proceedings 1981 IRCOBI Conference. Bergisch Gladbach (FRG). September 1988.
- (29) Aldman, B., et al., "A New Dummy for Pedestrian Test." Proceedings of Tenth International Technical Conference on Experimental Safety Vehicles. Oxford, Great Britain, July 1985.

## Annex 1

List of participants in EEVC Working Group 10:

Mrs. F. Brun-Cassan, APR, France  
 D. Cesari, INRET, France  
 G. Ferrero, Fiat, Italy  
 K.P. Glaeser, BAST, FRG  
 N.D. Grew, SMMT, U.K.  
 J. Harris, TRRL, U.K. Chairman  
 W. Heiss, Daimler-Benz, FRG  
 E. Janssen, TNO, Netherlands  
 G.J.L. Lawrence, TRRL, U.K.  
 H. Mellander, Volvo, Sweden

# NHTSA Pedestrian Head Injury Mitigation Research Program—Status Report —

**John Kessler and Michael Monk,**  
National Highway Traffic Safety Administration  
United States

## Abstract

This paper reports the current status of the National Highway Traffic Safety Administration's (NHTSA) pedestrian head-injury reduction research program. The pedestrian injury statistics of the United States are briefly reviewed and relationships between measured responses in laboratory testing and field injuries are offered.

The elements which are necessary to prescribe a test procedure are identified and discussed. Some possible test procedures are presented, and the data upon which a choice could be made is provided.

Various measurements of current U.S. vehicles are provided. These include geometrical measurements of the front ends, measurements of the underhood clearance and impact response measurements from testing with a pedestrian headform impactor. One vehicle is discussed which exhibited exceptional hood clearance and impact response measurements.

## Introduction

The National Highway Traffic Safety Administration (NHTSA) is continuing a research program aimed at reducing the numbers of deaths and injuries which occur in pedestrian head impacts. A tentative test procedure, the results of pedestrian accident reconstructions and limited production vehicle testing were presented at the 11th ESV Conference. (1)\* This paper provides a brief review of the earlier work and presents the results of analysis and testing performed since that time.

The functional relationship between HIC and the probability of death (POD) has been subjected to further analysis. The POD was earlier derived based upon a study of injuries to all body regions. Since all of the pedestrian accidents were analyzed based upon only head injuries, an analysis was conducted to derive POD functions based upon head injuries. Two approaches were used. The newly derived POD functions were used to derive HIC-POD functions based upon only head injuries. The degree of difference between the new relationships and the previous one is noted and discussed.

The elements necessary to define a pedestrian head-impact test procedure are identified and discussed. Options are identified for some of the elements and example test procedures are presented. Data are provided from which to select a test procedure. The overall testing scheme is defined and example schemes are given.

Three types of measurements of production vehicles are provided. These are the frontal exterior geometry, the

underhood clearance measurements and the headform impact responses. The measurement of underhood clearance is in process, so only two examples of complete results are provided.

One of the better performing vehicles is used as an example of the type of protection which can be provided. The underhood clearance map, limited structural description and impact response characteristics for this vehicle are provided.

## Outline of Pedestrian Program Elements

The research for the pedestrian head injury reduction program can be separated into six major elements. These are: 1. analysis of field accident data, 2. establishment of correlations between measured laboratory responses and field injuries, 3. development of test procedures, 4. measurement of production vehicle frontal geometry, underhood clearance and headform impact response, 5. demonstration of improved performance in hood region, and 6. development of injury mitigation concepts for the more difficult cowl and hood/fender regions.

## Analysis of Field Accident Data

Accident data analysis has shown that 35% of the harm (2) to pedestrians results from injuries to the head, for vehicle impact speeds of 30 mph or less. (3) Figure 1 shows the distribution of pedestrian harm by body region for this impact speed range. Forty percent of the harm is due to injuries to the thorax. Reduction of pedestrian thoracic injuries is being researched in a parallel NHTSA study. (4) Figure 2 illustrates the distribution of harm by injury source. The data from figures 1 and 2 were combined to form table 1, which shows the most harmful injury source/body region combinations. (3) Head impacts to hood, fenders and vehicle face account for approximately 19% of the harm.

## Correlations Between Measured Laboratory Responses and Field Injuries

Experimental reconstructions of selected pedestrian accidents were performed in order to better understand the relationships between responses which can be measured in the laboratory and the field injuries. These were presented at the 11th ESV Conference. (1) The accident cases were selected from the Pedestrian Injury Causation Study (PICS), a file of pedestrian accidents containing about 2000 cases collected from 1977 to 1980. The reconstruction testing was performed with a mechanical headform (this will be reviewed in a later section of this report) which was used to impact into the vehicle frontal surfaces. The severity was matched by adjusting the velocity and mass until the damage profile matched that of the accident case. The

\*Numbers in parentheses designate references at end of paper.

acceleration of the headform was recorded and used to compute the Head Injury Criterion (HIC). The HIC values were then correlated with various injury measures including the maximum AIS.

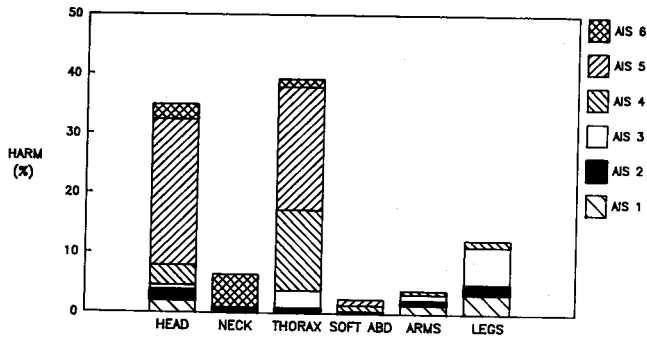


Figure 1. Distribution of pedestrian harm by body region and injury severity for impact speeds  $\leq 30$  mph.

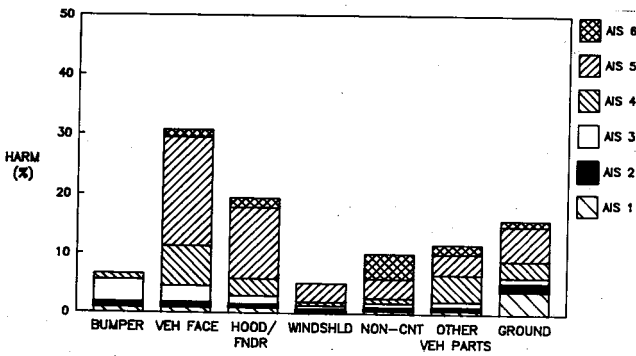


Figure 2. Distribution of pedestrian harm by injury source and injury severity for impact speeds  $\leq 30$  mph.

Table 1. Most harmful injury source/body region contacts for impact speeds  $\leq 30$  mph.

Injury Source/Body Region	Harm (%)
Vehicle Face/Thorax	17
Hood-Fenders/Head	11
Ground/Head	10
Other Vehicle Parts/Thorax	9
Vehicle Face/Head	8
Hood-Fenders/Thorax	7
Bumper/Legs	7
Non-contact/Neck	5
Windshield/Head	5
	79%

A plot of the measured HIC values for 14 adult pedestrian reconstructions along with the maximum AIS levels is shown in figure 3. The r-squared value is noted to be .68, which indicates fair correlation. The maximum AIS alone does not give a complete indication of the severity of the injuries to the pedestrian because of the other injuries which occurred. A method has been presented by which the 3 highest AIS levels are used to estimate the probability of death (POD) associated with the injuries. (5) This method was used to estimate the POD for each of the 14 pedestrian cases. The presentation of HIC and POD is shown in figure 4. This is noted to result in improved correlation, with an r-squared value of .94.

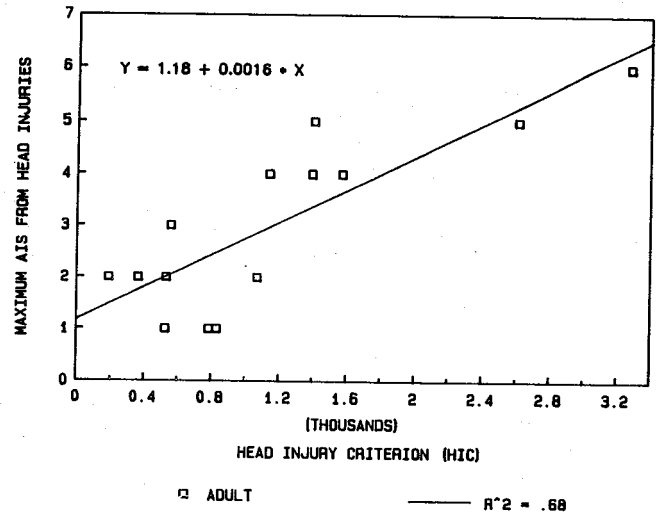


Figure 3. HIC reconstructions—normalized HIC versus maximum head AIS (adults only).

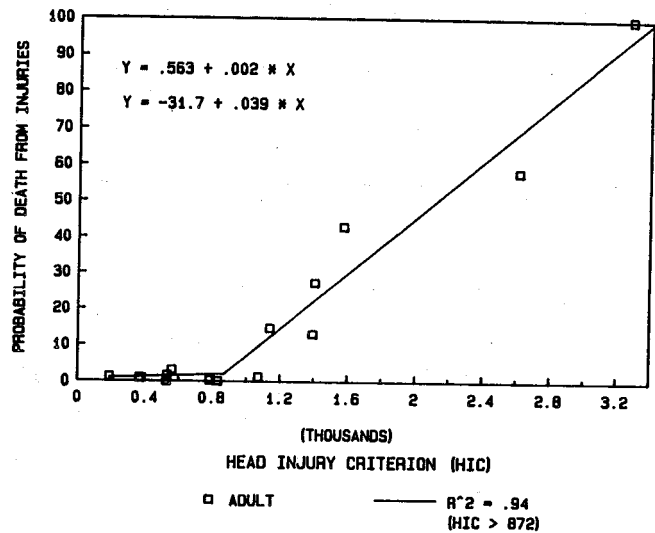


Figure 4. HIC reconstructions—normalized HIC versus probability of death (adults only).

The method of estimating POD was based upon the 3 highest AIS levels to all body regions. However, in the pedestrian reconstruction study, only head injuries were considered. This was a potential source of inaccuracy since the POD associated with 3 head injuries of given severity levels could differ from the POD associated with three injuries to other body regions with the same severity level. A separate analysis of POD was performed using only head injuries. (6) Two separate methods were explored, one being identical to the Ulman approach except that only head injuries were considered, and the other being the method reported by Eppinger in the 11th ESV. (7) The Eppinger method is based upon an optimization rather than regression approach. The details of the methods are contained in Reference 6.

Table 2 contains the POD for combinations of AIS. The first column is from the Ulman study, based upon 3 highest

AIS to all body regions, the second column is the same approach except applied to head injuries, and the third

column is the Eppinger approach. It is noted that the Eppinger approach utilizes only the 2 highest AIS codings.

Table 2. Death probabilities associated with Ulman model and regression and optimization methods.

	AIS Comb'n			Ulman Model	Regression Method	Optimiz'n Method
				'79-86 All Reg	Head Inj	'82-85 Head Inj
1	1	0	0	0.05	*	0.10
2	1	1	0	0.07	*	0.20
3	1	1	1	0.09	*	
4	2	0	0	1.09	1.00	0.00
5	2	1	0	1.28	1.55	0.10
6	2	1	1	1.45	2.22	
7	2	2	0	1.62	3.00	0.00
8	2	2	1	1.78	3.90	
9	2	2	2	1.93	4.92	
10	3	0	0	2.11	31.28	10.60
11	3	1	0	2.45	35.88	10.69
12	3	1	1	2.80	40.67	
13	3	2	0	3.17	45.63	10.60
14	3	2	1	3.56	50.76	
15	3	2	2	3.96	56.06	
16	3	3	0	4.38	61.52	20.08
17	3	3	1	4.81	67.12	
18	3	3	2	5.26	72.87	
19	3	3	3	5.72	78.77	
20	4	0	0	12.01	23.81	26.10
21	4	1	0	13.30	25.88	26.17
22	4	1	1	14.66	28.02	
23	4	2	0	16.08	30.23	26.10
24	4	2	1	17.58	32.52	
25	4	2	2	19.41	34.87	
26	4	3	0	20.78	37.28	33.93
27	4	3	1	22.48	39.77	
28	4	3	2	24.26	42.32	
29	4	3	3	26.10	44.93	
30	4	4	0	28.02	47.61	45.39
31	4	4	1	30.00	50.36	
32	4	4	2	32.06	53.17	
33	4	4	3	34.19	56.04	
34	4	4	4	36.39	58.97	
35	5	0	0	17.03	31.73	33.00
36	5	1	0	18.71	35.04	33.07
37	5	1	1	20.49	38.58	
38	5	2	0	22.39	42.37	33.00
39	5	2	1	24.40	46.42	
40	5	2	2	26.55	50.74	
41	5	3	0	28.82	55.33	40.10
42	5	3	1	31.22	60.22	
43	5	3	2	33.76	65.42	
44	5	3	3	36.44	70.92	
45	5	4	0	39.26	76.75	50.49
46	5	4	1	42.24	82.91	
47	5	4	2	45.37	89.42	
48	5	4	3	48.66	96.29	
49	5	4	4	52.11	100.00	
50	5	5	0	55.72	100.00	55.11
51	5	5	1	59.51	100.00	
52	5	5	2	63.48	100.00	
53	5	5	3	67.63	100.00	
54	5	5	4	71.96	100.00	
55	5	5	5	76.49	100.00	
56	6	-	-	100.00	100.00	100.00

The HIC-POD relationships derived from applying the 3 models of POD to the 14 adult reconstructions are contained in figure 5. The Ulman data was fit equally well with a linear curve, as shown in figure 4, or a power curve. The Eppinger (optimization) data was fit best with a power curve and for

this reason, all three versions were compared using power curve fits. The value of HIC at which the POD begins to increase sharply is nearly the same for all three methods, varying between 900 and 1000. It was concluded in the study of Reference 6 that given the increased level of

uncertainty resulting from the sparseness of the data when all but head injuries are eliminated, the differences in observed POD are not very significant.

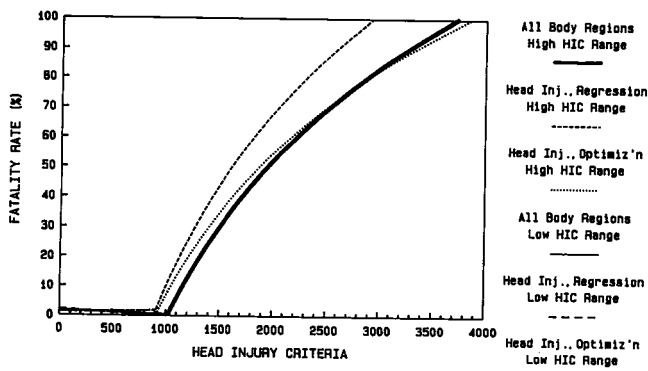


Figure 5. Fatality rate comparison/14 reconstructed cases.

## Test Procedure Development

In this section, several elements necessary to specify a test procedure will be identified. These elements will be discussed in terms of testing options. The hardware was documented in Reference 8 and will not be discussed in this paper.

### Pass/fail criteria

In the previous section, it was shown that the adult reconstructions resulted in a high degree of correlation between the measured HIC and the POD. It was also shown that the POD derived from head injury data did not differ markedly from the POD established in the Ulman study, which was derived from injuries to all body regions. The relationship of figure 4, derived from the Ulman study data, is used for reference here.

The POD begins to rise sharply beyond a HIC of 872 in the figure. At HIC=1000, the POD is 7%, and at HIC=2100, the POD is 50%. The only established use of HIC is FMVSS 208 which establishes 1000 as the pass/fail criterion. This appears to be supported by the pedestrian accident data as well.

### Definition of candidate zone

If testing for pedestrian head-impact protection is standardized, a target zone must be established. The target zone is that portion of the vehicle front end which is eligible for impact testing and which is required to meet the performance standard.

From the standpoint of pedestrian safety it is desirable to define the candidate zone as comprehensively as possible. The various zone alternatives will ultimately be weighed against the difficulty of meeting a proposed criterion. Some of the information relative to this trade-off will be shown.

A parameter called the "wrap around distance" (WAD) has been established to define where along the longitudinal direction of the vehicle the head impact occurs. The WAD is the distance from the ground to the head impact site, measured up and around the front surface of the vehicle. A

cumulative distribution of the WAD for the impacts occurring early in the PICS study (9) is shown in figure 6. It is noted that the slope of the line is somewhat constant at about 1.7% per inch of WAD. The "adult zone" defined in Reference 8 extends from 62 to 72 inches which includes about 26% of the population.

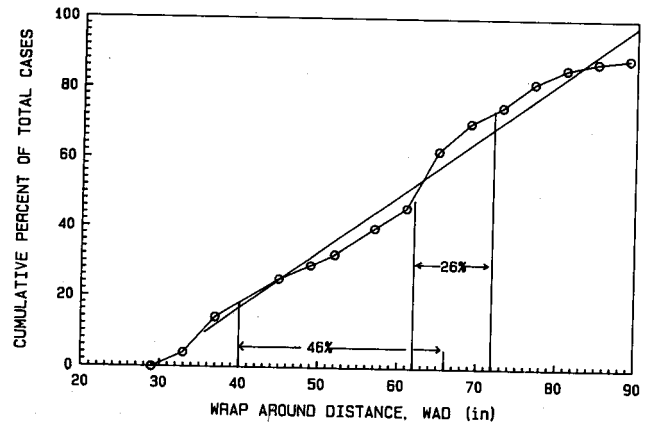


Figure 6. Cumulative percent distribution of accident cases with wrap around distance.

A similar presentation for the lateral distribution of head impacts is being prepared within the Agency. The longitudinal distribution of WAD and the lateral impact frequency distribution will provide the data for the definition of the candidate zone.

Again testing alternatives become apparent. The candidate zone could be ground based (tied directly to WAD) or vehicle based (referenced to vehicle components such as hood edges etc.). A possibility, given here only as an example, would be a zone of WAD and a lateral distance from the longitudinal centerline which falls within the hoods of most vehicles. For example, a zone extending from 40 to 66 inches WAD and 24 inches laterally from the centerline would define a zone of over 1248 square inches which would lie within the hood of most vehicles. This surface would include about 46% of the accidents based upon WAD but the actual percent would be less, based upon the portion of the lateral distribution not included.

An example of a vehicle based candidate zone might be the surface defined by the vehicle hood, or alternatively, all of the hood surface that is 6 inches from the outer edges. The latter definition would exclude the stiff region near the hood edges. One disadvantage of the vehicle based system is that it requires knowledge of the vehicle fleet in order to estimate benefits, since the accident data were collected using ground based rather than vehicle based references.

### Test mass

The testing discussed in Reference 8 was performed using both adult and child size impactors. It is most likely that any standardized test would be established based upon one mass of impactor. Currently the adult impactor being used by the Agency has a weight of 10 pounds.

## Test velocity

A possible test procedure presented by the Agency at the 11th ESV referenced a test velocity of 27 mph. It was pointed out that this was intended to represent the speed with which the head would impact the hood if the vehicle-to-pedestrian speed was 30 mph. The 30 mph impact speed was selected based upon the observation that approximately 90% of pedestrian impacts occur at speeds of 30 mph or less. (3)

The distribution of injuries (injuries and serious injuries to all body regions) with impact speed is shown in figure 7. It is noted that 87% of the injuries and 55% of the serious injuries occur at speeds of 30 mph or less. Table 3 contains the percentage of injuries and serious injuries corresponding to various accident speeds from 20 to 30 mph. The second column of the table indicates the head impact speed. Since very few vehicle HIC responses are below 1000 at the 27 mph impact speed, another possible test procedure option is to lower the test speed to an impact speed, another possible test procedure option is to lower the test speed to an impact speed corresponding to a 25 mph vehicle impact (23 mph head impact).

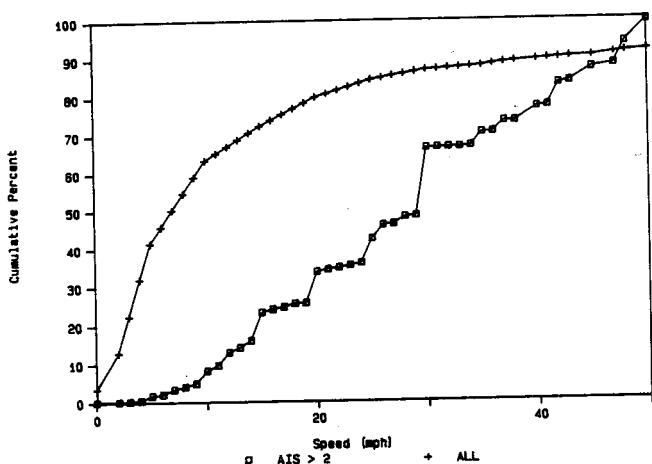


Figure 7. Vehicle impact speed vs. cumulative injuries for U.S. pedestrian accidents (Data Source: U.S. Nass, PICS).

Table 3. Cumulative injuries vs. accident and head impact speed.

Accident Impact Speed	Head Impact Speed	Percent All Injury Levels	Percent Serious Injury Levels
20	18.0	80%	30%
21	18.9	81%	33%
22	19.8	82%	35%
23	20.7	83%	38%
24	21.6	84%	40%
25	22.5	85%	43%
26	23.4	85%	45%
27	24.3	86%	48%
28	25.2	86%	50%
29	26.1	87%	53%
30	27.0	87%	55%

A study was performed to scale all of the production vehicle responses from 27 mph impacts to expected HIC responses at lower speeds. (10) The lower speed HIC is estimated from the following equation:

$$\text{HIC (low speed)} = \text{HIC (high speed)} * (\text{velocity ratio})^{2.93}$$

The exponent of 2.93 was derived empirically from a limited number of tests performed at differing speeds. The details of the study are contained in reference 10.

## Test scheme

The final element to a test procedure is the test scheme. Primarily, the test scheme identifies the number and location of tests within the candidate zone and the portion of the tests which have to meet the prescribed criterion.

The most simple scheme might be the performance of a single impact test at a randomly selected point within the candidate zone and require that the response meet the required HIC level. A more complex scheme might include the requirement that 15 impact locations be identified equally spaced within the zone, and that at least 9 must meet the HIC requirement.

If the scheme were based on a percentage of the zone passing the requirement, an option could be given to allow the designer to identify the location of a sub-zone with a particular percentage of the total area of the zone, in which the testing would be performed. This might then allow evaluation by performing only 1 (or a small number) test at a random position within the sub-zone identified by the designer.

The preceding discussion has identified various elements pertaining to test procedure development. The data pertinent to making trade-offs has been identified and for the most part provided. Examples of the types of test conditions which could be adopted have been given.

## Production Vehicle Measurement

The geometric measurements and headform impact response results of production vehicles will be presented and discussed in this section of the paper. The measurement of the frontal geometry of late model U.S. vehicles was recently performed (11), and the measurement of the underhood clearance of the same vehicles is currently underway. Most of the pedestrian head impact testing on production vehicles was documented in the 11th ESV. (1) These data along with test data on additional vehicles and responses scaled to a lower velocity will be presented.

## Measurement of frontal geometry

The frontal geometry of U.S. vehicles was documented by selecting a sample of late model vehicles and recording a variety of measurements and photographing each one. Vehicle selection was based on 1987 U.S. auto sales figures. (11) The top selling vehicle from each major manufacturer was selected. For some of the larger manufacturers, several of the top selling vehicles were selected. The 36 vehicles selected are listed in table 4. To insure that the 36 vehicles selected represented an approximate cross-section of the U.S. car, pickup truck, and van population, a number of factors were checked. These factors, and the comparative results between the vehicles selected and the actual 1987 fleet, are listed in table 5.

**Table 4. Representative cross section of 1987 U.S. vehicle fleet.**

NUMBER	MAKE	MODEL	TOTAL DOMESTIC SALES (1987)
1	Ford	F-Series	550 125
2	Chevrolet	Full-sized pickup	418 221
3	Ford	Escort	392 360
4	Ford	Taurus	354 971
5	Chevrolet	Cavalier	304 028
6	Chevrolet	Celebrity	306 480
7	Ford	Ranger	305 295
8	Hyundai	Excel	263 610
9	Toyota	Pickup	252 946
10	Oldsmobile	Cutlass Ciera	244 607
11	Honda	Accord	230 085
12	Chevrolet	S-10	224 807
13	Ford	Tempo	219 296
14	Pontiac	Grand Am	211 192
15	Cadillac	All	203 487
16	Toyota	Camry	186 633
17	Ford	Full-sized Van	184 413
18	Chevrolet	Caprice	177 344
19	Oldsmobile	Delta 88	168 853
20	Ford	Aerostar	159 149
21	Dodge	Caravan	153 191
22	Buick	Century	147 797
23	Buick	LeSabre	141 126
24	Chevrolet	Nova	134 956
25	Lincoln	All	126 009
26	Pontiac	6000	120 373
27	Nissan	Sentra	116 266
28	Mercury	Grand Marquis	113 972
29	Jeep	Cherokee	112 005
30	Mercury	Cougar	110 722
31	Plymouth	Reliant	105 919
32	Chrysler	LeBaron J	87 802
33	Dodge	Shadow	77 086
34	Mazda	323	76 212
35	Acura	Integra	54 757
36	Yugo	-----	48 812

Note: Figures taken from Automotive News, January 11, 1988 and January 18, 1989, issues.

**Table 5. Vehicle size and type distribution.**

O R I G I N	Selection Factor	Sample Of Vehicles Used In This Study (%)	1987 U.S. Car Population (%)
O R I G I N	% Domestic	75	69
	% Imports	25	31
C A T E G O R Y	% Light Pickup Trucks	8.3	11
	% Full-Size Pickup Trucks	5.5	8
	% Passenger Cars	77.5	73
	% Mini-Vans	5.5	5
	% Full-Size Vans	2.7	3
M A N U F A C T U R E R	% GM	36.1	35
	% Ford	27.7	23
	% Chrysler	13.9	14
	% Honda	2.7	5
	% Nissan	2.7	5
	% Toyota	5.5	6
U R E R	% Other	11.4	12
W E I G H T	Vehicle Weight: 0-2250 lb	21.4	25
	2250-2525 lb	21.4	25
	2525-2750 lb	25	14
	2750-3000 lb	3.6	9
H T	3000 lb & up	25	25

Adult and child head impact zones were determined using WAD's defined in Reference 8, which were based on average pedestrian height values. The adult wraparound region was 62-72 inches and the child wraparound regions was 30-51 inches. By overlaying the adult impact zone on the vehi-

cles, the proximity of the adult zone to the cowl and rear hood edge was gaged. The measurement results indicated that the adult zone extended to the lower windshield for 3 vehicles (8%). The adult zone extended to the rear hood edge for 10 vehicles (28%). (See figure 6)

**Table 6. Vehicle measurement data.**

Make	Model	Year	Total Domestic Sales (1987)	Overhead View Measurements						Profile View Measurements						
				Hood Width at Center of Adult Zone	Total width	MOP to:				Ground to:			MOP at hood fender edge	Bumper to hood front edge angle (Degrees)		
						Top Adult zone	Hood front edge	Front corner	Cowl line	Cowl line to top of Adult zone	Hood front edge to bottom child zone	Top of bumper			Lower hood edge	Upper hood edge
1	Ford F-150	1988	550,125	69.00	71	12.00	38.75	36.75	8.500	20.50	15.25	23.75	43.50	44.50	47.25	79
2	Chevrolet 1500 Pickup	1988	418,221	66.00	68.5	12.00	44.75	39.50	5.000	17.00	9.25	22.50	37.25	39.75	48.50	79
3	Ford Escort	1987	392,360	51.50	55	0.50	41.00	39.00	5.750	6.25	1.50	19.75	27.50	30.50	35.25	59
4	Ford Taurus L	1987	354,971	58.25	61	2.50	44.00	40.25	5.500	8.00	0.50	20.25	28.00	30.00	35.50	53
5	Chevrolet Cavalier	1988	307,028	54.50	58	3.25	47.25	42.75	7.250	10.50	-2.00	20.50	27.50	27.50	35.50	61
6	Chevrolet Celebrity	1987	306,480	58.00	61	3.75	45.25	43.00	8.175	11.93	0.50	20.50	28.25	30.25	35.75	56
7	Ford Ranger XLT	1988	305,295	57.00	60	3.00	38.50	37.25	6.750	9.75	6.50	21.75	36.50	39.75	42.00	83
8	Hyundai Excel GLS	1987	263,610	53.00	57	-1.50	40.50	38.00	5.500	4.00	0.00	19.50	28.00	28.50	36.00	57
9	Toyota 8200E Pickup	1988	252,946	53.75	56.5	-1.25	38.75	36.50	5.750	4.50	2.00	22.00	31.50	33.00	39.50	74
10	Oldsmobile Cutlass Ciera	1987	244,607	58.00	61	6.00	46.25	42.25	7.750	13.75	1.75	21.00	28.25	30.00	35.50	58
11	Honda Accord LX	1987	230,085	57.50	60	-1.75	41.50	39.00	4.375	2.63	-1.25	20.25	25.75	26.75	33.25	50
12	Chevrolet S10 Pickup	1988	224,807	56.75	62	5.00	39.00	37.25	5.500	10.50	8.00	22.75	36.25	37.50	41.25	77
13	Ford Tempo GLS	1987	219,296	51.50	57.5	-1.75	37.50	35.25	7.500	5.75	2.75	21.25	29.50	31.00	36.00	55
14	Pontiac Grand Am	1987	211,192	54.25	58	4.75	46.50	42.25	4.750	9.50	0.25	19.75	28.00	29.00	35.00	62
15	Cadillac Coup DeVille	1986	203,487	60.00	66	9.75	50.00	47.75	4.500	14.25	1.75	19.50	31.00	31.75	36.50	66
16	Toyota Camry	1987	186,633	56.25	60	2.75	44.75	40.25	4.500	7.25	0.00	20.75	28.00	29.25	34.50	60
17	Chevrolet Club Wagon - Van	1987	184,413	67.25	69.5	-7.50	22.50	21.50	7.250	-0.25	12.00	22.25	41.50	46.00	49.00	85
18	Chevrolet Caprice Classic	1986	177,344	64.50	68	22.00	60.50	56.25	4.750	26.75	3.50	20.25	31.50	32.75	37.50	60
19	Oldsmobile Delta 88	1986	168,853	59.75	62.5	8.50	50.25	47.25	4.500	13.00	0.25	20.00	28.75	29.00	36.00	55
20	Ford Aerostar XLT	1987	159,149	63.00	67	-16.75	19.75	18.00	9.000	-7.75	5.50	23.00	32.25	35.50	42.50	69
21	Dodge Caravan - SE	1987	153,191	60.50	61	-3.50	30.50	28.00	7.000	3.50	8.00	20.50	36.00	37.50	43.25	69
22	Buick Century	1987	147,797	57.75	61	5.25	48.00	44.25	8.250	13.50	-0.75	20.00	27.00	28.50	35.00	70
23	Buick LeSabre	1987	141,126	70.00	70	10.50	49.75	46.50	4.750	15.25	2.75	21.00	29.50	30.75	37.25	55
24	Chevrolet Nova	1986	134,956	53.00	56	2.00	42.00	39.75	4.000	6.00	2.00	19.75	26.50	27.50	34.75	60
25	Lincoln Town Car	1987	126,009	63.25	69.5	26.75	60.75	54.75	4.000	30.75	8.00	21.50	36.00	37.00	43.50	57
26	Pontiac 6000-LE	1987	120,373	58.25	61	2.25	44.00	42.00	8.175	10.43	0.25	20.00	29.00	29.25	35.50	57
27	Nissan Sentra	1987	116,266	54.75	58	-4.50	36.50	35.00	7.750	3.25	1.00	20.50	28.75	30.25	34.25	61
28	Mercury Grand Marquis	1987	113,972	63.00	69	20.25	59.50	55.50	4.250	24.50	2.75	20.25	31.75	32.50	36.50	63
29	Jeep Cherokee	1988	112,005	58.00	59.5	5.63	38.00	37.25	7.250	12.88	9.63	24.00	36.75	38.75	41.25	75
30	Mercury Cougar XR-7	1987	110,722	49.25	60.5	18.00	56.50	50.50	4.500	22.50	3.50	21.25	29.50	32.25	37.50	52
31	Dodge Aries K	1987	99,039	57.50	62.5	7.75	46.25	43.75	3.500	11.25	3.50	20.75	30.25	31.25	35.00	54
32	Chrysler LeBaron	1987	87,802	58.00	61	5.75	48.50	43.00	8.500	14.25	-0.75	19.25	27.50	27.50	34.50	54
33	Mazda 323LX	1987	76,212	52.25	56	-2.25	38.00	35.50	6.000	3.75	1.75	21.00	29.00	29.50	35.00	52
34	Plymouth Sundance	1987	75,883	56.25	58.5	0.75	42.00	38.00	7.000	7.75	0.75	20.00	27.50	28.25	35.75	53
35	Acura Integra-RS	1986	54,757	53.50	57.5	4.75	37.00	35.00	4.000	8.75	9.75	20.50	26.00	26.75	33.00	52
36	Yugo GV	1986	48,812	54.25	60	-8.00	31.50	29.50	4.500	-3.50	2.50	19.25	30.25	30.50	34.50	36

\* Measurements are in inches  
 \* The Mop (Measurement Origin Point) is defined as a horizontal line tangent to the curvature at the rear hood edge  
 \* The Cowl Line is defined as the line formed at the interface of the lower windshield and dashboard

Since the cowl, rear hood edge, and rear portion of the hood in the proximity of the rear edge are generally much stiffer than the central region of the hood, an estimate was made of the frequency that the adult zone extended into this stiffened region. It was noted, during preliminary testing, that approximately 6 inches of hood surface adjacent to the rear hood edge is stiffer than the central region. It was then determined what percent of the adult zone fell in this stiff region for each vehicle. The sales numbers were then used to find the weighted average percent. It was found that a typical vehicle has 33 percent of the adult zone surface in that stiff region.

Observations concerning the child head impact zone measurements included the following: child zones overlapped the leading hood edge for 89 percent of the vehicles, and the bottom of the child zone was within at least 6 inches of the leading hood edge for 100 percent of the vehicles.

### Available underhood clearance on late model vehicles

Results from adult headform impact tests into production car hoods at 27 mph indicate that sub-hood clearances of approximately 3 inches are necessary for HIC values less than 1000. For impacts of 23 mph the necessary clearance for a HIC value less than 1000 has been estimated to be 2.5 inches. A study has begun which will gauge the underhood

clearance available for the current U.S. fleet. The underhood clearance of a sample of the current fleet, identical to that used in the study of pedestrian head impact zones, is being mapped.

The surface of the hood is segregated into a grid of 2 in. by 2 in. squares. At the center of the square is a data point beneath which the distance from the hood underside to the nearest hard structure is measured. If a hood reinforcement lies beneath a data point, its depth is subtracted from the clearance distance (hood underside to nearest hard structure).

Plots, similar to the one shown in figure 8 (which contains about 700 measurements), will be produced for each vehicle in the sample. Figure 8 indicates that the 1988 Chevrolet Celebrity has at least 2.5 in. of space beneath 47.8% of the hood. This implies that head impacts of 23 mph or less into most of the 47.8% of the hood have the potential to result in HIC values less than 1000. Specific impact test results and the available underhood clearance for a 1985 Oldsmobile Ciera are contained in a later section of this report. Testing of other vehicles has begun to explore the relationships between the percentage of the hood area having at least 2 1/2 inches of sub-hood clearance and the number of 23 mph head impacts resulting in HIC values less than 1000, for a distributed area of tests across the hood.

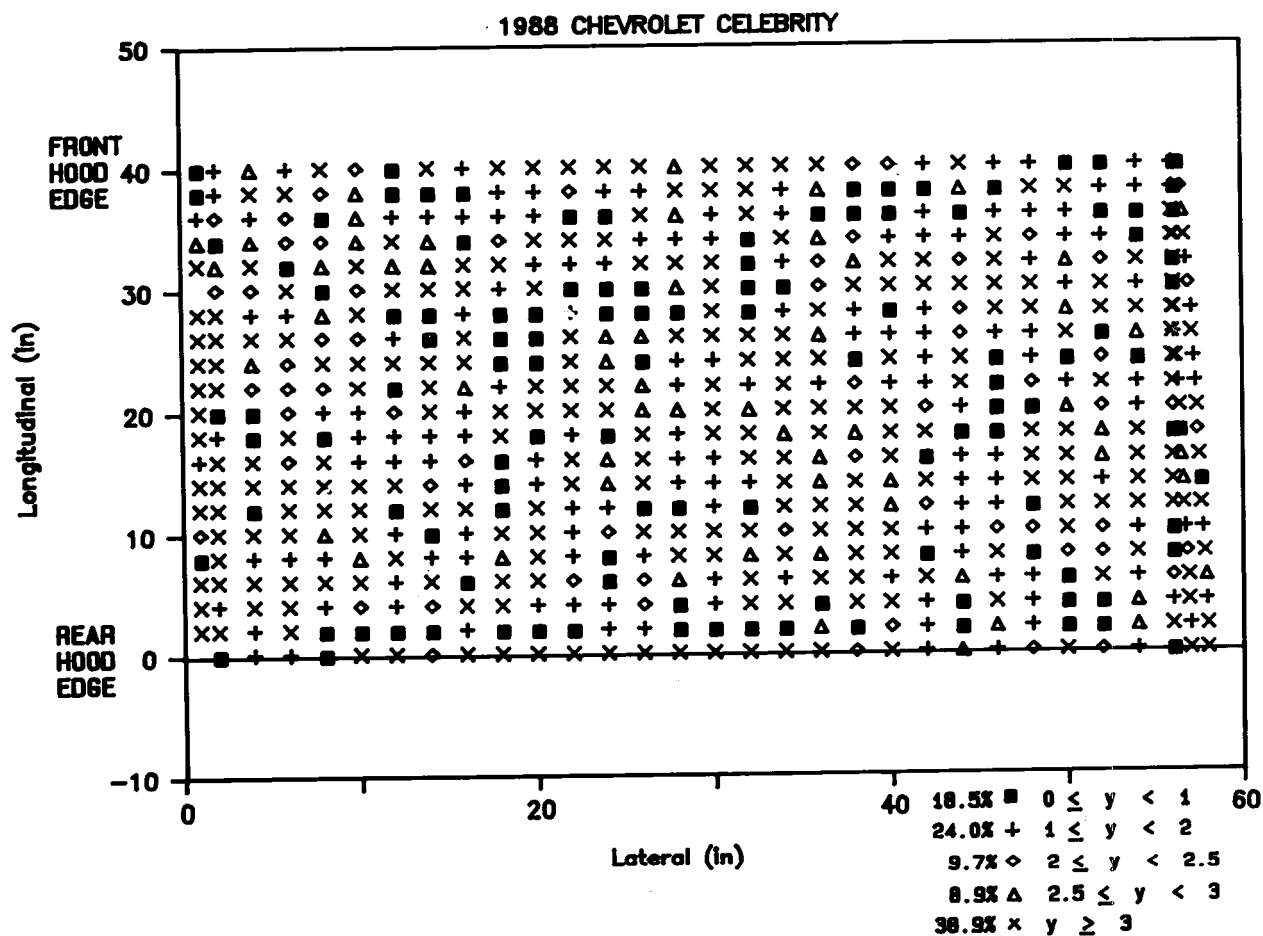


Figure 8. Hood/engine compartment clearance for 1988 Chevrolet Celebrity.

## Impact test results

Simulated adult and child head impacts were used together with the identified injury relationship to evaluate the current fleet. To date, approximately 120 tests were conducted on 22 passenger cars, (results from 16 of these were reported in the 11th ESV) (1) and 5 light trucks and vans. Headform impact test results indicated which designs showed a propensity for causing pedestrian head injury and

which ones represented injury reduction potential. A schematic diagram in figure 9 illustrates the simulated head impact test set up. Results from the passenger car tests, conducted with an adult headform impact velocity of 27 mph, are summarized in table 7. The 27 mph HIC results shown are actual test results. The 23 mph HIC results in the last column were mathematically scaled from the 27 mph results according to the relationship presented previously in the paper.

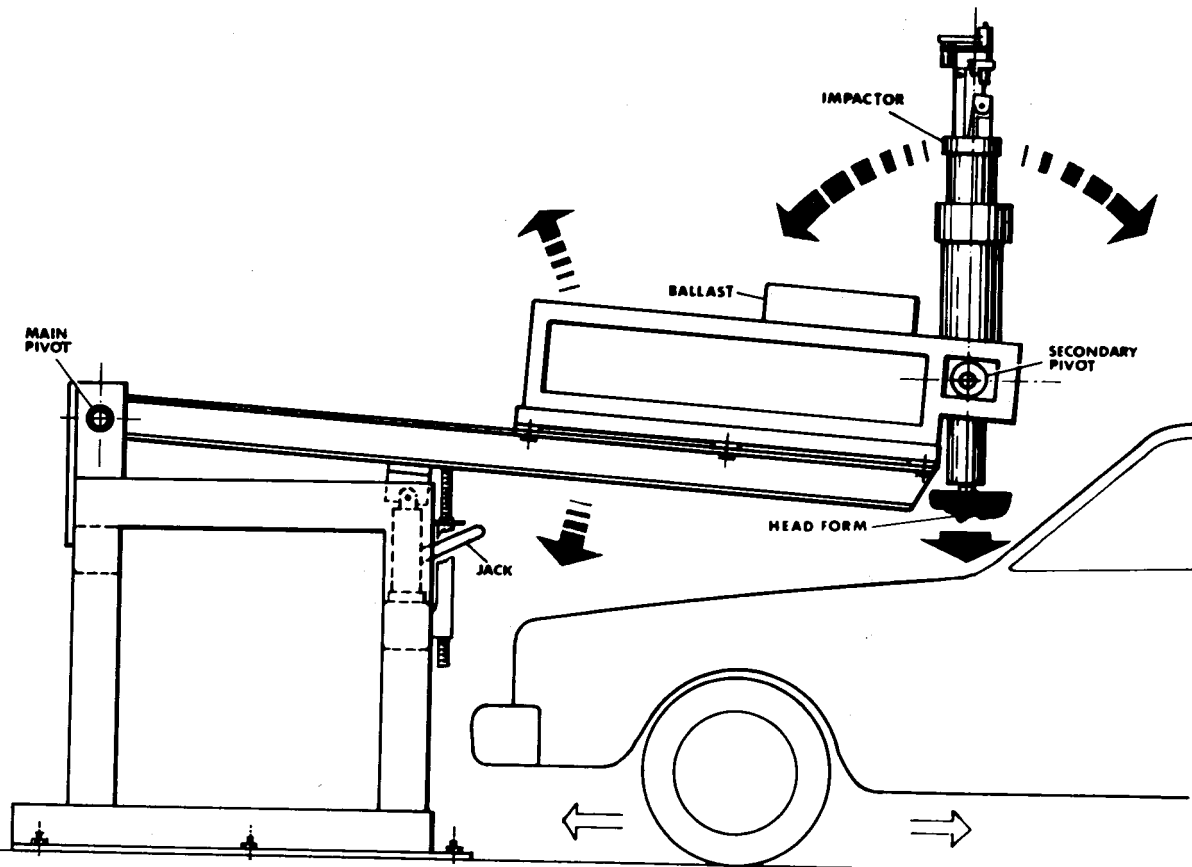


Figure 9. VRTC pedestrian head impact simulator.

Table 7. Production car test results—adult data.

IMPACT TYPE	TEST NO.	VEHICLE TYPE	HIC @ 27 MPH	PROB. OF DEATH (%) (HIC)	DYNAMIC DEFL. (in)	PEAK FORCE (lb)	IMPACT TIME DURATION (msec)	ENERGY ABSORBED (%)	MAXIMUM HOOD STIFFNESS (lb/in)	HIC @ 23 MPH
HOOD/OA	312	1983 Caprice	1748	36.5	2.6	2248	22.5	99.9	2696	1093
HOOD/OA	324	1983 Chevette	2133	51.5	2.3	1848	18.0	96.4	2250	1333
HOOD/OA	298	1985 Grand AM	1557	29.0	2.8	2042	22.5	95.9	2857	973
HOOD/OA	322	1985 LeBaron GTS	1444	24.6	2.8	1979	25.9	97.8	2130	903
HOOD/OA	292	1985 Sunbird	1717	35.3	3.1	2460	22.5	95.4	3000	1073
HOOD/OA	295	1985 Ciera	828	2.2	3.6	1413	28.1	98.9	1956	518
HOOD/OA	323	1983 Saab 900	1355	21.1	2.8	2000	31.5	98.1	2867	847
HOOD/OA	290	1983 Saab 900	1225	16.1	3.0	2109	25.3	96.4	2667	766
HOOD/OA	288	1985 LeBaron GTS	1303	19.1	2.8	2115	22.5	97.6	1981	815
HOOD/OA	321	1985 Mustang SVO	2178	53.2	2.4	2053	18.0	92.4	2295	1362

OA= open area

SS= substructure

Table 7. Production car test results—adult data (continued).

IMPACT TYPE	TEST NO.	VEHICLE TYPE	HIC @ 27 MPH	PROB. OF DEATH (%) (HIC)	DYNAMIC DEFL. (in)	PEAK FORCE (lb)	IMPACT TIME DURATION (msec)	ENERGY ABSORBED (%)	MAXIMUM HOOD STIFFNESS (lb/in)	HIC @ 23 MPH
HOOD/OA	361	1984 Celebrity	1667	33.3	2.3	1794	20.8	97.8	2885	1042
HOOD/OA	320	1985 Escort	1164	13.7	2.9	2086	25.3	96.3	2416	728
HOOD/OA	304	1985 Mustang SVO	1832	39.7	2.6	1810	22.5	94.3	3103	1145
HOOD/OA	308	1983 Thunderbird	1067	9.9	3.5	1922	25.9	96.6	2580	667
HOOD/SS	313	1983 Caprice	1634	32.0	2.8	2025	27.0	99.5	3043	1021
HOOD/SS	305	1985 Mustang SVO	5731	191.8	1.9	4434	7.9	99.0	7636	3563
HOOD/SS	358	1985 Fiero	5249	173.0	1.9	3144	14.6	85.4	4110	3281
HOOD/SS	315	1982 Cavalier	2799	77.5	2.4	1908	14.6	94.6	2857	1750
HOOD/SS	311	1983 Thunderbird	5461	181.3	2.8	3980	10.7	96.6	11470	3414
HOOD/SS	319	1985 Sunbird	1957	44.6	2.1	1952	16.3	97.6	2432	1223
HOOD/SS	286	1985 LeBaron GTS	3636	110.1	1.9	2624	11.3	97.4	3158	2273
HOOD/SS	291	1983 Saab 900	2086	49.7	2.9	1775	18.0	96.7	3673	1304
HOOD/SS	299	1985 Grand Am	2366	60.6	2.3	2133	16.9	96.1	3044	1479
HOOD/SS	360	1985 Fiero	10600	381.7	1.2	5880	10.1	85.1	15909	6626
HOOD/SS	293	1985 Sunbird	4759	153.9	1.8	4019	11.3	97.9	10263	2975
HOOD/SS	316	1982 Cavalier	5557	185.0	1.6	3219	9.6	96.1	4688	3474
HOOD/SS	302	1985 Escort	2230	55.3	2.7	2453	19.7	99.0	6154	1394
HOOD/SS	309	1983 Thunderbird	2452	63.9	2.7	2050	15.2	97.5	4200	1533
HOOD/SS	307	1985 Mustang SVO	4765	154.1	2.1	3446	10.1	92.8	10312	2979
HOOD/SS	301	1985 Escort	2483	65.1	2.0	2619	14.1	97.2	3478	1552
HOOD/SS	318	1982 Cavalier	2386	61.4	2.7	2037	14.6	96.3	5806	1492
HOOD/SS	296	1985 Ciera	5281	174.3	2.2	3786	9.0	97.4	18947	3301
HOOD/SS	327	1983 Chevette	1366	21.6	2.9	1802	22.5	97.5	1989	854
HOOD/SS	362	1984 Celebrity	7023	242.2	1.6	4332	7.9	94.9	15273	4390
HOOD/SS	325	1983 Chevette	2519	66.5	2.3	1918	18.6	95.8	3461	1575
HOOD/FENDER	317	1982 Cavalier	6831	100.0	1.2	3754	7.9	96.3	6735	4270
HOOD/FENDER	294	1985 Sunbird	5470	100.0	2.1	3320	12.4	95.1	7105	3419
HOOD/FENDER	326	1983 Chevette	4683	100.0	1.6	2765	11.3	94.9	6818	2927
HOOD/FENDER	287	1985 LeBaron GTS	5189	100.0	1.6	2948	9.0	96.6	5581	3244
HOOD/FENDER	363	1984 Celebrity	5363	100.0	1.3	3219	10.7	95.0	6383	3353
HOOD/FENDER	289	1983 Saab 900	3346	98.8	2.4	2400	14.1	92.9	7778	2092
HOOD/FENDER	310	1983 Thunderbird	4981	100.0	2.3	2923	11.3	94.9	12857	3114
HOOD/FENDER	314	1983 CAPRICE	4805	100.0	1.3	3161	9.6	96.7	6522	3004
HOOD/FENDER	303	1985 ESCORT	5112	100.0	1.7	3042	10.7	96.3	6000	3196
HOOD/FENDER	297	1985 CIERA	5554	100.0	1.6	3197	9.0	96.0	6000	3472
HOOD/FENDER	306	1985 SVO MUSTANG	5575	100.0	1.5	4466	9.0	93.1	6428	3485
HOOD/FENDER	359	1985 FIERO	10742	100.0	1.3	4687	8.4	84.3	3600	6715
HOOD/FENDER	300	1985 GRAND AM	5183	100.0	1.7	2755	9.6	94.8	5567	3240
COWL	101	1985 CIERA	1337	19.8	2.9	1203	22.0	94.7	3200	835
COWL	389	1985 CIERA	1508	26.4	2.5	951	27.0	94.6	800	943
COWL	395	1985 ESCORT	1804	37.9	1.9	955	21.9	90.6	1421	1128
COWL	390	1985 CIERA	1919	42.3	1.6	1318	21.4	93.6	6375	1200
COWL	100	1985 CIERA	2577	67.5	2.4	1673	14.0	92.9	3200	1611
COWL	103	1985 ESCORT	2656	70.6	2.1	1554	15.5	92.0	3200	1661
COWL	102	1985 ESCORT	3448	100.0	2.1	1759	12.5	93.2	1600	2155

OA= open area

SS= substructure

For headform impacts of 27 mph, a dynamic hood deflection of 3 to 3.5 inches is necessary to attain a reasonable injury level prediction (10% death probability) for the best

hood designs. This implies that at least 3 inches of space must be available beneath the hood to allow flexing of a reasonably stiff hood. Less severe injury predictions were

also seen when head contact with the hood lasted at least 25 milliseconds, the hood stiffness was less than 2000 lb/in and when the hood absorbed greater than 98% of the impact energy. It was noted that the only 27 mph test result less than HIC = 1000, was that on the open hood area of the 1985 Oldsmobile Ciera.

Based upon scaling the results to 23 mph, several of the open area tests, and at least one of the substructure and cowl tests resulted in predicted HIC values less than 1000. None of the hood/fender region tests resulted in predicted HIC values less than 1000.

## Demonstration of Improvement

This section will present information relative to provid-

ing pedestrian protection in the area of the vehicle hood.

Test results from the production vehicles test matrix indicated that the hood design of the 1985 Oldsmobile Ciera, having a 4 cylinder transverse engine, permitted the lowest injury predictions for adult head impacts into the central region of the hood. (8) (Central hood testing included impacts at least 6 inches from the outside edge of the hood.)

The clearance between the hood and the underlying structures for the Ciera is shown in figure 10 with a zone identified containing all of the surface of the hood except a 6 inch border along all 4 edges. The zone size was approximately 26 inches longitudinal by 48 inches lateral. Of the locations within the zone, 89% have more than 2.5 inches of underhood clearance.

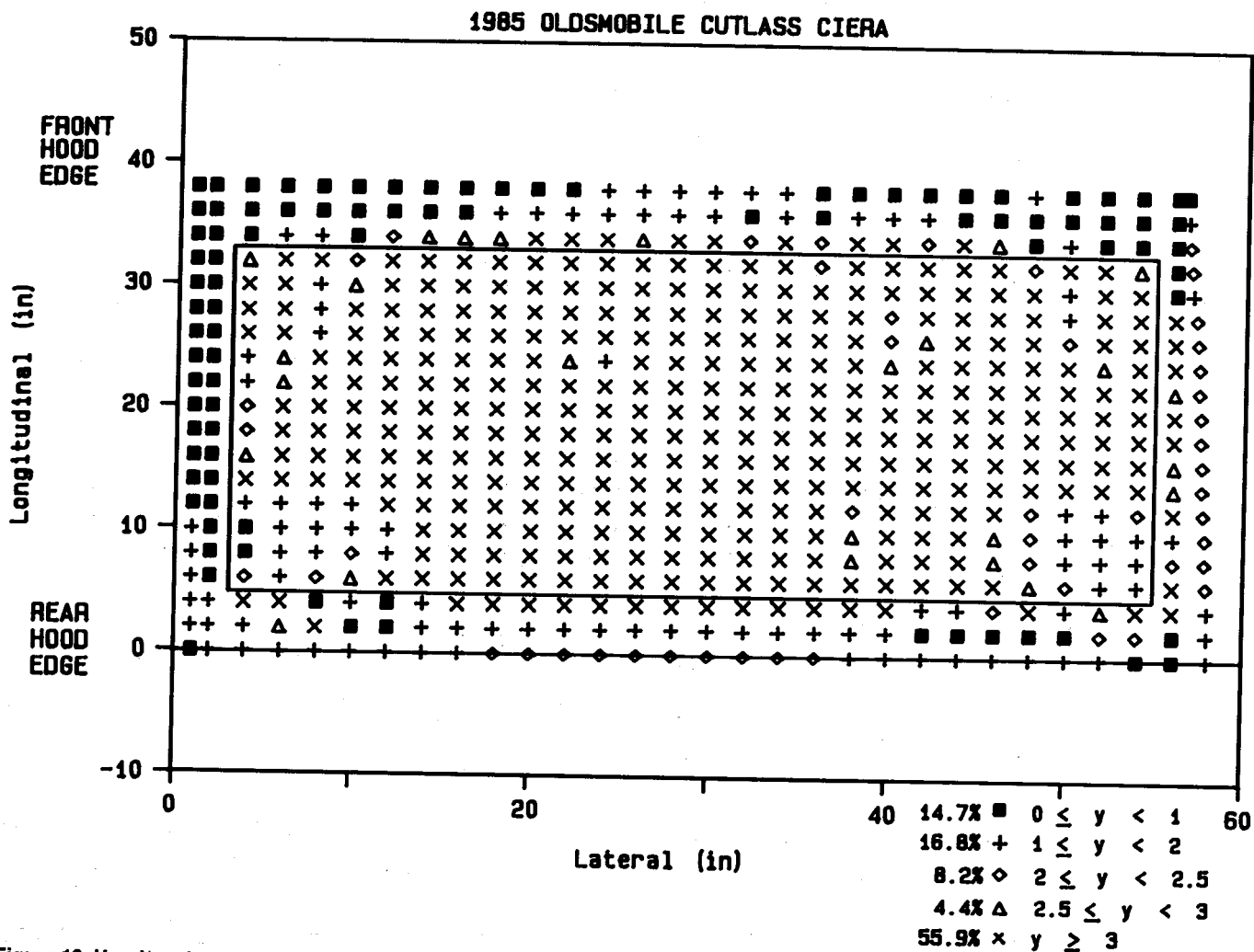


Figure 10. Hood/engine compartment clearance for 1985 Oldsmobile Ciera.

Because the impact tests performed during the production vehicle testing showed the vehicle to be promising in design, more extensive impact testing was performed. A grid of 5 longitudinal and 7 lateral locations within the zone was marked and 35 impacts were conducted, replacing the hood as necessary so that the

results were not affected by other damage to the hood. All of the tests were performed using the adult (10 lb.) headform at an impact velocity of 23 mph. The results of the impact tests are contained in figure 11. It is noted that 21 (60%) of the impact tests resulted in HIC values less than 1000.

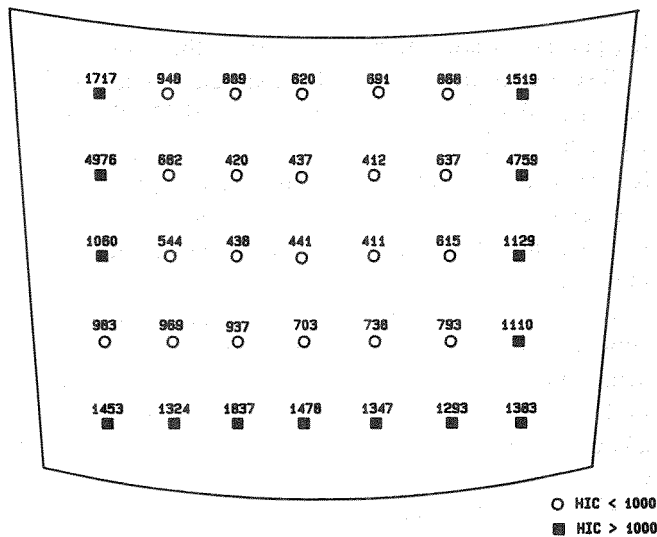


Figure 11. HIC values resulting from the distributed headform impact testing of the 1985 Oldsmobile Ciera. (Headform Impact Velocity—23 mph).

## Research Efforts on Injury Mitigation

Research to reduce the severity of pedestrian head injuries caused by contact with the hood, fenders, cowl, and leading hood edge has begun. To date some mitigation research has been conducted in the hood/fender and cowl region. Some success in reducing head injury severity was found, for impacts into the hood/fender interface region, by substituting a "full cover" hood (shown in figure 12) for the more conventional hood/fender design. A more detailed description of the full cover hood analysis is found in reference 8. Preliminary testing in the cowl/rear hood edge region indicates that headform impacts of 23 mph into the frangible plastic cowl design of the 1985 Ciera can result in

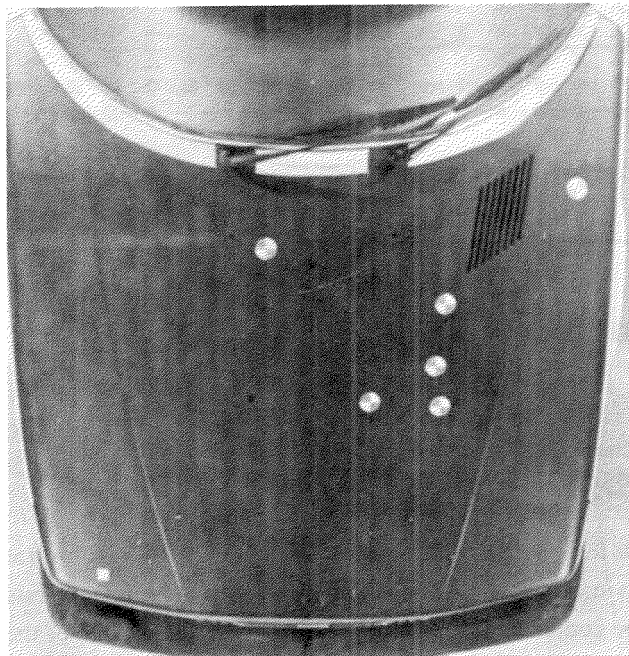


Figure 12. 1983 Saab 900 "Full Cover" hood.

HIC values less than 1000. (See table 7.) A more thorough study of typical cowl designs and possible alternative designs may be initiated based on the results of the head impact zone study and Ciera cowl test results.

## Conclusions

The following conclusions are offered as a result of this study:

1. A strong correlation was noted between measured/calculated HIC responses and the probability of death (POD) for 14 adult pedestrian accident reconstructions. It was found not to make a large difference whether the POD was derived from the Ulman approach, based upon injuries to all body regions, or on alternate approaches using POD's based upon only head injuries.

2. Although no specific test procedure was given, alternatives were identified and discussed. It was observed that simulation of 30 mph pedestrian impacts (with a 27 mph head impact speed), resulted in only 1 test with a HIC result below 1000. This was a hood open area test. Simulation of 25 mph pedestrian impacts (head impact speed of 23 mph) is expected to result in several vehicles which can satisfy HIC=1000 for all but the hood/fender seam region.

3. Vehicles which have sufficient clearance between the hood and the underhood structures have the potential of providing improved pedestrian protection. A target zone of 26 inches by 48 inches was marked in the central hood region of a 1985 Oldsmobile Cutlass Ciera. Eighty-nine percent of the hood surface within the zone was found to have sufficient (2.5 inches or more) clearance. A series of 35 impacts was conducted at evenly spaced locations on a target zone of 26 inches by 48 inches on the Ciera hood (replacing the hood as necessary). The impact speed was 23 mph. HIC values below 1000 were obtained at 60% of the impact sites.

## References

- (1) Kessler, J.W., "Development of Countermeasures to Reduce Pedestrian Head Injuries," Proceedings of the Eleventh International Technical Conference on Experimental Safety Vehicles, Washington D.C., May 1987.
- (2) Malliaris, A.C., Hitchcock, R. and Hansen, M., "Harm Causation and Ranking in Car Crashes," SAE Paper # 850090, February 1985.
- (3) MacLaughlin, T.F., Hoyt, T.A., Chu, S.M., "NHTSA's Advanced Pedestrian Protection Program," Proceedings of the Eleventh International Technical Conference on Experimental Safety Vehicles, Washington D.C., May 1987.
- (4) Elias, J.C. and Monk, M.W., "Status of NHTSA's Pedestrian Thoracic Protection Program," Proceedings of the Twelfth International Technical Conference on Experimental Safety Vehicles, Goteborg, Sweden, May 28-June 1, 1989.

(5) Ulman, M.S. and Stalnaker, R.L., "Evaluation of the AIS as a Measure of Probability of Death," Proceedings of the 1986 International IRCOBI Conference on the Biomechanics of Impacts, Zurich, Switzerland, June 2-4, 1986.

(6) Monk, M.W., "Injury Severity and Measured Response for Pedestrian Head Impacts," Interim Report for Project VRTC 86-0019, March, 1989.

(7) Eppinger, R., "On the Examination of Biases in the Abbreviated Injury Scale," Proceedings of the Eleventh International Technical Conference on Experimental Safety Vehicles, Washington D.C., May, 1987.

(8) Kessler, J.W., Hoyt, T.A. and Monk, M.W., "Pedestrian Head Injury Reduction Concepts," Final Report for VRTC Project SRL-101, June 1988.

(9) Pritz, H.B., "Effects of Hood and Fender Design on Pedestrian Head Protection," Final Report for VRTC

Project SRL-10, January 1984.

(10) Kessler, J.W. and Monk, M.W., "Scaling Pedestrian Head Injury Estimates for Changes in Impact Velocity," Progress Report for Project VRTC-86-0019, December, 1988.

(11) Kessler, J.W., Stoltzfus, D., and Monk, M.W., "Pedestrian Head Impact Zones on Late Model Cars and LTV's," Interim Report for Project VRTC 86-0019, August, 1988.

## Acknowledgements

The authors gratefully acknowledge the professional assistance of Joe Kokoruda in conducting the tests, Joan Jones and Ed Parmer in processing and analyzing the data, and Sonya Shuler in preparing the manuscript.

# NHTSA Pedestrian Thoracic Injury Mitigation Program—Status Report

**Jeffrey C. Elias and  
Michael W. Monk,**  
National Highway Traffic Administration,  
United States

## Abstract

The National Highway Traffic Safety Administration is conducting research at the Vehicle Research and Test Center for the reduction of pedestrian injury. Initial research in pedestrian thoracic injuries address translational side impact in child pedestrians. This paper reviews the development and current status of the child pedestrian program.

A brief overview of the development of the child thoracic surrogate devices is given while tentative threshold injury criteria values developed from accident reconstruction work using these devices are presented. Results of a baseline testing program of a selection of passenger vehicles, light trucks, and mini-vans is presented in terms of relative potential injury. Additional testing shows impact velocity affects on injury potential and indicates impact velocity ranges in which realistic benefits should be explored.

## Introduction

As part of the Pedestrian Protection Program, the National Highway Traffic Safety Administration (NHTSA) is conducting research at the Vehicle Research and Test Center (VRTC) for the reduction of pedestrian injury. Based on the results of a problem identification study (1),\* thoracic injuries caused by impact with the vehicle face comprise the largest and one of the most significant categories of pedestrian accidents (for impact speeds under

30 mph). Young pedestrians are over represented in this accident classification.

In order to develop a procedure in which laboratory simulations of pedestrian impacts could be performed, a series of thoracic surrogates were developed at VRTC which were capable of accurately reproducing the response characteristics of a child's thorax during lateral impact. Using information obtained from documented accident case files, pedestrian accidents were reconstructed using the thoracic surrogates. Original accident impact conditions were thus approximated under laboratory conditions. By relating injury levels observed in the original accidents to measurement data obtained using the thoracic surrogates, threshold response levels corresponding to a 20 percent probability of death were estimated for several variables commonly used for determining injury criteria.

Using the estimated injury criteria as a basis for comparison, a selection of passenger and light utility vehicles were tested using the thoracic surrogates at a 30 mph impact speed. Additional testing was performed at a series of lower impact speeds. The additional testing shows the effects of impact velocity on injury potential while defining impact velocity ranges in which realistic benefits can be achieved.

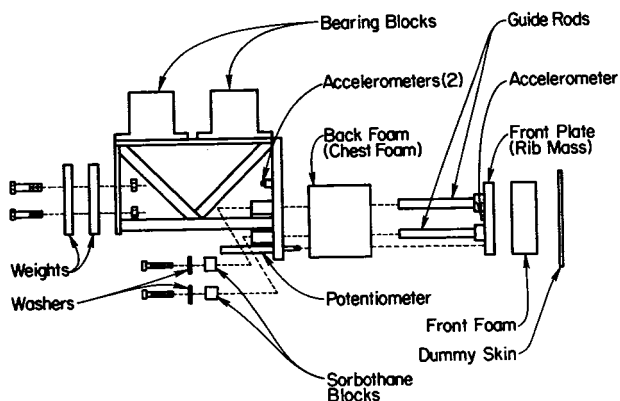
## Thoracic Surrogate (Development)

In order to conduct accident reconstruction, a device was developed to simulate the thorax of a child pedestrian (3). It was assumed that a struck pedestrian is generally traveling in a path perpendicular to that of the vehicle prior to impact. The selection of case studies included children ranging in age from 2 to 13 years old and estimated impact speeds ranging from 5 mph to 30 mph. A series of thoracic surrogates were developed to simulate lateral thoracic

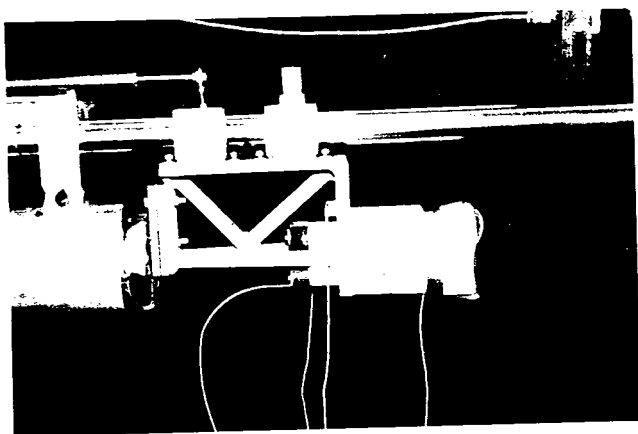
\*Numbers in parentheses designate references at end of paper.

impact response for the range of speeds and ages encountered.

Figure 1 pictures the six year old thoracic surrogate. With mounted weights to provide additional mass, this device is used to model the seven and eight year old pedestrian as well. The surrogate's design utilizes a lumped mass (discrete element) model. Cylindrical sections of Dow Ethafoam are used to represent the stiffness and damping characteristics of the ribs, thoracic viscera, and muscle tissue. The major components of this device as seen in figure 1 are:



(a) Exploded view of device.



(b) Assembled device.  
Figure 1. Six year old child lateral thoracic surrogate.

- A round metal plate—small mass used to simulate the child's rib mass.
- The sled structure with accompanying weights—to represent the spinal mass and remaining effective thoracic mass of the child.
- Cylindrical section of Dow Ethafoam 600—to simulate the stiffness and damping characteristics of the ribs and the thoracic content (viscera).
- Smaller section of Dow Ethafoam 220 and "dummy skin"—to simulate the skin and muscle tissue distal to the ribs.

The rib mass, spine mass and diameter of the foam inserts are adjustable to allow configuration of the surrogate for the full age range of interest (2 years to 13 years).

Instrumentation for the surrogate device consists of the following:

- One accelerometer mounted to the rib plate.
- Two accelerometers mounted to the spinal mass.
- Four inch linear potentiometer mounted between the rib plate and spinal mass.
- Twenty-five inch linear potentiometer mounted between the spinal mass (sled) and hydraulic ram (zero reference point).

This configuration allows the measurement of the rib and spine accelerations, relative displacement of the ribs referenced to the spine, and overall movement of the surrogate during impact.

The performance criteria used for development of the thoracic surrogate were force and deflection response curves of the fiftieth percentile 3, 6, 9 and 12 year old age groups. These curves were derived by scaling and normalizing the APR (Association of Peugeot-Renault) drop test data (adult cadaver lateral thoracic impact data). The normalization method and validation of the results are discussed in detail in reference 2. The surrogate design was restricted to uniaxial motion, and has resulted in a thoracic device which has good repeatability characteristics and shows good fit to the normalized APR data (3).

## Accident Reconstruction

Two databases were examined to obtain documented pedestrian accident cases involving children; the PICS study (Pedestrian Injury Causation Study) (4) and the PAIDS study (Pedestrian Accident Investigation Data Support) (5). Final selection of the accident cases were based on quality and completeness of photographic and measurement documentation, detail of accident and medical records, and availability of the vehicle year and model (for procurement of vehicle and parts for testing).

Three key parameters were considered for the reproduction of the conditions for each reconstruction:

1. Impact location.
2. Effective mass of the thorax.
3. Speed of impact (of the thorax).

Location of impact was determined from photographic records and measurements recorded from the actual accident vehicle in the PICS or PAIDS documentation. The effective thoracic mass was evaluated experimentally for a series of age groups (3, 6, 9 and 12 year-old children). The mass of the test device was adjusted to produce the derived performance criteria of the scaled and normalized adult cadaver test data (6). Figure 2 shows the total mass of the impactor required to produce the proper scaled response plotted as a function of the age of the child being modeled. This thoracic surrogate mass corresponds to the effective thoracic mass of the child of a given age group. The plot shows that relationship between age and effective thoracic mass is essentially linear through the range of ages of interest.

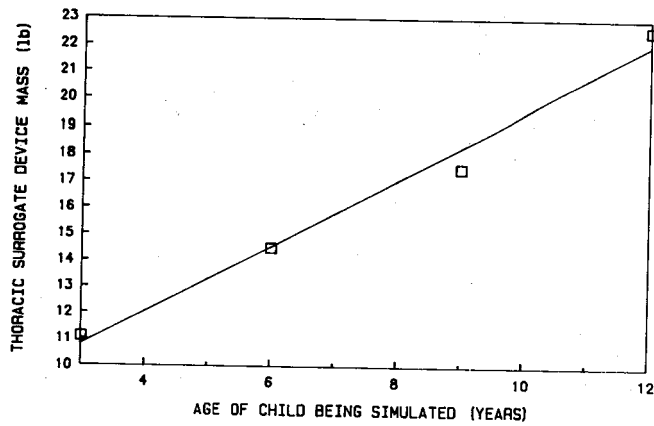


Figure 2. Thoracic mass versus representative age.

Initial estimates of thorax impact speed were obtained from the accident files using the investigator's "best estimate" of the vehicle's impact speed based on the physical evidence (skid marks) and on driver and eyewitness interviews. Reconstruction testing was conducted over a series of different speeds in order to determine the conditions which, upon visual inspection, best reproduced the physical damage documented in the original accident. Table 1 shows the tabulated results of the estimated vehicle speed and the thorax impact speed derived from the reconstruction tests.

Table 1. Impact speeds from case files and reconstruction tests.

Vehicle	Case File Vehicle Impact Speed (mph)	Nominal Thoracic Impact Speed of Best Reconstruction
1980 Tercel	29 - 32	30
1977 Monaco	05	05
1986 Camaro	15	16
1975 LeSabre	19	16
1975 Camaro	15	16
1973 Regal	18 - 21	10
1976 Cutlass	18 - 24	14
1974 Hornet	25	24
1973 Cutlass	10	10
1973 Chevy Pickup	14.9	13
1974 Dodge Van	26	25
1976 Olds 98	24	21
1977 Celica	15 - 24	19
1975 Marquis	14	14

The determination of the thoracic impact speed proved to be the most difficult parameter to accurately determine. Accident data is volatile in nature and often irretrievably lost within minutes of the occurrence. As a result, information in the subsequent data files could often be incomplete or contradictory. Even under ideal conditions, reproduction of the documented damage pattern was found to require much more subjective interpretation than was needed with the head impact reconstruction work described in reference 7.

Injury severity was the dependent variable in the study. MAIS (Maximum AIS) (8), ISS (Injury Severity Score) (8), and POD (Probability of Death) (9) were the injury potential scales considered in determining an injury criterion

relationship. Each of these injury potential scales uses AIS values (Abbreviated Injury Scale) as the basis for determining injury severity levels.

The independent variables considered were:

1. Peak Rib Acceleration.
2. Peak Spine Acceleration.
3. Average of the Peak Rib and Spine Accelerations.
4. Peak Chest Deflection.
5. Percent Chest Deflection.
6. Viscous Injury Criterion.

Rib and special accelerations were filtered using the procedure proposed for the SID dummy. The deflection data were filtered with a 100 hz. cutoff digital filter. The data processing and all six of these independent variables are presented in reference 6. In this paper, only three of these will be used for analysis. The peak chest deflection and percent chest deflection show very similar results. The percentage chest deflection, figure 3, allows some normalization of the deflection data with respect to the chest breadth across the range of age groups.

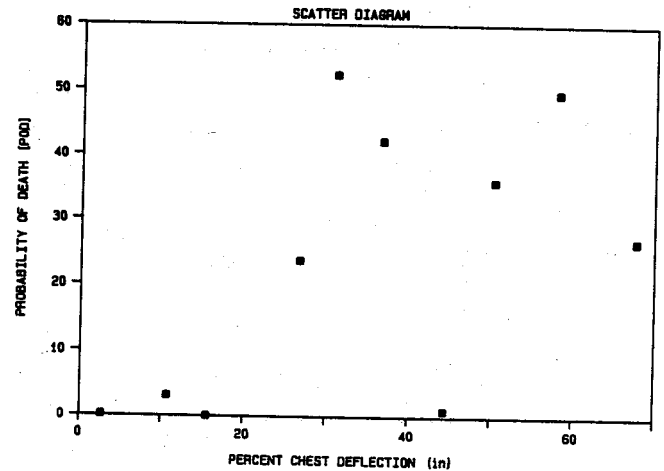


Figure 3. Probability of death versus percent chest deflection.

The viscous injury criterion, figure 4, is the product of compression (expressed as a percentage of the half chest breadth) and velocity (rate of compression) and is computed according to the procedure proposed by Viano and Lau (10).

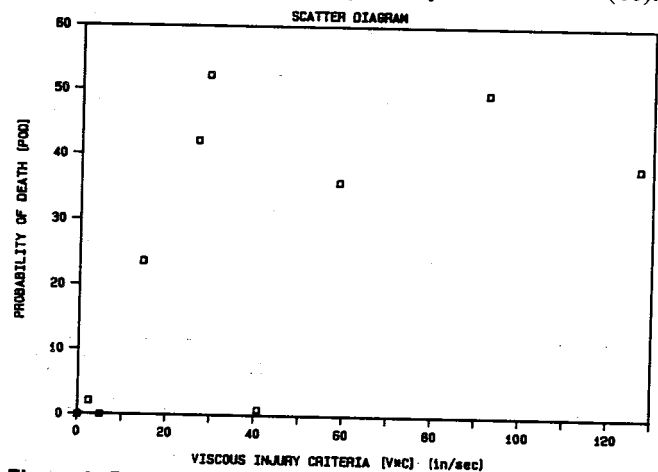


Figure 4. Probability of death versus V\*C.

The average of the peak rib and spine accelerations, figure 5, forms the core parameter for the Thoracic Trauma Index (TTI) (11). This criterion uses age and weight factors, based on the 50<sup>th</sup> percentile male, to modify the acceleration data. While the TTI is not intended for use with small children, the core parameter is included here for comparison.

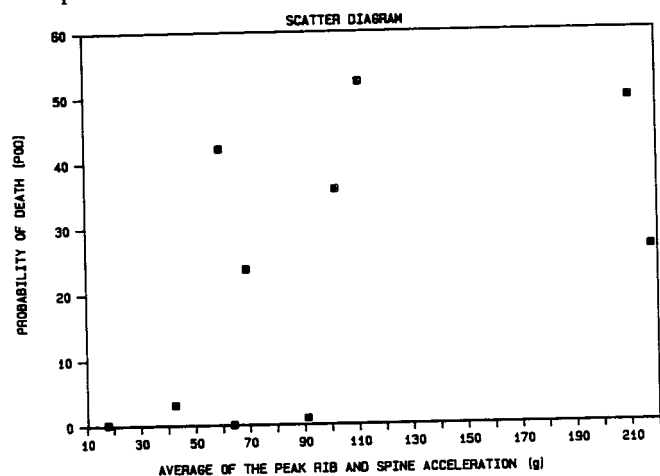


Figure 5. Probability of death versus average rib/spine acceleration.

It is noted that this test device is fairly unique and the application differs from that in which other types of devices are used. The results and observations in this paper are, therefore, not applicable to other devices or test environments.

As seen in the three preceding plots, results of the reconstruction work show a high degree of variability. Because of this, threshold values are effected rather than functional relationships between dependent and independent variables. The threshold values reported here are based on the onset of a 20 percent probability of death (POD). While these values should be viewed as tentative approximations subject to re-evaluation, they do provide some basic information for child impact response. The resulting values from the reconstruction work are the following:

1. Percent chest deflection = 25 percent.
2. Viscous injury criterion = 15 in/sec.
3. Average rib/spine acceleration = 60 g.

## Baseline Production Car Testing

The baseline vehicle testing was conducted to establish a general performance level for current production vehicles. Using the thoracic surrogates, pedestrian impacts were simulated in order to determine what vehicle design features may affect injury severity levels. Additional testing over a range of impact speeds showed the functional relationship between injury criteria and impact speed. This helped define impact velocity levels in which realistic benefits could be achieved.

Twenty-four passenger vehicles and five light trucks and vans (LTV) were used in the course of the testing. The

general impact location on each test vehicle was the upper leading edge of the hood or fascia. This height varied from vehicle to vehicle and determined the age group of pedestrian and the appropriate thoracic surrogate for the test. Each vehicle was impacted at three locations laterally across the face of the vehicle. The three locations were defined as:

1. *Headlight region*.—Point centered over the headlight or headlight region of the vehicle.
2. *Midline region*.—Point located in a position midway between the inner edge of the headlight region and the centerline of the vehicle.
3. *Centerline region*.—Point located on the centerline (horizontal axis) of the vehicle's face.

A study of pedestrian accident data (1) has shown that most pedestrians are struck at relatively low impact speeds. As much as 90 percent of these occur at impact speeds of 30 mph or less. Based on this and the reconstruction work, 30 mph was selected initially as the impact speed for the baseline testing. As testing progressed and the level of severity of this impact speed became apparent, a number of vehicles were tested at a lower impact speed of 20 mph. At the conclusion of the baseline testing, a subsample of six passenger vehicles was selected for retesting over a complete range of designs and response characteristics seen in the original test group. Each of these vehicles was tested at additional impact speeds of 5, 10, 15, 20 and 25 mph. The results of this testing show the sensitivity of the injury criteria to speed of impact, and demonstrate the levels of impact speed for which various levels of injury severity response can be realistically met.

## Result of the 30 mph Testing

Figure 6 shows the response range of one of the injury criteria used in the study. Due to the physical limitations of the test apparatus, the actual speed of impact generally had a variance of ( $\pm$ ) 1.0 mph with a small number of tests varying as much as ( $\pm$ ) 2.0 mph. For comparison, the data have been normalized to a 30 mph impact speed. While viscous injury criterion  $V \cdot C$  is shown here, very similar results are seen in the percent chest deflection data. The acceleration based data resulted in more variation, which might simply be due to hitting sheet metal with relatively small masses or

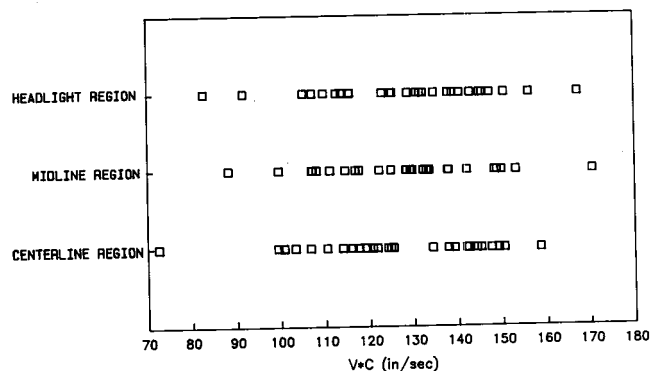


Figure 6.  $V \cdot C$  response range for 30 mph impact speed.

possibly to design problems in the device or a true sensitivity to structural response differences. Efforts are underway to improve the consistency of the acceleration responses. The same general trends are seen using this criterion as well. No judgment has been made on which is the better criterion for purposes of this test device.

The responses for the headlight, midline and centerline regions show little difference in terms of total range or distribution of response levels. This indicates that there is no region (i.e., headlights, central hood region, etc.) on the vehicle's face which consistently tests higher or lower in the predicted level of injury severity.

The minimum response for the 30 mph impacts is 70 in/sec. This is well above the 15 in/sec threshold response value suggested in the reconstruction studies. The 30 mph impact speed appears to be too severe to attempt the reduction of injury severity to the threshold levels.

While none of the vehicles tested could meet the desired threshold values, the range of response for the V\*C criterion is approximately 100 in/sec (70 in/sec—170 in/sec). This range and distribution of the V\*C values show that a considerable degree of improvement (in terms of the reduction of an injury criterion) may be possible on many production vehicles. Less clearly demonstrated is the accompanying reduction in injury severity since no clear relationship has been established between injury severity and an injury criterion for the more severe impact conditions.

## Velocity Sensitivity Results (V\*C)

The results of the 30 mph tests demonstrated the need for testing at lower impact speeds. Six vehicles representative of the range of geometrics and responses encountered in the baseline testing were selected for re-testing. Tests were conducted at impact speeds of 5, 10, 15, 20 and 25 mph.

Figure 7 shows the viscous injury criterion (V\*C) test results for the 1985 Ford Escort. The three impact locations, headlight, midline and centerline are shown over the range of impact speeds tested. The fourth set of data points (using the triangle symbols) represents the average value for all three locations and for all six vehicles tested thus providing a benchmark for comparison. The lower speed impacts show the V\*C values approaching zero at an asymptotic rate, while the higher impact speeds can be accurately

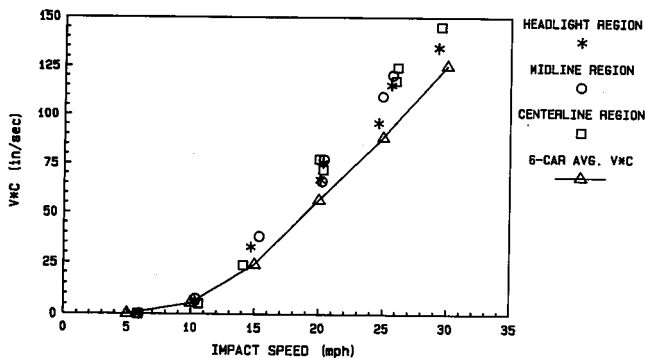


Figure 7. V\*C versus impact speed—1985 Ford Escort.

represented with a linear approximation. The Escort, with its relatively stiff front end (minimum sheet metal deformation and/or grill damage), resulted in higher than average values for nearly every impact.

Figure 8 shows the V\*C test results for the 1985 Pontiac Sunbird. The Sunbird has an unusually soft structure. The fascia is composed of a very compliant composite material backed with a light sheet metal substructure. This combination resulted in the lowest injury criteria values of any of the vehicles tested. As can be seen in figure 8, the impacts fall consistently below the average value curve but with the same general characteristic curve as seen with the Escort.

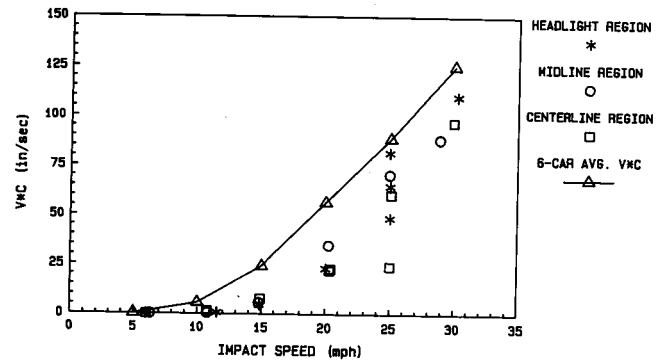


Figure 8. V\*C versus impact speed—1985 Pontiac Sunbird.

All of the vehicles tested showed similar patterns to the two shown. None of the vehicles tested met the threshold criteria of 15 in/sec at impact speeds of 20 mph or higher. Based on the results, 15/20 mph appears to be the maximum impact speed at which the threshold values of the injury criteria might be satisfied.

## Additional Criterion Results

Figures 9 and 10 show the results of the Peak Chest Deflection for the Ford Escort and the Pontiac Sunbird. The relationship for this criterion to increasing speed is essentially linear. At the very severe impact conditions seen in the 25 mph and 30 mph impact speeds, the thoracic surrogate approaches maximum compression. This can be seen in the average response curve and in the Escort test data. The data points for the 25 mph and 30 mph clearly depart from the slope defined by the data at the lower impact

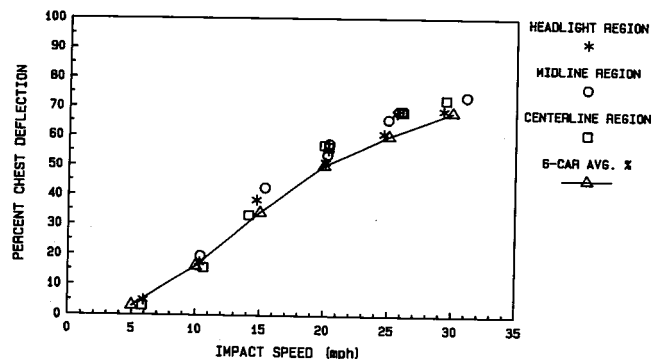


Figure 9. Percent chest deflection versus impact speed—1985 Ford Escort.

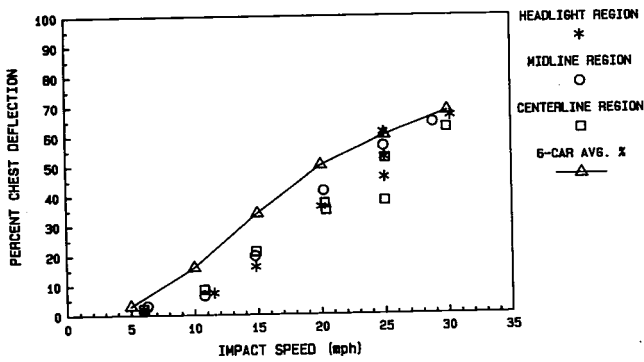


Figure 10. Percent chest deflection versus impact speed—1985 Pontiac Sunbird.

speeds. The Sunbird, with its "softer" front end, shows this deviation to a much lesser degree.

The acceleration data generally shows a higher degree of variability. This can be seen in figures 11 and 12, which are the results of the acceleration based data for the Escort and Sunbird tests. While the same overall trends are observed with the acceleration responses, some of the Sunbird results were higher than the average and some of the Escort responses were lower. Again, this could be due to hardware problems or to the response characteristics of sheet metal surfaces.

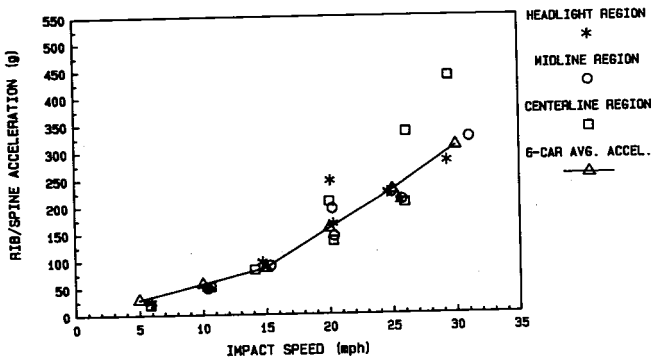


Figure 11. Average of peak rib and spine accelerations versus impact speed—1985 Ford Escort.

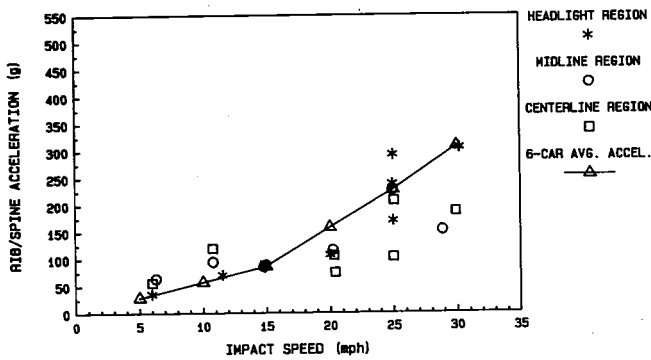


Figure 12. Average of peak rib and spine accelerations versus impact speed—1985 Pontiac Sunbird.

Figures 13, 14, and 15 are the response corridors and mean response values for the V\*C, percent chest deflection, and acceleration criteria respectively. Plot 13 shows the corridor for the V\*C criterion with the threshold value of 15

in/sec overlaid on the results. Similar overlays are shown in figures 14 and 15 for the peak chest deflection and acceleration criteria. From these corridors it can be seen that the maximum speed at which any of the tested vehicles were able to meet the threshold response levels (for any of the criterion) varies from 5 to 18 mph. Since a high frequency of pedestrian accidents occur at low impact speeds (1), a considerable improvement would be achieved if all vehicles were required to perform at response levels as low as the best of the vehicles shown in this test base.

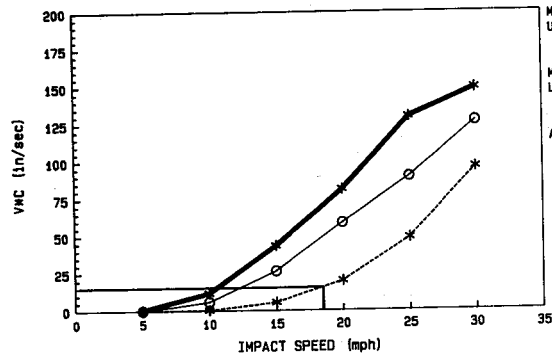


Figure 13. V\*C versus impact speed response corridor.

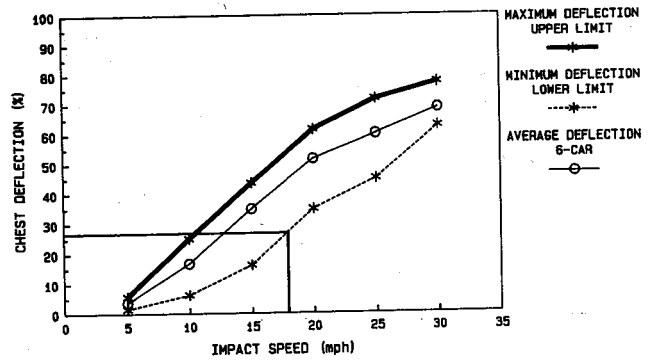


Figure 14. Percent chest deflection versus impact speed response corridor.

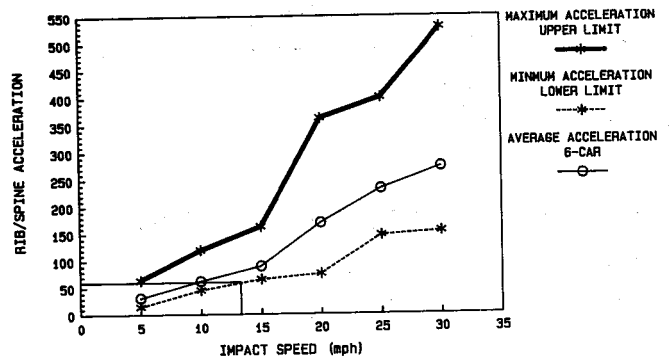


Figure 15. Average of the rib/spine acceleration versus impact speed—response corridor.

## Conclusions

1. The child thoracic surrogate devices developed at VRTC match the response corridors which were scaled from adult cadaver tests. The device is limited to translational impact.

2. There is a limited database of accident cases which adequately documents pedestrian accidents for laboratory reconstruction. The sparsity and variability of the data limits the correlation of measured response-injury severity to the estimation of threshold levels. These threshold values, based on the onset of a probability of death equal to 20 percent (roughly comparable to an AIS injury rating between AIS 4 with POD = 9% and AIS 5 with POD = 25%), are tentatively determined to be:

- a. Percent chest deflection = 25%.
- b. Viscous criterion ( $V \cdot C$ ) = 15 in/sec.
- c. Average of the peak rib and spine acceleration = 60 g.

3. Results of the baseline testing demonstrate that there are design features currently in use which can significantly reduce the observed injury criterion levels for pedestrian impact. However, the 30 mph impact speed is too severe a test condition for the pedestrian side impact studies. None of the vehicles selected for testing in the baseline study were capable of meeting the defined threshold response levels of a 20 percent probability of death.

4. The results of the six vehicles tested over a range of impact velocities show that the injury criteria increase in a predictable manner with increasing impact speed:

a.  $V \cdot C$  appears to have a higher order relationship (power curve regression) at lower impact speeds which becomes very linear in nature at the higher range of impact speeds tested.

b. Percent chest deflection increases in what appears to be essentially a linear function with increasing impact speed.

c. The acceleration responses from the pedestrian thorax device appeared to be more scattered than expected. This could indicate hardware problems or could be an outcome of hitting sheet metal surfaces with a relatively small mass surrogate. The data appear to have a higher order functional relationship (exponential or power) with increasing impact speed throughout the range of speeds tested.

5. Of the vehicles tested at 20 mph, none resulted in responses below the threshold values derived from the reconstruction testing. However, since some of the test responses were fairly close to the threshold values, it may be feasible to achieve this level of response at 20 mph. Below 20 mph, there is a sufficient range of impact response to

indicate that significant improvement is possible for injury reduction in pedestrian accidents.

## References

- (1) MacLaughlin, T.F., Hoyt, T.A. and Chu, S.M., "NHTSA's Advanced Pedestrian Protection Program," *Proceedings of the Eleventh International Conference on Experimental Safety Vehicles*, Washington, D.C., May 1987.
- (2) Hamilton, M.N., "Experimental Study of Thoracic Injury to Child Pedestrians," *Proceedings of the Eleventh International Conference on Experimental Safety Vehicles*, Washington, D.C., May 1987.
- (3) Hamilton, M.N., Chen, Hung-Hau and Guenther, D.A., "Adult to Child Scaling and Normalizing of Lateral Thoracic Impact Data," *Proceedings of the Thirtieth Stapp Car Crash Conference*, San Diego, October 27-29, 1986.
- (4) Pedestrian Injury Causation Study Data Files, National Highway Traffic Safety Administration, Research and Development, National Center for Statistics and Analysis, Washington, D.C.
- (5) Pedestrian Accident Investigation Data Supplement Files, National Highway Traffic Safety Administration, Research and Development, National Center for Statistics and Analysis, Washington, D.C.
- (6) Elias, J.C., Monk, M.W. and Hamilton, M.N., "Experimental Child Pedestrian Accident Reconstruction—Thoracic Impact," Vehicle Research and Test Center, Final Report, October 1988.
- (7) Hoyt, T.A., MacLaughlin, T.F. and Kessler, J.W., "Experimental Pedestrian Accident Reconstructions—Head Impacts," Vehicle Research and Test Center, Final Report #DOT HS 807 288, June 1988.
- (8) American Association for Automotive Medicine, "The Abbreviated Injury Scale," 1980 Revision.
- (9) Ulman, M.S. and Stalnaker, R.L., "Evaluation of the AIS as a Measure of Probability of Death," *Conference proceedings of the 1986 International IRCOBI Conference of the Biomechanics of Impact*, Zurich, Switzerland, September 1986.
- (10) Viano, D.C. and Lau, I.V., "Thoracic Impact: A Viscous Tolerance Criterion," 1985 NHTSA Symposium on Experimental Safety Vehicles, Oxford, England, June 1985.
- (11) Eppinger, R.H., Morgan, R.M., and Marcus, J.H., "Development of Dummy and Injury Index for NHTSA's Thoracic Side Impact Protection Research Program," SAE Paper No. 840885, May 1984.

# Evaluation of the Round Symmetrical Pedestrian Dummy Leg Behaviour

D. Cesari, C. Cavallero, H. Roche,  
INRETS-LCB,  
France

## Abstract

In a joint research programme Chalmers University (Sweden) and INRETS (France) developed a round symmetrical pedestrian dummy (1).\*

This dummy has a full instrumented leg in order to measure knee deformations as well as shearing force and bending moment at knee level.

Even if the new methods for pedestrian protection evaluation are not based on a full scale test with a dummy, a sub-system approach needs to use a mechanical leg model to predict the risk of leg injuries for a pedestrian.

In this work the behaviour of the leg of the Round Symmetrical Pedestrian Dummy (RSPD) is evaluated, as well its repeatability as its capability to predict pedestrian leg injuries.

## Description of the RSPD

Pedestrian experimental impacts showed that pedestrian dummies were not able to reproduce correctly the pedestrian kinematic, and moreover tests performed with such dummies had a poor repeatability. To solve these problems the RSPD dummy was designed.

Its leg is made of three main components: the foot, the lower leg, and the thigh.

The foot is in two parts: a wooden disk which remain on the ground during the impact, and a steel block attached to the lower leg through a steel bar.

The lower leg is made of a steel tube surrounded by a cylindrical foam flesh. The knee joint is simulated by a steel rod which would keep a permanent deformation after the impact test. The rod diameter, steel grade and the distance between leg and thigh are selected to provide a bending moment of 70 Nm at the beginning of plastic deformation.

The thigh is made of a steel tube surrounded by a conic wood block covered by a foam flesh. The thigh is attached to the pelvis through an adjustable ball and socket joint.

The instrumentation of the RSPD leg consists in ten sets of four strain gauges distributed along the leg to make possible to determine bending moment and shearing force about the joints.

## Test methodology

To make the evaluation of the round symmetrical pedestrian dummy, series of impact test were conducted. In these tests the dummy is hit by a car platform fitted with an adjustable bumper. The same model of bumper is used for all the tests, but before every test the platform is fitted with a new bumper.

This bumper is a model used on a mass production car, and is made of a hard plastic skin covering a steel sheet beam. This beam is attached to the platform structure through two force transducers which allow to determine the impact force between the bumper and the leg.

The dummy hanged up in a standing position is released just before the impact. Cadaver tests performed in the same conditions are used for comparison. In these tests, the cadaver is hit on its right side and is in walking attitude with the right leg in front and the left one at rear. Figure 1 shows the test set up.



Figure 1. Test set-up.

## Repeatability of the RSPD leg response

To make the evaluation of the repeatability of the RSPD leg response, six impact tests in the same conditions: bumper height 380mm (75% of knee level) impact speed 32 km/h.

The following parameters were recorded and their variation is analysed:

- Platform force
- Upper tibia acceleration
- Lower tibia acceleration
- Knee bending moment
- Upper tibia shearing force

Beside this upper and lower tibia speed were determined by integration of tibia acceleration, and leg kinematic related parameters were calculated and analysed.

Table 1 contains the average value and the coefficient of

Table 1. Repeatability evaluation of RSPD.

	Average	V.C. (%)
Platform force (N)	5 374	5.77
Upper tibia acceleration (g)	- 98.6	7.62
Lower tibia acceleration (g)	- 98.6	10.51
Upper tibia speed (m/s)	- 11.9	6.13
Lower tibia speed (m/s)	- 14.1	7.11
Shearing force (N)	4 159	6.22
Knee bending moment (N.m)	- 151.1	9.86
Knee angle (°)	- 23.4	11.24

(V.C. = 100 \* (Standard deviation/average value)

\*Numbers in parentheses designate references at end of paper.

variation of the main parameters. This table shows that standard deviation is within 10% of the average value except for lower tibia acceleration and knee angle variation.

Figure 2 shows the values of knee angle variation for the seven tests, and even if it is the worst correlated parameter, this figure shows a good repeatability of RSPD leg kinematic.

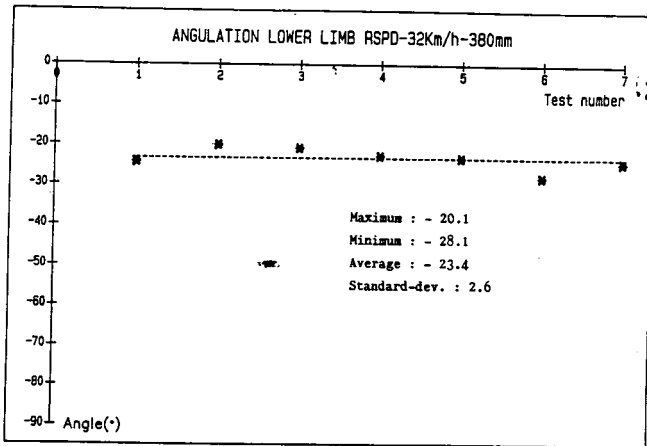


Figure 2. Knee angle variation.

It has to be noted that the repeatability evaluation is based on full scale tests which are necessarily not absolutely identical: impact speed, dummy attitude, bumper height at impact may vary in a small amount.

Generally speaking the RSPD was found to be repeatable, especially if we consider that at its present stage of development it is only a laboratory prototype, and an industrial production would probably improve its repeatability by choosing slightly different technical solutions to build it.

### Capability of RSPD leg to predict pedestrian leg injuries

Twelve RSPD tests were performed in the following conditions: bumper height equal to 300, 380, 445, and 510 mm above the ground (respectively 60, 75, 90, and 105% of knee level) and impact speed equal to 20, 32, and 39 km/h.

The same parameters were recorded as for repeatability tests, and each RSPD validation test was duplicated with a cadaver test performed in the same impact conditions.

Figure 3 compares the total bumper force recorded in RSPD tests and in cadaver tests. This figure shows that in dummy tests the bumper force is mainly correlated to impact speed. Bumper force is due to the inertia of the leg and then there is a rationale that this force increases with the impact speed. However for high speed impacts, the bumper force increases also with bumper height: the apparent mass of the leg depends on the impact location and a higher bumper would correspond to a greater leg apparent mass especially in high speed tests in which the knee bar cannot bend in phase with impact force.

In the average, bumper peak force is greater in dummy tests than in cadavers ones, the ratio being 3 to 2. The weight of the RSPD leg is approximately 1.5 times the weight of a

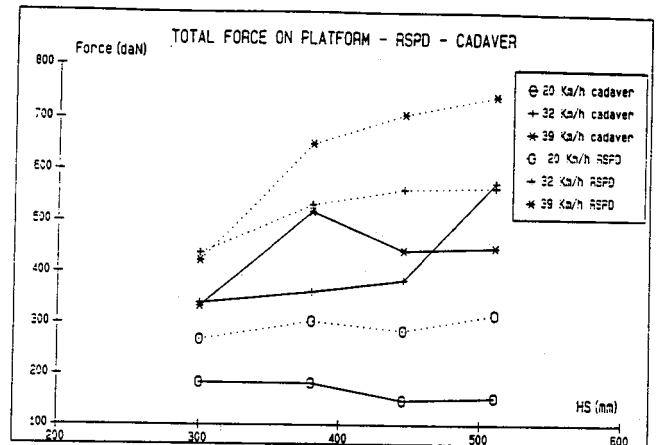


Figure 3. Bumper force—comparison between RSPD and cadavers.

human 50th percentile leg. This value was chosen considering that during a pedestrian impact the first impacted leg is fully involved whereas the second leg is only partly involved at the same time. In fact cadaver tests show that the maximum of the bumper force due to the first leg occurs when the second leg has almost no influence on the force/time history, as indicated on figure 4. Then the leg of the RSPD seems too heavy to simulate correctly a pedestrian hit by its side.

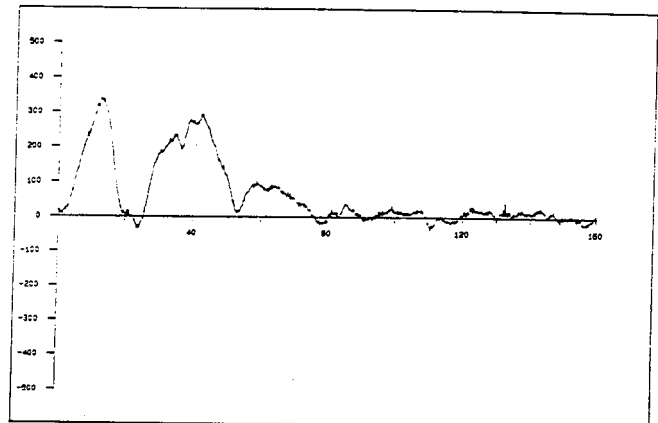


Figure 4. Cadaver test bumper force (32 km/h, 90% of knee level).

The RSPD dummy is able to record the bending movement applied to the knee, and it is possible to determine from film analysis the leg deformation at the knee level in terms of angle variation between the thigh and the lower leg.

Figure 5 shows the relationship between bending movement and variation of knee angle. This figure shows that for low knee angle variation (plus or minus 20°) the two parameters are linearly correlated, but when the knee angle value is below -20°, the bending movement increases slowly compared to knee angle. This is a realistic behaviour, as it has been found on cadavers that ligaments ruptures occur approximately at this value of knee deformation (2). When a ligament rupture occurs, the knee becomes less resistant, and then it can deform without an increasing of applied forces.

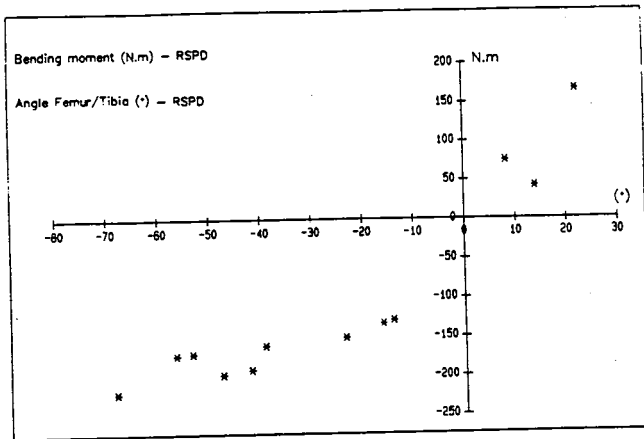


Figure 5. Relationship between bumper bending moment and leg bending deformation.

RSPD is also able to record shearing forces on the tibia just below the knee. Shearing forces appear to produce a specific deformation of the leg in which the upper and lower legs remain parallel and knee ligaments are torn (3).

Figure 6 shows the peak values of shearing force as a function of test conditions: the maximum of shearing force occur in tests with a 445 mm bumper height which corresponds to the closest impact point to transducer location. It seems also that shearing force depends on impact speed; this is especially true when comparing results of 20 and 32 km/h tests.

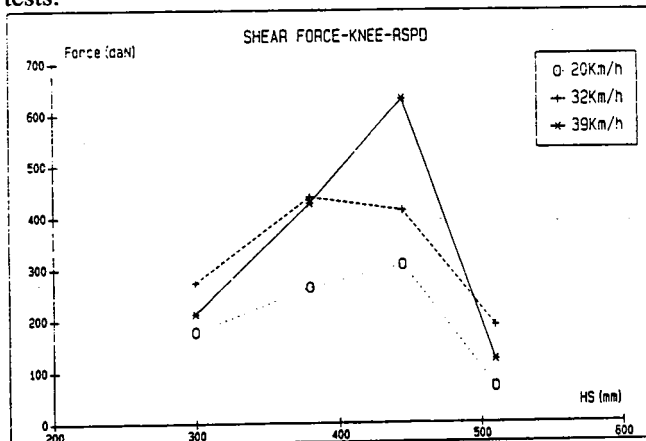


Figure 6. Shear force as a function of test conditions.

Comparison of RSPD and cadavers knee angle deformations shows that the two models perform in the same way, but the RSPD has a more predictable behaviour: the RSPD knee angle variation increases linearly with bumper height whatever is the impact speed.

## Conclusions

A sub system test has to take into account the mechanisms producing injuries. Evaluation of the leg of the round symmetrical pedestrian dummy shows that it is able to discriminate between the two mechanisms producing injuries in the knee area; however it loads the car front at the impact with a too high force due to a heavy dummy leg compared to one human leg.

Analysis of RSPD leg behaviour based on 7 tests performed in the same impact conditions shows a good repeatability, especially if we consider that the model used is only a laboratory prototype.

This study confirms that it is possible to develop a mechanical model of human leg to be used in a pedestrian protection evaluation sub-system test based on the main specifications of RSPD leg, but with some modifications especially a reduction of its weight.

## References

- (1) B. Aldman, J. Kajzer, D. Cesari, R. Bouquet, R. Zac, "A new pedestrian dummy for pedestrian tests" 10th ESV Conf. 1985.
- (2) D. Cesari, C. Cavallero, F. Cassan, Ch. Moffat, "Interaction between human leg and car bumper in pedestrian impact tests" 1988 IRCOBI Conference.
- (3) L. Grosch, J. Hochgeschwerder, "Experimental simulation of car/pedestrian and car/cyclist collisions" SAE paper 890751 in SP 782-1989.

## Acknowledgement

This validation study was done under contract with CCMC (Committee of Common Market Automobile Constructors) for which we are grateful.

## Bumper System Evaluation Using an Experimental Pedestrian Dummy

Janusz Kajzer, Bertil Aldman,  
Chalmers University of Technology, Sweden  
Hugo Mellander, Ingrid Planath,  
Kjell Jonasson  
Volvo Car Corporation, Sweden

### Abstract

Experimental studies have been undertaken using a rotationally symmetrical pedestrian dummy (RSPD) as a tool

for the assessment of car bumper aggressivity to pedestrians in low speed collisions (about 20 km/h). Aggressivity of different current bumpers, experimental foam bumpers and a standard bumper with an additional structure fitted below the bumper, was evaluated.

The frontal bumper is now required to protect certain car structures in lower speed collisions ( $\leq 8$  km/h). Such a bumper with extended structure mounted below would protect the adult pedestrian leg from knee injuries and probably lower leg fractures in pedestrian accidents at or below 20

km/h. This would require a structure which protrudes considerably in the front of the car and is designed to actively lower the contact point during impact. However, reasonably good protection can also be achieved if the scope is limited to a lower speed range. An additional structure fitted below a standard bumper is capable of transferring the forces necessary to accelerate the leg and reduce contact with the bumper. As an example results from tests with a structure which is only protruding about 30 mm in front of the standard bumper are shown.

## Introduction

The study presented in this paper is a result of two joint projects between the Department of Injury Prevention, Chalmers University of Technology and the Volvo Car Corporation.

In EEVC (1982) it was extensively reported that injury to the leg is one of the most common forms of trauma associated with pedestrian accidents.

The contact with the car bumper and the subsequent acceleration of the pedestrian leg result in a rather complex injury mechanism. The knee joint is subjected to a bending moment and often also to a shear force. The effect of this is compressive load on the nearest tibia condyle and tensile forces in the ligaments and the joint capsule. The inertia of the foot causes the lower leg to rotate with shear in the soft tissues and possibly torque is transmitted to the knee region.

## Experimental car fronts

Earlier studies by Aldman et al. (1985-b) of the biomechanics in car-pedestrian accidents have shown that two requirements must be met in order to achieve a reduction of the severity of injuries to the legs. The contact point between the car and the leg must be lowered and the contact forces must be limited.

Protection of pedestrians in collisions with cars is a complex problem. Analysis of this kind of accident shows that two body segments are overrepresented in the injury statistics, the lower limbs and the head. Ashton and Mackay (1979-b) reported that leg injuries were represented in about 60% of non-fatal injuries.

Several parameters influence the type and severity of lower limb injuries, e.g. the geometry of the car front and the properties of the structures. Pritz et al. (1975) showed that a lowering of the bumper level from 508 mm to 355 mm reduces adult knee injury. Aldman et al. (1979) showed that a 450 mm bumper level caused significantly more severe injuries than the same bumper at 250 mm. Harris (1976) proposed that the bumper should strike near the midpoint of the tibia. Jehu (1974) showed that bumpers should absorb energy also at pedestrian impacts.

During the 70's and 80's many research groups have designed experimental car fronts with the aim to protect pedestrians.

Pritz (1979) described the design of a modified production vehicle and indicated that a reduction in pedestrian injuries is possible through straightforward modification of existing production vehicles. Aldman et al. (1985-c) compared the standard bumper with one compliant bumper developed by NHTSA (like Pritz's construction) and made tests in two configurations with the bumper level 450 mm and 325 mm above the ground. A significant difference was found only between the standard bumper in the higher position and the compliant bumper in the lower position.

Harris and Radley (1979) presented a car designed for pedestrian protection. This car had energy absorbing bumper and bonnet leading edges. In another study Stcherbatcheff (1979) designed the Renault EPURE. Zones of impact were specially equipped to reduce the frequency of injury to the knee. Also Echavaidre and Gratadour (1979) presented a small car constructed for pedestrian protection.

Similar to the United States program Kruse (1976) and Richardson (1982) with its Research Safety Vehicle (RSV), Wollert et al. (1983) presented the development program for the UNI-CAR. The front end of this car had a so-called soft face developed on the basis of polyurethane foam.

A demonstration Pedestrian Safety Car was presented by Hobbs et al. (1985) based on the standard Austin Metro Car. The modification did not require the use of extra material, only changes to the car's styling were limited. Gaegauf et al. (1986) described a design of a car front with a pedestrian-activated displaceable hood.

## Current bumper design

Bumpers on today's cars are made of a variety of materials, like a simple plastic structure or a substantial energy absorbing arrangement conforming to low speed impact requirements such as US Standard Part 581 or ECE Regulation 42. As it is understood that most manufacturers will supply their cars with energy absorbing bumpers in the future, bumper configurations which will comply with these requirements were studied in the project presented in this paper.

Two different basic principles for energy absorbing bumpers are applied in production cars of today. The first type uses a strong exterior beam connected to the side members through energy absorbing dampers.

The other type consists of an energy absorbing foam or some other plastic cell structure in front of a strong beam across the side members. These arrangements normally have force-deflection characteristics which are too stiff to yield for a pedestrian leg.

The width and profile of different bumpers vary to a large extent. It seems evident, however, that there is a trend to integrate the bumper into the car's design.

In spite of the existing regulations or recommendations the height of different bumpers also vary significantly. The 62 most common car models in Sweden were studied regarding the differences in bumper level giving a mean value of 462 mm (figure 1).

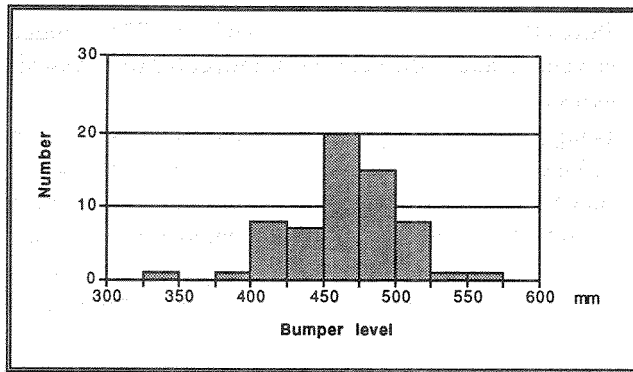


Figure 1. Bumper level distribution of car models registered in Sweden 1987 (n=62).

## Material and Methods

### Rotational symmetrical pedestrian dummy (RSPD)

All bumpers were evaluated with the RSPD (figure 2). The RSPD was developed in cooperation between INRETS in France and Chalmers University of Technology in Sweden (Aldman et al. 1985-a).

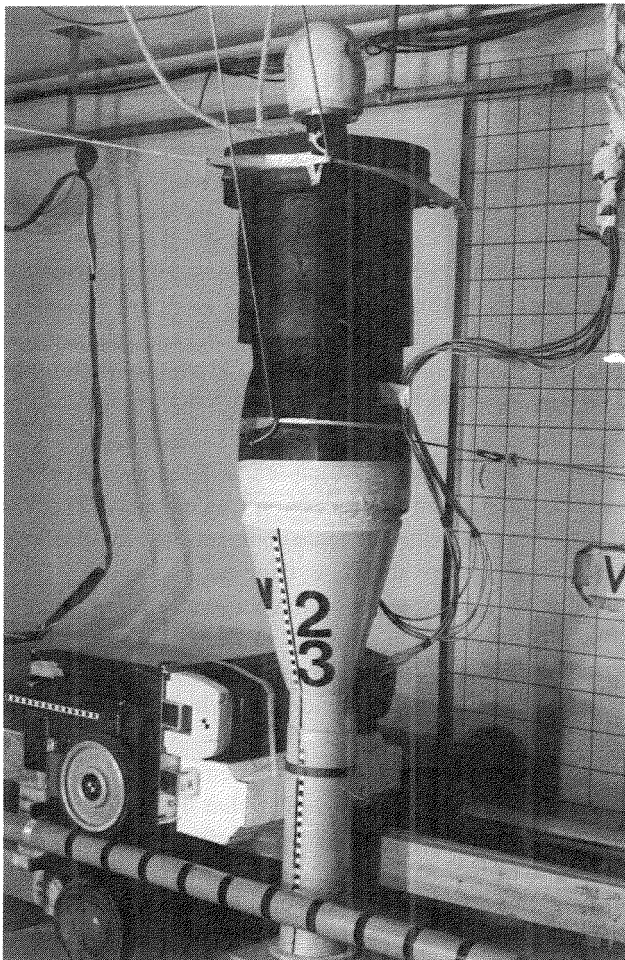


Figure 2. The RSPD dummy.

The dummy was used to study the bumper aggressivity to the lower limbs. This part of the RSPD is equipped with strain gauges, which are used to obtain bending moments and shear forces at the knee and the ankle levels. No measurements in the upper part of the dummy were made during the tests described in this paper.

The knee joint bar of the dummy is designed to deform plastically at a moment of 70 Nm. After each test the bar was replaced and the static bending angle was measured. In addition, the dynamic bending angle was determined by high speed film analysis.

### Test matrix

The study presented in this paper consists of three main phases. The first step was to perform tests with current bumper designs to define their aggressivity to the pedestrian. Results from this series gave input to the second part of the program: development of an experimental foam type bumper. In the third phase, a protruding structure was added below an unmodified current bumper. Different properties of the added structure were studied. A simplified test matrix is shown in table 1.

Table 1. Test matrix.

Phase	Main test object	Impact velocity	RSPD
1	3 different current bumpers	20 km/h	Yes
2	experimental foam bumper	20-40 km/h	Yes
	material and shape	30 km/h	No
3	additional protruding structure	20 km/h	Yes

Since it was difficult to distinguish the influence of different parameters in earlier experiments and with mathematical simulations with modified anthropometric test devices, the RSPD was designed. The leg of the RSPD is instrumented to enable the calculation of the bending moment, the shear and tensile forces and the torque about the knee and ankle joints. This makes it also possible to separately study the influence of various car front characteristics on these injury producing parameters. RSPD was used in all three phases.

### Bumper mounting

The bumpers, cut to the half width, were mounted on a trolley. The other frontal parts of the vehicle were not simulated. The experimental foam bumper was mounted 375 mm above the ground.

The standard bumper level was 442 mm above the ground. This level was measured to the vertical center of the bumper and includes a lowering of 15 mm representing loading and braking effect in real world accidents.

### Signal processing

The signals from all the transducers were after amplification filtrated with a low pass 500 Hz filter. The bending moments and the shear forces were calculated from the strain gauge signals.

High speed film (500 frames per second) was used to determine the maximum dynamic bending angle for the dummy knee.

### Damage criteria levels

In the evaluation of the tests performed, parameters and levels shown in table 2 were chosen.

**Table 2. Chosen damage criteria levels for the tests with the RSPD.**

Parameter	Level	Reference
Bending moment at knee level	≤70 Nm	Kramer 1973
Bending moment at ankle level	≤40 Nm	Kajzer 1989
Shear force at knee level	≤4.0 kN	Kajzer 1989
Bumper force	≤4.0 kN	Kramer 1973
Knee bar dynamic angle (used in relative evaluation between similar tests)	minimum	

The chosen damage criteria levels are based on the available biomechanical research and experience from the RSDP. They should be regarded as not yet fully verified.

Bending moment, is the primary parameter which generates injury in the knee joint, Aldman et al. (1985-b). Under dynamic conditions the magnitude of the shear force in the knee is less than the bumper force. This last parameter describes only local phenomena around the contact point between the bumper and the leg and can generate a fracture at the impact point. For complete information about the strain-stress response of the knee joint, both bending moment and shear force must be measured about this joint.

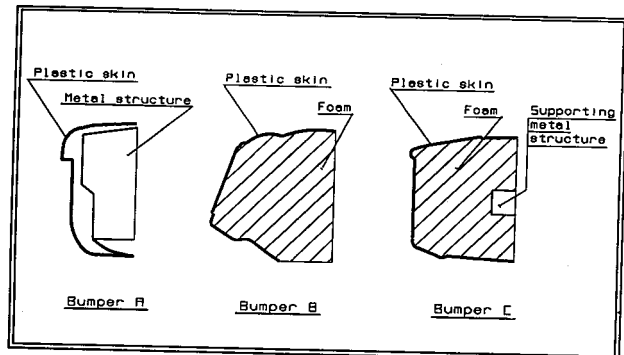
### Impact velocity

Farisse et al. (1981), Twigg et al. (1977), Appel et al. (1975) have concentrated on impact velocities of 30 km/h – 48 km/h (30 mph). These speeds correspond to accidents often resulting in very severe injuries, mainly to the head. However, Danner et al. (1979), Tharp and Tsongos (1976), Ashton and Mackay (1979-a) reported that many lower limb injuries occur at lower speeds. The tests described in this paper were mainly performed at velocity 20 km/h. However, in some initial tests the velocity was 40 km/h.

### Different current bumpers

Three current bumpers (figure 3) were tested with the RSPD. All three bumper types comply with US Standard Part 581.

**Figure 3. The current bumpers.**



The results from these tests formed the basis for the further work with modified bumpers. It was decided to study two different principles.

1. To limit the bumper force by changing the energy absorbing material.
2. To keep the standard bumper and add a structure below it to limit the bending moment at the knee level.

### Experimental foam type bumper

The objective of this work was to develop an energy absorbing bumper which would comply with existing low speed collision bumper requirements except for the bumper level and at the same time exhibit characteristics which would mitigate injuries to the leg of a struck pedestrian.

This phase of the project was performed in three steps.

1. Choice of material.
2. Pre-tests of the bumper.
3. Tests with instrumented leg.

It was decided that the principal system solution should use a stiff, supporting cross-member bolted to the side-members of the car and a plastic-foam core should act as an energy absorbing device.

The benefits of a reduced bumper fitting level have been shown in previous work (Aldman et al. 1985-b). It was therefore decided to mount the bumper at a level of 375 mm above the ground which was judged to be reasonable compromise between existing requirements and the need to have sufficient ground clearance for driving on to ramps.

The peak force which could be accepted by each side-member without permanent deformation was 40 kN.

### Test velocities

For the low speed collision tests, a test speed of 8 km/h (5 mph) was set.

For the pedestrian tests it was decided to start the evaluation process at a test velocity of 40 km/h. Later on in the test series it was, however, found that this was an unrealistic goal and the test velocity was reduced to 20 km/h.

### Standard bumper with additional structure

#### Principles of the additional structure

A number of different parameters were tested in this phase:

- Material, density.
- D, protruding depth (figure 4).
- h, active vertical height.
- H, level above ground.

The objective was to assess the minimum value of the protruding depth (D), which would fulfill the suggested damage criteria levels and still not affect the properties of the standard bumper.

Two different materials were used. Material M 1 was a

polyurethan foam with a density of 75 kg/m<sup>3</sup>. Material M 2 was a polypropene foam with a density of 55 kg/m<sup>3</sup>.

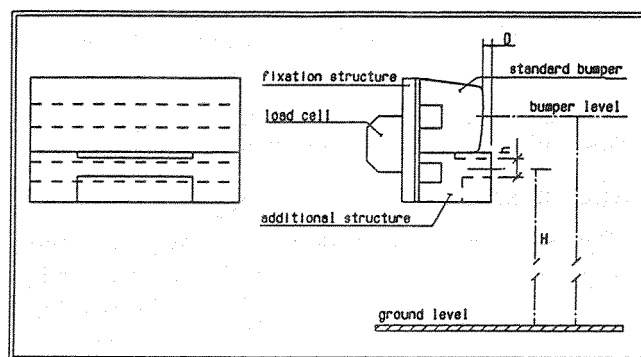


Figure 4. Set up for tests with the additional structure.

The standard bumper had a horizontal depth of 155 mm. The total horizontal depth of the additional structure was the sum of  $D$  and 155 mm.

## Results

### Different current bumpers

The results of the tests are presented in table 3.

Table 3. Results of the tests with current bumpers.

Test no	Bumper model	Bumper level (mm)	Bumper force (kN)	Measurements at knee level		
				Bending moment (Nm)	Shear force (kN)	Knee bar dynamic angle (°)
1	A	442	6.4	140	2.8	38
2	B	442	5.3	130	2.1	37
3	B	442	5.4	120	1.9	35
4	B	442	5.4	130	2.0	38
5	B	296	5.2	70	1.0	9
6	C	442	6.1	135	2.4	36
Chosen damage criteria levels			≤4.0	≤70	≤4.0	minimum

The bumper model B, which is not vertically symmetrical, was turned upside down in test no. 4. This resulted in an impact point about 50 mm lower than with the standard mounting. In test no. 5, model B was mounted at a level of 296 mm above the ground.

All bumper designs fulfilled the damage criteria level set for the shear force at the knee. When mounted at standard level, all models gave too high bumper forces and bending moments at the knee. Shear forces and bending moments at the ankle (not shown here) were acceptable in all tests.

From test no. 4 it was concluded that only a small change in the impact point was not enough to influence the results. When lowering the contact point between the bumper and the dummy leg more dramatically, as in test no. 5, the bending moment at the knee was reduced to an acceptable level. The knee bar dynamic angle confirmed the best result with the bumper configuration in test no. 5. The value in this test was lower than for the higher bumper contact points.

## Experimental foam type bumper

### Choice of material

To be able to select a plastic foam with the proper characteristics, a number of drop-tests with a tibia-like steel tube were performed on samples of interesting materials.

The purpose was to find a material with specific characteristics by a trial and error process. The material should be energy absorbing and give very little of the absorbed kinetic energy in rebound. The stiffness should be rate sensitive, meaning that at low speed it would be soft and at high speed it would be stiffer. This would prevent a bottoming out effect at higher speeds which otherwise could create high contact forces between the bumper and the pedestrian leg. The most efficient characteristics in terms of absorbed energy would be a square-wave force-deflection curve but in order to give protection also to the weaker part of the population it was decided to search for a material with a progressive linear deflection curve.

A material was specially developed and found to be in reasonable agreement with our requirements. The material was a polyether based polyurethan foam with a density of 60 kg/m<sup>3</sup>. In none of the tests, was there a skin covering over the foam core. The effect of such a skin was not studied.

A first prototype bumper was designed as seen in figure 5.

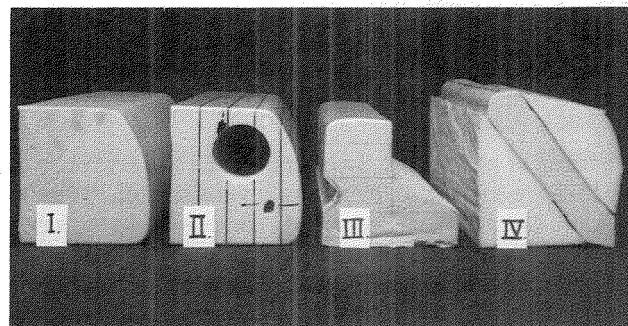


Figure 5. The prototype bumpers.

The depth and height of the bumper were arrived at after energy calculations for both the low speed impact conditions and the criteria levels to keep the forces acting on the leg below a certain level. The calculations were based on elementary theory in physics and will not be discussed here. It can be mentioned, however, that the effective mass of the leg was chosen to be 5 kg. The trolley weight was 240 kg. The depth and height of the bumper were 240 mm and 200 mm respectively.

### Performed pre-tests on the bumper

In order to find out whether it was advisable to move on to tests with the instrumented leg, drop tests with a cylinder with 50 mm diameter and a weight of 5 kg were performed on the prototype bumper. The objective was to keep the force below 4 kN. Due to restriction in height in the test hall the possible maximum speed was limited to 35 km/h.

The result showed that there was no bottoming-out and that the rebound velocity was 58% of the initial velocity.

The peak force was 4, 5 kN.

Despite the somewhat negative result in terms of rebound it was decided to move on to the bumper low speed collision tests. These were carried out in accordance with US Standard Part 581 with the exemption of the corner impact. The tests were successful without any permanent damage to the foam which recovered completely after the tests. The reacting forces in the side members were between 39.5 kN and 40.0 kN in each test.

### Test with instrumented leg

The prototype bumper No. 1 (figure 5) was tested initially at 40 km/h with the instrumented RSPD leg.

The results showed that the bumper force and the bending moment exceeded the chosen damage criteria levels (table 4).

**Table 4. Results of the tests with foam bumpers.**

Test no	Bumper prototype	Velocity (km/h)	Bumper force (kN)	Measurements at knee level		
				Bending moment (Nm)	Shear force (kN)	Knee bar dynamic angle (°)
7	I	40	5.8	135	2.0	29
8	II	40	5.0	115	1.7	20
9	III	40	5.0	120	1.6	18
10	IV	30	3.4	100	0.9	8
11	IV	20	2.4	90	0.6	5
Chosen damage criteria level			≤4.0	≤70	≤4.0	minimum

In order to lower the main load path, an 82 mm diameter hole was drilled (figure 5). This prototype was called No. II. The test showed that the bumper force was still too high (table 4).

A more drastic shape was tested in prototype No. III. Even with this design the bumper force was too high. It was also assumed that such a bumper would be impractical and easily damaged in real life. It was therefore decided to return to the original design but instead of having a homogeneous foam block, a diagonal 50 mm thick inner layer was positioned in the foam block (figure 5). The material in the diagonal part was polyurethane foam with a density of 60 kg/m<sup>3</sup> and the other material was polyurethane foam with very low density. This prototype was called No. IV. At this stage it was decided to lower the test speed to 30 km/h as it became more and more evident that the test objective was perhaps too stringent. All criteria levels were met except the bending moment at the knee which was on the limit (table 4). When lowering the velocity to 20 km/h all criteria levels were met except the bending moment which was just above the damage criteria level. With further optimization it is probable that this value could have been reduced below the level. Prototype No. IV did not meet the low speed collision requirements originally set up for this project.

### Standard bumper with additional structure

The results presented in the previous paragraph shows the difficulties in combining the low speed requirements with

improvements in pedestrian protection. A vehicle of normal weight would require a bumper with a very large horizontal depth. Therefore it was decided in a third phase of this project to keep the standard bumper and add a structure at the level of the air dam, i.e. below the bumper. The additional structure will lower the contact point on the pedestrian leg.

The results from the tests performed at 20 km/h with the RSPD are summarized in table 5.

**Table 5. Test results: The standard bumper with an additional structure.**

Test no	Material	D (mm)	h (mm)	H (mm)	Bumper force (kN)	Measurements at knee level		
						Bending moment (Nm)	Shear force (kN)	Kneebar dynamic angle (°)
12	M1	85	80	315	3.0	95	1.2	11
13	M1	85	80	315	2.8	95	1.2	10
14	M1	80	85	305	3.0	90	1.3	8
15	M1	80	85	305	3.0	90	1.3	9
16	M2	80	85	305	4.0	50	1.4	2
17	M2	30	85	305	4.5	60	1.3	2
18	M2	20	85	305	4.5	70	1.5	5
19	M2	20	85	305	4.5	70	1.5	5
Chosen damage criteria levels					≤4.0	≤70	≤4.0	minimum

Comparison of the materials (tests 14–16) shows that material M 2 gives a lower bending moment at the knee level. The bumper force is higher for material M 2.

Leg impact results in the additional structure bottoming out when material M 1 was used with values for D as in tests 12–15. A larger protrusion depth could have prevented this. With D = 85 mm the dummy leg was contacted by the bumper and experienced a more abrupt acceleration than when the additional structure did not bottom out, e.g. when material M 2 was used. The characteristics of M 2 allows construction of a non-bottoming out additional structure with D-values down to 30 mm. The lower knee bending moment and the knee bar dynamic angle for M 2 should be regarded as results of the combination of the material properties of M 2 and the non-bottoming out for this material.

For the same material, a slight change in the properties of the additional structure does not significantly affect the measurements (tests 12–15). Bottoming out occurs for the two values of D studied in these tests.

When varying the protruding depth of the additional structure most dramatically, the changes in the bending moment at the knee level and the knee bar dynamic angle are more obvious (test 16–19). D ≥ 30 mm gives a satisfactory bending moment, while 20 mm protruding depth proves to be insufficient to give results below the suggested damage criterion level. The bumper force is affected in a less significant way.

The shear forces at the knee level seem to be of the same order in all tests, with slightly higher values for material M 2.

The bumper forces exceed the suggested damage criterion level for all values of D when material M 2 is used. This finding confirms the difficulty in reaching compati-

bility between the existing low speed requirements and future pedestrian protection.

From the results in table 5 it can be concluded that the knee bending moment is less affected by variations in D than by the differences between the materials M 1 and M 2.

The best combination, when both considering vehicle and dummy measurements, appears to be a bumper of material M 2 with a protruding depth of 80 mm (test 16).

Not presented in table 5 are the shear forces and the bending moments at the ankle level. The value of these parameters increase when the contact point is lowered, but are in all tests below the suggested damage levels.

## Discussion

This project was performed under certain restrictions, e.g. geometrical conditions and simplicity of evaluation.

In the test method chosen, the impactor consisted of a trolley on which the bumper system had been mounted. The bonnet and the bonnet leading edge were not simulated. This might have affected the impact sustained by the leg, since possible bonnet leading edge impact to the femur was neglected. On the other hand, the current trend in car design is to give the front a more uniform slope, e.g. for aerodynamic purposes, thus eliminating the influence of the bonnet leading edge.

The different bumper systems have been evaluated by means of the RSPD. The measurements taken concentrate mainly on the impact sustained at the knee level. Injuries at this level are generally more severe than injuries to the long bones in the lower leg (Levine 1986). The RSPD is based on a fifty-percentile man, as are the criteria levels used. In future research the whole population at risk, including children and elderly, should be considered.

Phase two of the presented project pointed out the difficulty in combining compliance with low speed bumper requirements and pedestrian leg protection. Taking both these aspects into account in a conventional bumper only arrangement could result in considerable consequences on length, shape and design of the car front.

The experiments with different materials suggested that a bumper material which performs satisfactorily with respect to both low speed requirements and pedestrian protection probably can be found. Even if such a material obviously can be obtained, it is not yet readily available and has to be further developed with regard to the mass production process. Environmental aspects have also to be considered.

The addition of a protruding structure below the ordinary bumper proved to be a promising concept for the aims of this project. The dimensions resulting in the most satisfactory dummy readings should, however, be regarded as the most advantageous combination of the parameters tested. They do not claim to be the optimal solution. The purpose was merely to find out if the additional structure protruding below a standard bumper had an effect on the dummy lower leg measurements.

## Conclusion

Pedestrian protection of different bumper systems has been evaluated by means of the RSPD.

Two approaches to the construction of a pedestrian-friendly bumper system were studied.

1. Changes of ordinary bumpers by varying geometry, material and shape. The main disadvantages of this solution were the major design changes that would be needed, resulting in e.g. unrealistic long car fronts.

2. Addition of a protruding structure below the ordinary bumper. A major advantage with this approach is that it lowers the contact point of the pedestrian leg without affecting the low speed response of the ordinary bumper.

A system in accordance with point 2, with a polypropene additional structure protruding 30 mm and an active vertical height of 85 mm mounted below the ordinary bumper, resulted in the lowest bending and shearing at the pedestrian knee.

## References

- Aldman, B., Kajzer, J., Bunketorp, O., Eppinger, R. (1985-c). An Experimental Study of a Modified Compliant Bumper. Tenth Int Technical Conf on Experimental Safety Vehicles. Oxford England July 1-4, 1985. US Dept of Transportation, NHTSA pp 1035-1040.
- Aldman, B., Kajzer, J., Cesari, D., Bouquet, R., Zac, R. (1985-a). A New Dummy for Pedestrian Test, Tenth Int Technical Conf on Experimental Safety Vehicles. Oxford England, July 1-4. US Dept of Transportation NHTSA pp 176-185.
- Aldman, B., Kajzer, J., Anderlind, T., Malmqvist, M., Mellander, H., Turbell, T. (1985-b). Load Transfer From the Striking Vehicle in Side and Pedestrian Impacts, Tenth Int Technical Conf on Experimental Safety Vehicles. Oxford England, July 1-4. US Dept of Transportation, NHTSA pp 620-637.
- Aldman, B., Lundell, B., Thorngren, L., Bunketorp, O., Romanus, B. (1979). Physical Simulation of Human Leg-Bumper Impacts. Proc of the IVth International IRCOBI Conf on the Biomechanics of Trauma. Bron IRCOBI Secretariat pp 232-242.
- Appel, H., Stürtz, G., Gotzen, L. (1975). Influence of Impact Speed and Vehicle Parameter on Injuries of Children and Adults in Pedestrian Accidents., Proc of the 2nd Int Conf on Biomechanics of Serious Trauma. Birmingham Sept 9-11, IRCOBI Bron, France pp 83-100.
- Ashton, S.J., Mackay, G. M. (1979-a). Car Design for Pedestrian Injury Minimization. Proc 7th Int Techn Conf on ESV. Paris June 5-8, pp 630-640. US DOT NHTSA.
- Ashton, S.J., Mackay, G.M. (1979-b). Some Characteristics of the Population Who Suffer Trauma as Pedestrians When Hit by Cars and Some Resulting Implications. Proc of the IVth Int IRCOBI Conf on The Biomechanics of Trauma. Göteborg Sept 5-7, IRCOBI Bron France pp 39-48.

- Danner, M., Langwieder, K., Wachter, W. (1979). Injuries to Pedestrians in Real Accidents and Their Relation to Collision and Car Characteristics. Proc of Twenty-Third Stapp Car Crash Conf, Oct 17-19. San Diego pp 159-198. SAE Warrendale PA.
- Echavaidre, J., Gratadour, J. (1979). Peugeot VLS and Pedestrian Protection. Proc 7th Int Techn Conf on ESV. Paris June 5-8, pp 689-698. US DOT NHTSA.
- EEVC/CEVE (1982). Pedestrian Injury Accidents, Proc of the 9th ESV Conference. Kyoto pp 638-671.
- Farisse, J., Seriat-Gautier, B., Dalmas, J., Daou, N., Bourret, P., Cavallero, D., Cesari, D., Ramet, M., Billaut, P., Berthommier, M. (1981). Anatomical and Biomechanical Study of Injuries Observed During Experimental Pedestrian-Car Collisions. Proc of the VIth Int IRCOBI Conf on the Biomechanics of Impacts, Salon de Provence 8-10 September pp 342-354 IRCOBI Secretariat, Bron, France.
- Gaegauf, M., Kaeser, R., Meyer, E., Reif, G. (1986). Design of a Pedestrian Compatible Car Front. Proc Int IRCOBI Conf on The Biomechanics of Impacts. 2-3-4 September Zürich pp 205-219. IRCOBI Secretariat, Bron France.
- Harris, J. (1976). Research and Development Towards Improved Protection for Pedestrians Struck by Cars. Proc 6th Int Techn Conf on ESV Washington Oct 12-15 pp 724-733. US DOT NHTSA.
- Harris, J., Radley, C.P. (1979). Safer Cars for Pedestrians. Proc 7th Int Techn Conf on ESV. Paris June 5-8, pp 704-712. US DOT NHTSA.
- Hobbs, C A., Lawrence, G J L., Clarke, C S. (1985). PSC1-A Demonstration Car with Improvements for Pedestrian Protection, Tenth Int Technical Conf on Experimental Safety Vehicles. Oxford England, July 1-4. US Dept of Transportation, NHTSA pp 31-38.
- Jehu, V J. (1974) Towards Pedestrian Safety. Proc 5th Int Techn Conf on ESV London June 4-7, pp 533-534. US DOT NHTSA.
- Kajzer, J. (1989). Validation of RSPD with biological material. To be published.
- Kramer, M., Burow, K., Hegar, A., (1973). Fracture Mechanism of Lower Legs under Impact Load. Proc of the 17th Stapp Car Crash Conference pp 81-100. Oklahoma.
- Kruse, W L. (1976). Calspan-Chrysler Research Safety Vehicle Front End Design for Property and Pedestrian Protection. Proc 6th Int Techn Conf on ESV. Washington Oct 12-15, pp 426-442. US DOT NHTSA.
- Levine, R S. (1986). A Review of the Long-term Effects of Selected Lower Limb Injuries. Symposium on Biomechanics and Medical Aspects of Lower Limb Injuries, San Diego, California.
- Pritz, H B., Hassler, C R., Herridge J T., Weiss Jr., E B. (1975). Experimental Study of Pedestrian Injury Minimization Through Vehicle Design. Proc of 19th Stapp Car Crash Conf November 17-19. San Diego, California pp 725-751. SAE Warrendale PA.
- Pritz, H B. (1979). Vehicle Design for Pedestrian Protection. Proc 7th Int Techn Conf on ESV. Paris June 5-8, pp 699-703. US DOT NHTSA.
- Richardson, F G. (1982). Results of the United States Research Safety Vehicle Program. Proc 9th Int Techn Conf on ESV Kyoto Japan Nov 1-4, pp 41-48. US DOT NHTSA.
- Stcherbatcheff, G. (1979). Pedestrian Protection. Special Features of the Renault E.P.U.R.E. Proc 7th Int Techn Conf on ESV. Paris June 5-8, pp 660-673. US DOT NHTSA.
- Tharp, K J., Tsongos, N G. (1976). Injury Severity Factors—Traffic Pedestrian Collisions. Proc of the Meeting on Biomechanics of Injury to Pedestrians, Cyclists and Motorcyclists. Amsterdam Sept 7-8, IRCOBI Bron France pp 55-64.
- Twigg, D W., Ticher, J L., Eppinger, R H. (1977). Optimal Design Automobiles for Pedestrian Protection. SAE paper No 770094.
- Wollert, W., Blödorn, J., Appel, H., Kühnel, A. (1983). Realization of Pedestrian Protection Measures on Cars. Proc Pedestrian Impact Injury & Assessment. P-121. Int Congress & Exposition Detroit. Feb 28-March 4. SAE Warrendale pp 27-37.

## The Influence of Car Shape on Pedestrian Impact Energies and its Application to Sub-System Tests

Graham J.L. Lawrence,  
Transport and Road Research Laboratory,  
United Kingdom

### Abstract

In a collision between a car and pedestrian, the location and severity of impacts to the pedestrian vary considerably with respect to the shape of the car front. Consequently for the three primary areas of a car that are important for pedestrian safety (the bumper, bonnet leading edge, and bonnet top) the protection requirements will also vary considerably

according to the car shape. Any sub-system tests to assess the protection afforded by a particular design of car must take account of the important interactions between the vehicle structure and the corresponding body regions that are liable to suffer serious injury in an impact. In order to obtain further data to evaluate these interactions, the Transport and Road Research Laboratory has conducted two series of full scale tests with a range of simulated car shapes. Impact velocities, force and acceleration were measured at each of the three primary impact points and these have been used to derive effective mass and energy at each phase of an impact. This paper summarises results of tests at 40 km/h using

dummies representing a six year old child, and an adult pedestrian. The results show that bonnet height strongly influences impact energy for impacts to the bonnet leading edge and bonnet top. Bumper height influences the impact energy for bumper and bonnet leading edge contacts. The variations in impact severity are discussed with respect to their implications for sub-systems testing. The results in this paper can, for any style of car, identify structures where pedestrian protection requirements may be particularly demanding and also give guidance on the amount of protection required.

## Introduction

In a collision between a car and pedestrian, the location and severity of impacts to the pedestrian vary considerably with respect to the shape of the car front.

Research has shown that the important areas to consider with respect to pedestrian protection are the bumper, the bonnet leading edge and the bonnet top. Methods for evaluating pedestrian protection requirements for passenger cars are currently being developed and are concentrating on a sub-system form of test in which an impactor strikes each of these three regions of the car. The basic requirement of sub-system tests is that they should represent the important interactions between the vehicle structure that is under assessment and the corresponding body regions that are liable to suffer serious injury from striking it.

In order to obtain further data to evaluate these interactions with respect to both the size of pedestrian and the impact velocity, TRRL has conducted two series of full scale tests with a range of simulated car shapes. Impact velocities, force and acceleration were measured at each of the three primary impact points (i.e. bumper, bonnet leading edge and bonnet top) and have been used to derive effective mass and energy for each impact point. This paper summarises results of impact tests at 40 km/h using dummies representing a six year old child and an adult pedestrian.

The results are discussed with respect to impact requirements for sub-systems testing. The dominant trends in the variation of impact characteristics with respect to vehicle shape are identified. Values for impactor mass, velocity and direction of impact are given, based on the performance of dummies. These values may need to be adjusted to allow for the differences between the characteristics of the dummies and humans.

## Description of Tests

A range of simulated car shapes were mounted on a trolley to impact a standing adult or child dummy, at a nominal speed of 40 km/h, see figures 1 and 2. The dummy was supported from an overhead gantry and released electrically by the approaching trolley just before impact. In all tests kinematic data was digitised from high speed films and used in conjunction with outputs from transducers on the dummy in the computer analysis.

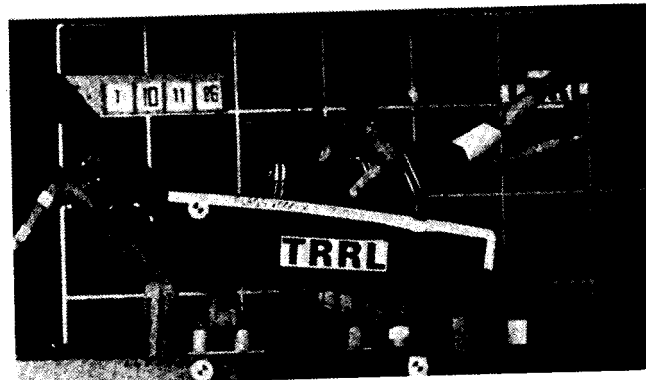


Figure 1. Typical test.

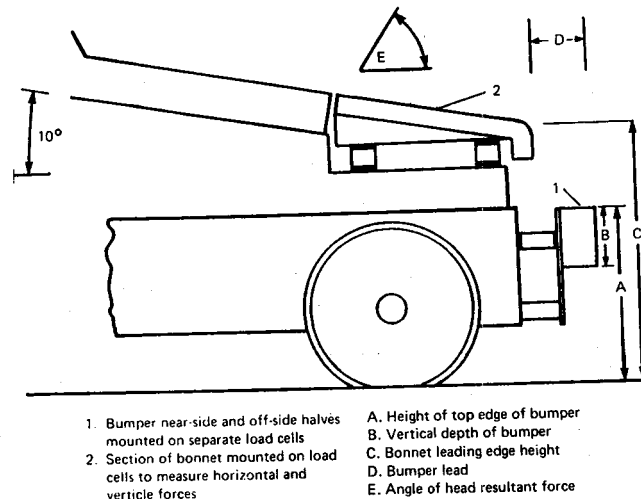


Figure 2. Vehicle simulation.

## Pedestrian dummies

The adult pedestrian dummy used was an Ogle 50th percentile male, 1.7 metres tall weighing 75 kg. Modified knee joints were fitted which incorporated clutches to simulate lateral bending at the knee resulting from ligamental strain (1)\*. Impact was square on to the left side, with the left leg backwards and the right leg forwards.

Miniature uni-directional accelerometers were attached directly to the steel leg bones under the "flesh" to measure the acceleration of the body region in contact with the car. The positions of the accelerometers were adjusted to be in the centre of bumper and bonnet impact points for each car shape.

To limit the number of test runs, the adult dummy head to bonnet impacts were not measured. These measurements would have required additional tests for each car shape, to identify the point of contact at which to relocate rear bonnet top force transducers.

The child pedestrian dummy used was an Ogle dummy represented a 6-year-old child, 1.19 metres tall weighing 23.6 kg. Two impact stances were used for each car shape. For the tests to assess bumper and bonnet leading edge contacts, the impact was square on to the left side, with the

\*Numbers in parentheses designate references at end of paper.

left leg backwards and the right leg forwards. To assess head to bonnet impacts the tests were repeated with the dummy turned to face 30 towards the car from directly sideways on. With this stance the head hit the bonnet without interference from the left shoulder.

The accelerations of body segments directly in contact with the vehicle were measured using pelvic and head tri-axial accelerometers and by accelerometers fitted to the leg and abdomen. Leg accelerations were measured by a miniature uni-directional accelerometer attached directly to the left leg bone under the flesh. For each test the accelerometer's height was adjusted to correspond with the centre of the impact point.

The abdominal and lower thoracic regions on a standard dummy have a poor resemblance to a human and there is no well defined structural form at the outer surface on which to mount an accelerometer. To overcome this difficulty an abdominal mass, made from a modified Eurosid dummy abdomen was installed to fill the gap between the pelvis and the diaphragm. The mass of the child dummy was kept standard by removing some ballast weights. Lateral and vertical accelerations were measured by two miniature accelerometers mounted in the abdomen mass, in the foam behind the layer weighted with lead, their height being adjusted to the centre of bonnet impact.

The use of a mass of this type will not give realistic instantaneous values of acceleration but the derived values should give a relative indication of the magnitude of the total impact to the bonnet leading edge.

### The impact trolley

The impact trolley weighed 1050 kg and consisted of an unsprung steel frame running on railway lines. The nominal test speed was 40 km/h. The trolley was braked after impact at a rate of 0.7 g. The car shapes simulated included variations in bonnet height, bumper lead and bumper height. The vertical bumper depth was 200 mm in all tests. In all cases the bonnet top sloped downward to the front at 10 degrees to the horizontal, see figure 2.

### Force measurement

The front section and the leading edge of the bonnet and the near-side and off-side halves of the bumper were separately mounted on load measuring transducers and covered in dense energy absorbing foam (Plastazote). The foam was 112 mm thick at the bumper and 62 mm at the bonnet leading edge. The general stiffness characteristics of this arrangement produced approximately sinusoidal force and acceleration time histories and were aimed to match the maximum forces generated by cars developed for pedestrian safety. The coefficient of restitution of the foam was low, giving little rebound velocity. The smooth time histories and low coefficient of restitution improved the accuracy with which force and acceleration curves could be used to derive energy.

Horizontal impact forces on the two halves of the bumper were measured using two pairs of load cells.

The bonnet leading edge and the first 0.57 metres of the bonnet top were mounted on a frame with four bi-axial load cells that measured both horizontal and vertical bonnet force.

## Discussion of Results

The results of the tests are shown in tables 1 to 9 for the adult dummy and tables 10 to 20 for the child dummy. For any given combination of bonnet and bumper dimensions the results for each dummy are from the same test, with the exception of child head results, where the tests were repeated as previously described.

### Velocity change due to bumper impact

Table 1 (adult first and second leg) and table 10 (child first leg), show the velocity change, up to common velocity, for the section of the leg in contact with the bumper.

**Table 1. Adult—velocity change first and second leg due to bumper impact, with respect to car shape.**

		Car dimensions mm					
Bonnet Height of leading edge	Bumper Height of top edge	Bumper lead			Bumper lead		
		50	150	250	50	150	250
		Velocity change of first leg m/s			Velocity change of second leg m/s		
600	400	11.0	10.8	----	11.5	11.2	----
700	400	10.7	10.6	11.1	11.4	10.8	11.5
750	400	11.1	10.9	11.0	11.8	11.1	11.2
850	400	10.7	11.0	11.1	11.7	11.4	11.7
750	350	----	11.0	----	----	11.6	----
750	400	11.1	10.9	11.0	11.8	11.1	11.2
750	450	----	11.1	----	----	11.3	----
750	500	----	10.9	----	----	11.2	----
750	550	----	10.9	----	----	11.3	----

**Table 10. Child—velocity change first leg due to bumper impact, with respect to car shape.**

		Car dimensions mm	
Bonnet Height of leading edge	Bumper Height of top edge	Bumper lead	
		150	250
		Velocity change of first leg m/s	
650	450	11.2	----
700	450	11.2	----
750	450	11.1	11.2
850	450	11.2	----
750	400	11.3	----
750	450	11.1	11.2
750	500	11.0	----
750	550	11.1	----

The values were derived from the leg accelerometer which was adjusted to coincide with the centre line of the bumper for each test. For both adult and child, the left leg was struck first. The velocity change was the same as the trolley impact velocity, and the small variations in the results arise from small frictional differences in the running

gear and braking system of the test rig. For the adult the impact velocity for the right leg is higher than the left leg in all cases, this being most marked for the 50 mm bumper lead, (table 1). The increase in velocity is due to the dummy rotating slightly as it is struck off-centre (legs apart) low down on the first leg. This swings the second leg towards the bumper. As the child was shorter than the adult the impact point is higher on its body, thus reducing the severity of the second leg impact. For this reason the only measurements made for the child second leg impact were the force time history.

### Energy of deformation for bumper to legs

Table 2 (adult first and second leg) and table 11 (child leg first), show the energy of deformation. This was derived for each half of the bumper from the measured bumper force and the displacement of each leg relative to the trolley, and was calculated up to the point of common velocity of the leg and bumper. The displacement was derived from the leg accelerometer which was adjusted to coincide with the centre line of the bumper for each test.

**Table 2. Adult—deformation energy of bumper from leg impact, with respect to car shape.**

		Car dimensions mm					
Bonnet	Bumper	Bumper lead			Bumper lead		
Height of leading edge	Height of top edge	50	150	250	50	150	250
		Energy of bumper deformation-first leg kJ			Energy of bumper deformation-second leg kJ		
		600	400	0.31	0.27	----	0.36
700	400	0.34	0.44	0.36	0.36	0.38	0.38
750	400	0.33	0.34	0.34	0.40	0.41	0.38
850	400	0.29	0.40	0.35	0.25	0.41	0.42
750	350	----	0.23	----	----	0.28	----
750	400	0.33	0.34	0.34	0.40	0.41	0.38
750	450	----	0.41	----	----	0.45	----
750	500	----	0.35	----	----	0.45	----
750	550	----	0.33	----	----	0.35	----

**Table 11. Child-deformation energy for bumper from leg impact, with respect to car shape.**

		Car dimensions mm	
Bonnet	Bumper	Bumper lead	
Height of leading edge	Height of top edge	150	250
		Energy of deformation of bumper by first leg to bumper kJ	
650	450	0.32	----
700	450	0.30	----
750	450	0.31	0.27
850	450	0.30	----
750	400	0.29	----
750	450	0.31	0.27
750	500	0.39	----
750	550	0.51	----

The results in the upper section of the table shows that, in general, the energy of bumper deformation is not strongly influenced by bonnet height or bumper lead.

The lower section of the tables shows the trend of energy against bumper height. For the adult legs (table 2) the deformation energy increases with bumper height until significant knee clutch deflections occur (table 3). When the bumper is high it impacts close to the joint, and the resulting clutch deflection has the effect of reducing mass and therefore energy. Operation of the knee clutch gives a measure of the effect of a broken knee joint or leg. For the child legs (table 11) the deformation energy also increases with bumper height, reflecting the increasing mass as the bumper top edge approaches the level of the pelvis.

### Knee clutch deflection

Table 3 (adult) shows the angle of lateral bending of the adult knee. The clutch simulating the knee ligaments was set to a torque of 200 Nm and a deflection angle of 6 degrees or more has been related to the onset of ligament failure (1). Impact in the vicinity of the knee results in high lateral bending moments across the knee, resulting in a large clutch deflection angle.

**Table 3. Adult—angle of knee lateral bending, with respect to car shape.**

		Car dimensions mm					
Bonnet	Bumper	Bumper lead			Bumper lead		
Height of leading edge	Height of top edge	50	150	250	50	150	250
		Knee lateral bending first leg degrees			Knee lateral bending second leg degrees		
		600	400	25	0	--	22
700	400	22	15	0	0	0	0
750	400	40	15	0	0	0	0
850	400	10	0	10	0	0	0
750	350	--	10	--	--	0	--
750	400	40	15	0	0	0	0
750	450	--	22	--	--	0	--
750	500	--	35	--	--	10	--
750	550	--	35	--	--	30	--

### Equivalent impactor mass for bumper to leg impacts

Table 4 (adult first and second leg) and table 12 (child first leg), show the equivalent impactor mass of the leg striking the bumper. This is the mass of an impactor which, when used in a sub-system test at the same velocity, will give the same energy of deformation to the vehicle as a full scale dummy test. Equivalent impactor mass was calculated from velocity change (table 1 for the adult and table 10 for the child) and energy of deformation for each leg impact (table 2 for the adult and table 11 for the child).

The upper sections of the table show that, in general, the leg to bumper equivalent impactor mass is not strongly influenced by bonnet height or bumper lead. This mass ranged between 3.6 and 7.7 kg for the adult and between 4.2 and 5.1 kg for the child.

The lower section of the tables shows the trend of equivalent impactor mass against bumper height. For the adult legs the mass rises with bumper height, until significant knee

clutch deflections occur with the higher bumpers, this having the effect of reducing mass. As with energy, operation of the knee clutch gives a measure of the effect of a broken knee joint or leg. For the child, raising the bumper increases the mass from 4.6 kg for the 400 mm bumper to 8.2 kg as the 550 mm bumper top edge approaches the height of the child pelvis.

**Table 4. Adult—equivalent impactor mass of first and second leg striking bumper, with respect to car shape.**

		Car dimensions mm					
Bonnet	Bumper	Bumper lead			Bumper lead		
Height of leading edge	Height of top edge	50	150	250	50	150	250
		Equivalent impactor mass of first leg kg			Equivalent impactor mass of second leg kg		
		600	400	5.12	4.63	----	5.44
700	400	6.00	7.73	5.86	5.51	6.43	5.80
750	400	5.37	5.63	5.62	5.72	6.72	6.06
850	400	5.04	6.58	5.70	3.65	6.23	6.19
750	350	----	3.80	----	----	4.12	----
750	400	5.37	5.63	5.62	5.72	6.72	6.06
750	450	----	6.57	----	----	7.11	----
750	500	----	5.81	----	----	7.16	----
750	550	----	5.43	----	----	5.48	----

**Table 12. Child—equivalent impactor mass of first leg striking bumper, with respect to car shape.**

		Car dimensions mm	
Bonnet	Bumper	Bumper lead	
Height of leading edge	Height of top edge	150	250
		Equivalent impactor mass of first leg to bumper kg	
		650	450
700	450	4.77	----
750	450	4.98	4.22
850	450	4.70	----
750	400	4.56	----
750	450	4.98	4.22
750	500	6.33	----
750	550	8.23	----

### Impulse of first and second leg striking bumper

Table 5 (adult) and table 13 (child), show the impulse, i.e. change of momentum, for the adult first and second leg and child first leg contact. The impulse for each half of the bumper was calculated up to the point of common velocity, for the section of the leg in contact with the bumper. The values were derived from the bumper force time histories.

The upper section of the tables shows that in general the impulse of the bumper impact is not strongly influenced by bonnet height or the 150 and 250 mm bumper leads, but with the 50 mm lead "adult" tests there is a tendency for the bonnet leading edge to off-load the bumper.

The lower section of the tables shows the trend of impulse against bumper height. For the adult legs (table 5) the

impulse increases with bumper height, until significant knee clutch deflections occur with the higher bumpers, this having the effect of reducing impulse. For the child legs (table 13) the impulse also rises with bumper height, with the 550 mm high bumper giving the largest value as the bumper top edge approaches the height of the pelvis.

**Table 5. Adult—impulse of first and second leg striking bumper, with respect to car shape.**

		Car dimensions mm					
Bonnet	Bumper	Bumper lead			Bumper lead		
Height of leading edge	Height of top edge	50	150	250	50	150	250
		Impulse of bumper to first leg N-s			Impulse of bumper to second leg N-s		
		600	400	70	63	----	76
700	400	71	93	88	76	84	87
750	400	69	83	83	83	88	79
850	400	61	91	88	50	77	89
750	350	----	57	----	----	79	----
750	400	69	83	83	83	88	79
750	450	----	90	----	----	92	----
750	500	----	75	----	----	100	----
750	550	----	68	----	----	74	----

**Table 13. Child—impulse of first leg striking bumper, with respect to car shape.**

		Car dimensions mm	
Bonnet	Bumper	Bumper lead	
Height of leading edge	Height of top edge	150	250
		Impulse of bumper to first leg N-s	
		650	450
700	450	79	----
750	450	85	70
850	450	97	----
750	400	76	----
750	450	85	70
750	500	98	----
750	550	128	----

### Velocity change due to bonnet leading edge impact

Table 6 (adult leg) and table 14 (child pelvis/abdomen) shown, for the section of the dummy in contact with the bonnet edge, the velocity change that resulted from the contact.

The values were derived from accelerometers mounted on the adult upper leg or child pelvis/abdomen. The positions of these accelerometers were adjusted to coincide with the centre line of the bonnet edge for each test, and their outputs were resolved into the horizontal plane using the kinematic data from the high speed films.

For both adult and child, the horizontal velocity change was greatest with the short bumper lead and high bonnet. In both cases the change approximated to trolley impact speed. It reduced as the bumper lead increased and the bonnet edge was lowered. Raising the bumper height also reduced the

horizontal impact velocity by up to 41 percent for the adult and by 66 percent for the child. Both of these trends reflect the influence of the bumper deflecting the dummy from impact with the bonnet edge as the bonnet becomes lower to and further behind the bumper.

**Table 6. Adult—velocity change of upper leg from impact with bonnet leading edge, with respect to car shape.**

Car dimensions mm							
Bonnet	Bumper	Bumper lead			Bumper lead		
Height of leading edge	Height of top edge	50	150	250	50	150	250
		Velocity change of upper leg - horizontal m/s			Velocity change of upper leg - vertical m/s		
600	400	8.0	1.2	----	1.8	2.1	----
700	400	10.7	6.7	4.4	2.3	3.9	4.2
750	400	11.1	8.1	5.5	2.9	4.0	4.8
850	400	10.7	10.3	8.5	0.0	3.7	5.6
750	350	----	8.2	----	----	4.4	----
750	400	11.1	8.1	5.5	2.9	4.0	4.8
750	450	----	6.5	----	----	5.2	----
750	500	----	5.2	----	----	5.4	----
750	550	----	4.8	----	----	4.3	----

**Table 14. Child—velocity change of pelvis/abdomen from impact with bonnet leading edge, with respect to car shape.**

Car dimensions mm					
Bonnet	Bumper	Bumper lead		Bumper lead	
Height of leading edge	Height of top edge	150	250	150	250
		Velocity change pelvis / abdomen - horizontal m/s		Velocity change pelvis / abdomen - vertical m/s	
650	450 +	3.8	---	1.6	---
700	450 *	7.8	---	5.7	---
750	450 *	9.6	8.8	3.2	5.7
850	450 *	10.9	---	1.1	---
750	400 *	10.8	---	2.2	---
750	450 *	9.6	8.8	3.2	5.7
750	500 *	8.3	---	2.6	---
750	550 *	4.1	---	2.5	---

Note + = pelvis accelerometers used  
\* = abdomen accelerometers used

### Energy of deformation for bonnet leading edge to upper leg impact

Table 7 (adult) shows the energy of deformation for the bonnet leading edge to upper leg impact. The horizontal energy of deformation was found from the measured bonnet forces and the displacement of the leg relative to the trolley, and was calculated up to the point of common velocity.

The leg displacement values were derived from the leg accelerometers whose positions were adjusted to coincide with the centre line of the bonnet edge for each test. The outputs were resolved into the horizontal plane using the kinematic data from the high speed films.

The upper section of the table shows that the energy of bonnet deformation (horizontal) increases as the bonnet is raised, the trend being similar to that of impulse shown in figure 8. The lower section and figure 9 show that the horizontal energy reduces as the bumper height is increased.

**Table 7. Adult—deformation energy of bonnet from upper leg impact, with respect to car shape.**

Car dimensions mm				
Bonnet	Bumper	Bumper lead		
Height of leading edge	Height of top edge	50	150	250
		Bonnet energy of deformation - horizontal kJ		
600	400	0.25	0.12	----
700	400	0.32	0.37	----
750	400	0.59	0.49	----
850	400	0.50	0.50	----
750	350	----	0.60	----
750	400	0.59	0.49	----
750	450	----	0.40	----
750	500	----	----	----
750	550	----	----	----

### Equivalent impactor mass for bonnet leading edge to upper leg impact

Table 8 (adult) shows the equivalent impactor mass of the upper leg striking the bonnet. This was calculated from velocity changes shown in table 6 and energy of deformation for upper leg impact in table 7.

**Table 8. Adult—equivalent impactor mass upper leg striking bonnet, with respect to car shape.**

Car dimensions mm				
Bonnet	Bumper	Bumper lead		
Height of leading edge	Height of top edge	50	150	250
		Equivalent impactor mass - horizontal kg		
600	400	7.8	*	----
700	400	5.6	16.3	----
750	400	9.6	14.9	----
850	400	9.1	9.3	----
750	350	----	17.7	----
750	400	9.6	14.9	----
750	450	----	18.7	----
750	500	----	----	----
750	550	----	----	----

\* Force and velocity change small.

The upper section of the table shows the trends for upper leg to bonnet equivalent impactor mass with regard to bumper lead and bonnet height. The horizontal component of mass generally reduces as the bumper lead reduces.

The lower section of the tables shows no significant change between equivalent impactor mass and bumper height, for the shapes tested.

### Impulse due to bonnet leading edge impact

Table 9 (adult) and table 15 (child) show the impulse, ie. change of momentum, for the section of dummy in contact with the bonnet leading edge. For the adult this figure was calculated up to the point of common velocity of the section of the leg in contact with the bonnet to eliminate the influence of rebound energy. For the child, it was calculated up to

the end of bonnet contact because the abdomen segment caused only a small proportion of the total impulse (see transfer of energy to dummy at end of this section). The value was derived from the bonnet horizontal and vertical force-time histories.

**Table 9. Adult—impulse of upper leg striking bonnet, with respect to car shape.**

Car dimensions mm							
Bonnet Height of leading edge	Bumper Height of top edge	Bumper lead			Bumper lead		
		50	150	250	50	150	250
		Impulse of upper leg to bonnet - horizontal N-s			Impulse of upper leg to bonnet - vertical N-s		
600	400	84	41	---	46	0	---
700	400	125	138	128	62	98	88
750	400	211	176	139	116	125	95
850	400	183	203	189	74	96	92
750	350	---	195	---	---	138	---
750	400	211	176	139	116	125	95
750	450	---	142	---	---	132	---
750	500	---	125	---	---	121	---
750	550	---	132	---	---	136	---

**Table 15. Child—impulse of pelvis/abdomen striking bonnet, with respect to car shape.**

Car dimensions mm					
Bonnet Height of leading edge	Bumper Height of top edge	Bumper lead		Bumper lead	
		150	250	150	250
		Impulse of pelvis / abdomen - horizontal N-s		Impulse of pelvis / abdomen - vertical N-s	
650	450	27	---	24	---
700	450	53	---	50	---
750	450	88	85	49	90
850	450	136	---	30	---
750	400	110	---	54	---
750	450	88	85	49	90
750	500	60	---	36	---
750	550	32	---	55	---

For both the child and adult the values of horizontal impulse increase strongly with respect to increasing bonnet height and decreasing bumper height (see also figures 8 and 9). The ratio of horizontal to vertical impulse also increases as the front of the car becomes more upright (ie. high bonnet and short bumper lead).

### Velocity change of child head due to bonnet top impact

Table 16 shows the resultant velocity change of the child dummy's head resulting from contact with the bonnet top. The value was derived from the outputs of the accelerometers mounted in the head.

The upper section of the table shows that the head velocity change is strongly influenced by bonnet height. Raising the bonnet from 650 to 750 mm reduces the velocity from 11.3 to 8.6 m/s. The influence of bumper lead was only shown by two tests in which the velocity reduced with

increased bumper lead. The lower section of the tables shows the bumper height has little effect on head velocity.

**Table 16. Child—resultant velocity change of child head striking bonnet, with respect to car shape.**

Car dimensions mm				
Bonnet Height of leading edge	Bumper Height of top edge	Bumper lead		Resultant velocity change of head to bonnet m/s
		150	250	
		650	450	
700	450	9.3	---	
750	450	8.6	6.1	
850	450	---	---	
750	400	7.6	---	
750	450	8.6	6.1	
750	500	8.8	---	
750	550	8.4	---	

### Resultant energy of deformation for child head striking bonnet top

Table 17 shows the resultant energy of deformation for the child head to bonnet top impact. This was found from the resultant of the measured bonnet forces and the resultant displacement of the head relative to the bonnet, and was calculated up to the point of common velocity. Displacement was derived from the resultant acceleration of the head.

**Table 17. Child—resultant deformation energy of bonnet from head impact, with respect to car shape.**

Car dimensions mm				
Bonnet Height of leading edge	Bumper Height of top edge	Bumper lead		Resultant energy of deformation of bonnet from head impact kJ
		150	250	
		650	450	
700	450	0.050	---	
750	450	0.034	0.037	
850	450	---	---	
750	400	0.051	---	
750	450	0.034	0.037	
750	500	0.042	---	
750	550	0.100	---	

The upper section of the table shows that the head deformation energy is influenced by bonnet height ranging between 0.034 and 0.11 kJ for the high and low bonnets respectively (see also figure 10). The influence of bumper lead was shown by two tests in which the energy increased slightly with increased bumper lead. The lower section of the tables shows that bumper height has no significant effect, except for the 550 mm high bumper, which acts as a low bonnet and the energy increases to 0.100 kJ.

## Equivalent impactor mass for child head striking bonnet top

Table 18 shows the equivalent impactor mass of the child head striking the bonnet. This was calculated from velocity changes shown in table 16 and energy of deformation in table 17.

**Table 18. Child—equivalent impactor mass of head striking bonnet, with respect to car shape.**

Car dimensions mm			
Bonnet	Bumper	Bumper lead	
		150	250
Height of leading edge	Height of top edge	Equivalent impactor mass of head striking bonnet kg	
650	450	1.74	----
700	450	1.16	----
750	450	0.93	2.02
850	450	----	----
750	400	1.77	----
750	450	0.93	2.02
750	500	1.09	----
750	550	2.83	----

The table shows that equivalent impactor mass ranged between 0.93 and 2.83 kg, which compares with the 2.73 kg static mass of the head and neck. Generally the mass increased with reduced bonnet height and increased bumper height. Both direction of head travel and the unpredictable forces acting through the neck affects the measured head mass.

## Angle of resultant force of child head striking bonnet top

Table 19 shows the angle of the resultant force of the child head striking the bonnet. This was derived from the ratio of vertical and horizontal bonnet forces (see figure 2). As with mass, both the direction of head travel and the force acting through the neck affects the measured angle of resultant force. The angle, which ranged between 62 and 90 degrees to the horizontal, showed no apparent trend with vehicle shape.

**Table 19. Child—angle of resultant bonnet force from head impact, with respect to car shape.**

Car dimensions mm			
Bonnet	Bumper	Bumper lead	
		150	250
Height of leading edge	Height of top edge	Angle of resultant bonnet force from head impact (relative to horizontal) degrees	
650	450	62	--
700	450	62	--
750	450	75	72
850	450	--	--
750	400	80	--
750	450	75	72
750	500	74	--
750	550	90	--

## Resultant impulse for child head striking bonnet top

Table 20 shows the impulse, ie. change of momentum, for the child head striking the bonnet top, and was calculated up to the point of common velocity. The value was derived from the bonnet horizontal and vertical force-time histories.

**Table 20. Child—resultant impulse of head striking bonnet, with respect to car shape.**

Car dimensions mm			
Bonnet	Bumper	Bumper lead	
		150	250
Height of leading edge	Height of top edge	Impulse of head striking bonnet N-s	
650	450	24	--
700	450	15	--
750	450	12	15
850	450	--	--
750	400	14	--
750	450	12	15
750	500	13	--
750	550	25	--

The table shows that the head impulse follows a similar pattern to that of deformation energy (see figure 10): generally the values lie between 12 to 15 N-s, except for the 650 mm high bonnet and 550 mm high bumper, which gave values of 24 and 25 N-s. For both these high values of impulse the dummy pivoted about a low front edge. In the case of the 550 mm high bumper it acted as a low bonnet, shielding the true bonnet edge.

Additional results are shown graphically in the following figures:

Figures 3 and 4 (adult) and 5 to 7 (child) show typical plots of force and acceleration against time.

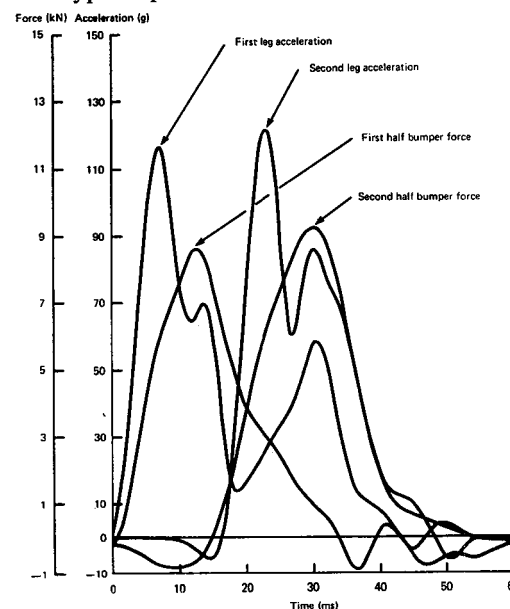


**Figure 3. Adult transducer outputs for bumper contact for car shape 750mm bonnet edge 400mm bumper top edge and 150mm bumper lead.**

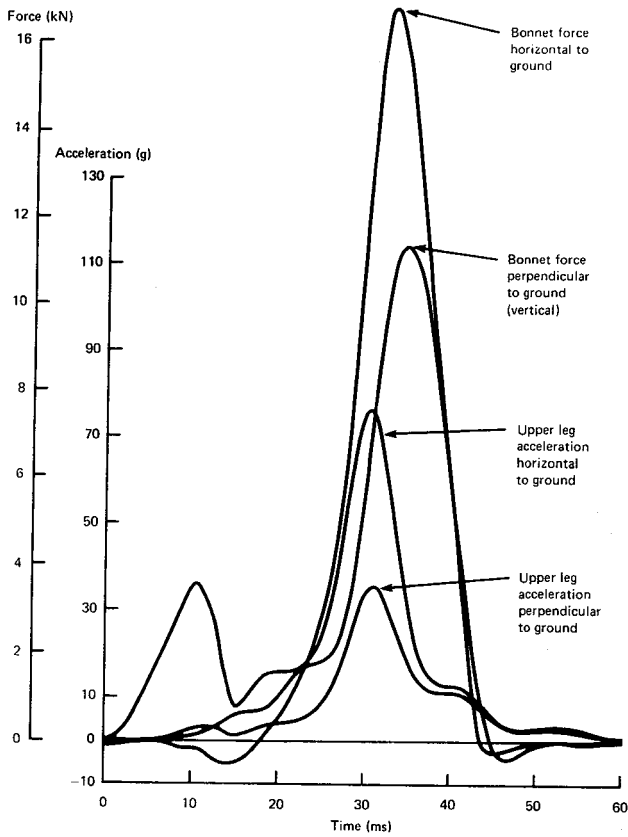


Figure 4. Adult transducer outputs for bonnet leading edge contact for car shape 750mm bonnet edge, 400mm bumper top edge and 150mm bumper lead.

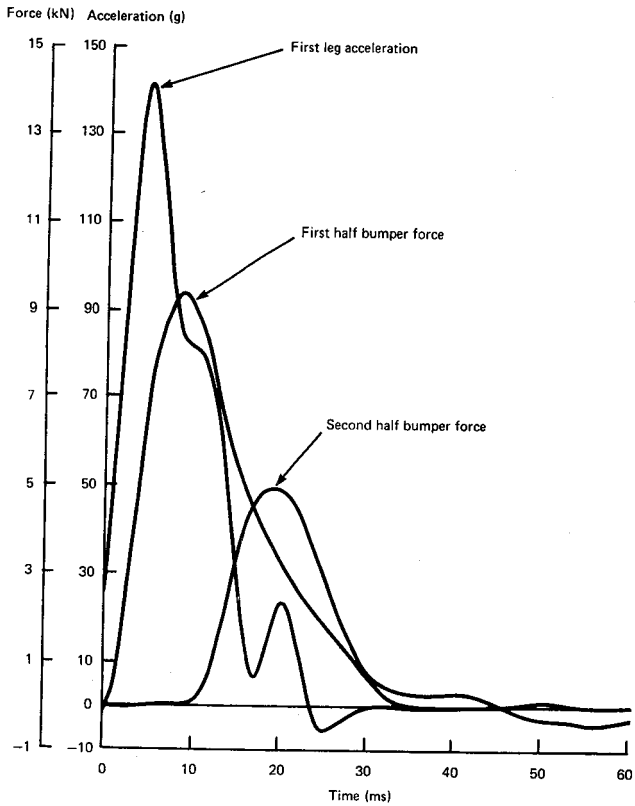


Figure 5. Child transducer outputs for bumper contact for car shape 750mm bonnet edge, 400mm bumper top edge and 150mm bumper lead.

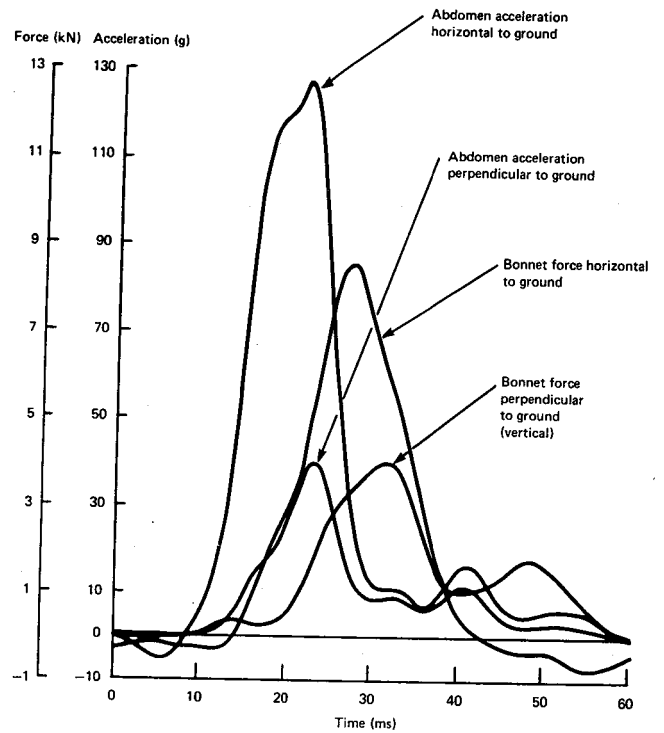


Figure 6. Child transducer outputs for bonnet leading edge contact for car shape 750mm bonnet edge, 400mm bumper top edge and 150mm bumper lead.

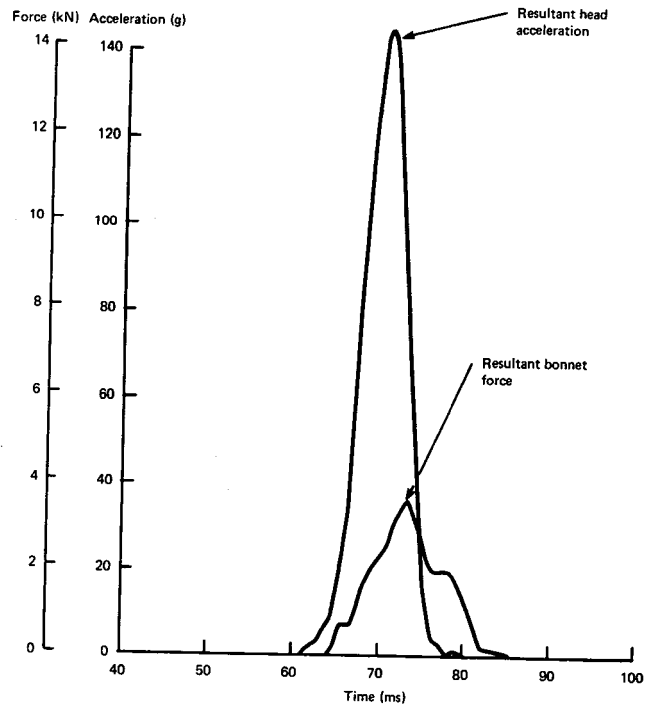


Figure 7. Child transducer outputs for bonnet top contact for car shape 750mm bonnet edge, 400mm bumper top edge and 150mm bumper lead.

Figure 8 shows the horizontal component of impulse at the bonnet edge with respect to bonnet height.

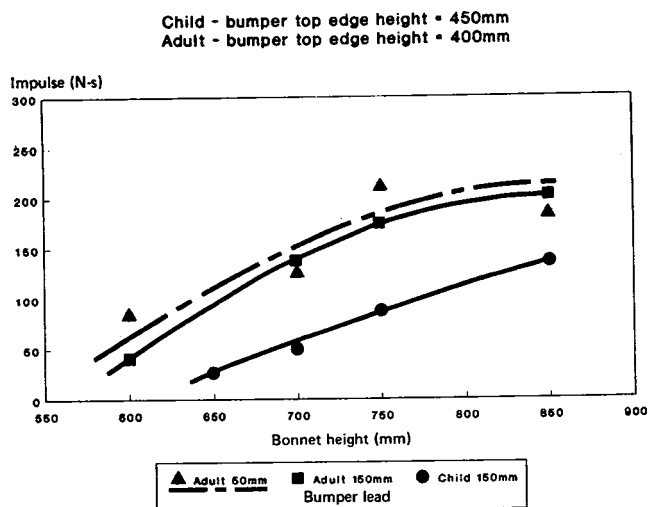


Figure 8. Bonnet leading edge impact horizontal component of impulse with respect to bonnet height.

Figure 9 shows the horizontal component of impulse and energy absorbed by the bonnet edge with respect to bumper height.

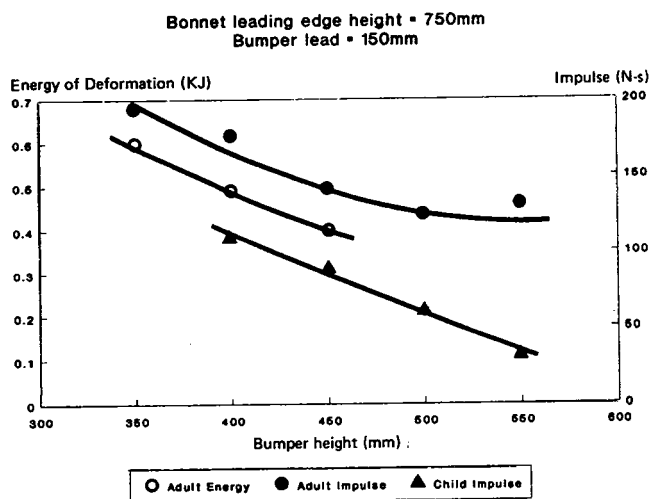


Figure 9. Horizontal component of impulse and energy absorbed by bonnet leading edge with respect to bumper height.

Figure 10 shows the impulse and energy absorbed by the bonnet top with respect to bonnet height.

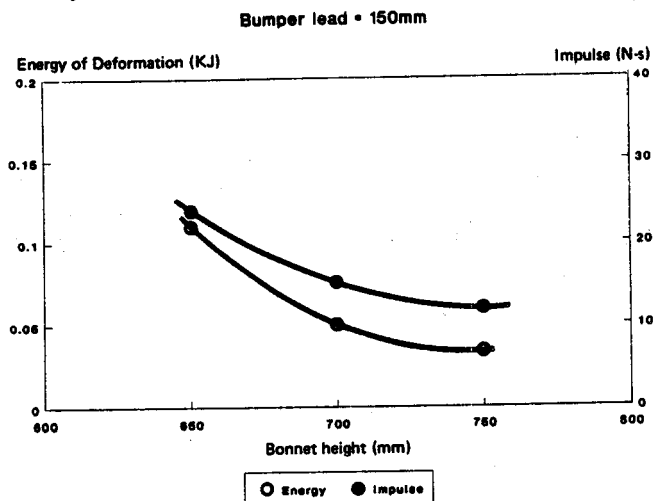


Figure 10. Child head to bonnet top impact resultant impulse and energy with respect to bonnet height.

### Transfer of energy to dummy

Study of the transducer outputs indicates generally two stages of energy transfer to the pedestrian for each of the main impact locations. In the first stage of an impact between a vehicle component and a segment of pedestrian, the bulk of the initial energy transfer goes to accelerating the contacted segment up to car speed. In the second stage of the impact, energy will go to accelerating (to some extent) the other sections of the pedestrian by acting through the joints attaching them to the struck segment. These two stages overlap, the magnitude and overlap depending on the compliance of the pedestrian's body regions, and severity of impact. This effect can be seen in figure 4 where the horizontal and vertical force between the bonnet and leg segment continues after the leg acceleration has essentially finished.

Figure 4 also shows horizontal upper leg acceleration well before bonnet edge contact, this resulting from the bumper impact to the lower leg.

For impacts to the skeletal parts of the dummies the impacted body segments achieved a common velocity with the trolley after peak structural force (or maximum penetration) had occurred. It was therefore possible to calculate the energy of structural deformation and the equivalent impactor mass from the force/displacement data.

For impacts to the abdomen of the child dummy, the two stages of energy transfer are somewhat different, with most of the deformation to the vehicle occurring in the second stage. Here, the relatively light abdomen mass was accelerated to car speed well before peak force was reached and before forces were transmitted to other segments of the dummy. Due to this action the abdominal accelerometer only registered the small amount of structural deformation resulting from the abdomen and did not respond to further and greater deformation resulting from later loading by other heavier dummy segments. The calculated values of

energy of structural deformation and equivalent impactor mass have therefore not been included in this paper. Values of impulse, calculated to the end of bonnet contact, which reflect the influence of the complete dummy, have however been included.

### Repeatability

In these tests only one run was completed for each configuration of vehicle tested. To give an indication of the repeatability of the test result, values have been compared of bumper to leg impacts with a bumper lead of 250 mm and a bumper height of 400 mm.

With this configuration the bumper impact is completed well before bonnet contact and the results should be similar. For these tests the values of energy of deformation, impulse and equivalent impactor mass all repeated within + or - 6 per cent. This compares either values of + or - 11 per cent for impacts to bumper, bonnet leading edge and bonnet top, obtained in previously reported tests at 32 km/h (2) in which tests were repeated. In configurations where there is little lead on the bumper the results are sometimes sensitive to precisely how the dummy is positioned at impact: a more severe impact with the bumper may be accompanied by a less severe impact with the bonnet leading edge i.e., or vice versa. This gives rise to additional variation in the results, but even so the important relationships have been clearly identified, and the consistency of the trends seen in interrelated variables lends confidence that the observed trends are genuine and not the result of random variation.

### Influence of vehicle shape

Trends in impact characteristics have been noted for contacts with the bumper, bonnet leading edge and bonnet top and these are summarised below together with the probable mechanisms that cause them.

For adult impacts between bumper and leg, the angle of deflection of the lateral knee clutch increases as the bumper is raised, particularly when it strikes close to the knee. The energy of bumper deformation, the equivalent impactor mass and the impulse all increase in value as the bumper is raised, until knee clutch lateral deflection becomes significant, which limits the moment across the knee joint. These increased values of energy and momentum are caused by the inertia of the increasing mass of the leg below the bumper as the bumper is raised.

Similar trends occur for the child, but in these cases the knee is not designed to bend laterally.

For contacts of the bonnet leading edge, the height of the bonnet edge is the dominant characteristic, with the impact velocity, energy of deformation and impulse all increasing as the bonnet edge is raised in height. Increases in these values also result from lowering the height of the bumper.

These increases in the value of energy and impulse partly result from the redistribution of impact energy between the bumper and the bonnet edge as the bumper is lowered in height. It also reflects the increased work done as the higher bonnets impact closer to the centre of gravity of the dummy.

Bumper lead was a less dominant characteristic and only influenced impact severity with the medium height bonnets.

The bumper tended to shield low bonnet leading edges from impact for all bumper leads tested and conversely gave no protection to the high bonnet leading edges. For medium height bonnets the shielding by the bumper of the bonnet leading edge increased as the bumper lead increased, particularly influencing adult impact velocity and impulse.

For the child head contact with the bonnet top, the impact velocity, energy of deformation and the impulse all increased as the bonnet height reduced. This resulted from the bonnet edge contact occurring further below the centre of gravity of the dummy and inducing a more rapid rotation of the head and torso onto the bonnet top.

### Comparison with computer simulation

Previously reported computer simulations of pedestrian impacts (3) included vehicle shapes that were similar to examples in this study and the results are compared below.

For the computer simulation (3) of adult dummy impacts the energy absorbed in deforming the bumper range between 0.46 and 0.58 kJ. In these tests, for vehicles of comparable shape values were on average 30 per cent lower and ranged between 0.27 and 0.45 kJ for each leg. No obvious reason could be determined for this difference.

The energies of deformation of the bonnet leading edge however gave good agreement, with simulation and test results varying between 0.06 and 0.55 and between 0.012 and 0.50 kJ respectively.

Child head resultant impact velocities to the bonnet top were calculated in the simulation model; these also gave good agreement for most vehicle shapes, ranging between 8.7 and 10.3 m/s for the simulation and between 6.1 and 11.3 m/s for the tests. The differences at the lower velocities may be partly due to the rapid change in head velocity prior to impact and the difficulty of accounting for the sensitivity of head velocity to neck stiffness in the simulation.

With respect to the basic trends in patterns of severity of impact:

(1) Both the computer simulation and the full scale tests showed the severity of the impact with bumper and the angle of knee lateral rotation increasing as the bumper is raised in height.

(2) The height of the bonnet leading edge is shown by both simulation and test to be an important influence on the severity of impact to the bonnet leading edge. The bumper lead also has an influence but this is less significant in the full scale tests.

(3) The velocity of the child head impact to the bonnet top is shown by both methods to be influenced primarily by the height of the bonnet leading edge.

### Sub-system Tests

The test data described in the preceding sections gives guidance on the impact requirements of sub-systems tests. Such tests can be used to examine the protection afforded by

the three primary areas of the front of cars important for the protection of the pedestrian (the bumper, the bonnet leading edge and the bonnet top) by impacting them with masses designed to represent contact with the appropriate part of a pedestrian. The data given in the preceding sections should be of value in determining the mass, the velocity and the direction of the impactors used in the sub-system tests.

The results show that in an impact with a pedestrian, the energy absorbed in the bonnet leading edge and the bonnet top varies with respect to the shape of the car. The velocity changes of the body regions in contact with the vehicle also vary, and in a similar manner. As already discussed, the impacts to each of the three primary areas of a car were considered in two distinct stages. In the first stage the vehicle structure deforms and the body segment in contact with the vehicle is accelerated to the velocity of the vehicle. In the second stage this body segment remains in contact with the vehicle, at the same time transmitting forces to the other parts of the dummy. In all of the body regions studied (except for the child abdomen), maximum deformation to the vehicle structure occurred before the impacted body region reached a common velocity with the vehicle. In order to understand the mechanism of these impacts, the following parameters have, where possible, been calculated for each of the main areas of contact:

Velocity change of the body region in contact with the vehicle.

Energy absorbed in deforming the vehicle structure.

Impulse of each impact (change of momentum).

The results show that in a sub-system test the initial kinetic energy of the impactor used to deform the car structure must be adjusted according to the vehicle shape and appropriate values of the energies of deformation are given in the results, for the range of vehicle shapes studied.

If the mass of the impactor is fixed, the different values of kinetic energy associated with different shapes of car may be achieved by adjusting the velocity.

However, greater realism may be obtained by using the velocity change quoted in the results as the sub-system test velocity, for respective shapes of car. In this case the required values of kinetic energy may be obtained by adjusting the mass of the impactor. Corresponding values of mass have been calculated and are shown in the results as equivalent impactor mass.

An impactor which is solely designed to cause the appropriate amount of structural deformation will not represent the additional mass which may continue the loading after the deformation stage is completed. In some circumstances this prolonged loading may increase the risk of injury. For instance a body region that bends may dynamically distort further, if the duration of the loading is extended, particularly if its natural frequency is relatively low. An indication of the momentum of impact that includes this additional loading is given by the impulse (change of momentum) shown in the results. This value is only approximate however as, with the exception of the child

abdomen, it has been stopped at the time of common velocity to avoid including the influence of restitution. For the child abdomen it was necessary to continue to the end of the contact, as explained previously, in order to include the influence of all the segments of the dummy, but in this case it will also contain the impulse of restitution. In consequence appropriate values for an abdomen impactor impulse are 20 percent less than those shown in the results to allow for the coefficient of restitution of the material used.

An impactor developed to include the additional mass needed to simulate prolonged contact will require compliance to absorb the associated increase in kinetic energy. The results from these tests identify the trends of the basic relationships of impact with respect to vehicle shape for pedestrian dummies.

These trends will be similar for impacts to the human frame but adjustments in the absolute values will be necessary to allow for the difference of the dummy and human impact characteristics.

### Summary of sub-system test conditions

The following summary of sub-system test conditions is based on the characteristics of child and adult dummies for a vehicle design speed of 40 km/h, and should be treated as indicative of basic trends and approximate values for a rigid impactor (except for child abdomen).

#### Bumper test for adult and child

Impact velocity—11 m/s

Impactor mass—5.7 kg adult (single leg)

—4.7 kg child (single leg)

Direction of impact—horizontal

Note—Bumper impact to a child involves a greater proportion of the total body mass than for the adult.

#### Bonnet leading edge test for adult and child

*Horizontal component of velocity*—Dependent on car shape: values ranged from 1.2 to 11.1 m/s for an adult and 3.6 to 10.9 m/s for a child (this value strongly dependent on bonnet and bumper height and bumper lead).

*Horizontal component of kinetic energy of impactor*—Ranged between 0.12 and 0.6 kJ for an adult (this value strongly dependent on bonnet and bumper height).

*Horizontal mass of impactor*—Dependent on car shape: values ranged from 5.6 to 18.7 kg for an adult.

*Direction of impact*—Dependent on car shape: values ranged between 22 and 45 degrees to horizontal for the adult, and 12 and 60 degrees to the horizontal for the child (derived from the ratio of horizontal and vertical change in momentum).

*Child abdomen compliant impactor horizontal mass*—Dependent on car shape: values ranged between 6.8 and 12.4 kg with an average of 8.75 kg for the shapes studied (derived from velocity change and impulse).

Note—For the adult the horizontal components of velocity and energy are given. The true test conditions should conform with the directions of impact shown.

## Bonnet top test for child

*Impact velocity*—Dependent on car shape: values ranged from 6.1 to 11.3 m/s (this value strongly dependent on bonnet height).

*Kinetic energy of impactor*—Dependent on car shape: values ranged from 0.034 to 0.11 kJ (this value primarily dependent on bonnet height).

*Mass of impactor*—Dependent on car shape: values ranged from 0.93 to 2.83 kg.

*Direction of impact*—Approximately 70 degrees from horizontal.

## Conclusions

The input conditions for sub-system testing using impactors striking a car's bodywork to evaluate the protection afforded to pedestrians must be chosen to reflect the influence of the shape of the front of a car. The main conclusions are as follows:

(1) In the design of an impactor the mass may be considered as having two components.

One component (referred to as the "equivalent impactor mass" in this paper) causes the structural deformation of the vehicle. It represents the mass of a rigid impactor that would reproduce the structural deformation that occurred in the tests when a complete pedestrian dummy was struck by the front of a car.

The second component of the mass prolongs the contact so that the injury potential of the complete impact may be assessed. The kinetic energy of this component is absorbed by compliance within the impactor.

These results give general support to the main trends in impact severity previously reported from mathematical simulations (3).

(2) In the tests with the adult dummy, the energy absorbed in deforming the bumper ranged between 0.27 and 0.45 kJ for each leg for most shapes of car tested. This compares with values ranging from 0.46 to 0.58 kJ previously reported from mathematical simulation (3). From these tests the equivalent impactor mass (i.e. the mass that would give comparable deformation energy) typically ranged between 5 and 7 kg and the impulse of the impact between 70 and 100 N-s. For the child the values were typically 0.5 to 0.6 kJ of energy with a mass of 4.2 to 5.1 kg and impulse of 70 to 100 N-s.

(3) For the bonnet leading edge, in the tests with the adult dummy the energy of deformation ranged between 0.12 and 0.5 kJ which compares with the values of 0.06 and 0.55 kJ previously reported from mathematical simulations (3). In these tests the

equivalent impactor mass (i.e. the mass that would give comparable bonnet deformation) ranged between 6 and 16 kg, and the impulse of the impact ranged between 40 and 200 N-s. For the child the impulse ranged between 27 and 136 N-s.

(4) For child head to bonnet contacts, the energy of bonnet top deformation ranged between 0.11 and 0.34 kJ and the corresponding effective mass between 2.83 and 0.93 kg. The impact velocity of the child head ranged between 6 and 11 m/s for the impact tests and between 8.7 and 10.3 m/s for the simulations (3). The differences at the lower velocities may be attributed to the rapid changes of head velocity just prior to impact and the difficulty of accounting for the sensitivity of head velocity to neck stiffness in the simulation.

(5) Variation in the impact energies and impulses as shown in figures 8 to 10 exhibit clear trends with respect to bonnet and bumper height for the bonnet leading edge impacts, and with respect to bonnet height for the bonnet top contacts.

This strong relationship between impact energy and vehicle shape may be used as a basis for determining the characteristics (i.e. weight, velocity and direction) for the sub-system tests.

## Acknowledgements

The work described in this paper forms part of the research programme of the Transport and Road Research Laboratory and the paper is published by permission of the Director.

## References

- (1) Fowler, J.E. and J. Harris, *Practical vehicle design for pedestrian protection*, Proceedings of the ninth International Technical Conference on Experimental Safety Vehicles, Kyoto, Japan November 1982.
- (2) Lawrence, G.J.L. and J. Harris, *Car to pedestrian impact energies and their application to sub-system testing*, Proceedings of the eleventh International Technical Conference on Experimental Safety Vehicles, Washington May 1987.
- (3) Harris, J. and N.D. Grew, *The influence of car design on pedestrian protection*, Proceedings of the tenth International Technical Conference on Experimental Safety Vehicles, Oxford July 1985.

Crown Copyright. Any views expressed in this paper are not necessarily those of the Department of Transport. Extracts from the text may be reproduced, except for commercial purposes, provided the source is acknowledged.

# Bumper Configurations for Conflicting Requirements: Existing Performance Versus Pedestrian Protection

L. Grösch, W. Heiss,  
Daimler-Benz AG,  
Federal Republic of Germany

## Abstract

The primary task of the bumper is to withstand minor impacts (e.g. with walls, poles, other vehicles) during parking or car-to-car collisions so as to prevent damage to the car or reduce the cost of repairs. In order to fulfill these requirements, the front bumper needs to be positioned relatively high, its protrusion from the body and its contact area should be large, and, most of all, it must absorb relatively high impact energy. In contrast to this, in order to reduce the severity of injuries to the lower legs of pedestrians and, in particular, to prevent injuries to the knee or ankle, the bumper design should be completely the opposite: i.e., the initial contact point as well as the bumper stiffness should be rather low. The problems resulting from these conflicting requirements are discussed in detail. It appears very difficult to fulfill both requirements—possibly with a system consisting of the conventional bumper and, in addition, a pedestrian friendly bumper positioned approx. 150 mm below and slightly protruding. However, the authors are not convinced that such a complicated and costly double bumper system will be the most efficient solution. Instead of this, measures to prevent any car-to-pedestrian collisions probably would be more suitable.

## Introduction

Although car accidents in the Federal Republic of Germany have increased in number by more than 40% since 1970, the number of fatalities has reduced by more than 50% and the number of injured persons by about 15% (5). The main reasons for this encouraging development are improvements in

- Belt usage rates
- Safety performance of the cars

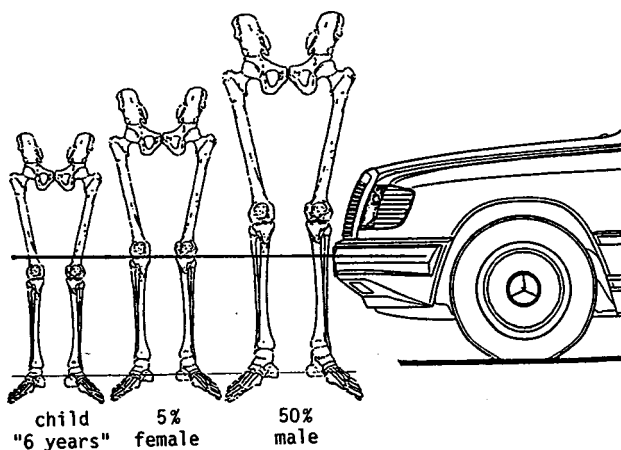


Figure 1. Loading of leg due to bumper impact.

- Rescue operations
- Accident surgery
- Traffic conditions

Nevertheless, the economic and social costs resulting from traffic accidents are enormous. Apart from this, a severe accident with the consequence of serious or even fatal injuries are grave to the persons involved and to their families.

This is why Daimler-Benz, conducting crash tests for more than 30 years, does not reduce its efforts in accident research, safety engineering and car safety performance. Unfortunately, there are some problems which make further improvements in safety more difficult, for example

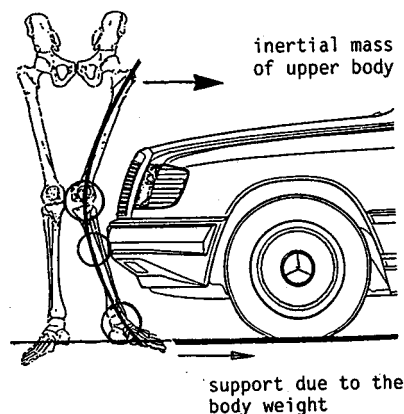
- Both tests with anthropometric dummies and mathematical modelling up to now do not provide complete and reliable information about injury patterns and mechanisms which would be necessary to derive the suitable design features,
- Customers frequently reject safety design features if the car becomes more expensive or less comfortable by it,
- Many safety requirements run counter to the necessities of practical use or regulations.

The latter is particularly true with respect to pedestrian protection measures which usually do not have any advantage for the car occupants. It is the purpose of this paper to discuss in detail the conflicting requirements in front bumper design and the possible solutions.

## Pedestrian Protection

### Loading of leg due to bumper impact/injury patterns and mechanisms

During the initial bumper contact, the leg is subjected to different loadings essentially depending on the bumper stiffness, height, protrusion from the body, the contact area and the size and position of the pedestrian (figure 1).



In addition to the local forces/pressure acting directly on the bone—either tibia/fibula or knee or femur—there is a bending moment, resulting from the support of the foot on the ground (due to static friction) on the

one hand and the inertial persistence of the upper body on the other hand. As a consequence, there are three distinct injury mechanisms and injury patterns (figure 2):

Long Bone Fractures of Tibia and Fibula

Tearing off of Ligaments

Joint Fractures/Crush of the head of Tibia/Fibula

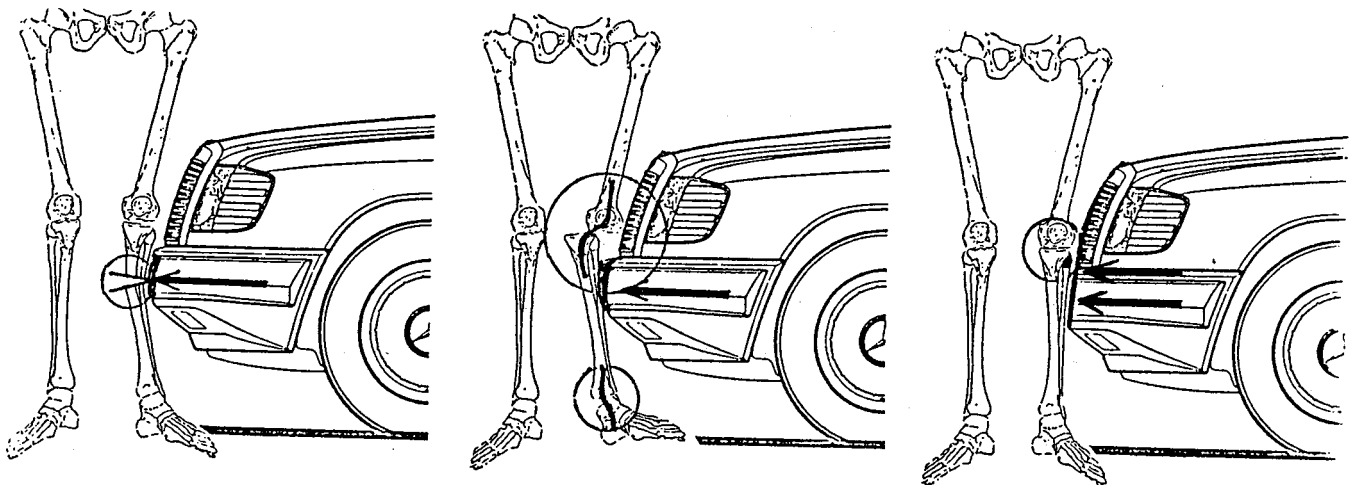


Figure 2. Injury patterns and mechanisms.

- Long bone fractures of tibia, fibula or femur:

Due to the bending and shearing forces, on the one hand and the local pressure, on the other hand, the bone is frequently breaking (1, 2, 3),\* either directly in the contact area or below. In minor cases occur oblique, dentate or comminuted fractures which may be harmless. However, if multiple or crush fractures or, in particular, open fractures are combined to soft tissue damages, healing up frequently is complicated and may cause long term impairments (5). It seems that the risk of long bone fractures can be reduced by

- larger contact area (local pressure reduced)
- lower bumper stiffness (both local force and bending moment reduced)
- lower bumper height (bending moment reduced).
- Overstressing/tearing off of ligaments:

If the lower leg is shifted with respect to the femur or if the angle between femur and lower leg ("knee deformation") exceeds the tolerance level in the knee, significant tensile and shear forces are acting on the ligaments in the knee joint. Furthermore, the ankle is subjected to bending and twisting moments. Ligamentum overstressing or even rupture are considered as serious injuries, sometimes with long time impairment. The risk of these injuries can be reduced by reducing the bumper stiffness, height, contact area and protrusion from the body.

- Direct joint fractures/crush of the head of tibia/fibula:

If the knee is directly impacted, fracture or even crush of the head of fibula or tibia may occur. The risk of such injuries can be reduced primarily with a very low bumper height, a large protrusion from the body, a soft bumper (including the vehicle face) and a small contact area.

### Pedestrian Friendly Bumper Design

Interestingly, there are some conflicting requirements with respect to avoiding lower leg fractures or injuries to the joints and, unfortunately, different opinions as to which is the lesser of the two evils. In the opinion of many accident surgeons, severe joint injuries have a higher priority than avoiding uncomplicated long bone fractures. However, according to a recent study (5) analyzing the consequences of injuries which people suffered in real world accidents with respect to both, permanent impairment and economic and social costs, open fractures of the lower leg rate significantly higher than injuries to the joints.

Nevertheless, some guidelines as to how a pedestrian-friendly bumper should be designed, can be established (table 1):

- It should be positioned as low as possible (2) in order to avoid direct impact to the knee even if small persons are involved and, furthermore, to reduce the bending moment to the leg and to prevent "overrunning",
- Both its protrusion from the body and its contact area should be relatively small to avoid shifting of

\*Numbers in parentheses designate references at end of paper.

- the lower leg with respect to the femur,
- Its stiffness should be rather low and, in particular, its local pressure to avoid soft tissue damages.

The question arises, of course, how these requirements fit both, the existing bumper performance and the bumper regulations.

**Table 1. Conflicting requirements with respect to pedestrian protection and performance/regulations.**

BUMPER-	PEDESTRIAN PROTECTION	BUMPER PERFORMANCE	BUMPER STANDARDS
STIFFNESS	low	high	either high and small or low and large
PROTRUSION	small	large	16 ... 20 inch
HEIGHT	low	high	large
CONTACT AREA	small or large	large	

## Existing Bumper Performance

The existing bumper performance is resulting from both, normal operating requirements and regulations. As everybody knows, the function of the bumper is to withstand minor impacts e.g. with a wall, a pole or another vehicle so as to prevent damages to the car body, in particular to fender, headlight or radiator grille, and avoid or reduce repair costs (figure 3).

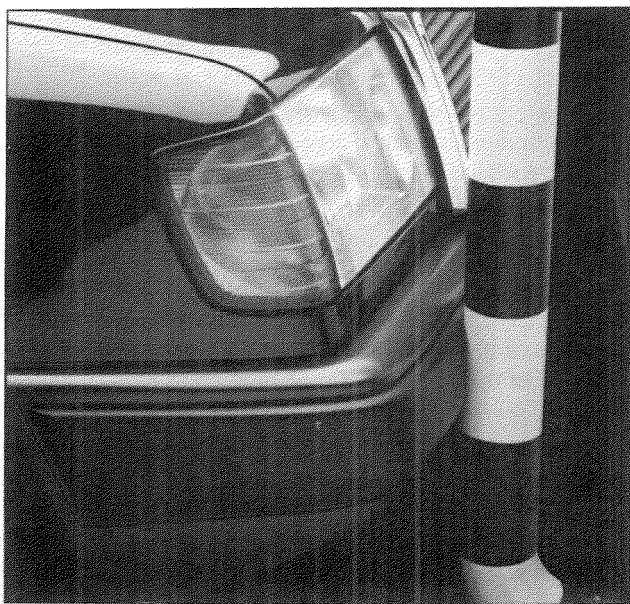


**Figure 3. Typical minor accident situation impact against a pole.**

Because petty damages like these are most frequent in real world accidents, even regulations have been prescribed by laws (e.g. U.S. Part 581, CMVSS 215, ECE-42, EWG 70/156—table 2, figures 5, 6) in order to protect consumers from unnecessary repair costs. These standards greatly restrict the bumper design with respect to

**Table 2. Existing bumper regulations.**

USA Part 581 Bumper Standard	CANADA CMVSS 215 Exterior Protection	EUROPE ECE Regulation No. 42
<b>barrier impact</b>	<b>barrier impact</b>	-----
with 2.5 mph = 4.02 km/h	with 5 mph = 8.04 km/h	
no damages at all	no damages which would restrict the functioning of the car in any way (e.g. to headlights, fuel system, radiator etc.)	
<b>pendulum test</b>	<b>pendulum test</b>	<b>pendulum test</b>
with 2.5 mph = 4.02 km/h to the center and with 1.5 mph = 2.41 km/h to the corner (30°) height: 16" and 20" mass of pendulum = mass of car	with 5 mph = 8.04 km/h to the center and with 3 mph = 4.82 km/h to the corner (30°) height: 16" and 20" mass of pendulum = mass of car	with 4 + 0.25 km/h to the center and with 2.5 + 0.1 km/h to the corner (30°) height: 18" mass of pendulum = mass of car
no damages at all	no damages which would restrict the functioning to the car in any way	no damages which would restrict the functioning to the car in any way

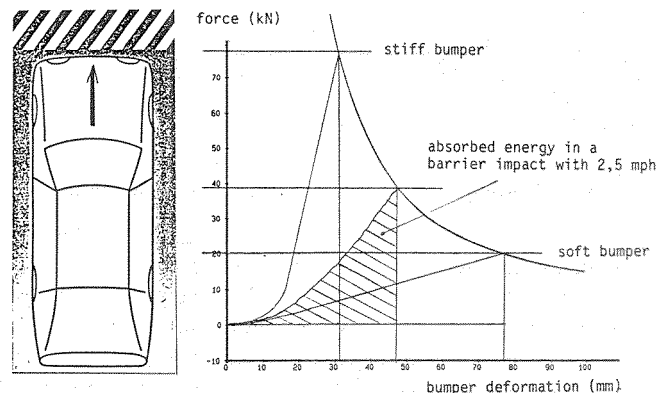


**Figure 5. Correlation of bumper stiffness with protrusion from the body, according to the energy absorption required in Part 581.**

- Bumper stiffness and protrusion from the body:

In order to absorb the required impact energy (e.g. approx. 1 kJ in a barrier impact of 1600 kg mass with 2,5 mph) either large protrusion of the bumper from the body or high bumper stiffness is necessary (figure 5).

- Bumper height and contact area:

In order to be properly contacted by the test pendulum (figure 4) the bumper needs to be positioned relatively high and its contact area should be as large as possible to cover the tested 16" and 20" range.

- Bumper height and protrusion from the body:

In order to meet the requirements with respect to angle of slope (figure 7), larger protrusion of the bumper from the body requires a higher bumper.

Although it is open to discussion whether the bumper standards achieve this purpose to the fullest, because in many real world accidents the bumper is impacted in

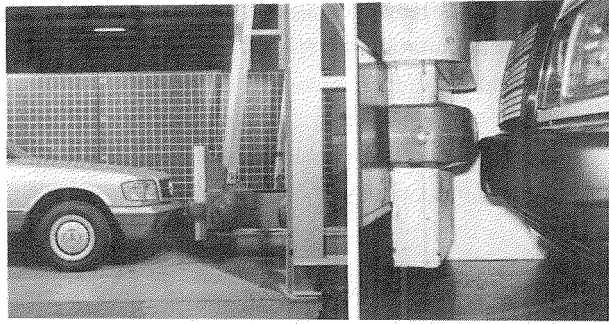


**Figure 4. Pendulum test according to bumper regulations (table 2).**

different ways as in the tests, there is no doubt at all that a bumper which

- Enables high energy absorption without damages
- Is rather stiff
- Has a high protrusion from the body
- Is positioned rather high
- Covers a large area of the vehicle's face

is advantageous in practical use.

### Conflicting requirements

A comparison of the conflicting requirements in bumper design (6) is given in table 1. It is interesting to note that each of the pedestrian friendly design features runs completely counter to the requirements of bumper regulations and of practical use. The question arises whether a bumper can be designed with due regard to both requirements, respectively, which problems would be resulting from designing the bumper more pedestrian friendly.

- Reducing the bumper height/contact area

Although positioning the front bumper very low would also be favourable in side impacts, because the side member would be loaded to a large extent instead of exclusively the doors and pillars, there would be problems, with respect to rear end collisions: In a rear end collision, the running car is usually braking and, as a consequence, driving with the front and therefore tends to underride the impacted car, in particular, if this car is also braking and, as a consequence, going up with the rear end (figure 6). With a sufficiently high front bumper and a large contact area, damages to headlights or radiator grille probably could be reduced, in particular, if both the stiffness of the bumper and its

protrusion from the body were sufficiently high. Further problems would result with respect to passing over curbstones, slopes or other obstacles (figures 7, 8). Because a lower front bumper necessarily requires a lower rear bumper (with similar problems with respect to angle of slope/low obstacles), an additional problem would be to support impact forces without damages in the rear end structure, in particular, where the rear end member sweeps over the rear axle (figure 9).

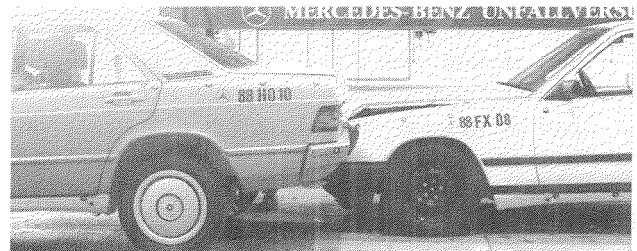


**Figure 6. Underriding of bumpers in rear end impact—both cars braking—front spring suspension compressing, front bumper going down; rear spring suspension extending, rear bumper going up; running car underrides impacted car.**

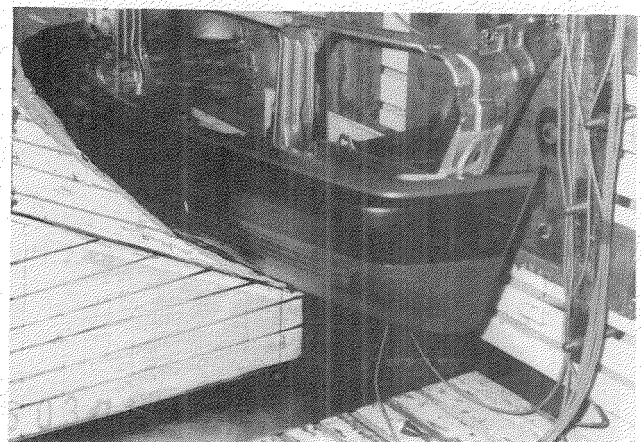
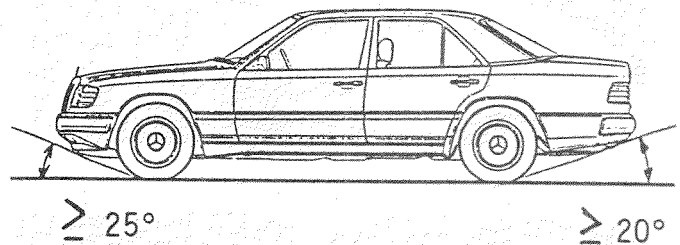


**Figure 7. Requirements with respect to angle of slope.**

- Reducing the bumper stiffness/protrusion

As mentioned above, because of the higher risk of injuries to the joints, a lower stiffness of the bumper must not be introduced at the expense of a larger protrusion from the body. Furthermore, a longer car would be disadvantageous with respect to space required in parking or maneuvering. A very interesting possibility to reduce the stiffness of the bumper during pedestrian impact, without the necessity to increase its protrusion distinctively with respect to bumper regulations, is to face the bumper with rigid foam. The essential advantage of rigid foam (4) is that its resistance to deformation is proportional to the contact area. That is, in a barrier impact involving a large contact area it reacts hard, absorbing much energy and in a lower leg impact, because of the small contact area, it is relatively soft

(figure 10). However, an extremely soft rigid foam, as it may be suitable with respect to pedestrian protection, would be disadvantageous in an impact against a pole (figure 3), which also involves only a small contact area. Furthermore, problems with respect to triggering the sensor of airbag or belt tensioner might arise.

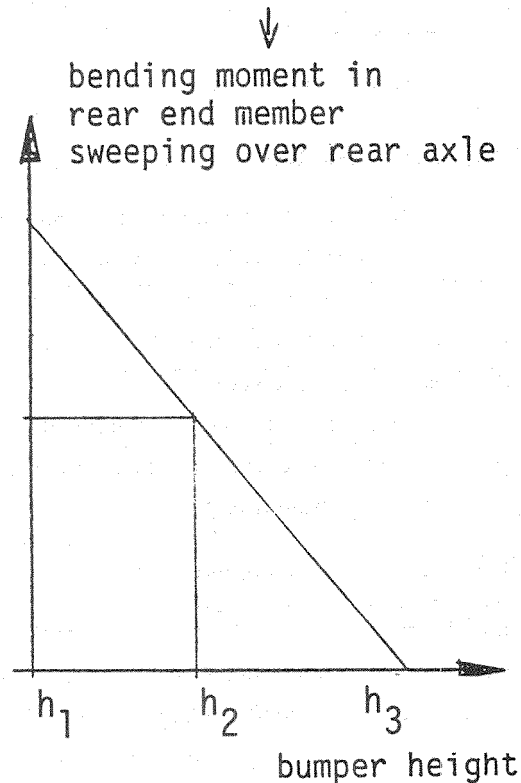
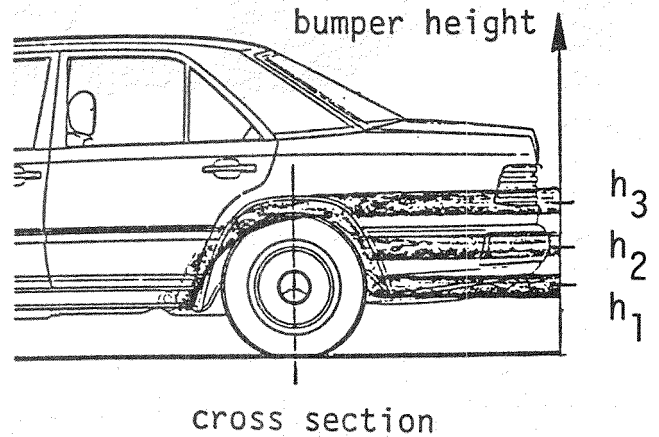


Figure 9. Bending moment in the rear end member due to different bumper heights.

### Possible solutions

In principle, there may be two ways to fulfill the conflicting requirements

- Finding a compromise with respect to bumper height, stiffness, protrusion and contact area,
- Looking for other systems than the conventional bumper, e.g. softnose or double bumper.



Figure 8. Passing over curbstone or other obstacle.

BUMPER FACED WITH ENERGY ABSORBING FOAM

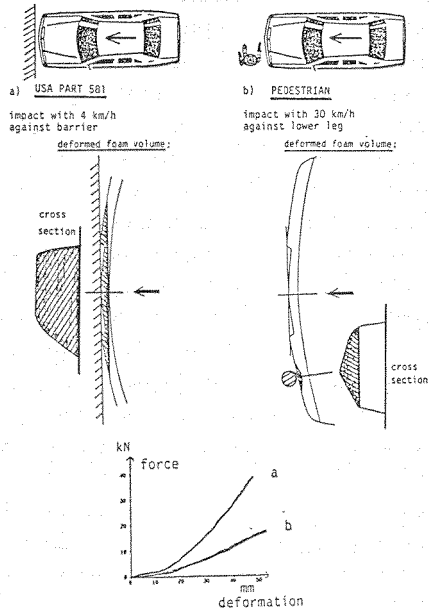


Figure 10. Deformation characteristics of rigid foam, resistance depending on volume of deformation.

Some of these bumper performances were tested at the Institute of Forensic Medicine in Hannover (3). The essential results are summarized in table 3:

Table 3. Typical injuries in cadaver tests (3) with different bumper performances (impact speed approx. 32 km/h).

BUMPER PERFORMANCE	TYPICAL INJURIES
RIGID FOAM, STIFF (small protrusion)	open crush fractures of fibula and tibia no injuries to knee and ankle
RIGID FOAM, SOFT (large protrusion)	both, injuries to the knee and ankle and fractures of fibula and tibia
BUMPER WITH SPOILER (large contact area)	injuries to ankle and fractures of the head of fibula
SOFTNOSE (bumper integrated)	both, injuries to knee and ankle and fractures of fibula and tibia
DOUBLE BUMPER SYSTEM (pedestrian bumper)	simple fracture of fibula or no injuries to bones or joints

(1) Variation of stiffness/protrusion (initial contact point approx. 360 mm above ground, size of cadavers larger than 160 cm).

Two rigid foams were tested:

- “Soft” foam, large protrusion from the body.
- Stiff foam, small protrusion.

As a result, with the relatively stiff bumper multiple fractures of fibula and tibia occurred, but no injuries to knee or ankle, whereas with the softer bumper, both, fractures and injuries to the joints occurred.

(2) Initial contact area extended to bottom (figure 11).

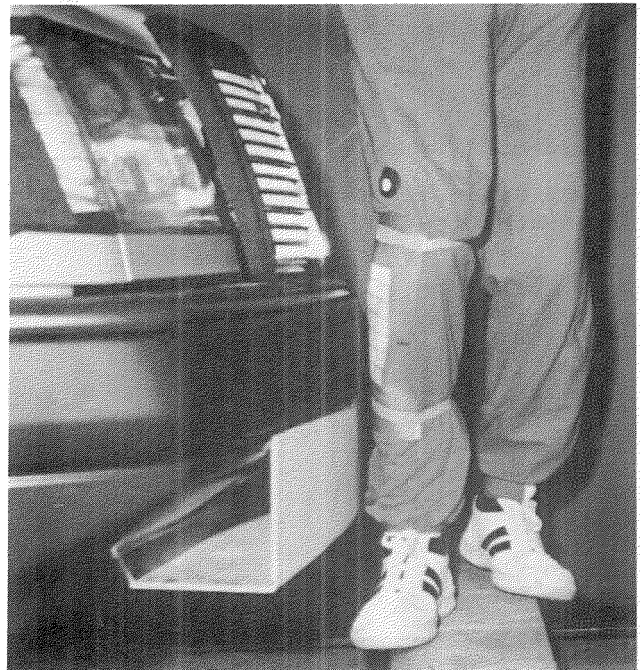


Figure 11. Bumper extended to bottom.

Both the local pressure to the bone and the bending moment to the leg can be reduced with a bumper which supports the lower leg in a large contact area. According to this, the bumper was considerably extended to bottom (spoiler). As a result, multiple fractures of fibula and tibia could be completely avoided. However, instead of this, serious injuries to knee and ankle occurred.

(3) Softnose/bumper integrated within the vehicle's face (figure 12):

In principle, there are two possibilities as to prevent car body damages in barrier impacts according to bumper regulations: Either the deformation of the bumper is lower than its protrusion from the body, or the vehicle's face (radiator grille) is yielding without permanent damages. In this case, the protrusion of the bumper from the body could be very small. In car-to-pedestrian collisions with such a softnose, the initial impact occurs not only at the lower leg, rather, the load

is distributed from top to bottom on both, lower leg and femur. However, even with this system both, long bone fractures and injuries to the joints occurred.

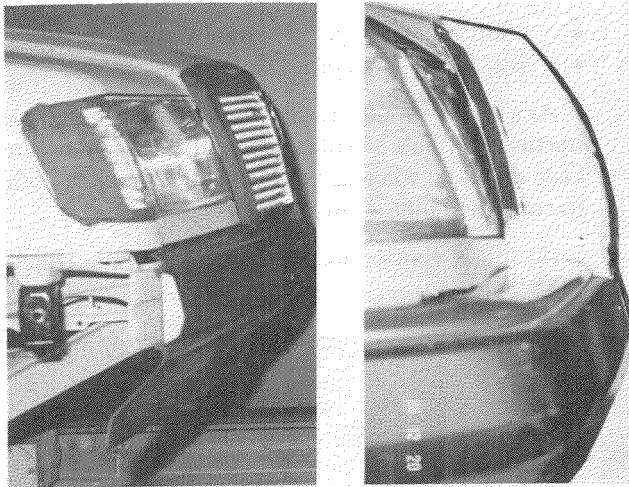


Figure 12. Softnose, different performances: bumper contour in line with radiator grille.

(4) Double bumper (figures 13, 14):

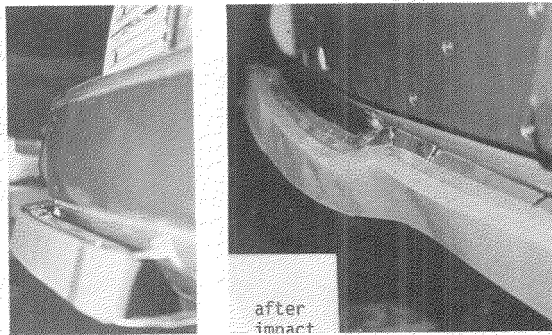


Figure 13. Double bumper, before and after pedestrian impact.



Figure 14. Project car A2000 (1981) with pedestrian friendly double bumper.

Evidently, it is difficult to fulfill contradictory requirements, pedestrian protection and normal operating requirements, with one simple bumper system. As a consequence, the possibility of two separated bumpers was investigated: the conventional one, relatively high positioned (approx. 450 mm) for energy absorption according to bumper standards and in minor collisions, and, in addition, another one positioned distinctively lower (initial contact height less than 300 mm), however slightly protruding (at least 20 mm) and significantly softer. In order to fulfill the bumper standards, the pedestrian friendly bumper must either be deformable without permanent damages or telescopic, above a vehicle speed of 5 mph. In cadaver tests, with such a system no serious injuries occurred. Obviously, the support of the feet on the ground is reduced in time before the impact with the upper bumper occurred. As a consequence, the lower leg is pushed away from the bumper and, as a result, the loading to the leg is reduced. As is illustrated in figure 13, the "pedestrian bumper" is deformed distinctively due to a lower leg impact with approx. 32 km/h.

## Consequences

Particularly, when certain measures in the development of a car serve a number of goals at the same time, these goals are more easily realized. In this way, the smooth-surfaced design which serves to improve aerodynamics is also beneficial in pedestrian protection. However, the existing bumper performance which results from both normal operating requirements and regulations, greatly restricts a pedestrian friendly design.

Of course, injuries which pedestrians suffer in collisions with moving cars certainly cannot simply be set off against damages to the car and repair costs in minor collisions. However, if on the one hand these injuries are damages to the car, economic aspects cannot be ignored in looking for technical solutions. Because, if a car is too expensive, customers may reject safety design features and may make their selection and decision by buying solely under financial aspects. This is particularly true with respect to pedestrian protection measures which do not have any benefit for the car owner. Under these circumstances, it is doubtful whether a complicated and expensive bumper performance such as the telescopic double bumper system, which may be a possible solution in the future even if designed as an aerodynamic spoiler, is a suitable design.

On the contrary, the reduction of fatalities and injuries in spite of an increased number of accidents indicates that other than technical solutions should be of higher priority, such as improvements in

- Traffic systems
- Road conditions
- Driver education.

In our opinion, of major importance would be to prevent car-to-pedestrian collisions altogether, in particular, by

dividing the traffic consistently into pedestrian and vehicle zones, i.e. pedestrian subways or bridges, pedestrian-only zones and restricted low speed limits near schools and within residential zones. Prevention of accidents is far better, more economic and, most of all, more humanitarian than anything else.

## References

(1) Kallieris, D.; Schmidt, G.: New Aspects of Pedestrian Protection: Loading and Injury Pattern in Simulated Pedestrian Accidents. Proceedings 32th Stapp Car Crash Conference, Atlanta, October 1988.

(2) Cesari, D.; Cavallero, C.; Roche, H.; Russo, J.L.: Evaluation of the Lower Limb of the Round Symmetrical Pedestrian Dummy Behaviour. Proceedings 12th International Technical Conference on Experimental Safety Vehicles, Göteborg, May 1989.

(3) Schroeder, G.; Windus, G.; Bosch, U.; Haas, N.; Tröger, H. D.: Injury Patterns of Lower Leg in Relation to Bumper Design in Simulated Car/Pedestrian Collisions. Proceedings 33th Stapp Car Crash Conference, Washington, October 1989.

(4) Grösch, L.; Hochgeschwender, J.: Experimental Simulation of Car/Pedestrian and Car/Cyclist Collision and Application of Findings in Safety Features on the Vehicle SAE-Technical Paper Series 890751, Warrendale.

(5) Mattern, R.; Eichendorf, W.; Reiß, S.; Alt, B.; Miksch, T.: Verletzungsfolgekosten nach Straßenverkehrsunfällen FAT Schriftenreihe Nr. 73, Frankfurt, Oktober 1988.

(6) Hoefs, R.; Heinz, M.: A Bumper for Both Pedestrian and Vehicle Body Protection; A Contradiction in Terms or a Soluble Conflict? Proceedings 11th International Technical Conference on Experimental Safety Vehicles, Washington, May 1987.

## Acknowledgement

The authors wish to acknowledge the strong support provided by the Institute of Forensic Medicine in Hannover (FRG) which conducted sled tests with dummies and cadavers. In particular, we appreciate their making available their results to us and thank them for their helpful advices and discussions.

## Pedestrian Casualties: The Decreasing Statistical Trend

Written Only Paper

**Harold Vallee, Christian Thomas, Claude Tarriere**

Laboratory of Physiology and Biomechanics  
PEUGEOT S.A./RENAULT

### Abstract

Protection of vulnerable road users and especially pedestrians is one of the problems to be solved in the field of road safety.

Since the beginning of the seventies, many changes have been observed in the magnitude of pedestrian casualties in most of the more motorized countries. The total number of pedestrian fatalities have been divided by 3 in West Germany (6,000 to 2,000) and by 2 for Japan and all Europe, while the vehicles in use greatly increased.

This interesting phenomenon is studied on the basis of available world road statistics. Differences between countries in terms of relative importance of pedestrian casualties, accident areas, alcohol influence, age of victims, violence of impact and risks are also given.

Consequences of these statistical facts on improvement in pedestrian protection are discussed.

### Introduction

The figures quoted in the first descriptive part of our survey are taken from documents entitled "Statistics of Road Traffic Accidents in Europe", published by the UNO.

The results given in the second part, devoted to various

factors of evolution or origin of improvements in safety as regards pedestrians, are taken from various investigations, the references of which are given at the end of the paper.

### Statistical Facts

The fact most worthy of note is most certainly the huge decrease in the number of pedestrian fatalities observed in western countries over the last fifteen years. It is in Japan and in the European Community that this evolution was the most appreciable since a reduction of around 50% of fatalities against close to 25% in the U.S.A. was recorded (37% for the period 1972-1986) (figure 1).

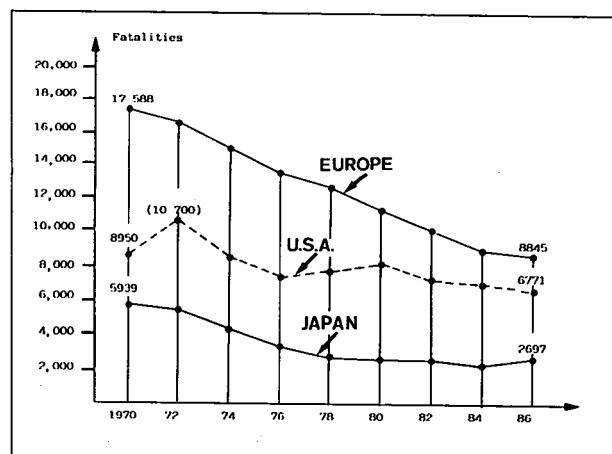


Figure 1. Evolution of the number of pedestrian fatalities between 1970 and 1986 in European Economic community, U.S.A. and Japan.

Within Europe, evolution varies according to the country. Thus, the greatest decreases especially affect the most motorized countries (West Germany: 66%; Denmark: 59%; Belgium: 56%; Italy: 53%; Netherlands: 48%; France: 49%) except for 2 countries where this decrease was lower (Ireland: 37%; United Kingdom: 34%). As for less motorized countries, either the decrease was much more modest (Spain: 5%), or there was a considerable increase (Greece: more than 20%). Another interesting fact, involving the classification of the various countries of the European Community in respect to the number of pedestrian fatalities in 1970, remains unchanged in 1986, except for Greece (figure 2).

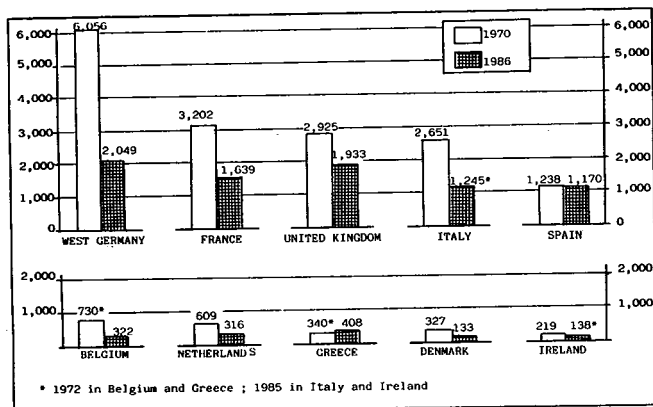


Figure 2. Evolution of the number of pedestrian fatalities between 1970 and 1986 in 10\* European countries.

\*Are not taken into account:  
—Portugal (data non available)  
—Luxembourg (weakness of cases)

In a context of diminution in number of road fatalities in western countries, the very considerable decrease in pedestrian fatalities is expressed by an exemplary reduction of their share among the total number of deaths. The reduction of this share was greater in Japan than in Europe (figure 3).

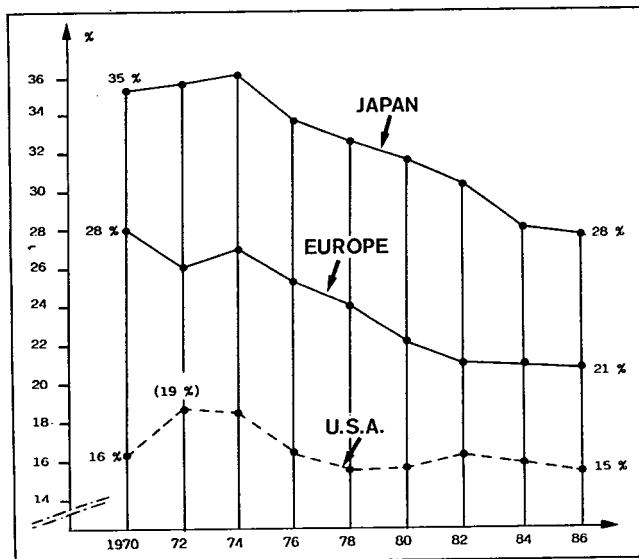


Figure 3. Evolution (in %) of the proportion of pedestrians killed among all road fatalities in Japan, Europe and USA during last fifteen years.

In 1970, for 7 EEC countries, more than a quarter of road fatalities were pedestrians. In 1986, this same proportion no longer applies to only 3 European countries (figure 4).

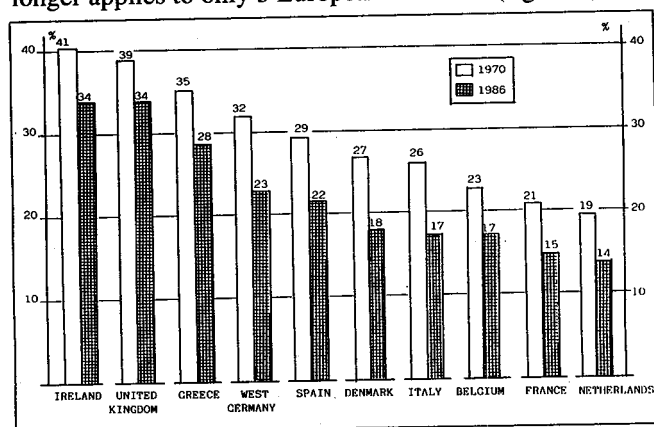


Figure 4. Evolution of the proportion (in %) of pedestrian fatalities among all road fatalities between 1970 and 1986 in 10\* European countries.

\*Are not taken into account:  
—Portugal (data non available),  
—Luxembourg (weakness of cases)

In 1986, within the EEC, only the United Kingdom and Ireland still record a third of all road deaths as being pedestrians.

Another pertinent sign is the pedestrian mortality rate (figure 5). Its evolution expresses a significant drop in all the countries of the European Community between 1970 and 1986. This rate has thus been divided by 2 (Denmark, Ireland, France and Italy) and even by 3 (West Germany, Netherlands). The drop is less in 3 other countries (United Kingdom: 36%, Spain: 17% and Belgium: 11%).

A relative equalizing of the rates around 3% is to be noted in 1986 (except for the Netherlands, where the risk for the pedestrian is lowest), while in 1970 their disparity was large.

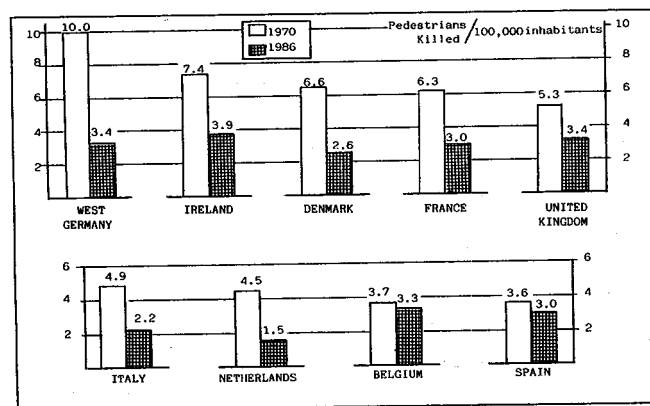


Figure 5. Evolution of pedestrian mortality rates between 1970 and 1986 in 9\* European countries.

\*Are not taken into account:  
—Greece and Portugal (data non available),  
—Luxembourg (weakness of cases)

The share of children under 16 years old<sup>1</sup> among all

<sup>1</sup> International statistics collections bring together children of under 16 years old. The finest distinctions reveal certain effects of size among pedestrians.

pedestrian fatalities dropped in Europe from 21% to 15% on average between 1976 and 1986 (figure 6). In 1986, this same share is variable from one country to another: in the region of 10% (West Germany, Italy) or around 15% (Spain, Belgium, France, United Kingdom, Denmark and Netherlands); the proportion of children among all pedestrians killed attains 28% in Ireland.

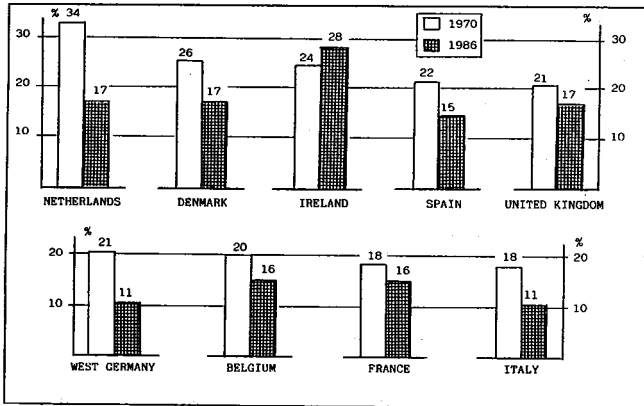


Figure 6. Evolution of the proportion of children (1 to 15 years old) among pedestrian fatalities between 1970 and 1986 in 9\* European countries.

\*Are not taken into account:

- Greece and Portugal (data non available),
- Luxembourg (weakness of cases)

In Europe over the same period, the demographic share of this age group fell from 24% to 19% on average. The 2 countries in which the drop in demographic share of children under 16 years old is greatest (West Germany and Netherlands) are those where the decrease in the share of children among all pedestrian fatalities was the most appreciable.

Except from 3 countries (United Kingdom, Denmark and Ireland), the share of elderly people among pedestrian fatalities is rising: their share, which was 39% in 1970, amounted to 42% on average for Europe in 1986 (figure 7).

The demographic share of elderly people more than 64 years old is rising slightly: it passed from 13% to 14% on average for Europe between 1970 and 1986.

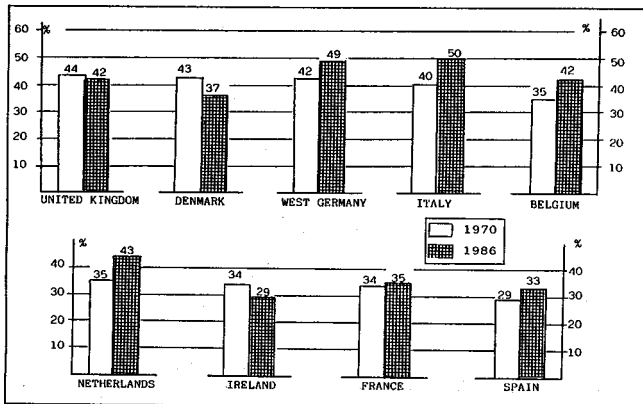


Figure 7. Evolution of the proportion of elderly people (64 years old) among pedestrian fatalities between 1970 and 1986 in 9\* European countries.

\*Are not taken into account:

- Greece and Portugal (data non available)
- Luxembourg (weakness of cases)

For all European countries, the distribution of pedestrian fatalities according to area remained stable, on average, over the last 15 years (around 31%). However, countries where the share of fatalities outside built-up areas is on the decrease (Denmark, France, Netherlands and West Germany) are those in which the highest drop in pedestrian fatalities is recorded (figure 8).

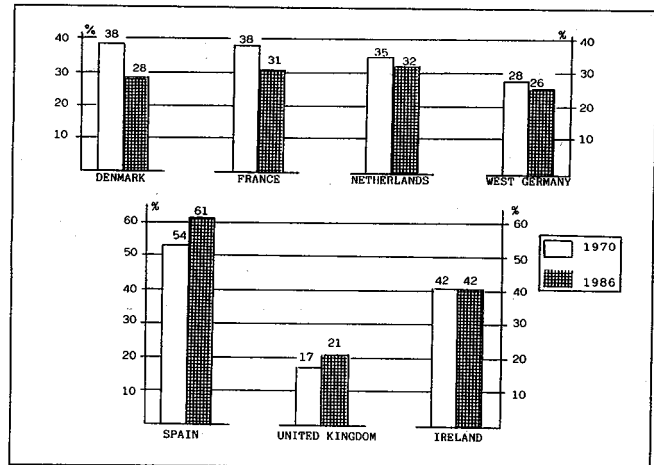


Figure 8. Evolution of the proportion of pedestrians killed in rural areas (in %) among all pedestrian fatalities between 1970 and 1986 in 7\* European countries.

\*Are not taken into account:

- Belgium, Greece and Portugal (data non available)
- Luxembourg (weakness of cases)

## Factors of Evolution

These are multiple. Some are the product of social changes. Others are due to actions undertaken in the fields of primary safety and secondary safety.

### Social factors

The extent of their respective influence is difficult on account of their tight overlapping. Two of them have unquestionable effects.

(1) The drop in birthrate observed in western countries for several decades is one of the reasons for the decrease in the share of children among pedestrian fatalities.

For elderly people, their increase in the population explains them maintaining the place they occupy among pedestrians killed. However, various observations allow it to be thought that the share of elderly people among pedestrian victims could diminish. An American survey (1)\* (table 1) shows that the share of trips made on foot by elderly people is constantly decreasing in favour of trips in motor cars.

This same survey notes the constant increase of driving licence holders among elderly people: 43% licence holders among people more than 65 years old in 1969 and 62% in 1983.

\*Numbers in parentheses designate references at end of paper.

**Table 1. Distribution of person trips by age and mode of transportation.**

Year	Mode	Age			All Ages
		65-74	75-84	85 +	
1977	Passenger Car	83.1	75.8	70.1	83.8
	Walk	12.2	20.7	25.9	9.3
	Other	4.7	3.5	5.0	6.9
		100	100	100	100
1983	Passenger Car	86.4	84.0	78.8	84.7
	Walk	9.8	12.6	13.7	8.9
	Other	3.8	3.4	7.5	6.4
		100	100	100	100

The effect of rural depopulation (61% of the French population was urban in 1960 against 69% in 1982), which is going to continue according to all the forecasts, will continue to lead to a reduction in pedestrian fatalities: the pedestrian mortality rate in Europe in 1986 was 15 killed for 100 victims outside built-up areas against 3 killed for 100 victims in built-up areas.

### Primary safety

This is the framework of all accident prevention actions certainly involving the public community, but also car manufacturers.

The knowledge acquired by the survey on behaviour of children at crosswalks (2) (3) has enabled education programs to be worked out, where the child, as pedestrian, then motor cyclist and future car driver, is trained in the rules of road traffic. Evaluation studies of such programs are at present lacking, but we think that the effect of such is real.

Numerous surveys have revealed the important role of alcohol in pedestrian accidents. In France, according to (4), among those presumed responsible for fatal accidents, pedestrians, with alcohol blood count 45% higher than the legal rate, constitute the class of users most frequently under the effect of alcohol. In Great Britain, according to (5), 74% of the pedestrians killed during "drink-drive hours" (from 10 p.m. to 4 a.m.) had a positive alcohol blood count, against 14% outside those hours. In the U.S.A., according to (6), in 49% of fatal pedestrian accidents, either the pedestrian, or the driver of the vehicle involved, or one and the other, had a positive alcohol blood count. This finding has enabled the embodiment of a policy of prevention by education or repression by alcohol tests at and away from accidents. The installation of devices preventing vehicles from being started by drunken drivers is technically feasible for habitual offenders.

In the field of road infrastructure, numerous efforts have already produced results. These basically cover better management of crossroads and separation of traffic: diversion of inter-urban road traffic towards motorways and expressways has the effect of leading to a reduction in pedestrian fatalities outside built-up areas.

In the automotive technology sector, the enhanced performances of braking systems and the improvement in visibility from the driving position have also individually contributed towards the decrease in accidents.

### Secondary safety

Since the beginning of the seventies, numerous research programs have been conducted in that direction and the results have already been applied to motor vehicle construction.

Such is the case of the reduction of aggressivity of bumpers in relation to pedestrians' lower limbs: elimination of metal "blade" type bumpers, replacement by shields consisting of materials with fibre base (in 10 years, the thickness of bumpers of newly registered vehicles has doubled). The disappearance of sharp angles on the front edges of bonnets and wings, retractable exterior rearview mirrors, elimination of gutter channels on windscreen pillars, gluing of laminated windscreens opposing severe impact of the head of pedestrian against the dashboard or the steering wheel, recessing of windscreen wiper shafts under the back end of the bonnet constitute a list, not exhaustive, of various recent appointments in zones struck by the heads of pedestrians.

These appointments are directly inspired by the lessons drawn from the construction of experimental safety vehicles undertaken as far back as the middle of the seventies. Table 2 summarizes the principal characteristics of a few experi-

**Table 2. Characteristics and estimated gain for 4 experimental safety vehicles.**

Experimental vehicle	AUSTIN ROVER - PSC1 (7)	PEUGEOT SA - ULS 104 (8)	RENAULT - E.P.U.R.E. (9)	PEUGEOT SA - U.S.S. (10)
Vehicle size	small	small	small	long
Appointment zones	- bonnet - bonnet top - bumper and bumper nose (soft nose)	- bonnet - bumper and bumper nose (soft nose) - windscreen frame	- bonnet - bonnet top - windscreen frame	- bonnet - scuttle bay - wing tops
Pedestrians protected	especially children	children and adults	children and adults	children and adults
Bodily areas protected	- lower limbs - head	- lower limbs - head	- head	- head
Protection limit	up to 40 km/h	up to 40 km/h	up to 30 km/h	up to 40 km/h
Reduction in mortality	Very low. Perhaps a slight gain for pedestrians hit at speeds lower than 40 km/h, but it principally involves elderly pedestrians whose tolerance to shock is mediocre.			
Reduction in gravity	This potentially* concerns 30 to 80 % of injured pedestrians (according to age of victims) for collisions up to 40 km/h.  * Notwithstanding the following correction factors: - Roughly 20 % of injured pedestrians are not hit by cars. - 47 % of lesions to the head and 33 % of lesions to the lower limbs are not attributable to the vehicle.			

mental vehicles together with an estimation of the gain obtained by the appointments incorporated. It is to be noted that the only beneficiaries would be the injured, as fatal accidents take place at speeds lying beyond the performances of the counter-measures tested (figures 9-10-11 and 12).

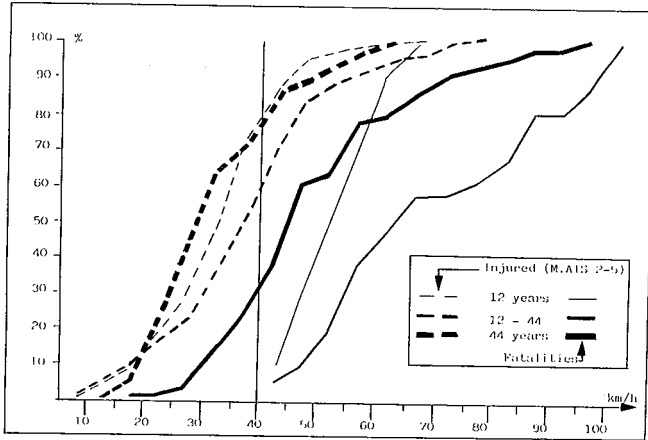


Figure 9. Cumulative impact speed distribution for non minor injuries and pedestrian fatalities.

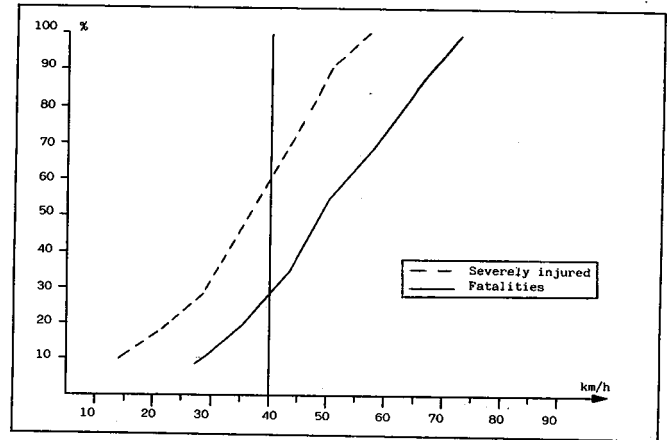


Figure 12. Cumulative impact speed distribution for severely injured and pedestrian fatalities.

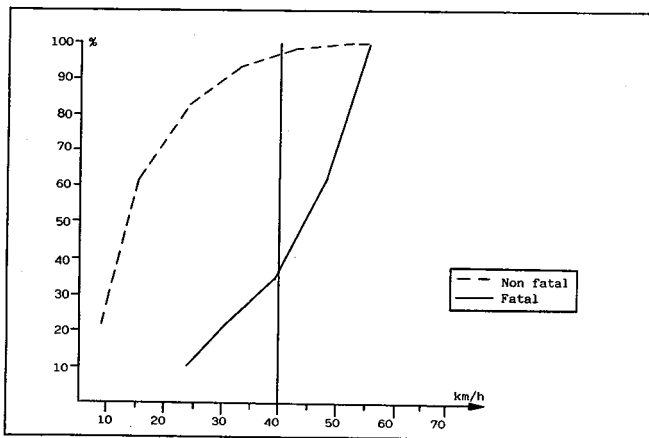


Figure 10. Cumulative impact speed distribution for fatal and non fatal pedestrian collisions.

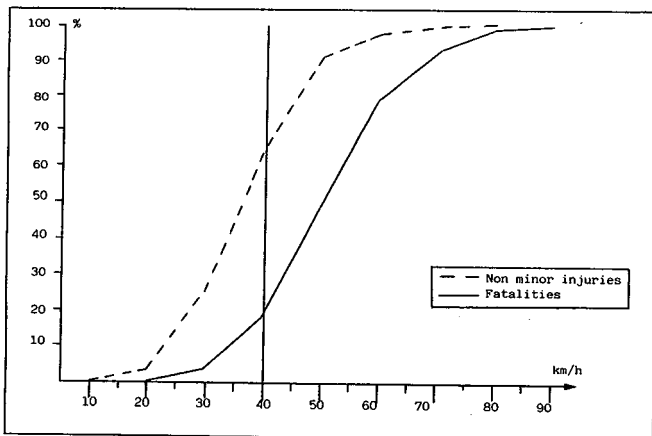


Figure 11. Cumulative impact speed distribution for non minor injuries and pedestrian fatalities.

## Discussion

Demographic changes, current upheavals in modes of transportation used, together with better assimilation of individuals to "civilization of the automobile", on their own combine to the continuing decrease in pedestrian victims in western countries.

It is nevertheless possible to take action to accelerate this favourable evolution. We think however that the perspectives offered by secondary safety will be limited to less severe collisions only. There are several reasons for this.

- The limits dictated by the performances of experimental counter-measures exclude any influence on pedestrian mortality in the present state of knowledge.
- Research has not succeeded in overcoming certain contradictions. Thus, for example: a raised bonnet nose tends to reduce the velocity of impact of the head of an adult pedestrian, but it contributes to aggravating the impact of the thorax of a child.
- The dimensional constraints to which cars are subjected oppose installation of the best performing "soft noses".
- Some appointments risk being the source of wastage: taking into account the discounted performances of the counter-measures; in consideration of their low "statistical profitability" taking into account the evolution of the fall in risk per motor vehicle (division by 2 of the number of pedestrians killed and increase of around 60% in the number of registered vehicles over the last 15 years); by entailing rising repair costs for low-speed impacts against other obstacles (15).

Primary safety seems to be the most realistic way, and we can be allowed to think that it is by pursuing all the prevention actions led in that direction, that the most substantial improvements for the community will be observed in the future.

## Conclusions

The statistical evolutions of the last 15 years have modified the order of priorities of safety actions for western countries. In Japan and in Europe, the number of pedestrian fatalities has been divided by two.

Several of the causes of this evolution are independent of the actions undertaken in the field of safety (demographic factors, rural depopulation). According to all the forecasts, their effect should continue in the years to come.

The reduction of the most aggressive zones on cars has contributed to reducing the gravity of collisions with pedestrians. The performances demonstrated with experimental safety vehicles do not allow a reduction in mortality to be envisaged if the appointments tested were generalized on motor cars.

Primary safety actions (infrastructure, education, alcohol) seem to be the most realistic and efficient.

## References

- (1) "Transportation in an aging society" National Research Council, Washington D.C. 1988.
- (2) "Behaviour of children and accompanying adults at a pedestrian crosswalk", Hugo Van Der Molen, University of Groningen Netherlands, in journal of safety Research, 1982, volume 13, number 3.
- (3) "A parent training program for the road safety education of preschool children", M. Limbourg and D. Gerber, University of Tübingen, Federal Republic of Germany, in Accident, Analysis and Prevention, September, 1981.
- (4) Rapport du Haut Comité d'Etudes d'Information sur

l'Alcoolisme en France, année 1984, Documentation Française, Service du Premier Ministre.

(5) Road accidents Great Britain, 1987, Department of Transport.

(6) Fatal accident reporting system, 1987, US Department of Transportation (NHTSA).

(7) PSC1—A demonstration car with improvement for pedestrian protection, Transport and Road Research Laboratory, 10th ESV 1979.

(8) ULS 104 Peugeot and pedestrian protection, 7th ESV 1979.

(9) "Pedestrian protection: Special features of Renault EPURE", G. Tchetchatcheff, 7th ESV 1979.

(10) "Aménagement d'un véhicule sûr pour le piéton", USS action thématique programmée 1974, Ministère des Transports.

(11) "Rappels accidentologiques concernant les piétons impliqués dans les accidents de la route", C. Thomas et H. Vallée, Société des Ingénieurs de l'Automobile, France n. 1983-2.

(12) "An analysis of fatal pedestrian accidents", J.W. Garret Calspan Field Service, PCIS, SAE 810323.

(13) "Some characteristics of the population who suffer trauma as pedestrian when hit by car and some resulting implications", S.J. Ashton and G.M. Mackay, IV IRCOBI, 1979.

(14) "Cost of injuries by vehicle front shapes and elements in real pedestrian accidents", G. Stürtz, SAE 770941.

(15) "A bumper for both pedestrian and vehicle body protection a contradiction or a soluble conflict?", R. Hoefs, M. Heinz, Porsche AG, 11th ESV.

# Technical Session 6B

## Motorcycle Safety

Chairman: Hiroshi Kizawa, Japan

### Risk of Leg Injuries to Motorcyclists—Present Situation and Countermeasures

A. Sporner, K. Langwieder, J. Polauke,  
HUK-Verband  
Federal Republic of Germany

#### Introduction

Leg protection, a safety element which, in recent times, has been attracting more and more attention, since it seems to represent an unlimited reduction of the risk of injury to motorcyclists involved in accidents.

How can this be assessed from the point of view of real-life accidents?

There is no doubt that it is the lower extremities of a motorcyclist in an accident which are especially exposed to a high injury risk. But, in addition to this, a large number of concomitant injuries result, which, however, in terms of frequency and severity, also influence the overall injury picture.

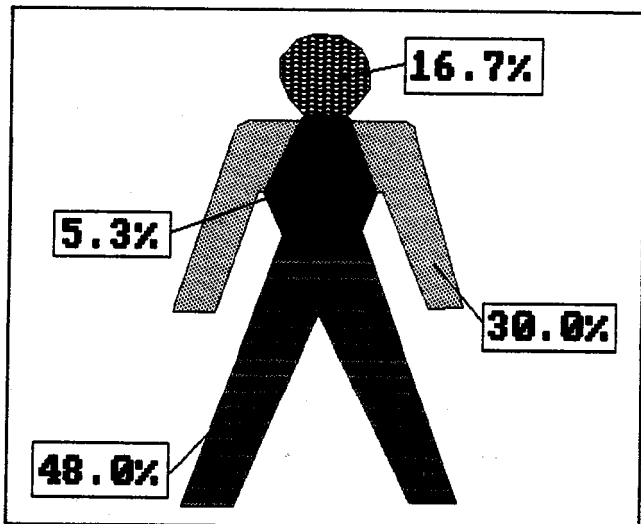


Figure 1. Total injuries of a motorcyclist involved in an accident.

The fact that simple injuries occur extremely rarely in motorcycle accidents and that the motorcyclist's body is always injured in several places also indicates the difficulties which can arise when parts of the accident sequence are examined in isolation.

This paper will therefore try to describe those parameters from real-life accidents which are mainly responsible for causing the injuries, and, moreover, to present an assessment of what influence the injury mechanics have on the injury picture, while paying special regard to the problems surrounding the lower extremities.

#### Case material

The data base of the Automobile Engineering Department of the HUK-Verband contains 1,062 traffic accidents involving motorised two-wheelers. The structure of this data material, which has been compiled from insurance records, police reports and expert opinions, corresponds closely to the distribution of the individual vehicle types and the consequences of the accidents according in the official statistics. All those cases have been filtered out of this data material in which the lower extremities of the motorcyclist were injured in the accident. Here the lower extremities include the following parts of the body: foot, lower leg, knee, thigh and the pelvic region, the latter covering only injuries to the bones. The lower leg injuries were broken down into injuries to the flesh and to the bones.

This resulted in material for the study from 487 traffic accidents with a distribution of the vehicle types and accident consequences according to figures 2a and 2b.

#### According to official statistics

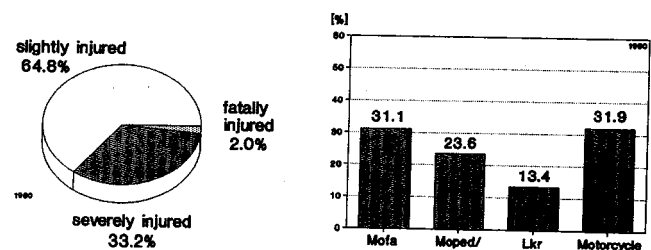


Figure 2a. Distribution of the accident (according to official statistics).

#### According to HUK material

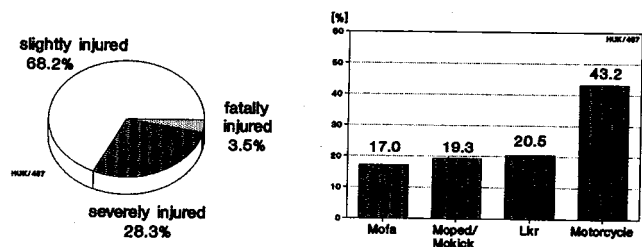


Figure 2b. Distribution of the accident (according to HUK material).

The removal of a specific subset from the total amount of material resulted in a shift in the distribution of the vehicle types, since the proportion of the lighter two-wheelers decreased.

This might be a first indication that the sequence of the accident will be of significance when injuries are caused to the lower extremities, because this clearly differs in the case of lighter and heavier motorcycles.

All the considerations that follow therefore refer to this subset.

## Injuries

First, the distribution of injuries to the lower extremities is shown without comparison and only with an indication of the individual degrees of severity, so that it is possible to assess the frequencies within this region of the body.

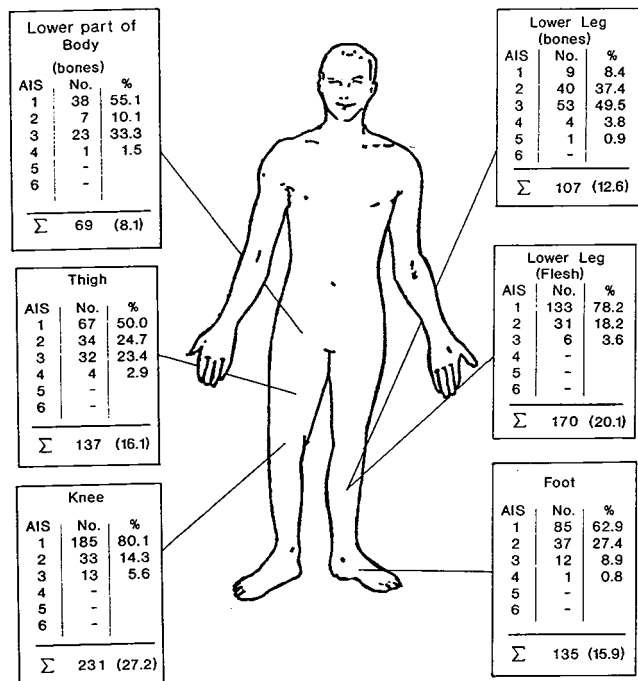


Figure 3. Frequency and severity of injuries to the lower extremities.

Injuries to the knee amount to 27.2% and thus range at the top of the frequency distribution. If the injury severity is also included, it can be seen that the most serious injuries occur to the lower leg, even if the single case of an AIS 5 is not taken into consideration.

## Comparison with the overall injury picture

The presentation of the distribution of the injuries to the lower extremities alone says nothing about the significance of the leg injuries. Only in conjunction with the overall injury picture is it possible to make an assessment. The following figures are therefore intended to supply a comparison between individual injuries and the overall injury severity (MAIS), both for the injuries to the lower extremities and in comparison with them for the head injuries.

Figure 4 shows the injuries to the lower extremities from the degrees of severity 1 to 5. There are no cases of AIS 6, which indicates that no motorcyclist has directly died as a result of injuries to the lower extremities at the scene of the

accident. The proportion of those severely and fatally injured (MAIS 5 and 6) shows the frequency that can be expected for the consequences to the whole body, although the injuries to the legs, for example, were only slight.

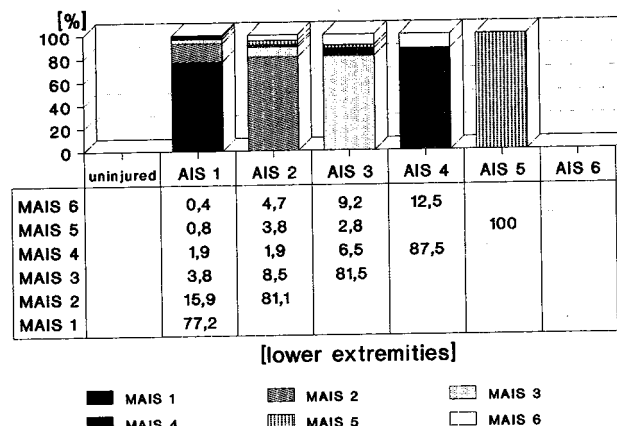


Figure 4. Injuries to the lower extremities compared with the overall injury severity. (Comparison of AIS lower extremities with MAIS.)

For the degrees of injury severity to the head a similar picture emerges up to AIS 2, since here, too, the total injury severity may be higher than the injury to the head. About 40% of all the motorcyclists injured sustained more severe injuries than to the head, when the latter had a maximum AIS of 2. But it can be said that from AIS 3 the head injury determines the total injury severity, because there is no case in which the MAIS was higher than the head injury.

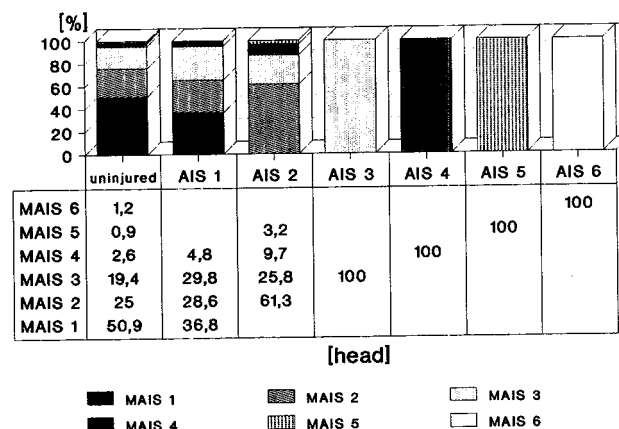


Figure 5. Injuries to the head compared to the overall injury severity. (Comparison of AIS head with MAIS.)

This presentation can be made even more specific, if the body regions head, trunk and upper extremities are included in the comparison.

In this case, the question is: Which injuries to the head, trunk or to the upper extremities does a motorcyclist sustain when he has an injury to the lower extremities with an AIS of 1, 2 or 3? The result is summarised in the next chapter.

## Upper parts of the body in comparison to the severity of the injuries to the lower extremities

In these descriptions the body is divided up into 4 regions. In each case the lower extremities are shown in conjunction with the head, the trunk and the upper extremities. Each figure shows the maximum degree of severity AIS 1 to 3 for the lower extremities. This group of injured persons is connected in each case with all the possible degrees of severity of injuries to the head, the trunk and to the upper extremities.

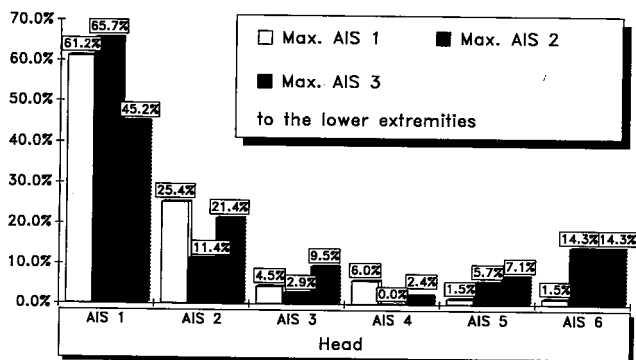


Figure 6. Maximum AIS to the lower extremities in comparison to the injuries of the head.

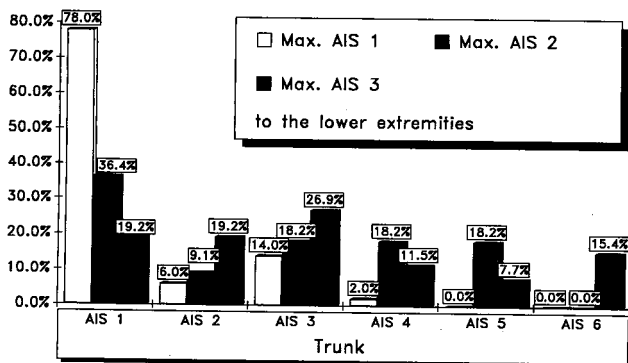


Figure 7. Maximum AIS to the lower extremities in comparison to the injuries of the trunk.

The comparison with the head injuries shows that even in the case of an AIS 1 to the leg 38.8% of the head injuries are above AIS 1. If the motorcyclist sustains an injury to the leg with a maximum AIS of 2 it can be assumed that in about 34% of the cases an injury to the head occurs which is equally severe or more severe.

On the other hand, it can be concluded from the presentation that in the case of an AIS of 3 to the lower extremities about two-thirds sustained only slight head injuries, i.e., a head injury of an AIS of 1 or 2.

For the body regions of the trunk and upper extremities more diversified accident consequences result. Here, too, it is clear that fatal consequences are not to be expected in the case of injuries in the area of the arms. But the diagram also shows, especially in the case of injuries to the trunk, the first

influence of the effect of the forces affecting the motorcyclist's body in an accident.

From AIS 2 to the lower extremities the injuries to the trunk are greater than, for example, to the head. This allows the conclusion that when there is an impact during the accident resulting in an injury to the lower extremities with an AIS of 2, the energy has to be so great that even the motorcyclist's trunk is detrimentally affected.

In 54.6% of the cases in which the motorcyclist had an injury with a maximum AIS of 2 the injuries to the trunk were above AIS 2. It is even more negative if the AIS 3 injuries to the lower extremities are compared in connection with the slight injuries to the trunk (AIS 1 and 2). In this case only 38.4% of the motorcyclists involved in an accident have slight injuries to the trunk.

The comparison between upper and lower extremities produces less information which is helpful in solving the injury problems of the lower extremities.

It emerges that the majority of the injuries range between AIS 1 and 3, and the probability of sustaining an equivalent AIS to the upper extremities increases with the injury severity to the lower extremities.

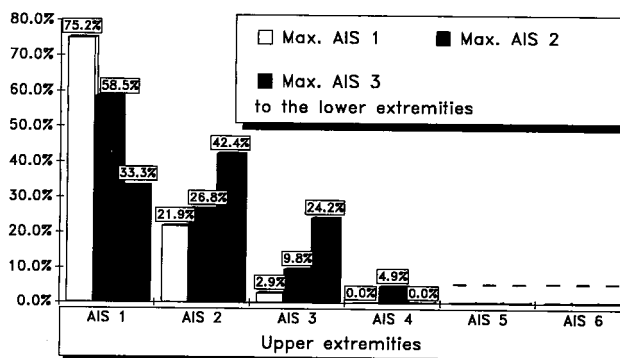


Figure 8. Maximum AIS to the lower extremities in comparison to the injuries of the upper extremities.

The injuries to the lower extremities therefore represent an essential part of the injury picture of a motorcyclist involved in an accident. So every effort to lower this risk should be examined to ultimately achieve an improvement. But as the sequence of movements in a motorcycle accident contains a large number of possible variants it is necessary to analyse in even greater detail the way in which the injuries develop so that no unwanted side effects are obtained. The next thing that is necessary to do is therefore to clarify the origin of the injuries and to describe the various accident sequences which result in the corresponding injuries. Insofar as the case material allows, the vehicle type will also be examined as a parameter, since the different accident sequences are also due to the vehicle. The knowledge thus obtained will then help in making decisions which will lead to the optimum design of a leg protection element.

## The cause of injuries

In the search for improvements the most important question is the one involving the origin of injuries. For a motor-

cyclist involved in an accident, the injuries principally result from three parameters.

1. Injuries through the forces exerted by the accident opponent
2. Injuries through falling after separation from the motorcycle
3. Injuries caused by the motorcyclist's own vehicle

In real-life accidents the third point can only be seen in the rarest cases without the involvement of an accident opponent. In most cases these injuries arise through the leg being wedged in or, in the case of glance-off collisions, when the leg has no room to escape. But even in these cases the effect of the accident opponent is responsible for causing the injury. In our case material, in collisions with a car, the proportion of injuries which resulted from the influence of the accident opponent was 80%. In 20% of all motorcycle collisions there was no contact between the accident opponent and the motorcyclist's lower extremities. In these cases the injury resulted from the circumstances of skidding on the road or hitting an obstacle.

A more detailed breakdown of the cases in which a contact between a motorcyclist and a car as an accident opponent occurred shows that the edges in the front area of the car produced about two-thirds of the injuries and were thus the main cause.



Figure 9. Typical damage to edges of a car.

### Impact areas of the accident opponent

In a collision with a car, part of the car always touches the motorcyclist. Below, the vehicle areas are presented which first come into contact with the motorcycle. In the course of an accident it is quite possible that further damage is caused to the accident opponent, but this has not been taken into consideration here.

The front of the accident opponent, in our case of the car, is the area which most frequently comes into contact with the motorcycle. It is the edges, that is the transition point between the bonnet and the mudguards, which rank first in the distribution within the front section.

The side areas are dominated by the left side of the car, while the rear section of the car is only of secondary impor-

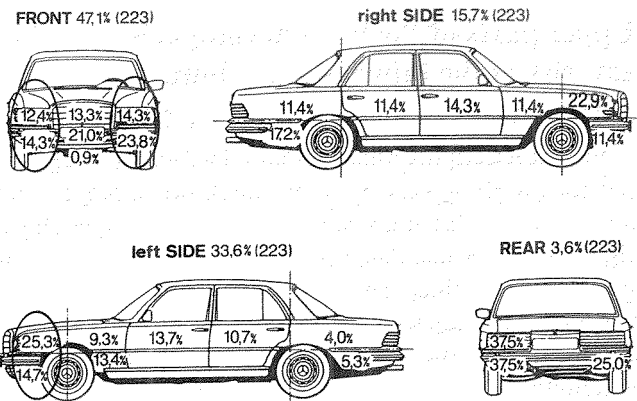


Figure 10. First contact in a collision with a two-wheeler.

tance. So much on the question as to which part of the vehicle causes the injuries when a collision with a car occurs. But it cannot be concluded from this account what the directions of the forces are which affect the motorcycle. This question will be answered in the next chapter, which deals with the directions of the impact against the motorcycle.

### Impact directions against the motorcycle

The influence of the vehicle type on the accident type and thus on the aggressive direction of the forces has already been clearly presented from previous works.

Smaller motorized two-wheelers are hit more frequently by the accident opponent, while larger and heavier motorcycles more frequently collide head-on with their accident opponent. This systematic pattern naturally also has considerable influence on the cause of the injuries. The following diagram shows the distribution of the impact directions against the two-wheelers, broken down into the groups Mofa, Moped, Mokick and light powered motorcycle (German = Leichtkraftrad, Lkr), motorcycle.

In the case of the heavier motorcycles, the main impact direction is in the front of the bike, while in the case of the lighter two-wheelers it is less in the front than the sides of the vehicle, particularly the left side, which are struck more often. This difference results, as already mentioned, from the distribution of the accident types. But the collision speeds of the vehicles involved are also dependent on the accident type and they, in turn, provide information on the energy applied. For the collision speeds of motorized two-wheelers the following picture emerges for the combined areas front, side and rear.

About 10% of all accidents occur when the speed of the two-wheeler is over 60 kph. In the case of impact areas at the front of the two-wheeler, the higher speeds predominate, although here, too, no more than 13.5% were above 60 kph. The main speeds range from 16 to 60 kph. If the collision speed of an accident opponent's car is examined, it becomes clear that here the essential speeds are even lower, namely between 16 and 45 kph.

For the findings of this chapter the evaluation was supplemented by a question regarding the first contact between the

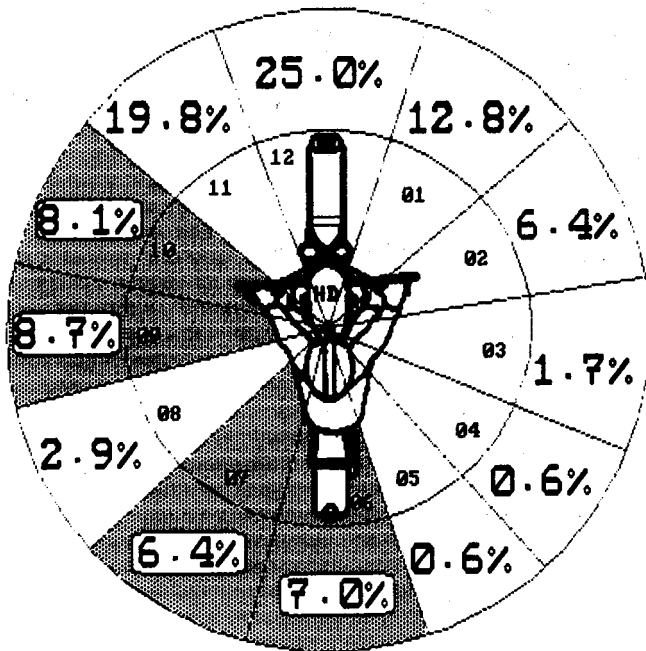


Figure 11. Impact directions against the motorcycle.

Collision speeds of the two-wheeler impact areas front, side, rear on the two-wheeler

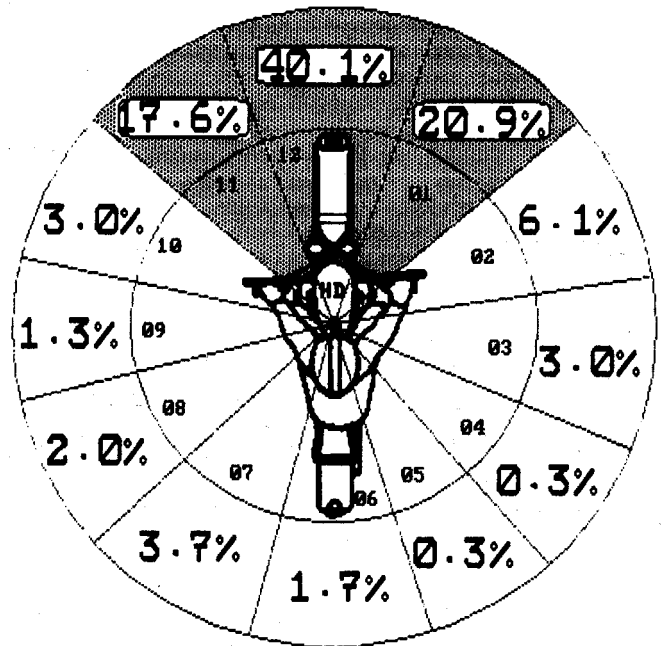
$V_K$	Front	Side	Rear	Total <sup>221</sup>
[kph]	%	%	%	%
> 100	0.6	0.0	0.0	0.5
81-100	3.1	0.0	7.1	2.7
61-80	9.8	2.3	0.0	7.7
46-60	28.8	9.1	7.1	23.5
31-45	28.2	43.1	7.1	29.9
16-30	22.7	34.1	50.2	26.7
- 15	6.8	9.1	21.4	8.1
0	0.0	2.3	7.1	0.9
	100	100	100	100

Figure 12. Collision speeds of the two-wheeler and collision areas of the two-wheeler.

Collision speed of the car impact areas front, side, rear on the two-wheeler

$V_K$	Front	Side	Rear	Total <sup>251</sup>
[kph]	%	%	%	%
> 100	0.0	0.0	0.0	0.0
81-100	0.5	2.1	20.0	1.6
61-80	3.1	0.0	30.0	3.6
46-60	3.1	8.5	0.0	4.0
31-45	4.1	10.6	10.0	5.6
16-30	20.1	31.9	30.0	22.7
- 15	65.0	46.9	10.0	59.3
0	4.1	0.0	0.0	3.2
	100	100	100	100

Figure 13. Collision speeds of the opponent car and collision area of the two-wheeler.



MOFA Moped Mokick

two-wheeler driver or vehicle and the accident opponent. For this purpose, the two-wheeler was divided up into the following areas:

- A. Front wheel.
- B. Side of front wheel with fork.
- C. Motor, tank and driver's leg.
- D. Rear part of the motorcycle without leg.
- E. Rear wheel.

The following picture emerged from the information known, broken down according to vehicle types.

		Moped.	Motorcycle	Total
Area of the first contact with the two-wheeler	A	32.6%	42.2%	38.8%
	B	30.4%	24.8%	26.9%
	C	28.2%	29.9%	29.3%
	D	4.4%	2.1%	2.9%
	E	4.4%	0.8%	2.1%

Figure 14. Area of the first contact with the two-wheeler.

The impact directions described above are very similar to this picture; the deviations result from the fact that this picture includes all the accident opponents—from the car to the truck—and the areas were defined differently. But the result is completely confirmed.

In about 70% of the cases the first contact and thus the first application of force, too, occurs with such parts of the vehicle as the front wheel, side of the front wheel or the rear wheel. In about 30% of the cases, the lower extremities are struck first, or the area of the two-wheeler which is covered by the lower extremities.

The differences between the vehicle types again indicate the different accident types in which the smaller motorized two-wheelers are more often struck in the side and the heavier motorcycles collide more often head on with the accident opponent.

If only the areas in which a part of the lower extremities are struck, that is the area of the motor and the tank, are concentrated upon, it is again possible to estimate the load applied from the distribution of the collision speeds.

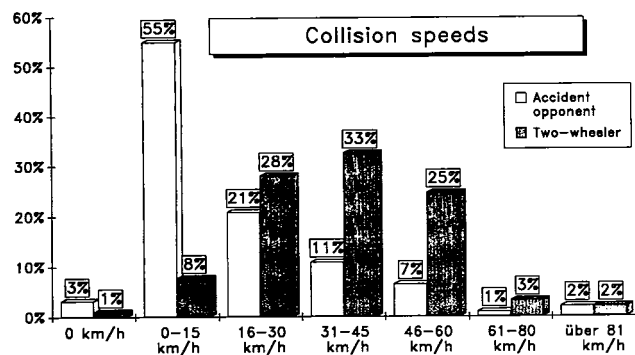


Figure 15 Collision speeds of the two-wheeler and accident opponent when the first contact was in the area of the two-wheeler driver's leg.

The speeds of the accident opponent are relatively low. Over 50% of the accident opponents were stationary or not moving faster than 15 kph when the contact between the two road-users took place.

The speeds of the two-wheeler are at a higher level. In this case over 50% of the two-wheeler's collision speeds are over 30 kph. Here, too, the first findings can be inferred for the conception of a leg protection, since the energy applied by the accident opponent and the two-wheeler's kinetic energy require different solutions. Excessive energy from the accident opponent causes almost insoluble problems, while, on the other hand, solutions can be found when the two-wheeler's kinetic energy dominates. Here, however, the further effects of the kinetic energy of the two-wheeler and of its driver must also be taken into account. More on this in the chapter on the influence of leg protection on the trajectory.

Next only the area of the two-wheeler is to be examined which is covered by the lower extremities of the driver, or, in other words, only those accidents in which the forces were directed to the middle of the two-wheeler, i.e. the leg and the corresponding parts of the two-wheeler. To simplify this both sides are combined.

As was expected, the main directions of the forces are between 0 and 75 degrees. But this time the area directly at the front is not struck so frequently as was observed from the impact directions against the whole vehicle. In this case it is mainly a question of glance-off collisions which do not play a dominant role in the accident scene but which, nevertheless, cannot be ignored. The consequences of glance-off collisions of this kind can be disastrous, since in these cases it is often necessary to amputate limbs. An impact of forces

from behind and at an angle from behind are relatively seldom. Nevertheless, here, too, suitable protective elements should be sought, since leg injuries, especially in view of the costs they cause to the national economy, are a significant factor. More on this in the next chapter.

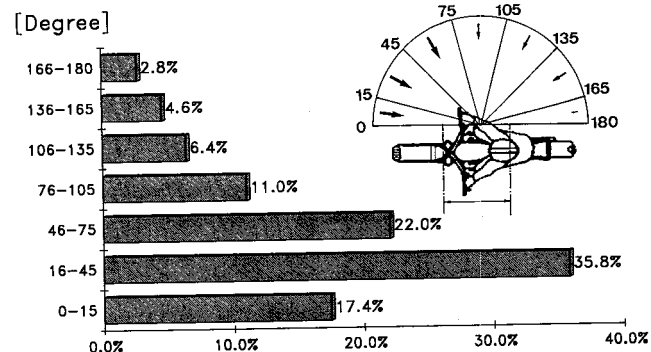


Figure 16 Impact directions when impact was in the leg area.

### Costs of the accidents consequences

The division into AIS-values is a possible way of classifying the consequences of traffic accidents. But it only considers the personal consequences, and does not allow an assessment of the equally important social effects. For this reason an attempt has been made in the following tables to relate the severity of the injuries which are caused to the different parts of the lower extremities to the costs which arise.

Publication No. 73 of the "Forschungsvereinigung Automobiltechnik" was used for ascertaining the costs of the accident consequences. In this work the costs of the consequences are broken down into costs of treatment (for in- and out-patients) and into economic costs, which are worked out by a special calculation. The economic costs (abbreviated EC) per case are, to a large extent, determined by the "reduction in the capacity to work" and by the "pension for injured persons" that has been granted. For a more detailed description of how these costs arise you are referred to the literature.

An examination of the HUK-material shows that 487 people received a total of 948 individual injuries to the lower extremities. This results on average therefore to 1.7 injuries to the lower extremities per person.

For all the injuries to the individual parts of the motorcyclist's lower extremities there is a wide gap between the costs of treatment and the economic costs. On average the EC exceed the costs of treatment by a factor of 10.

Particularly in the case of the lower leg it becomes clear that there is not necessarily a linear connection between the degree of accident severity and the costs. Open fractures require more intensive treatment than closed multiple fractures. The effect of wound infection in the case of open injuries is clearly more prominent in the table showing the costs of injury consequences.

A comparison of pelvis, hip and thigh with the knee, lower leg and foot reveals a difference in the level of the

economic costs. It is noteworthy that the follow-on costs for injuries to those parts of lower extremities which are furthest from the vital organs amount up to more than 100,000.-DM in accordance with AIS 2 or more. So here, too, it again emerges that an injury to the lower extremities is of a significance which should not be underestimated.

Abdomen (bones) (pelvis, hip joint)				Thigh		
AIS*	Inj. description	Treatment costs- [DM]	Economic costs- [DM]	Inj. description	Treatment costs- [DM]	Economic costs- [DM]
1	Bruises	5,240	25,000	Bruises	5,240	25,000
2	Fracture	8,370	27,000	Fracture (simple)	6,040	77,000
3	Fracture	28,900	214,000	Fracture (dislocated)	17,510	193,000
4	Fracture	25,630	284,000	Fracture (open, amputation)	47,170	319,000

Knee				Lower leg (flesh)		
AIS*	Inj. description	Treatment costs- [DM]	Economic costs- [DM]	Inj. description	Treatment costs- [DM]	Economic costs- [DM]
1	Bruises	5,290	35,000	Bruises, grazes	7,710	39,000
2	Fracture (simple)	14,470	124,000	Flesh wound (deep)	12,940	190,000
3	Fracture (dislocated, open)	17,720	199,000	Flesh wound (extensive)	?	?

Lower leg (bones)				Foot		
AIS*	Inj. description	Treatment costs- [DM]	Economic costs- [DM]	Inj. description	Treatment costs- [DM]	Economic costs- [DM]
1	Bruises	7,710	39,000	Bruises	6,870	42,000
2	Fracture (simple)	19,490	141,000	Fracture (closed)	12,810	113,000
3	Fracture (open, dislocated)	28,190	211,000	Fracture (multiple)	8,690	123,000
4	Fracture (multiple s. closed)	23,490	200,000	Fracture (open)	25,620	194,000
5	Fracture (multiple s. open)	18,200	213,000			

\* According to material of 487 cases  
 \* According to FAT...

Figure 17 Costs of the accidents consequences.

### The sequence of movements

All the results from the analysis of the real-life accidents and the considerations of the economic effects of leg injuries to motorcyclists involved in an accident that have been mentioned above call for an intensive search for suitable safety elements. Knowing these results, one is far too easily tempted to snatch at an isolated solution to the problem, i.e. to pursue a solution which only concentrates on reducing leg injuries. The rest of this paper is intended to help avoid this danger.

The injuries to the lower extremities have to be seen together with the other possible injuries. In most cases the impact which results in an injury to the lower extremities is also responsible for the whole of the trajectory of the motorcyclist in an accident.

An analysis of the available cases, supported by publications which have already appeared, shows two groups of accident sequences which contain an essential difference in the way the injuries are caused.

In the first group, all those accidents are combined which are characterized by the collision speed and thus by the kinetic energy of the accident opponent. The sequence of the accident is similar to that with a pedestrian; the motorcyclist is struck and his speed is adjusted to the speed of the accident opponent. As already shown, this group contains mainly lighter motorized two-wheeler vehicles.

The remaining accidents make up a group which is characterized by the motorcyclist's own kinetic energy. While in the first group, referred to below as Energy Type I, the motorcyclist is stationary or is only moving slowly, in this group the speed of the motorcycle is higher and thus the dominant factor. These basic differences also emerge when

the corresponding vehicle parts in the first contact during the accident sequence are examined.

In the following two tables the parts of the motorcycle and the areas of the accident opponent which are the first to touch each other in the accident are contrasted. Of course, it is the front of the accident opponent in Energy Type 1 which is most frequently the first contact area. The corresponding parts on the motorcycle are distributed in the following order: leg area/front wheel and rear area.

In just over 40% of the accidents the leg area is struck by the front of the accident opponent. Another area of the accident opponent's vehicle which comes into contact with the leg area of the motorcyclist is the side of the accident opponent's vehicle. This, less aggressive, contact between the two vehicles results from accident situations which show a relatively acute angle in the direction of the collision speeds.

Two-wheeler	Accident opponent				
	Front	Side area	Rear		
Rear area (without leg)	22.7	83.3	11.1	16.7	100%
Leg area	40.9	69.2	44.5	30.8	100%
Fork	-	-	33.3	100.0	100%
Front wheel	36.4	80.0	11.1	10.0	100%
	100%	100%	100%		

Figure 18 Energy Type I. Collision of the car over 30 kph.

Two-wheeler	Accident opponent						
	Front	Side area	Rear				
Rear area (without leg)	6.1	100.0	-	-	100%		
Leg area	47.0	53.5	30.7	44.2	33.3	2.3	100%
Fork	16.3	33.3	24.2	62.5	33.4	4.2	100%
Front wheel	34.1	34.1	45.1	63.6	33.3	2.3	100%
	100%	100%	100%				

Figure 19 Energy Type II. Collision speed of the two-wheeler over 30 kph.

In the second group, Energy Type 2, it is the accident opponent's side area which is struck most frequently, namely in 63.6% of the cases. About two-thirds of the motorcycles touch this part of the accident opponent first with their front wheel or with the side of the front wheel.

Making this distinction between the different accidents reveals an important aspect which it is essential to observe when developing a safety element for the lower extremities. There are accidents in which the impact takes place directly against the lower extremities, and there are cases in which the impact takes place indirectly against the motorcyclist's leg. While in the first case, the possible protection, i.e. destroying the energy of the impact, must be applied in the immediate vicinity of the leg, in the second case the space of time between the first contact of the accident opponent and

the injury caused to the leg the motorcyclist's trajectory can be decisively changed.

What effects does this difference have on the pattern of injuries to the rest of the body?

It can be gathered from the publications already mentioned that one factor for causing serious head injuries is the rotation of the upper part of the motorcyclist's body. This rotation of the upper part of the body occurs when a force is applied below the body's overall point of gravity. In a normal case the motorcyclist in a collision slides in a straight line on his saddle in a forward direction until he meets the first obstacle. Without leg protection and in a frontal collision with another road user this is, as a rule, the tank. When the lower part of the body comes into contact with the tank the head and the trunk begin to rotate about this contact point.

This kind of movement sequence also occurs when the motorcyclist's knee strikes the leg pad, since the forces are passed on to the hip via the thigh. As early as 1982 we therefore recommended the introduction of pads in front of the motorcyclist's leg only in conjunction with a handle-bar which forced the motorcyclist to sit in an upright position.

In tests and in mathematical simulation models it was observed that the rotation of the upper part of the body can be shifted so far that any lowering of the head becomes acceptable. It will never be possible to rule it out completely, unless the motorcycle is equipped with an airbag.

Another equally undesirable rotation of the upper part of the body occurs when the first contact between the two vehicles takes place in the leg area and not at the motorcycle's front wheel, i.e. when the injuries are caused directly. In this kind of accident sequence the force is also applied below the overall point of gravity, and the decelerations which occur at this point are extremely rapid.

Protective elements, which in this case are located in front of the motorcyclist's legs and which possess certain deceleration properties, can here reduce the rotation of the upper part of the body, since the maximum deceleration rates can be reduced. At any rate, an acceleration of the rotation motion is not to be expected.

The question is therefore: Which rotation of the upper part of the body can be accepted or is its influence on the causes of head injury too great?

Padding elements or leg protection elements in front of the motorcyclists legs will always have some effect on the movement of the whole body, especially when there is a delay in passing on the impact to the body.

## Conclusion

Leg injuries characterize the injury picture quite decisively. Every second motorcyclist involved in an accident is injured in the area of the lower extremities. On average 1.7 injuries are caused to the various parts of the lower extremities. The motorcyclist's knee is struck most frequently, and the lower leg is injured most severely. If the injuries to the lower extremities are related to the overall

injury severity the proportion of MAIS values higher than the injury severity to the lower extremities is about one-fifth.

A comparison of the different regions of the body head, trunk and upper extremities shows that, especially in the case of injury to the trunk, the injury severity of the lower extremities plays a subordinate part. On the other hand, a comparison with the head injuries produces a proportion of about two-thirds of all cases in which, in spite of AIS 3 to the leg, only a slight injury to the head could be observed.

The causes of the injuries can be divided into two groups, which also show differences depending on the kind of two-

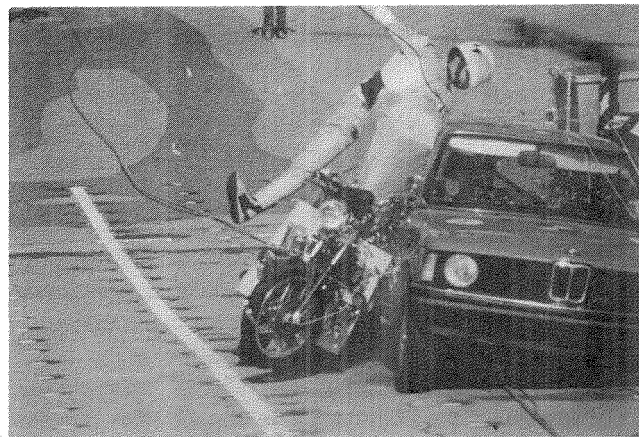
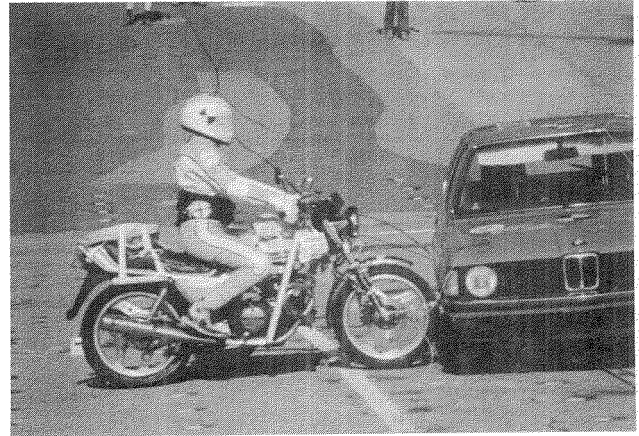


Figure 20 Test with airbag at 50 kph and both vehicles in motion.

wheeler involved. For lighter and less powerful motorized two-wheelers it can be said that as a rule the impact resulting in the injury is directly due to the contact with part of the accident opponent. Here it is the edge of car's front which is dominant. The direction of the force is concentrated on front and front-side contact in the area of the leg.

In the case of motorcycles there is a group of collision types in which the first contact with the accident opponent is not in the immediate area of the lower extremities. Here, because of the available time of about 100 ms up to the impact of the legs against the accident opponent, changes in the motion sequence can occur which produce effects on the motorcyclist's overall injury picture. In this connection the rotation of the upper part of the body should be mentioned as a negative effect, and it may mean additional loading for the head.

A solution might be found by combining leg protection with an airbag. This gives a motorcyclist's body extra height and exactly in that part which is otherwise pressed downwards as a result of the rotation of the upper part of the body. This possibility, at the moment unfortunately still in the experimental stage, was examined in a series of tests carried out by us in cooperation with the DEKRA.

It was possible to show in these tests that the direct impact of the head against the area of the edge of the roof is avoided. The additional rotation of the upper part of the body was also cushioned by the airbag.

The safety motorcycle of the future must consist of several safety elements which influence each other. Although individual solutions may be successful for a short time in the complex motion sequences during a motorcycle accident, when attention is focused on the overall injury picture only an integrated solution will, in the long run, increase passive safety.

## References

Verletzungsfolgekosten nach Straßenverkehrsunfällen  
Forschungsvereinigung Automobiltechnik e.V. FAT  
Schriftenreihe Nr. 73, Frankfurt, 1988.

Motorisierte Zweiradunfälle, eine Statistik der Berufsgenossenschaftlichen Unfallklinik Frankfurt a.M. aus den Jahren 1977 bis 1980, Börner M., 1. Workshop, Institut für Zweiradsicherheit, IFZ, Bochum-Wattenscheid.

The problem of Leg Injuries in Motorcycle Riders, Nordentoft E. et al, IRCOBI 1984, Delft.

Experimental investigation of motorcycle safety, Taneda K. IRCOBI 1976, Amsterdam.

Leg Protection for Motorcycles, Chinn B.P., TRRL, IRCOBI 1984, Delft.

Leg Protection for Riders of Motorcycles, Chinn B.P., Hopes P., TRRL, 10. ESV Conference 1985, Oxford.

A Study of Motorcycle Leg Protection, Tadokoro, H., Fukuda, S., Miyazaki, K., JAMA, JARI, 10. ESV Conference 1985, Oxford.

Motorcycle Rider Protection in Frontal Impacts, Chinn B.P., Donne G., Hopes P., TRRL, 10. ESV Conference 1985, Oxford.

Leg Protection for Motorcyclists, Chinn B.P., Macaulay M.A., TRRL, IRCOBI 1986, Zürich.

Experimentelle und mathematische Simulation von Motorradkollisionen im Vergleich zum realen Unfallgeschehen, Spörner A., Dissertation TU München, 1982.

Development of a safety concept for motorcycles: Results of accident analysis and of crash tests. Spörner, A., Langwieder, K., Polauke, J., 11. ESV Conference, 1987, Washington.

Versuchsreihe in Zusammenarbeit mit Dekra und schweizer Winterthur Versicherung, HUK-Verband, Büro für Kfz-Technik München Pressekonferenz vom 22.02.88.

## Acknowledgements

The authors are particularly indebted to all the member insurance companies of the HUK-Verband for making their claims records readily available for this study, to Messrs. Helmut Klein and Dieter Raßhofer, who were responsible for handling the data base and the accident analysis, and to Geoffrey P. Burwell for his assistance with the translation.

## Leg Protection and its Effect on Motorcycle Rider Trajectory

**B.P. Chinn, P.D. Hopes, and  
Melanie P. Finnis,**  
Department of Transport,  
United Kingdom

### Abstract

66% of serious injuries incurred by motorcyclists in Great Britain are leg injuries. Surveys of motorcycle accident data which show the collision configurations and speeds which typically cause leg injuries are reviewed. The majority of these injuries occur at fairly moderate speeds

(<50Km/hr) and at oblique angles of impact between the motorcycle and the opposing vehicle. Leg protection devices have, for some time, been considered to reduce the likelihood or severity of leg injuries in these types of impact.

A series of tests was devised using a Norton Interpol II, to examine the performance of leg protectors, designed to the

draft United Kingdom leg protection specification. The test series, equipment and test procedure are described. The purpose of the test series was twofold. The first aim was to show the effect of leg protection on potential leg injuries in those type of impacts where leg injuries are common. The second purpose was to demonstrate that leg protectors do not increase the risk of injury to other parts of the body in these, or in other impact configurations, e.g. head-on collisions, where serious and fatal upper body injuries are more prevalent. Various methods are employed to assess the potential injury and the results are discussed with respect to these considerations.

## Introduction

TRRL has reported (1, 2, 3, 4, 5) on numerous impact tests of motorcycles of various sizes with mainly stationary targets (barrier and cars) in order to assess the effect and likely benefits of leg protection. This report describes the results of impacts of a large motorcycle with (i) a moving vehicle (3 configurations) and (ii) a stationary vehicle (2 configurations), a total of 13 impacts. The purpose of these tests is to evaluate the performance of leg protection designed to the UK draft specification (6) by comparison with the standard faired machine, and in two instances a similar machine unfaired.

The potential injuries are analysed in two distinct ways. The first by an assessment from the output of transducers fitted to the dummy and the second by the use of high speed film data to determine the trajectory and velocity of the dummy rider. The effect of leg protection on the trajectory of the motorcycle is also analysed in these two ways.

If leg protection is to be of benefit not only must leg injuries be reduced but the potential for injuries to other parts of the body particularly the head must not be increased. The detailed analysis in this report focuses strongly on this point, which is why the analysis is in two parts. Information from transducers is extremely valuable but is subject to variations which are inevitable in impact testing not the least of which is the variation in the stiffness of different parts of the car. The transducer analysis from which injuries are predicted explicitly is compared and supported by the trajectory analysis which describes an implied and thus broader potential for injury. In analysing the trajectory the velocities calculated are related carefully to the motion and position of the impacted vehicle. This is essential if the values quoted are to have any meaning in terms of potential injury.

It is important when testing a safety device that the impact configurations chosen are those which have been reported in accident studies as the most likely to cause the type of injury against which the device is designed to protect. It is also important that the device is tested in impacts in which injuries to other important areas of the body (notably the head) are known to occur and to ensure that these are not made worse. Hence there is a brief review of accident

studies which report on the accident configurations most likely to cause leg and head injuries.

## Accident Configuration Review

Various studies have attempted to identify the type, direction and speed of impacts which cause leg injuries and to determine which of these impacts causes each type of injury.

### Injury mechanisms

Otte et al. (7) found that the highest injury severity tends to occur when a two-wheeled motor vehicle collides obliquely with the front of a car, either when the motorcycle is ridden into the car or the car drives into the motorcycle. This was also the conclusion of Stcherbatcheff et al. (8) and Bourret et al. (9). The injury depended on the part of the car contacted. The bumper produced tibia and fibula fractures (easy to repair) but if contact was made with the larger less smooth parts of the vehicle, i.e. radiator grill, several fractures of the leg occurred. These fractures were associated with serious injuries to the soft tissue, the most serious being where muscle tissue is torn away from the bone, referred to as stripping. A study by Meyrueis et al. (10) also highlights oblique impacts as the most frequent cause of lower limb injuries with the rider often sustaining open fractures of the knee-cap and femur.

Hight et al. (11) looked at 126 injured motorcyclists from California and reported that their accidents could be divided into three groups: a. Non-ejected (remained with motorcycle); b. Ejected (thrown off during impact); c. Deflected (direction of motorcycle and rider changed on impact, i.e. glancing blow). The percentages of riders with moderate to serious leg injuries in each of these groups were a. 83%, b. 72% and c. 93%. The nature of the leg injuries was:

Group a. Mainly knee and femur injuries from direct impact through the patella.

Group b. Produced general injuries to the legs from impact with the car's bonnet and the ground. Generally much less severe than those seen in a. or c.

Group c. Serious leg injuries were sustained when the riders struck with a glancing blow the vehicle or object that they were trying to avoid. Crushing and retarding forces were transmitted to, and through, the leg. Typical injuries seen were multiple fractures of the femur, tibia and fibular and traumatic amputation.

Direct impact force in oblique collisions caused 73 percent of the lower-limb and pelvic fractures in a study by Ramet et al. (12) whilst 27 percent were caused by force transmitted through the knee. Of the total, 68 percent of lower-limb and associated pelvic fractures were to the upper leg (including the knee) and pelvis. Bear et al. (13) have reported on pelvic injuries associated with traumatic distension of the leg, 33% were fatal, and all occurred when the rider's knee impacted the front corner of an oncoming vehicle. Mackay (14) found that there are two general mecha-

nisms of leg injury, direct impact with the other vehicle and crushing between the machinery and the other vehicle. Hurt et al. (15) state that in angled collisions the rider's ankle, foot and lower leg become trapped in contact between the automobile rear corner and the engine transmission side. Pedar and Newman (16) have shown that all major leg injuries resulted from impact with the striking vehicle while the rider is still on the machine, and Nyquist et al. (17) emphasises the phenomenon of rider near-side lower leg injury as a result of the pinching action experienced when the cycle "slaps" against the car. A comprehensive analysis of the type of impact associated with leg injuries and head injuries is that of Larder (18) who concludes that fatal accidents (from mainly head injuries) occur in "head on" impacts and the victims do not generally have leg injuries.

The conclusion is that leg injuries occur mainly in glancing impacts to the side, front and rear of cars where the legs are likely to make direct contact with the opposing vehicle.

### Speed and angle analysis

The most detailed estimates of accident impact speeds are given by Whitaker (19) and although they are stated to be very approximate they agree with implications for speed summarised in (20). The mean speeds for a motorcycle to car collision are 24 mile/h (39 km/h) for the motorcycle and 14 mile/h (23 km/h) for the car. Over 60 percent of motorcycle casualties occurred in the speed band 0–10 mile/h (0–16 km/h) for the car and 50 percent for the speed band 20–30 mile/h (32–48 km/h) for the motorcycle. Also in 75 percent of all the accidents the motorcycle was travelling at less than 30 mile/h (48 km/h) and in 93 percent less than 40 mile/h (64 km/h). The mean accident speed for conventional motorcycles was given as 27 mile/h (43 km/h) and for step throughs and mopeds as 19 mile/h (31 km/h).

Fuller and Snider report (21) that "the most prevalent speed of motorcycle was in the range 25–35 mile/h. Speeds of the adverse vehicle ranged from 10–45 mile/h with the most often speed at the low end of that range". These speeds are slightly higher than those given by Whitaker but a more detailed analysis by Hurt et al. (15) found that the median speed was 21.5 mile/h for all cases, and that 78% of accidents occurred at a motorcycle speed of 30 mile/h or less. He also found that 78% of injuries (all severities) and 85% of injuries AIS 1–3 occurred in the range 0–30 mile/h. (Almost all leg injuries are classified AIS 1–3).

Otte et al. (7) and Whitaker (19) conclude that over 80% of collisions occur within  $\pm 30^\circ$  from the front of the motorcycle, Harms (22) states that 72% occur within  $\pm 15^\circ$ . This information indicates where the impact to the motorcycle occurs but does not give the angle of collision between the machine and target. Fuller and Snider (21) state in their analysis of femur injuries that the angle of collision between the two vehicles is usually less than  $30^\circ$ . Hight et al. (23) indicate that the majority of leg injuries occur when the angle of collision is between  $15^\circ$  and  $25^\circ$ . These analyses of angles are in complete agreement with the other studies which relate leg injuries to "glancing" blows. Finally, in

the most recent and comprehensive analysis of leg injury mechanisms, Harms (22) (available at this conference) has shown that 92% of casualties sustained their leg injuries whilst still with the machine, and thus are likely to benefit from a properly designed leg protector.

### Vehicles Equipment and Tests

The system for launching the motorcycle into a moving car has been described previously (5). The type of car used in the majority of the tests was either a Vauxhall Cavalier 1.6 (Mk II) or a Ford Sierra 2.0, the same model being used in each pair of tests. These cars were chosen because they are the most popular medium sized saloon cars in the UK. The type of motorcycle used was a Norton Interpol II which was tested in three forms, unfaired, fitted with the standard fairing and fitted with an ESM3 (24) type fairing incorporating leg protection to the UK draft specification (6). The leg protection consists of a glass-fibre outerskin, an energy absorber which absorbs the energy of the impact between the motorcycle and the target vehicle, an energy absorber positioned ahead of the knee and designed to react against the knee such that the axial force generated does not exceed the knee-femur-hip tolerance, and a strong rigid element designed to hold the energy absorbing regions in position and attach the system to the motorcycle. Details of the specification relating to the leg protector components can be obtained from the paper describing ESM 4 (25), available at this Conference. Also described in this paper are the component test procedures and results of tests of some typical components.

The impact configurations chosen for the tests (see figure 1) are based on many accident studies, including those outlined above and are designed to be typical of impacts in which leg and head injuries are prominent. Thirty degrees to the front and side, and offset-front are typical leg injury impacts. Ninety degrees into the side of a car is a typical fatal head injury impact. Sixty degrees into the side, (near the front) is an intermediate type of impact designed to expand the information on the performance of leg protection across the entire range of accident configurations. Included in the series of  $90^\circ$  tests is one using the ESM3 safety system complete with an air-bag in conjunction with the leg protector, though for this test the impact car was a Morris Marina.

The dummy is the OPAT as used in all TRRL motorcycle testing and with the exception of the  $90^\circ$  tests the injury indicating aluminum honeycomb leg developed at TRRL and previously described in reference (1) was used. In the  $90^\circ$  tests the standard leg incorporating a femur load cell was used to be consistent with previous work on air bag testing. The dummy was fitted with triaxial accelerometers in the head, chest and pelvis, and the upper legs which were specially developed at TRRL were fitted with strain gauges to measure torsion and axial forces. Accelerometers were fitted to the motorcycle engine, approximately at the centre of gravity, to indicate fore-aft and lateral acceleration. An

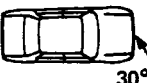
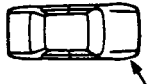
Impact configurations	Car		Motorcycle condition	Vel. MS-1
	Type	Vel MS-1		
30° front 	Ford Sierra	6.7	Faired	13.4
	Sierra	6.7	U.K. LP	13.4
30° side 	Sierra	6.7	Faired	13.4
	Sierra	6.7	U.K. LP	13.4
0° offset front 	Cavalier	0	Unfaired	13.4
	Cavalier	0	Faired	13.4
	Cavalier	0	U.K. LP	13.4
60° front corner 	Vauxhall Cavalier	6.7	Faired	13.4
	Cavalier	6.7	U.K. LP	13.4
90° side 	Cavalier	0	Unfaired	13.4
	Morris Marina	0	Faired	13.4
	Cavalier	0	U.K. LP	13.4
	Marina	0	U.K. LP & Air bag	13.4

Figure 1. Impact configurations.

impact event was used to trigger a flash to correlate the impact point with the instrumentation and film analysis. The analogue output from the instrumentation was filtered with an anti-aliasing filter and then digitally recorded. Digital filters were used in accordance with SAE J211b.

## Results

### Instrument predicted injuries in impacts 0-60°

**Leg injuries.**—The leg injuries are assessed using the aluminum honeycomb to indicate the energy impacted into the upper and lower legs and strain gauges to indicate the torsion and axial load sustained by the upper leg. For clarity the legs are considered as “included” and “non included” where the included leg is the one on the side of the machine facing the target on impact, i.e. the one most likely to be injured. For the 0° and 30° (glancing) impacts only the measurements for the “included” leg are given as the non included leg suffered little damage. However for the 60° impacts, measurements for both legs are given because the motorcycle rotated away from the target and so both legs were likely to be injured.

Figure 2 shows the energy impacted with the upper and lower leg for each test and figure 3 shows the upper leg strain gauge measurements. The results show that for the

glancing impacts the energy impacted into the included lower leg was always significantly lower in the tests where leg protection was fitted. The 0° offset front tests show that in this respect a faired machine is also beneficial for the lower leg. The upper leg results show again that leg protection significantly reduces the energy impacted into the upper leg, from above human tolerance levels to well below them in two instances. The results from the 60° tests show that the energy impacted with both lower legs is fairly low and the values are almost identical with and without protection (20, 21J respectively for the included leg and 16, 15J respectively) for the non included leg. The results for the upper leg are more complex, and are considered in conjunction with the strain gauge measurements.

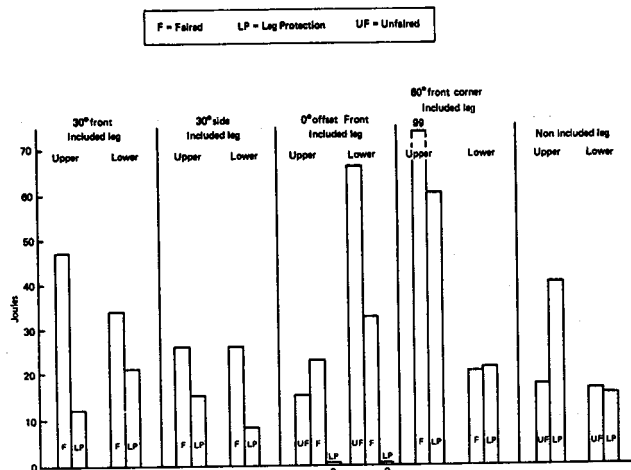


Figure 2. Energy absorbed by aluminium honeycomb legs.

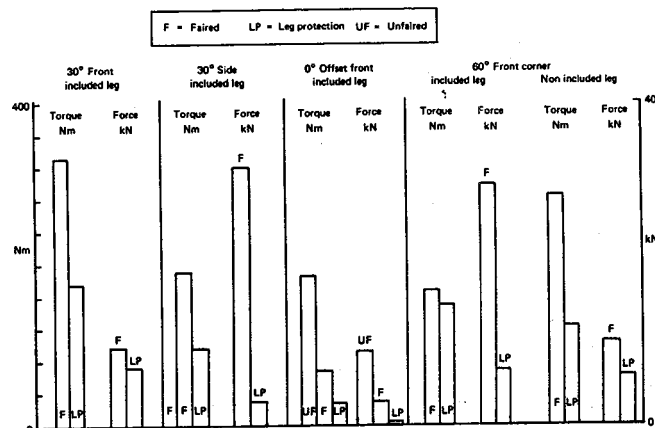


Figure 3. Femur torque and axial forces, 0°-60° impacts.

Of the different types of femur fracture torsion is considered to be the most harmful and in this respect the leg protector is shown to have significant benefits in all the tests (0-60°) see figure 2. High axial loads affect not only the femur but also the knee and pelvis and again the protector is beneficial in all tests. This was most noticeable in the 30° and 60° side impacts where the energy absorbing material of the knee protection element was most crushed.

The results are given for both legs for the 60° tests. They show that for the included upper leg there was a significant

reduction in impact energy with the leg protector fitted but for the non included leg there was an increase. However the motorcycle rotated more when the leg protector was fitted, so the impact to the leg is more to the side of than axial to the femur. This is verified by the very high torsional and axial loads sustained by both legs in the test with a standard machine. Consequently in this configuration also, as well as in all the other configurations tested, the protector offers a worthwhile reduction in injury risk.

To clarify the potential for injury and to provide a concise map of the performance of leg protection, the measurements were compared with current human tolerance criteria and the results presented in figure 4. The criterion for femur torsion is 192 Nm, for axial loading it is 10 kN and 8 kN must not be exceeded for more than 10 ms (6). The values for energy are taken from (26, 27) and are based on a mean of 54J for the tibia and 43J for the femur. The criteria (4 per leg) were exceeded or equalled in 12 out of 24 instances (50%) without leg protection and in only 2 out of 20 instances (10%) with leg protection. In the instances where the criterion was exceeded with a leg protector it was also exceeded in the test with the standard machine and by a greater amount. Thus at no time did the leg protector worsen the potential for leg injury. It is worth noting that in one instance with the standard machine the measured value was 3 times, and in two instances it was more than twice the criterion.

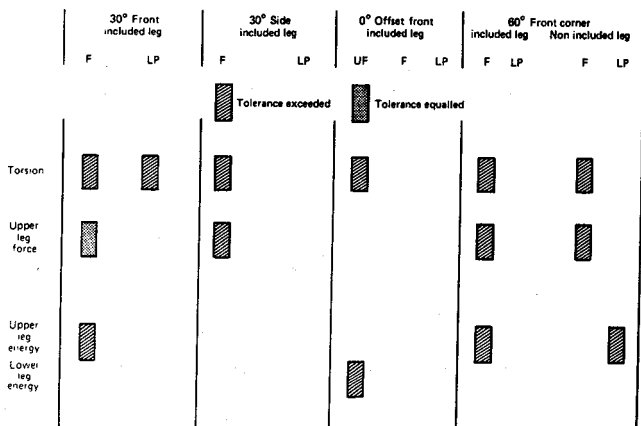


Figure 4. Instances where the human tolerance for the leg was exceeded, 0°-60° impacts.

**Head, chest and pelvis injuries.**—The results for the head chest and pelvis are shown as peak accelerations in figure 5.

The most significant differences and the most significant benefits that leg protection afforded the rider occurred in the 30° side and 0° offset front impacts. In both cases the head was prevented from hitting the vehicle whereas with the standard machines the peak accelerations from the head impact were over 90g. The benefits to the pelvis were also significant. In particular the dummy on the unfaired machine in the 0° offset front impact suffered extensive splaying of the right leg, synonymous with traumatic distension of the pelvis. This type of injury was reported (13) to have been fatal in 33% of the cases studied. *In the 30°*

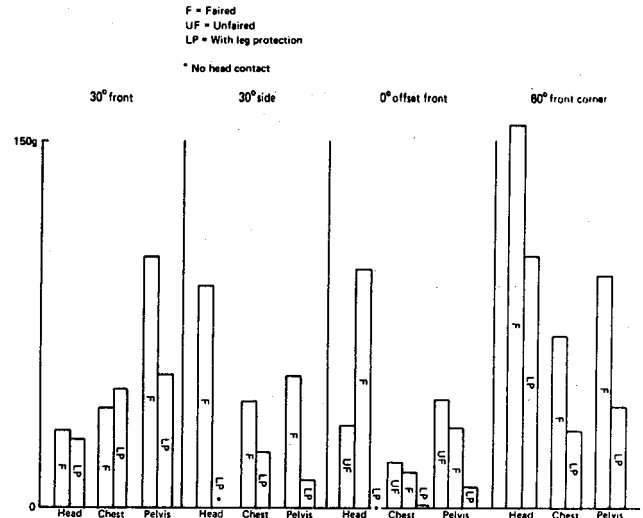


Figure 5. Head chest and pelvis, peak resultant accelerations (0°-60° impacts).

*front impact there was a slight increase in the peak chest acceleration with leg protector fitted (41-49g), however this difference is too small to be significant.*

Overall the highest levels recorded for all three body regions were in the 60° front corner impacts and the standard machine was significantly worse than the one with leg protection. In particular the head peak acceleration of 157g was by far the highest recorded. This result is consistent with accident studies where the majority of fatal head injuries are from "head on" impacts between machine and target.

Across the spectrum of tests leg protectors have not increased the injury risk significantly to any part of the body.

### Instrument predicted injuries on impacts—90°

This group of 4 impacts was designed to research the behaviour of a dummy rider in the type of impact associated with fatal head injuries rather than leg injuries. However it is vital, as stated earlier, to ensure that leg protection does not worsen the potential for head injuries, and that it works well in conjunction with frontal restraint devices designed to reduce the severity of head injuries. Thus the four machines used were unfaired, faired, with UK leg protection, and with a complete safety system incorporating a 120 litre air-bag with the UK leg protection.

To be consistent with other tests conducted at TRRL to research the potential for air-bags, the standard dummy legs were used, and so the only leg measurements recorded were axial femur loads. Figure 6 shows the resultant head chest and pelvic accelerations and the femur forces. The most significant results are those for the head where largest acceleration recorded was with the unfaired machine 133g, the faired machine was 128g and the UKLP was 123g. However with the air-bag the acceleration was only 33g, a significant reduction. These results demonstrate that leg protection

does not increase the potential for head injury. Also that an air-bag would significantly further reduce the likelihood.

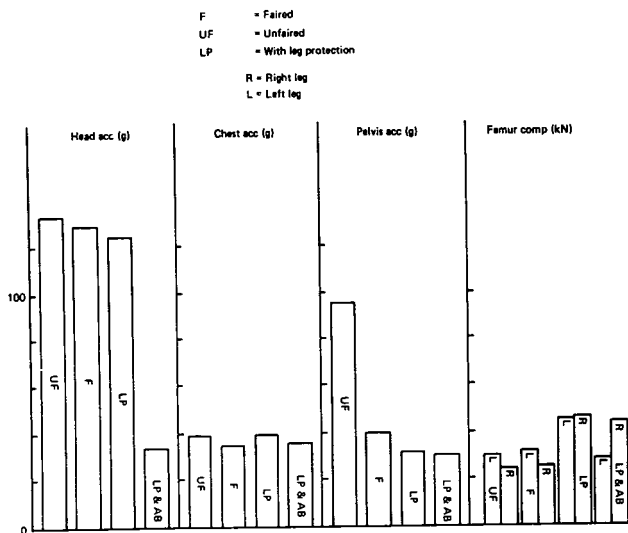


Figure 6. Head, chest and pelvis, peak resultant accelerations and femur peak axial force for 90° side impacts.

The leg and chest results are all well below the levels at which serious injury is likely to occur. This is also true for the pelvis with one notable exception, that of the unfaired machine. The high pelvis acceleration recorded, (95g), was caused by interaction between the legs and the handlebars, and it seems that there is some benefit from a standard fairing in this type of impact. The leg protectors actually increased femur compression slightly in this configuration because the knees impacted directly onto the energy absorbing pads. The forces are however well below tolerance, and it is precisely this interaction which slows the rider somewhat and so reduces head acceleration.

### Rider trajectory and velocity analysis

The rider trajectory analysis is an important complement to the instrumentation analysis and provides information on the potential for injury implied by the trajectory and velocity of a rider after the first contact of an accident. Velocities can be measured at any time during an impact but to have any relevance to the potential for injury the direction and position relative to the target must be known. For this purpose an axis system using the car as a reference is defined in figure 7. The car is regarded as the region of vulnerability and for motion of the rider to be considered to be potentially injurious it must have entered or have the potential to enter the vulnerable region. In describing the motion, the x axis lies longitudinally along the car, the y axis is vertical, and the z axis is at right angles to the x and y axes. In presenting analysis of this type there are several factors to be considered. On impact the rider will generally have a component of velocity in the x and z directions, therefore the results in the x and z direction are compared with the impact velocity and expressed as a percentage change. Absolute values are given for velocity in the y direction as it is assumed that there is no vertical motion until after the impact. Analysis is

restricted to the motion of the head as this is the most vulnerable part of the body, and given for each test are the maximum velocities and those 20ms before impact of the head with the target. If the head does not hit, only the maximum is given. It is considered that up to head-impact the rider's trajectory will be influenced by the presence or otherwise of leg protection, but after head-impact it will depend on the target and so analysis after head-impact is not considered analytically.

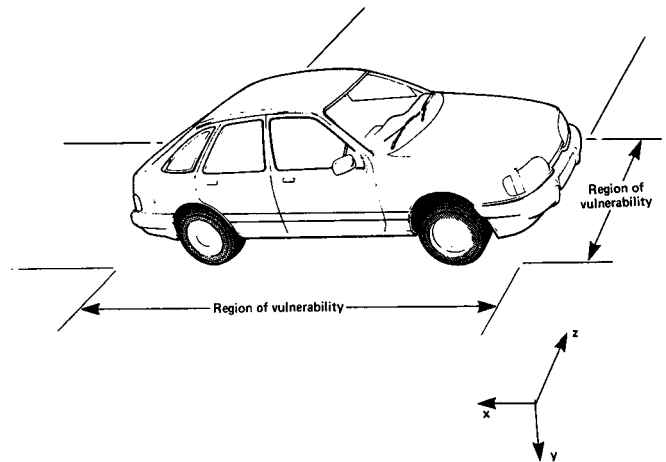


Figure 7. Displacement and velocity axis reference.

Figures 8–12 are diagrams showing the trajectory of the rider in each set of tests. Figure 13 shows the velocities in the x, y and z direction relevant to each impact configuration.

30° front (figure 8).—The trajectory of the rider in each test was similar, in both there was rotation about the hips and the rider's head hit the bonnet. For the rider of the standard machine there was a greater percentage increase in the hori-

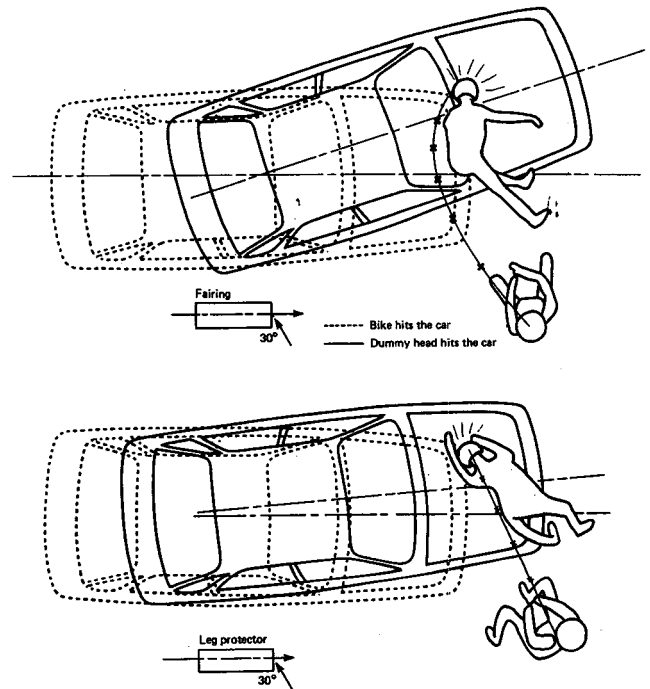


Figure 8. Rider/car motion for 30° front impacts.

zontal velocity ( $x$ ) indicating a greater potential to reach the "hard" parts of the car, i.e., the windscreen surround. Figure 8a shows that this is indeed what happened and the films show that the rider somersaulted across the screen with the potential for the back to be struck by the windscreen surround. The rider of the machine with leg protection slid across the bonnet well away from the screen. The vertical velocity ( $y$ ) was greater for the rider of the machine with leg protection but it is worth noting that this agrees with the philosophy of pedestrian protection, i.e., to throw the victim onto the bonnet which is soft and one of the least injurious parts of a car.

*30° side (figure 9).*—The fairing of the standard machine broke on impact and the rider's knee hit the car causing the head to be thrown violently downwards into the side of the car, whereas with leg protection the head did not hit the car. The difference in motion is reflected in the results, particularly for the vertical velocity, 6.3 m/s (std machine) is compared with 1.8 m/s (leg protector). In the  $z$  direction the peak velocity was similar for both vehicles and in the  $x$  direction there was a relevant velocity only for the standard machine because with leg protection the rider's head did not reach the region of vulnerability.

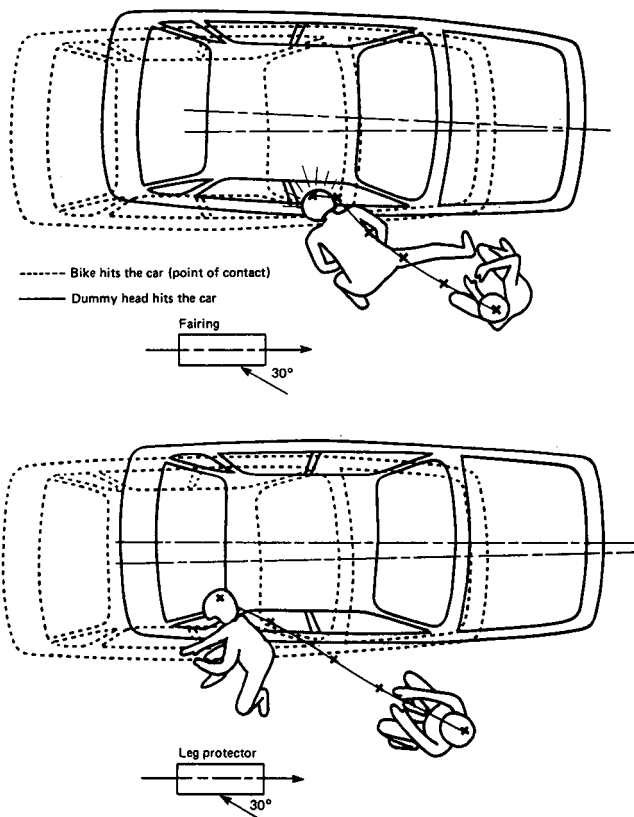


Figure 9. Rider/car motion for 30° side impacts.

*Offset front 0° (figure 10).*—Three types of machine were used in this configuration: unfaired, faired and with leg protection. The trajectory of the motorcycle and rider was very different for each test. The machine with leg protection glanced off the car with very little movement of the rider

toward the car. The rider of the unfaired machine impacted the car headlamp with a knee and consequently the leg was splayed and thrown into the air [known to cause distension of the pelvis], while the head was thrown downwards but not violently. The faired machine interacted violently with the car and the rider was thrown forwards onto the bonnet and windscreen. The vertical head velocities were 5.4 m/s for the faired machine, 3.7 m/s for the unfaired machine and 0 m/s for the machine with leg protection. The velocity change in the  $x$  direction was relevant only for the faired machine and was -51% just before head impact.

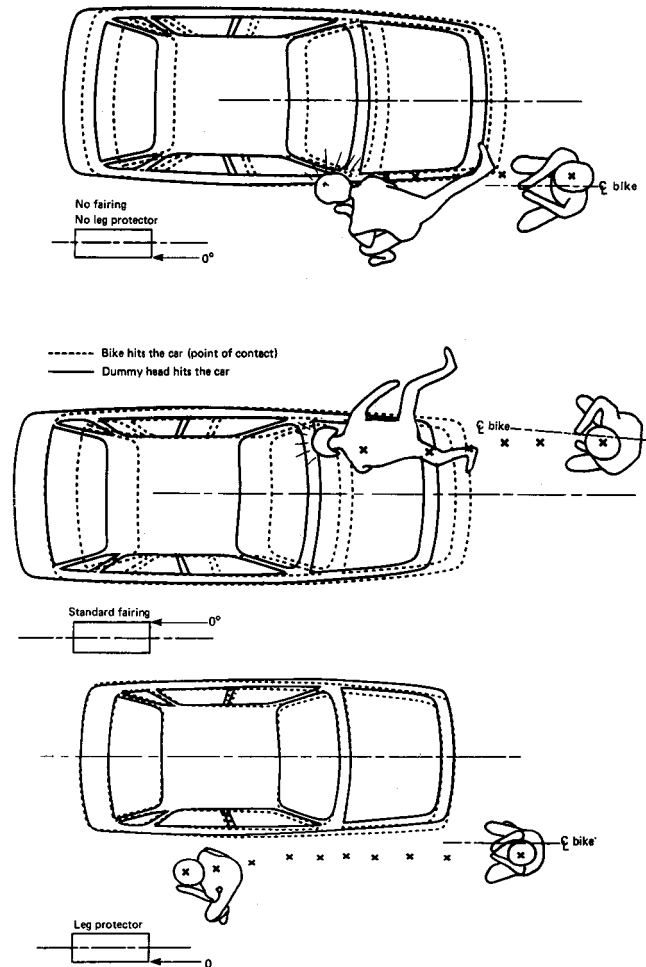


Figure 10. Rider/car motion for 0° offset front impacts.

*60° Front Corner (figure 11).*—With the standard machine the rider was thrown into the windscreen head-first and then over the roof of the car where a leg penetrated the rear screen. The rider of the machine with leg protection was not violently ejected and fell on the ground to the side of the car and away from the machine. The head struck the car's wing mirror. It was not possible to analyse the head vertical velocity for the machine with leg protection as the trajectory caused it to be hidden from view during the critical part of the impact. The peak value for the unfaired machine was 6.4 m/s. Similar difficulties occurred in the  $x$  and  $z$  direction. Because of this inability to track the head on film, the

velocity analysis is inconclusive, but it is nevertheless quite clear that the rider of the machine fitted with leg protection has greatly benefitted by not being thrown into the car windscreen and surround.

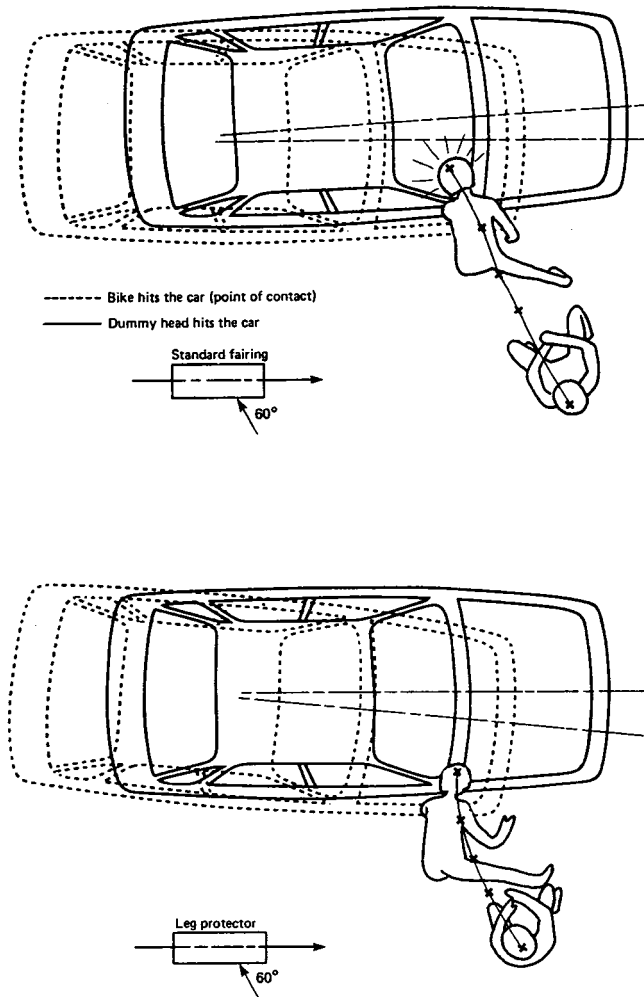


Figure 11. Rider/car motion for 60° front corner impacts.

90° side (figure 12).—The analysis and velocity comparisons in this configuration are less complex than previously as the motion is largely 2 dimensional consisting mainly of z (horizontal) and y (vertical) components. The horizontal velocity is the most significant as this indicates the potential for hitting the car, which happened in all of the tests except the one with the air bag, and it was invariably the head which first contacted the vehicle. A peak velocity change of +23% (relative to the impact velocity) was seen in the test with the unfaired machine, but the change 20 ms before impact was only -2%. The lack of a fairing allowed the rider to move rapidly forward relative to the machine, until the pelvis impacted the tank and induced rotation followed by the legs impacting the handlebars, the head then hit the roof just beyond the cant rail. In the test with the leg protector the % change in velocity just before impact was -11% and with the standard fairing it was 0%. Thus without an air bag the potential for injury was least with a leg protector and greatest with the unmodified machine.

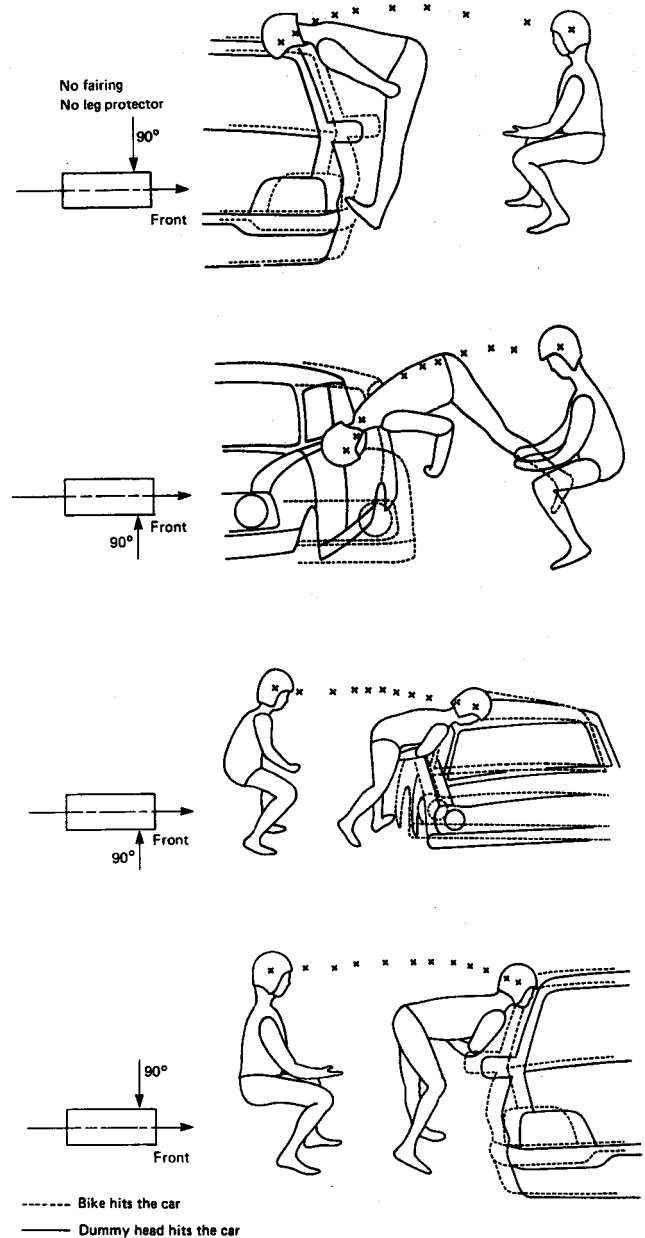
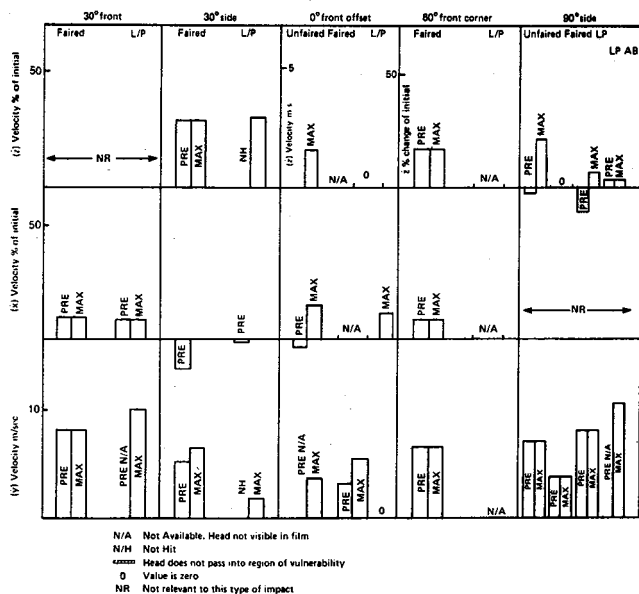


Figure 12. Rider/car motion for 90° side impacts.

Vertical head velocity in the context of these tests is likely to be potentially injurious only if the rider can strike the car or other hard object during the vertical motion. This was demonstrated during the test with the air bag where the highest peak velocity was measured (10.6 m/s), but the lowest head acceleration was recorded because the head motion was directed toward the air bag. In the test with the leg protector the rotation occurred earlier in the impact resulting in more of a glancing blow to the car rather than direct impact with the roof and cant-rail as with the unfaired machine. The peak vertical velocities were 8.0 m/s with the leg protector and 7.0 m/s with the unfaired machine. The rider of the faired machine rotated less rapidly (peak 3.8 m/s), the head impacted the car roof and the chest impacted the cant rail.



**Figure 13. Head velocity analysis, y m/s, x, z percent change of initial.**

### Motorcycle motion

Table 1 gives the motorcycle frame fore-aft (F/A) and lateral peak (L) acceleration for each test where appropriate. Also given is the average angular velocity (R) over the first 100 ms for the motorcycle in plan view.

**Table 1. Rotation and frame accelerations.**

Impact Type	Unfaired	Faired	UK Leg.Pro	UK L/P & Air Bag
30° FRONT F/A L R		34 22 +5.4	28 33 +4.4	g g rad/sec
30° SIDE F/A L R		28 13 +1.9	17 16 +6.1	g g rad/sec
0° OFFSET F/A L R	12 14 +1.3	18 10 -3	1 4 + .7	g g rad/sec
60° F/CORNER F/A L R		39 25 -3.1	95 15 -4.4	g g rad/sec
90° SIDE F/A	25	35	29	67 g

F/A = FORE AND AFT ACCELERATION  
L = LATERAL ACCELERATION  
R = ROTATION + TOWARD THE TARGET

In the 30° front and side impacts the machine with leg protection sustained a greater lateral and a lower fore-aft acceleration than the standard faired machine.

In the offset-front tests both accelerations tended to be lower with leg protection, particularly the fore-aft, because in this configuration the leg protector substantially reduces the motorcycle to car interaction. The results for the 60° impacts are anomalous with a high fore-aft acceleration recorded for the machine with (95g) leg protection compared with 39g for the standard machine. This difference

arose because the machine with leg protection hit the car front wheel initially whereas the standard machine impacted the much softer wheel arch. Even so, as the dummy results show, the presence of the leg protector provided a net reduction in injury risk.

The notable result in the 90° impacts is the high fore-aft acceleration sustained by the machine with an air bag. The interaction between the rider and machine through the air bag increases the overall effective mass. This causes greater intrusion and to the point where the car stiffness greatly increases. The other results are not directly comparable because of the different cars used.

The angular velocity exhibits no obvious trend except that in the 30° and 60° impacts the values are more consistent (4.4, 6.1, 4.4 rad/s) for the machine with leg protection than for the standard machine (5.4, 1.9, 3.1 rad/s).

### Conclusions

(1) Accident studies show that leg injuries and head injuries to motorcyclists do not occur in the same accident configurations. Head injuries occur in impacts "head-on" to the motorcycle and leg injuries occur in glancing impacts ie at angles of up to 30° between the longitudinal axis of the motorcycle and the target face.

(2) Accident studies show that the majority (92%, in one study) of leg injuries occur while the rider is with the machine. Two types of injury dominate (a) "trapped and crushed" where the motorcycle has swung toward the target and the leg is trapped between the target and the machine (b) "Direct Impact" where the rider's leg (often a knee) impacts directly on part of the target vehicle.

(3) More than 75% of motorcycle impacts occur at a speed of 30 mile/h or less for the motorcycle, and over 60% occur at a speed of 10 mile/h or less for the car.

(4) In the impacts at 0° (offset front), 30° to the front, 30° to the side and 60° to the side front wing, significant reductions in the potential leg injuries were measured with the motorcycle fitted with leg protection designed to the UK specification when compared with the standard faired motorcycle. When assessed against human tolerance criteria for torque, axial load and energy for the femur, and energy for the tibia, the criteria were exceeded or equalled in 12 out of 24 instances with the standard machine and in only 2 out of 20 instances when leg protection was fitted. There were no instances where the potential for leg injury was made worse with leg protection fitted.

(5) In all the impacts potential head injury was assessed from the peak resultant acceleration measured. There were no instances where the peak was greater with leg protection than for the standard machine. In the 60° impacts the peak was significantly less with leg protection, and in the 30° side and 0° offset front impacts head contact was eliminated. In the 90° impacts the peak acceleration was significantly reduced when an air-bag was fitted to a machine with leg protection. With leg protection only, there was little difference compared with the faired machine.

(6) Both the observed and measured trajectories of the rider were significantly different with and without leg protection, and in each case the differences were to the potential benefit of the rider's legs and head. In particular with the 0° and 30° side impacts the dummy rider remained seated: in the 0° grazing incidence configuration the rider may well remain in control of the machine.

(7) Leg protection has been shown to reduce significantly the potential for leg injury and in some cases head injury in glancing impacts and not to increase the risk of head injury in "head-on" impacts.

## References

- (1) Chinn, B.P., M.A. Macaulay, "Leg Protection for Motorcycles." International I.R.C.O.B.I. Conference on the Biomechanics of Impacts, 1984. P265.
- (2) Chinn, B.P., "Injuries to Motorcyclists Legs: Testing Procedures and Protection." PhD Thesis, Brunel University, Uxbridge, 1985.
- (3) Chinn, B.P., Hopes, P. and M.A. Macaulay, "Leg Protection for Riders of Motorcycles." Tenth International Technical Conference on Experimental Safety Vehicles 1985.
- (4) Chinn, B.P., M.A. Macaulay, "Leg Protection for Motorcyclists." International I.R.C.O.B.I. Conference on the Biomechanics of Impacts. 1986.
- (5) Chinn, B.P., "Protecting Motorcyclists Legs." Eleventh International Technical Conference on Experimental Safety Vehicles, Washington 1987.
- (6) Draft Specification: "Leg Protection for Riders of Motorcycles." Vehicle Standards and Engineering Division, Dept. of Transport, 2 Marsham Street, London SW1P 3EB UK.
- (7) Otte, D., P. Kalbe and E.G. Suren. Typical injuries to the soft body parts and fractures of the motorised two-wheelers. Proceedings of the meeting on the Biomechanics of Impacts. IRCOBI 1981 p. 148-165.
- (8) Stcherbatcheff, G., P. Duclos, C. Tarriere, C. Got and A. Patel. Kinematics of a pedestrian and a two-wheeler impacted by the front of a car. Proceedings of the meeting on Biomechanics of Injury to Pedestrians, Cyclists and Motorcyclists. 1976-09, p 311-21. IRCOBI.
- (9) Bourret, P., P. Sejourne, P. Orsoni and C. Cavallen. Lower limb injuries of two-wheeler riders. Proceedings of the VIth Int. IRCOBI conference on biomechanics of impacts. 1981-09 p. 206-18.
- (10) Meyrueis, J.P, D. Morin, B. le Saint and J. Vialla. Injuries to the lower limbs among motorcyclists. Arm med acid. traffic 1980-09 n25 p. 15-8. Paris, France. (In French, translation available).
- (11) Hight, P.V., A.W. Siegel and A.M. Nahum. Injury Mechanisms and Motorcycle Design. Proceedings of the meeting on Biomechanics of Injury to Pedestrians, Cyclists and Motorcyclists. 1976-09. p65-80.
- (12) Ramet, M., D. Cesari, A. Dedoyaw. Two Wheeler Accidents. Proceedings of the meeting on the Biomechanics of Impacts IRCOBI 1981. p 193-205.
- (13) Beard, J.D., C.M. Davidson, D.J.A. Scott, and A.G. Turner. "Pelvic Injuries Associated with Traumatic Abduction of the Leg." Injury: The British Journal of Accident Surgery (1988) vol 19/no5.
- (14) Mackay, M. "Lower Limb Injuries to Riders of Motorcycles." S.A.E. Symposium on the Biomechanics of Leg Injuries. Detroit 1985.
- (15) Hurt, H.H., Jr., J.V. Quellet, D.R. Thom. Motorcycle Accident Cause Factors and Identification of Countermeasures Vol I: Technical Report. Cont No. D.O.T HS-5-01160 U.S. Dept. of Transportation N.N.T.S.A.
- (16) Pedar, J.B., J.A. Newman. After Helmets—Is There Anything Else? Biokinetics and Associates, Canada. I.R.C.O.B.I. Sept 87 Birmingham, UK.
- (17) Nyquist, G.W., C.M. Savage, and D.L. Fletcher. Dynamics and Biomechanics of Motorcycle-to-Car Glancing Impact: Theory and Experiment 29th Proceedings American Association for Automotive Medicine Washington, DC Oct 85.
- (18) Larder, D. Analysis of Serious Two-Wheeled Motor Vehicle Accidents. Department of Transport, UK (Unpublished contract report 1984).
- (19) Whitaker, J. A survey of motorcycle accidents. T.R.R.L. Laboratory Report LR 913. 1980. UK.
- (20) Accidents Impliquent des Motocyclettes:
  - a. Revue Bibliographique. November 1983 Cahiers D'E'tudes, ONSER 2 Avenue du General-Malleret—Joinirlle 94114 Arcueil Cedex.
- (21) Fuller, P.M., J.N. Snider. Injury Mechanisms in Motorcycle Accidents. I.R.C.O.B.I. Sept 87 Birmingham UK.
- (22) Harms, P.L. Leg Injuries and Mechanisms in Motorcycling Accidents. Twelfth International Conference on Experimental Safety Vehicles, Gothenburg May 89.
- (23) Hight, P.V., P.E. Newhall, K. Landwieder, G.M. Mackay. An international review of motorcycle crash-worthiness I.R.C.O.B.I. Zurich Sept 86.
- (24) Watson, P.M.F., ESM3. A motorcycle demonstrating progress for safety. Eleventh International Technical Conference on Experimental Safety Vehicles. Washington, May 1987.
- (25) Watson, P.M.F., ESM 4—A Lightweight Safety Motorcycle. Twelfth International Technical Conference on Experimental Safety Vehicles. Gothenburg May 89.
- (26) Yamada, H. Strength of Biological Materials. The Williams and Wilkins Company, 428E Preston Street, Baltimore, Maryland 21202, USA. 1970.
- (27) Mather, B.S. Observations on the Effects of Static and Impact Loading on the Human Femur. Journal of Biomechanics Vol. 1 (1968) p.331-335.

Crown Copyright. The views expressed in this paper are not necessarily those of the Department of Transport. Extracts from the text may be reproduced, except for commercial purposes, provided the source is acknowledged.

## Acknowledgements

The work described in this paper forms part of the programme of the Transport and Road Research Laboratory and the paper is published by permission of the Director.

## Motorcycle Accident Impact Conditions as a Basis for Motorcycle Crash Tests

**Jocelyn B. Pedder,**  
Biokinetics and Associates Ltd., Ottawa  
**Hugh H. Hurt,**  
University of Southern California  
**Dietmar Otte,**  
Medizinische Hochschule, Hannover

### Abstract

This paper describes the preliminary results of an analysis of motorcycle accident data bases to identify the frequency and severity of different types of motorcycle/car collisions. Data from three primary accident studies conducted in the United States of America and Europe were utilized.

From this analysis specific accident impact conditions, of known frequency and severity can be selected as one possible basis for motorcycle crash tests.

### Evaluation of Accident Data

The identification of the true nature of motorcycle accidents and associated trauma depends on accident studies. Established records provide only limited information. Detailed field accident investigations facilitate a better understanding of the crash sequence and the source of the riders' injuries. Among other things, such accident data is seen as the key to isolating the problem areas and to identifying ways to reduce riders' injuries.

The effectiveness of potential protective systems can be determined through testing. Full-scale motorcycle/car crash testing could provide valuable insight into injury mechanisms (if the requirements for biofidelity in the crash dummy are met).

The overall consequences of equipment design changes can best be determined if the crash tests are based on "real life" accidents. Field accident data can be used to guide the selection of those crash accident test configurations (speeds, angles, impact points, etc.), which are representative of real accidents.

This paper describes one method of analyzing motorcycle accident data bases for this purpose.

### The Accident Data Bases

A summary of the three accident data bases used in this analysis is presented in table 1.

Table 1. Summary of data bases.

	TRAFFIC SAFETY CENTER CALIFORNIA, USA	ACCIDENT RESEARCH UNIT BIRMINGHAM, UK		MEDIZINISCHE HOCHSCHULE HANNOVER, FRG
Study Area	City of Los Angeles	Urban and Rural		Urban and Rural
Study Period	1976-1977	1977-1979	1981-1982	1973 ongoing
Sample Size (Accident)	900	197	96	534
Selection Criteria	all severities random selection	fatal random selection	serious random selection	all severities random selection
Investigation Technique	In-depth 617 on scene 283 follow-up	In-depth follow-up	In-depth follow-up	In-depth on-scene

The accident investigation procedures utilized in each study were essentially the same. The accidents were investigated at the scene or within 24 hours by multi-disciplinary and skilled accident investigation teams. Comprehensive data was collected on each accident. Injury data were extracted and interpreted by medical personnel. Each accident was reconstructed.

An extensive analysis of the original data from the California study is presented in the final contract reports (1, 2)\*. Since the completion of this work, some of the data has been re-evaluated to examine the effect of leg protective devices (3, 4). The "re-evaluated" data was used in the present analysis. The initial findings of the Birmingham and Hannover studies have been published elsewhere (5-10). The raw data files which formed the basis of these publications were utilised for the present paper.

### Comparison of accident data bases

The selection criteria for the accidents included in the original California and Hannover data bases were essentially the same, viz., a representative sample of all injury producing motorcycle accidents. In the Birmingham studies, data was collected on two distinct injury severities; fatally and seriously injured riders.

The motorcycle accident samples reflect two notable regional differences; helmet legislation and motorcycle type. In comparison to California, helmet wearing is mandatory in Birmingham and Hannover. The Hannover legislation was introduced in stages from 1976 to become mandatory for all motorcycle riders in 1985. Differences in the distribution of motorcycle types in Europe and California are reflected in the accident data. In Europe

\* Numbers in parentheses designate references at end of paper.

mopeds or mopeds and smaller motorcycles are popular. In California larger motorcycles predominate.

## Selection of motorcycle/car collision sub-samples

Accident cases considered relevant to the present analysis were those in which the opposing vehicle was a passenger car; the motorcycle driver was seated in normal riding position and there were no passengers. A breakdown of the cases selected is given in table 2.

**Table 2. Selection of motorcycle v. passenger car collision sub-samples.**

	California Study	Hannover Study	Birmingham	
			Fatal	Serious
Total Sample (accidents)	900	534	197	96
Multiple Vehicle	663	433	108	61
Passenger Car	588	321	66	48
M/C Driver Seated	528	250	50	41
M/C Driver Alone	439	228	35	35

As the Birmingham data base includes two accident samples preselected on the basis of injury severity, it is considered separately from the California and Hannover data in the following analysis.

## Analysis of California and Hannover data bases

The California and Hannover data were categorized using five primary impact variables; motorcycle and car impact locations, relative impact angle, motorcycle and car impact speeds. A comparison of the data collected on these selected variables and the injury data and some of the limitations of this data pertinent to the present analysis are considered below.

### Vehicle impacts locations

The point of impact on both the motorcycle and car was recorded for every accident in each of the 3 data bases. In this preliminary analysis the California contact data was grouped into 7 contacts, the Hannover into 3 contact locations.

### Relative impact angle

In the Hannover data base, the relative positions of the vehicles at impact were described by a single collision configuration code. The estimated angle of impact was also independently coded.

In the California data file, the angle of impact variable is coded as an acute angle between impacting surfaces which does not account for relative vehicle orientations. In the present analysis, to enable comparisons with the other data bases, a new angle variable which ranged from 0–360 degrees was defined. This new impact angle is based on the originally coded impact angle and the relative pre-crash bearings of the impacting vehicles. The relative bearing of

each vehicle, as seen from the other vehicle, is coded using a 12 hour clock.

### Impact speeds

The California and Hannover data includes crash speeds of involved vehicles. Accident reconstruction, vehicle damage, post-crash trajectories, skid and scuff marks were used to determine these speeds.

Speed estimates from witnesses or involved drivers and passengers may be unreliable. Speed calculations based on accident reconstruction data can be effected by many variables for example, elevation of back of motorcycle on impact, tumbling of rider, varying surface friction, collapse characteristics of different wheel types, etc. As such, the impact speed data were used prudently as fair estimates rather than exact values.

### Injury data

Injury data in each of the data bases are coded using the Abbreviated Injury Scale, AIS (12,13). Additional injury details including the precise location, nature and source of the injuries are recorded in each data base in a different manner. Overall this data is, however, reasonably comparable. The present analysis utilized maximum AIS values determined for each casualty.

## Variable groupings used in analysis

Within each variable, the data were classified as follows:

*Motorcycle contact.*—3 contacts; front, side and rear.

*Car contact.*—California data base:

7 contacts; front, front corner, side front, side middle, side rear, rear, rear corner.

Hannover data base:

3 contacts; front, side, rear.

*Impact angle.*—5 codes; using increments of 45 degrees and defined as the angle between the center lines of the vehicles as illustrated in Figure 1.

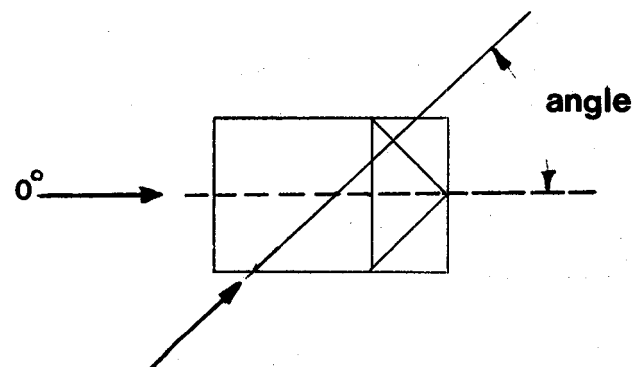


**Figure 1. Relative impact angle.**

Comparable impact angles on opposite sides of the car were matched to give the following five groups:

1. 338-22
2. 23-67, 293-337
3. 68-112, 248-292
4. 113-157, 203-247
5. 158-202

*Impact speeds.*—The motorcycle and car impact speeds were grouped as follows:

**Car impact speed**

- 0-9 mph
- 10-19
- 20-29
- 30-39
- 40 and over

**Motorcycle impact speed**

- 0-19 mph
- 20-39
- 40 and over

**Rationale for selected variables groupings**

The groupings were selected to reflect the accuracy and resolution of field accident data collection. At the same time, the largest possible increments were used without including “dissimilar” accidents to minimize the total number of possible configurations and maintain a meaningful number of cases in each cell.

The basis for partitioning the data in the given groups is as follows:

*Impact locations*

Impacts along the front or along the rear of a car typically involve similar structures. So the two categories, front and rear were considered sufficient for impacts at these locations. In contrast, impacts with the corner or side of a car involve structures of varying stiffness and profile. To isolate the different rider trajectories and injury patterns, impacts to the side of the car structures were divided into front, middle, and rear; and corner impacts were classified separately.

*Impact angle*

The 45 degree increment was selected to reflect the accuracy of the field data and repeatability of crash test work. In recognition of the tendency of accident investigators to describe angles to the nearest 45 degrees, i.e. 0°, 45°, 90° etc., the groupings were selected to avoid splitting such clusters.

*Impact speeds*

Car speeds can be relatively precisely estimated from skid marks, post-crash trajectories, and vehicle damage. The determination of motorcycle impact speeds in real accidents is more difficult. The accuracy of motorcycle speed estimates largely reflects the precision of the accident reconstruction. The broader motorcycle speed groupings were adopted to account for the varying levels of accuracy.

**Costing methods**

The cost estimates derived from the concept of “harm” by Malliaris (11) was utilized in the present analysis. Maximum AIS values were used in the calculation of the “harm” costs.

Notwithstanding the limitations of the costing method used by Malliaris, the present analysis utilizes his 1981 cost values. These are presented in table 3.

**Table 3. Estimated costs as a function of injury severity.**

<b>Injury Severity (AIS)</b>	<b>Average Cost<sup>1</sup> (with or without survival)</b>
1	0.7
2	3.9
3	10.2
4	107.1
5	264.5
6	307.8

<sup>1</sup>In thousands of 1981 US dollars

It should be noted that cost values used in the following analysis serve as a comparative tool and the meaningfulness of the individual figures per se is arguable.

**Catalogue of collision configurations**

The California and Hannover accidents were categorised using the 5 impact variable groupings into one of the possible 1575 combinations. Only 199 of these combinations were present in the California sub-sample, and 107 in the Hannover sub-sample. These configurations were subsequently listed with their respective frequency and costs utilising “harm” values. These lists are presented in Appendices A and B respectively. Cases with unknown values on the selected variables were excluded from these lists. The potential application of these catalogues in the selection of crash test parameters is considered later.

**The Birmingham data bases**

The relatively small number of cases of seriously injured riders in the Birmingham sample which met the selection criteria (N=35) disallowed extensive analysis of this data base at this time.

Of greater immediate interest to the present analysis is the data from the Birmingham study of fatalities. The injury characteristics of the sample of fatally injured riders is one of severity and multiplicity. The extremely violent nature of the fatal motorcycle/car collisions is reflected in the patterns of injuries presented in table 4.

**Selection of parameters for crash tests**

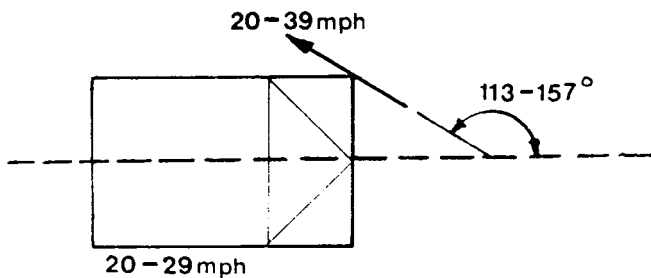
This paper has provided a rationally organized set of data that could be used in determining some of the parameters in

**Table 4. Patterns of injuries for Birmingham fatalities.**

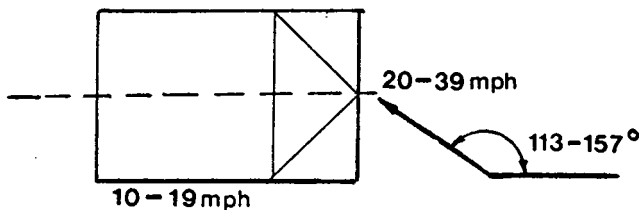
	% with AIS	
	>=3	>=5
Head	67.7%	58.8%
Neck	26.5	11.8
Chest	67.7	29.4
Abdomen	44.1	41.2
Arms	20.6	0
Legs	41.2	0

motorcycle crash tests. The tables in the appendix are, however, not definitive. Different configurations may be appropriate for different reasons.

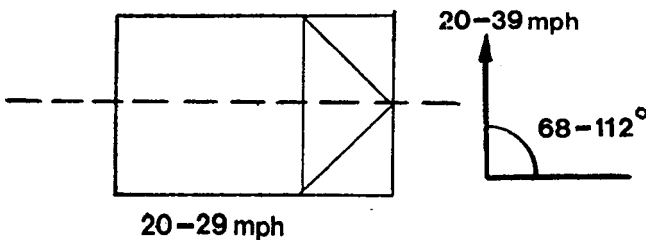
For example, the appended lists would indicate that out of all the California accident configurations, the single most expensive configuration is:



However, this configuration type or "bin" involves only two accidents. The next most expensive configuration may be more appropriate in that it includes thirteen cases:



Neither of these collision configurations are the same as the most "expensive" Hannover collision category:



The costs of accidents as presented here may have been skewed by fatalities which may be beyond the limits of foreseeable protective systems.

The appended list must be augmented by other considerations, such as the nature and severity of injuries to different body regions before it can be used effectively to select crash test configurations to evaluate specific protective systems.

What this preliminary analysis has provided is something of a "universe" of motorcycle collision configurations. Some configurations just do not occur. It also serves to initiate the process whereby real accident data can contribute to future crash test planning.

## Summary and Conclusions

The present analysis has used existing accident data to identify specific impact configurations of known frequency and costs.

This information is one element to be considered in the development of full-scale motorcycle/car crash tests. In addition, consideration should be given to:

- The specific injuries addressed by a particular protective system.
- The characteristics of that system.
- Effects of vehicle size differences.
- Performance in single vehicle crashes, etc.

Finally, all accident data are estimates. Crash speeds, impact angles, etc., associated with any data base must be interpreted accordingly.

## References

- (1) Hurt, H.H. Jr., Ouellet, J.V. and Thom., D.R. Final Report, Motorcycle Accident Cause Factors and Identification of Countermeasures, Volume 1: Technical Report, Contract No. DOT HS-5-01160, U.S. Department of Transportation, National Highway Traffic Safety Administration, Washington, D.C., January 1981.
- (2) Hurt, H.H., Jr., Ouellet, J.V., and Thom., D.R. Final Report, Motorcycle Accidents Cause Factors and Identification of Countermeasures, Volume II: Appendix/ Supplemental Date, U.S. Department of Transportation, National Highway Traffic Safety Administration, Washington D.C., January 1981.
- (3) Hurt, H.H. Jr., Ouellet, J.V., and Jennings, G. "Motorcycle Crash Bar Effective: A Re-Evaluation Using AIS-80". Twenty-Eight Annual Proceedings, American Association for Automotive Medicine, Denver, Colorado, October 8-10, 1984.
- (4) Ouellet, J.V., Hurt, H.H. Jr., and Thom, D.R. "Collision Performance of Contemporary Crash Bars and Motorcycle Rider Leg Injuries". SAE Paper No. 87063, Accident Reconstruction: Automobiles, Tractor-Semi Trailers, Motorcycles and Pedestrians, P-193, Society of Automotive Engineers, Warrendale, Pennsylvania, February 1987.

(5) Pedder, J.B., Hagues, S.B., and MacKay, G.M. "A Study of 93 Fatal Two-Wheeled Motor Vehicle Accidents". Proceedings of the Fourth International Conference on the Biomechanics of Trauma, Goteborg, Sweden, September, 1979.

(6) Pedder, J.B., Hagues, S.B., and MacKay, G.M. "Head Protection for Road Users with Particular Reference to Helmets for Motorcyclists". AGARD Conference, Cologne, April, 1982.

(7) Pedder, J.B. and Newman, J.A. "After Helmets—Is There Anything Else?" Proceedings of 1987 International Conference on the Biomechanics of Impacts, Birmingham, United Kingdom, September, 1987.

(8) Otte, D. "A Review of Different Kinematic Forms in Two-Wheeled Accidents—Their Influence on Effectiveness of Protective Measures". SAE Paper No. 801314, 24th Stapp Car Crash Conference, Detroit, October, 1980.

(9) Otte, D., Kalbe, P. and Suren, E.G. "Typical Injuries to the Soft Body Parts and Fractures of the Motorized Two-Wheelers". Sixth International IRCOBI Conference on the Biomechanics of Impacts, Salon de Provence, France, September, 1981.

(10) Otte, D., Appel, H. and Suren, E.G. "Recommendations for Improvement of the Injury Situation for the Users of Two-Wheel Vehicles". International IRCOBI Conference on the Biomechanics of Impacts, Zurich, Switzerland, September, 1986.

(11) Malliaris, A.C., Hitchcock, R., and Hedlund, J. "A Search for Priorities in Crash Protection", SAE Paper 820242, Crash Protection SP-513, International Congress and Exposition, Detroit, Michigan, February, 1982.

(12) The Abbreviated Injury Scale (AIS), 1976 Revision, American Association for Automotive Medicine, Morton Grove, Illinois, 1976.

(13) The Abbreviated Injury Scale (AIS), 1980 Revision, American Association for Automotive Medicine, Morton Grove, Illinois, 1980.

## Information Note on Appendices

Bins are sorted according to their classification categories in the following order:

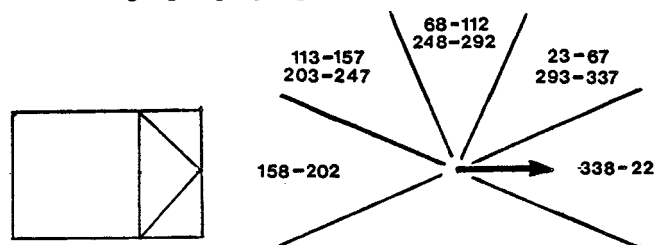
1. Car impact location
2. Motorcycle impact location
3. Relative heading angle (0–360°)
4. Car speed (mph)
5. Motorcycle speed (mph)

### Impact location definition

Car FO = front  
 FC = front corner  
 SF = side front  
 SM = side-middle  
 SR = side rear

M/C F = front  
 S = side  
 R = rear

Angles are expressed in terms of the 5 group classification system as illustrated below. For convenience only the first angle grouping is presented in the catalogues.



% represents percentage of total sub-sample population contained in a bin.

**Harm** is expressed in thousands of 1981 U.S. dollars and is based on maximum AIS value.

**Ave Harm** is Harm/N

% **Total Cost** is percentage of total sub-sample population harm.

**Appendix A: Catalogue of California  
Data—Motorcycle/Car Collision Subsample (N = 423)**

Bin #	Car Contact	M/C Contact	Angle	Car Speed	M/C Speed	N	% Total	Maximum AIS						Ave Harm	Harm	% Total Cost	
								1	2	3	4	5	6				
1	FO	F	68-112	10-19	0-19	1	0.2		1						3.9	3.9	0.1
2	FO	F	113-157	0-9	0-19	3	0.7	3							0.7	2.1	0.0
3	FO	F	113-157	0-9	40+	1	0.2			1					10.2	10.2	0.1
4	FO	F	113-157	10-19	20-39	2	0.5	2							0.7	1.4	0.0
5	FO	F	113-157	20-29	20-39	1	0.2						1		307.8	307.8	3.7
6	FO	F	158-202	0-9	0-19	2	0.5	2							0.7	1.4	0.0
7	FO	F	158-202	0-9	20-39	1	0.2	1							0.7	0.7	0.0
8	FO	F	158-202	0-9	40+	1	0.2			1					10.2	10.2	0.1
9	FO	S	338-22	0-9	0-19	1	0.2	1							0.7	0.7	0.0
10	FO	S	338-22	40+	20-39	1	0.2		1						3.9	3.9	0.1
11	FO	S	23-67	0-9	0-19	1	0.2	1							0.7	0.7	0.0
12	FO	S	68-112	0-9	0-19	2	0.5	1	1						2.3	4.6	0.1
13	FO	S	68-112	0-9	20-39	3	0.7	1		2					7.0	21.1	0.3
14	FO	S	68-112	10-19	0-19	3	0.7	3							0.7	2.1	0.0
15	FO	S	68-112	10-19	20-39	3	0.7	2					1		103.1	309.2	3.7
16	FO	S	68-112	20-29	0-19	3	0.7	2		1					3.9	11.6	0.1
17	FO	S	68-112	30-39	20-39	1	0.2			1					10.2	10.2	0.1
18	FO	S	113-157	0-9	0-19	2	0.5	2							0.7	1.4	0.0
19	FO	S	113-157	0-9	20-39	3	0.7	2	1						1.8	5.3	0.1
20	FO	S	113-157	10-19	0-19	6	1.5	4		2					3.9	23.2	0.3
21	FO	S	113-157	10-19	20-39	13	3.2	6		6			1		25.4	329.9	4.0
22	FO	S	113-157	20-29	0-19	2	0.5		1				1		134.2	268.4	3.2
23	FO	S	113-157	20-29	20-39	2	0.5			2					10.2	20.4	0.2
24	FO	S	113-157	40+	0-19	1	0.2				1				107.1	107.1	1.3
25	FO	S	158-202	0-9	0-19	2	0.5	1		1					5.4	10.9	0.1
26	FO	S	158-202	10-19	0-19	3	0.7	3							0.7	2.1	0.0
27	FO	S	158-202	10-19	20-39	2	0.5			2					10.2	20.4	0.2
28	FO	S	158-202	20-29	0-19	1	0.2	1							0.7	0.7	0.0
29	FO	S	158-202	20-29	20-39	1	0.2	1							0.7	0.7	0.0
30	FO	S	158-202	20-29	40+	1	0.2			1					10.2	10.2	0.1
31	FO	R	338-22	0-9	0-19	2	0.5	2							0.7	1.4	0.0
32	FO	R	338-22	10-19	0-19	6	1.5	6							0.7	4.2	0.1
33	FO	R	338-22	20-29	0-19	3	0.7	1	1	1					4.9	14.8	0.2
34	FO	R	338-22	30-39	0-19	1	0.2	1							0.7	0.7	0.0
35	FO	R	338-22	40+	20-39	4	1	1	2				1		79.1	316.3	3.8
36	FO	R	338-22	40+	40+	2	0.5	1		1					5.4	10.9	0.1
37	FC	F	68-112	10-19	20-39	2	0.5	2							0.7	1.4	0.0
38	FC	F	113-157	0-9	20-39	1	0.2	1							0.7	0.7	0.0
39	FC	F	113-157	10-19	0-19	1	0.2	1							0.7	0.7	0.0
40	FC	F	113-157	10-19	20-39	2	0.5		1	1					7.0	14.1	0.2
41	FC	F	158-202	0-9	0-19	1	0.2	1							0.7	0.7	0.0
42	FC	S	338-22	0-9	0-19	1	0.2	1							0.7	0.7	0.0
43	FC	S	338-22	10-19	0-19	1	0.2	1							0.7	0.7	0.0
44	FC	S	338-22	10-19	20-39	1	0.2						1		264.5	264.5	3.2
45	FC	S	338-22	30-39	20-39	1	0.2		1						3.9	3.9	0.1
46	FC	S	338-22	30-39	40+	1	0.2			1					10.2	10.2	0.1
47	FC	S	338-22	40+	20-39	1	0.2	1							0.7	0.7	0.0
48	FC	S	338-22	40+	40+	1	0.2			1					3.9	3.9	0.1
49	FC	S	23-67	0-9	0-19	1	0.2	1							0.7	0.7	0.0
50	FC	S	23-67	0-9	20-39	5	1.2	2	1	2					5.1	25.7	0.3
51	FC	S	23-67	10-19	0-19	2	0.5	1		1					5.4	10.9	0.1
52	FC	S	23-67	10-19	20-39	3	0.7	1		2					7.0	21.1	0.3
53	FC	S	23-67	20-29	0-19	1	0.2			1					3.9	3.9	0.1
54	FC	S	23-67	20-29	20-39	2	0.5	1	1						2.3	4.6	0.1
55	FC	S	68-112	0-9	0-19	2	0.5	2							0.7	1.4	0.0
56	FC	S	68-112	0-9	20-39	2	0.5	1	1						2.3	4.6	0.1

## Appendix A: Catalogue of California Data—Motorcycle/Car Collision Subsample (N = 423)

Bin #	Car Contact	M/C Contact	Angle	Car Speed	M/C Speed	N	% Total	Maximum AIS						Ave Harm	Harm	% Total Cost	
								1	2	3	4	5	6				
57	FC	S	68-112	10-19	0-19	2	0.5		2						3.9	7.8	0.1
58	FC	S	68-112	10-19	20-39	6	1.5	2	1	3					6.0	35.9	0.4
59	FC	S	68-112	20-29	0-19	3	0.7	1	2						2.8	8.5	0.1
60	FC	S	68-112	20-29	20-39	1	0.2		1						3.9	3.9	0.1
61	FC	S	68-112	30-39	20-39	1	0.2			1					10.2	10.2	0.1
62	FC	S	68-112	40+	0-19	1	0.2			1					10.2	10.2	0.1
63	FC	S	68-112	40+	20-39	1	0.2							1	307.8	307.8	3.7
64	FC	S	113-157	0-9	0-19	2	0.5		2						3.9	7.8	0.1
65	FC	S	113-157	0-9	20-39	7	1.7	2	2	2			1		42.0	294.1	3.5
66	FC	S	113-157	10-19	0-19	2	0.5	1		1					5.4	10.9	0.1
67	FC	S	113-157	10-19	20-39	6	1.5	2	3	1					3.9	23.3	0.3
68	FC	S	113-157	20-29	20-39	2	0.5						1	1	286.1	572.3	6.9
69	FC	S	113-157	30-39	0-19	1	0.2	1							0.7	0.7	0.0
70	FC	S	158-202	0-9	20-39	3	0.7		1	2					8.1	24.3	0.3
71	FC	S	158-202	10-19	20-39	3	0.7		1	2					8.1	24.3	0.3
72	FC	S	158-202	40+	20-39	1	0.2			1					10.2	10.2	0.1
73	SF	F	23-67	0-9	20-39	2	0.5	1			1				53.9	107.8	1.3
74	SF	F	68-112	0-9	0-19	5	1.2	4	1						1.3	6.7	0.1
75	SF	F	68-112	0-9	20-39	3	0.7		3						3.9	11.7	0.1
76	SF	F	68-112	0-9	40+	1	0.2		1						3.9	3.9	0.1
77	SF	F	68-112	10-19	0-19	1	0.2	1							0.7	0.7	0.0
78	SF	F	68-112	10-19	20-39	11	2.7	6	3	1			1		26.4	290.6	3.5
79	SF	F	68-112	10-19	40+	2	0.5			1	1				58.6	117.3	1.4
80	SF	F	68-112	30-39	40+	1	0.2						1		264.5	264.5	3.2
81	SF	F	113-157	0-9	20-39	1	0.2	1							0.7	0.7	0.0
82	SF	F	113-157	10-19	0-19	2	0.5	2							0.7	1.4	0.0
83	SF	F	113-157	10-19	20-39	7	1.7	3	2	1	1				18.2	127.2	1.5
84	SF	S	338-22	0-9	20-39	1	0.2	1							0.7	0.7	0.0
85	SF	S	338-22	10-19	0-19	1	0.2	1							0.7	0.7	0.0
86	SF	S	338-22	10-19	40+	1	0.2						1		264.5	264.5	3.2
87	SF	S	338-22	20-29	20-39	3	0.7	1	2						2.8	8.5	0.1
88	SF	S	338-22	20-29	40+	1	0.2			1					10.2	10.2	0.1
89	SF	S	338-22	40+	0-19	1	0.2			1					10.2	10.2	0.1
90	SF	S	23-67	0-9	0-19	1	0.2	1							0.7	0.7	0.0
91	SF	S	23-67	0-9	20-39	5	1.2	3	1				1		54.1	270.5	3.3
92	SF	S	23-67	10-19	20-39	2	0.5	2							0.7	1.4	0.0
93	SF	S	23-67	20-29	0-19	1	0.2			1					10.2	10.2	0.1
94	SF	S	23-67	20-29	40+	1	0.2							1	307.8	307.8	3.7
95	SF	S	68-112	0-9	0-19	1	0.2	1							0.7	0.7	0.0
96	SF	S	113-157	0-9	0-19	1	0.2	1							0.7	0.7	0.0
97	SF	S	113-157	10-19	0-19	1	0.2	1							0.7	0.7	0.0
98	SM	F	23-67	20-29	0-19	1	0.2	1							0.7	0.7	0.0
99	SM	F	68-112	0-9	0-19	1	0.2	1							0.7	0.7	0.0
100	SM	F	68-112	0-9	20-39	4	1	2		2					5.4	21.8	0.3
101	SM	F	68-112	10-19	0-19	2	0.5	1	1						2.3	4.6	0.1
102	SM	F	68-112	10-19	20-39	8	2	3	2	1	2				29.3	234.3	2.8
103	SM	F	68-112	20-29	0-19	2	0.5	2							0.7	1.4	0.0
104	SM	F	68-112	20-29	20-39	1	0.2	1							0.7	0.7	0.0
105	SM	F	68-112	20-29	40+	1	0.2						1		264.5	264.5	3.2
106	SM	F	68-112	30-39	20-39	3	0.7		1	1	1				40.4	121.2	1.5
107	SM	F	68-112	40+	0-19	1	0.2		1						3.9	3.9	0.1
108	SM	F	113-157	0-9	0-19	1	0.2		1						3.9	3.9	0.1
109	SM	F	113-157	0-9	20-39	1	0.2	1							0.7	0.7	0.0
110	SM	F	113-157	10-19	0-19	1	0.2	1							0.7	0.7	0.0
111	SM	F	113-157	10-19	20-39	5	1.2	1	4						3.3	16.3	0.2
112	SM	F	113-157	20-29	20-39	1	0.2			1					10.2	10.2	0.1

## Appendix A: Catalogue of California Data—Motorcycle/Car Collision Subsample (N = 423)

Bin #	Car Contact	M/C Contact	Angle	Car Speed	M/C Speed	N	% Total	Maximum AIS						Ave Harm	Harm	% Total Cost	
								1	2	3	4	5	6				
113	SM	S	338-22	0-9	0-19	1	0.2	1							0.7	0.7	0.0
114	SM	S	338-22	10-19	20-39	1	0.2	1							0.7	0.7	0.0
115	SM	S	338-22	20-29	0-19	1	0.2	1							0.7	0.7	0.0
116	SM	S	338-22	20-29	20-39	3	0.7	2	1						1.8	5.3	0.1
117	SM	S	23-67	0-9	20-39	4	1		3	1					5.5	21.9	0.3
118	SM	S	23-67	10-19	0-19	2	0.5	2							0.7	1.4	0.0
119	SM	S	23-67	20-29	0-19	1	0.2	1							0.7	0.7	0.0
120	SM	S	23-67	20-29	20-39	1	0.2	1							0.7	0.7	0.0
121	SM	S	23-67	30-39	0-19	1	0.2	1							0.7	0.7	0.0
122	SM	S	68-112	0-9	0-19	1	0.2	1							0.7	0.7	0.0
123	SM	S	68-112	10-19	0-19	1	0.2	1							0.7	0.7	0.0
124	SM	S	68-112	10-19	20-39	2	0.5	1					1		132.6	265.2	3.2
125	SM	S	68-112	20-29	20-39	2	0.5	1	1						2.3	4.6	0.1
126	SM	S	113-157	0-9	0-19	2	0.5	2							0.7	1.4	0.0
127	SM	S	113-157	0-9	20-39	1	0.2			1					10.2	10.2	0.1
128	SM	S	113-157	10-19	0-19	1	0.2		1						3.9	3.9	0.1
129	SM	S	113-157	10-19	20-39	3	0.7			3					10.2	30.6	0.4
130	SM	S	113-157	20-29	0-19	1	0.2	1							0.7	0.7	0.0
131	SM	S	113-157	20-29	20-39	2	0.5			2					10.2	20.4	0.2
132	SM	S	113-157	40+	0-19	1	0.2			1					10.2	10.2	0.1
133	SM	S	158-202	0-9	20-39	1	0.2			1					10.2	10.2	0.1
134	SM	S	158-202	10-19	0-19	1	0.2	1							0.7	0.7	0.0
135	SR	F	23-67	10-19	20-39	1	0.2	1							0.7	0.7	0.0
136	SR	F	68-112	0-9	0-19	1	0.2	1							0.7	0.7	0.0
137	SR	F	68-112	10-19	0-19	4	1	4							0.7	2.8	0.0
138	SR	F	68-112	10-19	20-39	9	2.2	5	1	2		1			32.5	292.3	3.5
139	SR	F	68-112	10-19	40+	2	0.5			1			1		159.0	318.0	3.8
140	SR	F	68-112	20-29	0-19	2	0.5	1	1						2.3	4.6	0.1
141	SR	F	68-112	20-29	20-39	4	1	3				1			66.6	266.6	3.2
142	SR	F	68-112	30-39	0-19	1	0.2	1							0.7	0.7	0.0
143	SR	F	113-157	0-9	20-39	1	0.2	1							0.7	0.7	0.0
144	SR	F	113-157	0-9	40+	1	0.2				1				107.1	107.1	1.3
145	SR	F	113-157	10-19	20-39	4	1	2	1	1					3.9	15.5	0.2
146	SR	F	113-157	10-19	40+	1	0.2	1							0.7	0.7	0.0
147	SR	F	113-157	20-29	0-19	2	0.5	2							0.7	1.4	0.0
148	SR	F	113-157	20-29	20-39	4	1	1		3					7.8	31.3	0.4
149	SR	S	338-22	0-9	20-39	1	0.2	1							0.7	0.7	0.0
150	SR	S	338-22	10-19	0-19	2	0.5	1	1						2.3	4.6	0.1
151	SR	S	338-22	20-29	20-39	1	0.2	1							0.7	0.7	0.0
152	SR	S	338-22	30-39	40+	1	0.2	1							0.7	0.7	0.0
153	SR	S	338-22	40+	40+	2	0.5	2							0.7	1.4	0.0
154	SR	S	23-67	0-9	0-19	1	0.2	1							0.7	0.7	0.0
155	SR	S	23-67	30-39	0-19	1	0.2			1					10.2	10.2	0.1
156	SR	S	23-67	40+	40+	1	0.2					1			264.5	264.5	3.2
157	SR	S	68-112	0-9	0-19	1	0.2		1						3.9	3.9	0.1
158	SR	S	68-112	0-9	20-39	1	0.2			1					10.2	10.2	0.1
159	SR	S	68-112	10-19	0-19	1	0.2	1							0.7	0.7	0.0
160	SR	S	113-157	0-9	0-19	1	0.2	1							0.7	0.7	0.0
161	SR	S	113-157	10-19	0-19	4	1	3	1						1.5	6.0	0.1
162	SR	S	113-157	10-19	20-39	5	1.2	3	1	1					3.2	16.2	0.2
163	SR	S	113-157	20-29	20-39	1	0.2	1							0.7	0.7	0.0
164	SR	S	158-202	10-19	20-39	1	0.2	1							0.7	0.7	0.0
165	RC	F	338-22	0-9	0-19	1	0.2	1							0.7	0.7	0.0
166	RC	F	338-22	0-9	40+	1	0.2			1					10.2	10.2	0.1
167	RC	F	338-22	40+	20-39	1	0.2			1					10.2	10.2	0.1
168	RC	S	338-22	0-9	0-19	1	0.2	1							0.7	0.7	0.0

**Appendix A: Catalogue of California  
Data—Motorcycle/Car Collision Subsample (N = 423)**

Bin #	Car Contact	M/C Contact	Angle	Car Speed	M/C Speed	N	% Total	Maximum AIS						Ave Harm	Harm	% Total Cost	
								1	2	3	4	5	6				
169	RC	S	338-22	0-9	20-39	2	0.5	1	1						2.3	4.6	0.1
170	RC	S	338-22	0-9	40+	1	0.2			1					10.2	10.2	0.1
171	RC	S	338-22	10-19	20-39	2	0.5	1		1					5.4	10.9	0.1
172	RC	S	338-22	10-19	40+	1	0.2		1						3.9	3.9	0.1
173	RC	S	338-22	20-29	0-19	1	0.2	1							0.7	0.7	0.0
174	RC	S	338-22	20-29	20-39	1	0.2	1							0.7	0.7	0.0
175	RC	S	338-22	30-39	20-39	1	0.2	1							0.7	0.7	0.0
176	RC	S	338-22	40+	40+	1	0.2	1							0.7	0.7	0.0
177	RC	S	23-67	0-9	0-19	1	0.2	1							0.7	0.7	0.0
178	RC	S	23-67	0-9	20-39	2	0.5	1		1					5.4	10.9	0.1
179	RC	S	23-67	10-19	20-39	2	0.5	2							0.7	1.4	0.0
180	RC	S	68-112	0-9	0-19	1	0.2	1							0.7	0.7	0.0
181	RC	S	68-112	10-19	0-19	1	0.2		1						3.9	3.9	0.1
182	RC	S	113-157	10-19	40+	1	0.2		1						3.9	3.9	0.1
183	RO	F	338-22	0-9	0-19	6	1.5	5	1						1.2	7.4	0.1
184	RO	F	338-22	0-9	20-39	5	1.2	4	1						1.3	6.7	0.1
185	RO	F	338-22	10-19	0-19	2	0.5	2							0.7	1.4	0.0
186	RO	F	338-22	10-19	20-39	7	1.7	5	1	1					2.5	17.6	0.2
187	RO	F	338-22	20-29	20-39	1	0.2	1							0.7	0.7	0.0
188	RO	F	338-22	20-29	40+	2	0.5	2							0.7	1.4	0.0
189	RO	F	338-22	40+	40+	1	0.2	1							0.7	0.7	0.0
190	RO	F	23-67	0-9	20-39	1	0.2	1							0.7	0.7	0.0
191	RO	F	68-112	0-9	0-19	1	0.2	1							0.7	0.7	0.0
192	RO	S	338-22	0-9	0-19	2	0.5	1					1		154.2	308.5	3.7
193	RO	S	338-22	0-9	20-39	4	1	2		2					5.4	21.8	0.3
194	RO	S	338-22	10-19	0-19	1	0.2		1						3.9	3.9	0.1
195	RO	S	338-22	10-19	20-39	1	0.2		1						3.9	3.9	0.1
196	RO	S	23-67	0-9	0-19	1	0.2	1							0.7	0.7	0.0
197	RO	S	23-67	10-19	20-39	2	0.5			2					10.2	20.4	0.2
198	RO	S	68-112	0-9	0-19	2	0.5	1		1					5.4	10.9	0.1
199	RO	S	68-112	10-19	0-19	1	0.2	1							0.7	0.7	0.0

## Appendix B: Catalogue of Hannover Data—Motorcycle/Car Collision Subsample (N = 211)

Bin #	Car Contact	M/C Contact	Angle	Car Speed	M/C Speed	N	% Total	Maximum AIS						Ave Harm	Harm	% Total Cost	
								1	2	3	4	5	6				
1	FO	F	68-112	10-19	20-39	1	0.5			1					10.2	10.2	0.18
2	FO	F	68-112	20-29	20-39	1	0.5		1						3.9	3.9	0.07
3	FO	F	113-157	0-9	20-39	1	0.5	1							0.7	0.7	0.01
4	FO	F	113-157	10-19	20-39	1	0.5		1						3.9	3.9	0.07
5	FO	F	113-157	10-19	40+	2	0.9				1		1		207.4	414.9	7.46
6	FO	F	113-157	20-29	0-19	1	0.5						1		307.8	307.8	5.53
7	FO	F	113-157	20-29	40+	1	0.5		1						3.9	3.9	0.07
8	FO	F	158-202	0-9	0-19	1	0.5		1						3.9	3.9	0.07
9	FO	F	158-202	0-9	20-39	2	0.9	2							0.7	1.4	0.03
10	FO	F	158-202	0-9	40+	1	0.5			1					10.2	10.2	0.18
11	FO	F	158-202	10-19	40+	1	0.5		1						3.9	3.9	0.07
12	FO	F	158-202	20-29	20-39	3	1.4		2	1					6	18	0.32
13	FO	F	158-202	20-29	40+	1	0.5	1							0.7	0.7	0.01
14	FO	S	338-22	10-19	0-19	1	0.5		1						3.9	3.9	0.07
15	FO	S	338-22	30-39	0-19	1	0.5				1				107.1	107.1	1.93
16	FO	S	338-22	40+	0-19	1	0.5			1					10.2	10.2	0.18
17	FO	S	23-67	10-19	0-19	1	0.5		1						3.9	3.9	0.07
18	FO	S	23-67	10-19	20-39	1	0.5			1					10.2	10.2	0.18
19	FO	S	23-67	20-29	0-19	1	0.5		1						3.9	3.9	0.07
20	FO	S	23-67	30-39	0-19	1	0.5			1					10.2	10.2	0.18
21	FO	S	23-67	40+	0-19	2	0.9			1	1				58.6	117.3	2.11
22	FO	S	23-67	40+	40+	1	0.5			1					10.2	10.2	0.18
23	FO	S	68-112	0-9	0-19	7	3.3	4	2	1					4	20.8	0.37
24	FO	S	68-112	0-9	20-39	6	2.8	2	2	2					4.9	29.6	0.53
25	FO	S	68-112	0-9	40+	1	0.5			1					10.2	10.2	0.18
26	FO	S	68-112	10-19	0-19	12	5.7	4	5	3					4.4	52.9	0.95
27	FO	S	68-112	10-19	20-39	2	0.9		1		1				55.5	111	2
28	FO	S	68-112	20-29	0-19	8	3.8	4	2	2					3.9	31	0.56
29	FO	S	68-112	20-29	20-39	1	0.5		1						3.9	3.9	0.07
30	FO	S	68-112	30-39	0-19	9	4.2	2	2	1	2	2			84.7	762.6	13.71
31	FO	S	68-112	30-39	20-39	1	0.5			1					10.2	10.2	0.18
32	FO	S	68-112	40+	0-19	4	1.9		2	1					81.4	325.8	5.86
33	FO	S	68-112	40+	20-39	1	0.5					1			264.5	264.5	4.75
34	FO	S	113-157	0-9	20-39	5	2.4	2	2				1		63.4	317	5.7
35	FO	S	113-157	10-19	0-19	7	3.3	3		4					6.1	42.9	0.77
36	FO	S	113-157	10-19	20-39	5	2.4	2	1	2					5.1	25.7	0.46
37	FO	S	113-157	20-29	0-19	3	1.4		2	1					6	18	0.32
38	FO	S	113-157	20-29	20-39	2	0.9			2					10.2	20.4	0.37
39	FO	S	113-157	30-39	0-19	2	0.9		1				1		155.8	311.7	5.6
40	FO	S	113-157	40+	0-19	1	0.5		1						3.9	3.9	0.07
41	FO	S	158-202	10-19	0-19	1	0.5	1							0.7	0.7	0.01
42	FO	S	158-202	20-29	40+	1	0.5			1					10.2	10.2	0.18
43	FO	S	158-202	30-39	0-19	4	1.9	1		2		1			71.4	285.6	5.13
44	FO	S	158-202	30-39	20-39	2	0.9		1	1					7	14.1	0.25
45	FO	S	158-202	30-39	40+	1	0.5		1						3.9	3.9	0.07
46	FO	R	338-22	20-29	0-19	2	0.9	1	1						2.3	4.6	0.08
47	FO	R	338-22	40+	0-19	1	0.5						1		307.8	307.8	5.53
48	FO	R	23-67	10-19	0-19	1	0.5		1						3.9	3.9	0.07
49	SM	F	338-22	0-9	0-19	1	0.5	1							0.7	0.7	0.01
50	SM	F	338-22	0-9	20-39	1	0.5		1						3.9	3.9	0.07
51	SM	F	338-22	0-9	40+	1	0.5					1			264.5	264.5	4.75
52	SM	F	23-67	0-9	20-39	3	1.4		2	1					6	18	0.32
53	SM	F	23-67	0-9	40+	2	0.9		1	1					7	14.1	0.25
54	SM	F	23-67	10-19	20-39	2	0.9	2							0.7	1.4	0.03
55	SM	F	68-112	0-9	0-19	6	2.8	3	2	1					3.3	20.1	0.36
56	SM	F	68-112	0-9	20-39	3	1.4		2	1					6	18	0.32

## Appendix B: Catalogue of Hannover Data—Motorcycle/Car Collision Subsample (N = 211)

Bin #	Car Contact	M/C Contact	Angle	Car Speed	M/C Speed	N	% Total	Maximum AIS						Ave Harm	Harm	% Total Cost	
								1	2	3	4	5	6				
57	SM	F	68-112	0-9	40+	1	0.5		1						3.9	3.9	0.07
58	SM	F	68-112	10-19	0-19	2	0.9	2							0.7	1.4	0.03
59	SM	F	68-112	10-19	20-39	2	0.9	1		1					5.4	10.9	0.2
60	SM	F	68-112	10-19	40+	1	0.5			1					10.2	10.2	0.18
61	SM	F	68-112	20-29	0-19	3	1.4				3				10.2	30.6	0.55
62	SM	F	68-112	20-29	40+	1	0.5	1							0.7	0.7	0.01
63	SM	F	68-112	30-39	0-19	1	0.5		1						3.9	3.9	0.07
64	SM	F	68-112	30-39	20-39	1	0.5			1					10.2	10.2	0.18
65	SM	F	113-157	0-9	0-19	1	0.5	1							0.7	0.7	0.01
66	SM	F	113-157	0-9	20-39	2	0.9		1	1					7	14.1	0.25
67	SM	F	113-157	0-9	40+	2	0.9		2						3.9	7.8	0.14
68	SM	F	113-157	10-19	0-19	1	0.5	1							0.7	0.7	0.01
69	SM	F	113-157	10-19	20-39	1	0.5	1							0.7	0.7	0.01
70	SM	F	113-157	10-19	40+	1	0.5				1				107.1	107.1	1.93
71	SM	F	113-157	20-29	0-19	1	0.5				1				10.2	10.2	0.18
72	SM	F	113-157	20-29	40+	1	0.5		1						3.9	3.9	0.07
73	SM	S	338-22	0-9	0-19	1	0.5	1							0.7	0.7	0.01
74	SM	S	338-22	0-9	20-39	3	1.4	2		1					3.9	11.6	0.21
75	SM	S	338-22	10-19	0-19	1	0.5		1						3.9	3.9	0.07
76	SM	S	338-22	20-29	20-39	1	0.5	1							0.7	0.7	0.01
77	SM	S	338-22	30-39	20-39	1	0.5				1				10.2	10.2	0.18
78	SM	S	23-67	0-9	0-19	2	0.9	1		1					5.4	10.9	0.2
79	SM	S	23-67	0-9	20-39	2	0.9	2							0.7	1.4	0.03
80	SM	S	23-67	0-9	40+	1	0.5		1						3.9	3.9	0.07
81	SM	S	23-67	10-19	20-39	8	3.8	7	1						1.1	8.8	0.16
82	SM	S	23-67	10-19	40+	2	0.9		1		1				55.5	111	2
83	SM	S	23-67	30-39	0-19	1	0.5		1						3.9	3.9	0.07
84	SM	S	23-67	40+	0-19	1	0.5	1							0.7	0.7	0.01
85	SM	S	68-112	0-9	0-19	2	0.9	1		1					5.4	10.9	0.2
86	SM	S	68-112	0-9	20-39	1	0.5	1							0.7	0.7	0.01
87	SM	S	68-112	10-19	0-19	1	0.5	1							0.7	0.7	0.01
88	SM	S	68-112	20-29	20-39	1	0.5		1						3.9	3.9	0.07
89	SM	S	68-112	20-29	40+	1	0.5	1							0.7	0.7	0.01
90	SM	S	113-157	0-9	40+	1	0.5			1					10.2	10.2	0.18
91	SM	S	113-157	10-19	20-39	1	0.5		1						3.9	3.9	0.07
92	SM	S	113-157	20-29	0-19	1	0.5		1						3.9	3.9	0.07
93	SM	S	113-157	20-29	40+	1	0.5		1						3.9	3.9	0.07
94	SM	S	158-202	0-9	20-39	1	0.5		1						3.9	3.9	0.07
95	SM	S	158-202	10-19	0-19	2	0.9	1	1						2.3	4.6	0.08
96	SM	S	158-202	10-19	40+	1	0.5					1			307.8	307.8	5.53
97	SM	S	158-202	20-29	20-39	1	0.5		1						3.9	3.9	0.07
98	RO	F	338-22	0-9	0-19	2	0.9	2							0.7	1.4	0.03
99	RO	F	338-22	0-9	20-39	2	0.9		1		1				55.5	111	2
100	RO	F	338-22	0-9	40+	2	0.9		1	1					7	14.1	0.25
101	RO	F	338-22	10-19	20-39	1	0.5		1						3.9	3.9	0.07
102	RO	F	338-22	20-29	40+	2	0.9			1		1			137.3	274.7	4.94
103	RO	F	23-67	10-19	40+	1	0.5			1					10.2	10.2	0.18
104	RO	S	338-22	0-9	0-19	1	0.5		1						3.9	3.9	0.07
105	RO	S	338-22	0-9	20-39	1	0.5	1							0.7	0.7	0.01
106	RO	S	338-22	10-19	20-39	1	0.5		1						3.9	3.9	0.07
107	RO	S	113-157	0-9	20-39	1	0.5	1							0.7	0.7	0.01

### Acknowledgement

This paper was prepared with the assistance of Dynamic Research Inc., California.

# Design of a Motorcyclist Anthropometric Test Device

A. St-Laurent, T. Szabo,  
N. Shewchenko, J.A. Newman,  
Biokinetics and Associates Ltd.  
Ottawa, Canada

## Introduction

Anthropometric Test Devices (ATD's) have a long history of use as surrogates in crash type environments. The environments have included cars, motorcycles, high performance fighter aircraft, etc. Each environment has presented specific challenges to those designing the tests. Car crash testing presents a relatively controlled environment with relatively little dummy motion. Further, the needs of the industry have evolved to require high levels of biofidelity (mostly in terms of impact response), repeatability, and reproducibility. The use of ATD's with high performance aircraft has been for the study of ejection seats where the governing factors are biofidelity (relative to joint range of motion), durability and the need to allow the dummy unimpeded motion within his environment.

The environment of a motorcyclist in a crash situation lies somewhere between the two described above. Injury prediction is of primary importance and biofidelic response of the surrogate to impact is emphasized. Since the motorcycle crash environment is relatively unconstrained and since many individual events occur during the relatively long period of the collision, keeping a surrogate's motion true to that of a human is vital to the assessment of injury potential. This is of particular importance in the later stages of a crash when the structural collapse of a lower extremity component and the presence of a data transmission cable (1) (umbilical cord) may influence body motion.\*

Following an assessment of the merits of contemporary ATD's, the "pedestrian" version of the Hybrid III (2) was selected as the basis for the motorcyclist crash dummy. This ATD has the capacity to monitor for a variety of injuries including those of closed head injury, chest trauma, femur compressive injury, and others. However, it has no capacity to monitor directly for fractures or dislocations of the lower extremities and transducers are connected to a data acquisition system by means of an umbilical cord.

This paper presents the results of an attempt to address these matters through the redesign of the Hybrid III lower extremities and the adaptation of on-board data acquisition. Bones that break, joints that dislocate and the removal of the umbilical cord are considered to be significant improvements to the Hybrid III ATD.

## Leg bone design

### Design Factors

The skeletal elements of interest are the thigh bone (the femur) and the lower leg bones (the tibia and fibula). Structurally, these elements are non-symmetrical and anisotropic. However, for purposes of this preliminary design, the femur and the tibia/fibula were each represented by straight circular tubes.

To achieve a humanlike response to impact, it is necessary to match certain physical characteristics of human bone. The parameters chosen for this study were the following:

- Torsional stiffness up to failure
- Torsional strength
- Bending stiffness up to failure
- Bending strength
- Compressive strength

The measurement of human bone stiffness and strength has been the subject of considerable research (3-5). The results of such studies depend upon the test protocol and may include such variables as loading rate, test site, sex, age, specimen preparation, etc.

Loading rate is especially troublesome when attempting to design an appropriate bone surrogate. Response to impact is a function of the structural characteristics of the component materials, the visco-elastic or strain rate sensitivity of the materials, and of the inertial properties of the body segments in question.

Results of existing studies are thus of limited value in an engineering design context. Such tests do however provide a means to validate an eventual design if it can be shown that the response of the model equates to that of the original specimens. Cadaver tests by Nyquist et al (6) for example, provide such data.

The strain rate sensitivity of femur bone to axial compression (3) is such that a 40% increase in stiffness and yield strength for both tibia and femur over the published quasi-static values seemed appropriate for the dynamic values. The following values were thus selected for the dynamic properties of the surrogate bones.

Table 1. Frangible leg bone design criteria.

	Femur	Tibia
Dynamic Bending Allowable (Nm)	328	294
Dynamic Torsion Allowable (Nm)	192	136
Bending Deflection at Failure (mm)	12	10
Torsional Rotation at Failure (degree)	18	17

### Bone design

The lower extremity "skeleton" of the standard Hybrid III is shown in figure 1.

\*Numbers in parentheses designate references at end of paper.

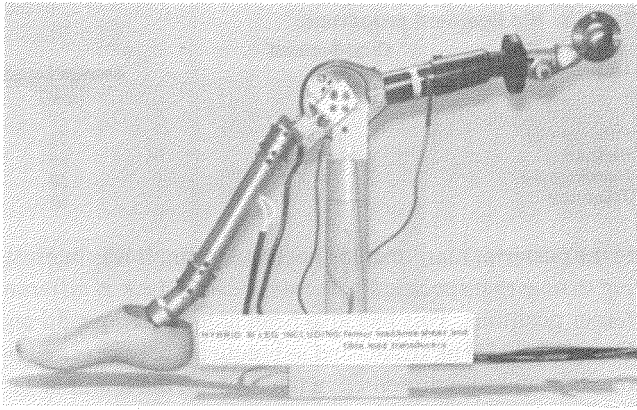


Figure 1. Standard Hybrid III lower leg.

To meet the required strength and stiffness characteristics, and to be compatible with the Hybrid III, necessitated a material which permitted a broad range of structural properties. It was determined that composite fibre materials such as glass, carbon, or polyamides in various resin matrices, provided the necessary flexibility of design. By orienting the fibres appropriately, it was possible to achieve the desired mix of properties.

Sixty example frangible bones, representing about 15 design configurations, were fabricated and tested. Orientation of the fibres were along the longitudinal axis of the bones, at  $\pm 30$  deg and at  $\pm 60$  deg to the long axis of the bones. The bending strength was constant around the circumference and along the length of the bone except for the end reinforcements. A bone fitted to a Hybrid III lower leg is shown in figure 2.

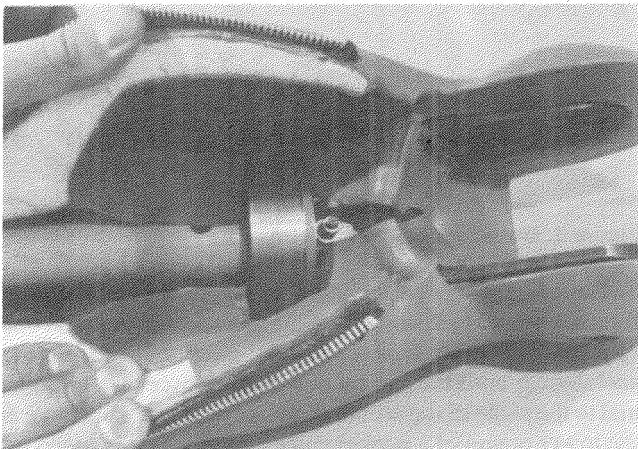


Figure 2. Lower leg bone fitted in calf flesh.

In addition to the static torsion and bending tests used in this design process, dynamic bending tests of the candidate designs were also performed. The dynamic tests were run utilizing a computer controlled hydraulic actuator, with a load cell and displacement feedback loop.

Table 2 below summarizes the percentage differences between the frangible composite bones and the corresponding design values for human bones.

Table 2. Percentage difference between frangible composite bones and human bones.

	Femur	Tibia
Dynamic Bending Allowable	+2	-3
Dynamic Torsion Allowable	+7	+8
Bending Deflection at Failure	+10	+10
Torsion Deflection at Failure	+9	+8

## Hip design

### Dislocation mechanism

The most prominent injuries to the hip are to the ligaments and pelvis bone. They are induced by excessive strains or loads, and may result in hip dislocation. It was the aim of this preliminary study to gain an understanding of the ligament injuries related to hip dislocations and to adapt this to a hip joint for the motorcyclist anthropometric test device.

Field accident data studied by Stewart et al (4), has shown that dislocations may occur in almost any direction in the plane of the acetabular rim. Posterior dislocations have been noted to account for the majority (80%) of the dislocation injuries. Suracci (5) also encountered a large percentage of posterior dislocations. Fractures of the acetabulum socket, acetabular rim and fracture of the head or neck of the femur can also be associated with hip dislocation. In an automotive environment, hip dislocations were often attributed to large axial forces applied to the femur when it is flexed and adducted. The femur is driven towards the posterior portion of the acetabulum where the femoral head is least supported by the acetabulum and the restraining effects of the ligaments are the least. (7). Figure 3 depicts the typical loading conditions.

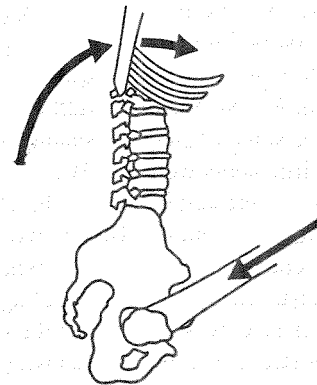


Figure 3. Posterior hip dislocation.

To assess hip dislocation mechanisms, it is necessary to consider the geometry of the hip joint, the restraining forces afforded by the ligaments and muscles, and the physical properties of the bone and ligaments. For this study, muscle involvement and bony fractures were excluded. The relationship between femur angle, ligament involvement and dislocation forces could not be discerned from available biomechanical data. Therefore, the force required to dislo-

cate the hip in the posterior direction and to strain the ligaments to the point of injury was not available.

Quantification of these forces was realized through the construction of a physical replica of the hip joint and capsule. The model, depicted in figure 4, was constructed from plastic replicas and the joint capsule was modelled by placing elastic bands at the lateral and medial portions of the iliofemoral, ischiocapsular, and pubocapsular ligaments. The geometry was confirmed with 50 percentile three dimensional data established by Reynolds et al (8). The model allowed the femur to be oriented relative to the pelvis and the strains and orientations to be measured. The model allowed the elastic ligaments to assume their natural paths thereby accounting for wrapping around the femoral head and neck. The ligament strains and orientations were measured with a three dimensional digitizer.

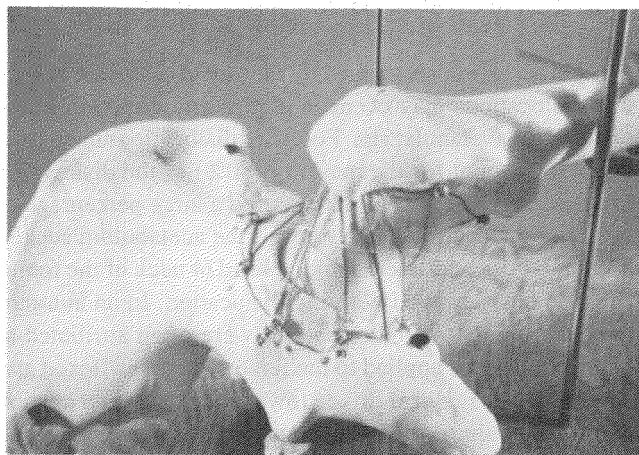


Figure 4. Hip joint model.

To ascertain the total resisting force acting on the hip due to ligament strains, the mechanical properties of the ligaments must first be known. Insufficient physiological and biomechanical data for the hip ligaments necessitated the use and extrapolation of force-strain data from knee ligaments. It was assumed that the mechanical properties of the knee and hip ligaments were similar.

Noyes et al (9) presented data on the elastic modulus of the anterior cruciate ligament. Based on this data, a value of 111 MPa was chosen to represent the dynamic elastic modulus in the elastic region for the target age group. A maximum strain of 30% was chosen for the onset of ligament tearing and a strain of 25% was chosen as the inflection point between the elastic and plastic regions.

The cross sectional areas of the ligaments and their average lengths were derived from basic cadaver measurements and model dimensions. A summary of the results is given in table 3.

With the approximate properties and available measuring techniques, it was possible to determine the resistive forces acting at the hip. Data was collected with the femur at maximum extension, flexion, and mid-position. In flexion, measurements were taken with the femoral head fully seated in the acetabulum and also with the head dislocated

Table 3. Hip ligament properties.

Ligament	Cross-Sectional Area (mm <sup>2</sup> )	Average Length (mm)
Pubocapsular	127	72
Ilio-femoral	362	65
Ischiocapsular	96	58
Transverse	58	69

to the posterior margin of the acetabular rim. It was interesting to note that specific ligaments became slack at different femur positions. This had also been noted by Kapandji and Gray (10, 11). The strains and subsequent forces exerted by the ligaments are presented in table 4 with the femur at 115 degrees flexion and 10 degrees adduction. The coordinate system has its origin at the center of hip joint rotation with the X-Y plane parallel to the rim of the acetabulum.

Table 4. Force components acting on the hip.

Component	Force (N)
X (posterior-anterior)	-1671
Y (inferior-superior)	-864
Z (medial-lateral)	-4185

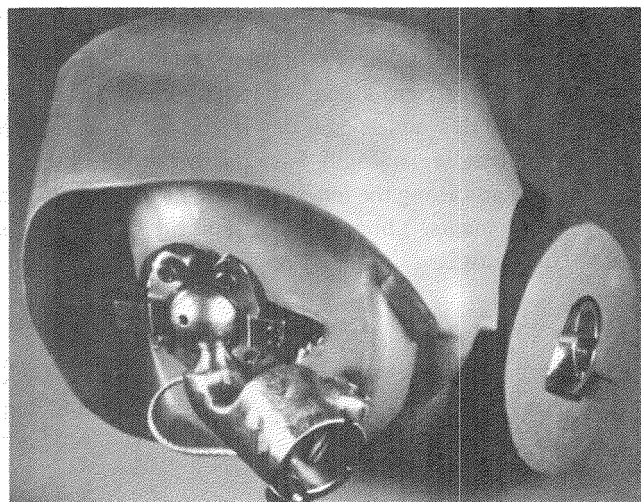


Figure 5. Motorcyclist ATD hip joint.

The current design depicted in figure 5 preserves the forces required to dislocate the hip. The design consists of a split ring assembly which retains the femoral head in the acetabulum until the critical dislocation force of 4 kN, normal to the plane of the acetabulum, is exceeded. This force is the lower bound of a performance corridor as it is based on the femur orientation when it is most likely to dislocate. The Hybrid III pelvic structure and femur head are used as the basis for the design. The hip region has been modified to represent the 50 percentile geometry of the acetabulum. The two arms which clamp the femur head are mounted to the pelvis. The arms pivot at one end and are retained at the other by shear pins. Failure of the pins occur when the critical load has been surpassed. The arms include a 70 degree opening at the posterior portion to provide an unobstructed displacement path for the dislocated femur. The design preserves the joint contact force vectors with a low

friction plastic lined acetabulum. In addition, joint torsional resistance may be adjusted to aid in the positioning of the ATD's legs.

Refinements to the design shall include improved bio-fidelity and the ability to monitor for ligament injuries. The concept, illustrated in figure 6, introduces a joint capsule which replicates the geometry and response found for humans. The capsule incorporates thermoplastic/elastomer ligaments with stress-strain characteristics similar to those of real ligaments. Although this concept has not been completed, full fruition of the design is expected in future work.

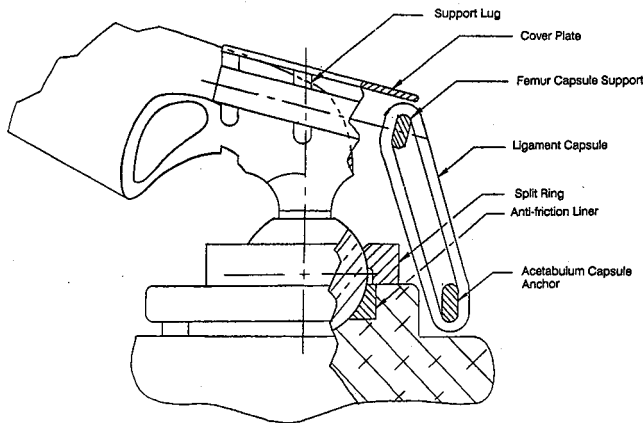


Figure 6. ATD hip joint capsule concept.

## Knee design

Modes of failure in the human knee may involve various combinations of bony, ligamentous, muscular, and cartilaginous structures. The reaction of structures in the knee to loading is dependant on the rate at which it is strained as bone, ligaments, cartilage and muscle are strain rate sensitive. Finally the degree to which the surrounding musculature is contracted significantly affects potential failure mechanisms.

A perfect surrogate knee would incorporate all of the above factors in its design and monitor for them in an accurate and repeatable manner.

It was decided to limit the design considerations to those factors which were deemed the most relevant to the motorcycle accident environment. The following points address this issue:

- Failures induced by combined loading (i.e., torsion and lateral shear) were not monitored for due to their complexity. Rather, the motions of the knee were considered uncoupled when incorporating tolerance data.
- It was decided not to monitor for patellar fractures given their low severity.
- Since the most readily accessible tolerance data is quasi-static in nature, while the loading anticipated in motorcycle crashes is dynamic, static tolerance data adjusted for dynamic effects was used in the design.

Four loading modes were identified as the most likely to cause knee injuries in the motorcycle accident environment. These are:

- Varus-valgus (inward-outward) rotation of the tibia relative to the femur
- Torsional rotations of the tibia relative to the femur
- Anteroposterior (A-P) shear
- Lateral shear

Of these motions, the only one currently possible in the Hybrid III is A-P shear. However, the current A-P mechanism is susceptible to binding during combined loadings and was excluded from the design.

No failure data was found on the other three motions. Consequently, dedicated cadaver tests were conducted (12). The knees of fresh frozen specimens were obtained from male cadavers, aged 23, 26, and 23. All specimens were deemed "healthy".

Two knees underwent 90 degrees of quasi-static tibia rotation about the axis of the femur (in valgus, or outward rotation), while one knee underwent 90 degrees of quasi-static tibia rotation about the axis of the tibia (in external torsional rotation). Torque-rotation curves were obtained from all tests. The knee flexion angle was set at 90 degrees for all tests.

Experimental limitations prohibited the testing of lateral shear to failure.

### Valgus rotation

Failures of the anterior cruciate and the medial collateral ligaments were observed in the applied range of movement. These failures coincided with a drop in torque observed at approximately 30 degrees. The mean maximum torque observed just prior to these failures was 95 Nm while the mean stiffness in the linear range up to failure was 4.3 Nm/deg. These were established as the static criteria values for valgus knee failure.

As an approximation, response to varus (inward) rotation of the tibia was considered similar to that of valgus (outward) rotation.

### Torsional rotation

Failures of the medial collateral and anterior cruciate ligaments were observed in the applied range of torsional rotation. These failures coincided with a drop in torque observed at approximately 50 degrees. The mean maximum torque observed just prior to this drop was 57 Nm while the static stiffness in the linear range prior to failure was 2.4 Nm/deg. Low resistance of the knee to torsional rotation observed in the first 20 degrees of motion was not incorporated into the knee unit, as much of this movement is currently accounted for by rotation in the Hybrid III ankle. The obtained values were adjusted for dynamic effects and used as design criteria for torsional rotation. As an approximation, response to internal rotation of the tibia was considered similar to that of external rotation.

In order to adapt the quasi-static values to a dynamic environment, the strain rate dependency of ligaments was considered. A 42% increase in ligament strength was observed in one study when the strain rate was increased from  $0.036 \text{ sec}^{-1}$  to  $0.14 \text{ sec}^{-1}$  (13). It is also known that as the loading rate to a joint increases the chances of sustaining a purely ligamentous (as opposed to bony) failure increase (14). This phenomenon has been attributed to a higher strain rate dependency of bone than ligament. Given these facts, coupled with a dynamic increase factor of 40% used for bone, it seemed not unreasonable to assign an increase of 30% to both the static yield strengths and stiffnesses of the knee. The criterion values for quasi-static knee failure in valgus rotation were thus adjusted to reflect this increase. Table 5 shows the target values for both varus-valgus and torsional rotation.

**Table 5. Design criteria for knee element.**

Motion	Stiffness	Failure Load
Varus-valgus rotation	5.6 Nm/deg	124 Nm at 30°
Torsional rotation	3.1 Nm/deg	74 Nm at 30°

### Knee design

The frangible knee components bolt to the base of the clevis of the existing Hybrid III knee, but do not affect the knee in terms of flexion and extension. Figures 7 and 8 show schematics of the assembled knee.

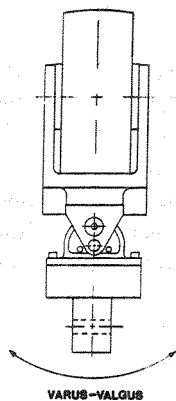


**Figure 7. Knee assembly in frontal plane.**

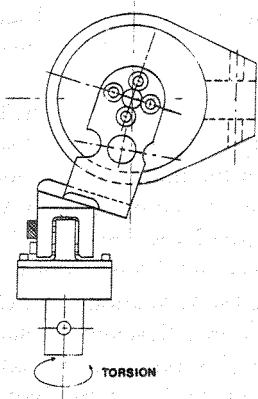


**Figure 8. Knee assembly in sagittal plane.**

The knee design contains two brass pins which act as fuses, shearing when the load in either torsional or varus-valgus rotation exceeds the established tolerance levels. Human-like response prior to failure is accomplished via plastically deformable springs which compress during torsional or varus-valgus movement. The springs are designed such that when the rotation in varus-valgus motion is between 25 and 30 degrees, and/or rotation in torsional motion is between 30 and 35 degrees, the compressive resistance is sufficient to shear the appropriate pin. In addition, the knee is equipped with a steel bolt which can shear in the event of extremely high lateral and/or axial loads. This occurrence could be indicative of complete knee amputation. The knee unit is shown in figure 9.

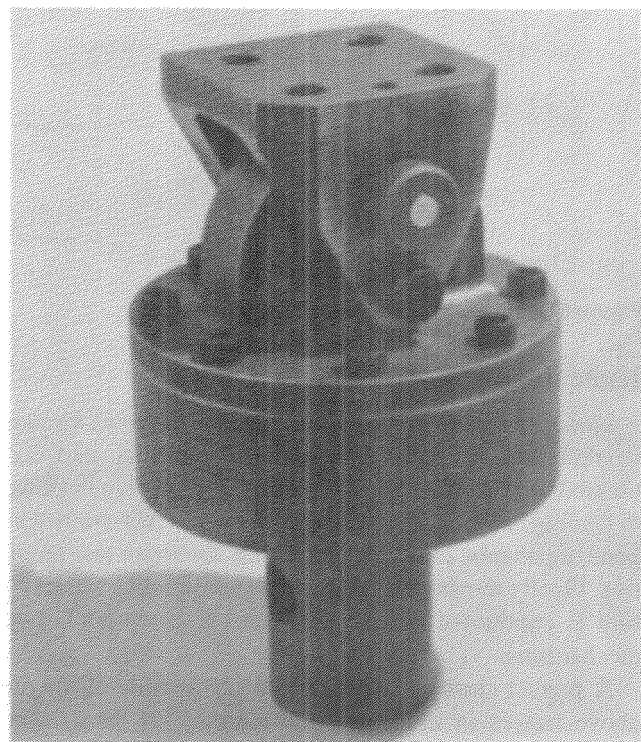


**Figure 9. Frangible knee assembly.**

The device was tested on the same equipment as was used for the cadaver tests. Figures 10 and 11 show the response curves with the corresponding cadaver curves (adjusted for dynamic effects).

The surrogate knee response curves end at the points where their respective shear pins failed. These points are 132 Nm at 29 degrees, and 72 Nm at 32 degrees, for varus-valgus and torsional rotations, respectively. These values are all within 7% of the target values listed in table 5. Although the stiffnesses were not directly calculated (due to their varying nature), it can be seen that the resistance up to failure is, to a degree, human-like for both movements. The resistance to rotation post-failure is zero for both rotation modes.

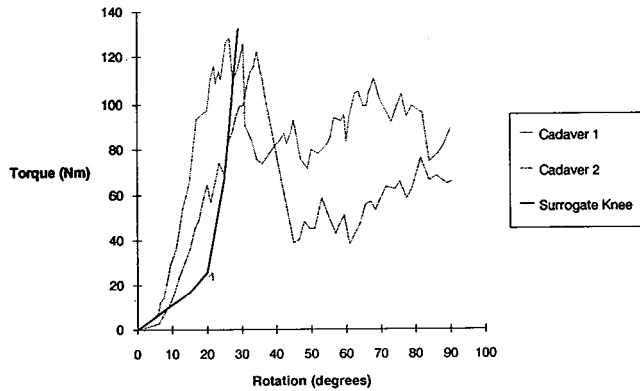


Figure 10. Response to Valgus rotation of the tibia.

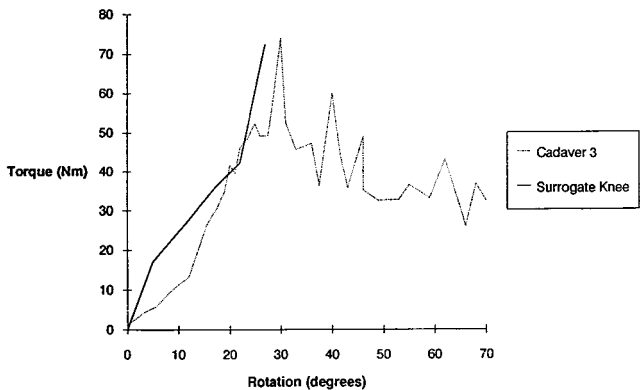


Figure 11. Response to External Torsional Rotation of the Tibia.

## Data acquisition system

The on-board data acquisition system developed is an extremely sophisticated piece of equipment whose production was made possible only by recent developments in integrated circuit technology. For such a system to be truly useful, it was decided from the outset that it should:

- Be durable enough to withstand the rigors of motorcycle testing.
- Be relatively easy to use and operate in a test environment.
- Provide for an appropriate combination of sensors, to allow for the accurate assessment of multiple injuries to various body parts.
- Result in data which is compatible with, and transferable to, commonly used computer systems.
- Not affect weight and mass distribution of the ATD.
- Not interfere with the response of the ATD.

These objectives were largely achieved. Any deviations relate to the size, weight, and location of the data acquisition system and are discussed further on.

## Transducers

The motorcyclist ATD is fitted with four types of transducers. Accelerometers are used in the head, chest, and pelvis; load cells are used in the neck, and in the proximal

femurs; strain gauges are applied to the knee clevis, distal femur, and tibia; and the use of the chest potentiometer standard in the Hybrid III has been retained. In all, 55 of the possible 64 channels are used. A detailed list of the transducers and the measurements taken is presented in table 6.

Table 6. Transducers used with the motorcyclist ATD.

Location	Measurement
Head	Linear Accelerations, Angular Accelerations
Neck	Forces, Moments
Chest	Linear Accelerations, Deflection
Pelvis	Linear Accelerations
Left Proximal Femur	Forces, Moments
Right Proximal Femur	Forces, Moments
Left Distal Femur	Forces, Moments
Right Distal Femur	Forces, Moments
Left Knee	Clevis Load
Right Knee	Clevis Load
Left Proximal Tibia	Moments
Right Proximal Tibia	Moments
Left Distal Tibia	Axial Load, Moments
Right Distal Tibia	Axial Load, Moments

For the most part, the transducers used equate to those found on a fully equipped Hybrid III ATD and all kinetic data that can be monitored by the Hybrid III is retained by this modified dummy. The differences between the two are as follows:

- Three angular accelerometers have been added in the head.
- The chest deflection potentiometer, although in use, provides data of limited value due to reduced deflection space and altered compliance of the chest.
- The 6 channel upper leg transducers are not situated where they are normally found on a Hybrid III. These units, specially designed by Denton are located just proximal to the bend in the femur.
- The sliding knee potentiometer has been eliminated.
- The standard lower leg transducers were not included.
- A large number of strain gauges have been placed on the frangible bones. For the lower legs, the values provided replace those previously furnished by the transducers. For the femurs, they supplement data obtained from other sensors.

## Data acquisition

The data acquisition system designed and built for the motorcyclist ATD consists of several units which are described in detail in reference (15). Some of these units are used for setup, calibration and data retrieval and are only connected to the acquisition system when necessary. This minimizes the volume required by the system.

The heart of the data acquisition system is the Durable Electronic Logging Violent Event Recorder or DELVER. Eight DELVERs are used for the motorcyclist ATD to provide a total capability of 64 channels. These have been

placed in an aluminum box which fits inside the chest cavity and wraps around the spine box. This arrangement is shown in figure 12.

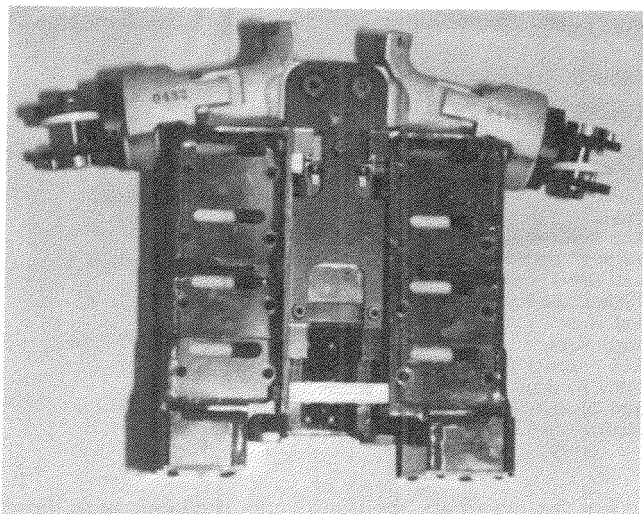


Figure 12. DELVER housing inside Hybrid III chest.

The data acquisition system did not entirely meet all of the design objectives. The mass and center of gravity as well as the available deflection and compliance of the chest have been affected.

Ballasting at the base of the thoracic spine was removed to compensate at least partially for the mass of the data acquisition system. Nevertheless, the chest mass of this version of the motorcyclist ATD has increased by approximately 7 kg. The mass distribution has changed slightly thereby raising the position of the center of gravity by close to 2 cm.

The size of the aluminium box also makes it impossible to retain the full amount of deflection normally possible in the chest. The box also interfered with the curvature of the ribs. The damping material had to be cut away in the front outside corners in order that the ribs fit on the ATD. As an additional modification, the ribs had to be cut at the spine into left and right sections. These changes are shown in figure 13. At

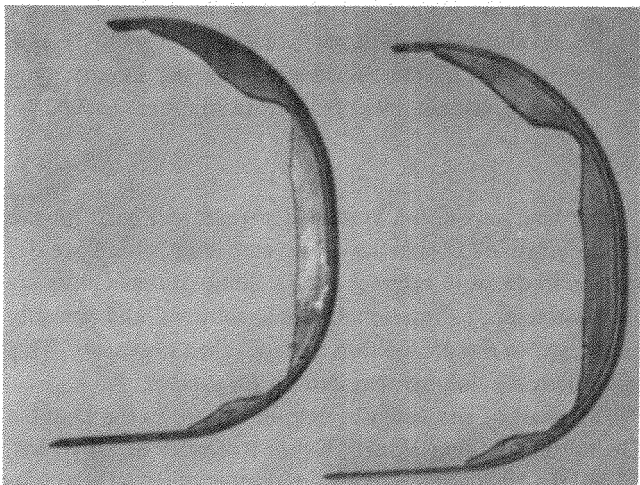


Figure 13. Modified Hybrid III ribs.

present, the configuration allows for only approximately 2 cm, and that, only when compressed directly from the front. The degree of biofidelity of this new thorax has not yet been assessed.

The overall instrumentation system block diagram is shown in figure 14. A description of the principal components follows.

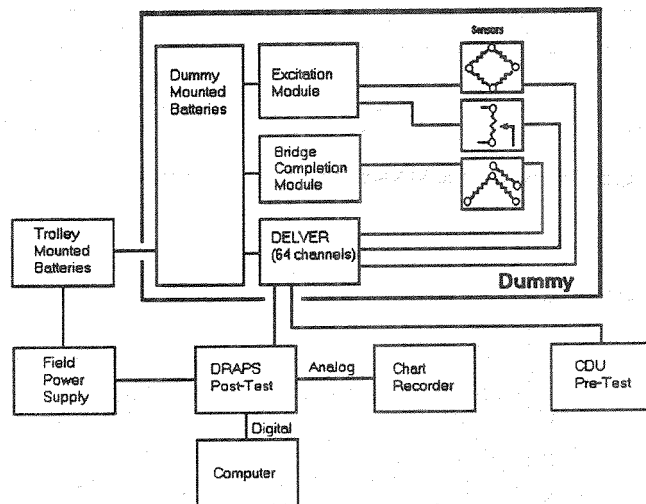


Figure 14. DELVER block diagram.

*Bridge Completion Module.* This unit fits within the thoracic spine box of the Hybrid III. Its function is to provide bridge completion circuitry for 350  $\Omega$ , 2 arm and 1 arm piezoresistive sensors. The bridge completion circuitry includes a precision potentiometer to provide circuit balancing capability. This circuitry has been mounted on the stem which fits inside the Hybrid III spine box. The unit is shown in figure 15.

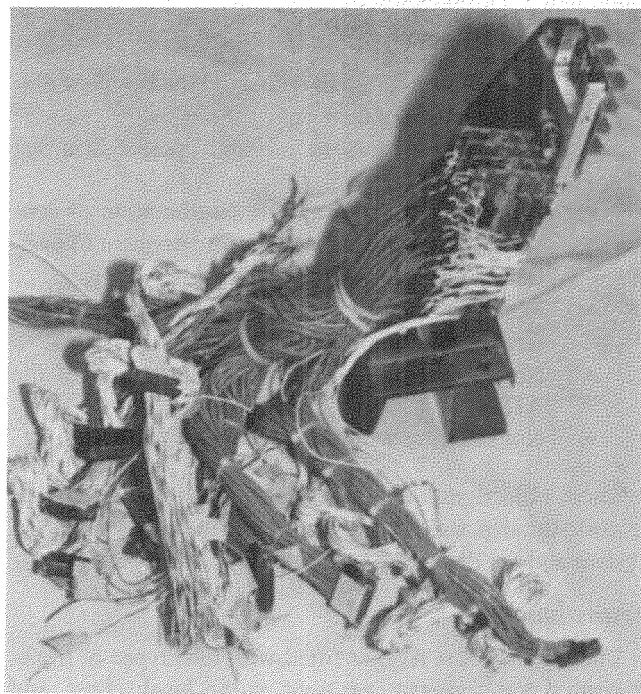


Figure 15. Circuitry mounted on Hybrid III stem.

*Voltage Excitation Module.* This module is also located within the spine box of the Hybrid III. The circuitry is designed to provide the appropriate excitation required to support the previously described list of dummy sensors.

*DELVER.* The primary specifications for the data channels include:

- 10,000 samples per second per channel.
- Solid state digital memory.
- 8 bit resolution, 0.78% accuracy.
- 13.1 seconds of data storage.
- Shock and vibration resistant.
- Compatible with low level and high level differential DC inputs.
- Per channel DC gain adjustments from 1 to 500.
- Anti-aliasing filtering with the -3db point set at 2,500 Hz.
- Per channel full scale signal offset capability.

*Field Power Supply.* This component supplies 24 VDC to the batteries and dummy during pre and post-test operations when line power is available. The unit is compatible with input voltages between 85 VAC and 132 VAC.

*Batteries.* There are three sets of batteries used with this system. Trolley mounted batteries can provide up to 10 minutes of power before a test. Dummy mounted batteries provide 30 seconds of full power during a test and a second set of dummy mounted batteries can provide up to 1,000 hours of power for data retention only. This arrangement is used to minimize the mass and volume of batteries housed within the dummy.

*Calibration/Diagnostic Unit (CDU).* During pre-test operations, this unit is used to ascertain the operational status of the DELVER as well as assist the user in setting the gains and offsets for the individual data channels.

*Data Retrieval and Playback System (DRAPS).* This unit, used during post-test operations, is a solid state, high capacity mass storage system designed to retrieve test data from DELVER. DRAPS is the communications link required between DELVER and digital computers or analog recorders. The download of DELVER data to DRAPS is a non-destructive read process at the original sample rate, which is typically too fast for most computers. DRAPS records DELVER data and then is capable of transferring the data to different types of equipment at various selectable playback rates.

## Summary

Using newly developed structural materials and methodologies, frangible leg bones for a Hybrid III test dummy were designed, fabricated and validated to match the currently available dynamic strength properties of the human upper and lower leg bones. The stiffness and failure criteria were met within 10%.

The frangible bones are comparable in weight to human bones, however they weigh considerably less than the standard Hybrid III bones. The Hybrid III bones though,

represent a much larger percentage of the total mass of the lower extremities than the human. Future refinements will endeavour to better match the overall mass distribution to that of the human through soft tissue development.

Modification to the lower leg soft tissue permitted the frangible bones to be easily installed and, following testing, be readily replaced. The provision of a series of strain gauges mounted to the surface of the bones, replaces the lower leg transducers normally fitted to the Hybrid III and enables monitoring for potential bone failure through stress strain analysis.

Finally, the structure is such that inspection of tested parts which were caused to fail in bending and in torsion are visually different from each other. The failure characteristics are distinctive enough that, with the strain gauge data, insight into the failure mechanisms in full-scale tests is possible.

The current effort has demonstrated the feasibility of composite material design in achieving a bone model with humanlike structural properties. The present solution however, should be regarded as interim. Improvements to be considered in the future include:

- Better representation of impact properties;
- Improved methods for predicting soft tissue injury;
- Variable strength properties along and around the bone;
- Improved quality control techniques for such frangible elements.
- Better mass and inertial representation.

Laboratory tests have verified the performance of the hip design. Full scale crash tests are ensuing and should prove the feasibility of such a device for the monitoring of hip joint injuries due to dislocations.

The knee design mimics the human knee well in its response to loading in both torsional and varus-valgus movements. Complete knee dissociation is monitored for, although comparative cadaver data was not obtained. Future improvements to be considered include:

- Refining post-failure resistance to loading to be more human-like;
- Reducing complexity of assembly;
- Conducting dynamic testing to verify response;
- Conducting tests to dissociate knee completely to establish "amputation" loads.

A digital data acquisition system has been designed to fit within the chest cavity of the Hybrid III.

An instrumentation package has been developed to provide the most complete kinematic and kinetic history ever achieved in motorcycle testing.

With the partial exception of chest compliance, all of the original design specifications have been met. It must still be realized, that the chest compliance issue for motorcycle crash testing does not bear the same relevance as in car crash testing.

Finally, the data acquisition system of the motorcyclist ATD has worked well in preliminary tests.

## References

(1) Tadokoro, H., Fukida, S. Miyazaki, K.; "A Study of Motorcycle Leg Protection". The Tenth International Technical Conference on Experimental Safety Vehicles, Oxford, July, 1985.

(2) Foster, J.K., Kortge, J.O., Walanin, N.J.; "Hybrid III: A Biomechanically-Based Crash Test Dummy". Proceedings of the Twenty-First Stapp Car Crash Conference, Society of Automotive Engineers, 1977.

(3) McElhaney, J.H.; "Dynamic Response of Bone and Muscle Tissue". *J. Applied Physiology*, 21, 1966.

(4) Stewart, M.J., McCarroll, H.R., Mulhollan, J.S., "Fracture—Dislocations of the Hip". *Acta Orthop. Scand.*, Volume 46, 507–525, 1975.

(5) Suracci, A.J., "Distribution and Severity of Injuries Associated with Hip Dislocations Secondary to Motor Vehicle Accidents". *The Journal of Trauma*, Volume 26, No. 5, 1986.

(6) Nyquist, G.W., Cheng, R., Ahmed, El-Bohy, King, Albert, I.; "Tibia Bending: Strength and Response". Twenty-Ninth Stapp Car Crash Conference Proceedings, SAE #851728, Washington, D.C., October, 1985.

(7) Armstrong, J.R., "Traumatic Dislocation of the Hip Joint". *The Journal of Bone and Joint Surgery*, Volume 30–B, No. 3, August, 1948.

(8) Reynolds, H.M., Snow, C.C., Young, J.W., "Spatial Geometry of the Human Pelvis".

(9) Noyes, F.R., Grood, E.S., "The Strength of the Anterior Cruciate Ligament in Human and Rhesus Monkeys". *The Journal of Bone and Joint Surgery*, Vol. 58–A, No. 8, December, 1976.

(10) Kapandji, I.A., "Physiologie Articulaire; Schemas Commentes de Mecanique Humaine". Libraire Maloine S.A., Paris, Fourth Edition.

(11) Gray, H., "Anatomy; Description and Applied". Longmans, Green and Co., New York, Twenty Fourth Edition, 1930.

(12) "Requirements for an ATD for Motorcycle Crash Testing". Biokinetics and Associates Ltd. Contract Report R88–11d.

(13) Kennedy, J.C., Hawkins, R.J., Willis, R.B. and Danylchuck, K.D., "Tension Studies of Human Knee Ligaments". *The Journal of Bone and Joint Surgery*, Volume 58–A, No. 3, April, 1976.

(14) Cabaud, H.E., "Biomechanics of the Anterior Cruciate Ligament". *Clin. Orthop. and Related Research*, Volume 172, 1983.

(15) Wiley, K.D., Zellner, J.W., White, R.P., Gustin, T.W.; "Summary of Data Acquisition System for Motorcycle ATD". Draft Report DRI–TM–89–4, submitted to the International Motorcycle Manufacturer's Association (IMMA), February, 1989.

## Acknowledgements

The authors wish to extend their gratitude and appreciation to the many individuals and organizations who have made this development a reality. To the material specialists at AVI who made bones that not only break like humans, but look like them; to the electronic wizards at SRL who packaged more self-supporting data collecting power in a crash dummy than was ever thought possible; to the biomechanics experts at McGill University who generated biomechanical data heretofore unknown, and to the fine engineers at DRI who helped make sure it all went together properly, Biokinetics extends its compliments and highest regards.

## A Combined Anti-lock Brake System for Motorcycles

**G.L. Donne**

Transport and Road Research Laboratory, UK

### Abstract

There is evidence that many motorcyclists use only one brake, usually that on the rear wheel. This technique seriously limits the deceleration available to the vehicle, particularly in emergencies. Combined braking systems in which the brakes of both wheels are actuated by a single control have been available for many years but not used in large numbers. Such systems ensure the use of both brakes by virtue of their design but problems related to distribution of effort have remained unresolved. The addition of anti-lock devices to a Combined brake system is discussed in the paper, along with results obtained from braking tests using a sample of riders.

### Introduction

Papers which discussed the difficulties faced by riders in the braking of motorcycles have been presented at previous ESV Conferences (DONNE and WATSON, 1985) (DONNE and CART, 1987) and elsewhere. Two-wheeled vehicles remain unusually susceptible to accidents which involve braking problems, such as skidding or excessive stopping-distance. In some cases, rider technique appeared to be inadequate, particularly under emergency conditions. For example, a study of the behaviour of riders (SHEPPARD ET AL, 1985) indicated serious deficiencies in the way in which many riders attempted to brake. It was observed that even during emergency braking over 20 per cent of riders used only one brake, generally that on the rear wheel. In "normal" braking only about half the riders

observed used both brakes. If such a pattern of behaviour is widespread, many motorcyclists are failing to brake in the most effective way, since, failure to use the front brake limits the deceleration available to the vehicle and can lead to unnecessarily long stopping-distances. The relevance of this has been illustrated in an accident study made in Australia (MCLEAN ET AL 1979). This indicated that 30 per cent of the accidents investigated might have been avoided if the available braking capacity of the motorcycle had been fully utilized. The education and training of riders to use both brakes might improve the situation but available evidence (HURT ET AL, 1981) indicates that attempts at this have been unsuccessful in the past.

Combining the operation of the brakes on both wheels to a single actuation system could be a means of "enforcing" the use of both brakes. A few manufacturers have produced commercially-available machines with such systems, the first more than sixty years ago. Moto Guzzi (MANICARDI, 1979) and Yamaha (in the US market) appear to be the only producers in recent years. A previous assessment at TRRL of a machine equipped with a combined system showed that intrinsically such an arrangement could not achieve results which were better than those obtained by an expert rider using a conventional system. Indeed, the results indicated that on a good road-surface, the conventional arrangement produced vehicle decelerations which were significantly higher than those obtained with the linked system alone (with an expert rider). However, another study (MORTIMER, 1986) found that there were significant benefits in using a combined brake system when non-expert riders were involved.

Generally, combined systems assessed previously had a fixed relation between front and rear brake-effort, dependent on the dimensions of components of the brake-system. Inevitably, this was a compromise and was found to limit the deceleration which was available to the vehicle on good surfaces. This was because the rear wheel locked before maximum brake-force was developed by the front wheel. On Moto Guzzi machines a supplementary brake was provided on the front wheel to overcome this problem. However, in extreme condition the rider was faced with the need to adjust front and rear effort just as with a conventional arrangement.

A logical extension of the combined brake system would consist of the addition of anti-lock brake devices on each wheel. Any need to attempt balance between front and rear brake effort would be unnecessary. Under maximum or panic braking conditions the operation of the anti-lock systems would ensure that both wheels were producing a brake-force which was near the optimum.

This paper describes and discusses measurements of braking-distance made to assess an anti-lock equipped combined brake system on a motorcycle. Comparisons were made with the performance of other brake operating configurations. As this was a preliminary investigation, intended to assess the possible benefits of the system, only a

relatively-small number of test-riders was used. However, care was taken to ensure that they had a range of experience and ability and that the test-procedure was well-controlled.

The results indicated that the use of the combined brake system with anti-lock was advantageous, particularly for riders braking on a slippery surface. In all cases, the use of the linked system (both with and without anti-lock operating) gave results which were superior to those obtained using the rear brake alone.

## Test Method

### Motorcycle

One machine was used. This was a BMW K100 which had been fitted with Lucas Girling anti-lock devices in the brakes of both wheels. Safety skids were fitted to protect the rider from the effects of capsize when tests were undertaken with the anti-lock devices immobilised. In its standard form the machine was equipped with brake systems of a configuration which has become the norm for large motorcycles, with two disc-brakes on the front wheel and a single disc-brake on the rear wheel. These were operated respectively by master-cylinders mounted on the handlebar and near the right foot-rest.

For the purposes of this investigation the pipework of the standard brake-systems was modified to provide an additional configuration referred to as a linked system. In this mode, the handlebar master-cylinder actuated one of the brakes on the front wheel and the single rear brake. Both the second brake on the front wheel and the rear master-cylinder were isolated in the linked configuration. Manually-controlled valves were provided to enable any of the possible modes of operation to be selected, with or without the anti-lock devices operating.

### Brake configurations

Measurements were made in each of the following brake configurations: rear brake only; front and rear brakes (separate operation); front and rear brakes (linked system), each with the anti-lock devices immobilised; front and rear brakes (separate operation); front and rear brakes (linked system), in each case with anti-lock devices activated.

Ideally, in the linked mode, both brakes on the front wheel of the motorcycle would have been operated in order to maintain the original braking capacity. In practice, it was not possible to obtain a suitable master-cylinder capable of operating three brakes simultaneously. However, the arrangement used was able to illustrate the possible benefits of a linked system, as a principle, despite the reduced brake force available at the front-wheel compared with the conventional configuration.

### Riders

A total of ten riders took part. They ranged in age from about 20 years to about 55 years and had a variety of motor-

cycling experience. None claimed to be an expert rider and not all were practising motorcyclists at the time of the tests.

### Road surfaces

Measurements of braking distance were made on two test surfaces of the research track at the Transport and Road Research Laboratory in the UK. These were: "Bridport" gravel, a macadam with a rough, polished texture and a peak coefficient of friction of about 0.4 when wet; fine, cold asphalt with a smooth, harsh texture and a peak coefficient of friction in excess of 0.7, wet or dry, at the speed used in this investigation.

### Speed measurement

A speed-measuring system was installed on each of the test surfaces. This measured the time taken by the motorcycle to cover the distance (one metre) between two parallel rubber tubes fixed to the road-surface at the approach to the braking area. The passage of the vehicle generated pulses in the tubes which operated switches. These, in turn, operated an electronic timer. The equipment was situated approximately two metres in advance of a line marked by two traffic-cones which indicated to the rider where to commence braking. Although all measurements were made using a nominal speed of 50km/h (30 mile/h) this arrangement enabled an accurate measurement of the actual speed of the motorcycle just prior to braking.

### Order of testing

As far as was practical the order of testing was randomised across conditions for each rider. This was intended to reduce any effects arising from increasing familiarity with the task among riders.

Each rider was asked to make five attempts at each test-condition; failed attempts were repeated and a note made of the reason for failure (usually loss of control).

### Results

Average vehicle-decelerations obtained by each rider with each brake configuration are shown in tables 1 and 2. Table 3 compares the average decelerations obtained with each configuration, as a multiple of that achieved by using the rear brake only. Riders' subjective comments are shown in the Appendix.

#### "Bridport" gravel surface (table 1)

Several comparisons may be made. First, the average deceleration obtained using the rear brake only compared with that for each of the other configurations (in which brakes were applied on both wheels). In the case of the two arrangements without anti-lock, the average deceleration achieved was about 70 per cent higher than that using the rear brake alone (table 3). With anti-lock operating, the two configurations which used brakes on both wheels gave average decelerations about twice that obtained using the rear brake alone (table 3).

**Table 1. Deceleration (g) obtained using various brake operating configurations on wet Bridport gravel surface, from 50 km/h.**

Rider	Brake Configuration				
	Rear Only No A/L	Separate No A/L	Separate with A/L	Linked No A/L	Linked with A/L
1. 10 years experience. Active rider	0.21 (1)	0.47 (2)	0.48	0.53	0.50
2. 6 years experience	0.29	0.56	0.54	0.54	0.64
3. 8 years experience	0.22	0.45	0.41	0.41	0.48
4. 16 years experience. Not riding regularly at present.	0.27	0.38	0.46	0.44	0.59
5. Active rider	0.22	0.36	0.52	0.29	0.45
6. Little experience	0.21	0.38	0.43	0.43	0.49
7. Novice	0.25	0.43	0.46	0.40	0.51
8. Some experience. Not riding regularly at present	0.28	0.46	0.50	0.40	0.57
9. 3 years experience. Active rider. Instructor in training scheme	0.21	0.41	0.42	0.41	0.53
10. 30 years experience Active rider.	0.27	0.39	0.49	0.39	0.55
Average	0.25	0.43	0.48	0.43	0.53

Figures are the average of 5 runs in each configuration  
Figure in brackets indicates number of occasions on which rider lost control.

Second, the average decelerations obtained by the use of linked and separated configurations did not appear to indicate any benefit intrinsic in the use of the former (without anti-lock). However, there is subjective evidence (Appendix) that riders perceive advantages in having to operate only one control to apply the brakes on both wheels.

Third, the average decelerations obtained in the two configurations with anti-lock were 11 and 23 per cent higher than those obtained in similar configurations with the anti-lock devices immobilised.

No pattern was apparent with regard to the decelerations obtained by various riders. It appeared that experience and regularity of riding were not factors which affected the performance achieved by riders in this assessment. However, the same general pattern of deceleration obtained across the various configurations was obtained for all riders.

#### Fine textured asphalt surface (table 2)

The limited brake-force available at the front wheel of the test motorcycle in the two linked-brake configurations has been discussed. It was evident that this factor affected the results obtained on this surface, which has a coefficient of friction about twice that of the Bridport gravel. The pattern of results was less consistent in this case but similar comparisons can be made.

First, the two configurations without anti-lock (in which brakes were applied on both wheels) produced decelera-

**Table 2. Deceleration (g) obtained using various brake operating configurations on wet fine textured asphalt surface, from 50 km/h.**

Rider	Brake Configuration				
	Rear Only No A/L	Separate No A/L	Separate with A/L	Linked No A/L	Linked with A/L
1. 10 years experience. Active rider	0.46	0.64	0.86	0.72	0.71
2. 6 years experience	0.40	0.90	0.87	0.67	0.71
3. 8 years experience	0.47	0.70	0.75	0.82	0.86
4. 16 years experience. Not riding regularly at present.	0.45	0.73	0.67	0.65	0.56
5. Active rider	0.37	0.47	0.60	0.45	0.51
6. Little experience	0.37	0.73	0.78	0.64	0.81
7. Novice	0.37	0.74	0.76	0.66	0.63
8. Some experience. Not riding regularly at present	0.38	0.66	0.75	0.65	0.74
9. 3 years experience. Active rider. Instructor in training scheme	0.42	0.73	0.76	0.65 <sup>(1)</sup>	0.78
10. 30 years experience Active rider.	0.46	0.67	0.72	0.62	0.75
Average	0.42	0.70	0.75	0.65	0.71

Figures are the average of 5 runs in each configuration  
Figure in brackets indicates number of occasions on which rider lost control.

**Table 3. Ratios of average decelerations obtained using various brake operating configurations on two surfaces—rear brake only as base.**

	Rear only No A/L	Separate No A/L	Separate with A/L	Linked No A/L	Linked with A/L
Bridport Gravel Surface	1.0	1.7	1.9	1.7	2.1
Fine Textured Asphalt Surface	1.0	1.7	1.8	1.5	1.7

tions which were typically about 60 per cent higher than that using the rear brake alone (table 3). When anti-lock was operating, average decelerations were about 75 per cent higher than those obtained using only the rear brake.

Second, consideration of differences in the results obtained with linked and separate braking systems indicated a small disbenefit of the use of the former. This was the case both with and without the operation of anti-lock. The limited brake-force available at the front wheel in the linked configuration appeared to be a factor in this instance.

Third, the average decelerations obtained with the two configurations with anti-lock were between 7 and 10 per cent higher than those obtained with the similar configurations without anti-lock.

As with the results obtained on the Bridport gravel surface, there was no pattern apparent with regard to the experience and degree of practice of riders.

## Discussion and Conclusions

The main purpose of the work described in this paper was to make a preliminary assessment of the benefits of fitting a novel type of brake system to motorcycles. Namely, a system with not only a unified means of actuation but also anti-lock devices applied to each brake. Despite the practical difficulties relating to the conversion of the experimental motorcycle it was apparent that there were advantages in the use of the linked-system with anti-lock. This was particularly the case when used on the more slippery of the surfaces employed in this assessment. The performance of the linked-operation configurations (with and without anti-lock) was slightly inferior to the conventional operation (with anti-lock) systems on the fine-textured asphalt surface. This was undoubtedly a result of applying only one of the two front-wheel brakes in the linked-configuration.

In a practical installation which used a combined braking system, actuation by the foot would be more appropriate than the hand operation used on the experimental machine. This would have the advantages of leaving the right hand free to operate the throttle and steering. Comments from the riders involved in this trial suggested that operation by the foot was preferable to hand operation.

Currently, the regulations which govern the design and provision of brake systems on motorcycles call for two, separate means of application. This is the case throughout Europe and in most other countries. Consideration has been given to changing the regulations to accommodate combined braking systems with anti-lock devices.

Despite the fact that no attempt was made to isolate hydraulically the two anti-lock devices on the test-machine there appeared to be no adverse interaction between them. However, this might not apply to all designs of anti-lock device and the use of a dual master-cylinder would be beneficial.

Secondary information was provided by the results of this trial. This related to the differences in the braking performance available with only the rear brake compared with the performance available if brakes on both wheels were used. This was an important result when it is considered how many riders habitually brake only the rear wheel.

Although a more extensive trial than that described would be needed before any firm or generally-applicable conclusions could be drawn, these preliminary results suggest that linking the operation of front and rear brakes is beneficial. The use of both brakes would be "enforced" by the provision of such a system. Combined with anti-lock any problems related to load-transfer and brake distribution would be reduced. In any extended investigation of the benefits of such a system, the provision of a test-machine equipped with either load-sensing or pressure-limiting valves in the rear brake would be advantageous. Such an addition would reduce the effects of over-modulation of the rear wheel and perhaps eliminate criticism by riders that the

rear anti-lock system operates too readily. A field-trial of machines fitted with combined braking systems and anti-lock devices could operate in a similar way to one already operating in the UK (DONNE and CART 1987).

## References

Donne, G L and J Cart, 1987. A Field trial of Motorcycles fitted with an Anti-lock Brake System. 11th International Conference on Experimental Safety Vehicles. Washington (NHTSA).

Donne, G L and P M F Watson, 1985. Aspects of Motorcycle Braking. 10th International Conference on Experimental Safety Vehicles. Oxford (NHTSA).

Hurt, H H, J V Ouellet, and R Thom, 1981. Motorcycle Accident Cause Factors and Identification of Countermeasures. Technical Report (University of Southern California).

Manicardi, S, 1979. Integral or Combined Braking System for Motorcycles. 7th International Conference on Experimental Safety Vehicles. Paris (NHTSA).

McLean, A J, N D Brewer, C Hall, B L Sandow and P Tamblyn, 1979. Adelaide In-depth Accident Study. Adelaide (Road Accident Research Unit, University of Adelaide).

Mortimer, R G, 1986. Braking Performance of Motorcyclists with Integrated Brake Systems. SAE Technical Paper No. 861384. Dearborn (SAE).

Sheppard, D, B A K Hester, Sonya Gatfield and Monica Martin, 1985. Motorcyclists' Use of Their Front Brakes. TRRL Report, RR 20. Crowthorne. (TRRL).

Crown Copyright. Any views expressed in this paper/article are not necessarily those of the Department of Transport. Extracts from the text may be reproduced, except for commercial purposes, provided the source is acknowledged.

## Appendix

### Riders' comments regarding brake configuration

During the trial described in the main body of the report, some riders volunteered comments. These were related mainly to the novel aspects of the trial, particularly linked

operation and anti-lock. The main comments are given below with, in some cases, explanatory remarks where appropriate, in brackets.

1. "I am surprised at how good linked braking actually feels. I thought it would be terrible". (Several riders expressed a similar view).

2. "Could be improved if rear wheel did not lock so easily." As tested, the motorcycle was underbraked on the front wheel, in the linked configurations. However, with anti-lock operable, "over-braking" of the rear wheel did not reduce vehicle deceleration to a significant extent).

3. "I am surprised at how long the rear-brake only stop was. It would be advantageous to demonstrate this to all riders as a part of their training."

4. "Even if linked braking gives shorter braking distances, there may be times when separate brakes would be necessary. (Effective anti-lock systems should make any separation of operation unnecessary).

5. "Perhaps it (linked operation) would have been better if operated by the foot instead of the hand." (It is envisaged that a practical system would use foot operation).

6. "It (linked operation) was good because I did not need to think about two brakes."

7. "During normal riding one should use both brakes so why not link their operation." (The evidence is that many riders do not use both brakes. Sheppard et al 1985).

8. "Experienced riders might find it difficult to become accustomed to linked operation but the system would be easy to handle for a beginner."

9. "Good idea, but not sure about the split." (Between front-wheel and rear-wheel brake-force. Effective anti-lock systems can eliminate problems caused by overbraking of either wheel. The limitations of the arrangement used on the test-motorcycle have been discussed in the body of the report).

10. "Would have been better if allowed to practice before each group of tests." (The results obtained from braking measurements obtained without practice must be more representative of the situation in the field than those obtained after practice).

## Acknowledgements

The work described in this paper forms part of the programme of the Transport and Road Research Laboratory and the paper is published by permission of the Director.

## Car Driver Behavior During Differing Driving Maneuvers

**P.A. Hancock, G. Wulf, and D. Thom,**  
Institute of Safety and Systems Management  
University of Southern California  
**P. Fassnacht,**  
Motorcycle Safety Foundation, Irvine, CA

### Abstract

Motorcycle-automobile accidents occur predominantly when the car driver turns left across the motorcyclist's right-of-way. Efforts to decrease this specific collision configuration, through increase in motorcycle conspicuity, have concentrated on the physical parameters of the motorcycle and

its rider. The work reported here focuses on the interaction between the observer (car driver) and the characteristics of the object to be observed (motorcycle and rider). Investigations are directed toward the examination of car-driver behavior during the left-turn sequence. Two experiments are reported which used simultaneous video-taping of the drivers themselves and the forward-looking display scene. In the first experiment, individuals followed a preset on-road course and were observed for workload responses such as probe-response time, subjective assessment, physiological activation, and manifestations of physical behaviors. Results indicated that there were significant increases in workload during turn sequences compared to straight driving. The second experiment included partial replication of previous performance assessment but examined principally driver eye movement and fixation, while isolating the separate effects of head movement. Subjects drove round a one square block course making repetitive left turns at intersections. One of the intersections was controlled by a traffic light and involved very heavy traffic, pedestrians, and other distractors. The other intersection was a two-way stop and involved light traffic flow. Descriptive data concerning behavior at these intersections is presented. Overall results indicate that turning maneuvers tax the information processing system more, result in higher workload and so increase the potential for detection failure. Such a propensity is increased by the higher structural interference that can be expected during turns. All left turns are not the same. The second experiment provides initial indications that eye/head behaviors are highly contingent upon the precise turn configuration. This argues that a taxonomy of left-turns is needed. Even with such differentiation, further understanding of the dynamics of driver behavior is required to increase recognition of on-coming motorcycles during this critical maneuver.

## Introduction

The leading cause of death of young people in urbanized societies is road traffic accidents. Such fatalities are not evenly distributed across different types of vehicle. Comparative data from a number of sources indicate the significantly higher propensity for fatality while using a motorcycle compared to other vehicles. While automobiles comprised 74.5% of the 1986 vehicle registrations in the United States and were involved in 62.4% of fatal accidents, motorcycles (including motor scooters and motor bikes) comprised 2.9% of the total vehicle registrations but were involved in 7.9% of the fatal accidents (National Safety Council, 1987). This problem is not confined to the United States alone. Comparable accident data are even less favorable for motorcyclists in other countries. In West Germany in the same year, 4.4% of all registered vehicles were motorcycles.

Their overall accident involvement, however, was 12.5% and their involvement in fatal accidents was even greater at 15.6% (Allgemeiner Deutscher Automobil-Club, 1987).

Using miles traveled as a baseline, the death rate in the U.S. for motorcycle riders is approximately 35 per 100,000,000. This is about 13.6 times higher than the overall death rate of 2.57 per 100,000,000 miles (National Safety Council, 1987). In West Germany, the kilometer-death rate is 44 times higher for motorcyclists than for automobile drivers (Appel, Otte, & Wüstemann, 1986). The high fatality rate of motorcyclists leads to a dominant and prevailing misconception that it is the motorcycle itself, or its control characteristics in conjunction with its driver, that are the source of the problem. Analysis of actual accidents indicates otherwise. In nine out of the leading ten accident configurations involving a motorcycle and automobile, it is the automobile driver's violation of the motorcyclist's right-of-way that leads to the critical incident (Hancock, Hurt, Ouellet, & Thom, 1986; Hurt, Ouellet, & Thom, 1981). Subsequent analyses of automobile-motorcycle collisions show the dominance of a single accident configuration (e.g., Waller, 1972; Olson, Hallstead-Nussloch, & Sivak, 1979; Weber & Otte, 1980; Hurt, Ouellet, & Thom, 1981). This type of accident is portrait on occasions when the automobile driver violates the motorcyclist's right-of-way by making a left turn into the path of the on-coming motorcycle. We have represented this situation schematically in figure 1. In post-accident interviews, the driver frequently claims not to have seen the motorcycle.

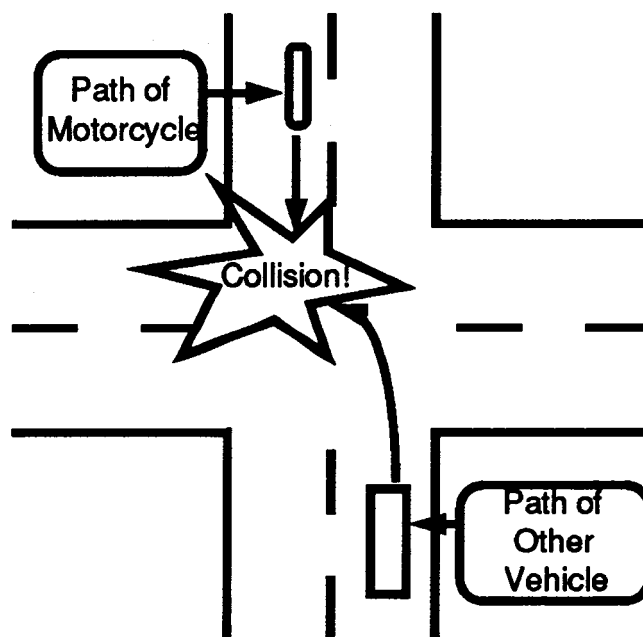


Figure 1. Predominant automobile-motorcycle accident configuration.

Attempts to reduce the frequency of motorcycle-automobile collisions have directed considerable effort to the question of the physical characteristics of the motorcycle and its rider. These manipulations have tried to improve the probability to detect the motorcycle through changes in its *conspicuity*. Conspicuity can be defined as the

degree to which an object can be distinguished from an environmental display, that is, its visual prominence due to its physical characteristics. Clearly, this distinction has to be specified upon a number of axes, which are typically those of a dynamic visual environment, e.g., object size and constancy, reflected wavelength, etc. These factors which represent the physical qualities of an object that can be compared using external reference measures, should more appropriately be referred to as *sensory conspicuity* (Engel, 1976). Numerous studies have focused on motorcycle characteristics, such as running the headlight during the daytime (e.g., Janoff & Cassel, 1971; Janoff, 1973; Fulton, Kirkby, & Stroud, 1980; Dahlstedt, 1986) or fairings which increase the frontal surface area (Williams & Hoffmann, 1977, 1979), and motorcyclist characteristics, such as the wearing of fluorescent garments (e.g., Stroud & Kirkby, 1976; Stroud, Kirkby, & Fulton, 1980; Donne & Fulton, 1985; Olson, Hallstead-Nussloch, & Sivak, 1979a, b, 1981) to enhance sensory conspicuity. These studies are reviewed by Wulf, Hancock, and Rahimi (1989).

A second form of conspicuity is *cognitive conspicuity*; it is specifically contingent upon the characteristics of the observer, and relies critically on the *saliency* of the target, or its meaning with respect to the observer's existing goals. Cognitive conspicuity depends on the previous experience and momentary intentions of the observer. There are indications that this aspect of conspicuity plays a role in failures to detect motorcycles. Post-accident interviews by Hurt, Ouellet, and Thom (1981) indicate that automobile drivers involved in collisions with motorcycles were generally "unfamiliar" with motorcycles. Also, Weber and Otte (1980) report for West Germany that among automobile drivers involved in a collision with a motorcycle, those without a driver's license for a motorcycle were overrepresented. It is our contention in the present work, that the failures of detection are the result of a complex interplay between the observer and the object to be observed. While many studies have manipulated elements of the object, few have examined the characteristics of the observer while involved in the task of on-road control.

The present experiments examined limitations in automobile drivers' information processing and the competition for limited processing resources which affect the driver efficiency in detecting on-coming motorcycles during left-turn sequences. In the first experiment, such capabilities were assessed using measures such as probe-response time and associated error, as well as eye-blink frequency. These measures have been found useful in measuring mental workload (Hancock & Meshkati, 1988). Furthermore, head-reversal frequency was used to determine possible structural limitations to visual information processing. The second experiment was used to provide partial replication of the first experiment, but the major focus was on eye movement and eye fixation (gaze) patterns. Our initial concerns were for the driver's behavior with respect to static and dynamic distractors during the left-turn sequence.

## Experiment 1—Method

### Subjects

Eighteen subjects (10 female and 8 male) were recruited from the staff and faculty of the Institute of Safety and Systems Management, University of Southern California. Their age range was between 21 and 50 with a mean age of 30 years. Subjects were not paid for their participation and all were naive as to the purpose of the experiment. Each subject possessed a current California State driver's license and the visual capabilities that the license requires.

### Task and procedure

The driver's task was to negotiate a pre-set course of major Los Angeles non-freeway urban streets. It consisted of 10 left turns and 10 right turns with interspersed straight sections. The time required to complete the route varied with the individual driver and traffic but was between 12 and 18 minutes. Each subject was guided through the course by an experimenter sitting in the passenger seat of the car. The experimenter also activated a switch to turn on a probe light at random intervals during various turn and straight sequences. The probe light was mounted on the dashboard directly in front of the driver. The subject was required to turn off the light as rapidly as possible upon detection by pressing a button that was attached to the dashboard to the left of the steering wheel. In addition to these measures, the subjects were asked to complete two subjective mental workload procedures, which are described below. Each procedure required the subject to complete portions before and following the driving sequence, while one of the procedures also elicited response during driving.

### Workload assessment techniques

The two procedures chosen to assess subjective workload response were the NASA *Task Load Index* (TLX) procedure and the USAF *Subjective Workload Assessment Technique* (SWAT) (see Hart & Staveland, 1988; Reid & Nygren, 1988). Their administration is described below. The TLX consists of a two-step sequence, one step of which is completed prior to the experimental procedure, and one which follows performance termination. In the first step, the participant compares the six dimensions of workload against each other in pairs to establish which of each pair is perceived to contribute the greater source of load. The dimensions are: mental demand (md), physical demand (pd), temporal demand (td), effort (ef), performance (op), and frustration (fr). The weight for each scale depends upon the number of times a scale is selected in the fifteen total comparisons. The weights therefore can vary between zero and five. The second step of the TLX process requires the subject to rate the load of the drive on a 0–100 scale for each of the six dimensions. These are the raw scores for each scale. The raw scores are multiplied by their respective weights to derive weighted scores, and the overall workload value is the sum of all weighted scores divided by fifteen, the origi-

nal number of pair comparisons. In the present experiment, the subjects rated the driving sequence they had just performed against a nominal drive of equivalent duration that they experience in their normal commute to work. It was these data that were subject to analysis.

The SWAT technique also consists of two components. The first is a card sort procedure in which the participant sorts twenty-seven cards that contain statements about the time, effort, and stress load of performance. Each card consists of three statements which describe three ascending load conditions on each scale. It is the matrix of three scales by three loads in combination that give the twenty-seven possible combinations. The subject sorts these combinations in perceived ascending load, and a workload scale is derived from the individual's responses. The second phase is the event scoring phase in which subjects rate the event which has just occurred on one of three levels for each of the time, effort, and stress scales. In the present experiment, subjects rated performance following the driving sequence, and as with the TLX, compared this with a nominal commute to work. In addition, some subjects were asked to give three number SWAT ratings during the driving sequence. Each participant was probed twice during the left-turn, the right-turn and the straight driving sequence. These overall data were subjected to analysis as reported below.

## Apparatus

Automobile-driver behavior was recorded through the use of simultaneous linked videorecorders. All experimental trials were conducted in a 1988 Ford Ltd. Crown Victoria. To analyze drivers' head and eye movements, "split-screen" video recording was used. This technique time locked the two video cameras. One camera was mounted above the windshield in front of the driver, focusing on the driver's face. The other camera was mounted on the roof of the car, directly above the driver's head, and recorded the visual field of the driver. A light connected in series with the probe light on the dashboard was attached to the headrest of the driver's seat, and recorded by the first camera. The subject's activation of the throttle and brake lights was monitored as well. This was achieved by using microswitch activated light-emitting diodes (LED's). Microswitches mounted on the floor of the car were activated by slight pressure on the throttle or brake pedal, and lit the respective LED. The LEDs were attached to the headrest of the driver's seat, along with the probe light. The output was such that approximately half of the image of the first camera occupied the lower portion of the video screen, and half of the image of the second camera occupied the upper portion of the screen.

## Results

A digital time display was located on the split-screen tape. The block gave time in terms of hours, minutes, seconds, and frames (30 per second). The time required to respond to the probe light, as well as the time for each turn

and straight-lane sequence was recorded, together with the associated error rate. The start and end of each turn sequence was defined by the deactivation of the throttle LED and the achievement of a car position parallel to the street, respectively. For each turn sequence the number of eye blinks and head reversals were recorded and their rate per second was derived for analysis. The dependent variables were then analyzed against the driving sequence in which they occurred. Analyses of variance were performed for each dependent variable. For probe-response time and probe-response error, one-way ANOVAs were performed on the three driving maneuvers, i.e., left turns, right turns, and straight sequences. The analyses for eye-blink frequency and head-reversal frequency involved 2 (probe condition)  $\times$  3 (maneuver) models. Fisher-PLSD test was used for *post-hoc* comparisons of means.

## Probe-response time

For probe-response time, the ANOVA revealed a significant effect of maneuver,  $F(2,235) = 9.34, p < .001$ . *Post-hoc* analysis indicated that the times to respond to the stimulus light were significantly ( $ps < .05$ ) longer for both left-turn (2.01 sec) and right-turn sequences (1.84 sec), as compared to straight-lane driving (1.48 sec) (see figure 2). Left turns and right turns did not differ significantly from each other. The intra-individual variability (variance) in probe-response time differed only minimally for the three driving maneuvers (.702, .501, and .592, for left turns, right turns, and straight sequences, respectively). One possible explanation for the first finding is that during the execution of turn sequences, drivers turned their head away from the centrally placed stimulus light, a form of interference not encountered during straight driving. To examine this possibility, probe response times were analyzed depending upon the type of turn. Those turns which did not require monitoring for cross traffic, i.e., controlled intersections showed no

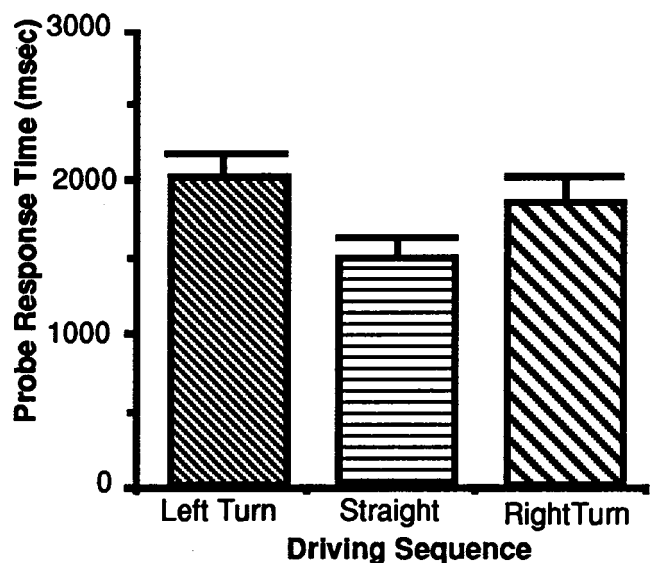


Figure 2. Probe-response time in different driving sequences.

difference in response time from those that did (2.05s vs. 2.01s). This finding contradicts a simple explanation that structural interference due to head position was responsible for the probe difference recorded.

### Probe-response error

Response times of more than 5 seconds were classified as response errors. The number of response errors was about twice as high for left turns (13.8%) and right turns (12.0%), relative to straight sequences (5.5%). In keeping with the results for the response times, subject made more errors during turns. This finding contradicts a simple speed-accuracy trade-off in responses to the probe light in this task. Analysis of left turns that did not require head movement to monitor cross traffic indicated a 13.2% frequency. So, the failure to notice the stimulus light during turns cannot be attributed simply to an interference effect. Both latency and accuracy of probe responses point to the increase in central processing time during the more difficult turn sequences.

### Eye-blink frequency

For eye-blink frequency, there was no significant effect of probe condition, or interaction of probe condition and driving maneuver. The main effect of maneuver, however, was significant,  $F(2,610) = 5.68, p < .01$ . Overall, the number of eye blinks per second was lower for both left turns (.310) and right turns (.290) than for straight sequences (.376) (see figure 3). *Post-hoc* comparisons indicated that the differences between both turn conditions and the straight-driving condition were significant ( $ps < .05$ ), while there was no significant difference between left and right turns. The intra-individual variance in eye-blink frequency was about 2.5 times higher during straight driving sequences (.100) than during left (.037) and right turns (.039).

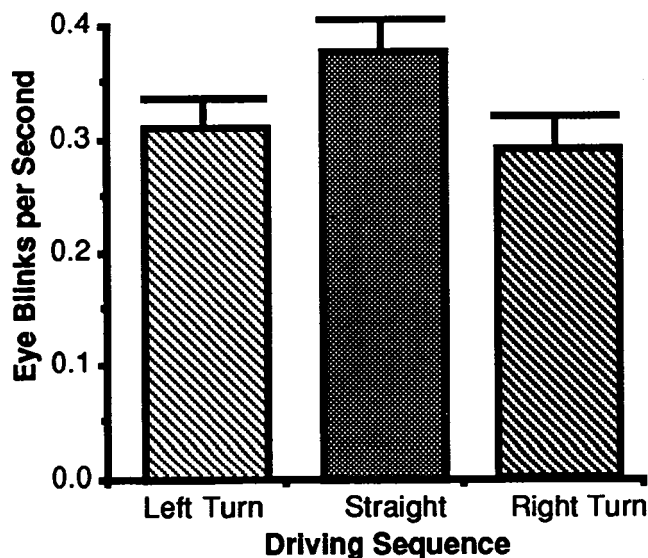


Figure 3. Eye-blink frequency in different driving sequences.

### Head-reversal frequency

With regard to the head-reversals frequency, there was a significant effect of probe condition,  $F(1,625) = 7.33, p < .01$ . The number of head reversal per second was generally higher for the sequences that included a probe (.209) than for maneuvers without a probe (.169). No significant interaction between probe condition and driving maneuver was found. The main effect of maneuver was statistically significant,  $F(2,625) = 24.37, p < .001$ . The head-reversal frequency per second was higher during left turns (.255) and right turns (.253) than during straight-lane driving (.127) (see figure 4). *Post-hoc* tests indicated that both the differences between left turns and straight-lane driving, and between right turns and straight driving were significant ( $ps < .05$ ). Also, the intra-individual variances were significantly ( $ps < .001$ ) higher for both left turns (.055) and right turns (.055) than for straight-lane driving (.021).

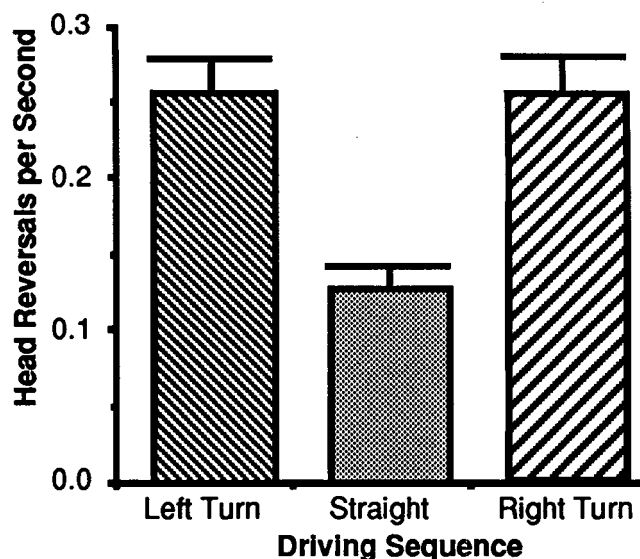


Figure 4. Head-reversal frequency in different driving sequences.

### Subjective workload responses

The first analysis of workload concerned the comparison of the present drive versus a nominal drive to work. If the analysis had found any differences it would suggest that the present driving sequence was different from a normal commute. However, analysis indicated no significant differences in perceived workload of the present test sequence in comparison to a normal drive to work. This finding was consistent for both the TLX and SWAT procedures. Interestingly, there was a significant difference for the TLX score for gender. While this did not interact with the test versus nominal driving sequence, responses indicated a higher perceived load of driving for males compared to female drivers (Males = 42.33, Females = 27.6). However, this finding was not replicated in the SWAT scores. For the SWAT scores taken during the driving sequence there was no significant difference between the three noted conditions. However, there was a trend in the direction noted for

the performance variables and other measures of workload given in the results above (left turn = 27.58, straight = 25.42, right-turn = 34.29).

## Experiment 2

The purpose of this experiment was to observe eye and head-movement activities while executing a series of left-turn maneuvers. The number of eye and head movements were recorded from the post-processed video tapes. This set-up was particularly designed for in-car experimentation with minimum degree of intrusion from the measurement equipment. The primary objective of this technique was to observe eye and head movements related to the location of objects in the field of vision.

## Method

### Subjects

The subjects were four members of the staff and faculty of the Department of Safety Science at the University of Southern California. Each individual was in good health, had 20/20 or adjusted 20/20 vision and held a current State of California driver's license. No subject was under prescription medication at the time of testing. There were two male and two female drivers.

### Task and procedure

In this experiment, a one square block driving route was identified in which the diagonal corners represented two distinctly different intersections—a busy intersection with a number of potentially distracting elements, and a quiet intersection with little distraction. The busy intersection was controlled by traffic lights, but the left-turn was not controlled with a separate green arrow. Consequently, the driver had to either cross between traffic if a space became available, or wait until the light turned amber and turn when the on-coming traffic stopped. The quiet intersection was a two-way stop where the driver faced one of the stop signs. The driver had to monitor the presence of on-coming traffic at the facing stop and had to complete the left turn between any cross traffic. As this was a quiet intersection, cross traffic was light. The driver was required to drive around the block completing four left-turns for each circuit. The total time involved in the turn, the number of eye and head movements and the pattern of gaze were recorded from the post-processed video tape, and it was this digitized information that was used in subsequent analysis.

### Apparatus

The technique used two synchronized video cameras—one on the roof of the car and the other mounted on the driver's head. The synchronization was obtained through time-lock electronic circuitry. The head-set was designed with a mirror attached which allowed eye movements to be observed via the head camera. The spatial position of the eyes in relation to the objects in the scene could be calibrated at the beginning of each experimental session, and

subsequently recorded during driving. A real-time clock was embedded in both camera images in the post production editing.

## Results

In the present work, the descriptive results from the first subject are reported. Initially, to code the videotape data, the forward visual scene was divided into four potential sectors of gaze. These are illustrated in figure 5. As can be seen, they represent the potential locations of conflicting traffic. Figure 6 gives the descriptive breakdown by percentage time of the eye movement pattern with respect to the busy

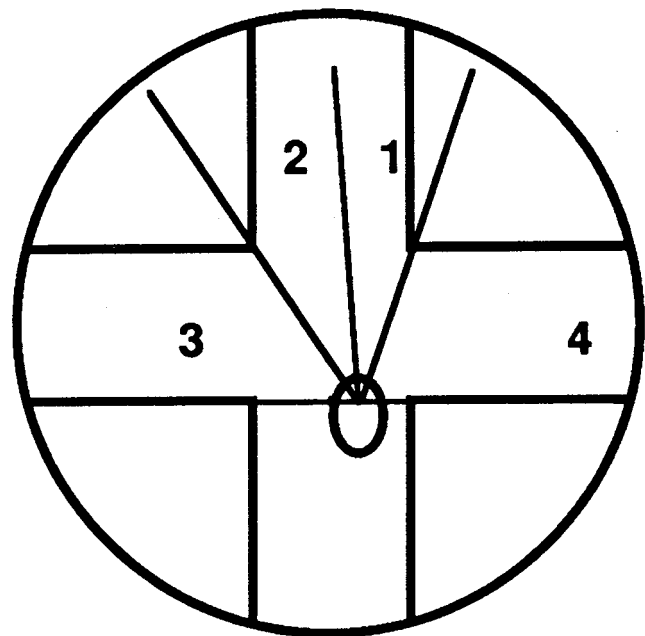


Figure 5. Descriptive regions for eye fixation.

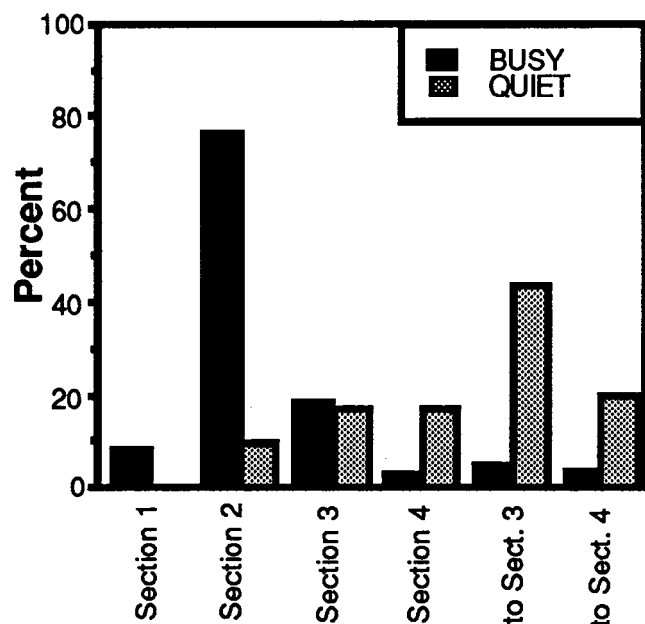


Figure 6. Descriptive breakdown of eye-fixation location, relative to total turn time.

and quiet intersections. While each sector is identified, two additional categories are given. They represent eye movements into sectors 3 and 4, respectively.

## Discussion

With respect to detection failures that occur during the left-turn sequence, there are two lines of evidence to be considered. The first centers around the significant increase in head movements. Detection failures due to looking in the other direction are regarded as *structural interference*. This can take two forms. The most common form is the masking of the on-coming vehicle by some visual obstruction. The alternate form relates to the restriction of the visual system. We have limited access to the 360 degree visual field, and structural interference can arise because the driver is simply looking in the other direction. To the experimentalist these are rather mundane findings, however, our evidence from the increasing propensity to head movement during turns warns that such behavior can be an important source of detection failure. Data indicate that there was no significant difference between head movements for the left and right turn sequences. However, the result of a detection failure when turning across traffic is clearly different than the result of such a failure when turning with no opposing on-coming vehicles. It is also reasonable to suggest that structural interference due to head movement is more liable to result in missed targets with smaller frontal surface area rather than larger frontal surface area simply from the absolute intensity with which such a target impacts the retina.

The second line of evidence addressed by the present data is *resource competition*. It is postulated that there are some limits to the central processing capability. Differing performance demands tax the central processing capability to differing degrees. One theory that uses the concept of a limited central capability is the unitary attentional resource model of human information processing. Despite extensions into multiple resource constructs (Wickens, 1987), which provide explanatory power at the expense of additional degrees of freedom, the unitary resource model (Kahneman, 1973) is usually taken as the model construct through which to interpret secondary task information. The basic rationale is that the performance of the secondary (probe) task, is a reflection of the residual attention left after performance on the primary (driving) task is accomplished. There are numerous discussions about the validity of this model and particularly this assumption (see Kantowitz, 1987). The length of time taken to respond to the secondary probe is taken as a measure of the residual attention. In the present findings, it is clear that processing time to the secondary task is increased with the difficulty of the driving maneuver between turning and straight driving. These findings are in line with those of Miura (1986; 1987). He examined driver response to a stimulus lights on the windshield that were illuminated at differing spatial locations and at random intervals. Miura found that as the situational demands increased (driving in high-crowded

downtown traffic compared to a low-crowded one-way route), the associated reaction time also increased. Also, higher demands resulted in a narrower functional visual field. In a number of experimental procedures (see Hancock & Meshkati, 1988), processing time to the secondary task is taken as a direct reflection of the mental workload demanded by the task. In our experiments, this assertion was supported by the findings for the physiological reflection of workload as reflected in eye blinks per second (Hancock, Meshkati, & Robertson, 1985). It has been observed that as subjects increase mental effort, particularly with respect to a visual task, the eye blink response is suppressed. In the first experiment, we found a significant depression, depending upon driving sequence, that followed the probe response time.

The findings for subjective workload response presented a somewhat supportive pattern of data. First, it was established that there was no significant difference between the test drive and a nominal commute with similar road conditions. While a number of cautions have been raised concerning the influence of memory on subjective ratings (Eggemeier, Melville, & Crabtree, 1984), the present data indicate that subjects found driving the test car of similar load to their usual commute. The data from the subjective workload probes inserted into the driving sequence indicated no significant effects for driving maneuver on perceived workload. However, examination of the actual response indicates a propensity toward higher workload during turn sequences in accord with the other workload measures. As with all recorded responses, however, there were dominating effects for individual differences. Indeed, one of the major findings of the first experiment was the range of responses recorded across differing individuals each faced with the same common performance task. In summary, the results from the first experiment all point to the conclusion that the responses involved with turning sequences are liable to increase detection failures through increasing structural interference and through the reduced central processing capability that remains when a more difficult performance response is demanded. In the latter condition, less residual attention is available to monitor the surrounding environment for potential sources of threat. This finding dovetails nicely with the observations of performance under stress where a functional attentional "narrowing" occurs as greater stress is imposed (Easterbrook, 1959). In the present case, the stress is the increased demand of driving difficulty. Also, the present findings are allied to previous use of mental workload techniques to evaluate driving performance (for a critique see Noy, 1987).

As yet, evidence from the second experiment is sparse and provides only initial indications of behavior during the turn sequences. However, the methodology that we, and some of our colleagues are developing (Rahimi & Briggs, 1989), may be able to relate gaze patterns to environmental targets and distractors during carefully preanalysed maneuvers. An initial question concerns the temporal

duration of the turn. From an initial point of opportunity to the completion of the turn there was an unsurprising three-fold increase in duration from the quiet to the busy intersection. This highlights an important question as to the appropriate scales upon which to base comparisons across the numerous types of left-turn. Clearly, there is a need for a taxonomy of left-turn configurations to form a framework upon which to base comparative inference. It is upon this work that our laboratory is presently engaged. Understanding perception-action systems in a complex visual world is a difficult challenge. Understanding the etiology of rare collision events where actual information about pre-collision behavior is inaccessible is even more so. The price of ignorance with respect to such understanding is the continuation of serious and often fatal injury to motorcycle riders.

## References

- Allgemeiner Deutscher Automobil-Club (1987). *Mitteilungen der Hauptabteilung Verkehr*. Reg. NR. 03.15/228, München (West Germany).
- Appel, H., Otte, D., & Wüstemann, J. (1986). Epidemiologie von Unfällen motorisierter Zweiradfahrer in der Bundesrepublik Deutschland: Sicherheitsaspekte. In: H. Koch (Ed.), *Der Motorradunfall: Beschreibung, Analyse, Prävention* (pp. 48–92). Bremerhaven (West Germany): Wirtschaftsverlag.
- Dahlstedt, S. (1986). A comparison of some daylight motorcycle visibility treatments. Väg-och Trafik-Institutet, Linköping (Sweden).
- Donne, G.L., & Fulton, E.J. (1985). The evaluation of aids to the daytime conspicuity of motorcycles. Department of Transportation, Transport and Road Research Laboratory, *Report No. LR 1137*, Crowthorne.
- Easterbrook, J.A. (1959). The effect of emotion on cue utilization and the organization of behavior. *Psychological Review*, *66*, 183–207.
- Eggemeier, F.T., Melville, B.E., & Crabtree, M.S. (1984). The effect of intervening task performance on subjective workload ratings. *Proceedings of the Human Factors Society*, *28*, 954–958.
- Engel, F.L. (1976). Visual conspicuity as an external determinant of eye movements and selective attention. Eindhoven University of Technology.
- Fulton, E.J., Kirkby, C., & Stroud, P.G. (1980). Daytime motorcycle conspicuity. Transport and Road Research Laboratory, Dept. of the Environment, Dept. of Transport, Supplementary Report 625.
- Hancock, P.A., Hurt, H.H., Ouellet, J.V., & Thom, D.R. (1986). Failures of driver sustained attention in the etiology of motorcycle-automobile collisions. *Proceedings of the Annual Meeting of the Human Factors Society of Canada*, Vancouver, Canada.
- Hancock, P.A., & Meshkati, N. (1988). *Human mental workload*. Amsterdam: North-Holland.
- Hancock, P.A., & Meshkati, N., & Robertson, M.M. (1985). Physiological reflections of mental workload. *Aviation, Space and Environmental Medicine*, *56*, 1110–1114.
- Hart, S.G., & Staveland, L.E. (1988). Development of NASA-TLX (Task Load Index): Results of empirical and theoretical research. In: P.A. Hancock and N. Meshkati (Eds), *Human Mental Workload* (pp. 139–183). North-Holland: Amsterdam.
- Hurt, H.H., Jr., Ouellet, J., & Thom, D.R. (1981). Motorcycle accident cause factors and identification of countermeasures, Vol. 1: *Technical Report*. Traffic Safety Center, University of Southern California, Los Angeles.
- Janoff, M.S. (1973). Motorcycle noticeability and safety during the daytime. *Proceedings of the Second International Congress on Automotive Safety*, Paper No. 73034, San Francisco.
- Janoff, M.S., & Cassel, A. (1970). Effect of distance and motorcycle headlight condition on motorcycle noticeability. *Highway Research Record*, *377*, 64–67.
- Kahneman, D. (1973). *Attention and effort*. Prentice-Hall: Englewood Cliffs, N.J.
- Kantowitz, B.H. (1987). Defining and measuring pilot mental workload. *Proceedings of the 1987 Mental State Estimation Workshop*. Hampton, VA: NASA-Langley Research Center.
- Miura, T. (1986). Coping with situational demands: A study of eye movements and peripheral vision performance. In: A.G. Gale (Ed.), *Vision in vehicles*. North-Holland: Amsterdam.
- Miura, T. (1987). Behavior oriented vision: Functional field of view and processing resources. In: J.K O'Regan and A. Levy-Schoen (Eds.), *Eye movements: From physiology to cognition*. North-Holland: Amsterdam.
- National Safety Council (1987). *Accident facts*. Chicago: National Safety Council.
- Noy, Y.I. (1987). Theoretical review of the secondary task methodology for evaluating intelligent automobile displays. *Proceedings of the Human Factors Society*, *31*, 205–209.
- Olson, P.L., Hallstead-Nussloch, R., & Sivak, M. (1979a). Development and testing of techniques for increasing the conspicuity of motorcycles and motorcycle drivers. Technical Report No. DOT HS 805 143, U.S. Department of Transportation.
- Olson, P.L., Hallstead-Nussloch, R., & Sivak, M. (1979b). Means of making motorcycles more conspicuous. *The HSRI Research Review*, *10*, September-October.
- Olson, P.L., Hallstead-Nussloch, R., & Sivak, M. (1981). The effect of improvements in motorcycle/motorcyclist conspicuity on driver behavior. *Human Factors*, *23*, 237–248.
- Rahimi, M., & Briggs, R.P. (1989). A field evaluation of driver gaze patterns toward environmental targets and distractors. Internal Report, Motorcycle Conspicuity Group, May, 1989.
- Reid, G.B., & Nygren, T.E. (1988). The subjective workload assessment technique: A scaling procedure for measuring mental workload. In: P.A. Hancock and N.

Meshkati (Eds.), *Human mental workload* (pp. 185–214). North-Holland: Amsterdam.

Stroud, P.G., & Kirkby, C. (1976). A study of the conspicuity of the motorcyclist in a daylight urban environment. Institute for Consumer Ergonomics, Department of Transport Technology, University of Technology, Loughborough, Leicestershire.

Stroud, P.G., Kirkby, C., & Fulton, E.J. (1980). Motorcycle conspicuity. *Proceedings of the International Motorcycle Safety Conference*, Volume IV, 1705–1722.

Waller, P.F. (1972). An analysis of motorcycle accidents with recommendations for licensing and operation. The University of North Carolina Highway Safety Research Center.

Weber, H., & Otte, D. (1980). Unfallauslösende Faktoren bei motorisierten Fahrrädern. Bundesanstalt für Straßenwesen, Köln (West Germany).

Wickens, C.D. (1987). Attention. In: P.A. Hancock (Ed.), *Human factors psychology* (pp. 29–80). North-Holland: Amsterdam.

Williams, M.J., & Hoffmann, E.R. (1977). The influence of motorcycle visibility on traffic accidents. Department of Engineering, University of Melbourne.

Williams, M.J., & Hoffmann, E.R. (1979). Conspicuity of motorcycles. *Human Factors*, 21, 619–626.

Wulf, G., Hancock, P.A., & Rahimi, M. (1989). Motorcycle conspicuity: An evaluation and synthesis of influential factors. *Journal of Safety Research*, in press.

## Acknowledgements

This research was supported by the Motorcycle Safety Foundation and American Honda Motor Co. We would like to thank Professor H.H. Hurt for his valuable comments on an earlier draft of this manuscript, and Andrew Chu for his help with the data collection, and the subjects for their time and effort in the realization of this project.

## Difficulties in Leg Protection Research

**Shinichi Sakamoto**

Japan Automobile Manufacturers Association,  
Inc.

### Abstract

Following the announcement of a leg protection draft specification by the United Kingdom's Department of Transport (UKDTP) in July 1987, we carried out a full-scale test to observe the effects of the UK-proposed leg protectors for the motorcycle rider. The leg protectors were designed, fabricated and verified to meet the performance requirements by the draft specification. Then, by repeating Transport and Road Research Laboratory (TRRL) testing technique, we tested motorcycle 30 degree angle collisions with a fixed barrier, using a dummy with metallic leg bones, and compared the test results with those of TRRL. Subsequently, we tested three collision modes, including a motorcycle-to-car both moving collision. A dummy utilizing "breakable" leg components, unlike the TRRL metal leg components, was used as the motorcycle occupants. Our studies evidence that the utilization of breakable leg bones is preferable as such permits required evaluation of post impact dummy dynamics. As were shown in our former researches (Refs 1 and 2), the leg protectors studied in some cases had the potential of reducing the motorcyclist's lower leg fracture; however, they also indicated the potential of increasing overall injury which results in a dilemma. In this series of tests, the possibility of reducing rider's lower leg fracture with the leg protector is not observed moreover, the possibility of increasing overall injury is indicated again.

---

In sum, the dilemma in motorcycle leg protection research remains.

## Introduction

Research into devices which potentially might protect the legs of motorcycle riders and passengers, without increasing injuries to other parts of the body, has continued over the last 2 decades. To date, this research has not found a viable solution. This is partly due to the basic nature and properties of motorcycles as vehicles; but is also due to the very wide range of crash conditions under which such devices should not create injuries. The research has also been limited by the need for better test methodologies for the assessment of rider injuries, especially in the areas of the leg and the achievement of realistic dummy behaviour.

Notwithstanding this situation, the UK Draft Specification for Leg Protectors (UKDS, Refs 3 and 4) was introduced by the UK Department of Transport in July 1987. However, until now, there has been a lack of any published information or data for devices which actually comply with the UKDS. Also the work of TRRL has been severely limited by methodological problems, as have been documented elsewhere. For these reasons, and in order to understand and comment on the UKDS in a timely way, the Japan Automobile Manufacturers Association and Japan Automobile Research Institute conducted a preliminary full scale evaluation of a leg protector which met the UKDS.

The results of this research are presented in this report.

## Test Method

### Test motorcycle

A Yamaha XS400SP motorcycle, the same model used in the Ref 3 test programme was selected as representative of "medium" sized motorcycles. This was based on epidemiological studies (e.g. Ref 5) which have indicated that the 50th percentile crash situation involved motorcycles which are in the "medium" category. This machine falls within the UKDS "Category 3 (less than 200 kg)" range.

Table 1. Specifications of test motorcycle.

Manufacturer	:	Yamaha
Model	:	XS400SP
Overall length	:	2070mm
Overall Width	:	870mm
Overall height	:	1140mm
Weight	:	170 kg (190,3kg for the UKDLP type)
Appearance	:	Figures 1 and 2.

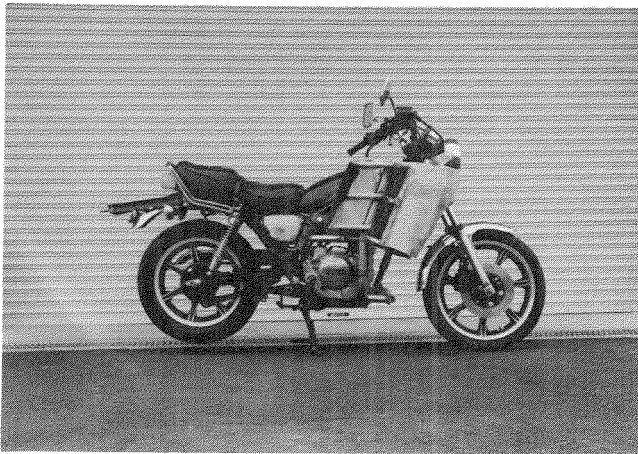


Figure 1. Side view of motorcycle with UKDLP.

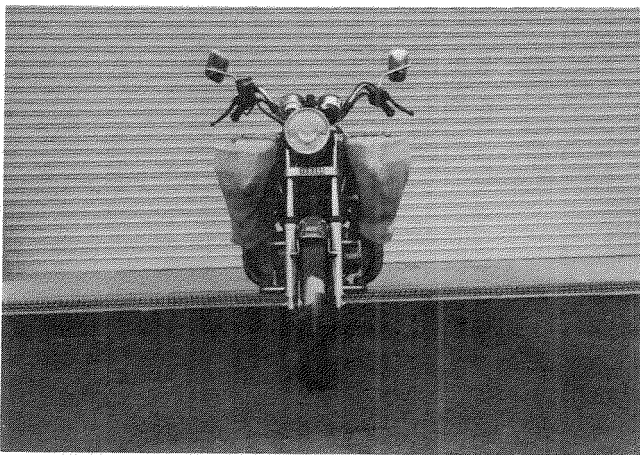


Figure 2. Front view of motorcycle with UKDLP.

### Example UK draft specification leg protector (UKDLP)

A leg protector which complied with the UK Draft Specification was designed, fabricated and laboratory tested. As

specified in the Draft Specification, the three main elements of the example UKDLP are described below.

### Primary impact element (PIE)

The example PIE consisted of aluminium honeycomb and polyurethane foam. Figure 3 shows the displacement characteristics of this PIE when tested using the UKDS impact test procedure.

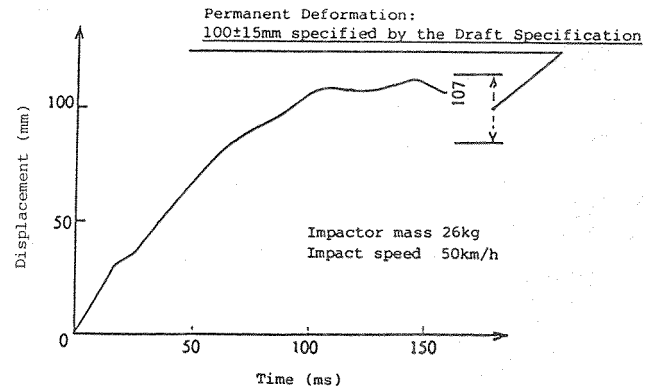


Figure 3. Displacement characteristics of PIE.

### Knee protection element (KPE)

The example KPE consisted of polyurethane foam. Figure 4 shows the kneeform impactor load response during impact with the example KPE when tested using the UKDS impact test procedure.

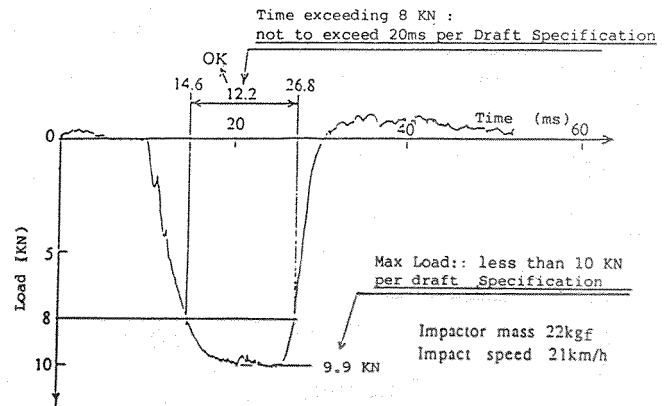


Figure 4. Kneeform impactor load response KPE energy absorption test.

### Rigid support element (RSE)

The example RSE was fabricated from tubular and sheet steel. Figures 5 and 6 show the static load/displacement characteristics and dynamic displacement response of the RSE, respectively.

Analysis indicated that the stiffness of the example RSE was greater than that of the CLP (Crushable Leg Protector) used in the Ref 2 tests.

Table 2 shows the specifications of the PIE, KPE, and RSE materials.

This means a test result which indicates that the device meets the requirements of the draft specification

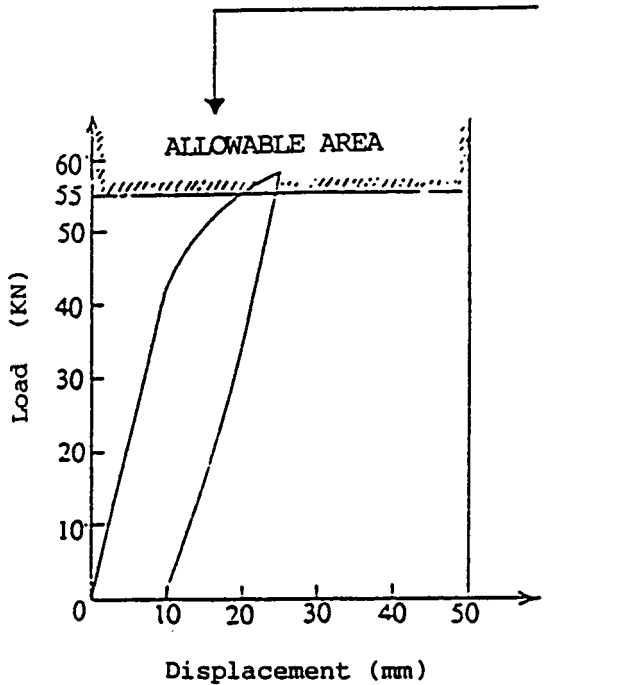


Figure 5. Static load/displacement characteristics of RSE.

Impactor mass 26kgf  
Impact speed 50km/h

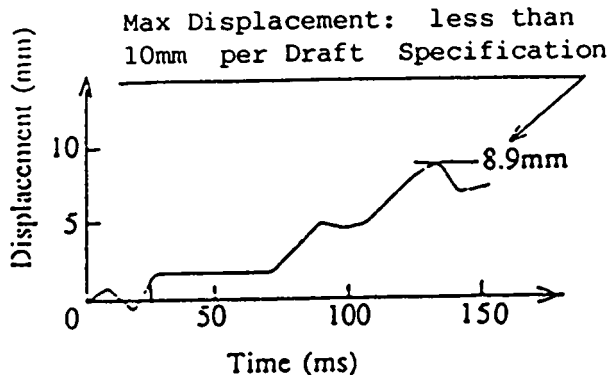


Figure 6. Dynamic displacement response of RSE.

### Fixed Barrier

In order to duplicate the TRRL test method, a fixed barrier 1.23 m high and covered with plywood was fabricated and used in the barrier impact test. While a fixed barrier impact is not realistic, these tests allowed comparisons with tests reported by TRRL, many of which used a fixed barrier. For the same reason, steel dummy leg bones were used in the barrier tests only.

### Opposing Automobile

The Toyota Crown passenger automobile was selected as the opposing vehicle. This automobile, the same size and

Table 2. Specification of example UKDLP (construction).

<u>Primary Impact Element</u>	
Construction	: Polyurethane form and aluminum honeycomb on steel sheet
Energy absorbing component size	: Thickness 145mm(75mm) (Polyurethane foam) 145mm (Aluminum honeycomb)
Aluminum honeycomb	: Manufacture : Hexcel & Showa Model No. : AL 3/8-5052-0.0015N Compression characteristic: 5,0kg/cm <sup>2</sup> Density : 0.026 gr/cm <sup>3</sup>
Polyurethane foam	: Manufacture : Toyo Rubber Industry Model No. : W80 Compression characteristic: 8.7kg/cm <sup>2</sup> Porosity : 93% Density : 0.078 gr/cm <sup>3</sup>
Steel sheet	: SPHC, 6.0mm (JIS G 3131)
<u>Knee Protection Element</u>	
Construction	: Polyurethane on steel sheet
Energy absorbing component size	: Thickness 90mm
Polyurethane foam	: Manufacture : Toyo Rubber Industry Model No. : W80 Compression characteristic: 8.7kg/cm <sup>2</sup> Porosity : 93% Density : 0.078 gr/cm <sup>3</sup>
Steel sheet	: SPHC, 3.2mm (JIS G 3131)
<u>Rigid Support Element</u>	
Composition	: Steel tube structure
Steel tube	: STKM13A OD25.4 x t1.6 (JIS G 3445) STKM13A OD38.1 x t2.0 (JIS G 3445) SGP OD42.7 x t3.5 (JIS G 3452)
	OD : Outer diameter, t : thickness

shape as the Ref 2 test vehicle, although of a different model year, was selected based on accident statistics (e.g. Ref 2) which show that about 80% of the opposing vehicles in motorcycle accidents are passenger automobiles. The Toyota Crown, which is representative of a medium sized automobile when viewed from a worldwide perspective, was believed to be appropriate for the kinematic analysis. The specifications of the automobile are given in table 3.

Table 3. Specifications of opposing automobile.

Manufacturer	: Toyota
Model	: Crown
Overall length	: 4690mm
Overall width	: 1690mm
Overall height	: 1440mm
Weight	: 1380kg
Appearance	: Figure 7 and 8

### Test conditions

For this preliminary evaluation, motorcycle speeds of 24 and 48 km/h, and opposing automobile speeds of 48 and 0 km/h were selected (Ref 2).

The test conditions used for these preliminary tests are summarized in table 4. Motorcycles are involved in diverse types of accidents covering a broad range of vehicle speeds and impact geometries. A representative sampling of this wide spectrum is beyond the scope of this initial study. However, to the extent practical, except for the barrier impacts, the test conditions chosen are believed to be examples of some real world collisions.



The motorcycle was transported to the point of impact by a four-wheeled trolley, on which the motorcycle was held in place by attachments at the handlebar, lower section of the wheels, and at the upper rear section of the frame until its release just prior to impact. Figures 11 and 12 are front and side views of the trolley and motorcycle.

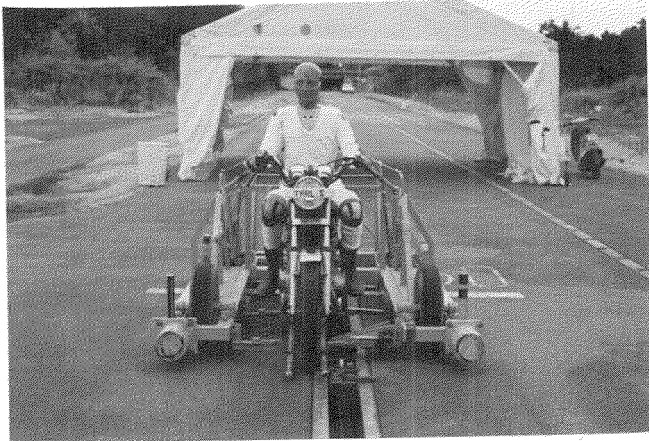


Figure 11. Front view of the trolley.

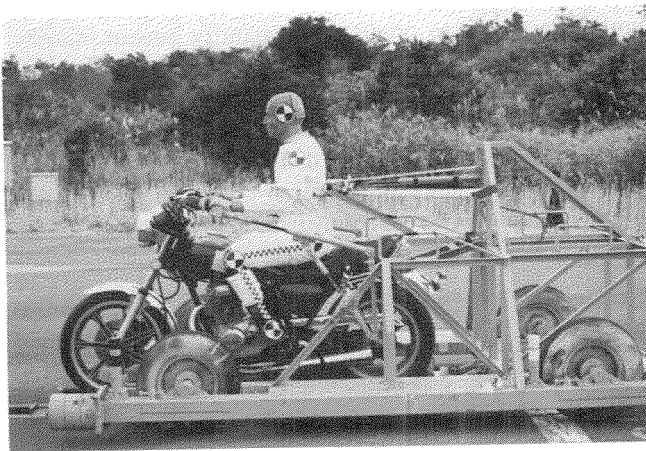


Figure 12. Side view of the trolley.

## Test Measures

### Motorcycle behaviour

The translational and rotational velocities of the motorcycle were determined from high speed film analysis.

### Leg fracture

The fracture modes of the breakable bakelite leg bones were observed to evaluate the leg protective effects of the example UKDLP.

### Dummy behaviour and head velocity

Since past studies indicated that reinforced leg protection structures possessed a potential for increased injuries to the head and chest, the head velocity of the dummy was studied from film analysis to determine the effect of the example UKDLP on head velocity.

## Test Results

### Barrier tests

Table 6 contains velocity data for the barrier impacts. These include motorcycle impact velocity, exit velocity, mean angular velocity, and dummy head forward velocity. Also included in table 6 for comparison are previously reported TRRL data from Ref 8. The post impact velocity was determined at 100 ms after impact and compared with the impact velocity to determine the velocity reduction.

Table 6. Velocity data for 30° fixed barrier impacts.

Motorcycle configuration	Motorcycle				Dummy head Forward* velocity (m/s)
	Impact velocity (m/s)	Exit velocity (m/s)	Velocity reduction (%)	Mean angular velocity (rad/s)	
S T D ( Test No. L-1) Unmodified Motorcycle (TRRL Test)	13.3	8.9	33.1	7.0	8.3
	13.4	9.2	31.3	6.7	13.7
U K D L P (Test No. L-2) Soft cone Protector (TRRL Test)	13.4	9.3	30.6	4.1	7.4
	13.7	6.7	51.1	2.6	12.1

\* 100 ms After Impact

The exit velocity of the standard motorcycle was slightly lower (reduced by 33.1%) compared to that of the example UKDLP motorcycle (reduced by 30.6%). In contrast, Ref 8 showed a larger reduction of motorcycle velocity with the TRRL prototype device (51.1%) when compared to the unmodified motorcycle (31.3%). Thus, the present evaluation and the TRRL tests show some difference in this respect.

Figure 13 and table 6 show that the mean angular velocity of the example UKDLP motorcycle was clearly lower than that of the standard motorcycle. This result was similar to the TRRL Ref 8 tests results.

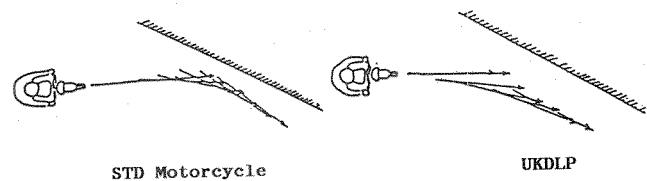
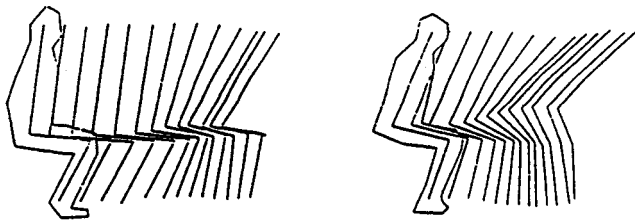


Figure 13. Plane view of motorcycle trajectory during barrier impact (0-120ms).

The dummy forward head velocity reduction was larger for the example UKDLP than for the standard motorcycle. This agreed with the TRRL finding that the head velocity reduction was larger for the motorcycle with the device than for the unmodified motorcycle. On the other hand, an evaluation of the head velocity 100 ms after impact, as suggested by TRRL, may be meaningless in this test configuration, since the shoulder had already contacted the barrier and the head motion had changed due to the reaction force from the barrier, as shown in figure 14.

The dummy behaviour shown in figure 14 indicates that lifting of the hip and pitching of the torso were more accentuated with the example UKDLP motorcycle than with the standard motorcycle, which agreed with the TRRL test results.



STD motorcycle

UKDLP

Figure 14. Side view of trajectory of dummy hip, shoulder, and leg (0-120ms).

Overall, for the barrier tests there was general agreement between the results of the present evaluation and the Ref 8 TRRL results. Quantitative discrepancies may be due to the differences in the test motorcycles (shape, size, weight, the position of center of gravity, etc.), the test device, test dummy and in different test conditions such as road surfaces and friction coefficients between the motorcycle and the barrier.

## Tests Involving Passenger Cars

### Leg fracture

Although research continues into bone fracture mechanisms, breakable bakelite bones were considered capable of providing some indication of the likelihood of leg fracture. The breakable bakelite bones provided data indicating whether or not the loads were sufficient to cause fracture. They also enabled an evaluation of various fracture modes by analysis of its fracture section surface shape.

The fracture terminology utilized herein is for descriptive purposes. It is recognized that generally both the bending and the compression fractures are more appropriately termed transverse fractures.

In this report: "bending" fracture means a transverse fracture resulting from a bending moment applied to the bone; "compression" fracture means a transverse fracture which results from axial loading applied along the longitudinal axis of the bone.

Table 7 includes the leg fracture occurrence data for the present evaluation series, and also from Ref. 2.

Table 7. Leg fracture data.

Collision configuration	Angled			Brookside			Offset frontal			
	Test No..	A-3	A-4	A-5	B-3	B-4	B-5	C-1	C-2	C-3
Motorcycle configuration	STD	CLP	UKDLP	STD	CLP	UKDLP	STD	CLP	UKDLP	
Mode of fracture	Upper leg	C	C	B,C,T	C	C	B,C	None	C	C
	Lower leg	B	B	B	B	None	B	B	None	B

B...Bending C...Compression T...Torsional  
"CLP" denotes the crushable leg protector used in Ref 2.

Experimentally, the nature of the fracture was determined by an examination of the shape of the fracture point and by film analysis of the dummy behaviour.

The present test results indicate that bone fractures occurred in both the upper and lower leg in all collision configurations with the example UKDLP motorcycles.

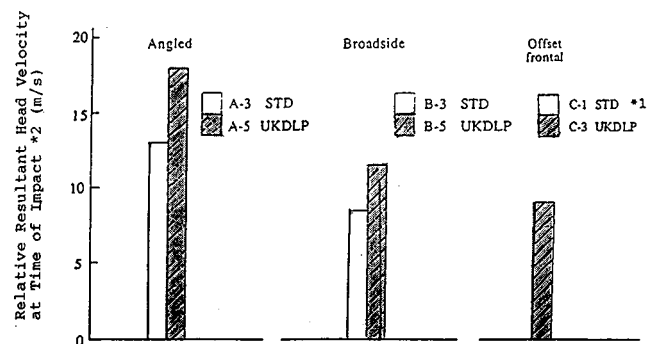
From the standpoint of leg fracture occurrence and fracture severity, the example UKDLP motorcycle is clearly more harmful than both the standard motorcycle and the CLP motorcycle used in Ref 2. The effects of the example UKDLP on the dummy can be summarized as follows:

- In the 45 degree angled collision (A-5), the example UKDLP caused combined (torsional, bending and compression) fractures in the leg.
- In the broadside collision (B-5), the example UKDLP caused a more severe combined (compression and bending) fracture.
- In the offset frontal collision (C-3), the example UKDLP caused a fracture in the upper leg which did not occur in the case of the standard motorcycle.

### Head velocity

The analysis of injury to the head and chest is necessarily incomplete. Not only is there lack of agreement in the medical field concerning injury criterion, but in addition, appropriate dummy technology is lacking.

In the case of the angled and broadside collisions, where head impact to the bonnet seemed likely, the possibility of head injury was evaluated by comparing the resultant head velocity relative to the opposing automobile. Figure 15 shows the effect of the example UKDLP on the relative resultant head velocity.



\*1 : No data: No impact on the ground occurred with STD, the dummy stayed on the motorcycle.

\*2 : In the case of the angled and broadside collision, head velocity at the moment right before any part of the dummy's upper body contacts the bonnet of the opposing automobile. And in the case of the offset frontal collision, head velocity at the moment right before the dummy's head hits the ground.

Figure 15. Comparison of relative resultant head velocity.

- The relative resultant head velocity at the time of impact was increased by the example UKDLP in the angled collision (A-5). The dummy behaviour also indicated a high degree of dummy restraint by the example UKDLP. The initial impact, along with the intrusion of the example UKDLP and leg under the bonnet, resulted in combined fractures of the upper leg.

- In the broadside collision (B-5), because the leg space appeared to be preserved by the RSE of the example UKDLP, the upper body of the dummy was violently ejected, causing the head velocity to be increased. This indicates that the example UKDLP has the potential of increasing head injury.
- In the case of the offset frontal collision (C-1), the dummy stayed on the motorcycle and fell down together on the ground. On the other hand, in the case of the example UKDLP in the offset frontal collision (C-3), severe pitching motion of the dummy was observed as described in page 24.

### Dummy behaviour

To determine the tendency to eject the dummy from the motorcycle, the hip lift was measured. The results are shown in figure 16.

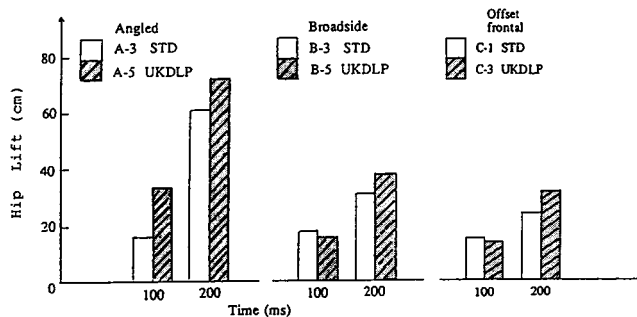


Figure 16. Comparison of hip lift.

These results suggest that the example UKDLP has somewhat more tendency to cause higher hip lift and a more violent ejection of the dummy.

The major features of the dummy behaviour in each collision configuration are as follows:

- In the angled collision (A-5), because the left lower leg is firmly restrained by the KPE and intrudes under the bonnet, the occupant was pushed back by the opposing vehicle, which increased the impact on the leg and thus caused a leg fracture. Further, the occupant's torso pitched violently, increasing the head movement towards the bonnet, causing the neck to be flexed severely.
- In the broadside collision (B-5), because leg space was preserved by the RSE of the example UKDLP, the upper body of the motorcycle occupant was violently ejected towards the opposing automobile. On the other hand, no damage to the PIE was observed, indicating that the example UKDLP absorbed little of the collision energy. In this collision configuration, therefore, the example UKDLP produced the negative effect of causing a more violent body ejection perhaps associated with the preservation of leg space.
- In the offset frontal collision (C-3), although the motorcycle was decelerated violently by the relatively high stiffness of the RSE, the knee was restrained by the KPE as the occupant continued

to move in the initial forward direction. The resulting deceleration of the motorcycle and the occupant's knee caused the upper body to pitch violently, and the dummy to eject and hit the road head first. At the same time, because the KPE restrained lateral movement of the knee, the left lower leg was initially forced to roll to the right with the motorcycle while the upper torso continued forward. In summary, the upper and lower body tended to move in different directions, placing an extremely large load on the femur and pelvis. This bone fracture mechanism was clearly visible in the film analysis.

### Motorcycle motion

As in the case with the CLP motorcycle, Ref 2, the example UKDLP motorcycle tumbled after impact with the opposing automobile in the broadside collision configuration. The fact that the motorcycle equipped with the leg protector tumbled in both the Ref 2 test and the present test is a serious problem, since tumbling can involve and injure third parties in an accident.

### Discussion

It was found, in general, that the barrier impact results obtained in this study were similar to those reported by the TRRL, although there were some quantitative differences in some specific measurement items.

The results of these preliminary evaluations indicated that a protector complying with the UK draft specification not only failed to reduce leg injury in all three of the collision configurations but also induced more serious, combined, upper leg fractures, strongly suggesting that such a device can actually increase leg injuries. The degree of harm caused by this device was greater than those of the side protection device used in the Ref 1 experiments and the crushable leg protector used in the Ref 2 experiments.

In addition, it was found that the dummy was pushed back together with the motorcycle by the opposing automobile in an angled collision. The upper body of the occupant pitched violently, increasing the head movement towards the automobile, causing the neck to be flexed severely while the head was accelerated downward. Obviously this may tend to increase head injuries, neck and spinal cord damage, and other injuries to the motorcycle occupant.

In the offset frontal collision, the occupant sustained not only lower leg fractures but also more complex injuries to the upper leg and other body parts because the lower leg was restrained and forced to move with the motorcycle.

In a broadside collision, the upper body of the dummy was ejected violently towards the opposing automobile, causing an increase in the head velocity, as found in past investigations. This suggests that the occupant may sustain more serious head injuries with the example UKDLP.

In the broadside collision, it is important to note that the motorcycle with the example UKDLP tumbled after impact with the opposing automobile. Past studies have also

observed a similar type of tumbling caused by proposed leg protective devices. This is a serious negative effect that should not be overlooked, since tumbling can involve third parties in accidents.

## Conclusion

The results of the present evaluation clearly indicate that the example UKDLP was not only unable to reduce lower leg fractures, but could result in more serious upper leg fractures and damage to other parts of the body, including the head, in some cases.

As noted in other studies, it is important to continue to work toward the improvement of test and evaluation methods used in rider protection research, for use in evaluating any future leg protector proposals.

## References

- (1) Uto, T., "Side Collision Test of Motorcycles Equipped with Side Protection Devices", JAMA, December, 1975.
- (2) Tadokoro, H., S. Fukuda, and K. Miyazaki, "A Study of Motorcycle Leg Protection", The 10th International Technical Conference on Experimental Safety Vehicles, Oxford, July, 1985.
- (3) "Draft Specification: Leg Protection for Riders of Motorcycles", June, 1987. Vehicle Standards and Engineering Division Department of Transport UK.
- (4) Chinn, B.P., "Leg Protectors for Riders of Motorcycles, Explanatory Report to Motorcycle Leg

Protector Specification", Transport and Road Research Laboratory, August, 1987.

(5) Hurt, H.H., Jr., J.V. Ouellet, and D.R. Thom, "Motorcycle Accident Cause Factors and Identification of Countermeasures, Volume II": Appendix/Supplemental Data, DOT-HS-5-01160, January 1981.

(6) Tadokoro, H., "Load Measuring Method of Occupant's Leg on Motorcycle Collision", The 11th International Conference on Experimental Safety Vehicles, Washington D.C., May, 1987.

(7) Fuller, P.M., and J.N. Snider, "Lower Leg Injuries Resulting from Motorcycle Accidents", The 11th International Conference on Experimental Safety Vehicles, Washington D.C., May, 1987.

(8) Chinn, B.P., and M.A. Macaulay, "Leg Protection for Motorcycles", International IRCOBI Conference on the Biomechanics of Impacts, 1984.

(9) Motoshima, T., "Studies on the Strength for Bending of Human Long Extremity Bones", Magazine of Kyoto Prefectural, University of Medicine, Vol. 68, No. 6, pp. 1377-1397, Sept. 14, 1960 ed.

## Acknowledgement

This study described herein was performed by the Motorcycle Rider Protection Subcommittee of JAMA. The tests used for this study were conducted at the Japan Automobile Research Institute (JARI), JAMA expresses its appreciation to Mr. MIYAZAKI and other members of JARI for conducting the experiments used in this study.

## A Study on Required Field of View for Motorcycle Rear-View Mirrors

**Masanori Motoki,**  
Japan Automobile Research Institute, Inc.  
**Tsuneo Tsukisaka,**  
Japan Automobile Manufacturers Association,  
Inc.

### Abstract

In this study, with the overall goal object to determine the desired field of view for motorcycle rear-view mirrors, we examined the role of the direct rearward field of view by head check and the role of the indirect rearward field of view by mirror check. The following three research items were selected:

(1) Head check duration and frequency, mirror check duration and frequency, category Judgment for the rearward field of view were obtained on actual roads using a test motorcycle with various rear-view mirror fields of view and a test car with typical rear-view mirrors.

(2) The ratio by number of riders who used the direct rearward field of view by head check was measured with a sample of riders in typical traffic situations, such as lane changes and lane merges, in which the rider needed rearward information.

(3) The limits of the direct rearward field of view by head check within which the rider could perceive a following car were measured.

As the results of these studies, we suggest considerations for performance requirements (required field of view) and design requirements (i.e. rear-view mirror curvature, size and mounting position) relating waiting to possible designs for motorcycle rear-view mirror field of view in the future period.

## Introduction

In order to help determine future design requirements (such parameters as the rear-view mirror curvature, size, and mounting position) and possible performance requirements (field of view reference) for the field of view of the motorcycle rear-view mirror, the following prerequisites should be clarified:

- (1) A method of eye point determination as a reference point for field of view measurements.
- (2) A measurement method of field of view for motorcycle rear-view mirror.
- (3) The necessary field of view for motorcycle rear-view mirrors.

Among these, concerning the eye point determination method and the development of a 3-dimensional motorcycle manikin for use in establishment of the eye point, we have already made a report based upon data from 155 American riders at the 10th ESV Conference (Motoki, M. and Asoh, T., 1985) (1).\*

Also, concerning the measurement method of field of view for motorcycle rear-view mirrors using a 3-dimensional manikin on actual motorcycles as well as computer simulation for assessment of the field of view for rear-view mirror in the design stage, we have already made a report based upon data from 26 American riders at the 11th ESV Conference (Motoki, M. and Tsukisaka, T., 1987) (2).

Accordingly, in order to help determine future design requirements and possible performance requirements for the field of view for motorcycle rear-view mirrors, there is the further necessity for clarifying the necessary field of view for rear-view mirrors.

For this reason this study took its objective in the clarification of the desired field of view for motorcycle rear-view mirrors, making comprehensive considerations of the role of the direct rearward field of view when actually turning the head (hereafter referred to as the 'head check'), as well as the role of the indirect rearward field of view through the rear-view mirror (hereafter referred to as 'mirror check') (figure 1).

Work was carried out over four items listed below:

- (1) Survey on use of direct rearward field of view and indirect rearward field of view.  
Concerning the proper use of direct rearward field of view and indirect rearward field of view in typical

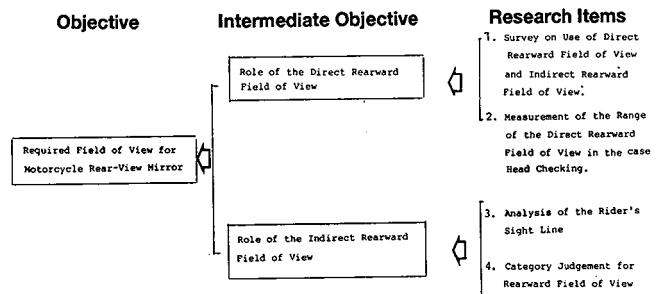


Figure 1. Study process.

traffic situations (lane changing and merging) in which rear information is necessary, a survey was carried out on a large number of non-specified drivers on public roads.

(2) Measurement of the range of the direct rearward field of view in the case of head checks.

Measurements were made of the range of vehicles coming from behind that can be seen by direct rearward field of view through head checks on riders driving on a test course.

(3) Analysis of rider's sight line.

Analysis of the sight line of riders when changing lanes driving on a test course provided a determination grasp of the time span and frequency of both head checks and mirror checks.

(4) Category judgment of rearward field of view.

Test vehicles with altered rear-view mirror fields of view were driven on public roads in order to obtain rider's category judgment of the rear-view mirror field of view, as well as to determine the time span and frequency of both head checks and mirror checks in actual traffic situations (lane changing and merging).

## Survey on Use of Direct Rearward Field of View and Indirect Rearward Field of View

### Purpose

In situations where rear information is necessary, riders obtain it by use of their direct rearward field of view through head checks and of their indirect rearward field of view through mirror checks.

Here a determination was achieved of the actual condition in the use of direct rearward field of view and indirect rearward field of view for obtaining the rear information necessary in typical traffic situations (lane changing and merging).

### Method

*Survey on lane changing situation.*—This survey was carried out by observation vehicles (passenger cars) travelling at a speed of 60km/hr in the outside lane of 2-lane expressways (Tohoku Expressway and Higashi Meihan Expressway). Observation of the behavior of riders of vehicles coming from behind and changing lanes to pass was ob-

\*Numbers in parentheses designate references at end of paper.

served and filmed with a video camera to investigate the presence or absence of head checks (figure 2).

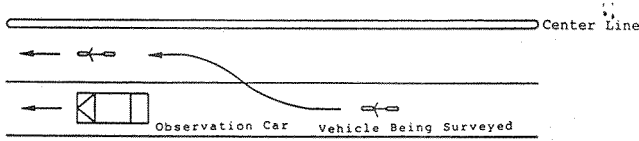


Figure 2. Survey conditions in a lane changing situation.

*Survey on merging situation.*—The survey was carried out by observation and filming with video cameras from the road side or a walk bridge near the merging position from an expressway to a highway or a road or vice versa to investigate the presence or absence of head checks (figures 3 and 4).

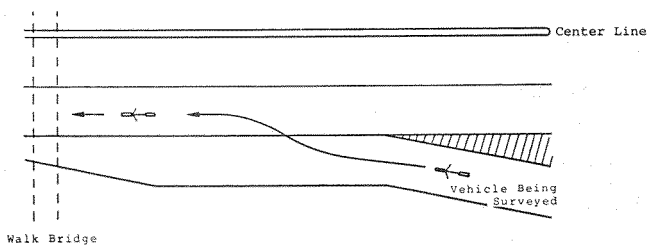


Figure 3. Survey conditions in a merging situation.

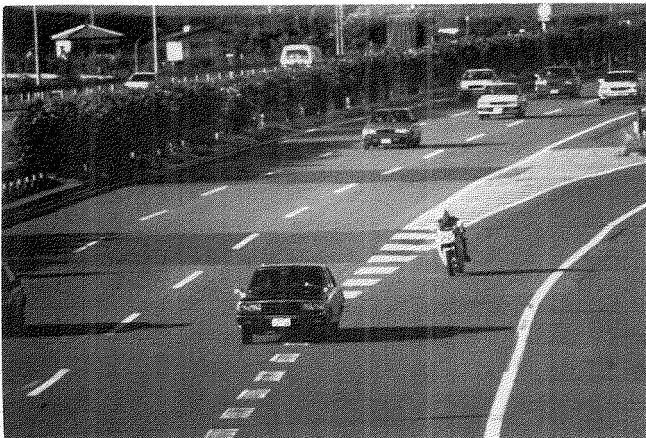


Figure 4. An example of a head check in a merging situation.

The following three types of observation positions were utilized:

- (a) Merging position from the expressway to a road (near Kameyama Interchange).
- (b) Merging position from the expressway to a highway (near Yawahara Interchange).
- (c) Merging position onto the expressway (Yawahara Interchange).

Further, at survey position (a), investigation of the presence or absence of head checks among drivers of 4-wheeled vehicles (passenger cars) was also carried out.

## Results and considerations

The surveyed number of motorcycle riders was 515 and of 4-wheeled vehicles was 246.

The ratio of drivers who made head checks in lane changing and merging situations is shown by observation position in table 1 and figure 5.

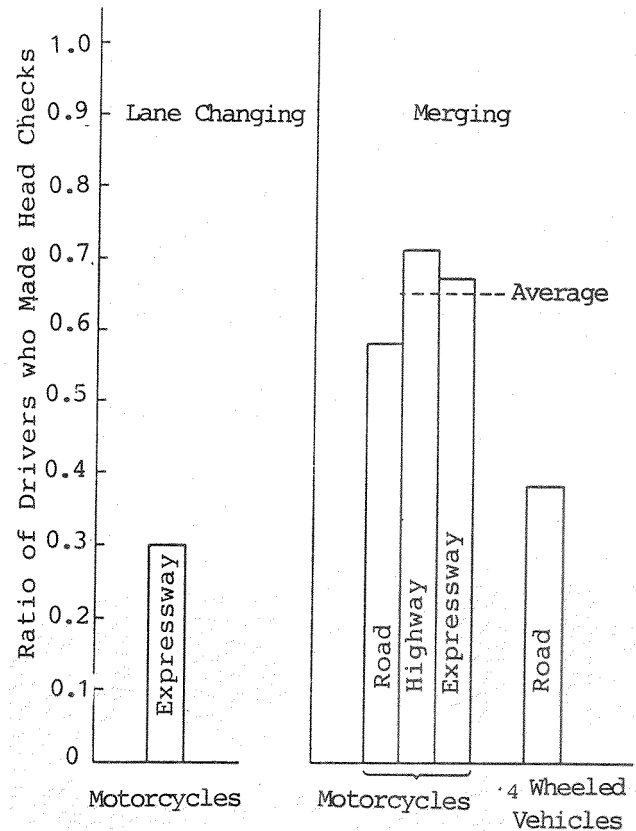


Figure 5. Ratio of drivers who made head checks both lane changing and merging situations.

Table 1. Ratio of drivers who made head check.

Traffic Situation	Observation Position	Vehicles	
		Motorcycle	4-Wheeler
Lane Changing	Expressway	0.30 (33/110)	No Data
	Road	0.58 (140/242)	0.38 (93/246)
Merging	Highway	0.71 (45/63)	No Data
	Expressway	0.67 (67/100)	No Data

(NOTE) Figures in parenthesis indicate the number of drivers who made head check and the number of drivers taken as survey subjects

The percentage of riders who made head checks in lane changing situations was 30%, meaning that about one in three made head checks.

The percentage of riders who made head checks in merging situations was from 58% to 71%, meaning that around two in three made head checks.

Also, the percentage of 4-wheeled vehicle drivers who made head checks in merging situations was 38%, meaning that around two in five made head checks.

Compared with lane changing situations, the ratio was more than double for riders who made head checks in merging situations. It is thought that the major reason behind this

is that due to differences in road lane shapes. It is more difficult to obtain rear information with any other method than head checks (including use of the rear-view mirror field of view) for merging than for lane changing.

Thus, in situations where rear information is necessary, it has become clear that both motorcycle riders and 4-wheeled vehicle drivers make head checks depending on the traffic conditions.

## Measurement of the Range of the Direct Rearward Field of View in the Case of Head Checks

### Purpose

A determination grasp of the direct rearward field of view range is made by measuring the range at which a rear vehicle can be seen through head checks by riders while driving.

### Method

*Test vehicle.*—European type motorcycles on which the rear-view mirror is mounted on the fairing were utilized (see figures 6, 7 and table 2). A video system was installed on the test vehicles for the purpose of recording the rider's sight lines and the rear traffic conditions as well as the rider's

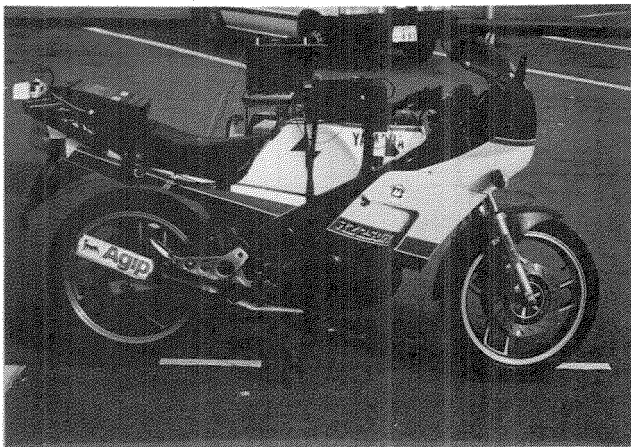


Figure 6. Test vehicle.

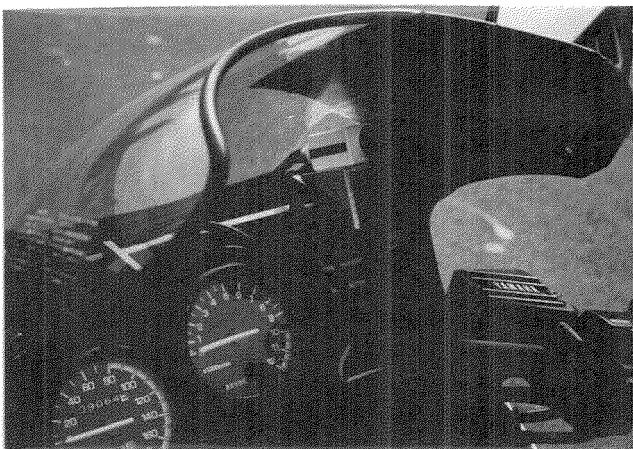


Figure 7. Small video camera for recording sight line.

Table 2. Location of reference point and rear-view mirror specifications.

Type	Item	Related to Riding Position			Related to Rear-View Mirror	
		R Point	G Point	F Point	M Point	Rear-View Mirror Specification
European Type	X	0	743	135	996	Vertical Height: 104 Lateral Width: 125 Curvature Radius: 1200
	Y	0	±260	±243	±295	
(R' Point Height: From G/L: 800)	Z	±60	±160	-440	+325	

(NOTE) The express method for vehicle reference point is in accordance with JASO 005

R Point: Design Standard Point that Corresponds to the Hip Point  
G Point: Center Point of the Upper Surface of the Effective Portion of the Handgrip  
F Point: Center Point of the Upper Surface of the Effective Portion of the Footrest  
M Point: Center Point of the Mirror Surface

voice (two small video cameras, and image synthesizer unit, and a video recorder).

*Helmet.*—In cases where the forward inclination angle of the rider's posture is large, the direct rearward field of view by head checks is sometimes limited by the helmet.

Here two types of helmets were utilized. One example has the standard full-face opening (hereafter referred to as the 'Standard Helmet'), and the other is a full-face helmet with the opening expanded downward from that of the Standard Helmet (hereafter referred to as the 'Improved Field of View Helmet') (figure 8).

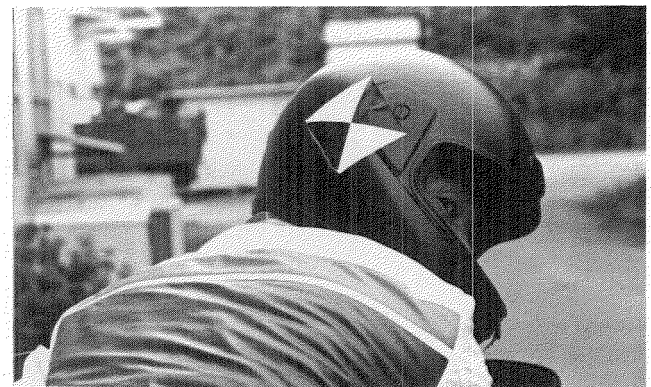


Figure 8. Helmets used in measuring.

*Test course.*—A 2-Lane one-way (with 3.0m wide lanes) flat and straight road (of about 400m in length) was used.

*Measuring procedures.*—

(1) The test rider wears a full-face helmet, and drives the test vehicle at a specified speed (about 40km/h) down the center of the lane.

(2) The test rider carries out a head check when passing the half-way position of the test course (marked by a cone), and reports by means of either turning signal or voice whether or not he was able to see the rear vehicle (driving down the center of the passing lane) through direct field of view (figure 9).

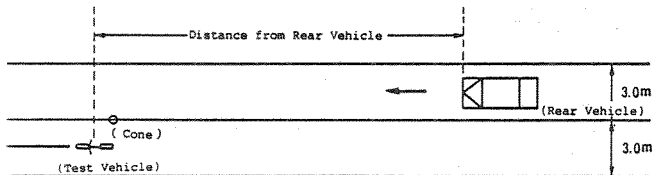


Figure 9. Test course and test conditions (measurement of direct rearward field of view range by head check).

(3) The distance between the test vehicles and the rear vehicle which the driver is to look at is changed for each measurement (beginning with a distance of more than 40m, and gradually shortening the distance to determine the seeing limit distance for each test rider and each situation).

*Measuring conditions.*—For each test rider, measurements were carried out in accordance with the following three conditions:

- (1) Wearing a Standard Helmet when the rear vehicle is a 4-wheeler (passenger car).
- (2) Wearing a Standard Helmet when the rear vehicle is a motorcycle.
- (3) Wearing an Improved Field of View Helmet when the rear vehicle is a 4-wheeler (passenger car).

*Test rider.*—Fourteen male American riders who use motorcycles in their daily lives, average age 31, average weight 80kg, average height 1768mm, average arm length 783mm.

The build of the test riders for this study was about the same with those in eye point measurement (1985) (1) and arm contour measurement (1987) (2) (see table 3).

Table 3. Comparison of anthropometric data among American riders (mean value).

Item \ Measuring Period	1985 (Eye Point Measurement) N = 155	1987 (Arm Contour Measurement) N = 26	1989 (This Study) N = 14
1. Age	29	29 ( 0 )	31 (+2)
2. Weight	80	77 (-3)	80 ( 0 )
3. Height	1775	1754 (-21)	1768 (-7)
4. Arm Length	780	779(-1)	783 (+3)

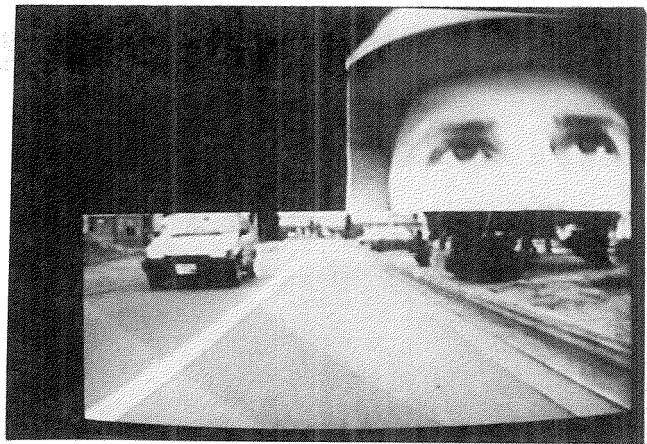
Unit: Age (years)

Weight (Kg)

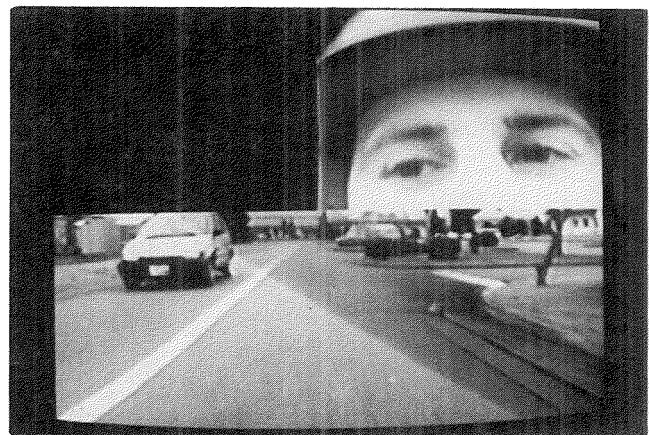
Dimensions (mm)

(NOTE) Values shown in parenthesis are those that differ from the 1985 data

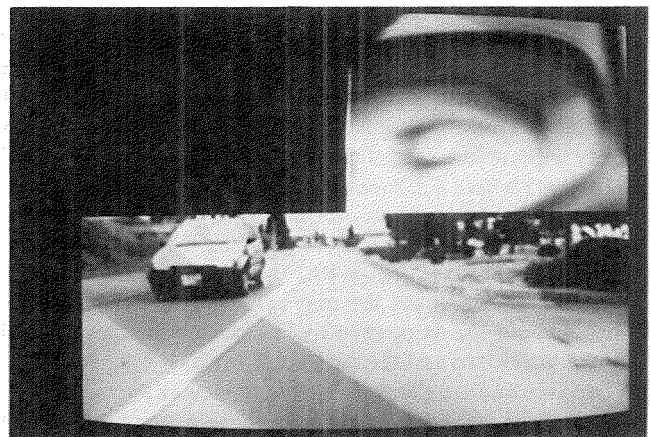
*Data processing.*—Records of sight lines and rear traffic conditions (in video tape, figure 10) were processed by an image analyzer to determine the distance between the test vehicle and the rear vehicle (between the rider's eye point and the front end of the rear vehicle) at the time of the head check by measuring the size of the rear vehicle in the image.



When looking forward.



When looking at right-side rear-view mirror.



When starting a head check.

Figure 10. Record of sight lines and rear traffic conditions (Test Course).

## Results and considerations

The seeing limit distance of the rear vehicle driving in the neighboring lane was determined for each test rider in each situation.

Seeing limit distance was divided up into 5 stage classes (class width difference of 10m), the number of test riders in

each class is shown in table 4, and the number of test riders and their ratios are shown for each class in cases where the rear vehicle was a 4-wheeler in figure 11.

**Table 4. Number of test rider's by seeing limit distance.**

Seeing Distance	Standard Helmet		Improved Field of View Helmet
	4-Wheeled Vehicle	Motorcycle:	4-Wheeled Vehicle
Less than 10m	1 (7m)	1 (8m)	0
10 m - 19 m	1 (16m)	1 (12m)	1 (16m)
20 m - 29 m	0	0	0
30 m - 39 m	0	0	1 (30m)
More than 40m	12	12	12

(NOTE) Figure in parenthesis are the seeing Distances for each test rider (only figures below 40m are indicated) UNIT: Number of Persons

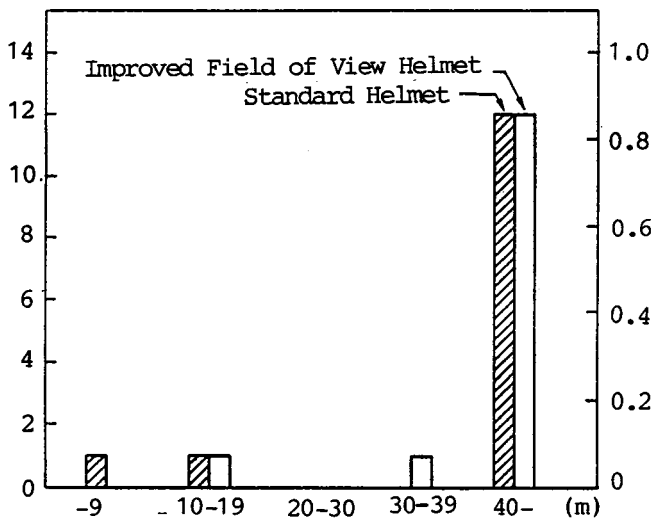


**Figure 11. Number of test rider's and ratios versus seeing limit distance (when rear vehicle is a 4-wheeler).**

*In cases where a standard helmet was worn and the rear vehicle was a 4-wheeler.*—Among the 14 test riders, there were only 2 whose seeing limit distance was less than 40m (one of which was less than 10m), while all the other 12 test riders were able to see the rear vehicle at more than 40m.

*In cases where a standard helmet was worn and the rear vehicle was a motorcycle.*—Among the 14 test riders, there were only 2 whose seeing limit distance was less than 40m (one of which was less than 10m), while all the other 12 test riders were able to see the rear vehicle at more than 40m. This is about the same result as in cases where a standard helmet was worn and the rear vehicle was a 4-wheeler.

*In cases where an improved field of view helmet was worn and the rear vehicle was a 4-wheeler.*—Among the 14 test riders, there were only 2 whose seeing limit distance was less than 40m (neither of which was less than 10m), while all the other 12 test riders were able to see the rear vehicle at more than 40m.

In the case of test riders who wore a Standard Helmet and had a seeing limit distance of less than 40m, an improvement of the helmet's field of view almost doubled the seeing limit distance. As a result, it was noted that there were no test riders who still had a seeing limit distance of less than 10m.

*The role of the direct rearward field of view.*—The results of this measurement are summarized below:

(1) The majority of the test riders (86%) were able to see the rear vehicle driving in the neighboring lane at a distance of more than 40m to the rear through direct field of view.

(2) Only on (7%) of the test riders had a seeing limit distance of less than 10m, and even in this case, when an Improved Field of View Helmet was worn, the seeing limit distance was extended to 16m.

Based on the data for these riders, these helmets, and this example motorcycle, when establishing the field of view standards for motorcycle rear-view mirrors, it is thought that there is no problem involved in considering the role of the seeing of rear vehicles in neighboring lanes at a distance of less than 10m as a role of direct rearward field of view.

## Analysis of the Rider's Sight Line

### Purpose

The time span and frequency of mirror checks and head checks were measured through analysis of the sight line of riders making lane changes while driving on the test course.

### Method

*Test vehicles.*—The same motorcycle and 4-wheel vehicle (passenger car) were used as in the visible range measurement.

*Test course.*—The same as the visible range measurement.

### Measurement procedures

(1) *Rear-view mirror aiming.*—The optical axis traveling to the center of the mirror surface (M point) from the eye point of the test rider riding the test vehicle in a normal position should be reflected horizontally and in a parallel manner in relation to the center line of the vehicle by adjusting the angle of the mirror surface. Adjustment should be made using the optical axis from the left eye for the left side rear-view mirror and from the right eye for the right side rear-view mirror (figure 12). Rear-view mirror aiming adjustment is carried out for each test subject.

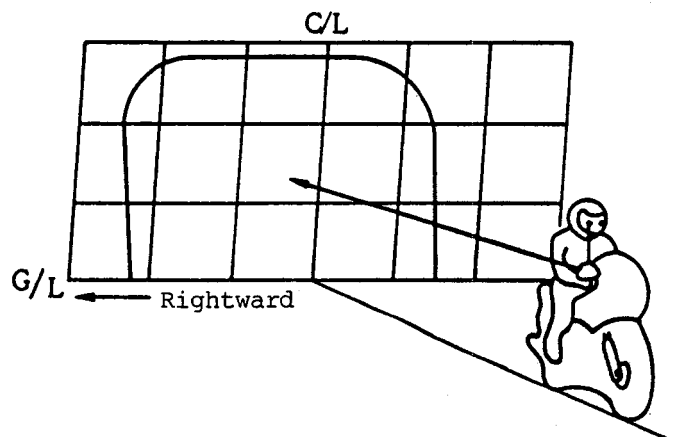


**Figure 12. Rear-view mirror aiming method.**

Also, concerning the interior rear-view mirrors of 4-wheeled vehicles, test riders were allowed to make their own adjustments, for the example vehicle used.

(2) *Driving method.*—The test riders were made to drive the example test vehicle along the center of the driving lane at a specified speed (about 40 km/h), and to change lanes to the passing lane when reaching the vicinity of the half-way position (where there is a marking cone) of the test course (figure 13). Test Subjects were given the freedom to choose for themselves whether or not and how frequently they made mirror checks and head checks. They were instructed to make the lane change in as natural a manner as possible.

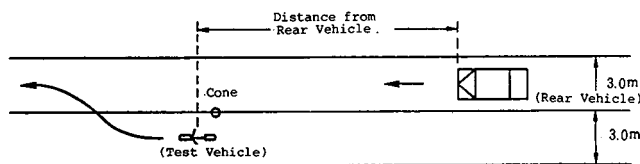


Figure 13. Test course and test conditions (analysis of rider's sight lines). Note.—In Japan traffic is left hand.

The rear vehicle (4-wheeler) was made to drive along the center of the passing lane and the distance between the rear vehicle and the test vehicle was altered for each measurement (beginning with a distance of over 40m and gradually reducing the distance, see figure 13).

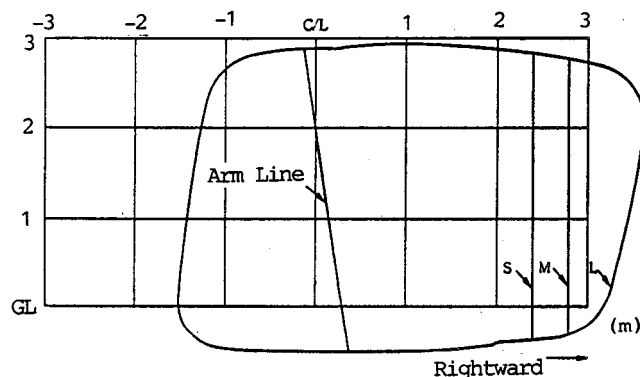


Figure 14. Field of view of right-side rear-view mirror of the test vehicles in binocular condition (motorcycles).

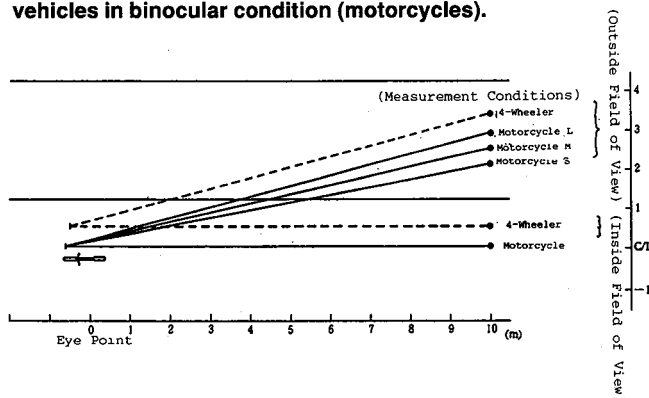


Figure 15. Field of view of right-side rear-view mirror of test vehicle in binocular condition (ground level of 10m behind the eye-points).

## Measurement conditions

In this measurement, three conditions were realized: the first two were that the test vehicle was a motorcycle and that it has differing rear-view mirror outside field of view, and the third was that the test vehicle was a 4-wheeler (see figures 14 and 15).

Measurements were carried out on each test rider 8 times in accordance with the following three conditions:

(1) An example test vehicle which is a motorcycle with no limitations on the mirror surface (referred to as Motorcycle L from here on).

Under this condition, the limit of the outside field of view from binocular eye points was set at 3.2m outward from the vehicle center line on the ground surface 10m behind the eye points.

(2) An example test vehicle which is a motorcycle with partial limitations on the mirror surface (referred to as Motorcycle M from here on).

Under this condition, the limit of the outside field of view from binocular eye points was set at 2.8m outward from the vehicle center line on the ground surface 10m behind the eye points.

(3) An example test vehicle which is a 4-wheeler with no limitations on the mirror surface (referred to as 4-Wheeler).

Under this condition, the limit of the outside field of view from binocular eye points was set at 3.7, outward from the vehicle center line on the ground surface 10m behind the eye points.

*Test subjects.*—The same 14 male American riders as in the visible range measurement.

*Data processing.*—The following items were determined by analyzing the record (video tape, see figure 10) of sight line and rear traffic conditions through an image analyzer.

(1) Frequency of mirror checks and head checks.

(2) Duration from the beginning of eye movement for mirror checks and head checks to the return of the gaze to the front (including movement time of both the eyeballs and the head).

(3) Distance between the test vehicle and the rear vehicle just prior to lane change (from the rider's eye point to the front end of the rear vehicle).

Also, time was determined by the number of frames and distance was determined by the size of the rear vehicle in the image.

## Results and considerations

Choice was made from the 8 data for each test rider and each condition of the typical data of set distances nearest to the set distance from the rear vehicle (in 3 stages of 10m, 20m, and 40m).

Next, using the above typical data, frequency of mirror checks and head checks for each run; time span of mirror checks and head checks within each run (referred to as time

span from here on); duration for each mirror check and head check (time span/frequency) (see figure 16).

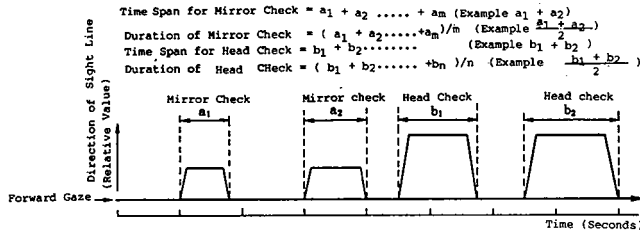


Figure 16. Method for analyzing time spans of mirror checks and head checks (example).

Table 5 shows the frequency, time span, and duration of mirror checks and head checks by condition and set distance. Mean values for all 14 test riders were used for each condition.

Table 5. Frequency and time of mirror checks and head checks (mean values—test course).

Check	Item	Conditions								
		Motorcycles M			Motorcycle L			4-Wheeler.		
		.10m	20m	40m	10m	20m	40m	10m	20m	40m
Mirror Check (Right-side Mirror)	Time Span	2.20	2.14	1.74	2.49	1.97	1.58	2.56	2.08	1.74
	Frequency	3.07	2.43	2.50	2.79	2.57	2.21	3.00	2.64	2.14
	Duration	0.72	0.88	0.69	0.89	0.77	0.71	0.85	0.79	0.81
Mirror Check (Room Mirror)	Time Span							0.56	0.56	0.73
	Frequency							0.64	0.79	0.79
	Duration							0.88	0.70	0.93
Head Check	Time Span	1.21	1.04	0.99	1.27	1.03	1.03	0.74	0.78	0.65
	Frequency	0.86	0.86	0.79	0.86	0.79	0.79	0.57	0.64	0.64
	Frequency	1.40	1.21	1.25	1.47	1.30	1.30	1.30	1.22	1.01
Mirror Check + Head Check	Frequency	3.41	3.18	2.72	3.76	3.00	2.60	3.87	3.42	3.12
	Ratio	(0.88)	(0.93)	(0.87)	(0.97)	(0.88)	(0.83)			
	Frequency	3.93	3.29	3.29	3.64	3.36	3.00	4.12	4.07	3.57
Interval (Forward Gaze)	Time Span	4.30	3.77	4.42	4.47	4.63	4.71	5.06	5.68	5.48
	Frequency	3.21	2.50	2.93	3.21	3.00	2.71	3.14	3.21	2.86
	Duration	1.34	1.51	1.51	1.39	1.54	1.74	1.61	1.77	1.91

(NOTE 1) Duration = Time Span/ Frequency

(NOTE 2) The values in parenthesis are ratios of the check time for each condition for motorcycles compared each condition for 4-wheeler Vehicles

UNIT: Frequency (number of times)  
Time (seconds)

Frequency of mirror checks and head checks.—Figure 17 shows the frequency (mean values) of mirror checks and head checks versus the distance from the rear vehicle by mirror conditions.

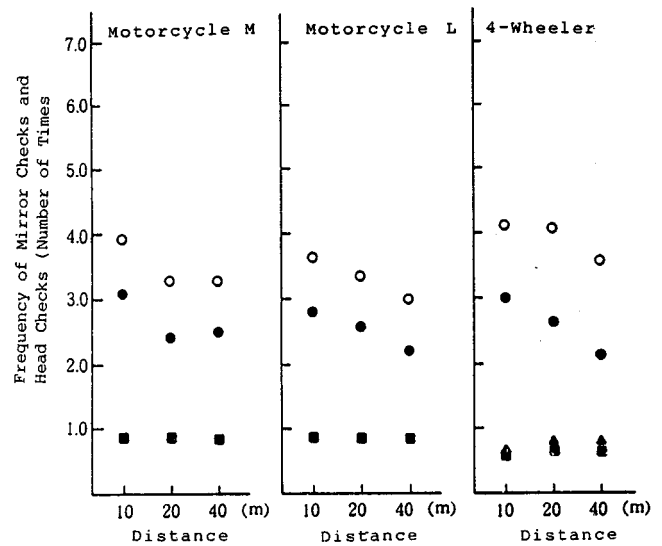
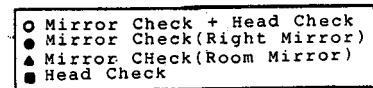


Figure 17. Frequency of mirror checks and head checks in relation to the distance from the rear vehicle (mean values—test course).

In all rear-view mirror conditions, the frequency of right rear-view mirror checks tended to diminish as the distance from the rear vehicle became longer.

In the case of motorcycle test vehicle, right rear-view mirror checks were from 2.5–3.1 times and head checks 0.8 times.

In the case of 4-wheeled test vehicle, right rear-view mirror checks were 2.1–3.0 times, interior rear-view mirror checks were 0.7 times, and head checks were 0.6 times.

As seen above, it was made clear that either mirror checks or head checks were carried out several times in the case of lane changes.

Time span of mirror checks and head checks.—Figure 18 shows the time span of mirror checks and head checks versus the distance from the rear vehicle by mirror conditions.

In all rear-view mirror conditions, the time span of right rear-view mirror checks tended to diminish as the distance from the rear vehicle became longer. Also, the total time of the mirror check time span and the head check time span tended to diminish as distance from the rear vehicle became longer.

In the case of motorcycle test vehicles, the time span for mirror checks was 1.6–2.5 seconds and the time span for head checks was 1.0–1.3, bringing the total time span to 2.6–3.8 seconds. Also, the duration of each check was around 0.8 seconds for mirror checks and around 1.3 seconds for head checks.

In the case of 4-wheeled test vehicles, right side rear-view mirror checks were 1.7–2.6 seconds, interior rear-view mirror checks were 0.6–0.7 seconds, and head checks were 0.7 seconds, bringing the total time span to around 3.1–3.9

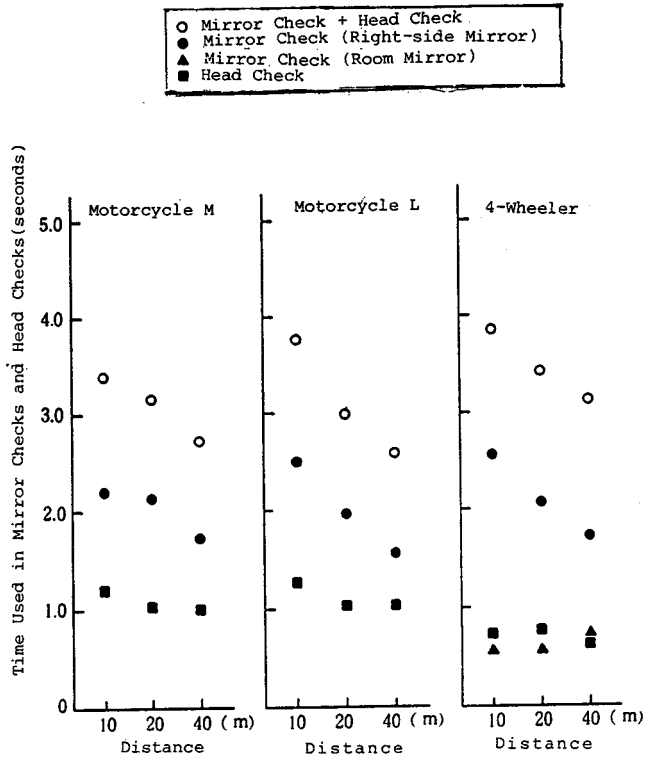


Figure 18. Time used for mirror checks and head checks in relation to the distance from the rear vehicle (mean values—test course).

seconds. Also the duration of each check was around 0.8 seconds for mirror checks and around 1.2 seconds for head checks. These results are about the same as those for motorcycles.

*Comparison of total time used for mirror checks and head checks.*—Figure 19 shows comparisons of the total time used for mirror checks and head checks by distance from the rear vehicle for the test configurations used.

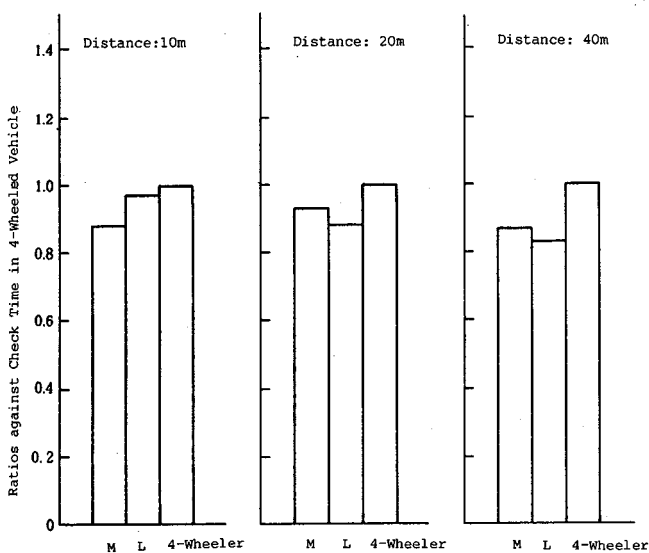


Figure 19. Ratio of total time used.

Throughout all distances and rear-view mirror conditions, the total time used by motorcycles was around 90% of

the total time used by 4-wheeled vehicles, making their time somewhat shorter.

Neglecting variations in visual field content and related factors, if the total time spent when the gaze is shifted away from the road ahead in order to obtain rear information is taken as the assessment standard for the field of view of the rear-view mirror (the assessment is low when the time gaze is shifted from the road ahead is long), it can be assessed as nearly equal to that of 4-wheeled vehicles for motorcycle rear-view mirror conditions, M and L alike.

## Category Judgment for Rearward Field of View

### Purpose

Test vehicles with example altered rear-view mirror field of view were driven on both highways and expressways in order to obtain category judgment for rear-view mirror field of view and to determine the time span and frequency of mirror checks and head checks in actual traffic situations (lane changing and merging).

### Method

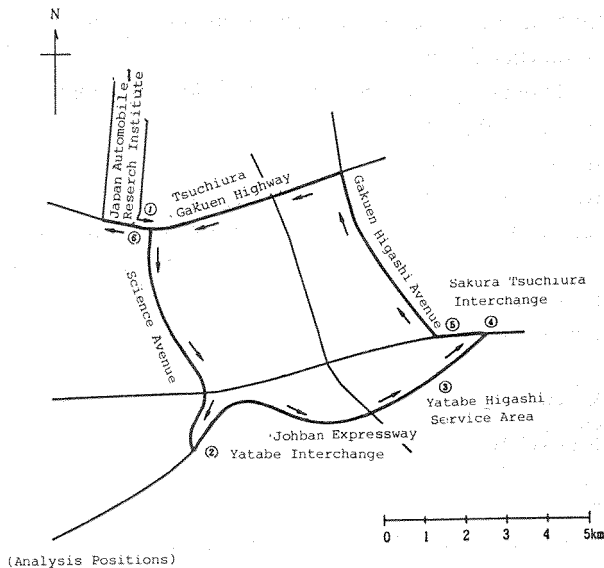
*Test vehicles.*—The test vehicles are as described in the sight line measurement. A video system (3 small video cameras, an image synthesizer unit, and a video recorder) was installed on the test vehicles to record the forward traffic conditions, the rear traffic conditions, and the rider's sight line and voice.

*Driving course.*—The driving course was set on highways and expressways in the vicinity of the Japan Automobile Research Institute. The course was 24km long, and the roads used were 2- or 3-lane roads (figure 20).

*Measurement procedures.*—

- (1) The test rider received an explanation of the direction to drive on the driving course.
- (2) The test rider drove around the driving course once in a passenger car (with the examiner on board) in order to memorize the route.
- (3) Rear-view mirror aiming was carried out before measuring (in accordance with the same procedures as the sight line measurement).
- (4) The test rider made a run on the above mentioned driving course using the test vehicle. Presence or absence and frequency of head checks and mirror checks were left up to the decision of the test rider, and he was instructed to drive as naturally as possible.

(5) After completion of driving, the test rider made a report on category judgment values of the rear-view mirror field of view. Category standards were set in 5 categories (see table 6), but the test riders were instructed that they could use intermediate values (for instance 3.5) as well.



- ① Lane change into passing Lane
- ② Merging into Expressway
- ③ Merging into Expressway
- ④ Merging into Highway
- ⑤ Lane Change into Passing Lane
- ⑥ Lane Change into Passing Lane

Figure 20. Driving course.

Table 6. Category judgment for rear-view mirror field of view.

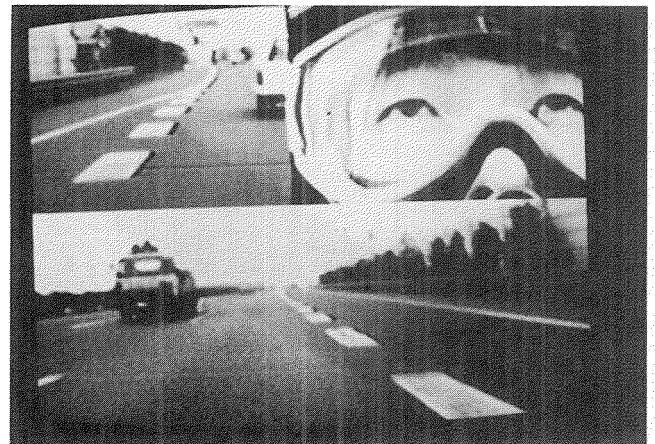
Test Subject	Range of Rear-View Mirror Field of View			
	S	M	L	4-Wheeler
1	2.0	3.0	4.5	5.0
2	2.0	3.5	4.0	4.0
3	3.0	4.0	4.0	4.5
4	1.0	2.0	3.0	4.0
5	1.0	3.0	3.0	3.0
6	1.0	1.5	2.0	3.0
7	2.0	2.5	4.0	5.0
	2.0	3.0	4.0	4.0

Categories for Field of View

- 5 — Very Good
- 4 — Good
- 3 — Moderate
- 2 — Somewhat Insufficient
- 1 — Insufficient

Measurement conditions.—In these measurements, a total of 4 conditions were set, including that test vehicle be motorcycles with 3 different mirror surface areas, and one that the test vehicle be a 4-wheeler (see figures 14 and 15).

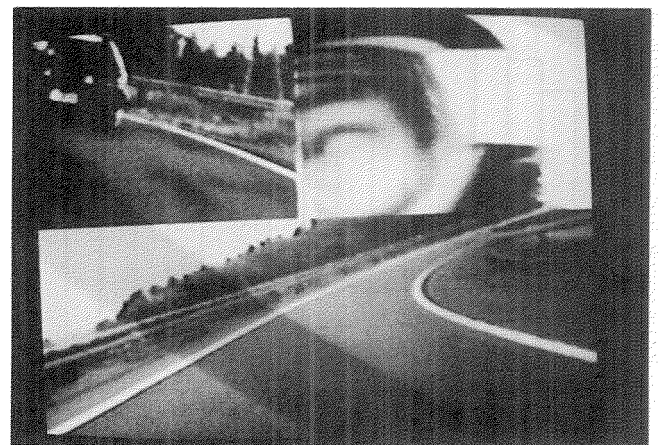
- (1) The condition that the test vehicle be an example motorcycle with no limitations on the mirror surface (Motorcycle L).



When looking straight ahead.



When looking at the right-side mirror.



When starting head check.

Figure 21. Record of sight lines, traffic conditions both forward and backward (highway and expressway).

(2) The condition that the test vehicle be an example motorcycle with partial limitation on the mirror surface (Motorcycle M).

(3) The condition that example test vehicle have greater limitations on the mirror surface than that of condition M (referred to as Motorcycle S from here on). Under these conditions, the limits of the outside field of view from binocular eye points was set 2.4m outside of the vehicle center line on the ground surface.

(4) The condition that example test vehicle be a 4-wheeler with no limitations on the mirror surface (4-Wheeler).

**Test riders.**—Seven male Japanese Riders who use motorcycles in their daily lives, average age 29, average weight 70kg, average height 1744mm, average arm length 746mm.

Compared to the American riders who were test riders in the previous measurement, they were 10kg lighter, 24mm shorter in height, and 37mm shorter in arm length.

**Data processing.**—Records of sight lines and forward and rear traffic conditions (figure 21) were processed by an image analyzer, and the following items were determined:

- (1) Frequency of mirror checks and head checks.
- (2) Duration from the beginning of eye movement for mirror checks and head checks to the return of the gaze to the front (including movement time of both the eyeballs and the head, see figure 16).

## Results and considerations

**Category judgment of rear-view mirror field of view.**—Table 6 shows the category judgment for each measurement condition of the rear-view mirror field of view:

(1) **Category judgment of motorcycle S.**—Six out of the 7 test riders gave judgments of “somewhat insufficient” or “insufficient”, making the median value correspond to the “somewhat insufficient” value.

(2) **Category judgment of motorcycle M.**—Among the 7 test riders, one gave a judgment between “insufficient” and “somewhat insufficient”; one gave “somewhat insufficient”; and one gave between “somewhat insufficient” and “moderate”. No one gave a judgment of “insufficient”. Thus the median value was the “moderate” value.

(3) **Category judgment of motorcycle L.**—Only one out of the 7 test riders gave a judgment of “somewhat insufficient”, and none gave a judgment of “insufficient”. Thus the median value was the “good” value.

(4) **Category judgment of 4-wheeled vehicle.**—None of the 7 test riders gave the judgment of either somewhat insufficient or insufficient, making the median value the “good” value.

If the median value of the 7 test riders is taken as a typical value, the value for the rear-view mirror field of view of Motorcycle M is “moderate”, and that for Motorcycle S is “somewhat insufficient”, for the traffic conditions that prevailed at the time.

**Comparison of total time used for mirror checks and head checks.**—For use as analysis positions, three positions for lane changes from the driving lane to the passing lane, and three positions for merging into an expressway or a highway (figure 20) were selected.

At the above mentioned measuring positions, records of sight lines and traffic conditions (figure 21) were made to determine the frequency, the time utilized (referred to as time span from here on), and the duration time (time span/frequency) of one lane change or merge (see figure 16).

Table 7 shows the frequency, time span and duration of mirror checks and head checks. The mean values of 3 positions X 7 test riders were utilized.

**Table 7. Frequency and time of mirror checks and head checks (mean values—highway and expressway).**

Check item	Mirror Traffic Situation	Motorcycle S		Motorcycle M		Motorcycle L		4-Wheeler	
		Lane change	Merging	Lane change	Merging	Lane change	Merging	Lane change	Merging
		Mirror check (Right-side Mirror)	Time Span	1.88	2.66	1.65	1.99	1.40	2.69
	Frequency	2.21	3.00	2.00	2.52	2.00	2.87	2.10	3.31
	Duration	0.86	0.89	0.83	0.80	0.70	0.94	0.73	0.98
Mirror check (Room Mirror)	Time Span							0.37	0.21
	Frequency							0.48	0.36
	Duration							0.77	0.58
Head check	Time Span	0.58	1.63	0.32	1.21	0.50	1.01	0.10	0.57
	Frequency	0.53	1.37	0.33	0.91	0.40	0.85	0.14	0.55
	Duration	1.09	1.19	0.97	1.33	1.25	1.19	0.71	1.04
Mirrorcheck	Time Span	2.46	4.29	1.07	3.21	1.90	3.68	2.02	4.03
	Ratio	(1.22)	(1.06)	(0.98)	(0.80)	(0.94)	(0.91)		
Head check	Frequency	2.74	4.37	2.34	3.43	2.40	3.72	2.72	4.22
Interval (Forward Gaze)	Time Span	2.97	2.71	2.43	2.89	3.11	2.66	3.80	3.36
	Frequency	2.59	3.68	2.00	3.10	2.30	3.23	2.67	3.79
	Duration	1.15	0.74	1.22	0.93	1.35	0.82	1.42	0.89

(NOTE 1) Continuous Time=Necessary Time/Frequency  
 (NOTE 2) The Values in parenthesis are Ratios of the Check time for each condition for 4-wheeled Vehicles compared with each conditions for Motorcycles

UNIT: Frequency (Number of Times)

(1) **Frequency of mirror checks and head checks.**—Figure 22 shows the frequency of mirror checks and head checks for rear-view mirror conditions by traffic situation.

In lane changing situations, in the case of motorcycles, mirror checks were carried out 2.0–2.2 times, and head checks 0.4 times. In the case of 4-wheeled vehicles, checks of the right side rear-view mirror (Note: In Japan traffic is left hand) were carried out 2.1 times, and checks of the interior rear-view mirror 0.5 times, but there were hardly any head checks at all.

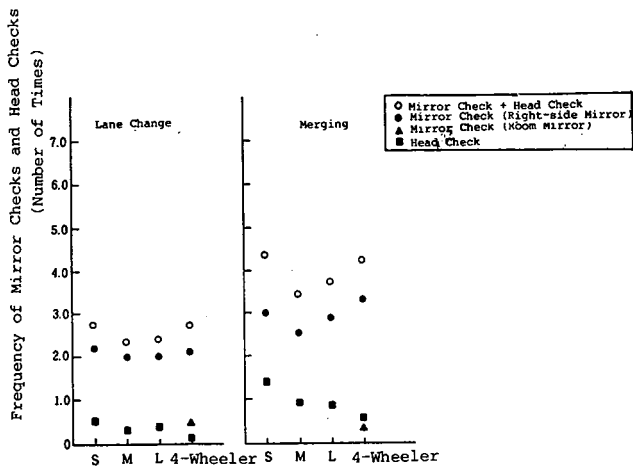


Figure 22. Frequency of mirror checks and head checks (mean values—highway and expressway).

In merging situations, in the case of motorcycles, mirror checks were carried out 2.5–3.0 times and head checks 0.9–1.4 times. In the case of 4-wheeled vehicles, checks of the right side rear-view mirror were carried out 3.3 times, checks of the interior rear-view mirror 0.4 times, and head checks 0.6 times.

In the above mentioned tests, it has become clear that in actual traffic situations, in the case of both lane changing and merging, mirror checks and head checks are carried out several times.

(2) *Time span of mirror checks and head checks.*—Figure 23 showed the time span of mirror checks and head checks versus rear-view mirror conditions by traffic situation.

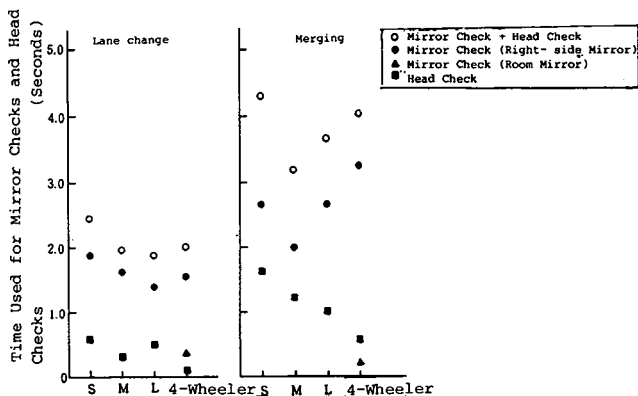


Figure 23. Time used for mirror checks and head checks (mean values—highway and expressway).

In lane changing situations, in the case of motorcycles, the time used for mirror checks was 1.4–1.9 seconds, for head checks 0.3–0.6 seconds, making the total time span 1.9–2.5 seconds. Also, the duration for a single check was 0.8 seconds for mirror checks and 1.1 seconds for head checks.

In lane changing situations, in the case of 4-wheeled test vehicle, the time span for checking of the right side rear-view mirror was 1.5 seconds, and checking of the

interior rear-view mirror was 0.4 seconds, making the total time span 2.0 seconds. Also, the duration for each check of the right side rear-view mirror was 0.7 seconds. This is about the same as in the case of motorcycles.

In merging situations, in the case of motorcycle test vehicle, the time span for mirror checks was 2.0–2.7 seconds and for head checks, it was 1.0–1.6 seconds, making the total time span 3.2–4.3 seconds. Also, the duration for each check was 0.9 seconds for mirror checks and 1.2 seconds for head checks.

In merging situations, in the case of 4-wheeled test vehicle, the time span for checking right side rear-view mirrors was 3.3 seconds, for interior rear-view mirrors it was 0.2 seconds, and for head checks it was 0.6 seconds, making the total time span 4.0 seconds. Also the duration for each check was 1.0 seconds for both right side rear-view mirrors and head checks.

(3) *Comparison of total time used for mirror checks and head checks.*—Figure 24 shows comparisons of total time used for mirror checks and head checks by traffic situation.

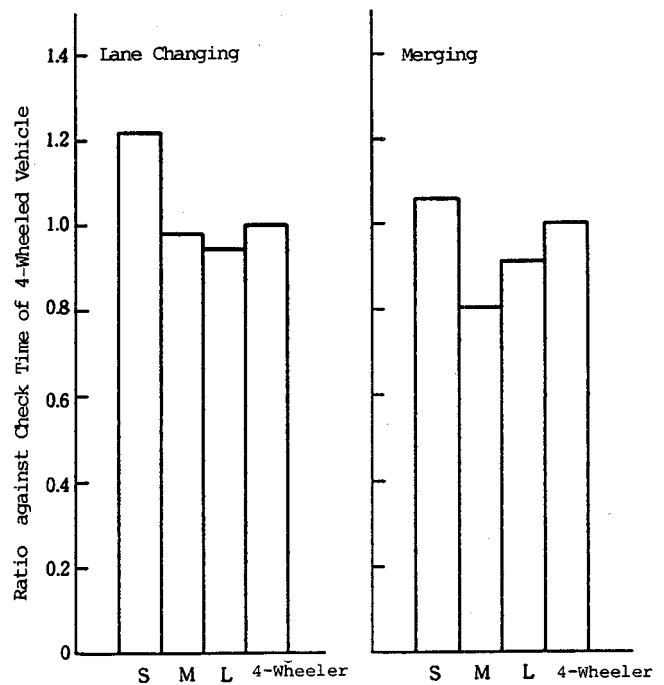


Figure 24. Ratio of total time used (highway and expressway).

A comparison of total time used in lane changing situations shows that the time span was somewhat shorter for Motorcycles L and M than for 4-wheeled vehicles (94%–98%), but it was longer for Motorcycle S than for 4-wheeled vehicles (122%).

A comparison of total time used in merging situations shows that the time span was shorter for Motorcycle L and Motorcycle M than for 4-wheeled vehicles (80%–90%), but it was longer for Motorcycle S than for 4-wheeled vehicles (106%).

If the total time spent when the gaze is shifted away from the road ahead, in order to obtain rear information, is taken for the field of view of rear-view mirror assessment standard (the assessment is lower when the time the gaze is shifted away from the road ahead is longer), almost equal assessment can be made of Motorcycle L, Motorcycle M, and 4-wheeled vehicles, but it is thought to be somewhat lower than 4-wheeled vehicles in the case of Motorcycle S.

## **Summary of Test Results**

In this study, the purpose was to clarify the desired field of view for motorcycle rear-view mirrors. In order to accomplish this purpose, considerations were made of the role of direct rearward field of view by head checks and the role of indirect rearward field of view by mirror checks.

The following is a summary of the results obtained by this study, based on the example vehicle and helmets used, and the traffic conditions encountered.

### **Survey on use of direct rearward field of view and indirect rearward field of view**

It became clear that in situations where rear information is necessary, both motorcycle riders and 4-wheeled vehicle drivers used both mirror checks and head checks depending upon the traffic conditions, and other factors.

### **Measurement of the range of the direct rearward field of view in the case of head checks**

The majority of the test riders were able to see rear vehicles driving the neighboring lane at a distance of more than 40m by direct field of view through head checks. It became clear that test riders who had a limited seeing distance of less than 10m were the exception, and even in the rare cases where this did occur, when an example Improved Field of View Helmet was worn, the limit seeing distance rose to over 10m.

Accordingly, concerning confirmation of the presence of rear vehicles at a rear distance of less than 10m in the neighboring lane, there is no problem in using mainly the direct rearward field of view.

### **Analysis of the rider's sight line**

When a rider changes lanes while driving on the test course, he carried out 2-3 mirror checks and 1 head check, with a total check time of 3 seconds.

Neglecting traffic conditions and other sources of variability, if the total time spent when the gaze is shifted away from the road ahead in order to obtain rear information is taken as the assessment standard for the field of view of rear-view mirror, almost equal assessment can be made for both condition M and L motorcycle rear-view mirrors and 4-wheeled vehicles.

### **Category judgment of rearward field of view**

When category judgment was made of the rear-view mirror field of view in the case of example motorcycles with

altered mirror surface area driven in actual traffic situations, assessments of "moderate" were obtained for condition M motorcycle rear-view mirrors and "somewhat insufficient" for condition S.

Again, neglecting other sources of variability, if the total time spent when the gaze is shifted away from the road ahead in order to obtain rear information is taken as the assessment standard for the field of view of rear-view mirror, almost equal assessment can be made for Motorcycle M and Motorcycle L condition rear-view mirrors and 4-wheeled vehicles, but it is somewhat lower than 4-wheeled vehicles in the case of Motorcycle S.

## **Required Field of View for Motorcycle Rear-View Mirrors**

### **Basic requirement for the field of view of motorcycle rear-view mirrors**

When setting the desired field of view for motorcycle rear-view mirrors, it was hypothesized that the following considerations would apply, and it was on this premise that this study was initiated:

(1) 'That in actual traffic situations, the motorcycle rear-view mirror has essentially equal usefulness as that of the rear-view mirrors of 4-wheeled vehicles depending on the motorcycle configuration'.

(2) 'Combined utilization of mirror checks and head checks makes it possible to minimize the occurrence of obstruction angles in the rearward field of view.'

In order to investigate consideration (1), example motorcycles with altered rear-view mirror fields of view and 4-wheeled vehicles were used as test vehicles. Measurements were made of the time used for obtaining rear information and a category judgment was carried out on the size of the rear-view mirror field of view. As a result, it was found that in the case of Condition M, the motorcycle rear-view mirror field of view is almost equally as useful as that of the 4-wheeled vehicle rear-view mirror.

In order to investigate consideration (2), a survey was made of the use of direct rearward field of view and indirect rearward field of view in typical traffic conditions where rear information is necessary. As a result, it became clear that both 4-wheeled vehicle drivers and motorcycle riders use both mirror checks and head checks depending upon the traffic conditions. Further, measurements were made of the rear visible range of head checks by motorcycle riders, and direct rearward field of view ranges were set. As a result, when the motorcycle rear-view mirror field of view was greater than Condition M, it was confirmed that a combination of indirect rearward field of view and direct rearward field of view serve to avoid occurrence of obstruction angles in rearward field of view (the same was true even in the case of test riders with the smallest rear visible ranges, see figure 25).

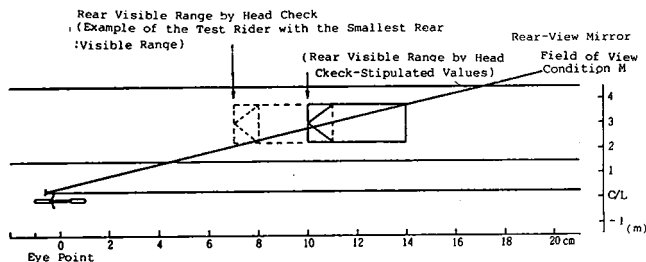


**Figure 25. Relationship of rear visible range by head checks and rear-view mirror field of view.**

From the above, and for the test motorcycle and configurations used, it became clear that when the motorcycle rear-view mirror field of view is equal to or greater than Condition M, both considerations are satisfied.

### Proposal for required field of view for future motorcycle rear-view mirrors

Concerning the desirable field of view for future motorcycle rear-view mirrors, and based on the example configurations studied, it was judged that rear-view mirror Condition M is most appropriate, and the following proposal is suggested for future field-of-view requirements (see figure 26).

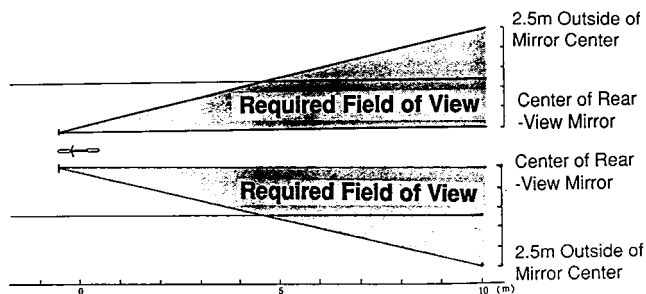


**Figure 26. Required field of view for future motorcycle rear-view mirror (10m behind eye-points on ground in binocular condition).**

(1) The outside field of view from the binocular eye points should be equal to or greater than 2.5m outside the mirror center at a point on the ground surface 10m to the rear of the eye points (corresponding to the field of view of rear-view mirror Condition M).

(2) The inside field of view from the binocular eye points should be equal to or inside the rear-view mirror center on the ground surface 10m to the rear of the eye points.

However, the eye point establishment method which was used as the reference point for the field of view measurement was taken from Reference Material (1), while the mirror aiming method which stipulates the direction of the rear-view mirror field of view and the arm line establishment method which stipulates the inside rear-view mirror field of view was taken from Reference Material (2).

## Design Considerations in Determining the Field of View for Motorcycle Rear-View Mirrors

### Purpose

In order to try to confirm whether or not the desired field of view is satisfied for motorcycle rear-view mirrors, one could consider measuring the rear-view mirror field of view by using a 3-dimensional manikin for motorcycle on actual vehicles or evaluating the rear-view mirror field of view by means of computer simulation.

Because of the complexity of and difficulties connected with the elaboration of these two options, an interim measure based on design requirements is suggested here, in order to satisfy the motorcycle field of view requirements proposed in this report.

### Method

We use two example types of test vehicles, one with the rear-view mirror mounted on the fairing and the other on the handlebar, and carried out computer simulation with CAD.

*Computing procedures.*—The computing procedures are as follows (in accordance with reference (2)):

(1) Set the binocular eye points (in accordance with JASO T005 (3)).

(2) Set the rear-view mirror specifications.

(3) Set the angle of the mirror surface. In this case, the mirror angle is adjusted in such a way that optical axis from the reference eye point to the center of the mirror surface (M-point) reflects in a parallel and horizontal manner to the center line of the vehicle. Concerning the left side rear-view mirror, the optical axis from the left eye is used to make the setting, and concerning the right rear-view mirror, the optical axis from the right eye is used to make the setting (See figure 12).

(4) Set the arm line.

(5) Compute and display the rear-view mirror field of view as it is projected on a screen 10m behind the eye point.

*Evaluation criteria.*—Evaluations were made through a field of view on the ground surface 10m behind the eye point (see figure 26). In other words, the outside field of view from the binocular eye points is more than 2.5m outside the center of the rear-view mirror, and when the inside field of view is inside the center of the rear-view mirror it is evaluated as having satisfied the desired field of view.

*Test considerations.*—With the design position of the handgrips and the rear-view mirror of the test vehicles taken as the standard position, we made changes in the following items. But this is with the shape of the rear-view mirror being square (the standard size is 100×100mm):

(1) Curvature radius of the rear-view mirror (1000,1200,1400mm)

- (2) Change in the longitudinal location of the rear-view mirror (-60, 0, +60 mm)
- (3) Change in the vertical location of the rear-view mirror (-60, 0, +60 mm)
- (4) Change in the lateral location of the rear-view mirror (-60, -20, 0, +20, +60 mm)
- (5) Change in the lateral location of the handgrips (-60, 0, +60 mm)
- (6) Size of the rear-view mirror (60×60, 80×80, 100×100, 120×120, mm)

## Results and considerations

**Relationship between the curvature radius and the rear-view mirror field of view.**—Even when the curvature radius of the rear-view mirror was changed, there was very little change in the inside field of view determined by the arm line, but the outside field of view diminished to a certain extent when the curvature radius was enlarged (figure 27). Compared to a rear-view mirror with a curvature radius of 1200mm, the outside field of view diminished by about 140mm with a rear-view mirror with a curvature radius of 1400mm.

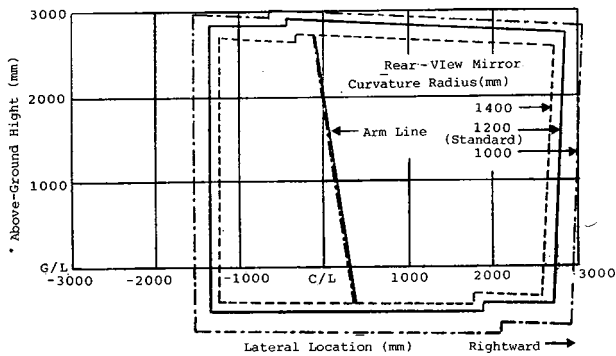


**Figure 27.** Changes in right-side rear-view mirror field of view resulting from rear-view mirror curvature radius changes (fairing mount, 100×100mm).

**Relationship between the longitudinal location of the rear-view mirror and the rear-view mirror field of view.**—Even when the location of the rear-view mirror was moved 60mm backward or forward, there was very little change in the outside field of view or the inside field of view (figure 28).

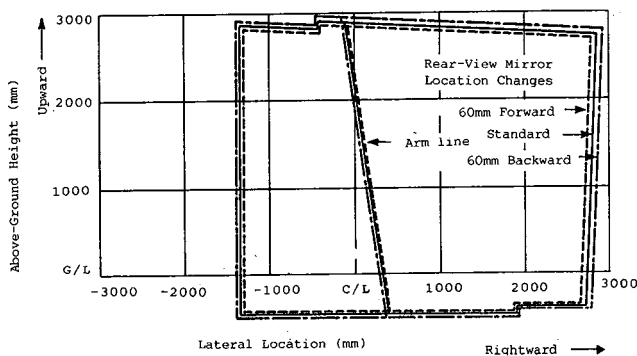


**Figure 28.** Changes in right-side rear-view mirror field of view resulting from rear-view mirror longitudinal location changes (fairing mount, 100×100mm, 1200R).

**Relationship between the vertical location of the rear-view mirror and the rear-view mirror field of view.**—Even when the location of the rear-view mirror was moved up or down 60mm, there was very little change in the outside field of view, but when the location of the rear-view mirror was moved upward, the inside field of view determined by the arm line increased slightly (figure 29). When the location of the rear-view mirror was moved upward 60mm, the inside field of view increased by about 140mm.

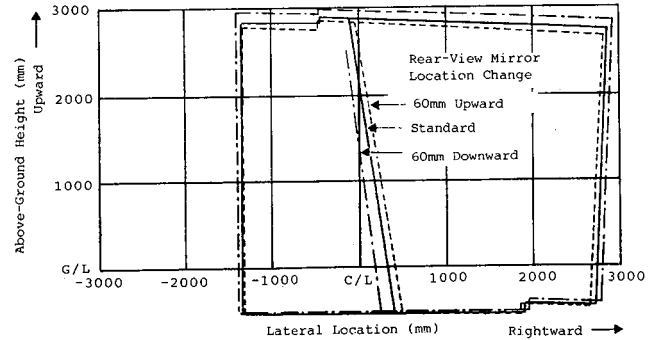


**Figure 29.** Right-side rear-view mirror field of view changes resulting from rear-view mirror vertical location changes (fairing mount, 100×100mm, 1200R).

**Relationship between the lateral location of the rear-view mirror and the rear-view mirror field of view.**—Even when the location of the rear-view mirror was moved 60mm to the outside or the inside, there was very little change in the outside field of view, but there was a large change in the inside field of view determined by the arm line (figure 30). When the location of the rear-view mirror was moved 60mm to the outside, the inside field of view increased by about 840mm.

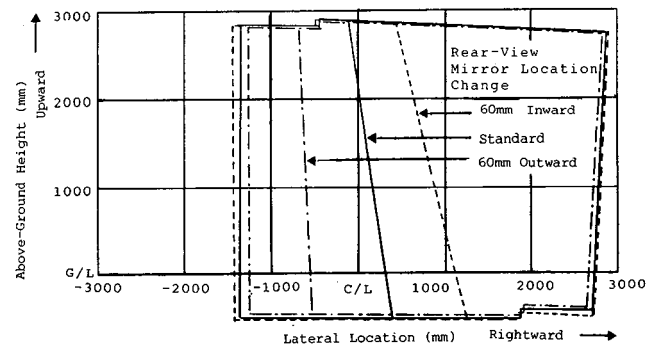


**Figure 30.** Right-side rear-view mirror field of view changes resulting from rear-view mirror lateral location changes (fairing mount, 100×100mm, 1200R).

**Relationship between the lateral location of the handgrips and the rear-view mirror field of view.**—Even when the location of the handgrips was changed 60mm to the outside or the inside, there was no change at all in the outside field of view, but there was a large change in the inside field of view determined by the arm line (figure 31). When the location of the handgrips was moved 60mm to the outside, the inside field of view diminished by about 700mm for this example configuration.

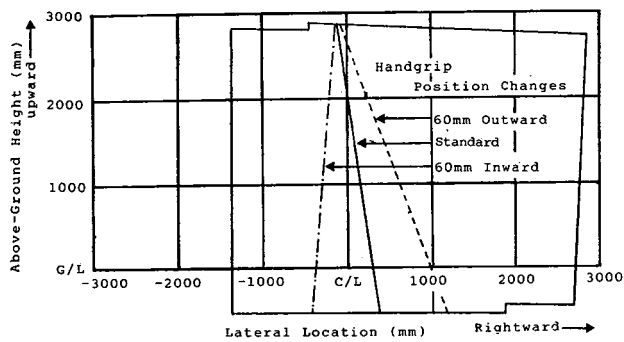


**Figure 31. Right-side rear-view mirror field of view changes resulting from handgrip lateral location changes.**

Compared to the change of the inside field of view resulting from changes in the lateral location of the rear-view mirror, the change of the inside field of view resulting from changes in the lateral location of the handgrips is about 83%.

*The lateral distance from the handgrips to the rear-view mirror and the rear-view mirror field of view.*—The relationship between the lateral distance from the center of the handgrips (G-point) to the center of the rear-view mirror and the inside field of view is shown in figure 32. For the two types of test vehicles, condition (-20, 0, +20 mm) data was plotted against the lateral location change of the rear-view mirror.

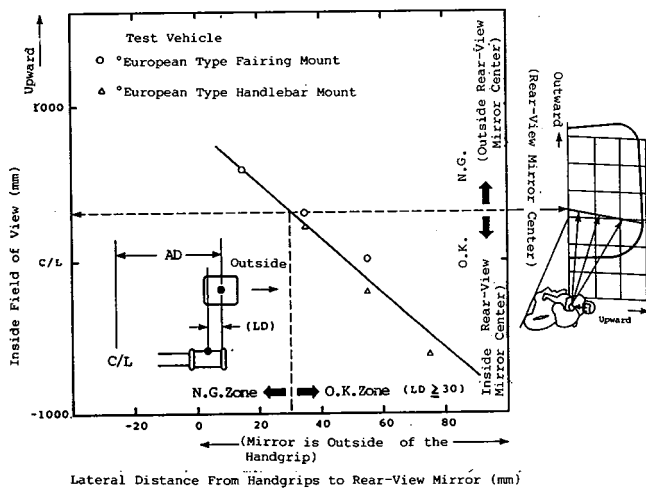


**Figure 32. Inside field of view relating to the lateral distance from handgrips to rear-view mirror (100x100mm, 1200R).**

As the lateral distance from the handgrips to the rear-view mirror increased (placing the rear-view mirror further outside), the inside field of view determined by the arm line increased linearly. Since the inside field of view from the binocular eye points is inside of the center of the rear-view mirror at a point on the ground surface 10m behind the eye point, it may be desirable to locate the center of the rear-view mirror more than 30mm outside the center of the handgrips.

*Relationship between the size of the mirror surface and the rear-view mirror field of view.*—Even when the size of the surface of the rear-view mirror was changed, there was

no change at all in the inside field of view determined by the arm line, but there was a large change in the outside field of view for the example configurations used (figure 33). Compared to a rear-view mirror of 100x100mm in size, the outside field of view diminished by about 340mm with a 80x80mm rear-view mirror. Since the outside field of view from the binocular eye points was more than 2.5m outside the center of the rear-view mirror (more than 2.8m outside the center line of the vehicle) at a point on the ground surface 10m behind the eye points, it may be desirable for the surface of the rear-view mirror to have a width of equal to or more than 100mm (figure 34).

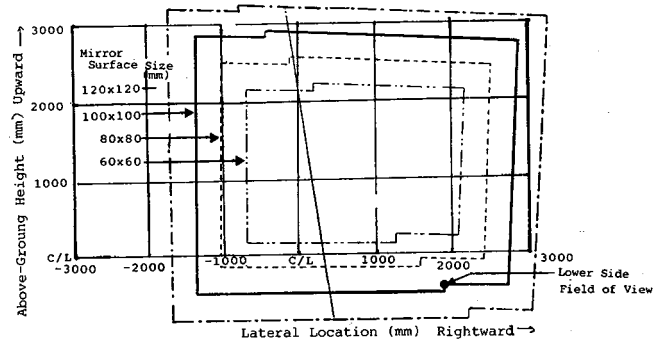


**Figure 33. Right-side rear-view mirror field of view change resulting from mirror surface size change (fairing mount, 1200R).**

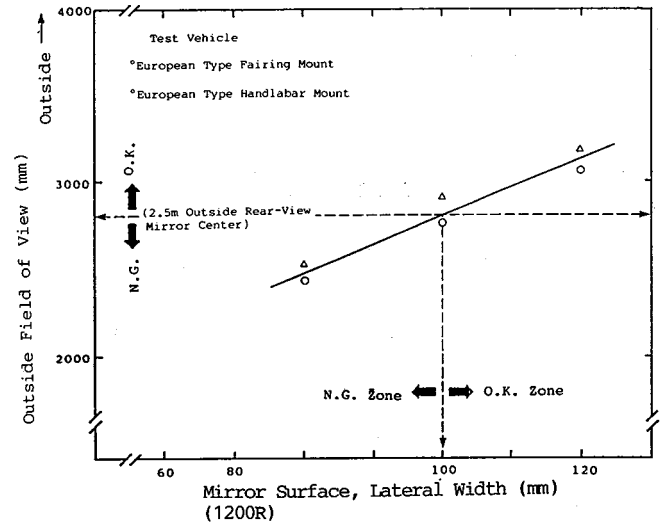


**Figure 34. Outside field of view in relation to lateral width of mirror surface.**

Also, since the lower field of view is lower than the ground surface 10m behind the eye point (meaning that it is possible to see the ground surface ahead from at 10m behind the eye point), it was indicated that it may be desirable for the vertical height of the surface of the rear-view mirror to be equal to or more than 75mm.

### Factors for determination of rear-view mirror field of view

(1) *Determination factors for the inside field of view.*—The data suggest that the inside field of view of the rear-view mirror is determined by the vertical location of the

rear-view mirror, the lateral location of the rear-view mirror, and the lateral location of the handgrips. Among these, influence of the vertical location of the rear-view mirror is comparatively small, while the other two factors have a share of 17–20%. Also, the inside field of view is not determined by the absolute values of either the lateral location of the rear-view mirror or the lateral location of the handgrips. Rather, it was made clear that it is the relative lateral distance between the two that determines the field of view.

From the above, it is thought that “positioning of the center of the surface of the rear-view mirror equal to or more than 30mm outside the center of the handgrips” might be utilized as a future consideration for the inside field of view.

(2) *Determination factors for the outside field of view.*—The results indicate that it is the curvature radius of the rear-view mirror and the size of the rear-view mirror that determine the outside field of view of the rear-view mirror.

Among these, it has been reported (4) that 1000–1200mm is most appropriate for the curvature radius of the rear-view mirror and one European Regulation (EEC Directive 80/780/EEC) is requiring this range.

More recent European Regulations however (like ECE Regulation 81) allow for wider range (1000–1500mm). It is also true that 1200mm is a fairly typical volume for the radius of curvature of today’s motorcycle rear-view mirrors.

“From the above, it is thought that it is most appropriate to base further considerations on this typical value of 1200mm when setting up design requirements for rear-view mirror field of view”.

Assuming the curvature radius at the 1200mm level, it is thought that “setting the rear-view mirror surface lateral width at equal to or more than 100mm” could be utilized as a future design requirement for the outside field of view.

Also, when establishing the curvature radius at around 1200mm, it is thought that “setting the vertical height of the rear-view mirror surface at equal to or more than 75mm” could be utilized as a future design requirement for lower side field of view.

### **Proposal for design considerations for motorcycle rear-view mirrors**

It is thought that, because of the difficulties in elaborating a rear-view mirror field of view measurement method using a 3-dimensional manikin for motorcycle on actual vehicles and a rear-view mirror field of view evaluation method using computer simulation, design considerations for the motorcycle rear-view mirror field of view are necessary as interim measures. In the face of this situation, and based on the example results available, the two items below are proposed as future design considerations for helping to ensure the desirable field of view for motorcycle rear-view mirrors.

However, this is on the premise that a rear-view mirror curvature radius of 1200mm be utilized.

(1) The rear-view mirror surface center should be located equal to or more than 30mm outside the center of the handgrips.

(2) The lateral width of the rear-view mirror surface should be equal to or more than 100mm, and its vertical height should be equal to or more than 75mm.

### **Postscript**

The objective of this study was to clarify the desired field of view of motorcycle rear-view mirrors. For this objective, consideration on both the role of direct rearward field of view through head checks and the role of indirect rearward field of view through mirror checks was made. Also, from these results, a proposal was made for the desired field of view of motorcycle rear-view mirrors that might be adopted in the future.

However, since the scale (in terms of number of test riders, types of test vehicles and helmets, types of specified traffic situations, etc.) of this study is not necessarily sufficient, basically mean values or median values as typical values of the data were utilized. Accordingly, in the future, in order to obtain data that shows a distribution, it is thought that it is possible that it could be useful to carry out a larger scale study.

### **References**

- (1) Motoki, M., and Asoh T., Measurement of Motorcycle Rider’s Eye Locations, The Tenth International Technical Conference on Experimental Safety Vehicles, (1985).
- (2) Motoki, M., and Tsukisaka, T., A Study on Measurement Method of Field of View of Rear-View Mirror for Motorcycle, The Eleventh International Technical Conference on Experimental Safety Vehicles, (1987).
- (3) JASO T 005; Motorcycle Rider’s Eye Range, (1985).
- (4) Tsukisaka, T., A Study of Rear Visibility of Motorcycles, International Motorcycle Safety Conference, (1975).

### **Acknowledgement**

The authors wish to express their appreciation to members of the Motorcycle Safety Structure Subcommittee, Japan Automobile Manufacturers Association, Inc., and Maj. L.D. Maahs, TSgt. C.F. Carson and Mr. Noboru Horikoshi, Safety Department, Yokota Air Force Base, U.S. Air Force, for their great help; to Mr. Shiro Tomimoto, Mr. Hironao Adachi, and Mr. Kazunari Ohara, Yamaha Motor Co., Ltd. for conducting the computer simulation, and to all the American and Japanese Motorcycle riders for their willing cooperation.

## ESM-4—A Lightweight Safety Motorcycle

---

**PMF Watson and G.L. Donne,**  
Transport and Road Research Laboratory,  
United Kingdom

### Abstract

The United Kingdom has previously shown safety motorcycles based on large machines. These have incorporated the findings of research into both primary safety and secondary safety features. However, a large proportion of the machines used in the UK are of small capacity and many accidents occur to inexperienced riders. Consequently the exhibit for the 1989 ESV Conference is based on a 125 cm<sup>3</sup> motorcycle which satisfies the UK regulations as a machine which can be ridden under a learner's licence. ESM-4 incorporates features designed to enhance conspicuity, anti-lock brakes, protection for the rider in frontal impacts, by means of an air-bag system, and a leg-protecting fairing. The paper discusses the design of these features and compliance with relevant specifications.

### Introduction

At the seventh International Technical Conference on Experimental Safety Vehicles in Paris, June 1979 the United Kingdom exhibited their first Experimental Safety Motorcycle ESM 1 (Watson, 1979). This vehicle, based on a Triumph 750cc motorcycle, incorporated both primary and secondary safety features at a prototype development stage, to provide solutions to the problems of motorcycle safety, identified in studies by the Transport and Road Research Laboratory (TRRL) since 1974. The second Experimental Safety Motorcycle ESM 2 (Watson, 1985) was exhibited by the United Kingdom at the tenth International Conference on Experimental Safety Vehicles at Oxford in 1985. This vehicle was based on a BMW 800cc twin cylinder motorcycle to Police Specification and showed progress made to those safety features that were originally fitted to ESM 1.

On the occasion of the eleventh International Conference on Experimental Safety Vehicles in Washington the United Kingdom exhibited their third Experimental Safety Motorcycle ESM 3 (Watson, 1987) based on the Norton Interpol II rotary piston engine motorcycle nominally of 600cc. This vehicle showed the progress of the development of safety features from the prototype in 1979 to the production stage, providing safety features which could readily be incorporated into machines in daily use.

These three safety motorcycles were constructed using standard large motorcycles designed for use on public roads, retro fitted with safety features which had been developed using a systems approach.

For the occasion of the twelfth International Conference on Experimental Safety Vehicles the United Kingdom now exhibits its fourth Experimental Safety Motorcycle ESM 4. This machine again incorporates primary and secondary safety features but departs from its predecessors in so far as

its basis is a small lightweight motorcycle of 125cc capacity. This represents a typical machine that learner riders are limited to riding in the United Kingdom prior to passing their Department of Transport Driving Test for motorcycles. The safety aspects of these smaller motorcycles are particularly relevant as all future new riders will have their first motorcycling experience on these machines. The safety features for both primary and secondary safety are again retro-fitted to a standard machine using a systems approach. This fourth safety motorcycle demonstrates that the knowledge gained in previous research and development of large motorcycles can readily be transferred to much smaller lightweight machines, to produce a perfectly satisfactory and practical commercial motorcycle.

### Primary Safety—Accident Avoidance

#### Brakes

Research on motorcycle braking has been carried out by TRRL for over 25 years as the instability of these vehicles during braking is known to be a contributory cause of accidents. More recently the laboratory has carried out work to provide a solution to the problem of water on disc brakes (Donne and Watson, 1981) and the international braking regulations have since been amended to control the disparity between wet and dry performance. Anti-lock brake systems have featured on all previous ESM's and in 1985 the TRRL launched the first field trial with Police forces using motorcycles fitted with anti-lock. The system used was a fully tested and productionised unit developed by Lucas Girling which was retro-fitted to motorcycles to Police specification. This year the German motorcycle manufacturers BMW became the first manufacturer to offer anti-lock brake devices on their motorcycles for sale to the public.

ESM 4 is fitted with a re-developed unit which had originally been used by TRRL in the 1970s (Watson et al, 1976) and was fitted to the first safety motorcycle ESM 1 (Watson, 1979). The unit was fitted to both wheels with independent brake operation and in this form had been successfully tested by NHTSA in 1978 (Zellner and Weir, 1978). This was the first motorcycle anti-skid system with a fully-satisfactory performance and suitable for normal, everyday use.

The system developed for these smaller machines can use either mechanical or electronic sensing. The braking system is however a combined system whereby the brakes on both wheels are applied by a single operation of the rider. Studies by TRRL observing riders on the road (Sheppard, 1985) have shown that braking behaviour of many riders is far from ideal. Many apply only one brake. To overcome this deficiency a single application to apply the brakes on both wheels can now be used, in conjunction with the anti-lock device which prevents the inadvertent wheel locking which previous coupled systems with fixed ratio brakes could

induce. Work on coupled brake systems at the TRRL is summarised in the paper by G.L. Donne in the proceedings of this conference.

Although the practicality of anti-lock for large motorcycles has been established by BMW in commercial production, a challenge exists for safety engineers to provide advanced braking for those small motorcycles and mopeds which are not fitted with hydraulic brakes. At the ESV Conference at Oxford in 1985 TRRL exhibited an early prototype of mechanical anti-skid of simple design for very light machines which is still under development. The system fitted to ESM 4 requires hydraulic operation but it has the potential to be produced relatively cheaply and is suitable for use on all but the smallest and cheapest two-wheelers.

TRRL has been involved in considerable research on conspicuity for day (Donne et al, 1985) and night conditions (Donne and Fulton, 1987). Recommendations for daytime conspicuity are now contained in the U.K. Highway Code, and the night time results have already been recognised in the vehicle regulations. The requirement for vehicles to be fitted with dim/dip lighting<sup>1</sup> equipment excluded motorcycles as it was found that the brightness of motorcycle lamps in ambient traffic had a beneficial effect on the conspicuity of the motorcycle.

Identification of a vehicle as a motorcycle at night presents a difficult problem. The most effective treatment was found to be the fitting of two strip lights vertically on either side in front of the rider's lower legs. Such a solution is contained in the safety fairing of ESM 4. Use of the relatively large headlight will aid conspicuity in daytime.

## Secondary Safety—Rider Protection

Protection of the rider by engineering treatments to the motorcycle has provided a reduction in risk of injury, as measured in full-scale impact tests using a dummy rider, to an extent which a decade ago would not have seemed possible. There had been two approaches to reducing injuries in accidents, total restraint of the rider on the motorcycle or free ejection, both having benefits and disadvantages. Work at TRRL has concentrated on preferential restraint to provide the rider with some protection in those accident configurations found to be important in investigations of accidents and injuries. In other situations the motorcycle design allows the rider to leave the machine, as in the case of "down on the road" single vehicle accidents, without introducing unnecessary injuries caused by non separation during the crash phase.

### Frontal impacts

Each of the experimental safety motorcycles shown at previous ESV Conferences (Watson, 1979, 1985, 1987) demonstrated a system which was intended to reduce the effects of frontal collisions. These were designed to reduce

<sup>1</sup>Dim/dip lighting equipment provides for two levels of intensity of the dipped beam of the vehicle headlamps. In good street lighting the intensity emitted from the vehicle is reduced to about 10 per cent of standard.

the exit-velocity of the rider compared with that from a standard machine. The systems on ESM 2 and ESM 3 were based on prototype air-bags used in combination with modified fairings. These modifications were intended to enhance the effectiveness of the air-bag by providing a secondary load-path designed to reduce the pitch of the vehicle during the impact, and knee-restraints at the rear of the fairing designed to absorb energy and to modify the trajectory of the rider. The air-bag of 120 litre capacity fitted to ESM 3 was assessed in controlled impacts. It was found that the air-bag could reduce the horizontal component of the rider's velocity to zero, measured at the plane of impacts. This result represented a very significant reduction in the rider's energy compared with that when a standard machine was tested.

The previous experimental safety motorcycles were all large machines which provided the maximum scope for the provision of safety features, particularly with regard to space and accommodation of weight. ESM 4 is a much smaller and lighter machine. However it was considered to be possible to incorporate an air-bag system of similar capacity to that used effectively on ESM 3.

Accordingly, ESM 4 has been fitted with an air-bag of approximately 130 litre capacity deployed with a single inflator produced by Bayern. Both are mounted at the rear of the fuel-tank. When deployed the bag tapers in both plan and elevation to its maximum cross-section at the forward end in order to make the most effective use of its capacity.

Initiation of the bag is by an air-damped inertia-switch which is designed to trigger at a vehicle deceleration of 10g, with a time-period threshold. Work remains to be done to assess typical accelerations experienced on motorcycles during normal use to ensure that initiators used in safety-systems operate at realistic levels without the risk of spurious deployment.

ESM 4 incorporates features which are designed to complement the operation of the air-bag. Knee-protecting elements are fitted at the rear of the fairing as part of the leg-protection system. In frontal impacts these are designed to absorb energy from the lower part of the rider's body and to impart rotation. This is intended to translate the motion of the rider into a component which can be most effectively controlled by the air-bag.

**Table 1. Main results of impact tests made with standard machine and one fitted with the ESM 4 secondary protection devices.**

(90° Impact into side of stationary car - Nominal speed of m/c = 30 mile/h)

	Standard Machine	ESM 4
HIC	414	59
Resultant deceleration-peak g		
Head	123	27
Chest	58	28
Pelvis	47	26
Horizontal exit-velocity of rider - m/s (From 14 m/s impact)	12	1.6

Table 1 compares the main results obtained in impact tests with a standard machine and one modified in the same way as ESM 4.

## Leg protection

The concept of leg protection was introduced on ESM 1 in 1979 (Watson, 1979) using the hard prototype leg protector. TRRL carried out experimental work on different kinds of leg protection devices which led to a less stiff energy-absorber designed to break away at high impact velocity, and installed on ESM 3 in 1987 (Chinn and Hopes). It was in that year that the Department of Transport issued its Draft Specification "Leg Protection for Riders of Motorcycles" (Department of Transport, 1987) for comment.

Since then there has been considerable controversy over the efficacy of leg protectors. Opposition from the enthusiast element of motorcycle user-groups, who object to any imposed change in their machines or freedom of use, is not surprising given the same lobby's opposition to helmet legislation. The recent objections from the motorcycle manufacturer's organisation, IMMA, have been more surprising, especially so since TRRL first published the potential benefits of leg protection ten years ago.

It has been suggested that head injuries can be made more severe and injuries may be transferred from the lower leg to the upper leg when leg protectors are fitted. However, these objections (Dynamic Research Inc., 1988) (Motorcycle Association, 1988) seem to be based on information supplied by the Japanese Automobile Research Institute (JARI) about results from a very small number of tests using a leg protector design which, from visual inspection of the test film, is very much bulkier than the TRRL device and which violates the draft DTp specification in at least one respect. As the paper by Chinn and Hopes (1989), presented to this Conference, shows, a series of tests of leg protectors fitted to a large motorcycle gives consistently large reductions in leg injuries, as measured on a test dummy specially constructed to indicate damage to the legs. Beyond this, TRRL has conducted over 100 full-scale impact tests comparing motorcycles of various sizes and designs, with and without leg protectors, at a variety of impact speeds, angles and configurations, and into rigid barriers and stationary and running cars. In almost all cases leg protectors provided a worthwhile reduction in leg injury, quite often dramatically so, and in no case was injury to any part of the body increased. In several instances the leg protectors also reduced head injury by slowing the rider down before he left the motorcycle. It is also argued that leg protectors increase the width of the machine and may involve it in collisions which the bare machine might avoid. This criticism applies equally to fair-aid machines, yet normal fairings offer little, if any, protection from injury, and there are certainly instances where the fairings actually add to injury. The energy absorption and protection provided by a properly designed leg protector fitted inside a fairing far outweigh any possible disadvantage from the greater width, which in any case is only

marginally outside the envelope defined by the rider's legs, and which often protrudes less than the handlebars. Without the fairing, it would be the legs which were making contact with the object in collision. And it is quite clear from ESM 4, and the previous ESM 3, that this protection can be designed into the machine to give an aesthetically pleasing appearance, in a fully practical and commercially acceptable machine.

A great deal of effort has been spent investigating leg injuries which, considered together with the engineering and physical principles of the impact, and underpinned by work on mathematical modelling, provides a very sound basis for safety engineers to design a system for controlling energy during impact. The latest analysis of motorcycle accident and injury data is contained in the paper by P.L. Harms, in the proceedings of this conference. Harm's findings underline the need for leg protection for motorcycles, and identify the most important circumstances under which leg injuries occur. Caution is required when assessing presentations of injury data, since it is important to identify those accident situations where useful protection can be achieved, and not confuse the debate by diverting attention to situations and configurations where survival is unlikely whatever type of protection the motorcycle designer tries to provide. Leg injuries are rarely fatal, but they often cause permanent disability, and of course most of the victims are young. The total cost of motorcycle leg injuries in the UK (in terms of hospitalisation, loss of earnings, pain and suffering, etc) is currently £150 million per year. We estimate that fitting leg protectors to all motorcycles could save at least £50 million of this, even after allowing for the extra costs of designing leg protectors into the machines, and recent results from testing suggest that even this large saving might be an underestimate. ESM 4 is fitted with a safety fairing incorporating leg protection devices meeting the Draft Specification (Department of Transport, 1987).

Table 2 (Appendix) sets out the main requirements specified for the performance of the three elements of a leg protector and gives results of the tests made to assess this. These results are for a protector intended for a category 3(ii) motorcycle.

The performance of leg-protectors in simulated accidents is discussed in the paper by Chinn and Hopes in the proceedings of this conference (Chinn and Hopes, 1989).

## Conclusion

There has been great interest shown in TRRL's series of previous safety motorcycles, both at the International Technical Conferences where they have been exhibited and afterwards. The progress which has been made towards incorporating new safety features in production machines, since the experimental systems on ESM 1, is encouraging and supports the forum of the ESV Conferences for introducing vehicle safety research and developments.

The concept of secondary safety for motorcycles in particular, offers great scope for benefits in the future and a

challenge in design for those involved in promoting safety now. Motorcycling carries much greater risk of both accident and injury than most other modes of travel. The rider is unavoidably exposed and vulnerable yet it is possible by thoughtful design and engineering to provide a much higher level of protection in accidents than is currently offered by motorcycle manufacturers. Realistic testing of the devices developed through research has been most encouraging. The disappointment lies in the apparent reluctance of motorcycle manufacturers to adopt them.

## References

Chinn, B.P. and P.D. Hopes, 1987. Protecting Motorcyclists' Legs. 11th International Conference on Experimental Safety Vehicles. Washington (NHTSA).

Chinn, B.P. and P.D. Hopes, 1989. Leg Protection and its Effect on Motorcycle Rider Trajectory. 12th International Conference on Experimental Safety Vehicles. Gothenburg (NHTSA).

Department of Transport, 1987. Leg Protection for Riders of Motorcycles. Draft Specification, London. (Department of Transport).

Donne, G.L. and P.M.F. Watson, 1981. The influence of Brake System Properties on Motorcycle Braking Performance. Society of Automotive Engineers Technical Paper 810406. Warrendale (SAE).

Donne, G.L., E.J. Fulton and P.G. Stroud, 1985. Motorcycle Conspicuity in Daylight. 10th International Conference on Experimental Safety Vehicles. Oxford (NHTSA).

Donne, G.L. and E.J. Fulton, 1987. Safety Considerations of Motorcycle Lighting at Night. 11th International Conference on Experimental Safety Vehicles. Washington (NHTSA).

Dynamic Research, Inc., 1988. Comments on the UK Draft Specification for Leg Protection for Riders of Motorcycles. Torrance, California (Dynamic Research Inc).

Harms, P. and J.K. Meades, 1989. Motorcyclists' Leg Injuries, Mechanisms and Potential for Remedial Action. 12th International Conference on Experimental Safety Vehicles. Gothenburg (NHTSA).

Motorcycle Association, 1988. Motorcycle Leg Protectors—Response of MCA of GB Ltd to DTp Legislative Proposals. Coventry (MCA Ltd).

Sheppard, D., B.A.K. Hester, Sonya Gatfield and Monica Martin, 1985. Motorcyclists' Use of Their Front Brakes. TRRL Report RR 20. Crowthorne (TRRL).

Watson, P.M.F., F.T.W. Lander and J. Miles, 1976. Motorcycle Braking. International Conference on Automobile Electronics. London (Institution of Electrical Engineers).

Watson, P.M.F., 1979. Features of the Experimental Safety Motorcycle ESM 1. 7th International Conference on Experimental Safety Vehicles. Paris (NHTSA).

Watson, P.M.F., 1985. A Motorcycle Demonstrating Improved Safety Features. 10th International Conference on Experimental Safety Vehicles. Oxford (NHTSA).

Watson, P.M.F., 1987. ESM 3—A Motorcycle Demonstrating Progress for Safety. 11th International Conference on Experimental Safety Vehicles. Washington (NHTSA).

Zellner, J.W. and D.H. Weir, 1978. Evaluation of the Mullard/TRRL Anti-lock Brake System. Contract No DOT-HS-6-01381. Hawthorne, California (Systems Technology Inc).

## Acknowledgements

TRRL acknowledges the support of Marling Industries plc in supplying the experimental air-bag equipment. The work described in this paper forms part of the programme of the Transport and Road Research Laboratory and the paper is published by permission of the Director.

Crown Copyright. The views expressed in this paper are not necessarily those of the Department of Transport. Extracts from the text may be reproduced, except for commercial purposes, provided the source is acknowledged.

## Appendix

### Development of leg-protection to draft specification

As part of the development of leg-protecting devices for motorcyclists the UK Department of Transport has produced a draft specification. This set out general provisions and stated requirements for both the location and performance of the elements considered to be necessary in an effective leg-protector.

These elements are:

(i) *Primary impact element*.—intended to absorb energy from the vehicle impact.

(ii) *Knee protection element*.—intended to absorb energy from impact between the rider's lower leg and the motorcycle, at a force below human tolerance.

(iii) *Rigid support element*.—the structure which supports (i) and (ii) in the correct position.

This appendix describes the development of these elements for ESM 4 and includes details of the main tests used to ensure compliance with the specification.

The design of the leg-protection elements is critically dependant on the mass of the motorcycle. The specification therefore provides for different levels of performance for devices used on machines of different mass. ESM 4 is classed as a Category 3(i) machine.

Energy-absorbing and structural-integrity tests were made on each of the elements, as specified.

(a) *Primary impact element*.—a dynamic test was done using an impactor of 26kg mass moving at 50 km/h. The angle of impact was set at 30° to the centre-line of the motorcycle as specified. The performance requirements of this test were specified as follows:

(i) The permanent deformation (measured at the first contact point and in line with the direction of impact) should be 100mm ± 15mm.

(ii) Peak dynamic force must be not more than 20 per cent greater than the average crushing force.

(iii) Recoil energy should be not more than 5 per cent of the energy absorbed.

(iv) External profile should be smooth and not likely to interact.

(b) *Knee protection element*.—a dynamic test, using a cylindrical steel cylinder of mass 22 kg ± 1 kg, was specified for the energy-absorbing material used in this element. The striker diameter was specified at 80mm and the end making contact with the energy absorbing material was hemispherical. The striker was suspended in a double bifilar configuration and the test-speed was 21 km/h.

The characteristics of the energy-absorbing material were specified to be such that the loads sustained by the striker should be less than 10kN with 8kN not exceeded for periods totalling more than 20 ms.

(c) *Rigid support element*.—a dynamic test similar to that for the primary impact element was specified except that the test speed should be 100 km/h (or with the mass/speed combination adjusted to provide the same energy input). Alternatively a static test, using a flat test-surface and applying a load of 55kN, can be made. In both cases, the element should resist the applied energy such that either the deformation, measured in line with the direction of loading does not exceed 50mm or the support becomes detached from the motorcycle without leaving any sharp edges or projections. In the case of ESM 4, the mountings were designed to permit the latter.

The draft specification does not limit the design of the leg-protection system to the use of particular materials, but determines the performance to be achieved by each element. In the case of ESM 4, experience gained in the design of protectors used on large machines was used. The elements were constructed and tested as follows:

*Primary impact element*.—This was constructed of light-gauge mild-steel sheet of modified part-conical form and was filled with closed-cell plastic foam. After initial development using quasi-static testing the complete protector was tested dynamically on the TRRL impact rig according to the draft specification.

*Knee protection element*.—Aluminium honeycomb material was used for this element. Initial tests showed that this material was promising although the grades available did not provide characteristics which met the draft specification. Attempts were made to stiffen soft grades by filling the cells with plastic foam. However, the main problem appeared to be concerned with the hemispherical end of the striker of the knee-form specified. With penetration of the energy-absorbing material the increasing cross-sectional area of the stiker resulted in a progressively rising deceleration.

An energy-absorbing material of corresponding change of stiffness was implied if a constant deceleration was to be experienced by the striker. Consequently an energy absorber was developed which comprised laminations of honeycomb of different grades. The element used on ESM 4 comprised of three components, namely a 3mm rubber facing, 30mm of aluminium honeycomb of grade 2.3 – 0.25 –

**Table 2. Specified performance and test results for the three elements of a leg protector—category 3(ii) motorcycle.**

Primary Impact Element (PIE)

Specified Test Conditions

	REQUIREMENT	RESULT
IMPACT MASS	32 kg ± 2 kg	32kg
IMPACT SPEED	13.89 m/s ± 0.55 m/s	14.14 m/s
IMPACT ENERGY	2667J TO 3547J	3199J

Results

	REQUIREMENT	RESULT
DEFORMATION IN PIE TEST	100mm ± 15mm	88.9mm
ENERGY ABSORBED IN PIE TEST	2667J to 3547J	2830J
RECOIL ENERGY AS % OF TOTAL ENERGY ABSORBED IN PIE TEST	5%	2.7%
DEFORMATION IN STATIC TEST	100mm ± 15mm	88.2mm
ENERGY ABSORBED IN STATIC TEST	2667J to 3547J	2705J

\* NOT A REQUIREMENT FOR STATIC TEST, INCLUDED FOR INFORMATION

Rigid Support Frame

Specified Test Conditions

	REQUIREMENT	RESULT
IMPACT MASS	32kg ± 2kg	83kg *
IMPACT SPEED	27.78 m/s ± 0.55 m/s	17.73 m/s *
IMPACT ENERGY	11116J to 13647J	13046J

\*OR THE EQUIVALENT ENERGY INPUT

Results

	REQUIREMENT	RESULTS
DYNAMIC DEFLECTION IN PIE TEST	<10mm	7.2mm
LOAD AT FAILURE OF BREAKAWAY	70kN	58.9kN
MOUNTS IN STATIC TEST		
PROTECTOR MUST BREAK OFF LEAVING NO SHARP EDGES		COMPLIED WITH

Knee Protection Element  
Specified Test Conditions

	REQUIREMENT	RESULT
IMPACT MASS	22kg ± 1kg	21.65kg
IMPACT SPEED	5.83 m/s	5.83 m/s
IMPACT ENERGY	357.3J to 391.3J	384.9J

Results

	REQUIREMENT	RESULT
MAXIMUM FORCE ON	10kN	9.875kN
KNEE FORM	>8kN FOR <20 m s	>8kN FOR 7 ms

10 (5052) T, and 40mm of honeycomb of grade 3.4 – 0.25 – 15 (5052) T.

Results of the tests of ESM 4 installation were not available as this paper was printed. However, Table 2 gives the main results of similar tests made on a leg-protector for a category 3(ii) motorcycle.

This report discusses only the most important of the requirements of the UK draft specification. For full details, reference should be made to the specification (Department of Transport, 1987).

## Assessment of Motorcycle Braking Performance and Technical Perspectives for Enhanced Braking Safety

Alois Weidele,  
 Department of Automotive Engineering,  
 University of Darmstadt, West Germany

### Introduction

As a result of their static instability, single-track vehicles are dependent on dynamic stabilization, which means working gyroscopic effects and sufficient adhesion reserves, as far as all the driving maneuvers are concerned. This is of a special importance for the braking procedure of a motorcycle, because there is the possibility of a falling away of the gyroscopic moments and the adhesion reserves at the same time. Concerning the slope of brake force and the distribution of brake force the conventional standard brake is controlled by the driver and it doesn't offer any reliability in case of a lock of wheels. National and international studies demonstrate—in spite of an obligatory statistical insufficiency—that braking faults have, as primary or secondary reasons for accidents, an immense part on these accidents on roads. Regarding these background, the Department of Automotive Engineering of the University of Darmstadt carries out investigations about the behaviour of brakes and the stability of driving under consideration of the influence of driver, vehicle and roadway. In this respect, especially the braking in the bend is driving dynamically because of lateral dynamic effects of a single-track vehicle.

### Physical foundations of stationary driving with a single-track vehicle

Above a certain minimum of speed, that is dependent on the vehicle, the single-track vehicle is stabilized almost exclusively by the gyroscopic effects of its rotating parts

(1)\*. This is in like manner valid for the stationary cornering than for the straight ahead driving, which can be seen as a special case of cornering (with unlimited radius of the bend). The gyroscopic moments, which are necessary to counterpoise around the roll axis, respectively the track line, are dependent on permanent derangements around the vertical axis, that are however hardly realised by the driver. Close by this fact, there is in higher speeds the possibility of derangement caused by increasing oscillations (2).

The physical roll angle  $\lambda_{th}$ , that results in case of stationary cornering on plain road form vectorial addition of lateral and vertical acceleration (= acceleration due to gravity), is enlarged through geometrical influences (notice 3) by the additional angle  $\lambda'$  and through gyroscopic moments (4) by the angle  $\lambda''$  caused by the yawing motion, of the rotating parts around the center of the curve, as presented arithmetically for a motorcycle of the 1000 cm<sup>3</sup> class in figure 1.

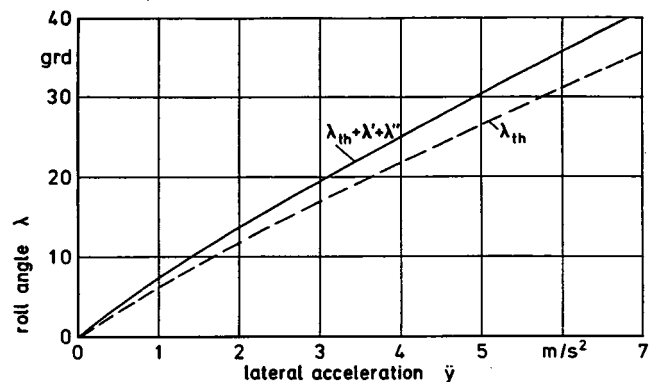


Figure 1. Physical roll angle  $\lambda$  and additional roll angle  $\lambda'$  and  $\lambda''$  as a function of lateral acceleration.

\*Numbers in parentheses designate references at end of paper.

The center of gravity of the whole system, that turns the scale for the angle beside the breadth of the tyre, also reduces by stationary cornering with increasing lateral acceleration and as a consequence of the increased pseudo weight of the vehicle, with correspondant body work compression, figure 2. The fact, that the center of gravity is dependent on the role angle, has a permanent modification of the ideal distribution of the brake force as a consequence. This effect and additional influences like load or pitch, are responsible for the very problematical distribution of the brake force, that is regulated by the driver. Only a dynamical load dependent combined brake is able to recognize such oscillations and to take them regulating into consideration.

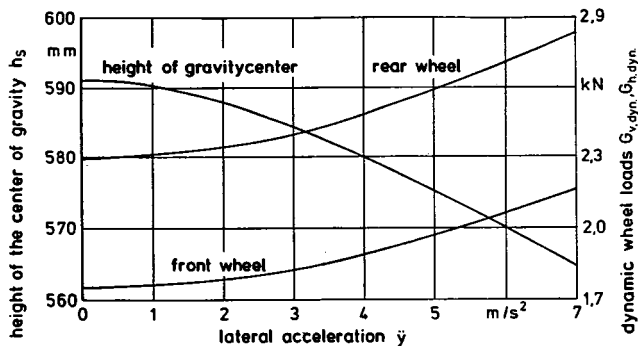


Figure 2. Height of the center of gravity and dynamic wheel loads as a function of lateral acceleration.

The dynamical wheel loads (figure 2), which increase by the lateral acceleration, are not identical with the wheel normal load (= wheel load, vertical to the roadway), that are responsible for the transfer of wheel circumference and cornering force. On roads, which are not lateral inclined, the wheel normal loads correspond by any cornering with those in straight ahead driving; as far as roads are concerned, that increase towards the center of the curve, the wheel normal loads fall off overproportionally. In superelevated curves, these forces can increase until the amount of the dynamical wheel loads as schematically presented in figure 3.

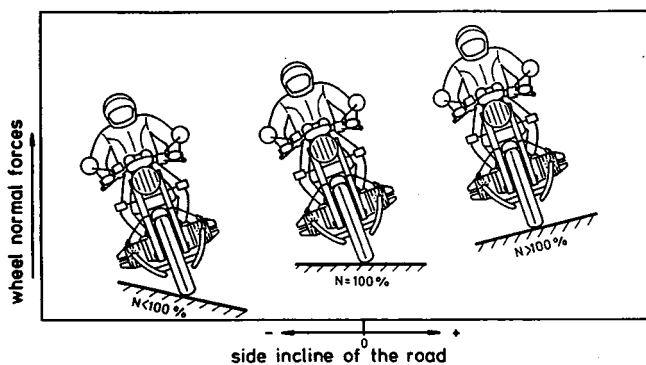


Figure 3. Influence of the side incline of the road on the wheel normal forces.

### Theoretical considerations of braking in the bend

Similar to multi-track vehicles, there is, concerning the motorcycle, a basical superimposition—in the case of brak-

ing in the bend—of the cornering force and the wheel circumference force on the respective wheel, geometrically to the total tangential force. As a consequence of the trigonometrical relations between cornering, brake and total friction force, there is the possibility—if one is not driving with the threshold value of cornering speed—that there are decelerations which are astonishingly high. Moreover the transferable brake forces increase quickly with reducing speed, while the radius of the curve is constant, because of the quadratic dependence of the lateral acceleration on the speed. These brake forces approximate after a short break time on the threshold value of the straight ahead braking in an asymptotical way. Both effects are presented in figure 4 with a theoretical ideal brake system for a medium friction coefficient ( $\mu^0 = 0,8$ ).

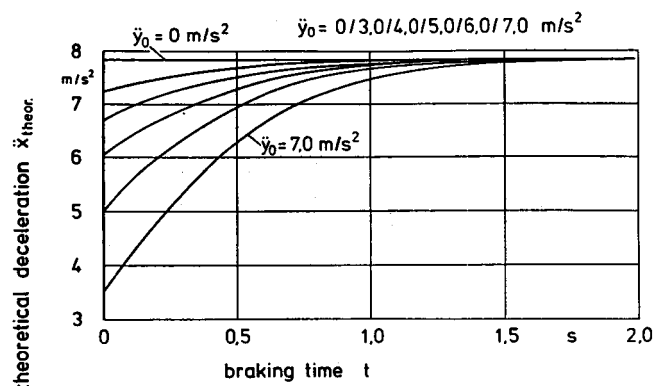


Figure 4. Theoretical time history of the deceleration in curve braking ( $\mu^0 = 0.8$ ;  $V^0 = 50$  km/h).

The theoretically possible medium decelerations are situated on a similar high level above a wide area of lateral acceleration, figure 5. In practise the level of deceleration is a little bit lower, as a consequence of constructive influences, like the loss time of the brake, the relaxation of the wheel, and so on . . . and diving dynamical derange like the unevenness of the roadway or the discharge of a wheel that is caused by the lift. The onliest way to reach this level is to use a brake system which is secure concerning the locking of wheels, because otherwise the risk of a sudden fall is very high.

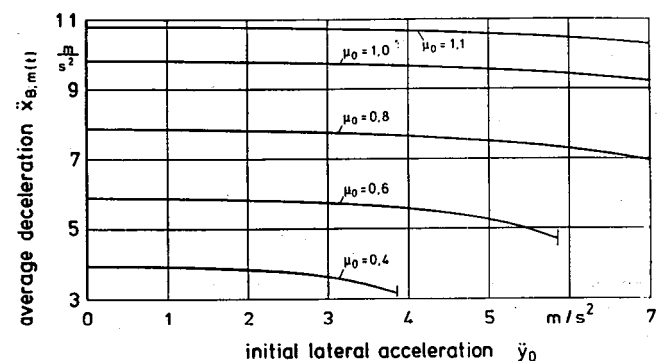


Figure 5. Theoretical average deceleration as a function of the initial lateral acceleration.

The curve of the ideal distribution of the brake force, which is already subjected to fluctuations by straight ahead driving because of the strongly marked pitch, is additionally influenced in cornering: On the one hand the body of the vehicle springs more and more in, with increasing dynamical wheel loads, that are dependent of the lateral acceleration. On the other hand the efficient radius of the wheel diminish with the increasing roll angle of the motorcycle. Both factors have a reduction of the center of gravity as a consequence, shown in figure 6.

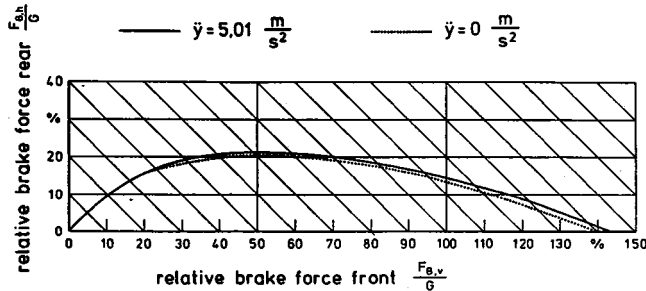


Figure 6. Ideal brake force distribution for straight ahead and curve braking.

In lateral dynamical respect, the braking in the bend of the single-track vehicle is influenced by two factors, which disturb: The brake-steering-moment (Bremslenkmoment) and the lateral wheel slip. The brake-steering-moment arises by the emigration of the efficient center of wheel brake force, that moves with an increasing roll angle to the inner side of the curve. The lateral movement of the center of the wheel contact area, compared with the vehicle's plane of symmetry and as a consequence also with the steering axis, has been measured for a motorcycle of the 1000 cm<sup>3</sup> class and is plot as a function of the total roll angle, figure 7. As it can be seen, it has, dependent on the width of the tyre, considerable quantities. With the aid of these quantities, the brake steering moment, that is calculated for the case of total utilisation of the possible adhesion reaches with increasing lateral acceleration more than 150 Nm, figure 8. During the driving experiments, maximas of 120 Nm have been measured. It is impossible to compensate these quantities by the driver because they are varying or pulsating and

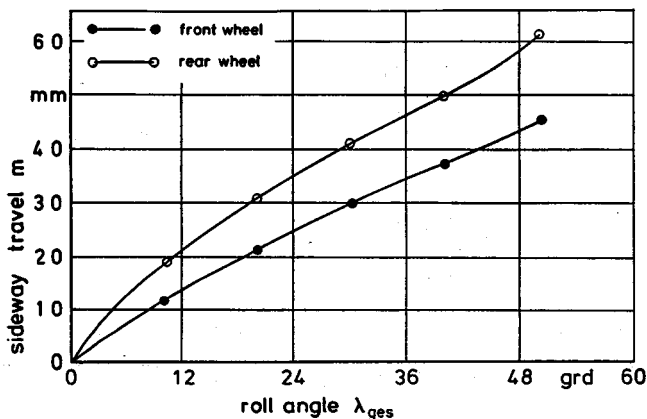


Figure 7. Sideway travel of the tyre contact point as a function of the roll angle.

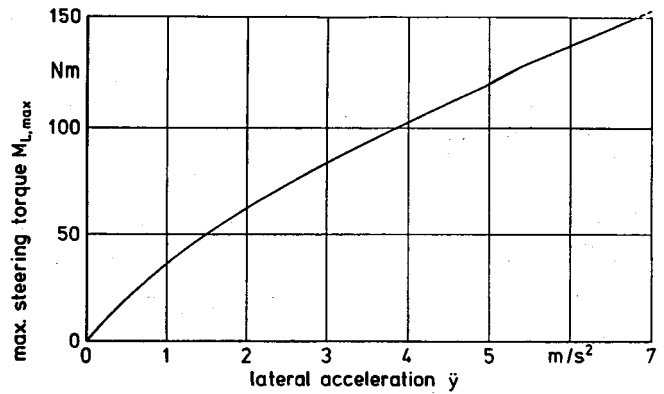


Figure 8. Maximum steering torque while braking as a function of the lateral acceleration (theoretical,  $\mu^0 = 1,1$ ).

this leads, in consequence of its effect, that diminish the radius of the curve and consequently enlarge the centrifugal power, to the feared tangential left of the circular path. Possible helps are a limitation of the brake force, a compensation of the steering moment or a constructive elimination of the steering offset.

### Driving dynamical analysis

To verify the theoretical observations and to analyse the influences, that are difficult to obtain by calculation, like for example the behaviour of the driver, extensive driving dynamical measurements have been carried out. Therefore two powerful motorcycles have been taken, that were equipped, besides the normal standard brake system, with a combined brake system, which can be operated by the feet, and an ABS-system, which can be inserted. To draw all relevant circumferential, vertical and lateral measuring values, a data acquisition system with 19 channels on the basis of a micro-computer has been developed and carried along with the motorcycle. The results have been reviewed with a micro-computer and finally they were evaluated on a mini-computer, figure 9.

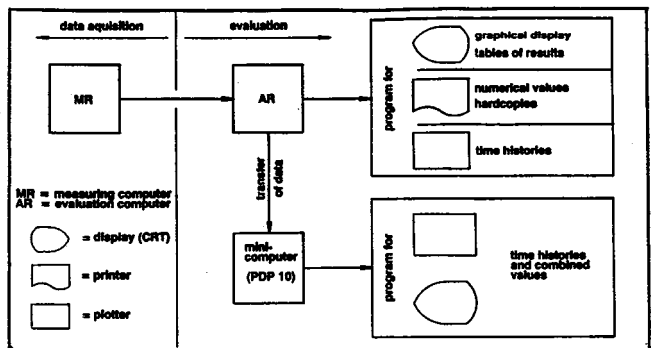


Figure 9. Path of evaluation.

All important driver-, vehicle- and road-dependent parameter have been varied in the driving tests (carried out in the "closed-loop"-method):

- Height, weight and degree of training of the driver,

- Braking system (standard, combined, ABS), the sort of tyres; driving with and without co-driver, initial brake velocity,
- Surface of the roadway, adhesion coefficient, radius of the curve (inclusive lateral acceleration), crossfall.

The measurements with the vehicles are completed by experimental determination of the tyre's way to transfer forces with the help of a special trailer, made for the research on motorcycle tyre. This trailer allows the realistical variation of the measuring speed, the wheel load, the camber and the lateral slip. The map of lateral force, figure 10, shows an appearance, this is typical for the tyres of a motorcycle: A considerable part of the cornering force is brought up by the camber force; cornering without lateral force would only be possible with a negative slip angle.

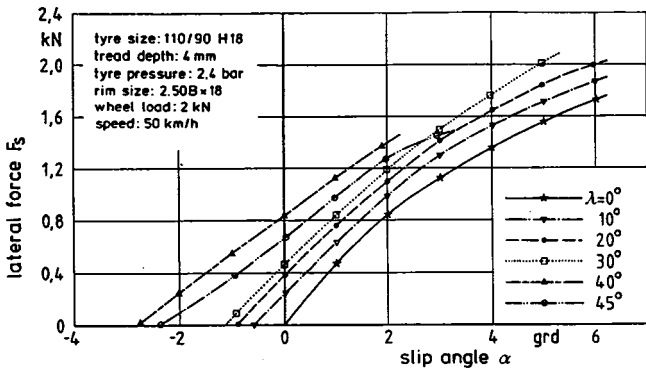


Figure 10. Lateral force as a function of slip angle.

At the moment, a teststand is tested, that allows the analysis of the braking of a stillstanding motorcycle, fixed in the center of gravity, on a translational moved, plain roadway (5). Besides the riskless simulation of braking in high speeds (until 200 km/h), the teststand offers, among other things, the direct measurement of the actual dynamic wheel loads.

### Results (selection)

The tested ABS-system use as regulation dimension only the change of the spin of the road wheels. However especially the electronic ABS-system is indirect sensible for lateral acceleration as it can be seen in figure 11, where an illustration of the hydraulic brake pressure of the front wheel is quoted. The heel and toe curve, which is typical for the ABS-regulation, persists clearly longer in the range of the maximum transferable brake pressure in the case of higher initial lateral acceleration. The reason for this phenomenon is to discover in the  $\mu$ -s-curve, that becomes more flat with an increasing utilisation of the possible lateral slip and the flattening of the maximum of the adhesion coefficient at the same time. As a result of the charged lapse of the graph of the brake pressure, a bigger area under the graph of the brake pressure, which is a gauge for the translated braking work, is filled. This results in an increase of the average deceleration, that is reachable with the electronic ABS, as a

function of the initial lateral acceleration, figure 12, while the other systems exhibit the expected moderate decrease of the deceleration with an increasing initial lateral acceleration. However, it must be mentioned that this gain of deceleration is bought with greater lateral dynamical disturbances.

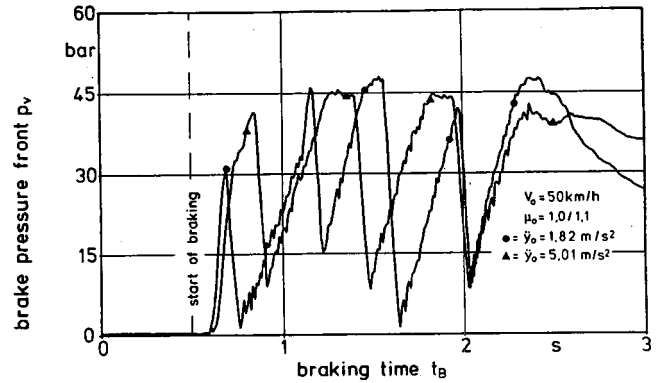


Figure 11. Time history of brake pressure at different initial lateral accelerations.

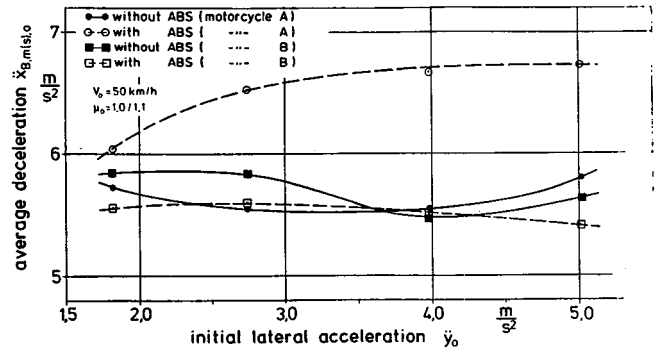


Figure 12. Average deceleration as a function of initial lateral acceleration.

Figure 13 illustrates by the example of the steering angle declination and the steering moment that the lateral dynamical disturbances in the case of increasing lateral acceleration are much greater with the ABS-regulated brake than with the driver-regulated one. The reason therefore is the low frequent pulsating of the brake force if the ABS-regulation works. Nevertheless, the risk of destabilisation with the driver-regulated standard brake is greater as a consequence of the permanent danger of a locking wheel.

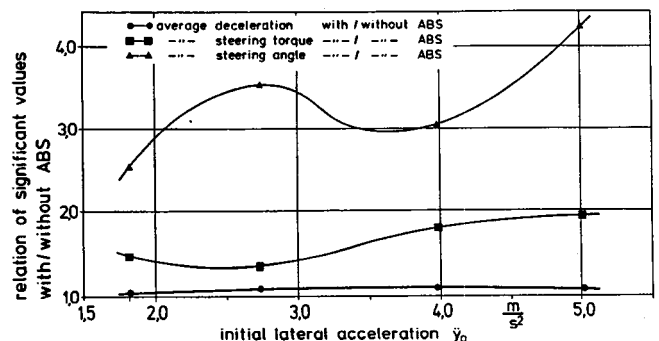


Figure 13. Relation of deceleration, steering torque and steering angle with and without ABS as a function of initial lateral acceleration.

With an increasing initial lateral acceleration the utilisation of the possible brake force takes a more and more unsatisfying development as the lapses of the brake pressure (frontwheel) demonstrate (figures 14 and 15). The driver stays, especially at the beginning of braking, while the speed is still high, far below the possible maximum of brake pressure. He also interprets the transgression of certain amounts of the steering moment and especially of the steering moment velocity as a signal for imminent lockings of a wheel. As a consequence the driver loosens the brake totally or partly. The ABS-regulated brake makes, under identical experimental conditions, a considerable level of brake pressure available, figure 16, with the result of the already

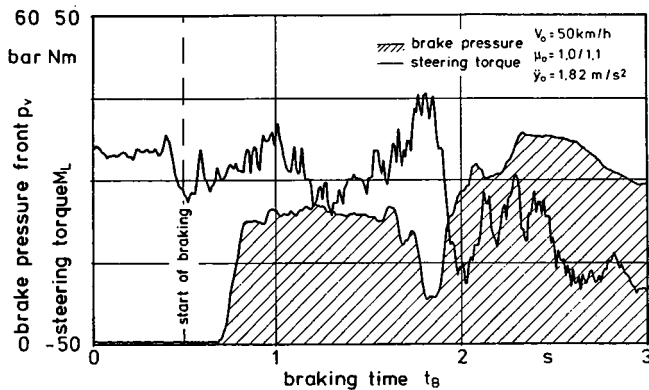


Figure 14. Time history of brake pressure (front wheel) and steering torque at curve braking (standard brake).

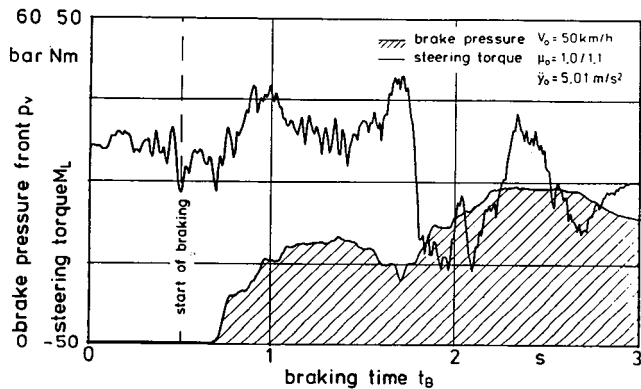


Figure 15. Time history of brake pressure (front wheel) and steering torque at curve braking (standard brake).

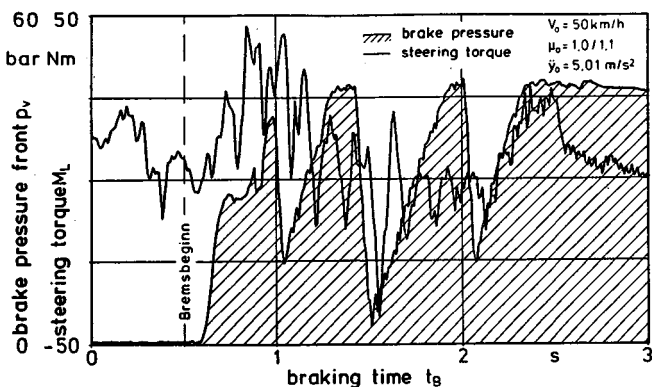


Figure 16. Time history of brake pressure (front wheel) and steering torque at curve braking with ABS.

described favourable average deceleration. However the figure also shows a corresponding turbulent lapse of time of the braking moment with big declinations and steep gradients.

The brake-steering-moment and the change of the steering angle, besides slip angle and sideslip angle, are two lateral dynamical disturbances during braking which are important for the objective driving stability and the subjective feeling of security of driving. As a characteristic value for the security of braking, the increase of steering disturbance (Lenkunruheanstieg) has been defined as a product of the appearing brake-steering-moment and the steering angle velocity, realized as a reaction of the driver. With its help the stability of the course of the straight ahead braking and the braking in the bend is to be valued likewise. Due to figure 17, the increase of steering disturbance of the unregulated brake shows obviously lower values in the whole range of lateral acceleration than the one of the ABS-system (a consequence of the heel and toe regulation). The situation is similarly favourable at the "ABS-protected" braking. The driver is requested to brake nearby the maximum of the adhesion, however without an activation of the regulation of the ready to act ABS-system. This procedure allows high decelerations while the lateral dynamical stability is acceptable. The lapse of the second employed driver is therefore more disadvantageous because he chooses the increase of the brake force that he is occasionally surprised by a dynamic over-braking of the frontwheel (notice 3), connected with a single activation of the ABS-system.

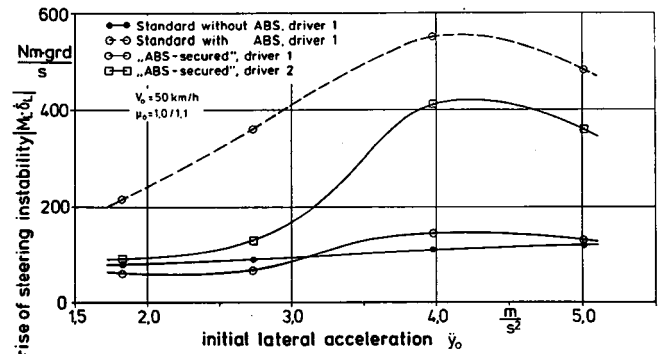


Figure 17. Rise of steering instability as a function of initial lateral accelerations beginning of the braking quiet steep to have the favour of a utmost high deceleration.

One statement has been obviously again and again of not uninteresting importance: The less sophisticated the used brake system is, the bigger is the effect of the driver's training. In figure 18 there is shown the reached distribution of slip on the unregulated braked front wheel at the beginning and at the end of the driving dynamical measurements. It is confirmed, that with an increasing practice, the frequency of braking at the slip level with best adhesion increases as well, but the instable area of high slip or even of the blockade of the wheel ( $s > 95\%$ ) are extensively avoided. With driver of less routine this progress, which is conditioned by practice, is even more obviously.

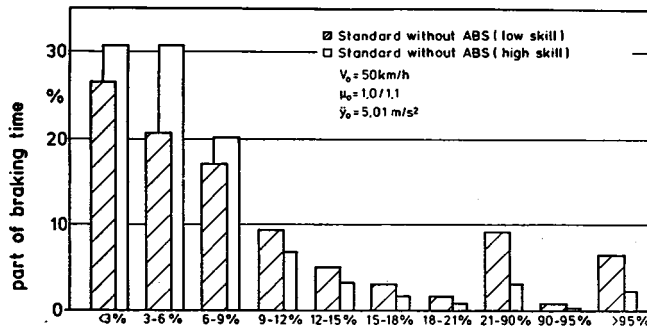


Figure 18. Front wheel slip spectrum (influence of the skill).

## Conclusions and Views

The driver regulated standard brake allows stable braking with high deceleration only under controlled conditions with a trained driver; situations of panic or a lack of routine concerning the driver, have unsatisfactory effects and security of braking as a consequence. A combined brake, which is load dependent, with an ABS-system that has effects on both wheels, unburdens the driver concerning the brake force distribution and allocation and relieves him a secure conduction of the vehicle. The complex driving dynamic of braking in the bend shows the limits of all the up-to-date systems of motorcycle brakes: The standard brake is, concerning the security of braking—the risk of a sudden fall is impossible to calculate (because of the possible wheel locks)—out of the question. ABS-regulated brakes improve the security of braking considerably, they produce, however, pulsating brake-steering-moments which are

dependent on the deceleration and the lateral acceleration. These brake-steering-moments can only be compensated up to a driver dependent limit and moreover, they are able to impair the stability of the course up to a tangential left of the curve track.

Improvements seem to be possible by ABS-regulated systems, which are measuring cornering and adhesion, and also by a constructive elimination of the brake-steering-moments or a compensating steering action. Solutions concerning these possibilities are explored at the moment of the research institute.

## References

- (1) Breuer, B., B. Bayer, M. Pyper u. A. Weidele: Motorräder. Darmstadt 1985. Skriptum for lessons.
- (2) Bayer, B.: Untersuchungen zur Fahrdynamik von Krafträdern unter besonderer Berücksichtigung konstruktiver Einflußparameter auf die Hochgeschwindigkeitsstabilität. Diss. Darmstadt, 1987.
- (3) Weidele, A. u. B. Breuer: Kraftradbremsten-Kombibremsten und ABS. Deutsche Kraftfahrforshung und Straßenverkehrstechnik, Heft 301. Düsseldorf: VDI-Verlag 1984.
- (4) Weidele, A., B. Breuer u. M. Schmieder: Kraft-radbremsten—ABS und Kurvenbremsung. Forschungsbericht Nr. 112/89 des Fachgebiets Fahrzeugtechnik der Technischen Hochschule Darmstadt, 1989, not published.
- (5) Weidele, A.: Fahrdynamik-Prüfstand für Motorräder. In: Radmarkt Nr. 9/1988, S. 125ff., Bielefelder Verlag-sanstalt, 1988.

## Motorcycle Safety Research and Development—State of the Art

**Dr. Hubert Koch,**  
Institut für Zweiradischerheit e. V.,  
Federal Republic of Germany

In the last years a multitude of projects have been carried out around the world to investigate motorcycle accidents. The findings obtained have been published in a wide-ranging spectrum, for example (22, 24, 23, 36, 55, 1, 13, 34, 54).<sup>1</sup>

### Findings From Motorcycle Accident Research

On the basis of a differentiated analysis of the available reports, the following central findings of motorcycle accident research can be summarized as follows:

The percentage of accidents involving only a **single vehicle accident** is approximately 30% (55, 54, 22).

The main **collision partners** are cars (approximately 75%) (22, 55, 35, 33).

The main **type of collision** is turning off (generally turning left, or right in countries which drive on the

left) of a car which leads to a collision with an oncoming or overtaking motorcycle (22, 55, 13, 54).

The **main accident locations** are crossroads (approximately 45%). Bends make up for around 32% of accident locations, whereas slopes and gradients account for around 11% (22, 55, 13, 54).

The **accident causes** are predominantly not observing the right of way of the motorcyclist by other road users (approximately 67%) (22, 1).

The **apportioning of blame** in car-motorcycle collisions is approximately 61% for the car drivers and approximately 35% for motorcyclists (22, 55, 13).

The pattern of injuries in accidents involving motorcycles has also been subjected to a highly differentiated study. The following findings can be regarded as being reliable:

**Head injuries** can be registered in approximately 52% of motorcycle accidents (1, 35, 29, 17). They lead most frequently to severe injuries and to fatalities (17).

**Leg injuries** dominate clearly in the injury frequency (up to 83%) (45, 35, 55, 3).

<sup>1</sup>Numbers in parentheses denote references at end of paper.

The **points of impact** in collisions between cars and motorcycles differ in the resulting injury severity and the injury patterns. Particularly the impact with the front wind-screen frame, the roof edge and A, B, C, D-posts leads to serious injuries (47, 19, 35).

The **direction of the collision** is most frequently the 90° lateral collision (approximately 58%) (46, 35, 13, 34).

The **collision type** which has the least severity of injury for the motorcyclist is flying over the car as collision obstacle (39, 46, 17).

On the basis of the analysis of actual accidents described above, a multitude of laboratory experiments, as a rule collision tests, were carried out in order to investigate the kinematics of the motorcycle accident in more detail. The aim here was to obtain more detailed findings on the sequences of movements and more precise data on the causes of injuries so that protection possibilities for motorcyclists could be developed on this basis (32, 40, 46, 36, 19, 6, 43, 7, 9, 48).

## **Constructive Conversion of the Results of Motorcycle Accident Research**

Using the basis of both the actual accident investigations and also the laboratory experiments, a series of protection possibilities for motorcyclists was developed which improve the passive safety and therefore reduce the severity of injury. Certain examples should be mentioned here:

**Protectors** to reduce the danger from the posts of **crash barriers** which are aggressive both in their form and material (25, 11, 27).

**Optimized crash helmets** (41, 26, 47, 19, 21, 42, 44, 15, 5, 14, 28).

Improved and/or newly developed **protective motorcycle clothing** (protective suits) (51, 2, 37, 38, 41, 4, 52, 53).

**Motorcycle airbags** as restraint systems and/or structural elements to influence the line of flight (56, 46, 8, 30).

**Leg protection** (23, 36, 48, 16, 9, 7, 43, 20, 6).

Concepts for **safety motorcycles** with elements such as leg protection, special designs of the fuel tank-seat line, airbag, protective claddings, optimized handlebar design and seat fixing or lateral collision protection (18, 31, 30, 49, 50, 10, 46).

## **Leg Protection—a Controversially Discussed Structural Element to Increase Passive Safety**

**Leg protection**, although it has been under discussion for many years, can serve as the latest example of a development, which has been directly derived from collision investigations and which was already a basis for a political initiative (England).

For this reason this development in passive accident protection should be looked at more closely in order to—*pars pro toto*—demonstrate the current state of research-supported motorcycle safety development.

An analysis of the scientific literature published in the last few years around the world produces in part completely different findings in spite of the comparable investigation design.

The following illustrates the contrary statements on the positive and negative consequences of leg protection for motorcycles using the most important sources as a basis.

### **Positive aspects of leg protection:**

Leg protection leads to a reduction both in the frequency and the severity of leg injuries (6, 7, 9).

Leg protection positively influences the line of flight by a put up moment (6, 7, 9).

Leg protection reduces the number and the severity of head injuries (6, 7, 9).

### **Negative aspects of leg protection:**

Leg protection leads neither to a reduction in the frequency nor the severity of leg injuries, according to the latest investigation findings even leads to an increase of the frequency of leg injuries (43, 48, 18).

Leg protection can induce additional thigh and hip injuries and also increase the flight speed of the rider after the collision (catapult effect) (48, 43).

Leg protection can lead to an increase in the number and severity of injuries to the upper part of the body and the head (43, 38).

These contradictory findings can be explained with an exact comparable analysis of the fundamental research work. There are a multitude of highly differing conditional factors:

The leg protection units used in the tests are clearly different in their design and were installed on completely different types of motorcycles (48, 6, 46).

The impact simulation was carried out using artificial barriers on the one hand and test cars on the other (6, 43, 7, 9, 48).

The impact speeds selected in setting up the tests did not always agree (43, 7).

The impact angles used in the tests did not cover the same spectrum in every case.

The vehicle configurations differed clearly (e.g. shape of handlebars, seat position, form of the fuel tank-seat line, etc.) (48, 6, 46).

The ergonomic parameters of the dummies used in the tests did not agree (7, 43).

## **Attempts to Define the Goals of Motorcycle Safety Research**

The problems illustrated clearly show a basic dilemma of motorcycle accident research:

At the present time there is a lack of defined and standardized tests. There are no generally valid guidelines for the performance of the tests and there are no uniform measuring processes. There are not even uniform test equipment or measuring methods.

In order to solve the last-mentioned problem it would certainly be helpful to develop and use a measuring dummy specially designed for motorcycle impact tests, which was presented at the 1989 ESV Conference in Gothenburg (125).

The Hybrid III-ATD stands out because it takes particular account of the human movement behaviour and the vulnerability particularly of the lower body extremities and of the head area. Modified measured value recorders were adapted to the specific situation of a motorcycle accident and permit more exact measurements and more valid transfers of the measured results.

Although this technical innovation is without a doubt a step in the right direction, the decisive deficit in present accident research cannot be corrected by this. This deficit is the lack of clearly defined research aims and the resulting research work acceptable to all research scientists. Such a clear definition of the aim, as for example in the automobile industry many years ago, the survival of an impact against a solid wall at a speed of 50 km/h could make the research and development work clearer, more exact and more efficient.

If motorcycle accident research and safety development were to be orientated towards such defined aims, then the complexity of the research item would be clearer and the conditional factors would stand out more clearly.

The following is an attempt to formulate certain potential wide-ranging aims of motorcycle safety development. The basis of the formulations is among others an international questionnaire study of motorcycle accident researchers prepared by the Institut für Zweiradsicherheit e. V. (publication in progress).

Of decisive importance is the close networking of the findings from actual motorcycle accident research with the type and results of laboratory experiments. The concentration on particularly serious accident sequences which dominate in their frequency and injury severity promises an efficient improvement of the output.

The projected aim named most frequently by the questioned accident researchers can be seen in parallel to automobile accident research: the lateral collision of a motorcycle with a moving car at a speed of approximately 50 km/h should be able to be survived by the motorcyclist.

In general, the concentrated activities of international research institutes with an efficient safety element would lead considerably earlier to a consensus on the most effective design so that an appropriate introduction into series production and therefore an improvement to the actual accident events could be achieved.

It is also of crucial importance that the findings obtained from the individual structural safety elements are integrated into an overall concept so that negative interactions of combined individual components can be avoided and that

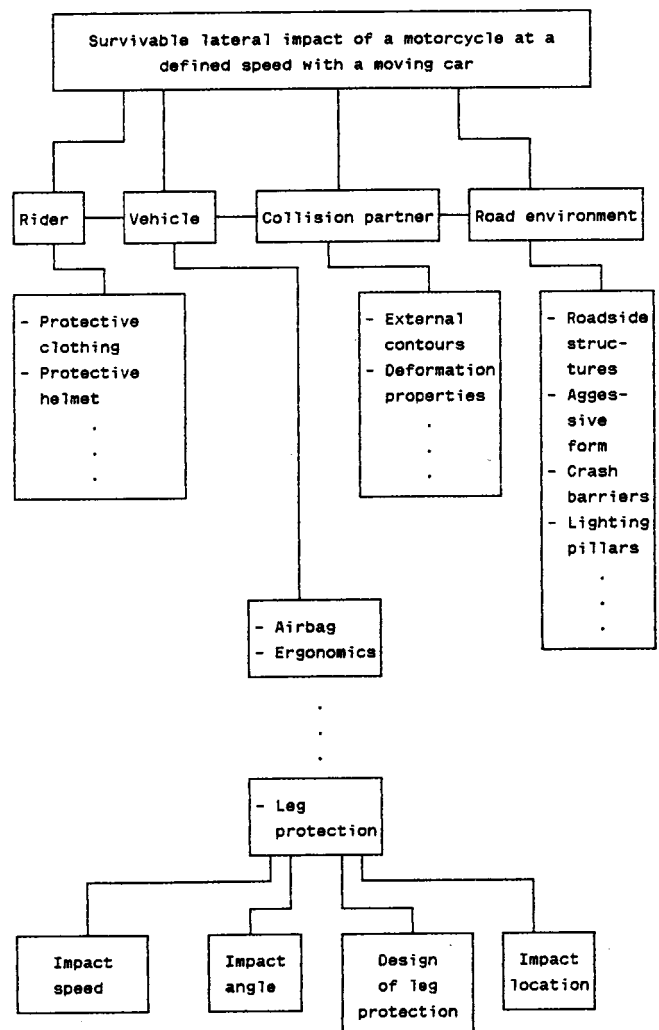
the ideal case could simultaneously lead to an even greater combined increase in the safety level.

The safety development of the motorcycle cannot be carried out in an isolated fashion, but directly in parallel with the design of other vehicles (cars, trucks, etc.), the development of protective clothing for the rider, the reduction in the dangers of the road environment, etc. This is the only way to comprehend the interactions which are present in accident events.

The following diagram serves as an example to illustrate in which conditional structure the research and development work in leg protection stands, if it is orientated towards a higher aim. It should also be taken into consideration that leg protection must not only be effective in the context given for the collision type here, but must also prove its worth in all other occurring collision and accident types; as a minimum it must have a neutral effect.

## Integration of Leg Protection in a Networked Model of Motorcycle Safety Research

Integrated model of motorcycle safety research using leg protection as an example.



The diagram shown above provides an exemplary overview of the components to be taken into consideration and the relevant possibilities for improvement. However, these must not be investigated and taken into account in isolation, but in their interactive combinations during both research and development. The guideline for all actions is the higher aim, in this case the survivability of the lateral impact with a moving car at a defined speed. Here it must be precisely formulated which partial components in the overall accident events can make which contribution to achieve the overall aim. In addition such a method of proceeding permits the formulation of further precise aims, which can be defined to be more realistic, more valid and more comprehensive.

## Perspectives

The following results as a perspective for the future of motorcycle safety research:

It is not the continued accumulation of new individual findings from empirical investigations which are important, but the development of an achievable, realistic catalogue of aims, orientated towards the actual accident events.

An overall research and development concept can be based on this catalogue of aims.

This method of proceeding permits the prevention of short-term, political (wrong) decisions, and at the same time concentrates the available research capacities, and, using the same resources, can supply more and better results to further improve the safety level of motorcycle traffic.

## References

(1) Adelaide in-depth accident study: 1975–1979 / A.J. McLean [u.a.]. The University of Adelaide, Road Accident Research Unit.—Adelaide, 1979.

(2) Aldman, Kajzer, Gustafsson, Nygren, Tingvall  
Schutzwirkung eines besonders entwickelten Anzugs für Motorradfahrer IN: Passive Sicherheit für Zweiradfahrer: Referate d. 2. Bochumer Workshops für Zweiradsicherheit / hrsg. von Hubert Koch.—Bochum, 1987.—S. 57–76 (Forschungshefte Zweiradsicherheit; 5).

(3) Appel, Herrmann; Otte, Dietmar; Wüstemann, Joachim: Epidemiologie von Unfällen motorisierter Zweiradfahrer in der Bundesrepublik Deutschland: Sicherheitsaspekte IN: Der Motorradunfall: Beschreibung, Analyse, Prävention / hrsg. von Hubert Koch. Institut für Zweiradsicherheit.—Bremerhaven, 1986.—S. 47–92 (Forschungshefte Zweiradsicherheit; 3).

(4) Bayer, Bernward; Breuer, Bert: Experimentelle Untersuchungen an Motorradfahrerschutzbekleidung unter besonderer Berücksichtigung von Schutzhandschuhen IN: Der Motorradunfall: Beschreibung, Analyse, Prävention / hrsg. von Hubert Koch. Institut für Zweiradsicherheit.—Bremerhaven, 1986.—S. 241–276 (Forschungshefte Zweiradsicherheit; 3).

(5) Berge, Wilfried Untersuchungen an Motorradhelmen im Windkanal IN: Passive Sicherheit für Zweiradfahrer:

Referate d. 2. Bochumer Workshops für Zweiradsicherheit / hrsg. von Hubert Koch.—Bochum, 1987.—S. 3–25 (Forschungshefte Zweiradsicherheit; 5).

(6) Chinn, B.P.: Injuries to motorcyclists' legs: testing procedures and protection.—Uxbridge University Thesis 1985.

(7) Chinn, B.P.; Hopes, P.D.; Finnis, Melanie P.: Leg protection and its effect on motorcycle rider trajectory. Paper presented to the 12th International Technical Conference on experimental safety vehicles. Gothenborg 1989 (printing in progress).

(8) Chinn, B.P.: Motorcycle impact simulation and practical verification IN: The eleventh International Technical Conference on Experimental Safety Vehicles: May 12–15 Washington, DC.; 20 years of progress in highway safety / U.S. Department of Transportation, National Highway Traffic Safety Administration.—Washington, D.C., 1987.—S. 858–864.

(9) Chinn, B. P.; Hopes, P. D.: Protecting motorcyclists legs IN: The eleventh International Technical Conference on Experimental Safety Vehicles: May 12–15 Washington, D.C.; 20 Years of progress in highway safety / U.S. Department of Transportation, National Highway Traffic Safety Administration. Washington, D.C., 1987.—S. 902–909.

(10) Danner, Max; Langwieder, Klaus; Sporer, Alexander: Unfälle motorisierter Zweiradfahrer: Sicherheitserhöhung durch techn. Maßnahmen aus d. Kenntnis d. realen Unfallgeschehens IN: Der Motorradunfall: Beschreibung, Analyse, Prävention / hrsg. von Hubert Koch. Institut für Zweiradsicherheit.—Bremerhaven, 1986.—S. 215–239 (Forschungshefte Zweiradsicherheit; 3).

(11) Domhan, Martin: Passive Sicherheit von Schutzplanken bei Anprall von Motorradfahrern IN: Passive Sicherheit für Zweiradfahrer: Referate d. 2. Bochumer Workshops für Zweiradsicherheit / hrsg. von Hubert Koch.—Bochum, 1987.—S. 163–176 (Forschungshefte Zweiradsicherheit; 5).

(12) Engels, Klaus: Analyse des Unfallgeschehens mit motorisierten Zweirädern auf der Basis des von der Polizei erhobenen Unfalldatenmaterials IN: Der Motorradunfall: Beschreibung, Analyse, Prävention / hrsg. von Hubert Koch. Institut für Zweiradsicherheit.—Bremerhaven, 1986.—S. 93–112 (Forschungshefte Zweiradsicherheit; 3).

(13) Erhebungen am Unfallort / Dietmar Otte [u.a.]. Bundesanstalt für Straßenwesen, Bereich Unfallforschung.—Köln, 1982.

(14) Facial protection of motorized two-wheeler riders: new features of a specification for "full face" helmet IN: 1984 International IRCOBI Conference on the Biomechanics of Impacts: 4–5–6 Sept. Delft (The Netherlands); proceedings / Delft, 1984 S. 193–211.

(15) The fracturing of helmet shells IN: 1984 International IRCOBI Conference on the Biomechanics of Impacts: 4–5–6 Sept. Delft (The Netherlands); proceedings

/ International Research Committee on Biokinetics of Impacts.—Delft, 1984.—S. 99–110.

(16) Fuller, Peter M.; Snider, John N.: Lower leg injuries resulting from motorcycle accidents IN: The eleventh International Technical Conference on Experimental Safety Vehicles: May 12–15 Washington, D.C.; 20 years of progress in highway safety / U.S. Department of Transportation, National Highway Traffic Safety Administration.—Washington, D.C., 1987.—S. 865–869.

(17) Gahr, R.H.: Der Motorradunfall aus der Sicht des Notarztes IN: Dortmunder Notarztkolloquien: präklin. Versorgung aus interdisziplinärer Sicht / hrsg. von G. Kramer u. R.H. Gahr. Unter Mitarb. von M. Andres [u.a.].—Erlangen, 1987.—S. 99–109 (Notfall Medizin; 16).

(18) Gaukler, Conradin: Gedanken zu einem zukünftigen Sicherheitsmotorrad IN: Verkehrsunfall—und Fahrzeugtechnik.—23(1985)3.—S. 89–92.

(19) Grandel, Jürgen; Schaper, Dieter: Der Schutzhelm als passives Sicherheitselement: Anforderungen an künftige Entwicklungen aus Sicht der Unfallforschung IN: Passive Sicherheit für Zweiradfahrer: Referate d. 2. Bochumer Workshops für Zweiradsicherheit / hrsg. von Hubert Koch.—Bochum, 1987.—S. 109–130 (Forschungshefte Zweiradsicherheit; 5).

(20) Harms, P.L.: Leg injuries and mechanisms in motorcycling accidents Paper presented to the 12th International Technical Conference on experimental safety vehicles. Gothenborg 1989 (printing in progress).

(21) Harms, P.L.: A study of motorcyclist casualties with particular reference to head injuries IN: 1984 International IRCOBI Conference of the Biomechanics of Impacts: 4–5–6 Sept. Delft (The Netherlands); proceedings / International Research Committee on Biokinetics of Impacts.—Delft, 1984 S. 91–98.

(22) Hurt, H. H.; Quellet, J. V.; Thom, D. R.: Motorcycle accident cause factors and identification of countermeasures: final report / Traffic Safety Center, University of Southern California. Prepared for U. S. Department of Transportation, National Highway Traffic Safety Administration.—Los Angeles, Calif., 1981. Vol. 1. Technical report. Vol. 2. Appendix / Supplemental data.

(23) Hurt, Hugh H.; Quellet, James V.; Jennings, Gordon: Motorcycle crash bar effectiveness: a re-evaluation using AIS-80 IN: 28th Annual proceedings American Association for Automotive Medicine: Oct. 8–10, 1984.—Colorado, II.—S. 237–246.

(24) Hurt, H. H.: Status report of accident investigation data: motorcycle accident cause factors and identification of countermeasures / Traffic Safety Center, University of Southern California. Prepared for U. S. Department of Transportation. National Highway Traffic Safety Administration.—Los Angeles, Calif., 1979.

(25) Jessl, Peter: Anprallversuche an Leitplanken mit Dummies IN: Passive Sicherheit für Zweiradfahrer: Referate d. 2. Bochumer Workshops für Zweiradsicherheit / hrsg. von Hubert Koch.—Bochum, 1987.—S. 141–161 (Forschungshefte Zweiradsicherheit; 5).

(26) Jessl, P.; Christ, W.; Decker, H.-J.: Sicht durch Helmvisiere IN: Aktive und passive Sicherheit von Krafträdern: Tagung Berlin, 8.—9. Oktober 1987 / VDI-Ges. Fahrzeugtechnik.—Düsseldorf, 1987.—S. 245–261.

(27) Der Körperanprall gegen Schutzplanken beim Verkehrsunfall motorisierter Zweiradbenutzer / von Florian Schüler u.a.—Bremerhaven, 1984 (Forschungshefte Zweiradsicherheit; 2).

(28) Köstner, H.; Stöcker, U.: Mathematische Analyse der Stoßabsorption im Schutzhelmmaterial IN: Aktive und passive Sicherheit von Krafträdern: Tagung Berlin, 8.—9. Oktober 1987 / VDI-Ges. Fahrzeugtechnik.—Düsseldorf, 1987.—S. 211–244.

(29) Den Kopf hingehalten: Dummies fahren bei Opel Motorrad / Adam Opel.—Rüsselsheim, 1985.

(30) Langwieder, K.; Spörner, A.; Polauke, J.: Ansatzpunkte zur Erhöhung der passiven Sicherheit: Erkenntnisse der Unfallforschung IN: [Hundert] 100 Jahre Motorrad: Tagung München, 10. u. 11. Okt. 1985 / VDI-Ges. Fahrzeugtechnik. Verein Dt. Ingenieure.—Düsseldorf, 1986.—S. 171–190.

(31) Langwieder, K.; Spörner, A.; Polauke, J.: Stand der passiven Sicherheit für Motorradfahrer und mögliche Entwicklungstendenzen IN: Aktive und passive Sicherheit von Krafträdern: Tagung Berlin, 8.—9. Oktober 1987 / VDI-Ges. Fahrzeugtechnik.—Düsseldorf, 1987.—S. 29–52 (VDI-Berichte; 657).

(32) Lindenmann, Max: Unfall- und Aufprallforschung mit Motorrädern IN: Sicherheit für Zweiradfahrer: 1. Schweiz. Fachtagung für Zweiradsicherheit; 26./27. Februar 1987 / Schweiz. Motorradfahrerverband.—Wohlen, 1987.—6 S.

(33) Mechanism of lower limb injuries amongst motorcyclist casualties: preliminary findings IN: 1984 International IRCOBI Conference on the Biomechanics of Impacts: 4–5–6 Sept. Delft (The Netherlands); proceedings / International Research Committee on Biokinetics of Impacts.—Delft, 1984 S. 243–251.

(34) Otte, Dietmar; Jessl, Peter; Suren, Ernst Günter: Impact points and resultant injuries to the head of motorcyclists involved in accidents, with and without crash helmets IN: 1984 International IRCOBI Conference on the Biomechanics of Impacts: 4–5–6 Sept. Delft (The Netherlands); proceedings / International Research Committee on Biokinetics of Impacts.—Delft, 1984.—S. 47–64.

(35) Otte, Dietmar; Suren, Ernst-Günter; Appel, Herrmann: Lösungsansätze zur Verbesserung der Verletzungssituation des motorisierten Zweiradbenutzers IN: Passive Sicherheit für Zweiradfahrer: Referate d. 2. Bochumer Workshops für Zweiradsicherheit / hrsg. von Hubert Koch.—Bochum, 1987.—S. 3–25 (Forschungshefte Zweiradsicherheit; 5).

(36) Ouellet, James V.; Hurt, Hugh H.; Thom, David R.: Collision performance of contemporary crashbars and motorcycle rider leg injuries IN: Accident reconstruction; automobiles, tractor—semi-trailers, motorcycles and

pedestrians; International Congress and Exposition, Detroit, 23–27, 1987 / Society of Automotive Engineers.—Warrendale, Pa., 1987 S. 131–145.

(37) Protective clothing for motor cyclists / a study made by the insurance company Folksam. Project leader: Hans Gustafsson . . .—[o.o., ca. 1984].

(38) The protective effect of a specially designed suit for motor-cyclists / B. Aldman [u.a.] IN: The tenth International Technical Conference on Experimental Safety Vehicles July 1–5, 1985 Oxford / U.S. Department of Transportation, National Highway Traffic Safety Administration.—Washington, D.C., 1987.—S. 1095–1100.

(39) Rau, Hartmut: Simulation von Zweiradkollisionen IN: Sicherheit bei motorisierten Zweirädern / Kolloquium d. Instituts für Verkehrssicherheit im Technischen Überwachungs-Verein Rheinland e.V., . . . ; Veranstaltung der TÜV-Akademie Rheinland am 4. Dez. 1980 in Köln-Poll.—Köln, 1980.—S. 212–255.

(40) Rau, Hartmut; Pasch, Reinhard; Rattaj, Horst: Der Zusammenstoß Pkw—Zweirad: Ergebnisse experimenteller Untersuchungen IN: Der Verkehrsunfall.—(1979)10.—S. 205–211; 11.—S. 227–232.

(41) Schüler, Florian: Der Beitrag von Straße, Verkehrseinrichtungen und persönlicher Schutzausrüstung zur passiven Sicherheit von Motorradaufsassen IN: [Hundert] 100 Jahre Motorrad: Tagung München, 10. u. 11. Okt. 1985 / VDI-Ges. Fahrzeugtechnik. Verein Dt. Ingenieure.—Düsseldorf, 1986 S. 191–212 (VDI-Berichte; 577).

(42) Schüler, Florian; Schmidt, Georg: Unfallanalytische und biomechanische Aspekte des Motorradunfalles unter besonderer Berücksichtigung der Funktion von Kraftfahrerschutzhelmen IN: Der Motorradunfall: Beschreibung, Analyse, Prävention / hrsg. von Hubert Koch. Institut für Zweiradsicherheit.—Bremerhaven, 1986.—S. 197–214 (Forschungshefte Zweiradsicherheit; 3).

(43) Shinichi, Sakamoto: Difficulties in leg protection research Paper presented to the 12th International Technical Conference on experimental safety vehicles. Gothenborg 1989 (printing in progress).

(44) Schutzhelme für motorisierte Zweiradfahrer / Bundesanstalt für Straßenwesen, Bereich Unfallforschung.—Bergisch Gladbach (Forschungsberichte der Bundesanstalt für Straßenwesen, Bereich Unfallforschung; . . . ) Bericht zum Forschungsprojekt 7806. H. Laboruntersuchungen / Peter Jessl [u.a.]—1983. I. Auswertung von Zweiradunfällen / Dietmar Otte; Ernst Günter Suren.—1985 J. Unfallanalyse / Gundolf Beier [u.a.]—1985 K. Helmvisiere / Walter Christ [u.a.]—1987.—Teil I-II.

(45) Skanda, Peter: Unfälle mit dem motorisierten Zweirad und ihre Verletzungsfolgen: 1975–1978.—

Heidelberg, 1979.

(46) Spörner, Alexander: Experimentelle und mathematische Simulation von Motorrad-Kollisionen im Vergleich zum realen Unfallgeschehen.—München, 1982.

(47) Stöcker, Ulrich: Optimierung von Kraftfahrerschutzhelmen IN: Passive Sicherheit für Zweiradfahrer: Referate d. 2. Bochumer Workshops für Zweiradsicherheit / hrsg. von Hubert Koch.—Bochum, 1987.—S. 91–106 (Forschungshefte Zweiradsicherheit; 5).

(48) Tadokoro, Hidetoshi; Fukuda, Shigehisa; Miyazaki, Kyoichi: A study of motorcycle leg protection IN: The tenth International Technical Conference on Experimental Safety Vehicles July 1–5, 1985 Oxford / U.S. Department of Transportation, National Highway Traffic Safety Administration.—Washington, D.C., 1987.—S. 1100–1108.

(49) Watson, Peter M. F.: ESM 3 [three]—a motorcycle demonstrating progress for safety IN: The eleventh International Technical Conference on Experimental Safety Vehicles: May 12–15 Washington, D.C.; 20 years of progress in highway safety / U.S. Department of Transportation, National Highway Traffic Safety Administration.—Washington, D.C., 1987.—S. 883–888.

(50) Watson; Donne: ESM-4, a lightweight safety motorcycle. Paper presented to the 12th International Technical Conference on experimental safety vehicles. Gothenborg 1989 (printing in progress).

(51) Weidele, Alois: Untersuchung des Unfallverhaltens für Motorradschutzbekleidung.—1980.

(52) Weidele, Alois: Schutzkleidungsprüfung und Entwicklungsmöglichkeiten IN: Aktive und passive Sicherheit von Krafträdern: Tagung Berlin, 8.–9. Oktober 1987 / VDI-Ges. Fahrzeugtechnik.—Düsseldorf, 1987.—S. 263–279 (VDI-Berichte; 657).

(53) Weidele, Alois: Schutzkleidung aus Synthetik: Alternative zu Leder IN: Sicherheit für Zweiradfahrer: 1. Schweiz. Fachtagung für Zweiradsicherheit; 26./27. Februar 1987 / Schweiz. Motorradfahrlehrerverband.—Wohlen, 1987.—14 S.

(54) Whitaker, J.: A survey of motorcycle accidents / by J. Whitaker. Transport and Road Research Laboratory.—Crowthorne, 1980 TRRL Laboratory report 913.

(55) White, James G.: Motorcycle accident study: a report / prepared by the Road and Motor Vehicle Traffic Safety Branch, Transport Canada by James G. White.—Ottawa, Ontario, Canada, 1980.

(56) Yamamoto, Takenori: Some basic considerations on occupant restraint systems for motorcycles IN: Sicherheit bei motorisierten Zweirädern / Kolloquium d. Instituts für Verkehrssicherheit im Technischen Überwachungs-Verein Rheinland e.V., . . . ; Veranstaltung der TÜV-Akademie Rheinland am 4. Dez. 1980 in Köln-Poll.—Köln, 1980.—S. 258–278.

# Load Measuring Method of Motorcyclist's Leg During Motorcycle Collision

Written Only Paper

**Kyoichi Miyazaki and Masami Kubota,**  
Japan Automobile Research Institute, Inc.,  
**Shinichi Sakamoto,**  
Japan Automobile Manufacturers Association

## Abstract

In spite of considerable effort of researchers, an effective leg protection device for motorcyclists free from undesirable side effects has not been developed yet. In order to explore the feasibility in the development of an effective motorcycle leg protection device, it is beneficial to analyze the mechanism of leg injury. Progress in measuring methods of leg load will contribute to research into leg protection devices. Following the earlier report (reference 1), further investigation of leg load measuring methods has been continued.

## Introduction

Many researchers have been working to develop leg protection devices for motorcyclists. Although the purpose of a leg protection device is to preserve leg space to prevent leg injuries, it must be attained without increasing the risk of injuries to other parts of the body. One research step for achieving this is to measure and analyze the degree of leg injury quantitatively. Leg load can be considered to be one of the factors influencing the degree of injury.

Through our research into leg protection, we have recognized the importance of continuing to study leg load measuring methods. In the previous report, a leg load measuring system using many sensors attached to the leg bones of a Hybrid III dummy (references 2, 3) was examined by impact tests. While the possibility of specifying load points, load values and load direction was indicated, some points requiring further improvement were also revealed.

In addition, it was indicated that the dummy's behavior at the time of impact could be hindered by its nonbreakable metallic leg bone. Accordingly, we have conducted experiments using three different types of leg bone structures, under more realistic impact conditions in furtherance of this research.

## Method

If the dummy leg is made of non-breakable material such as steel, it offers the advantage of allowing load measurement beyond the level at which a human leg bone would fracture. However, because the bone does not break at these measured load values, these values naturally differ from the actual ones and also the dummy's behavior is adversely affected. In the hopes of resolving these problems, three kinds of leg bone structures utilizing

materials and sensors were adapted and tested in this research.

## Dummy leg bone structure

To evaluate rider safety in motorcycle collision experimentally, it is useful to simultaneously measure leg loads and observe rider behavior. To do this, we made the leg joints of the Hybrid III dummy we had used before more compact and unified the sensor mounts. More compact sensor system with reduced cross-sensitivity was developed, the three kinds of dummy legs used were:

- A steel bone with sensors at the end of each tibia (hereafter, "steel-sensor bone");
- A breakable bakelite bone without sensors (hereafter, "all bakelite bone") (reference 4);
- A breakable bakelite bone with sensors at each end (hereafter, "bakelite-sensor bone").

These leg's structural outline is described in table 1.

Table 1. Structural summary of dummy's lower legs.

LEG	MEASUREMENT ITEMS	COMMENTS
Hybrid III	Upper: Mx, My Lower: Mx, Fy, Fz	No sensor interchangeability, sensors too large
All bakelite bone	Fr <sub>x</sub> *: Yes/No & Mode	Difficult to obtain information without breaking
Bakelite-sensor bone	Upper: Fx, Mx, My, Lower: Fx, Mx, My, Fr <sub>x</sub> *: Yes/No & Mode	Breakable part is short, sensor damage possible
Steel-sensor bone	Upper: Fx, Mx, My, Lower: Fx, Mx, My,	Non-breakable, influences dummy behavior

\* Fr<sub>x</sub>: Fracture  
x,y,z: See Ref. 2

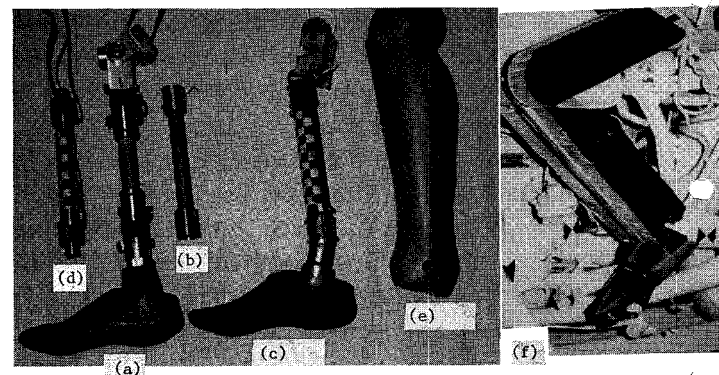


Figure 1. Lower legs of dummy for collision testing.

Figure 1 shows existing lower legs, with (a), (b) and (c) representing the three kinds of lower legs explained before. The steel-sensor bone is (a), (b) is the bakelite-sensor bone and (c), the all bakelite bone.

More compactly modified knee joint of the Hybrid III dummy is attached to the bakelite-sensor bone and is shown as (b), it is also applicable to both (a) and (c).

Lower leg (d) is made to the standard measurements for the Hybrid III dummy, while (e) is the lower-leg "flesh" for (a)—(d). For reference, (f) is the lower leg used by the United Kingdom Transport and Road Research Laboratory (reference 5). It features a square steel plate, to the left and right of which are attached of aluminum honeycomb. Figure 2 shows the detail of the bakelite-sensor bone. As can be seen from this figure, sensors are located at the upper and lower tibia, with the bakelite bone held by metal adapters.

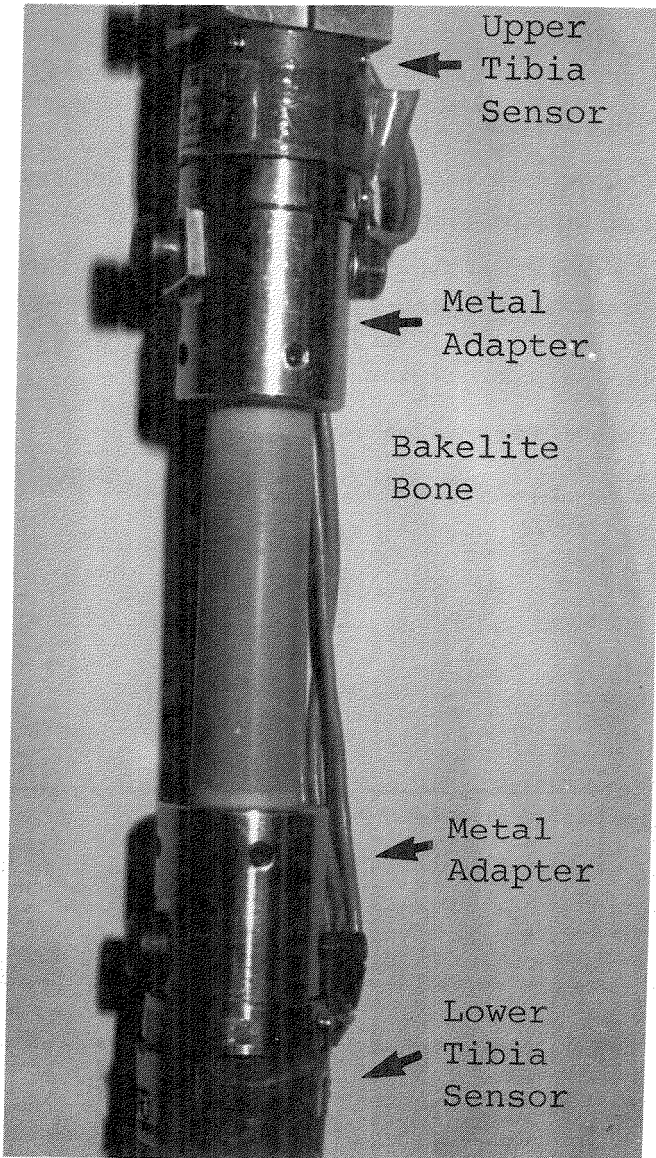


Figure 2. Bakelite-sensor bone.

### Types of validation tests

Development and testing of the three types of dummy legs was performed as shown in figures 3 to 6 for the four items listed in table 2. They are as follows:

Table 2. Test outline.

TEST NAME	SPECIMEN	NUM. OF TESTS	IMPACTOR	SUPPORT	DIRECTION	OBJECTIVE
Static	Simple bone elements	9	Cross head	pin-both end	frontal	physical characteristics
Dynamic Impact (cart)	Knees & tibia	54	cart	pin-both end inertia-free	frontal angled	Compare with human bone characteristics
Dynamic Impact (Pendulum)	full-articulated dummy	60	Sharp-edge impactor	actual dummy systems	broad-side	dynamic loading characteristics
Full-scale	full-articulated dummy	3	car-front structure	actual dummy systems	broad-side	dummy behaviour

- In the static laboratory test, a loading test machine was used to examine the static bending load and deformation of the bone element (see figure 3).

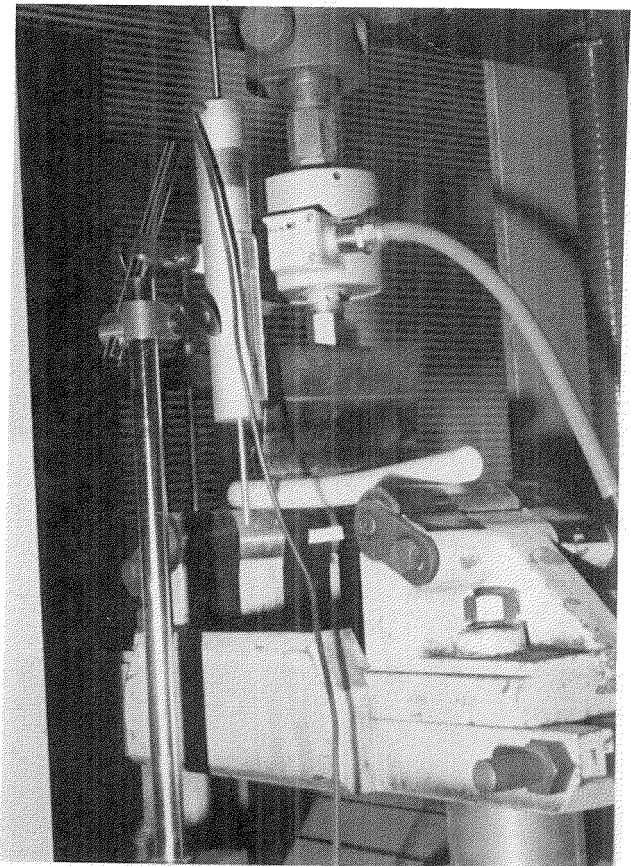


Figure 3. Static test.

- In the dynamic laboratory test, a movable cart with an impactor at the University of Tennessee, U.S.A. (reference 6) was used; dynamic bending tests of lower leg units were performed on the three types of dummy legs (see figure 4).
- In the next dynamic laboratory test, a pendulum impactor was used; a dummy was seated on a motorcycle, then the load and fracture by the impact (dynamic bending) to each type of lower leg were analyzed (see figure 5).



Figure 4. Leg impact cart test.

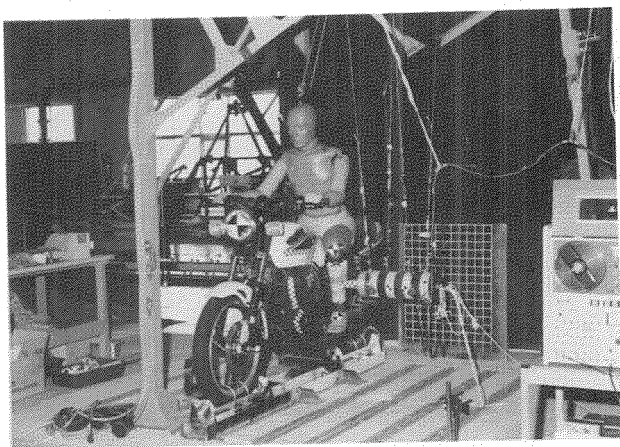


Figure 5. Pendulum impact test.

- The final test was the full-scale impact test; a dummy was seated on a motorcycle and its behavior when a car struck the left side of a motorcycle was analyzed. All three leg types were tested (see figure 6).

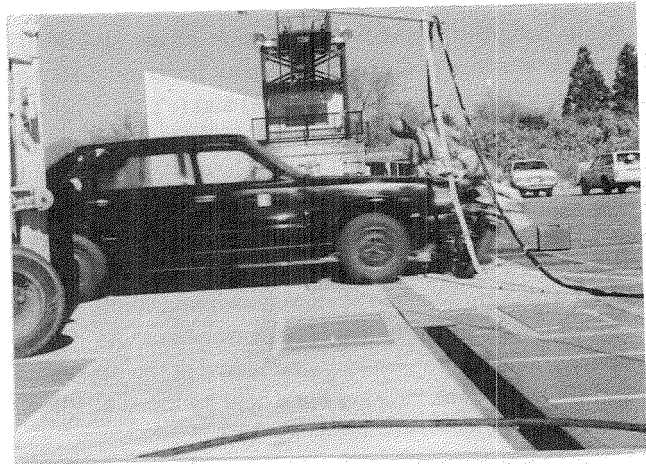


Figure 6. Full scale collision test.

## Test Results and Considerations

### Comparison of three kinds of bone structures and measurement data in elastic region

Measurement data for the three kinds of leg bone structures were compared under the same conditions after the series of tests. Table 3 shows the result of the static bending test and the dynamic bending test.

Table 3. Data comparison of three bone types.

Bone Type	STATIC *1 LOAD(W)(Kgf)	Correction Ratio	DYNAMIC *2 LOAD(Kgf)	Correction Ratio
Bakelite Bone	21.5	1.00	151.8	1.00
Bakelite sensor	33.4	0.64	208.5	0.73
Steel sensor	648.6	0.03	467.4	0.32



Note:

\*1 Bending Stiffness=W/S S = 2.0mm

\*2 Impact Condition=Impactor Mass 30kgf  
Impact Velocity 3.1 m/s

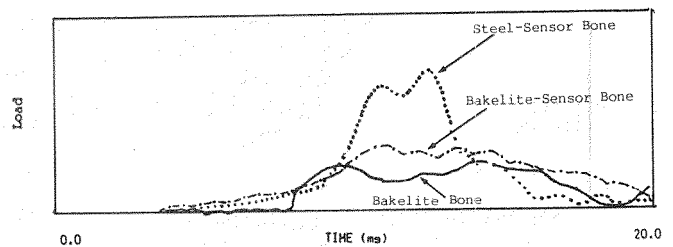


Figure 7 shows the load-time history curves of the dynamic bending tests.

The dynamic bending test is the one using a pendulum impactor and a dummy seated on a motorcycle. Here the dynamic load is derived from multiplying the impactor acceleration and the impactor weight.

The static bending stiffness (W/S) in elastic region calculated from Table 3 is as follow: 10.75 kgf/mm for the all bakelite bone, 16.70 kgf/mm for the bakelite-sensor bone and 324.30 kgf/mm for the steel-sensor bone. It is quite

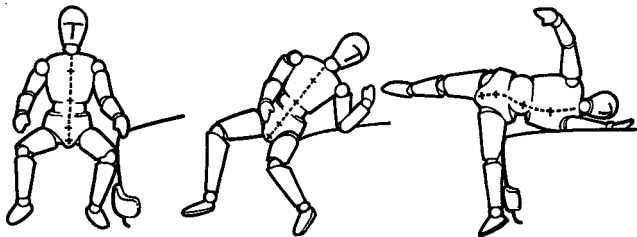
obvious that the steel-sensor bone has extreme stiffness. The dynamic bending load can be represented by the impactors peak load and it is; 151.8 kgf for the all bakelite bone, 208.5 kgf for the bakelite-sensor bone and 467.4 kgf for the steel-sensor bone. Here again, the steel-sensor bone shows much higher load than the others.

Using a stiff material such as steel possibly causes problems in analyzing measured load by requiring large correction ratio, while the use of a bakelite bone which more closely simulates the character of actual human bone presents few problems (reference 1).

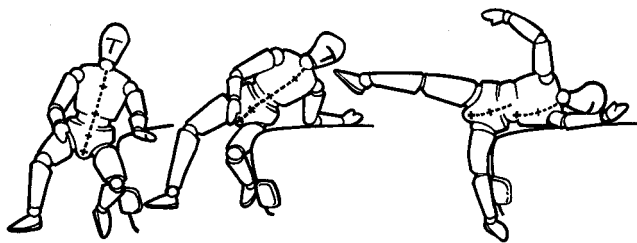
### Leg bone structure's influence on dummy's behavior

In our previous report (reference 1) it was pointed out that the dummy behavior during an impact test could be affected by the fact of whether or not the fracture of lower leg bone occurred. Accordingly, the three kinds of lower legs developed here were attached to a dummy and were examined by full scale impact tests to see their influence on the dummy behavior. However, since it was already recognized in the previous report that the steel bone influenced dummy behavior, the bakelite-sensor bone, which could give more information than the others during the fracture, was mainly compared with the all bakelite bone.

#### All bakelite bone



#### Bakelite-sensor bone



#### Steel-sensor bone

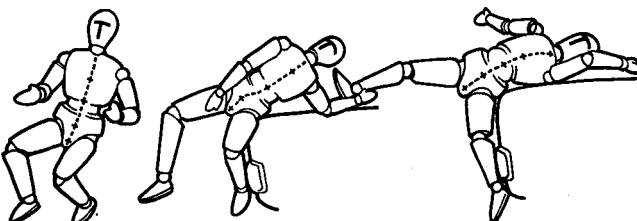
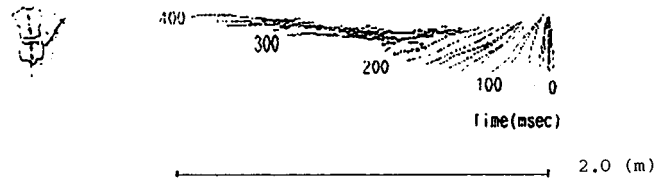
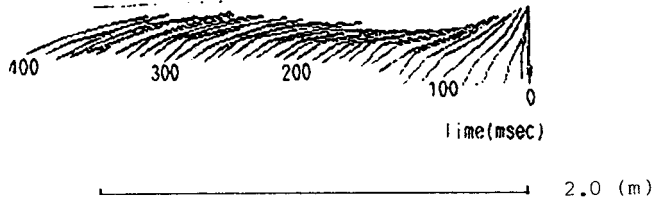


Figure 8. Difference in rolling motion depending on leg bone structure.

#### (a) All bakelite bone



#### (b) Bakelite-sensor bone



#### (c) Steel-sensor bone

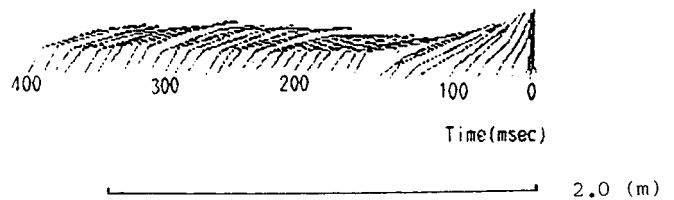


Figure 9. Comparison of dummy's torso and pelvis stick motion for three types of leg bone structure.

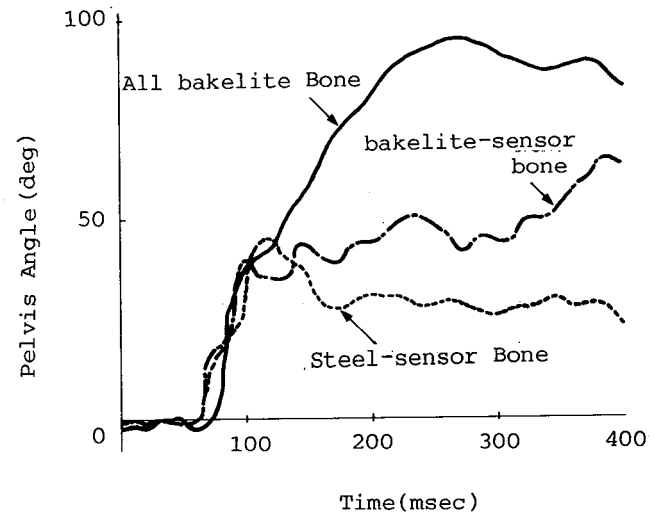


Figure 10. Pelvis angle relative to vertical line.

The dummy behavior focused on here is the rolling motion of unrestrained upper body, and it is caused by the excessive loads transmitted to the lower leg, knee and upper leg through joints to restrain the pelvis.

The sketches of dummy behavior during impact is shown in figure 8. Figure 9 describes the stick motion represented by two target marks on each of the dummy's torso and pelvis at each 10 msec. interval. In figure 10 we see the angle of pelvis relative to vertical line. And figure 11 shows the time history of the relative angle of torso and pelvis, that is, the lumbar-spine flexion angle.

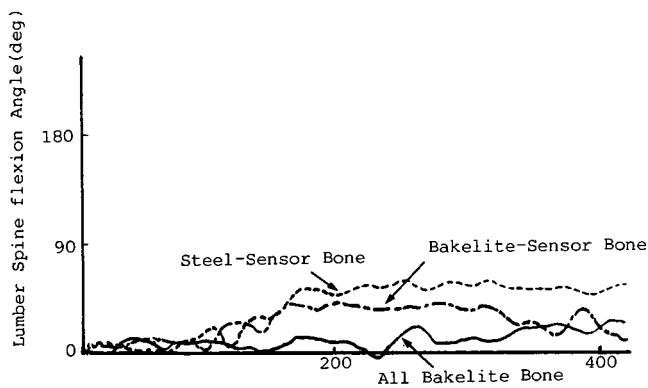


Figure 11. Lumbar spine flexion angle.

These figures show a similarity in that the lower leg is trapped between the car and motorcycle right after impact, however, subsequent behavior differs considerably.

Difference in pelvis motion is quite noticeable. Using the breakable bakelite bone, fracture of the lower leg and the upper leg can occur during impact, allowing the pelvis to move and roll easily. The dummy's upper body and pelvis move easily over the car's hood and then the pelvis bounces up.

As shown in figures 10 and 11, the breakable bakelite-sensor bone did not allow the same behavior as the all bakelite bone. But rather, it brought about a kind of intermediate behavior between those of all bakelite bone and the steel-sensor bone.

From these results we can conclude that:

- A suppression of the pelvic rolling motion was revealed with the steel bone and with the bakelite-sensor bone.
- The flexion of the lumbar spine is most remarkable in case of the steel bone and is slightly noticeable in case of the bakelite-sensor bone.
- The tendency to prevent the pelvis from bouncing up is most noticeable in case of the steel-sensor bone and less so in case of the bakelite-sensor bone.

It is reconfirmed so far that the non-breakable characteristic of the steel-sensor bone tend to interfere with the natural dummy behavior. The bakelite-sensor bone was de-

veloped to simulate bone fracture and bring load information during fracture. Although it was recognized to be quite informative, it still has some room for improvement when compared with the all bakelite bone structure.

In other words, the all bakelite bone could be more useful if some methods were developed to extract load information during fracture.

United Kingdom Transport and Road Research Laboratory is also executing their own research to evaluate lower leg damage using honeycomb leg structure shown in figure 1.

It can be considered to have some influence over dummy behavior during impact.

## Conclusion

To develop a more effective dummy for motorcycle leg protection research, it is desirable to improve its fidelity to the human legs. In this paper, experiments were carried out on three types of leg bone structures. The breakable bakelite bone offers the advantage of allowing distinction of the load mode by watching the fracture cross-section, apart from the timing of fracture. However, quantitative load analysis below the fracture point is not readily achieved and, as this report demonstrates, it is desirable to develop some quantitative load measuring method without shortening the breakable portion of the bone structure.

Besides the leg bone itself, it is also desirable for the other parts of legs to be as human-like as possible. Approaches to solve these problems are the subjects of future research.

## References

- (1) H. Tadokoro "Load Measuring Method of Occupant's Leg on Motorcycle Collision" 11th ESV Conf. May 1987.
- (2) 49CFR PART 572 "Anthropomorphic Test Dummies" Dockets NO. 74-14 Notice 45, Federal register/Vol. 51, No. 143 Jul. 1986.
- (3) R.A. Denton, et al "An Over view of Existing Sensors for the Hybrid III Anthropomorphic Dummy" 11th ESV Inter. Conf. pp 353-363, May 1987.
- (4) S. Fukuda, et al "A Study of Motorcycle Leg Protection" 10th ESV Inter. Conf. July 1985.
- (5) B.P. Chinn, et al "Protecting Motorcyclists' Leg" 11th ESV Inter. Conf. PP 902-909. May 1987.
- (6) J.N. Snider, et al "The Response of the Human Lower Leg to Impact Loading" Inter. IRCOBI Conf. Sep. 1988.

## The Application of a New Data Recovery System for Automotive/Motorcycle Dynamic Testing

Written Only Paper

Richard P. White, Jr. and Thomas W. Gustin,  
Systems Research Laboratories, Inc.

### Abstract

The accurate recording of dynamic data in a hostile environment has been a challenge since this type of data has

been recorded. Based on the technology developed for a computer-controlled data system for processing and storing dynamic data measured on manikins during aircraft ejection tests, a small, ruggedized high speed data logger has been developed. This small (2.2" × 3.1" × 4.75"), lightweight (1½ pounds) battery-powered recorder samples data up to

10,000 samples per second, recording times up to 100 seconds for eight analog sensor signals and five event signals. This recorder has the advantage of not requiring a hard ground line link which can restrict the dynamic motions of the object being tested. While this system has been developed for recording dynamic data in many different hazardous environments, its initial use for recording data during automotive/motorcycle crash investigations will be the subject of this paper. The unique features of the recorder and its adaptability and usefulness in the automotive/motorcycle crash test program will be discussed in detail.

## Introduction

This paper will present two main topics. First, a detailed discussion about the data acquisition system's recorder will be presented. The second half will focus attention on modifications to the recorder, support systems, and the overall system configuration for a test manikin being used in automotive/motorcycle crash tests by JAMA at the Japan Automobile Research Institute, Inc.

## The Recorder

The "Durable Electronic Logging Violent Event Recorder" (DELVER) is a multichannel, ruggedized, high speed, solid state data logger with many enhanced data acquisition system features. Its generic structure permits it to be used in many test environments, some of which were previously of such configurations that valid physical event information was not attainable. Gathering data that are generated by a wide variety of sensors on small vehicles and test articles in violent test environments has been done in the past primarily by using either an umbilical cable or via radio or light telemetry. An umbilical cable imposes severe restrictions on mobility and, therefore, adversely affects the natural reactions of the test article during the event, subsequently affecting the data. Radio telemetry is subject to loss of data due to misalignment of antennas, many forms of radio interference, and test/environmental extremes.

The DELVER now makes it feasible to install "black-box" recorders on high performance aircraft ejection seats and on privately owned light aircrafts. The DELVER is self-contained; therefore, it can operate in a totally unconstrained test/event environment allowing vehicle and passenger safety testing to be conducted in an untethered, free-flight manner. The DELVER's selectable midpoint trigger feature enables the user to obtain important event information both before and after a critical event; and a channel's high threshold level, which often occurs during violent events, can be used as an automatic trigger if needed. These features, and many others, will be discussed in greater detail later.

The DELVER is physically composed of five densely packed printed circuit boards sandwiched together and mounted in a durable, lightweight container with the DELVER's battery and interface connector. This data acquisition system's structure, as presented in the block

diagram of figure 1, and its features combine to form a versatile and easy-to-use piece of sampling hardware, which is the subject matter of U.S. Patent Application Serial No. 305-038, dated 2 February 1989; entitled: "Data Recorder Including a Recirculating Nonvolatile Memory," and invented by the author.

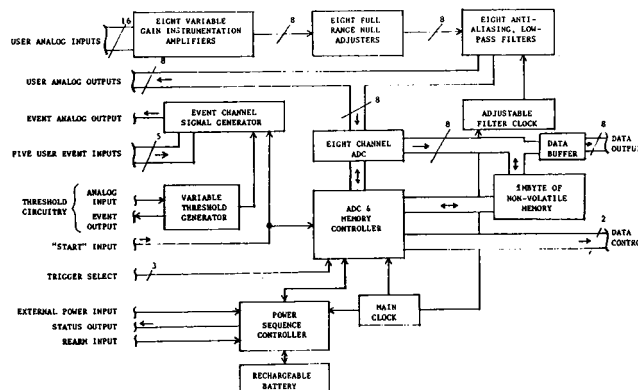


Figure 1. DELVER block diagram.

The DELVER contains eight channels of analog signal conditioning, a high speed eight-channel analog-to-digital converter, storage capacity for 1048576 samples, a variable threshold generator, an event channel signal generator, a rechargeable integrated battery, and a very sophisticated sequential-state-machine controller.

## DELVER Details

Figure 2 presents one (of eight) of the analog signal conditioning circuits. The sensor's input interface is to a differential input, variable gain, low power, monolithic instrumentation amplifier. The gain range is factory set (as needed) in one of two ranges: 0.5 to 100, and 9 to over 500, on a per channel basis. The ranges were split to provide the user good command of gain adjustments in the high gain regions of both ranges. The input impedance is greater than 300 Mohms, and the input's common mode voltage plus signal envelope should be maintained between  $\pm 2.5$  volts (referenced to ground) to ensure accurate (no clipping) amplification. This means that sensors attached to DELVER will typically require bipolar excitation about ground. The overvoltage protection circuitry on the analog inputs protect the DELVER to  $\pm 2.5$  volts (referenced to ground).

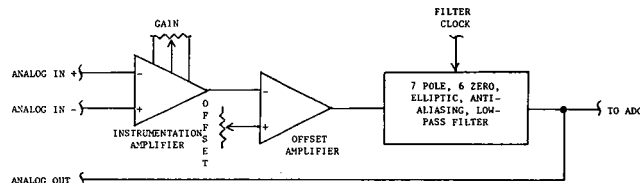


Figure 2. Analog signal conditioning.

The output of the inverting instrumentation amplifier is fed to the inverting input of the unity gain offset amplifier. The offset adjustment provides a means for nulling a sensor over a  $\pm 2.5$  volt spectrum and is placed so that it can also

remove offset errors from the instrumentation amplifier, the offset amplifier circuitry, and the channel's filter. Since the sampling spectrum of the DELVER's analog-to-digital converter (ADC) is from ground (zero volts) to +2.5 volts, most sensors generating bipolar signals will have their channel's null state typically established at +1.25 volts.

The unity gain bandwidth of the prefilter circuitry discussed so far is flat to 75 KHz, and is flat to 20 KHz at a channel gain of 1000.

The analog signal conditioning circuitry is terminated (perchannel) with a switched-capacitor, seven-pole, six-zero, elliptic, low pass filter, which serves as a channel's bandwidth limiter for anti-aliasing protection. The filter clock (set at the factory) establishes a -3 dB point at 2500 Hz, 1250 Hz, 625 Hz, 313 Hz, 156 Hz, or 78 Hz. Note that 2500 Hz is dropped as an option if the DELVER's sampling rate is 5000 samples per second per channel; 2500 Hz and 1250 Hz are not available if sampling at 2500 Hz; and only the three lower bandwidths are made available if DELVER is running at its slowest sampling rate of 1250 samples per second per channel. These limitations are imposed to guarantee no aliasing error by DELVER.

Each of the eight filter outputs is fed simultaneously to both the user's interface connector and to the ADC. The eight interface connector lines are made available for monitoring during system calibration and verification procedures for setting and checking each channel's gain and offset values. Additionally, any one of these eight lines can be tied back into the analog input to the threshold generator circuitry to develop a bistate (digital) signal, which can, in turn, be used as the parametric "START" trigger for the saving of event data.

The eight analog signals are also sent to the ADC, which is depicted in figure 3. This state-of-the-art CMOS device is a greatly enhanced (pin compatible) upgrade to the industry standard ADC0808 and ADC0809. A typical sampling cycle starts with the ADC controller circuitry selecting and latching a multiplexer address that gates one of the eight analog inputs (from the filter outputs) through the multiplexer to the sample and hold circuitry. During the first few clock cycles following the subsequent issuance of a "start conversion" command pulse, the selected analog input signal and the ground reference are simultaneously and differentially sampled by the auto-zero comparator, after which they are held for conversion processes. The ADC uses a successive approximation register (SAR) to generate the digital code that defines the analog signal's voltage level. The digital-to-analog converter (DAC) used in this ADC is unique in that it uses a switched capacitor array for the four most significant bits, and a resistor array for the four least significant bits, which enables superior linearity and accuracy between 16 elements each, instead of the 256 elements found in conventional designs. When the conversion is complete, the ADC signals its controller to write the newly converted data into memory, and then the process is restarted with the next channel.

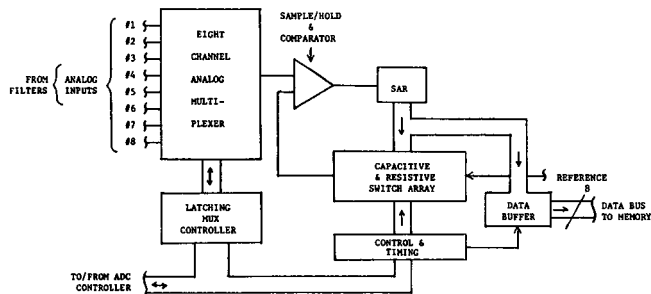


Figure 3. Analog-to-digital converter.

Before memory control is discussed, it is best to first present the main control functions of the DELVER, as depicted in figure 4, the power sequence controller (PSC). The "XPOWER" input is one of two control inputs that define DELVER's mode. This +9 to +32 volts input serves as an indicator to DELVER to turn on its digital power, and if data are not being saved in memory from a previously captured event, it also turns on memory power and analog power, and DELVER starts sampling and saving data. If data were being saved from a prior test or event, the memory power will already be on (from the DELVER's battery) prior to the application of XPOWER. In this latter case, when XPOWER is applied, it then turns on digital power and replaces the DELVER battery as the power source for the memory power; analog power is not turned on, and no data are sampled for storage, thus protecting the data in memory. Following any application of XPOWER, the "STATUS" output line will be high if DELVER is sampling and storing data, and it will be low if it is saving data from a prior event/test.

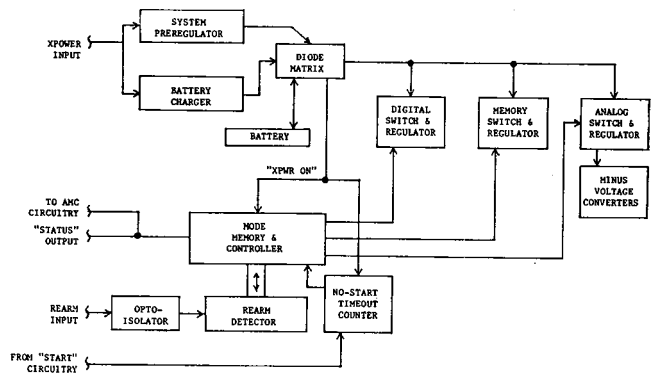


Figure 4. Power sequence controller.

The XPOWER input also serves as a supplemental source of power to the internal DELVER battery, for both the running of DELVER and for trickle-charging the DELVER battery to keep it as fully charged as possible, regardless of mode of operations.

The "START" input, which is conditioned and used by other circuitry (see figure 5), is the other DELVER mode and function control input. Its use in figure 4 is that of controlling the no-start timeout counter. If a START signal is not received within 16 seconds following the removal of XPOWER, the DELVER shuts off power to all sections

(memory, digital, and analog) and remains rearmed so that it will start sampling and storing data again once XPOWER is reapplied. During the 16-second interval between the removal of XPOWER and the shutdown of all DELVER operations, the DELVER battery is the only source of power for all of the DELVER circuitry. If a START signal is received during the 16-second period following the removal of XPOWER, DELVER will perform data acquisition duties as defined by the trigger input selector, finish acquiring event information using DELVER battery power only, and then shut off all digital and analog power, while maintaining memory power for subsequent data retrieval operations. A typical scenario that could use such a power sequence technique might be like those encountered during ejection seat and parachute testing, as well as live ejection operations. More will be presented on the START signal during figure 5 discussions.

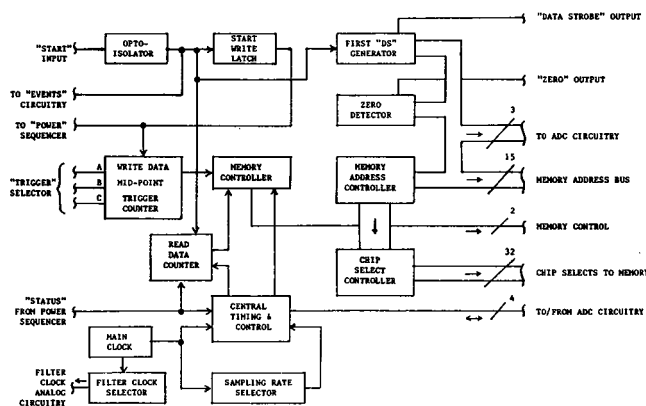


Figure 5. ADC and memory controller.

The last circuitry to be presented in figure 4 is that of the "REARM" circuitry. As previously covered, a low STATUS line (with XPOWER applied) indicates that valid event data are stored within DELVER, and the DELVER will prevent the overwriting of those data by refusing power to the analog section of DELVER and by write-protecting the memory. The application of a REARM (special format) signal from the Data Retrieval And Playback System (DRAPS) or Calibration/Diagnostics Unit (CDU) resets this safety logic and allows the resumption of data sampling and storage processes, which destroys (overwrites) the old event data. A successful rearm operation is indicated by the STATUS line going from a low to a high state. XPOWER must be applied for the application of a REARM signal to reset the DELVER's mode from "save data" to "take data" operations.

Figure 5 presents the ADC and memory controller circuitry (AMC). This circuitry performs all of the clocking and gating control functions in DELVER based upon the mode as established by the PSC circuitry of figure 4 and user control inputs. Its primary elements are the START circuitry, the memory address and timing controller, the write-to-memory and read-from-memory counters, the

main clock and filter clock generators, ADC controller including the sampling rate selector, and the digital port's handshake control lines.

The START input circuitry found in the AMC section of DELVER consists of a special opto-isolated signal conditioner, and a sequencing control latch that is functional during the times when DELVER is actually writing data to memory. This input serves as the "capture data" trigger for the DELVER, and is also used to initiate the start of a data dump from DELVER during data retrieval operations.

The START input is a single-ended (referenced to ground) input into a bipolar opto-isolator with an input impedance of about 10 Kohms. The input signal range is logic level compatible, with a capability of operating on absolute value signals. A signal increasing above about +2.5 volts or decreasing below about -2.5 volts will generate a valid START signal. The AMC circuitry is leading edge sensitive, with only the first edge causing mode and control changes. The output of this circuitry is also internally hardwired to the most significant bit of the event signal generator for data stream recording of the START signal if desired. The minimum input pulse time for a valid START action is about 500 microseconds. The output of the threshold signal generator, which is discussed later, is designed to drive this input directly for automatic parametric starts.

During a data capture operation, the first START occurrence is latched and this information is used to control both the duration of the write to memory and to inform the PSC that after the current writing to memory is completed, a change in modes to data retention is required. Any further applications of a START signal serves as initiation signals for the read of DELVER data, one complete dump of memory per valid input. The conditioned START input also presets circuitry designed to generate a first Data Strobe (DS) only on channel 1 for proper synchronization of channel information during data retrieval operations.

The AMC's memory control functions are two-fold. The address controller keeps track of the current loop pointer for both write and read operations. It also provides the ADC's multiplexer address for determining which analog signal is to be converted to digital information. The address controller provides all of the direct address lines as well as the decoder for four banks of octal chip select circuitry for the 1MByte of memory within the DELVER. The second memory controller function in the AMC section is that of providing the write protection logic for the memory when the DELVER is in a "save data" mode, as well as generating the proper number and sequencing of write pulses when the DELVER is in a "take data" mode. The latter function is closely coupled to two other functional elements depicted in figure 5. The read data counter provides the proper number of address controller increments when data are being retrieved from DELVER, while the write data midpoint trigger counter performs the same function when data are being stored within DELVER based upon the three trigger selector inputs.

The three trigger select lines provide the user with a means of selecting the location of the START signal with relationship to the total event time captured with the DELVER. There are three middata locations available, each providing various amounts of data stored before and after the application of the START signal. The default option is that which causes the DELVER to save equal amounts of data before and after the leading edge of the START signal. This is implemented when neither TRIG-B nor TRIG-C are connected to TRIG-A. The second trigger location that is selectable places the START signal at the location where 75 percent of the data occur before the START signal's first leading edge, and 25 percent of it after. This option is excersized by connection TRIG-A to TRIG-C (leaving TRIG-B open). The last option places the START signal very late in the data event sequence with about 87 percent of the data occurring before the leading edge of the START signal and about 13 percent of it after. This option occurs when TRIG-A is connected to TRIG-B (leaving TRIG-C open).

The main clock provides all of the clock signals necessary for the system's sequential and asynchronous timing circuitry. It provides the four different sampling rate clocks, one of which is wired into the central timing and control circuitry at manufacturing time. The four binary options are 10000, 5000, 2500, and 1250 samples per second per channel for a system sampling rate of 80000, 40000, 20000, and 10000 samples per second, respectively.

The main clock also provides the primary frequency required to develop the six cutoff frequency clocks that are available within DELVER. As noted in the earlier discussions on the filter, one of six, five, four, or three bandwidth options are available, and is hardwired to the filters at manufacturing time.

There are two digital output port control lines developed by the AMC section. The "ZERO" output, an active low 0.50 microsecond pulse, is generated everytime channel one is processed, with an output rate equivalent to the per channel sampling rate. The "DS" output, an active high 0.50 microsecond pulse, is used by peripheral equipment for the latching of digital data presented by the DELVER during both data capturing and data retrieval modes of operation, and it has an output rate equivalent to the system sampling rate. Because the START signal can occur asynchronously during data capturing processes, the first "DS" generator withholds the Data Strobe pulses during a read operation until the first occurrence of a channel one read attempt, thereby providing a means for external channel synchronization with host/peripheral computer processing equipment and the DRAPS.

The first of two auxiliary built-in circuits is presented in figure 6. The event signal generator develops an analog signal representation of seven bistate event channels, five from the user and two internally generated. The signals were combined because 128 discrete states (out of a possible 256) better utilizes the voltage spectrum than just two discrete states.

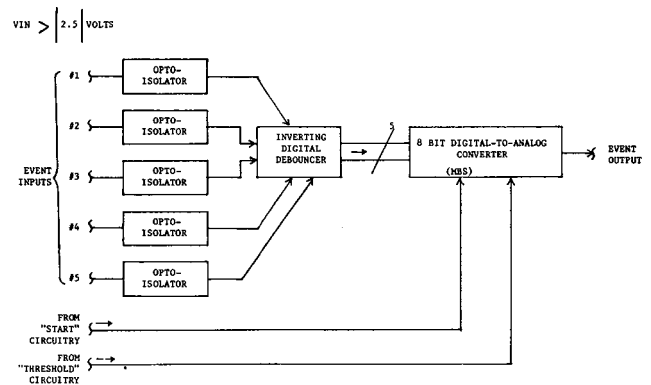


Figure 6. Event circuitry.

The five user event inputs are identical, and they are similar to the START input except for a few parameters. The event input impedance is about 2.5 Kohms, and the response time is much slower than that of the START input. All five of the user's event inputs are digitally debounced to remove noise and to bring their bandwidths more in line with those of the analog section. As mentioned earlier, the conditioned (unlatched) START signal is also applied to this circuitry, at the most significant bit location so that it causes a half full scale change for easy spotting in posttest analysis work. The next weight bit location is hardwired to the output of the threshold generator circuitry (to be discussed next). The hardwiring of these two important internal signals simplifies the user's interface with the DELVER.

The analog output from this circuitry can be externally tied to any of the analog channel inputs on this or another DELVER (provided the ground references are identical) for inclusion of event information in the event data set. This is accomplished by connecting the event output line to a signal plus input line and by grounding its corresponding signal minus input line. Then adjust that analog channel's gain for one and its offset adjusts to zero. That channel's analog output and its digitized data will provide a full report of all seven event inputs, in standard binary format. Note that the five user inputs are inverted by the debouncer. This is important for posttest reconstruction work.

The second of two auxiliary built-in circuits is presented in figure 7. The threshold generator circuitry provides the user with an optional way of generating event information for inclusion in the data set as either just an alarm channel or that of the parametric START generator. This single bit DAC has a variable threshold that is typically set via the CDU. If the analog input presented to this circuitry is below the threshold adjust level, the output will be low; if it is above the threshold level, the output will be high. The input impedance is about 10 Kohms and the output impedance from the ground clamper is about 1 Kohm, which will directly drive the DELVER's START input if this circuitry is used as the parametric START signal generator. Typically, the input signal to this circuitry will be an analog output from the same DELVER (or another DELVER provided the ground reference is the same), but it can be any

analog signal source within the  $\pm 2.5$  volts spectrum (referenced to ground) of this circuitry.

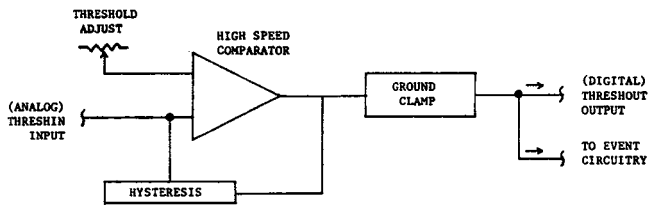


Figure 7. Threshold generator.

Interface with the DELVER is accomplished through a single 51 pin interface connector. Most of these lines have been discussed in detail. Twenty-four lines are used for analog inputs and outputs for the eight analog channels of signal conditioning. There are five event input lines and an event output line. The threshold generator has two lines, one for analog input and a digital output line. The digital port consists of eight data lines, and the two control lines of ZERO and DS. The START signal, along with the three trigger select lines determine when a valid event has occurred and where that START pulse should occur in the stored data set. In addition to the STATUS and REARM lines, there is a line to monitor the DELVER's battery status. With XPOWER input, and the DELVER's system ground point line, the list is complete.

This completes the detailed description of the DELVER itself. Time and space do not allow for discussions into all of the possible DELVER configurations.

## The Test System

Figure 8 presents the system configuration for a fully instrumented test manikin designed to evaluate "injuries" incurred by a motorcyclist involved in automobile impacts at various speeds and angles, with and without different types of experimental safety equipment.

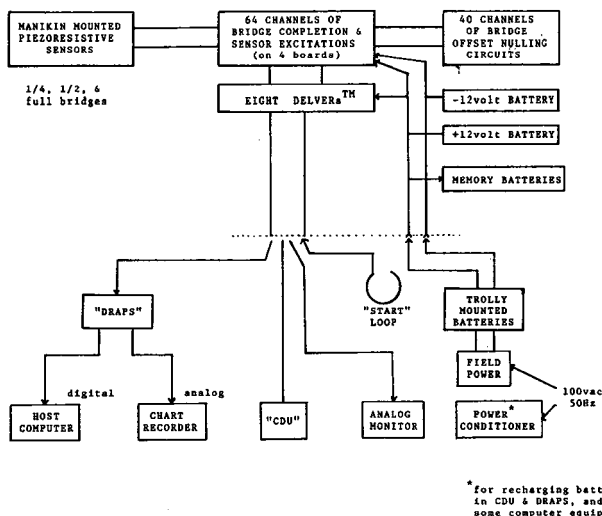


Figure 8. Fully instrumented system configuration.

The typical sensors deployed on this manikin, nicknamed (and hereafter called) SPIKE, include: single, double, and

four-arm piezo-resistive force sensors including: strain gauges, force and moment load cells, accelerometers, and rate gyros. Most of the strain and load cell measurements are configured for detailed analysis of leg, knee, and hip injuries in the initial configuration, with important physical phenomenon information also being collected in the head, neck, and chest regions. The purpose for the sensors and their placements is in the evaluation of "where did SPIKE get hurt and how bad is it?" Within the modified spine of SPIKE, there is a group of five boards that provide 64 channels of sensor bridge completion circuitry, offset (null) adjustment capabilities for the less-than-full bridge sensors, excitation for 64 sensors, and sensor and DELVER interface cabling. SPIKE also contains two rechargeable batteries that contain sufficient power to run all sensors and eight DELVERs for about 10 minutes in a totally unconstrained test configuration.

Also shown in figure 8 is a block labeled "memory batteries," which is the first clue to a modified DELVER system. The normal configuration for a DELVER is that it contains its own integrated rechargeable battery. To save room, the DELVER batteries and their battery charging circuits were removed and separate memory batteries with their own dedicated trickle chargers were installed; one per two DELVERs. This necessarily required the use of two additional wires from each DELVER for connection to these memory batteries. The DELVERs were removed from their normal enclosures and installed into special carriers which then fit snugly into two vertical boxes attached on either side of the spine box from the rear of SPIKE. The sensor-to-DELVER channel assignments were chosen to maximize survivability of critical event data. Most of the sensors located on the left side of SPIKE went to DELVERs located on the right side of SPIKE's chest, and vice versa. Because this mounting scheme did not provide continual open access to the gain and offset adjustments on the DELVERs, they are slid backwards out of their slots far enough to gain access when adjustments are necessary. The memory batteries were placed in special boxes below the DELVER boxes with access panels opening downward into the pelvic region of SPIKE. The offset (null) adjustments are made accessible through an access panel at the top rear of the SPIKE's spine box. The sensor interface wiring staging area is in the pelvic region of SPIKE, as is the -12 volt onboard battery. The +12 volt onboard battery is on the front surface of the spine box, between the two DELVER boxes, for maximum survivability protection.

## Support Equipment

As depicted in figure 8, many pieces of support equipment are deployed for an actual test scenario. The CDU is typically used prior to DELVER installation to set and verify gain and offset settings for the DELVERs. "Trolley batteries" and an ac powered supply are used as a source of power for SPIKE in all constrained modes of operations, including pretest setup and checkout procedures

as well as in-the-field power for SPIKE while on the motorcycle with totally unconstrained (internal battery only) operations occurring just prior to impact with an automobile. This power scheme permits a continual trickle charge to be applied to all SPIKE's batteries in all modes except for the impact test itself. A special harness was designed to provide (constrained) access to all of the analog outputs from the DELVERs. This analog output harness is connected to a special "analog monitor" box which permits the test team to verify the static and dynamic status of every SPIKE channel during laboratory preparations, and in the field while sitting on the motorcycle just prior to a test. This simple yet valuable tool provides the required system status information to make test-abort decisions if necessary. All eight REARM inputs for the DELVERs were tied together and made accessible to a CDU and/or a DRAPS for easy rearming of all systems during pretest checkout operations. This technique makes it easy to transport SPIKE in a fully powered-down condition by just implementing a START sequence prior to transportation, and rearming SPIKE for more checkout procedures or for an actual crash test. For this test configuration, SPIKE receives a start signal when a looped wire is disconnected by a tether during the launch sequence of the motorcycle SPIKE is riding from the trolley that is used to provide it the velocity required for the crash test. All eight START inputs were tied together for the DELVERs, and were resistor pulled-up to the +12 volt battery in SPIKE's chest. This START input line is made accessible to the start loop, along with ground. When the start loop is pulled, either by the separation of motorcycle and trolley, or in the preparation laboratory, the START line loses its ground and is pulled high to generate a simultaneous START signal for all eight DELVERs.

The power conditioner shown in figure 8 is a special device that is needed for the tests in Japan. While the ac field power supply was chosen to handle the low power available in Japan, other pieces of support equipment (CDU, DRAPS, and some computer support equipment) require the use of this device to boost the ac power to that which they were designed.

The DRAPS is a battery operated, solid state, high capacity, mass storage system designed to retrieve test/event data from up to ten DELVERs and present those data in any of three playback methods for posttest data analysis purposes. The DRAPS is the communications formatting link that is typically required between the DELVER(s) and the eventual data target.

The DRAPS retrieves data from the DELVER to which it is attached at the same rate the DELVER originally acquired data. Once the data transfer is complete, the DRAPS permits the rearming of the DELVER to take place because the data have been removed from the DELVER at least once. The DRAPS also prohibits the writing of new DELVER information into the same memory field just used by the previous DELVER until after it has been read from the DRAPS at least once, in parallel or serial modes. These safeguards are intended to prevent the accidental loss of

valuable test data. SPIKE has two separate DRAPS supporting it. One is populated with enough memory for five DELVERs, and the other has memory for three DELVERs. If one DRAPS fails, the other one can still remove all of SPIKE's test data by retrieving some of it, offloading it to the host computer, and then going after more of the test data until it is all retrieved. Redundant data retrieval operations are always recommended, especially for expensive tests. SPIKE's data are first played back on strip chart recordings, and then the data are played into an FM magnetic recording machine using the same analog outputs as those used to make the strip chart recordings, and then transferred to the host computer system via an RS-422 serial link at 9600 baud (18+ minutes per DELVER). Multiple data bases ensure that the data are most likely to be permanently saved for future analysis.

## Instrumentation System Details

The first section of this paper presented a detailed description of the DELVER. The following discussions are more details on the remaining elements of SPIKE's instrumentation system, excluding support equipment.

There are four boards that provide 64 channels of bridge completion and sensor excitation (BCE) circuitry, each enough for 16 sensors feeding signals to two DELVERs, all contained within the spine box. Each of the 16 BCE channels per board consists of a generic bridge completion circuit that can be configured for completing sensor bridges with the addition of two or three 0.01 percent Vishay resistors, and each can be coupled to the offset adjust board (OAB), which is also located in the spine box above the four BCE boards. Each channel's excitation can be individually configured for  $\pm 5$  volts or  $\pm 2$  volts excitation. The lower excitation is typically used for strain gauges located on poor heat sink materials to minimize self-heating effects.

Each BCE board contains DELVER monitor and power switching circuitry to turn off all power to their attached sensors once both DELVERs attached to that BCE have finished collecting data and have gone into "save data" modes. This conserves main battery power enabling it to supplement the DELVER memory batteries in their data retention activities.

Excitation voltages for each board are generated from common source, high precision voltage regulators. Each sensor's excitation potential is buffered from the common source and all other sensors attached to each of them to prevent crosstalk effects. Every sensor has its own high and low frequency excitation filtering network to prevent noise problems. Excitation voltages are jumper selectable for ease of field changes if they are required.

Sensor interface to the BCE boards is accomplished via custom 100-pin high density connectors providing up to five lines per channel ( $\pm$ signal,  $\pm$ excitation, and a shield), although the number of lines actually used is a function of the type of sensors attached.

DELVER interface to the BCE boards is accomplished via two custom 51-pin high density connectors, one for

each DELVER. Eight shielded twisted pair lines per DELVER connector are all that attach to the BCE boards, with the rest being used in other functions (described below) or being tied off as spares.

Eight analog output lines per DELVER interface connector are brought out (via one of two large MS-style connectors) to the analog monitor, previously described. The other lines brought out of the 51-pin DELVER connector include: the START, REARM, XPOWER, STATUS, and GROUND lines, all previously discussed. The remaining lines for event inputs, threshold circuitry, and the digital interface are bundled as spare lines in the current system configuration.

The offset adjustments on all nonfull bridge sensor channels is accomplished via a fixed resistor and potentiometer across one of the bridge completion resistors. The OAB is capable of performing this function for 40 channels, even though only 20 channels over the four BCE boards currently utilize this feature. The 25-turn potentiometers are accessible from the rear of the spine box after it is installed for easy fine tuning.

The internal +12 volt batteries were wired to be directly connected (in parallel) across the trolley batteries when they are attached. The four memory batteries in SPIKE are attached to the internal +12 volt battery through diodes and dropping resistors, with values selected to maintain the proper float charge for maximum performance during data retention activities. The DELVER's XPOWER lines are also directly connected to the internal +12 volt battery.

This section concludes with a few of the system specifications. In the current configuration, 54 channels are currently active with the remaining held as future spares. There are no event channels being used. There are 20 channels with bridge completion and offset adjustment circuitry. All DELVER gains are set for the high range (from 9 to 500), with most of them actually being in the 30 to 70 range. All operational offsets are at or very near the typical midpoint value of +1.25 volts. All eight DELVERs are sampling at 10000 samples per second per channel with all channel bandwidths set at 2500 Hz. The DELVER recording time is 6.5536 seconds of data before the START signal, and 6.5536 of data after the START signal. The data format is eight bits (binary) per sample, with a total of 8388608 samples being taken per test. The worst case full power requirements for SPIKE are +12 volts at about 2 amps and -12 volts at about 1 amp. Based on tests conducted so far, the following estimates are provided. In a fully unconstrained configuration, SPIKE will operate all systems without error for about 10 minutes on internal batteries alone, with this time being increased to about 40 minutes when running on trolley batteries without being powered by the ac field power supply. As will be seen, SPIKE needs to run on internal power only for about 7 seconds, and on trolley batteries for about 5 minutes. Due to the nonstandard DELVER battery configuration, the poststart data retention time is only about 100 hours, which is more than sufficient for data retrieval operations.

## Physical Installation of Instrumentation System

Under contract to Dynamic Research, Inc., Systems Research Laboratories, Inc., incorporated an instrumentation system into a highly modified Hybrid III manikin to be used to obtain injury data for a motorcyclist during car/motorcycle impacts at speeds up to 50 mph. The requirements for the on-board instrumentation system were the following:

- Onboard signal conditioning and storage for 64 channels of analog data.
- A system that would operate successfully in a severe, dynamic G field.
- A system that would survive when the manikin was subjected to severe impact damage.
- Be self-contained so that an umbilical line would not hinder the dynamic response of the manikin during the crash sequence.
- Minimize the effect of the instrumentation system on the manikin mass properties.

The system that was utilized to provide the required instrumentation needs was the DELVER Data Acquisition System developed by Systems Research Laboratories, Inc., in 1987 and 1988.

In addition to the onboard instrumentation data system, SRL designed, fabricated, and installed electronic circuitry to provide bridge completion networks for 64 data channels and voltage excitation ( $\pm 5V$  and  $+2V$ ) for all the sensors incorporated into the highly instrumented manikin. The following sections of the papers will describe the manner by which the instrumentation and onboard voltage excitation system were incorporated within the manikin.

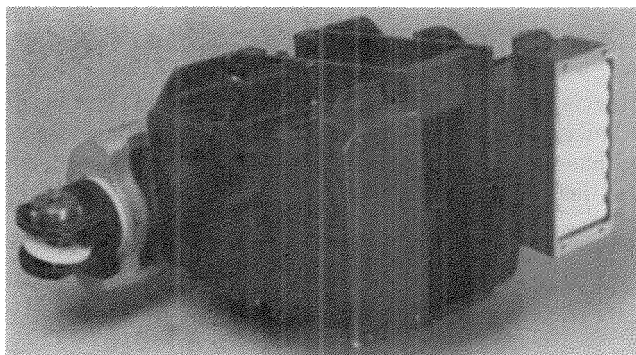


Figure 9. Aluminum instrumentation housing.

In order to provide the maximum protection for the instrumentation, minimize changes to the manikin mass properties, and use the best available space, it was decided to incorporate the entire instrumentation system in the chest cavity inside the rib cage, next to the spine. Figure 9 shows a photograph of the lightweight aluminum structure that was placed around and attached to the steel spine. Four DELVER units were placed on each side of the spine within this aluminum enclosure. The rechargeable Nicad batteries,

to support the DELVER units, were placed on each side at the bottom of the aluminum case to assist in maintaining the proper torso center of gravity and minimizing the inertial contribution of these mass-dense items. The batteries, located on each side, supported the four DELVER units placed on the same side of the spine. Figure 10 shows the modified upper torso enclosed within the rib structure. The plastic sternum/shoulder bib is not attached in this photograph in order to illustrate how the complete instrumentation system fits within the rib structure. With the instrumentation system incorporated, approximately 1 inch of frontal rib deflection could still be obtained before the ribs contacted the aluminum support structure. One of the Nicad batteries, used to support sensor excitation, can be seen attached to the spine in the center of the torso. A second battery was attached to the lumbar spine/pelvic attachment block, located in the abdomen. The dual battery location was selected to minimize the effect of the instrumentation weight on the manikin CG location.

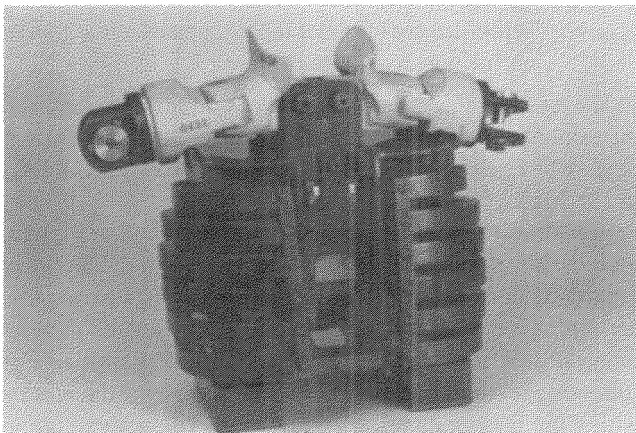


Figure 10. Torso assembly with instrumentation housing.

Figure 11 shows a photograph of a DELVER Data Acquisition System incorporated within the holder especially designed for installation of the unit within the manikin. Fore and aft G loadings on the instrumentation system were resisted by the front and back aluminum plates, and lateral G loadings were resisted by the sides of the

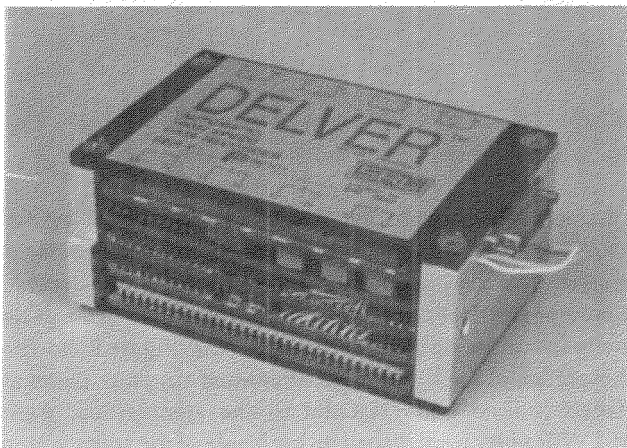


Figure 11. The DELVER data acquisition system.

aluminum holding fixture. The two wires extending from the front of the unit are the memory battery lines, and the 51-pin provides supports the instrumentation system interface lines. The null and gain adjust potentiometers, for each data channel, can be seen running fore and aft on each side, just under the cover plate.

Figure 12 shows how the DELVER units were inserted into the aluminum housing. When fully inserted, the unit was bolted to the front of the aluminum housing by two cap screws (figure 11). The machined protrusion in the rear aluminum support of the DELVER fits into the mating slot in the housing to resist G loading in the vertical direction.

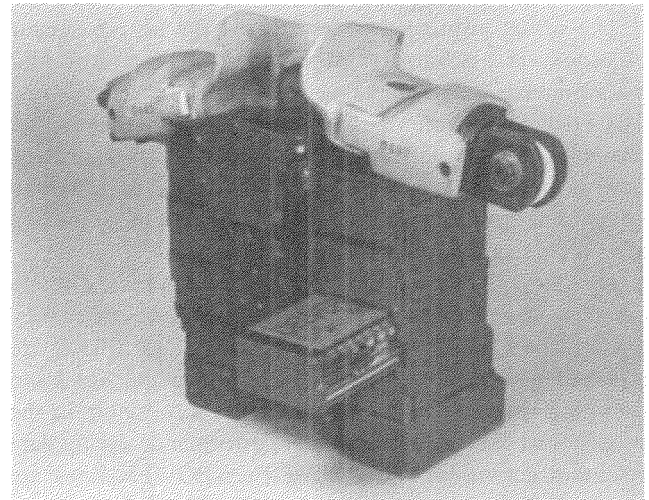


Figure 12. DELVER incorporation within torso housing.

Figure 13 is a photograph of part of the instrumentation system that provides the bridge completion networks and the voltage excitation for all the transducers located within the manikin. This part is mounted to the spine insert after the standard 5.3 pounds of ballast weight were removed. The small board in the right of the photograph incorporated the

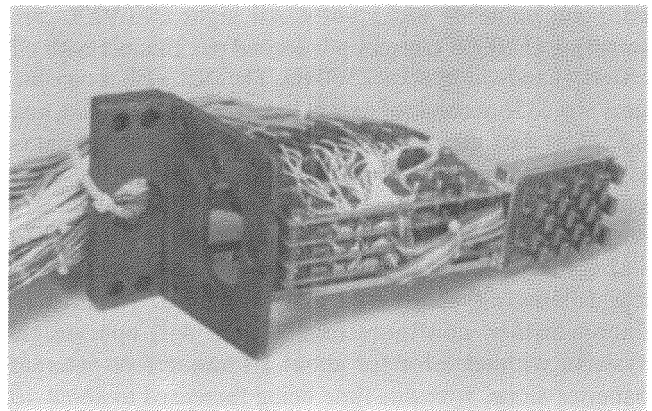


Figure 13. Bridge completion/voltage excitation circuitry.

20 precision trim potentiometers for the offset adjustment channels. Figure 14 shows how the entire system is inserted within the spine, and figure 15 shows how the offset potentiometers can be accessed through the upper back of the spine when the spine cover plate is removed.

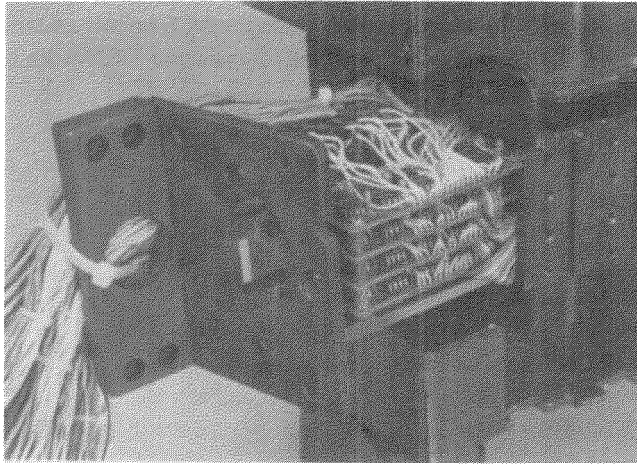


Figure 14. Insertion of BCE circuitry into spine.

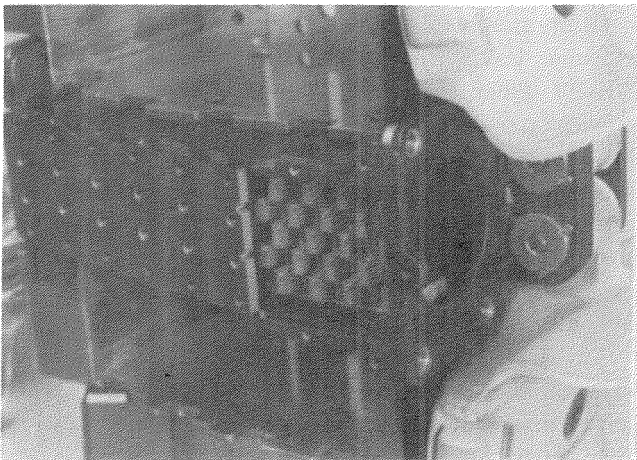


Figure 15. Access to trim potentiometers inside torso.

The effect of adding the instrumentation to the mass properties of the thorax is shown in table 1. Since these properties were measured before and after all modifications were made, the separate effects on the mass properties of the DELVER system and the bridge completion-voltage excitation circuits plus battery cannot be determined. As can be seen from the data presented in table 1, while the total manikin weight increased by about 11 percent with the accompanying increase in inertia, the center of gravity did not change significantly in the torso.

Table 1. Effect of instrumentation on torso mass properties.

Parameter	Before Modification	After Modification	Difference
Weight (lbs)	37.59	53.26	15.67
Principal Moments of Inertia (lbs/inches <sup>2</sup> )			
I <sub>xx</sub>	1011.94	1416.10	404.16
I <sub>yy</sub>	788.40	989.26	200.86
I <sub>zz</sub>	670.24	865.14	194.90
CG Location (inches)			
X <sub>sc</sub>	0.33	0.24	0.09
Y <sub>sc</sub>	0.33	0.16	0.17
X <sub>sc</sub>	4.83	5.28	0.75

Figures 16 and 17 show photographs of the support equipment for the DELVER system. The CDU (figure 16) is used in conduct diagnostics and calibration checks of the DELVER units prior to a test. DRAPS (figure 17) is used to download the DELVER units in the field immediately after a test. The DRAPS is then downloaded to a host computer in a laboratory environment. Both the CDU and DRAPS are battery powered so that they can be effectively utilized in the field when external power is not available.



Figure 16. Calibration/diagnostic unit (CDU).

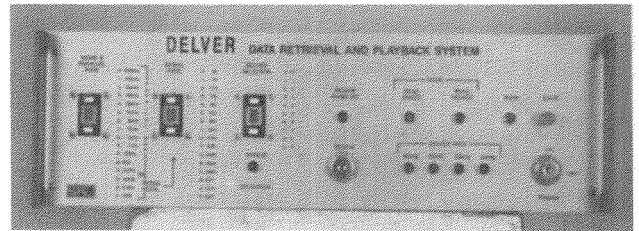


Figure 17. Data retrieval and playback system.

Initial use of the DELVER system in a series of motorcycle/automobile crash tests, in late April at the Japanese Automotive Research Institute (JARI), demonstrated that the DELVER system operated successfully in the severe environment for which it was designed.

During four violent crash tests, the instrumentation system collected all data for later analysis in the laboratory. The tests are continuing at JARI during the month of May, and it is anticipated that the DELVER system will continue to be a unique asset in collecting all the dynamic data in the violent environment.

The DELVER system is currently being fabricated for use in manikins supporting very high speed parachute testing in Canada. Many other unique uses of DELVER in hazardous environments are expected in the near future.

## Scenario of Typical Test

This completes the technical presentation portion of this paper. The following is a short scenario of a typical motorcycle crash test, including some of the pretest checkout operations. This does not include the prior posttest manikin refurbishment that typically is required due to the many mechanical failures that occur during such violent tests.

## HIT HIM ONCE! HIT HIM HARD!

The scene is a large table surrounded by several people working on SPIKE, whose torso is deribbed and separated from its pelvic section. The posttest calibration verification on all eight DELVERs revealed that all channels maintained their gain and offset values at the values set several tests prior to the one coming up. The ac power supply is on line, charging a laboratory set of trolley batteries, which are also linked into SPIKE's internal batteries, thereby providing a full charge to all internal batteries. The eight DELVERs have been reinserted into their boxes, numbers 1, 3, 4, and 6 on the right side and numbers 2, 5, 7, and 8 on the left side. Their retention bolts are in place but no power is applied to them. Because the DELVERs are off, the BCE boards have removed all power to all sensors. The legs have been completely replaced/repared from the previous test, and the left hip was repaired. There are no skins on the lower legs yet, and the chest is without skins and ribs.

The analog monitor box is hooked into the two MS-style connectors and a voltmeter is inserted into ground and a test point for DELVER #1. A REARM source is attached to the common REARM line, and the START loop is attached to the tethered start lines of SPIKE. The 51-pin connector for DELVER #1 is attached (but not bolted) to DELVER #1, and a REARM function is performed. A successful rearm sequence is confirmed by an increase in power (BCE #1 is on with all of its sensors and DELVER #1 is on) and by the fact that the sensor channel being monitored by the voltmeter on the analog monitor registers a reading of +1.25 volts. A quick scan of all active channels for DELVER #1 confirms that all channels are working. Then all sensors are individually checked for activity by bending, twisting, pulling, pushing, hitting, and dropping as needed to confirm their operational status. The START loop is pulled, and about 6.5 seconds later the power drops to a very low standby level and DELVER #1 is off. DELVER #1 connector is removed and DELVER #2 connector is attached. The same REARM and checkout procedures are conducted, with the START loop finally checking the DELVER's data capture timing capabilities. If a nonfull bridge sensor is significantly off the null value of +1.25 volts, then its corresponding offset adjust potentiometer is adjusted to bring it back on center. Typically this does not happen, even with bone replacement occurring between every test, because the gauge tolerances are very tight.

DELVER #2 is disconnected and DELVER #3 is brought on line with the same REARM procedure as before. The power requirement is higher than before because DELVER #3 has turned on BCE board #2 which has 16 active sensors attached to it (BCE #1 has some spare channels). The same tests are conducted for all 64 channels. All spare unused channels have their offset values adjusted to maintain some fixed voltage value above ground, and this is also checked during these procedures.

After DELVER #8 has gone through its sensor check and has shut down following a START signal activation, all

eight DELVERs are connected into the BCE boards and the memory batteries are connected to the eight DELVERs at this time also. A REARM sequence and power check reveals that all systems appear to be operating, with the current monitors indicating approximately +2 amps and -1 amp being supplied. A quick scan of all channels indicate that all active sensors are at their null values. Pulling the START loop activates a data capture sequence one more time, and 6.5 seconds later the power drops to a very low standby (trickle charge) value indicating that all eight DELVERs successfully started on command.

The DELVER connectors are bolted into place. The torso is attached to the pelvis. The cabling is carefully placed into the pelvic region. The leg skins are installed. And SPIKE is then positioned for final assembly. The 12 ribs are attached, front and back, with careful placement of wires being carefully monitored. The chest skin is installed and partially zippered, leaving the analog monitor box connectors, the START tether, the trolley battery connector, a ground connector, and the REARM line all hanging out SPIKE's lower back region. SPIKE and the trolley batteries (without ac power now) and the analog monitoring and rearming equipment are taken to the test pad. While hanging from a forklift, SPIKE is outfitted with a motorcycle outfit, including boots. It is then placed on the test motorcycle which has been previously installed into the trolley.

SPIKE is removed from the portable trolley batteries and is reconnected to the trolley-installed set of batteries, which have temporarily also received power from an ac powered field supply. The eyehook is removed from SPIKE's head and the helmet is installed. SPIKE is carefully positioned on the motorcycle, with many measurements and documentation operations being performed. When SPIKE is properly positioned, the trolley mounted START tether is attached to SPIKE, and a REARM sequence is generated. The power monitor is checked, and all channels are again checked for their null states. The REARM line and the analog monitor are then disconnected, and the chest skin is finished being zippered, now fully operational and ready to test. At about 1 second before impact, the motorcycle separates from the trolley, which mechanically removes the trolley batteries from SPIKE, placing it on internal batteries only, and it also pulls the START loop, indicating to the DELVERs that an important event needs to be captured.

## CRASH—OUCH!

After the high speed cameras have stopped, after the car has stopped, after the motorcycle has stopped, and after SPIKE has stopped, the DELVERs stop. The BCE boards turn off all power to all sensors, and the internal batteries maintain the test data. Following the posttest photo session, access to SPIKE is permitted. Loose limbs and broken legs are carefully positioned so that the torso is accessible. The tattered and torn motorcycle suit is removed, as is the helmet. The chest skin is removed and so are the ribs. The

eight DELVER connector bolts are removed in preparation for data retrieval operations.

The DELVER #1 connector is removed and the DRAPS is connected to DELVER #1. The DRAPS start button is pushed and the DRAPS indicates that a transfer has started. The transfer is complete 13.1 seconds later, the DRAPS is disconnected, and the BCE to DELVER #1 connector is reinstalled. The same procedure is performed for all eight DELVERs using the two different DRAPS units. The DELVER connectors are reinstalled to maintain memory retention power from the main +12 volt battery. This minimizes the need to draw power from memory batteries which is the last line of defense. The data will not be purged from the DELVERs until after all of the data are transferred from the DRAPS units to strip charts, FM magnetic tape, and to the host analysis computer. If a failure in one or more pieces of data retrieval equipment had occurred, the DELVERs would still have the data for subsequent retrieval attempts.

Following the last transfer of data from DELVER #8 to the DRAPS, both DRAPS are returned to the host computer area, and SPIKE is returned to the refurbishment area for another test (usually in 24 hours). The DRAPS feed a strip chart recorder the test results for quick-look analysis of the test, and for verification that successful data transfers took place between the DELVERs and the DRAPS units. The DRAPS then offload the analog version of the data to FM magnetic tape as a backup source of data. The DRAPS are then individually linked to the host computer for serial transfers of all eight files (at about 18 minutes a transfer).

After the files are established and massaged, window plots of the crash event are generated and compared against the strip chart recordings to confirm that the data are stored in the computer. Only then are the DELVERs permitted to have their test data purged for the pretest setup and checkout procedures for the next test.

While these procedures take much longer to perform than to describe, they are about as simple as they sound. As many more tests are conducted, the procedures will be refined and simplified where possible. SPIKE and its instrumentation system have ushered in a new era of advanced, unconstrained, data acquisition operations under extremely violent test conditions, and has survived (been revived) to repeatedly perform the tasks it was designed to do.

## Acknowledgements

The author would like to extend a word of appreciation to the SRL "DELVER team," whose hard work made the instrumentation system possible. I would like to also express my gratitude to Dynamic Research, Inc., for the opportunity to help create and test SPIKE, especially to Mr. Ken Wiley (who also provided "Hit him once, hit him hard"), and to Mr. John Brubacher (who named SPIKE), for their excellent team contributions in the technical aspects of this program, and for providing greatly needed support during our shared long hours of hard work. A note of thanks is also due to our JAMA and JARI hosts. Their long hours of support, both technically and culturally is greatly appreciated.

## Study of Antilock Brake Systems for Motorcycles

---

Written Only Paper

**Takumi Okayama, Tomoo Nishimi, Tsuyoshi Katayama, Akira Aoki,**  
Japan Automobile Research Institute, Inc.

### Abstract

Studies of Antilock Brakes (hereinafter called "ALB") for motorcycles have been accomplished in various countries in recent years, and evaluation test methods have been studied within the ECE. We have also studied this area since the spring of 1986, in order to investigate the effectiveness and the range of the effect of ALB for motorcycles, to obtain data related to possible evaluation methods, and to analyze ALB behaviour using a mathematical model. While detailed analysis is still in progress, some preliminary results can be described.

ALB designs using an electronic control system were trial manufactured for this experimental work. They were applied to the front and rear wheels of 4 motorcycles: 2 each with displacement of 750cm<sup>3</sup> and 400cm<sup>3</sup>. Eleven items were measured to analyze the operation of the ALB and the behaviour of the vehicle.

The following preliminary results have been obtained from this study: (1) they are effective over a certain range of road surface and straight line braking, (2) it is technically difficult to optimize the ALB characteristics especially for the front wheel during braking in a turn, (3) though momentary locking of wheel may occur while the ALB is operating, it does not necessarily affect the straight running stability for a moderately long time, (4) it may be useful to change the characteristics of the vehicle in order to match the properties of the ALB.

### Introduction

To improve vehicle behaviour under some braking conditions and reduce driver workload, ALB has been installed in some four wheel vehicles in recent years. This includes adopting it to a range of passenger cars as well as Japan, and it has been mounted to four wheel drive cars which present somewhat different characteristics.

The effectiveness of motorcycle ALB has been studied in various ways in several countries (1, 2, 3), and a manufacturer in West Germany has a version on the market

for example. Also in Japan, motorcycle ALB is being actively studied, and some interim results can be reported.

With regard to possible standards, on the other hand, a brake performance evaluation test method for motorcycle ALB has been addressed by WP29/GRRF. Although the work is still in progress, a part of the results can be presented as a progress report.

## Outline of Study on Motorcycle ALB

Motorcycle ALB has been studied in various countries in recent years, and possible evaluation test methods have been studied within ECE. We have also carried forward a study of motorcycle ALB, and the purposes can be summarized as follows:

- (1) To study the effectiveness of ALB and assess the range of its effect during operation,
- (2) To study possible evaluation test methods, and
- (3) To analyze the behaviour using a kinematic model.

An additional objective was to study whether performance evaluation using only the straight line braking method proposed by ECE is adequate, recognizing that it is desirable that any testing method adopted for certification should be brief. Consideration is also being given to ALB evaluation test methods used four wheel vehicles. For these reasons, we have considered the following evaluation test items for motorcycle ALB:

- (1) Straight line braking (including the braking test based on GRRF R.143).
- (2) Braking in a lane change.
- (3) Braking in a turn.
- (4) Obstacle avoidance during braking.

In each case, the riders' best braking by an expert rider can be compared with ALB braking, in terms of the braking distance, behaviour stability during braking, etc.

The schedule for the study has been as follows:

*First year.*—We designed and manufactured the ALB system for experimental study, measured the basic braking performance of a comparable motorcycle with a conventional braking system, measured the tire characteristics, vehicle data, etc., required for simulation analysis, and studied the performance evaluation test method for the motorcycle with ALB. The experimental methods include: (1) Straight Line Braking, (2) Braking In A Lane Change, and (3) Braking In A Turn. In addition, the basic analysis model for braking the motorcycle was studied.

*Second year.*—We performed braking tests using the evaluation test method examined in the first year, and braking experiments based on GRRF R.143, and mounted the trial manufactured ALB system on the test vehicle for tuning and operational checkout. In the process, we studied various problems with the trial

manufactured ALB system, the compatibility with a motorcycle, the effectiveness of the ALB, etc. We also analyzed ALB behaviour in straight line braking using the kinematic model.

*Third year.*—We studied further the problems of the ALB system which were identified in the second year, made the modifications required to adapt the ALB to the motorcycle, and studied the effectiveness of the motorcycle ALB by repeating the braking test used in the second year, and doing the obstacle avoidance during braking test. We are in the third year, and the results are being analyzed at present. Using the kinematic model, the behaviour when the steering and braking are in combined operation is planned to be analyzed.

The motorcycle ALB system used in this series of studies was newly trial manufactured for this study, as discussed below. It should be specially noted commercial factors such as cost, weight and reliability were not considered in the manufacture of this trial manufactured ALB system.

## Description of Motorcycle ALB System used in the Experimental Work

The trial manufactured motorcycle ALB system is summarized in table 1. It includes wheel velocity sensors for the front and rear wheels, control systems which detect the respective wheel rotation condition via the input signal

Table 1. Antilock brake system for motorcycle.

1	Sensor	⊙ Wheel Velocity Sensor
2	Control	⊙ Electronic Control ⊙ Front And Rear Wheel Independently
3	Hydraulic Control System	⊙ Single Hydraulic Power Supply ⊙ Hydraulic Control: Front And Rear Wheel Independently, Dual Independent System ⊙ Pressure Modulation: Variable Volume Type

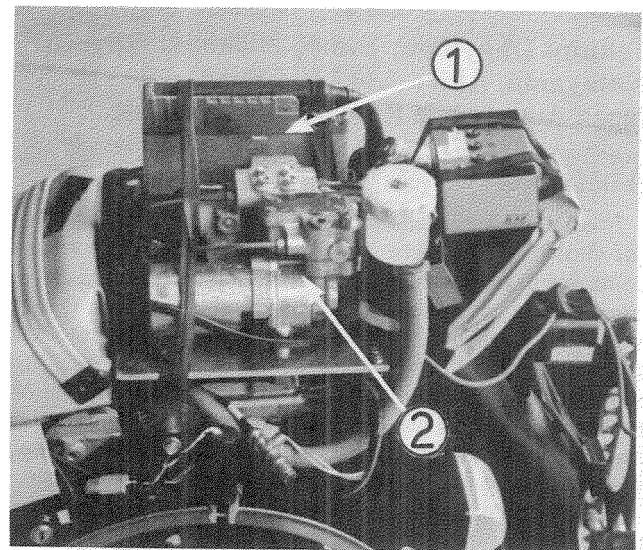


Figure 1. Trial manufactured antilock brake unit.

- ① Electronic Control Unit
- ② Hydraulic Control Unit

from the sensor to control the brake hydraulic pressure, and a hydraulic system which produces the braking force by changing the brake hydraulic pressure by means of the controller. The control and hydraulic systems comprise a dual independent system, in which the front and rear wheels are individually controlled. The hydraulic control is of the variable volume type.

Figure 1 shows the trial manufactured ALB unit, and the electronic controller and the hydraulic control unit are identified. Figure 2 shows the wheel velocity sensor unit for the ALB, fitted to the front and rear wheels.

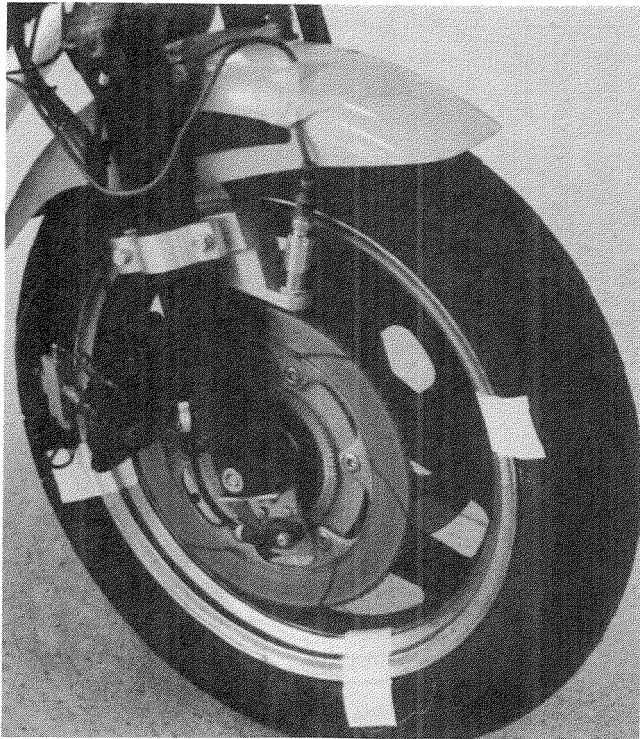


Figure 2. Wheel velocity sensor unit.

## System operation

Figure 3 shows the operational flow chart for the ALB system, figure 4 shows the composite block diagram when the ALB system is not operating, and figures 5 and 6 show it in operation.

*When ALB system is not operating.*—As shown in figure 4, the cutoff valve opens, the inlet and outlet valves are closed, and the master cylinder hydraulic pressure is directly applied to the wheel brake cylinder. At this time, the pressure control piston does not operate, and the hydraulic source remains at a static pressure.

*When ALB system is operating.*—When the controller judges from the input signal from the wheel velocity sensor that the wheel is tending to lock, the cutoff valve closes and the wheel cylinder goes into a «(PRESSURE HOLD)» state. At this time, the pump operates to maintain the hydraulic source at the regulated pressure.

If the locking tendency increases further, the outlet valve opens to shift the pressure control piston to the right, and the

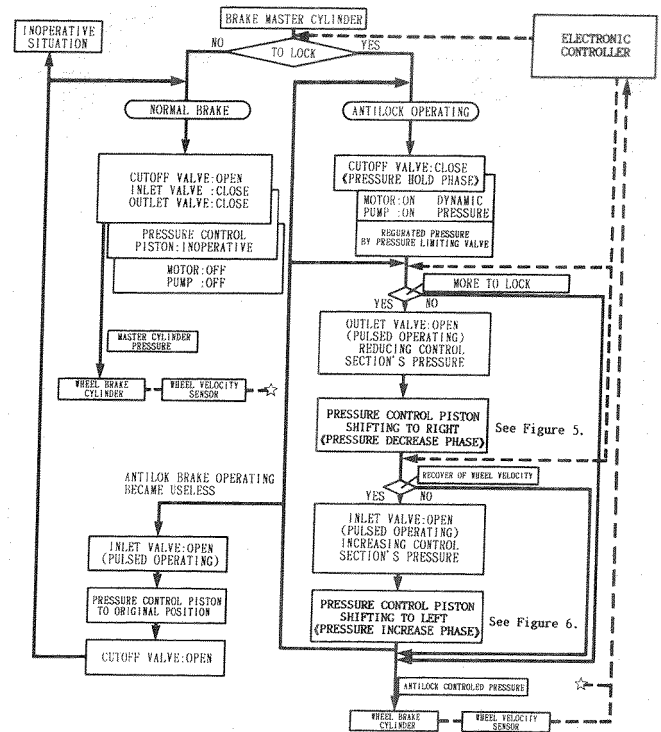


Figure 3. Operation flow chart for motorcycle ALB system.

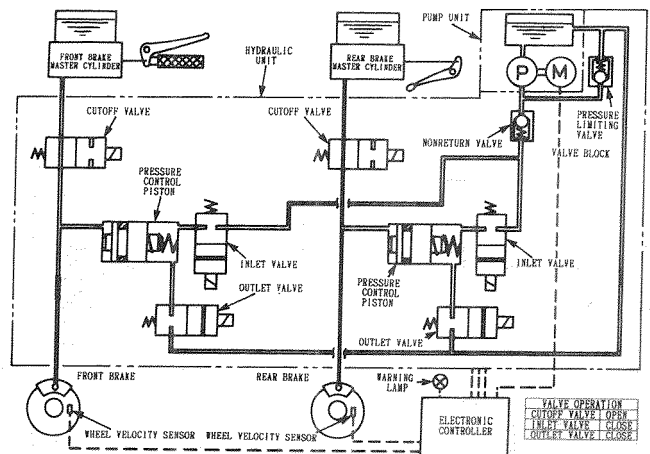


Figure 4. Block diagram when motorcycle ALB is not operating.

wheel cylinder goes into a «(PRESSURE DECREASE)» state (see figure 5).

When the wheel velocity begins to recover, the inlet valve opens and the pressure of the hydraulic source is applied to the pressure control piston to shift it to the left and the wheel cylinder goes into a «(PRESSURE INCREASE)» state (see figure 6).

As mentioned above, the «(PRESSURE HOLD)», «(PRESSURE DECREASE)», and «(PRESSURE INCREASE)» modes change to control the brake hydraulic pressure in accordance with the rotation state of the wheel. Also when the antilock is not operating, the inlet valve opens to return the pressure control piston to its original position, and the cutoff valve opens.

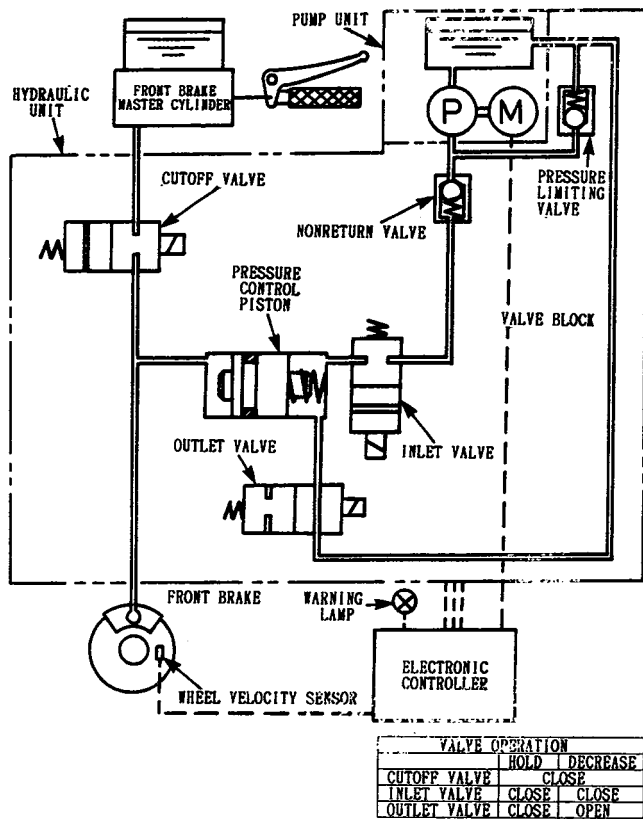


Figure 5. Block diagram when motorcycle ALB is operating (pressure decrease phase).

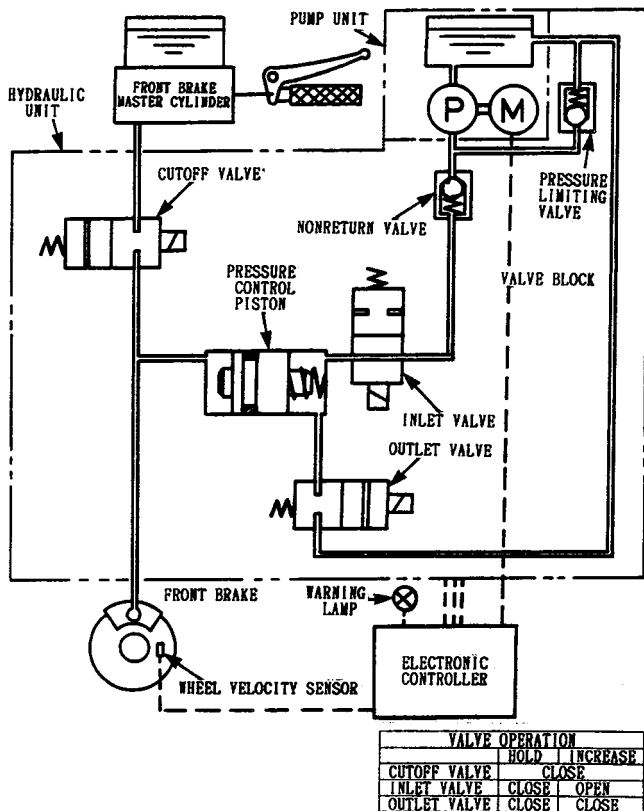


Figure 6. Block diagram when motorcycle ALB is operating (pressure increase phase).

## Outline of the Test

### Test procedures and road surface

Three test procedures were used: (1) straight line braking on various road surfaces, (2) braking in a lane change on various road surfaces, and (3) braking in a turn. The course layout for the braking in a lane change test was based on SAE J46 JUN80 (4) as shown in figure 7, and the braking in a turn test is shown in figure 8.

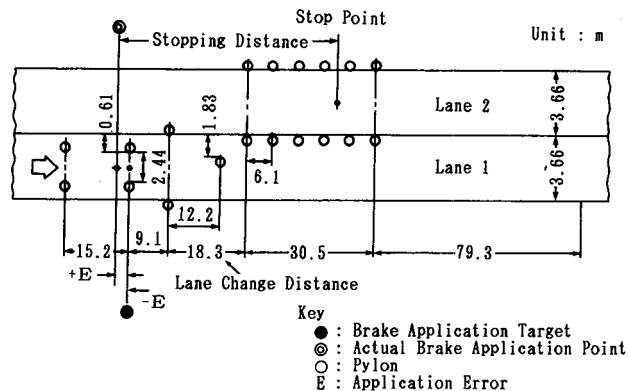


Figure 7. The course layout for braking in a lane change test.

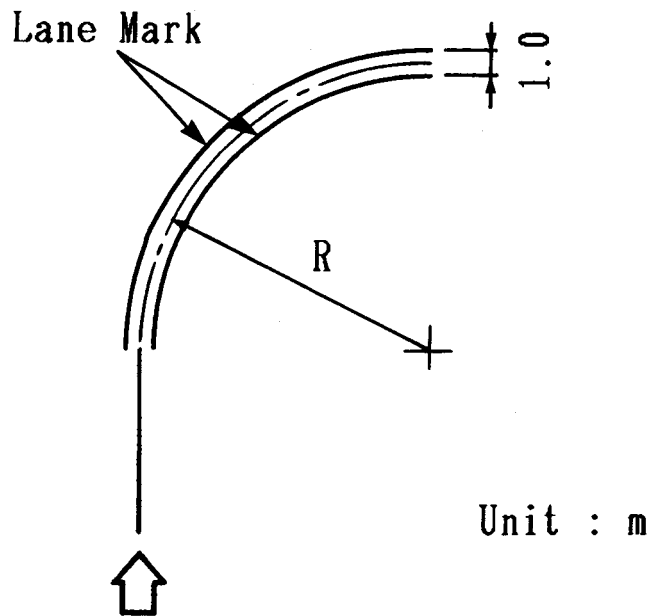


Figure 8. The course layout for braking in a turn test.

In the straight line braking test, the changing friction braking test specified in GRRF R.143 was also performed together. For all of the test items and test conditions, the riders' best braking and ALB braking were performed for three conditions: front wheel braking, rear wheel braking and both wheels braking. Table 2 shows the test items and conditions.

**Table 2. Test items and test conditions.**

Test Item	Surface	Surface Condition	Friction Coefficient of Surface		Initial Braking Velocity (km/h)
			SN	Adhesion Coeff. ( K Value )	
Straight Line Braking	High	Dry	79	0.77~1.03	50,80,100
	Medium	Wet	57	0.63~0.89	50
Braking	Low	Wet	14	0.21~0.34	50,80
Braking In A Lane Change	High	Dry	79	0.77~1.03	at the Highest Velocity
	Medium	Wet	57	0.63~0.89	at the Highest Velocity
Braking In A Turn	Low	Wet	14	0.21~0.34	at the Highest Velocity
	High	Dry	79	0.66~0.84	50,57,62 ( R=50 m ) 72 ( R=100 m )
	Medium	Wet	57	0.61~0.79	50 ( R=50 m )

- Key) 1.SN : Skid Resistance Number ( by ASTM measuring method )  
 2.K Value : The extent of four test vehicles by GRRF R.143 measuring method using Cut Valve in Straight Line Braking, and obtained by riders' best braking in Braking In A Turn.  
 3.K Value of Braking In A Turn is for turning radius R=50 m.

**Test vehicles and measurement items**

Four test motorcycles were used: each test vehicle equipped with disk brakes on the front and rear wheels as shown in table 3. In order to ensure safety during the test, each test vehicle was equipped with an outrigger capable of changing the mounting angle in accordance with the test procedure. The outrigger was the wheel type for vehicle A, and a sled type construction for vehicles B, C, and D (see figures 9 and 10).

**Table 3. The general specification of the test vehicles.**

Test Vehicle	A	B	C	D	
Displacement (cm <sup>3</sup> )	750	400	750	400	
Vehicle Mass (kg)	240	198	200	188	
Wheel Base (m)	1.495	1.425	1.430	1.385	
Caster Angle (°)	28.2	25.5	26.0	26.0	
Trail (mm)	96	83	107	100	
Tire	Front	120/80-16 60H	100/90-16 54H	110-80VR18 V260	100/90-16 54H
	Rear	130/80-18 66H	130/90-16 67H	150-70VR18 V260	120/80-18 62H
Inflation Pressure (kPa)	Front	221	196	221	196
	Rear	221	221	245	221
Brake Effective Diameter (mm)	Front	DUAL DISK 245	DUAL DISK 242	DUAL DISK 264	DUAL DISK 235
	Rear	SINGLE DISK 265	SINGLE DISK 216	SINGLE DISK 186	SINGLE DISK 214

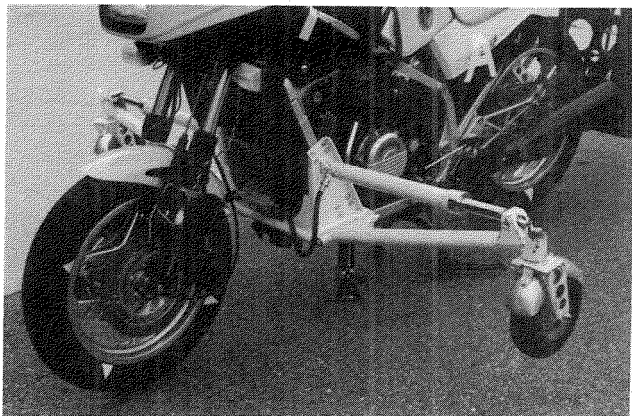


**Figure 9. Test vehicle with the wheel type outrigger.**

The measures and sensors were the 11 items shown in table 4. They were recorded on a small-sized data recorder. The forward velocity was measured by mounting a third wheel to the test vehicle. Figures 11 and 12 show the instrumentation of the test vehicle and a test in progress.

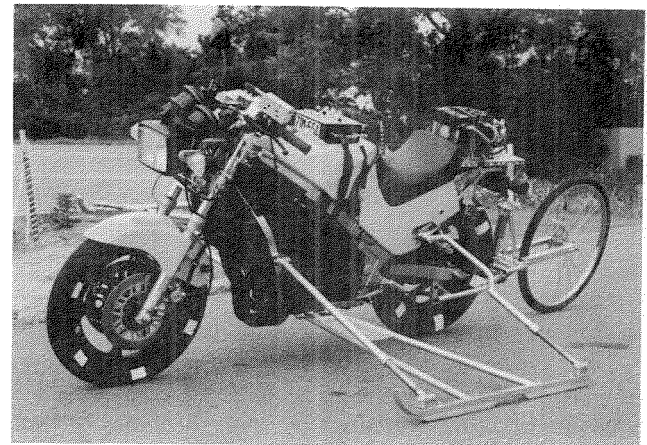


**Figure 10. Test vehicle with the sled type outrigger.**

**Table 4. Measurement items and sensors.**

	Measurement Items	Sensors
1	Velocity	3rd Wheel, Magnetic Pickup
2	Front Wheel Velocity	Magnetic Pickup
3	Rear Wheel Velocity	Magnetic Pickup
4	Front Brake Pressure	Pressure Transducer
5	Rear Brake Pressure	Pressure Transducer
6	Front Suspension Displacement	Potentiometer
7	Rear Suspension Displacement	Potentiometer
8	Steer Angle	Potentiometer
9	Steer Torque	Potentiometer
10	Rolling Velocity	Rate Gyroscope
11	Yawing Velocity	Rate Gyroscope

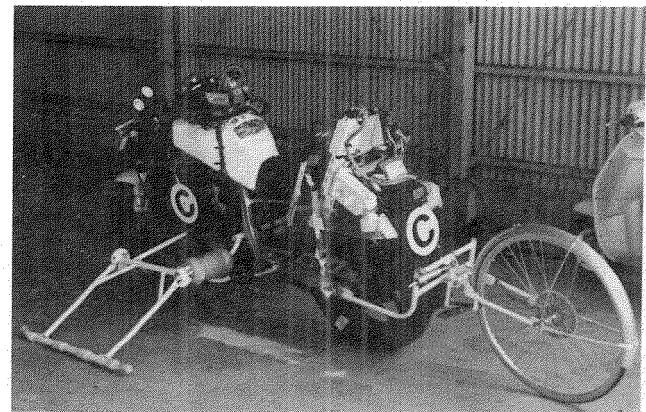


**Figure 11. Test vehicle equipped with ALB system, measuring system and the outrigger.**

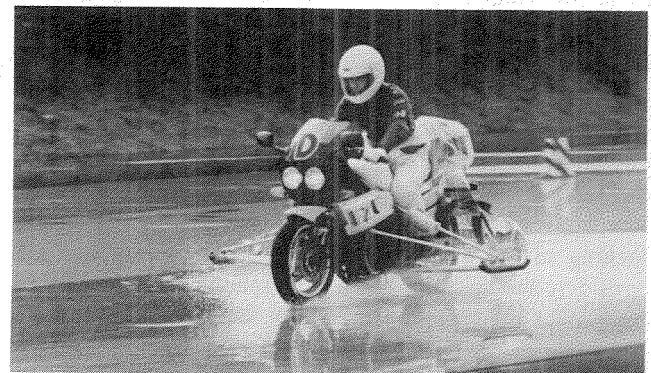


**Figure 12. Straight line braking test on a low friction surface.**

## Test Results and Discussion

### Various issues arose during tuning of the trial manufactured ALB system

In the process of tuning trial manufactured ALB system mounted on the test vehicle, it was discovered that ALB tuning can be a complex process. For example, it was necessary to improve the control logic for the ALB system, to adjust the brake fluid flow rate, and to adjust the fitting to the motorcycle. Some of these issues are discussed below.

*Lowered control performance of ALB due to occurrence of front fork vibration.*—As mentioned in the reports of R. J. Miennert (5) and J. W. Zellner (6) et al., there may be cases where a resonant vibration of the front fork occurs due to the pulsing control of the ALB. In that case, the accuracy of the forward velocity estimate may be degraded by the fluctuation in the wheel velocity, and the control performance of ALB may lower because of improper increased/decreased pressure control due to said fluctuations. To overcome these difficulties for this particular prototype ALB and this particular motorcycle, it was necessary to increase the rigidity of the front fork, to change the essential characteristic of the motorcycle by increasing the rigidity of the main frame, and to review the characteristics of the brake pads and tires.

*Occurrence of full increase in pressure after first control cycle for the front wheel.*—In the initial braking of the front wheel, the trial manufactured ALB system detects a wheel lock tendency before the load transfer due to braking, and operates the cutoff valve in the ALB unit to intercept the input hydraulic pressure from the master cylinder. Thereafter, the braking force may be small compared with the increased front wheel load due to load transfer and there may be room for generating more braking force, and the ALB control may increase the pressure. If, however, this increase in hydraulic pressure is insufficient, and locking does not tend to occur after the pressure has been increased more than a certain number of times, the cutoff valve will open. Then, the input hydraulic pressure from the master cylinder will be directly applied to the wheel cylinder, and the wheel may suddenly tend to lock.

Since a motorcycle typically has a larger ratio of the height of center of gravity to the wheel base than passenger cars, a larger load transfer during braking may occur. As a result, the control logic should consider load transfer in order to account for the possible situation described above.

*Occurrence of momentary locking of wheel due to a change in the surface friction.*—During braking tests when the surface friction changed (medium friction surface → low friction surface), based on GRRF R.143, momentary locking of the wheel occurred in some cases. This was considered to be caused by a slow speed of response in the hydraulic control valve, which was adapted from a passenger car design. However, even though a moderately long momentary locking of the wheel occurred, the straight running stability did not appear to be adversely affected.

*The trial manufactured system properties allowed wheel lock on a very low friction surface in some cases.*—Front wheel brake for motorcycles is usually performed by the hand brake. The brake hydraulic pressure can be much lower than for passenger cars, and the coefficient of friction for some of these tests was very low. Since the trial manufactured ALB system was adapted from a passenger car design, the hydraulic pressure could not be reduced to a low enough in the pressure decrease phase in some cases. As a result, wheel lock occurred in some cases.

### Straight line braking test

*Adhesion coefficient of road surface.*—As shown in table 2, the adhesion coefficients (based on GRRF R.143) of the road surfaces used for this test were 0.77 to 1.03 for high friction surface, 0.63 to 0.89 for medium friction surface, and 0.21 to 0.34 for low friction surface, for the four test vehicles. The high friction surface for all vehicles except one and the low friction surface for all the vehicles conformed to the requirement:  $K \geq 0.8$  and  $K \leq 0.45$  as specified in GRRF R.143. One test surface had a very low value,  $K=0.21$ , and on such a low coefficient of friction it can be difficult for a motorcycle to accelerate and turn in some cases. To determine the K value of the road surface, the procedure required braking three to eight times on the high and medium friction surfaces. On the other hand, we had to make 12 braking tests on the low friction surface to measure the friction, since the wheel locked and the vehicle tended to become unstable.

*Braking performance.*—Figure 13 shows a recorded time history data example for test vehicle C on a medium friction surface. Figure 14 shows the braking performance,  $\epsilon$  expressed as the ratio of ALB braking deceleration to test riders' best braking's it, for the straight line braking test. In terms of the ratio  $\epsilon$  specified in GRRF R.143 at this time, we measured 0.80 to 1.19 on the high friction surface, 0.86 to

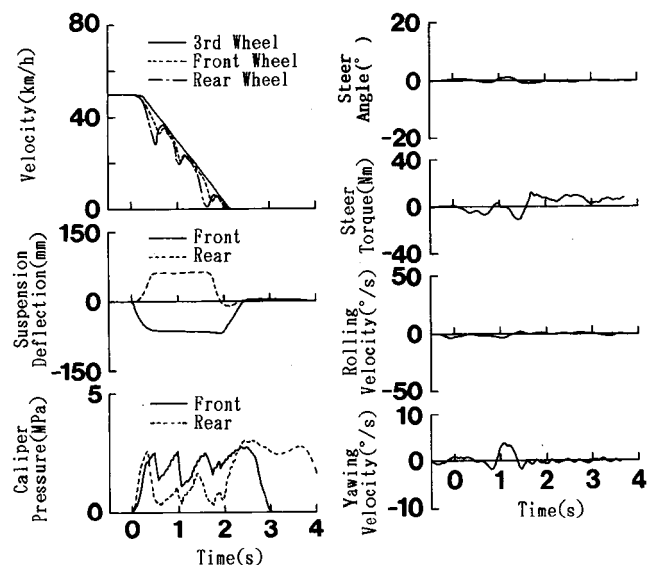


Figure 13. A recorded time history data example for straight line braking test on medium friction surface (test vehicle: C).

1.30 on the medium friction surface and 0.91 to 1.85 on the low friction surface, which numerically conforms to GRRF R.143. In general, the lower the adhesion coefficient of the road surface, the greater the potential effect of the ALB. Since the results on the high friction surface have variations depending upon the final ALB tuning, the variation in braking distance may reflect such factors. However, the generally shortened braking distances shown can be expected from the operation of ALB on a wet road surface, especially if it has low friction surface. These example results demonstrate this for the trial manufactured system.

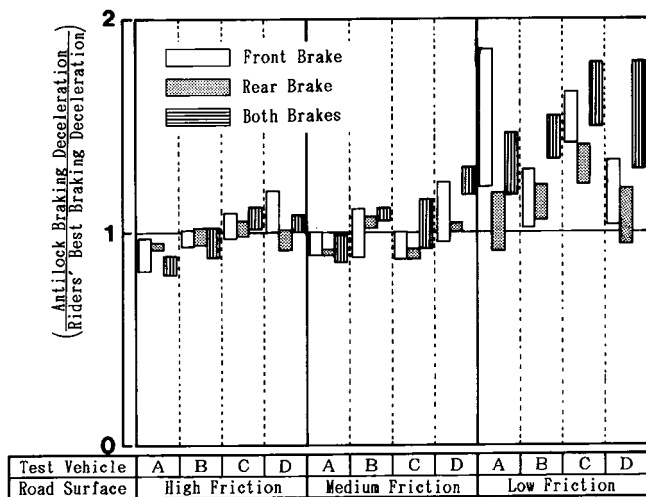


Figure 14. Example braking performance ( $\epsilon$  value by GRRF R.143) for straight line braking test (50km/h).

It should be noted, however, that variations in this value  $\epsilon$  can be large, depending upon ALB adjustment and the degree to which it is matched to each test vehicle. Such variations can result from an ALB system with inadequate settings in the ALB control logic, hydraulic unit, etc. Care should be taken to correctly determine  $Z_m$  value (maximum braking ratio while ALB is not operating) which is a standard to calculate  $\epsilon$  value, and the  $\epsilon$  value can be directly affected in turn, by the variations in  $Z_m$  value. We plan to study this issue in future tests and analysis for the example trial manufactured system.

*Stability during straight line braking.*—To compare the lateral stability between during riders' best braking and during ALB braking, we analyzed the steer angle, steer torque, and maximum values of rolling velocity and yawing velocity as reflecting possible characteristic values of stability.

Figure 15 shows the results of braking tests for vehicle C on a low friction surface. In the case of front wheel braking and both wheels braking, variations and maximum values of all characteristic values during riders' best braking are greater than during ALB braking, and the stability during braking tends to be improved with the trial manufactured ALB operating. This is because the possibility of wheel lock due to over-braking is reduced by the operation of ALB. In the case of rear wheel braking, the stability is hardly affected for these examples even if wheel lock temporarily

occurs due to over-braking, and therefore the differences between riders' best and ALB are small. On the other hand, with front wheel ALB braking and both wheels ALB braking, all characteristic values tend to increase slightly on high friction surface and medium friction surface with the trial manufactured system, and these changes are considered to be within the allowable range. In the case of rear wheel braking, the difference is slight as on the low friction surface.

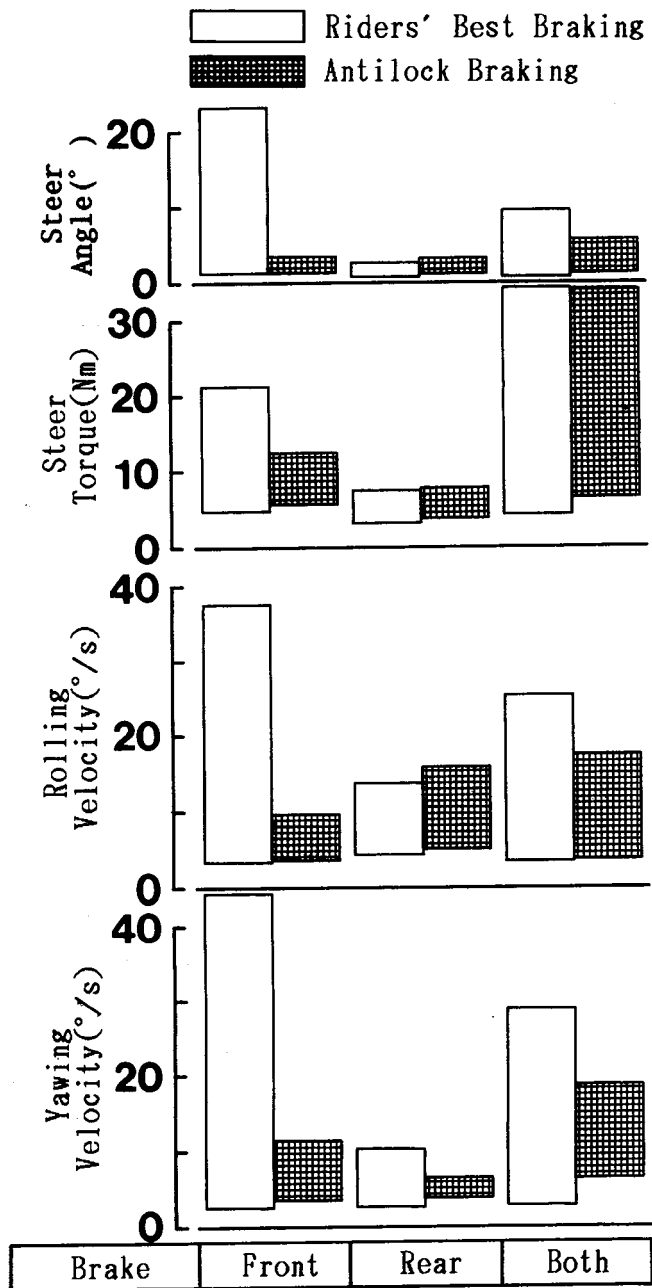


Figure 15. Measures of the vehicle behaviour for straight line braking on low friction surface (test vehicle: C, 50km/h).

Figure 16 shows the comparison between the stability during changing friction braking and uniform friction surface braking with the example ALB system. During changing friction braking from medium friction surface to

low friction surface, the momentary locking data are also included in the figure, and no particular difference is seen between the two in the independent front and rear wheel braking. In the case of both wheels braking, the maximum value for rolling velocity is slightly larger, and the steer angle, steer torque and yawing velocity are on nearly the same level as seen with the uniform friction surface. Even if a momentary locking of 0.14 second duration occurs, the running stability of the vehicle as reflected in the maximum

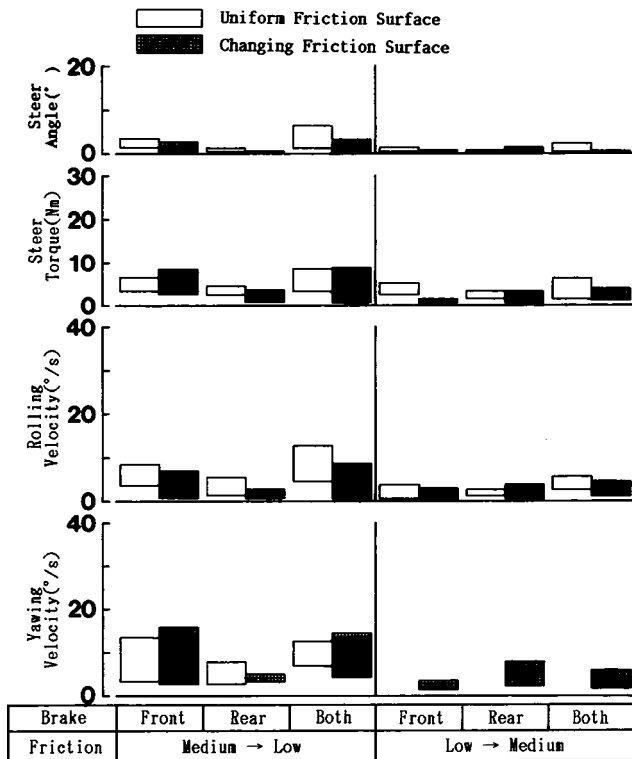


Figure 16. The comparison between measures of the vehicle behaviour for changing friction surface braking test and uniform friction surface braking test (test vehicle: A).

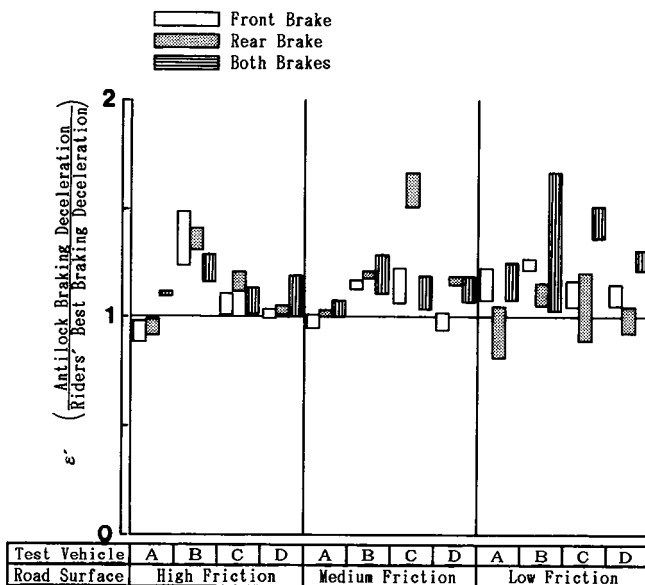


Figure 17. The braking deceleration ratio of ALB braking to the riders' best braking for braking in a lane change test.

rolling velocity does not seem to be affected much for these example cases.

### Braking in a lane change test

**Braking deceleration.**—Figure 17 shows the braking deceleration ratio of ALB braking to the riders' best braking. This figure shows that the braking deceleration for the four test vehicles with ALB braking is relatively high during front wheel braking on a low friction surface, and during both wheels braking on high, medium and low friction surfaces. This is intended to show the braking effectiveness with an ALB which can allow steering while braking the front wheel. Since, however, the difference is not clear in these examples during front wheel braking on high friction surface and medium friction surface, we plan further study.

**Stability during braking in a lane change.**—Figure 18 shows the steer angle, steer torque, maximum values for yawing and rolling velocity when braking test vehicle C. During ALB braking with front wheel braking and both wheels braking for this example system, the maximum characteristic values tend to slightly increase as compared with the riders' best braking, however the stability is hardly affected.

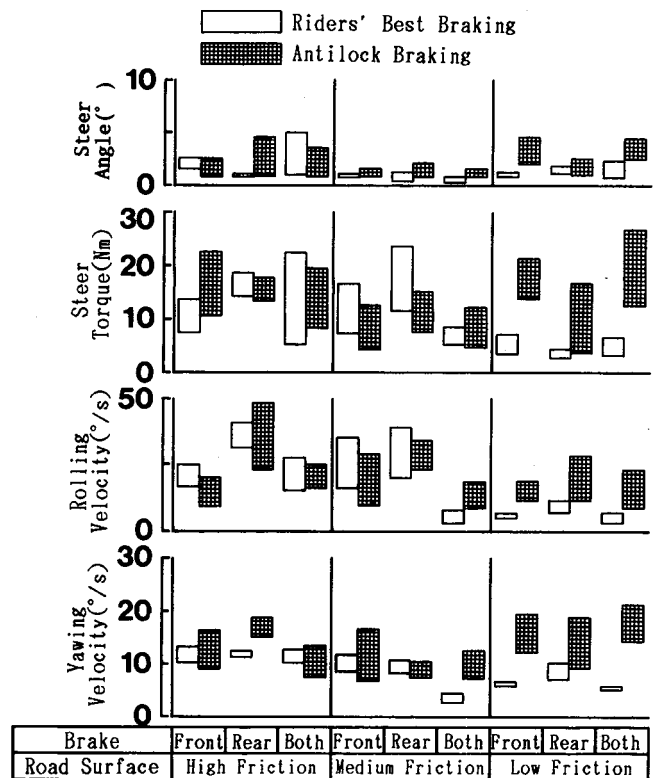


Figure 18. Measures of the vehicle behaviour for braking in a lane change (test vehicle: C).

### Braking in a turn test

**Adhesion coefficient of road surface.**—Table 2 shows the adhesion coefficient during braking in a turn (turning radius 50m) determined in the same manner as for straight line braking as specified in GRRF R. 143. The range for the four test vehicles was 0.66 to 0.84 for the high friction surface,

and 0.61 to 0.79 for the medium friction surface. The former is about 84% and the latter is about 93% as compared with those adversed during straight line braking. Braking in a turn on a low friction surface could not be performed as the test course was restricted.

**Braking deceleration.**—Figure 19 shows a recorded time history data example for the braking in a turn for test vehicle C, and figure 20 shows the braking deceleration for riders' best braking and ALB braking during both wheels braking. For braking in a turn with a radius of 50m on the high friction surface, only vehicle A was able to brake up to 62km/h (initial lateral acceleration  $6m/s^2$ ) in these examples. The both wheels braking procedure at 50km/h (initial lateral acceleration  $3.8m/s^2$ ) in this example could not be performed for test vehicles B, C and D. However, there were cases where independent front and rear wheel braking was possible up to 62km/h. When the braking deceleration ratio (the ratio of braking deceleration of ALB braking to the riders' best braking) was calculated, vehicle A showed so that the braking performance is improved (higher deceleration) by ALB. But, the stability which could be maintained during straight line braking was lost for this example. A main factor during braking in a turn is that the vehicle behaviour may become unstable because of a momentary locking and a large drop in the wheel velocity, it is occurs.

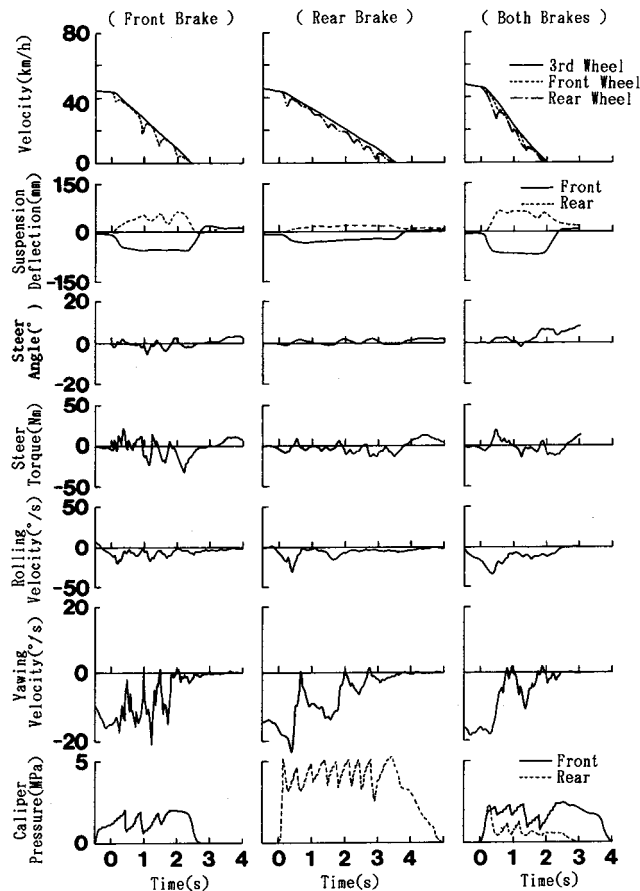


**Figure 19.** A recorded time history data example for braking in a turn test on medium friction surface (Test vehicle: C, turning radius: 50m).

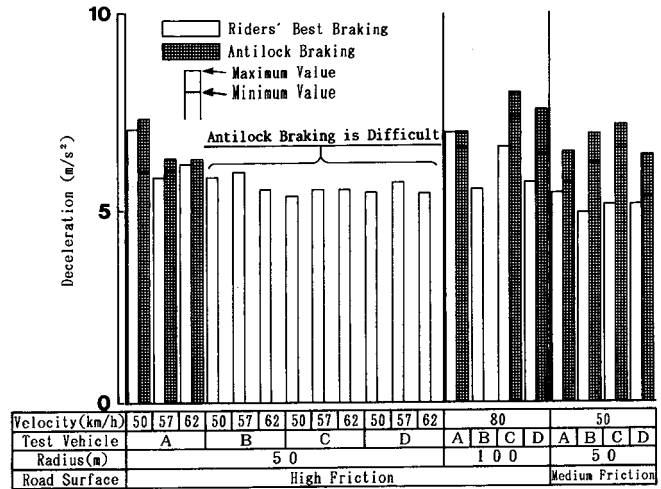


**Figure 20.** The braking deceleration for riders' best braking and ALB braking during both wheels braking.

A turning radius of 100m on a high friction surface, with braking at 80km/h (initial lateral acceleration  $4m/s^2$ ) could be accomplished by all vehicles, except test vehicle B. Also, a turning radius of 50m on a medium friction surface, with braking at 50km/h (initial lateral acceleration  $3.8m/s^2$ ) was possible for all vehicles. In the case of a turning radius of 50m on a medium friction surface, ALB braking for all vehicles gave a shorter braking distance than the riders' best braking for these example cases.

**Stability during braking in a turn.**—The recorded time history data example in figure 19, shows an interval where the steer torque, rolling and yawing velocity fluctuate with the increase and decrease in the hydraulic pressure for ALB control, especially for the front wheel.

To evaluate the stability during braking in a turn, we compared the riders' best braking and ALB braking cases in terms of the steer angle, steer torque, maximum rolling velocity, maximum yawing velocity value and yawing velocity variation as the characteristic values. The maximum yawing velocity value has been normalized by the stationary yawing velocity values. Figure 21 shows the results of a braking in a turn test on a high friction surface for vehicle A which has the highest braking performance among the four test vehicles. At 50km/h, there was not much difference between the riders' best braking and ALB braking, other than the maximum rolling velocity value. The peak rolling velocity occurs in a direction to raise the vehicle body immediately after braking, and this may lower the course tracking property, though the upright running is not affected. Overall the example results show that it did not deviate from the course with a course width of 1 m.

In the example of 57km/h, however, response values for ALB braking become larger in all indexes, and the steer angle and steer torque needed to maintain the course become larger. The stability appears lower at the same time, in this case.

Figure 22 shows the results of a braking in a turn test for test vehicle C on a high friction surface. In the cases of both

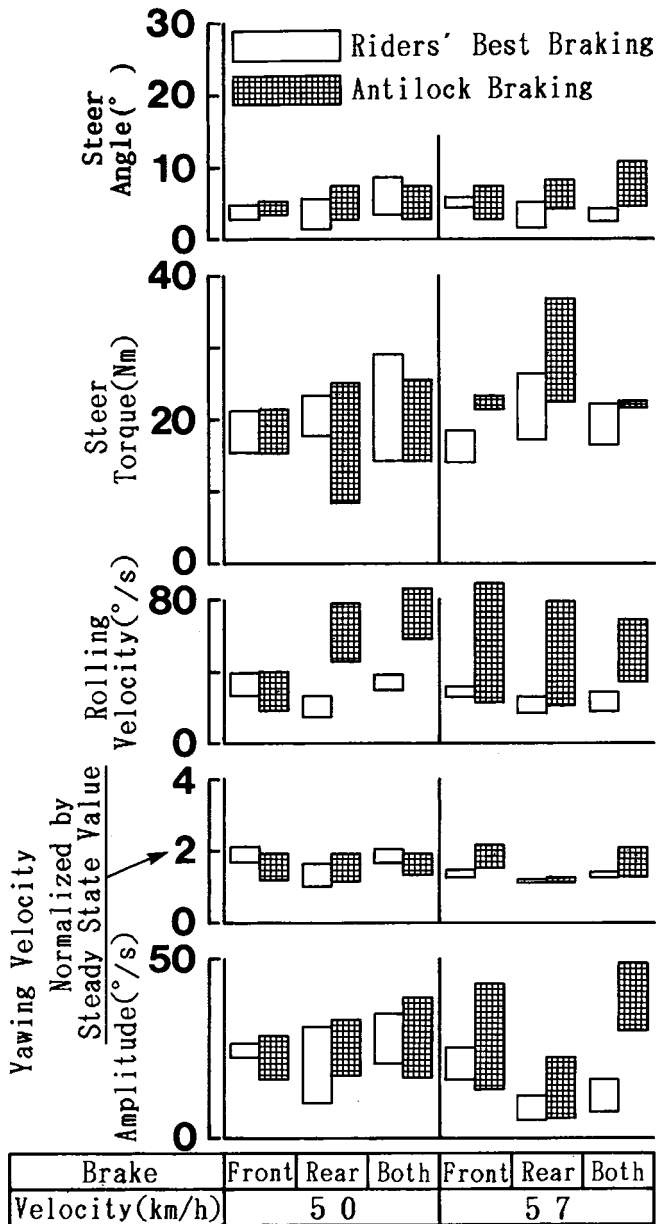


Figure 21. Measures of the vehicle behaviour for braking in a turn test on high friction surface (test vehicle: A, turning radius: 50m).

wheels braking at 40 km/h, and front wheel braking at 50km/h, the vehicle behaviour with ALB braking becomes unstable with this particular example trial manufactured system. This indicates one possible difficulty with ALB control on the front wheel brake but it depends on the system details. In the case of rear wheel braking, the characteristic velocity values increase during ALB braking, however, the behaviour is not much affected by the velocity, and is comparatively stable.

## Conclusion

To investigate the effectiveness and range of effect of the ALB for motorcycles, we developed a trial manufactured ALB system for experimental work, mounted it on four motorcycles and performed tests of straight line braking,

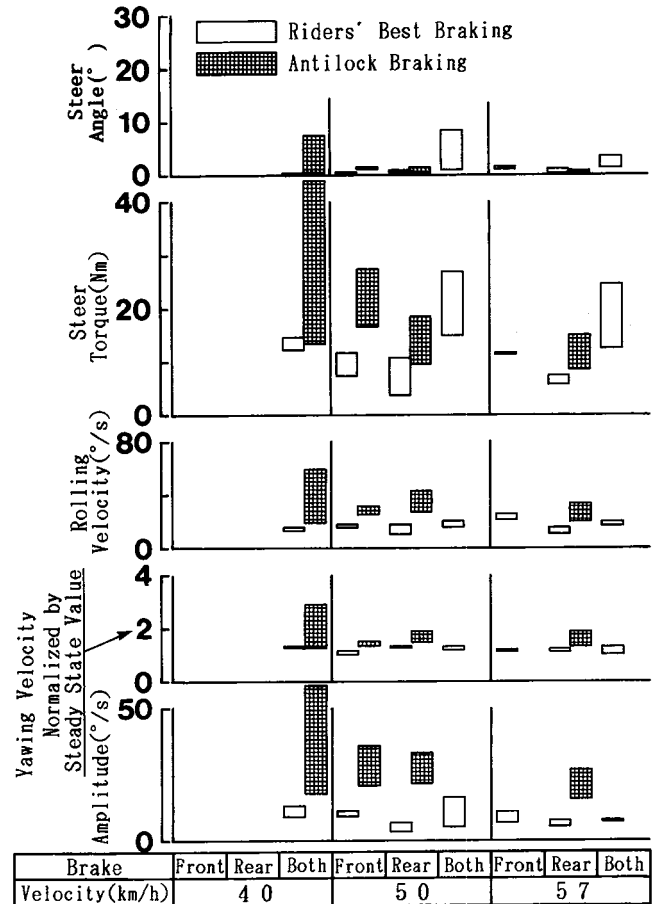


Figure 22. Measures of the vehicle behaviour for braking in a turn test on high friction surface (test vehicle: C).

braking in a lane change and braking in a turn test under various road surface and velocity conditions. Though it was discovered that this trial manufactured ALB system has various problems and further improvements should be made in future, we reached the following interim conclusions, though the study has not yet been finished:

(1) When straight line braking from 50km/h on low friction surface (adhesion coefficient: 0.21 to 0.34), it is possible to shorten the braking distance more than the riders' best braking, and to prevent over-braking, and thereby improve the running stability. The effectiveness of ALB was recognized for this condition.

(2) Though momentary locking may occur during changing friction braking (changing from medium friction surface to low friction surface) even while ALB is operating, the straight running stability may not be much affected, even for a moderately long time.

(3) In the braking in a lane change on low friction surface, the steering property was retained by preventing over-braking of the front wheel ALB, and the braking effectiveness for this trial manufactured ALB was shown. However, the behaviour with this particular system was slightly unstable.

(4) Braking in a turn is difficult with the trial manufactured ALB system: during braking in a turn,

the vehicle behaviour tends to become unstable, and the course tracking property lowers. This tendency becomes especially apparent during front wheel braking, and it is technically very difficult to optimize the ALB characteristic for the front wheel.

(5) To apply the trial manufactured ALB system to motorcycles, there would be cases where the motorcycle would require a wide range of changes in its characteristics, such as changing the rigidity of the front fork and the main frame, and matching the hydraulic system with the ALB.

## References

- (1) J. Cart, An anti-lock braking system for motorcycle, C 188/85, I Mech E 1985.
- (2) A. Weidele, et al., Braking Performance and Stability of Motor Cycle With and Without Anti-Lock-Braking System, IPC-4, SAE Paper 871183.

## Riders' Control Behaviour of Lane Change

Written Only Paper

**Tomoo Nishimi, Tsuyoshi Katayama,  
Takumi Okayama, and Akira Aoki,**  
Japan Automobile Research Institute Inc.

### Abstract

This paper investigates by means of a mathematical model and running experiments how a rider controls a motorcycle while performing lane change, and proposes a rider model which reproduces the difference in riders' control patterns shown in the running experimental results.

The mathematical model of the motorcycle used here is a linear model having four degrees of freedom i.e. side slip, yaw, roll, and steering. The rider model consists of the upper body and the lower body, and the former has a degree of freedom for roll, and the latter has a degree of freedom for the lateral direction.

The running experiments of lane change were carried out as follows. In the experiments, five motorcycles with a displacement of 250 cc to 750 cc were used, and the lane changes were performed by 24 skilled riders.

The following results were obtained from the study on the running experiments and the simulations used by the mathematical model. In this running of lane change, the rider's steering pattern is mainly divided into two: smooth steering pattern and sharp steering pattern. The difference between the two is mainly based on the characteristic of the individual rider. The control of lane change is mainly performed by the steering torque. If the control by the steering torque is assisted by the control of the rider lower body torque, the lane change behaviour can be quickened as compared with only steering torque control.

(3) J. W. Zellner, Advanced Motorcycle Brake Systems—Recent Results, SAE Paper 830153.

(4) SAE J46 JUN80, Wheel Slip Brake Control System Road Test Code.

(5) R. J. Mienniart, Antilock Brake System Application to a Motorcycle Front Wheel, SAE Paper 740630.

(6) J. W. Zellner, D. H. Weir, Evaluation of the Mullard/TRRL Antilock-Brake System, DOT HS 804192(PB 297460).

## Acknowledgement

The study result described herein is a part of the study result that we have been entrusted on a three-year effort supported by Japan Automobile Manufacturers Association, Inc. (JAMA). We express our gratitude to JAMA's Motorcycle Brake Subcommittee for affording us this opportunity to publish this interim report.

## Introduction

The obstruction avoidance performance is one of the important manoeuvre-abilities of a motorcycle. When avoiding an obstruction, the motorcycle rider may not succeed even if he immediately turns the handle bar in the direction which avoids the obstruction, although the automobile driver turns the steering wheel in the avoidance direction. In the case of the motorcycle, the rider should roll the motorcycle in the direction for avoidance. For this purpose, the rider should add the steering torque which rotates the handle bar in the opposite direction to that of avoidance, or the rider should directly add a torque which rolls the motorcycle by moving his body. With the motorcycle, the movement of the rider's body affects the motion of the rider-motorcycle system, and plays a role on controlling the motorcycle. In this way, the motorcycles are basically different from the automobiles in their controlling method.

The control model of the motorcycle has been studied by many researchers, and it was disclosed that it is mainly controlled by the steering torque. However, concerning the detail of the control based on such rider's bodily movement as expressed by the lean angle, etc. of the rider, there has not been much information available.

The author et al. revealed in the previous study (1) the basic control operation of the rider while performing lane change using the rider's control model. Upon analyzing running experiment results by many riders thereafter, it was found out that only a single rider model does not always express the control operation of all riders.

As concerns this analysis of lane change performance, the rider's control operation is made clear in more detail on the basis of the simulations and running experiments.

This paper first presents the outline of the running experiments and the introduction of the rider-motorcycle model to be used in this study. The rider's control method is clarified, the applicability of the control model which is proposed here is investigated by comparing the simulations with the running experiments, and this rider-motorcycle model is applied to lane change performance. Finally the conclusion is described.

## Running Experiments

To throw light on the rider's control operation during transient operation of the rider-motorcycle system, the lane change experiments shown in figures 1 and 2 were performed. The rider traveled along these courses at various fixed speeds (40 km/h to 100 km/h). Five experimental motorcycles (A to E) with displacement of 250 cc to 750 cc were used, and driven by 24 skilled riders in all. The measurement items measured in the running experiments were steer torque, steer angle, yawing velocity, rolling velocity, forward velocity, rider lean angle and rider lateral movement as shown in table 1.

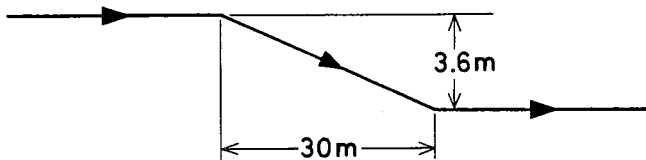


Figure 1. Single lane change course.

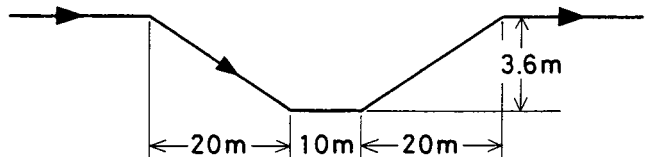


Figure 2. Double lane change course.

Table 1. Measurement items.

	Items
1	Steer torque
2	Steer angle
3	Yawing velocity
4	Rolling velocity
5	Forward velocity
6	Rider lean angle
7	Rider lateral movement

## Rider-motorcycle dynamics

The block diagram for the rider-motorcycle system used in this study is shown in figure 3. The movement of the motorcycle is basically the same as four-degree of freedom model of Sharp (2). The motorcycle has degrees of freedom for the following: side slip, yaw, roll, and steering. The tyre forces and moments which work on the motorcycle are lateral forces, aligning moments, and overturning moments due to side slip and camber of tyre. The dynamic characteristic of tyre shall be first order lag. In addition, the aerodynamic forces and moments are taken into consideration. It is drag, lift and pitching moment that greatly affects the movement of the motorcycle out of the aerodynamic forces and moments, and these affect the load on the front and rear wheels of the motorcycle.

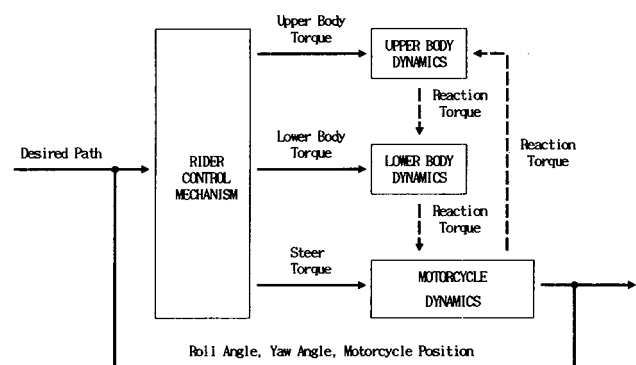


Figure 3. A block diagram of the rider-motorcycle system.

The rider is assumed to consist of two portions: upper and lower bodies as shown in figure 4. The upper body consists of the head, upper trunk, forearms and upperarms. The lower body consists of the parts other than the upper body, palms and feet. The upper body is secured to the lower body through a spring and a damper, and the lower body is also secured to the motorcycle through a spring and a damper in the same manner. The rider upper body rolls to the lower body, and the rider lower body moves laterally to the motorcycle. The lateral movement of the lower body is considered here to be replaced with the roll against the motorcycle with the ground point as the centre. The mechanical characteristic of the rider is described in the latest study (3).

The rider is assumed to input the lateral deviation to the desired course and the roll angle of the motorcycle, and output the steering torque, upper body torque and lower body torque as control torques.

These three control torques are the internal forces of this system. Therefore, these should follow the Third Law of Newton's Motion. It is assumed here that the steering torque reaction, the upper body torque reaction and the lower body torque reaction operate on the rider upper body, the rider lower body and the motorcycle respectively.

The coordinate system is downward to the right as shown in figure 4. The equations of motion for the rider-motorcycle system are described with reference to the projection point of the centre of gravity,  $G_m$  of the main frame on the

road surface shown in figure 4. The details of the equations of motions are shown in appendix I and II.

### Control method

It is generally considered that the rider controls the motorcycle by the steering torque, and at the same time controls the motorcycle and facilitates supporting his body by moving the body. However, the detail of the purpose and effects of the rider moving his body are not clearly known.

First, the basic control method by the steering torque and moving the body is described, and a control model is proposed, which represents the individual differences in the control methods seen in the running experimental results.

In the previous study, the rider's basic control behaviour during running of lane change as below was clarified. The rider controls the course tracking and the roll posture of motorcycle mainly by the steering torque. The rider moves his body in such a transient motion during lane change to control the motorcycle by its reaction. The movement of the rider's lower body assists the control by the steering torque. The movement of the rider's upper body does not directly control the movement of the motorcycle, but only the uprightness of the rider himself.

In the basic rider's control model taking into consideration the above movement of the rider, the rider inputs roll angle  $\phi$  of the motorcycle and heading deviation,  $\delta$ , from the

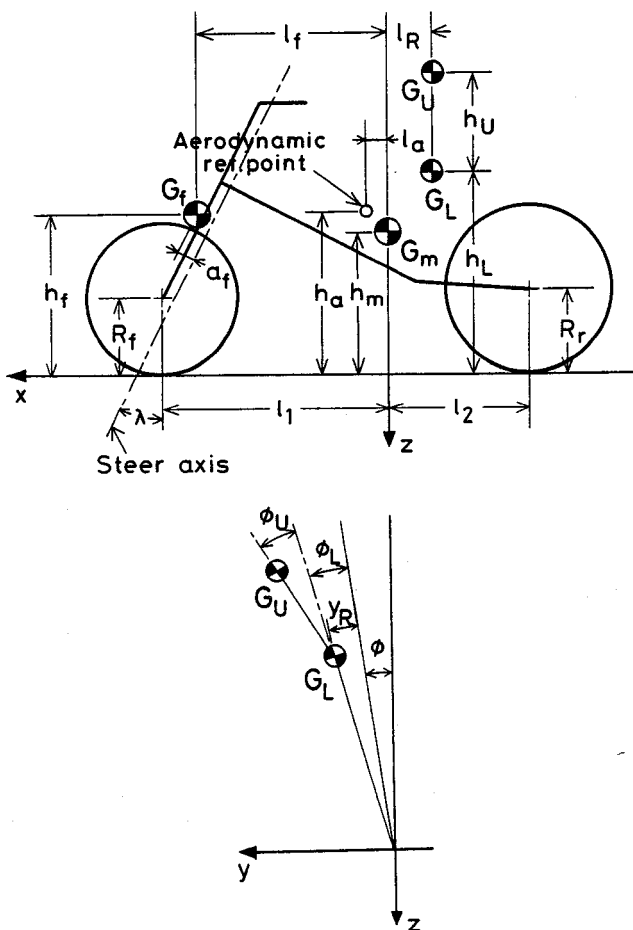


Figure 4. Rider-motorcycle system.

desired course, and outputs steering torque,  $\tau_s$ , lower body torque,  $\tau_L$ , and upper body torque,  $\tau_U$ . The detail of the basic rider model is specified in Appendix III.

This rider model well represents the basic features of the rider's control behaviour in lane change.

When, however, studying the experimental results in detail, some individual differences are seen in the riders' control behaviours in running under the same conditions. Figure 5 shows examples of double lane change at a speed of 40 km/h. The experimental motorcycle is motorcycle E (250cc) and was driven by riders i and j. The control behaviours during lane change this time are divided into two patterns. One is a smooth pattern represented by rider i, and the other is a control pattern with sharp peak represented by rider j.

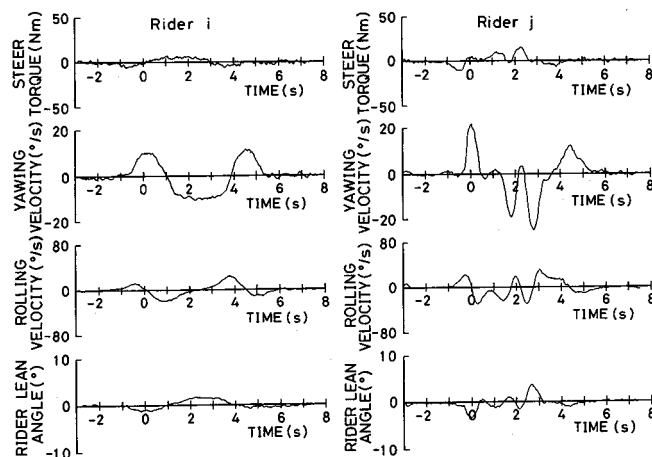


Figure 5. Results of experiments of double lane change (motorcycle E, velocity: 40 km/h).

The basic rider model nearly reproduces a control behaviour with a smooth pattern, however is not capable of reproducing its peak for a pattern with sharp peak. Therefore, a rider model is introduced which describes the rider's control behaviour of control pattern with sharp peak.

Figure 6 shows a steering torque trace of rider j. It can be seen from this figure that the rider of pattern with sharp peak represented by rider j suddenly controls before the desired course changes. It is considered that he is going to more

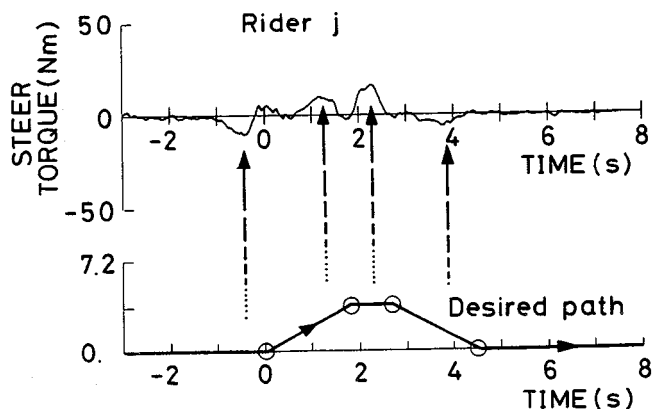


Figure 6. Steering torque trace of double lane change (motorcycle E, rider j, velocity: 40 km/h).

faithfully travel along the desired course. That is, it can be regarded that the rider of the pattern with sharp peak increases the gain to follow up the desired course before the turning point.

Therefore, in the rider model of the control pattern with sharp peak, the steering torque is assumed to be as follows:

$$\tau_s = k_{S\phi} + \left[ \sum_{i=1}^N w_i(x) + 1 \right] k_{sd} d,$$

where  $k_{S\phi}$  is a coefficient of roll angle input, and  $k_{sd}$  is a coefficient of heading deviation input.  $w_i(x)$  is a weighting function to correct the coefficient,  $k_{sd}$ , of heading deviation from the desired course.  $w_i(x)$  value becomes a maximum value before the turning point as shown in figure 7.

$$w_i(x) = H_i \exp[-2.77(x - x_i)^2/D_i^2].$$

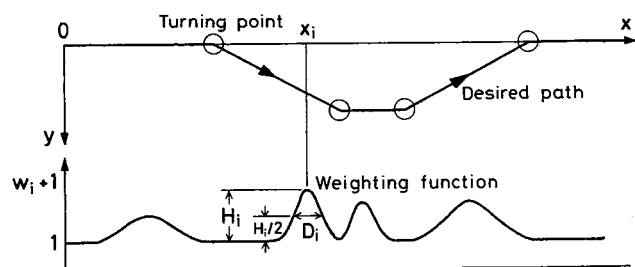


Figure 7. Weighting function of the steering torque gain.

Since the ratio of the roll angle to the heading deviation which cover the steering torque changes in this model, this model is called "the variable steering torque gain ratio model" here. The alternate basic model is called "the constant gain ratio model" since the ratio of the roll angle to the heading deviation remains unchanged.

These two rider models are used for analysis.

## Results of Simulations and Experiments

### Comparison of simulational results to experimental results

The rider model proposed in this study is applied to lane change performance, and it is compared with the running experimental results.

Figures 8 and 9 show examples of results of double lane change. The experimental motorcycle is motorcycle E, and the running speed 40 km/h.

Figure 8 shows the running result of a smooth steering pattern by rider i, and the constant gain ratio model is applied to simulation. Figure 9 shows the running result of a steering pattern with sharp peak by rider j, and the variable gain ratio model is applied to simulation. In the figures, the experimental result is expressed by a thin line and the simulation result by a bold line.

The constant gain ratio model nearly reproduces the rider's experimental result of a smooth steering pattern, while the variable gain ratio model more clearly reproduces a sharp peak which could not be reproduced by the constant gain ratio model. Combination of other experimental motorcycles or other riders shows the same result.

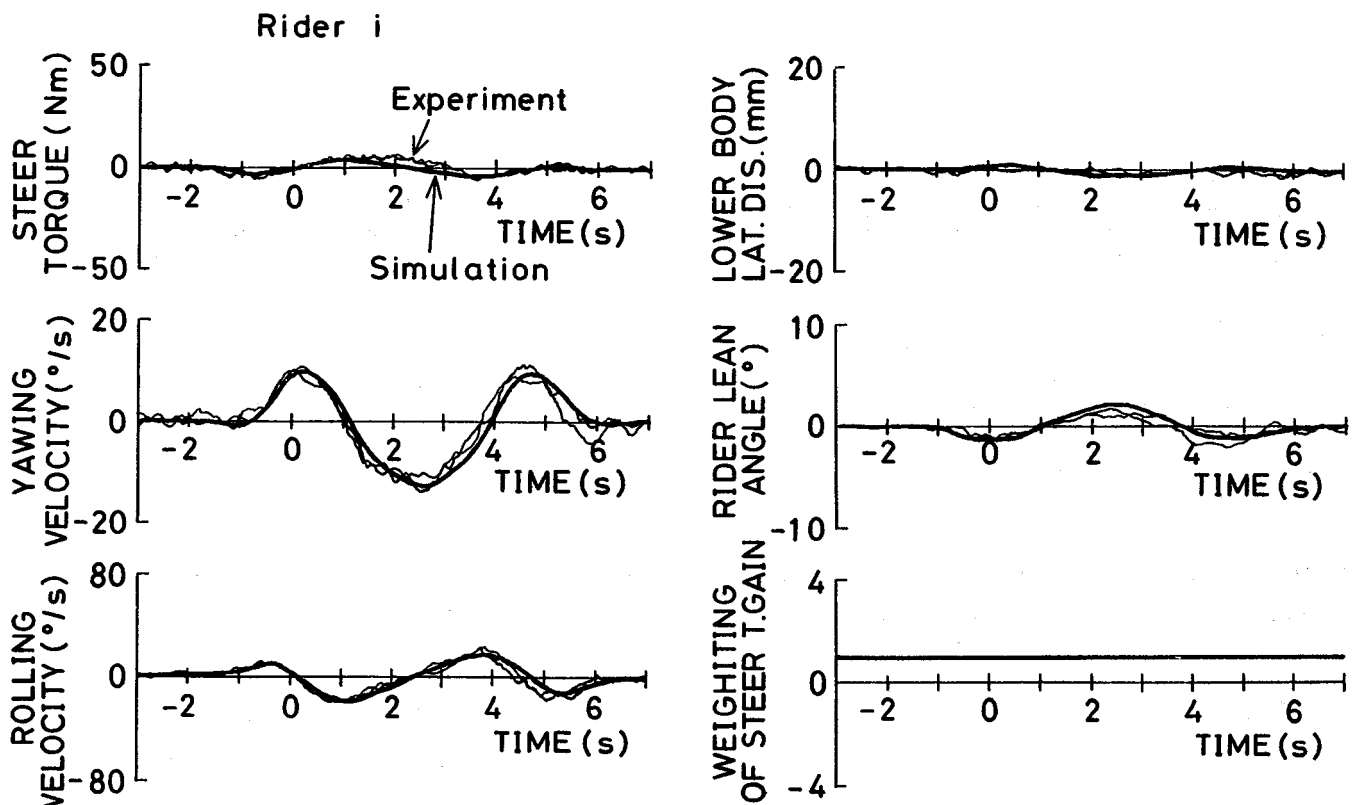


Figure 8. An example of double lane change manoeuvre (motorcycle E, rider i, velocity: 40 km/h).

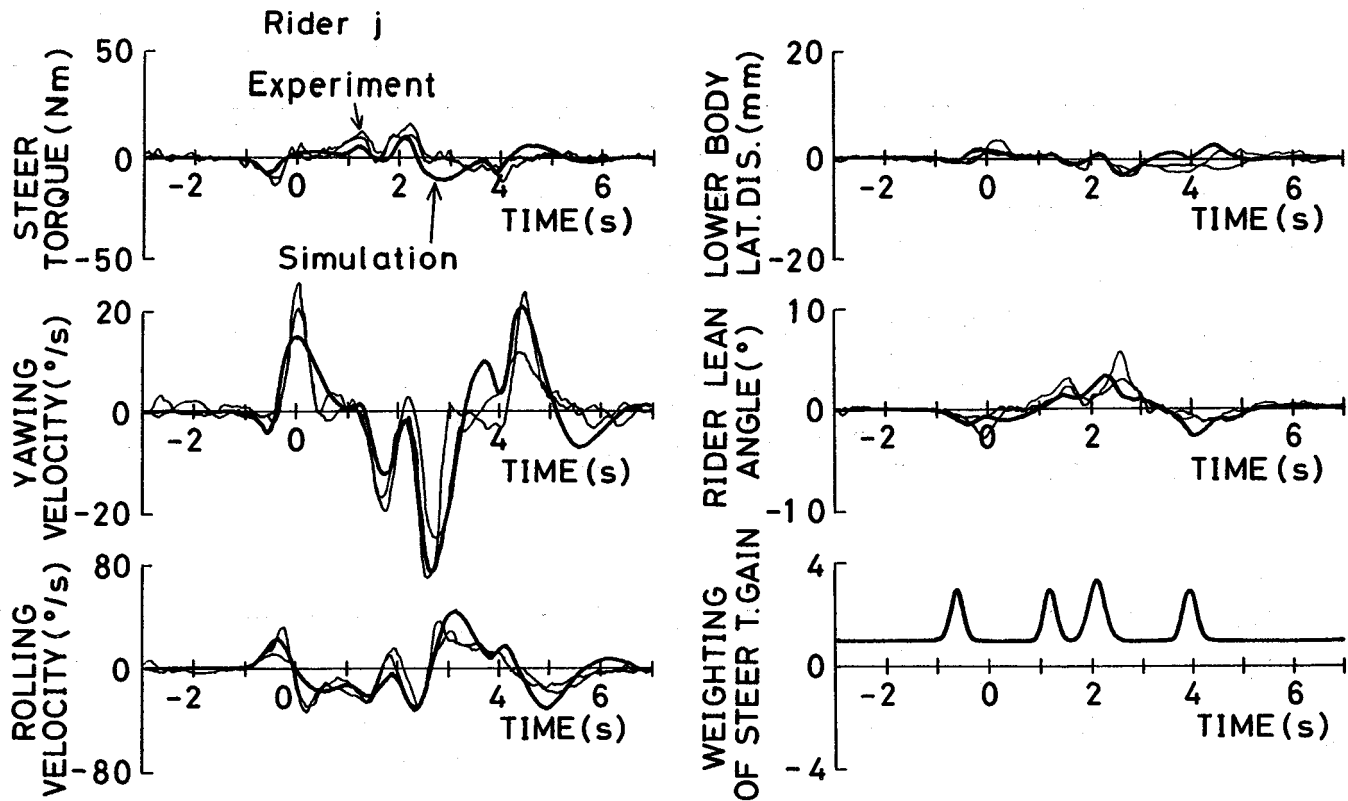


Figure 9. An example of double lane change manoeuvre (motorcycle E, rider j, velocity: 40 km/h).

Since the constant gain ratio model can be regarded as a special case where the weighting function,  $w_i(x)$ , of the variable gain ratio model has been set to zero, the lane change motion of the motorcycle by various riders can be represented by the variable gain ratio model proposed here.

Table 2. Riders' control patterns (single lane change).

Motor-cycle	Rider	Age years	Experi-ence years	Riders' Weight kg	Single lane change			
					40 km/h	60 km/h	80 km/h	100 km/h
E	a	22	4	61	●	●	○	○
	b	26	6	59	●	●	○	○
	c	29	6	62	●	●	●	●
	d	33	10	63	●	●	○	○
	e	22	1	70	●	○	○	○
	f	25	9	63	●	●	●	●
	g	25	5	67	●	●	●	●
	h	31	10	71	○	○	○	○
	i	26	5	72	○	○	○	○
	j	22	4	69	●	●	○	●
	k	32	10	68	●	●	○	○
l	24	5	58	○	○	○	○	

● : Variable gain ratio model is applied.  
○ : Constant gain ratio model is applied.

Table 3. Riders' control patterns (double lane change).

Motor-cycle	Rider	Age	Experi-ence	Double lane change		
				40 km/h	60 km/h	80 km/h
A	g	25	5	●	●	○
	h	31	10	○	○	○
	i	26	5	●	○	○
	j	22	4	●	●	○
	k	32	10	●	●	○
	l	24	5	○	○	○
E	g	25	5	●	○	○
	h	31	10	●	○	○
	i	26	5	○	○	○
	j	22	4	●	●	○
	k	32	10	●	●	○
	l	24	5	○	○	○

● : Variable gain ratio model is applied.  
○ : Constant gain ratio model is applied.

The riders are skilled. This is considered to apply also to other transient motions such as slalom motion as well as lane change.

By comparing the above simulation results using the variable and constant gain ratio models with the experimental results, the rider control pattern was classified by the rider model as shown in tables 2 and 3. On these tables, a black circle mark indicates an experimental result which can be explained by the variable gain ratio model in which the heading deviation coefficient,  $[\sum w_i(x) + 1] k_{sd}$ , of the steering torque has been changed into variable, while a white open circle mark indicates an experimental result which can be explained by the constant gain ratio model.

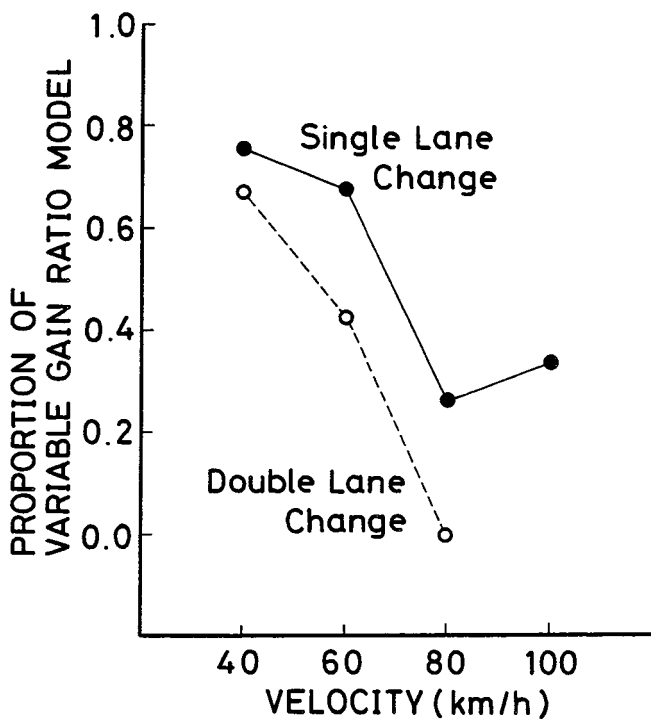


Figure 10. Proportion of the variable gain ratio model.

It can be seen from tables 2 and 3 that it depends upon the rider as to which rider model should be applied, and that the difference in the control pattern is based on the individual differences of the rider.

The results obtained by determining the proportion of variable gain ratio model to the running velocity from this result are shown in figure 10.

Figure 10 shows that the proportion of the variable gain ratio model decreases as the running velocity increases. Especially in double lane change at a speed of 80 km/h, that of the variable gain ratio model is zero.

When the lane change running experiment was performed, subjective estimate on the rate of facility for each experiment task was taken from six to twelve riders who drove each experimental motorcycle. The relationship between this subjective estimate on the rate of facility for each task and the proportion of the variable gain ratio model in the simulation result for each running experiment is

shown in figure 11. A point in the figure indicates the average of the subjective rating for each experimental motorcycles.

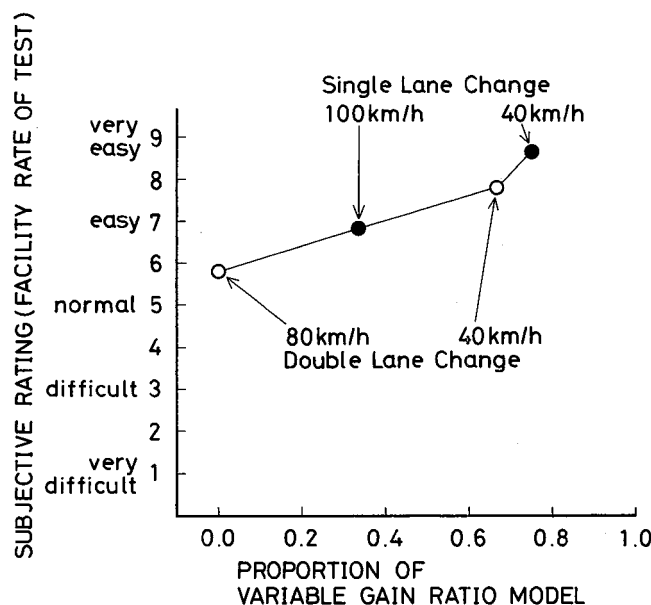


Figure 11. Subjective rating on the degree of facility for tasks.

According to this result, the task becomes naturally more difficult as the running speed increases. Also it can be seen that double lane change at 80 km/h is more difficult than single lane change at 100 km/h. From the foregoing, when the task becomes more difficult and room for performing the task becomes less, the rider model to be applied is reduced to one.

### Estimate function

Two estimate functions are introduced to analyze the simulation.

$$[\text{first estimation}] = \int (\text{heading deviation})^2 x^2 dt,$$

$$[\text{second estimation}] = \int (\text{steer torque})^2 x^2 dt,$$

The first estimation provides an index for accuracy of course tracking, and the second estimation is an index representing the degree of the rider's effort at the time. The respective estimations are multiplied by the square of  $x$ , which is the coordinate of the forward direction, since emphasis is placed on the second half of the running.

The comparison of the course tracking result between the variable and the constant gain ratio models using the first estimation is shown in figure 12. The course is single lane change, the motorcycle is the motorcycle E, and the running speed is 40 km/h. In the case of the constant gain ratio model when the sighting distance is about 17.5 m, the first estimation becomes minimum. The value is about 0.5. In the variable gain ratio model, the first estimation becomes minimum as the sighting distance is about 16.5 m. The value is about 0.2 and is smaller than that of the constant gain ratio model. The variable gain ratio model has been obtained by thus modeling the control behaviour of the rider who is going to follow up the course more faithfully.

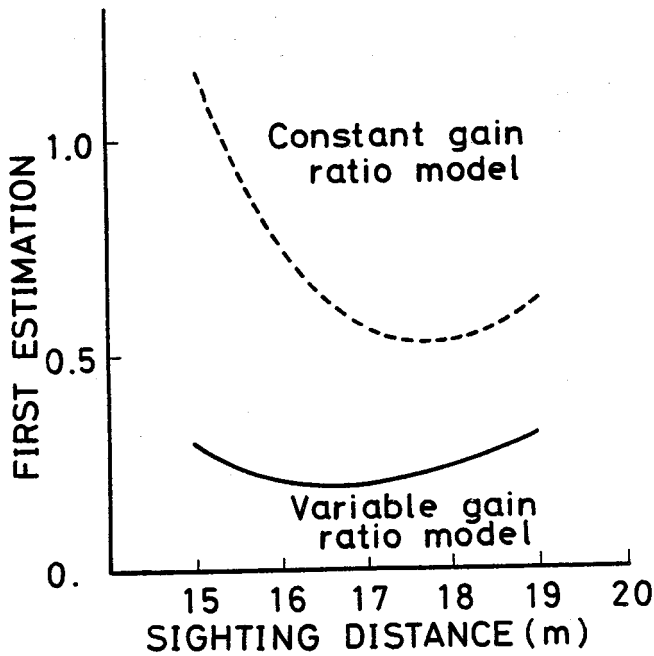


Figure 12. Tracking performance of the rider models.

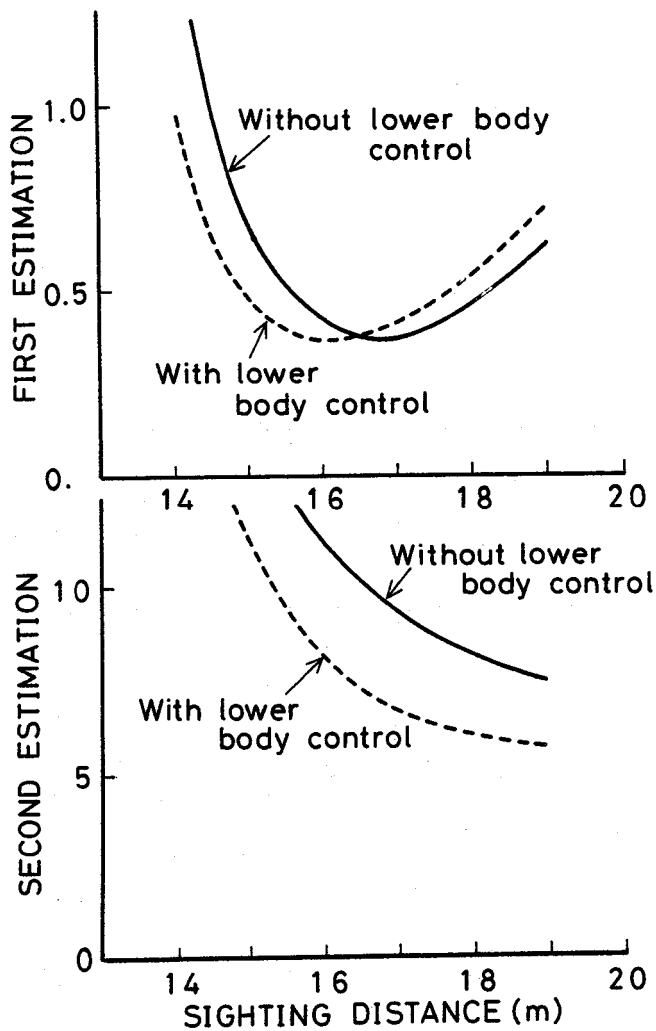


Figure 13. Effect of the lower body controlling torque.

## Effects of the rider's lower body controlling torque

As clarified in the previous study (1), the rider's lower body torque plays a role to assist the control by steering torque. It is studied how the running result changes when controlled by the lower body torque and when not controlled.

Figure 13 shows the results of the estimations when controlled by the lower body torque and when not controlled. The running course is single lane change, the speed is 40 km/h, and the experimental motorcycle is motorcycle B (400cc). For the rider model, the constant gain ratio model is applied. The results drawn in this figure show such a travel as to reduce the first estimation to a minimum at the respective sighting distance.

According to this result, the minimum value of the first estimation remains unchanged irrespective of the control of the lower body torque, and the control of the lower body torque does not affect the accuracy of course tracking. The sighting distance which minimizes the first estimation is shorter when controlled by the lower body torque. This is because the steering torque acts on the steering angle to generate tyre lateral force and this tyre force produces roll motion through yaw motion and lateral motion of the motorcycle, while the lower body torque directly produces roll motion of the motorcycle. Therefore, the motorcycle responds slightly more quickly when the control by the steering torque is assisted by the lower body torque. Therefore, the sighting distance is shorter when controlled by the lower body torque. The second estimation has a larger value when not controlled by the lower body torque than when controlled. When not controlled by the lower body torque, the second estimation becomes larger since the control to be done by the lower body torque is performed by the steering torque. Also in either case, when the sighting distance becomes larger, the second estimation becomes less. That is, when the control operation is started earlier, the control effort is reduced that much.

## Sighting distance versus forward velocity

Figure 14 shows the sighting distance versus forward velocity determined to minimize the first estimation for each experimental motorcycle. The running course is single lane change. The speed is 40 km/h to 100 km/h. The rider model is the constant gain ratio model.

Figure 14 shows that the optimum value for the sighting distance becomes longer as the running speed increases though the minor portions differ depending upon the experimental motorcycles. Even if, however, the running speed is doubled at this time, the optimum sighting distance is not doubled. When the sighting distance is converted to time, the time for forward sighting becomes shorter when the running speed becomes faster. This is because the response of the motorcycle becomes faster as the running speed increases.

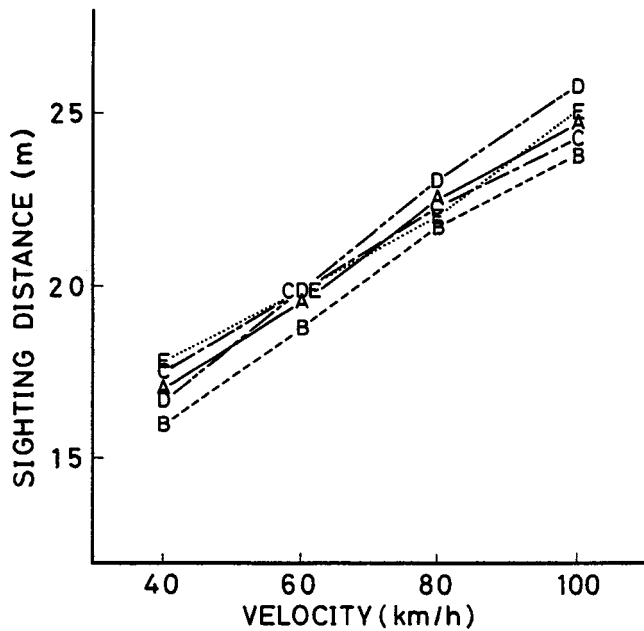


Figure 14. Sighting distance with the lowest first estimation value.

## Conclusion

This study proposed a rider model: a variable gain ratio model which reproduces the differences in control behaviour by riders during lane change performance, and investigated the propriety by comparing the operational characteristics of skilled riders.

The outline of the models proposed here is as follows: A motorcycle has four degrees of freedom for lateral motion, yaw, roll and steering. The rider consists of the upper and lower bodies. The rider's control inputs are the heading deviations from the desired path and the roll angle of the motorcycle, and the control outputs are the steering torque, the rider upper body torque and the lower body torque. The control torque reactions which are output from the rider act on the rider upper body, the rider lower body and the motorcycle respectively. The course tracking

characteristics and the posture for motorcycle roll are mainly controlled by the steering torque. The rider lower body torque is applied in proportion to the steering torque, and assists the control by the steering torque. The rider upper body torque control only the uprightness of the rider himself. The desired course follow-up gain of the variable gain ratio model varies in accordance with the preset value before the course change point.

The following conclusions have been obtained by applying this rider-motorcycle model to lane change:

(1) The variable gain ratio model is capable of almost representing the sharp peak waveform which could not be reproduced by the constant gain ratio model.

(2) During lane change, the motorcycle is mainly controlled by the steering torque. When, however, the control by the steering torque is assisted using control of the rider lower body, the behaviour of lane change can be quickened.

(3) In these running experiments of lane change, the control pattern can be mainly divided into two: a smooth steering pattern and a steering pattern with sharp peak. This difference is mainly based on the characteristic of the individual rider.

This rider model was applied to lane change performance this time, and it is thought that the model can be applied to other transient motions such as slalom.

## References

- (1) Katayama, T., Aoki, A., and Nishimi, T., Control Behaviour of Motorcycle Riders, *Vehicle System Dynamics*, 17-4 (1988).
- (2) Sharp, R.S., The Stability and Control of Motorcycles, *J. Mech. Engng Sci.* 13 (1971).
- (3) Katayama, T., Aoki, A., Nishimi, T., and Okayama, T., Measurements of Structural Properties of Riders, 4th International Pacific Conference on Automotive Engineering, (1987) Melbourne.

## Appendix I, Symbols

$a_f, h_f, h_m, h_L, h_U, h_a, l_f, l_R, l_a, l_1, l_2, t$	Linear dimensions (Figure 4)
$C_{F_x}, C_{F_y}, C_{F_z}$	Coefficients of aerodynamic forces
$C_{M_y}, C_{M_z}$	Coefficients of aerodynamic moments
$C_{r_{xx}}$	Product of inertia of main frame
$C_{x_{c1}}, C_{x_{c2}}$	Overturning moment coefficients due to camber angle (1:front, 2:rear)
$C_{x_{s1}}, C_{x_{s2}}$	Overturning moment coefficients due to sideslip angle
$C_{y_{c1}}, C_{y_{c2}}$	Camber stiffness
$C_{y_{s1}}, C_{y_{s2}}$	Cornering stiffness
$C_{z_{c1}}, C_{z_{c2}}$	Camber torque coefficients
$C_{z_{s1}}, C_{z_{s2}}$	Aligning torque coefficients
$C_s$	Damping constant of steering system
$F_{ax}, F_{ay}, F_{az}$	Aerodynamic forces
$F_{fy}, F_{ry}$	Tyre forces, cornering forces and camber forces
$F_{fz}, F_{rz}$	Tyre loads
$g$	Gravitational acceleration
$I_{fx}, I_{fz}$	Moments of inertia of front fork
$I_{rx}, I_{rz}$	Moments of inertia of main frame
$I_{Lx}, I_{Lz}$	Moments of inertia of rider lower body
$I_{Ux}, I_{Uz}$	Moments of inertia of rider upper body
$i_{cy}$	Polar moment of inertia of engine flywheel
$i_{fy}, i_{ry}$	Moments of inertia of front and rear wheel
$k_{sd}, k_{s\phi}$	Coefficients of steering control torque
$k_{ud}, k_{u\phi}$	Coefficients of upper body control torque
$M_f, M_m$	Mass of front fork and main frame
$M_L, M_U$	Mass of rider lower body and upper body
$T_{ax}, T_{ay}, T_{az}$	Aerodynamic moments
$T_{fx}, T_{rx}$	Overturning moments
$T_{fz}, T_{rz}$	Aligning torques and camber torques
$x, y$	Longitudinal and lateral positions of motorcycle
$\delta$	Steer angle
$\zeta_L, \zeta_U$	Damping ratios of lower and upper bodies
$\kappa_y$	Gear ratio between rear wheel and engine flywheel
$\lambda$	Caster angle
$\sigma_f, \sigma_r$	Relaxation lengths of front and rear tyres
$\tau_s$	Steer torque
$\tau_L, \tau_U$	Rider lower and upper body torques
$\phi$	Roll angle of motorcycle
$\phi_L, \phi_U$	Lean angles of lower and upper body
$\psi$	Yaw angle of motorcycle
$\omega_L, \omega_U$	Natural frequencies of lower and upper body

## Appendix II, Equations of motions

### Equation of equilibrium of lateral forces

$$\begin{aligned} & (M_f + M_m + M_L + M_U) \ddot{y} + [M_f l_f - (M_L + M_U) l_R] \ddot{\psi} + (M_f + M_m + M_L + M_U) \dot{x} \dot{\psi} \\ & + [M_f h_f + M_m h_m + M_L h_L + M_U (h_L + h_U)] \dot{\phi} + M_f a_f \dot{\delta} \\ & + [M_L h_L + M_U (h_L + h_U)] \dot{\phi}_L + M_U h_U \dot{\phi}_U - F_{ay} - F_{fy} - F_{ry} = 0 \end{aligned}$$

### Equation of equilibrium of yawing moments

$$\begin{aligned} & [M_f l_f - (M_L + M_U) l_R] \ddot{y} \\ & + [M_f l_f^2 + I_{fx} \sin^2 \lambda + I_{fx} \cos^2 \lambda + I_{mz} + (M_L + M_U) l_R^2 + I_{Lz} + I_{Uz}] \ddot{\psi} \\ & + [M_f l_f - (M_L + M_U) l_R] \dot{x} \dot{\psi} \\ & + [M_f h_f l_f + (I_{fz} - I_{fx}) \sin \lambda \cos \lambda - C_{rxz} - M_L h_L l_R - M_U (h_L + h_U) l_R] \dot{\phi} \\ & + (M_f a_f l_f + I_{fz} \cos \lambda) \dot{\delta} - i_{fy} / R_f \sin \lambda \dot{x} \dot{\delta} - [M_L h_L + M_U (h_L + h_U) l_R] \dot{\phi}_L - M_U h_U l_R \dot{\phi}_U \\ & - l_a F_{ay} - T_{az} - l_1 F_{fy} + l_2 F_{ry} - T_{fz} - T_{rz} = -\tau_s \cos \lambda \end{aligned}$$

### Equation of equilibrium of rolling moments

$$\begin{aligned} & [M_f h_f + M_m h_m + M_L h_L + M_U (h_L + h_U)] \ddot{y} \\ & + [M_f h_f l_f + (I_{fz} - I_{fx}) \sin \lambda \cos \lambda - C_{rxz} - M_L h_L l_R - M_U (h_L + h_U) l_R] \ddot{\psi} \\ & + [M_f h_f + M_m h_m + M_L h_L + M_U (h_L + h_U) + i_{fy} / R_f + (i_{ry} + i_{ey} \kappa_y) / R_r] \dot{x} \dot{\psi} \\ & + [M_f h_f^2 + M_m h_m^2 + I_{fx} \cos^2 \lambda + I_{fz} \sin^2 \lambda + I_{mx} + M_L h_L^2 + M (h_L + h_U)^2 + I_{Lx} + I_{Ux}] \dot{\phi} \\ & - [M_f h_f + M_m h_m + M_L h_L + M_U (h_L + h_U)] g \phi \\ & + (M_f a_f h_f + I_{fz} \sin \lambda) \dot{\delta} + i_{fy} / R_f \cos \lambda \dot{x} \dot{\delta} + (t Z_f - M_f a_f g) \delta \\ & + [M_L h_L^2 + M_U (h_L + h_U)^2 + I_{Lx} + I_{Ux}] \dot{\phi}_L - [M_L h_L + M_U (h_L + h_U)] g \phi_L \\ & + [M_U h_U (h_L + h_U) + I_{Ux}] \dot{\phi}_U - M_U h_U g \phi_U - h_a F_{ay} - T_{ax} - T_{fx} - T_{rx} = \tau_L \end{aligned}$$

### Equation of equilibrium of moments about steering axis

$$\begin{aligned} & M_f a_f \ddot{y} + (M_f a_f l_f + I_{fz} \cos \lambda) \ddot{\psi} + (M_f a_f + i_{fy} / R_f \sin \lambda) \dot{x} \dot{\psi} \\ & + (M_f a_f h_f + I_{fz} \sin \lambda) \dot{\phi} - i_{fy} / R_f \cos \lambda \dot{x} \dot{\phi} + (t Z_f - M_f a_f g) \phi \\ & + (M_f a_f^2 + I_{fz}) \dot{\delta} + C_s \dot{\delta} + (t Z_f - M_f a_f g) \sin \lambda \delta + t F_{fy} - T_{fz} \cos \lambda - T_{fx} \sin \lambda = \tau_s \end{aligned}$$

### Equation of equilibrium of leaning moments of rider lower body

$$\begin{aligned}
 & [M_L h_L + M_U (h_L + h_U)] \dot{y} \\
 & - [M_L h_L + M_U (h_L + h_U)] l_R \dot{\psi} + [M_L h_L + M_U (h_L + h_U)] \dot{x} \dot{\psi} \\
 & + [M_L h_L^2 + M_U (h_L + h_U)^2 + I_{Lx} + I_{Ux}] \ddot{\phi} - [M_L h_L + M_U (h_L + h_U)] g \phi \\
 & + [M_L h_L^2 + M_U (h_L + h_U)^2 + I_{Lx} + I_{Ux}] \dot{\phi}_L \\
 & + 2 \zeta_L \omega_L [M_L h_L^2 + M_U (h_L + h_U)^2 + I_{Lx} + I_{Ux}] \phi_L \\
 & + \omega_L^2 [M_L h_L^2 + M_U (h_L + h_U)^2 + I_{Lx} + I_{Ux}] \phi_L \\
 & + [M_U h_U (h_L + h_U) + I_{Ux}] \dot{\phi}_U - M_U h_U g \phi_U = \tau_L - \tau_U
 \end{aligned}$$

### Equation of equilibrium of leaning moments of rider upper body

$$\begin{aligned}
 & M_U h_U \dot{y} - M_U h_U l_R \dot{\psi} + M_U h_U \dot{x} \dot{\psi} + [M_U h_U (h_L + h_U) + I_{Ux}] \ddot{\phi} - M_U h_U g \phi \\
 & + [M_U h_U (h_L + h_U) + I_{Ux}] \dot{\phi}_L - M_U h_U g \phi_L \\
 & + (M_U h_U^2 + I_{Ux}) \dot{\phi}_U + 2 \zeta_U \omega_U (M_U h_U^2 + I_{Ux}) \phi_U + \omega_U^2 (M_U h_U^2 + I_{Ux}) \phi_U = \tau_U - \tau_U \sin \lambda
 \end{aligned}$$

### Equations of tyre forces and tyre moments

$$\begin{aligned}
 \dot{F}_{fy} + \dot{x}/\sigma_f F_{fy} &= -C_{Ys1}/\sigma_f \dot{y} - C_{Ys1} l_1/\sigma_f \dot{\psi} + C_{Ys1} t/\sigma_f \dot{\delta} \\
 & + C_{Yc1} \dot{x}/\sigma_f \phi + (C_{Ys1} \cos \lambda + C_{Yc1} \sin \lambda) \dot{x}/\sigma_f \delta \\
 \dot{F}_{ry} + \dot{x}/\sigma_r F_{ry} &= -C_{Ys2}/\sigma_r \dot{y} + C_{Ys2} l_2/\sigma_r \dot{\psi} + C_{Yc2} x/\sigma_r \phi \\
 \dot{T}_{fz} + \dot{x}/\sigma_f T_{fz} &= C_{Zs1}/\sigma_f \dot{y} + C_{Zs1} l_1/\sigma_f \dot{\psi} - C_{Zs1} t/\sigma_f \dot{\delta} \\
 & + C_{Zc1} \dot{x}/\sigma_f \phi - (C_{Zs1} \cos \lambda - C_{Zc1} \sin \lambda) \dot{x}/\sigma_f \delta \\
 \dot{T}_{rz} + \dot{x}/\sigma_r T_{rz} &= C_{Zs2}/\sigma_r \dot{y} - C_{Zs2} l_2/\sigma_r \dot{\psi} + C_{Zc2} x/\sigma_r \phi \\
 \dot{T}_{fx} + \dot{x}/\sigma_f T_{fx} &= C_{Xs1}/\sigma_f \dot{y} + C_{Xs1} l_1/\sigma_f \dot{\psi} - C_{Xs1} t/\sigma_f \dot{\delta} \\
 & - C_{Xc1} \dot{x}/\sigma_f \phi - (C_{Xs1} \cos \lambda + C_{Xc1} \sin \lambda) \dot{x}/\sigma_f \delta \\
 \dot{T}_{rx} + \dot{x}/\sigma_r T_{rx} &= C_{Xs2}/\sigma_r \dot{y} - C_{Xs2} l_2/\sigma_r \dot{\psi} - C_{Xc2} \dot{x}/\sigma_r \phi
 \end{aligned}$$

### Aerodynamic forces and moments

$$\begin{aligned}
 F_{ay} &= C_{Fy\beta} q (l_1 + l_2)^2 \dot{y}/\dot{x} & q &= 1/2 \rho \dot{x}^2 \\
 T_{ax} &= C_{Mx\beta} q (l_1 + l_2)^3 \dot{y}/\dot{x} \\
 T_{az} &= C_{Mz\beta} q (l_1 + l_2)^3 \dot{y}/\dot{x} \\
 F_{ax} &= C_{Fx} q (l_1 + l_2)^2 \\
 F_{az} &= C_{Fz} q (l_1 + l_2)^2 \\
 T_{ay} &= C_{My} q (l_1 + l_2)^3
 \end{aligned}$$

### Front and rear tyre loads

$$Z_f = Z_{f0} - F_{az}(l_2 + l_a)/(l_1 + l_2) - F_{ax}h_a/(l_1 + l_2) + T_{ay}/(l_1 + l_2)$$

$$Z_r = Z_{r0} - F_{az}(l_1 - l_a)/(l_1 + l_2) + F_{ax}h_a/(l_1 + l_2) - T_{ay}/(l_1 + l_2)$$

### Coefficients of tyre forces and tyre moments

$$C_* = C_{*1}Z_* + C_{*2}$$

$C_*$  : Tyre coefficients,  $C_{y*1}, C_{y*2}$  etc.

$C_{*1}, C_{*2}$  : Constants

$Z_*$  : Tyre loads

### Appendix III, Basic control method

In this appendix, basic control method is described.

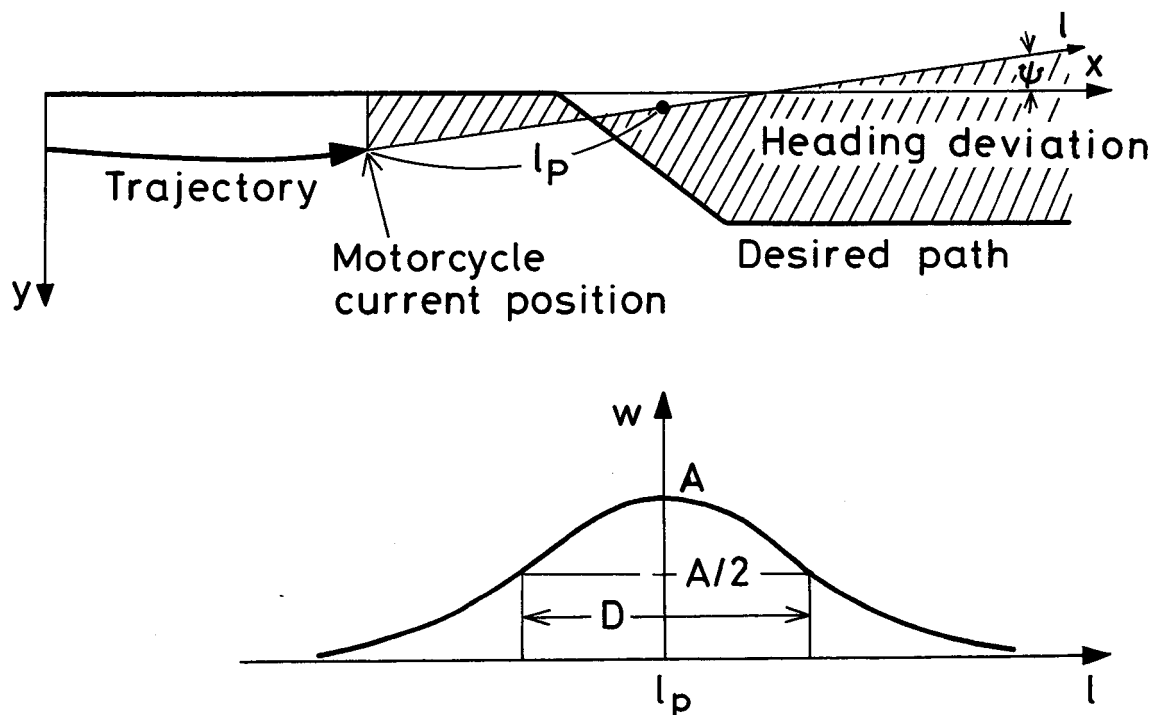
In this study, it is assumed that input informations of a rider are roll angle  $\phi$  of a motorcycle and heading deviation  $d$  from a desired path, and his control outputs are steer torque  $\tau_s$ , lower body control torque  $\tau_L$  and upper body control torque  $\tau_U$ . These control torques are given as follows:

$$\tau_s = k_{s\phi} \phi + k_{s_d} d,$$

$$\tau_L = 2 \tau_s,$$

$$\tau_U = k_{U\phi} \phi + k_{U_d} d,$$

where  $k_{s\phi}$  and  $k_{U\phi}$  are the coefficients of the roll angle input,  $k_{s_d}$  and  $k_{U_d}$  are the coefficients of the heading deviation input.



Attached figure 1. Geometrical configuration of a lane change manoeuvre.

The heading deviation  $d$  from the desired path is determined as follows: First, all forward heading deviations are calculated with motorcycle lateral position  $y$  and yawing angle  $\psi$  and the desired path  $f$  as is illustrated at Attached figure 1. Then these heading deviations are averaged using a weighting function  $w(l)$  drawn at Attached figure 1. The averaged heading deviation  $d$  is given by the following equation,

$$d = A \int_0^{\infty} \exp[-2.77(l - l_p)^2 / D^2] (f - y - l \sin \psi) dl,$$

where  $l_p$  is a rider's sighting distance, and  $D$  is a width of the weighting function at a half value of  $A$ .

## Appendix IV, Specifications of motorcycle models

Attached table 1. Specifications of motorcycle models.

Specification		A	B	C	D	E
$M_f$	kg	38.81	35.48	35.87	27.73	30.87
$M_m$	kg	200.8	173.3	206.2	179.7	166.6
$F_{fz}$	N	-1327.9*	-1036.8*	-1153.5*	-1176.0*	-1143.7*
$I_{fx}$	kgm	4.55	4.62	5.21	2.60	3.70
$I_{fz}$	kgm	0.774	0.715	0.745	0.431	0.843
$I_{mx}$	kgm	13.16	14.11	14.05	11.56	11.86
$I_{mz}$	kgm	26.56	21.75	29.61	16.98	25.77
$i_{fy}$	kgm	0.666	0.666	0.657	0.441	0.441
$i_{ry}$	kgm	0.696	0.725	0.608	0.657	0.598
$a_f$	m	0.044	0.035	0.040	0.026	0.048
$h_f$	m	0.554	0.563	0.579	0.483	0.562
$l_f$	m	0.740	0.813	0.851	0.700	0.668
$h_m$	m	0.503	0.491	0.478	0.550	0.536
$h_a$	m	0.627	0.627	0.573	0.641	0.633
$l_1$	m	0.888	0.998	1.038	0.808	0.803
$l_2$	m	0.609	0.482	0.514	0.572	0.550
$l_a$	m	0.065	0.106	0.121	0.049	0.052
$R_f$	m	0.318	0.320	0.320	0.284	0.299
$R_r$	m	0.315	0.304	0.308	0.314	0.312
$t$	m	0.095	0.102	0.128	0.090	0.086
$\lambda$	°	29.4	32.0	33.7	26.0	27.0
$C_{Fx0}$		-0.246	-0.273	-0.242	-0.275	-0.284
$C_{Fy\beta}$	(°) <sup>-1</sup>	-0.0113	-0.0102	-0.0102	-0.0128	-0.00975
$C_{Fz0}$		-0.0289	-0.0291	-0.0244	-0.0374	-0.0336
$C_{Mx\beta}$	(°) <sup>-1</sup>	-0.000235	-0.000155	-0.000088	0.000237	—
$C_{My0}$		0.0315	0.0323	0.0246	0.0407	0.0428
$C_{Mz\beta}$	(°) <sup>-1</sup>	-0.000134	-0.000431	-0.000866	-0.001582	-0.00127

NOTE \* : Values of  $F_{fz}$  are the values with a rider whose mass is 65kg.

Attached table 2. Tyre coefficients ( $C_0 = C_1 \times |F_{oz}| + C_2$ ).

			A	B	C	D	E
$C_{Ys1}$	$N(^{\circ})^{-1}$	$C_1$	0.1783	0.1984	0.1655	0.1471	0.1591
		$C_2$	8.62	36.26	7.45	18.03	60.76
$C_{Ys2}$	$N(^{\circ})^{-1}$	$C_1$	0.1276	0.1214	0.0557	0.1602	0.0850
		$C_2$	97.41	151.70	232.26	80.16	77.42
$C_{Yc1}$	$N(^{\circ})^{-1}$	$C_1$	0.02195	0.02085	0.01995	0.0176	0.0250
		$C_2$	-6.96	-3.07	-5.44	-3.57	-4.80
$C_{Yc2}$	$N(^{\circ})^{-1}$	$C_1$	0.02245	0.02220	0.01985	0.01860	0.02021
		$C_2$	-5.02	-9.14	4.13	-4.86	1.27
$C_{Zs1}$	$Nm(^{\circ})^{-1}$	$C_1$	0.0032	0.0044	0.00305	0.00275	0.00425
		$C_2$	-1.59	-1.43	-0.99	-0.95	-1.84
$C_{Zs2}$	$Nm(^{\circ})^{-1}$	$C_1$	0.00405	0.0057	0.00625	0.0046	0.0036
		$C_2$	-3.66	-4.16	-4.01	-3.90	-2.42
$C_{Zc1}$	$Nm(^{\circ})^{-1}$	$C_1$	0.00020	0.000105	0.00021	0.000025	0.000245
		$C_2$	-0.169	-0.014	-0.123	0.024	-0.107
$C_{Zc2}$	$Nm(^{\circ})^{-1}$	$C_1$	0.00042	0.000425	0.000465	0.00041	0.000255
		$C_2$	-0.310	-0.454	-0.180	-0.415	-0.029
$C_{Xs1}$	$Nm(^{\circ})^{-1}$	$C_1$	—	—	—	—	0.00315
		$C_2$	—	—	—	—	-2.41
$C_{Xs2}$	$Nm(^{\circ})^{-1}$	$C_1$	—	—	—	—	0.00277
		$C_2$	—	—	—	—	-3.02
$C_{Xc1}$	$Nm(^{\circ})^{-1}$	$C_1$	0.00135	0.00140	0.00135	0.00125	0.00120
		$C_2$	-0.208	-0.206	-0.108	-0.167	-0.255
$C_{Xc2}$	$Nm(^{\circ})^{-1}$	$C_1$	0.00175	0.00215	0.00315	0.00180	0.00157
		$C_2$	-0.358	-0.360	-0.958	-0.157	-0.588
$\sigma_f$	mm	$C_1$	0.0887	0.1329	0.1006	0.0830	0.1188
		$C_2$	4.71	31.07	19.37	33.66	29.00
$\sigma_r$	mm	$C_1$	0.0919	0.0640	0.0476	0.1190	0.0379
		$C_2$	29.40	87.90	144.9	6.32	82.00

### Acknowledgement

This paper is a part of the results of the research conducted by JARI for a long period of time under commission and finance by the Japan Automobile

Manufactures Association Inc. (JAMA). We would like to express our hearty appreciation to the Motorcycle Handling Stability Subcommittee of JAMA which supplied the experiment motorcycles and test riders for the running experiments of this research.

# Leg Injuries and Mechanisms in Motorcycling Accidents

Written Only Paper

**Peter L. Harms,**  
Transport and Road Research Laboratory,  
England

## Abstract

Concern has been expressed over the high proportion of motorcyclists who sustain serious leg injuries in road traffic accidents. This Paper reports on a targeted sample of motorcyclist casualties whose leg injuries were severe enough to warrant hospital in-patient care. Detailed mechanisms of injury were established for 115 casualties admitted to five hospitals in the same geographical location as the Transport and Road Research Laboratory.

Careful examination of the motorcycle and object struck (usually a car) enabled case profiles to be built up for each accident. There were two main mechanisms of injury: (a), entrapment and (b), direct impact to the injured leg. The upper leg sustained more direct blows from a car structure and any entrapment usually involved the motorcycle petrol tank and the car. The lower legs sustained more entrapment injuries between some part of the lower motorcycle structure and a car component, usually but not exclusively the bumper. The handlebars also caused femoral fractures.

Other related studies with larger samples are also reported and show that leg injuries predominate, both as a proportion of total injuries and also in relation to the length of stay in hospital required to treat these particular injuries. The findings of all these studies lend strong support to the provision of integral leg protectors as a means of reducing leg injuries sustained by accident-involved motorcyclists.

## Introduction

Out of 790 motorcyclist casualties attending one district hospital over a two year period, 61 percent sustained a leg injury of some severity. Concern over leg vulnerability, coupled with information from other studies, prompted an in-depth study on motorcyclist leg injury mechanisms. This was carried out over an eighteen month period with the cooperation of five district hospitals, two police authorities and various recovery garages. The machines and roadside structures/other vehicles involved were examined and photographed, correlated with injury details and other data in order to obtain a leg injury mechanism profile for each case. Preliminary results were reported earlier (1).<sup>\*</sup> This Paper finalises the work and also reports on, and integrates the results from, some related studies.

## Methodology

The five hospital sample was selected from casualties whose leg injury was severe enough the warrant either in-patient care or major out-patient treatment. The majority of the casualties sustained leg fractures. Injury information

plus brief accident circumstances were obtained by the participating medical staff who then notified TRRL investigators—usually within 24 hours of the accident. Vehicle location and further accident circumstances were obtained from the appropriate police Divisions. The vehicles were then traced to recovery garages (or exceptionally to a home address), fully examined to a standard procedure and photographed at the earliest opportunity. If appropriate, the casualty was questioned in more depth and external clothing worn at the time fully examined for contact marks (preferably in a discrete hospital location *before* the garments were taken home and washed by caring relatives!). The accident scene was visited and photographed if a roadside structure was involved. If another vehicle was involved in the accident, this was also traced, examined and photographed. However, since a number of these vehicles were still driveable following the accident, this sometimes meant arranging an evening visit to a home address. Full information on accident circumstances was obtained from police sources at a later date. The Abbreviated Injury Scale (AIS) was used to classify injury severity. It is appropriate to touch on several aspects of the methodology:

(a) Such a study involves handling confidential medical and police information at an early stage where the latter is often sub-judice. The sensitivity of these situations must be recognised and handled accordingly if the study is to succeed. The fact that the project involves *injury* causation as opposed to *accident* causation goes a long way to allaying any fears of a breach of confidentiality. The involvement of staff from a nationally recognised Research Laboratory whose task was perceived as being involved in injury prevention also gave further credibility. At any stage where casualties and others involved were interviewed, the investigators always left a letter to be read at a later time explaining the reason for the study and assuring those concerned of confidentiality. Names and addresses used for the initial search were eventually destroyed.

(b) The investigator is looking for interaction between a motorcycle/rider/pillion and a striking/struck object—usually a car. Therefore good lighting during the examination is essential and structures must be viewed from several angles. Ideally, clothing examination should take place and injury details noted *before* vehicle(s) are examined as vehicle paint traces or other marks are frequently present on the former which can then be correlated with the vehicle involved. Such marks usually take the form of a dulling of the vehicle paintwork in the area concerned and also fibres may have adhered due to the paint melting slightly during friction impact. Care should be taken when using photographic flash in order to avoid reflections from shiny body panels and glazed areas—both on the vehicle *and* the garage building.

<sup>\*</sup> Numbers in parentheses designate references at end of paper.

## Results

These are presented in a series of tables with brief comment. Percentages may not always equate to 100 due to rounding errors.

### The Accident

Although it is beyond the scope of this paper to discuss primary accident circumstances, it is considered worthwhile presenting some key factors. Information was available for 116 accident cases and is presented in tables 1, 2 and 3. Some of these factors could be considered in combination as contributing to accident causation.

**Table 1. Accident location of posted speed limit.**

LIMIT(miles/h) " ( km/h )	30/40 *	50/60/70 80/96/112	Limit NK " "
N.	60	41	15
(%) Known values	(59)	(41)	-

\* Built-up areas.

Almost 60 percent of the accidents occurred in built-up areas, which is in line with national figures. However, the speed of the motorcycle prior to impact may have been higher or lower than the posted speed limit. In many cases it was not possible to determine this with accuracy.

**Table 2. Accident location related to road layout.**

INVOLVING	Junction *	Non-junction	Roundabout	NK
N.	62	46	4	4
(%) Known values	(55)	(41)	(4)	-

\* Junctions of different types, including cross-roads.

It will be seen that a higher percentage of the accidents involved a junction where the potential for vehicle conflicts is greatest.

**Table 3. Day/night distribution.**

AMBIENT LIGHT	Daylight	Night with lights	Night w/out lights	Night, lights N	Ambient light
N.	72	21	12	5	6
(%) known values	(69)	(20)	(11)	-	-

The majority of the accidents occurred during daylight hours.

**Table 4. Road surface condition.**

ROAD CONDITION	Dry	Wet	NK
N.	84	17	15
(%) Known values	(83)	(17)	-

Wet road conditions did not appear to play a major role in these accidents.

### The accident-involved motorcycle

Motorcycle engine capacity is given in table 5.

**Table 5. Engine capacity of accident-involved motorcycles.**

CAPACITY (cc)	50-80	90-100	125	175	200-250	350-400	500-650	750	900-1100	Capacity NK
N.	25	17	20	3	14	9	9	7	5	3

The majority (62 percent) of the machines had an engine capacity of 125 cc or less. (For comparison, 75 percent of motorcycles and mopeds currently registered in the UK are under 150 cc).

The principal direction of force to the motorcycle in the accident is given in table 6. Secondary impacts usually involving the road surface invariably occurred. When there was no clear direction of impact e.g., when the machine skidded and went on its side, a 00 classification is given.

**Table 6. Clock direction of principal impact (12 o'clock is in line of travel).**

DIRECTION	08	09	10	11	12	01	02	03	04	00/NK
N (%)	1 (<1)	6 (5)	6 (5)	14 (13)	51 (46)	14 (13)	5 (5)	3 (3)	4 (4)	7 (6)

Seventy-two percent of the principal collisions were to the front (11-01 clock direction).

The principal object hit by the motorcycle is given in table 7 and show that almost three-quarters of the collisions were with cars. In many cases contact with the same object also caused the leg injury. The detailed injury mechanisms are presented in tables 10 to 16.

**Table 7. Principal object hit by motorcycle.**

OBJECT	Car	HGV/PSV	LGV	Trailer	Road	Wall/Tree	Other	NC*	NK
N. (%)	86 (74)	3 (3)	8 (7)	3 (3)	4 (3)	3 (3)	3 (3)	2 (2)	4 (3)

\* No significant contact to motorcycle

### The Casualty

Complete injury data for the casualties involved was available for a slightly smaller subset of 112 accidents. This involved 110 riders and 7 pillion passengers—all with severe leg and sometimes other injuries. All except one survived their particular accident.

The age distribution is given in table 8 and shows that 74 percent of the casualties for whom age was known were 21 years or under.

**Table 8. Age distribution of injured motorcyclists.**

AGE	16	17	18	19	20	21	22	23	24	25	26-30	31+	Age NK
N.	18	23	7	14	10	2	3	5	2	2	6	7	18

Of the 117 casualties, 108 sustained their leg injuries whilst still with the machine and 9 casualties whilst off the machine. There were two cases where the mechanism was not established.

Location of leg injuries of severity  $\geq$  AIS2 is given in table 9. Most of these were fractures—sometimes at more than one anatomical site.

**Table 9. Anatomical location of severe leg injuries (AIS >= 2).**

LOCATION	Pelvis	Thigh	Knee	Tibia *	Fibula	Tib+fib	Ankle	Foot
L. limb (% s/set)	- (0)	22 (30)	9 (12)	16 (22)	2 (3)	18 (24)	5 (7)	2 (3)
R. limb (% s/set)	7 (9)	25 (31)	8 (10)	16 (20)	3 (4)	16 (20)	4 (5)	2 (2)
TOTAL (%)	7 (4)	47 (30)	17 (11)	32 (21)	5 (3)	34 (22)	9 (6)	4 (3)

\* Includes 2 non-fracture but severe lower leg injuries.

(N.B. Because of the multiplicity of injuries, these exceed the number of casualties. Numbers are only exclusive relative to Left and Right Limbs).

There were five casualties with bilateral fractures of the femur and some casualties sustained fractures to both limbs but at different anatomical sites. Also one leg can have more than one significant injury. Lower leg injuries slightly predominated. In general, there appeared to be no significant difference in numbers of injuries to the left and right legs. However there were seven Right-sided pelvic injuries with none on the Left.

### Detailed mechanism of leg injuries

Mechanism of injury related to the unprotected road user is not always easy to determine. Unlike a vehicle occupant in an accident situation, the casualty is not contained and the lack of contact marks sometimes presents problems. However, interpretation based on experience and good investigative procedures will produce results on most occasions. It must be appreciated that the leg is often swept aside during the impact phase to a location other than the normal riding position and investigators must keep an open mind on contact location for both the machine and other structures. For the motorcyclist casualty, mechanisms of leg injury broadly fall into four main categories:

(a) When the leg is trapped between some part of the machine and the striking/struck object (usually part of a car exterior).

(b) The injury has been caused by a direct blow from some part of the striking/struck object. However, involvement of some part of the motorcycle acting in combination cannot be ruled out and some injuries in this category could have been caused by entrapment without leaving evidence.

(c) The injury has been caused by a direct and exclusive contact with some part of the machine. Typical situations are in frontal impacts when the machine remains in contact with the striking/struck object and the rider is projected forward causing the leg to strike the handlebars and/or a car front structure.

(d) The casualty has been thrown from the machine on impact and sustained leg injuries by striking an unyielding object (usually the road). Injuries to other body regions are sometimes sustained due to this mechanism.

A fifth category (e), is used when the injury mechanism cannot be established.

Aggravation of an injury can also take place following an initial impact e.g., (a), (b) or (c) followed by (d).

Results showing the numbers and percentages falling in each of the categories are given in table 10.

**Table 10. Broad categories of leg injury mechanisms.**

CATEGORY	Entrapment (a)	Direct (Other) (b)	Direct (M/C) (c)	Direct (Off M/C) (d)	Mechanism N.K. (e)
Leg injuries (N=157)	57	66	24	8	2
% Casualties (N=117) *	(49)	(56)	(21)	(7)	(2)
% Leg injuries	(36)	(42)	(15)	(5)	(1)

\* Due to a multiplicity of leg injuries in some cases, numbers and percentages are not necessarily exclusive.

The broad injury mechanisms were further divided into two anatomical groups: Pelvic area/upper leg/knee and, Lower leg/ankle/foot. The distribution is given in table 11.

**Table 11. Broad categories of injury mechanisms by leg region.**

MECHANISM LEG REGION	Entrapment (a)	Direct (Other) (b)	Direct (M/C) (c)	Direct (Off M/C) (d)	NK (e)	TOTAL
Upper N. (% sub-set)	13 (19)	38 (54)	15 (21)	3 (4)	1 (1)	70
Lower N. (% sub-set)	44 (51)	28 (32)	9 (10)	5 (6)	1 (1)	87
Both N. (%)	57 (36)	66 (42)	24 (15)	8 (5)	2 (1)	157

The results indicate that there is more entrapment to the lower leg than the upper. The precise mechanisms will be detailed in subsequent tables, again taking the upper and lower legs separately.

### Upper leg injury mechanisms

As would be expected, the petrol tank was responsible for a larger proportion of entrapment injuries to the upper leg—in combination with a variety of car structures (table 12).

**Table 12. Upper leg injury mechanisms—entrapment.**

OTHER STRUCTURE	Front Grille	Bonnet L/edge	Wing/door panels	Corner /Edge	Road	TOTAL
M/C STRUCTURE						
Petrol tank	2	2	3	1		8
M/C seat				2		2
Front wheel assembly		1				1
M/C part NK					2	2

There was a variety of contact locations for 'direct impact' mechanisms as shown in table 13. As previously stated, some of these injuries could have been caused by entrapment between the other structure and the motorcycle, but leaving no direct evidence on the latter.

**Table 13. Upper leg injury mechanisms. Direct impact by/to other structure.**

Grille /Boot	Bonnet L/edge	Wing/Door Panels	Wing Corner /Edge	Front Bumper	Torn Panels	Road Surf	Other
5	3	4	15	2	5	3	4

The car wing corner/edge predominates as an injury causing source in this mechanism category. There were also 15 occasions when handlebar contact alone caused upper leg injuries, mainly femoral fractures in frontal impacts. There was one upper leg injury where the mechanism could not be determined.

### Lower leg injury mechanisms

There was a higher proportion of entrapment injuries to the lower leg/ankle/foot compared to the upper leg (table 14).

**Table 14. Lower leg injury mechanisms—entrapment.**

OTHER STRUCTURE	Front Bumper	Front Grille	Panels	Corner /Edge	Air dam	Road	Soft Earth	Other
M/C								
Petrol /tank		1	1					
Engine /zone *	5	2		5		1		2
Front /wheel		1						
Gearbox /region	5		2	2				
Platform /Pedals					2	1		
Handlebar M/C Other	1			2				1
M/C, NK Other	2			1			2	1
						1		
TOTAL	13	4	3	10	2	3	2	4

\* Includes engine fins, frame, battery cover & exhaust.

Table 14 shows a wide range of structures giving rise to entrapment injuries of the lower legs. The combined engine area components give rise to most entrapment injuries in combination with a variety of car structures. The gearbox region is the principal individual part involved on the motorcycle, while the front bumper and corners of the car also feature prominently.

As for the upper legs, there was a wide variety of contact locations giving rise to 'direct blow' injuries to the lower legs, caused principally by the car bumper. A proportion was also caused by direct road contact when the rider was thrown from the machine, as shown in table 15. Again some of these injuries could be in the 'entrapment' category but leaving no evidence on the motorcycle.

**Table 15. Lower leg injury mechanisms direct contact by/to other structure.**

Front Grille	Wing Corner	Bumpers	Panels	Torn Panels	Bonnet L/Edge	Boot Rear	Car Other	HGV	Road
2	2	10	3	2	2	3	1	1	5

There were relatively few lower leg injuries caused exclusively by direct contact with some part of the motorcycle structure. They are listed in table 16 and show that no motorcycle structure predominates as an injury source in this particular mechanism category.

**Table 16. Lower leg injury mechanisms caused by motorcycle structure.**

Handlebars	Engine Bars	Pedals	Frame	Front Wheel	M/C Other	M/C NK
2	1	1	1	1	2	1

In addition to the injuries listed in tables 14 to 16, there was one case where the injury mechanism could not be determined.

## Additional Studies

### Casualty attendance at one hospital

An analysis was carried out of data from a separate hospital-based TRRL survey of casualties attending one large district hospital in Oxford (a different geographical area from the above and over a more extended period). The original data combined skeletal and other injuries so the distribution is not directly comparable to that given in previous tables. However similar headings have been used. The sample contained 1498 motorcyclist casualties of which there were 3748 separately identifiable injuries. The distribution according to severity and body region is presented in table 17. AIS 2 limb injuries were likely to include fractures. AIS 3 limb injuries would all be fractures.

**Table 17. Distribution of Injuries, 1498 motorcyclist casualties (N.B. numbers are not mutually exclusive).**

BODY REGION	Head /neck	Spine	Shoulder	Chest	Uppr limb	Abdo	Pelvis *	Lower limb
AIS [N] (%)								
1 [2537] (%)	273 (11)	5 (<1)	2 (<1)	22 (<1)	807 (32)	83 (3)	3 (<1)	1342 (53)
2 [705] (%)	252 (36)	12 (2)	101 (14)	16 (2)	168 (24)	2 (<1)	6 (<1)	148 (21)
3 [421] (%)	42 (10)	20 (5)	12 (3)	23 (5)	96 (22)	10 (2)	17 (4)	201 (48)
4-6 [85] (%)	34 (40)	5 (6)	-	22 (26)	-	23 (27)	1 (1)	-
TOTAL [3748] (%)	601 (16)	42 (1)	115 (3)	83 (2)	1071 (29)	118 (3)	27 (<1)	1691 (45)
2-3 [1126] (%)	294 (26)	32 (3)	113 (10)	39 (3)	264 (23)	12 (1)	23 (2)	349 (31)

\* Includes hip.

A more specific distribution for regions of the lower limb is given in table 18.

**Table 18. Number of injury sites.**

SITE	Pelvis *	Up leg	Knee	Lo Leg	Ankle/Foot	TOTAL
AIS 1 (%)	3 (<1)	285 (21)	15 (1)	730 (54)	312 (23)	1345 (100)
AIS 2-3 (%)	23 (6)	75 (20)	79 (21)	114 (31)	81 (22)	372 (100)
AIS 1-3 (%)	26 (2)	360 (21)	94 (5)	844 (49)	393 (23)	1717 (100)

\* Includes hip. (N.B. Sites are not mutually exclusive)

A rank order of injury sites by injury severity is given in table 19.

Out of this total sample of 1498 casualties, there were 3748 separately identifiable injuries of all severities. Of these, 45% were to the lower limbs of which about 50% were to the lower leg (excluding knees, ankles & feet).

**Table 19. Rank order of injury sites (%). 1498 motorcyclist casualties.**

AIS1 (N=2537)	AIS 2-3 (N=1126)	AIS 4-6 (n=85)	AIS 1-6 (N=3748)
Lo Limb (53)	Lo Limb (31)	Head/Neck(40)	Lo Limb (45)
Up Limb (32)	Head/Neck(26)	Abdomen (27)	Up Limb (29)
Head/Neck(11)	Up Limb (23)	Chest (26)	Head/Neck(16)
Abdomen (3)	Shoulder (10)	Spine (6)	Abdomen (3)
All Others(1)	Spine (3)	Pelvis (1)	Shoulder (3)
	Chest (3)		All Others(4)

There were 2537 separately identifiable injuries of AIS 1 severity. Of these, 53% were to the lower limbs of which 54% were to the lower leg (excluding knees, ankles & feet).

There were 1126 separately identifiable injuries of AIS 2-3 severity. Of these 33% were to the lower limbs of which 31% were to the lower leg (excluding knees, ankles & feet).

The lower limb ranked highest as the site of the maximum number of injuries of AIS 2-3 severity and all severities.

### Length of stay in hospital

Length of stay as a hospital in-patient depends, amongst other things, on severity of the injury, treatment regimen, bed availability, presence of other injuries and level of care available in the casualty's home. However previous clinical experience suggests that leg injuries produce longer stay periods as treatment procedures such as traction require the patient to remain in bed for extended periods with plaster, weights and a level of nursing care that is not available in the home situation.

Although length-of-stay data was not available from the above in-depth studies, information contained in the Scottish Hospital Inpatients (SHIPS) database enabled leg injuries and their specific in-patient care period to be assessed separately. Injury severity is classified using AIS converted from the International Classification of Diseases (ICD) and a fracture will be given a score of 2 or 3. Table 20 presents leg injury severity vs. length of stay in hospital for the treatment of that particular leg injury.

**Table 20. Length of stay versus leg injury severity: Motorcyclist casualties**

STAY (days)	0	1	2	3	4-10	11-30	31-100	101+	TOTAL
AIS									
1 (%)	11 (6)	47 (25)	24 (13)	29 (15)	51 (27)	21 (11)	5 (3)	0 (0)	188 (100)
2 (%)	16 (2)	76 (12)	81 (12)	54 (8)	243 (37)	146 (22)	36 (6)	1 (<1)	653 (100)
3 (%)	6 (1)	7 (1)	8 (1)	19 (3)	75 (14)	197 (38)	198 (38)	12 (2)	522 (100)
TOTAL (%)	33 (2)	130 (10)	113 (8)	102 (7)	369 (27)	364 (27)	239 (18)	13 (1)	1363 (100)

As expected and generally speaking, the more severe the injury, the more extended the stay in hospital. The distribution of stay for each injury level is shown graphically in figure 1 and illustrates this shift.

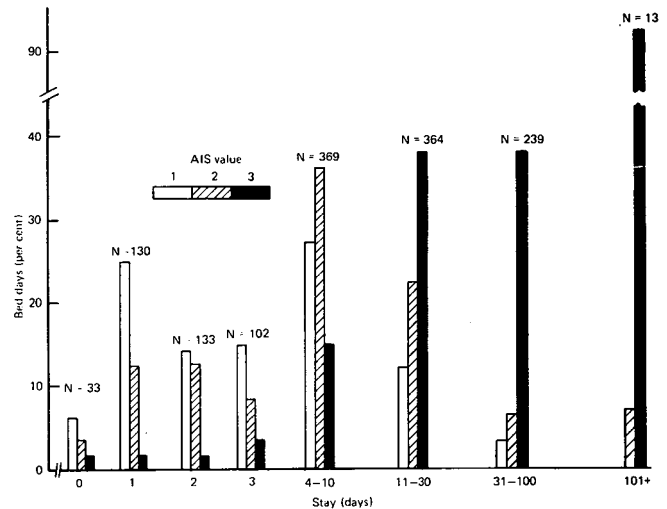


**Figure 1. Motorcyclist casualties with leg injuries (N = 1363). Length of in-patient stay (bed-days) (N.B. 'stay' scale is non-linear).**

### Discussion

Although there has been a decline in motorcyclist casualties in recent years in line with a decrease in motorcycle usage, the young motorcyclist continues to remain vulnerable to death and serious injury. Comparisons are often made between accident rates for motorcycle riders and car drivers and analysis of national accident figures show that these rates vary with age. For example, the estimated probability of death or serious injury for motorcycle riders in the 21-24 year age group per vehicle kilometre travelled is about 18 times that of car drivers of the same age (2).

Translating results from a targeted in-patient accident sample to national figures is not always possible. However the large sample involving some 1500 casualties reported in the Oxford study shows that leg injuries represent nearly half of the total injuries for which the motorcyclist casualty attended hospital. Of all the injuries in that sample, 45 percent were to the lower limbs. Experience has shown that a high proportion of these involve skeletal comminution requiring lengthy in-patient care. In addition, there is a strong possibility of protracted out-patient recovery with the added risk of permanent disability, either from the outset or in later life. Data from the Scottish Hospital In-Patient Study shows an increase in the in-patient stay period for the more severe leg injury.

In the five-hospital leg injury study, nearly two-thirds of the accidents occurred in built-up areas and a higher proportion involved a junction. Most took place during daylight hours. Wet roads did not appear to be a major factor in these accidents but a combination of ambient conditions could be a casual factor. Where ages were known, 74 percent of casualties in this study were 21 years of age or under. Most of them were riding machines with an engine capacity of 125cc or less.

Most of the primary collisions to the motorcycle were frontal (72% having a clock direction of between 11-01).

However, this may not always have a bearing on the subsequent leg injury mechanism due to the sometimes violent post-collision movement of the machine with the rider still astride. An obvious example is in a frontal vehicle collision followed by violent pivoting of the machine about the headstock causing entrapment of the leg between the machine and (usually) a car side. In the majority of cases (74 percent), the motorcycle was in collision with a car. This contact also gave rise to most of the leg injuries, often in combination with the motorcycle structure.

The majority of injuries were to the lower leg where most were to the tibia and/or fibula and 51 percent of these were caused by entrapment between the motorcycle and the other structure, usually a car. There was no significant difference between the number or severity of injuries to the left and right limbs. As expected, there were a variety of structures giving rise to these leg injuries. However, the majority in the entrapment category involved either front car corner structures, bumpers or wing/door panels. The motorcycle component involved in entrapment varied, but a high proportion were components of the engine area, the gearbox and petrol tank. Where injuries appeared to be caused by direct impact rather than entrapment (and entrapment was almost certainly underestimated because its identification requires visible evidence on *both* of the structures involved), the principal parts of the 'other vehicle' causing the impact injuries were again, corners, wing/door panels and bumpers. The predominant feature on the motorcycle giving rise to most direct-impact injuries (fractured femurs) was the handlebars in frontal impacts.

## Conclusions

The results reported in this Paper show that the greatest cause for concern in motorcyclist casualties is the predominance of severe leg injuries. These generally require an extended period in hospital and may lead to permanent disability. The studies have shown that most of these injuries occur when the rider/pillion passenger is still with the machine in the impact phase. There are two main types of injury mechanisms: (a), entrapment and (b), direct impact. A higher proportion of upper leg injuries are caused by direct impacts and more lower leg injuries are caused by entrapment between some part of the motorcycle and the struck/striking object. However some of the 'direct impact' injuries may in fact be entrapment injuries without any witness marks being left on the opposing structure.

The results from these injury studies strongly support to the need for some form of integral leg protector to be fitted

to the motorcycle structure in order to reduce leg injury morbidity amongst young riders. This in turn would reduce costly in-patient treatment and therefore the cost to the community. In addition to the obvious value of such a remedy, there is potential for improving parts of the car structure involved in motorcycling accidents. It is encouraging to note that proposals for modifying car front structures to lessen pedestrian injuries are currently being pursued by this Laboratory and others. This could also have great benefit in reducing motorcyclists leg injuries, as results from this Paper indicates that similar parts of the car's structure are involved in causing injuries to both types of road user.

## References

(1) Harms, P.L. et al., *Mechanism of Lower Limb Injuries amongst Motorcyclist Casualties—Preliminary Findings*. Proc. 10th IRCOBI Conference, Delft. September 1984.

(2) Broughton, J., *Casualty Rates by Age and Sex*. Road Accidents Great Britain 1987, the Casualty Report. Her Majesty's Stationery Office, London, England.

## Acknowledgements

Studies such as those reported in this Paper could not take place without the cooperation of many people. The author is grateful to the following:

Jeff Meades of the Vehicle Safety Division, TRRL for his contribution to the five-hospital study. Rob Tunbridge and Fred James of the Road Safety Division, TRRL. The former for providing the Oxford data and the latter for the SHIPS data. The origins of these two data sources are also acknowledged.

The Accident Consultants, their senior medical and nursing staff and the Medical Records personnel of the participating hospitals. Also the staff of the Accident Records offices and police officers of Thames Valley and Hampshire Police.

Recovery garages in the study catchment area and also the casualties, their relatives and others involved in the accidents investigated.

The work described in this Paper forms part of the programme of the Transport and Road Research Laboratory and the Paper is published by permission of the Director.

**Crown Copyright. The views expressed in this Paper are not necessarily those of the Department of Transport. Extracts from the text may be reproduced, except for commercial purposes, provided the source is acknowledged.**